



A University of Sussex PhD thesis

Available online via Sussex Research Online:

<http://sro.sussex.ac.uk/>

This thesis is protected by copyright which belongs to the author.

This thesis cannot be reproduced or quoted extensively from without first obtaining permission in writing from the Author

The content must not be changed in any way or sold commercially in any format or medium without the formal permission of the Author

When referring to this work, full bibliographic details including the author, title, awarding institution and date of the thesis must be given

Please visit Sussex Research Online for more information and further details

Building Molecules for the Modulation of Age-Related Diseases

Jessica E. Dwyer

Supervisor Prof M. C. Bagley

Submitted to the University of Sussex in part fulfilment of the requirements of the
degree of Doctor of Philosophy, June 2016

Declaration

I hereby declare that the work presented in this thesis was carried out at the University of Sussex under the supervision of Prof M. C. Bagley between the dates of September 2012 and March 2016. The work presented in this thesis is my own, unless otherwise stated, and has not been submitted in whole or in part form for award of another degree.

Jessica E. Dwyer

Acknowledgements

First and foremost I would like to express my gratitude to my supervisor, Prof. Mark Bagley. His constant guidance, exuberance and passion for chemistry have helped me become a more quizzical and enthusiastic chemist.

I would like to thank the School of Life Sciences (Sussex) and the EPSRC for funding my studies.

I would like to thank the staff at the University of Sussex chemistry department. My co-supervisor Dr John Spencer, for his helpful comments and discussions, Dr Alaa Abdul-Sada for performing mass spectrometry measurements, Dr Mark Roe for performing X-ray crystal diffraction experiments and Dr Iain Day for his guidance and tuition in the understanding and completion of NMR experiments. Also special thanks to Alex, Paul and Barry for all their help.

I would like to thank the staff and Ph.D. students who taught and supervised me during my undergraduate degree at the University of Sussex, especially Dr Eddy Viseux and Dr Chris Gallop.

I would like to thank my colleagues, past and present, David Neill-Hall, Hayley Rand, Irina Chuckowree, Alex Rand, Ayed Alnomsy, Hussein Sharhan, Tyler Nichols, Pierre Milbeo and Lorna Bringham. They have been a constant source of support and friendship throughout my degree, a shoulder to lean on and an avid audience for presentations when my confidence needed it.

I would like to thank my friends Vicki Greenacre, Gavin Roffe, Tom Moore, Rhiannon Jones, Adam Close, Oran O'Doherty, Irene Maluenda, Katie Duffell, Jess Frey, Laura Nicholls and Daniel Guest for their help and support through some difficult times, personal and professional. I would never have been able to get to this stage without their encouragement, kindness and jelly beans.

I would like to thank all my teachers from Colchester County High School for girls. They instilled in me a passion to succeed and zest for knowledge that has continued to flourish during my degree. My CCHS girls have been a constant touchstone, bringing me joy and encouragement in bucket loads.

Lastly I need to thank my family and closest friends. Always a support when I needed them, my parents have been the most wonderfully stubborn cheerleaders. I would also like to thank my brother, my granny, my partner Brendan, my aunts, my uncles and my cousins for all their love, support and faith in me throughout the last four years.

Abstract

Improved understanding of normal human ageing will provide important insights into major risk factors for many age-related diseases. Using the progeroid disease Werner syndrome (WS) as a model for accelerated ageing, this project aimed to investigate how modulation of protein function in the p38 α stress-signalling kinase cascade could affect ageing on the cellular level.

New rapid routes towards p38 α and MK2 inhibitors have been developed to evaluate their use as chemical probes to investigate the mechanisms of cellular ageing. The p38 α inhibitor RO3201195 has been synthesized and used as a probe to corroborate previously published evidence that inhibition of the p38 α protein kinase reverses the aged morphology of WS fibroblasts.¹

A new route for the synthesis of the MK2 inhibitor PF-3644022 was developed, exploring new methods for building the heterocyclic scaffold through a number of retrosynthetic strategies. Microwave-assisted organic synthesis was used extensively as a tool towards halogenated benzothiophenes² and fused quinoline systems, and in rapid Suzuki-Miyaura coupling and Buchwald-Hartwig *N*-arylation chemistry.³ This MK2 inhibitor can now be used as a readily accessible probe to further investigate the role of kinases downstream of p38 α and the role of MK2 in the premature ageing of WS cells.

The final part of the project focussed on the potential of a known p38 α inhibitor, BIRB 796, in the development of new chemical probes. BIRB 796 binds allosterically outside of the ATP-binding pocket of p38 α MAPK, which drives a conformational change of the kinase into an inactive form. Using rapid synthetic methods towards pyrazole and urea formation, the selectivity elements of the inhibitor were reviewed and a new library of analogues was synthesized. Upon testing against a small panel of kinases, it was found that through small changes the inhibitor potency for p38 α could be dramatically altered, and binding affinity for alternative kinases could be selectively enhanced.

Abbreviations

(±)-BINAP	(±)-2,2'-Bis(diphenylphosphino)-1,1'-binaphthalene
μmol	Micromole
ADME	Adsorption, distribution, metabolism and excretion
ATP	Adenosine triphosphate
Boc	<i>tert</i> -Butyloxycarbonyl
CDCl ₃	Deuterated chloroform
COMU	1-[(1-(Cyano-2-ethoxy-2-oxoethylideneaminoxy)dimethylamino morpholino-methylene)]methanaminiumhexafluorophosphate
COSY	Correlation spectroscopy
d	Doublet
DBU	1,8-Diazabicycloundec-7-ene
dd	Doublet of doublets
DDQ	2,3-Dichloro-5,6-dicyano-1,4-benzoquinone
DIEA/DIPEA	<i>N,N</i> -Diisopropylethylamine
DIPA	Diisopropylamine
DMAP	Dimethylaminopyridine
DMF	<i>N,N</i> -Dimethylformamide
DMSO- <i>d</i> ₆	Deuterated dimethylsulfoxide
DPPP	1,3-Bis(diphenylphosphine)propane
DSF	Differential scanning fluorimetry
EAS	Electrophilic aromatic substitution
EDCI	1-Ethyl-3-(3-dimethylaminopropyl)carbodiimides
EDG	Electron-donating group
EI	Electron ionisation
ESI-MS	Electrospray ionisation mass spectrometry
EWG	Electron-withdrawing group
h	Hours
HATU	<i>N</i> -[(Dimethylamino)-1 <i>H</i> -1,2,3-triazolo-[4,5- <i>b</i>]pyridin-1-yl-methylene]- <i>N</i> -methylmethanaminium hexafluorophosphate- <i>N</i> -oxide
HBA	Hydrogen bond acceptor
HBD	Hydrogen bond donor
HMBC	Heteronuclear multiple bond correlation

HOAt	1-Hydroxy-7-azabenzotriazole
HOBt	1-Hydroxybenzotriazole
HPLC	High performance liquid chromatography
HRMS	High resolution mass spectrometry
HSQC	Heteronuclear single bond correlation
HTS	High-throughput screening
IC ₅₀	Half maximal inhibitory concentration
IL-β	Interleukin-β
IR	Infra-red irradiation
<i>J</i>	Coupling constant (in Hz)
JNK	c-Jun kinases
LDA	Lithium diisopropylamine
M	Molar
m	Multiplet
<i>m/z</i>	Mass to charge ratio
MAPK	Mitogen activated protein kinase
MCR	Multi-component reaction
Me	Methyl
MeOH- <i>d</i> ₄	Deuterated methanol
MHz	Megahertz
Min	Minutes
MK2	Mitogen activated protein kinase-activated protein kinase 2
mL	Millilitre
Mmol	Millimole
Mr	Molecular Weight
<i>n</i> -BuLi	<i>n</i> -Butyl lithium
<i>n</i> -BVE	<i>n</i> -Butyl vinyl ether
NH ₃	Ammonia
NMR	Nuclear magnetic resonance
PD	Pharmacodynamics
pdd	Pseudo doublet of doublets
PK	Pharmacokinetics
pK _a	Acid dissociation constant
ppm	Parts per million

pt	Pseudo triplet
RP-LCMS	Reverse-phase liquid chromatography mass spectrometry
RT	Room temperature
s	Singlet
SAR	Structure-activity relationship
SIPS	Stress-induced premature senescence
SOSA	Selective optimization of side activities
t	Triplet
TBAB	Tetrabutylammonium bromide
TBAC	Tetrabutylammonium chloride
TFA	Trifluoroacetic acid
THF	Tetrahydrofuran
TLC	Thin layer chromatography
TNF- α	Tumor necrosis factor- α
W	Watts
WS	Werner syndrome
δ	Chemical shift
ν	Frequency

Table of Contents

Declaration.....	i
Acknowledgements.....	ii
Abstract.....	iii
Abbreviations.....	iv
1. Introduction	1
1.1. Ageing.	1
1.2. Werner syndrome.	2
1.3. P38 MAPK inhibitors.	4
1.3.1. The p38 MAPK cascade.	4
1.3.2. SB203580, the first p38 inhibitor.	6
1.3.2. The biaryl imidazole pharmacophore.	8
1.3.3. Extending the scope.....	11
1.3.4. Outlook for p38 inhibitors.....	13
1.4. MAPKAP kinase 2 (MK2) inhibitors.	14
1.4.1. Type 1 MK2 inhibitors.	14
1.4.3. Type 2 MK2 inhibitors.	18
1.4.4. Outlook for MK2 inhibitors.	20
1.5. Project aims.	21
1.6. Methods and techniques.	22
1.6.1. Microwave-assisted organic synthesis (MAOS).	22
1.6.2. Heterocycles.....	23
1.6.2.1. Azoles.	23
1.6.2.1.1. Synthetic routes towards functionalized pyrazoles.....	25
1.6.2.2. Pyridines.....	28
1.6.2.2.1. Synthesis of pyridines.	29
1.6.2.2.2. Reactions of pyridines.....	32

1.6.2.3. Quinolines.	35
1.6.2.3.1. Synthesis of quinolines.	35
1.6.2.3.2. Reactions of quinolines.	41
1.6.2.4. Benzo[<i>b</i>]thiophenes.	44
1.6.2.4.1. Synthesis of benzo[<i>b</i>]thiophenes.	46
1.6.2.4.2. Reactions of benzo[<i>b</i>]thiophenes.	48
1.6.3. Strategic bond forming reactions.	53
1.6.3.1. Amide bond forming reactions.	53
1.6.3.1.1. Coupling reagents.	54
1.6.3.1.2. Alternative coupling reagents.	58
1.6.3.1.3. Protecting group strategies.	59
1.6.3.1.4. Applications and advances: Solid phase peptide synthesis.	61
1.6.3.2. Metal-mediated cross-coupling.	62
1.6.3.2.1. The Mizoroki-Heck reaction.	65
1.6.3.2.1.1. Catalytic cycles for ligated and ligandless systems.	65
1.6.3.2.1.2. Regioselectivity.	68
1.6.3.2.1.3. Heck coupling of α,β -disubstituted alkenes.	69
1.6.3.2.2. Suzuki-Miyaura cross-coupling.	71
1.6.3.2.2.1. The catalytic cycle.	72
1.6.3.2.2.2. Applications in medicinal chemistry.	74
1.6.3.2.3. Buchwald-Hartwig <i>N</i> -Arylation.	75
1.6.3.2.3.1. Palladium-mediated <i>N</i> -arylation and catalytic cycle.	76
1.6.3.2.3.2. Catalyst and ligand systems.	79
1.6.3.2.3.3. Applications in medicinal chemistry.	80
1.7. Overall project objectives.	82
Chapter 2. RO3201195. Corroborating the role of p38 α MAPK on accelerated ageing in WS cells.	83
2.1. Background and aims.	83

2.1.1. RO3201195: Hit-to-lead optimization of a highly selective p38 MAPK inhibitor.	84
2.1.2. Application in WS cells.	85
2.2. Synthetic routes towards RO3201195.	87
2.2. Deconstructing RO3201195.	90
2.3. Synthesis of RO3201195.	91
2.3.2. Benzoylacetone synthesis.	91
2.3.2.1. Application of Heck coupling towards the synthesis of benzoylacetone nitriles. ..	91
2.3.2.1.4. Claisen condensation routes for the synthesis of benzoylacetone nitrile.	95
2.3.2. Pyrazole formation.	96
2.3.3. <i>O</i> -Alkylation and diol installation.	97
2.3.4. Conclusion.	98
2.4. Biological studies of RO3201195 in WS cells.	100
2.5. Overall conclusions and future perspectives.	103
Chapter 3. Synthesis of PF-3644022. Probing an MK2 inhibitor for the modulation of cellular ageing in WS cells.	104
3.1. Introduction.	104
3.1.1. Hit-to-lead identification of PF-3644022 (25).	105
3.1.2. Deconstructing PF-3644022 (25).	108
3.2. Retrosynthesis 1. Quinoline based scaffold.	110
3.2.1. Chloroquinoline synthesis and Suzuki coupling.	110
3.2.2. Synthesis of 6-amino-5-cyanoquinoline intermediates.	111
3.3. Retrosynthesis 2. Thieno[3,2- <i>f</i>]quinolone scaffold.	113
3.3.1. Thienoquinolone synthetic route.	114
3.4. Retrosynthesis 3. Halothieno[3,2- <i>f</i>]quinolone scaffold.	116
3.4.1. Synthesis of 3-bromobenzo[<i>b</i>]thiophene.	117
3.4.2. <i>N</i> -Functionalization of methyl 3-bromo-5-nitrobenzo[<i>b</i>] thiophene-2-carboxylate.	118
3.4.3. Acidic cyclization to thienoquinolone.	122

3.4.4. Chlorination to dihalogenated thienoquinoline and Suzuki coupling.	126
3.4.5. Conclusion.	128
3.5. Retrosynthesis 4. Benzo[4,5]thieno[3,2- <i>e</i>][1,4]diazepin-5-one scaffold.	129
3.5.1. Buchwald-Hartwig <i>N</i> -arylation and lactam ring formation.	130
3.5.2. <i>N</i> -Functionalization and acidic cyclization to quinolones.	134
3.5.3. Alternative cyclization methods.	137
3.5.3.1. Doebner-von Miller quinoline formation.	137
3.5.3.2. Multi-component Lewis acid-mediated quinoline formation.	139
3.5.3.2.1. Lewis acid-mediated quinoline formation.	139
3.5.3.2.2. Extending the model: thienoquinoline formation.	142
3.5.3.2.3. Application of convergent quinoline route to complex intermediates. ...	151
3.5.3.2.4. Assessing the viability of aromatic aldehydes.	154
3.5.4. Future perspectives.	155
3.6. Conclusion.	156
3.7. Biological studies.	158
3.7.1. Progress in the clinic.	158
3.7.3. Application in WS cells.	160
3.7.3. Development of more efficacious MK2 inhibitors.	163
3.7.4. Conclusion and future perspectives.	164
Chapter 4. Looking back 'upstream'. The potential of p38 MAPK inhibitors.	165
4.1. Introduction.	165
4.1.2. BIRB 796, a novel p38 α MAPK inhibitor.	165
4.1.2. Exploring the potential of the BIRB 796 pharmacophore.	168
4.1.3. Identifying structural features of initial interest.	169
4.1.3. Synthetic approaches to 3,5-disubstituted pyrazoles.	170
4.1.4. An introduction to ureas.	173
4.1.4.1. Synthetic approaches to ureas.	175
4.2. Synthesis of analogue library 1.	177

4.2.1. Synthesis of the core pyrazole	177
4.2.2. Synthesis of urea analogue library 1.....	179
4.2.3. Improving the synthesis.....	181
4.3. Biological evaluation of analogue library 1.....	183
4.3.1. Introduction to drug/fragment screening.....	183
4.3.2. Kinase screening panel.....	183
4.3.3. DSF results for analogue library 1.....	185
4.3.4. Conclusion.....	188
4.4. Analogue library 2. Taking the 'hit' forward.....	190
4.4.1. An introduction to fluorine. The C-F bond as a tool in medicinal chemistry.....	190
4.4.2. Pyrazole modification.....	192
4.4.3. Synthesis of pyrazole subset library.....	193
4.4.4. Synthesis of analogue library 2.....	196
4.5. Biological evaluation of analogue library 2.....	199
4.5.1. DSF results from analogue library 2.....	199
4.5.2. Conclusion.....	204
4.6. Future perspectives.....	205
4.6.1. Pharmacodynamics and verifying biological interactions.....	205
4.6.2. Pharmacokinetics.....	207
4.6.3. Conclusion.....	211
Chapter 5. Conclusions.....	212
Chapter 6. Experimental.....	215
6.1. Chapter 2.....	216
6.1.1. Methyl 3-methoxybenzoate (123)	216
6.1.2. 3-Methoxybenzoylacetone nitrile (107)	216
6.1.2.1. Claisen ester condensation	216
6.1.2.2. Heck reaction. Conductive heating.....	217
6.1.2.3. Heck reaction. Microwave-assisted method.....	217

6.1.3. 2-(3-Methoxybenzoyl)-3-(phenylamino)prop-2-enenitrile (124)	218
6.1.4. [5-Amino-1-(4-fluorophenyl)-1 <i>H</i> -pyrazol-4-yl]-3-methoxyphenyl ketone (125)	219
6.1.5. [5-Amino-1-(4-fluorophenyl)-1 <i>H</i> -pyrazol-4-yl]-3-hydroxyphenyl ketone (126)	220
6.1.6. 5-Amino-1-(4-fluorophenyl)-4-{3-[2(<i>S</i>)-3-dihydroxypropoxy]benzoyl} pyrazole (RO3201195) (10).....	221
6.1.6.1. Procedure for isolation of [5-Amino-1-(4-fluorophenyl)-1 <i>H</i> -pyrazo-4-yl]{3-[(<i>R</i>)- 2,2-dimethyl-1,3-dioxolan-4-yl)methoxy]phenyl} ketone (136).....	222
6.2. Chapter 3.....	223
6.2.1. 2-Chloro-6-nitroquinoline (151).....	223
6.2.2. General procedure for Suzuki coupling	223
6.2.2.1. 2-(6-Methylpyridin-3-yl)-6-nitroquinoline (153).....	224
6.2.2.2. 6-Nitro-2-(pyridin-3-yl)quinoline (152)	224
6.2.3. 6-Amino-5-cyanoquinoline (144)	225
6.2.4. Methyl 5-nitrobenzo[<i>b</i>]thiophene-2-carboxylate (162)	226
6.2.4.1. Conductive synthesis.	226
6.2.4.2. Microwave-assisted synthesis.	226
6.2.5. 5-Nitrobenzo[<i>b</i>]thiophene-2-carboxylic acid (167)	227
6.2.5.1. Conductive synthesis.	227
6.2.5.2. Microwave-assisted synthesis.	227
6.2.6. 3-Bromo-5-nitrobenzo[<i>b</i>]thiophene-2-carboxylic acid (168)	227
6.2.7. Methyl 3-bromo-5-nitrobenzo[<i>b</i>]thiophene-2-carboxylate (164).....	228
6.2.7.1. From 3-bromo-5-nitrobenzo[<i>b</i>]thiophene-2-carboxylic acid (168)	228
6.2.7.2. From methyl 3-amino-5-nitrobenzothiophene-2-carboxylate (170).....	229
6.2.8. Methyl 3-amino-5-nitrobenzothiophene-2-carboxylate (170)	229
6.2.8.1. Conductive method.....	229
6.2.8.2. Microwave-assisted synthesis.	230
6.2.9. Methyl 5-aminobenzo[<i>b</i>]thiophene-2-carboxylate (158)	230
6.2.10. Methyl 5-amino-3-bromobenzo[<i>b</i>]thiophene-2-carboxylate (165).....	231

6.2.11. (2 <i>E</i>)-3-Ethoxyprop-2-enoyl chloride.....	232
6.2.12. Methyl 3-bromo-5-{[(2 <i>E</i>)-3-ethoxyprop-2-enoyl]amino} benzo[<i>b</i>]thiophene-2-carboxylate (171)	232
6.2.12.1. Table 2, entry 1.	232
6.2.12.2. Table 2, Entry 2.	233
6.2.12.3. Table 2, Entry 3.	233
6.2.12.4. Table 2, Entry 4.	233
6.2.12.5. Table 2, entry 5.	234
6.2.13. 3,3-Dimethoxypropanoic acid (172)	234
6.2.14. Methyl 5-(3,3-dimethoxypropanamido)benzo[<i>b</i>]thiophene-2-carboxylate (174)	235
6.2.14.1. Conductive synthesis	235
6.2.14.2. Microwave-assisted synthesis	235
6.2.15. Methyl 3-bromo-5-(3,3-dimethoxypropanamido)benzo[<i>b</i>]thiophene-2-carboxylate (175)	236
6.2.15.1. Conductive synthesis.	236
6.2.15.2. Microwave-assisted synthesis.	237
6.2.15.3. Microwave synthesis, using COMU reagent	237
6.2.16. Methyl 7-oxo-6,7-dihydrothieno[3,2- <i>f</i>]quinoline-2-carboxylate (160A and 160B)	237
6.2.17. Methyl 1-bromo-7-oxo-6,7-dihydrothieno[3,2- <i>f</i>]quinoline-2-carboxylate (176A and 176B)	238
6.2.17.1. Using Methyl 3-bromo-5-{[(2 <i>E</i>)-3-ethoxyprop-2-enoyl]amino} benzo[<i>b</i>]thiophene-2-carboxylate (171).....	239
6.2.17.2. Using Methyl 3-bromo-5-(3,3-dimethoxypropanamido)benzo[<i>b</i>]thiophene-2-carboxylate (174).	239
6.2.18. Methyl 1-bromo-7-chlorothieno[3,2- <i>f</i>]quinoline-2-carboxylate (166)	239
6.2.19. Methyl 7-chloro-1-(6-methylpyridin-3-yl)thieno[3,2- <i>f</i>]quinoline-2-carboxylate (177)	240
6.2.20. (<i>R</i>)- <i>tert</i> -Butyl-(1-amino-1-oxopropan-2-yl)carbamate (182)	241

6.2.21. <i>tert</i> -Butyl ([2 <i>R</i>]-1-aminopropan-2-yl)carbamate (137).....	242
6.2.22. (<i>R</i>)-Methyl 3-((2-((<i>tert</i> -butoxycarbonyl)amino)propyl)amino)-benzo[<i>b</i>]thiophene-2-carboxylate (184)	243
6.2.22.1. Conductive synthesis.	243
6.2.22.2. Microwave-assisted synthesis.	243
6.2.23. (<i>R</i>)-Methyl 3-((2-((<i>tert</i> -butoxycarbonyl)amino)propyl)amino)-5-nitrobenzo[<i>b</i>]thiophene-2-carboxylate (185).....	244
6.2.24. (3 <i>R</i>)-3-Methyl-9-nitro-1,2,3,4-tetrahydro-5 <i>H</i> -[1]benzothieno[3,2- <i>e</i>][1,4]diazepin-5-one (178).....	245
6.2.25. (3 <i>R</i>)-9-Amino-3-methyl-1,2,3,4-tetrahydro-5 <i>H</i> -[1]benzothieno[3,2- <i>e</i>][1,4]diazepin-5-one (179).....	246
6.2.26. 3,3-Dimethoxy- <i>N</i> -((3 <i>R</i>)-3-methyl-5-oxo-2,3,4,5-tetrahydro-1 <i>H</i> -[1]benzo[4,5]thieno[3,2- <i>e</i>][1,4]diazepin-9-yl)propanamide (186)	247
6.2.26.1. EDCI-HOBt mediated microwave-assisted synthesis	247
6.2.26.2. COMU mediated microwave-assisted synthesis.....	247
6.2.27. Methyl 7-(pyridin-3-yl)thieno[3,2- <i>f</i>]quinoline-2-carboxylate (195A)	248
6.2.28. 6-Methylpyridine-3-carboxaldehyde (190).....	249
6.2.29. (<i>R</i>)-10-Methyl-3-(6-methylpyridin-3-yl)-9-10-11-12-tetrahydro-8 <i>H</i> -[1,4]diazepino[5',6':4,5]thieno[3,2- <i>f</i>]quinoline-8-one. PF-3644022 (25)	250
6.2.30. Methyl 7-phenylthieno[3,2- <i>f</i>]quinoline-2-carboxylate (199)	251
6.2.31. Methyl 7-(6-methylpyridin-3-yl)thieno[3,2- <i>f</i>]quinoline-2-carboxylate (200)	252
6.3. Chapter 4.....	254
6.3.1. 3- <i>tert</i> -Butyl-1-phenyl-1 <i>H</i> -pyrazole-5-amine (215).....	254
6.3.2. <i>N</i> -(3-(<i>tert</i> -Butyl)-1-phenyl-1 <i>H</i> -pyrazol-5-yl)- <i>N'</i> -(naphthalene-1-yl)urea (215A).....	255
6.3.3. <i>N</i> -(3-(<i>tert</i> -Butyl)-1-phenyl-1 <i>H</i> -pyrazol-5-yl)- <i>N'</i> -(naphthalene-2-yl)urea (215B).....	256
6.3.4. <i>N</i> -(3-(<i>tert</i> -Butyl)-1-phenyl-1 <i>H</i> -pyrazol-5-yl)- <i>N'</i> -(<i>o</i> -tolyl)urea (215C)	256
6.3.5. <i>N</i> -(3-(<i>tert</i> -Butyl)-1-phenyl-1 <i>H</i> -pyrazol-5-yl)- <i>N'</i> -(4-ethoxyphenyl)urea (215D)	257
6.3.6. <i>N</i> -(3-(<i>tert</i> -Butyl)-1-phenyl-1 <i>H</i> -pyrazol-5-yl)- <i>N'</i> -(4-fluorophenyl)urea (215E).....	258

6.3.7. <i>N</i> -(3,5-Bis(trifluoromethyl)phenyl)- <i>N'</i> -(3-(<i>tert</i> -butyl)-1-phenyl-1 <i>H</i> -pyrazol-5-yl)urea (215F)	259
6.3.8. <i>N</i> -(4-(Benzyloxy)phenyl)- <i>N'</i> -(3-(<i>tert</i> -butyl)-1-phenyl-1 <i>H</i> -pyrazol-5-yl)urea (215G)	259
6.3.9. <i>N</i> -(3-(<i>tert</i> -Butyl)-1-phenyl-1 <i>H</i> -pyrazol-5-yl)- <i>N'</i> -(3,5-dimethylphenyl) urea (215H)	260
6.3.10. <i>N</i> -(3-(<i>tert</i> -Butyl)-1-phenyl-1 <i>H</i> -pyrazol-5-yl)- <i>N'</i> -(5-fluoro-2-methylphenyl)urea (215I)	261
6.3.11. <i>N</i> -(3-(<i>tert</i> -Butyl)-1-phenyl-1 <i>H</i> -pyrazol-5-yl)- <i>N'</i> -(3,4-difluorophenyl) urea (215J)	262
6.3.12. <i>N</i> -(3-(<i>tert</i> -Butyl)-1-phenyl-1 <i>H</i> -pyrazol-5-yl)- <i>N'</i> -phenylurea (215K)	263
6.3.13. <i>N</i> -((3-(<i>tert</i> -Butyl)-1-phenyl-1 <i>H</i> -pyrazol-5-yl)carbamoyl)-4-methylbenzenesulfonamide (215L)	263
6.3.14. <i>N</i> -(3-(<i>tert</i> -Butyl)-1-phenyl-1 <i>H</i> -pyrazol-5-yl)- <i>N'</i> -(3-methoxyphenyl)urea (215M)	264
6.3.15. <i>N</i> -(3-(<i>tert</i> -Butyl)-1-phenyl-1 <i>H</i> -pyrazol-5-yl)- <i>N'</i> -(<i>p</i> -tolyl)urea (215N)	265
6.3.16. 3-(<i>tert</i> -Butyl)-1-(<i>p</i> -tolyl)-1 <i>H</i> -pyrazol-5-amine (217)	266
6.3.17. 3-(<i>tert</i> -Butyl)-1-methyl-1 <i>H</i> -pyrazol-5-amine (226)	267
6.3.18. 3-(<i>tert</i> -Butyl)-1-(4-fluorophenyl)-1 <i>H</i> -pyrazole-5-amine (227)	267
6.3.19. 3-(<i>tert</i> -Butyl)-1-(4-nitrophenyl)-1 <i>H</i> -pyrazol-5-amine (228)	268
6.3.20. 1,3-Di- <i>tert</i> -butyl-1 <i>H</i> -pyrazol-5-amine (229)	269
6.3.21. 1-(4-Bromophenyl)-3-(<i>tert</i> -butyl)-1 <i>H</i> -pyrazol-5-amine (230)	270
6.3.22. 1-Methyl-3-phenyl-1 <i>H</i> -pyrazol-5-amine (231)	270
6.3.23. 1,3-Diphenyl-1 <i>H</i> -pyrazol-5-amine (232)	271
6.3.24. <i>N</i> -(3,5-Bis(trifluoromethyl)phenyl)- <i>N'</i> -(3-(<i>tert</i> -butyl)-1-(<i>p</i> -tolyl)-1 <i>H</i> -pyrazol-5-yl)urea (217F)	272
6.3.25. <i>N</i> -(3,5-Bis(trifluoromethyl)phenyl)- <i>N'</i> -(3- <i>tert</i> -butyl-1-methyl-1 <i>H</i> -pyrazol-5-yl)urea (226F)	273
6.3.26. <i>N</i> -(3,5-Bis(trifluoromethyl)phenyl)- <i>N'</i> -(3- <i>tert</i> -butyl-1-(4-fluorophenyl)-1 <i>H</i> -pyrazol-5-yl)urea (227F)	274
6.3.27. <i>N</i> -(3,5-Bis(trifluoromethyl)phenyl)- <i>N'</i> -(3-(<i>tert</i> -butyl)-1-(4-nitrophenyl)-1 <i>H</i> -pyrazol-5-yl)urea (228F)	274

6.3.28.	<i>N</i> -(3,5-Bis(trifluoromethyl)phenyl)- <i>N'</i> -((1,3-di- <i>tert</i> -butyl)-1 <i>H</i> -pyrazol-5-yl)urea (229F)	275
6.3.29.	<i>N</i> -(3,5-Bis(trifluoromethyl)phenyl)- <i>N'</i> -(3-(<i>tert</i> -butyl)-1-(4-bromophenyl)-1 <i>H</i> -pyrazol-5-yl)urea (230F).....	276
6.3.30.	<i>N</i> -(3,5-Bis(trifluoromethyl)phenyl)- <i>N'</i> -(1-methyl-3-phenyl-1 <i>H</i> -pyrazol-5-yl)urea (231F)	277
6.3.31.	<i>N</i> -(3,5-Bis(trifluoromethyl)phenyl)- <i>N'</i> -(1,3-diphenyl-1 <i>H</i> -pyrazol-5-yl)urea (232F)	278
6.3.32.	<i>N</i> -(3,5-Difluorophenyl)- <i>N'</i> -(3-(<i>tert</i> -butyl)-1-(phenyl)-1 <i>H</i> -pyrazol-5-yl)urea (215O)	278
6.3.33.	<i>N</i> -(3,5-Difluorophenyl)- <i>N'</i> -(3-(<i>tert</i> -butyl)-1-(<i>p</i> -tolyl)-1 <i>H</i> -pyrazol-5-yl)urea (217O)	279
6.3.34.	<i>N</i> -(3,5-Difluorophenyl)- <i>N'</i> -(3- <i>tert</i> -butyl-1-methyl-1 <i>H</i> -pyrazol-5-yl)urea (226O)..	280
6.3.35.	<i>N</i> -(3,5-Difluorophenyl)- <i>N'</i> -(3-(<i>tert</i> -butyl)-1-(4-fluorophenyl)-1 <i>H</i> -pyrazol-5-yl)urea (227O)	281
6.3.36.	<i>N</i> -3-(<i>tert</i> -Butyl)-1-(4-nitrophenyl)-1 <i>H</i> -pyrazol-5-yl)- <i>N'</i> -(3,5-difluorophenyl)urea (228O)	282
6.3.37.	<i>N</i> -(3,5-Difluorophenyl)- <i>N'</i> -(1,3-(<i>tert</i> -butyl)-1 <i>H</i> -pyrazol-5-yl)urea (229O)	282
6.3.38.	<i>N</i> -(3-(<i>tert</i> -Butyl)-1-(4-bromophenyl)-1 <i>H</i> -pyrazol-5-yl)- <i>N'</i> -(3,5-difluorophenyl)urea (230O)	283
6.3.39.	<i>N</i> -(3,5-Difluorophenyl)- <i>N'</i> -(1-methyl-3-phenyl-1 <i>H</i> -pyrazol-5-yl)urea (231O)	284
6.3.40.	<i>N</i> -(3,5-Difluorophenyl)- <i>N'</i> -(1,3-diphenyl-1 <i>H</i> -pyrazol-5-yl)urea (232O)	285
7.	References.	287

1. Introduction

1.1. Ageing.

Strehler and Mildvan defined ageing as an inherent process that is progressive, intrinsic, degenerative and universal.^{4,5} Although it is possible to age in relatively good health, unhealthy ageing increases the probability of developing a range of age-related morbidities, including cancers, Alzheimer's and Parkinson's disease, and a much impaired lifestyle.⁶ By increasing understanding of the underlying causes of ageing, it is hoped that the process can be modulated to increase the human health span, as well as the human life span.

Biological studies of ageing have been defined by Faragher *et al.* as "roughly akin to the study of the consequences of wear and tear", as with age comes a reduced ability of an organism to handle stresses that younger organisms may be able to survive.⁵

There are many theories of how and why ageing occurs, though one of the most prolific models is the cellular senescence hypothesis. This model proposes that the progressive accumulation of senescent cells over time results in the development of the aged phenotype. Indeed, the build-up of senescent cells in aged individuals has been linked to the development of cancers and age-related conditions.⁷

Replicative senescence occurs when a cell has reached its set capacity for division, as determined by telomere erosion and controlled by tumour suppressor genes. Cells with short telomeres are potentially oncogenic and to prevent replication of these high risk cells they are put into a stable, non-dividing senescent state.⁷ In younger individuals this programmed senescence prevents the growth of malignant tumours, while in aged individuals the accumulation of senescent cells has been proposed to contribute to inflammatory conditions and cancer progression. Senescent cells are known to secrete pro-inflammatory and growth factors, and so Lockett *et al.* have postulated that these factors alter the immediate microenvironment to promote oncogenic mutations.⁷

Although it is likely that there is a broad spectrum of mechanisms which contribute to the normal aged phenotype,⁸ in order to better understand the ageing process, premature ageing diseases classed as progeroid syndromes have been widely studied. These disorders are phenocopies of normal ageing, exhibiting many of the same characteristics of normally aged individuals.⁹ Dependent upon the syndrome studied, individuals may not exhibit all of the clinical

characteristics generally associated with normal ageing. It is the segmented nature of these syndromes that allow them to be analyzed and studied in a tractable manner.¹⁰

1.2. Werner syndrome.

Werner syndrome (WS) is a rare genome instability and segmental progeroid disorder in which individuals exhibit the premature on-set of age-related conditions between the ages of 15 and 30, and a shortened median life span.¹¹ The prominent features of this age-related phenotype include short stature, skin atrophy, cataracts, greying hair and hair loss, in addition to a number of age-related inflammatory disorders including type II diabetes, osteoporosis and atherosclerosis.^{8,12,13} This “stunning mimicry” of normal human ageing has led to WS being used extensively as a model to investigate the mechanisms of normal human ageing.¹⁴



Figure 1: WS case at 48 years. General aged appearance, with loss of and greying hair.¹¹

On a cellular level, the dermal fibroblasts of WS patients show an extremely reduced replicative life span, resembling those of elderly individuals who have aged normally.^{14,15} Though the segmented nature of WS is evident in a lack of degradation of the central nervous system (CNS), and limited damage to T-cells and the immune system compared to normally aged individuals.^{5,9,12}

WS is caused by a genetic mutation of a member of the RecQ helicase family (WRN).¹³ In normal cells, this gene helps regulate DNA replication, recombination and prevents the collapse of replication forks.¹⁶ WS cells deficient in this gene experience interrupted and illegitimate recombination events and frequent DNA replication ‘fork stalling’.^{16,17} These events cause significant genomic stress and contribute to the reduced replicative lifespan of WS fibroblasts.⁹

Senescent WS fibroblasts resemble normal cells that have undergone stress-induced premature senescence (SIPS).^{14,18} They exhibit elevated levels of the stress-associated p38 mitogen-activated protein kinase (MAPK) and an enlarged morphology due to prominent F-actin stress fibres.^{14,18,19}

In order to investigate the role of p38 MAPK on the stressed morphology of WS cells, Davis *et al.* treated primary WS fibroblasts with the p38 α/β inhibitor SB203580 (**1**).^{14,18,19} The group found that upon treatment with **1** the aged morphology of the WS fibroblasts was reversed. The treated cells exhibited an extended replicative lifespan, a 20% increase in growth rate compared to DMSO controls, and a morphology resembling that of a normal young cell, with a dramatic reduction in stress fibre production.

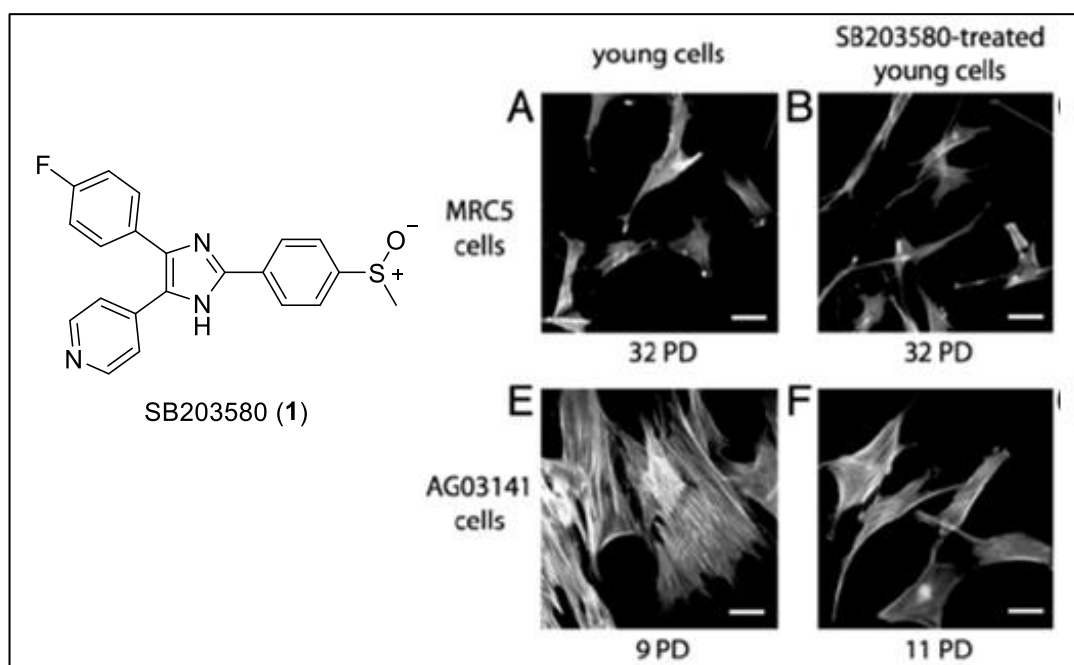


Figure 2: Visualization of F-actin stress-fibre production in normal (MRC5) and WS (AG03141) cells with p38 inhibitor SB203580 (**1**), with population doublings (PD) indicated.¹⁴

Figure 2 illustrates the F-actin stress fibre visualization completed by Davis *et al.* It can be observed that for normal young cells, treatment with **1** had no effect on the extent of F-actin stress fibres or growth rate. Though for the WS cells (AC03141), after treatment there was a dramatic reduction in F-actin stress fibres and a significant change in the morphology of the cells.¹⁴

These results supported a p38-mediated SIPS-like mechanism contributing to the aged morphology and accelerated senescence of WS cells. However, the p38 MAPK inhibitor SB203580 (**1**) is prone to off-target effects, and so it could have been the case that other kinases

were responsible for the reversal of the aged morphology.¹⁸ In order to understand more about the role of p38 and other MAPKs in the premature ageing phenotype, a number of p38 inhibitors have been used as probes in WS cells.

1.3. P38 MAPK inhibitors.

Protein kinases are enzymes which modify the functional properties of proteins through covalent phosphorylation, mediated by the co-enzyme adenosine triphosphate (ATP).²⁰ These kinases mediate signalling cascades in all eukaryotic cells to relay signals from extracellular stimuli to the nucleus and regulate most aspects of normal cellular function including protein synthesis, gene transcription and cell death.^{20,21}

The binding of ATP is essential to protein kinase function and so when the first protein kinase modulators were designed the ATP binding pocket was a prime target. Though this site is highly druggable, due to the existence of over five hundred protein kinases in the human kinome and the high degree of conserved structural domains, the design of selective kinase inhibitors can be a prodigious challenge.^{20,22}

1.3.1. The p38 MAPK cascade.

MAPK signalling cascades are extremely widespread across all eukaryotic cells, with the p38-mediated pathway one of many which responds to different extracellular stimuli. Stimuli can range from hormones and growth factors, to inflammatory cytokines like tumor necrosis factor- α (TNF- α) and interleukin- β (IL- β), to environmental stresses including osmotic shock, radiation and heat.^{21,23}

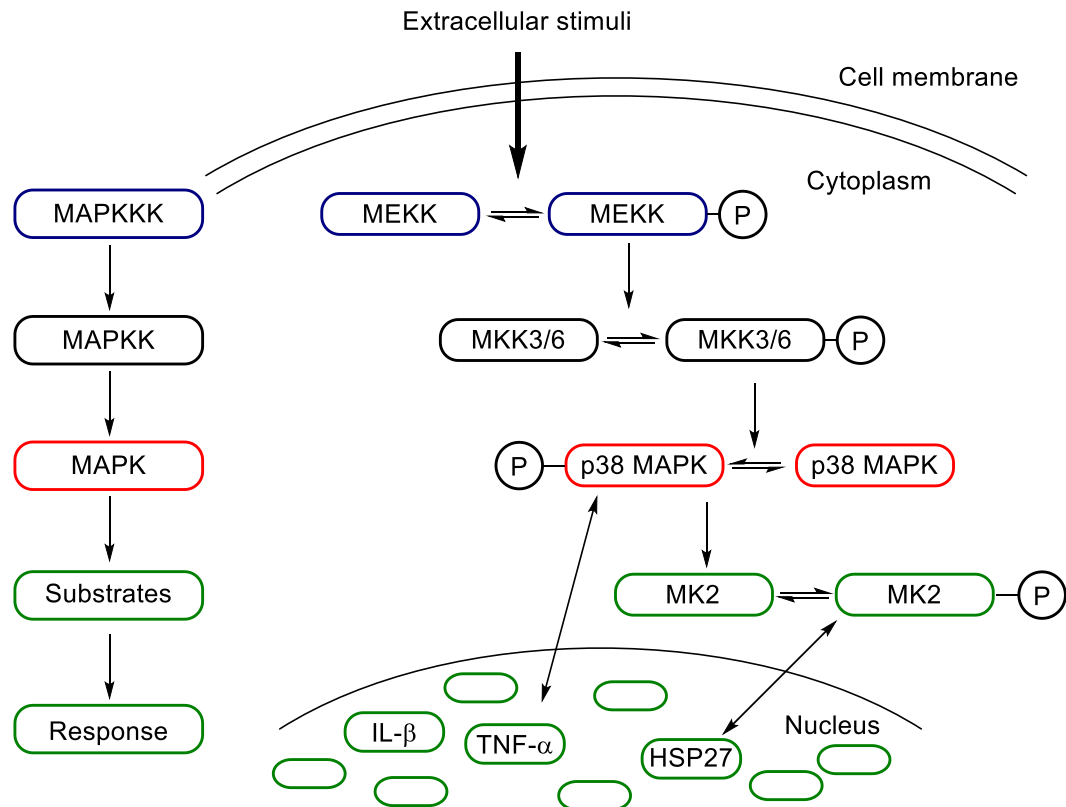


Figure 3: MAPK signalling cascade. Extracellular stimuli activate responses through mitogen activated protein kinases through phosphorylation, travelling downstream via p38 MAPK to elicit immunological responses.

Figure 3 illustrates the main stress-signalling pathway of interest in this project. MAPKs are the “middle-men” in the signalling cascade.²⁴ After receptor stimulation at the plasma membrane of the cell an MAP kinase kinase kinase (MAPKKK) is activated and phosphorylates a downstream MAP kinase kinase (MAPKK). For p38α the upstream MAPKKs are MKK3 or MKK6. P38 MAPK exists in four isoforms, with each eliciting a different immunological response. For instance, p38α and p38β, once activated, can bind to kinase targets like MAPK activated protein kinase 2 (MAPKAP-2, MK2), or translocate to the nucleus to activate other targets and promote immunological responses.²⁴ It should be noted there are many other targets downstream of the p38 MAPKs, and there is a significant amount of cross-talk that can occur between kinases in different inflammatory pathways.²⁴

The p38 MAPK stress-signalling cascade is activated by extracellular stimuli including stress, heat, and the pro-inflammatory cytokines TNF-α and IL-β.^{25,26} P38α MAPK is believed to be the primary member of the p38 MAPK family responsible for the regulation of inflammation,²⁷ with expression controlling regulation of the actin-cytoskeleton through heat shock protein HSP27, and production of pro-inflammatory cytokines TNF-α and IL-β.²³

Hence, over-activation of p38 α can result in a potential feedback loop to exacerbate inflammatory diseases mediated by these pro-inflammatory cytokines, including rheumatoid arthritis (RA), Crohn's disease and inflammatory bowel disease (IBD).^{24,25} As a result, p38 inhibitors have been studied extensively as potential anti-inflammatory agents, though the design of efficacious p38 inhibitors has encountered problems including severe off-target and cytotoxic side-effects.²⁸

1.3.2. SB203580, the first p38 inhibitor.

The pyridinylimidazole class of anti-inflammatory drugs were initially designed as dual cyclooxygenase (COX) and 5-lipoxygenase inhibitors, and were found to inhibit biosynthesis of the pro-inflammatory cytokine interleukin-1 (IL-1).^{29,30} Gallagher *et al.* at SmithKline Beecham expanded the pharmacophore of SK&F 86002 (**2**) using a structure-activity relationship (SAR) study to develop SB203580 (**1**).

They hypothesized that the 4-pyridinyl group was essential for inhibition of IL-1 biosynthesis, and they found incorporation of a *para*-sulfoxide substituted phenyl group at the imidazole C-2 enhanced potency, and good pharmacokinetics were maintained through the 4-fluorophenyl group.²⁹ Further studies identified **1** as an ATP-competitive inhibitor which binds selectively to p38 α and p38 β MAPKs, resulting in IL-1 biosynthesis inhibition by blocking the p38 MAPK cascade.^{27,31–33}

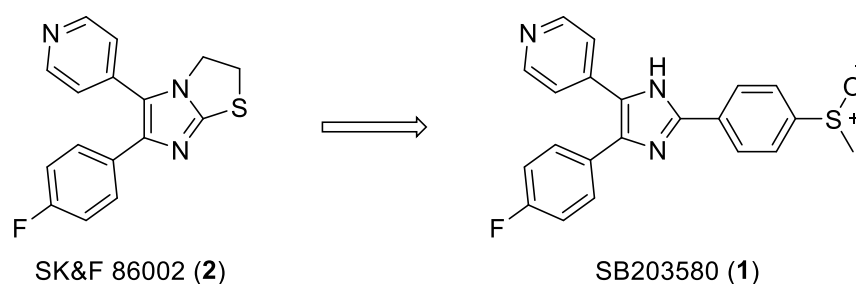


Figure 4: Gallagher *et al.*'s SAR led investigation to improve inhibitory activity towards IL-1 biosynthesis.²⁹

X-ray co-crystallization studies of ATP (**3**) with p38 identified the key binding interactions of the hinge region-ATP binding pocket of p38 (see **Figure 5**). Hydrogen bonding in the hinge region with the ATP adenosine ring was identified as essential for binding, allowing the correct orientation of the phosphate group to mediate phosphorylation of the kinase.^{10,34}

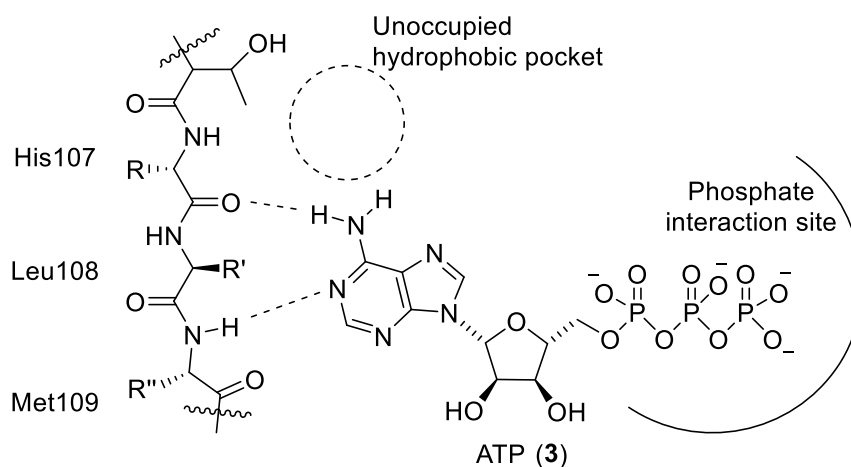


Figure 5: ATP bound to unphosphorylated p38 MAPK, illustrating key adenosine hydrogen bonding interactions in hinge region and an unoccupied hydrophobic pocket.¹⁰

X-ray co-crystallization of **1** with p38 α identified the 4-fluorophenyl group occupied a hydrophobic pocket that was vacant in the ATP-p38 complex (see **Figures 5** and **6**). Through occupation of that space, the entropy of binding was positively affected, with the expulsion of solvent from the pocket. X-ray co-crystallization also confirmed Gallagher *et al.*'s hypothesis of the importance of the 4-pyridinyl group to conduct essential hydrogen bonding with the p38 α hinge region akin to ATP (see **Figure 6**).^{29,31,35}

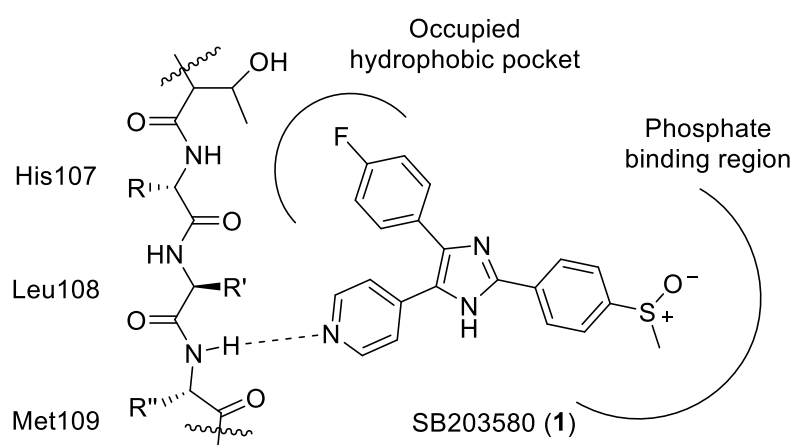


Figure 6: P38 MAPK inhibitor SB203580 (**1**) bound to the hinge region of p38, illustrating occupation of the hydrophobic pocket and phosphate binding region, and essential hydrogen bonding with hinge region.¹⁰

The aged morphology of WS cells was successfully reverted when treated with p38 α inhibitor **1**, with the lifespan and growth rate of the WS fibroblasts increased to within normal ranges.¹⁴ Unfortunately, **1** has been found to have significant cross-kinase activity, exhibiting potencies

similar to that with p38 α / β when bound to the stress-related c-Jun kinases (JNKs), casein kinase 1 (CK1) and growth related kinase cRaf1.^{18,28} Hence, these off-target interactions have hampered efforts to delineate the specific physiological role of the p38 α kinase in inflammatory conditions and WS.³² Additionally, **1** has been found to exhibit a significant toxicity profile, thereby limiting its use *in vivo*.²⁰

This lack of specificity and the resultant toxicity have been traits common to many p38 inhibitors.^{28,36} In recent years some very selective p38 inhibitors have been designed exploring a variety of different pharmacophores;³⁷ a selection of these will now be discussed with regards to their selectivity and binding modes with p38. Additionally, a number of p38 inhibitors have been used to probe the role of p38 in the premature aged phenotype of WS fibroblasts; a selection of these studies will also be discussed where pertinent.

1.3.2. The biaryl imidazole pharmacophore.

Since the development of SB203580 (**1**) there have been a number of iterations of p38 inhibitors designed, some of which were developed using the SAR of the pyridinylimidazole pharmacophore and others that have been identified through hits in high-throughput screening (HTS) programmes.

Goldstein *et al.* at Roche sought to enhance the inherent potency of the SmithKline Beecham (SB/SKB) biarylimidazole pharmacophore **2** by adapting the known SAR to an alternative scaffold.³⁸ X-ray co-crystallization studies had identified the imidazole N-lone pair of **2** as an important hydrogen bond acceptor (HBA), interacting with a lysine residue in the p38 ATP-binding pocket.³⁵ This interaction was postulated to stabilize the molecule in the binding pocket to enable further ligand-kinase interactions.

The group at Roche proposed that exchange of the imidazole ring for an azaindole would increase the intrinsic potency of the inhibitor through incorporation of a more basic nitrogen whilst retaining a similar structural geometry. Hence, 4-azaindole **4** was designed and found to be a potent inhibitor of p38 α , with an IC₅₀ value in the low nanomolar range (see **Figure 7**).

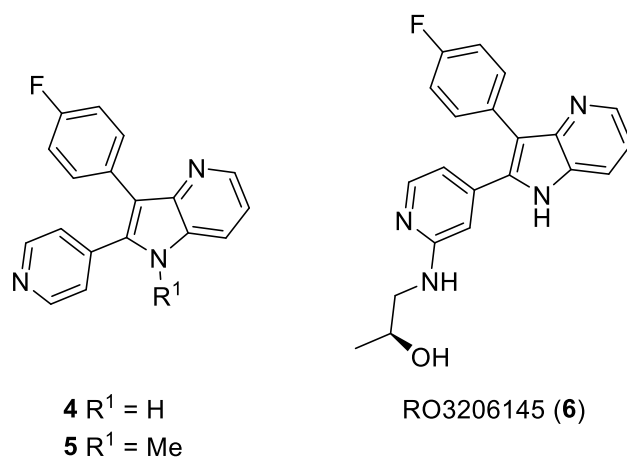


Figure 7: Compounds studied by Goldstein *et al.* in the design of p38 inhibitors based upon 4-azaindoles.³⁸

Alkylation of the indole group to give **5** increased compound bioavailability.³⁸ Unfortunately, **4** and **5** both exhibited high rates of oxidative metabolism at the pyridine ring, and so a metabolic shunt was installed α - to the pyridinyl nitrogen to give RO3206145 (**6**). The chiral (2-hydroxypropyl)amine group also helped to enhance bioavailability, inhibitor potency and endowed reasonable selectivity for p38 α against a panel of related kinases.³⁸

The spatial arrangement of the aryl rings fused to the indole ring in **6** accurately simulated the arrangement in biarylimidazole **1**, facilitating the same interactions with the p38 hinge region. Another potent p38 α inhibitor, which was very closely modelled on this pharmacophore, though based on a 6-membered heterocyclic core, is the Palau Pharma pyrazolopyridine UR-13756 (**7**).³⁹

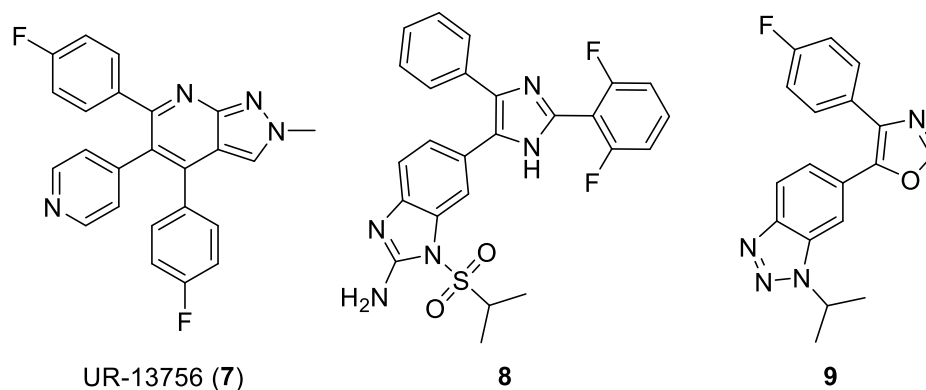


Figure 8: P38 α inhibitors adopting a similar binding motif to SB203580 (**1**): UR-13756 (**7**),⁴⁰ and alternative HBAs, 2-aminobenzimidazole (**8**) and benzotriazole (**9**).^{42,43}

A potent p38 α MAPK inhibitor in cellular assays and with favourable pharmacokinetic properties, **7** also demonstrated a much improved kinase selectivity profile over SB203580 (**1**), with selectivity for the p38 α isoform over p38 β .^{40,41} The inhibitory activity of **7** was confirmed

by Bagley *et al.* in telomere immortalised human cells and WS cells.⁴⁰ Treatment of WS cells with **7** resulted in inhibition of the p38 signalling pathway, with much reduced levels of phosphorylated MK2 (*p*-MK2) and phosphorylated HSP27 (*p*-HSP27) observed through Western blotting.⁴⁰ Though it has been noted by Davis *et al.* that the effect on the growth rate of WS^{tert} cellsⁱ was much less pronounced than upon treatment with SB203580 (**1**), with only a 10% increase observed at maximal concentrations.¹⁸

Other p38 inhibitors designed using the established SAR of SB203580 (**1**) include 2-aminobenzimidazole **8** and benzotriazole **9**, in which the pyridinyl ring has been exchanged for an alternative HBA (see **Figure 8**).^{42,43} The change in motif in **8** required the flexible hinge of the p38 ATP binding pocket to undergo a slight shift, to allow room for the larger size of the aminobenzimidazole compared to a 4-pyridinyl, which was confirmed by X-ray co-crystallization of **8** with p38 α .⁴² These studies also confirmed the imine nitrogen to act as a HBA with the p38 α hinge methionine residue, and that the isopropyl sulfonyl was exposed to a small lipophilic pocket not occupied by ATP or by **1**. A similar movement and hydrogen bonding interaction with the hinge region was confirmed through X-ray co-crystallization of benzotriazole **9** with p38 α .⁴³

Alternative pharmacophores to the classic pyridinylimidazole have been sought with the aim to improve kinase selectivity through new and interesting ATP-competitive binding motifs.⁴⁴

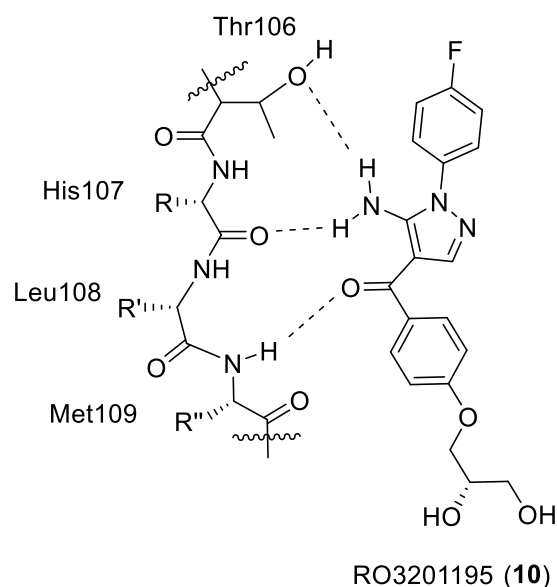


Figure 9: RO3201195 (**10**) bound into the ATP-hinge region of p38 α , with key binding interactions indicated between the hinge region of the ATP pocket and the *exo*-cyclic amine and benzoyl carbonyl group.⁴⁵

ⁱ WS^{tert} cells: WS cells immortalised by ectopic expression of telomerase.

The ATP-competitive 4-benzoyl-5-pyrazole p38 α / β inhibitor RO3201195 (**10**) was developed by Goldstein *et al.* at Roche from an initial HTS hit. Through X-ray co-crystallization with unphosphorylated p38 α , **10** was found to exhibit a unique binding mode through an *exo*-cyclic amine to a threonine residue (Thr 106) in the hinge region (see **Figure 9**).⁴⁵ Only 20% of kinases exhibit a threonine at this position in the hinge, and so it was hypothesized this interaction could convey improved selectivity. Additionally the 4-benzoyl carbonyl oxygen was identified as a methionine residue HBA. The diol chain was found to be exposed to solvent, a modification which was found to dramatically improve the pharmacokinetics of the compound (see **Chapter 2** for more detail).

The high selectivity of **10** towards p38 α highlighted this compound as a prime candidate for testing in WS cells to explore the role of p38 in premature cellular ageing. One aspect of this project will describe the development of a rapid synthesis of this molecule for testing in WS cells (see **Chapter 2**).

1.3.3. Extending the scope.

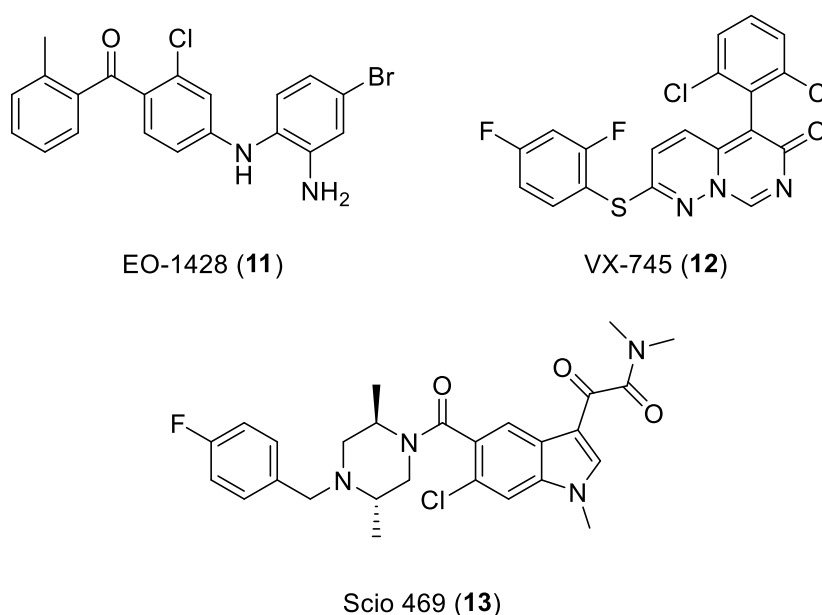


Figure 10: Alternative p38 inhibitor chemotypes: benzophenone EO-1428 (**11**), cyclic lactam VX-745 (**12**) and piperazine Scio 469 (**13**).

In an effort to reduce the promiscuity of imidazole based p38 inhibitor scaffolds, many groups sought to uncover alternative chemotypes with potency for p38. One such alternative pharmacophore was benzophenone; for example EO-1428 (**11**), designed by Leo

Pharmaceuticals for the treatment of inflammatory skin conditions. The carbonyl group was postulated to act as a HBA with the hinge methionine, akin to **10**, and the *ortho*-toluene ring occupied a hydrophobic pocket.⁴⁶ The fused lactam VX-745 (**12**), disclosed by Vertex Pharmaceuticals in 1999, has been postulated to conduct a similar carbonyl-methionine hydrogen bonding interaction, with the difluorophenyl group occupying the same hydrophobic pocket as the 4-fluorophenyl group of SB203580 (**1**).^{44,47}

With potent inhibition of p38 α and 1000-fold selectivity over related kinases JNK and MK2, **12** was investigated by Bagley *et al.* for its effect on WS cells.⁴⁸ They found **12** inhibited p38 α activity in normal cells and WS^{tert} cells with no inhibition of the related JNK kinases.⁴⁸ Davis *et al.* observed that **12** exhibited a similar effect on the growth rate of WS^{tert} cells as UR-13756 (**7**), with treatment causing an increase in the growth rate (approximately 10%) that was much less pronounced than treatment with SB203580 (**1**). Trials of both of these compounds have since been discontinued.⁴⁶

Another potent chemotype which follows a linear binding mode was developed by Scio Inc. based upon a 2,5-*trans*-dimethyl-substituted piperazine, Scio 469 (**13**). Molecular modelling suggested that the benzoyl amide acted as a HBA with the methionine hinge residue and the 4-fluorophenyl ring occupied a deep hydrophobic pocket.⁴⁴ However, despite progressing to phase 2 clinical trials, **13** was also discontinued as it was found to not be as effective as other treatments for RA.³⁷

Many of these inhibitors act by binding in multiple 'selectivity hotspots' in or near the ATP hinge region,³⁷ endowing them with enhanced potency compared to ATP.

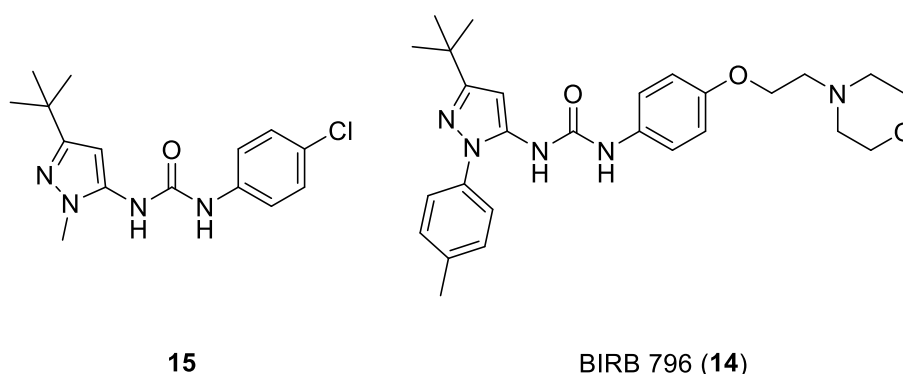


Figure 11: Type 2 p38 inhibitors developed by Boehringer Ingelheim.^{49–51}

One method that has been adopted widely to improve kinase selectivity has been the introduction of non-ATP-competitive, or type 2 inhibitors. For example, Boehringer Ingelheim's

high potency p38 α inhibitor BIRB 796 (**14**) was developed from an initial HTS hit (**15**) and was identified through X-ray co-crystallization studies to occupy an allosteric binding pocket outside of the ATP binding site (for more information on binding mode see **Chapter 4**).^{49–51}

Lead optimization of **14** resulted in installation of a chain-linked morpholino group, which was found to improve the potency of the inhibitor by reaching around to act as a HBA with the hinge region methionine residue.⁴⁹

Treatment of WS^{tert} cells with BIRB 796 (**14**) by Bagley *et al.* was found to fully inhibit p38 α activation and phosphorylation.⁵² Davis *et al.* also noted that upon treatment, the growth rate of WS cells was increased by 30%, an improved rate compared to treatment with SB203580 (**1**).¹⁸ The group postulated that this improved activity over **1** was potentially due to the inhibitor binding both allosterically and in the ATP-pocket, to block p38 activity and activation.

The unique binding mode of the *N,N'*-diaryl urea pharmacophore **14** has sparked a lot of interest in its application as a potent and selective method of binding.^{53,54} Part of this project will focus on exploring the potential of repurposing this pharmacophore to target alternative kinases and the development of new chemical probes to investigate MAPK stress-signalling pathways (see **Chapter 4**).

1.3.4. Outlook for p38 inhibitors.

For the development of therapeutics, despite the promise of p38 inhibitors for the modulation and treatment of inflammatory disorders, it has been surmised by a number of experts in the field that “the era of optimism surrounding the use of p38 MAPK inhibition for the treatment of RA is over”.²⁶

Due to the promiscuity of many p38 inhibitors initially hailed as ‘specific’, for the probing of the p38 MAPK stress-signalling pathways, Bain *et al.* have suggested testing inhibitors in parallel.³² For instance, use of two inhibitors such as SB203580 (**1**) and BIRB 796 (**14**) which do not overlap in their off-target activities can be used to extrapolate data on the only overlapping interaction: p38 α .³² This will be discussed with regards to the role of p38 α in the premature aged phenotype of WS fibroblasts in further detail in **Chapter 2**.

Severe physiological side effects have been a major contributor to the failure of many of the p38 inhibitors that have entered clinical trials.⁵⁵ It has been suggested that targeting p38 may not be the optimal strategy as p38 is an important checkpoint kinase, controlling feedback loops in the

inflammatory cascade, and plays a key role in other important immune system responses.⁵⁶ Hence, inhibition of p38 could interrupt or hyperactivate these other pathways, resulting in unwanted physiological side effects.^{55,56}

The significance of the p38 MAPK cascade in the modulation and regulation of inflammatory diseases is undeniable, and so alternative targets upstream and downstream of p38 have been suggested as alternative therapies.^{22,36}

1.4. MAPKAP kinase 2 (MK2) inhibitors.

MAPK activated protein kinase 2 (MK2) is a downstream target of p38 α , which once phosphorylated activates the heat shock protein HSP27 to regulate and stabilize the actin cytoskeleton and production of F-actin stress fibres (see **Figure 3**).⁵⁷ These stress fibres are a prominent feature of senescent WS cells, resulting in an engorged morphology to resemble a normal cell that has undergone SIPS. Hence MK2 has been implicated as a key kinase in the stress-signalling cascade contributing to the aged phenotype of WS cells.¹⁰

The viability of MK2 as a target *in vivo* is supported by the fact that MK2 knockout mice possess a normal healthy phenotype, exhibiting a significant reduction in TNF- α levels,⁵⁸ while the removal of the p38 α gene is lethal to growing embryos.^{22,59} Cells lacking MK2 also exhibit a significant reduction in levels of p38, implying that MK2 has a stabilizing effect on p38, though the exact mechanism for this stabilization is not clear.⁵⁸ Additionally, the MK2/HSP27 pathway has been implicated to play a key role in remodelling and cell migration during cancer cell invasion and metastasis, hence modulation of this pathway could help in the development of anticancer therapies.⁵⁵

From this evidence, MK2 has presented itself as a prime candidate for inhibition in the development of anti-inflammatory agents, for the treatment of p38 MAPK mediated conditions, and as a target to probe the stressed and aged phenotype of WS fibroblasts.^{3,60}

1.4.1. Type 1 MK2 inhibitors.

The majority of existing MK2 inhibitors belong to the type 1, ATP-competitive inhibitor class.⁵⁵ The ATP binding site of MK2 is characterized by a narrow and deep groove, resulting from the

closed conformation of the kinase. **Figure 12** illustrates how adenosine diphosphate (ADP, **16**) binds into the MK2 ATP binding site.^{55,61}

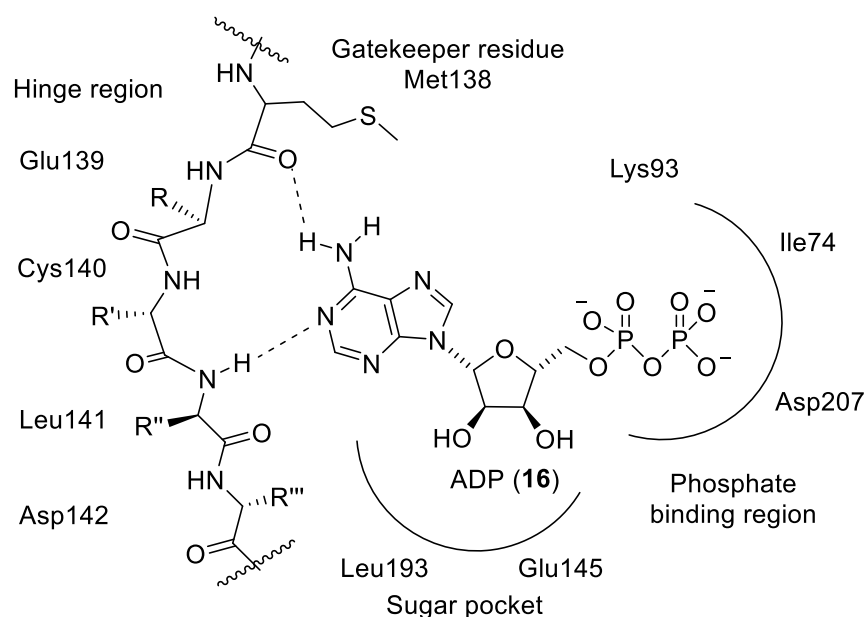


Figure 12: MK2 hinge region bound to ADP (**16**) indicating the hinge region, gatekeeper residue, sugar pocket and phosphate binding region.^{55,61}

The hinge region of MK2 is defined by a Glu139, Cys140, Leu141 and Asp142 residue sequence, with the Glu139 and Leu141 residues forming hydrogen bonds with the adenine residue of ADP. There is a methionine gatekeeper residue which closes off the ATP binding pocket, reducing its size compared to other kinases.⁵⁵ As a result, planar compounds tend to be better tolerated, although improving kinase selectivity is complicated as a consequence.⁵⁵ Additionally, the MK2 ATP-binding site is structurally very similar to a number of other kinases, including MK3 and MK5, further complicating the design of selective inhibitors.

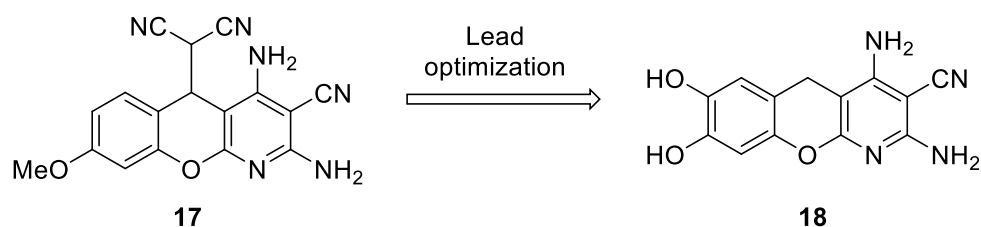


Figure 13: Anderson *et al.*'s development of an aminocyanopyridine class of ATP-competitive MK2 inhibitors.⁶²

Aminocyanopyridines were one of the first chemotypes discovered as potent and selective MK2 inhibitors.²² Anderson *et al.* at Pfizer identified the initial benzopyranopyridine scaffold **17**

through HTS and optimized the structure to reduce potential toxicity of the malononitrile moiety on the pyran ring.⁶² Potency was increased through installation of the 7- and 8-hydroxy groups (**18**). It was inferred that these groups were involved in hydrogen bonding with the ATP binding pocket, as alkylation resulted in a severe loss in potency. **18** was found to be active in rat models *in vivo*, reducing TNF- α production. Subsequently Davis *et al.* established that this compound inhibited the MK2/HSP27 stress-signalling pathway in normal cells, but found that treatment of WS^{tert} cells with **18** gave inconclusive results (see **Chapter 3**).⁶³

Anderson *et al.* at Pfizer also identified pyrrolopyridine **19** as an inhibitor of MK2 through HTS.⁵⁹ Working from data generated from the X-ray co-crystal structure of ATP bound to MK2, the group carried out docking studies to provide a rationale for improving the SAR of **19**. It was found that substitution at the pyridine 2-position (**20**) improved potency for MK2 over the unsubstituted pyridine **19**. Further exploration led to the discovery of an extremely potent 3-quinoline derivative **21**. However it was found that **21** still demonstrated some cross-kinase activity with MK3 and MK5, which have very similar amino acid sequences and larger hinge regions which are able to accommodate the pyridine-2-substituent.

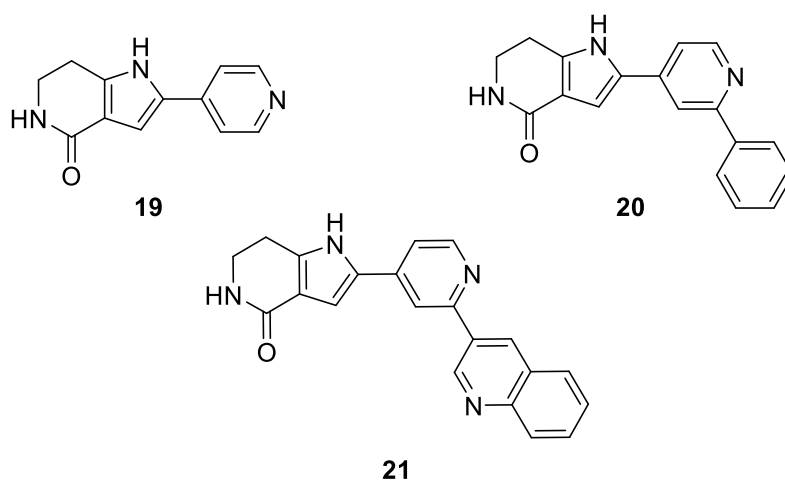


Figure 14: Hit to lead identification of pyrrolopyridine based MK2 inhibitors designed by Anderson *et al.* at Pfizer.⁵⁹

X-ray co-crystallization studies of **21** with MK2 identified that the pyridinyl nitrogen acts as a HBA with the hinge leucine NH and that the lactam ring forms two hydrogen bonds with the lysine and aspartic acid residues of the phosphate region of MK2 (see **Figure 15**).⁵⁹ The group also identified close Van der Waals interactions between **20** and the gatekeeper methionine residue.⁶⁴ Davis *et al.* used pyrrolopyridine **21** to probe the role of MK2 in WS cells, although inconclusive results were again obtained (see **Chapter 3**).⁶⁰

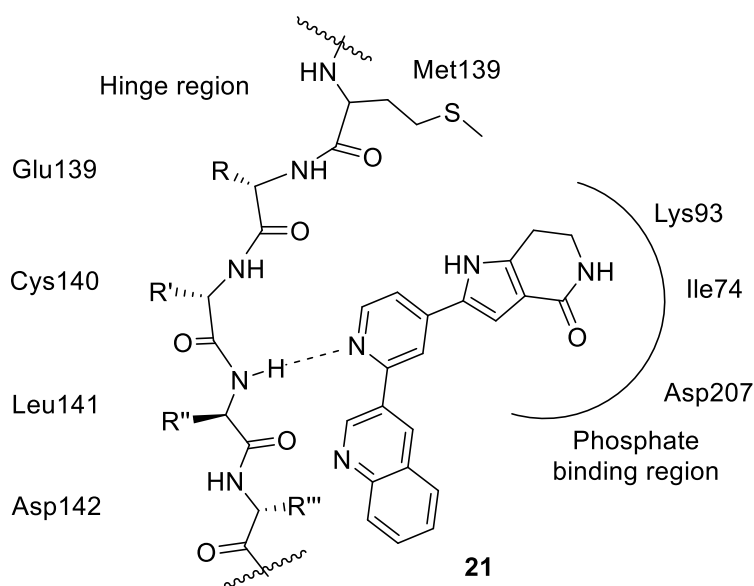
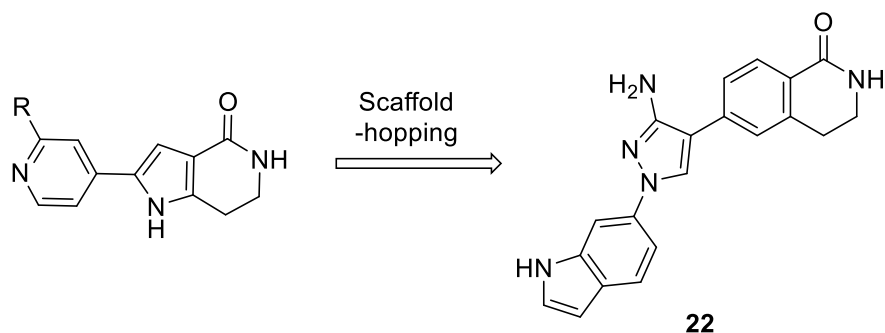


Figure 15: Pyrrolopyridine MK2 inhibitor **21** complexed with the MK2 ATP-binding site showing hydrogen bonding between the pyridine moiety and Leu141 in the hinge region, and interaction with the phosphate binding region.⁵⁹

Many of the key binding regions established using the pharmacophore of Anderson's pyrrolopyridine MK2 inhibitor **21** have become ubiquitous to type 1 MK2 inhibitors. For instance, Velcicky *et al.* adopted a 'scaffold-hopping' strategy from analogues of **20** and **21** to develop the 3-aminopyrazole MK2 inhibitor **22**.⁶⁵



Scheme 1: Velcicky's 'scaffold-hopping' strategy for the development of novel 3-aminopyrazole MK2 inhibitors (**22**).⁶⁵

The group aimed to exchange the pyrrole of **21** for a phenyl ring, and so proposed a five-membered heterocyclic HBA to maintain the same spatial arrangement between the binding sites. A 3-aminopyrazole scaffold was found to improve kinase activity over a simple pyrazole group, and extension of the 1*H*-aryl group revealed a new selectivity element. Using X-ray co-crystallization studies the group discovered that when a 1-(1*H*-indol-6-yl)pyrazole was installed (**22**), a conformational rearrangement occurred through an additional hydrogen bonding

interaction of the indole. This conformational shift exposed a new hydrophobic pocket behind the hinge region of the kinase, endowing **22** with an enhanced selectivity for MK2 over other similar kinases.⁶⁵

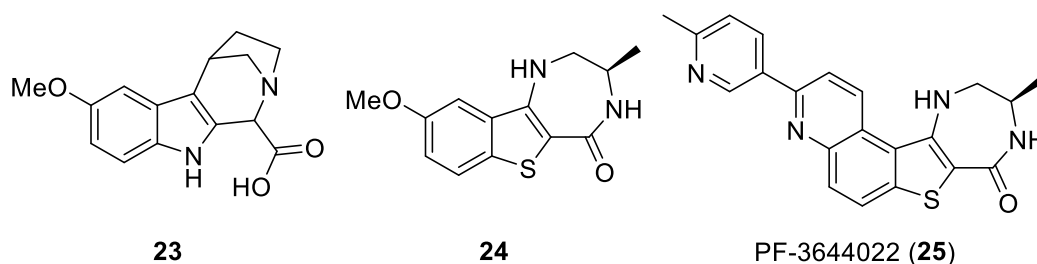


Figure 16: β-Carboline and benzo[*b*]thiophene based MK2 inhibitors designed by Pfizer with similar pharmacophoric properties.^{66–68}

The β-carboline and benzothiophene MK2 inhibitors **23**,⁶⁶ **24** and **25** developed by Pfizer also shared a number of binding traits with the pyrrolopyridine pharmacophore. β-Carboline **23** was developed before the crystal structure of MK2 was available,⁶⁶ though with comparison with benzothiophene analogues **24** and **25**, the key binding interactions can be inferred.^{67,68} The methoxy groups of **23** and **24**, and the pyridine ring of **25** act as HBAs with the hinge leucine residue, while the carboxylic acid of **23** and the fused lactam rings of **24** and **25** interact with the phosphate binding region.

Fused heterocyclic benzo[*b*]thiophene based MK2 inhibitor PF-3644022 (**25**) is a highly potent inhibitor for MK2, with a nanomolar IC₅₀, good projected ADME characteristics and high selectivity for MK2 against a panel of two hundred kinases.⁶⁹ It was proposed that this new pharmacophore would be an interesting compound to test in WS cells to probe the role of MK2 on the aged phenotype of WS fibroblasts. Thus, the main thrust of this report will discuss efforts to develop a new total synthesis of the fused heterocyclic benzo[*b*]thiophene based MK2 inhibitor PF-3644022 (**25**), ready for testing in WS cells. The development of new methods of heterocycle synthesis will be discussed, and the benefits of microwave-dielectric heating techniques for the development of a more efficient synthetic route will be explored (see **Chapter 3**).

1.4.3. Type 2 MK2 inhibitors.

The high affinity of MK2 for ATP and high concentrations of ATP *in vivo* tend to result in a poor biochemical efficiency (BE) for type 1 MK2 inhibitors. Additionally, given the significant similarity

between the ATP-binding pocket of MK2 and a number of other kinases, the design of efficacious type 2, non-ATP-competitive inhibitors has been proposed as a route to more selective and potent therapeutics.^{55,70} A limited number of type 2, non-ATP-competitive MK2 inhibitors have been designed, with the most extensive studies completed by Merck.

Huang *et al.* at Merck identified the furan-2-carboxamide scaffold (**26**) as a potential non-ATP-competitive MK2 inhibitor using an affinity selection-mass spectrometry (AS-MS)-based HTS method using an automated ligand identification system (ALIS). This method exposes the target biomolecule to a library of compounds, and then uses size-exclusion chromatography to separate out the unbound ligands and compounds, with subsequent analysis of complexes conducted using reverse-phase liquid chromatography-mass spectrometry (RP-LCMS) and electrospray ionization (ESI) mass spectrometry.⁵⁵

Initial hit compound **26** exhibited good pharmacokinetic and ADME characteristics and the non-ATP-competitive binding mode was confirmed through NMR spectroscopic and enzymatic studies. Lead optimization was undertaken to improve cell potency and pharmacokinetic properties.

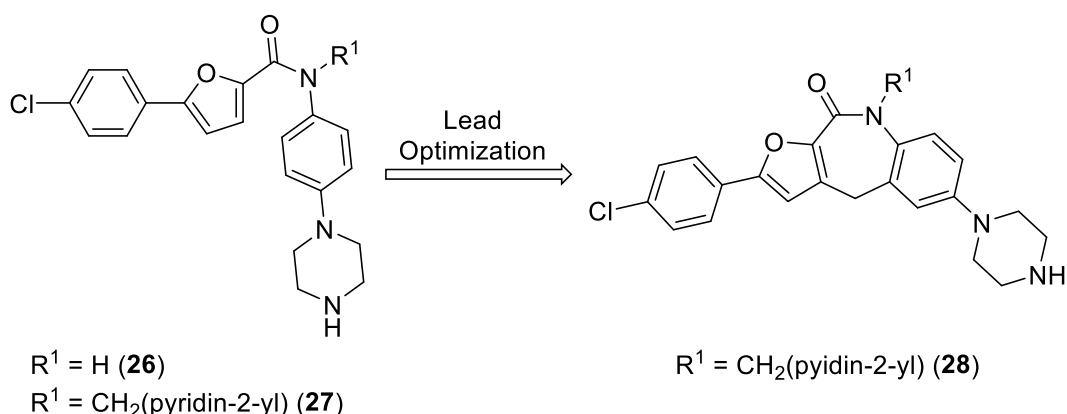


Figure 17: Merck's hit to lead identification of non-ATP-competitive MK2 inhibitors. From initial hit **25** to the development of tricyclic lactams **27** and **28**.^{70,71}

It was found that functionalization of the secondary amide NH dramatically influenced compound potency, with installation of a pyridine ring (**27**) resulting in a compound with high selectivity against a panel of 150 kinases, a good toxicity profile and favourable pharmacokinetics in rat models.⁷⁰ Compound **27** was also found to inhibit pro-inflammatory cytokine production in a concentration-dependent manner in human cells.

It was proposed by the group that the increased potency from **26** to **27** was due to an energetically-favoured conformational change from the linear (*Z*) to the bent (*E*) conformer.⁷¹

The group proposed that through constraining the geometry of the amide the potency of the compound should benefit. The synthesis of tricyclic lactam **28**, supported this theory, with a significant increase in inhibitor efficiency and single digit nanomolar IC₅₀ values.

1.4.4. Outlook for MK2 inhibitors.

A variety of pharmacophores have been explored in the development of ATP-competitive MK2 inhibitors,²² although the majority have been found to suffer from poor solubility, low cell permeability and low cell potency due to the high levels of ATP. As such, efforts to improve the pharmacokinetics and binding potency of these compounds is still a priority.⁵⁵

The development of non-ATP-competitive MK2 inhibitors has been embraced as a potential route for the development of more viable therapeutic candidates. Studies into optimizing these compounds are still ongoing.

1.5. Project aims.

This project aims to explore the development of new methods for the synthesis of a number of heterocyclic targets and their use as chemical probes to investigate the p38 stress-signalling cascade and its role in the modulation of the aged phenotype of WS cells. Its findings will be described in three sections.

Firstly, a rapid synthetic route towards the p38 α inhibitor RO3201195 (**10**) will be described. The aim of this investigation was to develop an improved total synthesis towards the pyrazole based inhibitor, adopting new chemical methods towards key bond-forming reactions and improving on methods published in the literature. Once synthesized, the compound was tested in WS cells, the results of which will be described in detail.

Secondly, efforts to develop a new total synthesis of the MK2 inhibitor PF-3644022 (**25**) will be discussed. A number of different retrosynthetic strategies will be discussed, exploring a variety of heterocycle forming reactions and alternative disconnective routes to those described in the literature. The use of MK2 inhibitors as probes in WS cells will then be reflected upon, including the application of **25**.

Lastly, the pharmacophore of the p38 α inhibitor BIRB 796 (**14**) will be probed for its potential towards drug repurposing. The unique binding mode of the *N,N'*-diaryl urea will be explored to target alternative kinases for the development of new, selective chemical probes to investigate the MAPK signalling cascade.

1.6. Methods and techniques.

Throughout the course of this synthetic organic project a number of different chemical and synthetic methods and techniques were adopted. The most prevalent will now be discussed.

1.6.1. Microwave-assisted organic synthesis (MAOS).

Over the past two and a half decades, microwave-assisted synthesis has been recognized within mainstream organic chemistry as a clean and efficient way of achieving fast, high-yielding transformations.⁷² With the development of new instruments offering a greater degree of control, microwave-assisted synthesis has emerged as one of the most convenient and practical methods for conducting organic synthesis in industry and academia.⁷³

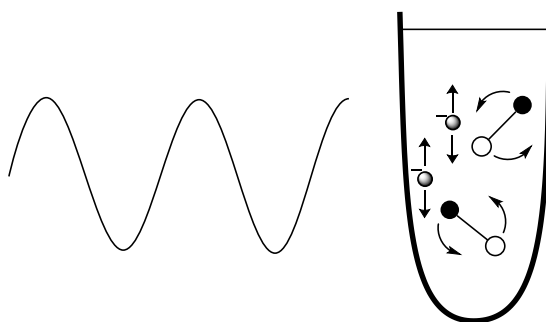


Figure 18: Effects of a rapidly oscillating electric field on molecules in solution, showing rotation of polar molecules and rapid movement of charged particles to align with the changing field.

Microwave dielectric heating is promoted by two mechanisms as a consequence of the rapidly oscillating electric field component of electromagnetic radiation. When a polar molecule is subjected to an external electric field, dipolar polarization occurs and the molecule rotates as it attempts to align with the undulating field (see **Figure 18**). The frequency of radiation determines how quickly the molecule rotates. However, if the frequency is too high the molecule will not have enough time to adjust and rotate and will remain stationary.

The energy window of microwave radiation lies at a frequency that is low enough to allow a polar molecule to start rotation into alignment, but not too low to allow full alignment before the phase of the wave changes. This creates phase differences which cause friction and collisions between the molecules in solution and loss of energy as heat.

The addition of ions to solution can increase the rapidity of heating through a conductive mechanism. Ions rapidly align with the oscillating electric field and travel swiftly through the

solution to collide with other molecules (see **Figure 18**), converting kinetic energy into heat energy. Hence, the addition of ions to a non-polar solvent will enable the solution to be heated using microwave energy.

Through a combination of these mechanisms rapid temperature gradients can be achieved. The use of sealed vessels allows solvents to be heated above their atmospheric boiling point and this creates energy profiles which are not easy to safely reproduce by conventional means.

Microwave technology has been embraced as a reliable, efficient technique to accelerate drug design and discovery. Readily-adaptable from small to large scale, it is widely utilized in research and development with applications in metal-mediated reactions, combinatorial and library synthesis, solid-phase synthesis, and multi-component tandem reactions.^{72,74}

MAOS was adopted throughout this project as a means to facilitate rapid and efficient synthetic procedures, with specific applications to heterocyclic synthesis and metal-mediated reactions.

1.6.2. Heterocycles.

Heterocycles are ubiquitous in drugs and natural products, often acting as scaffolds from which further functionalization and diversification can be cultivated, and that are able to conduct electronic and hydrogen bonding interactions with biological targets.

The most prominent heterocyclic scaffolds which appear throughout this project will now be discussed, including their synthesis, reactivity and applications in medicinal chemistry and other industries.

1.6.2.1. Azoles.

Clean, simple and efficient routes towards 5-membered heterocycles of the azole class, including pyrazoles (1,2-azole), imidazoles (1,3-azole) and oxygen containing oxazoles and isoxazoles, are highly desirable in medicinal chemistry and drug discovery as they can act as highly substituted scaffolds, while reducing lipophilicity compared to carbon-based scaffolds.⁷⁵

The incorporation of heteroatoms can facilitate numerous additional interactions with amino acid residues of proteins and kinases through hydrogen bonding and Van der Waals interactions. However, it is notable that pyrazoles do not exist in nature due to an inability of living organisms

to form N-N bonds.⁷⁶ A selection of pyrazole and imidazole containing p38 MAPK inhibitors have already been discussed (see **Chapter 1.3.1**) including SB203580 (**1**), and the pyrazolopyridine UR-135756 (**7**). **Figure 19** illustrates some examples of current drugs and agrochemicals which contain azoles.

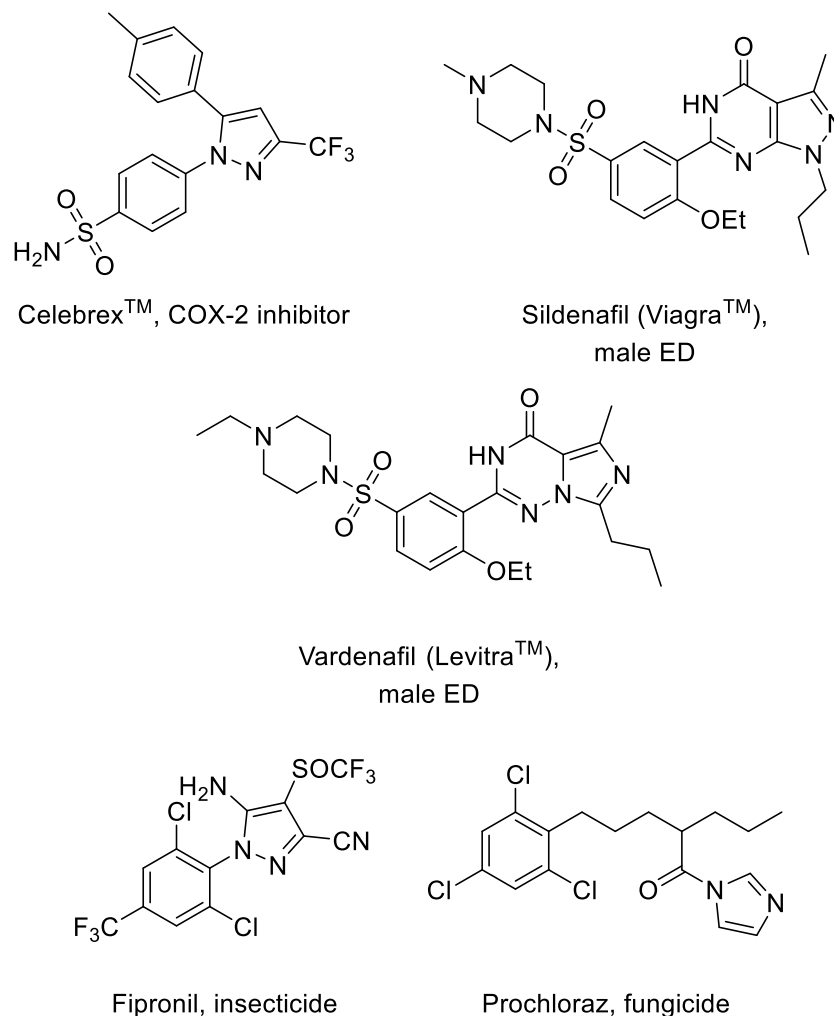


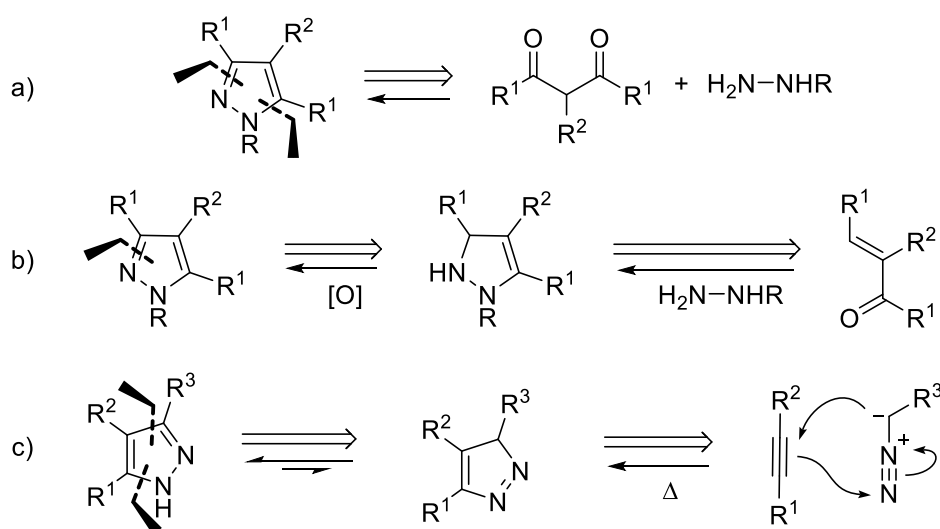
Figure 19: Examples of azoles in pharmaceuticals and agrochemicals.

Celebrex is a pyrazole-containing COX-2 inhibitor and anti-inflammatory drug. Sildenafil and Vardenafil contain a pyrazole and imidazole respectively, and are both phosphodiesterase type 5 (PDE5) inhibitors and vasodilators used in the treatment of male erectile dysfunction (ED).⁷⁷

The agrochemicals Fipronil and Prochloraz also contain azoles. Fipronil is an insecticide which acts through blocking the chloride ion channel of the γ -aminobutyric acid (GABA) receptor, and has a particular toxicity towards insects compared to vertebrates due to higher GABA receptor sensitivity in that species.⁷⁸ Prochloraz is a fungicide which operates through inhibition of a

cytochrome P450-dependent pathway which is essential for building the cell membrane of fungi.⁷⁹ The binding relies upon association of the imidazole to the iron core of cytochrome P450, but it is not very specific and affects a number of other P450-dependent pathways. Reports have advised that use of Prochloraz be reduced, as it has been found to exhibit endocrine disruptive effects in animals and humans, leading to disruptions in hormone levels during fetal development.^{79,80}

1.6.2.1.1. Synthetic routes towards functionalized pyrazoles.



Scheme 2: Different disconnection strategies towards pyrazoles.

There are many routes for the synthesis of pyrazoles, of which the most widely used is the condensation of 1,3-dicarbonyl compounds and hydrazines to give di- or tri-substituted pyrazoles.⁸¹ The bis-nucleophilic hydrazine is able to react with each carbonyl in turn, with unsymmetrical dicarbonyl compounds potentially giving a mixture of regioisomers unless the reaction is carefully controlled (**Scheme 2a**).⁸² The reaction of an α,β -unsaturated aldehyde or ketone with hydrazine provides an alternative approach, giving an intermediate which must be oxidized in order to generate the poly-substituted pyrazole (**Scheme 2b**).^{83,84} Another method of synthesis is via the 1,3-dipolar cycloaddition of an alkyne or alkene with a diazoalkane or nitrilimine, which on tautomerization gives the desired pyrazole (**Scheme 2c**).⁸⁵ Synthetic methods for the synthesis of 3,5-disubstituted pyrazoles will be discussed later in **Chapter 4.1.2**.

The aminopyrazole scaffold is prominent in pharmaceutical agents and agrochemicals, with 5-aminopyrazoles representing a useful building block in drug design as well as demonstrating significant biological activity.^{76,86} Examples of 5-aminopyrazoles of biological significance include the GABA inhibitor pesticide Fipronil (see **Figure 19**);⁷⁸ the lymphocyte-specific protein kinase p56^{lck} inhibitor **29**,⁸⁷ and the human neuropeptide Y5 (NPY5) receptor antagonist **30**.⁸⁸

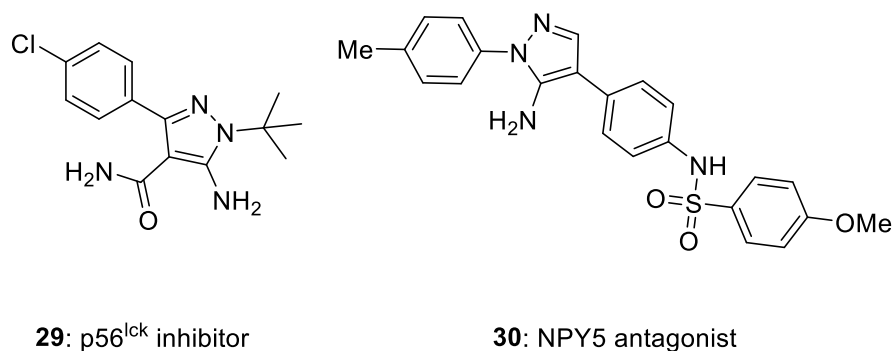
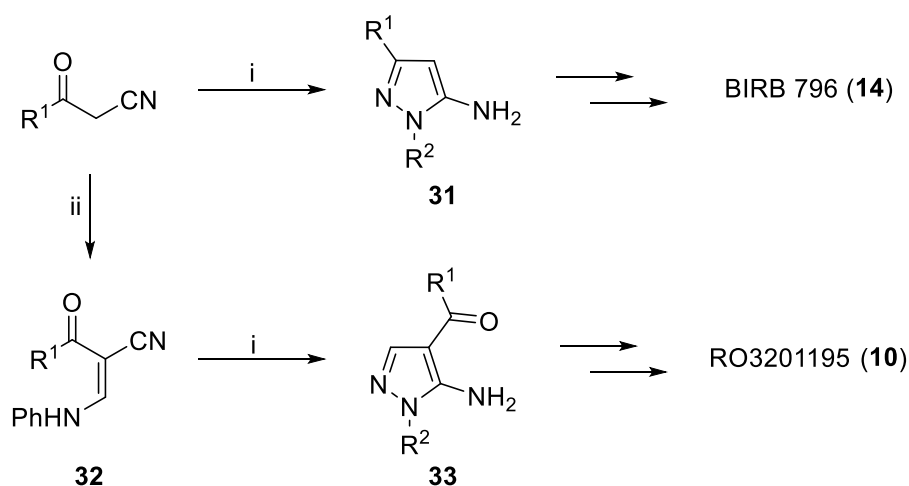


Figure 20: Examples of 5-aminopyrazole-containing pharmaceutical agents.^{87,88}

5-Aminopyrazoles can be synthesized by the condensation of β -ketonitriles and hydrazines.⁷⁶ This route was adopted by Regan *et al.* in the synthesis of the 1,3-disubstituted-5-aminopyrazole BIRB 796 (**14**) and by Goldstein *et al.* towards the 1,4-disubstituted-5-aminopyrazole RO3201195 (**10**) (see **Scheme 3**, and **Chapter 4.3** and **Chapter 2.2**).⁵⁰

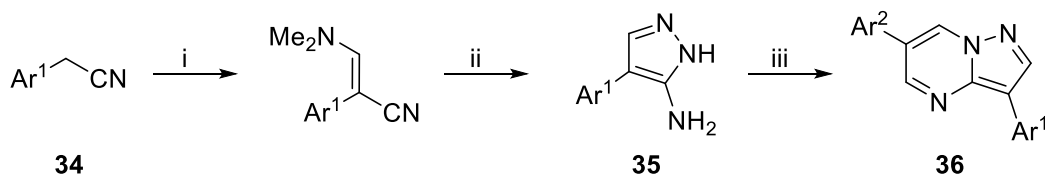


Scheme 3: Methods for the synthesis of two differently substituted 5-aminopyrazoles in the preparation of p38 α MAPK inhibitors from β -ketonitriles. Reaction conditions: i) H_2NNHR^2 ; ii) N,N' -diphenylformamidine.

Starting from a β -ketonitrile starting material, Goldstein *et al.* accessed different substitution patterns on the 5-aminopyrazole through β -ketonitrile homologation using N,N' -diphenylformamidine. The aminoacylonitrile **32** preferentially underwent cyclocondensation

with the hydrazine to change the pyrazole ring substitution pattern from a 3- to 4-substituted-5-aminopyrazole, **31** and **33** respectively.

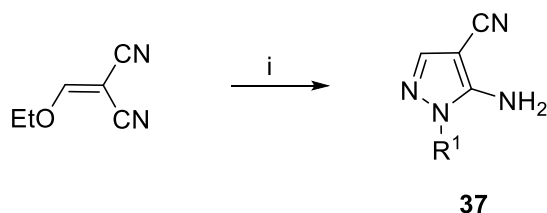
Daniels *et al.* adopted a similar homologation approach to synthesize 5-aminopyrazole intermediates (**35**) in the preparation of pyrazolo[1,5-*a*]pyrimidines (**36**) and pyrazolo[3,4-*b*]pyrimidines as new lead compounds for cancer and neuroscience programmes (see **Scheme 4**).⁸⁹



Scheme 4: Microwave-mediated synthesis of pyrazolo[1,5-*a*]pyrimidine **36** from 4-aryl-5-aminopyrazole **35**. Reaction conditions: i) DMFDMA, PhCF₃, MW 150 °C, 10 min; ii) N₂H₄, MW 140 °C, 10 min, 85%; iii) malondialdehyde, 5% AcOH/EtOH, MW 150-170 °C, 10 min, 85-98%.⁸⁹

Their method of homologation started from arylacetonitrile **34** and used *N,N*-dimethylformamide dimethyl acetal (DMFDMA) as a single carbon unit donor.⁹⁰ Daniels *et al.* adopted microwave-assisted dielectric heating to facilitate a more efficient synthesis of 5-amino-4-arylpyrazole **35**. Doing so they were able to reduce reaction times from over 72 h to just 20 minutes, and increased their yields from 55-75% to 88% over two steps in one pot.⁸⁹ Acid-mediated thermal cyclocondensation with malondialdehyde gave pyrazolopyrimidine product **36**.

Another popular method for the synthesis of 4-substituted-5-aminopyrazoles starts from unsaturated malononitriles which can be reacted with hydrazine to give 4-cyano-5-aminopyrazoles **37** (see **Scheme 5**).^{91,92}



Scheme 5: Synthesis of 1-substituted-4-cyano-5-aminopyrazoles synthesis. Reaction conditions: i) H₂NNHR¹, EtOH, Δ.⁹³

Bagley *et al.* explored this route by reacting ethoxymethylenemalononitrile with monosubstituted alkyl and aryl hydrazines and synthesized 1-substituted-4-cyano-5-aminopyrazole **37** with total regiocontrol.⁹³ These pyrazole derivatives have found use as

potential purine antagonists,^{91,93} and as building blocks towards A_{2A} adenosine antagonists (see **Figure 21**).⁹⁴

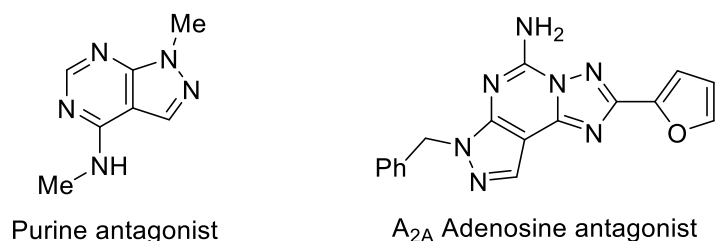


Figure 21: 1-Substituted-4-cyano-5-aminopyrazoles **37** are building blocks for the synthesis of purine antagonists⁹¹ and A_{2A} adenosine antagonists.⁹⁴

1.6.2.2. Pyridines.

The prevalence of pyridine in nature, medicinal chemistry and industry is undeniable. Pyridine-containing natural products include vitamins B₆ (pyridoxine) and B₃ (nicotinic acid) which are essential nutrients for human life. Nicotinamide adenine dinucleotide phosphate (NADP) is an essential co-enzyme in the body which mediates redox reactions and is derived from vitamin B₃ (see **Figure 22**).^{95,96}

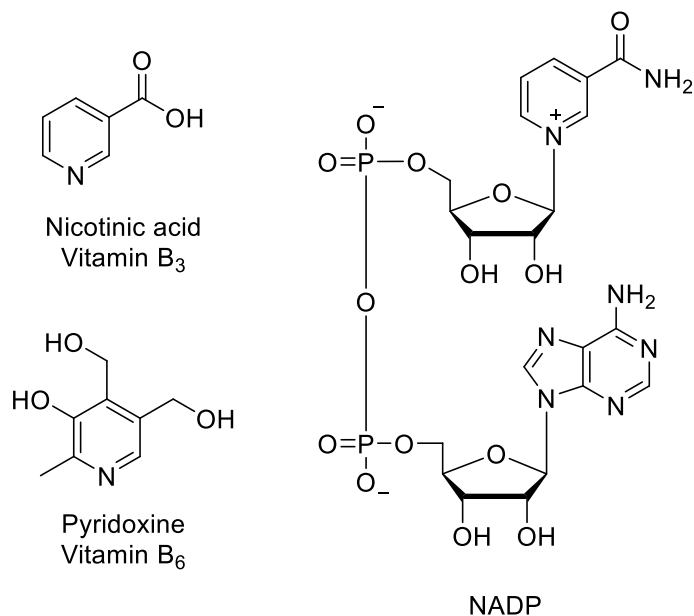


Figure 22: Natural pyridine-containing compounds: vitamin B₃, vitamin B₆ and NADP.

In a survey conducted by Roughley and Jordan and published in 2008, 90% of all heterocycle-forming reactions carried out in medicinal chemistry generated *N*-containing rings, with pyridine

constituting almost 25% of all heteroaromatic compounds.⁹⁷ A few examples of pyridine-containing pharmaceutical agents and drug candidates are detailed in **Figure 23**, including the antibiotic isoniazid (**38**), a prodrug used to treat tuberculosis. Activated by oxidation in the bacterium, the mechanism of action of this agent is postulated to operate through a nitric oxide radical.⁹⁸ Further examples include the highly-bioavailable 2-pyridinemethylamine based 5-HT_{1A} receptor agonist **39**, an antidepressant that can travel across the blood-brain barrier and bind to 5-HT receptors and activate them,⁹⁹ and the A₃ adenosine receptor antagonist **40**, which is an anti-inflammatory and anti-asthmatic that binds to and blocks adenosine receptors.¹⁰⁰

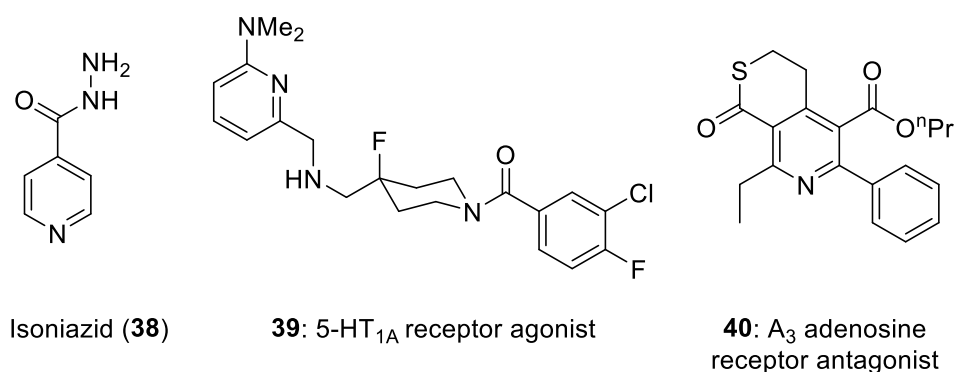


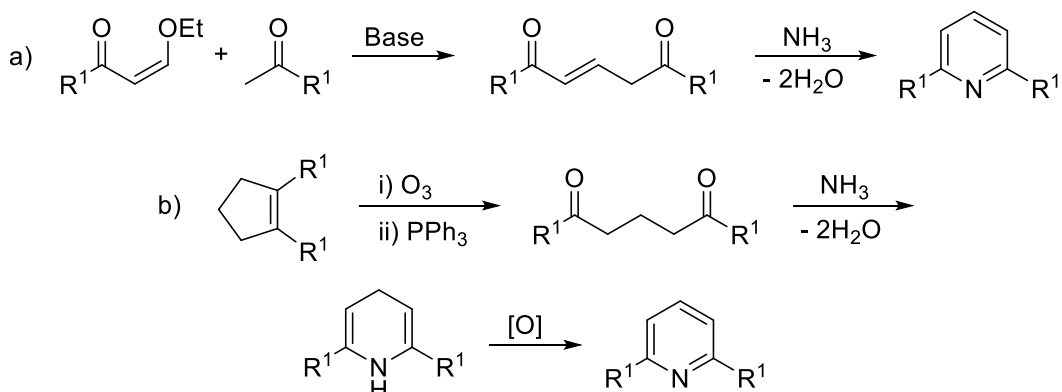
Figure 23: Examples of pyridine-containing pharmaceutical agents and drug candidates: Isoniazid (**38**), a 2-pyridinemethylamine based 5-HT_{1A} receptor agonist (**39**) and an A₃ adenosine receptor antagonist (**40**).

1.6.2.2.1. Synthesis of pyridines.

Pyridine was originally isolated from a number of sources, including by-products of bone pyrolysis, via condensation of various aldehydes and ketones with ammonia,⁹⁶ and for a long time directly from coal tar.⁸¹ With increasing understanding of their biological and practical applications, many new methods of pyridine synthesis have been discovered starting from simple materials.

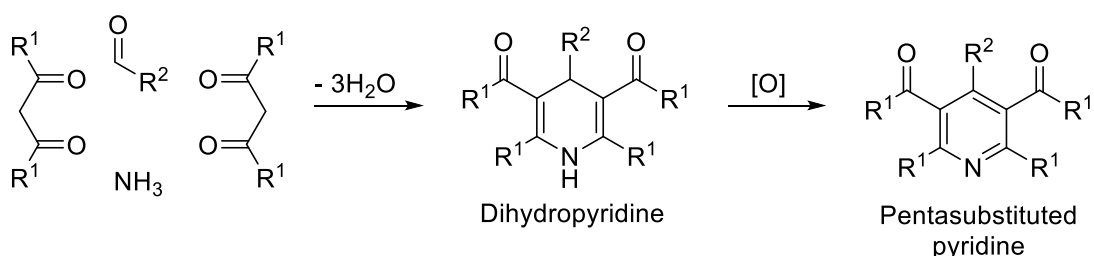
Depending upon the complexity of the target molecule there are numerous different disconnection routes available for the synthesis of pyridines. The classical [5+1] condensation reaction of ammonia and a 1,5-dicarbonyl compound gives 1,4-dihydropyridines, which can be oxidized to the corresponding pyridine. 1,5-Dicarbonyl compounds can be accessed by a number of routes, including via Michael addition of enolates and enones, or by ozonolysis of

cyclopentenes (see **Scheme 6a** and **6b** respectively). Through the use of hydroxylamine the final oxidation step can be avoided, giving the aromatic pyridine on elimination of water.



Scheme 6: [5+1] Connective strategies for the synthesis of 2,6-disubstituted pyridines. a) Michael addition of an α,β -unsaturated ketone and a methyl ketone under basic conditions. Subsequent condensation with ammonia gives 2,6-disubstituted pyridines. b) Ozonolysis of cyclopentene, condensation with ammonia, and subsequent oxidation.

The Hantzsch dihydropyridine synthesis adopts a [2+2+1+1] connective strategy.⁹⁶ Classically two equivalents of a 1,3-dicarbonyl are condensed with one equivalent of an aldehyde and ammonia, with oxidation subsequent to cyclization affording the symmetrical pyridine (see **Scheme 7**). Mechanistically, the precise sequence of condensations is not explicitly known, though it is likely to be dependent upon the reagents used.

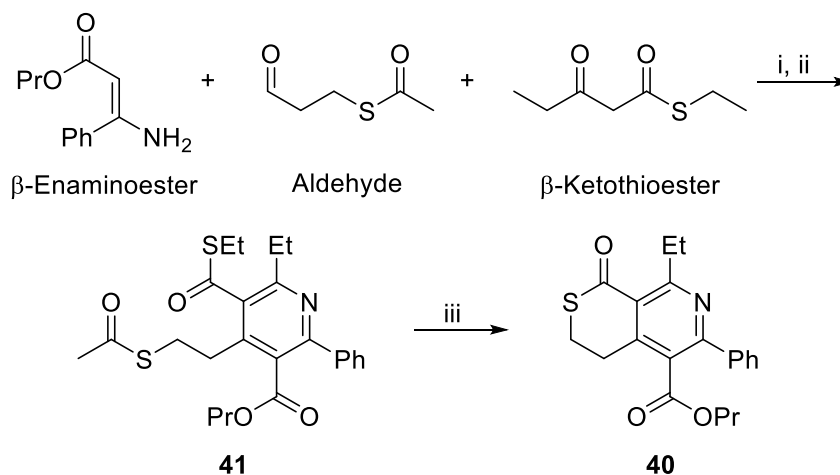


Scheme 7: Hantzsch dihydropyridine synthesis. Condensation with loss of three equivalents of water to give the dihydropyridine. Oxidation gives the final tetrasubstituted pyridine.

Unsymmetrical pyridines can be formed by condensing ammonia and a 1,3-dicarbonyl compound to form an intermediate β -ketoenamine, and then reacting with an aldehyde and another 1,3-dicarbonyl compound. Oxidation to the dihydropyridine can be conducted using nitric acid, ceric ammonium nitrate, manganese dioxide or iodine with KOH .⁸¹

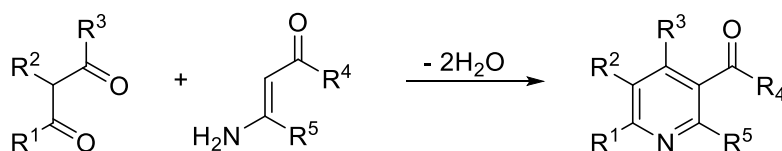
The Hantzsch pyridine synthesis is commonly used for the synthesis of pentasubstituted pyridines. For instance, towards the A_3 antagonist **40**, Li *et al.* condensed a β -aminoester with a functionalized aldehyde and β -ketothioester to give the 1,4-dihydropyridine intermediate,

which was oxidized using tetrachloroquinone to afford pentasubstituted pyridine **41** (see **Scheme 8**).¹⁰⁰ It was found that potency of the antagonist could be increased through a more conformationally constrained system. Hence **41** was deprotected and subjected to intramolecular transesterification using sodium thiomethoxide to afford **40** in high yield.¹⁰⁰



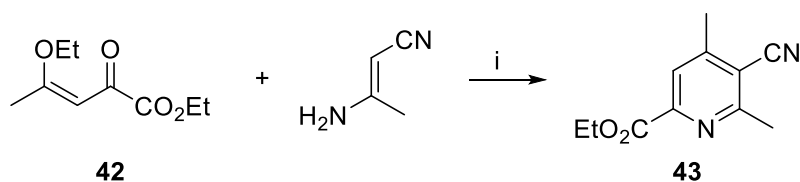
Scheme 8: Synthesis of A₃ adenosine receptor antagonist **40**. Reaction conditions: i) EtOH, 80 °C, 24 h; ii) tetrachloroquinone, THF, Δ , overnight; iii) NaSMe, MeOH, RT, 30 min, 98%.¹⁰⁰

Pyridines can also be synthesized through [3+3] connective routes, for instance from the reaction of 1,3-dicarbonyl compounds and 3-aminoenones or 3-aminoacrylates (see **Scheme 9**).⁸¹



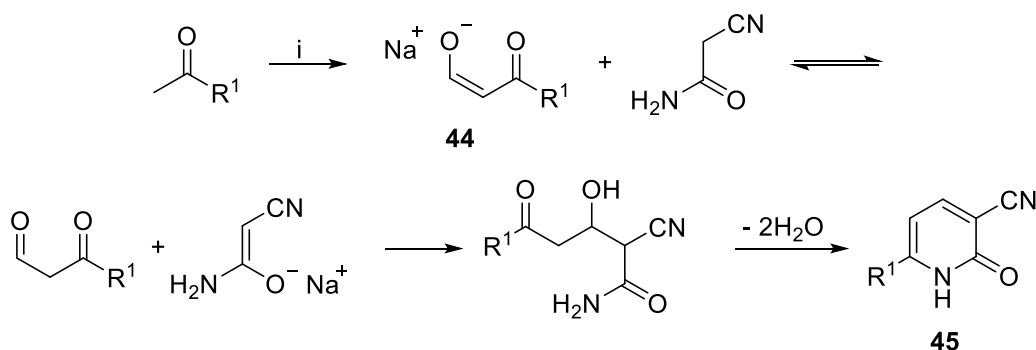
Scheme 9: Pyridine [3+3] connective synthesis from 1,3-dicarbonyl compounds and 3-aminoenones or acrylates.

The Guareschi synthesis is a variation on this route wherein a 3-aminocrotonitrile undergoes cyclocondensation with an ethoxyenone (**42**) via Michael addition to give the 6-ethoxycarbonyl-3-cyanopyridine (**43**) (see **Scheme 9**).^{81,96}



Scheme 10: [3+3] Guareschi pyridine synthesis: Reaction conditions: i) K₂CO₃, 73%.⁹⁶

Through use of cyanoacetamide, 3-cyano-2-pyridones can be synthesised directly (see **Scheme 11**). Claisen condensation of ethyl formate and a methyl ketone gives the stable enolate **44**. Proton exchange can then occur in situ on treatment with cyanoacetamide, to facilitate the intermolecular aldol reaction.^{101,102} Intramolecular condensation and loss of water then affords the final 3-cyano-2-pyridone **45**.

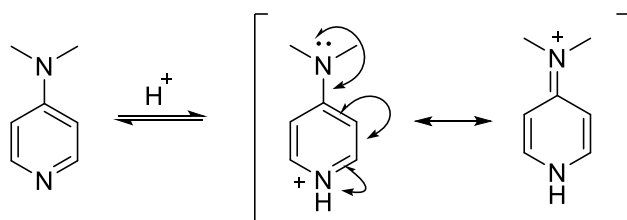


Scheme 11: Synthesis of Pyridones. Reaction conditions: i) HCO_2Et , NaOMe .¹⁰²

2-Pyridones can tautomerize to 2-hydroxypyridines, but the amide tends to predominate due to the strong $\text{C}=\text{O}$ bond.¹⁰¹ Pyridones can be useful intermediates in synthesis. Alkylation will readily occur at oxygen and conversion to the corresponding 2-chloropyridine can be carried out by reaction with phosphorous oxychloride (POCl_3).¹⁰¹

1.6.2.2.2. Reactions of pyridines.

The reactivity of pyridine is very different from its carbocyclic analogue benzene. Exchange of a methine unit for nitrogen introduces a permanent dipole on the heterocycle and a new sp^2 hybridized lone pair in the plane of the ring.⁸¹

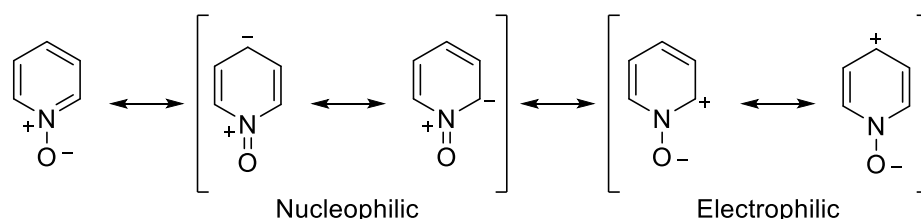


Scheme 12: Resonance stabilization of protonated dimethylaminopyridine (DMAP).

The lone pair of the pyridine nitrogen makes the ring slightly basic, with pK_{aH} 5.2 in water. It acts similarly to a tertiary amine and is open to attack by external electrophiles, resulting in formation

of the pyridinium cation.⁸¹ The basicity of the nitrogen lone pair can be tuned through the substituents on the ring, with electron-donating groups (EDG) increasing basicity, and the α - and γ -positions having a more pronounced effect. For example, 4-dimethylaminopyridine (DMAP) is a strongly basic analogue of pyridine, due to further resonance stabilization of the pyridinium cation (see **Scheme 12**), and is used commonly in synthetic organic reactions.

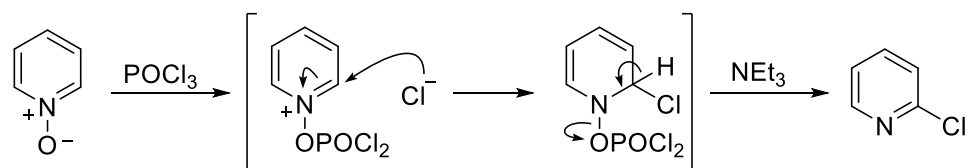
Reactions that can occur at the nitrogen include nitration, oxidation, acylation and alkylation. Oxidation of pyridines to the pyridine *N*-oxide using *m*CPBA or peroxides can be used as a method to augment reactivity, enhancing the electrophilicity or nucleophilicity of the α - and γ -positions. This contrasting effect can be viewed as being due to inductive withdrawal of electron density by the nitronium cation, or donation of electron density from the oxy anion (see **Scheme 13**).⁸¹ For instance, alkylation and protonation of pyridine *N*-oxides will occur initially at the oxygen, thereby amplifying electrophilicity of the pyridinium ring at the α - and γ -positions.⁸¹



Scheme 13: Pyridine *N*-oxide canonical forms explain the increased reactivity on the ring towards attacking electrophiles and nucleophiles.⁸¹

Pyridine *N*-oxides can undergo nucleophilic attack through addition-elimination on functionalization of the oxide. For instance, reaction with POCl_3 will result in formation of the 2-chloropyridine. The oxide initially reacts with the oxophilic phosphorous to enhance electrophilicity of the α -position. Nucleophilic attack by a chloride anion is then proposed to occur, with elimination giving the rearomatized pyridine ring (see **Scheme 14**).¹⁰³

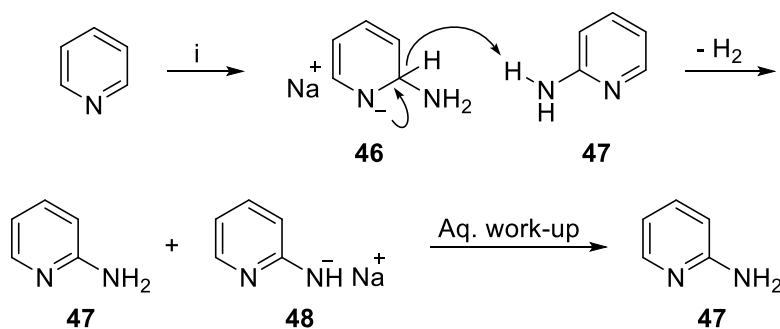
Chlorination will also tend to occur at the γ -position, with a 7:3 ratio of 2- and 4-chloropyridine products.¹⁰³ However, Jung *et al.* found that through the use of stoichiometric amounts of NEt_3 , elimination of the more acidic proton at C-2 was promoted, and that chlorination could be carried out almost selectively at the α -position (90% yield, 99.2% selectively).¹⁰³ The same method can be used with acetic anhydride to give the 2-acetoxypyridine.⁸¹



Scheme 14: Chlorination of pyridine *N*-oxide using POCl₃ and triethylamine base.¹⁰³

Electrophilic substitution of pyridines at carbon occurs less readily than for benzene in part due to preliminary formation of a pyridinium cation. Through the use of bulky alkyl groups at the α -carbons, electrophilic attack at nitrogen can be disfavoured, promoting electrophilic aromatic substitution (EAS) at the β -carbons.⁸¹

Nucleophilic substitution on to the pyridine ring is much more favourable due to the electron-deficient nature of the ring. For instance, pyridine amination can be carried out through the Chichibabin reaction. Using sodium amide the reaction is believed to occur through formation of an anionic intermediate (**46**). Hydride transfer to the amine product **47** eliminates hydrogen gas to give the aminopyridine conjugate base **48** and the 2-aminopyridine **47** on aqueous work-up (see **Scheme 15**).



Scheme 15: Chichibabin amination of pyridines. Reaction conditions: i) NaNH₂, PhNMe₂, 100 °C, 75%.⁸¹

Pyridines are extremely versatile intermediates in organic synthesis and exhibit a variety of interesting biological activities. Their fused analogues tend to demonstrate similar reactivities and are similarly important, biologically, with one major class being quinolines.

1.6.2.3. Quinolines.

Highly regioselective methods for the synthesis of quinolines are desirable as, much like pyridines, quinoline derivatives elicit a range of biological responses and are present in natural and synthetic products.^{104,105}

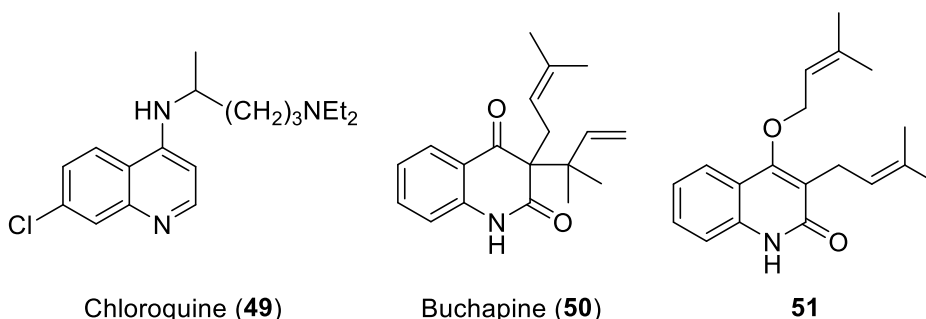


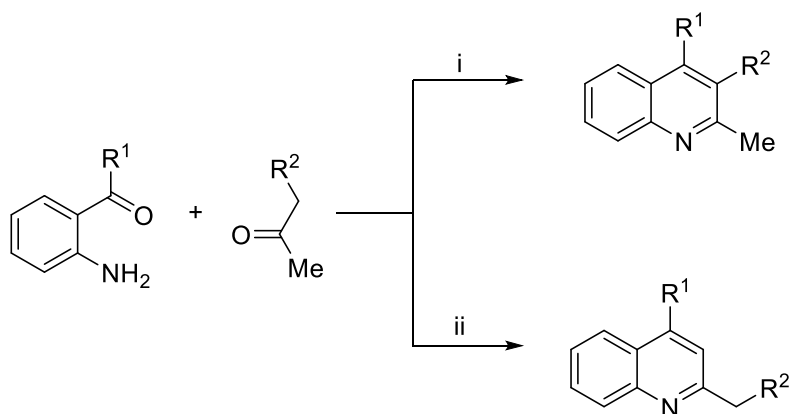
Figure 24: Quinoline containing drugs and natural products. Antimalarial chloroquine (**49**), and anti-HIV agents buchapine (**50**) and quinolin-2-one **51**.^{105,107}

For instance, the antimalarial agent chloroquine (**49**) is a quinoline-containing drug that was designed in the 1940s. It is believed to act by binding to DNA in blood, which is then ingested by the malaria parasite to inhibit its digestive pathway.¹⁰⁶ Numerous natural quinoline and quinolinone alkaloids have been isolated from plants, animals and microbes and have been found to exhibit very interesting biological properties, including the anti-HIV activity of extracts from *Evodia roxburghiana* which contain quinoline-2-ones buchapine (**50**) and **51**.¹⁰⁷

1.6.2.3.1. Synthesis of quinolines.

Synthesis of quinolines or quinolones can be conducted through a number of different disconnective strategies, though most adopt anilines as the nitrogen containing component. The reactions tend to occur either through an initial C-N bond forming reaction between aniline and a 4-carbon synthon before cyclization onto the benzene ring, or reaction with a 2-carbon unit through C-C bond formation to an aniline *ortho*-substituent.

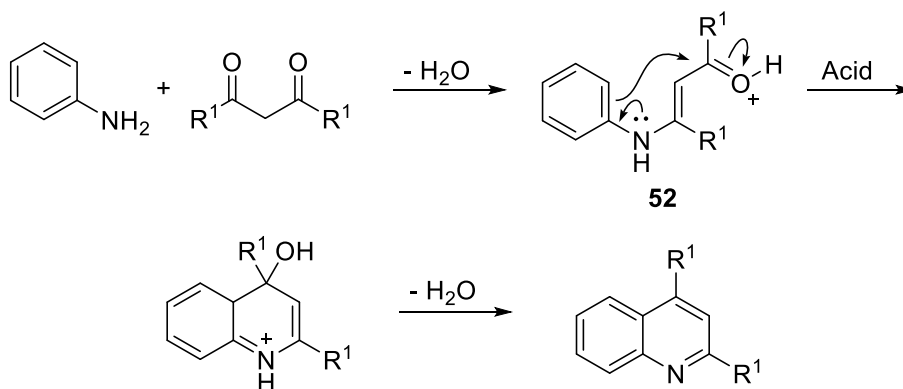
The Friedländer quinoline synthesis is an example of the latter route, proceeding through a [4+2] cyclocondensation of an *ortho*-acyl-arylamine and a ketone or aldehyde (with an α -methylene group) to give substituted quinolines (see **Scheme 16**). The choice of conditions is very important for this reaction when using unsymmetrical ketones, as the orientation of condensation is highly dependent upon the enol or enolate that is formed.



Scheme 16: Friedländer quinoline synthesis, a [4+2] cyclocondensation. Reaction conditions: i) conc. H_2SO_4 (cat.), AcOH , Δ ; ii) aq. KOH , EtOH , 0°C .⁸¹

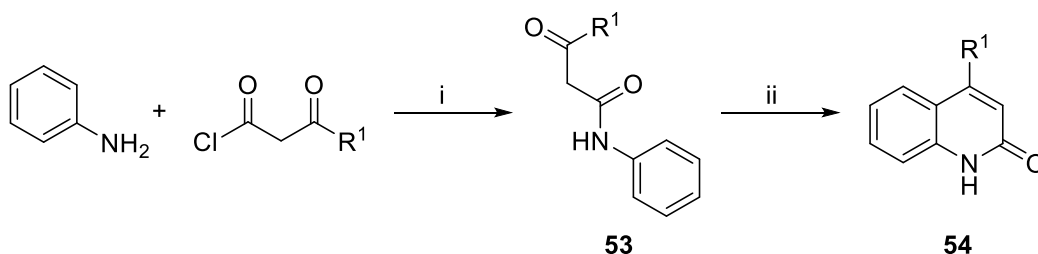
For example, in **Scheme 16** the acid-mediated reaction of an α -methyl ketone results in a 2,3,4-trisubstituted quinoline. Though the mechanism of the Friedlander has not been defined explicitly,¹⁰⁸ this reaction could either occur through an initial intermolecular aldol condensation or via a Schiff base formation. On the other hand, the base-mediated reaction affords the 2,4-disubstituted quinoline through deprotonation of the terminal α -proton of the α -methyl ketone, with subsequent aldol cyclocondensation.

Most other methods of quinoline synthesis using anilines tend to proceed through a [3+3] connective route. The Coombes quinoline synthesis adopts the traditional 1,3-dicarbonyl coupling partner to give 2,4-disubstituted quinolines (see **Scheme 17**). The reaction proceeds through initial condensation to form the β -ketoenamine (**52**), which can cyclize under acidic conditions via an EAS mechanism.



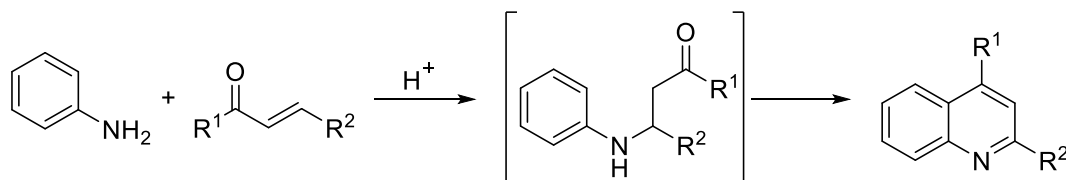
Scheme 17: Coombes quinoline synthesis, an acid-mediated [3+3] cyclocondensation of anilines and 1,3-dicarbonyl compounds.

A related method that gives 2-quinolones directly is the Knorr-carbostyryl synthesis.^{109,110} Initial formation of a β -keto acid anilide **53** can be conducted using traditional amide bond forming reaction conditions with a carboxylic acid or acid chloride.¹¹¹ Elevated temperatures or strongly acidic conditions promote EAS to afford the 2-quinolone **54** (see **Scheme 18**).⁸¹



Scheme 18: Knorr-carbostyryl synthesis of 2-quinolones under acidic conditions. Reaction conditions: i) Coupling reagents; ii) conc. H_2SO_4 .¹¹⁰

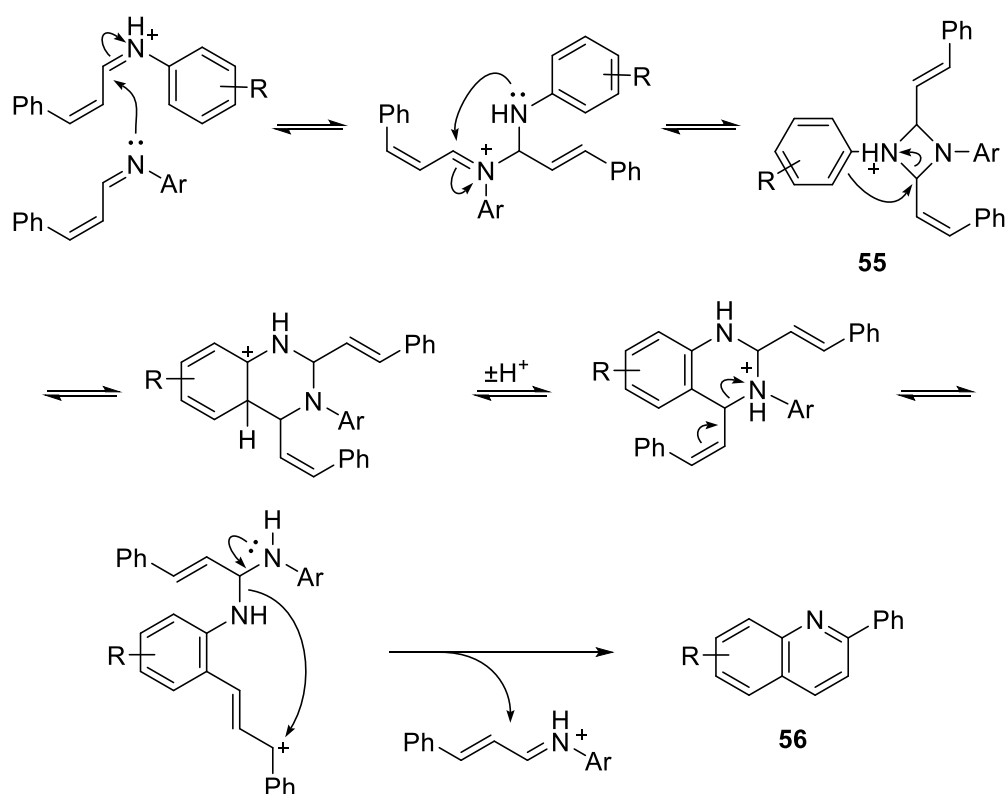
The Skraup is a classic method for the synthesis of quinolines, traditionally carried out as a “witch’s brew” combining aniline, glycerol, an acid and an oxidizing agent in one pot.^{101,112,113} This traditional method tended to suffer from poor reproducibility, and hence in modern laboratories more reliable, step-wise routes have been adopted.¹⁰¹



Scheme 19: Michael addition of α,β -unsaturated carbonyls onto aniline. Skraup reaction when $\text{R}^1 = \text{R}^2 = \text{H}$. Doebner-von Miller when $\text{R}^1 = \text{akyl}$ or aryl, $\text{R}^2 = \text{H}$, alkyl, aryl.

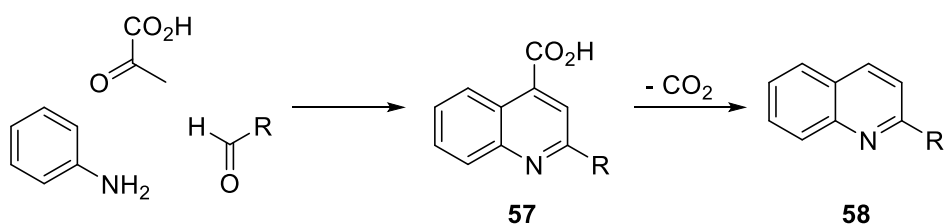
Analysis of the mechanism revealed that dehydration of glycerol occurred in the Skraup reaction to give acrolein, which undergoes conjugate addition with the aniline. Acidic cyclization and subsequent oxidation affords the aromatic product.¹¹⁴ The Skraup reaction is an ideal route to quinolines which are unsubstituted on the heteroaromatic ring (see **Scheme 19**).⁸¹

The Doebner-von Miller reaction follows a similar mechanistic course. The substitution pattern obtained from the Doebner-von Miller was used as evidence that the mechanism of the Skraup occurs by Michael addition of the aniline, rather than formation of a Schiff base (see **Scheme 19**).⁸¹ Though, mechanistic studies conducted by Eisch and Dluzniewski have suggested that Schiff base formation does indeed occur first and that rearrangement proceeds in situ through a bimolecular intermediate diazetidinium ion **55** to give 2-quinoline **56** (see **Scheme 20**).¹¹⁴



Scheme 20: Eisch and Dlugosz proposed bimolecular mechanism for the Doebner-von Miller quinoline synthesis.¹¹⁴

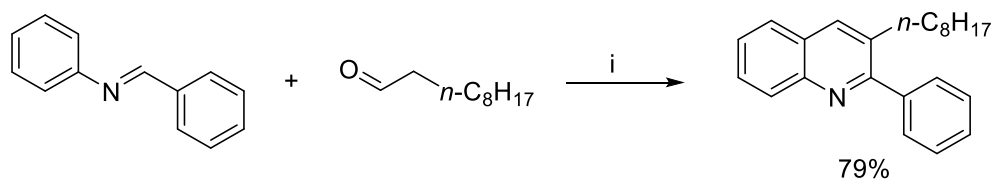
The Doebner quinoline synthesis is another slight variation on this route, adopting a multi-component reaction (MCR) to enable access to a more diverse array of potential products. Traditionally carried out using an aniline, aldehyde and pyruvic acid to give the quinoline-4-carboxylic acid **57**; decarboxylation then affords the 2-substituted quinoline **58** (see **Scheme 21**).^{115,116}



Scheme 21: Doebner multi-component quinoline synthesis via quinoline-4-carboxylic acid.

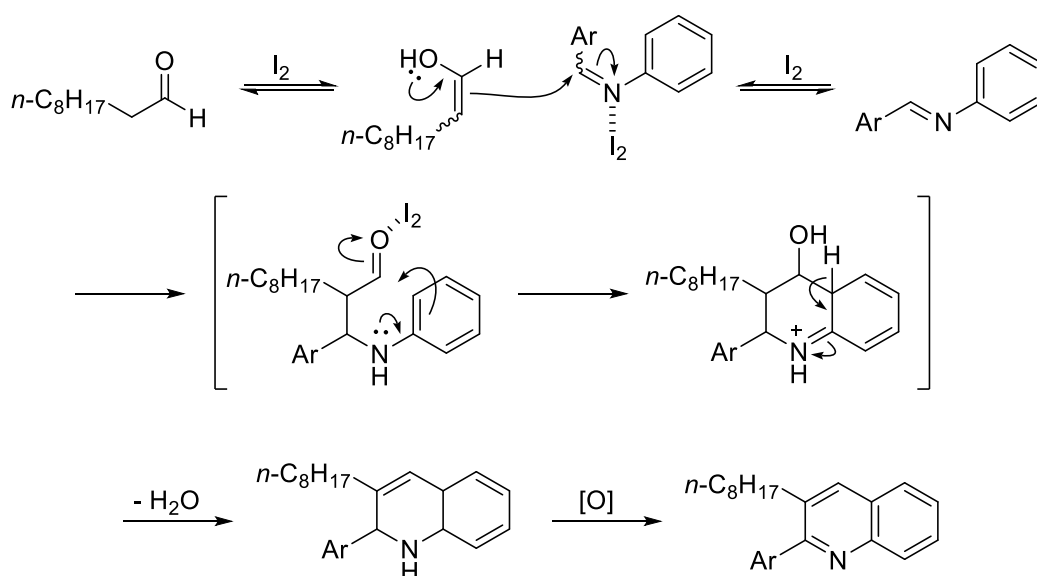
Mechanistically, the reaction could occur through initial condensation of the aniline and aldehyde or the aldehyde and pyruvic acid, depending upon which is more kinetically favoured. A common variant of the reaction is to pre-form the Schiff base intermediate before addition of the second carbonyl derivative.¹¹⁷ For instance, in 2006 Wang *et al.* reported the synthesis of

2,3-disubstituted quinolines in a mild and efficient one pot-procedure from the reaction of an aniline Schiff base with aliphatic aldehydes (see **Scheme 22**).¹¹⁸



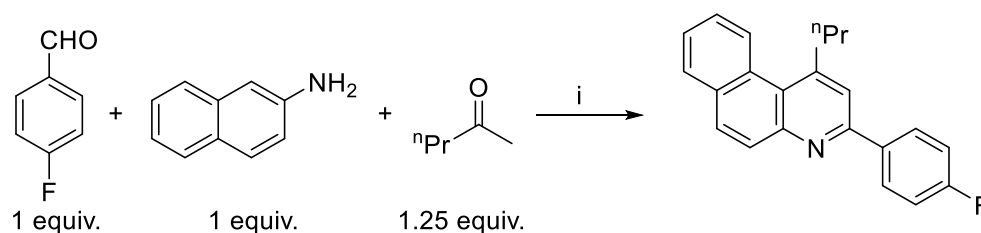
Scheme 22: Wang *et al.*'s synthesis of substituted quinolines. Reaction conditions: i) I_2 (1 mol%), benzene, Δ , 0.5 h, 79%.¹¹⁸

The group found catalytic amounts of a Lewis acid were essential for the reaction to proceed, and deemed molecular iodine as the most efficient catalyst for the reaction. They proposed the reaction to proceed through Lewis acid-mediated activation of the Schiff base and aldehyde, with a fast aldol-type addition of the enol tautomer to the Schiff base. Subsequent Friedel-Crafts cyclization onto the ring would then afford the 1,2-dihydroquinoline which oxidized in air to give the disubstituted quinoline (see **Scheme 23**).



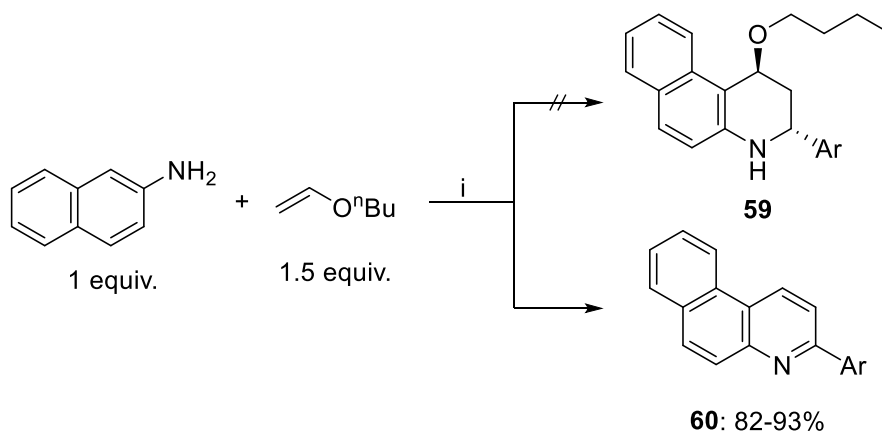
Scheme 23: Proposed mechanistic course for iodine-mediated quinoline formation, with tautomerization and activation of the reactive partners.¹¹⁸

The group of Xiang-Shan Wang *et al.* extended this method further, exploring the use of ketones in addition to aldehydes, and developed a Lewis acid-mediated MCR towards benzo[*f*]quinolines and benzo(naphtho)quinolines.^{119–122} The one-pot process reacted naphthalene-2-amines and aromatic aldehydes to give the Schiff base, which combined with an enolizable ketone as a two-carbon unit (see **Scheme 24**).



Scheme 24: Wang *et al.*'s MCR for the synthesis of naphthoquinolines. Reaction conditions: i) I_2 (5 mol%), THF, Δ , 89%.¹²⁰

A number of different variations on the original scaffold were explored, with cyclic ketones used to synthesize benzo[*f*]cyclopenta[*c*]quinoline and benzo[*f*]cyclododeca[*c*]-quinoline derivatives, of interest for their biological and pharmaceutical properties.¹²¹ However, when exploring the utility of vinyl ethers, rather than generating the expected 1-butoxy-1,2,3,4-tetrahydro-3-arylquinoline derivative **59** using *n*-butyl vinyl ether (*n*-BVE), it was found that re-aromatization and elimination of butanol occurred to give the 3-substituted arylbenzo[*f*]quinoline **60** (see **Scheme 25**).¹²³ This method offers a mild, efficient and regioselective route towards fused α -substituted quinolines.



Scheme 25: Wang *et al.*'s synthesis of 2-substituted benzo[*f*]quinolines (**50**). Reaction conditions: i) ArCHO (1 equiv.), I_1 (10 mol%), THF, Δ , 8-12 h.¹²³

1.6.2.3.2. Reactions of quinolines.

Quinolines have a very similar reactivity to pyridines, with primary reaction of electrophiles occurring at the nitrogen lone pair, reducing reactivity towards EAS. For this reason, electrophilic attack tends to occur on the carbocyclic ring (see **Figure 25**).

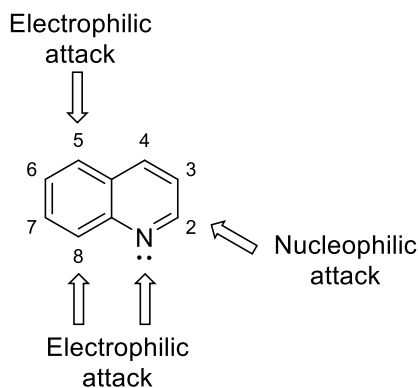
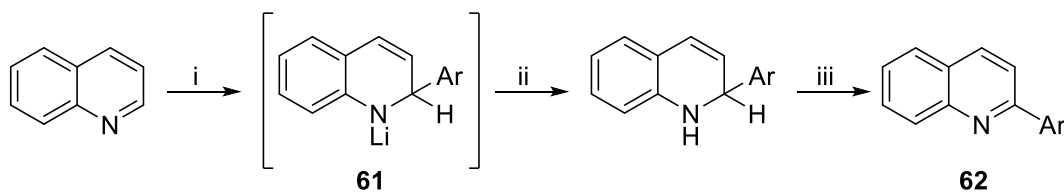


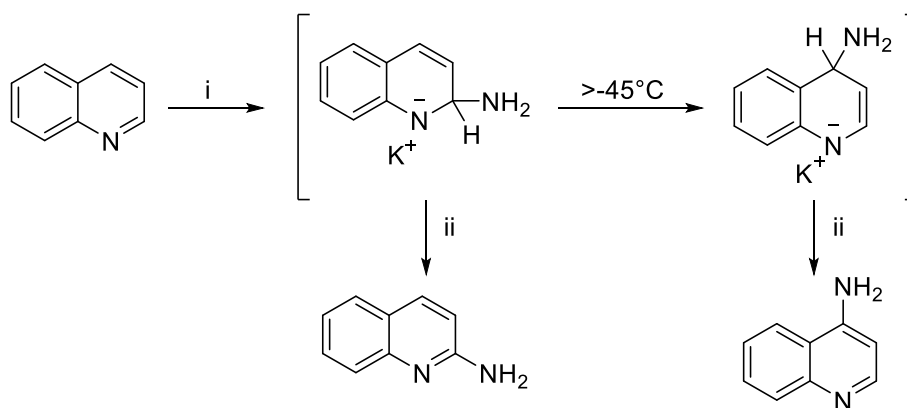
Figure 25: Major points of reactivity for quinoline rings.

Nucleophilic attack tends to occur at the 2-position of quinolines, with analogous reactivity to pyridines. For instance, alkylation using aryl or alkyl lithium reagents gives the 1,2-dihydroquinoline *N*-lithio salt (**61**), which on oxidation gives the corresponding 2-alkyl- or 2-arylquinoline derivative (**62**) (see **Scheme 26**).⁸¹



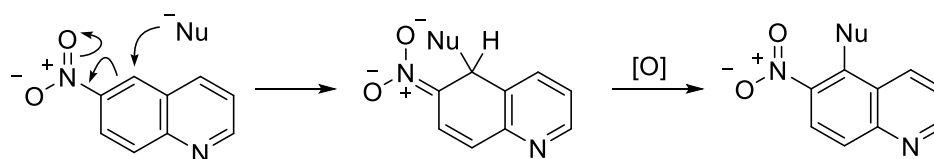
Scheme 26: Synthesis of 2-arylquinolines (**62**) using an aryllithium reagent. Reaction conditions: i) ArLi ; ii) H_2O ; iii) PhNO_2 .⁸¹

Similarly, Chichibabin amination occurs with quinolines using potassium or sodium amide. At temperatures higher than $-45\text{ }^\circ\text{C}$ rearrangement of the 2-amine adduct to the more stable 4-amine will occur. Either adduct can be isolated through oxidative trapping (see **Scheme 27**).^{81,124}



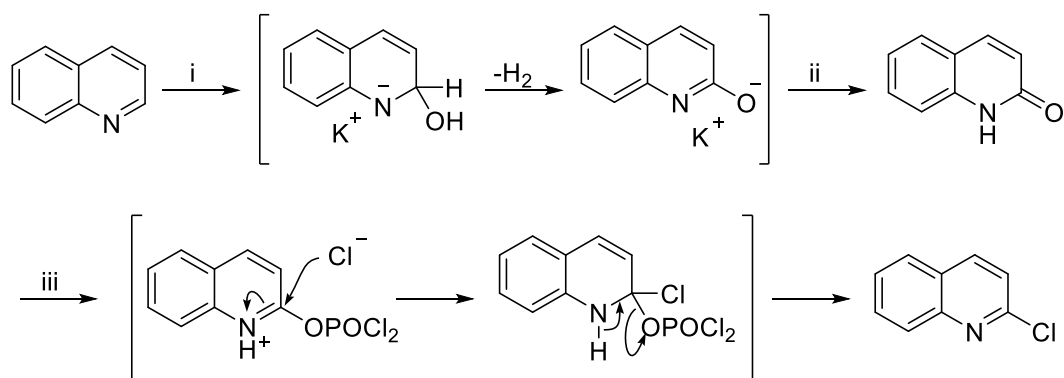
Scheme 27: Chichibabin amination of quinolines. Reaction conditions: i) KNH_2 , NH_3 (liq.), -66°C ; ii) KMnO_4 .¹²⁴

Oxidative amination can be promoted at other positions on the fused ring system if a nitro group is present to promote a vicarious nucleophilic substitution.^{125–127} The electron-withdrawing nitro group enhances electrophilicity of the *ortho*-positions, analogous to the electron-withdrawing action of a pyridine *N*-oxide or quinoline *N*-oxide (see **Scheme 28**). Oxidation to the quinoline can be mediated by the nitroquinoline or air.¹²⁸



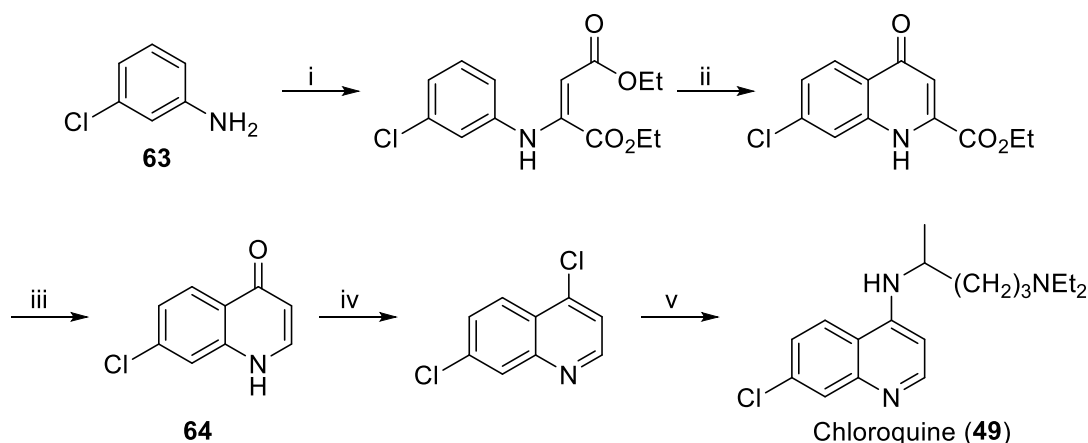
Scheme 28: Vicarious nucleophilic substitution mediated by nitro-substituents on quinoline.

Hydroxylation of quinoline to give the 2-quinolone or ‘carbostyryl’ can be conducted by heating to high temperatures in the presence of KOH (see **Scheme 29**). Quinolones exhibit similar reactivity to pyridones, and so can be converted to the chloroquinoline on treatment with POCl_3 or phosphorous pentachloride (PCl_5). Chlorinated quinolines can be used to direct nucleophilic substitution, with displacement of the halide as a good leaving group, or to facilitate metal-mediated coupling reactions.



Scheme 29: Hydroxylation of quinoline to 2-quinolone and subsequent chlorination. Reaction conditions: i) KOH, NaOH, 240 °C; ii) H₂O; iii) POCl₃, heat.⁸¹

For instance, in the synthesis of chloroquine (**49**), designed by Surrey and Hammer in 1946, chlorination of a quinolone was essential to install a directing group for nucleophilic substitution. Condensation of diethyl oxalpropionate and 3-chloroaniline (**63**) was used to construct the quinoline framework, with cyclization to the 4-quinolone at elevated temperatures.¹²⁹ Base-mediated saponification and subsequent decarboxylation gave the 7-substituted-4-quinolone **64**, which was chlorinated using POCl₃. The chlorine was then used as a leaving group for S_NAr using a primary amine to give chloroquine (**49**) (see **Scheme 30**).



Scheme 30: Synthesis of chloroquine (**49**). Reaction conditions: i) Diethyl oxalpropionate, AcOH, 40 °C; ii) 250 °C; iii) aq. KOH, EtOH, then 270 °C; iv) POCl₃, Δ; v) H₂NCH(Me)(CH₂)₃NEt₃, 180 °C.^{81,129}

Anderson *et al.* adopted the quinoline motif in their design of PF-3644022 (**25**) in order to take advantage of the structural rigidity of the aromatic ring system, as well as the nitrogen lone pair as a HBA for hinge binding in the ATP-pocket of MK2.⁶⁸

1.6.2.4. Benzo[*b*]thiophenes.

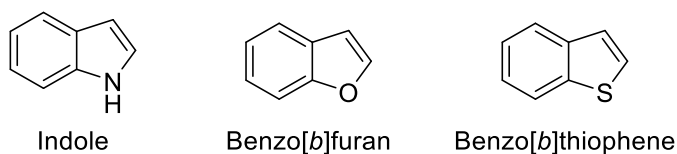


Figure 26: Benzo[*b*]fused heterocyclic aromatic rings.

Benzo[*b*]thiophenes are naturally-occurring heterocycles that can be isolated from petroleum deposits and as complex glycoside derivatives from the roots of the Chinese *Echinops grijissi* plant.^{2,130} They are sulfur analogues of the nitrogen containing indole and oxygen containing benzo[*b*]furan (see **Figure 26**). They possess interesting π -delocalization properties due to the larger bonding radius of sulfur compared to the Group 2 heteroatoms nitrogen and oxygen, and the intermediate electronegativity of sulfur compared to those two heteroatoms. Due to these properties, benzo[*b*]thiophenes have been explored extensively in the development of organic semi-conductors.^{131–133}

Benzo[*b*]thiophenes have found widespread application as privileged structures and building blocks in drug discovery. The fused ring system has been shown to exhibit a range of biological activities including anti-fungal, anti-bacterial and anti-inflammatory effects.¹³⁴ Additionally, incorporation of the benzo[*b*]thiophene scaffold has been demonstrated by Romagnoli *et al.* to improve the pharmacokinetics (PK) of tubulin polymerization inhibitors, and to enhance solubility and activity compared to hydrocarbon analogues.¹³⁵

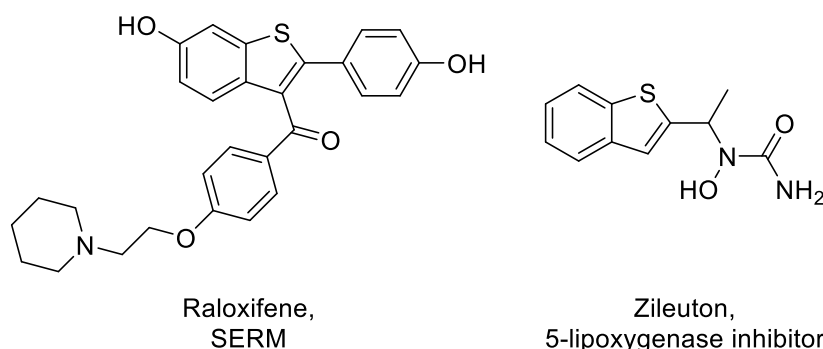


Figure 27: Examples of benzo[*b*]thiophenes in clinical agents. Raloxifene, and Zileuton.^{137,139}

Benzo[*b*]thiophenes can be found in a number of clinical agents including Raloxifene, a selective estrogen receptor modulator (SERM) used in the treatment and prevention of breast cancer and osteoporosis;^{136,137} and Zileuton, a 5-lipoxygenase inhibitor used in the prevention and

treatment of chronic asthma by modulating production of leukotrienes, which can trigger contractions of the smooth muscle lining of the bronchioles (see **Figure 27**).^{138,139}

In the design of novel kinase inhibitors, in addition to the benzo[*b*]thiophene scaffold present in MK2 inhibitor PF3644022 (**25**), benzo[*b*]thiophenes have also been explored as inhibitors for LIM kinases and PIM kinases.

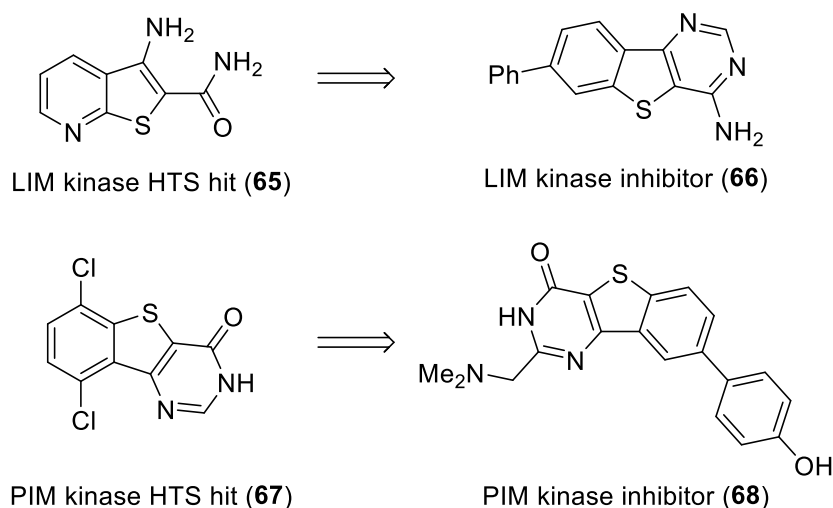


Figure 28: LIM kinase and PIM kinase benzo[*b*]thiophene-based scaffolds, from initial HTS hit to optimized kinase inhibitor.^{140,141}

LIM kinases mediate regulation of the actin-cytoskeleton and have been postulated to play a role in determining the metastatic potential of tumour cells. Baell *et al.* used HTS to identify 3-aminothieno[2,3-*b*]pyridine-2-carboxamide (**65**) as a potent inhibitor of LIMK1, and were able to develop the tricyclic LIMK-1 inhibitor **66** via an SAR-based lead investigation.¹⁴⁰

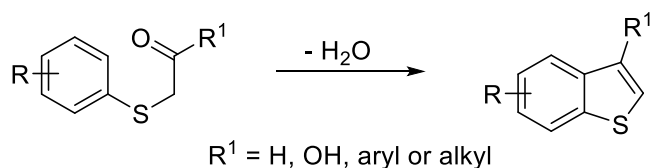
The PIM kinase family (Pim-1, Pim-2 and Pim-3) have been found to be overexpressed in a variety of malignancies and lymphomas, inferring a role for these kinases in tumorigenesis. Tao *et al.* proposed that simultaneous targeting of all PIM kinases may offer an alternative, superior cancer therapy.¹⁴¹ Benzo[*b*]thiophene based scaffold **67** was identified as a potential inhibitor through HTS, and lead optimization generated biaryl phenol **68** which exhibited a low nanomolar potency for all PIM kinases, a high bioavailability and excellent kinase selectivity (see **Figure 28**).¹⁴¹

There is a continued interest in the development of novel strategies towards the synthesis of benzo[*b*]thiophenes and their functionalized derivatives.^{2,142} The reactivity of benzo[*b*]thiophenes is somewhat reduced in comparison with many other heteroaromatic

scaffolds, and so functionality tends to be installed during cyclization of the fused heteroaromatic ring.

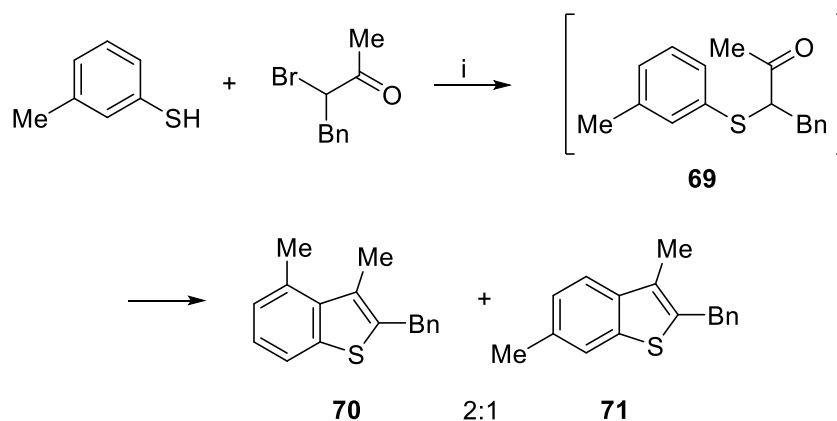
1.6.2.4.1. Synthesis of benzo[*b*]thiophenes.

More traditional methods of synthesis follow routes very similar to those adopted for pyridine and quinoline synthesis, for instance, via intramolecular cyclocondensation of a 2-arylthioaldehyde, ketone or acid onto a benzene ring (see **Scheme 31**).



Scheme 31: General reaction scheme for synthesis of benzo[*b*]thiophenes from 2-arylthioaldehydes, ketones, or acids.⁸¹

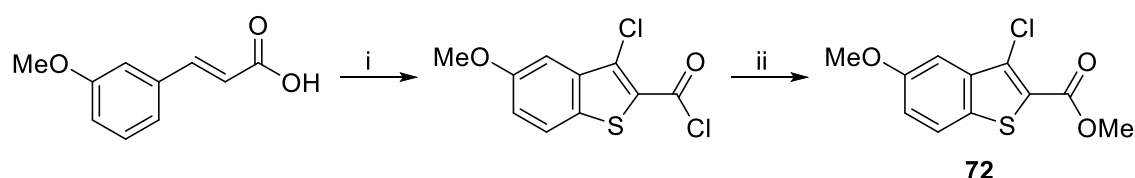
This method does not always control regioselectivity in the synthesis of benzo-substituted benzo[*b*]thiophenes. For instance, the acid mediated reaction of 2-arylthio ketone **69** resulted in a 2:1 ratio of the 2,3,4- and 2,3,6-trisubstituted benzo[*b*]thiophenes **70** and **71**, respectively (see **Scheme 32**). Aoyama *et al.* carried out this reaction using solid-supported reagents to facilitate a one-pot base/acid-mediated reaction.¹⁴³ With almost complete conversion to the benzo[*b*]thiophene products, this method offered an alternative to stepwise formation and isolation of reaction intermediates.



Scheme 32: Solid-supported reagent-mediated benzo[*b*]thiophene formation from 3-methylthiophenol. Reaction conditions: i) $\text{Na}_2\text{CO}_3\text{-SiO}_2$, PPA-SiO_2 , PhCl , 135°C , 6 h, 95%.¹⁴³

In order to circumvent regioselectivity problems, the strategic use of substituents can help direct cyclization on to the ring. For instance, Higa and Krubsack developed a regioselective route

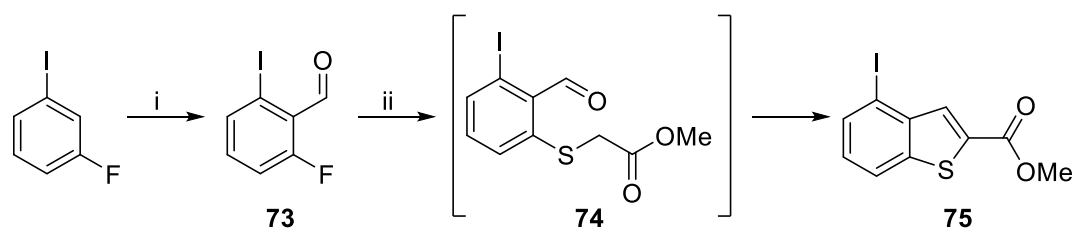
towards 5-functionalized benzo[*b*]thiophenes via “electrocyclization” of *meta*-substituted cinnamic acids using thionyl chloride (SOCl₂) and base.¹⁴⁴ Using a *meta*-electron-donating group (EDG), Higa and Krubsack found that cyclization was directed to the *para*-position, to afford the 3-chloro-5-substituted benzo[*b*]thiophene-2-acid chloride (see **Scheme 33**), whereas a *meta*-directing electron-withdrawing group (EWG), such as a nitro group, was found to deactivate the ring and give a mixture of cyclization products.



Scheme 33: Higa and Krubsack's benzo[*b*]thiophene formation from *meta*-substituted cinnamic acids, adopted by Anderson *et al.* Reaction conditions: i) SOCl₂, pyridine, 140 °C;¹⁴⁴ ii) MeOH.⁶⁷

This method of benzo[*b*]thiophene formation was adopted by Anderson *et al.* at Pfizer for the synthesis of their initial benzo[*b*]thiophene MK2 inhibitor hit compound **24** (see **Figure 16**). Key intermediate **72** was synthesized from 3-methoxycinnamic acid and SOCl₂ and then esterified to give methyl carboxylate **72** (see **Scheme 33**).⁶⁷

In order to circumvent regioselectivity problems, alternative methods have been explored. One such method is the base-mediated intramolecular aldol condensation of *ortho*-arythioacetic acids or esters (see **Scheme 34**).¹⁴⁵ Synthesis of the cyclization precursor **74** can be conducted by thioglycolate displacement of a halogen or nitro group *ortho* to a carbonyl moiety. Fluoro and nitro groups exhibit a faster rate of reaction, usually augmented by the electron-withdrawing α -carbonyl group.^{146,147}

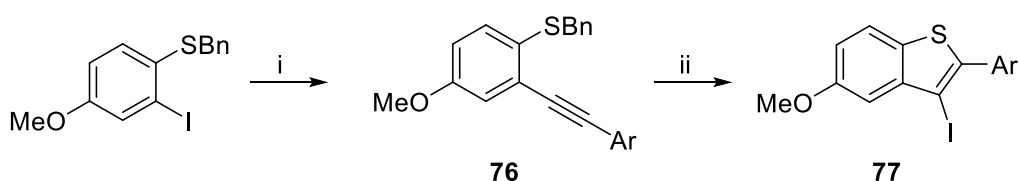


Scheme 34: Lee *et al.*'s methyl 4-iodobenzo[*b*]thiophene-2-carboxylate synthesis. Reaction conditions: i) LDA, THF, -78 °C then DMF, 60-95%; ii) Methyl thioglycolate, K₂CO₃, DMF, 65-95%.¹⁴⁵

For example, Lee *et al.* synthesized dihalogenated benzaldehyde cyclization precursor **73** by *ortho*-deprotonation using lithium diisopropylamide (LDA), followed by treatment with dimethylformamide (DMF). The fluoride was then preferential displaced under base-mediated

reaction conditions with methyl thioglycolate to afford **75** after intramolecular aldol condensation of **74** (see **Scheme 34**).¹⁴⁵

For 3-halo-2-substituted benzo[*b*]thiophene synthesis, only a limited number of routes are available. The 5-*endo-dig* halocyclization of *ortho*-alkynyl thioethers is a regioselective and efficient route, though it suffers the disadvantage of necessitating installation of the alkyne moiety, usually by a metal-mediated method.^{131,148–150} Intramolecular attack by sulfur onto the alkyne can be promoted by halogen-containing electrophiles, such as iodine, bromine or *N*-bromosuccinimide (NBS), to give the desired 3-halogenated benzo[*b*]thiophene (see **Scheme 35**).



Scheme 35: Flynn *et al.*'s halocyclization to give 2,3-disubstituted benzo[*b*]thiophenes. Reaction conditions: i) Phenylacetylene, 2 *n*-BuLi, THF, then ZnCl₂, Pd(PPh₃)₂Cl₂, 95%; ii) I₂, CH₂Cl₂, 98%. Ar = *para*-methoxyphenol.¹⁴⁹

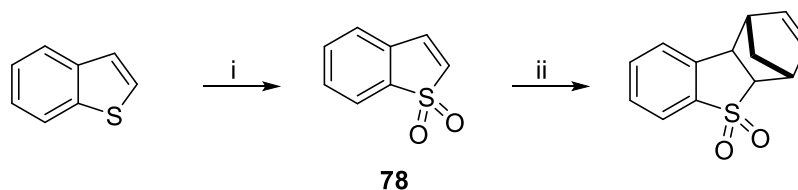
Flynn *et al.* adopted this halocyclization route using molecular iodine as the electrophile to synthesize a library of 3-iodo-2-arylbenzo[*b*]thiophenes (**77**) in the development of novel tubulin binding agents (see **Scheme 35**).¹⁴⁹ The group synthesized their alkyne precursors (**76**) via palladium-mediated coupling of the relevant phenylacetylene-zinc adduct and aryl iodide, with subsequent cyclization affording the corresponding benzo[*b*]thiophene in high yield.

1.6.2.4.2. Reactions of benzo[*b*]thiophenes.

The regioselectivity of reaction of benzo[*b*]thiophenes with electrophiles is not as explicit as for many other heteroaromatic and fused systems. Reaction still generally occurs on the more electron-dense heteroaromatic ring, but depending upon the substituents, the C2 and C3 positions can exhibit almost the same reactivity.^{2,81,151–153}

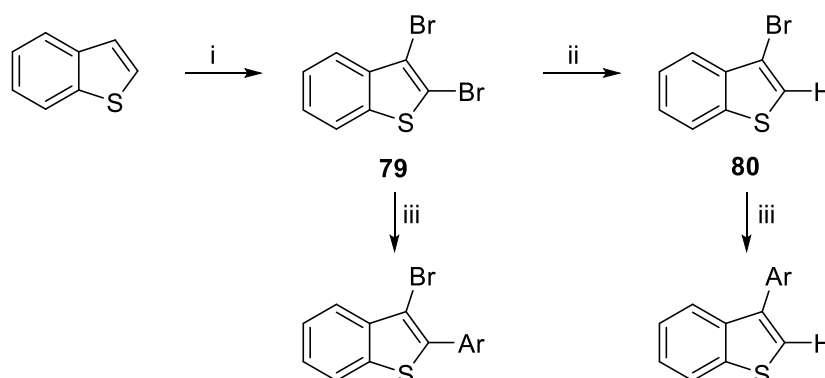
It has been calculated by Martinez *et al.* using density functional theory (DFT) that the most reactive sites on a benzo[*b*]thiophene ring towards electrophilic attack should theoretically be sulfur and carbon-3, though the products of attack on sulfur are rarely seen due to their instability.¹⁵⁴ These studies complement general experimental evidence of reactivity.^{155–157} However it is important to note that Martinez *et al.*'s calculations were conducted on an unsubstituted model.

Sulfur in benzo[*b*]thiophene is very nucleophilic, and its lone pair will readily react with electrophilic alkylating agents in solution to form benzothiophenium salts.⁸¹ Additionally, oxidation of the sulfur centre can be effected to give the 1,1-dioxide **78**, which can act as a dienophile, for example, with cyclopentadiene as illustrated in **Scheme 36**.¹⁵⁸



Scheme 36: 1,1-Dioxide formation and cycloaddition with cyclopentadiene. Reaction conditions: i) H₂O₂, AcOH, 95 °C, 76%; ii) cyclopentadiene, xylene, 180 °C, 56%.^{81,158}

For reactions on carbon, bromination of unsubstituted benzo[*b*]thiophenes will preferentially occur at the 3-position under controlled conditions, though the yields are moderate. Therefore it can be more efficient to synthesize the 2,3-dibromobenzo[*b*]thiophene (**79**) followed by regioselective bromine-metal exchange and hydrolysis at the 2-position in order to access 3-bromothiophene (**80**) (see **Scheme 37**).^{81,159} This method was adopted by Heynderickx *et al.* for the synthesis of 2- and 3-arylbenzo[*b*]thiophenes via Suzuki-Miyaura cross-coupling.¹⁵⁹ The group found that 2,3-dibromobenzo[*b*]thiophene preferentially coupled at the 2-position under Suzuki conditions. Therefore to selectively couple at the 3-position the group removed the 2-bromo substituent before coupling.

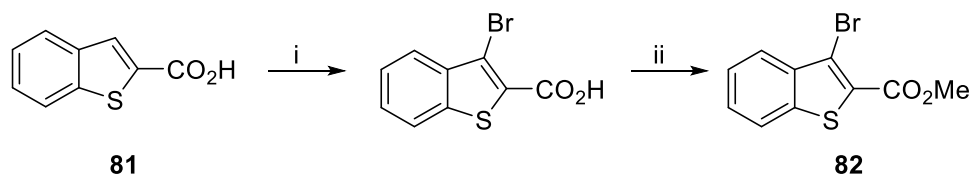


Scheme 37: Heynderickx *et al.* selective bromination route for directed Suzuki-Miyaura coupling. Reaction conditions: i) Br₂, CHCl₃, RT, 18 h, 93%. ii) BuLi, Et₂O, −78 °C, 20 min, then −20 °C for 1 h, then aq. NH₄Cl; iii) ArB(OH)₂, Pd(PPh₃)₄, aq. Na₂CO₃, DME-EtOH, Δ, 63-95%.¹⁵⁹

For 2-substituted benzo[*b*]thiophenes, the heteroaryl ring can be activated towards EAS at the 3-position. For example, Martin-Smith and Reid conducted a number of bromination studies on benzo[*b*]thiophenes in the 1950s and found that benzo[*b*]thiophene-2-carboxylic acids were

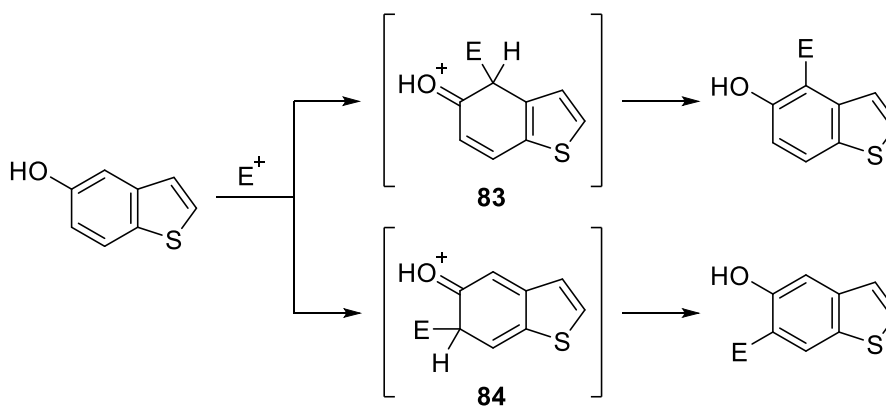
deactivated towards electrophilic attack at the 3-position, but that reactivity was reinstated upon formation of the conjugate base.¹⁵²

This method was adapted by Mbere *et al.* in their synthesis of prospective anti-bacterial agents based upon benzo[*b*]thiophene-2-carboxamides.¹⁶⁰ Regioselective bromination of benzo[*b*]thiophene-2-carboxylic acid **81** at the 3-position was facilitated by in situ conjugate base formation and reaction with molecular bromine, with subsequent esterification affording the methyl ester **82** (see **Scheme 38**).



Scheme 38: Mbere *et al.*'s benzo[*b*]thiophene bromination. Reaction conditions: i) AcOH , NaOAc , then Br_2 , 55°C , 49%; ii) MeOH , H_2SO_4 , 97%.¹⁶⁰

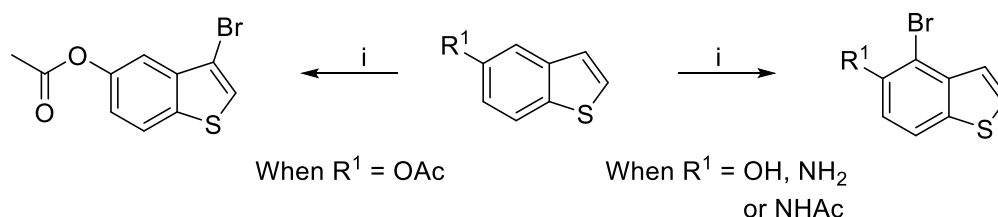
With regards to reactions involving the carbocyclic ring of a benzo[*b*]thiophenes, it is generally necessary to install an activating group onto the benzene ring to direct the attack. Bordwell and Stange conducted a number of studies in 1955 into the relative reactivity of differently 5-substituted benzo[*b*]thiophenes towards nitration and bromination.¹⁶¹ They proposed that EAS would preferentially occur at the 4-position, as the transition state to prepare this intermediate (**83**) maintained stabilizing aromaticity in the thieno ring. The transition state from EAS at the 6-position would provide a less stabilized conjugated triene intermediate (**84**) (see **Scheme 39**).



Scheme 39: Bordwell and Stange's explanation of EAS at the 4- and 6-positions of a 5-hydroxybenzothiophene.¹⁶¹

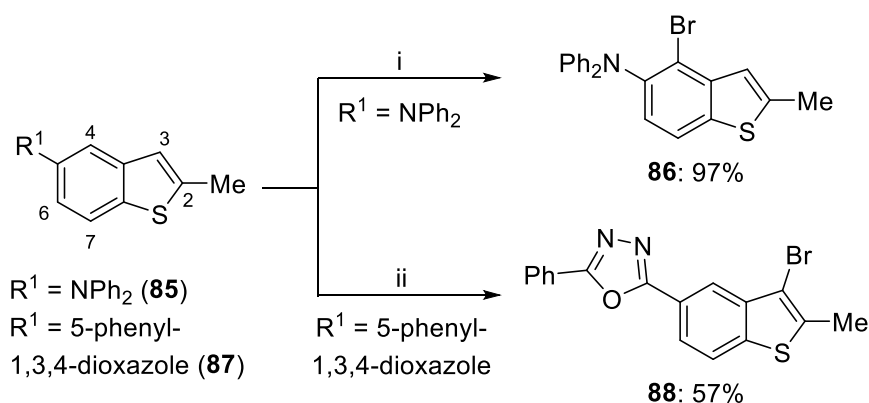
Using 5-hydroxy, 5-acetoxy, 5-acetamido and 5-aminobenzo[*b*]thiophenes, Bordwell and Stange found that mononitration predominantly afforded the 4-nitro product. Under bromination conditions, 5-hydroxy, 5-acetamido and 5-aminobenzo[*b*]thiophene gave the 4-bromides,

whereas 5-acetoxybenzo[*b*]thiophene afforded 5-acetoxy-3-bromobenzo[*b*]thiophene (see **Scheme 40**). Hence, Bordwell and Stange concluded that the acetoxy group was not strongly activating enough to promote bromination on the benzene ring over the heteroaryl ring.¹⁶¹



Scheme 40: Bromination experiments completed by Bordwell and Stange. Reaction conditions: i) Br_2 , AcOH , H_2O , 100°C .¹⁶¹

These studies have been supported more recently through DFT studies completed by Wu *et al.* to investigate what appeared to be an “abnormal” bromination reaction of 5-diarylamino-2-methylbenzo[*b*]thiophene (**85**). The group had expected the reaction to afford the 3-bromo-5-diarylamino-2-methylbenzo[*b*]thiophene, but found the reaction gave the 4-bromo analogue **86** with very high regiocontrol (see **Scheme 41**).



Scheme 41: Wu *et al.*'s "abnormal" bromination pattern. Reaction conditions: i) NBS , CH_2Cl_2 , -15°C to -20°C ; ii) Br_2 , Fe , CHCl_3 , Δ .³⁷⁴

The group conducted a number of DFT calculations and generated an electrostatic potential map of **85**. This map inferred a significantly higher concentration of electron-density at the 4-position compared to the 3-position of the aromatic ring due to activation by the electron-donating diarylamine. In order to verify their theory, bromination was induced at the 3-position through installation of an EWG at the 5-position. Indeed, it was found that when 5-oxadiazole analogue **87** was brominated under similar conditions, only the 3-bromobenzo[*b*]thiophene **88** was produced.

These studies confirmed that, even though the carbocyclic ring of benzo[*b*]thiophenes might be considered to have a lower overall charge density, it can be activated towards EAS through the use of strategic functionalization. The required activating or deactivating substituents can usually be installed during initial heterocyclization and so careful consideration of the sequence of reaction steps must be considered in approaches towards any complex benzo[*b*]thiophene-based scaffold.

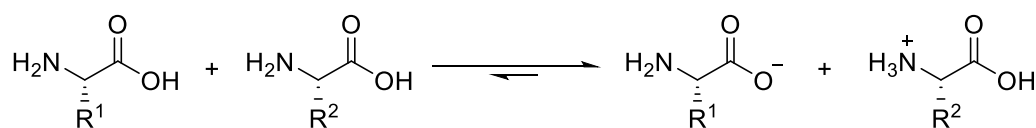
1.6.3. Strategic bond forming reactions.

In addition to heterocycle forming reactions and general oxidation, reduction and functional group interconversions, there are a number of key carbon-carbon and carbon-heteroatom bond forming reactions which have been adopted throughout the course of this project to facilitate the synthesis and connection of core scaffold molecules. These include amide bond formation, and metal-mediated Suzuki-Miyaura cross-coupling, the Mizoroki-Heck reaction and Buchwald-Hartwig *N*-arylation. Each of these reactions will now be discussed in turn for their relevance and applicability as tools in organic synthesis.

1.6.3.1. Amide bond forming reactions.

The amide bond is an essential building block for life, linking the framework of all peptides and proteins in the human body. Protein synthesis occurs in the human body through the condensation reaction of α -amino acids and peptides. The reaction is mediated by numerous macromolecules in order to translate predetermined sequences of amino acids from genes in DNA to the new peptide on a single molecule scale.¹⁶²

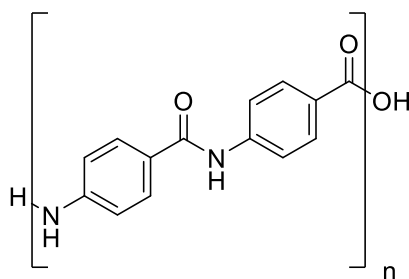
The condensation reaction of amines and carboxylic acids to form amide bonds is thermodynamically disfavoured, with formation of the carboxylate salt being much more energetically favourable in solution (see **Scheme 42**). Hence, the body employs enzymes to mediate formation of a more reactive amino ester from one of the α -amino acid coupling partners. This will then condense with the *N*-terminus of another α -amino acid in a much less energetically demanding macromolecule-mediated process.¹⁶²



Scheme 42: Thermodynamically favoured salt formation from the combination of two α -amino acids.

Amide bonds are ubiquitous in medicinal chemistry, present in approximately two thirds of drug candidates (as of 2006),¹⁶³ and a quarter of all pharmaceuticals on the market.^{164,165} Therefore it is unsurprising that, in a survey conducted by Roughley and Jordan in 2008, amide bond forming reactions constituted at least 70% of acylation reactions in medicinal chemistry.⁹⁷ Polymers

based upon the strong amide bond have also found extensive use in synthetics such as nylons and Kevlar, as adhesives in wound healing, and as drug delivery systems.^{166,167}



Kevlar

Figure 29: Kevlar, a synthetic polymer with high strength.

1.6.3.1.1. Coupling reagents.

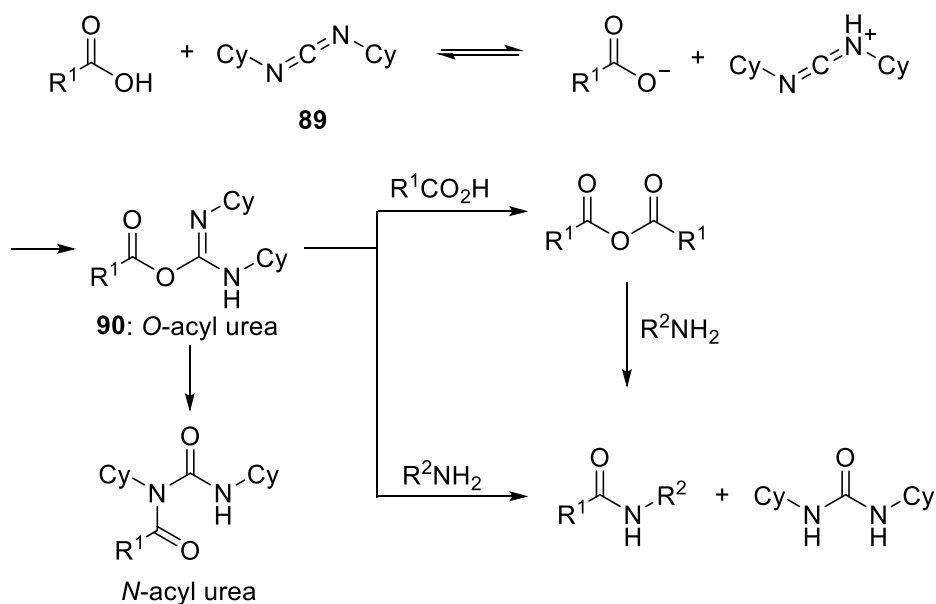
Medicinal chemists have faced many challenges regarding amide bond forming reactions for the synthesis of polypeptide chains and small molecules. Although the condensation reaction of a carboxylic acid and an amine can be conducted directly, very high temperatures are required and that could denature other functionalities in the molecule. In order to facilitate milder reaction conditions and overcome the substantial energy barriers, a plethora of technologies and methods have been designed.^{162,164,168,169}

‘Coupling reagents’ are widely used as stand-alone reagents to activate carboxylic acids, transforming them into mixed anhydrides, active esters or carbonic anhydrides. This activation lowers the energetic barrier towards subsequent nucleophilic substitution. Coupling reagents can be used for general small molecule synthesis and in parallel, peptide and library synthesis.

The choice of coupling reagent is very important and is dependent upon the reaction substrates. For instance, in a library-based synthesis, the coupling reagent must enable the reaction to run under mild enough conditions to limit side-reactions and racemization, but activating enough for a wide range of amines.¹⁶⁹ Additionally, for peptide coupling of α -amino acids, maintaining absolute stereochemistry of the peptide chain is paramount, and the choice of coupling reagent is vital when trying to reduce epimerization of asymmetric carbons.

Carbodiimides were the first broadly-used coupling reagents, with the use of *N,N'*-dicyclohexylcarbodiimide (DCC, **89**) pioneered by Sheehan and Hess in 1955. An improvement over the moisture-sensitive mixed anhydride methods of the time, the reaction could be carried

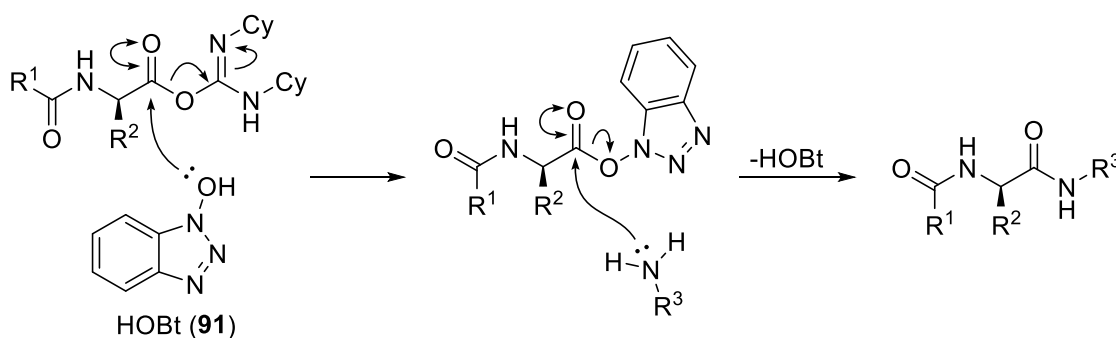
out in aqueous solvents, and the insoluble urea condensation side product could be removed relatively easily.¹⁷⁰



Scheme 43: O-Terminal activation of a carboxylic acid using DCC (**89**) and subsequent coupling with a primary amine to give an amide, with potential side and by-products.¹⁶⁹

Unfortunately, epimerization of the activated *O*-acyl urea (**90**) was a prevalent issue associated with this method, and prominent side products included the *N*-acyl urea derivative and the carboxylic acid anhydride (see **Scheme 43**). However, thereafter the anhydride could undergo further reaction with the amine to afford the required amide product.

In an effort to reduce epimerization and increase reactivity, in 1970 König and Geiger introduced additives to the amide coupling reaction mixture.¹⁷¹ Addition of 1-hydroxyl-1*H*-benzotriazole (HOBT, **91**) and a non-nucleophilic base such as diisopropylethylamine (DIEA) to a DCC activated α -amino acid coupling was found to react in situ with the *O*-acyl urea to form a more activated ester (see **Scheme 44**). This in situ transformation resulted in improved yields and reduced levels of epimerization compared to the same reaction carried out with just DCC. It was believed that, in addition to improving the electrophilicity of the ester, the benzotriazole ring stabilized the approach of the nucleophilic amine in solution through hydrogen bonding.¹⁶⁹



Scheme 44: HOBt (**91**) as an additive in peptide coupling α -amino acids with DCC, forming a more activated ester for attack by an external amine.

Since these first innovations, various alternative carbodiimides and benzotriazole reagents have been designed to improve reaction efficiency. For example, the urea side products formed from reactions with diisopropylcarbodiimide (DIC) and DCC can be difficult to remove, and so more soluble unsymmetrical and cationic carbodiimides were designed (see **Figure 30**), including phenyl isopropyl carbodiimide (PIC) and 1-ethyl-3-(3-dimethyl aminopropyl)carbodiimide (EDC or EDCI), and the hydrochloride salts of these compounds.¹⁶⁹

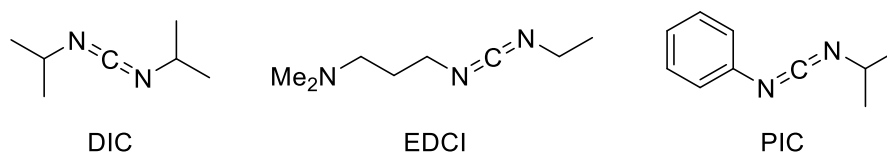
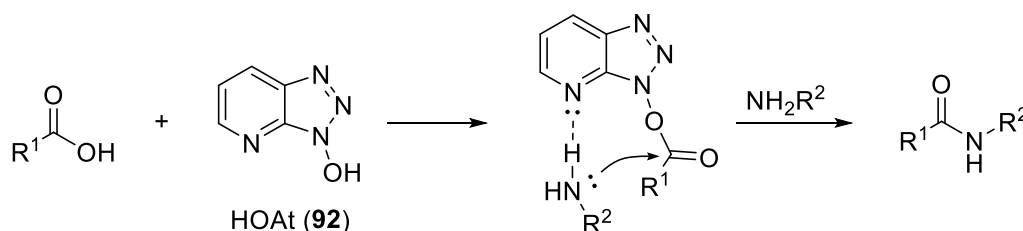


Figure 30: Examples of carbodiimide reagents: diisopropylcarbodiimide (DIC), phenyl isopropyl carbodiimide (PIC) and 1-ethyl-3-(3-dimethylaminopropyl)carbodiimide (EDCI)

Hydroxy-7-azabenzotriazole (HOAt, **92**) was designed as an alternative to HOBt, and has been largely found to be a more efficient coupling reagent. This is believed to be due to additional chelation of the approaching amine with the pyridinyl ring (see **Scheme 45**).¹⁷²



Scheme 45: HOAt (**92**), a coupling reagent with enhanced chelation of the pyridinyl ring with the nucleophilic amine.

In the development of more economical coupling reactions, a number of onium salts based upon the 1*H*-benzotriazole units HOBt and HOAt have been developed which are able to mediate amide bond formation without the need for an additional carbodiimide reagent. **Figure 31** illustrates some examples, with HATU (**93**), the most commonly used onium coupling reagent,¹⁷³ and the phosphonium salts AOP and BOP, based upon HOAt and HOBt respectively, which are used less often nowadays due to toxic side products.

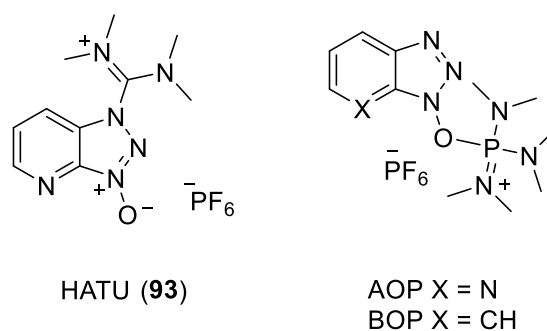
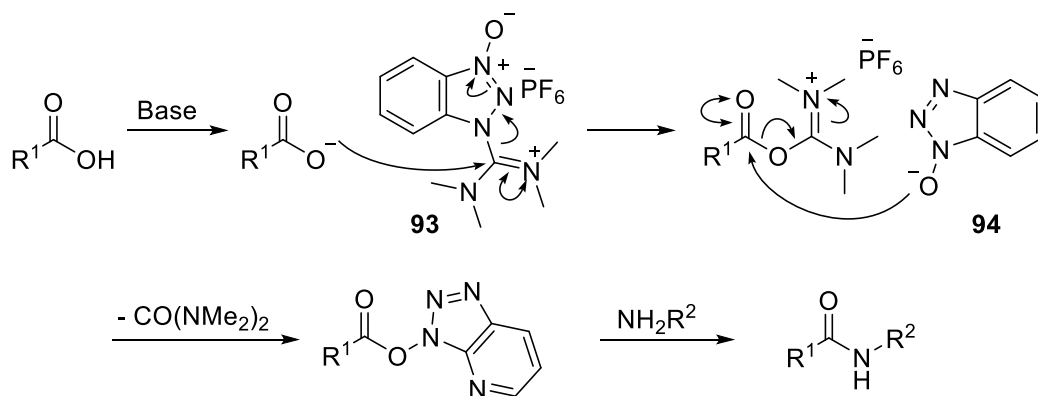


Figure 31: Onium salts of 1*H*-benzotriazoles used as coupling reagents.

Amide bond formation mediated by these salts occurs through nucleophilic attack by the carboxylate on the guanidinium salt, with expulsion of the HOAt conjugate base **94**. This then attacks the ester to give the *O*-acyl intermediate, which reacts with the amine coupling partner (see **Scheme 46**).



Scheme 46: Activation of carboxylic acid for amide bond formation using onium salt HATU (**93**).¹⁶⁹

For the coupling of two sterically hindered amino acids, El-Faham *et al.* found that aminium and phosphonium salts (HBTU, HATU, AOP and BOP) in the presence of DIEA base were more effective activators than DCC in the presence of HOAt.¹⁷⁴ However it should be noted that 1-hydroxybenzotriazole compounds have been noted for their potentially explosive properties, with a relatively high sensitivity to friction and sparks.¹⁷⁵

There have been many efforts to design new 1*H*-benzotriazole coupling reagents with improved reactivity and stability; however, comparison tends to reveal little improvement over those reagents already available.¹⁶⁹ One example that has exhibited somewhat improved characteristics is COMU (**96**), a member of a new class of uronium coupling reagents which has a less-hazardous reaction profile and an enhanced reactivity.¹⁷⁶

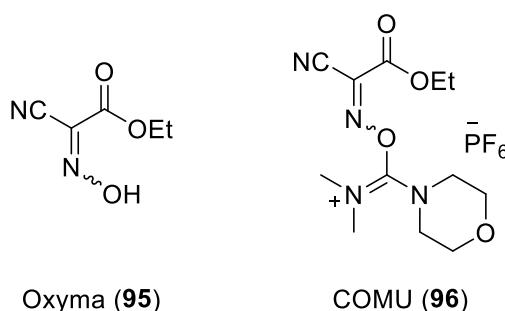


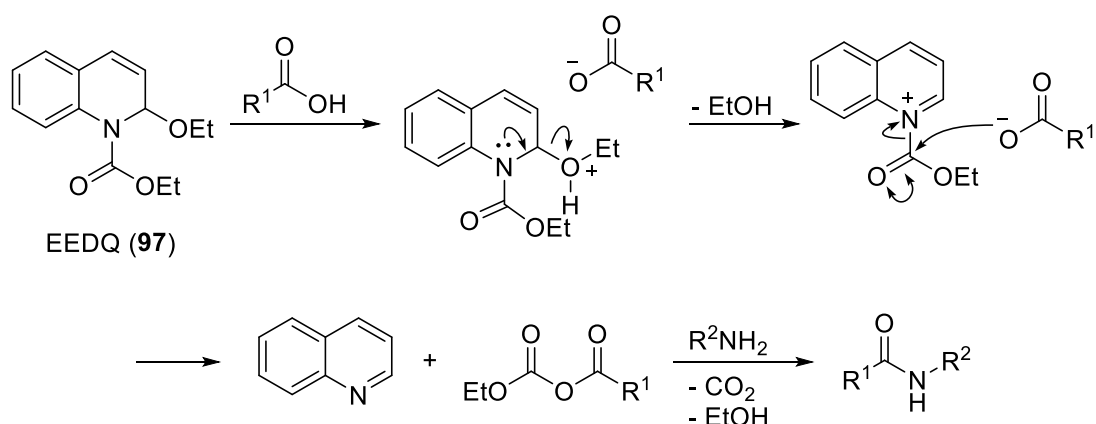
Figure 32: Alternative coupling reagents Oxyma (**95**) and uronium salt COMU (**96**).¹⁷⁶

El-Faham *et al.* had previously demonstrated that acidic oxime Oxyma (**95**) could be used as an alternative coupling reagent, with high activity and low racemization in peptide formation.¹⁷⁷ The uronium salt COMU (**96**) was developed to incorporate the oxyma residue as a leaving group, reminiscent of the mechanism of action of the onium salt HATU (**93**).¹⁷⁶ COMU (**96**) has been found to be more stable than HATU (**93**) and its derivatives, and exhibits enhanced polarity, solubility and reactivity endowed through incorporation of the morpholino group.^{169,178,179}

The use of carbodiimides and 1*H*-benzotriazole, or their oxonium salt derivatives, is potentially the most prevalent method for amide bond formation and peptide coupling. However there are many other alternative ‘coupling reagents’, as well as alternative methods for amide bond formation.^{162,169}

1.6.3.1.2. Alternative coupling reagents.

Acid chloride formation is one of the easiest methods of carboxylic acid activation, formed through reaction of a carboxylic acid and thionyl chloride (SOCl₂), oxalyl chloride ((COCl)₂) or POCl₃.¹⁶² However, these reagents are limited in their practicality due to formation of HCl as a by-product, limiting *N*-protecting group strategies, and the propensity of acid chlorides towards hydrolysis and racemization under basic conditions.



Scheme 47: Mechanism for amide bond formation using carbonic anhydride EEDQ (**97**).¹⁶²

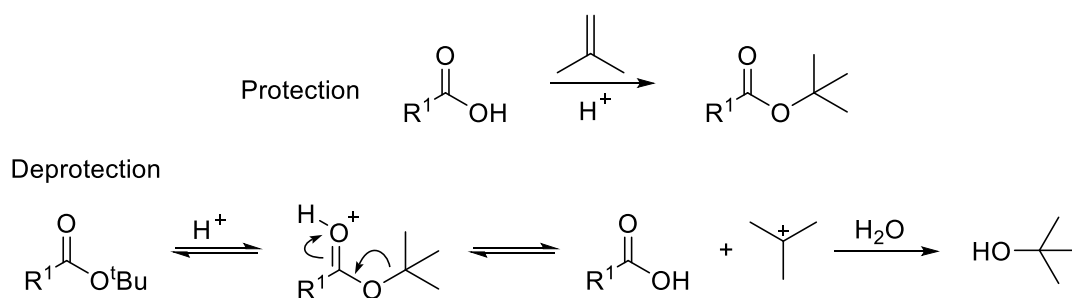
Formation of mixed anhydrides is a popular method of carboxylic acid activation. For instance, EEDQ (**97**) generates the reactive carbonic anhydride of the carboxylic acid. The reaction occurs through deprotonation of the acid by the highly basic ethoxy moiety on EEDQ, with anhydride formation then driven by re-aromatization of the quinoline (see **Scheme 47**). This anhydride then reacts rapidly in solution with external nucleophiles, limiting the extent of side reactions and potential epimerization.^{169,180,181}

There are many other coupling routes available,^{162,164,169} including the use of chloroformate to activate the carboxylic acid, Staudinger ligation and native chemical ligation, although the latter route employs thioester intermediates, limiting reaction applicability to amino acids and peptides containing terminal cysteines or thiol-functionalized serine or threonine residues.

1.6.3.1.3. Protecting group strategies.

Most of the coupling reagents discussed have been considered with respect to the reaction of amino acids in forming new peptide bonds. However, it is imperative when reacting amino acids that appropriate protecting group strategies be adopted.

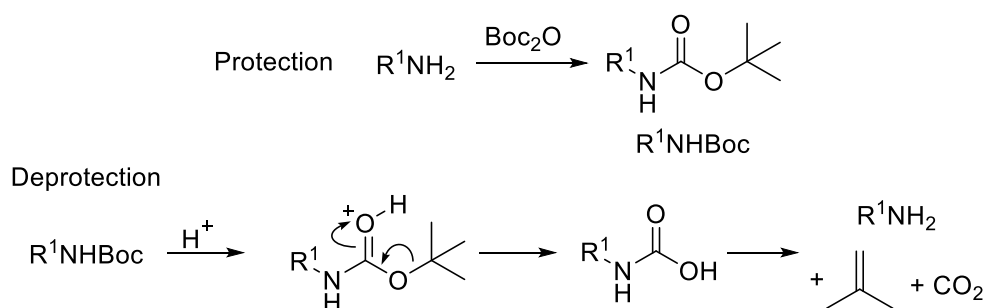
For solution phase synthesis, there must be two orthogonal protecting groups employed for the NH_2 (*N*-terminus) and CO_2H (*C*-terminus), which can be removed under different, mild conditions to enable selective modification of the requisite end of the peptide. Common *C*-terminus protecting groups include benzyl or *tert*-butyl esters, the latter formed through reaction of the carboxylic acid and isobutene under acidic conditions.



Scheme 48: C-terminal protecting group strategies using *tert*-butyl esters.¹⁰¹

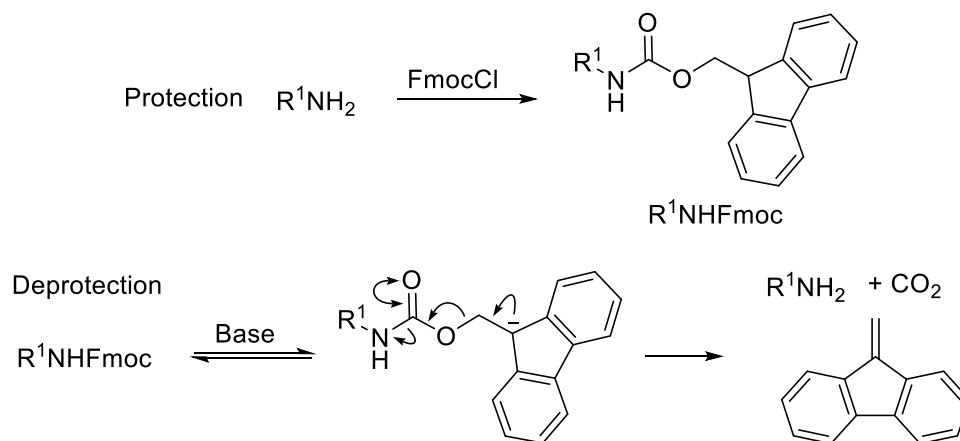
This protecting group is stable under basic conditions as the bulky group prevents attack by nucleophiles in solution. Under acidic conditions the protonated carboxyl group will collapse to give the stabilized *tert*-butyl cation, which is quickly hydrolyzed in solution, and the deprotected acid (see **Scheme 48**).¹⁰¹

Popular *N*-terminus protecting groups for peptide synthesis include the acid labile Boc (*tert*-butyloxycarbonyl) group and the base labile Fmoc group. The Boc group is a carbamate derived protecting group, formed through reaction of the amine with the anhydride Boc₂O. Deprotection occurs under acidic conditions, with loss of the *tert*-butyl cation collapsing to the volatile isobutene and decarboxylation giving the free amine (see **Scheme 49**).



Scheme 49: *N*-terminal acid protecting group strategy with the acid-labile Boc-group.

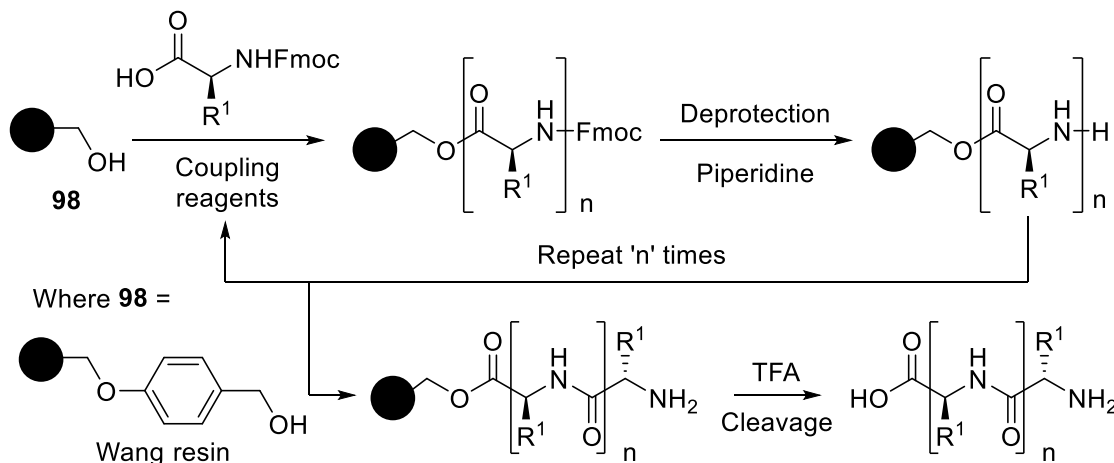
Fmoc (fluorenylmethyloxycarbonyl) is formed through reaction of Fmoc chloride and the free amine. Deprotection is usually carried out through deprotonation of the highly acidic proton on the fluorenyl ring system using a tertiary amine like piperidine, to produce a 14-electron anionic aromatic group (see **Scheme 50**). Fmoc protection is a popular strategy in peptide synthesis as most C-terminal protecting group strategies adopted are acid labile.¹⁶²



Scheme 50: *N*-terminal protecting group strategies with the Fmoc group.

1.6.3.1.4. Applications and advances: Solid phase peptide synthesis.

Despite innovations in protecting group strategies and coupling reagents, solution phase peptide synthesis can be problematic for the synthesis of long chain peptides. This is due to problems of purification and solubility with increasing chain length. Solid phase peptide synthesis (SPPS) was introduced by Merrifield to circumvent these problems.¹⁸²



Scheme 51: Example SPPS using acid labile Wang resin and base labile Fmoc *N*-protection strategy.

By mounting the nascent peptide chain covalently onto a solid support a step-wise process of coupling, washing, deprotection and cycle repetition can be conducted to build-up a peptide before cleavage from the resin (see **Scheme 51**). Protecting group strategies are paramount to this process, as the bond to the solid support must be stable to all reaction conditions, and the deprotection must be mild enough to not disrupt the stereochemical purity of the product.

For example, Wang resins are hydroxybenzyl-based resins (see **Scheme 51, 98**) which are base stable and bind to the C-terminus of an amino acid.¹⁸³ SPPS using these resins can therefore be conducted in collaboration with a base labile *N*-protecting group, such as Fmoc. The completed peptide chain can then be selectively cleaved using trifluoroacetic acid (TFA), mindful of side chain stability and protecting group strategies that may still be employed.

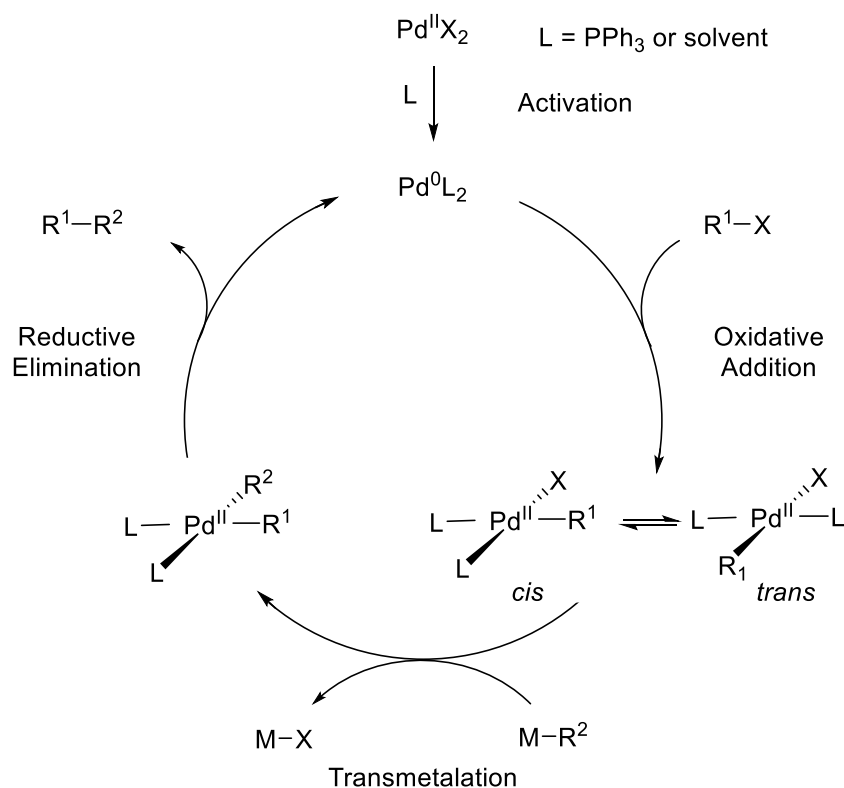
Amide bond forming reactions were used in this project as an essential tool in approaches towards the fused heterocyclic core of PF-3644022 (**25**) and its advanced intermediates (see **Chapter 3**).

1.6.3.2. Metal-mediated cross-coupling.

Metal-mediated cross-coupling reactions have become an essential item in the synthetic organic chemist's 'toolbox', facilitating bond formations that may otherwise be severely energetically disfavoured.¹⁰¹ Early reports were documented at the end of the 19th century, with copper, organo-alkali-metals and organo-magnesium to mediate homocoupling reactions. Examples include seminal work by Glaser and Ullmann into the homocoupling of arylacetylenes,^{184,185} and the development of nucleophilic Grignard reagents.¹⁸⁶ Over the following century, the reactive scope was extended to the selective formation of carbon-carbon bonds between different fragments, encompassing all hybridization states of carbon, the incorporation of heteroatoms, and the use of catalytic amounts of metals.

Huge advances have been made in the field over the past 40 years, with ground-breaking work completed by Heck, Negishi and Suzuki in the 1970s earning them the Nobel prize in Chemistry in 2010 for their discoveries and development of the field of C-C bond construction.^{186,187} Their work led to major advances in the use of the group 10 metals in cross-coupling and catalysis.^{97,186–189} Palladium (Pd) has emerged to dominate the field as the choice metal catalyst and as a "jack of all trades" for carbon-carbon bond forming reactions; offering enhanced chemo- and regioselectivity, high tolerance for a wide range of functional groups, and the ability to modulate reactivity through the use of ligands.^{101,186}

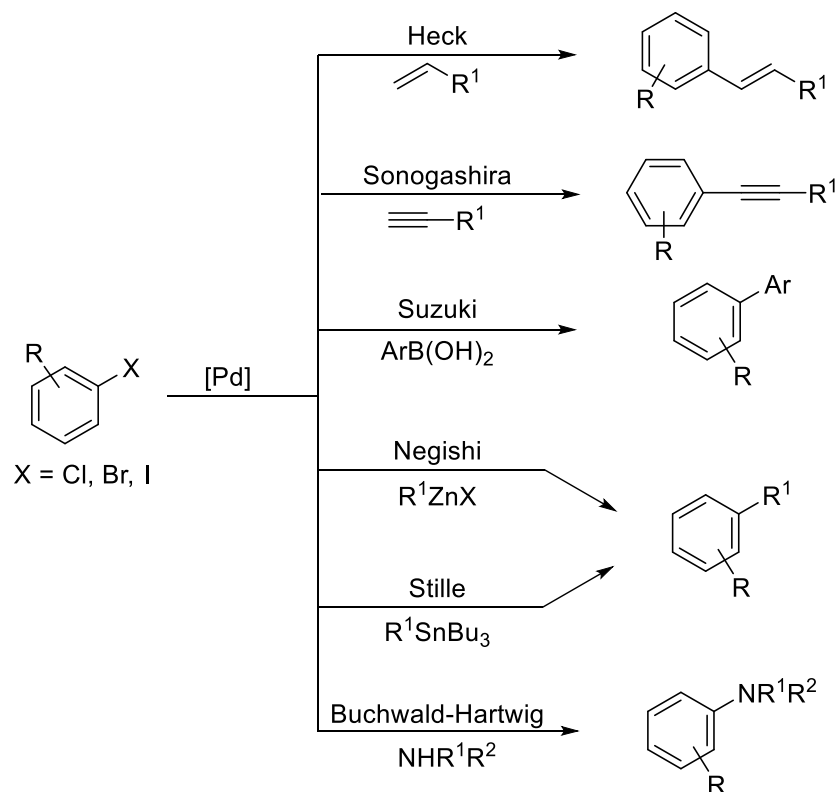
The general catalytic cycle for a palladium-mediated cross-coupling reaction proceeds through four principle steps: catalyst activation, oxidative addition, transmetalation and reductive elimination (see **Scheme 52**).



Scheme 52: General catalytic cycle for palladium mediated cross-coupling.

Palladium catalysts tend to require an activation step to form the unsaturated Pd(0) catalyst. Hence, saturated Pd(0) and Pd(II) complexes, like $\text{Pd}(\text{PPh}_3)_4$ and $\text{Pd}(\text{OAc})_2$, must undergo a loss or exchange of ligands, or react with nucleophiles in solution.^{101,190} Unsaturated Pd(0) is then able to activate C-X bonds through an oxidative addition step to form Pd(II) organopalladium complexes. The Pd(II) square-planar complex can then undergo transient *cis*- to *trans*-isomerization to form the most thermodynamically stable complex. Organometallic reagents (pre-formed, or formed *in situ*) can then undergo a slow transmetalation step, with transfer of the organic component to the palladium centre and loss of a metal halide. To enable reductive elimination the palladium complex usually needs to isomerize back into the *cis*-configuration, a step which can be slow and energetically demanding. Once the two organic ligands are arranged in the *cis*-configuration, reductive elimination of the ligands as the coupled product regenerates the zerovalent Pd(0) active catalyst to facilitate the next cycle.

The organometallic component that undergoes transmetalation can be based upon zinc, tin, silicon, magnesium, aluminium or boron. The RX component can be a halide or pseudo-halide, and the organic ligand must not have a β -hydrogen, as this can decompose via β -hydride elimination with palladium. Some examples of palladium-catalyzed reactions are illustrated in **Scheme 53**.

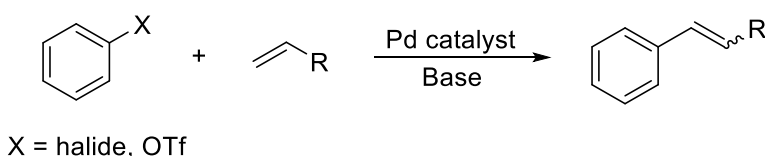


Scheme 53: A few examples of palladium-catalyzed cross-coupling reactions.

The catalytic cycles for the Heck and Sonogashira reactions occur via slightly different pathways than the one illustrated in **Scheme 52**. Sonogashira coupling occurs via formation of an organometallic species in situ, through reaction of a terminal alkyne with a copper halide co-catalyst and base in solution.¹⁰¹ The Heck reaction has an additional π -coordination and migratory insertion step which will now be discussed in more detail.

1.6.3.2.1. The Mizoroki-Heck reaction.

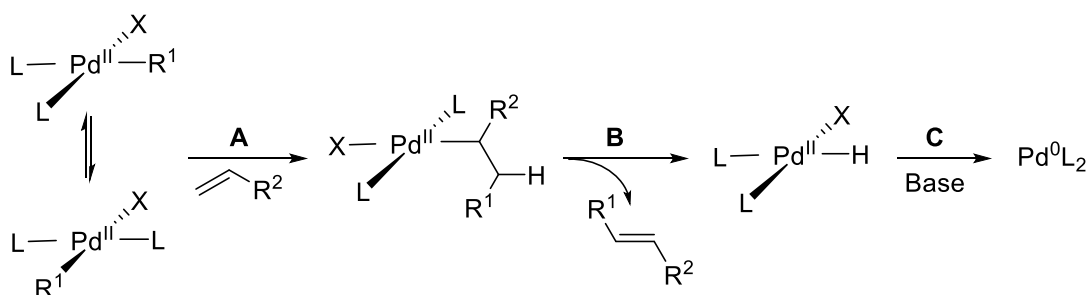
The Mizoroki-Heck reaction (here on referred to as the Heck reaction) is a widely explored and flexible method of C-C bond formation between two sp^2 hybridized carbon centres, usually for the coupling of aryl (or vinyl) halides or pseudo-halides and activated alkenes in the presence of a base (see **Scheme 54**).^{190–192}



Scheme 54: General reaction scheme for Mizoroki-Heck coupling.

The reaction is quite accommodating in its requirements, though an optimal system has yet to be devised, with reaction conditions often referred to as a catalyst ‘cocktail’.^{193–195} For example, reactions have been conducted successfully under anhydrous conditions,¹⁹⁶ in the presence of water¹⁹⁷ and in water-organic mixtures.^{190,197} The source and amount of palladium required for catalytic activity has been widely discussed, including the role of palladium nanoparticles and homeopathic palladium.^{198,199} The use of ligands has been widely explored, initially used to extend reactivity beyond just iodides and to help maintain stereochemistry,²⁰⁰ and an extensive variety of phosphine and *N*-heterocyclic carbene (NHC) based ligands have been described in the literature,^{196,201–204} in addition to a number of ligand-free systems.²⁰⁵

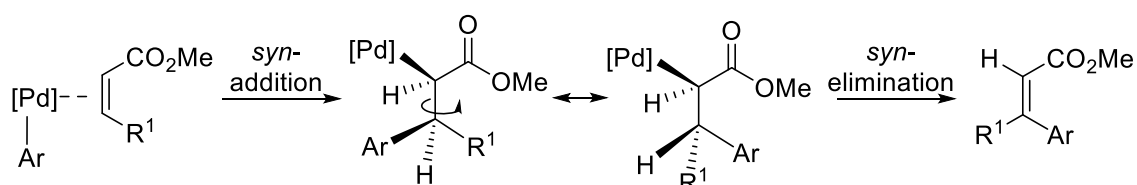
1.6.3.2.1.1. Catalytic cycles for ligated and ligandless systems.



Scheme 55: Additional steps of the Heck catalytic cycle. **A:** Migratory insertion. **B:** β -Hydride elimination. **C:** Base-assisted reductive elimination.

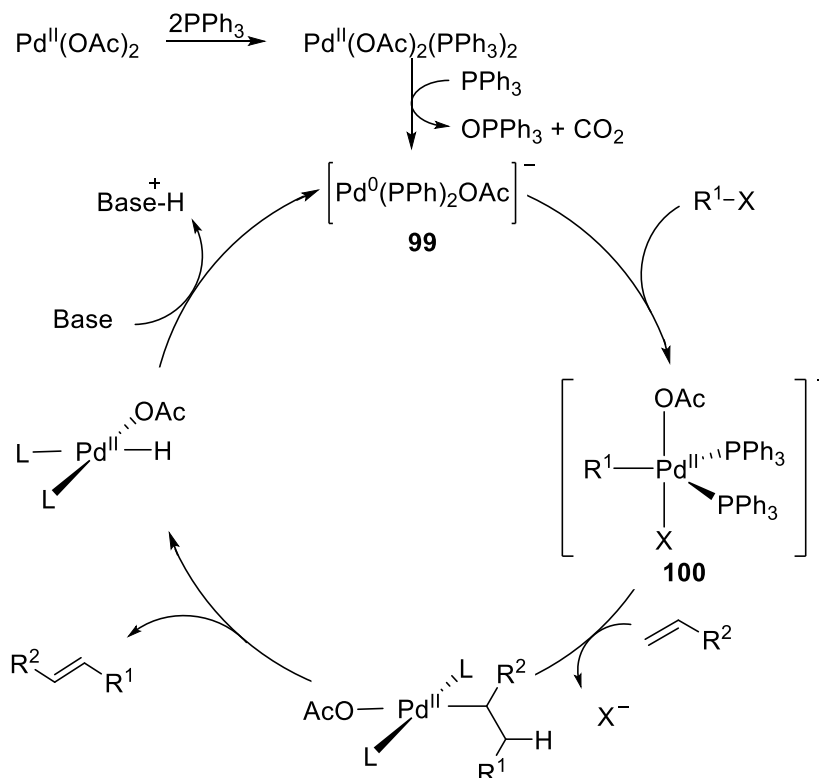
The classical mechanism of the Heck coupling reaction is similar to that illustrated in **Scheme 52**, though with an additional migratory insertion step of the alkene (see **Scheme 55**). Transient π -

complexation of the alkene is proposed to occur with the organopalladium(II) complex, with *syn*-migratory insertion into the palladium-carbon bond (step **A**).²⁰⁰ The saturated chain must then rotate to enable β -hydride elimination (step **B**). The most stable transition state is usually the one in which the R groups eclipse the smallest group possible, leading to predominantly *trans*-alkene products (see **Scheme 56**). Finally, base-assisted reductive elimination of HX returns the active Pd(0) catalyst (step **C**).



Scheme 56: Illustrative mechanism of how the *syn*-addition and *syn*-elimination steps of the palladium complex determine the stereochemistry of the product alkene.

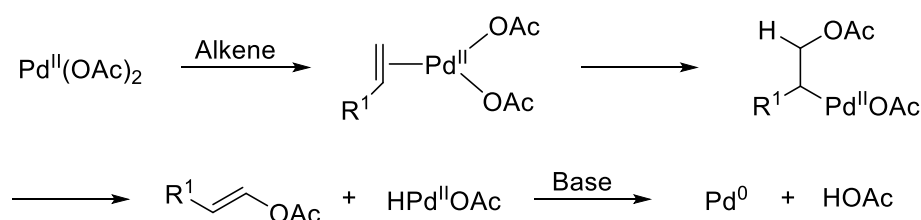
Numerous studies have been conducted since the initial publication of the Heck reaction, and it has been found that the mechanism is much more complex than initially thought.²⁰⁶ An alternative mechanism postulated by Amatore and Jutand occurs via an anionic catalytic species, and has been proposed to be applicable to most ligated, homogeneous systems (see **Scheme 57**).^{207,208}



Scheme 57: Amatore and Jutand's postulated mechanism for palladium-mediated catalysis via an anionic palladium complex.²⁰⁷

Based upon a catalytic system involving use of triphenylphosphine (PPh_3) and $\text{Pd}(\text{OAc})_2$, they proposed formation of an anionic 16-electron palladium species (**99**) as the active catalyst. Oxidative addition with RX forms a transient pentacoordinated aryl $\text{Pd}(\text{II})$ anionic complex **100**, which eliminates the additional halide anion to give the neutral species. Coordination and migratory insertion of the electron-rich alkene can then occur following the traditional steps of the mechanism (see **Scheme 57**), and reaction of the $\text{Pd}(\text{II})$ complex with base in solution regenerates the anionic $\text{Pd}(\text{0})$ catalyst.^{203,209}

The most popular ligand-free Heck reaction was developed by Jeffery, operating under generally milder, phase-transfer conditions.^{210,211} Classical Jeffery conditions are usually run at or near room temperature, using an excess of base, with a palladium(0) catalyst (for example, $\text{Pd}(\text{OAc})_2$) and a phase-transfer agent such as tetrabutylammonium chloride or bromide (TBAC and TBAB, respectively).²¹⁰ Even Jeffery's conditions tend to involve a catalyst 'cocktail', with yields highly dependent upon changes in the choice and concentration of phase-transfer agent, the choice of base, and the presence of water, which can be detrimental or beneficial dependent upon the system.²¹¹



Scheme 58: Generation of the active $\text{Pd}(\text{0})$ catalyst in ligand-free Heck reactions.²⁰⁶

Generation of the active palladium species from $\text{Pd}(\text{OAc})_2$ in a ligand-free system is believed to occur through a sacrificial alkene and base-mediated mechanism, to produce $\text{Pd}(\text{0})$ in solution (see **Scheme 58**).²⁰⁶ Evidence has been found to support the agglomeration of $\text{Pd}(\text{0})$ atoms into nanoparticles or colloids, which are stabilized by bulky ammonium cations under Jeffery conditions.²⁰⁵

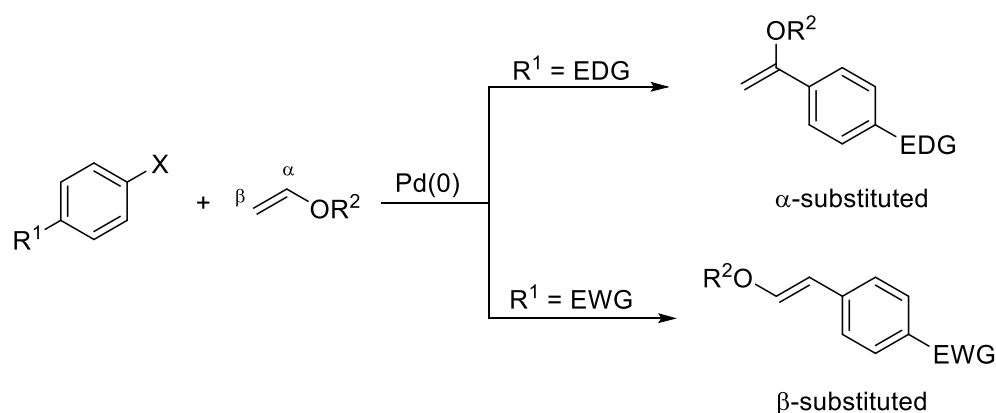
It has been proposed that subsequent catalysis then occurs on the surface of the nanoparticles akin to a heterogeneous catalyst system,^{198,212} or through solubilization of the palladium clusters and oxidative addition with RX to form organopalladium intermediates RPdX or RPdX_3^{2-} which then enter the catalytic cycle.²⁰⁵

The use of quaternary ammonium salts as additives has also been found to be beneficial for a number of ligated systems, with proposed roles including as a source of additional anions in

solution to act as promoters, in the stabilization of un-ligated Pd(0) in solution, or as phase-transfer agents for reactions mediated by solid salts (solid-liquid) or aqueous solvents (liquid-liquid).^{190,203} Indeed, Amatore *et al.* proposed that the presence of bulky cations in solution could help to regenerate and stabilize the active anionic species **99** and **100**.²⁰⁸

1.6.3.2.1.2. Regioselectivity.

Regioselectivity of the Heck reaction is determined during the migratory insertion step of the alkene into the palladium-carbon bond, as the aryl (or alkenyl) group undergoes a β -shift from the palladium centre to the alkene to form the new C-C bond. Usually a concerted step, migration tends to be directed by steric factors of the alkene, with the aryl group moving to the least substituted and often more electron-deficient carbon.^{213,214} In the case of electron-rich alkenes, like enol ethers, migration of the aryl group tends to be directed to the more electron-deficient α -position. However, this is dependent on the electronics of the palladium complex and migrating group, as an electron-poor aryl group will favour migration to the electron-rich β -position of the alkene (see **Scheme 59**).^{194,215}

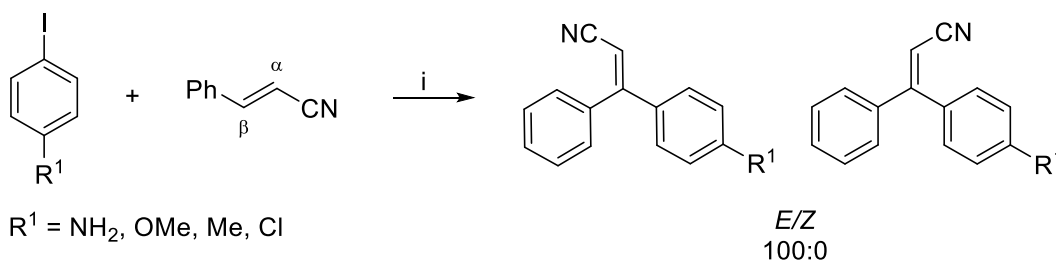


Scheme 59: Changes in regioselectivity with the use of enol ethers. Substituting at the α - or β -position depending on the electron density of the aromatic ring.

Additionally, electronic effects of the palladium complex have been studied to explore their influence on regioselectivity. For instance, von Schenck *et al.* conducted a number of studies into the use of neutral and anionic palladium complexes with symmetrical and unsymmetrical ligand systems and found that, through tuning the electronics of the catalyst, migratory insertion could be directed to alter the regioselectivity of the reaction.²¹⁶

1.6.3.2.1.3. Heck coupling of α,β -disubstituted alkenes.

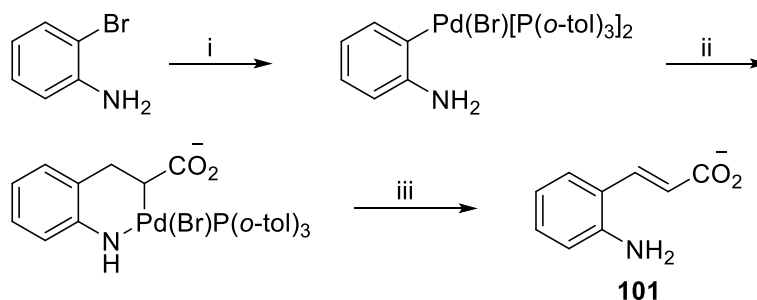
α,β -Disubstituted alkenes are much less reactive towards Heck coupling than their monosubstituted or 1,1-disubstituted counterparts.¹⁹⁶ However, there are a number of examples of electron poor α,β -disubstituted alkenes that have been coupled successfully in Heck reactions, including cinnamates and crotonates,^{194,217} alkoxypropenes,²¹⁵ methyl 3-methoxyacrylates,²⁰¹ and 3-substituted acrylonitriles.²¹⁸



Scheme 60: Masllorens *et al.*'s stereoselective synthesis of 3,3-disubstituted acrylonitriles using Heck coupling. Reaction conditions: i) $\text{Pd}(\text{OAc})_2$, KOAc , $n\text{Bu}_4\text{NBr}$, DMF , $80\text{--}100^\circ\text{C}$, 2-3 days.²¹⁸

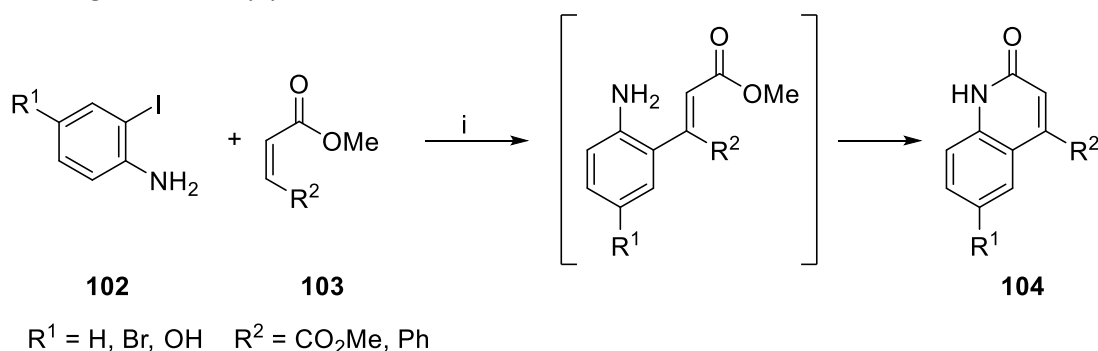
Masllorens *et al.* conducted Heck coupling between 3-substituted acrylonitriles and aryl iodides under Jeffery's conditions with total control of regioselectivity; to substitute at the β -position, and with complete stereocontrol giving the (*E*)-isomer.²¹⁸ Electron-rich and electron-poor aryl iodides both coupled at the β -position, and *trans*- to the nitrile group, though more electron-poor aryl iodides required longer reaction times (see **Scheme 60**).

The versatility of the Heck reaction using α,β -disubstituted alkenes has been explored as a route towards the synthesis of quinolone and coumarin derivatives. Heck *et al.* developed a one pot method, coupling α,β -disubstituted malonates with 2-iodoanilines in an effort to promote cyclization to the heterocycle in situ.²¹⁷ Use of monosubstituted alkenes, including acrylic acid and methyl acrylate, returned only the (*E*)-alkene (**101**) after coupling with 2-bromo and 2-iodoaniline. It was concluded that β -hydride elimination of these derivatives must occur at a faster rate than the desired cyclization (see **Scheme 61**).



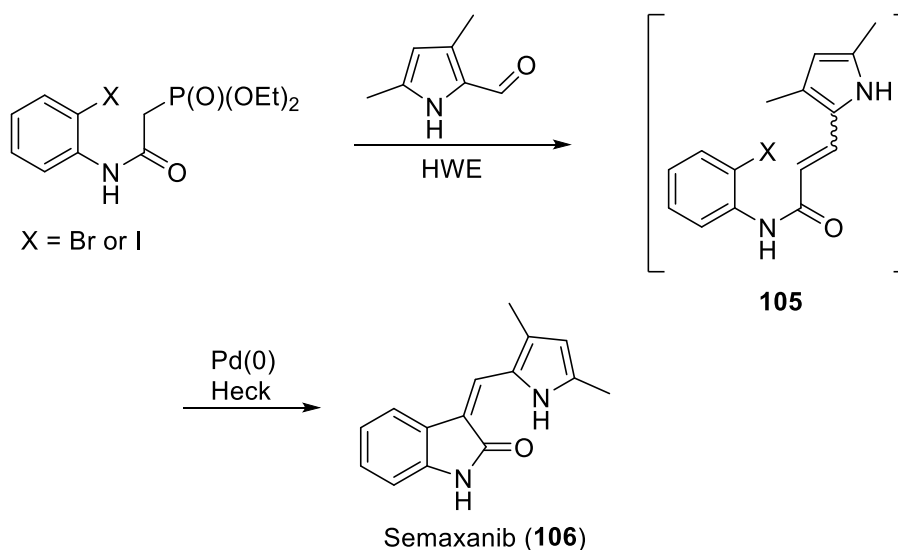
Scheme 61: Heck *et al.*'s attempted 2-quinolone formation via Heck coupling of a monosubstituted alkene and a 2-bromoaniline. Reaction conditions: i) $\text{Pd}[\text{P}(\text{o-tolyl})_3]_2$; ii) acrylic acid, base; iii) $\text{P}(\text{o-tol})_3$, Et_3N .²¹⁷

It was hypothesized that use of a 1,2-disubstituted alkene, specifically the (*Z*)-isomer of an acrylate derivative (**103**), would couple with iodide **102** and possess the correct stereochemistry for cyclization to occur. It was also proposed that conducting the reaction in the absence of any additional triarylphosphine should help slow the final β -elimination step, thus enabling the desired cyclization to occur (see **Scheme 62**). Heck *et al.* did experience some problems with isomerization of intermediates, but achieved yields of up to 72% of their desired 2-quinolone **104** using this one step procedure.



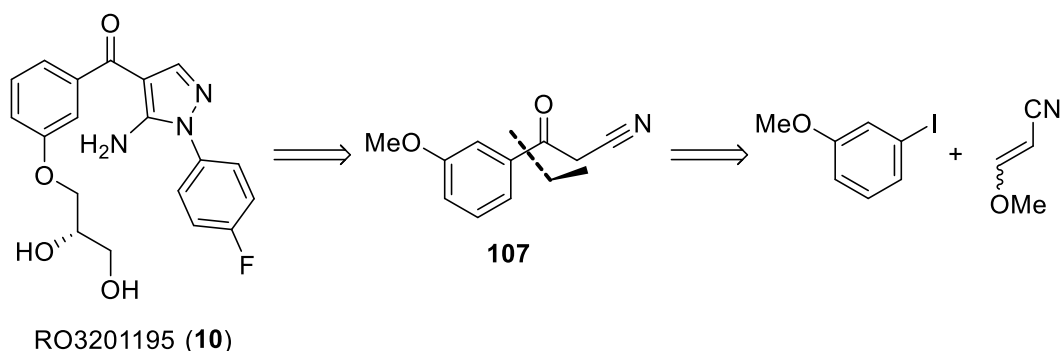
Scheme 62: Heck *et al.* one pot synthesis of 2-quinolones using 2-iodoanilines and (*Z*)-3-substituted acrylates. Reaction conditions: i) Pd(OAc)₂, Et₃N, MeCN 100 °C.²¹⁷

The utility of this Heck-mediated synthetic route towards quinolones has since been demonstrated in the total synthesis of Tipifarnib, a potent and orally-bioavailable inhibitor for farnesyl protein transferase,²¹⁹ and in the synthesis of Semaxanib (**106**), a tyrosine-kinase inhibitor and cancer therapeutic (see **Scheme 63**). A tandem Horner-Wadsworth-Emmons (HWE)/Heck process, provided alkene **105** which was then subjected to an intramolecular Heck reaction to form the 3-methylidene-oxindole **106**, Semaxanib.²²⁰



Scheme 63: Synthesis of Semaxanib (**106**), via a tandem HWE and Heck reaction.²²⁰

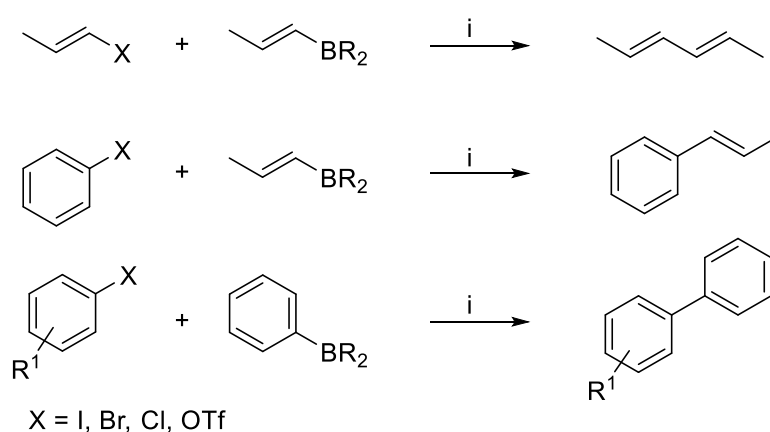
Given the adaptability and flexibility of the Heck reaction,¹⁹⁰ it presented itself as a prime method to be explored in this project for the total synthesis of RO3201195 (**10**), specifically for the preparation of benzoylacetone nitrile intermediate **107** (see **Scheme 64**).



Scheme 64: Retrosynthetic strategy for Heck coupling towards benzoylacetone nitriles.

1.6.3.2.2. Suzuki-Miyaura cross-coupling.

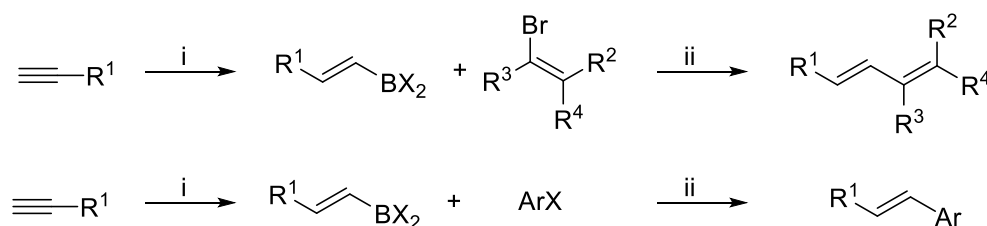
The Suzuki-Miyaura reaction (hereon referred to as the Suzuki or Suzuki-coupling reaction) is one of the most prolific cross-coupling reactions, observed in approximately 40% of C-C bond forming reactions in medicinal chemistry,⁹⁷ and earned Suzuki a share of the Chemistry Nobel prize in 2010.^{187,221} Suzuki reactions can be more generally classified as the coupling of an organoborane and an organic electrophile, usually an organohalide or triflate, in the presence of a base (see **Scheme 65** for examples). Over the course of this project, Suzuki coupling was relied upon as an efficient and reliable method for the formation of biaryl linkages.



Scheme 65: Prototypical Suzuki coupling reactions. Reaction conditions: i) Palladium catalyst and base.

1.6.3.2.2.1. The catalytic cycle.

Suzuki *et al.* first reported their coupling method in 1979, for the stereoselective synthesis of (*E*)-arylalkenes²²² and (*E*)-aryldienes.²²³ The desired 1-alkenylborane was synthesized through hydroboration of the relevant alkyne, and coupled with aryl halides, haloalkynes or haloalkenes in the presence of base and catalytic tetrakis(triphenylphosphine)palladium ($\text{Pd}(\text{PPh}_3)_4$) (see **Scheme 66**). The reaction scope was quickly extended to the synthesis of symmetrical and unsymmetrical biaryls via palladium catalyzed coupling of arylboronic acids and esters with aryl halides in the early 1980s.²²⁴



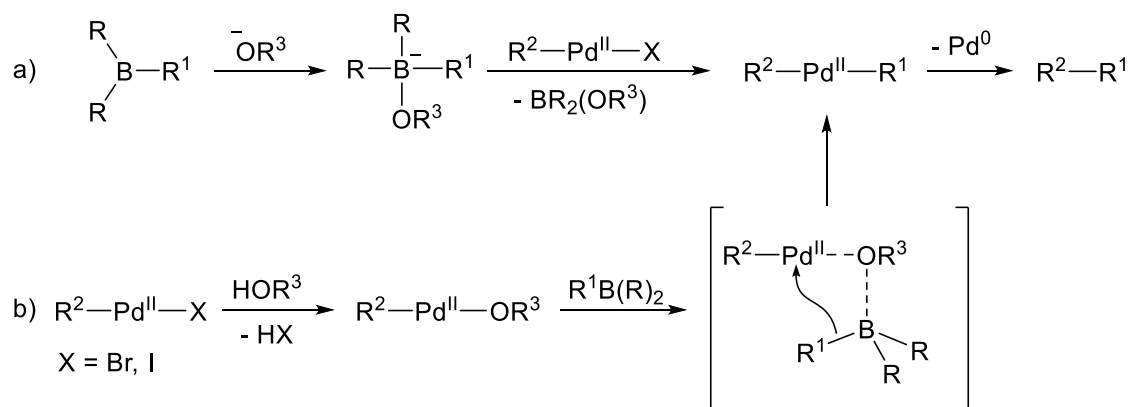
Scheme 66: Suzuki's first published reactions using the "Suzuki" coupling system. Reaction conditions: i) Bis(1,2-dimethylpropyl)borane; ii) $\text{Pd}(\text{PPh}_3)_4$, base.

Suzuki coupling occurs through the traditional catalytic cycle detailed in **Scheme 52** (Section 1.6.3.2). Activation of the catalyst affords an unsaturated $\text{Pd}(0)$ complex, with oxidative addition of the organic halide, transmetalation of the organoboron reagent and reductive elimination affording the coupled product.^{225,226}

Suzuki coupling offers several advantages over other C-C bond forming reactions, including high functional group tolerance, mild reaction conditions, ease of removal of side products and amenability towards aqueous and heterogeneous reaction conditions.²²¹ These features are almost entirely due to the chemical nature of the organoboron coupling partner.^{225,227}

Stability of organoboron reagents can be attributed to the small dipole moment of the carbon-boron bond and low nucleophilicity of the organic component. Since the conception of Suzuki coupling, a plethora of new organoborane reagents have been designed with improved stability and reactivity, to facilitate cleaner, more efficient and selective reactions.²²⁸

The presence of a base in Suzuki reactions is paramount to activation of the organoboron, though there have been abundant discussions over its precise role.^{225,229} One theory is that the base coordinates with Lewis acidic boron to create a four coordinate 'ate' complex, to increase the nucleophilicity of the carbon component and facilitate transmetalation onto the $\text{Pd}(\text{II})$ complex (the "boronate pathway", see **Scheme 67a**).^{225,228,230}



Scheme 67: Potential reaction pathways for base-mediated Suzuki-Miyaura coupling: a) The boronate pathway; b) The oxo-palladium pathway.

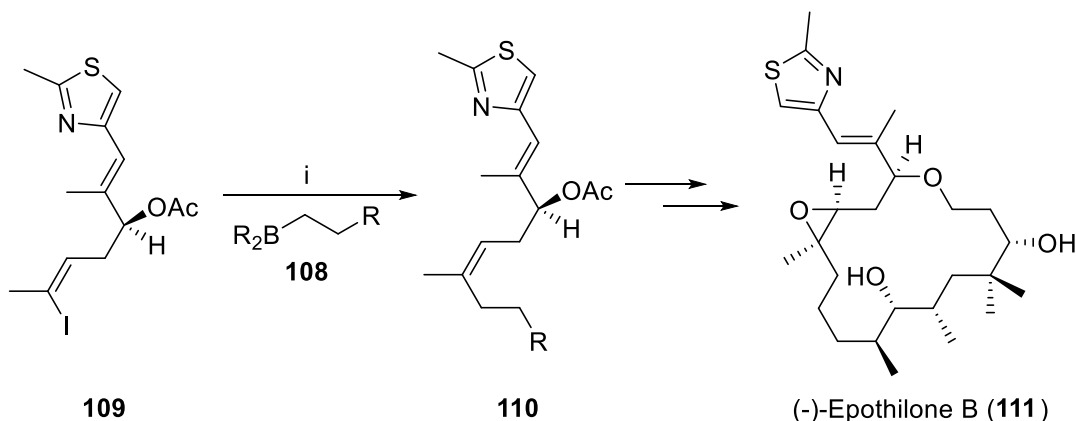
An alternative pathway has been proposed to occur via ligand exchange of the anionic base and halide on the Pd(II) complex. This forms a new hydroxy-, alkoxy- or acetopalladium(II) active complex. The oxo-palladium(II) complex then acts as a Lewis base to coordinate with the oxophilic organoboron and promote transmetalation (the “oxo-palladium” pathway, see **Scheme 67b**).^{225,226,228} Studies by Suzuki and Miyaura support this second mechanism of reaction, with transmetalation found to occur readily under neutral conditions between organoboron reagents and alkoxy-palladium(II) complexes, for example, formed from oxidative addition of epoxybutenes,²³¹ propargyl carbonates,^{226,232} allylic acetates and phenoxides.^{233,234}

In early studies the most common catalytic systems used in Suzuki coupling were Pd(PPh₃)₄, PdCl₂(PPh₃)₂ and Pd(OAc)₂, the latter with the addition of phosphine ligands.²²⁶ In order to carry out the catalytic cycle it is necessary for the catalyst to undergo activation to form an unsaturated Pd(0) species, which was generally facilitated by ligand dissociation or reaction in solution with an additional ligand, nucleophile or base, as discussed in **Section 1.6.3.2**.

Miyaura claimed that, in some cases, the choice of a suitable base was more important than the choice of the catalyst.²²⁹ Nonetheless, some of the great advances that have been achieved in extending the scope of Suzuki coupling can be attributed to improvements in the stability and reactivity of metal catalysts and the use of supportive ligands. For instance, the use of bulky, linked bisphosphines, chiral phosphines, and *N*-heterocyclic carbene ligands have led to advances including reactions with aryl chlorides, hindered substrates and asymmetric reactions, in addition to conducting reactions at a lower temperature and with lower catalyst loadings (for more information on ligands, see **Chapter 1.6.3.2.3**).^{235–237}

1.6.3.2.2.2. Applications in medicinal chemistry.

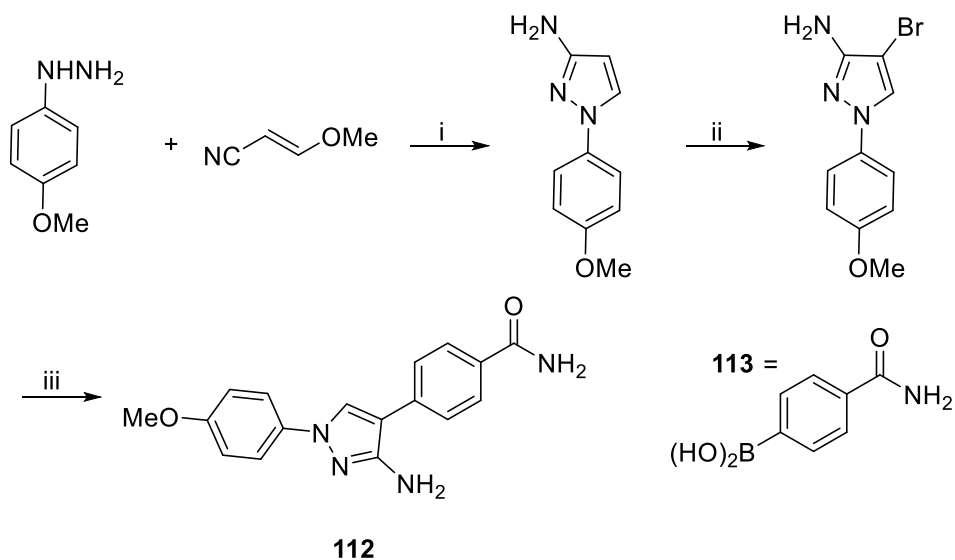
The extent of the applications of Suzuki coupling in pharmaceutical, agrochemical and engineering industries is widespread.²²¹ For example, Danishefsky *et al.* adopted Suzuki coupling for the formation of a *Z*-trisubstituted alkene (**110**) in their total synthesis of the natural product (–)-epothilone B (**111**), a compound of interest due to its antifungal and cytotoxic properties.²³⁸



Scheme 68: Danishefsky *et al.*'s Suzuki-mediated synthesis of (–)-epothilone B (**111**). Reaction conditions: i) Pd(dppf), Cs₂CO₃, Ph₃As, H₂O, DMF, RT, 77%.²³⁸

Boron alkyl **108** was generated via hydroboration of the relevant alkene with 9-borabicyclo[3.3.1]nonane (9-BBN) and reacted with vinyl iodide **109**, synthesized via a complex Wittig reaction. Using [Pd(dppf)₂] (dppf = 1,1'-bis(diphenylphosphino)ferrocene) with Cs₂CO₃ and AsPh₃ in water and DMF, Suzuki coupling was conducted in high yield (77%) at room temperature to generate exclusively the (*Z*)-alkene **110** (see **Scheme 68**). Further functionalization and macroaldolization followed, with deprotection of the hydroxyl groups and chemoselective epoxidation affording (–)-epothilone B (**111**).

Suzuki coupling has also been used successfully to synthesize a number of MK2 inhibitors.³ For instance, Velcicky *et al.* used Suzuki coupling extensively in the synthesis of pyrrolopyridine MK2 inhibitor **22** (see **Chapter 1.4.1**).⁶⁵ Bagley *et al.* proposed this chemotype as a prime candidate to investigate the role of MK2 in WS cells.³ However, when conducting their own synthesis of **22**, problems were encountered when conducting the halogenation of intermediates for the Suzuki coupling step. Therefore, the group synthesized the simplified target **112**, which maintained the majority of pharmacophoric traits important for binding in MK2 (see **Scheme 69**).



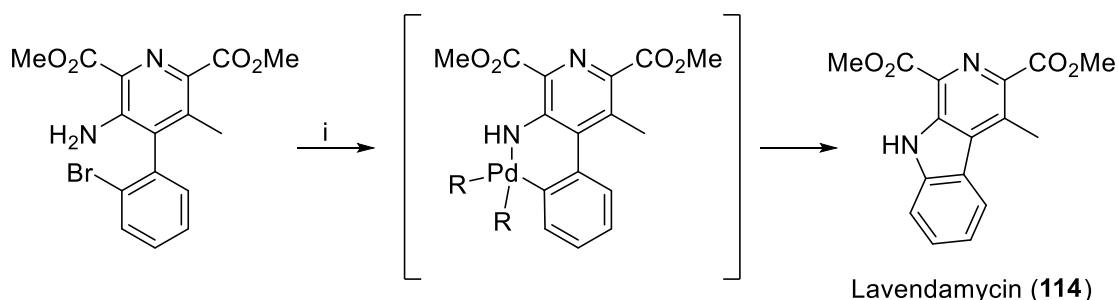
Scheme 69: Bagley *et al.*'s Suzuki-mediated synthesis of aminopyrazole MK2 inhibitor analogue **112**. Reaction conditions: i) NaOEt, EtOH, MW 150 °C, 2 h, 85%; ii) NBS, THF, MW 150 °C 2 h, 77%; iii) **113**, PdCl₂(PPh₃)₂, K₂CO₃, *i*-PrOH, H₂O, MW 150 °C, 2 h, 54%.³

Suzuki coupling was adopted to install the pyrazole 4-aryl substituent onto the ring, using aryl boronic acid **113**. Adopting microwave-assisted dielectric heating, the coupled product **112** was obtained in reasonable yield (54%) after heating at 150 °C for 2 h in aqueous solvent (see **Scheme 69**). WS cells grown in the presence of **112** were found to have a slightly extended life-span compared to controls, though only very low levels of MK2 inhibition was noted, making it difficult to draw significant conclusions about the role of MK2 from these results.³

1.6.3.2.3. Buchwald-Hartwig *N*-Arylation.

Before the advent of palladium-mediated *N*-arylation, methods available for aryl-nitrogen bond formation were very limited and generally required quite harsh conditions. Suitable methods include, for instance, copper-mediated nucleophilic displacement reactions of aryl halides using various nitrogen nucleophiles,²³⁹ strongly acidic nitration and subsequent reduction to the aniline, and radical nucleophilic aromatic substitution (*S*_{RN}1) using alkali metals and ammonia, which could return a mixture of products through benzyne formation.²⁴⁰

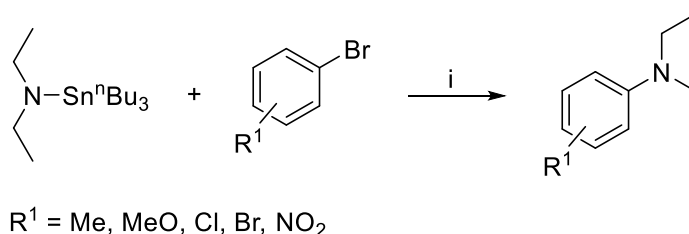
1.6.3.2.3.1. Palladium-mediated *N*-arylation and catalytic cycle.



Scheme 70: Boger and Panek's Pd(0)-mediated aryl C-N bond formation in the synthesis of lavendamycin (**114**). Reaction conditions: i) Pd(PPh₃)₄ (1.5 equiv.), THF, 80 °C, 21 h, 84%.²⁴¹

In the development of milder, functional group tolerant and regiospecific reactions, palladium was explored as a catalyst and reaction mediator in the mid-1980s. Boger and Panek published an intramolecular palladium(0) mediated aryl C-N bond formation in 1984 in the synthesis of the natural product lavendamycin (**114**).²⁴¹ They used super-stoichiometric amounts of Pd(PPh₃)₄ in THF to effect 5-membered cyclization of a linked aryl amine and aryl bromide (see **Scheme 70**). They proposed formation of a 6-membered σ-bonded palladacycle intermediate.

Only one year before, in 1983 Migita *et al.* published a study using catalytic amounts of PdCl₂[P(*o*-tolyl)₃]₂ to mediate aryl C-N bond formation.²⁴² Using aryl bromides and diethylamino-tributyltin as coupling partners, the group screened a number of palladium complexes and found that catalytic amounts of PdCl₂[P(*o*-tolyl)₃]₂ returned much higher yields of the coupled product than when Pd(PPh₃)₄ or PdCl₂(PPh₃)₂ were used (see **Scheme 71**).

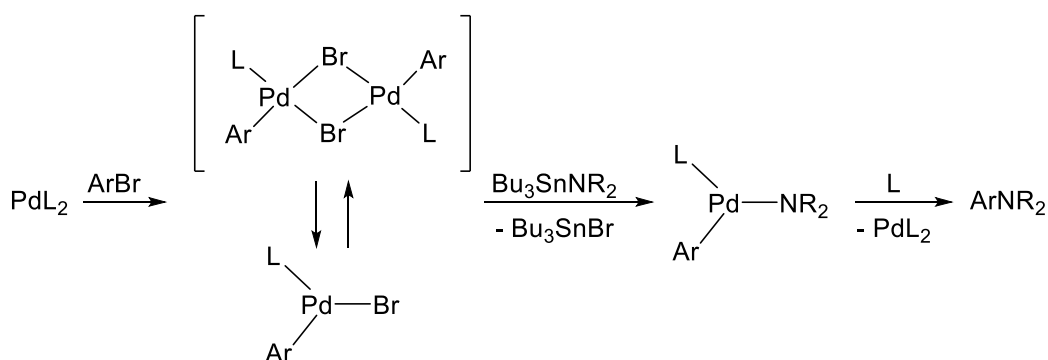


Scheme 71: Migita's original *N*-arylation reaction from 1984. Reaction conditions: i) PdCl₂[P(*o*-tolyl)₃]₂ (1 mol%), toluene, Ar, 100 °C, 3 h, 33-79%.²⁴²

In 1994, Buchwald and Hartwig both separately published work extending the scope of this coupling reaction. Hartwig recognized the similarity between the work of Migita and Stille, using tin-based reagents to mediate C-N and C-C bond formation, respectively.²⁴³ The group

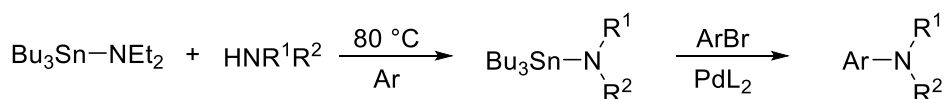
conducted work to identify the key intermediates of the reaction and the oxidation state of the active palladium species to elucidate the mechanistic aspects of the reaction.

The group isolated the Pd(II) dimer complex $[\text{PdArBr}(\text{P}(o\text{-tolyl})_3)]_2$, formed after oxidative addition of ArBr onto the monophosphine $\text{Pd}^0[\text{P}(o\text{-tolyl})_3]$ active complex. In this primary publication, it was proposed that transmetalation could occur onto either the monomer or dimer of this complex,²⁴³ with later studies confirming reductive elimination to occur via a three-coordinate monomeric species to give the coupled arylamine (see **Scheme 72**).²⁴⁴



Scheme 72: Hartwig's original proposed reaction pathway for *N*-arylation. L = $\text{P}(o\text{-tolyl})_3$.²⁴³

Concurrently, Buchwald *et al.* extended the scope of Migita *et al.*'s work by developing a method for the transamination of tributyltin amines. They recognized that aminostannanes tended to be unstable, and proposed that an in situ transamination reaction would enable access to a wider variety of substrates.²⁴⁵



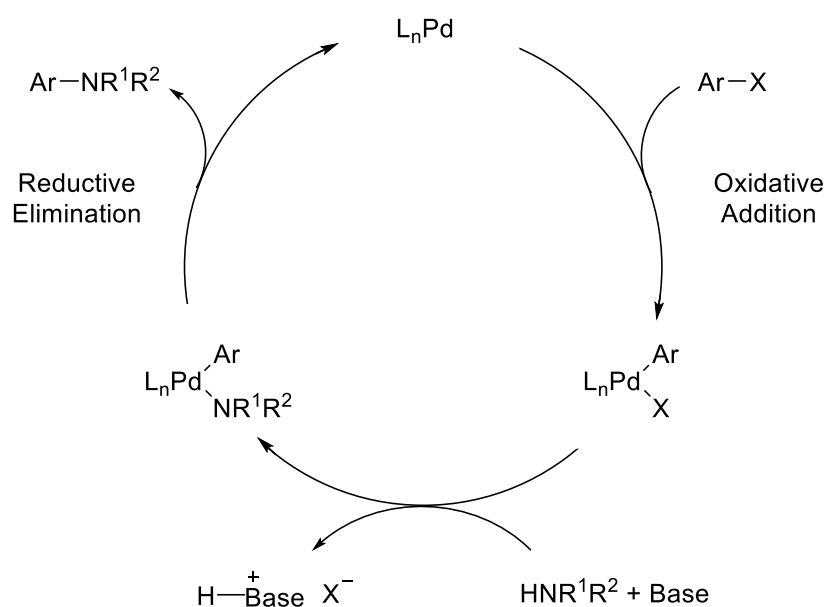
Scheme 73: Buchwald *et al.*'s transamination and palladium-mediated arylamine formation.²⁴⁵

Heating together an aminostannane derived from a highly volatile amine (such as diethylamino-tributyltin) with a free amine that possessed a higher boiling point in toluene resulted in exchange of the amino groups, with the more volatile amine removed by purging the vessel with argon. Immediate palladium-mediated *N*-arylation could then be conducted. This method enabled access to a much wider variety of amine coupling partners, including primary and secondary alkyl and aryl amines (see **Scheme 73**).

Buchwald *et al.* also confirmed that use of alternative ligands such as PPh_3 , dppf and linked diphosphine $\text{PPh}_2(\text{CH}_2)_3\text{PPh}_2$ instead of Migita's original ligand of choice, $\text{P}(o\text{-tolyl})_3$, gave inferior results. It was also confirmed that more electron-poor aryl bromides reacted faster in the oxidative addition step, and that the sterics and electronics of the aminostannane were very important in determining intrinsic reactivity. For instance, larger aminostannanes derived from *n*-hexylamine and *N*-methylcyclooctylamine did not react under the conditions tested. This was presumed to be due to the steric bulk of the $\text{P}(o\text{-tolyl})_3$ ligands obstructing ligand exchange.²⁴⁵

Despite the importance of these transamination reactions for extending the scope of C-N coupling reactions, it was a year later that both Buchwald and Hartwig published work detailing the development of tin-free coupling of primary and secondary amines with aryl bromides, through the use of an additional bulky base.^{246,247}

Buchwald *et al.* detailed the use of a slight stoichiometric excess of sodium *tert*-butoxide (NaO^tBu) in conjunction with $[\text{PdCl}_2(\text{P}(o\text{-tolyl})_3)_2]$ or $[\text{Pd}(\text{dba})_2]/2 \text{P}(o\text{-tolyl})_3$ to couple primary and secondary amines with aryl bromides. They found that when K_2CO_3 or NaOMe were used there was no conversion to the product. Hartwig *et al.* detailed the use of lithium silylamide $\text{LiN}(\text{SiMe}_3)$ (LHMDS) as base to successfully conduct *N*-arylation reactions, and noted much slower conversions were obtained using LiO^tBu or NaO^tBu as the base.²⁴⁷



Scheme 74: Buchwald-Hartwig catalytic cycle for palladium- and base-mediated *N*-arylation.²⁴⁸

Hartwig *et al.* proposed that the dimeric Pd(II) complex would break-down into the monophosphine complex to facilitate addition of the amine, and once conjugated the acidity of the amine proton would be enhanced.²⁴⁷ Deprotonation using the bulky silyl amide base would result in formation of an amido complex, which would rapidly undergo reductive elimination to afford the arylamine product. This proposed catalytic cycle, as shown in **Scheme 74**, has since been largely maintained as the accepted mechanism for the Buchwald-Hartwig coupling reaction.²⁴⁸

1.6.3.2.3.2. Catalyst and ligand systems.

Through the use of bidentate and bulky phosphine ligands, the scope of the Buchwald-Hartwig *N*-arylation reaction has advanced significantly. The use of P(*o*-tolyl)₃ ligands had been strongly emphasized by Buchwald, Hartwig and Migita, with the general consensus that the enhanced steric constraints of the *o*-tolyl group helped to reduce formation of bisphosphine-palladium complexes.²⁴⁹ This was desirable as it had been proven by Hartwig that the monophosphine palladium complex was the active species in the catalytic cycle.²⁴³ However, significant β -hydride elimination was noted when this ligand system was used for the coupling of primary amines and aryl bromides.

Buchwald *et al.* found that, through the use of the chelating bisphosphine ligand BINAP and the bispalladium catalyst Pd₂(dba)₃ in the presence of NaO^tBu, yields of *N*-arylation using primary amines were drastically improved.²⁴⁹ Reduction in the extent of β -hydride elimination was speculated to be due to inaccessibility of the unsaturated three-coordinate monophosphine from the BINAP ligated complex.

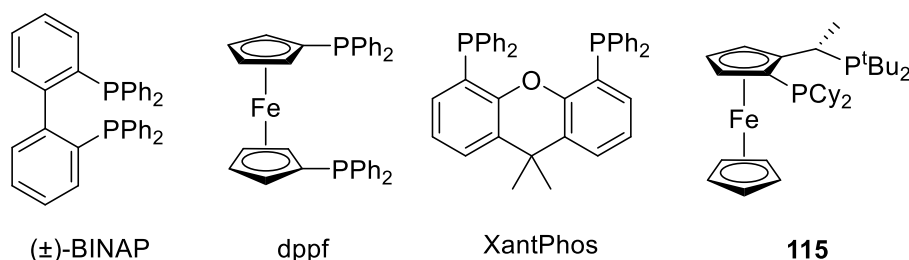


Figure 33: Examples of bisphosphine ligands: racemic BINAP, dppf, XantPhos and hindered ferrocenyl alkyl bisphosphine **115**.²⁵²

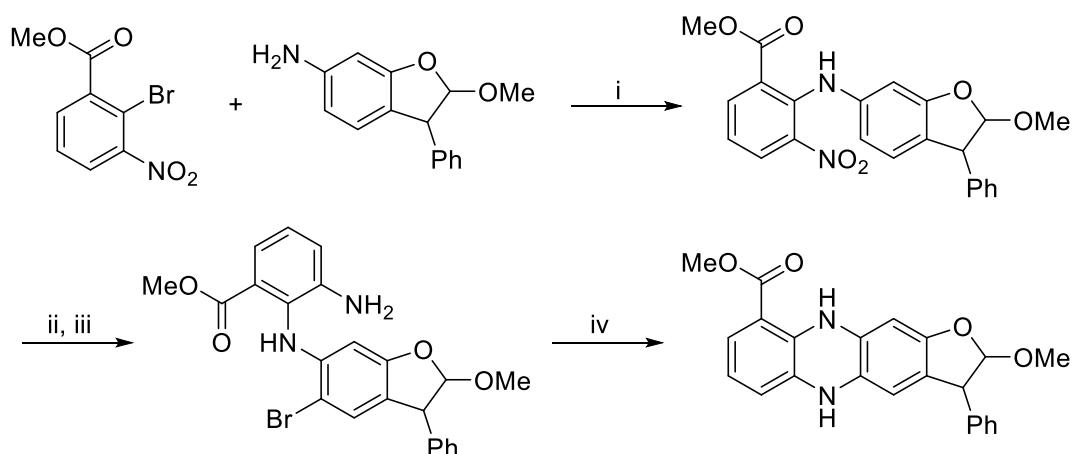
There have been a number of generations of catalyst-ligand systems developed for Buchwald-Hartwig coupling, including integration of more complex aromatic bisphosphine ligands such as

dppf and XantPhos used similarly to BINAP (see **Figure 33**). More sterically-hindered alkyl monophosphines and NHCs have been used for the activation of less-reactive aryl halides,^{248,250,251} and the use of hindered ferrocenyl alkyl bisphosphines (for example, **115**) have been documented to extend catalyst lifetimes to improve catalyst efficiency.²⁵²

1.6.3.2.3.3. Applications in medicinal chemistry.

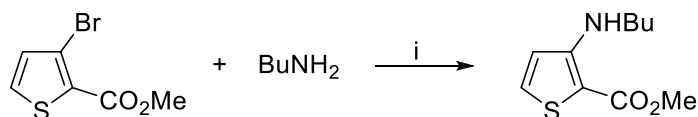
The impressive advances that have been made in the coupling of aryl halides and amines using Buchwald-Hartwig chemistry has opened up a whole field of efficient and tolerant methods for the synthesis of pharmaceutically and industrially-relevant compounds.²⁵³

For example, Kamikawa *et al.* in their preparation of polysubstituted phenazines, which have been noted for their interesting biological activities, adopted two sequential Buchwald-Hartwig *N*-arylation reactions to construct a fused heterocyclic ring system (see **Scheme 75**).²⁵⁴



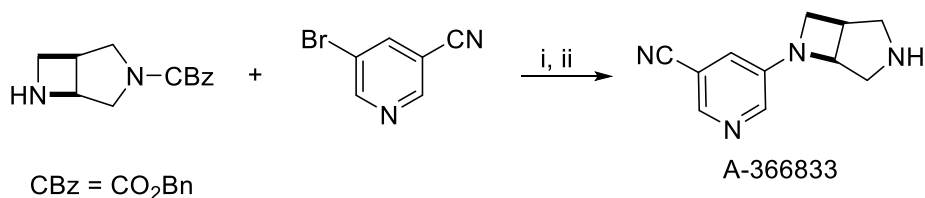
Scheme 75: Kamikawa *et al.*'s Buchwald-Hartwig mediated synthesis of phenazines. Reaction conditions: i) Pd(OAc)₂, BINAP, Cs₂CO₃, toluene, 100 °C, 99%; ii) H₂, Pd(C), EtOAc, 100%; iii) Br₂, NaHCO₃, CHCl₃, 91%; iv) Pd(OAc)₂, BINAP, Cs₂CO₃, toluene, 100 °C, 50%.²⁵⁴

The base and catalyst system used in this total synthesis was a slight variation on those discussed previously, with the use of the milder base Cs₂CO₃ endowing wider functional group tolerance.²⁵⁵ For instance, Luker *et al.* developed a milder *N*-arylation route to couple methyl 3-bromothiophene-2-carboxylates and primary amines, using Cs₂CO₃ with Pd₂(dba)₃ or Pd(OAc)₂ and BINAP in toluene (see **Scheme 76**).²⁵⁶ They found that use of other metal carbonates or tertiary amines as the base gave inferior results, and that use of NaO^tBu resulted in formation of the amide side product.



Scheme 76: Luker *et al.*'s Buchwald-Hartwig coupling of methyl bromobenzothiophene-2-carboxylates. Reaction conditions: i) $\text{Pd}_2(\text{dba})_3$, BINAP, Cs_2CO_3 , toluene, 94%.²⁵⁶

The analgesic and selective $\alpha 4\beta 2$ neuronal nicotinic receptor (NNR) antagonist A-366833 has also been constructed using Buchwald-Hartwig coupling in the final step of the total synthesis.²⁵⁷ The group developed a convergent synthetic route, separately building an enantiomerically pure fused diazabicyclo[3.2.0]heptane unit, before coupling with an aryl bromide using the $\text{Pd}_2(\text{dba})_3$ /BINAP catalytic system.



Scheme 77: Ji *et al.*'s Buchwald-Hartwig coupling step for the synthesis of NNR antagonist A-366833. Reaction conditions: i) $\text{Pd}_2(\text{dba})_3$, BINAP, Cs_2CO_3 , toluene, 100 °C, 40 h, 73%; ii) TFA, 65 °C, 1 h, 93%.²⁵⁷

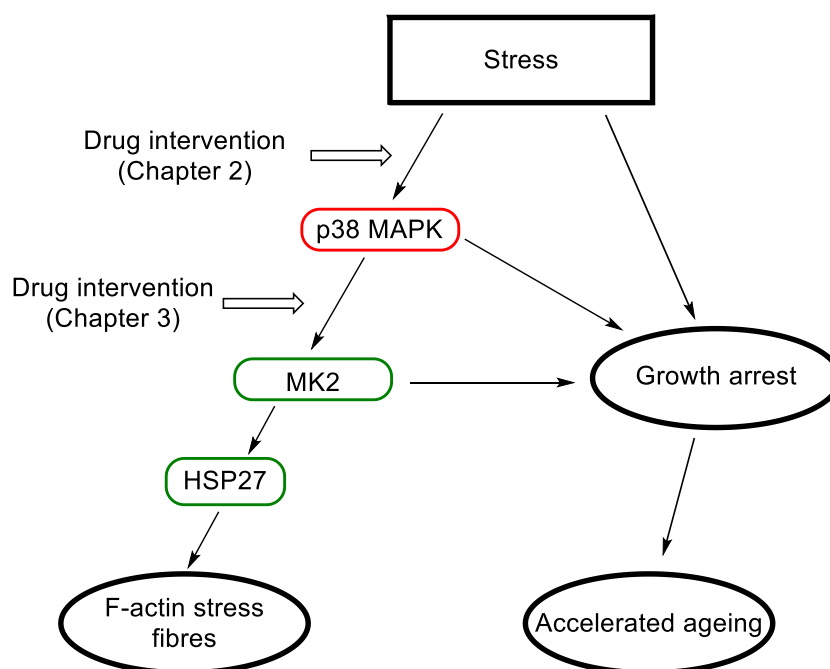
The group found that when they used $t\text{BuONa}$ as base for the coupling, only a 47% yield was achieved after 10 h, with significant production of the *tert*-butoxide exchange partner. However, through the use of Cs_2CO_3 this was circumvented, and the CBz (benzyl carbamate) protecting group could be safely removed to give the final product in high yield (see **Scheme 77**).

Buchwald-Hartwig *N*-arylation is a mild and efficient method for the synthesis of aryl amines, and was adopted as the method of choice for a key *N*-arylation step during the construction of the fused heterocyclic scaffold for PF-3644022 (**25**) in this project (see **Chapter 3**).

1.7. Overall project objectives.

The goals of this project were to deconvolute the stress-signalling pathways which contribute to accelerated ageing in the progeroid syndrome WS. The project aims were to corroborate previous biological studies completed on WS cells using p38 MAPK inhibitors, to establish the major p38-mediated pathways contributing to premature cellular senescence and to explore the potential of p38 MAPK inhibitors to be re-purposed as chemical probes.

Therefore the aims of this project were to synthesize the p38 MAPK inhibitor RO3201195 (**10**) and the MK2 inhibitor PF-3644022 (**25**) in sufficient yields and purity for biological studies, to verify the ability of the inhibitor to modulate their target in WS cells, and ascertain the role of the targets in accelerated ageing in WS (see **Scheme 78**).



Scheme 78: Investigating the stress-signalling pathways which contribute to accelerated ageing in Werner syndrome.

Additionally, studies were to be completed to explore the potential of the p38 MAPK inhibitor BIRB 796 (**14**) towards drug-repurposing. By altering the steric and electronic features of the *N,N'*-diaryl urea pharmacophore an analogue library would be synthesized. This library would then be tested against a panel of kinases of interest for their role in the MAPK stress-signalling cascade, in cell-proliferation and in age-related diseases such as cancer and Alzheimer's disease.

Chapter 2. RO3201195. Corroborating the role of p38 α MAPK on accelerated ageing in WS cells.

2.1. Background and aims.

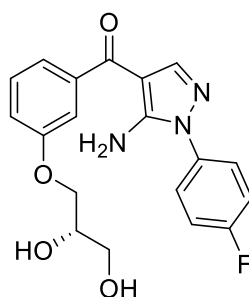
One of the biggest limitations in the development of small molecule p38 α inhibitors for therapeutic use has been their lack of selectivity.²⁸ Bain *et al.* identified this lack of selectivity to be true for a number of ‘specific’ inhibitors and urged caution in their application, instead suggesting parallel testing of inhibitors targeting the same protein to assess and confirm physiological effects.³²

One of the most promising p38 α inhibitor pharmacophores identified over the past decade is that of the 5-aminopyrazole ketone RO3201195 (**10**). This chemotype demonstrated a unique binding mode, exploiting an amino acid residue in the p38 ATP-binding pocket that is rare to the human kinome, endowing an additional degree of selectivity not present in other type 1 p38 α MAPK inhibitors (see **Section 1.3.2.**).

The aim of the first part of this project was to synthesize RO3201195 (**10**) to explore its biological properties in WS cells, to investigate new routes towards key intermediates and utilize microwave-assisted dielectric heating to improve efficiency and yields. The efficacy of RO3201195 (**10**) as a p38 α inhibitor in WS^{tert} fibroblasts has been verified by Bagley *et al.*,²⁵⁸ and this project aimed to advance this research by investigating the effect of RO3201195 (**10**) on the rate of proliferation of WS primary cells. By drawing a direct comparison against the prototypical p38 α inhibitor SB203580 (**1**) it was hoped that a better understanding of the function of p38 α and the MAPK stress-signalling pathway and their roles in the premature aging of WS cells could be gained.^{14,19}

2.1.1. RO3201195: Hit-to-lead optimization of a highly selective p38 MAPK inhibitor.

RO3201195 (**10**) was developed as one candidate in an extensive drug discovery programme led by Goldstein *et al.* at Roche towards the development of novel and selective small molecule inhibitors of p38 α , for the modulation of TNF- α and IL- β cytokine production.⁴⁵



RO3201195 (**10**)

Figure 34: Selective p38 α MAPK inhibitor RO3201195 (**10**).

HTS at Roche identified the 4-benzoyl-5-aminopyrazole **116** as a new lead in the development of potent and selective p38 α inhibitors.⁴⁵ Co-crystallization of **116** with unphosphorylated p38 α identified a novel hydrogen bonding interaction between the *exo*-cyclic amine and the side chain hydroxyl group of threonine 106, as discussed in Section 1.3.2. It was postulated that this *exo*-cyclic amine could bestow significant kinase selectivity to the inhibitor.

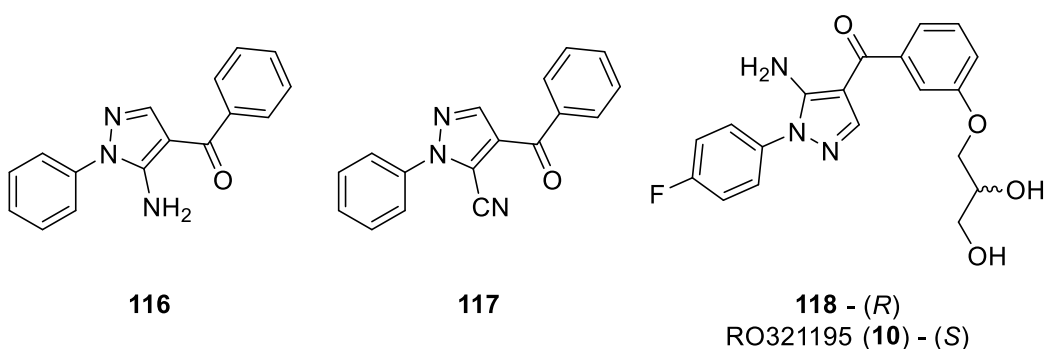


Figure 35: Hit-to-lead optimization of 5-aminopyrazole p38 inhibitors.⁴⁵

Preliminary studies by Goldstein *et al.* confirmed the importance of the 5-amino group, with complete loss of binding affinity for p38 α observed for 5-hydroxyl or 5-cyanopyrazole analogues (such as **117**). Additionally, it was found that only small hydrophobic substituents were tolerated on the 1*N*-pyrazole aryl substituent, with the most favourable group found to be a 4-

fluorophenyl. Subsequent X-ray co-crystallization studies rationalized this as, when bound to the kinase, the phenyl ring slotted into a hydrophobic region at the back of the ATP-binding pocket, and so any large or hydrophilic substituents would not be well tolerated.

Initial stages of lead optimization concentrated on improving the pharmacokinetics (PK) of the pyrazole group, as the compounds had been found to be extremely insoluble. Installation of ionizable and polar groups connected via linkers at the *meta*-position of the benzoyl ring were found to dramatically improved solubility, but also resulted in severe off-target effects. Therefore, the group focused on non-ionizable solubilizing groups, and incorporated amides, ethers and alcohols into their scaffold.

The glycerol based diols **118** and **10** were both found to be extremely potent inhibitors, though the (*S*)-enantiomer (**10**) demonstrated enhanced PK properties, with higher relative bioavailability, a lower rate of clearance, and favourable pharmacodynamics (PD) with a high selectivity for p38 α against a panel of 105 kinases.

In pharmacological studies, Goldstein *et al.* found that RO3201195 (**10**) decreased production of pro-inflammatory cytokines, including TNF- α and IL- β , in a concentration dependent manner *in vitro* and *in vivo*.

2.1.2. Application in WS cells.

Continuing their work into the effect of p38 α inhibitors on the growth rate of WS fibroblasts (see **Chapter 1**), Bagley *et al.* sought to verify the activity of RO3201195 (**10**) and related 5-aminopyrazol-4-yl ketones as p38 α inhibitors in WS cells.²⁵⁸

An aspect of great interest for the group was to ascertain whether **10** exhibited any off-target activity, especially with respect to Jun N-terminal kinases (JNKs). JNKs are another MAPK subfamily and a well-known subject of off-target activity for many p38 α inhibitors, including SB203580 (**1**) and BIRB 796 (**14**).^{10,259} Hence, when using RO3201195 (**10**) as a probe for p38 α activity in WS fibroblasts, ascertaining its propensity for off-target activity with other stress-signalling kinases was an issue of high priority.

The inhibitors were tested through the use of ELISA and immunoblot assays,ⁱⁱ using telomerase immortalized human cells and WS^{tert} cells. ELISA assays rely on antibodies which detect the

ⁱⁱ ELISA: Enzyme-linked immunosorbent assay. All biological testing for Bagley *et al.* BMCL 2008 conducted at the Department of Pathology, Cardiff University.²⁵⁸

activity of specific kinases and calculate the ratio of phosphorylated kinase to total protein. The cells were treated with relevant concentrations of respective inhibitors and activated with anisomycin, an antibiotic which up-regulates stress-signalling kinases. Blank and activated controls of the cells were grown to provide baseline and maximal activity of the kinases under investigation.

Through the use of ELISA assays on telomerase immortalized human cells, the activity of RO3201195 (**10**) as asserted by Goldstein *et al.* was verified, with inhibition of anisomycin-induced activity of p38 α observed upon treatment with **10** in a concentration-dependent manner.²⁵⁸ Anisomycin-induced JNK activation did not appear to be inhibited. However, no definitive target-specific conclusions could be drawn as the ELISA assay could not differentiate between JNK1 and JNK2 activation. Hence it was unclear whether **10** exhibited its inhibitory effects specific to one of the isoforms of JNK.

Treatment of WS^{tert} cells with RO3201195 (**10**) was analyzed using Western blot, phosphorylation state of anisomycin-activated p38 α , MK2 and HSP27 proteins (see **Figure 36**).

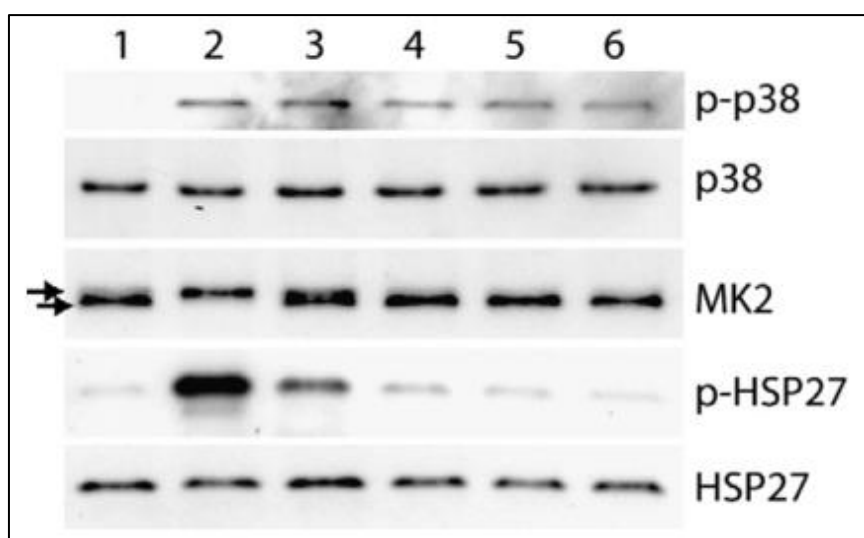


Figure 36: Bagley *et al.*'s Western blot analysis of WS^{tert} cells treated with RO3201195 (**10**). Lane 1: Control cells; Lane 2: Activated cells; Lane 3-5: Activated WS^{tert} cells, pre-treated with **10** at 2.5, 10.0 and 25.0 μ M concentration, respectively; Lane 6: Activated WS^{tert} cells, pre-treated with SB230580 (**1**) at 2.5 μ M concentration.²⁵⁸

In the immunoblot analysis, the control WS cells (Lane 1) showed low levels of activated p38 α as assessed by the presence of activated MK2, as indicated by the upper band in the MK2 row. This is indicative of the upregulation of this stress-signalling pathway in WS^{tert} cells.¹⁰

WS^{tert} cells were pre-treated with three different concentrations of **10** before activation with anisomycin, and it was found that activity of the p38 stress-signalling cascade was inhibited in a

concentration-dependent manner, with progressively lower levels of *p*-HSP27 (phosphorylated HSP27) observed across lanes 3 to 5 as the concentration of **10** increased from 2.5 to 25 μ M.

Lane 6 was a comparative immunoblot using the prototypical p38 inhibitor SB203580 (**1**), to observe whether the two different p38 α inhibitors affected WS cells in distinct ways. It was found that pre-treatment with **10** at 10 and 25 μ M concentration exhibited very similar profiles to pre-treatment with SB203580 (**1**) at 2.5 μ M (**Figure 36**, lanes 4, 5 and 6). Very low levels of *p*-HSP27 similar to that of control lane 1 were observed, and no activation of MK2, as indicated by the lack of the upper band in the MK2 row.²⁵⁸

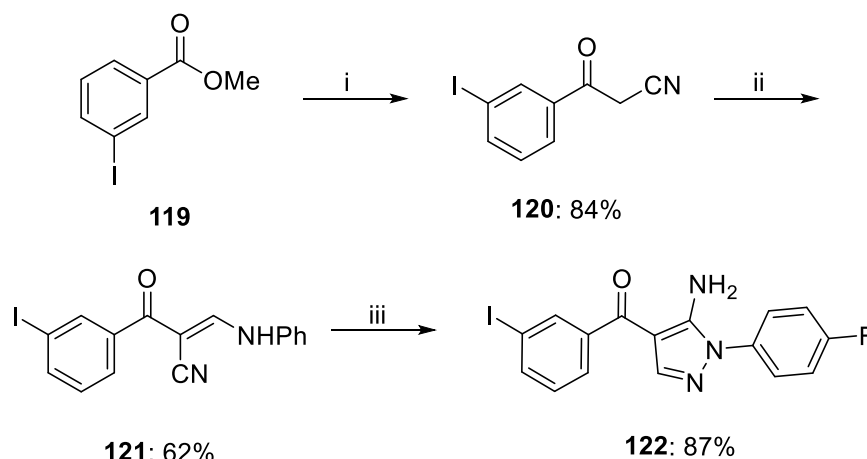
From this data, it was inferred that both SB203580 (**1**) and RO3201195 (**10**) inhibited the stress-signalling pathway mediated by *p*-p38 α and MK2 activation in WS^{tert} cells; the stress-signalling pathway believed to transduce genomic stress in WS cells.^{10,14}

It was determined that further tests needed to be conducted in order to ascertain whether the p38 α -selective inhibitor **10** would exhibit the same effect on the rate of WS fibroblast cell proliferation observed following treatment with SB203580 (**1**) (**Chapter 1.2**), and to determine unequivocally whether **10** inhibited either of the JNK isoforms to any significant extent.

2.2. Synthetic routes towards RO3201195.

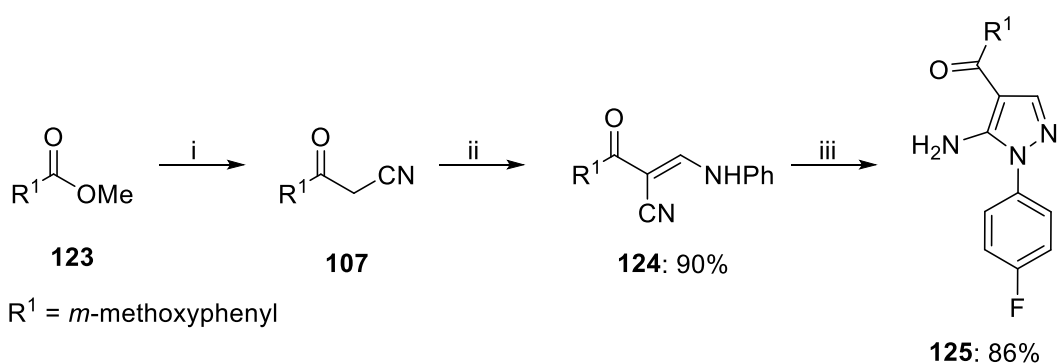
Goldstein *et al.*'s original publication on the discovery, synthesis and biology of RO3201195 (**10**) was not accommodating for replication of the synthesis, with no yields or experimental methods given that directly related to the total synthesis of **10**.⁴⁵ Bagley *et al.* developed their own synthetic route towards **10** in order to verify its activity as a p38 α inhibitor in WS cells, and adopted microwave-assisted techniques to facilitate higher yields and shorter reaction times.²⁵⁸

For synthesis of their benzoylpyrazole library, Goldstein *et al.* chose a combinatorial approach, with pre-functionalized or functionalizable groups installed on the phenyl ring prior to cyclocondensation of the pyrazole. For instance, towards **122** (see **Scheme 79**), Claisen ester condensation of methyl 4-iodobenzoate (**119**) with acetonitrile (MeCN) gave benzoylacetonitrile **120**, and homologation with *N,N*-diphenylformamidine afforded enamine **121**. Cyclocondensation of **121** with a functionalized hydrazine afforded the 1,4-disubstituted-5-aminopyrazole **122** in high yield.⁴⁵



Scheme 79: Goldstein *et al.*'s synthesis of intermediate 5-aminopyrazoles. Reaction conditions: i) MeCN, *n*-BuLi, DIPA, THF $-50\text{ }^{\circ}\text{C}$, 3 h, 84%; ii) *N,N'*-diphenylformamidine, toluene, Δ , 8 h, 62%; iii) 4-fluorophenylhydrazine, EtOH, Δ , 30 min, 87%.⁴⁵

When a halogen was installed on the aromatic ring, such as in iodinated intermediate **122**, Goldstein *et al.* were able to readily functionalize the aryl ring through metal-mediated coupling techniques to assess the viability of different substituents and substitution patterns on the benzoyl ring for their binding affinity with p38 α .

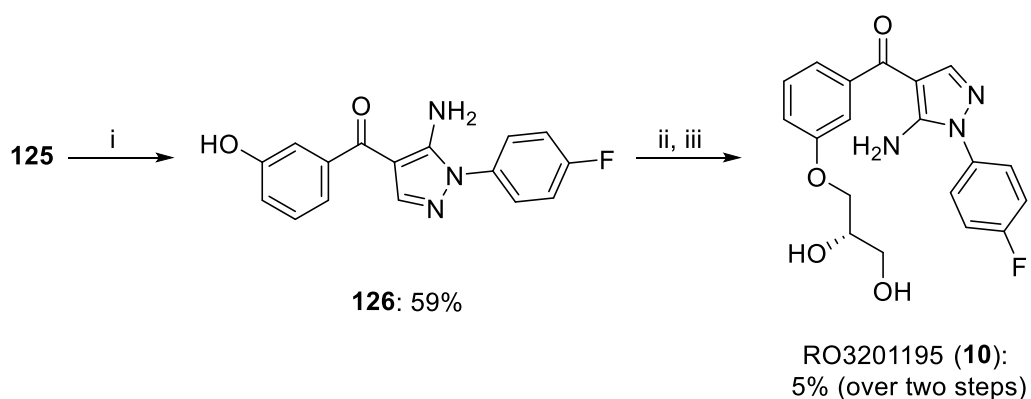


Scheme 80: Bagley *et al.*'s microwave-mediated synthesis of 1,4-disubstituted-5-aminopyrazole **125**. Reaction conditions: i) MeCN, NaOEt, $80\text{ }^{\circ}\text{C}$; ii) *N,N'*-diphenylformamidine, xylenes, MW $180\text{ }^{\circ}\text{C}$, 20 min, 90%; iii) 4-fluorophenylhydrazine hydrochloride, NEt_3 , EtOH, MW $140\text{ }^{\circ}\text{C}$, 1 h, 86%.²⁵⁸

Bagley *et al.* adopted a similar constructive strategy, forming intermediate **107** through Claisen condensation of methyl ester **123** with MeCN and NaOMe (no yields provided). Formylation with *N,N'*-diphenylformamidine provided enamine **124** in 85% yield, after heating to reflux for 2 h in dry xylenes. The group adopted microwave-assisted techniques to shorten reaction times and improve yields, with irradiation at $180\text{ }^{\circ}\text{C}$ for 20 minutes giving **124** in 90% yield (see **Scheme 80**).²⁵⁸ 5-Aminopyrazole **125** was synthesized in 86% yield when **124** was irradiated with 4-fluorophenylhydrazine hydrochloride and NEt_3 in ethanol for 1 h at $140\text{ }^{\circ}\text{C}$. This method was also

used by Bagley *et al.* in their synthesis of a small pyrazoyl library based upon the RO3201195 (**10**) pharmacophore for use as probes in WS cells.^{1,260}

Functionalization of **125** to RO3201195 (**10**) was conducted similarly by both Goldstein *et al.* and Bagley *et al.*, though Goldstein did not publish yields or experimental procedures for some steps. Protodemethylation of **125** using boron tribromide conducted by Bagley *et al.* proceeded to give a reasonable yield, though subsequent *O*-alkylation of **126** using an acetal-protected chiral glycerol tosylate and acidic deprotection towards **10** suffered from low yields (see **Scheme 81**). Nevertheless, for their purposes, enough material was synthesized to conduct the biological tests described in **Chapter 2.1.2**.



Scheme 81: Bagley *et al.*'s synthesis of RO3201195 (**10**).²⁵⁸ Reaction conditions: i) BBr_3 , CH_2Cl_2 , 0 °C to RT, 2.5 h, 59%; ii) (*S*)-L- α,β -isopropylidenglycerol- γ -tosylate, K_2CO_3 , DMF, 80 °C, 24 h, 9%; iii) *p*-TsOH, MeOH, H_2O , 50 °C, 18 h, 48%.²⁵⁸

2.2. Deconstructing RO3201195.

Over the course of this project several alternative synthetic methods were explored for the construction of RO3201195 (**10**), in addition to adapting the routes tried and tested by Goldstein *et al.* and Bagley *et al.* Endeavours were made to explore new synthetic methods towards intermediates and, when adapting routes used previously in the literature, every effort was made to improve yields, and to construct an overall more efficient, streamlined total synthesis of **10**.

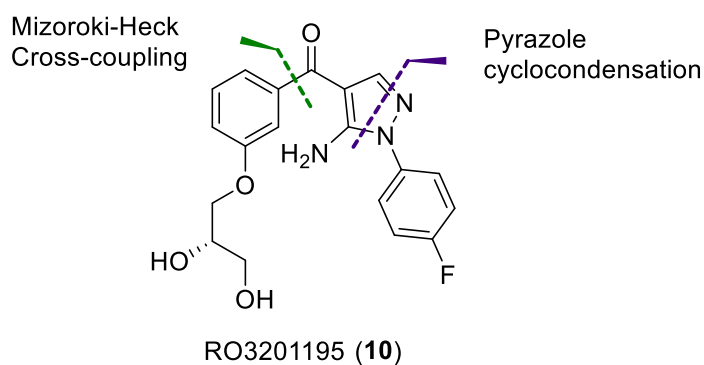


Figure 37: Retrosynthetic strategy for the synthesis of RO3201195 (**10**). Proposed Mizoroki-Heck aryl cross-coupling and pyrazole constructive strategy.

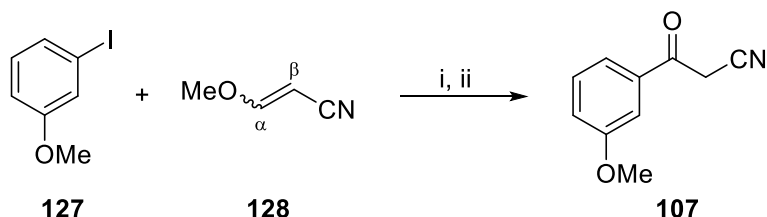
One of the major adaptations explored in an effort to facilitate a more efficient and streamlined synthesis was an alternative carbon-carbon bond forming reaction using the metal-mediated Mizoroki-Heck coupling (see **Figure 37** and **Chapter 1.6.3.2.1**).

The spatial arrangement of substituents on the pyrazole pharmacophore is extremely important for optimal ligand-kinase interactions with p38 α . There are many methods to synthesize pyrazoles; however for this specific substitution pattern there are a limited number of routes available (see **Chapter 1.6.2.1**).

2.3. Synthesis of RO2301195.

2.3.2. Benzoylacetonitrile synthesis.

As mentioned in **Chapter 1.6.3.2**, it was hypothesized that rather than adopting traditional Claisen condensation chemistry towards benzoylacetonitrile **107**, an alternative route was proposed through the use of palladium-mediated Heck coupling of iodoanisole **127** and acrylonitrile **128** (see **Scheme 82**).

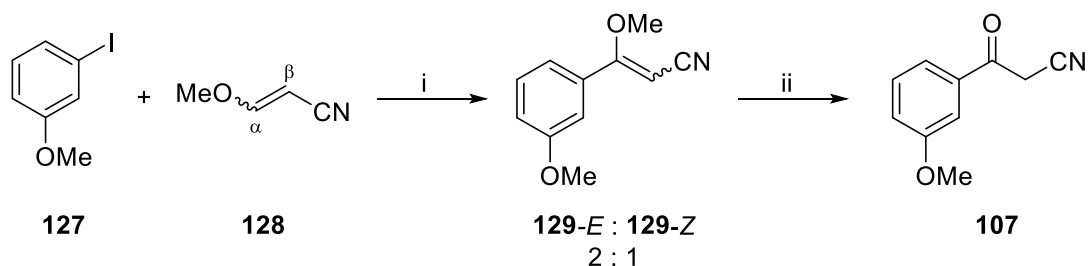


Scheme 82: Proposed Heck coupling towards intermediate benzoylacetonitrile **107**. Reaction conditions: i) Heck coupling conditions; ii) acidic hydrolysis.

It was predicted that coupling would occur at the α -position of the alkene to generate an intermediate enol ether, with subsequent acidic hydrolysis of the coupled product affording the desired benzoylacetonitrile **107**.¹⁹⁶

2.3.2.1. Application of Heck coupling towards the synthesis of benzoylacetonitriles.

For the desired coupling of 3-iodoanisole **127** and 3-methoxyacrylonitrile **128**, it was found that Jeffery's conditions had been used to great effect for related acrylonitriles¹⁹⁷ and α -methoxyacrylates²⁶¹ using TBAB, Pd(OAc)₂ and an inorganic base in an aqueous-solvent mixture.²¹¹ Coupling trials using this system were conducted to test the feasibility of the reaction.



Scheme 83: Heck coupling of 3-iodoanisole **127** and 3-methoxyacrylonitrile **128**. Reaction conditions: i) Pd(OAc)₂ (10 mol%), TBAB (10 mol%), K₂CO₃ (2 equiv.), MeCN-H₂O (3:1), MW 130 °C, 1.5 h; ii) conc. HCl-MeOH (1:4), MW 110 °C, 30 min, 20%.

3-Iodoanisole was reacted with an excess of 3-methoxyacrylonitrile in an MeCN-H₂O mixture using Pd(OAc)₂ (10 mol%) catalyst, TBAB (10 mol%) additive, and two equivalents of K₂CO₃ base. The reaction mixture was irradiated using microwave-assisted dielectric heating to 130 °C in a sealed vessel for 1.5 h (see **Scheme 83**). Formation of the desired α -aryl enol ether **129** was confirmed by ¹H NMR spectroscopic analysis, after aqueous work up, as a mixture of (*E*)- and (*Z*)-diastereoisomers in an approximate 2:1 ratio (see **Figure 38**).

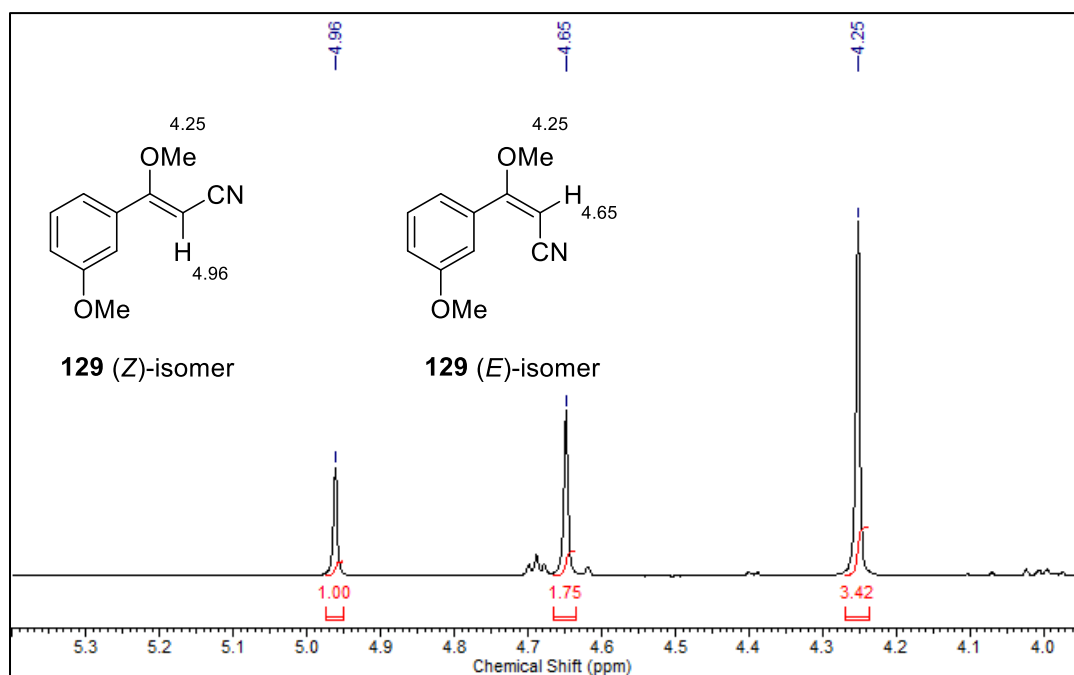


Figure 38: Crude ¹H NMR spectrum (500 MHz, CDCl₃, δ_H 5.5 - 4.0 ppm) illustrating the two alkenyl protons of the (*E*)- and (*Z*)-isomers of **129**. Integration of peaks gives the diastereomeric ratio as approximately 2:1.

The diastereoisomers could be separated by flash column chromatography, though they were isolated in variable and poor yield. The two diastereoisomers were differentiated by two-dimensional ¹H NMR spectroscopic NOSEY analysis (see **Figure 39**) and by reference to similar 3-aryl-3-ethoxyacrylonitriles in the literature.²⁰¹

The mixture of diastereoisomers and poor isolated yield were not anticipated to be an issue for the total synthesis of RO3201195 (**10**) as it was intended that the crude material would be hydrolyzed directly to form benzoylacetone nitrile **107**.

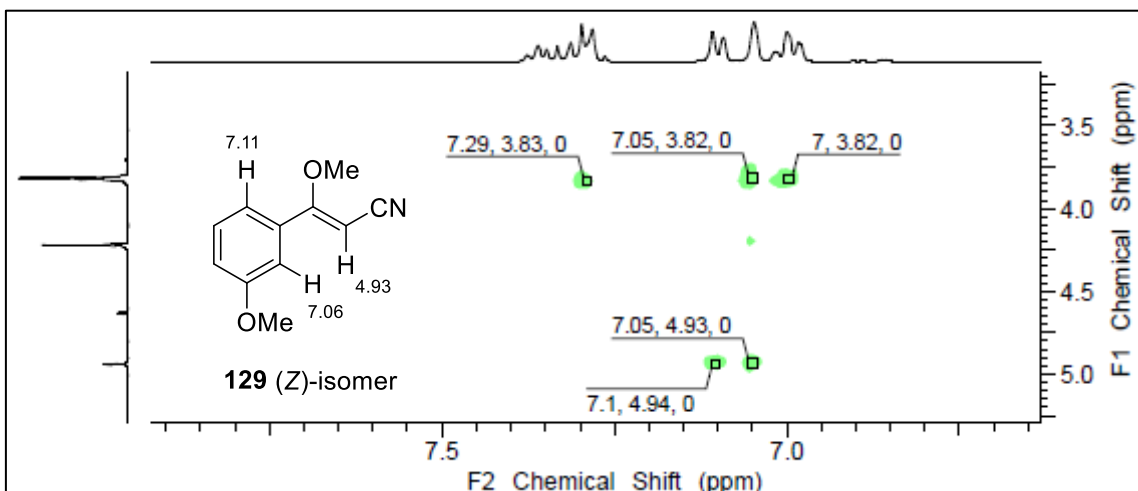
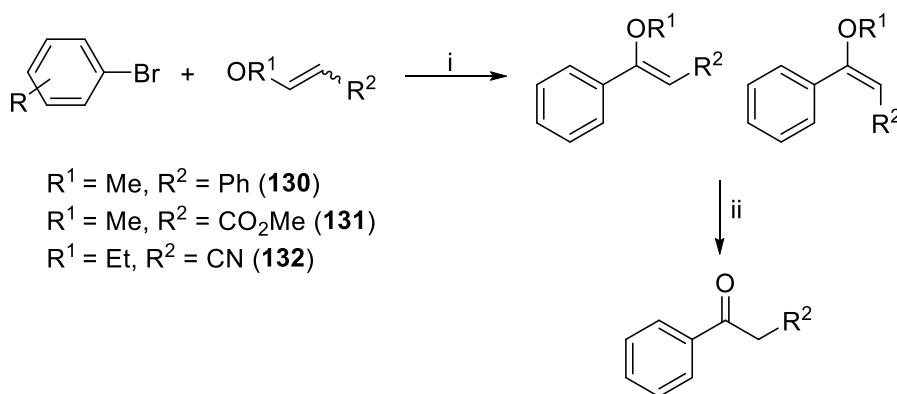


Figure 39: ^1H NMR 2D NOSEY experiment (X-axis δ_{H} 8 - 6.5 ppm, Y-axis δ_{H} 5.5 - 3 ppm). (Z)-isomer of **129** identified from through-space interaction of alkenyl proton at δ_{H} 4.93 ppm and the *ortho*-benzoyl protons at δ_{H} 7.11 and 7.06 ppm.

Unexpectedly, it was found that the enol ether intermediate **129** was quite stable under typical acidic hydrolysis conditions. Doucet and Santelli worked with α - and β -disubstituted enol ethers when exploring the utility of a new tetraphosphane/palladium complex for Heck arylations, including β -methoxystyrene (**130**), methyl 3-methoxyacrylate (**131**) and 3-ethoxyacrylonitrile (**132**) (see **Scheme 84**).¹⁹⁶ They successfully synthesized the α -enol ether intermediates of all derivatives and hydrolyzed them to the 1-arylpropanones under relatively mild conditions, using a THF/ H_2O /HCl mixture.²⁰¹ However, it was notable that they did not hydrolyze the 3-aryl-3-alkoxyacrylonitriles.



Scheme 84: Doucet and Santelli's Heck reaction to form benzoylacrylates. Reaction conditions: i) $[\text{Pd}(\text{C}_3\text{H}_5\text{Cl})_2]/0.5$ Tedicyp, DMF, NaHCO_3 , 150°C ; ii) HCl or H_2SO_4 , THF, H_2O , 25°C .¹⁹⁶

Towards benzoylacetonitrile **107**, the diastereomeric mixture of **129** was eventually hydrolyzed successfully using microwave-assisted dielectric heating of the crude mixture, after aqueous work up, at 110 °C for 30 minutes in a solution of concentrated HCl and MeOH. Application of this method to the aforementioned crude material, gave modest yields of **107** after purification by flash column chromatography over the two steps (**Table 1**, entry 4, 20%).

Table 1: Heck reaction conditions for the synthesis of benzoylacetonitrile 107 (Scheme 83). ^a					
Entry	Time (h)	Base	Additive	Temp (°C)	% Yield ^b
1	24	K ₂ CO ₃	TBAB	90 ^c	36
2	24	NaHCO ₃	TBAB	90 ^c	34
3	1	K ₂ CO ₃	TBAB	130 ^d	26
4	1.5	K ₂ CO ₃	TBAB	130 ^d	20
5	1.5	NaHCO ₃	TBAB	130 ^d	37
6	1	K ₂ CO ₃	TBAB	140 ^d	19
7	1.5	K ₂ CO ₃	DPPP	150 ^d	31

^a Reaction conditions: 3-Iodoanisole (**127**) (1 equiv.), 3-methoxyacrylonitrile (**128**) (4 equiv.), base (2 equiv.), additive (10 mol%) and Pd(OAc)₂ (10 mol%) in MeCN:H₂O (3:1) under given conditions.
^b Isolated yield after aqueous work-up, microwave irradiation at 110 °C for 30 min in conc. HCl- MeOH (4:1) and purification by flash column chromatography.
^c Conductive heating.
^d Microwave dielectric heating. Held at temperature for indicated length of time through modulation of the initial power (150 W).

Under conductive heating conditions the viability of the popular inorganic bases K₂CO₃ and NaHCO₃ were assessed.^{197,201,211,261} After 24 h at 90 °C using the above mentioned conditions there was some improvement in the yield over the microwave-assisted conditions, with K₂CO₃ giving a modest yield (**Table 1**, entry 1, 36%) and a slight improvement over NaHCO₃ (entry 2, 34%).

Microwave-assisted heating in a sealed tube at elevated temperatures was further probed. With K₂CO₃ as the base, irradiation at 130 °C for 1 h (entry 3, 26%) and 1.5 h (entry 4, 20%) gave lower yields compared to the conductive heating route. The use of NaHCO₃ improved the yield modestly under microwave-assisted heating (entry 5, 37%), comparable to those yields achieved under conductive heating. Raising the reaction temperature to 140 °C was found to be detrimental to yields (entry 6).

A ligated system using the bidentate ligand 1,3-bis(diphenylphosphine)propane (DPPP) was also investigated. After irradiation at 150 °C for 1.5 h and the established acidic work-up, a lower

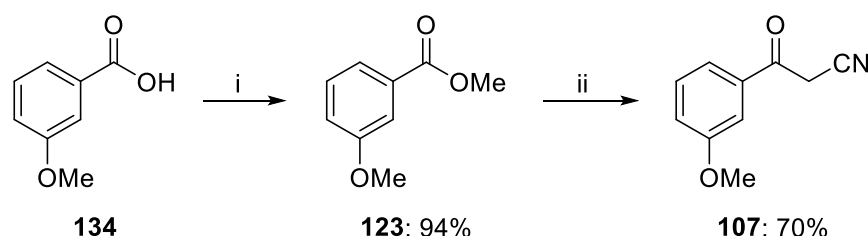
yield was achieved than the ligand-less systems (entry 7, 31%), corroborating that Jeffery's conditions were better suited for this coupling reaction.

These studies illustrated that, though a Heck-mediated synthetic route towards **107** was viable, the additional step required for hydrolysis, and the modest yields achieved (**Table 1**, entry 5, 37%), did not support this method as the most efficient route for the synthesis of RO3201195 (**10**). Therefore, alternative methods were explored for their utility and compared with the Heck-mediated route.

2.3.1.4. Claisen condensation routes for the synthesis of benzoylacetoneitrile.

A more traditional Claisen condensation approach, akin to those adopted by Goldstein *et al.* and Bagley *et al.* in their total syntheses, was acknowledged as potentially a more efficient route towards the benzoylacetoneitrile **107**.

Following the route illustrated in **Scheme 85**, Fischer esterification of 3-methoxybenzoic acid (**134**) gave methyl 3-methoxybenzoate (**123**) in excellent yields (90%) after heating to reflux with MeOH and catalytic sulfuric acid (H₂SO₄) for 3 h. Yields were improved upon subjecting the same reaction mixture to microwave-assisted heating in a sealed vessel at 110 °C for 10 minutes (94%).



Scheme 85: Fischer esterification and Claisen condensation for the synthesis of benzoylacetoneitrile **107**. Reaction conditions: i) Catalytic conc. H₂SO₄, MeOH, MW 110 °C, 10 min, 94%; ii) *n*-BuLi, DIPA, MeCN, THF -50 °C, 3 h, 70%.

Traditional Claisen condensation of methyl ester **123** had been explored by previous members of our research group using NaOMe or NaOEt as base to generate the acetonitrile anion. However, the immediate formation of intractable mixtures upon addition of the base frustrated these attempts and gave poor yields of the product (9%).¹

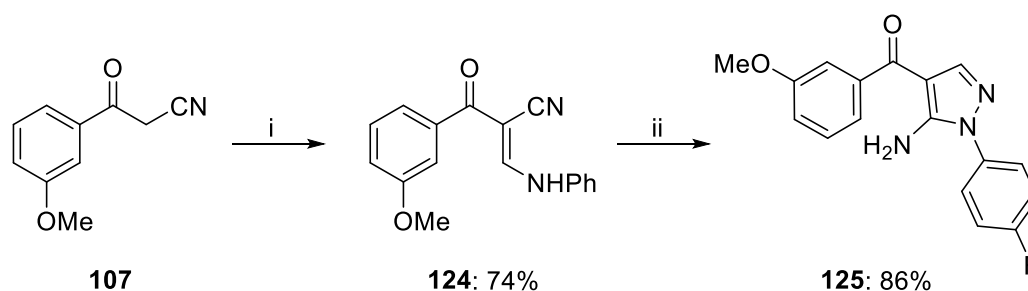
In order to improve this method two alternative, stronger bases were explored for the formation of the acetonitrile anion. Use of sodium hydride (NaH) in dry toluene and heating to 90 °C for 16

h gave **107** in 34% yield after aqueous work-up and purification by flash column chromatography. Further improvements were achieved with in situ formation of the bulky base lithium diisopropylamine (LDA), from the reaction of *n*-butyl lithium (*n*-BuLi) and diisopropylamine (DIPA) at $-50\text{ }^{\circ}\text{C}$. Slow addition of dry MeCN, followed by methyl 3-methoxybenzoate (**123**), and stirring at $-50\text{ }^{\circ}\text{C}$ for 3 h gave the desired benzoyl acetonitrile **107** in 70% yield after purification.

Given the improved yield and efficiency of this two-step approach, compared to the Heck coupling route, it was decided that the esterification-condensation method would be adopted to access the key benzoylacetonitrile intermediate.

2.3.2. Pyrazole formation.

The central 1,4-disubstituted-5-aminopyrazole scaffold of **10** was synthesized via a homologation and cyclocondensation strategy (see **Scheme 86**). A slight excess of *N,N'*-diphenylformamidine was used to conduct a Knoevenagel-type condensation with **107**. Microwave-assisted heating in a sealed vessel at $180\text{ }^{\circ}\text{C}$ for 20 minutes in dry xylenes gave enamine **124** in 74% yield after trituration with hexanes. Identification of the product was confirmed by ^1H NMR spectroscopic analysis, with a distinct loss of the methylene CH_2 protons of **107**, seen previously at δ_{H} 4.07 ppm, and addition of the enamine NH proton broad resonance downfield at δ_{H} 12.76 ppm (in CDCl_3).



Scheme 86: Synthesis of pyrazole scaffold **125**. Reaction conditions: i) *N,N'*-Diphenylformamidine, dry xylenes, MW $180\text{ }^{\circ}\text{C}$, 20 min, 74%; ii) 4-fluorophenylhydrazine hydrochloride, NEt_3 , EtOH, MW $140\text{ }^{\circ}\text{C}$, 1 h, 86%.

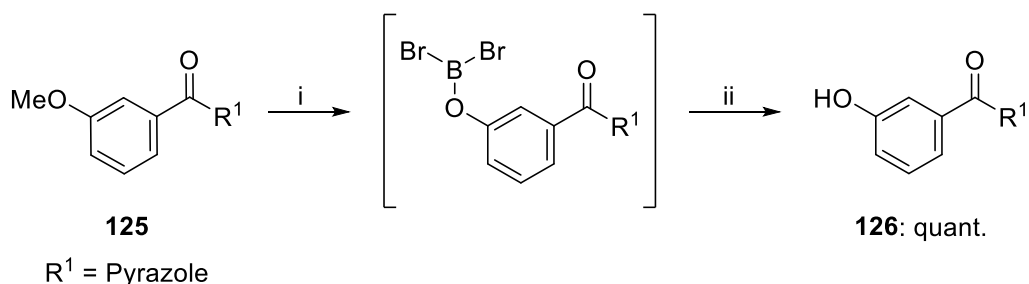
Enamine **124** was reacted with 4-fluorophenylhydrazine hydrochloride with catalytic amounts of NEt_3 , mediated by microwave-assisted heating in a sealed vessel at $140\text{ }^{\circ}\text{C}$ for 1 h, to afford pyrazole **125** in high yield (86%) after purification by flash column chromatography. The yield achieved was an improvement on that quoted by Bagley *et al.* for the same reaction conducted on a similar scale (124 mg; 68%).²⁵⁸

2.3.3. O-Alkylation and diol installation.

In order to functionalize the benzoyl ring, the methoxy protecting group was cleaved to expose the phenol group of **126**. Traditional ether deprotection methods can be very harsh, including conditions such as refluxing in HBr.²⁶² In order to improve functional group tolerance, milder deprotective strategies have been developed, employing nucleophilic displacement routes such as base-mediated reactions with thiols and mildly Brønsted acidic and Lewis acidic techniques.²⁶² Boron tribromide (BBr₃) is a popular Lewis acidic reagent for protodemethylation of aryl methyl ethers that can operate at or below room temperature, and has a high tolerance for other functional groups. Thus it was decided that BBr₃ would be used for the penultimate step of the synthesis.

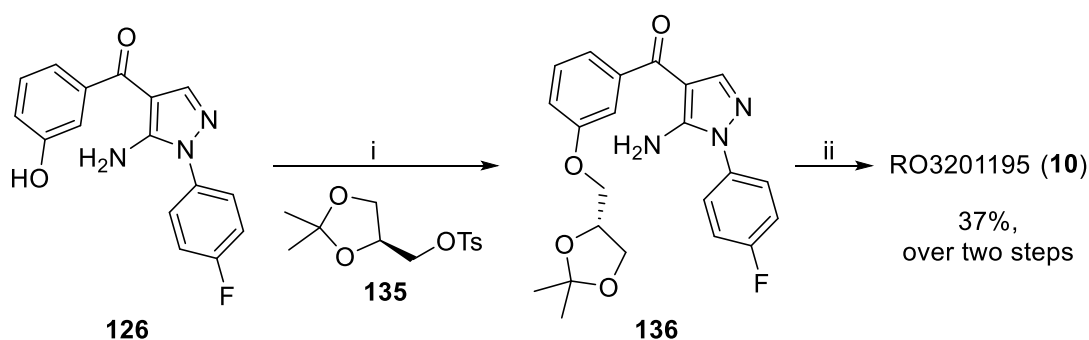
The mechanism for protodemethylation using BBr₃ is generally thought to occur via complexation of the strongly Lewis acidic boron with the methoxy lone pair, which on formation of an alkyl bromide gives the ether-BBr₂ adduct. Hydrolysis of this adduct then affords the desired phenol. However, new evidence has suggested a bimolecular reaction pathway, wherein two ether-BBr₂ adducts interact to effect the same outcome.²⁶³ This suggests that more sterically hindered methyl ethers may not be amenable to BBr₃-mediated protodemethylation.

Aryl methyl ether **125** was subjected to an excess of BBr₃ in dry CH₂Cl₂ and stirred at room temperature under argon for 20 h to afford phenol **126** in quantitative yields after aqueous work up (Scheme 87).



Scheme 87: Protodemethylation of **125** with BBr₃. Reaction conditions: i) BBr₃ (1 M in CH₂Cl₂), 0 °C - RT, 20 h; ii) aqueous work up, quant.

O-Alkylation was conducted through an S_N2 displacement reaction with (S)-2,2-dimethyl-1,3-dioxolan-4-ylmethyl *p*-toluenesulfonate (**135**) under basic conditions (see **Scheme 88**). This reaction had been reported to occur in very low yield by Bagley *et al.* in their 2008 publication (9%).²⁵⁸ However, by changing the solvent from DMF to DMSO and heating the reaction mixture to 100 °C for 25 h, it was possible to isolate **136** in a much increased 42% yield. However, there were still issues which complicated the reaction.



Scheme 88: O-Alkylation and deprotection to RO3201195 (**10**). Reaction conditions: i) **135**, K_2CO_3 , DMSO, 100 °C, 40 h ii) *p*-TSA. H_2O , MeOH- H_2O , 50 °C, 18 h, 37%.

The tosylate **135** was a viscous liquid and was used in excess to promote the reaction, hence it was found that the crude product was quite gelatinous. After flash column purification on silica gel and confirmation of purity by 1H NMR spectroscopic analysis, the product still tended to be quite gelatinous in nature. Recrystallization from hot EtOAc returned **136** as a colourless powder, though this led to a significant loss of material and no improvement in purity by 1H NMR spectroscopic analysis. Therefore, it was decided that for the final step of the synthesis, **136** would be carried forward once determined pure by 1H NMR spectroscopic analysis.

Deprotection of the diol was completed using *para*-toluenesulfonic acid monohydrate in a MeOH-water solution. Heating at 50 °C for 18 h, purification by flash column chromatography and recrystallization gave final product RO3201195 (**10**) in 37% yield over two steps. Comparison of spectroscopic data with the literature confirmed product formation.

2.3.4. Conclusion.

RO3201195 (**10**) was successfully synthesized over seven steps in an overall yield of 15%. A new palladium-mediated route towards β -ketonitriles was developed using microwave-assisted heating, albeit in low yield. Alternative classical condensation methods were found to be more suitable for the total synthesis of RO3201195 (**10**) and were achieved in high yield. The scale of

reactions carried out and the overall yield of the synthetic process were improved compared to previously published data, and the target compound was synthesized in sufficient purity for biological studies, as ascertained by comparison with previous data.¹

2.4. Biological studies of RO3201195 in WS cells.

Bagley *et al.* verified RO3201195 (**10**) to be a potent p38 α inhibitor in WS cells, albeit with a lower potency than SB203580 (**1**).²⁵⁸ In collaboration with Dr Terence Davis at Cardiff University, the aim of these new biological studies was to investigate what effect, if any, **10** had on the rate of proliferation of WS cells. It was hoped that direct comparison of results with prototypical p38 MAPK inhibitor SB203580 (**1**) would help advance understanding of the role of the p38 α -mediated stress-signalling pathway in the premature ageing phenotype of WS cells.ⁱⁱⁱ

Due to limited supplies of primary WS cells, initial biological tests were conducted on WS^{tert} cells, which should demonstrate similar rates of proliferation as primary WS cells, and hence demonstrate similar responses when treated with p38 α inhibitors.

Firstly, the optimal concentration of each inhibitor to effect total inhibition of p38 α was determined for WS^{tert} cells. This was done by growing WS^{tert} cells in a medium of each inhibitor and monitoring the extent of protein activation by ELISA. For SB203580 (**1**) the optimal concentration was found to be 1 μ M and above, and 10 μ M for RO3201195 (**10**).¹ The higher optimal concentration of **10** was due to a lower intrinsic potency for p38 α in WS^{tert} cells than SB203580 (**1**). However, this lower potency was not of concern for these studies as **10** was only being used as a probe *in vitro*.

Observing the rate of proliferation for WS^{tert} cells grown in the presence of SB203580 (**1**) at 2.5 μ M concentration, the rate of growth increased by approximately 22% compared to DMSO control cells. For RO3201195 (**10**) at 10 μ M concentration, the rate of proliferation also increased, with a 19% increase compared to DMSO controls.¹

Figure 40 illustrates the rate of cell proliferation as % p38 activity against % population growth of WS^{tert} cells. The sigmoidal curves recorded for SB203580 (**1**) and RO3201195 (**10**), at 2.5 and 10 μ M respectively, were almost identical. This indicated that as the p38 activity in the cells decreased the rate of population growth increased. This data confirmed the contributory role of p38 α MAPK in reducing the rate of cell proliferation in WS cells.

ⁱⁱⁱ Biological testing as conducted by Dr Terence Davis, Institute of Cancer and Genetics, Cardiff University.

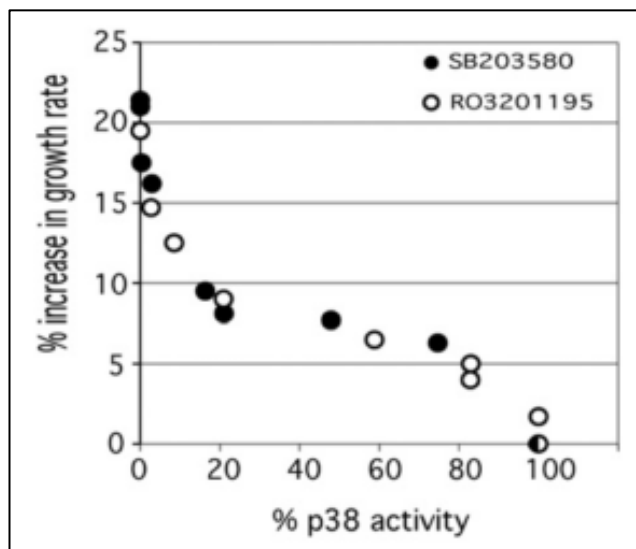


Figure 40: Plot of % p38 activity against % population growth for WS^{tert} cells growth in 2.5 μ M SB203580 (**1**) and 10 μ M RO3201195 (**10**) concentration.¹

SB203580 (**1**) has been noted to have off-target activity with JNKs, another stress-signalling kinase family which could potentially play a role in the premature ageing seen in WS fibroblasts. Western blots were completed in order to ascertain whether inhibition of JNKs occurred at the maximal concentrations established in these studies. **Figure 41** illustrates the blots, in which the extent of activation of phosphorylated-HSP27 (*p*-HSP27), HSP27, phosphorylated JNK (*p*-JNK) and JNK were monitored upon treatment with the optimal concentrations of SB203580 (**1**) and RO3201195 (**10**), with blank control cells and activated cells grown in DMSO for comparison.

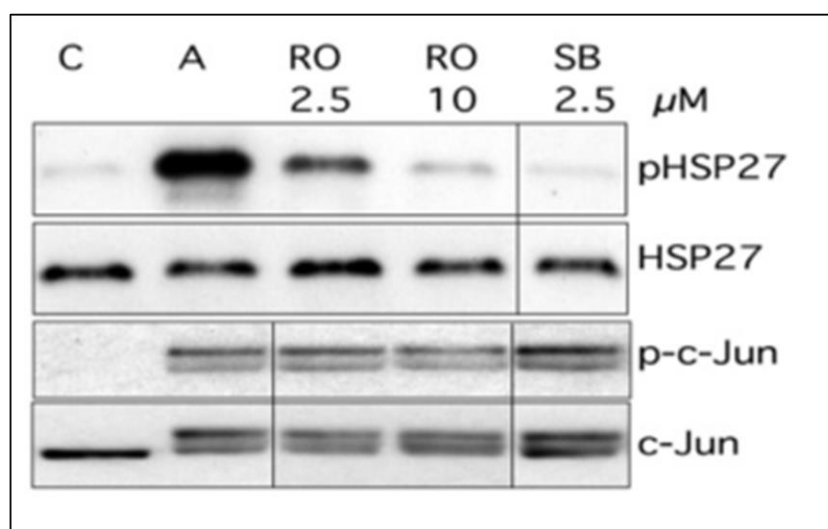


Figure 41: Western blot of RO3201195 (**10**) and SB203580 (**1**) against WS^{tert} cells. Blot key; C: Control, run in DMSO; A: run in DMSO and activated with anisomycin. RO 2.5 and RO 10; cells run at 2.5 μ M and 10 μ M RO3201195 (**10**); SB 2.5: cells run at 2.5 μ M SB203580 (**1**).¹

From the blot it could be seen that *p*-HSP27 was greatly reduced when the WS^{tert} cells were pre-treated with RO3201195 (**10**) at 10 μ M and with SB230580 (**1**) at 2.5 μ M, matching the profile of the lane 1 control. This confirmed that the p38 α -mediated stress-signalling pathway was being inhibited at these concentrations. It can also be seen that there was no inhibition of JNK signalling at any inhibitor concentration, with lanes 3-5 all showing the same extent of *p*-c-JNK and c-JNK activation as the anisomycin-activated control in lane 2.

From this evidence it can be concluded that inhibition of JNK was not responsible for the increased rates of proliferation observed in these studies.¹

Investigation into the effect of treatment with RO3201195 (**10**) and SB203580 (**1**) on the aged morphology of WS cells at the established optimal concentrations was then conducted. A primary strain of WS fibroblasts that was determined close to replicative senescence was treated with SB203580 (**1**) and RO3201195 (**10**), at 2.5 and 10 μ M concentrations, respectively. The cells were fed the optimal concentrations of the inhibitors and left for 88 days (**Figure 42**).

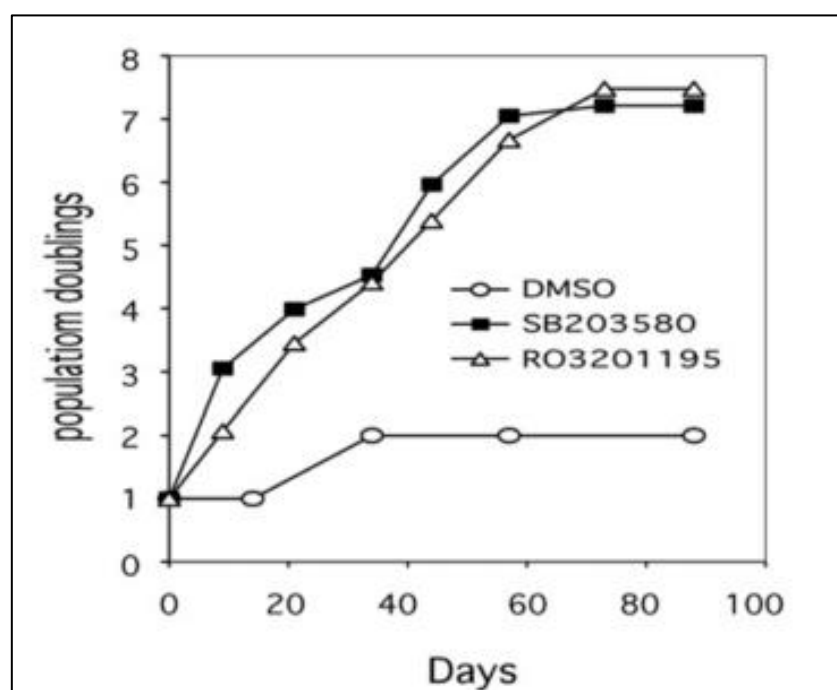


Figure 42: Proliferation of primary WS fibroblasts in the presence of SB203580 (**1**) at 2.5 μ M and RO3201195 (**10**) at 10 μ M, measured as population doublings against days.¹

A control sample of DMSO-fed primary WS fibroblasts was observed to only undergo one population doubling in this time. On the other hand, the inhibitor-treated cells had a much increased rate of proliferation, reaching 7.5 population doublings before growth arrest, with essentially no difference in the rate of growth between the two inhibitors.¹

The two p38 α inhibitors SB230580 (**1**) and RO3201195 (**10**) demonstrate very different kinase selectivity profiles, with p38 α being the only common target. Hence, it can be inferred that the remarkably comparable effect of these two inhibitors upon the rate of proliferation of primary WS cells must result from inhibition of the p38 α MAP kinase.

2.5. Overall conclusions and future perspectives.

A new synthetic route towards p38 inhibitor RO3201195 (**10**) and its intermediates has been developed, with an improved overall yield over preceding published routes and an increased efficiency established through the use of microwave-assisted heating in a number of the steps.

Biological testing of RO3201195 (**10**) established an astounding correlation in activity with the prototypical p38 inhibitor SB203580 (**1**) in WS cells. Comparative studies conducted at the lowest optimal concentrations of the two inhibitors found that the two inhibitors demonstrated almost identical profiles to increase the rate of cell proliferation of WS^{tert} cells and extended the replicative lifespan of primary WS cells. Off-target JNK inhibition by SB203580 (**1**) has been disproven as a contributing factor in effecting the increased replicative life span of WS cells at the concentrations used in these studies; confirming that the results observed were due to inhibition of the p38 stress-signalling pathway.

These studies demonstrated that RO3201195 (**10**) can be adopted as a very useful chemical tool to investigate the stress-signalling pathways of human cells, to corroborate results of alternative p38 α inhibitors and to help further our understanding of the effects of p38 α inhibitors on cell proliferation in WS and progeroid fibroblasts.

Chapter 3. Synthesis of PF-3644022. Probing an MK2 inhibitor for the modulation of cellular ageing in WS cells.

3.1. Introduction.

Having found that inhibition of p38 α positively affects the proliferation rate of WS cells, it was desirable to gain a better understanding of the mechanism by which this occurs. One method proposed was to target kinases downstream of p38. However, as mentioned in **Chapter 1.3**, p38 mediates a number of important stress-signalling pathways.

MK2 mediates activation of the small heat shock protein HSP27 (see **Chapter 1.4**),¹⁹ which regulates and stabilizes the actin-cytoskeleton and production of F-actin stress fibres.⁵⁷ These fibres have been found to be up-regulated in senescent WS cells and greatly reduced in WS cells grown in the presence of the p38 α inhibitor SB203580 (**1**).^{14,264} These findings support MK2 as a key kinase in the p38 α -mediated pathway inhibited by SB203580 (**1**).

MK2 presents itself as a therapeutically viable target as MK2 knockout mice exhibit normal healthy phenotypes, while p38 knockout mice are lethal.⁵⁹ A variety of MK2 inhibitors have been developed spanning a range of chemotypes,²² though most tend to exhibit poor activity in cellular models and *in vivo* (see **Chapter 1.4**).⁶⁹ The benzothiophene based MK2 inhibitor PF-3644022 (**25**) however possesses nanomolar potency, good projected ADME characteristics and selectivity against a panel of 200 kinases.^{68,69} It was therefore proposed that the MK2 inhibitor

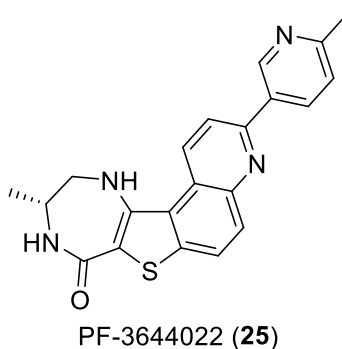


Figure 43: MK2 inhibitor PF-3644022 (**25**).⁶⁸

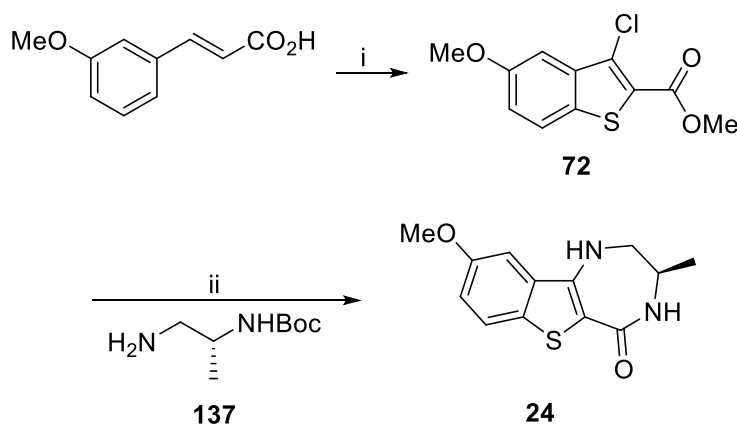
PF-3644022 (**25**) should be synthesized and used to investigate the role of MK2 in the premature senescence of WS cells.

Efforts were made to design a novel, rapid and efficient route towards the inhibitor, ready for testing in normal human cells and WS cells to assess its viability as a selective MK2 inhibitor, and its effect, if any, upon the rate of proliferation of primary WS cells.

3.1.1. Hit-to-lead identification of PF-3644022 (**25**).

Anderson *et al.* at Pfizer completed a number of projects towards the development of MK2 inhibitors as therapeutics for inflammatory conditions, such as rheumatoid arthritis (RA) and Crohn's disease. Their specific target of interest was to inhibit production of TNF- α , a cell-signalling cytokine modulated by MK2.⁵⁹

PF-3644022 (**25**) arose from an SAR-led investigation of a new benzo[*b*]thiophene-based chemotype **24** that had not been previously explored towards inhibition of MK2, though it shared a number of pharmacophoric similarities to previous MK2 inhibitors (see **Chapter 1.4**, **Figure 16**).^{59,62,66,265–267}



Scheme 89: Synthesis of benzothiophene-based scaffold **24**. Reaction conditions: i) SOCl₂, chlorobenzene, 120 °C then MeOH; b) Pd₂(dba)₃, (±)-BINAP, Cs₂CO₃ toluene, 110 °C, 24 h, then TFA/CH₂Cl₂ and NaOMe/MeOH.⁶⁷

Anderson *et al.* synthesized **24** through cyclization of 3-methoxycinnamic acid with thionyl chloride (SOCl₂) to afford the 3-chlorobenzo[*b*]thiophene intermediate **72** (see **Chapter 1.6.2.4.1**, **Scheme 33**).⁶⁷ Buchwald-Hartwig *N*-arylation of the chloride with a chiral mono-Boc-protected diamine (**137**) and subsequent deprotection and lactamization gave the cyclized benzothiophene lactam **24**. Carbon and sulfur analogues of the lactam ring and alternative

functionalities at the 3-position were used to explore the inhibitor SAR with MK2 (see **Figure 44**).

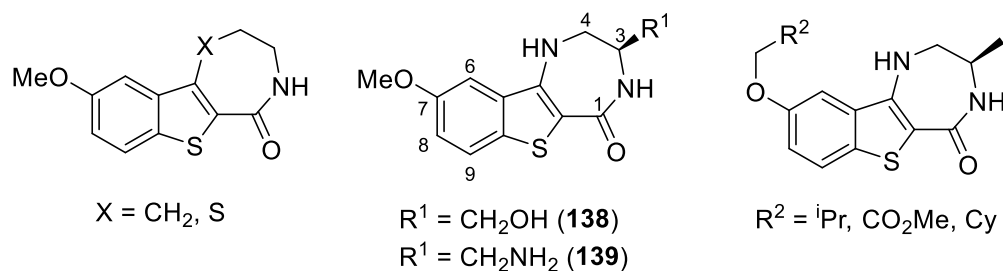


Figure 44: Fused benzothiophene-lactam compounds explored for MK2 inhibitor viability by Anderson *et al.*⁶⁷

Nitrogen-containing rings demonstrated enhanced binding to MK2, though by X-ray co-crystallization studies there were no direct amino acid interactions that could be observed. It was postulated that the nitrogen was modulating electron density through the thiophene π -system to enhance HBA properties of the carbonyl group.⁶⁷

Substitution at the 3-position of the diazepinone was explored, with the (*R*)-enantiomers found to be about 10-fold more potent inhibitors for MK2. Introduction of a heteroatom onto the substituted chain (**138** and **139**) was found to improve potency of binding with MK2, though cell permeability and cell potency were found to be dramatically reduced.⁶⁷

Hydrogen bonding of the methoxy group of **24** was determined to be an essential interaction for binding with the hinge region of MK2. Based upon previous work,⁵⁹ Anderson *et al.* speculated that interaction with the hinge region of the kinase may be enhanced through a more rigid structure, hence the group proceeded to synthesize a small collection of furan and pyridine analogues of **24** (see **Figure 45**).

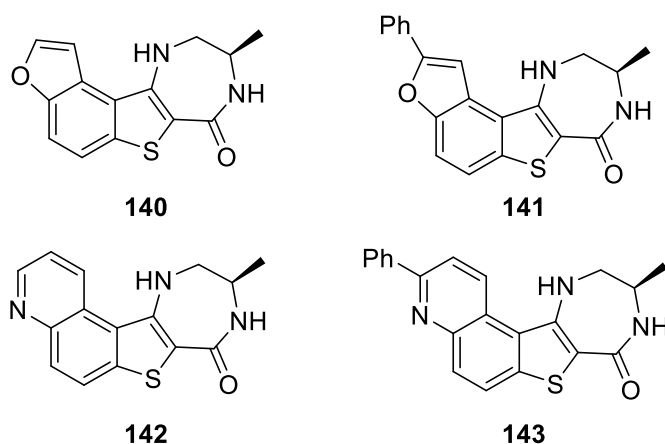
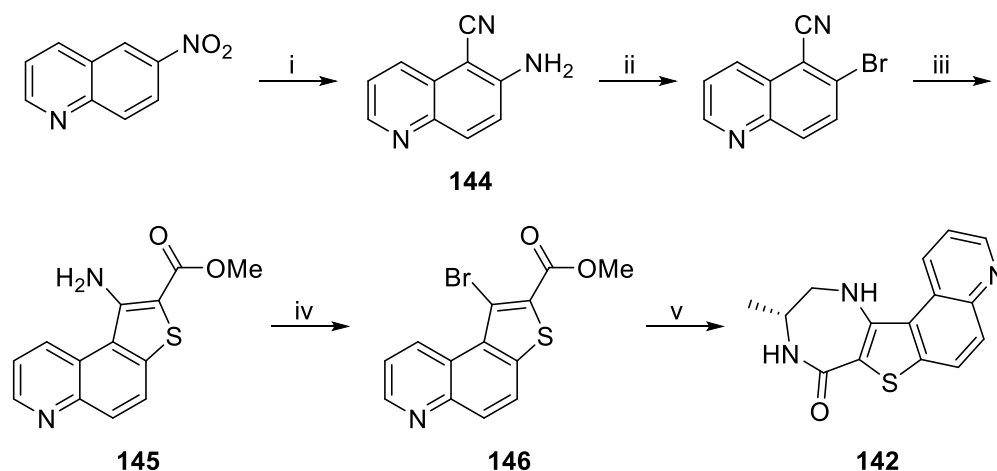


Figure 45: Anderson *et al.*'s heteroaromatic fused ring systems, exploring inhibitor binding to the hinge region of MK2.⁶⁸

The group found that when a fused furan system was incorporated (**140**) there was a significant increase in potency of binding with MK2 compared to **24**. In an effort to improve inhibitor selectivity, a 2-phenyl ring was introduced onto the furan (**141**). However, it was found that **141** exhibited reduced cell and inhibitor potency.

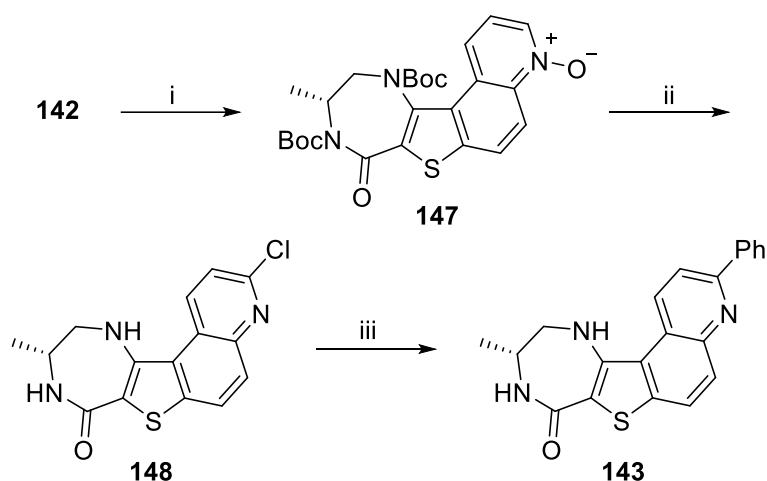
For the pyridine analogues **142** and **143** there was a similar reduction in cell and inhibitor potency upon addition of a phenyl ring, though the reduction was much less severe and an increased specificity for MK2 over other structurally similar kinases was observed.⁶⁸

To synthesize pyridine analogues **142** and **143**, the group started from a 6-nitroquinoline, converting it to 6-amino-5-cyanoquinoline (**144**) using ethyl cyanoacetate and potassium hydroxide (KOH) (see **Scheme 90**). Deaminative bromination via diazotization of the amine enabled benzo[*b*]thiophene (**145**) formation through cyclocondensation with methyl thioglycolate under basic conditions. A second deaminative bromination step was carried out to give the Buchwald-Hartwig precursor **146**, which was then coupled with the desired Boc-protected amine (**137**). Acidic Boc-deprotection, and lactamization under basic conditions afforded the final cyclised product **142**.



Scheme 90: Synthesis of fused pyridine-benzothiophene analogue **142**. Reaction conditions: i) Ethyl cyanoacetate, KOH, DMF, then HCl; ii) NaNO₂, then HBr; iii) Methyl thioglycolate, NaOMe MeOH; iv) ^tBuONO, CuBr₂; v) Buchwald Hartwig conditions, **137**, acidic deprotection and basic cyclization.⁶⁸

In order to synthesize the biaryl pyridine analogue **143**, Anderson *et al.* settled upon a Suzuki-Miyaura cross-coupling approach. *N*-Protecting groups were installed on the diazepinone ring, and the pyridine ring was oxidized to the pyridine *N*-oxide **146** using *m*CPBA, and functionalized to 2-chloropyridine **147** using oxalyl chloride ((COCl)₂) followed by Boc-deprotection. Suzuki coupling was carried out using phenylboronic acid under basic conditions to give **142** (see **Scheme 91**).



Scheme 91: Synthesis of biaryl phenyl-pyridine fused analogue **143**. Reaction conditions: i) Boc_2O , DMAP, NEt_3 then *m*CPBA; ii) $(\text{COCl})_2$, DMF, then HCl; iii) PhB(OH)_2 , $\text{Pd(PPh}_3)_4$, Na_2CO_3 , 80 °C.⁶⁸

Analogues of **143** were explored by coupling the advanced 2-chloropyridine intermediate **148** with a variety of aromatic rings, through which PF-3644022 (**25**) was identified as the most promising drug candidate, with nanomolar potency for MK2.⁶⁸

Since initial publication of its biological activity, **25** has been of major interest as a probe to delineate the mechanisms of stress-signalling in the body and as a potential therapeutic for inflammatory conditions.

3.1.2. Deconstructing PF-3644022 (**25**).

The synthetic route published by Anderson *et al.* for PF-3644022 (**25**) was driven from lead optimization, with functionalization of a late-stage intermediate affording their candidate compound. It was proposed that a more streamlined total synthesis of **25** could be designed.

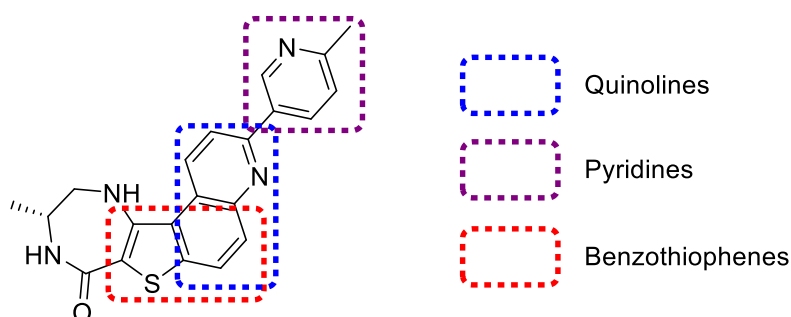


Figure 46: Key heterocycles of PF-3644022 (**25**).

Over the course of this project a number of retrosynthetic approaches were investigated. Each one utilized a different heterocyclic component of the core scaffold and explored how it could be functionalized and built-up to the target compound.

There are three main heterocycles which are fused or linked together to form PF-3644022 (**25**): a pyridine, quinoline and benzothiophene (see **Figure 46**). Each of these has been discussed in **Chapter 1.6.2**. To diversify the main heterocyclic scaffold, a number of essential carbon-carbon and carbon-heteroatom bond-forming reactions were used over the course of this project, including Suzuki-Miyaura cross-coupling, Buchwald-Hartwig *N*-arylation and amide bond formation (see **Figure 47**). These reactions have been discussed in detail in **Chapter 1.6.3**.

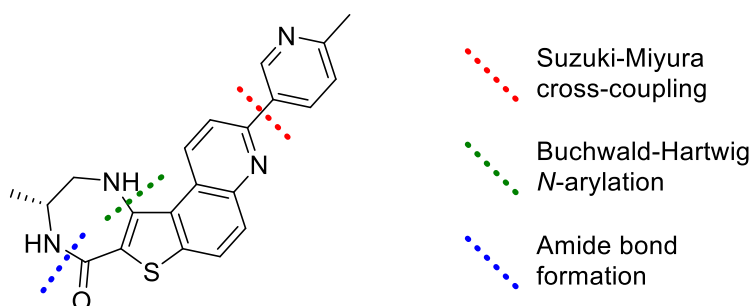
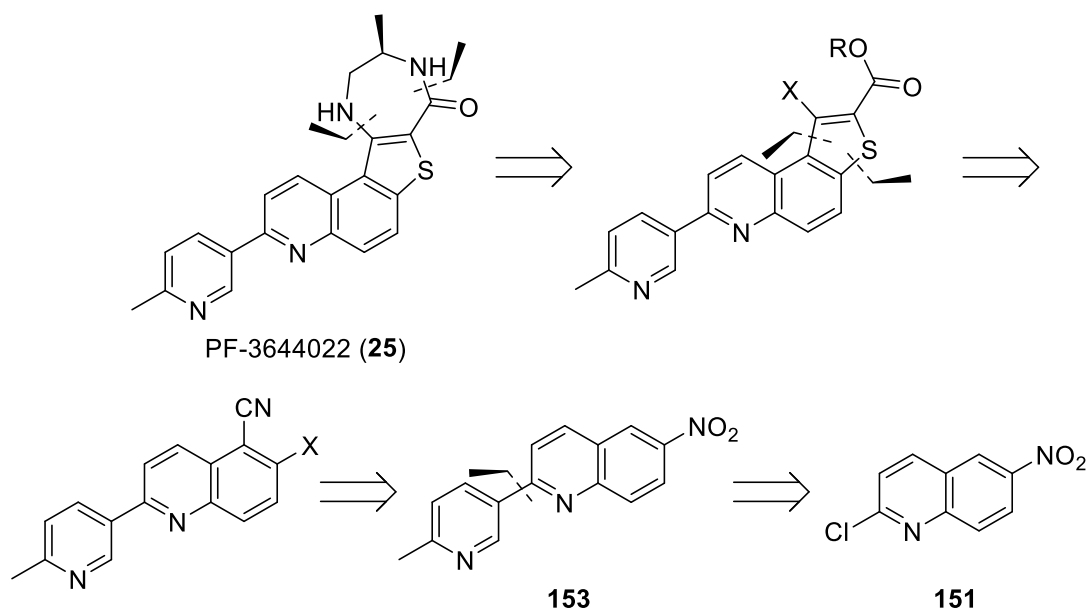


Figure 47: Key bond-forming reactions in approaches towards PF-3644022 (**25**).

A number of different disconnection strategies presented themselves as viable options for the synthesis of PF-3644022 (**25**). Though not all were successful in affording the final product due to issues of reactivity, reproducibility and tractability of intermediates, through each iteration of the synthesis a cumulative knowledge was accrued which led to an overall diverse and innovative route towards PF-3644022 (**25**). Each of these routes will be discussed in turn.

3.2. Retrosynthesis 1. Quinoline based scaffold.

The initial route explored was closely related to Anderson *et al.*'s synthetic route towards pyridine-fused benzothiophene **142**. It was proposed that the total synthesis could be streamlined through installation of the biaryl unit using Suzuki coupling at the beginning of the reaction (see retrosynthetic **Scheme 92**).



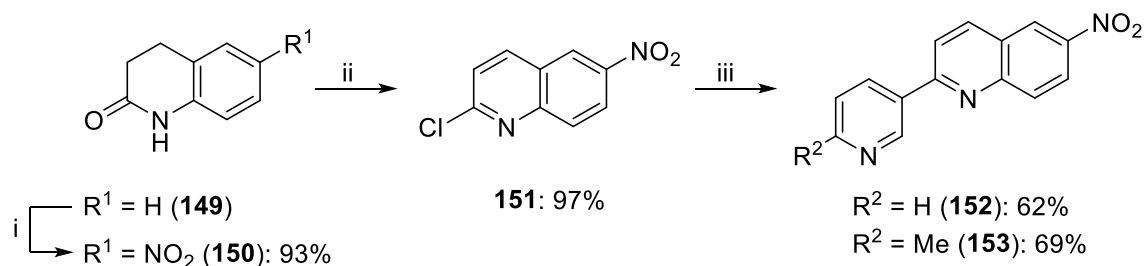
Scheme 92: Retrosynthesis 1. Quinoline based scaffold with early stage Suzuki coupling.

It was anticipated that the thieno ring could be installed on the quinoline in a manner similar to Anderson *et al.*, with aspirations to incorporate microwave-assisted techniques to reduce reaction times and improve yields. Final stage *N*-arylation and lactamization of the chiral amine would then negate the need for additional protective steps, to deliver the final enantiopure product.

3.2.1. Chloroquinoline synthesis and Suzuki coupling.

Suzuki precursor **151** was synthesised through nitration of 3,4-dihydroquinol-2(1*H*)-one (**149**), using a concentrated HNO₃/H₂SO₄ mixture to give **150** in high yield,^{iv} and subsequent tandem chlorination and oxidation with POCl₃ in the presence of 2,3-dichloro-5,6-dicyano-*p*-benzoquinone (DDQ) (see **Scheme 93**).

^{iv} Step completed and yields given for result obtained by Dr Irina Chuckowree.³



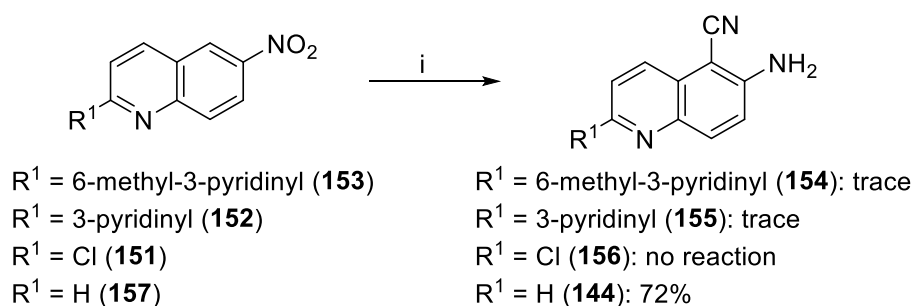
Scheme 93: 2-Chloroquinoline synthesis and Suzuki coupling. Reaction conditions: i) HNO_3 , H_2SO_4 , 0°C , 15 min, 93%; ii) POCl_3 , DDQ, DMF, RT, 1 h, 97%; iii) Pyridinyl-boronic acid, Na_2CO_3 , $\text{PdCl}_2(\text{PPh}_3)_2$, $\text{MeCN-H}_2\text{O}$, MW 140°C , 15 min.

Microwave-assisted Suzuki-Miyaura cross-coupling was completed using 3-pyridineboronic acid to test viable conditions. Using $\text{PdCl}_2(\text{PPh}_3)_2$ catalyst and Na_2CO_3 base in $\text{MeCN-H}_2\text{O}$, microwave-assisted heating at 140°C in a sealed vessel for 15 minutes gave the biaryl cross-coupled product **152** in reasonable yield. Thus the reaction was completed using 6-methylpyridin-3-boronic acid under the same conditions to give **153** in very agreeable yield (69%). Given the satisfying results of this catalytic system, no others were probed.

3.2.2. Synthesis of 6-amino-5-cyanoquinoline intermediates.

In order to facilitate formation of the fused thieno ring, the nitroquinoline needed to be functionalized. Anderson *et al.* adopted Yamazaki *et al.*'s vicarious nucleophilic substitution method of nitration and reduction using ethyl cyanoacetate under basic conditions.^{68,268,269}

However, it was found after reacting **153** with ethyl cyanoacetate, KOH and DMF for 72 h at room temperature, with subsequent hydrolysis in 5% NaOH aqueous solution, only trace amounts of the desired product **154** were collected after purification by flash column chromatography (see **Scheme 94**).



Scheme 94: Cyanation of nitroquinolines. Reaction conditions: i) Ethyl cyanoacetate, KOH, DMF, RT, then 5% NaOH, H_2O , Δ , 3h.^{268,269}

This meagre yield was unexpected given the apparent ease of use in Anderson *et al.*'s synthesis.⁶⁷ It was speculated that under basic conditions, the acidity of the 2-methylpyridine group of **153** may have impacted the reaction unfavourably. Hence, related substrates were investigated for their viability under the same reaction conditions (see **Scheme 94**).

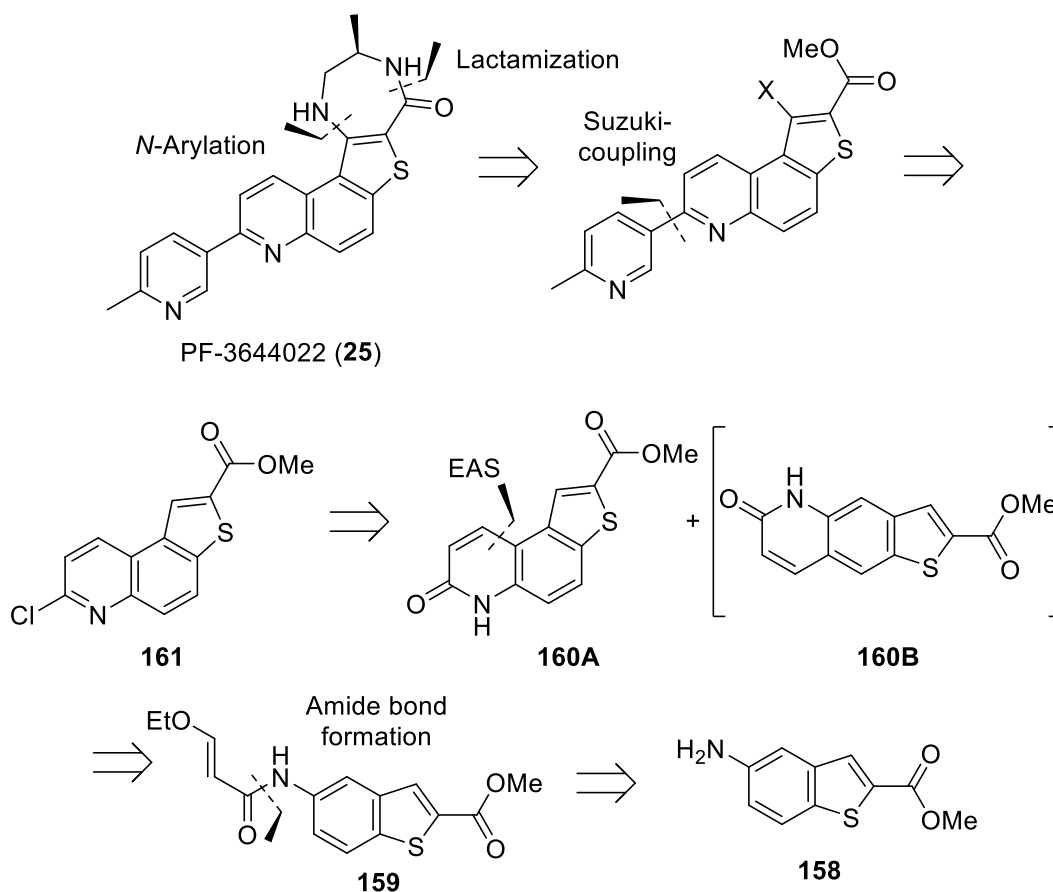
Unsubstituted biaryl **152** was reacted under the same conditions and only a trace of product **155** was observed by ¹H NMR spectroscopic analysis. The 6-nitroquinolone intermediate **150** was found to be inert under the reaction conditions, and the chlorinated intermediate **151** afforded a complex mixture of products after 64 h and subsequent hydrolysis, with none of the desired product **156** observed to be present.

As a control, the reaction was conducted on 6-nitroquinoline **157** using the same conditions and reagents. After purification, a 72% yield of 6-amino-5-cyanoquinoline **144** was achieved confirming the reaction was a viable method of cyanation, though it appeared to be incompatible with the 6-nitro-2-pyridinylquinolines **152** and **153** and their earlier intermediates.

Potential reasons why this method was not viable for the biaryl-pyridine-quinoline compounds could include deprotonation of **153**, resulting in a mixture of side products under the reaction conditions, competing reaction of the pyridine ring or deactivation of the nitro group as an *ortho*-director (see vicarious nucleophilic addition, **Chapter 1.6.2.3.2**), perhaps through complexation. Nevertheless, this method was deemed inappropriate for the total synthesis of PF-3644022 (**25**), and thus alternative disconnective strategies were investigated.

3.3. Retrosynthesis 2. Thieno[3,2-*f*]quinolone scaffold.

Reviewing the heterocyclic analysis of PF-3644022 (**25**), it was postulated that the next viable strategy would be to start from the benzo[*b*]thiophene ring **158** (see retrosynthetic **Scheme 95**). As has been discussed, it is possible to synthesize quinolones and quinolines from anilines through intramolecular EAS (see **Chapter 1.6.2.3.**). It was proposed that an intermediate fused thienoquinolone system **160A** could be built via intramolecular EAS from **159**. Chlorination would then give chlorothienoquinoline **161** ready for Suzuki coupling. Installation of the diazepinone ring was proposed for the closing steps of the synthesis through halogenation of the benzothiophene, to enable Buchwald-Hartwig *N*-arylation and lactamization as the final step to give **25**.

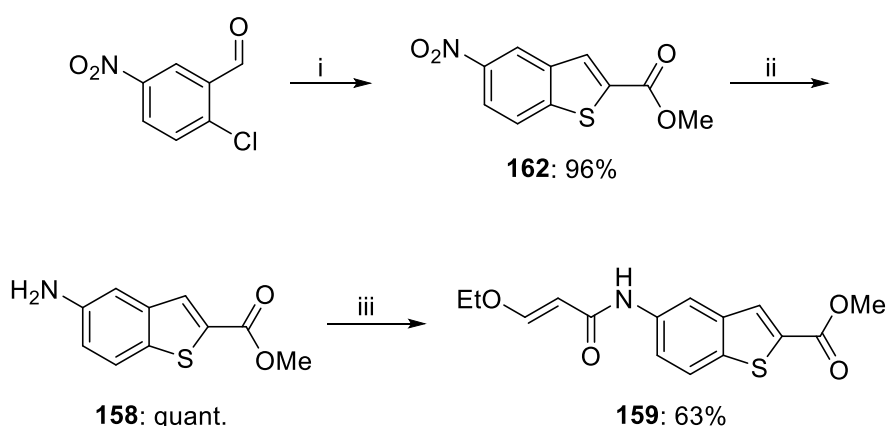


Scheme 95: Retrosynthesis 2, via thienoquinolone based scaffold.

Mid-stage Suzuki-coupling by this route would still avoid any additional protective steps for the diazepinone ring, though it was recognized at the outset that there was the potential for regioselectivity issues during the cyclization step from **159** to **160A**, with potential formation of the alternative thienoquinolone **160B**.

3.3.1. Thienoquinolone synthetic route.

The first approach to the thienoquinoline scaffold was completed in the group by Dr Irina Chuckowree, as illustrated in **Schemes 96** and **97**, but has a bearing on our approach.^v Benzo[*b*]thiophene **162** was synthesized by cyclocondensation of methyl thioglycolate and 2-chloro-5-nitrobenzaldehyde under basic conditions in high yield (93%). Reduction of the nitro group using palladium on charcoal (Pd/C) under an atmosphere of hydrogen gave **158** in quantitative yields, and subsequent amide bond formation with 3-ethoxyacrylic acid was completed using peptide coupling reagents EDCI.HCl and HOBt at room temperature to give **159** in reasonable yields (63%).



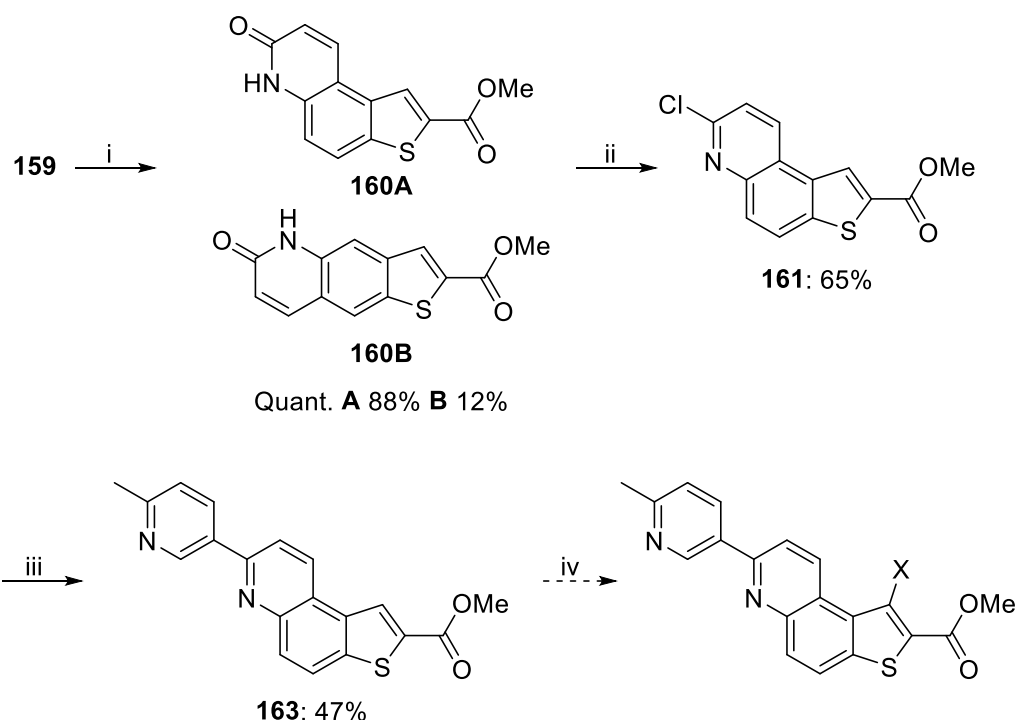
Scheme 96: Synthesis of thienoquinoline precursor **159** completed by Dr Irina Chuckowree. Reaction conditions: i) Methyl thioglycolate, K₂CO₃, DMF, RT, overnight, 96%; ii) H₂ (1 atm), Pd/C, MeOH, RT, 3 h, quant.; iii) 3-ethoxyacrylic acid, EDCI.HCl, HOBt.H₂O, DIEA, DMF, RT, overnight, 63%.

Subsequent thienoquinoline formation was conducted under Knorr-carbostyryl cyclization conditions, stirring in conc. H₂SO₄ at 0 °C and warming to room temperature over 3 h (see **Scheme 97**).¹⁰⁹ Quantitative conversion to the quinoline was obtained, with a mixture of the two regioisomers in an 88:12 ratio in favour of the desired thieno[3,2-*f*]quinoline **160A**, as ascertained by ¹H NMR spectroscopic analysis (see **Scheme 97**).

The crude mixture was subjected to chlorination by heating to reflux in POCl₃ for 3 h, and the desired chloroquinoline **161** was isolated from its regioisomer in reasonable yields after purification by flash column chromatography on SiO₂ (65%). Microwave-assisted Suzuki coupling of **161** was conducted using a non-aqueous system to avoid hydrolysis of the ester functionality, but gave reduced yields of biaryl **163** compared to the Suzuki coupling of nitroquinoline **150** (see

^v Dr Irina Chuckowree, Prof. M. C. Bagley, unpublished results, 2013.

previous section, **Chapter 3.2.1**). This lower yield was most likely due to poor solubility, as the compounds became a lot less tractable once the thienoquinoline scaffold had been constructed.



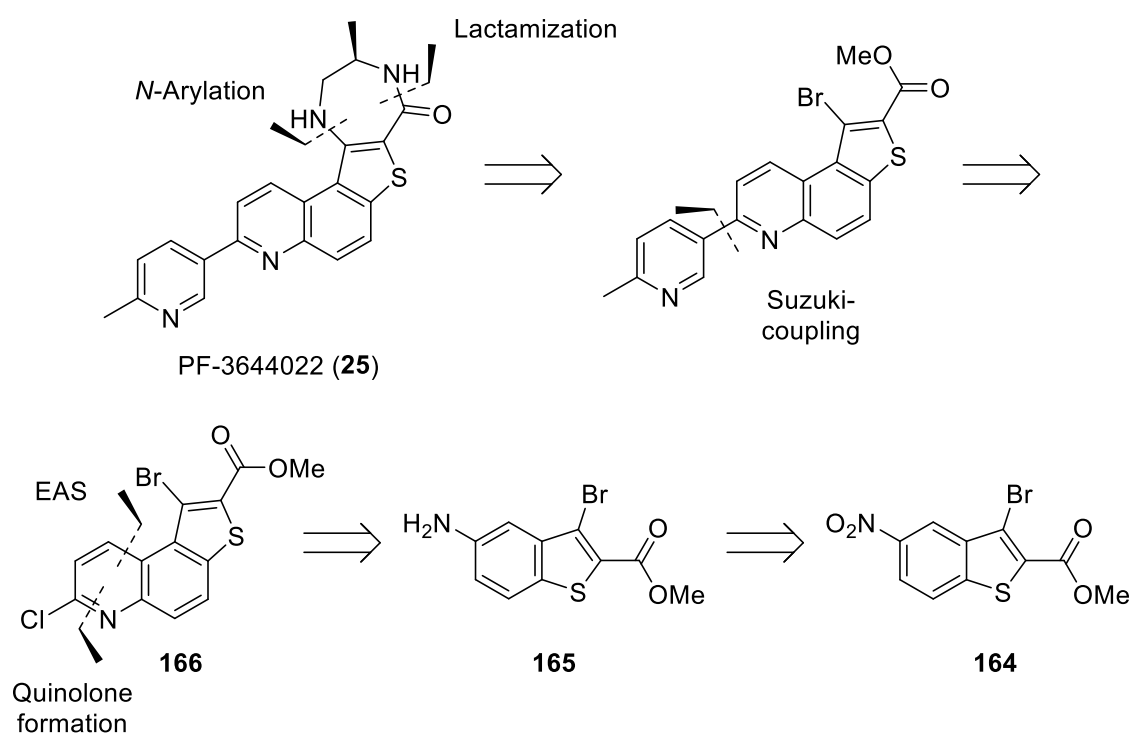
Scheme 97: Cyclization to form thienoquinolones **160A** and **160B**, and functionalization to biaryl quinoline **163**. Reaction conditions: i) Conc. H_2SO_4 , RT, 3 h, quant.; ii) POCl_3 Δ , 2 h, 65%; iii) 6-Methylpyridinyl-3-boronic acid, Cs_2CO_3 , $\text{PdCl}_2(\text{PPh}_3)_2$, 1,4-dioxane, MW 140 $^\circ\text{C}$, 1 h, 47%; iv) NBS, no reaction.

Further problems were encountered upon attempting halogenation of the thieno ring. Use of *N*-iodo, bromo or chlorosuccinimide (NIS, NBS, NCS) were all investigated with no success. A variety of different solvent systems were investigated, with additional Lewis acids and mineral acids used in an attempt to promote the reaction, however only the starting material **163** or a complex mixture of multi-halogenated products was returned.

Halogenation of the thienoquinoline scaffold at an earlier stage was also investigated. Treatment of **161** with NBS, NIS, NCS or bromine with zinc chloride also either resulted in multiply halogenated products, or returned unreacted starting material. It was concluded that in order to proceed with a synthetic strategy via a thieno[3,2-*f*]quinolone scaffold, a much earlier-stage halogenation would be required.

3.4. Retrosynthesis 3. Halothieno[3,2-f]quinolone scaffold.

Having established synthetic routes towards a number of key intermediate frameworks, including the Knorr-carbostyryl quinolone formation and Suzuki coupling procedures to 2-(pyridin-3-yl)quinolines, it was desirable to maintain these key steps in the total synthesis. It was decided that an alternative strategic route towards PF-3644022 (**25**) would require only slight alteration. Synthesis of halobenzo[*b*]thiophene **164** was proposed as the first step, followed by reduction to aminobenzothiophene **165** which should facilitate functionalization to dihalogenated intermediate **166** (see Scheme 98).



Scheme 98: Retrosynthesis 3, via halothieno[3,2-*f*]quinoline and dihalogenated intermediate.

The proposed sequence of cross-coupling steps was to conduct the Suzuki coupling at this intermediate stage, followed by final Buchwald-Hartwig *N*-arylation and lactam ring formation. It was noted that the presence of two halogens during the Suzuki coupling of **166** could cause issues of chemoselectivity.

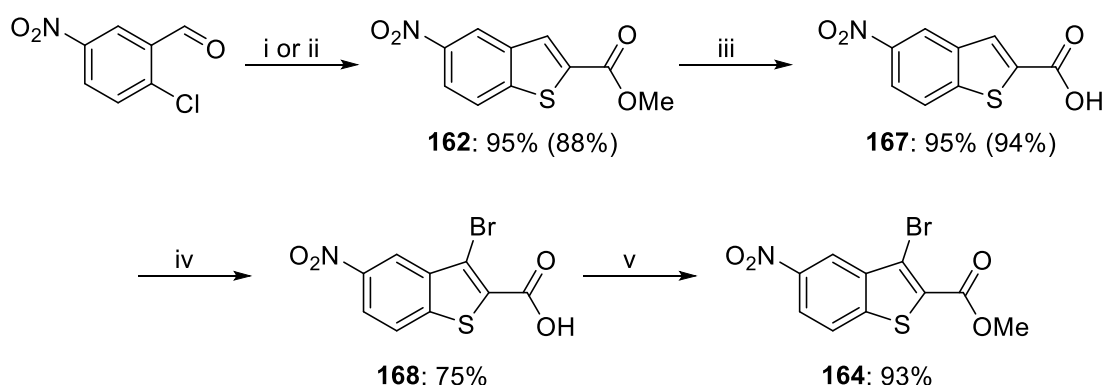
It had been decided that the halogen to be installed in **164** would be a bromine, as this is most commonly used in Buchwald-Hartwig *N*-arylation reactions. C-Br bonds are typically more activated towards oxidative addition at a metal centre than C-Cl bonds. However, at this stage

it could not be anticipated whether the high reactivity endowed to the C-Cl bond at the 2-chloroquinoline centre would challenge this order of reactivity. In order to probe the amenability of this route, it was proposed that the dihalogenated intermediate **166** be synthesized and tested for its reactivity towards Suzuki conditions. With most steps of the synthesis already validated in related systems, it was anticipated that repurposing the reaction conditions for the synthesis of **166** would not be too problematic.

3.4.1. Synthesis of 3-bromobenzo[*b*]thiophene.

Initial routes explored direct bromination of benzo[*b*]thiophene **162**. As discussed in **Chapter 1.6.2.4**, the heteroaromatic ring of benzo[*b*]thiophenes tends to be more reactive, however, due to the electron-withdrawing 5-nitro group of **162**, it was expected that the benzothiophene would be somewhat deactivated towards EAS.

As discussed in **Section 1.6.2.4**,^{152,160} bromination can be directed to the 3-position of a benzothiophene-2-carboxylic acid when converted to the carboxylate salt. Hence Mbere's route was explored for its applicability to methyl 5-nitrobenzo[*b*]thiophene-2-carboxylate (**162**) (see **Scheme 99**).



Scheme 99: Bromination of methyl 5-nitrobenzo[*b*]thiophene-2-carboxylate (**162**). Reaction conditions: i) Methyl thioglycolate, K₂CO₃, DMF, RT, 17 h, 95% ii) methyl thioglycolate, K₂CO₃, DMF, MW 90 °C, 15 min, 88%; iii) NaOH aq. (1 M sol.), MeOH, Δ, 3 h (or MW 100 °C, 3 min), then 1 M HCl, 95% (94%); iv) Br₂, NaOAc, AcOH, 55°C, 17 h, 75%; v) MeI, K₂CO₂, DMF, RT, 3 h, 93%.

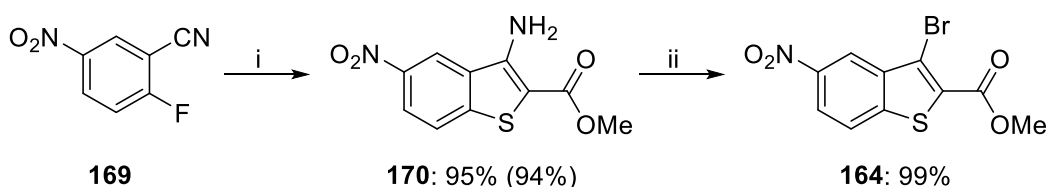
Methyl 5-nitrobenzo[*b*]thiophene-2-carboxylate (**162**) was synthesized from condensation of 2-chloro-5-nitrobenzaldehyde under basic conditions with methyl thioglycolate in 95% yield after 17 h at room temperature. To facilitate a potentially more rapid synthetic route, the application of microwave-assisted dielectric heating was explored. Irradiation at 90 °C in a sealed vessel reduced the reaction time to 15 minutes and maintained high yields. Saponification to carboxylic

acid **167** was also amenable to microwave-assisted techniques, with the reaction time shortened from 3 h with conventional reflux to a 3 minute irradiation in a sealed vessel at 100 °C, with no detrimental effect on the yield (see **Scheme 99**).^{vi}

5-Nitrobenzo[*b*]thiophene-2-carboxylic acid (**167**) was then subjected to Mbere *et al.*'s bromination conditions, using excess bromine and anhydrous sodium acetate (NaOAc) in glacial AcOH, and heated to 55 °C for 17 h. The brominated carboxylic acid **168** was isolated successfully and esterified to methyl ester **164** in high yield using methyl iodide under basic conditions.

Unfortunately, the bromination step was found to be quite variable in its efficiency, often returning mixtures of **162** and **164**. Therefore an alternative route for bromination using diazotization chemistry was explored via methyl 3-amino-benzothiophene-2-carboxylate **170**.

Beck established the cyclocondensation of 2-nitrobenzonitrile with methyl thioglycolate to form benzo[*b*]thiophenes in 1971, and this method has been adapted by a number of groups to set up substrates for *ortho*-halogen displacement.^{147,270–272} To this end, a microwave-assisted method towards **170** was designed (see **Scheme 100**). Methyl thioglycolate and 2-fluoro-5-nitrobenzonitrile (**169**) were condensed under basic conditions using triethylamine in DMSO to give aminobenzothiophene **170** in very high yield, either via conductive heating at 100 °C for 2 h (95%) or microwave-assisted heating at 130 °C for 11 minutes (94%). Subsequent deaminative bromination using copper(II) bromide and *tert*-butyl nitrite (*t*-BuNO₂) in MeCN afforded the brominated benzo[*b*]thiophene **164** in excellent yield (99%).²



Scheme 100: Synthesis of 3-bromobenzothiophene **170**. Reaction conditions: i) Methyl thioglycolate, NEt₃, DMSO, 100 °C, 2 h, 95% or MW 130 °C, 11 min, 94%; ii) CuBr₂, *t*-BuNO₂, MeCN, 0 °C to RT, 2 h, 99%.²

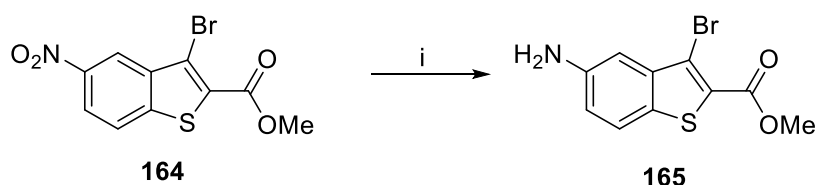
3.4.2. N-Functionalization of methyl 3-bromo-5-nitrobenzo[*b*]thiophene-2-carboxylate.

Now that a viable route for the synthesis of 3-bromo-5-nitrobenzothiophene **164** had been established, it was necessary to append a group onto the carbocyclic ring ready for cyclization

^{vi} Microwave-mediated saponification optimised by Alexander Rand, University of Sussex, 2013

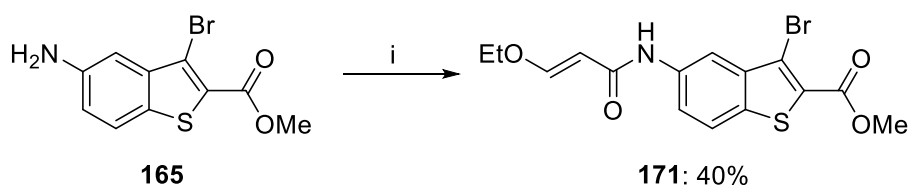
to thienoquinoline **166** by EAS. It was intended that this would be conducted through *N*-functionalization with a suitable electrophile bearing carboxylic acid.

In order to transform nitrobenzothiophene **164** to the corresponding amine **165**, it was found that the traditional hydrogenation procedure conducted under an atmosphere of hydrogen gas and promoted by catalytic Pd/C, used previously in **Scheme 96 (Chapter 3.3)**, was not a viable route to **165**, affording the hydrodehalogenated product. Thus, an electron transfer and protonation method was investigated with the reaction of **164** with tin(II) dichloride (SnCl₂) in a conc. HCl-EtOH solvent system affording the desired methyl 5-amino-3-bromobenzo[*b*]thiophene-2-carboxylate **165** in excellent yield (97%) after heating to reflux for 3 h (see **Scheme 101**).



Scheme 101: Electron transfer and protonation to afford 5-amino-3-bromobenzo[*b*]thiophene **165**. Reaction conditions: i) SnCl₂·2H₂O, conc. HCl, EtOH, Δ, 3 h, 97%.

The amide bond forming conditions used previously by Dr Chuckowree returned quite disappointing yields. After stirring amine **165** with 3-ethoxyacrylic acid for 24 h, in the presence of peptide-coupling reagents EDCI·HCl, HOBT·H₂O and DIEA as base in DMF at RT, the coupled product **171** was isolated in 40% yield after purification by flash column chromatography (see **Scheme 102**).



Scheme 102: Amide bond formation to quinolone precursor **171**. Reaction conditions: i) 3-Ethoxyacrylic acid, EDCI·HCl, HOBT·H₂O, DIEA, DMF, N₂, RT, 24 h, 40%.

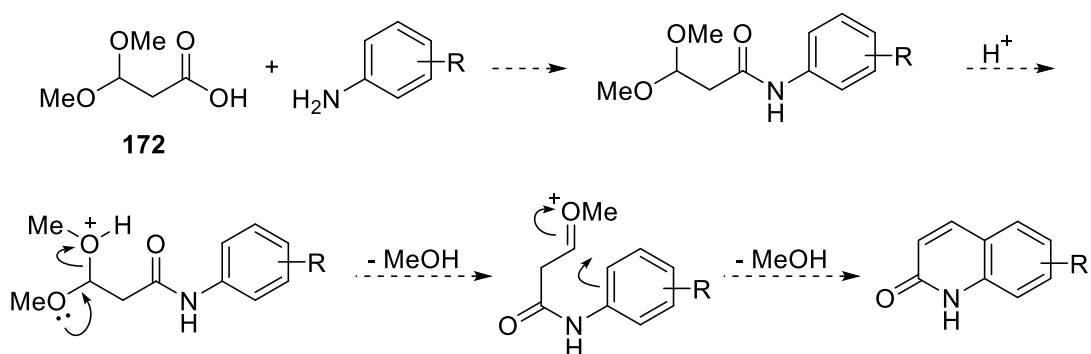
In order to try and improve yields alternative conditions were explored, as illustrated in **Table 2**. These included the use of DMAP as an alternative acyl-transfer agent instead of HOBT (entries 2-4).²⁷³ Similarly the use of pyridine was explored as an additive, aprotic solvent and proton scavenger. However, lower yields than the original peptide-coupling system were obtained (10-15%). The use of Schotten-Baumann type conditions with an acid chloride, 3-ethoxyacryloyl

chloride, and catalytic amounts of DMAP in pyridine-CH₂Cl₂ were unsuccessful with no isolable products (entry 5).¹⁶²

Table 2: Amide bond formation trials for synthesis of 171 (see Scheme 102). ^a				
Entry No.	Coupling reagents	Additive	Solvent	Yield (%) ^b
1	EDCI.HCl, HOBT.H ₂ O	DIEA	DMF	40
2 ^c	EDCI.HCl, DMAP ^d	Pyridine	DMF	10
3	EDCI.HCl, DMAP	Pyridine	DMF	10
4	EDCI.HCl, DMAP ^d	n/a	Pyridine	15
5 ^e	Pyridine	DMAP ^d	CH ₂ Cl ₂	n/a

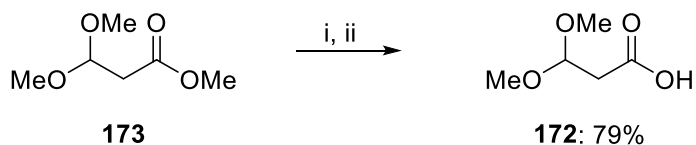
^a Reaction conditions: **165**, 3-ethoxyacrylic acid (1.1 equivalents), coupling reagents and additives were stirred at RT for 24 h, unless otherwise indicated.
^b Isolated yield after purification by flash column chromatography.
^c Reaction stirred for 17 h.
^d Used catalytically.
^e Reaction conducted using the acid chloride, 65 h reaction time.

From these trials it was determined that the original peptide-coupling strategy was the best route. However, upon repetition it was apparent that the yields were quite inconsistent and often fell below 40%, with a lot of degradation observed during purification. It was postulated that the carboxylic acid may be acting as a Michael acceptor in solution, to undergo a number of side reactions. Due to these issues alternative coupling partners were investigated, with consideration of the desired subsequent acidic activation step required for the Knorr-carbostyryl quinolone reaction. Considering an acid-mediated cyclization, the required cyclization partner would need to be able to form an oxonium ion under acidic conditions for intramolecular EAS. Thus it was proposed that 3,3-dimethoxypropanoic acid (**172**) could be an appropriate alternative acyl partner for coupling (see **Scheme 103**) and so was investigated.



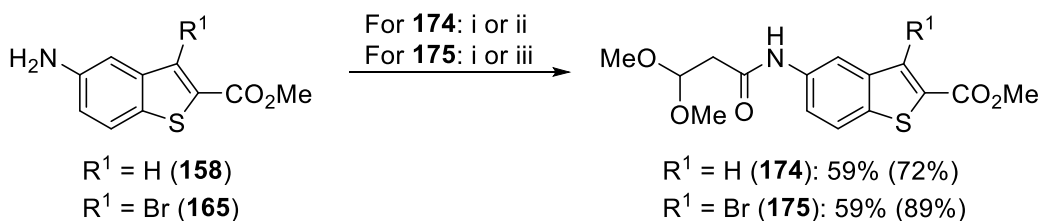
Scheme 103: Proposed acid-mediated Knorr-carbostyryl mechanism using 3,3-dimethoxypropanoic acid (**172**), via formation of an oxonium ion.

Saponification of methyl ester **173** gave 3,3-dimethoxypropanoic acid (**172**) in high yields as a clear, colourless oil after careful acidification (see **Scheme 104**).



Scheme 104: Synthesis of 3,3-dimethoxypropanoic acid **172**. Reaction conditions: i) Aq. NaOH (4 M in H₂O), 110 °C, 30 min; ii) 6 M HCl, 79%.

Using the EDCI.HCl, HOBT.H₂O coupling system, **172** was coupled with non-brominated **158** to ascertain the reaction viability. After stirring at RT for 24 h, a reasonable yield of coupled product **174** (59%) was obtained after purification by flash column chromatography (see **Scheme 105**). Use of a higher reaction temperature and submission of the reaction mixture to microwave-assisted dielectric heating in a sealed vessel at 78 °C for 1 h, gave amide **174** in an improved yield (72%). Thus, the same set of conditions were applied to methyl 5-amino-3-bromobenzo[*b*]thiophene-2-carboxylate (**165**), with similar yields obtained after stirring at RT for 24 h (59%), though slightly lower yields were observed after microwave-assisted heating at 80 °C for 1h (56%).

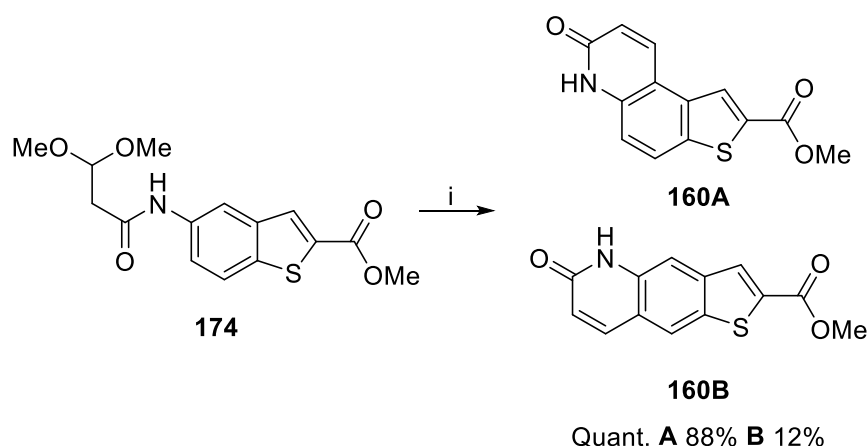


Scheme 105: Amide bond formation using carboxylic acid **172**. Reaction conditions for the synthesis of **174**: i) **158**, **172**, EDCI.HCl, HOBT.H₂O, DIEA, N₂, RT, 24 h or ii) MW 78-80 °C, 1 h. Reaction conditions for synthesis of **175**: i) **165**, **172**, EDCI.HCl, HOBT.H₂O, DIEA, N₂, RT, 24 h or iii) **172**, COMU, DIEA, DMF, N₂, MW 120 °C, 30 min. Microwave-mediated yields given in parentheses.

Yields of the coupling reaction of **165** was further improved through use of the new coupling reagent COMU as a substitute for both HOBT and EDCI. With an excess of carboxylic acid **172**, DIEA and 1.5 equivalents of COMU, microwave-assisted heating under a nitrogen atmosphere at 120 °C for 30 minutes gave **175** in excellent yield (89%).

3.4.3. Acidic cyclization to thienoquinolone.

With the advent of a new cyclization precursor, it was uncertain how successful the quinolone formation would be and if the ratio of regioisomers would be affected. Hence the non-brominated dimethoxy cyclization precursor **174** was stirred with conc. H₂SO₄ at 0 °C and allowed to warm to room temperature over 3 h. Isolation by pouring into iced water and collection of the solid by vacuum filtration gave **160** in quantitative yields, with a ratio of 88:12 of **160A**:**160B** (see **Scheme 106**), ascertained by ¹H NMR spectroscopic analysis (see **Figure 48**).



Scheme 106: Acidic cyclization of non-brominated precursor **174**. Reaction conditions: i) Conc. H₂SO₄, RT, 3 h, quant., 88:12 **160A**:**160B**.

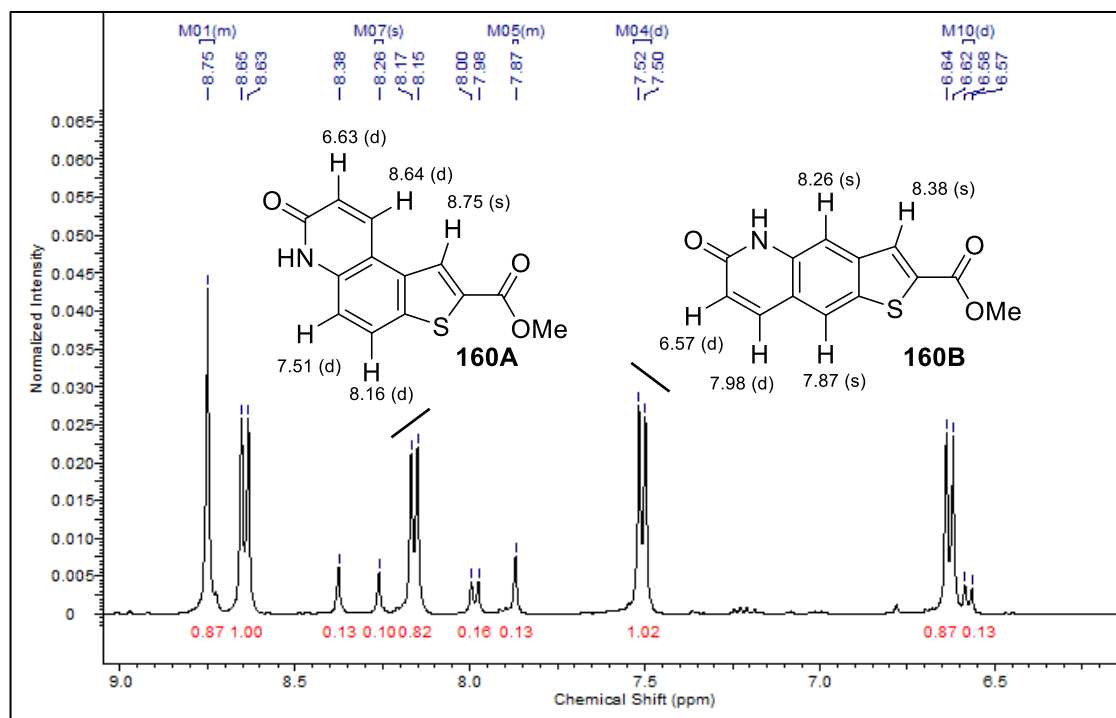


Figure 48: ¹H NMR spectrum (DMSO-*d*₆, 500 MHz, δ_H 9.0 - 6.0 ppm) of crude quinolone mixture **160A** and **160B** from acidic cyclization of **174**. Quinolones with chemical structures annotated with chemical shift assignments. Ratio of products calculated by averaging the integration of peaks for each chemical structure: 88:12 ratio **A**:**B**.

The two regioisomers were easily differentiated by ^1H NMR spectroscopic analysis due to their very different coupling patterns. As illustrated in **Figure 48**, for thieno[3,2-*f*]quinolone **160A**, each of the two quinolone fused rings had two vicinal protons which coupled strongly but had very different chemical shifts. The 9-CH proton in **160A** was much more deshielded by the electron-withdrawing carbonyl, which resulted in a more downfield resonance (δ_{H} 8.64 ppm) than the 8-CH proton (δ_{H} 6.63 ppm). The shielding of the 9-CH resonance in **160B** was much less pronounced.

The two protons of the carbocyclic ring were more similar in their chemical environments, constituting an AB system with 'roofing' of the doublets apparent in the ^1H NMR spectrum (as illustrated on **Figure 48**). This AB relationship confirmed that the fused benzo ring was *para*-disubstituted.¹⁰¹ As the difference in the chemical shifts of the two protons was still quite large, the 'roofing' effect was only slight.

These coupling relationships were confirmed through 2D COSY ^1H NMR spectroscopic experiments (see **Figure 49**). For **160B**, due to the manner of cyclization, the protons of the carbocyclic ring were *para* to one another and hence would only give rise to a very small coupling and appeared as singlets in the ^1H NMR spectrum at δ_{H} 8.26 and 7.87 ppm.

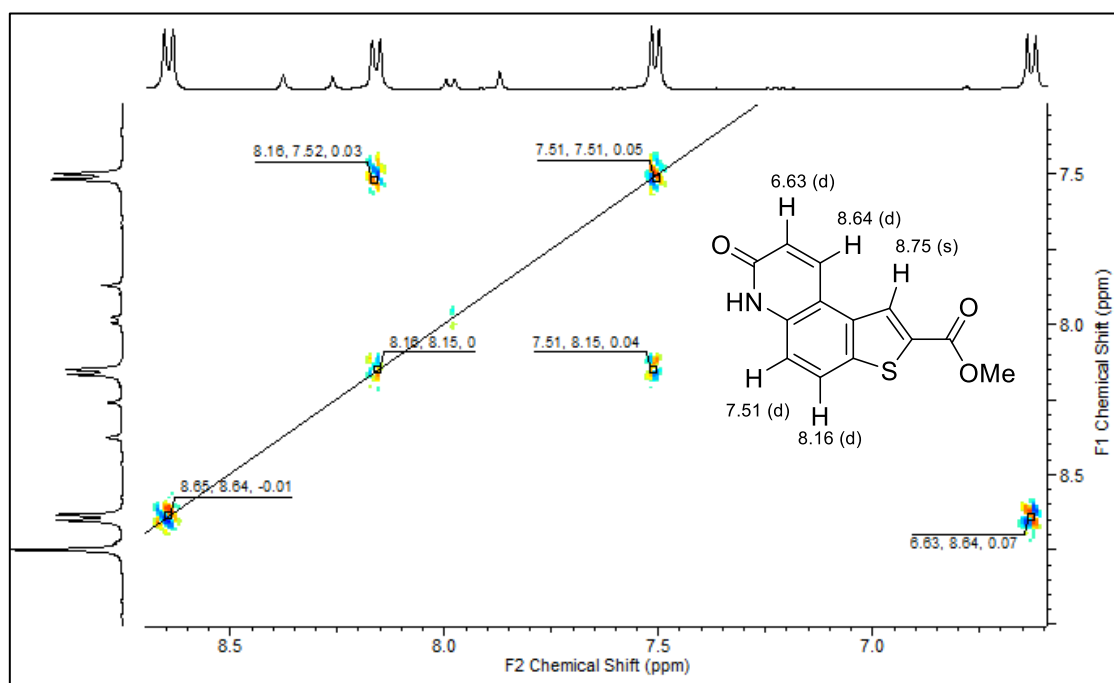
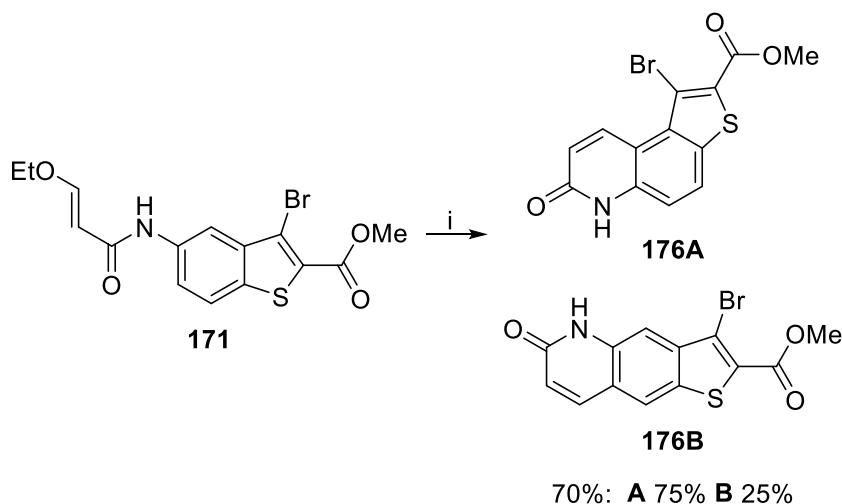


Figure 49: 2D COSY ^1H NMR experiment for crude quinolone mixture **160A** and **160B** ($\text{DMSO}-d_6$, 500 MHz). The higher concentration of **160A** resulted in only the proton-proton coupling relationships of this compound being visible in the spectrum.

The ratio of quinolone products echoed those reported by Dr Chuckowree from the alternative cyclization precursor **159** (see **Chapter 3.3.1**). Hence it was ascertained that the regioselectivity of reaction had not changed significantly from a change in the cyclization precursor and so the brominated cyclization precursors **171** and **175** were subjected to the acidic cyclization conditions (see **Scheme 107**).



Scheme 107: Acidic cyclization of ethoxyprop-2-ene amide **171**. Reaction conditions: i) Conc. H_2SO_4 , RT, 3 h, 70%. 70:30 ratio of **176A**: **176B**

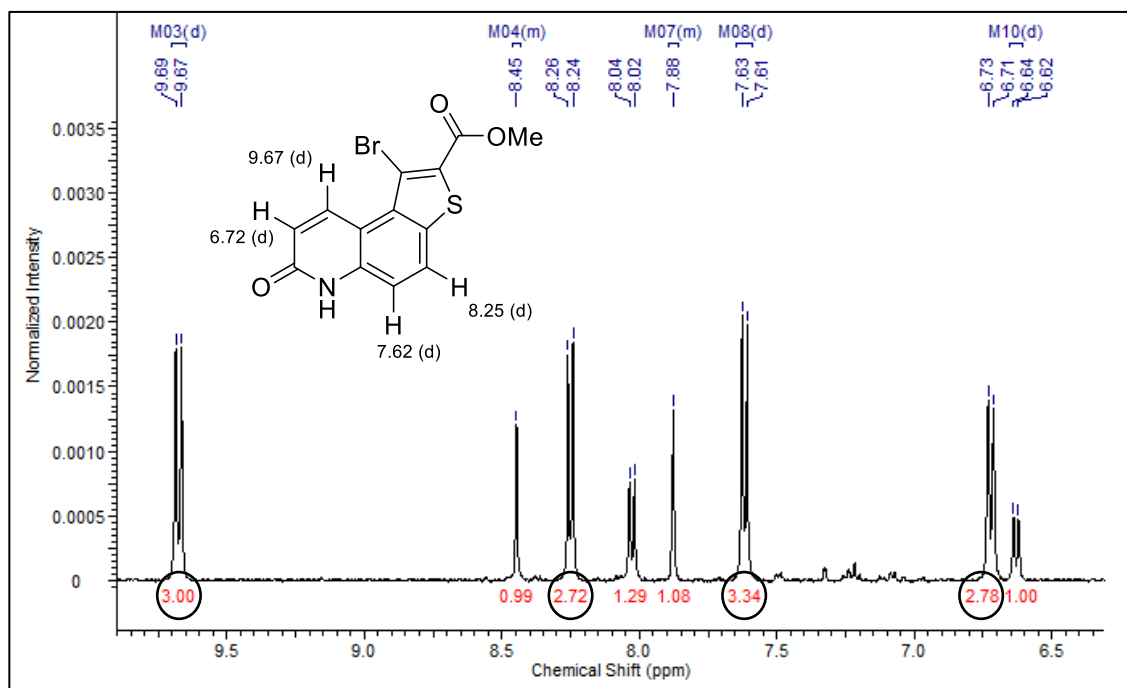


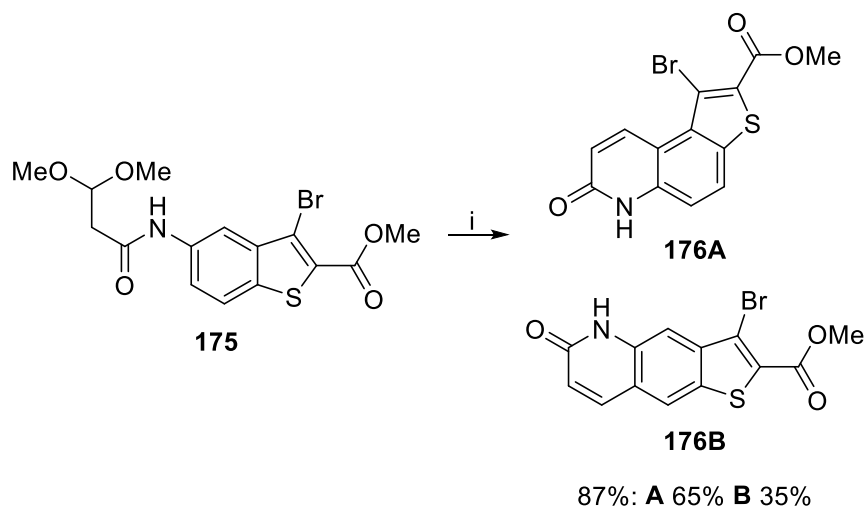
Figure 50: ^1H NMR spectrum ($\text{DMSO}-d_6$, 500 MHz, δ_{H} 9.8 - 6.4 ppm) for crude mixture of quinolones **176A** and **176B**. Signals associated with **176A** illustrated with integrations circled. Averaged integration gave the ratio of products as approximately 3:1.

By ^1H NMR spectroscopic analysis, it was found that there was a change in the ratio of regioisomers. The major product was still the desired thieno[3,2-*f*]quinolone **176A**, but it was

found that the overall yield had reduced to 70% and there was an approximate 3:1 ratio of **176A** to **176B** (see **Scheme 107** and **Figure 50**). The two regioisomers were assigned as previously, with inference from the coupling patterns, relative integrations of the peaks and the 2D COSY ^1H NMR data.

The change in quinolone regioisomer ratio with the addition of the bromine group may be due to a reduction in electron density at the 4-position of the benzothiophene, reducing the difference in activation energy for EAS at the 4- and 6-positions, or it could be due to steric effects. Nevertheless, the reaction proceeded in favour of the desired regioisomer, and so the alternative cyclization precursor **175** was subjected to the same reaction conditions.

From the dimethoxy precursor **175**, the reaction yields and ratios were found to be more variable than those from **171**. The proportion of **176A** to **176B** was found to be more comparable than in any previous cyclization, with a 65:35 ratio of products, though the best yields obtained were slightly higher than the previous iteration (87%, see **Scheme 108**).

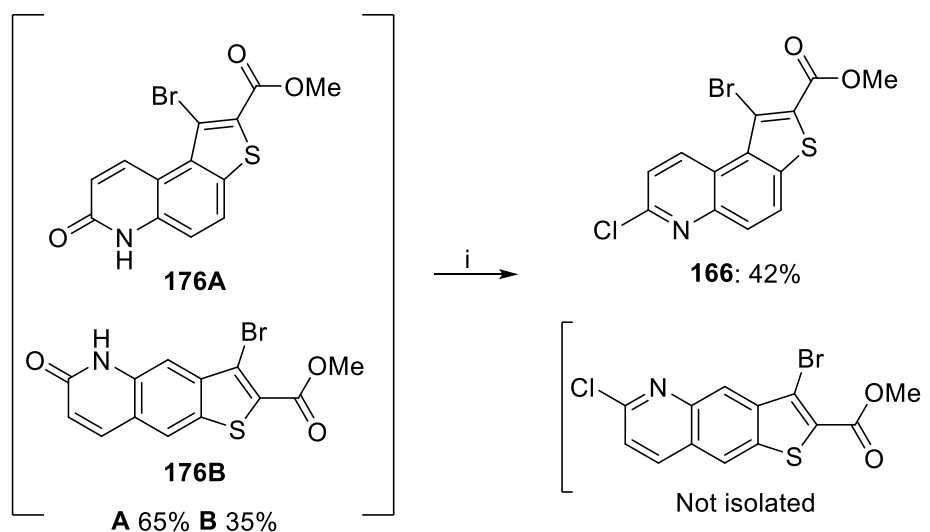


Scheme 108: Reaction scheme for acidic cyclization of (3,3-dimethoxypropanamido)benzothiophene **175**. Reaction conditions: i) conc. H_2SO_4 , RT, 3 h, 87%. 65:35 ratio **176A** to **176B**.

Though this change in the ratio and yield of cyclized products was inconvenient, it was reasoned most likely to be due to small changes in reaction profile. It was proposed that the crude cyclization product should be carried forward to determine the viability of the Suzuki coupling step before undertaking optimization of the cyclization step.

3.4.4. Chlorination to dihalogenated thienoquinoline and Suzuki coupling.

Chlorination using POCl₃ was completed using the previously described method (see **Chapter 3.3.1**). The crude quinolone mixture **176** (**Scheme 108**) was heated to reflux in neat POCl₃ for 2.5 h, and purified by flash column chromatography to give chloroquinoline **166** in 42% yield (see **Scheme 109**).



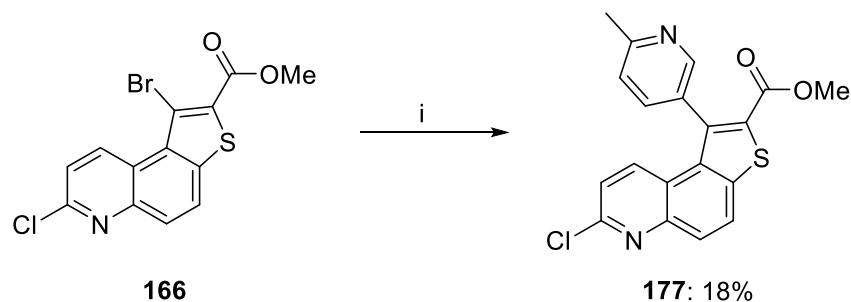
Scheme 109: Chlorination of crude mixture of thienoquinolone **176**. Reaction conditions: i) POCl₃, Δ, 2.5 h, 42%.

Upon purification, the presence of protodemethylated side products was noted. Additionally, the purification was somewhat complicated by the poor solubility of the crude material. Nevertheless, given the ratio of quinolone regioisomers in the crude starting material, the yield of the chlorothieno[3,2-*f*]quinoline regioisomer **166** that was collected was extremely reasonable and could be improved further in parallel with any improvements in the quinolone regioisomeric ratio.

Given successful isolation, the Suzuki coupling of **166** with 6-methylpyridine-3-boronic acid was investigated. The aqueous reaction system used in **Chapter 3.1** for the Suzuki coupling of 2-chloro-6-nitroquinoline was found to protodemethylate the reactants, and so an alternative non-aqueous system was adopted using caesium fluoride (CsF) as base and PdCl₂(PPh₃)₂ as catalyst in anhydrous 1,4-dioxane.

Unfortunately, after microwave-assisted heating at 140 °C for 30 minutes and purification by flash column chromatography, exclusively the unwanted bromine-substituted coupling product

177 was collected in 18% yield (see **Scheme 110**). This was confirmed through ^1H NMR spectroscopic analysis and high-resolution mass spectrometry (HRMS), in which the two chlorine isotopes of the parent ion could be clearly differentiated in a characteristic 3:1 ratio.



Scheme 110: Suzuki coupling of dihalogenated intermediate **166**. Reaction conditions: i) 6-Methylpyridinyl-3-boronic acid, CsF, $\text{PdCl}_2(\text{PPh}_3)$, 1,4-dioxane, N_2 , MW 140 $^\circ\text{C}$, 30 min, 18%.

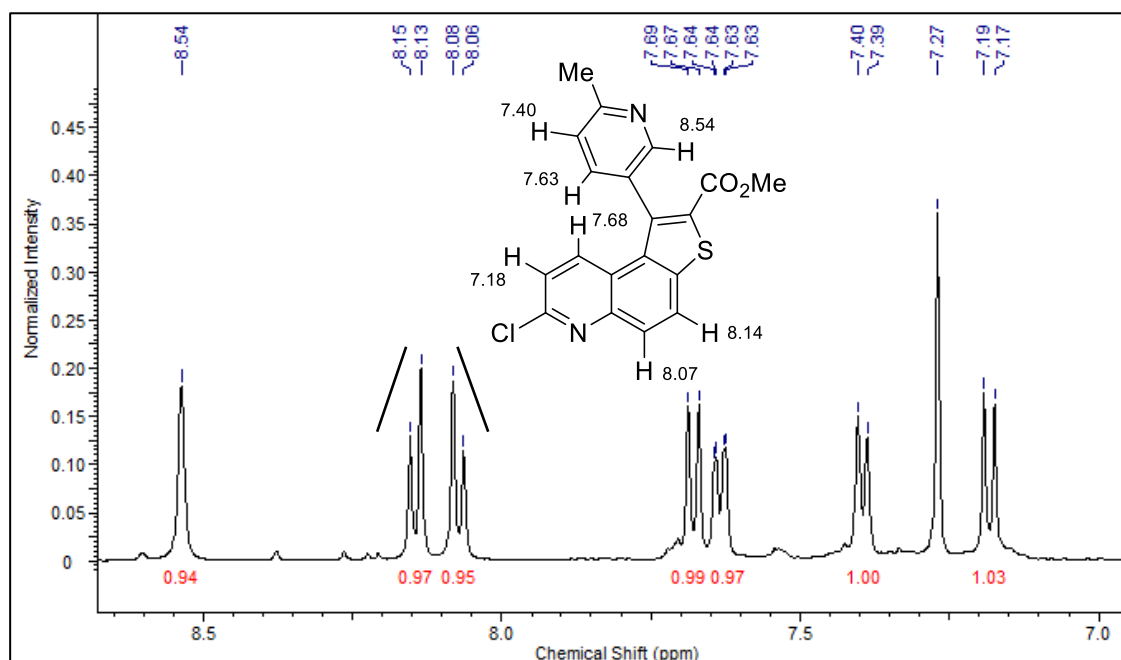


Figure 51: ^1H NMR spectrum ($\text{DMSO}-d_6$, 500 MHz, δ_{H} 10.5 - 7 ppm) of **177**, illustrating the 7 aromatic proton peaks. Chemical structure labelled with those peaks visible in the spectroscopic window.

By ^1H NMR spectroscopic analysis, the AB system of the benzo ring protons was significantly more pronounced, with the extent of ‘roofing’ illustrative of how the chemical environments of the 4-CH and 5-CH protons were much more similar than in the quinolone system (illustrated in **Figure 51**). The additional proton peaks of the 6-methylpyridine were differentiated through their coupling patterns and a 2D COSY ^1H NMR spectroscopic experiment.

Figure 52 illustrates the proton-proton interactions of the 4'-CH proton with 2'-CH and 5'-CH. The 2'-CH proton (δ_{H} 8.54 ppm) was strongly deshielded by proximity to the pyridine nitrogen

and appeared as a broad singlet due to residual coupling with the *meta*-proton 4'-CH (δ_{H} 7.63 ppm), whereas 4'-CH appeared as a doublet of doublets due to vicinal and meta-coupling with the pyridine 5'-CH and 2'-CH protons, respectively.

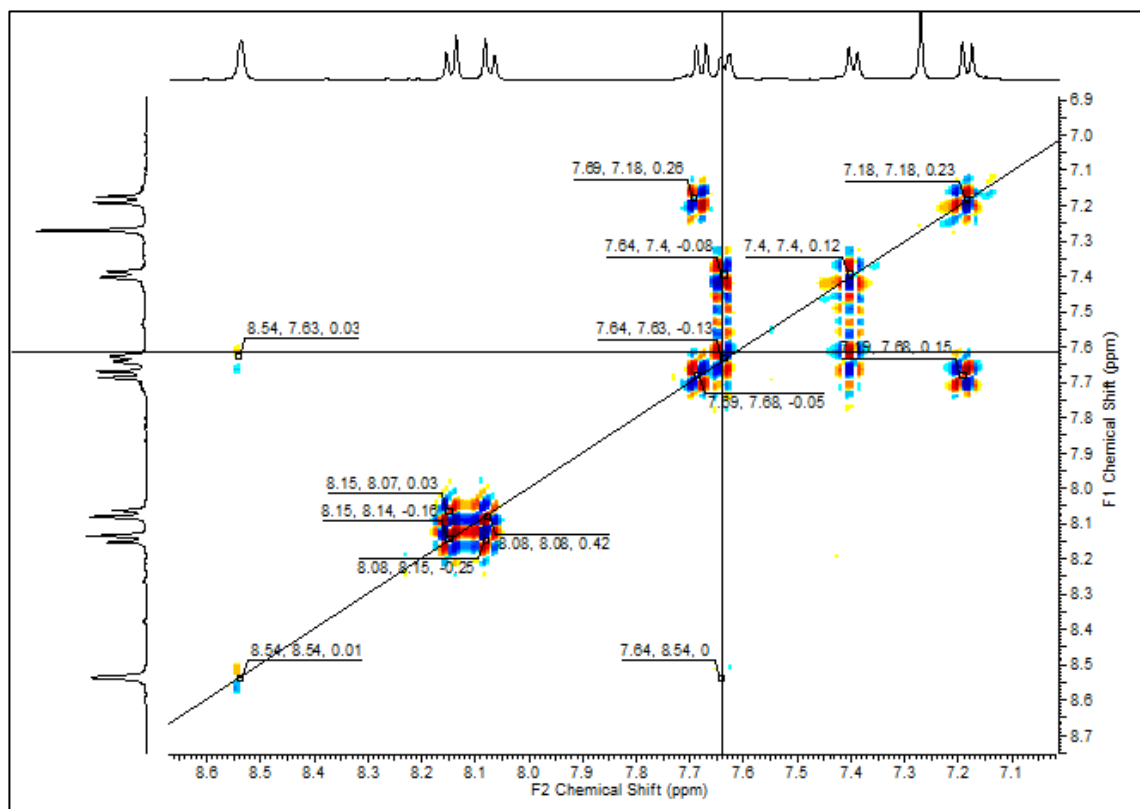


Figure 52: 2D COSY ^1H NMR spectroscopic experiment for **177**, used to differentiate between the two aromatic ring systems. Gridlines indicate the proton-proton interactions of the 4'-CH proton at δ_{H} 7.63 ppm.

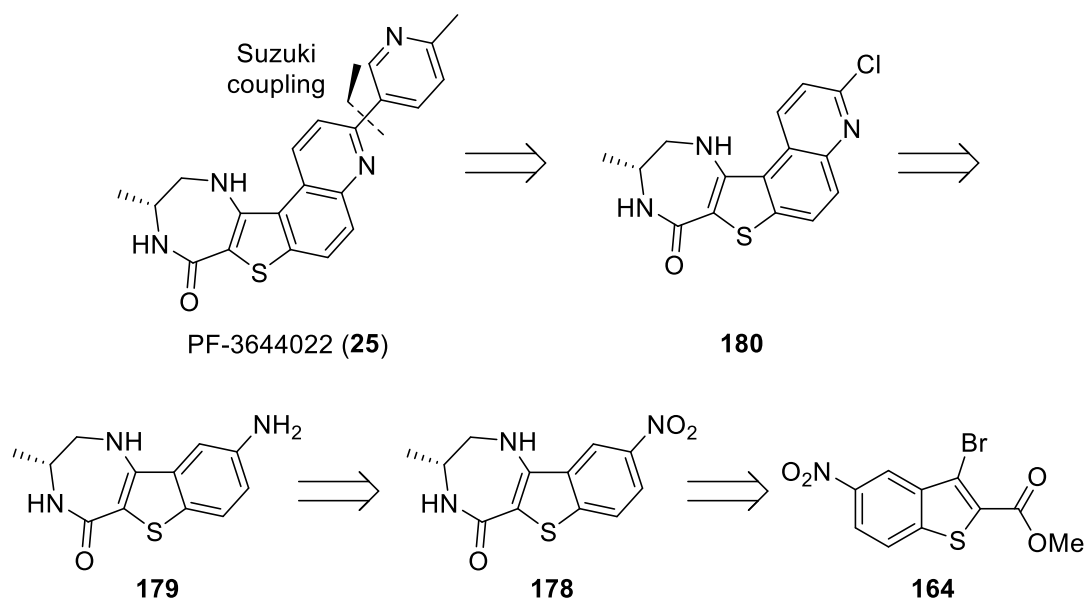
3.4.5. Conclusion.

It was concluded that Suzuki coupling of the dihalogenated intermediate was not a suitable route for the total synthesis of PF-3644022 (**25**). Despite this set-back in completing the synthesis, very important synthetic methods towards key intermediates had been designed and carried out in high yield. These included a new microwave-assisted synthetic route towards methyl 3-bromo-5-nitrobenzothiophene-2-carboxylates² and a new approach for regioselective thienoquinoline synthesis using amide bond formation with COMU as the coupling reagent, which gave excellent yields of cyclization precursors via microwave-assisted synthesis.

3.5. Retrosynthesis

4. Benzo[4,5]thieno[3,2-*e*][1,4]diazepin-5-one scaffold.

Early stage installation of the diazepinone ring of PF-3644022 (**25**) had been avoided up until this point as the ring contained a number of potentially reactive functional groups. However, at this stage of the project, the synthetic options available towards alternative intermediates were becoming more limited, and so it was decided this approach would now be adopted, and that protecting group strategies could be used if found to be necessary.



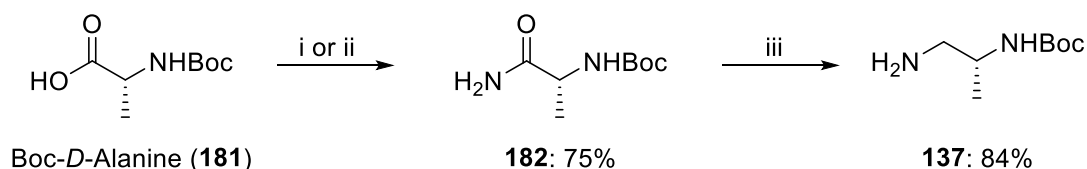
Scheme 111: Retrosynthesis 4, via benzo-thieno-diazepin-one intermediates **178** and **179**.

As illustrated in **Scheme 111**, a new retrosynthetic strategy was proposed with final stage Suzuki coupling, from a 2-chloroquinoline derived from a thieno[3,2-*f*]quinoline-diazepinone (**180**). It was proposed that the lactam ring would be built up via Buchwald-Hartwig *N*-arylation using methyl 3-bromo-4-nitrobenzo[*b*]thiophene-2-carboxylate (**164**), and cyclized thereon to form the diazepinone ring in **178**. Reduction of the nitro group thereafter to **179** would ensure no homocoupling of the aminobenzothiophene under the Buchwald-Hartwig coupling conditions. Subsequent amide bond formation with carboxylic acid **172** was proposed, to be carried forward as established in **Chapter 3.4**, via the Knorr-carbostyryl quinolone reaction and subsequent chlorination ready for final-stage Suzuki coupling to afford PF-3644022 (**25**).

3.5.1. Buchwald-Hartwig *N*-arylation and lactam ring formation.

Buchwald-Hartwig *N*-arylation was chosen to construct the scaffold for diazepinone ring formation as it is a mild, functional group tolerant and generally high-yielding method (see **Chapter 1.6.2.3**). Additionally, through this method it should be possible to install the asymmetric centre without significant racemization. For the chiral centre of PF-3644022 (**25**), enantiopure Boc-*D*-alanine (**181**) was used to derive the mono-Boc-protected diamine **137** ready for *N*-arylation.

Initially, carboxylic acid **181** was converted to the amide using a mixed anhydride method, through reaction with ethyl chloroformate under basic conditions and substitution with ammonia to give amide **182** in up to 41% yield.²⁷⁴ However, it was found that a peptide coupling strategy using EDCI.HCl and HOBT.H₂O with DIEA and ammonia boosted yields to 75% (see **Scheme 112**).



Scheme 112: Amide bond formation and reduction of Boc-*D*-Alanine to chiral Boc-protected diamine **137**. Reaction conditions: i) NEt₃, ethyl chloroformate, THF, N₂, 0 °C, 45 min, then NH₃ (aq. 35%), THF, 0 °C, 45 min 41%; ii) EDCI.HCl, HOBT.H₂O, DIEA, CH₂Cl₂, 0 °C to RT, 30 min, then NH₃ (aq. 35%), 0 °C to RT, 30 min, 75%; iii) BH₃•SMe₂, THF, N₂, 0 °C to RT, 18 h, then MeOH, 84%.

Reduction of the amide group was completed using a Lewis acidic borane complex. **182** was stirred with borane dimethylsulfide (BH₃•SMe₂) at 0 °C under an inert atmosphere and allowed to warm to room temperature overnight. Heating the reaction was found to decompose the Boc group. Once reaction completion had been confirmed by thin layer chromatography (TLC) analysis, the excess BH₃•SMe₂ was removed under reduced pressure and the residues washed with MeOH to decomplex the borane.²⁷⁵ Purification by SCX-2 chromatography gave the chiral mono-Boc-protected diamine **137** in high yield (84%). Characterization of the amine by ¹H NMR spectroscopic analysis confirmed the presence of two diastereotopic protons. Each of these protons coupled with the 2-CHMe centre and with each other, resulting in a doublet of doublets for each proton (see **Figure 53**, δ_H 2.75-2.5 ppm).

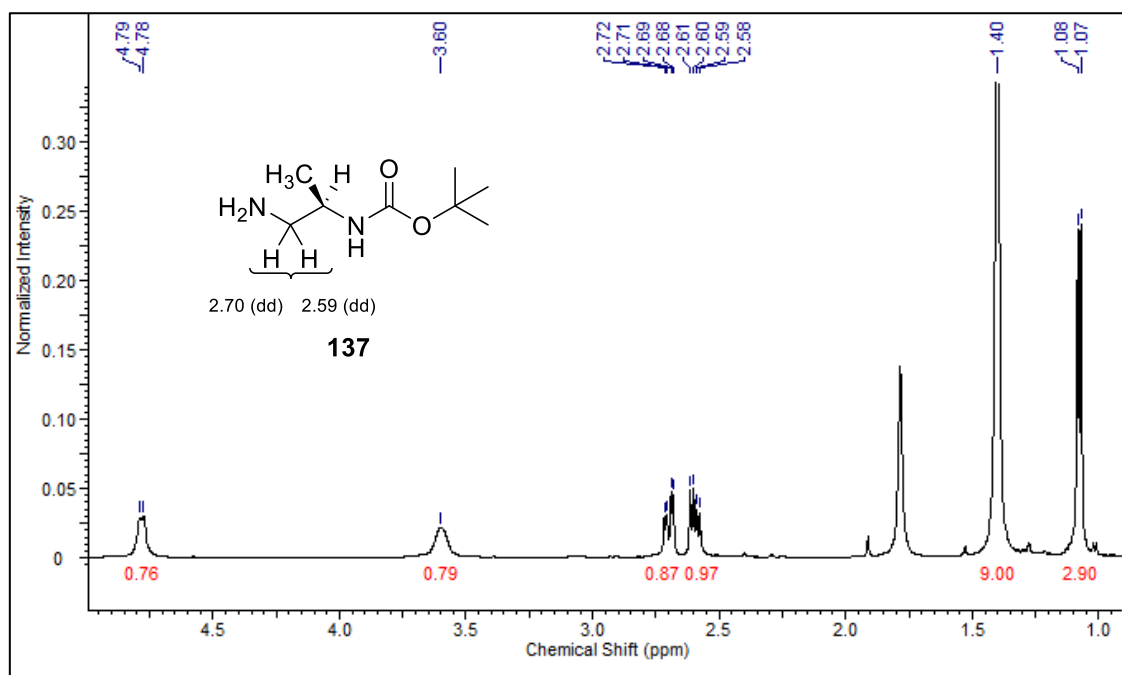
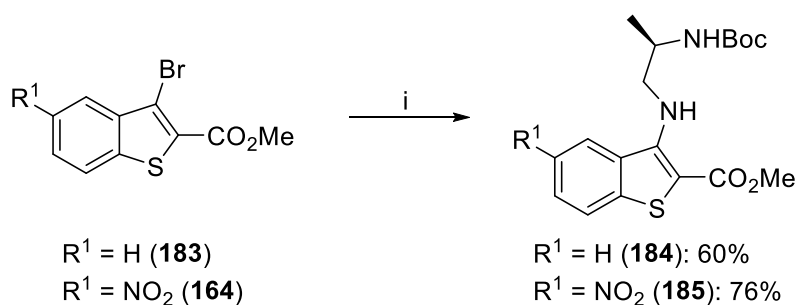


Figure 53: ^1H NMR spectrum (CDCl_3 , 500 MHz, δ_{H} 5.0 – 1.0 ppm) of **137**, illustrating the doublet of doublet peaks for the diastereotopic protons.

For the Buchwald-Hartwig *N*-arylation of **164**, reaction conditions were adapted from studies completed by Queiroz *et al.* for the coupling of aryl amines and electron-rich and electron-poor 3-halogenatedbenzo[*b*]thiophenes.²⁷⁶



Scheme 113: Buchwald-Hartwig *N*-arylation of bromobenzo[*b*]thiophenes **183** and **164**. Reaction conditions: i) **137**, Cs_2CO_3 , (\pm)-BINAP, $\text{Pd}(\text{OAc})_2$, toluene, MW 150 $^\circ\text{C}$, 1.25 h.

Initial trials were conducted using methyl 3-bromobenzo[*b*]thiophene-2-carboxylate (**183**) (see **Scheme 113**, and **Table 3** entries 1-3). Conductive heating routes were investigated first, using equimolar benzothienophene and amine with Cs_2CO_3 (2 equiv.), (\pm)-BINAP (10 mol%) and $\text{Pd}(\text{OAc})_2$ catalyst (5 mol%) in dry toluene and heating to reflux for 24 h. After purification quite a low yield of the coupled product **184** was isolated (entry 1, 27%), and some formation of the transesterification side product was noted.

Through the use of microwave-assisted dielectric heating in a sealed vessel, the reaction time was dramatically reduced from 24 h to 1-1.25 h, with achieve similar yields of **184** achieved (entry 2, 25%). Additionally, the amount of base was reduced, which helped reduce the extent of transesterification.

Table 3: Buchwald-Hartwig <i>N</i> -arylation trial reactions, see Scheme 113 . ^a				
Entry No.	Precursor	Time (h)	Temperature (°C)	Yield (%) ^b
1	183	24	110	27 ^c
2	183	1	150	25
3	183	1.25	150	60
4	164	1.25	150	76
5	164	2	150	69

^a Reaction conditions: Equimolar methyl 3-bromobenzo[*b*]thiophene-2-carboxylate and **137**, Cs₂CO₃ (1.5 equiv.), (±)-BINAP (15 mol%) and Pd(OAc)₂ (5 mol%) in dry toluene, under N₂, were irradiated at 150 °C for the stated time using microwave dielectric heating.

^b Isolated yield after purification by flash column chromatography on SiO₂

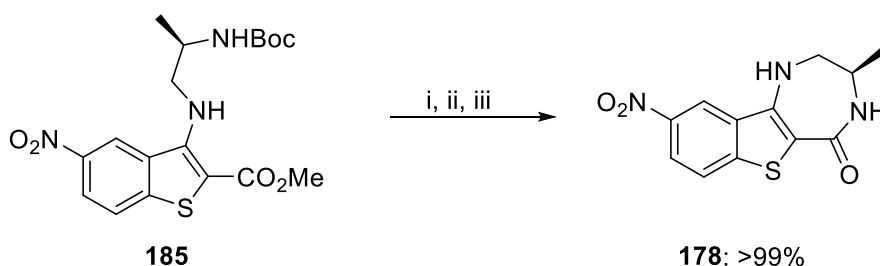
^c Conductive heating, and 2 equiv. Cs₂CO₃.

By extending the reaction time to 75 minutes, the yield of **184** was increased significantly (entry 3, 60%). Coupling of 3-bromo-5-nitrobenzothiophene **164** to amine **137** under these conditions was found to produce the coupled product **185** in excellent yield (entry 4, 76%). However, attempts to improve the yield through prolonged heating gave a slightly diminished yield (entry 5, 69%).

Given the success of the conditions explored and the improved efficiency achieved through application of microwave-assisted heating, no other methods were investigated and the synthesis was carried forward.

Using a general procedure, Boc-deprotection was carried out using a 10% solution of trifluoroacetic acid (TFA) in CH₂Cl₂, stirring the mixture at room temperature overnight (see **Scheme 114**). Attempts to reduce the reaction time through heating resulted in decomposition of materials. Upon confirmation the reaction was complete by TLC analysis, volatile components were carefully removed and subsequent basic cyclization was conducted using a procedure reported by Khatana *et al.* and applied to similar benzothieno-1,4-diazepin-5-one frameworks.²⁷⁷ The TFA salt was stirred with NaOMe in MeOH and heated to 50 °C for 2 h before heating at reflux for an additional 2 h. The crude mixture was then poured into iced water and

neutralized using 1 M HCl aqueous solution. Isolation by vacuum filtration gave **178** as a red powder in quantitative yields.

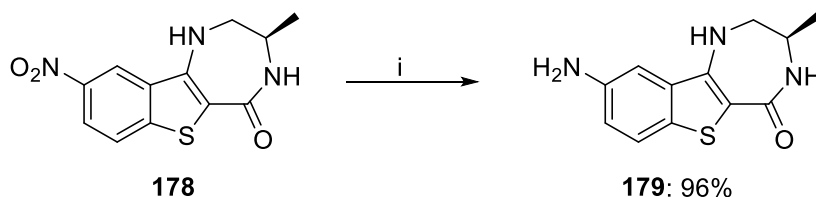


Scheme 114: TFA deprotection and base-mediated lactam ring formation: Reaction conditions: i) TFA (10% in CH₂Cl₂), RT, overnight: ii) NaOMe (25 w% in MeOH), MeOH, 50 °C, 2 h, then Δ, 2 h. iii) 1 M HCl, >99%

Upon attempted reduction of **178** to **179**, it was again found that some conventional methods were not applicable. This was attributed to be due to poor or limited solubility of **178** in most solvents, as many hydrogenation methods rely upon heterogeneous catalysis with adsorption of a soluble reactant onto the solid catalyst surface.

Hydrogenation using H₂ gas with Pd/C in MeOH, EtOAc and AcOH all resulted in either decomposition or return of starting materials. Electron transfer and protonation using SnCl₂·H₂O in acidic ethanol returned a mixture of products, with similar results when ammonium formate and zinc were used. The use of acidic solvents was explored thoroughly as a method to reduce in situ catalyst poisoning through complexation of the basic nitrogen formed. However, even despite this precaution, no reduction product was observed.

The best route found was developed by Spencer *et al.* as a microwave-mediated route for the reduction of poly-functionalized nitroaromatics using molybdenum hexacarbonyl (Mo(CO)₆) and 1,8-diazabicycloundec-7-ene (DBU) in ethanol.^{278,279} A highly functional group tolerant method, the reaction is believed to occur through formation of a metal nitrene complex, with deoxygenation of the nitrogen and loss of carbon dioxide (CO₂) via metal carbonyl mediated carbonylation.²⁸⁰ The non-nucleophilic base DBU was used as an additive as it is known to aid CO liberation from Mo(CO)₆,²⁸¹ and so facilitate generation of open coordination sites for nitro complexation. Once deoxygenated, protonolysis of the nitrogen affords the primary amine.²⁸⁰



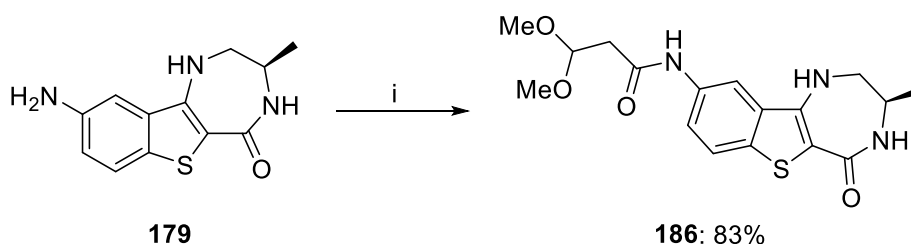
Scheme 115: Mo(CO)₆-mediated reduction of aminobenzothiophene **178**. Reaction conditions: i) Mo(CO)₆, DBU, EtOH, MW 150 °C, 30 min, 96%.²⁷⁹

Microwave-assisted heating of **178** with one equivalent of Mo(CO)₆ and three equivalents of DBU in EtOH in a sealed vessel at 150 °C for 30 minutes^{vii} and purification by flash column chromatography gave **179** in excellent yield (96%, see **Scheme 115**).

Characterization by ¹H NMR spectroscopic analysis confirmed nitro reduction, with significant upfield shift of the carbocyclic ring proton resonances. Additionally, when the ¹H NMR spectrum was conducted in DMSO-*d*₆ as the solvent medium, the NH₂ proton resonances were visible as a broad singlet at δ_H 5.04 ppm.

3.5.2. *N*-Functionalization and acidic cyclization to quinolones.

To form the acidic cyclization precursor **186**, the amide bond formation methods screened towards in **Chapter 3.4.2** were again trialled.



Scheme 116: Amide bond formation to give acidic cyclization precursor **186**. Reaction conditions: i) **172**, COMU, EDCl.HCl, DIEA, DMF, MW 120 °C, 1 h, 83%.

After irradiation at 120 °C for 15 minutes using traditional peptide coupling reagents, **186** was collected in low yield after a problematic purification by flash column chromatography (**Table 4**,

^{vii} Caution was taken when preparing the reaction vessel for microwave irradiation, as liberation of CO₂ gas over the course of the reaction could lead to a significant build-up of pressure. It was important to ensure enough headspace was left in the reaction vessel to allow for this.

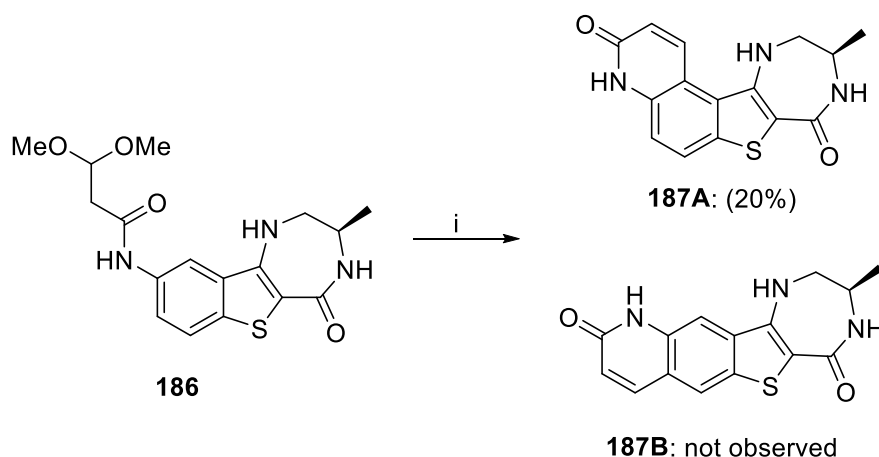
entry 1, 36%). The yield using these reagents was improved through extending the reaction time to 1 h and 40 minutes and use of SCX-2 chromatographic purification (entry 2).

Table 4: Amide bond formation to give acidic cyclization precursor 186 (see Scheme 116). ^a				
Entry No.	Coupling reagents	Temperature (°C)	Hold time (h)	Yield (%) ^b
1	EDCI.HCl, HOBT.H ₂ O	120	0.25	36 ^d
2	EDCI.HCl, HOBT.H ₂ O	120	1.7	43
3	COMU	120	1	70 ^d
4	COMU, EDCI.HCl	120	1	83 ^e
^a Reaction conditions: Benzothiophene 179 and carboxylic acid 172 , the coupling reagents stated and two equivalents of DIEA in DMF were irradiated under argon at 120 °C for the indicated hold time. ^b Isolated yield after SCX-2 purification. ^c Isolated yield after purification by flash column chromatography on SiO ₂ . ^d 50% purity, by LCMS trace. ^e >85% purity, by LCMS trace.				

Application of COMU as the coupling-reagent dramatically improved the isolated yield (entry 3, 70%). However the isolated product was deemed only approximately 50% pure after SCX-2 chromatography, as determined by reverse-phase liquid chromatography mass spectrometry (RP-LCMS).^{viii} The purity of the sample and the isolated yield were greatly improved through the combined use of COMU and EDCI.HCl under the same reaction conditions (entry 4, 83%, **Scheme 116**), with a >80% purity determined by RP-LCMS.

Acidic cyclization of **186** was then conducted as previously described in **Chapter 3.4.3**, before isolation by vacuum filtration. Isolation of the crude solid was very problematic, and the yield obtained was greatly reduced compared to previous studies (20%, see **Scheme 117**).

^{viii} LCMS data was recorded on a Waters 2695 HPLC using a Waters 2487 UV detector and a Thermo LCQ ESI-MS. Samples were eluted through a Phenomenex Lunar 3μ C18 50 mm × 4.6 mm column, using acetonitrile and water acidified by 0.01% formic acid. Samples were eluted using acetonitrile and water (1:9 to 9:1) acidified by 0.01% formic acid, at a flow rate of 3 μl/min.



Scheme 117: Acidic cyclization of advanced intermediate **186**. Reaction conditions: i) Conc. H_2SO_4 , 0 °C to RT, 3 h.

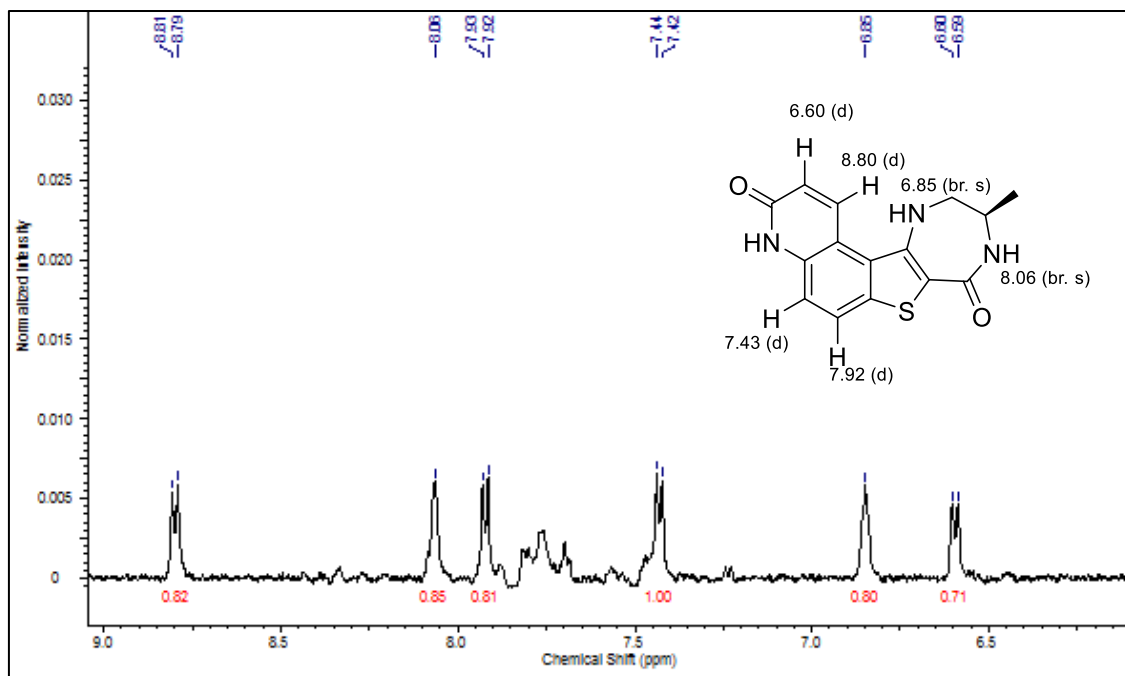


Figure 54: ^1H NMR spectrum ($\text{DMSO}-d_6$, 500 MHz, δ_{H} 9.0 - 6.0 ppm) of crude acidic cyclization product. Only regioisomer **187A** was clearly observed. Illustrative chemical structure labelled with proton chemical shifts (only those visible in this spectral window).

Surprisingly, the only regioisomer that could be clearly observed in the crude ^1H NMR spectrum was the thieno[3,2-*f*]quinolone regioisomer **187A** (see **Figure 54**). It was identified with inference from previous acidic cyclization products. The diazepinone NH protons were visible in the ‘aromatic’ region of the spectrum using $\text{DMSO}-d_6$ as solvent medium, and have been labelled as such in **Figure 54**.

Due to solubility issues the signals of the ^1H NMR spectrum were very weak. Upon repeating the ^1H NMR experiment with a more concentrated sample it was found that the crude material rapidly decomposed. Additionally, mass spectrometry showed significant fragmentation.

In case decomposition was occurring in the reaction vessel, the reaction was repeated using a more dilute acidic system and longer reaction time; however this resulted in a mixture of unidentifiable products by ^1H NMR spectroscopic analysis.

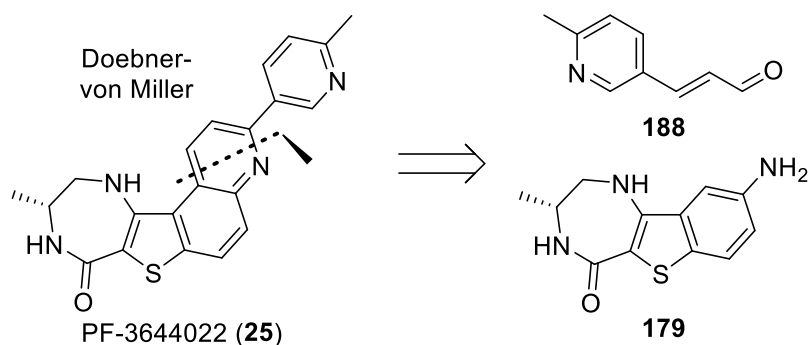
Unfortunately, it appeared that the harshly acidic conditions were decomposing the diazepinone-based intermediates, a possible outcome that had been speculated on at the beginning of this chapter. It was concluded that alternative cyclization procedures should be investigated.

3.5.3. Alternative cyclization methods.

As was described in **Chapter 1.6.2.3**, there are a number of different routes towards multi-functionalized quinolines. Towards 2-substituted quinolines a number of routes were discussed based upon the Skraup and Doebner-von Miller quinoline cyclizations. Most reactions tend to proceed through intramolecular EAS of an aniline derivative, similar to those routes adopted in **Chapters 3.2** and **3.3**.

3.5.3.1. Doebner-von Miller quinoline formation.

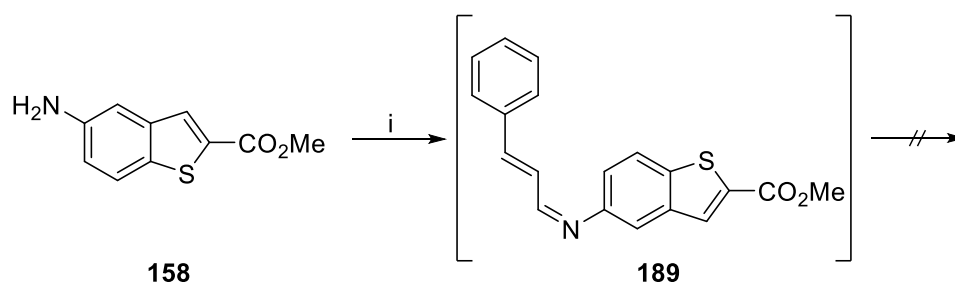
The Doebner-von Miller reaction proceeds from a starting aniline, with *N*-functionalization via Michael addition of an α,β -unsaturated aldehyde to give an intermediate imine. It was proposed that a Doebner-von Miller cyclization may be a viable method to synthesize a thienoquinoline from the advanced aniline intermediate **179** and a pyridine-derived cinnamaldehyde (see **Scheme 118**).



Scheme 118: Retrosynthesis 4.1. Proposed Doebner-von Miller quinoline formation from advanced intermediate **179** and pyridine-derived cinnamaldehyde **188**.

Trial reactions were completed to assess the viability of the reaction using a simplified model with methyl 4-aminobenzo[*b*]thiophene-2-carboxylate (**158**) and cinnamaldehyde (see **Scheme 119**). As described by Matsugi *et al.* in their synthesis of 2-methylated quinolines,²⁸² a two-phase system of aqueous acid and organic solvent was adopted in order to reduce unwanted aldehyde polymerization, by keeping the aldehyde in the organic phase whilst the protonated aniline occupies the aqueous phase. However, after heating to reflux for 2 h in a 6 M HCl-toluene (4:1) solution, only the starting materials were collected.

The use of phase-transfer catalysts TBAB or TBAC was explored to aid the interfacial movement of reagents, but only the Schiff base condensation product **189** was collected.^{283,284} Use of more forcing conditions, including heating to reflux overnight and stirring the isolated Schiff base in neat concentrated HCl overnight, resulted in decomposition of materials.



Scheme 119: Doebner-von Miller reaction of model aminobenzothiophene **158**. Reaction conditions: i) Cinnamaldehyde, TBAB/TBAC, 6 M HCl-toluene (4:1), Δ , 2 h, no reaction.

There are various mechanisms postulated for the Doebner-von Miller quinoline reaction, with debate over whether the reaction proceeds through initial Schiff base formation¹¹⁴ or a Michael addition of the aniline, with subsequent EAS at the carbonyl centre (see **Chapter 1.6.2.3**).⁸¹ For this reaction, it may be that the cinnamaldehyde was too bulky to allow Michael addition to

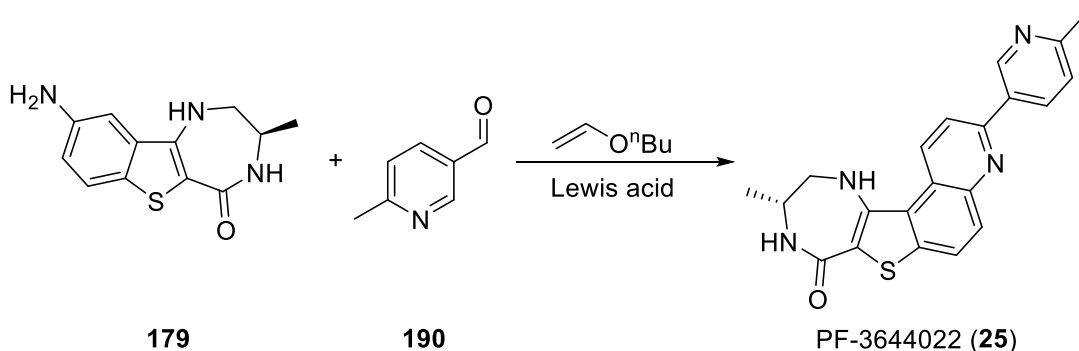
occur or that the benzothiophene ring was not electron dense enough to promote intramolecular EAS. Therefore alternative methods of cyclization were investigated.

3.5.3.2. Multi-component Lewis acid-mediated quinoline formation.

The multi-component Doebner quinoline synthesis was traditionally conducted between an aniline, functionalized aldehyde and pyruvic acid to give the 2-substituted-4-carboxyl quinoline, which could then be decarboxylated to give the 2-substituted quinoline.^{115,116}

As has been discussed in **Chapter 1.6.2.3**, the Doebner multi-component quinoline synthesis has been explored extensively by Wang *et al.* to develop a one-pot multi-component reaction (MCR) for the synthesis of fused quinoline ring systems.^{119–123} Specifically, they developed a route towards 2-substituted quinolines using *n*-butyl vinyl ether (*n*-BVE) as the reactive ethene unit, with proposed loss of butanol upon aromatization.¹²³

This method offered an alternative path for synthesis of the quinoline unit in PF-3644022 (**25**) under mild conditions. It was proposed that a Doebner-type multi-component convergent cyclization reaction could be conducted between advanced intermediate **179**, 6-methylpyridine-3-carboxaldehyde (**190**) and *n*-BVE under Lewis acidic conditions to give direct access to **25** in a one-pot procedure (see **Scheme 120**)



Scheme 120: Proposed Doebner-type multi-component quinoline synthesis to PF-3644022 (**25**).

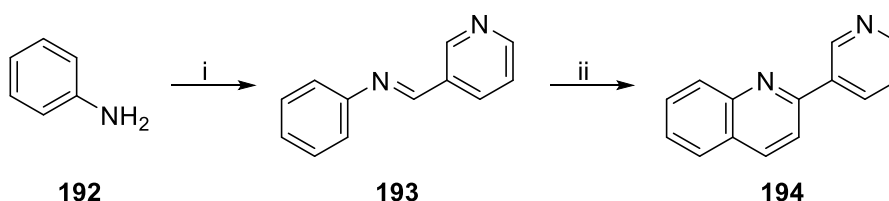
3.5.3.2.1. Lewis acid-mediated quinoline formation.

A trial system had been briefly investigated by Lorna Brigham, a summer student in the research group,^{ix} to ascertain the viability of reacting together pyridine-3-carboxaldehyde (**191**) and

^{ix} Experiments and analysis of results completed by Lorna Brigham, M.C. Bagley, University of Sussex, 2015, unpublished.

aniline (**192**) to promote this type of cyclization and to investigate the applicability of Wang *et al.*'s published methods.

It was found that using Wang *et al.*'s procedure with a higher quantity of molecular iodine (50 mol%), equimolar quantities of aldehyde **191** and aniline (**192**), and 1.5 equivalents of *n*-BVE, heating to reflux for 20 h in tetrahydrofuran (THF) resulted in quinoline **194** formation (see **Scheme 121**), as ascertained by ¹H NMR spectroscopic analysis of the crude material after aqueous work-up. A number of side products were also observed, but efforts to isolate the pure quinoline by flash column chromatography on SiO₂ were complicated by significant co-elution of components.



Scheme 121: Trial multi-component quinoline synthesis. Reaction conditions: i) Pyridine-3-carboxaldehyde (**191**), solvent; ii) *n*-BVE, Lewis acid, Δ, 20 h, or MW 100 °C, 1 h.

Bagley and Brigham found that pre-stirring the aniline and aldehyde in the minimum amount of solvent at room temperature for 1 h to form the Schiff base (**193**) before addition of the Lewis acid and *n*-BVE, helped reduce the amount of side products formed. Also, microwave-assisted dielectric heating in a sealed vessel at 120 °C for 1 h was found to improve the ratio of quinoline to side products in the crude reaction mixture. Alternative Lewis acids were also briefly examined before the project was handed over, with similar product conversions observed by ¹H NMR spectroscopic analysis when the reaction was mediated by SnCl₂·2H₂O as for iodine.

Upon taking over these studies, it was decided that a few additional conditions would be examined before swiftly moving onto closer analogues of PF-3644022 (**25**).

Alternative solvents were screened for their viability, including toluene, MeCN and THF. The use of less iodine was also investigated for its impact on the reaction conversion. Furthermore, analysis of the crude material was conducted using RP-LCMS in addition to ¹H NMR spectroscopic analysis. The microwave-assisted method developed by Bagley and Brigham was utilized, as it reduced reaction times and increased efficiency.

Use of toluene as solvent resulted in a number of unknown side products being generated, as ascertained by RP-LCMS and ¹H NMR spectroscopic analysis, and so was ruled out as a potential solvent. The crude reaction mixtures of the THF- and MeCN-mediated reactions, after aqueous

work-up, appeared to contain far fewer side-products, though there was still a significant side reaction occurring. The RP-LCMS chromatographic trace of the crude reaction mixtures tended to indicate at least two major UV-active species were present (see **Figure 55** and **56**).^x

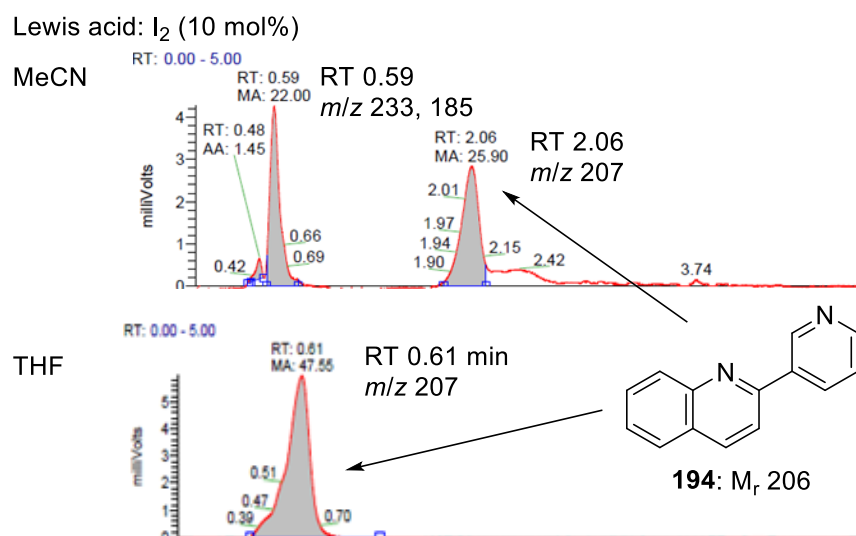


Figure 55: RP-LCMS chromatogram of the crude reaction mixture from **Scheme 121**, using I₂ (10 mol%) as Lewis acid via microwave-assisted heating, illustrating the UV traces corresponding to compound of interest **194**: $m/z = 207$ (MH⁺).

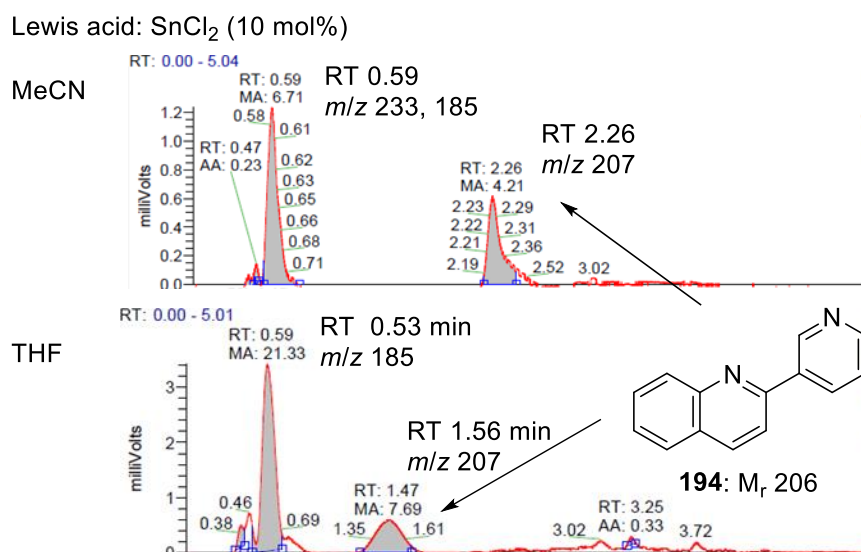


Figure 56: RP-LCMS chromatogram of the crude reaction mixture from **Scheme 121**, using SnCl₂ (10 mol%) as Lewis acid, via microwave-assisted heating, illustrating the UV traces corresponding to compound of interest **194**: $m/z = 207$ (MH⁺).

^x LCMS data was recorded on a Waters 2695 HPLC using a Waters 2487 UV detector and a Thermo LCQ ESI-MS. Samples were eluted through a Phenomenex Lunar 3μ C18 50 mm × 4.6 mm column, using acetonitrile and water acidified by 0.01% formic acid. Samples were eluted using acetonitrile and water (1:9 to 9:1) acidified by 0.01% formic acid, at a flow rate of 3 μl/min.

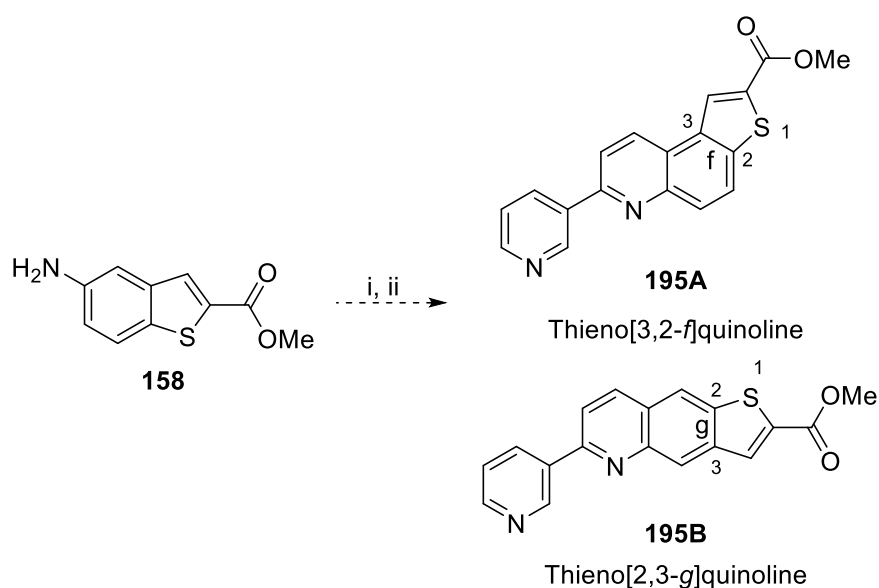
Product conversion, as ascertained by integration of the UV active peaks of the chromatogram, appeared to be fairly similar when the reaction was mediated by the two different Lewis acids in MeCN (**Figure 55** and **56**, top row). The mass ion of the second UV active peak at retention time 2.05-2.25 minutes correlated to the protonated quinoline **194** ($m/z = 207$ [MH^{+}]), confirming product formation.

However, for the THF-mediated reactions, there were inconsistencies between the two different Lewis acid-mediated reactions. The mass ion was still present on analysis of the crude reaction mixtures, confirming reaction conversion (**Figure 55** and **56**, bottom row), however, it was apparent that molecular iodine was only poorly soluble in THF, and hence MeCN became the solvent of choice for further reactions.

In these reactions, the equivalents of Lewis acid had been reduced compared to the previous trials conducted by Bagley and Brigham, from 50 mol% to 10 mol%. It was speculated that this may have been detrimental to the reaction conversion and so for further reactions the equivalence was increased back to 50 mol%.

3.5.3.2.2. Extending the model: thienoquinoline formation.

Having established the viability of a simple model, the compatibility of this method for thienoquinoline formation was probed, using methyl 5-aminobenzo[*b*]thiophene-2-carboxylate (**158**) and reacting with pyridine-3-carboxaldehyde (**191**) (see **Scheme 122**).

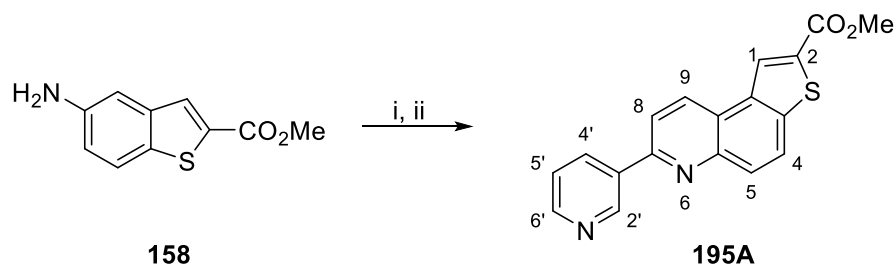


Scheme 122: Proposed thienoquinoline formation reaction microwave-assisted heating. Reaction conditions: i) Pyridine-3-carboxaldehyde (**191**) (1 equiv.), RT, 1 h; ii) *n*-BVE (2 equiv.), Lewis acid (50 mol%), MW heating.

Wang *et al.* had reported high regioselectivity for the cyclization of naphthalene-2-amines to occur at C-1 (see **Chapter 1.6.2.3.1, Scheme 24**),¹²³ though it was uncertain whether this trend in reactivity would favour formation of thieno[3,2-*f*]quinoline **195A**.

However, across previous work there had been a positive distribution in favour of the thieno[3,2-*f*]quinoline in the ratio of acidic cyclization products. Additionally, as discussed in **Chapter 1.6.2.3**, 5-aminobenzothiophenes can favour EAS at the 4-position over the 6-position (see **Scheme 41**), most likely due to a combination of kinetic and electronic effects. Consequently, the regioselectivity of this MCR method towards our model was approached with an optimistic outlook.

A simple model reaction of **158** with pyridine-3-carboxaldehyde (**191**) was completed as illustrated in **Scheme 123**, using iodine as the Lewis acid (50 mol%) in THF with two equivalents of *n*-BVE under microwave-assisted dielectric heating in a sealed vessel at 120 °C for 1 h (**Table 5**, entry 1). Fortunately, purification by flash column chromatography after an aqueous work-up gave a single thienoquinoline product, identified as the desired thieno[3,2-*f*]quinoline **195A** by ¹H NMR spectroscopic analysis and HRMS.



Scheme 123: Reaction scheme for thieno[3,2-*f*]quinoline formation from **158**. Reaction conditions; i) Pyridine-3-carboxyaldehyde (**191**) (1 equiv.), THF, RT, 1 h; ii) Iodine (50 mol%), *n*-BVE (2 equiv.), MW 120 °C, 1 h, 7%.

Characterization and differentiation between the pyridine and quinoline ring systems was inferred by reference to previous spectra and using 2D COSY ¹H NMR spectroscopy experiments. The pyridine ring had characteristically high chemical shifts for the 2'-CH and 6'-CH protons due to deshielding by the adjacent nitrogen (see **Figure 57**). The multiplet at δ_{H} 8.74 ppm which integrated to two protons was identified as overlapping resonances from the 9-CH and 6'-CH protons. This was confirmed through the 2D COSY ¹H NMR experiment, with proton-proton interactions between the δ_{H} 8.74 ppm multiplet and 8-CH of the quinoline and 5'-CH of the pyridine (at δ_{H} 8.06 and 7.5 ppm respectively), as illustrated in **Figure 58**. The 5'-CH exhibited a much more upfield resonance due to the comparatively shielded environment.

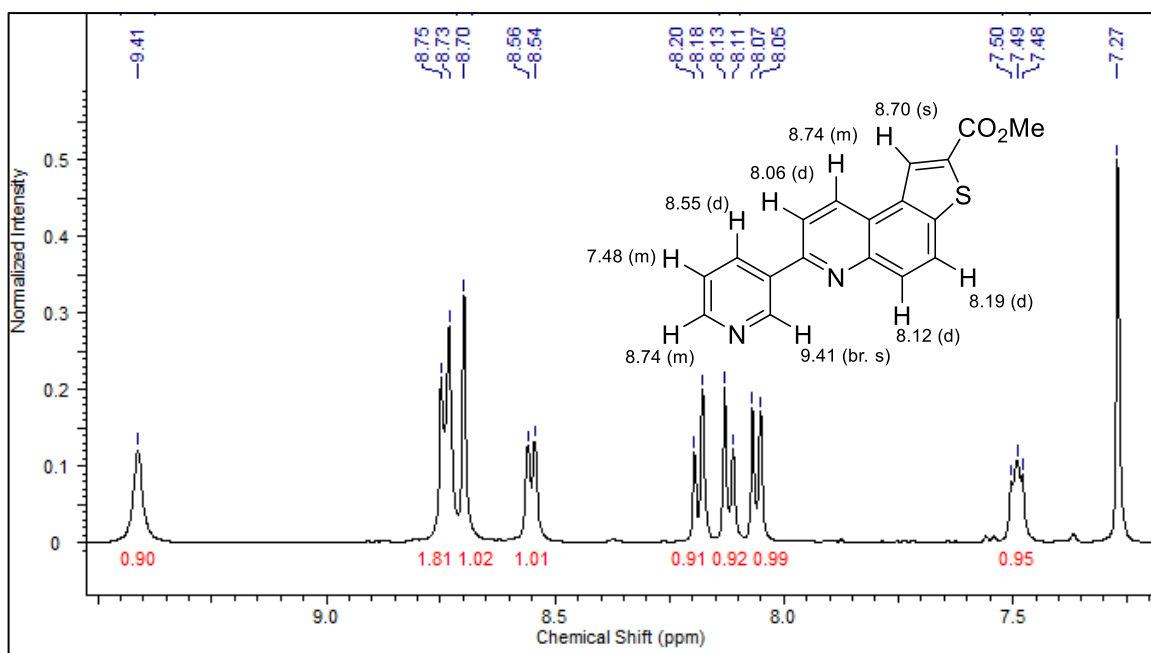


Figure 57: ^1H NMR spectrum (CDCl₃, 500 MHz, δ_{H} 9.7 – 7.0 ppm) of thieno[3,2-f]quinoline **195A** with chemical structure annotated with chemical shifts of protons within the spectral window.

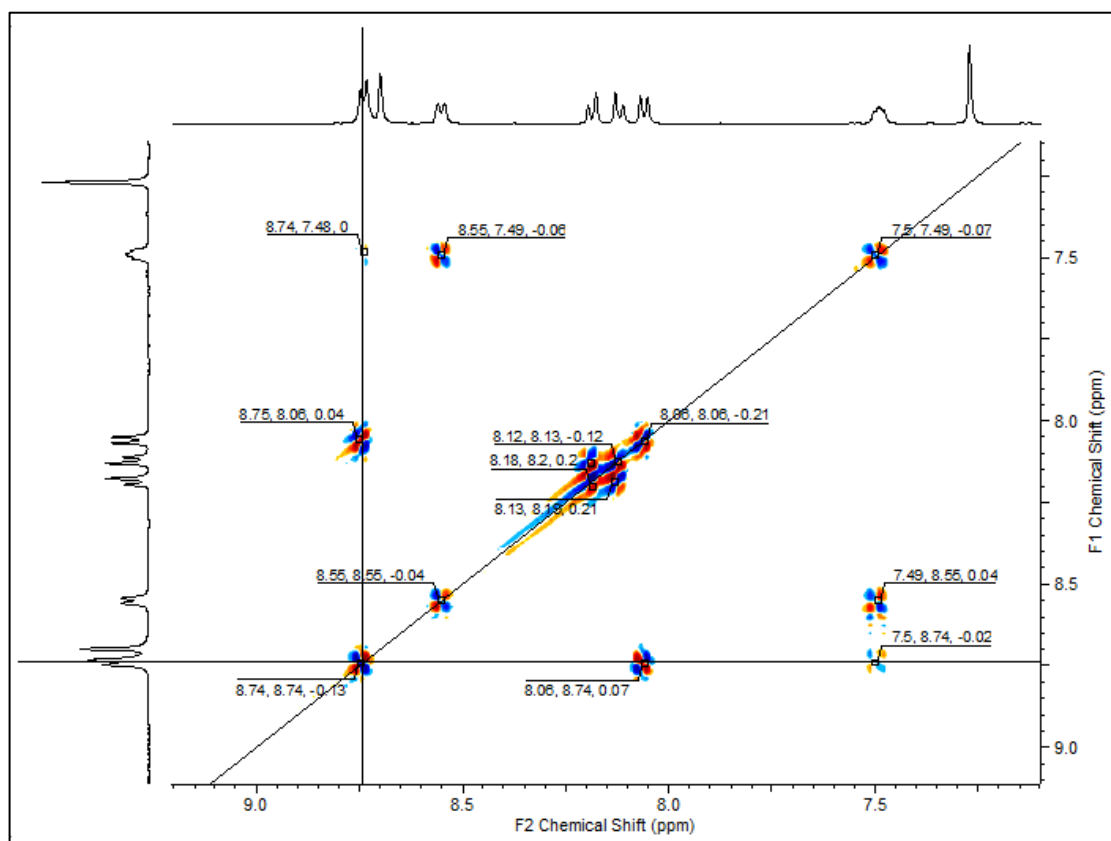


Figure 58: 2D COSY ^1H NMR experiment for **195A**, with gridlines illustrating the proton-proton relationships associated with the two 9-CH and 6'-CH protons of the δ_{H} 8.74 ppm multiplet.

The quinoline ring was characterized in the ^1H NMR spectroscopic analysis with inference from previous spectra, with large chemical shift differences noted between the 9-CH and 8-CH protons, and characteristic roofing of the 4-CH and 5-CH AB system (see **Figure 57**). Hence it was confirmed that only the thieno[3,2-*f*]quinoline (**195A**) had been isolated.¹⁰¹

The ^{13}C NMR spectrum of **195A** was interpreted through the use of a heteronuclear single bond correlation (HSQC) and heteronuclear multiple bond correlation (HMBC) experiments.

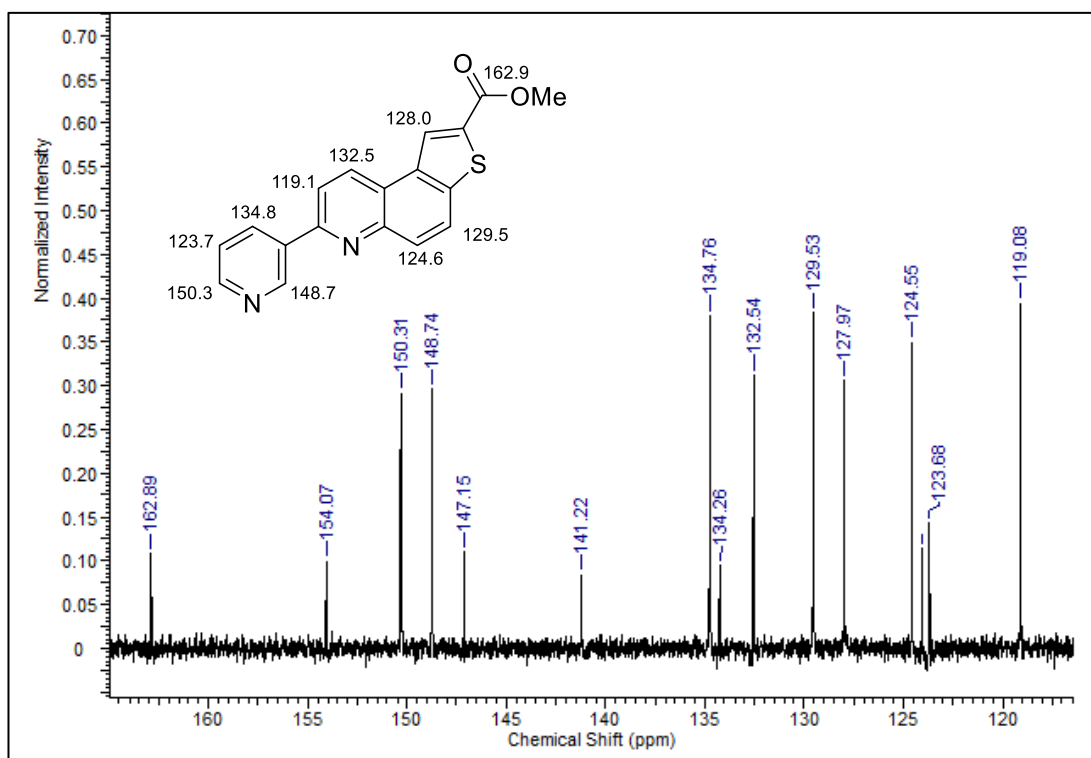


Figure 59: ^{13}C NMR spectrum (CDCl_3 , 100 MHz, δ_{C} 165–115 ppm) for **195A**, with chemical structure annotated.

From the ^{13}C spectrum, the sp^2 hybridized carbons could generally be differentiated from the quaternary carbons due to their characteristically stronger signals. This phenomenon is due to the proximity of the proton nucleus speeding up the rate of relaxation of the excited carbon nuclei between scans, resulting in stronger signals for sp^2 and sp^3 hybridized carbons (see **Figure 59**).¹⁰¹ The more downfield ^{13}C peaks correlated with the extremely deshielded carbonyl and α -pyridine quaternary carbons, with 2'-CH and 6'-CH centres at δ_{C} 148.7 and 150.3 ppm respectively. The other pyridine carbon centres 5'-CH and 4'-CH were identified using the HSQC experiment, at δ_{C} 134.8 and 123.7 ppm, respectively (see **Figure 59** and **60a**).

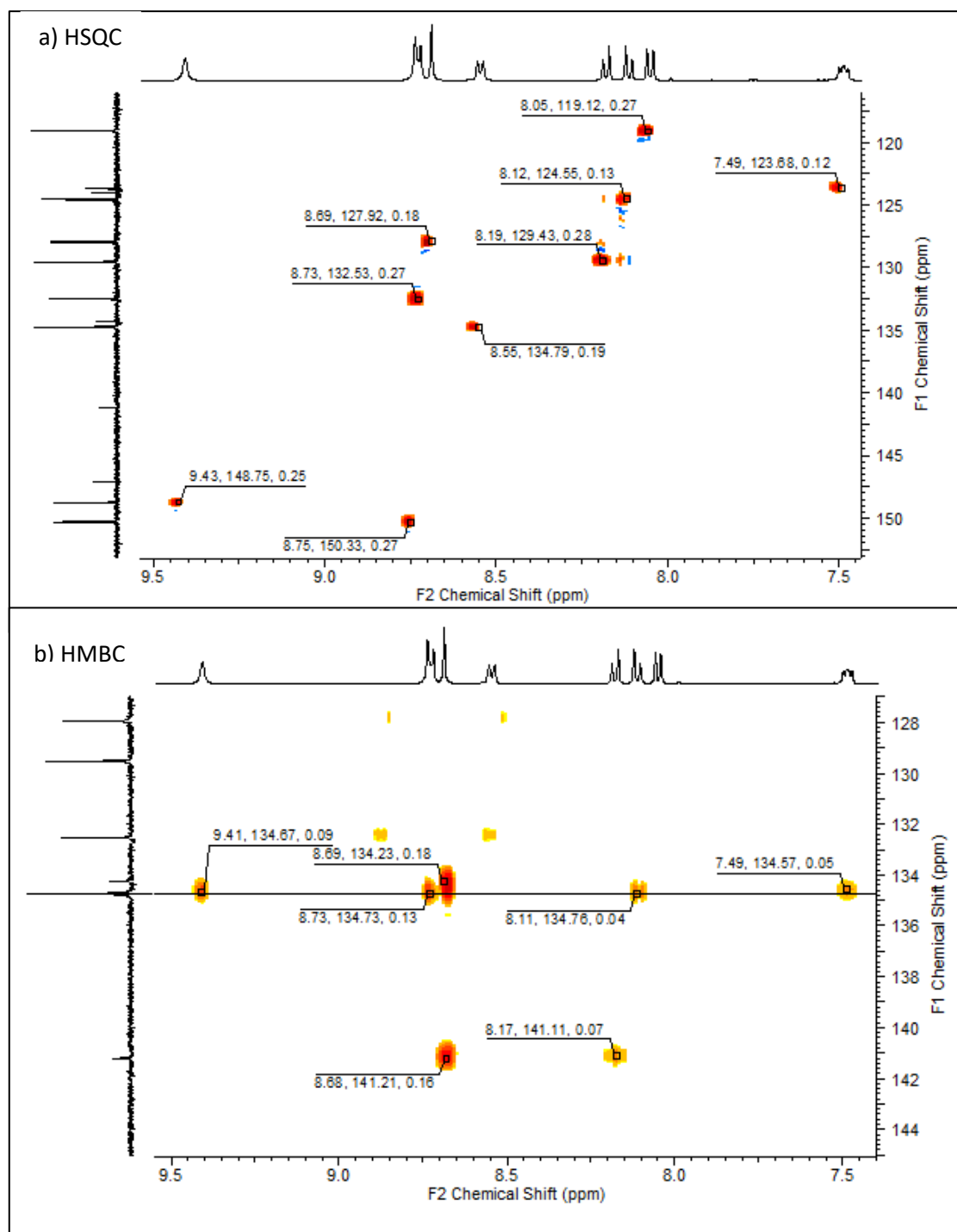


Figure 60: ^1H and ^{13}C correlation experiments for **195A**. a) HSQC experiment plot, illustrating single-bond interactions between protons and carbons of the molecule; b) HMBC, illustrating more distant proton-carbon relationships, specifically highlighting the interactions of the ^{13}C shift at δ_{C} 137.8 ppm.

The sp^2 hybridized carbons of the quinoline were identified similarly, with the 9-CH carbon centre significantly deshielded compared to 8-CH (δ_{C} 132.5 and 119.1 ppm, respectively). One quaternary carbon was not observed in the spectrum, but it was believed to have coalesced with the resonance of an sp^2 hybridized carbon at δ_{C} 134.8 ppm. This was ascertained using an HMBC experiment, which detects through bond interactions over longer ranges than the HSQC.

Through the two-dimensional HMBC experiment notable interactions were observed between the ^{13}C resonance at δ_{C} 137.8 ppm and two proton peaks at δ_{H} 9.41 and 8.11 ppm, correlating to protons of the pyridine and quinoline ring respectively (see **Figure 60b**). From this cumulative data, it was concluded that quinoline product **195A** had been successfully isolated.

Unfortunately, the yield of **195A** from this initial reaction was very low (**Table 5**, entry 1, 7%). A variety of conditions were screened in an attempt to improve the reaction outcome, as shown in **Table 5**. Adjustments were made to the equivalents of *n*-BVE, the temperature, hold time of the reaction and the solvent used.

Table 5: Thienoquinoline formation, using model aminobenzothiophene 158 and pyridine-3-carboxaldehyde (191) (see Scheme 123). ^a					
Entry No.	<i>n</i> -BVE (equiv.)	Time (h)	Temp. (°C)	Solvent	Yield (%) ^b
1	2	1	120	THF	7
2	1.5	1	120	THF	11
3	1.5	1	100	THF	11.5
4	2	1	120	MeCN	9.5
5	1.5	0.5	100	MeCN	5
6	1.5	1.5	100	MeCN	14
7	1.5	3	100	MeCN	27
8 ^c	1.5	3	100	MeCN	10
9	1.1	3	100	MeCN	10.5
10 ^d	1.5	3	100	MeCN	13
11 ^e	1.5	24	Reflux	MeCN	5.5
^a Reaction conditions: An equimolar amount of benzothiophene 158 and pyridine-3-carboxaldehyde (191) were stirred for 1 h at RT in solvent, then I_2 (50 mol%) and <i>n</i> -BVE were added and solution irradiated in a sealed vessel. ^b Isolated yield of 195A after purification by flash column chromatography; quoted to the nearest 0.5%. ^c 1.25 equiv. of aldehyde were used. ^d Trimethyl(vinyloxy)silane was used instead of <i>n</i> -BVE. ^e Conductive heating at reflux.					

Broadly speaking, it was found that the isolated yield improved upon changing the solvent from THF to MeCN (**Table 5**, entry 1, 7%; and entry 4, 9.5%) and upon lowering the equivalents of *n*-BVE (entry 2, 11%). Additionally, lowering the temperature was found not to affect the yield detrimentally (entries 2 and 3).

Once these small changes had been confirmed as beneficial to the isolated yield, the hold time for the reaction was evaluated. Reducing the reaction time to 30 minutes reduced the yield

(entry 5, 5%), while incrementally increasing the hold time resulted in significant improvements. After 90 minutes (entry 6, 14%) and 3 h (entry 7, 27%) at 100 °C in MeCN with 1.5 equivalents of *n*-BVE the yields improved incrementally, though the isolated yields were still quite low.

Analysis of the side products of the reaction indicated formation of an alternative thienoquinoline framework. HRMS and ^1H NMR spectroscopic analysis was used to deduce that the side product was methyl 6-methylthieno[2,3-*g*]quinoline-2-carboxaldehyde (**196**).

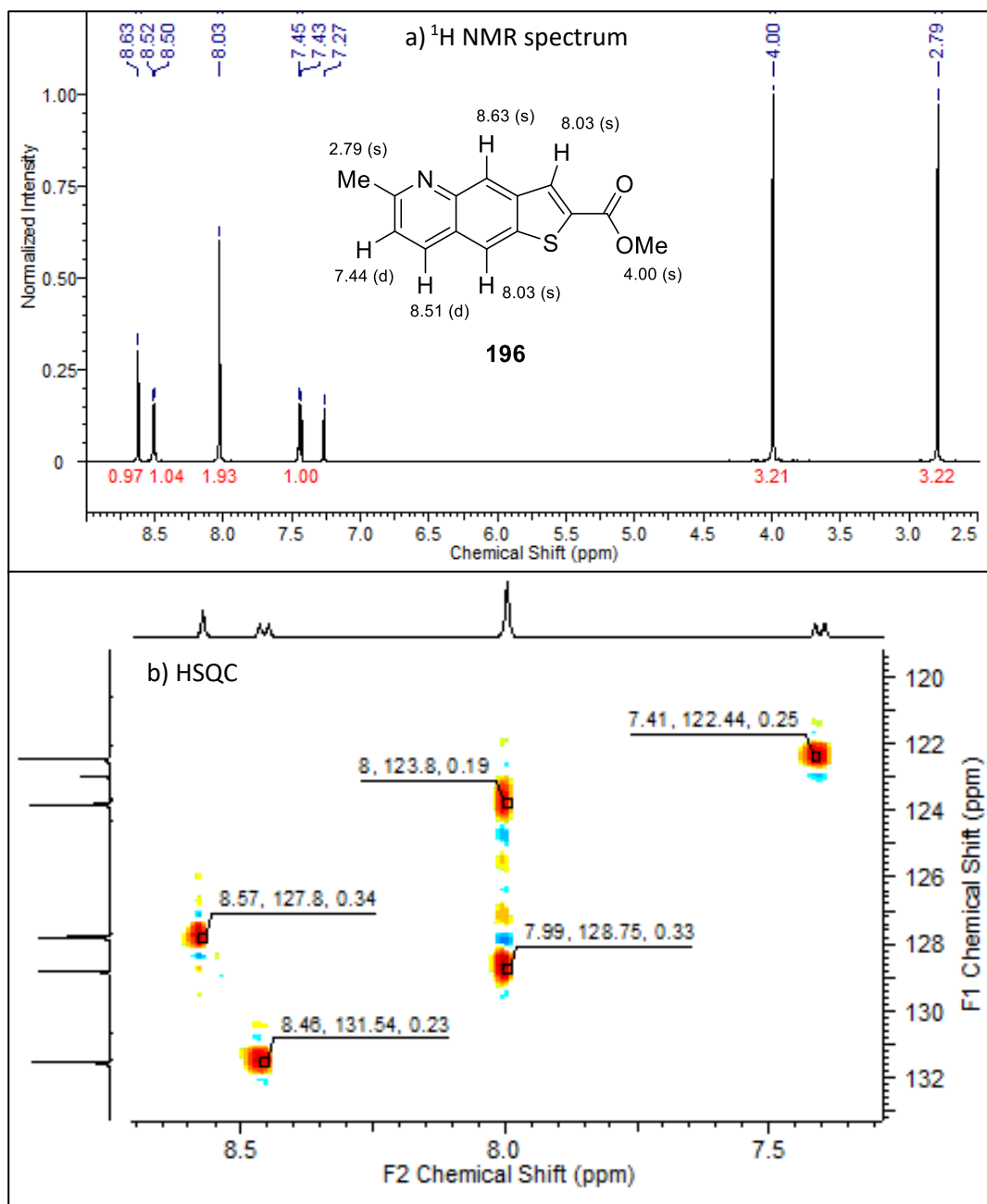
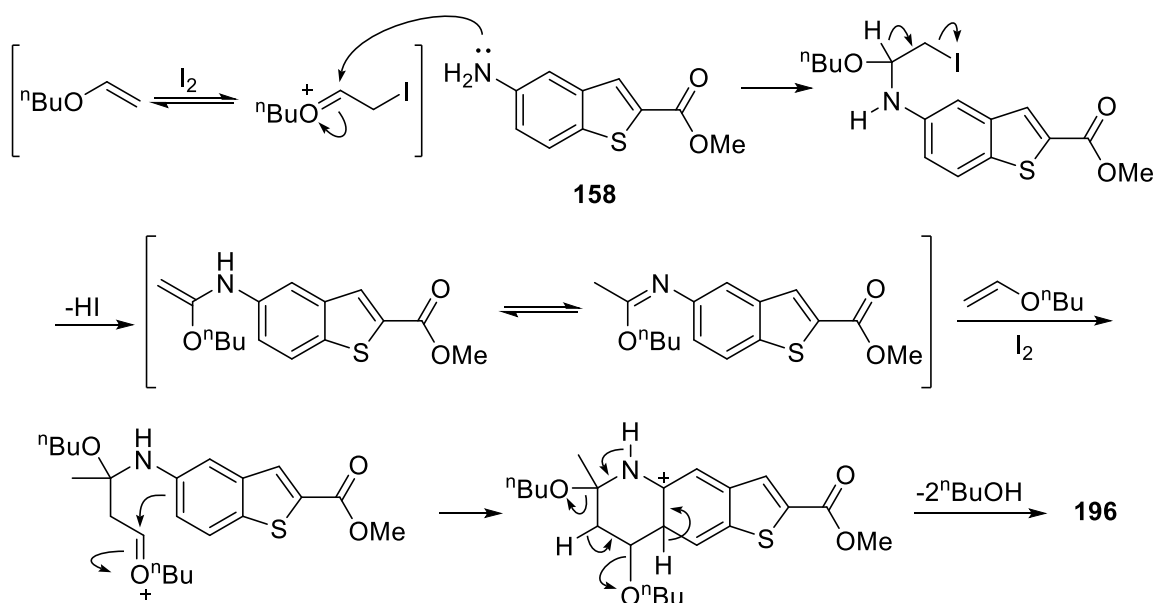


Figure 61: a) ^1H NMR (CDCl₃, 500 MHz, δ_{H} 9.0 - 2.5 ppm) of side product **196** and b) 2D HSQC experiment used to confirm two protons from different environments had coalesced into one peak at δ_{H} 8.03 ppm in the ^1H NMR spectrum.

Characterization by ^1H NMR spectroscopic analysis was completed, with two very prominent singlets which both integrated to three protons; one at δ_{H} 4.00 ppm, typical of the CO_2Me group, and one at δ_{H} 2.79 ppm. The integration and chemical shift of this new peak inferred it to be a new methyl group.

In the aromatic region, there were two doublets and two singlets, though one of those singlets integrated to 2 protons (at δ_{H} 8.03 ppm, see **Figure 61a**). Using a 2D HSQC experiment, it was ascertained that the two protons resonating at δ_{H} 8.03 ppm could be attributed to two protons on different carbon centres. Considering the frameworks being constructed, it was proposed that the overlapping resonances at δ_{H} 8.03 ppm were the 1- and 4-CH peaks of a thieno[2,3-*g*]quinoline, with the other singlet assigned as the 9-CH proton and the two doublets inferring that the 7-C centre was occupied by the methyl group. HRMS was used to verify the identity of the side product, with a parent ion found with m/z 258.0578, corresponding to $[\text{MH}]^+$, $\text{C}_{14}\text{H}_{12}\text{NO}_2\text{S}$.

It was proposed that this side product could form through a reversible Schiff base intermediate, with **158** reacting with two equivalents of *n*-BVE via an alternative Schiff base pathway (see **Scheme 124**). Additionally, it was interesting to observe that the cyclization of this alternative Schiff base favoured the alternative thieno[2,3-*g*]quinoline, with EAS at the 6-position of the benzothiophene ring.



Scheme 124: Postulated mechanism for formation of methyl thienoquinoline side product **196**.

Attempts to reduce the extent of this side reaction included trial reactions with an excess of pyridine-3-carboxaldehyde (**191**) (Table 5, entry 8, 10%) and reducing the equivalents of *n*-BVE to just over one equivalent (entry 9, 10.5%). Unfortunately, the yields were considerably lower than for previous reactions and side product **195** was still formed.

The alternative vinyl ether trimethyl(vinyloxy)silane was probed in this process, as it was hypothesized that a different profile of reactivity could modulate the reaction outcome. Alas, the isolated yield of the reaction was found to suffer (entry 10, 13%).

A conductive heating trial confirmed microwave-assisted heating in a sealed vessel was the superior method of heating for this reaction, with low yields obtained after heating the reaction mixture to reflux for 24 h (entry 11, 5.5%).

Having determined the best conditions using iodine as the Lewis acid, a number of other acids and Lewis acids were investigated (see Table 6). Additionally, the equivalents of *n*-BVE were lowered to try and reduce the extent of side reactions that were occurring.

Table 6: Exploring different acids and equivalents of <i>n</i> -BVE, in the synthesis of 195A . ^a				
Entry No.	Acid (mol%)	<i>n</i> -BVE (equiv.)	Time (h)	Yield (%) ^b
1	-	1.1	1.5	-
2	AcOH (50)	1	3	-
3	ZnBr ₂ (38)	1.1	3	14.5
4	SnCl ₂ (36)	1.1	3	9.5
5	TiCl ₄ (50)	1.1	3	4 ^c
6	FeCl ₃ (50)	1.1	3	- ^d
^a Reaction conditions: Equimolar amounts of benzothiophene 158 and pyridine-3-carboxaldehyde (191) were stirred for 1 h at RT in MeCN, then the Lewis acid and <i>n</i> -BVE were added and the solution irradiated at 100 °C for the stated time. ^b Isolated yield after purification by flash column chromatography; quoted to the nearest 0.5%. ^c ≤50% pure by ¹ H NMR spectrum analysis. ^d Only Schiff base 193 was isolated.				

No reaction occurred when there was no Lewis acid present or when the Brønsted acid AcOH was used (Table 6, entries 1 and 2). This result confirmed the necessity of a Lewis acid rather than a protic acid to facilitate Schiff base activation in this quinoline formation (see Chapter 1.6.2.3.1 for discussion of the mechanism).

Other Lewis acids were probed including SnCl₂·2H₂O, zinc(II) bromide (ZnBr₂) (used in reduced quantity as it has been documented that 30-35 mol% resulted in better Lewis acidic properties²⁸⁵), iron(III) chloride (FeCl₃) and titanium tetrachloride (TiCl₄).

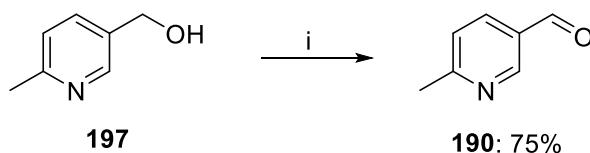
Using the reactions mediated by 50 mol% iodine under similar conditions as the benchmark reaction (**Table 5**, entry 9, 10.5%), the yields obtained using ZnBr₂ showed a slight improvement in the isolated yield (**Table 6**, entry 3, 14.5%), though the results were not consistent between experimental runs, with notable co-elution of products and decomposition occurring in one experiment.

SnCl₂ gave a very similar isolated yield to the use of iodine (**Table 6**, entry 4, 9.5%), though both Lewis acids also resulted in significant side product formation. Use of TiCl₄ gave a much lower yield of the quinoline, with significant impurities detected by ¹H NMR spectroscopic analysis (entry 5, 4%), and it was found that use of FeCl₃ did not mediate the cyclization, with only the Schiff base intermediate formed.

The best yield obtained in these trials was mediated by ZnBr₂. However, the co-elution and decomposition noted during the reaction was troubling. Hence, it was decided that iodine would be progressed into trials with advanced intermediates, and that use of ZnBr₂ should be further investigated in future studies.

3.5.3.2.3. Application of convergent quinoline route to complex intermediates.

In order to conduct the final synthetic step towards PF-3644022 (**25**), 6-methylpyridin-3-carboxaldehyde (**190**) was synthesized by oxidation of alcohol **197**. Initially oxidation using Dess-Martin periodinane (DMP) was investigated, as a mild and functional group tolerant reagent.²⁸⁶ Typically oxidations mediated by DMP occur quickly at room temperature. However, after stirring **197** in dry CH₂Cl₂ under argon with 2.5 equivalents of DMP for 3 h, the isolated yield of **190** was still very low (11%).

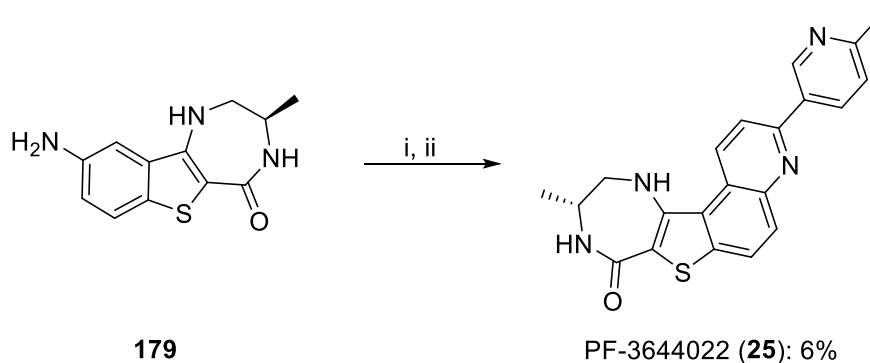


Scheme 125: Oxidation of (6-methylpyridine)alcohol (**197**) to 6-methylpyridine-3-carboxaldehyde (**190**). Reaction conditions: i) (COCl)₂, DMSO, NEt₃, CH₂Cl₂, -78 °C, 75%.

Adopting Swern oxidation conditions greatly improved the reaction yield (see **Scheme 125**). Reacting oxalyl chloride and DMSO in dry CH₂Cl₂ at -78 °C, before slow addition of **197**, with subsequent deprotonation of the sulfur ylide by addition of NEt₃ base, afforded aldehyde **190** in high yield (75%) after purification by flash column chromatography.

Reaction of **179** and aldehyde **190** was carried out using the best conditions from the model system, with 1 h pre-stir of the aniline and aldehyde at room temperature in MeCN, and then addition of iodine (50 mol%) and *n*-BVE (1.5 equiv.) and heating the reaction mixture using microwave-assisted dielectric heating in a sealed vessel at 100 °C for 3 h (see **Scheme 126**).

The reaction was carried out a number of times on a small scale and the yields were found to be very low. Isolation of the product and purification by flash column chromatography were both problematic, with poor purity ascertained by ¹H NMR spectroscopic analysis. Trituration of the contaminated product with diethyl ether did help remove impurities, but this method was not consistent. Recrystallization was found to be an impractical method of purification on the small scale used. Only when an excess of aldehyde **190** was used did purification by flash column chromatography return a clean product, ascertained by ¹H NMR spectroscopic analysis, giving a final yield of 6%.



Scheme 126: Multi-component reaction towards PF-3644022 (**25**). Reaction conditions: i) **190** (1.4 equiv.), MeCN, RT, 1 h; ii) I₂ (50 mol%), *n*-BVE (1.6 equiv.), MW 100 °C, 3 h, 6%.

Identity of the product was confirmed through ¹H NMR spectroscopic analysis and HRMS. The alkyl protons of the diazepinone ring were assigned using 2D COSY ¹H NMR correlation experiments. The diazepinone NH protons were notable between δ_H 6.40 and 5.40 ppm (in CDCl₃), and the aromatic quinoline and pyridine protons were assigned by reference to previous spectra, recognizable coupling patterns and use of 2D COSY and HSQC NMR correlation experiments (see **Figure 62**).

The ¹³C NMR spectrum was assigned with inference from previous spectra and through use of HSQC and HMBC NMR correlation experiments. There was one quaternary carbon not observed, but this had been noted for the similar pyridinyl-thieno[3,2-*f*]quinoline **195A**, and so it was inferred that a similar coalescence of a quaternary carbon signal had occurred.

From the cumulative spectroscopic data, it was concluded that final compound PF-3644022 (**25**) had been synthesized successfully.

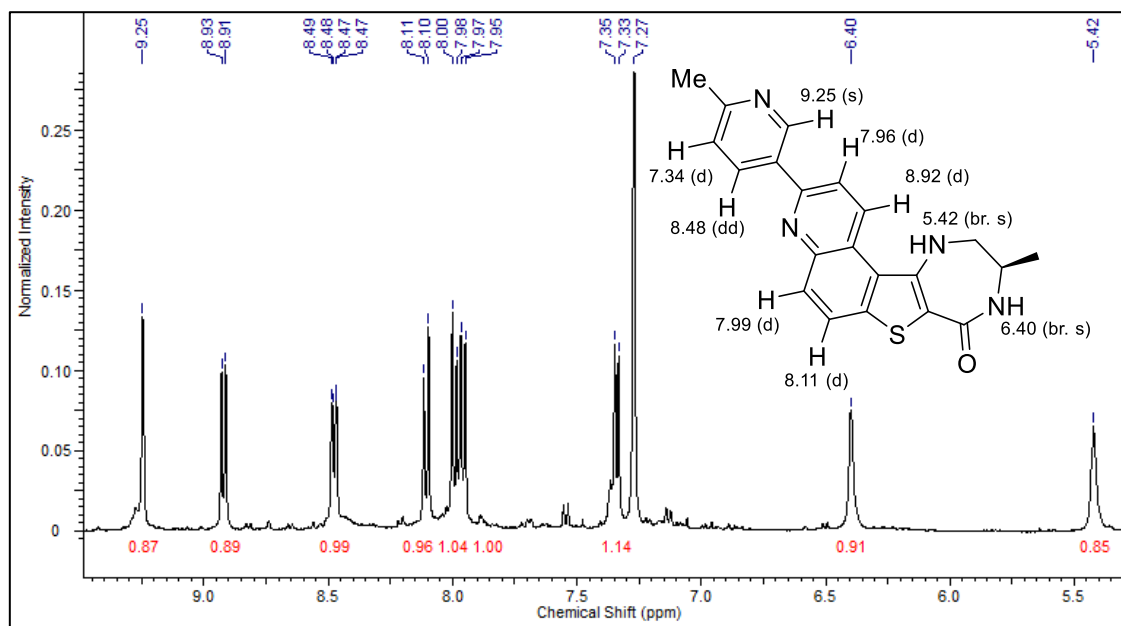


Figure 62: ^1H NMR spectrum (CDCl_3 , 500 MHz, δ_{H} 9.8 - 5.3 ppm) of PF-3644022 (**25**), with annotated chemical structure, illustrating the shifts visible in the spectral window.

Upon purification of the crude reaction mixture from the reaction of diazepinone **179** and pyridine-3-carboxaldehyde **190** (see **Scheme 126**), unreacted pyridinyl-carboxaldehyde and the α -methylthienoquinoline side product **198** were often also isolated.

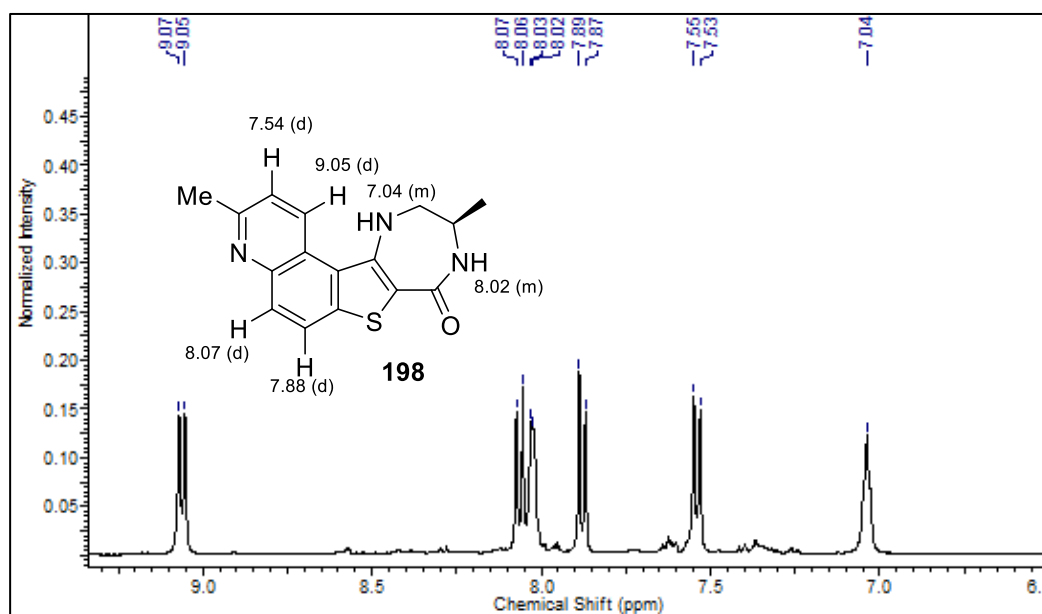


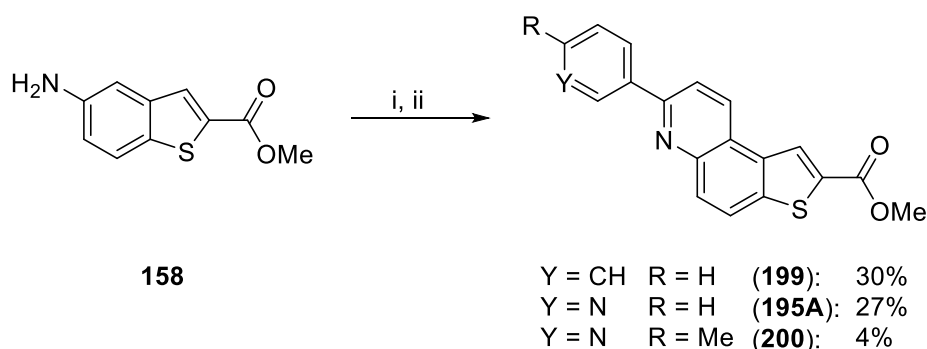
Figure 63: ^1H NMR spectrum ($\text{DMSO}-d_6$, 500 MHz, δ_{H} 9.5 - 6.5 ppm) of α -methylthienoquinoline side product **198**, with annotated chemical structure, illustrating the proton resonances visible in the spectral window.

Characterization of **198** was conducted through ^1H NMR spectroscopic analysis, with characteristic roofing of the two carbocyclic protons indicating that the thieno[3,2-*f*]quinoline product from the alternative reaction pathway had been formed (see **Figure 63**).

It was postulated that the alternative reaction product had been formed due to subtle changes in the electronic and steric demands of the system, favouring the alternative condensation rather than Schiff base formation. Nevertheless, it was clear that the reaction was not proceeding as favourably as anticipated, and so some further investigations were conducted using the benzothiophene based system.

3.5.3.2.4. Assessing the viability of aromatic aldehydes.

The yields achieved in this convergent MCR for quinoline synthesis were significantly lower than those documented by Wang *et al.*, who reported yields of 82-93% for reactions mediated by *n*-BVE.¹²³ Furthermore, the substantial difference in yields between the model system (see **Scheme 123**, 27%) and those achieved for PF-3644022 (**25**) (see **Scheme 126**, 6%) implied there may be some additional, fundamental reduction in reactivity of the substrates.



Scheme 127: Convergent quinoline synthesis, exploring the viability of aromatic aldehydes. Reaction conditions: i) aromatic aldehyde, MeCN, RT, 1 h; ii) I_2 , *n*-BVE, MeCN, MW 100 °C, 3 h.

A limited set of trial reactions were run using the aromatic aldehydes benzaldehyde, pyridine-3-carboxaldehyde (**191**) and its methyl analogue **190** (see **Table 7**). It was hoped that these trials would help ascertain whether the lower reactivity and reaction yields were due to the electronics of the pyridine-3-carboxaldehyde, some interaction of the Lewis acid with the pyridine heteroatom or due to changing steric demands.

Table 7: Convergent quinoline synthesis with alternative aromatic aldehydes (Scheme 127). ^a			
Entry No.	Y	R	Yield (%) ^b
1	CH	H	30
2	NH	H	27
3	NH	Me	4

^a Reaction conditions: An equimolar amount of benzothiophene **158** and aldehyde was stirred in MeCN for 1 h at RT in MeCN, then I₂ (50 mol%) and *n*-BVE (1.5 equiv.) were added and solution irradiated at 100 °C for 3 h.

^b Isolated yield after purification by flash column chromatography.

There was a slight improvement in the isolated yield of the cyclized quinoline product when **159** was reacted with benzaldehyde under the standard conditions (**Table 7**, entry 1, 30%) compared to reaction with unsubstituted pyridine analogue **191** (entry 2, 27%). Interestingly, it was found that the yield for reaction of **159** with 6-methylpyridine-3-carboxaldehyde (**190**) was very low (entry 3, 4%).

Wang *et al.* reported consistent yields upon altering the electronic properties of the aromatic aldehyde in their synthesis of fused quinoline systems,¹²³ though these results indicated there was a clear reduction in efficiency when the aromatic aldehyde was altered.

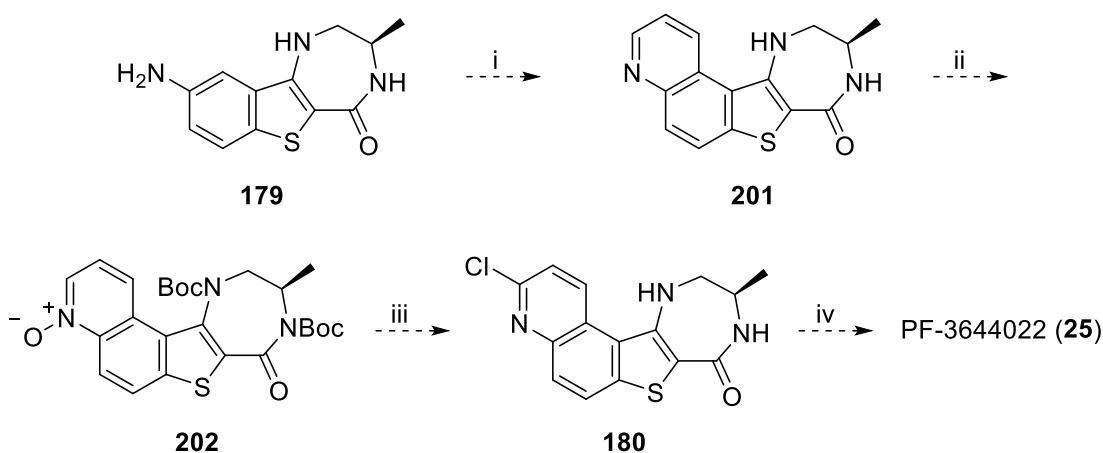
At this stage it could not be determined whether the unfavourable change in the yield of the quinoline product was due to the change in electron density of the aromatic group, some association between the heteroatom and the Lewis acid in solution, or because of subsequent degradation due to the pyridine α -methyl group of **25** that could readily tautomerize under the Lewis acidic reaction conditions.

3.5.4. Future perspectives.

The low efficiency of the cyclization method designed by Wang *et al.*¹²³ was noted for the convergent synthesis of advanced intermediates diazepinone **179** and 6-methylpyridine-3-carboxaldehyde (**190**). Low yields were achieved of the final compound PF-3644022 (**25**, 6%) and also in the reaction of a simple 5-aminobenzothiophene with different aromatic aldehydes giving fused quinolines **195A**, **199** and **200**. In order to optimize this route towards the desired substrates, there are a number of options available.

Further investigation of alternative Lewis acids would be beneficial, as the screening conducted herein was by no means exhaustive and would benefit from further experimentation with models and with **190** as the carboxaldehyde coupling partner.

Exploration as to the cause of the reactivity issues would also be beneficial, although it would seem that this reaction is just not ideal for this highly complex target. Therefore, it has been proposed that an alternative method to synthesize our final target, could be conducted via a Skraup cyclization from advanced intermediate **179** to give unsubstituted quinoline **201**.²⁸⁷ Using the chemistry established by Anderson *et al.* (see **Chapter 3.1.1, Scheme 91**), the pyridine ring could then be functionalized to the *N*-oxide (**202**) and chlorinated to give **180**, ready for subsequent Suzuki coupling to afford PF-3644022 (**25**) (see **Scheme 128**). Work on this chemistry is currently ongoing in our research group.

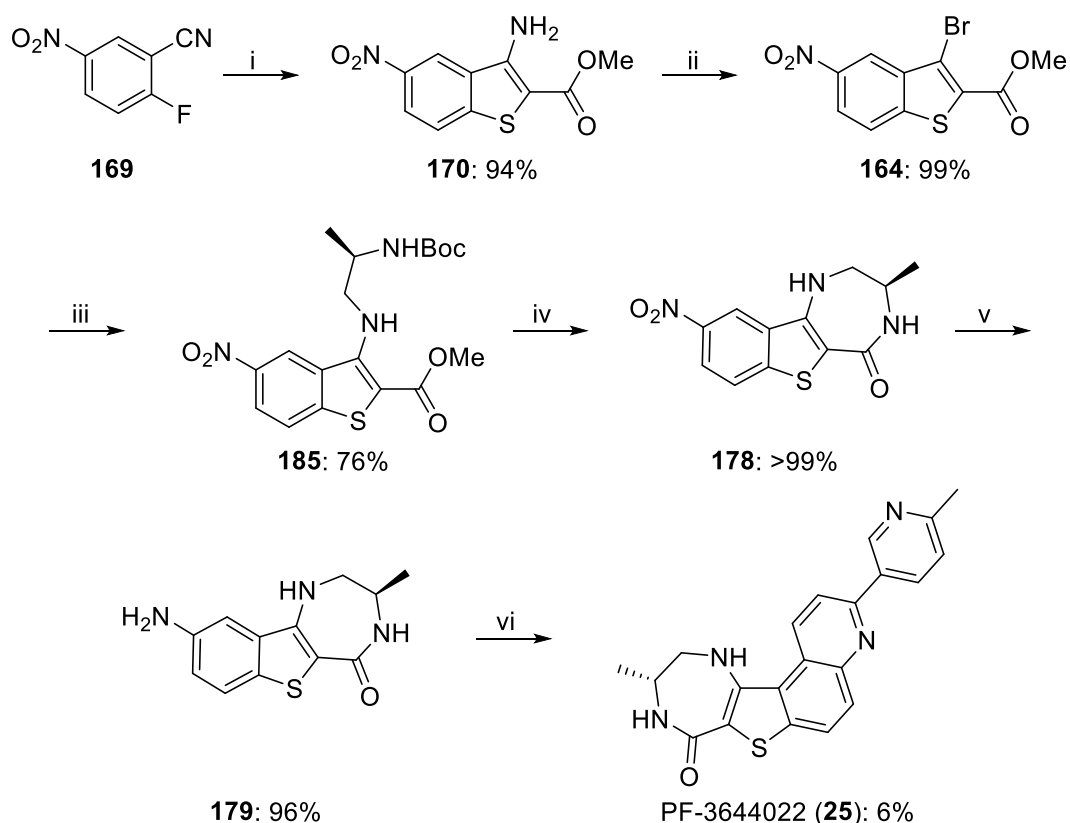


Scheme 128: Proposed alternative route for the synthesis of PF-3644022 (**25**). Reaction conditions: i) Glycerol, H₂SO₄, B(OH)₃, Ac₂O, Fe₂(SO₄)₃;²⁸⁷ ii) Boc₂O, DMAP, NEt₃ then *m*CPBA; iii) (COCl)₂, DMF, then HCl; iv) 2-methylpyridinyl-5-boronic acid, Pd(PPh₃)₄, Na₂CO₃, 80 °C.⁶⁸

3.6. Conclusion.

The MK2 inhibitor PF-3644022 (**25**) was synthesized in 6 steps and 4% overall yield (see **Scheme 129**). New methods and syntheses have been developed and optimized towards a number of advanced intermediate scaffolds through a variety of different disconnective strategies. These included a new and efficient microwave-assisted route towards 3-amino and 3-halobenzo[*b*]thiophenes, improved microwave-assisted amide bond forming reactions using 5-aminobenzo[*b*]thiophenes for synthesis of acidic cyclization precursors, and the development of new microwave-assisted routes towards thieno[3,2-*f*]quinolines.

The development of PF-3644022 (**25**) towards a viable therapeutic candidate has been progressed by Pfizer, with pre-clinical studies conducted on **25** and a number of more pharmacokinetically-viable candidates. The application of a variety of MK2 inhibitor chemotypes, including **25**, have been explored by Davis *et al.* in WS cells with some intriguing results obtained when compared to treatment with the prototypical p38 inhibitor SB203580 (**1**).



Scheme 129: Total synthesis of PF-3644022 (**25**). Reaction conditions: i) Methyl thioglycolate, NEt₃, DMSO, MW 130 °C, 11 min, 94%; ii) CuBr₂, ^tBuONO, MeCN, 0 °C to RT, 2 h, 99%; iii) **137**, Cs₂CO₃, (±)-BINAP, Pd(OAc)₂, toluene, MW 150 °C, 75 min, 76%; iv) a) TFA (10 % in CH₂Cl₂), RT, 16 h; b) NaOMe (25 w% in MeOH), MeOH, 50 °C, 2 h, then Δ, 2 h; c) 1 M HCl, >99%; v) Mo(CO)₆, DBU, EtOH, MW 150 °C, 30 min, 96%; vi) **190**, I₂, *n*BVE, MeCN, MW 100 °C, 3 h, 6%.

3.7. Biological studies.

Initial screenings of MK2 inhibitor PF-3644022 (**25**) by Pfizer found it to possess good kinase selectivity across a panel of two hundred protein kinases, with potency on the nanomolar scale and projected ADME (adsorption, distribution, metabolism and excretion) characteristics suitable for oral human dosing.^{68,69,288} Hence, it was considered an ideal candidate to take forward into pre-clinical trials.

3.7.1. Progress in the clinic.

Despite good projected ADME characteristics, pre-clinical investigations of the *in vivo* activity of PF-3644022 (**25**) at Pfizer by Daniels *et al.*, in 2013, found that it caused acute liver damage and hepatotoxicity in dogs.²⁸⁸ The group completed an *in vitro* ADME analysis on transfected human cells and found that **25** underwent hepatic bioactivation and inhibited a number of important transporter proteins which regulate the movement of toxic substances around the hepatobiliary system.

In previous work, the group had found that fused thiophene-diazepinone scaffolds were liable to undergo bioactivation in the liver into glutathione conjugates, and that installation of a metabolic shunt could temper this unwanted reaction. It was important that the diazepinone section of the molecule be maintained, as it had been found through X-ray co-crystallization studies to be involved in critical binding interactions with MK2 and that the biaryl linkage was important for kinase selectivity.^{67,68} Therefore efforts to improve the pharmacokinetics (PK) of the PF-3644022 (**25**) chemotype were completed while bearing these important pharmacophoric properties in mind.

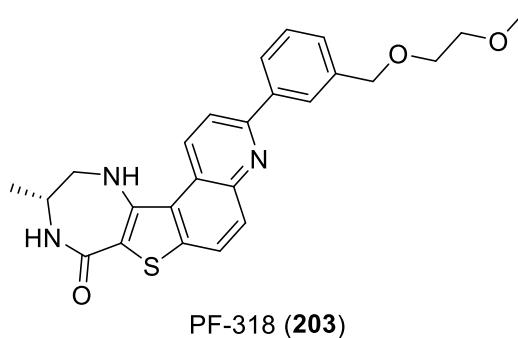


Figure 64: First alternative candidate (**203**) to improve the pharmacokinetic properties of PF-3644022 (**25**).²⁸⁸

PF-318 (**203**) was synthesized, with a new polyether chain installed as a metabolic shunt on the distal aryl group. **203** maintained inhibitory potency akin to **25** and was confirmed to preferentially undergo *O*-dealkylation upon metabolism. However, severe liver injuries were still noted in dogs when given a single oral dose of **203**.

Further *in vitro* studies identified **203** to be an even more potent inhibitor towards hepatobiliary efflux transporter proteins than **25**, with enhanced distribution and exposure characteristics. To reduce this unwanted transporter protein inhibition, the group used studies completed by Pedersen *et al.* which identified a number of prevalent characteristics to distinguish between inhibitors and non-inhibitors of transporter proteins.²⁸⁹ For instance, inhibitors generally tended to have a higher average molecular weight, with higher degrees of aromaticity and to be either anionic or neutral at physiological pH.

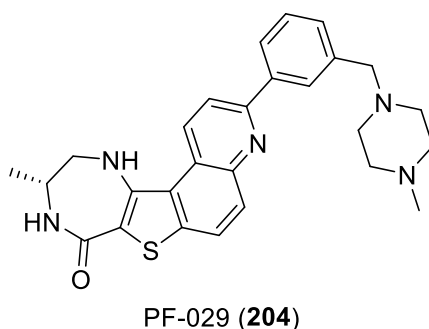


Figure 65: Daniels *et al.*'s second candidate (**204**) to improve the pharmacokinetics of PF-3644022 (**25**).

MK2 inhibitors **25** and **203** both possessed pK_{aH} values of around 4, and so were more likely to be neutral at physiological pH. To increase basicity, a piperazine group was installed via a methylene linkage to give PF-029 (**204**). This new candidate possessed a pK_{aH} of approximately 8, and so the majority of molecules would be present as the cationic conjugate acid at physiological pH. Tests completed by Daniels *et al.* validated their approach and found that **204** did not inhibit transporter proteins or result in liver toxicity *in vivo*.²⁸⁸

These pharmacokinetic improvements at the pre-clinical stage of development for PF-3644022 (**25**) were very fortuitous for Pfizer, as toxicity is one of the major factors which leads to attrition in late stage drug design.²⁹⁰

Originally designed towards the development of therapeutics for inflammatory disorders, PF-3644022 (**25**) was designed to target MK2 as an alternative to the typical p38 targeting inhibitors.^{67,69} Since its design and publication, **25** has been used as a chemical tool to probe

MAPK stress-signalling pathways in a variety of cell types. For example, Cao *et al.* used **25** to probe links between p38 and MK2 in Sonic Hedgehog (Shh) pathways in breast cancer cells.²⁹¹

Shh is a member of the Hedgehog (Hh) family of proteins, and is overexpressed in breast cancer cells.²⁹¹ The exact role of Shh in breast cancer signalling is unclear, though it is known to be involved in developmental processes, including cancer pathology and tissue regeneration. It was postulated that there was some cross-talk between the Shh and MAPK signalling pathways, and so MK2 inhibitor PF-3644022 (**25**) and p38 inhibitor SB203580 (**1**) were used as tools to investigate the mechanism of action of Shh. It was found that upon treatment with these inhibitors there was a reduction in phosphorylation of one of the key members of the Shh signalling pathway, demonstrating direct involvement of the p38-MK2 pathway in the cell proliferation of breast cancer cells.^{55,291}

3.7.3. Application in WS cells.

As has been discussed in **Chapter 1.2**, the p38 α /MK2-mediated stress-signalling pathway has been postulated to play a key role in the stressed and aged morphology of prematurely aged WS cells. This is due in part to prominent F-actin stress fibres observed in senescent WS cells, production of which is mediated by MK2 phosphorylation of HSP27.

P38 α MAPK has been confirmed to play a crucial role in the stress-signalling events of WS cells, leading to the stressed and aged morphology of WS cells and premature cellular senescence.^{1,14} In order to gain a better understanding of the mechanisms of the prematurely aged phenotype, and for the development of more therapeutically-viable drug candidates, the role of the kinases downstream of p38 α have become of more prominent interest.

Unfortunately, investigations into the MAPK stress-signalling pathway in WS cells using MK2 inhibitors have been largely inconclusive due to a pervasive cessation of cell growth.⁶⁰ Cessation in these tests did not appear to be a direct effect of MK2 inhibition, but predominantly due to the small therapeutic window of the compounds.⁶³

For instance, Davis *et al.* found that although the aminocyanopyridine ATP-competitive MK2 inhibitor **18** inhibited the MK2/HSP27 stress-signalling cascade in normal cells,^{62,63} growth studies completed on WS^{tert} cells were inconclusive.⁶⁰

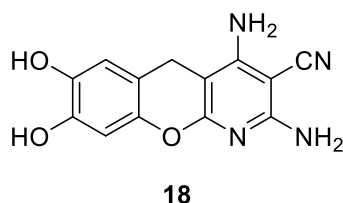


Figure 66: Diaminocyanopyridine MK2 inhibitor **18**.⁶²

After treatment with **18**, WS^{tert} cells exhibited a reduction in cell growth and no effect on the extent of F-actin stress fibre production. Davis *et al.* determined from these results that either MK2 inhibition was limiting cell growth, which was inconsistent with the role of MK2 established from cell cycle arrest pathways,^{55,60} or that the inhibitor had some off-target or toxic effects. Hence it was determined that more selective and potent MK2 inhibitors would be required for conclusive results.

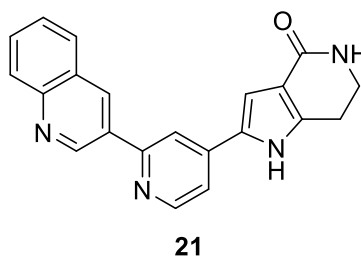


Figure 67: Tetrahydropyrrolo[3,2-c]pyridine-4-one MK2 inhibitor **21**.⁵⁹

In 2013 Davis *et al.* published a selection of studies on the use of MK2 inhibitors in WS cells, including the tetrahydropyrrolo[3,2-c]pyridine-4-one **21**,⁶⁰ an MK2 inhibitor designed by Pfizer with high potency and target specificity (see **Chapter 1.4.1**).⁵⁹ Tests on primary WS cells showed a notable increase in their replicative capacity and little comparative effect on normal human cells.⁶⁰ Additionally, it was found that continuous treatment with **21** resulted in a dramatic reduction in F-actin stress fibres.⁶⁰

Treatment of the same primary WS cells with the p38 inhibitor SB203580 (**1**) still resulted in a more enhanced increase in the replicative capacity. Though it was found that **21** exhibited a higher efficacy at reverting the production of stress fibres in WS primary cells to resemble those of normal cells.

From this evidence Davis *et al.* inferred that, although the accelerated senescence of WS cells was at least partially due to activation of MK2, the results were not conclusive. Additionally, the studies confirmed that MK2 inhibitor **21** was not as effective at extending the replicative capacity as the p38 α inhibitor SB203580 (**1**).

It was speculated that there could be several reasons why MK2 inhibitor **21** did not elicit the same response as SB203580 (**1**), including the possibility that the therapeutic window of **21** may have been too small, causing off-target effects and inhibition of cell growth at higher concentrations.⁶⁰ Also, it was proposed that the superior effect of SB203580 (**1**) could have been due to off-target effects, or that there may be multiple kinases downstream of p38 α which have a role in mediating the cellular response to treatment.

Biological tests of MK2 inhibitor PF-3644022 (**25**) have been run by Davis *et al.* on primary WS cells, although the extent of tests has been restricted due to limited supplies of primary WS cells.³ The results collected complement those collected previously using the MK2 inhibitor **21**.⁶⁰

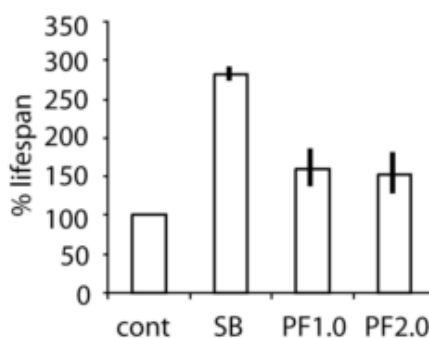


Figure 68: Graph representing % increased lifespan of primary WS cells. Cont = control. SB = SB203580 (**1**) at 2.5 μ M. PF1.0 and PF2.0 = PF-3644022 (**25**) 1.0 μ M and 2.0 μ M, respectively.³

Primary WS cells grown in the presence of PF-3644022 (**25**), at a concentration where MK2 was fully inhibited (1.0 μ M and 2.0 μ M), were found to show a replicative lifespan extended by approximately 50% compared to controls (see **Figure 68**). Comparative studies using SB203580 (**1**) on the same cell line demonstrated a higher cellular lifespan extension.

More informatively, the stressed morphology of the WS cells was corrected upon treatment with **25**. As shown in **Figure 69**, the comparison of treated cells with control WS cells clearly illustrated the extent to which stress fibre production had been reduced after treatment with **25** (comparative data for SB203580 (**1**) not available).³

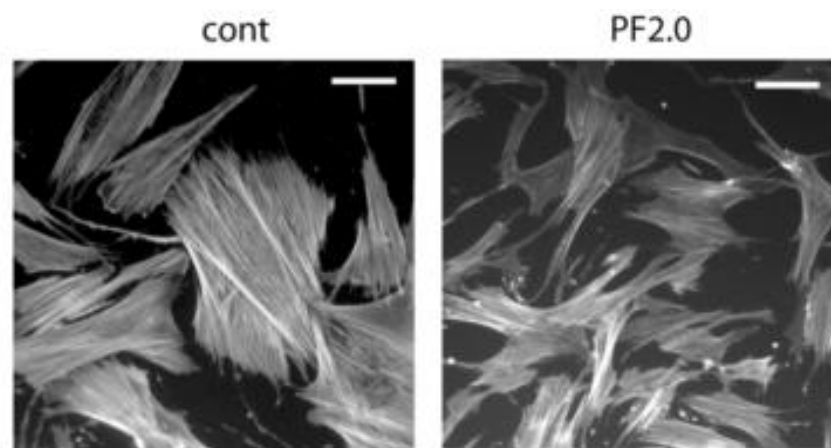


Figure 69: F-actin stress fibres in primary WS cells. Cont = control grown in DMSO. PF2.0 = Grown in 2.0 μ M PF-3644022 (**25**).³

Unfortunately, similar to **21**, it was ascertained that the therapeutic window of PF-3644022 (**25**) was too small to gain an accurate representation of the effect of MK2 inhibition on reversing the aged phenotype of primary WS cells.²⁹²

These results support further investigation of MK2 and its role in the accelerated senescence of WS cells. In order to conduct these tests more therapeutically viable candidates with higher selectivity and cell potency would be required to give firmer conclusions as to the role of MK2 in the premature senescence of WS cells.

3.7.3. Development of more efficacious MK2 inhibitors.

Significant developments have been made over the past few years towards more potent and selective MK2 inhibitors (see **Chapter 1.4**), though one of the major limitations in the development of ATP-competitive MK2 inhibitors has been low biochemical efficiency (BE).⁵⁵

Manetii *et al.* published a perspective recognizing a trend in ATP-competitive MK2 inhibitors and a large disparity between the cell based potency (EC_{50}) and the enzymatic assay potency (IC_{50}). The group speculated this to be due to ATP's very high affinity for MK2 and a trend in low solubility and cell permeability of the MK2 inhibitors that have been developed and widely studied.⁵⁵ Hence, even if an inhibitor exhibited a high binding affinity (K_i), its cellular response would be limited due to an inability to enter the cell and access the active site, as well as intense competition for binding with the high concentrations of ATP in the cell. To counteract low BE and achieve reasonable potency, higher drug concentrations tend to be required,²⁹³ though with

increasing concentrations there is a higher probability of cytotoxicity, off-target effects and drug attrition.⁵⁵

Therefore, Manetti *et al.* postulated that non-ATP-competitive inhibitors would offer much higher selectivity profiles.⁵⁵ A limited number of non-ATP-competitive MK2 inhibitors have been designed, with some examples discussed in **Chapter 1.4.2**. Given that theoretically lower concentrations of these inhibitors should be necessary to effect a desirable inhibitory response in cells, problems of cytotoxicity and off-target effects should be reduced. Consequently, it may be beneficial to shift the scope of MK2 inhibitors being probed in WS cells to non-ATP-competitive or allosterically binding candidates.

3.7.4. Conclusion and future perspectives.

Inconclusive results have been obtained so far when MK2 inhibitors have been used to investigate the premature ageing phenotype of WS cells. This has been postulated to be due to low cell potency and a typically small therapeutic window, often resulting in cessation of cell growth. Therefore there is still a need for the development of more selective and therapeutically viable MK2 inhibitors.

One repository that has a wealth of potential is the use of non-ATP-competitive MK2 inhibitors. These compounds should offer an enhanced cell potency and kinase selectivity profile, lowering the concentration of the inhibitor required and so reducing the probability of cytotoxicity from off-target effects.

Additionally, it may be beneficial for future studies to be completed using an alternative standard p38 inhibitor for comparison. The prototypical p38 inhibitor SB203580 (**1**) has been used extensively as a standard against which MK2 inhibitors have been measured, despite its known off-target effects.²⁸ As a result, further questions tend to be raised, specifically as to whether specific inhibition of p38 α is indeed eliciting the cellular responses being recorded.¹⁸ Therefore, in future studies it may be beneficial to conduct comparative assays additionally against the p38 α inhibitors RO3201195 (**10**) or BIRB 796 (**14**), both of which demonstrate much more selective profiles towards p38 α , and have a similar effect upon the proliferation rate of WS cells.^{1,18}

Chapter 4. Looking back ‘upstream’. The potential of p38 MAPK inhibitors.

4.1. Introduction.

Despite the precedent for MK2 inhibitors to act as an effective method for inhibition of the p38 α /MK2-mediated stress-signalling pathway, thus reversing the aged phenotype of WS cells,^{19,58} it was found that the cellular response was much reduced when compared to the prototypical p38 inhibitor SB203580 (**1**).⁶⁰

It has been postulated that when the signalling cascade is interrupted downstream, other kinases can compensate for the disruption and use alternative pathways to regulate and elicit the desired immunological response.³⁶ Therefore, continuing to probe the ‘upstream’ kinases remains a viable avenue of investigation.

4.1.2. BIRB 796, a novel p38 α MAPK inhibitor.

Though a wide variety of structural chemotypes have been investigated as potential p38 inhibitors (see **Chapter 1.3**),³⁷ the prevalence of ATP-competitive inhibitors is quite apparent. Boehringer Ingelheim’s p38 α MAPK inhibitor BIRB 796 (Dormapimod) (**14**) binds allosterically to the kinase outside the ATP-binding pocket,^{50,51} to exhibit a unique binding mode that induces a conformational change to catalytically inactivate the enzyme.²⁹⁴

The key binding interactions were identified by Regan *et al.* through co-crystallization of BIRB 796 (**14**) with p38 α (see **Figure 70**).⁵¹ In addition to binding allosterically outside the ATP-pocket, BIRB 796 (**14**) interacts through an ether-linked methionine residue in the ATP-hinge region. This additional hydrogen-bonding interaction was found to improve the binding efficiency of the molecule,⁵⁰ and classified **14** as a type 2 inhibitor.²⁹⁴

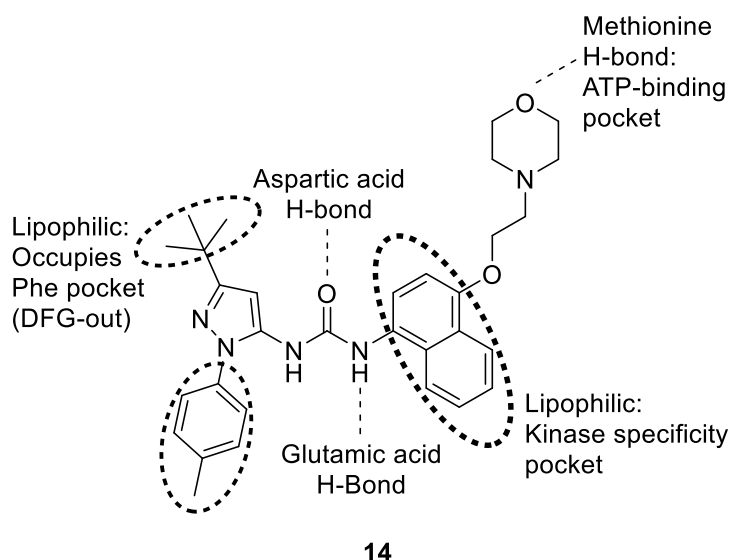


Figure 70: BIRB 796 (**14**), illustrating the key interactions when bound to p38 α , as identified by Regan *et al.*⁵¹

The molecular mechanism for inhibition of p38 α by BIRB 796 (**14**) is through a major conformational change of the activation loop, or DFG motif (Asp-Phe-Gly). When the kinase is in its active form, the activation loop adopts the DFG-in conformation, wherein the phenylalanine (Phe) residue occupies a hydrophobic pocket between the two lobes of the kinase.⁴⁹ When bound to BIRB 796 (**14**) this loop is flipped 'out' relative to the active state, into a DFG-out conformation.

From X-ray co-crystallization studies of p38 α with BIRB 796 (**14**), it has been identified that the Phe residue has moved out of this hydrophobic pocket, to be replaced by the *tert*-butyl group of the pyrazole.⁵¹ It has been speculated that the pyrazole moiety is crucial as a scaffold for positioning the *tert*-butyl group into this pocket,⁴⁹ and helps slow dissociation rates of the ligand from the kinase.⁵¹

Schneider *et al.* endeavoured to emulate the DFG-out conformation and slow dissociation rates of BIRB 796 (**14**) by adopting the same scaffold in their design of CDK8/CycC inhibitors (see **Figure 71**).²⁹⁵ They synthesized **205**, with a residence time calculated to be up 1600 minutes. However they determined this extended residence time to be due to the number of productive ligand interactions rather than restriction of the kinase into the DFG-out conformation.^{295,296}

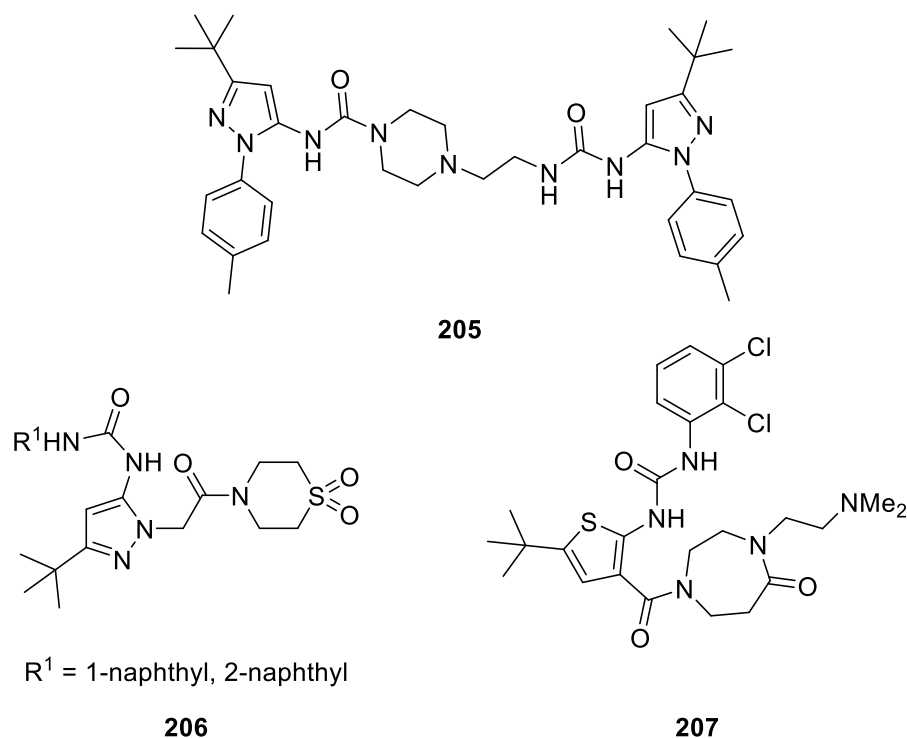


Figure 71: Drug candidates based upon the BIRB 796 (**14**) chemotype: Schneider *et al.*'s CDK8/CycC inhibitor **205**²⁹⁵ and Moffett *et al.*'s azole-based p38 α inhibitors **206** and **207**.⁵³

Moffett *et al.* also investigated the allosteric binding potential of BIRB 796 (**14**), adopting the pyrazole-urea pharmacophore as a model with the aim to improve drug-likeness and reduce off-target activity through removal of the ATP hinge binding element.⁵³ Using computationally assisted hypotheses, the group synthesized potential candidates, some of which are detailed in **Figure 71**. The *tert*-butyl group and urea backbone were conserved, with the use of thiophenes in addition to pyrazoles explored as the 5-membered heterocyclic scaffold. It was found that through replacement of the toluene group with a dioxothiomorpholine (**206**) or diazepanone group (**207**), and the use of extended linkers, new binding interactions could be achieved. Upon exploring the kinase selectivity pocket, occupied by the naphthalene group in BIRB 796 (**14**), it was found that **207** exhibited a similar binding efficiency with p38 α as BIRB 796 (**14**) with improved oral bioavailability in animal efficacy models.

Interestingly, Moffett *et al.* found that, in a broad kinase selectivity screening against 150 kinases, the only other kinase that was inhibited by **207** within a 150-fold range of the p38 α MAPK IC₅₀ value was the p38 β isoform; a great improvement in selectivity over BIRB 796 (**14**). In the same panel BIRB 796 (**14**) was found to exhibit cross-kinase activity with 29 out of the 150 screened kinases.⁵³

Indeed, despite being a very potent inhibitor for p38 α , BIRB 796 (**14**) has been reported to exhibit significant binding affinity for a number of kinases,²⁹⁷ including the other isoforms of p38 (p38 α , p38 β , p38 γ and p38 δ) and the Jun N-terminal kinases (JNK);²⁵⁹ an alternative MAPK-signalling subfamily and a subject of great interest in the development of therapeutics for inflammatory diseases.²⁴

The significant promiscuity of BIRB 796 (**14**), despite the selectivity elements designed by Regan *et al.* and its novel binding mode, inspired a project to explore the potential of the BIRB 796 pharmacophore, upon repurposing, as a chemical tool.

4.1.2. Exploring the potential of the BIRB 796 pharmacophore.

The identification of new and more pharmacologically-viable drug candidates through the modification of other drugs is known as the repurposing or reengineering of drugs, and is becoming a more prevalent trend in drug discovery.^{298–300} The studies conducted by Schneider *et al.*²⁹⁵ and Moffett *et al.*⁵³ are prime examples of how medicinal chemists can adapt lead candidates or unsuccessful drugs, abandoned or rejected from previous development programmes, and repurpose them towards new targets with hindsight from former failure.

Another emerging method is the selective optimization of side activities (SOSA). Unlike traditional high-throughput screening (HTS) methods employed by industry, and becoming acknowledged as a large investment with potentially little gain,³⁰¹ SOSA methods tend to adopt a small screening library consisting of drug-like, bioavailable molecules. This method reduces the likelihood of failure at late-stage development, and tends to enable the screening of a wide variety of pharmacophores to ensure diversity in potential candidates.³⁰¹ For instance, the triarylimidazole core of SB203580 (**1**) was originally designed as a dual inhibitor for cyclooxygenase (COX) and 5-lipoxygenase, and was found to inhibit the biosynthesis of interleukin-1 (IL-1).^{29,30} With further studies, the pyridinylimidazole chemotype was found to be a selective inhibitor for p38 α MAPKs, leading to the widespread use of SB203580 (**1**) as a model p38 α inhibitor and chemical tool (for more information, see **Chapter 1.3.2**).^{31,32}

These new advents in drug discovery and the potential of utilizing the novel binding mode of BIRB 796 (**14**) promoted a SOSA-inspired project with the aim of investigating the potential of the BIRB 796 (**14**) scaffold for the design of new chemical probes. Chemical probes are very important tools for target validation in drug discovery. They can help evaluate the roles and

mechanisms of kinases *in vivo* and *in vitro* and give some return on investments by companies in the drug discovery program.^{302,303}

For this project, focus was placed on adapting the selectivity elements of BIRB 796 (**14**), in particular its side activities, to find what other potential targets could be explored and if it was possible to increase selectivity for those kinases, whilst reducing ligand binding affinity with p38 α .

4.1.3. Identifying structural features of initial interest.

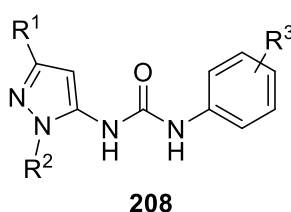


Figure 72: Scaffold **208**. R¹, R² and R³ illustrate the points of interest of the BIRB 796 (**14**) chemotype that will be altered and explored over the course of this project.

In order to reduce affinity for p38 α , a step-wise approach was adopted in which incremental changes were made to the structural features of BIRB 796 (**14**) identified by Regan *et al.* as important for p38 α selectivity (**Figure 70**). One section of the molecule was focused on at a time, as illustrated in **Figure 72**, and a small library of compounds was synthesized varying the electronic and steric effects of R¹, R² or R³ of **208**. This library was then screened for binding potential against a small profile of kinases and the biological results were used to determine the direction of further enquiries.

In this project initial studies concentrated on modification of the aromatic ring attached to the urea: altering R³ of **208**. The presence of an aromatic ring at this position had been a consistent feature, even in the early stages of Boehringer Ingelheim's project, and so exploring its importance to p38 α recognition was of great interest.^{304,305} Computational modelling by Regan *et al.* to compare the binding of SB203580 (**1**) and BIRB 796 (**14**) when bound to p38 α MAPK found that both inhibitors had aromatic rings occupying the same kinase selectivity pocket (see **Figure 73**).⁵⁰ From SAR studies of theseazole-based inhibitors Regan *et al.* determined the

presence of the phenyl group at this position to be paramount for p38 α inhibitor potency and kinase specificity.^{50,306}

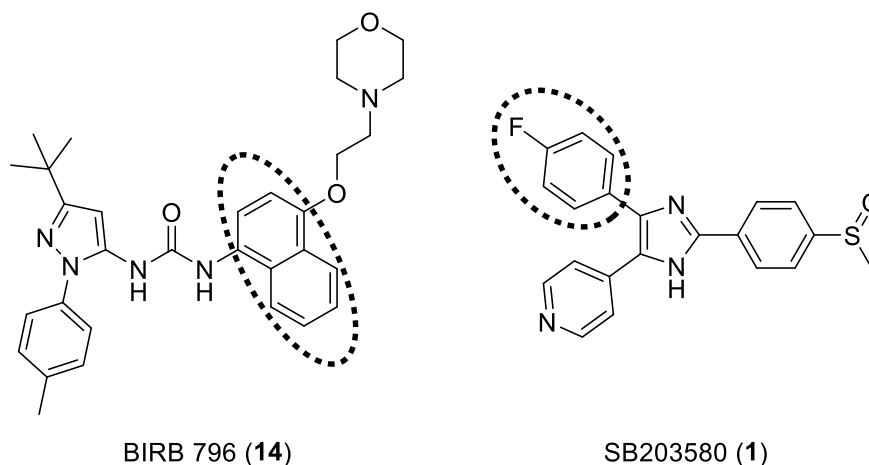
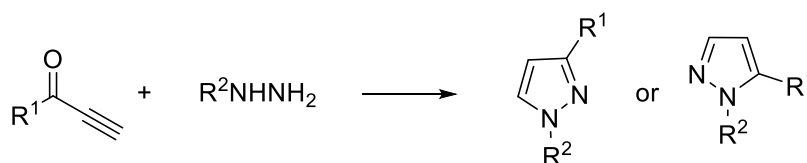


Figure 73: BIRB 796 (**14**) and SB203580 (**1**) highlighting the aromatic ring regions that occupy the same space when bound to p38 α .

Therefore, it was hypothesized that by modifying the electronic and steric factors of this ring it could be possible to quickly determine other kinases which would bind to this structural chemotype, while reducing binding affinity for p38 α . Thus the synthesis of a small library of compounds based upon scaffold **208** was proposed. This library would be generated by synthesizing an initial aminopyrazole building block and reacting it with a selection of isocyanates to produce a range of ureas with three potential points of diversity.

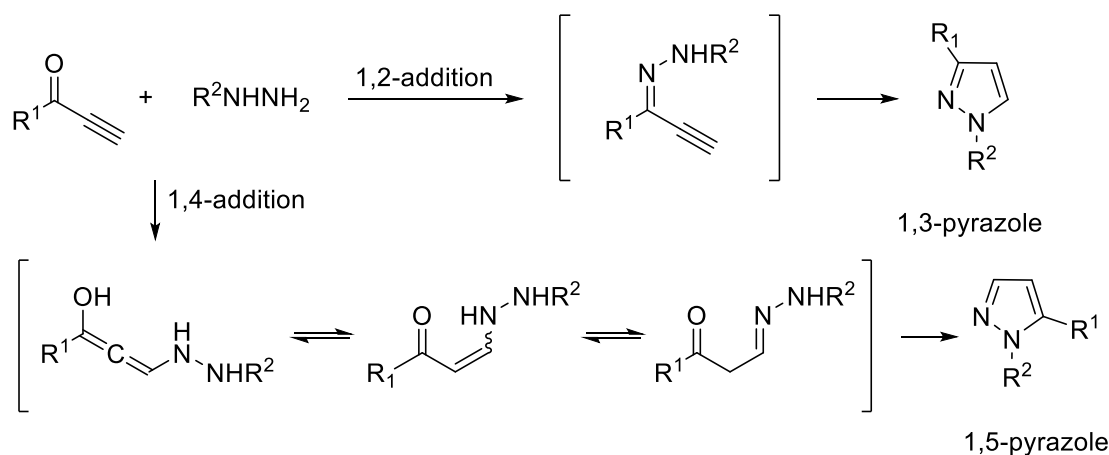
4.1.3. Synthetic approaches to 3,5-disubstituted pyrazoles.

For a general introduction to pyrazoles, and synthetic approaches towards pyrazoles, see **Chapter 1.6.2.1**. For the synthesis of 3,5-disubstituted pyrazoles, like BIRB 796 (**14**), issues of regioselectivity must be considered. For instance, in the cyclocondensation of ethynyl ketones and hydrazines, though a well-established route to both 3- and 5-substituted pyrazoles, the regioselectivity of these processes can be quite low.^{307,308} Bagley *et al.* conducted a study to explore the regioselectivity of reactions between mono-substituted hydrazines and ethynyl ketones (**Scheme 130**) and developed a metal-free route using microwave-assisted techniques to facilitate rapid conversion to 3- and 5-substituted pyrazoles.³⁰⁸



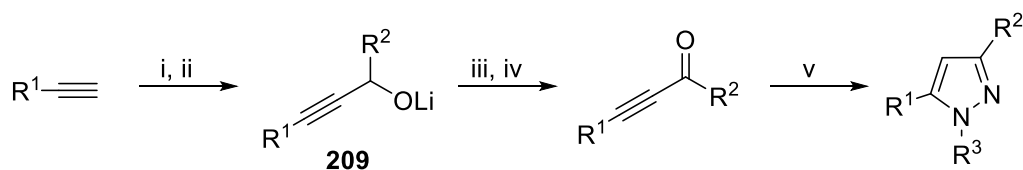
Scheme 130: Synthetic route towards 1,3- or 1,5-pyrazoles investigated by Bagley *et al.*³⁰⁸

It was found that a two-step process, with initial condensation of the ethynyl ketone and hydrazine, followed by addition of acid and conductive heating or microwave-assisted heating, generally improved regioselectivity to favour formation of the 1,3-pyrazole. Additionally, it was found that microwave-assisted heating reduced reaction times significantly, from refluxing for 4 to 15 h in acidified methanolic solution, to just 2 minutes heating in a sealed vessel at 120 °C.



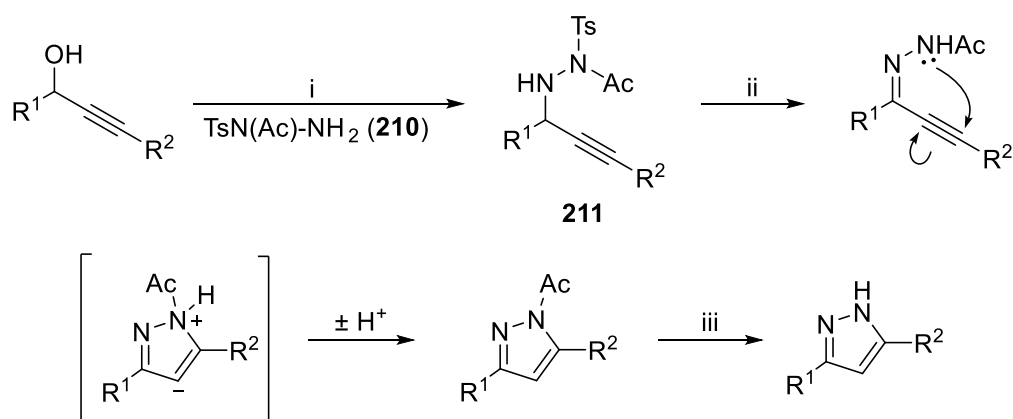
Scheme 131: Mechanistic reasoning for regioselectivity of pyrazole formation.

The ratio of regioisomers still varied, depending upon the substrate, but some trends in reactivity were observed. The mechanism for the reaction was proposed to occur either through a 1,4-Michael addition of the hydrazine and the ethynyl ketone, or by 1,2-addition (see **Scheme 131**). Under acidic conditions, the latter process was generally observed, forming an intermediate ethynyl hydrazone, which on cyclization gave the 1,3-pyrazole. In the absence of acid, or when certain very electron-rich ethynyl ketones were used, 1,4-Michael addition was favoured, which on cyclocondensation, gave the 1,5-pyrazole.



Scheme 132: Togo *et al.*'s proposed route for synthesis of 3,5-disubstituted pyrazoles via mono-substituted alkynes, aldehydes and hydrazines. Reaction conditions: i) *n*-BuLi; ii) $R^2\text{CHO}$; iii) I_2 ; iv) K_2CO_3 ; v) H_2NNHR^3 .³⁰⁹

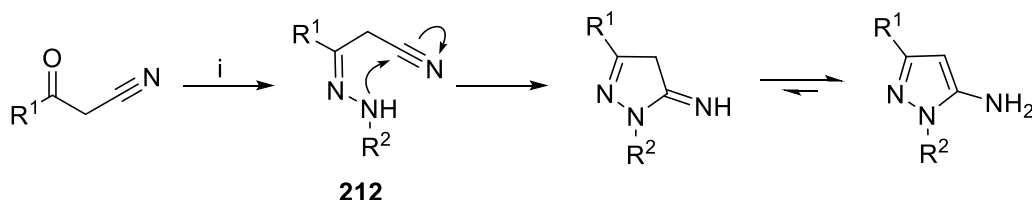
Togo *et al.* developed a regioselective, one-pot route for the synthesis of 1,3,5-trisubstituted pyrazoles in 2014 from mono-substituted alkynes, aldehydes and hydrazines (see **Scheme 132**).³⁰⁹ Deprotonation of the alkyne using *n*-butyl lithium (*n*-BuLi), followed by reaction with a functionalized aldehyde, was proposed to form a propargylic alkoxide intermediate (**209**). Treatment with iodine and base gave a functionalized ethynyl ketone in situ, which reacted smoothly with hydrazine when heated to reflux to give the desired pyrazole with high regioselectivity in yields of 75-99%, with no need for purification of intermediates.



Scheme 133: Reddy *et al.*'s proposed mechanism for the synthesis of 3,5-disubstituted pyrazoles from propargyl alcohols and *N,N*-disubstituted hydrazines.³¹² Reaction conditions: i) $\text{BF}_3 \bullet \text{Et}_2\text{O}$; ii) KO^tBu , iii) Base.

Propargyl alcohols have also been used to direct the 1,2-addition of hydrazines to form intermediate propargyl hydrazines suitable for cyclization to the pyrazole. Yoshimatsu *et al.*³¹⁰ and Zhan *et al.*³¹¹ developed routes employing a tosylhydrazine and catalytic Lewis acids, including AuCl , $\text{Sc}(\text{OTf})_3$, and AgOTf to promote nucleophilic attack at the alcohol α -carbon. Independently, Reddy *et al.* developed a metal-free route, reacting *N*-acetyl-*N*-tosylhydrazine **210** with propargyl alcohols in the presence of 10 mol% $\text{BF}_3 \bullet \text{Et}_2\text{O}$ to form an intermediate propargyl hydrazine (**211**). The *N,N*-disubstituted hydrazine could then be reacted under basic conditions to give the 3,5-disubstituted pyrazole via a proposed 5-*endo-dig* cyclization (see **Scheme 133**).³¹²

The key scaffold in BIRB 796 (**14**) is a 5-aminopyrazole. One popular route towards 5-aminopyrazoles is by condensation of a β -ketonitrile and hydrazine to form an intermediate hydrazone (**212**), which undergoes 5-*exo-dig* cyclization and tautomerization in air to give the pyrazole (see **Scheme 134**, and **Chapter 1.6.2.**).⁷⁶



Scheme 134: Synthesis of 5-aminopyrazoles from a functionalized hydrazine and β -ketonitrile via a 5-*exo-dig* cyclization. Reaction conditions i) H_2NNHR^2 .

Regan *et al.* adopted this route to build the scaffold of BIRB 796 (**14**), by derivatization of the 5-aminopyrazole as a urea through reaction with an isocyanate at room temperature.⁵⁰ The utility of this method towards 1,3-disubstituted-5-aminopyrazoles was verified by Bagley *et al.* and, through the use of microwave-assisted techniques, they were able to improve yields and shorten reactions times from hours to minutes.⁵²

On this basis, it was proposed that the most efficient route towards the new analogue library would be to proceed via the microwave-mediated synthesis of 1,3-disubstituted 5-aminopyrazoles. Using β -ketonitriles and functionalized hydrazines as starting materials, this route had the potential to be rapid and high yielding, as well as readily-amenable to further functionalization of scaffold **208** at R^2 and R^3 at later stages in the project (see **Figure 72**).

4.1.4. An introduction to ureas.

In medicinal chemistry, ureas have been found to be very useful as scaffolds due to their structural rigidity. For example, cyclic ureas have been used in the design of seven-membered scaffolds as HIV protease (HIV PR) inhibitors (**Figure 74**).³¹³

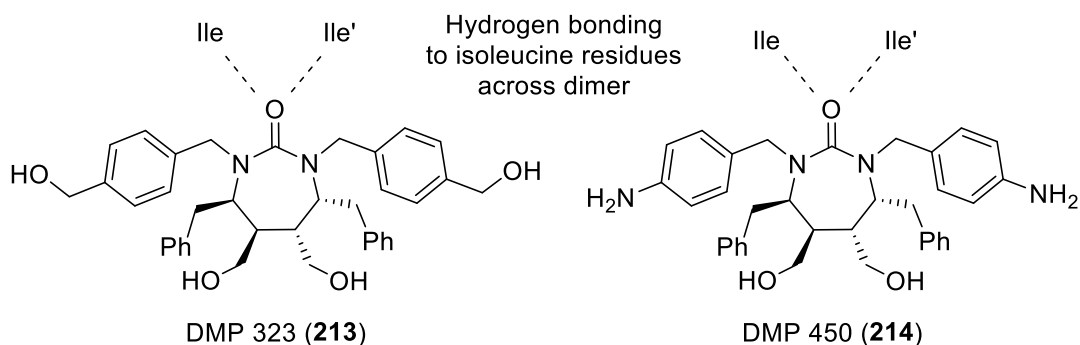
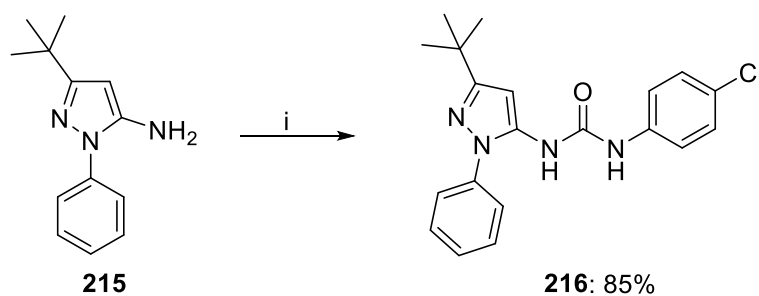


Figure 74: HIV Protease (HIV PR) inhibitors, employing a cyclic urea to form a rigid scaffold, and hydrogen bonding across the dimer of the enzyme.

The carbonyl groups of ureas **213** and **214** mimic the interactions of a key water molecule normally ligated to the protease which is unique to the retroviral proteases. The carbonyl oxygen forms two hydrogen bonds with isoleucine residues on either side of the symmetrical HIV PR dimer backbone. Lam *et al.* hypothesized that displacement of the water molecule should be energetically favourable and the rigid structure of the cyclic urea would provide a positive entropic effect.³¹⁴ Initial lead DMP 323 (**213**) was found to have good oral bioavailability in dogs and mice, and a relatively high potency.³¹⁴ However, it had reduced bioavailability in humans due to poor water solubility. Hence DMP 450 (**214**) was designed to have an enhanced bioavailability, through installation of weakly basic residues with a pK_{aH} of 4.6, so that the molecule would be protonated in the stomach and neutral in the cell.³¹⁵

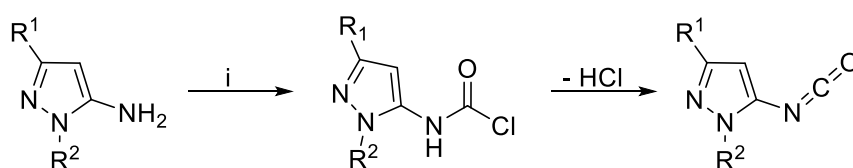
The urea group in BIRB 796 (**14**) is very important for binding to p38 α , as ascertained by Regan *et al.* in their initial investigations.⁵⁰ X-ray co-crystallization studies identified a complex hydrogen bonding network between the urea and glutamic acid and aspartic acid residues (see **Figure 70**). The importance of these interactions was confirmed through exchange of the secondary amide NH groups for tertiary NMe and methylene bridge units, which resulted in huge reductions in binding affinity. Also, when a thiourea was used as the central scaffold there was a 60-fold decrease in potency, confirming the importance of the urea moiety for binding, in addition to maintaining the geometry of the scaffold.

4.1.4.1. Synthetic approaches to ureas.



Scheme 135: Regan *et al.*'s synthesis of the initial lead compound **216** in the development of BIRB 796 (**14**). Reaction conditions: i) 4-chlorophenyl isocyanate, THF or CH₂Cl₂, 25 °C, overnight, 85%.⁵⁰

Regan *et al.* synthesized their original HTS 'hit' urea compound **216** by reacting together 5-aminopyrazole **215** and 4-chlorophenyl isocyanate, with stirring at room temperature in THF or CH₂Cl₂, affording **216** in high yield (85%) (see **Scheme 135**).⁵⁰ However, as their molecular target became more complex, alternative methods of synthesis were necessitated.

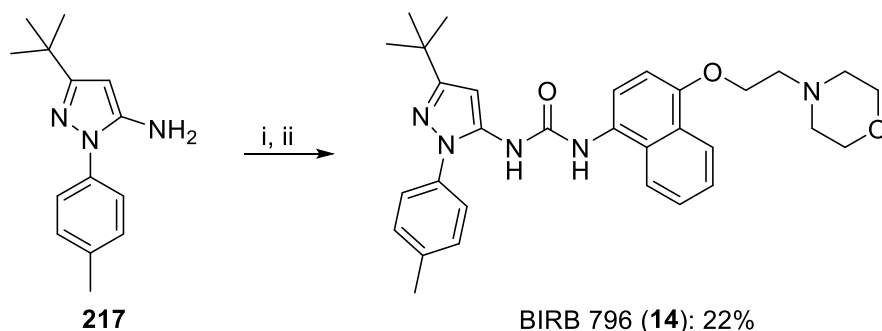


Scheme 136: Isocyanate formation from 5-aminopyrazoles and phosgene. Reaction conditions: i) phosgene, aq. NaHCO₃, CH₂Cl₂.⁵⁰

Their chosen method was via in situ formation of an isocyanate through reaction of 5-aminopyrazole with phosgene (COCl₂). In this reaction, COCl₂ reacts with the amine to form a carbamoyl chloride with elimination of HCl. This intermediate can then collapse or undergo a second nucleophilic attack to eliminate another equivalent of HCl and give the isocyanate (see **Scheme 136**).³¹⁶ Typically, this reaction is conducted through slow addition of the amine to cold phosgene to prevent build-up of the amine and carbamoyl chloride together in solution. An excess of phosgene is typically used to promote initial nucleophilic attack and dehydrohalogenation to the isocyanate.

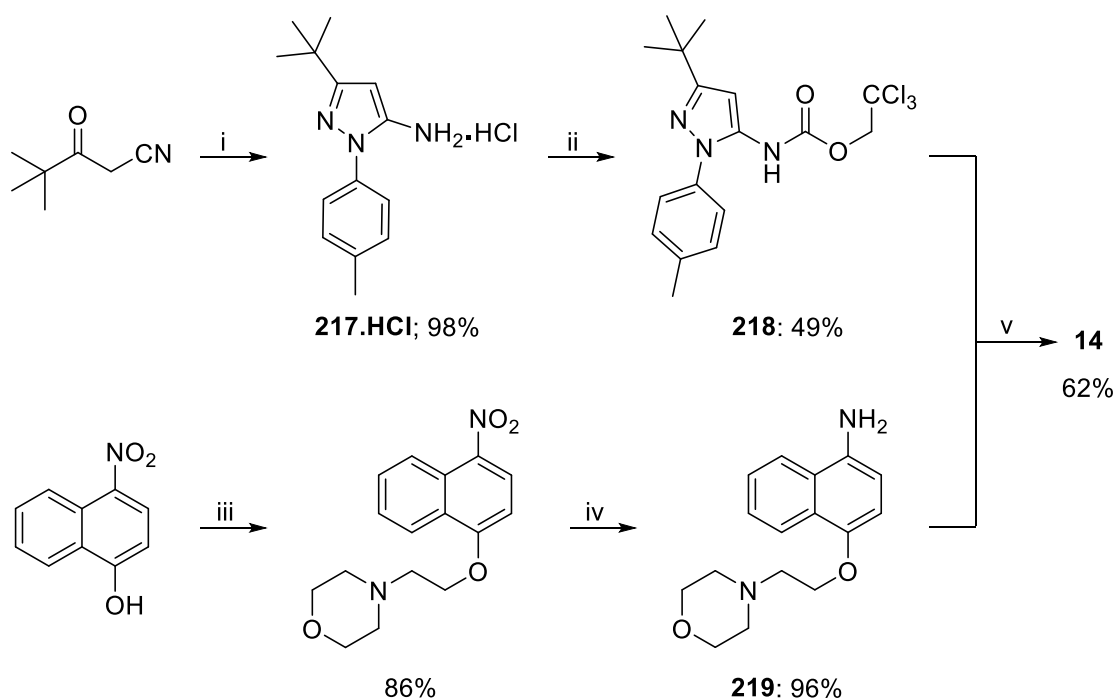
Regan *et al.* conducted their phosgene-mediated reactions in the presence of saturated aqueous sodium hydrogen carbonate solution (NaHCO₃) to neutralize the HCl produced in solution. In order to synthesize BIRB 796 (**14**), 5-aminopyrazole **217** was reacted with phosgene. Once the isocyanate was formed, addition of the aminonaphthalene **219** afforded a 22% yield of **14** (see

Scheme 137). However, phosgene is highly toxic, and will react with amines and amino acids in the body, and so alternative methods of urea formation are highly desirable.



Scheme 137: Regan *et al.*'s synthesis of BIRB 796, using intermediate isocyanate formation. Reaction conditions: i) phosgene, NaHCO₃, toluene, 0 °C; ii) aminonaphthalene **219**, DIEA, THF, RT, overnight, 22%

Bagley *et al.* developed a microwave-assisted synthetic route towards BIRB 796 (**14**) in order to test the p38 inhibitor in WS cells.⁵² They developed a route that negated the addition of phosgene and afforded the final urea in much improved yields (see **Scheme 138**).



Scheme 138: Bagley *et al.*'s microwave-assisted synthesis of BIRB 796 (**14**). Reaction conditions: i) *p*-tolylhydrazine hydrochloride, MeOH, MW 120 °C, 40 min, 98%; ii) 2,2,2-trichloroethyl chloroformate, NaOH, EtOAc-H₂O, 0 °C to RT, 3 h, 49%; iii) 4-(2-chloroethyl)morpholine hydrochloride, NaOH, K₂CO₃, NMP, 100 °C, 2 h, 86%; iv) Pd/C, NH₄CO₂H, EtOH, MW 100 °C, 15 min, 96%; v) DMSO, MW 100 °C, 30 min, 62%⁵²

Rather than forming an isocyanate in situ, the group synthesized intermediate carbamate **218** in moderate yield from the pyrazole-5-amine hydrochloride salt **217.HCl** by reacting under basic

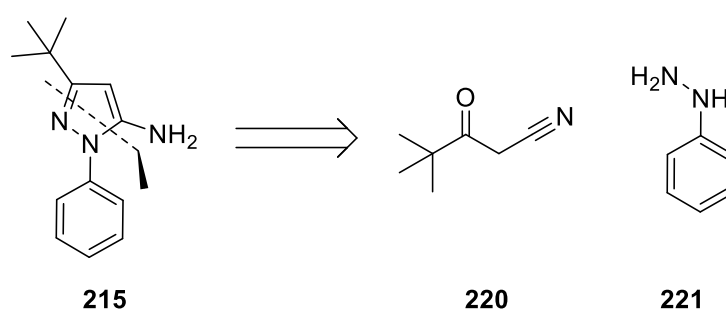
conditions with 2,2,2-trichloroethyl chloroformate.⁵² Concurrently, morpholine-linked naphthyl amine **219** was synthesized by a base catalyzed alkylation of 4-nitronaphth-1-ol, and reduced via microwave-assisted palladium-catalysed transfer hydrogenation. The two fragments were then combined, and microwave-assisted heating at 100 °C in DMSO afforded **14** in higher overall yield than Regan *et al.*'s published route.

For the synthesis of the first analogue library, it was determined that the reaction of 1,3-disubstituted-5-aminopyrazoles and a diverse range of isocyanates would likely be the most rapid and efficient method to generate a broad spectrum of ureas. The biological results of the first library would determine the direction of further study. It was noted that the synthesis of intermediate carbamates or isocyanates may be necessitated at this later stage in order to investigate any areas highlighted to be of specific interest through biological studies.

4.2. Synthesis of analogue library 1.

4.2.1. Synthesis of the core pyrazole.

For initial investigations the potential of the aromatic ring directly attached to the urea scaffold **208**, was investigated to identify alternative targets which would bind in a distinct fashion to the BIRB 796 (**14**) chemotype. It was resolved that the pyrazole section of the molecule would be kept consistent through the first iteration of screening, with an unsubstituted phenyl group at the 1*N*-pyrazole position and a *tert*-butyl group at the 3-*C* centre (**215**).



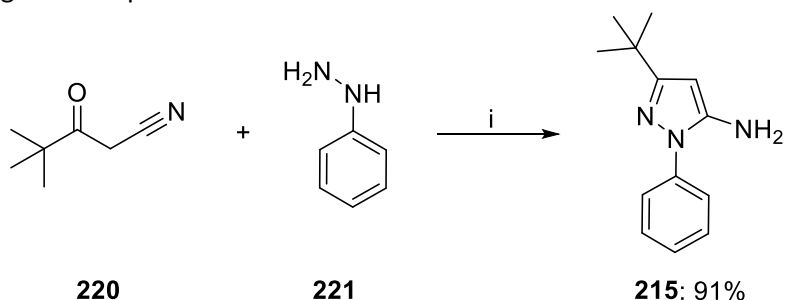
Scheme 139: Retrosynthesis for urea formation from isocyanates and 5-amino pyrazoles.

Following the literature approach towards **215**,⁵² a solution of 4,4-dimethyl-3-oxopentanitrile (**220**) and phenyl hydrazine (**221**) (1:1 ratio) in methanol was heated to 120 °C for 40 minutes in a sealed vessel using a microwave synthesizer. However, purification of **215** by trituration in light petroleum was problematic due to low conversion to product. Efforts to improve the reaction

included conducting the reaction under an inert atmosphere, increasing the reaction temperature to 140 °C, extending the reaction time and using alternative methods of purification, including flash column chromatography on silica and by SCX-2 chromatography.

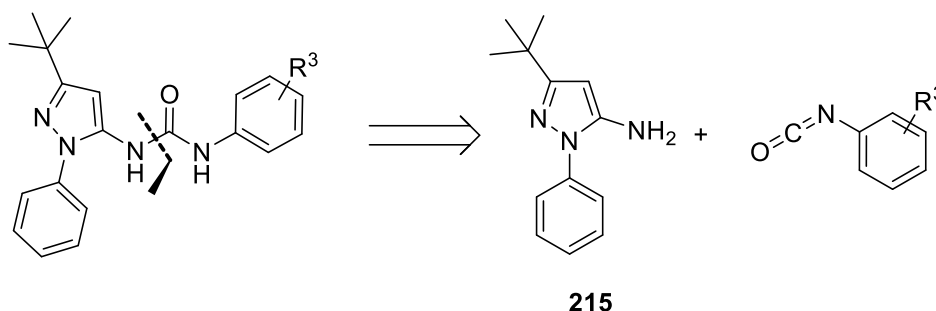
Yields were inconsistent across all methods when methanol was used as the reaction solvent, ranging from zero to 76% isolated yield. The best yield was achieved by microwave-assisted heating in a sealed vessel at 140 °C for 60 minutes hold time and purification by SCX-2 chromatography. By ^1H NMR spectroscopic analysis, conversion to the product could be easily confirmed through loss of the 2-CH₂ proton resonance of **220** at δ_{H} 4.23 ppm, and a new resonance at δ_{H} 5.40 ppm for the 4-CH pyrazole proton of **215**.

Yield and reproducibility of the reaction were improved through the use of a toluene and glacial AcOH mixture (5:1), and microwave-assisted heating at 120 °C for 40 minutes in a sealed vessel, with yields of up to 91% achieved after purification by flash column chromatography (see **Scheme 140**).³¹⁷ After initial investigations, it was found a slight excess of the hydrazine favoured complete reaction and more efficient purification procedures, preventing any unreacted nitrile from co-eluting with the product.



Scheme 140: Synthesis of 1-phenyl-3-*tert*-butylpyrazol-5-amine **215**. Reaction conditions: i) Toluene-AcOH (5:1), MW 120 °C, 40 min, 91%.

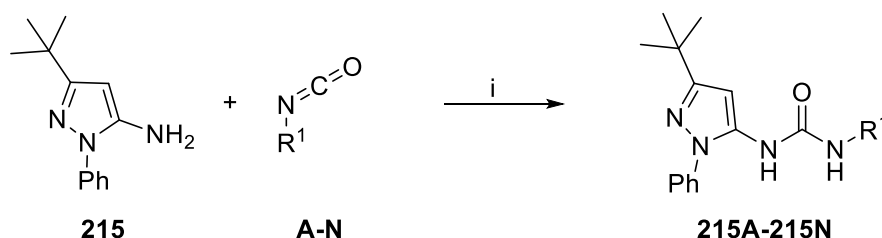
4.2.2. Synthesis of urea analogue library 1.



Scheme 141: Retrosynthesis of urea scaffold, with reference to R³ of scaffold **208**.

Once a reliable route towards **215** was established, synthesis of the first urea library was completed as illustrated in **Table 8**. A selection of isocyanates was chosen to be investigated, each selected to explore how changes in the steric, electronic and lipophilic properties of the aromatic ring might affect the selectivity of binding to p38.

Following this synthetic route, **215** was stirred with the relevant isocyanate for 20 minutes at room temperature (unless otherwise stated in **Table 8**). The reaction mixture was then evaporated and the residues triturated with light petroleum to afford the urea product, with additional recrystallization from hot methanol if required (see **Scheme 142**).



Scheme 142: Reaction scheme for the synthesis of analogue library 1. Reaction conditions i) CH₂Cl₂, 20 min, RT.

Overall, the results obtained were extremely satisfactory, with all isolated yields of the urea product being in excess of 60% and half of them being formed in >80% yield. However, in some cases additional purification by recrystallization was required.

Table 8: Analogue library 1 (see Scheme 142). ^a			
Entry No.	Compound No.	R ¹	Yield (%) ^b
1	215A	1-Naphthalene	65 ^d
2	215B	2-Napathalene	81 ^e
3	215C	<i>o</i> -Toluene	53
4	215D	4-Ethoxyphenyl	86 ^f
5	215E	4-Fluorophenyl	87
6	215F	3,5-Bis(trifluoromethyl)phenyl	88
7	215G	4-(Benzyloxy)phenyl	82
8	215H	3,5-Dimethylphenyl	89
9	215I	5-Fluoro-2-methylphenyl	67
10	215J	3,4-Difluorophenyl	67
11	215K	Phenyl	85 ^c
12	215L	<i>p</i> -Toluenesulfonyl	75
13	215M	3-Methoxyphenyl	65
14	215N	<i>p</i> -Toluene	62 ^c
^a General reaction conditions: an equimolar mixture of aminopyrazole 215 and isocyanate was stirred at RT for 20 min in CH ₂ Cl ₂ , unless otherwise stated. ^b Yield after evaporation <i>in vacuo</i> and trituration with light petroleum. ^c Yield after recrystallization from hot methanol. Extended reaction time: ^d 90 min, ^e 30 min, ^f 25 min.			

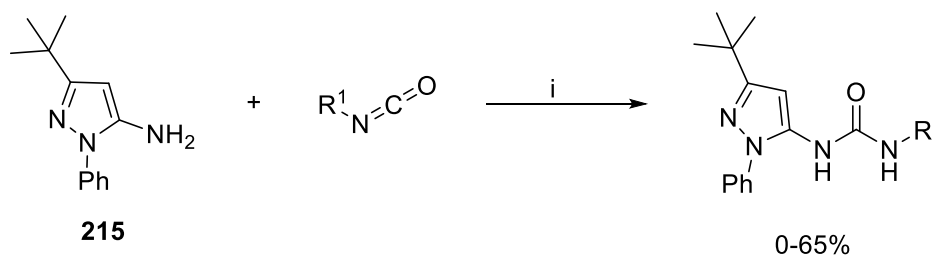
There were specific difficulties in the purification of products synthesized from 4-fluorophenyl isocyanate and 3,5-bis(trifluoromethyl)phenyl isocyanate (**Table 8**, entries 5 and 6). The starting isocyanates in these cases were viscous oils and consequently handling them was quite problematic, especially upon purification. If any starting isocyanate remained, trituration became very challenging with the product often trapped within an intractable, viscous mixture. Perseverance with trituration and accurate attention to stoichiometry was essential to facilitate the purification of these analogues, with very agreeable results.

All products were obtained as off-white or colourless powders and structural identification was conducted through ¹H NMR spectroscopic analysis in DMSO-*d*₆. The final product could clearly be identified from a shift of the 4-CH pyrazole singlet resonance downfield and two broad singlet resonances for the urea protons between δ_H 9.5-8.5 ppm, depending upon the electron density of the attached aromatic group. In the ¹³C NMR spectroscopic analysis, the appearance of a new carboxyl signal was observed at approximately δ_C 155-150 ppm and 2D NMR ¹H-¹³C correlation experiments were essential to assign the different aromatic peaks of the carbon spectrum. For

instance, the carboxyl and the pyrazole 3-C centre had very similar carbon shifts in all spectra. Differentiation could only be achieved with analysis of through-bond interactions using HMBC experiments, with the pyrazole 3-C centre assigned by a distinctive interaction with the nearby 4-CH pyrazole proton. Additionally, correlations between the NH proton of the urea and *ortho*-protons on the aromatic ring were required for complete assignment of resonances.

4.2.3. Improving the synthesis.

Though mostly satisfactory yields were obtained for the urea products, efforts were made to further optimize reaction efficiency. The reaction time was considered first, with some results in **Table 8** taken from reactions run over slightly longer periods (entries 1, 2 and 4); overall it was found that the yields were extremely acceptable after just 20 minutes reaction time. The effect of temperature was also briefly examined; heating reactions to 25-30 °C, again, gave only negligible improvements to the yield compared to reactions run at 20-22 °C (room temperature).



Scheme 143: Reaction scheme for exploring the effect of changing solvents on urea formation. Reaction conditions: i) DMF, THF, MeOH or toluene-AcOH (5:1)

Table 9: Exploring the effect of changing solvent on urea formation (Scheme 143). ^a			
Entry	R ¹	Solvent	Yield (%) ^b
1	<i>o</i> -Toluene	DMF	-
2	<i>o</i> -Toluene	THF	36 ^c
3	4-Ethoxyphenyl	DMF	-
4	4-Ethoxyphenyl	MeOH	23
5	4-Ethoxyphenyl	THF	65 ^c
6	3,5-Dimethylphenyl	Toluene:AcOH (5:1)	65

^a General reaction conditions: An equimolar mixture of aminopyrazole **215** and isocyanate was stirred at RT for 20 min.
^b Yield after evaporation *in vacuo* and trituration with light petroleum.
^c 25 °C, overnight.

There were a number of problems with the solubility of both starting materials and products, with precipitation tending to be observed quite early in the reaction. In order to try and maintain homogeneity and boost yields, alternative solvents were investigated, as illustrated in **Table 9**.

Solvents chosen as potential reaction media included CH₂Cl₂ (solvent used in library synthesis), DMF and THF; the solvent of choice in Regan *et al.*'s original route to BIRB 796 (**14**).⁵⁰ However, when comparing the reaction of **215** with 4-ethoxyphenyl isocyanate in CH₂Cl₂ (**Table 8**, entry 4) and in THF (**Table 9**, entry 5), the yield was significantly reduced, from 86% to 65%, even after stirring overnight at 25 °C. When reactions were conducted in DMF, despite all reactants dissolving, the reaction failed to result in product formation after the 20 minute reaction time (**Table 9**, entries 1 and 3).

Methanol was proposed as a desirable solvent to design a one-pot urea formation reaction, as acidified methanol or ethanol was the desired reaction medium for the synthesis of pyrazoles from hydrazine hydrochloride salts (see **Chapter 4.5.3** for alternative pyrazole synthetic route). Thus a one-pot synthesis of ureas from the starting β-ketonitrile and hydrazine was hypothesized, in which simultaneous addition of all reactants could be conducted, negating additional time-consuming purification, to improve the efficacy of the total urea synthesis. However, yields were very low when reacting with 4-ethoxyisocyanate in methanol (23%) (entry 4). Similarly, when using toluene-AcOH (5:1) solvent mixture (entry 6), investigated for the same aforementioned reasons, yields were greatly diminished when compared to the use of CH₂Cl₂ as solvent; from 89% (**Table 8**, entry 8) to 65%. Hence, plans to develop a one-pot synthetic method were abandoned in favour of the higher yielding step-wise route.

After these studies, it was decided that the original synthetic method was the most reliable to provide a broad range of acceptable yields. Once the first library was complete, all compounds were purified by recrystallization from hot methanol before biological evaluation by the Structural Genomics Consortium (SGC) against a panel of kinases to assess their binding affinity compared to BIRB 796 (**14**).

4.3. Biological evaluation of analogue library 1.

4.3.1. Introduction to drug/fragment screening.

To assess the potential affinity and selectivity of the urea analogues in library 1, and their prospects as chemical probes, the thermal shifts for the ligands when bound to a range of protein kinases were completed using differential scanning fluorimetry (DSF) in collaboration with the SGC at Oxford.^{xi} DSF is a measure of the thermal stabilization endowed by a ligand when bound to a protein.³¹⁸ The procedure is carried out by melting the ligand-bound protein and comparing its melting temperature with that of the unbound protein. If the ligand binds strongly, more energy will be required to unfold the protein and break the new bonds, raising the melting temperature. The range over which the protein melts is measured using a fluorescence probe, and the change in melting temperature gives the thermal shift (T_m).

The fluorescent probe used in these tests was designed to fluoresce in non-polar environments and quench in aqueous environments. Hence, as the protein unfolded and the hydrophobic areas were exposed to solvent, the probe in solution bound to those regions, protecting them from the solvent, would fluoresce. The fluorescence intensity was plotted as a function of increasing temperature and the melting temperature (T_m) was recorded at the mid-point of increasing fluorescence.

This technique tends to be used as a rapid screening method, with any positive results carried forward into further biological assays for verification and to estimate the extent to which the compound could inhibit, activate or modulate the target process.

4.3.2. Kinase screening panel.

Analogue library 1 was screened in triplicate when bound to p38 α , SRPK1, SRPK2, PIM1, CLK1 and DYRK1A, kinases which are currently of interest to the SGC for the development of new chemical probes.

^{xi} Completed by Dr Ana Clara Redondo, Professor Stefan Knapp, Structural Genomic Consortium at the University of Oxford.

Provirus integration site for Moloney murine leukemia virus (PIM-1) is a protein kinase encoded by the Pim1 gene and classified as a proto-oncogene.^{319,320} It plays an important role in the regulation of cell cycle progression and apoptosis, and has been found to be overexpressed in haematological malignancies and solid tumours, implicating an important role for it in tumour growth. Hence PIM kinases have been widely explored as drug targets for anticancer therapeutics.

Cdc2-like kinase (CLK1) protein kinases are dual specificity kinases that can phosphorylate serine-threonine and tyrosine sites.³²¹ CLK1 is the primary member of the CLK family that has been shown to be involved in the activation of members of the MAP kinase cascade and plays a role in regulating pre-mRNA splicing.^{322,323} Serine-arginine protein kinases (SRPK) are also heavily involved in pre-mRNA splicing, and both SRPK and CLK1 have been shown to phosphorylate the serine-arginine (SR)-rich splicing protein ASF/SF2, though they exhibit distinct specificities.³²⁴

SRPK1 and SRPK2 are very similar in structure and function, both phosphorylating the serine-arginine rich domains of SR proteins; a family of nuclear RNA binding proteins (RBPs) essential for recruiting maturing pre-mRNA for splicing.³²⁵ Pre-mRNA splicing is essential to allow alternative splicing, which is a key step in controlling gene expression and increasing organismal complexity. SR proteins demonstrate key roles in regulating splice site selection,³²⁶ and their activity is modulated by reversible phosphorylation. SRPK1 and SRPK2 are the main mediators of this phosphorylation and help to maintain levels of phosphorylated SR proteins even under conditions of stress and shock.³²⁵

Dual specificity tyrosine-phosphorylation-regulated kinase 1A (DYRK1A) is also an important protein in the alternative splicing of genes, and has become a protein kinase of specific interest in the development of treatments for Downs syndrome (DS) and Alzheimer's disease (AD).^{32,327} It has been reported that individuals with neurodegenerative diseases, including DS and AD, exhibit increased activity of DYRK1A in the brain, with the percentage of DYRK1A positive nuclei in AD brains at about 10% compared to 0.5% in normal brains.³²⁷

These protein kinases are a just a small set of the over 500 protein kinases in the human kinome,³² and though they have been studied widely, the development of new chemical probes with a high degree of selectivity are desirable for target validation and to gain a better understanding of the roles of these proteins *in vivo* and *in vitro*.^{302,303}

4.3.3. DSF results for analogue library 1.

Table 10: DSF results for BIRB 796 (14) against the panel of kinases selected. ^a						
Compound	Thermal shift (T _m) (°C)					
	P38α	SRPK1	SRPK2	CLK1	DYRK1A	PIM1
BIRB 796 (14)	20.56	12.53	1.16	1.69	0.40	0.48
^a Thermal melting experiments were carried out using a Stratagene Mx3005p Real Time PCR machine (Agilent Technologies). SYPRO Orange (Molecular Probes) was added as a fluorescence probe, excitation and emission filters for the SYPRO-Orange dye were set to 465 nm and 590 nm, respectively. The temperature was raised with a step of 3 °C per minute from 25 °C to 96 °C, and fluorescence readings were taken at each interval. The observed temperature shifts, ΔT _m ^{obs} , were recorded as the difference between the transition midpoints of sample and reference wells containing protein without ligand in the same plate and determined by non-linear least squares fit. Experiments were performed in triplicate and data were analyzed as previously described. ³¹⁸						

Table 11: Analogue library 1 (215A-215N) T _m shifts as measured by DSF when bound to p38α and SRPK1. ^a				
Entry No.	Compound No.	R ¹	T _m Shift (°C)	
			P38α MAPK	SRPK1
1	215A	1-Naphthalene	15.80	2.92
2	215B	2-Naphthalene	10.64	8.55
3	215C	<i>o</i> -Toluene	13.08	1.34
4	215D	4-Ethoxyphenyl	7.59	8.02
5	215E	4-Fluorophenyl	12.25	7.13
6	215F	3,5-Bis(trifluoromethyl)phenyl	2.03	9.19
7	215G	4-(Benzyloxy)phenyl	4.56	5.75
8	215H	3,5-Dimethylphenyl	7.88	4.39
9	215I	5-Fluoro-2-methylphenyl	12.09	2.82
10	215J	3,4-Difluorophenyl	12.43	11.69
11	215K	Phenyl	12.30	3.91
12	215L	<i>p</i> -Toluenesulfonyl	0	0
13	215M	3-Methoxyphenyl	9.60	4.38
14	215N	<i>p</i> -Tolyl	11.40	4.71
15	BIRB 796 (14)		20.56	12.53
^a Thermal melting experiments carried out as detailed in Table 10.				

As a comparison, BIRB 796 (**14**) was also screened against the panel of kinases for its activity (see **Table 10**). A thermal shift (T_m shift) above 7 was indicative of good stabilization of binding with the protein. BIRB 796 (**14**) strongly stabilized p38 α and SRPK1, with T_m shifts of 20.6 and 12.5 °C respectively, however against the other kinases in the panel there was a very low binding affinity.

For analogue library 1 similar results were observed, with most compounds exhibiting some stabilizing effect when bound to p38 α and SRPK1, and very low affinities for SRPK2, PIM1, CLK1 and DYRK1A (for full data see supplementary information). **Table 11** illustrates the results of the DSF screening for analogue library 1 against p38 α and SRPK1. Heat mapping has been used to help illustrate the results obtained, with red for the high, white for the average, and green for the low T_m shift values.

From these results, a number of trends were observed. With regards to p38 α activity, the addition of polar groups seemed to reduce affinity of the ligand for p38 α . For instance, compounds **215D** and **215M**, with thermal shifts of 7.59 and 9.60 °C, respectively, had a much reduced affinity compared to the non-functionalized phenyl derivative **215K**, with a thermal shift of 12.30 °C (see **Figure 75**). Conversely, the polar 4-(benzyloxy)phenyl derivative **215G** had a lower thermal shift value of 4.56 °C, but this may have been due to unfavourable steric clashes or entropic changes due to movement of the benzyloxy-chain when bound to the kinase, reducing its binding affinity.

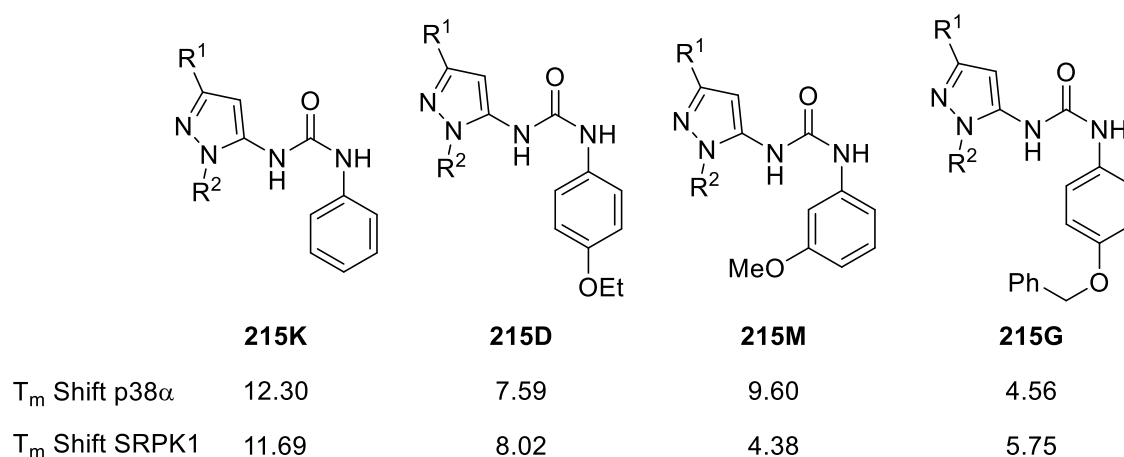
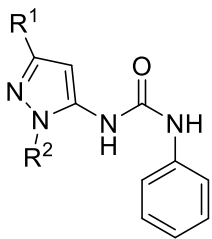
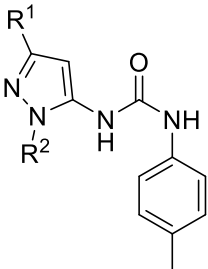
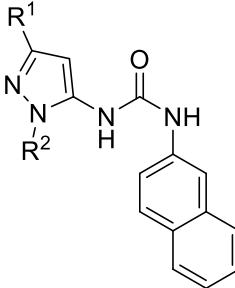


Figure 75: Analogue library 1. Thermal shift data (°C) when R^1 = *tert*-butyl, R^2 = phenyl, observing the effect of addition of polar groups on the degree of stabilization when bound to p38 α and SRPK1.

Despite increasing lipophilicity in 3,5-disubstituted compounds **215F** and **215H**, a characteristic that Regan *et al.* claimed to contribute to p38 α binding affinity,⁵⁰ when bound to p38 α there was a decrease in the thermal shift when compared to the fairly lipophilic **215K** and **215N** (see

Figure 76). However, it was found that when a large, lipophilic aromatic group was substituted onto the compound, such as with naphthalene based molecule **215B**, the stabilizing effect when bound to p38 α was significantly higher. This suggested that the positioning of the lipophilic groups at the *meta* positions of the phenyl ring could be important to destabilizing binding with p38 α .

			
	215K	215N	215B
T _m Shift p38 α	12.30	11.40	10.64
T _m Shift SRPK1	3.91	4.71	8.55

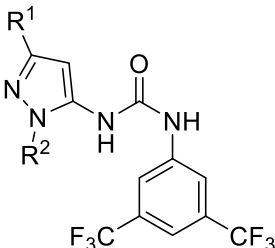
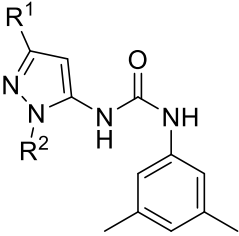
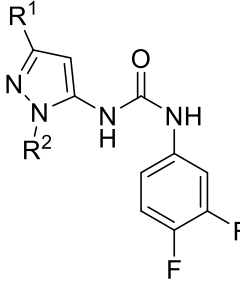
			
	215F	215H	215J
T _m Shift p38 α	2.03	7.88	12.43
T _m Shift SRPK1	9.19	4.39	11.69

Figure 76: Analogue library 1. Thermal shift data (°C) when R¹ = *tert*-butyl, R² = phenyl, observing the effect of lipophilicity and steric factors on T_m shift when bound to p38 α and SRPK1.

Looking at binding affinity with SRPK1, two interesting trends were observed. The first was the propensity of fluorine-containing substituents on the ring to enhance the binding affinity. For instance, the 3,4-difluorophenyl based urea **215J** had the strongest binding affinity for SRPK1 of all the tested molecules, with a thermal shift of 11.69 °C (see **Figure 76**). Despite offering no selectivity for SRPK1, exhibiting a high thermal shift when bound to p38 α as well, the stabilizing effect endowed by this compound when bound to SRPK1 presented itself as a good prospective lead for the design of the next library.

The 3,5-bis(trifluoromethyl) analogue **215F** also exhibited a high degree of stabilization for SRPK1, and a lower affinity for p38 α when compared to its protonated equivalent **215H** (see **Figure 76**). Thus it was decided that the potential of fluorinated analogues would be further explored in analogue library 2, with special attention to *meta*-substituted derivatives, to further assess the potential destabilization of binding with p38 α .

The second trend observed was that when an electron-donating substituent was in the *para* position of the ring, affinity of binding with p38 α was reduced (see **Figure 75**, **215D** and **215G**), while binding with SRPK1 appeared to exhibit a higher stabilizing effect. For instance, the 4-ethoxyphenyl compound **215D** had a higher stabilizing effect on SRPK1 than the unsubstituted phenyl **215K**, with thermal shifts of 8.02 and 3.91 °C, respectively. Though it should be noted that 4-(benzyloxy)phenyl (**215G**) had a lower thermal shift with SRPK1 of 5.75 °C; though, again, this may have been due to additional steric factors or ligand flexibility. Nevertheless, an increase in the electron density of the aromatic ring bound to the urea through the addition of small electron-donating substituents at the *para* position could be another avenue of investigation.

4.3.4. Conclusion.

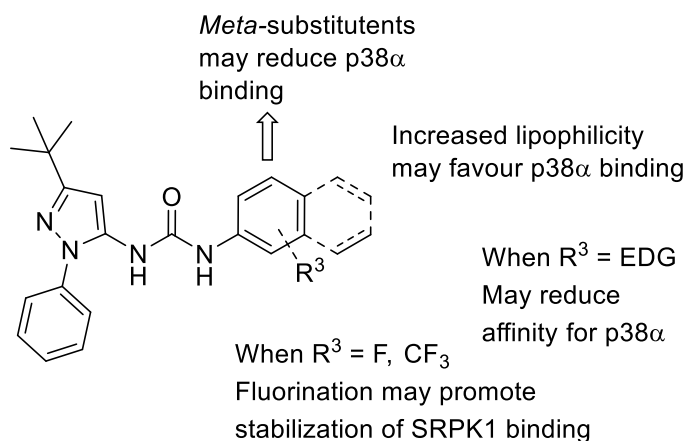


Figure 77: Inferred SAR from analysis of DSF data generated by analogue library 1.

Using the data collected from the biological studies of analogue library 1, it was decided that another library would be synthesized to focus on the 'hit' compound 3,5-bis(trifluoromethyl)phenyl urea **215F**. This compound exhibited an increase in stabilization when bound to SRPK1 whilst also dramatically reducing affinity for p38 α .

From the biological assay, an inferred structure-activity relationship (SAR) was assembled (**Figure 77**) exploring how substitution on the aromatic ring might have affected binding to p38 α and SRPK1. It was decided that development of analogue library 2 would continue to probe the characteristics found to be conducive to reducing p38 α affinity, with additional exploration of the potential to increase SRPK1 stabilization through the use of *meta*-substituted fluorinated aromatics. Hence, in addition to the 3,5-bis(trifluoromethyl)phenyl, it was decided that 3,5-difluorophenyl ureas would be an interesting pharmacophore to explore.

4.4. Analogue library 2. Taking the ‘hit’ forward.

A second library of compounds was designed to probe the role of the pyrazole substituent in selectivity and binding, whilst retaining those characteristics found to be most promising for SRPK1 activity, most notably, the incorporation of fluorinated aromatics.

4.4.1. An introduction to fluorine. The C-F bond as a tool in medicinal chemistry.

The carbon-fluorine single bond is one of the strongest known, with a bond strength only surpassed by the silicon-fluorine bond (485 and 582 kJ mol⁻¹, respectively¹⁰¹). This is due to silicon being slightly more electropositive and polarizable than carbon. The dipole of the carbon-fluorine bond is so extreme that the bond can be considered to have more electrostatic than covalent character. Hence this functionality tends to interact intermolecularly through electrostatic interactions, specifically dipole-dipole or point charge-dipole interactions. Time-dependent interactions, including ion-induced dipole, dipole-induced dipole and dispersion interactions however are not as common due to the low polarizability of the bond.³²⁸ The fluorine in the carbon-fluorine bond also has suppressed nucleophilicity compared to other halogens, and so will tend not to act as a HBA in solution, though such interactions have been observed in the gas phase and are possible when there is an excess of proton donors present.^{328,329}

Fluorine is widely used in medicinal chemistry as a method to improve the pharmacokinetics (PK) of molecules, to reduce molecular susceptibility to metabolism and as probes to investigate the metabolic stability of certain functional groups in lead development.

The size of fluorine makes it a good candidate to exchange with protons and oxygens when investigating their potential roles in ligand-kinase binding. For instance, exchange of a fluorine for a proton can help elucidate its significance while conserving the steric environment. This exchange can result in significant changes to the electronic properties of the molecule, for example, lowering the pK_a of neighbouring functional groups, which in some instances can increase solubility and improve PK.³³⁰

Exchange of fluorine for oxygen does not significantly affect the electronic properties of a structure, as both are very electronegative atoms, but can be used to probe the significance of

π -bonding and proton acidity. For example, exchange of a carbon-oxygen double bond in favour of a carbon-fluorine single bond, or a CF_2 group, necessitates a change in the hybridization state of carbon. Exchange of a carbon-oxygen single bond, like in C-OH, for a C-F group, removes the acidic proton and can help probe potential significance as a HBD. This method can also be used to investigate the relative importance of hydrogen bonding versus polarisation for a C-OH unit, exploiting the 'polar hydrophobic'³²⁸ nature of C-F relative to C-OH; as fluorine reduces polarizability and increases hydrophobicity.³²⁹

As a tool to improve the PK of a drug candidate, not only does fluorine improve solubility and hence absorption and distribution, but it can also affect drug metabolism and excretion. The excretion of drug molecules from the body is very important to prevent the build-up of foreign toxins in cells and fatty-tissues. Foreign compounds that cannot be assimilated into normal pathways of excretion are metabolized to make them more soluble, often through addition of polar groups, or conjugation with more hydrophilic groups to enable excretion through urine or bile.^{331–333}

The extent of metabolism can be predicted from the physicochemical characteristics of the molecule, including lipophilicity, pK_a , molecular weight and the sites open to potential metabolic modification. Since the carbon-fluorine bond is so strong, exchange of a hydrogen for a fluorine can block metabolism as well as increase polarity. Additionally, fluorine can inductively reduce electron density of groups to diminish the extent of oxidation. Hence, *para*-fluoro substitution of electron rich aromatic compounds is a common method to protect the ring from oxidative enzymes, whilst retaining the steric environment.

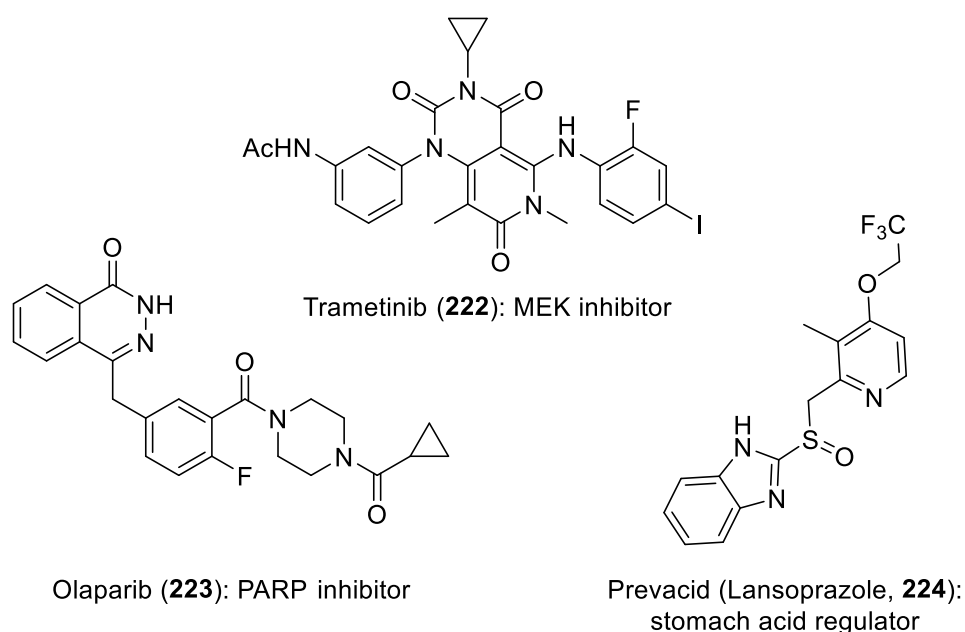


Figure 78: Fluorine containing drugs; Trametinib (222), Olaparib (223) and Prevacid (224).^{334,335}

Examples of fluorine-containing drugs are detailed in **Figure 78**, including Trametinib (**222**), a MEK (MAPK/ERK kinase) inhibitor used in the treatment of melanomas with BRAF^{V600E/K} mutations. Installation of the 2-fluoroaniline substituent increased hydrophobicity and antitumor potency 4-fold.³³⁴ Olaparib (**223**), a poly(ADP-ribose) polymerase (PARP) inhibitor, developed for treatment of numerous cancers when combined with DNA-damaging agents. Introduction of fluorine on the central benzene ring enhanced cellular activity whilst maintaining potency. Additionally it was speculated that repulsive electrostatic interactions between the fluorine and the C-3 carboxyl group restricted rotation, lowering the molecular entropy to enhance cell permeability of the compound.³³⁵ And the trifluoromethyl-containing Prevacid (**224**) is a 'proton-pump inhibitor' which reacts with acid in the stomach to undergo rearrangement to a sulfenamide, which then binds irreversibly to the K⁺/H⁺ ATPase via a cysteine residue.³³⁴

With the number of new and approved drugs containing fluorine increasing from an estimated 20% in 2010³³⁶ to approximately 30% in 2016, the impact of fluorine upon medicinal chemistry has been dramatic, especially as a tool in lead optimization.³³⁴

4.4.2. Pyrazole modification.

Regan *et al.* found early on in their hit-to-lead development towards BIRB 796 (**14**) that substitution of a phenyl group at the 1*N*-pyrazole position could improve ligand binding affinity 40-fold, when compared to a methyl group in the same position.⁵⁰ X-ray co-crystallization studies identified that the phenyl ring conducted important lipophilic ligand-kinase interactions and acted as a 'water shield' for the urea moiety, protecting it from solvation and enabling the urea oxygen and NH to act as HBA and HBD with aspartic acid and glutamic acid residues in the allosteric binding pocket. Regan *et al.* deemed these interactions essential for the strong binding of the inhibitor, and to stabilize the DFG-out conformation.⁵⁰

These studies implied that altering the phenyl ring may result in dramatic changes to p38 α binding affinity. Hence, for analogue library 2, the potential of 3,5-bis(trifluoromethyl)phenyl (**F**) and 3,5-difluorophenyl (**O**) derived ureas were explored with a range of 1*N*-pyrazole substituents, as illustrated in new scaffold **225**. Changes to R² concentrated on the importance of steric bulk and changes to the lipophilicity of the phenyl ring, in addition to the importance of the aromatic group for SRPK1 activity, with analogues exchanging the phenyl ring in favour of an aliphatic group.

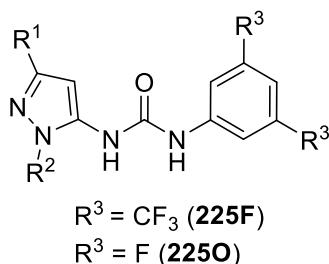


Figure 79: Analogue library 2 scaffold, with a fluorine-containing 3,5-disubstituted phenyl ring, varying R^1 and R^2 substituents on the pyrazole.

Another moiety of interest was the *tert*-butyl group of the pyrazole (**225**, R^1), another consistent feature in Regan *et al.*'s development of a suitable clinical candidate.⁵⁰ The group found even small alterations resulted in dramatic changes to activity, with reduction in size to a methyl group causing complete loss of activity and addition of polar groups reducing binding affinity. They inferred the importance of a lipophilic unit at 3-C to enable p38 α binding, with X-ray co-crystallization studies used to confirm that the *tert*-butyl group occupied a Phe pocket vacated upon binding with BIRB 796 (**14**), helping to maintain the DFG-out conformation (see **Chapter 4.1**).⁵¹ It was decided that only slight changes should be made for analogue library 2, with further investigation to be considered in light of any interesting results from this screening iteration.

In order to generate a new analogue library incorporating all these features, a new pyrazole precursor subset library was synthesized.

4.4.3. Synthesis of pyrazole subset library.

Using the same retrosynthetic approach as described previously, 3-oxopentanitrile derivatives were reacted with substituted hydrazines or hydrazine hydrochloride salts to prepare the desired precursor subset.

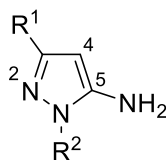
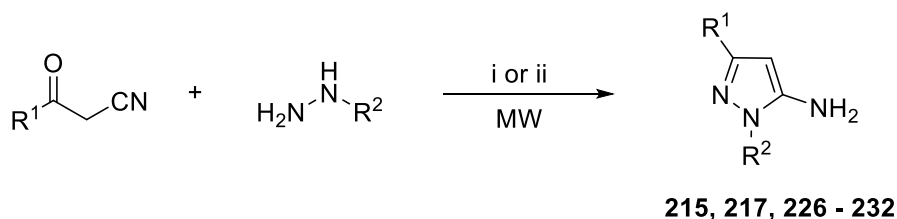


Figure 80: Pyrazole model for the design of a new subset library.

For the hydrazine free-base derived reactions, conditions were employed as previously stated, with microwave-assisted heating at 120 °C for 40 minutes in toluene-glacial AcOH (5:1), and purification by flash column chromatography. For reactions adopting the hydrazine

hydrochloride salt precursor, the nitrile and hydrazine salt were reacted at 130 °C for 20 minutes using microwave-assisted heating in a sealed vessel, in the presence of a catalytic amount of conc. HCl in ethanol. The hydrazine salt tended to be used in slight excess to promote complete reaction and the excess was easily removed through a basic work-up to give the pure product, usually without the need for further purification.

All members of the pyrazole subset library were isolated and carried forward as the free base, and the synthetic results are shown in **Table 12**. For compound **229** (entry 6), 1,3-di-*tert*-butyl-1*H*-pyrazol-5-amine, the mixture was heated overnight at reflux. This was because it had previously been reported that conducting the reaction in a closed vessel could result in an explosive rupture of the tube⁵² due to a build-up of pressure, possibly as a result of the production of isobutene gas.³¹⁷



Scheme 144: Synthesis of pyrazole subset library. Reaction conditions: i) toluene-AcOH (5:1); ii) MeOH, cat. conc. HCl. (**Table 12**).

Table 12: Synthetic results of pyrazole subset library.				
Entry No.	Compound No.	R ¹	R ²	Yield (%)
1	215	<i>tert</i> -Butyl	Phenyl	91 ^a
2	217	<i>tert</i> -Butyl	4-Methylphenyl	83 ^b
3	226	<i>tert</i> -Butyl	Methyl	95 ^a
4	227	<i>tert</i> -Butyl	4-Fluorophenyl	88 ^b
5	228	<i>tert</i> -Butyl	4-Nitrophenyl	48 ^a
6	229	<i>tert</i> -Butyl	<i>tert</i> -Butyl	61 ^{b,c}
7	230	<i>tert</i> -Butyl	4-Bromophenyl	58 ^b
8	231	Phenyl	Methyl	50 ^{a,d}
9	232	Phenyl	Phenyl	91 ^{a,d}
Microwave-assisted reaction conditions: A mixture of 4,4-dimethyl-3-oxopentanitrile (220) (1 equiv.) and ^a hydrazine (1.01 equiv.) in toluene-AcOH (5:1) were irradiated at 120 °C (initial power 100 W) for 40 minutes; or ^b hydrazine.HCl (1.01 equiv) in EtOH with catalytic conc. HCl was irradiated at 130 °C (initial power 200 W) for 20-30 min. Reaction times refer to hold times at the given temperature through modulation of the initial power.				
^c Reflux conditions, 18 h reaction time.				
^d Using benzoylacetone nitrile.				

From the results in **Table 12**, it was clear that the use of the hydrazine free-base or the hydrochloride salt did not adversely impact the isolated yields, which overall were very high. However there were some compounds which were problematic in their synthesis and isolation.

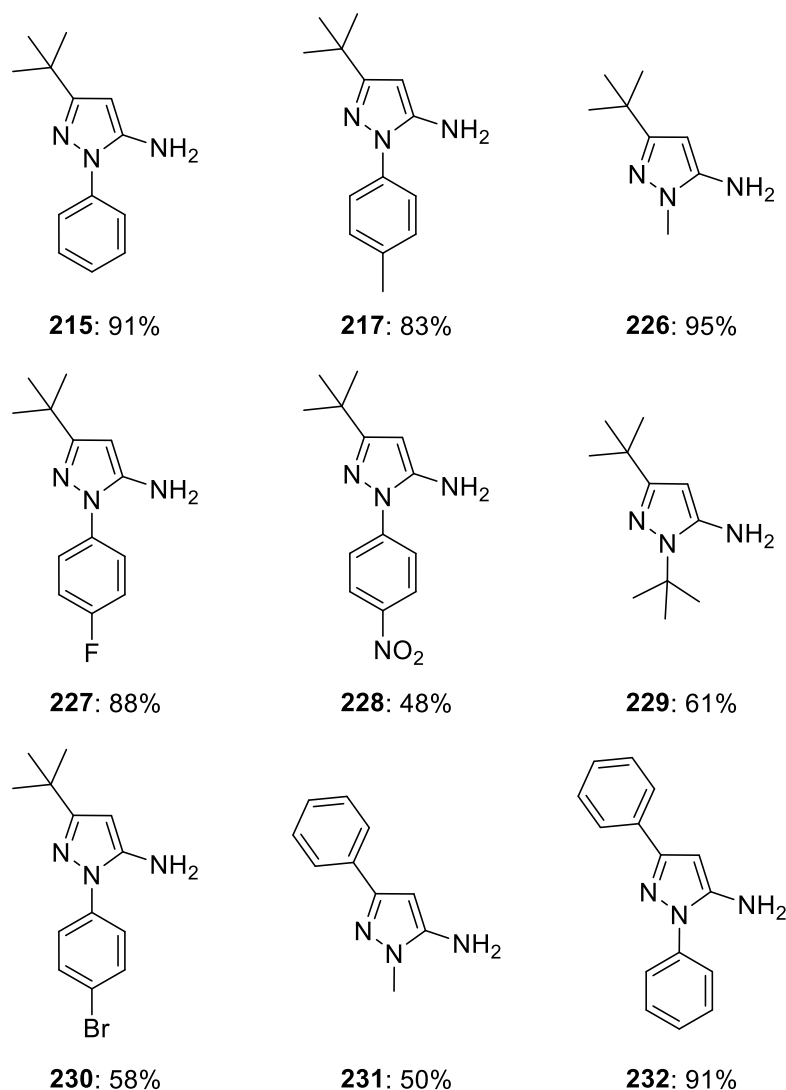
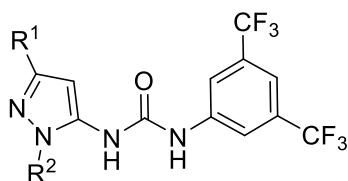


Figure 81: Pyrazole subset library. Yields given as shown in **Table 12**.

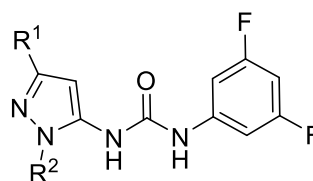
The synthesis of **228** and **230** (entries 5 and 7), under the chosen reaction conditions, did not go to completion, resulting in residual nitrile in the crude reaction mixture which caused complications during flash column chromatography purification. Extending the reaction time (overnight reflux towards **229**) and using a large excess of the hydrazine did not improve the conversion. The reason for this poor reactivity was most likely due to the electron-withdrawing group on the phenyl hydrazine, as both the 4-nitro and 4-bromophenyl substituents would reduce the nucleophilicity of the hydrazine.

For **231**, the yield was also quite low, but this was due to an accidental excess of the hydrazine being used, resulting in co-elution during purification by flash column chromatography. Recrystallization of the crude material afforded the final product in 50% yield.

4.4.4. Synthesis of analogue library 2.



217F, 226F - 232F



215O, 217O, 226O - 232O

Table 13: Synthesis of analogue library 2.^a

Entry No.	Compound No.	R ¹	R ²	Yield (%) ^b
1	217F	CMe ₃	<i>p</i> -Tolyl	40 ^c
2	226F	CMe ₃	Methyl	30 ^c
3	227F	CMe ₃	4-Fluorophenyl	75
4	228F	CMe ₃	4-Nitrophenyl	35 ^c
5	229F	CMe ₃	<i>tert</i> -Butyl	72
6	230F	CMe ₃	4-Bromophenyl	59
7	231F	Phenyl	Methyl	73
8	232F	Phenyl	Phenyl	65 ^c
9	215O	CMe ₃	Phenyl	49 ^c
10	217O	CMe ₃	<i>p</i> -Tolyl	64
11	226O	CMe ₃	Methyl	78 ^c
12	227O	CMe ₃	4-Fluorophenyl	40 ^c
13	228O	CMe ₃	4-Nitrophenyl	25 ^d
14	229O	CMe ₃	<i>tert</i> -Butyl	69 ^c
15	230O	CMe ₃	4-Bromophenyl	54 ^c
16	231O	Phenyl	Methyl	85 ^c
17	232O	Phenyl	Phenyl	70 ^c

^a Reaction conditions: 1.1 equivalents of 5-aminopyrazole and the corresponding isocyanate was stirred at RT for 20 min in CH₂Cl₂.

^b Isolated yield after evaporation *in vacuo* and trituration with light petroleum .

^c Yield after recrystallization from hot methanol.

^d Reaction was stirred at RT for 18 h

Using 3,5-bis(trifluoromethyl)phenyl (**F**) isocyanate and 3,5-difluorophenyl (**O**) isocyanate, synthesis of analogue library 2 was carried out as described previously, by stirring a solution of the respective 5-aminopyrazole and isocyanate in CH₂Cl₂ for 20 minutes at room temperature, followed by product isolation by trituration and recrystallization where necessary. The results of the synthesis of analogue library 2 are detailed in **Table 13**.

Overall the reactions yields were far lower than those of analogue library 1, though this was mostly due to problems with product purification. As previously mentioned (**Chapter 4.2.2**) the fluorinated isocyanates were viscous oils and this complicated trituration if any unreacted isocyanate remained. It was also necessary for most of the ureas to be recrystallized as, unlike for library 1, trituration was seldom sufficient to remove all impurities.

In particular, isolation and purification of the 4-nitrophenyl and 4-bromophenyl derivatives, **228F**, **228O**, **230F** and **230O**, were problematic. Poor reproducibility of reactions, low reactivity and poor stability of products became prevalent issues, especially when reacting the respective 5-aminopyrazoles with 3,5-difluorophenyl isocyanate. For instance, when reacting **228** with 3,5-difluorophenyl (**O**) isocyanate only starting material was isolated upon trituration after stirring at room temperature for 20 minutes. An overnight reaction was necessary for product formation in these cases, with a 25% yield of **228O** achieved after recrystallization (**Table 13**, entry 13).

Isolation of 3,5-difluorophenyl derived urea **230O** was also extremely problematic. When first attempted the reaction gave a reasonable yield with no substantial issues, however reproduction of results was inconsistent, with reaction mixtures necessitating isolation by flash column chromatography and additional trituration to provide enough compound for biological evaluation. Efforts to further purify **230O** by recrystallization only returned an oily residue, and so a sample was submitted for biological testing following ¹H NMR spectroscopic analysis without prior recrystallization.

Structural characterization of these products was carried out by ¹H and ¹³C NMR spectroscopic analysis. In the ¹H NMR spectrum, a downfield shift of the pyrazole 4-CH proton resonance was characteristic of urea formation, and differentiation of resonances in the two aromatic rings was facilitated by analysis of fluorine-proton and fluorine-carbon splitting patterns. Identification of resonances in the ¹³C spectrum for the 3,5-bis(trifluoromethyl)phenyl (**F**) and the 3,5-difluorophenyl (**O**) rings were unambiguously clarified by carbon-fluorine splitting.

For the 3,5-difluorophenyl rings, interesting splitting patterns were noted, especially for the 2,6-CH carbons, which exhibited second order coupling with the fluorine. For example, *N*-(3,5-

difluorophenyl)-*N'*-(3-(*tert*-butyl)-1-(*p*-tolyl)-1*H*-pyrazol-5-yl)urea (**2170**) featured an AA'XX' spin system, and was observed upon ^{13}C NMR spectroscopic analysis (see **Figure 82**). This splitting pattern arose as a result of the two fluorines of the ring being chemically equivalent but magnetically inequivalent,³³⁷ resulting in the unusual resonance at δ_{c} 100.9 ppm correlating to the 2,6-CH aromatic carbons. This splitting pattern was consistently observed in all ^{13}C NMR spectra generated from the **O**-derived urea compounds.

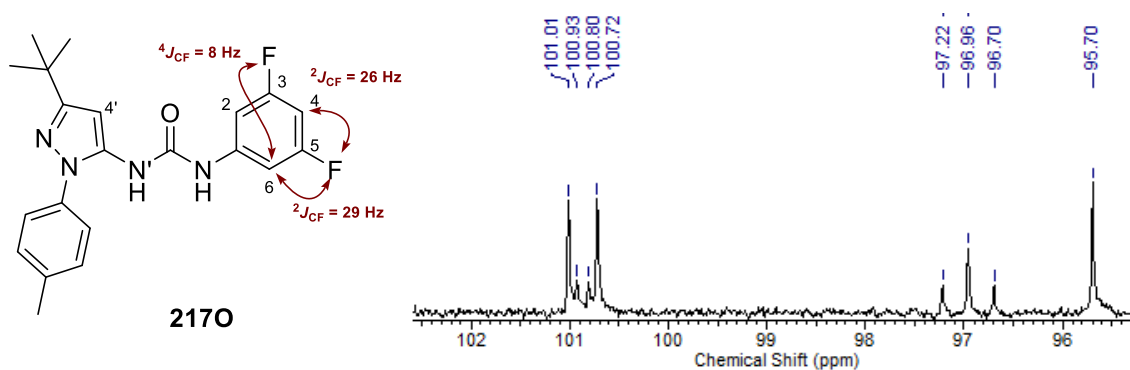


Figure 82: ^{13}C NMR spectrum (δ_{c} 103 - 95 ppm) of *N*-(3,5-difluorophenyl)-*N'*-(3-(*tert*-butyl)-1-(*p*-tolyl)-1*H*-pyrazol-5-yl)urea (**2170**), illustrating the second order C-F coupling.

4.5. Biological evaluation of analogue library 2.

4.5.1. DSF results from analogue library 2.

Analogue library 2 was screened against the same panel of kinases as investigated previously, with calculation of the thermal shifts conducted using identical DSF methods. Similar to library 1, there was minimal ligand binding with SRPK2, CLK1, DYRK1A and PIM1A (see supplementary information for full data), however, there were some interesting changes in the thermal shifts observed upon ligand binding to p38 α and SRPK1. **Table 14** contains the thermal shift data for all 3,5-bis(trifluoromethyl)phenyl (**F**) derived ureas and **Table 15** contains the data for all 3,5-difluorophenyl (**O**) derived ureas when bound to p38 α and SRPK1.

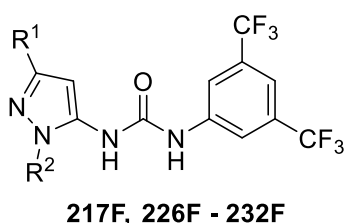
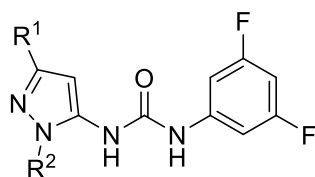


Table 14: DSF results for analogue library 2, compounds 217F, 226F-232F . ^a					
Entry No.	Compound No.	R ¹	R ²	T _m Shift (°C)	
				P38 α MAPK	SRPK1
1	217F	CMe ₃	<i>p</i> -Toluene	1.17	9.95
2	226F	CMe ₃	Methyl	1.24	11.80
3	227F	CMe ₃	4-Fluorophenyl	0.82	11.81
4	228F	CMe ₃	4-Nitrophenyl	1.54	-0.61
5	229F	CMe ₃	<i>tert</i> -Butyl	0.49	1.15
6	230F	CMe ₃	4-Bromophenyl	0.70	12.25
7	231F	Phenyl	Methyl	1.86	2.57
8	232F	Phenyl	Phenyl	0.81	1.72
^a Thermal melting experiments carried out as detailed in Table 10 .					

The first very noticeable aspect of these findings compared to the thermal shift data collected for analogue library 1 (**Table 11**) was that, in general, the affinity of the compounds for p38 α appeared to be greatly reduced, whilst the stabilizing effect upon binding to SRPK1 appeared to

be significantly higher; as can be seen through comparison of the heat maps between **Tables 11, 14 and 15**.



215O, 217O, 226O - 232O

Table 15: DSF results for analogue library 2, compounds 215O, 217O, 226O - 232O . ^a					
Entry No.	Compound no.	R ¹	R ²	T _m Shift (°C)	
				P38α MAPK	SRPK1
1	215O	CMe ₃	Phenyl	5.18	13.72
2	217O	CMe ₃	<i>p</i> -Toluene	6.48	14.82
3	226O	CMe ₃	Methyl	2.84	6.37
4	227O	CMe ₃	4-Fluorophenyl	5.33	12.62
5	228O	CMe ₃	4-Nitrophenyl	7.51	14.15
6	229O	CMe ₃	<i>tert</i> -Butyl	0.10	0.14
7	230O	CMe ₃	4-Bromophenyl	5.10	12.72
8	231O	Phenyl	Methyl	0.22	1.34
9	232O	Phenyl	Phenyl	2.59	2.27
^a Thermal melting experiments carried out as detailed in Table 10 .					

Regarding comparison of the two branches of analogue library 2, and the contrasting heat maps produced from the thermal shift data of the compounds, there were some notable differences upon altering the phenyl urea substituents.

The 3,5-difluorophenyl (**O**) ureas in **Table 15** exhibited, overall, a much higher degree of stabilization for binding with SRPK1, but appeared to result in some low to moderate stabilization when bound to p38α. When compared with the thermal shift data for all the 3,5-bis(trifluoromethyl)phenyl (**F**) ureas (**Table 11**, entry 6 and **Table 14**), the larger fluorinated substituents appeared to have a markedly more significant destabilizing effect when bound to p38α, whilst seeming to promote stabilization of binding with the SRPK1 kinase to a similar degree as the **O**-urea series.

Reviewing the pyrazole modifications, there were some changes which appeared to considerably affect binding to both kinases, though with varying degrees of severity. Foremost, the most significant loss of binding stabilization was when the 3C-pyrazole *tert*-butyl group (R^1) had been exchanged for a phenyl group; **231F**, **232F**, **231O** and **232O** all demonstrated thermal shifts below 3 °C for SRPK1 and p38 α (see **Figure 83**).

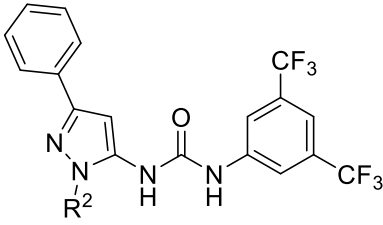
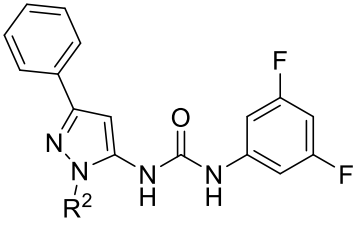
							
	R^2	P38 α T_m	SRPK1 T_m		R^2	P38 α T_m	SRPK1 T_m
231F	Methyl	1.86	2.57	231O	Methyl	0.22	1.34
232F	Phenyl	0.81	1.72	232O	Phenyl	2.59	2.27

Figure 83: Analogue library 2. Thermal shift data (°C) for compounds with reduced binding affinity when R^1 = phenyl.

In Regan *et al.*'s original findings they stated that the *tert*-butyl group at the pyrazole 3-position was essential to maintain the DFG-out conformation of p38 α , as it occupied a hydrophobic pocket vacated by a phenylalanine residue upon rearrangement (discussed in **Chapter 4.1**).⁵¹ Therefore, it could be concluded that a phenyl group cannot successfully sustain the same lipophilic interactions as the bulky *tert*-butyl group in the binding pocket. This would infer a conserved binding pocket in this region for p38 α and SRPK1, and suggested that retaining the *tert*-butyl group could also be important for SRPK1 activity. Further investigation of this binding pocket in SRPK1 could be conducted once more is understood about the ligand-binding of these models, for instance, through exploring the use of isopropyl or ethyl groups, or fluorinated variants.

The thermal shift data generated from the compounds in which the 1*N*-pyrazole phenyl ring (R^2) was exchanged for an alkyl group, with retention of the 3C-*tert*-butyl group, proved to be quite interesting. From the hypotheses of Regan *et al.* on the significance of the phenyl 'water shield',⁵⁰ it was expected that there would be a significant loss of binding affinity upon substitution of a methyl group, however this was not found to be the case (see **Figure 84**).

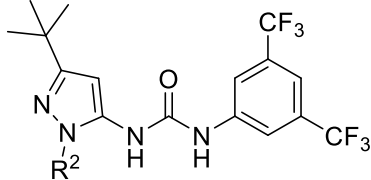
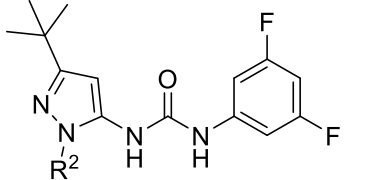
							
	R ²	P38α T _m	SRPK1 T _m		R ²	P38α T _m	SRPK1 T _m
226F	Methyl	1.24	11.80	226O	Methyl	2.84	6.37
231F	<i>tert</i> -Butyl	0.49	1.15	231O	<i>tert</i> -Butyl	0.10	0.14

Figure 84: Analogue library 2. Thermal shift data (°C) when R² = alkyl group when bound to p38α and SRPK1.

Though compounds **226F** and **226O** both exhibited very low thermal shifts when bound to p38α, these were not dissimilar to the other compounds of analogue library 2. Interestingly, for the 3,5-bis(trifluoromethyl)phenyl urea **226F**, the exchange actually increased the stabilization of binding to SRPK1 with a thermal shift of 11.80 °C, compared to when R² = *p*-toluene (T_m = 9.9 °C) (**Table 14**, entry 1).

This trend was not emulated by 3,5-difluorophenyl urea **226O**, which had only a moderate stabilization effect when bound to SRPK1 (see **Figure 84**). X-ray co-crystallographic studies of these compounds when bound to SRPK1 would help to elucidate this curious result, and potentially enable comparisons to be drawn between the hydrogen bonding networks present when SRPK1 and p38α were bound to this molecular pharmacophore.

Conversely, when the 1*N*-pyrazole position (R²) was substituted with a *tert*-butyl group, a dramatic reduction in binding affinity was observed for both incarnations of the urea in analogue library 2 (see **Figure 84**, **231F** and **231O**). This implied that steric bulk at the 1*N*-pyrazole position was not conducive to support stabilization of the complex when bound to p38α or SRPK1.

Looking at the effect of substituents on the phenyl ring at the pyrazole 1*N*-position in analogue library 2, when R² was 4-fluorophenyl (see **Figure 85**, **227F** and **227O**), the compounds appeared to exhibit a much higher degree of stabilization when bound to SRPK1. It was noted that 3,5-difluorophenyl urea **227O** still appeared to demonstrate moderate affinity for p38α; this was, as mentioned, a consistent trend for the 3,5-difluorophenyl series.

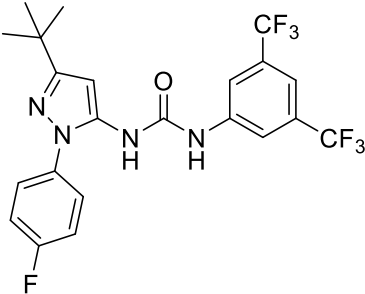
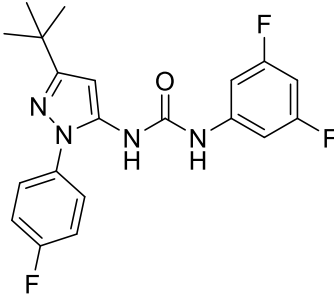
					
P38α T _m	SRPK1 T _m	P38α T _m	SRPK1 T _m		
227F	0.82	11.80	227O	5.33	12.62

Figure 85: Analogue library 2. Thermal shift data (°C) when R² = 4-fluorophenyl when bound to p38α and SRPK1.

The *para*-toluene 3,5-difluorophenyl urea derivative **217O** also resulted in a higher thermal shift when bound to SRPK1 than its trifluoromethyl counterpart **217F**, with thermal shift values of 14.82 and 9.95 °C respectively (**Figure 86. Table 14**, entry 1 and **Table 15**, entry 2). Therefore it may be worth investigating this aryl *para*-substituent further, either by substituting with larger alkyl groups or some fluorinated groups.

	R	P38 α T _m	SRPK1 T _m		R	P38 α T _m	SRPK1 T _m
217F	Methyl	1.17	9.95	217O	Methyl	6.48	14.82
228F	NO ₂	1.54	-0.61	228O	NO ₂	7.51	14.15
230F	Br	0.70	12.25	230O	Br	5.10	12.72

Figure 86: Analogue library 2. Thermal shift data (°C) when altering the *para*-phenyl substituent from slightly electron donating (Me) to electron withdrawing (NO₂).

An interesting change in activity between the different urea derivatives was seen with the 4-nitrophenyl pyrazole series (**228**). The 3,5-difluorophenyl urea analogue **228O** had a very high degree of stabilization for SRPK1, with a thermal shift of 14.15 °C and a marginal affinity for p38α (see **Figure 86. Table 15**, entry 5), whilst the 3,5-bis(trifluoromethyl)phenyl analogue **228F** exhibited a low affinity for p38α (T_m shift = 1.54 °C), and a negative thermal shift with SRPK1 (**Table 14**, entry 4). A negative value could be due to the compound binding preferentially to the

unfolded state of the protein or may indicate that the fluorescence of the compound had interfered with the fluorescence of the dye. Nevertheless, this change in activity was very interesting as these were the only compounds of the series which exhibited such dissimilar behaviour upon switching the urea phenyl ring.

One compound of particular interest was the 3,5-bis(trifluoromethyl)phenyl 4-bromophenyl pyrazoyl urea **230F**. This compound not only demonstrated a high affinity for SRPK1 and low affinity for p38 α (**Figure 86**), but also showed some binding affinity for the other kinases tested in the DSF assay: CLK1A and PIM1A, with thermal shifts of 19.53 and 11.48 °C respectively (see supplementary information). This was of particular interest as none of the other compounds exhibited this stabilizing effect. In order to confirm the apparent activity of **230F**, further biological tests could be carried out to ascertain why this activity was exhibited.

4.5.2. Conclusion.

Overall, from the thermal shift data heat map generated from analogue library 2, it could be observed that there was a much higher degree of stabilization for these compounds when bound to SRPK1 than observed for analogue library 1. Additionally, the affinity of binding for p38 α had been dramatically decreased, with most compounds in analogue library 2 exhibiting moderate to low thermal shifts when bound to p38 α . Therefore, from this data, it can be inferred that the BIRB 796 (**14**) chemotype has indeed been reengineered to favour a new target, with selective improvement in binding with SRPK1 and a dramatic reduction in binding affinity for the p38 α kinase.

Through fluorination of the urea aromatic ring, significant stabilization was observed when the molecules were bound to SRPK1. With further investigation, it was found that the size or nature of the fluorine substituents seemed to be an important factor in determining the extent of stabilization when bound to p38 α , with the larger 3,5-bis(trifluoromethyl)phenyl ureas exhibiting reduced affinity for p38 α compared to the 3,5-difluorophenyl ureas.

The potential of the bulky trifluoromethyl substituent, sometimes referred to as being “slightly larger” than an isopropyl group,³³⁰ may be worth further investigation. For instance, exploring the potential of isopropyl or CHF₂ substitution, or some larger substituents at the 3,5-positions, symmetrical and unsymmetrical, to further probe this region of chemical space.

Compound **227F** was determined to be the compound with the most promise for further development in the design of an SRPK1 probe. With a very low binding affinity for p38 α , and a high degree of stabilization when bound to SRPK1, the poly-fluorinated **227F** also presented itself as the most pharmacokinetically viable candidate (see **Figure 85**).

Bearing this 'lead compound' in mind, other potential aspects which could warrant further investigation include the importance of the 'water shield' 1*N*-pyrazoyl phenyl group (R²), and whether there is a similar hydrogen bonding network present when the urea scaffold is bound into SRPK1 as with p38 α . Also, exploring the potential of the *para*-substitution on the 1*N*-pyrazoyl phenyl group, including extending the group further into chemical space, with more varied substituents and the potential of heteroatoms and heteroaromatic rings.

4.6. Future perspectives.

In order to progress this work, the results of the thermal shift data needs to be verified through additional biological tests to validate the conclusions that have been drawn. From these additional tests, a better understanding of the compound pharmacodynamics (PD) with SRPK1 would be established, including the mode of binding, amino acids involved and the kinetics of binding; all insights which would help in the design of a third library.

Pharmacokinetics (PK) are extremely important to consider when designing any biological probe. For the probe to be useful *in vivo* it must be stable to metabolism in order to reach the target of interest. Hence the design of a new library should also concentrate on developing compounds with more drug-like properties, with an emphasis on improving the potential ADME characteristics of the compounds.

4.6.1. Pharmacodynamics and verifying biological interactions.

In order to verify the DSF results, there are a number of additional biological screens that would be beneficial before progressing in the design of a new library. For instance, isothermal titration calorimetry (ITC) is a method that can be used to determine the enthalpy of binding. This is done by measuring the heat released on binding a ligand to a protein against a blank sample.³³⁸ This method is widely used to validate initial hits, and the comparison of ITC values with the library DSF results could help direct efforts to further optimize binding.

NMR spectroscopic studies could also be used to observe the strength of ligand binding. Periodic spectra would be run of the target protein and ligand mixed in solution, with slow addition of a competitive ligand of known binding affinity. This method could also be used to help confirm whether the compounds of libraries 1 and 2 bind allosterically to SRPK1 and p38 α , through use of ATP as the competitive ligand.³³⁸

X-ray co-crystallization studies of a ligand-bound protein can be extremely beneficial in determining the SAR of a binding ligand. This technique can be used to determine where the ligand binds, what residues are important for that binding, whether it binds allosterically and if it is ATP- or non-ATP-competitive. It can also be used to determine if there are any amino acid residues in the binding pocket which could be used to improve binding, or any additional space which could be employed to improve kinase selectivity and binding affinity.

This method of investigation would be ideal to identify the best potential course of investigation for this compound series, as it would help to qualify the hypotheses already formulated. For instance, if increasing bulk at the 3- and 5-positions of the urea aromatic ring would be beneficial when binding with SRPK1, if extension of the pyrazole 1*N*-aromatic substitution might utilize additional interactions inside or outside of the pocket, and if the urea moiety plays a similar, important role when binding to SRPK1 as with p38 α in the BIRB 796 scaffold (see **Figure 87**).

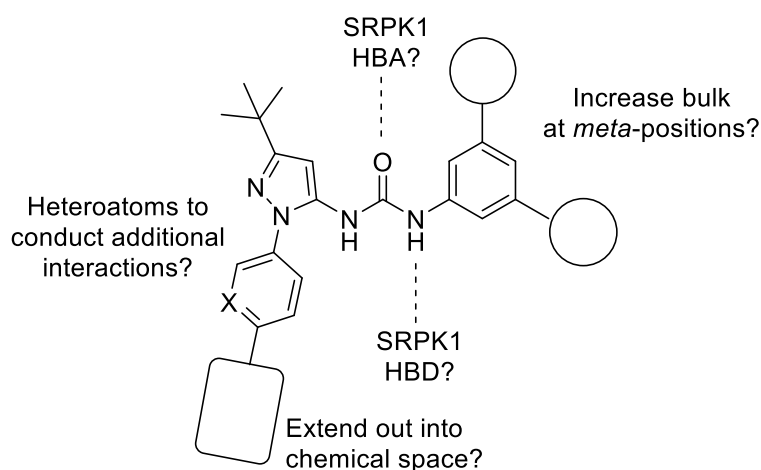


Figure 87: Areas of potential PD for the new *N,N'*-diaryl urea pharmacophore with SRPK1.

Still, more importantly, co-crystallization would help to confirm if the compounds of analogue libraries 1 and 2 are binding allosterically, in a similar mode to BIRB 796 (**14**), or if they are ATP-competitive compounds.

Recent work by Morooka *et al.* on the dual SRPK1 and CK2 inhibitor SRPIN340 (**233**) has included the solved X-ray co-crystal structure of this small molecule inhibitor bound to SRPK1 in the ATP-binding pocket.³³⁹ Extensive hydrophobic interactions between the inhibitor and the ATP-binding cleft of SRPK1 were identified and essential hydrogen bonding interactions were noted between the carbonyl oxygen and the kinase. Additionally, they identified that the trifluoromethyl group of **233** had induced a ‘flip’ of the main peptide chain from its position in the un-ligated kinase, and the CF₃ group occupied the region that had been vacated. It was identified that as a consequence of the ‘flip’, an additional hydrogen bonding interaction was facilitated between two peptide chains of the kinase, potentially stabilizing the binding of SRPIN340 (**233**) in the ATP-pocket.

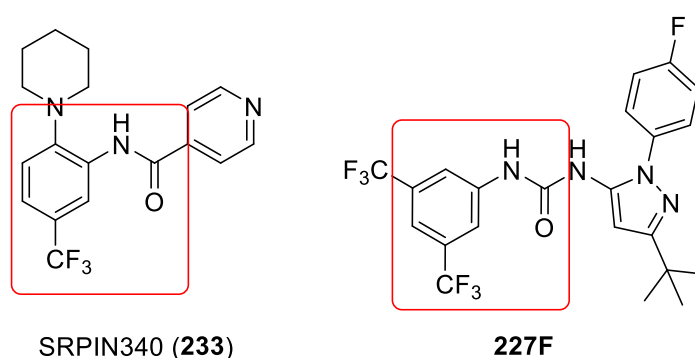


Figure 88: SRPK1 inhibitor SRPIN340 (**233**) and lead compound **227F**.

Figure 88 illustrates the important trifluoromethyl and carbonyl groups of SRPIN340 (**233**). Upon visual comparison with lead compound **227F** a high degree of similarity could be recognized in the spatial arrangement of substituents in these two compounds. Therefore it may be possible that the compounds of analogue library 2 interact with SRPK1 in a type 1, ATP-competitive fashion. However, only through additional biological testing could this be evaluated.

Until these studies are carried out, there are other aspects of the lead compound which could still be evaluated to improve PK, drug-likeness and viability as a chemical probe in biological systems.

4.6.2. Pharmacokinetics.

Lipinski's rule of 5 has been sacrosanct as a tool for the design of drugs since publication of the first seminal paper in 1997.³⁴⁰ In an effort to reduce rates of pipeline attrition in drug design, a

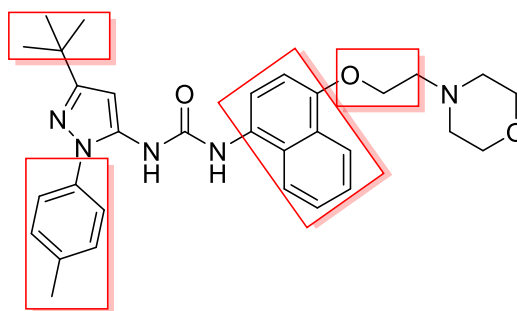
change in perspective to take these 'rules' as guidelines is helping hit-to-lead discovery expand its perspective and design candidates of a quality that are more 'fit for purpose'.²⁹⁰

One of the key features of drug-likeness is relative lipophilicity.³⁴¹ In order to be orally-bioavailable a drug must be able to solubilize in the blood and saliva, but also be lipophilic enough to permeate the cell membrane and pass through the stomach or gut cell-lining. Hence some believe "lipophilicity remains the single most important physical property to optimize".³⁴¹

Other important factors to consider include total polar surface area (TPSA),³⁴² defined as the sum of polar atom surfaces in a molecule. A good predictor of permeability, it can be used to help calculate whether a molecule is likely to permeate the gut and even the blood-brain barrier. Therefore it is a very important measure of bioavailability and potential toxicity.

The number of HBDs and HBAs is expected to affect permeability into cells, as they will tend to interact unfavourably with lipophilic cell membranes. A high proportion of tetrahedral carbon atoms are predicted to have a favourable effect on solubility and bioavailability, whilst reducing promiscuity and potential toxicity.^{290,343,344}

There is a vast array of factors that need to be considered over the course of a drug design project, and it is a balancing act to achieve a favourable ratio of each aspect whilst also retaining a high binding affinity for the target molecule.



BIRB 796 (14)

Figure 89: Areas of BIRB 796 (14) contributing to high lipophilicity, and at risk of oxidation and metabolism.

Upon examination of BIRB 796 (14) as a drug candidate, the ligand does not appear to be very drug-like, demonstrating a high-proportion of lipophilic areas at risk of phase 1 metabolism and oxidation (see **Figure 89**). The ether chain of BIRB 796 (14) is very important to the PD of the compound with respect to p38 α MAPK, and increases the favourable PK of the molecule by contributing a number of rotatable bonds and heteroatoms. However, this would most likely be a high risk area for metabolism, acting much like the metabolic shunt of Pfizer's alternative MK2

inhibitors PF-318 (**203**) and PF-029 (**204**). Additionally, as a very planar molecule, BIRB 796 (**14**) would be expected to have a low solubility, and has the potential to get trapped in lipophilic cell lining and DNA.²⁷⁶ There is a drive in the pharmaceutical industry to move away from highly unsaturated molecules, which have thrived through HTS and fragment-based lead identification, to develop more architecturally diverse, complex molecules and drugs which are more natural product-like.³⁴³

Indeed, despite advancing to phase 3 human clinical trials, BIRB 796 (**14**) did not demonstrate any sustained improvement in treating the disease³⁴⁵ and was reported to induce gastrointestinal distress, with other potentially drug-related side-effects including infections in the upper-respiratory tract, dizziness, rashes and abnormal liver function test.³⁷

In this project, the extensive π -system of BIRB 796 (**14**) was retained in the new analogue libraries. However, depending upon the substituents of the pyrazole and aromatic rings, the planarity of the molecule could be altered. For instance, X-ray crystallographic data collected for **2310**, a less active compound by DSF analysis, demonstrated the molecule to crystallize into a triclinic unit cell and adopt a flat, planar geometry. Three molecules crystallized to arrange themselves around three water molecules, interacting through the urea NHs and the pyrazole 2-N lone pair (**Figure 90**).^{xii}

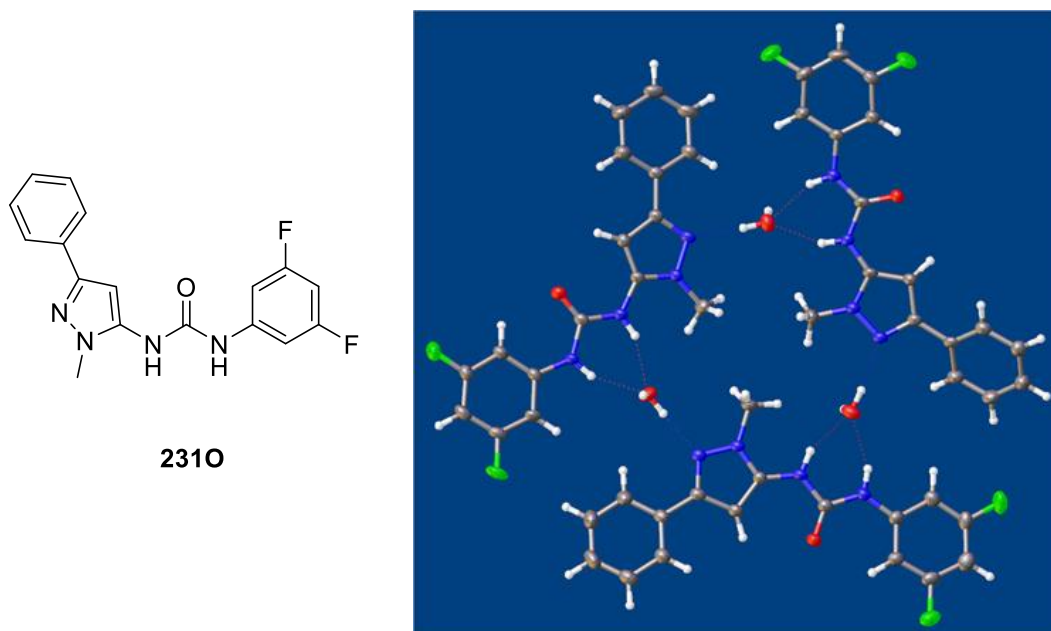


Figure 90: X-ray crystal structure of **2310**. Triclinic crystal, bound via three water molecules.

^{xii} Single crystal X-ray diffraction experiments were performed using an Agilent Excalibur with CCD plate detector using Cu-K α ($\lambda = 1.514184$ Å), and solved using SHELX.³⁷³ See supplementary information for complete CIF report.

Comparison with the hit compound from library 1, **215F**, the X-ray crystal structure illustrated the molecule to be much more twisted about the urea group (**Figure 91**). Crystallized into a monoclinic cell, the positioning of the phenyl and *tert*-butyl substituents on the pyrazole appeared to prevent the same water hydrogen bonding network from occurring as with **2310** in **Figure 90**.

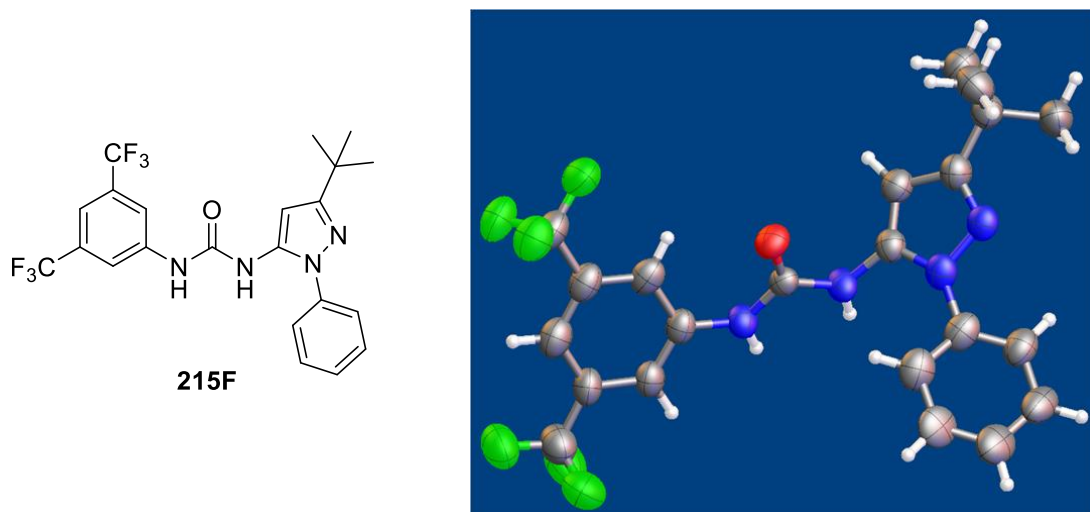


Figure 91: X-ray crystal structure of **215F**, demonstrating the twist in the molecule due to steric interactions of the pyrazole substituents.

Despite the observation that this slight twist removed some planarity in the molecule, there was still a high degree of sp^2 character to this molecule. In order to improve drug-likeness, a favourable change could be to increase the sp^3 character; for instance, through the incorporation of saturated rings. These changes could help increase solubility and evaluate the importance of π - π stacking within the protein binding pocket. Also the incorporation of saturated rings could potentially open up new areas of diversification to harness additional amino acid interactions.

When considering the potential ADME characteristics of lead compound **227F** compared to BIRB 796 (**14**), it could be observed that not all of the modifications made may be conducive towards improving compound PK. **Figure 92** highlights the areas of **227F** which have been altered from the BIRB 796 (**14**) pharmacophore. In blue are shown the areas which appear to have had a positive effect on the PD; to reduce affinity for p38 α and increase stabilization when bound to SRPK1. In red are highlighted the sites potentially still at risk of phase 1 metabolism. Though the number of sites at risk are reduced compared to BIRB 796 (**14**), and the addition of fluorinated groups should temper metabolism of the aromatic rings, there are still high risk areas on the molecule.

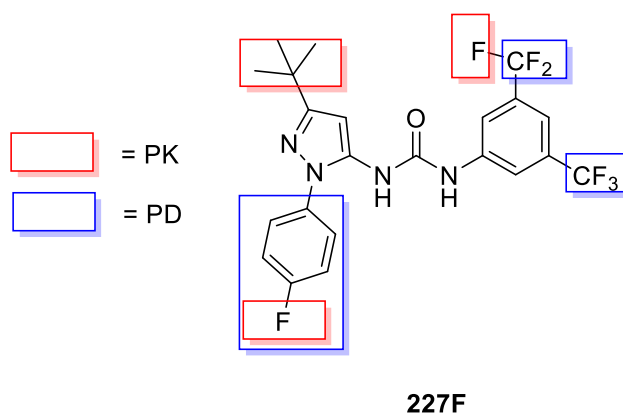


Figure 92: Highlighting the areas of significance for the PK and PD of lead compound **227F**.

Additionally, it should be noted that, with the loss of the ether-linked morpholine group of BIRB 796 (**14**), the number of rotatable bonds and heteroatoms in the molecule has been reduced, which may adversely affect the solubility and bioavailability of the molecule. Hence, the balancing act of developing an efficacious biological probe should continue with further investigation and the design of new compound libraries.

4.6.3. Conclusion.

There is a lot of potential work on this project that could be carried forward. Many avenues of investigation are available and this was only the first step in this, a promising project, the results of which were already astounding.

Further investigation of the potential of this library could conceivably lead to some very interesting and important discoveries on the role of SRPK1 in the human kinome, and towards the development of new, selective chemical probes to help in the validation of targets of interest for drug discovery programmes.

Chapter 5. Conclusions.

The major objectives of this research project have been to develop new, rapid routes towards p38 α and MK2 inhibitors, and to evaluate their use as chemical probes for investigating the mechanisms of ageing using WS as our model.

The p38 α inhibitor SB203580 (**1**) has been proven to reverse the aged morphology of WS fibroblasts; however, due to the cross-kinase activity of this inhibitor it could not be explicitly asserted that this was the key kinase being inhibited to elicit this effect. Hence, the alternative p38 α inhibitor RO3201195 (**10**), which is much more selective to p38 α , was synthesized through a rapid microwave-assisted route, and investigated in a comparative study of the two inhibitors.

The 4,5-disubstituted pyrazole inhibitor RO3201195 (**10**) was synthesized in 15% overall yield over seven steps, with three steps employing microwave-assisted heating, including the rapid formation of the key pyrazole ring scaffold of the drug.¹ Upon testing in WS fibroblasts it was found that RO3201195 (**10**) had an almost identical effect on the rate of cell proliferation as SB203580 (**1**). This evidence strongly supported previous assertions that the rate of proliferation of WS cells is subject to the activity of the p38 α stress-signalling pathway.² Additionally, the biological studies completed established RO3201195 (**10**) as a reliable tool for investigating stress-signalling pathways, as it is highly kinase specific and relatively potent compared to SB203580 (**1**).

In order to further probe the role of the p38 α MAPK stress-signalling pathway, synthesis of the MK2 inhibitor PF-3604422 (**25**) was investigated. MK2 is downstream of p38 α in the stress-signalling cascade and it was hypothesized that, by obstructing the cascade further downstream, the likelihood of off-target effects would be reduced. Testing an MK2 inhibitor in WS cells would give greater insight into the mechanism of premature ageing in WS fibroblasts, and potentially help in the development of efficacious therapeutics.

Initial synthetic routes to PF-3644022 (**25**) concentrated on building up a core quinoline unit and using Suzuki-coupling chemistry to establish the biaryl linkage,³ onto which the fused ring system would be installed, with final installation of the chiral centre. However, the yields and reproducibility of these reactions was not viable for a total synthesis.

An alternative route was investigated concentrating on the initial synthesis of a poly-substituted benzo[*b*]thiophene heterocyclic core, ready for further functionalization thereon to form the fused quinoline ring and chiral centre.² Through trial and error, the best sequential route was

determined to proceed via synthesis of the bromobenzo[*b*]thiophene,² with subsequent diazepinone formation and a final Doebner multi-component quinoline reaction to install the fused heterocyclic ring and the linked pyridine in one step. The total synthesis was completed in six steps and 4% overall yield. Future work on this project should focus on optimizing this yield.

Biological tests have been completed on WS fibroblasts using PF-3644022 (**25**) and found that treatment of cells with this MK2 inhibitor did indeed improve the growth rate, though comparative studies with the p38 inhibitor SB203580 (**1**) demonstrated a significantly higher growth rate.³ Additionally, due to the small therapeutic window of PF-3644022 (**25**) an accurate representation of the effect of MK2 inhibition could not be gleaned from the studies. Work is still ongoing into the potential of MK2 inhibitors as therapeutic agents and chemical probes.

Alongside these main projects, work has also been carried out to investigate the potential re-purposing of the potent non-ATP-competitive p38 α inhibitor BIRB 796 (**14**). The novel chemotype and binding mode of the inhibitor presented itself as a candidate for the design of new and selective chemical probes to be used to delineate mechanisms of kinase signalling pathways in cells.

Primary investigations focussed on the selectivity elements of BIRB 796 (**14**) to explore how changes to electronic and steric factors of the molecule might influence activity with a small selection of kinases. The first library of molecules was very fruitful, with an unexpected re-optimization of the kinase selectivity towards SRPK1 with congruent reduction in potency for p38 α . From these initial results, a second library of compounds was synthesized, to investigate how changing the substituents on the pyrazole ring might increase or decrease the newly established activity. Further biological studies are on-going with this project in association with the SGC, but initial DSF results have been very positive, continuing to maintain the affinity established for SRPK1 over p38 α . From the results of these biological studies, the potential of this project to be carried on will be assessed and taken forward in the research group.

The key objectives of the project have been met, with advances in our understanding of the WS premature-ageing stress-signalling pathway. Through the rapid and efficient synthesis of RO3201195 (**10**), a greater understanding of the role of p38 α in the premature aged phenotype of WS fibroblasts has been achieved. Synthesis of the MK2 inhibitor PF-3644022 (**25**) has been completed, exploring new synthetic routes towards advanced intermediates and the final compound. Though fairly low yields were achieved in the final steps of the synthesis, work is ongoing in the group to optimize the reaction. Unfortunately due to the small therapeutic window of PF-3644022 (**25**), the information gathered from tests in WS fibroblasts was limited, though

there was a positive correlation between the growth rate and treatment with the MK2 inhibitor. Additionally, new unexpected results have been obtained into how the p38 α inhibitor BIRB 796 (14) can be repurposed to target alternative kinases. This research has a great deal of potential for the development of chemical probes and tools to advance understanding of stress-signalling events in cells, and their influence on the ageing process *in vivo*.

Chapter 6. Experimental.

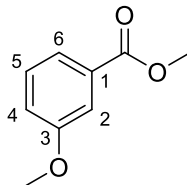
All procedures were completed in air unless otherwise stated. Commercially available reagents were used throughout without purification, with solvents dried by standard procedures. Light petroleum refers to the fractions with bp 40-60 °C. Analytical thin layer chromatography was carried out using aluminium-backed plates coated with Merck TLC Silicagel 60 F₂₅₄. Plates were visualized under UV light (at 254 and/or 360 nm), and/or with ninhydrin and potassium permanganate solutions. Microwave-assisted reactions were carried out using a CEM Discover™ with a CEM Explorer at the given temperature using the instrument's in-built IR temperature measuring device, by varying the irradiation power (initial power given in parentheses). Column chromatography was carried out on a Biotage Isolera Prime flash purification system. SCX-2 ion exchange chromatography was carried out using Biotage Isolute SPE SCX-2 flash columns.

Fully characterized compounds were chromatographically homogeneous. Melting points were determined using a Stanford Research Systems Optimelt and are uncorrected. IR spectra were recorded in the range 4000-600 cm⁻¹ using a Perkin Trans FT-IR Spectrum. NMR spectra were recorded using a Varian VNMRS instrument operating at 600, 500 or 400 MHz for ¹H NMR and 126 or 100 MHz for ¹³C NMR. *J* values were recorded in Hz and multiplicities were expressed in the usual conventions. ESI mass spectra were obtained using a Bruker Daltonics Apex III, with ESI source Apollo ESI, using methanol as the spray solvent. For EI mass spectra a Fissons VG Autospec instrument was used at 70 eV and were captured by Dr. Alla K. Abdul-Sada of the University of Sussex Mass Spectrometry Centre. A number of high resolution mass spectra were obtained courtesy of the EPSRC Mass Spectrometry Service at Swansea University, UK using the ionization methods specified.

LCMS data was recorded on a Waters 2695 HPLC using a Waters 2487 UV detector and a Thermo LCQ ESI-MS. Samples were eluted through a Phenomenex Lunar 3μ C18 50 mm × 4.6 mm column, using acetonitrile and water acidified by 0.01% formic acid. Samples were eluted using acetonitrile and water (1:9 to 9:1) acidified by 0.01% formic acid, at a flow rate of 3 μl/min.

6.1. Chapter 2.

6.1.1. Methyl 3-methoxybenzoate (123)

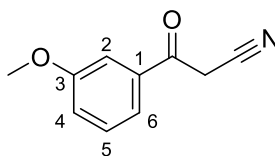


Chemical Formula: $C_9H_{10}O_3$

Mr: 166.18

3-Methoxybenzoic acid (1.48 g, 9.71 mmol) in MeOH (10 mL) and a catalytic amount of conc. H_2SO_4 (0.01 mL, 0.20 mmol) was irradiated at 110 °C for 10 min in a pressure-rated glass vial (35 mL) using a CEM Discover microwave synthesizer by moderating the initial power (200 W). After cooling in a flow of compressed air, the volatiles were removed and the residue partitioned between water and Et_2O . The organic fraction was washed with saturated aqueous $NaHCO_3$ solution, dried (Na_2SO_4), filtered and evaporated *in vacuo* to give the title compound (1.52 g, 94%) as a clear colourless oil, (Found [ESI⁺]: 189.0520. $C_9H_{10}O_3Na$ [MNa] requires 189.0522); IR (neat) ν_{max}/cm^{-1} : 2953 (C-H str), 1718 (C=O str), 1601 (C-C str), 1276 (C-O str), 1221 (C-O str); 1H NMR (500 MHz, $CDCl_3$) δ_H/ppm : 7.64 (1H, d, J = 8 Hz, 6-CH), 7.57 (1H, br. s, 2-CH), 7.35 (1H, t, J = 8 Hz, 5-CH), 7.11 (1H, dd, J = 8, 2 Hz, 4-CH), 3.92 (3H, s, CO_2Me), 3.86 (3H, s, OMe); ^{13}C NMR (126 MHz, $CDCl_3$) δ_C/ppm : 166.9 (C), 159.6 (3-C), 131.5 (1-C), 129.3 (5-CH), 122.0 (6-CH), 199.5 (4-CH), 144.0 (2-CH), 55.4 (OMe), 52.1 (CO_2Me); m/z (EI⁺): 166 (M^{+} , 14), 135 ($M-OMe^{+}$, 39), 93 (100).

6.1.2. 3-Methoxybenzoylacetonitrile (107)



Chemical Formula: $C_{10}H_9NO_2$

Mr: 175.19

6.1.2.1. Claisen ester condensation.

According to a modified procedure,⁴⁵ under argon, *n*-BuLi (2.5 M in hexanes; 5.3 mL, 13.2 mmol) was added dropwise to a solution of DIPA (1.9 mL, 13.6 mmol) in dry THF (2 mL) cooled to 0 °C, and allowed to stir at 0 °C for 10 min. In a separate flask, methyl 3-methoxybenzoate (**123**) (1.1 g, 6.6 mmol) and dry MeCN (0.5 mL, 9.5 mmol) in dry THF (5 mL) was cooled to –50 °C. The cold LDA solution was added dropwise and the reaction mixture was stirred at –50 °C for 3 h. Saturated aqueous NH₄Cl solution (10 mL) was then added. The solution was allowed to warm to RT, extracted with EtOAc (3 x 20 mL), washed with aqueous HCl solution (1 M; 20 mL) and brine (20 mL), dried (MgSO₄), filtered and evaporated *in vacuo*. Purification by flash column chromatography on SiO₂ (dry-load), gradient eluting with hexanes to EtOAc-hexanes (40:60), gave the *title compound* (0.82 g, 70%) as a yellow solid, mp 86.3-87.4 °C (MeOH) mp 87.3-88.2 °C (EtOAc) (lit³⁴⁶ 87-88), (Found [ESI⁺]: 198.0523. C₁₀H₉NO₂Na [MNa] requires 198.0525); IR (neat) ν_{max} /cm⁻¹: 2948 (C-H str), 2252 (C≡N str), 1694 (C=O str), 1580 (C-C str), 1451 (C-H bend), 1258 (C-O str), 1012 (C-O str); ¹H NMR (500 MHz, CDCl₃) δ_{H} /ppm: 7.49-7.41 (3H, m, 2, 5, 6-CH), 7.21 (1H, d, *J* = 8 Hz, 4-CH), 4.07 (2H, s, CH₂), 3.88 (3H, s, Me); ¹³C NMR (126 MHz, CDCl₃) δ_{C} /ppm: 186.9 (C), 160.2 (3-C), 135.7 (1-C), 130.1 (5-CH), 121.2 (4-CH), 120.9 (6-CH), 113.6 (CN), 112.8 (2-CH), 55.6 (Me), 29.4 (CH₂); *m/z* (EI⁺): 175 (M^{•+}, 36), 135 (M⁺-CH₂CN, 100).

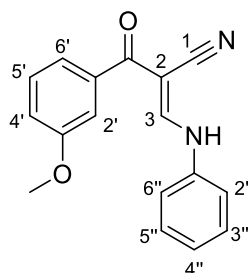
6.1.2.2. Heck reaction. Conductive heating.

Under argon, 3-methoxyacrylonitrile (0.24 g, 2.92 mmol) was added to a solution of 3-iodoanisole (0.14 g, 0.61 mmol), K₂CO₃ (0.24 g, 1.71 mmol), tetrabutylammonium bromide (39 mg, 0.12 mmol) and Pd(OAc)₂ (21 mg, 93 μ mol) in a solution of H₂O-MeCN ([3:1]; 3 mL) and heated at 90 °C for 20 h. Once cooled, the solution was partitioned between water and EtOAc, and the aqueous layer extracted with EtOAc (2 x 10 mL). The organic extracts were combined, washed with brine (1 x 20 mL), dried (Na₂SO₄), filtered and evaporated *in vacuo*. In air, the residue was taken up in MeOH (2 mL) and conc. HCl (10.2 M; 0.5 mL) and irradiated at 110 °C for 1 h in a pressure-rated glass vial (10 mL) using a CEM Discover microwave synthesizer by moderating the initial power (150 W). After cooling in a flow of compressed air, the solution was partitioned between water and EtOAc, and extracted into EtOAc (2 x 10 mL). The organic extracts were combined and washed with brine (1 x 20 mL), dried (Na₂SO₄), filtered and evaporated. Purification by flash column chromatography on SiO₂, (dry-load) eluting with hexanes to EtOAc-hexanes (4:6), gave the *title compound* as a yellow solid (39 mg, 36%) mp 87.0-87.6 °C (MeOH), with identical spectroscopic data.

6.1.2.3. Heck reaction. Microwave-assisted method.

Under argon, 3-methoxyacrylonitrile (0.26 g, 3.43 mmol) was added to a solution of 3-iodoanisole (0.17 g, 0.72 mmol), NaHCO₃ (0.15 g, 1.78 mmol), TBAB (30 mg, 93 μmol) and Pd(OAc)₂ (22 mg, 98 μmol) in a solution of H₂O:MeCN ([3:1]; 3 mL) was irradiated at 130 °C for 1.5 h in a pressure-rated glass vial (10 mL) using a CEM Discover microwave synthesizer by moderating the initial power (150 W). After cooling in a flow of compressed air the solution was partitioned between water and EtOAc, and the aqueous layer extracted with EtOAc (2 x 10 mL). The organic extracts were combined, washed with brine (1 x 20 mL), dried (Na₂SO₄), filtered and evaporated *in vacuo*. The residues were treated as above, irradiating in MeOH and with conc. HCl. Purification by flash column chromatography on SiO₂ (dry-load), gradient eluting with hexanes to EtOAc-hexanes (40:60) gave the *title compound* (47 mg, 37%) as a yellow solid, with identical spectroscopic data.

6.1.3. 2-(3-Methoxybenzoyl)-3-(phenylamino)prop-2-enenitrile (124)



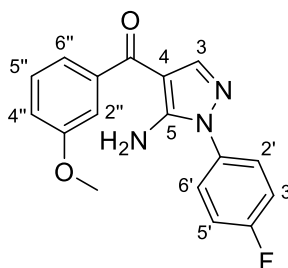
Chemical Formula: C₁₇H₁₄N₂O₂

Mr: 278.30

A solution of *N,N'*-diphenylformamidine (0.24 g, 1.20 mmol) and 3-methoxybenzoylacetonitrile (**107**) (0.20 g, 1.13 mmol) in dry xylenes (7.5 mL) was irradiated at 180 °C for 20 min under argon in a pressure-rated glass vial (35 mL) using a CEM Discover microwave synthesizer by moderating the initial power (200 W). After cooling in a stream of compressed air, the solution was diluted with hexanes and the precipitate isolated by gravity filtration to afford the *title compound* (0.23 g, 74%) as a colourless solid, mp 107.4-108.8 °C (lit³⁴⁷ 105 °C) (Found [ESI⁺]: 279.1126. C₁₇H₁₅N₂O₂ [MH]⁺ requires 279.1128); IR (neat) ν_{max}/cm⁻¹: 3062 (=C-H str), 2921 (C-H str), 2204 (C≡N str), 1634 (C=O str), 1596 (N-H bend), 1571 (C-C str), 1392 (C-C str), 1313 (C-N str), 1225 (C-O str), 1044 (C-O str), 990 (=C-H bend), 867 (N-H wag); ¹H NMR (500 MHz, CDCl₃) δ_H/ppm: 12.76 (1H, d,

$J = 13$ Hz, NH), 8.06 (1H, d, $J = 13$ Hz, 3-CH), 7.57 (1H, d, $J = 8$ Hz, 6'-CH), 7.46 (3H, m, 2'-CH, 3'', 5''-CH), 7.40 (1H, t, $J = 8$ Hz, 5'-CH), 7.30 (1H, m, 4''-CH), 7.23 (2H, d, $J = 8$ Hz, 2'', 6''-CH), 7.11 (1H, d, $J = 8$ Hz, 6'-CH), 3.89 (3H, s, CH₃); ¹³C NMR (126 MHz, CDCl₃) δ_c /ppm: 192.1 (C), 159.6 (3'-PhC), 154.1 (3-CH), 139.2 (1'-PhC), 138.1 (1''-PhC), 130.2 (3'', 5''-PhCH), 129.4 (5'-CH), 126.6 (4''-PhCH), 120.5 (6'-CH), 120.3 (1-CN), 118.9 (4'-CH), 117.9 (2'', 6''-PhCH), 112.7 (2'-CH), 83.5 (2-C), 55.5 (Me); m/z (EI+): 278 (M^{•+}, 49), 277 (M-H, 100), 135 (52).

6.1.4. [5-Amino-1-(4-fluorophenyl)-1H-pyrazol-4-yl]-3-methoxyphenyl ketone (125)



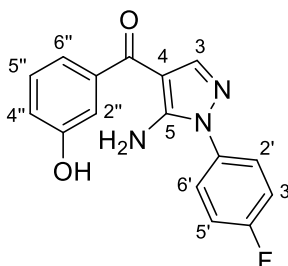
Chemical Formula: C₁₇H₁₄N₃O₂F

Mr: 311.32

A solution of 2-(3-methoxybenzoyl)-3-(phenylamino)prop-2-enenitrile (**X3**) (0.13 g, 0.46 mmol), 4-fluorophenylhydrazine hydrochloride (0.073 g, 0.47 mmol) and NEt₃ (0.02 mL, 0.14 mmol) in EtOH (3 mL) was irradiated at 140 °C for 1 h in a pressure-rated glass vial (10 mL) using a CEM Discover microwave synthesizer by moderating the initial power (100 W). After cooling in a stream of compressed air, the volatiles were removed *in vacuo*. Purification by flash column chromatography on SiO₂ (dry-load), gradient eluting with hexanes to EtOAc-hexanes (30:70), to give the *title compound* as a pink solid (0.11 g, 86%), mp 130.1-132.0 °C (Found [ESI+]: 312.1138. C₁₇H₁₅N₃O₂F [MH] requires 312.1143); IR (neat) ν_{\max} /cm⁻¹: 3318 (N-H str), 2925 (C-H str), 1610 (C=O str), 1595 (N-H bend), 1539 (C-C str), 1286 (C-N str), 1223 (C-O str), 1051 (C-O str), 838 (N-H wag); ¹H NMR (500 MHz, CDCl₃) δ_H /ppm: 7.81 (1H, s, 3-CH), 7.56 (2H, pdd, ³J_{HH} = 8 Hz, ⁴J_{HF} = 5 Hz, 2', 6'-CH), 7.42 (2H, m, 5'', 6''-CH), 7.35 (1H, s, 2''-CH), 7.25 (2H, pt, ³J_{HH}, ³J_{HF} = 8 Hz, 3', 5'-CH), 7.11 (1H, m, 4''-CH), 6.04 (2H, br. s, NH₂), 3.89 (3H, s, Me); ¹³C NMR (126 MHz, CDCl₃) δ_c /ppm: 189.4 (C), 162.2 (d, ¹J_{CF} = 250 Hz, 4'-CF), 159.8 (3''-C), 150.6 (5-C), 142.0 (3-CH), 141.1

(1''-C), 133.3 (d, $^4J_{\text{CF}} = 4$ Hz, 1'-C), 129.5 (5''-CH), 126.1 (d, $^3J_{\text{CF}} = 9$ Hz, 2', 6'-CH), 120.7 (6''-CH), 117.8 (4''-CH), 116.9 (d, $^2J_{\text{CF}} = 23$ Hz, 3', 5'-CH), 113.0 (2''-CH), 104.8 (4-C), 55.4 (OMe).

6.1.5. [5-Amino-1-(4-fluorophenyl)-1H-pyrazol-4-yl]-3-hydroxyphenyl ketone (126)

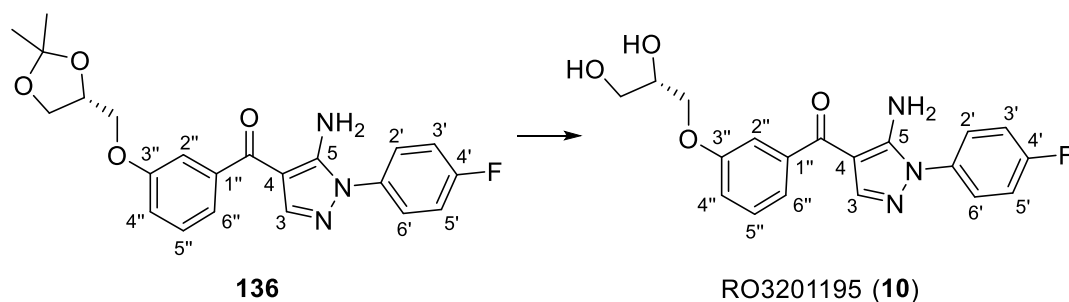


Chemical Formula: $\text{C}_{16}\text{H}_{12}\text{N}_3\text{O}_2\text{F}$

Mr: 297.29

Boron tribromide solution (1M in CH_2Cl_2 ; 1.7 mL, 1.70 mmol) was added dropwise to [5-amino-1-(4-fluorophenyl)-1H-pyrazol-4-yl]-3-methoxyphenyl ketone (**125**) (0.10 g, 0.34 mmol) in dry CH_2Cl_2 (1 mL) at 0 °C under argon and the mixture allowed to warm to RT and stirred for 20 h. Water (15 mL) was then cautiously added and the mixture extracted with EtOAc (3 x 15 mL). The organic extracts were combined, washed with brine (1 x 20 mL), dried (MgSO_4), filtered and evaporated *in vacuo* to give the *title compound* (0.10 g, quant.) as a brown solid, mp 192.2-194.9 °C (Found [ESI⁺]: 298.0984. $\text{C}_{16}\text{H}_{13}\text{N}_3\text{O}_2\text{F}$ [MH] 298.0986); IR (neat) $\nu_{\text{max}}/\text{cm}^{-1}$: 3320 (N-H str), 3204 (br. O-H), 3072 (C-H str), 1610 (C=O str), 1592 (N-H bend), 1538 (C-C str), 1310 (C-N str), 1126 (C-O str), 841 (N-H wag); ^1H NMR (500 MHz, $\text{MeOH}-d_4$) $\delta_{\text{H}}/\text{ppm}$: 7.78 (1H, s, 3-CH), 7.59 (2H, pdd, $^3J_{\text{HH}} = 9$ Hz, $^4J_{\text{HF}} = 5$ Hz, 2', 5'-CH), 7.37-7.29 (3H, m, 3', 5', 5''-CH), 7.23 (1H, d, $J = 7$ Hz, 6''-CH), 7.18 (1H, s, 2''-CH), 7.00 (1H, dd, $J = 7, 1$ Hz, 4''-CH); ^{13}C NMR (100 MHz, $\text{MeOH}-d_4$) $\delta_{\text{C}}/\text{ppm}$: 191.6 (C), 164.1 (d, $^1J_{\text{CF}} = 247$ Hz, 4'-CF), 159.2 (3''-C), 153.4 (5-C), 143.6 (3-CH), 142.7 (1''-C), 135.0 (d, $^4J_{\text{CF}} = 3$ Hz, 1'-C), 131.1 (5''-CH), 128.5 (d, $^3J_{\text{CF}} = 9$ Hz, 2', 6'-CH), 120.6 (6''-CH), 120.1 (4''-CH), 118.0 (d, $^3J_{\text{CF}} = 24$ Hz, 3', 5'-CH), 116.0 (2''-CH), 105.7 (4-C); m/z (EI⁺): 297 ($\text{M}^{\bullet+}$, 91), 296 ($\text{M}-\text{H}^+$, 100), 204 (31).

6.1.6. 5-Amino-1-(4-fluorophenyl)-4-{3-[2(*S*)-3-dihydroxypropoxy]benzoyl} pyrazole (RO3201195) (10)



Chemical Formula: C₁₉H₁₈N₃O₄F

Mr: 371.37

(*S*)-2,2-Dimethyl-1,3-dioxolan-4-ylmethyl *p*-toluenesulfonate (0.60 mL, 2.52 mmol) and anhydrous K₂CO₃ (0.59 g, 4.25 mmol) were added to a solution of [5-amino-1-(4-fluorophenyl)-1*H*-pyrazol-4-yl]-3-hydroxyphenyl ketone (**126**) (0.48 g, 1.61 mmol) in dry DMSO (15 mL) under argon and heated at 100 °C for 40 h. Once cooled, the solution was diluted with water (25 mL) and extracted into EtOAc (3 x 20 mL). The organic extracts were combined, washed with brine (1 x 20 mL), dried (MgSO₄), filtered and evaporated *in vacuo*. Purification by flash column chromatography on SiO₂ (dry-load), eluting with light petroleum to EtOAc-light petroleum (40:60), gave the crude intermediate [5-amino-1-(4-fluorophenyl)-1*H*-pyrazol-4-yl]{3-[(*R*)-2,2-dimethyl-1,3-dioxolan-4-yl]methoxy}phenyl ketone (**x6**), which was taken up in a MeOH-H₂O solution ([4:1]; 4 mL), *p*-toluene sulfonic acid monohydrate (0.04 g, 0.21 mmol) was added and the solution heated at 50 °C for 18 h. Once cooled, volatiles were removed *in vacuo* and the residue taken up in EtOAc (25 mL), washed with saturated aqueous NaHCO₃ solution (20 mL), dried (MgSO₄), filtered and evaporated *in vacuo*. Purification by flash column chromatography on SiO₂ (dry-load), gradient eluting with light petroleum to EtOAc, and recrystallization from hot EtOAc and hexanes gave the *title compound* (0.22 g, 37%) as a colourless solid, mp 154.1-154.6 °C (EtOAc) (Found [ESI⁺]: 372.1353. C₁₉H₁₉N₃O₄F [*MH*] requires 372.1354); [α]_D²² -28 (*c* 0.2, EtOAc), [α]_D²² +6.5 (*c* 0.6, MeOH); IR (neat) ν_{max} /cm⁻¹: 3440 (N-H str), 3330 (O-H str), 3229 (O-H str), 2896 (C-H str), 1633 (C=O str), 1597 (NH₂ str), 1540 (C=N str), 1498 (C-C str), 1292 (C-O str), 1222 (C-F str), 1053 (C-O str), 839 (NH₂ wag.); ¹H NMR (500 MHz, DMSO-*d*₆) δ_{H} /ppm: 7.80 (1H, s, 3H), 7.61 (2H, pdd, ³*J*_{HH} = 8 Hz, ⁴*J*_{HF} = 5 Hz, 2', 6'-CH), 7.47-7.37 (3H, m, 3', 4', 5''-CH), 7.33 (1H, d, *J* = 7 Hz, 6''-CH), 7.25 (1H, m, 2''-CH), 7.14 (3H, m, 4''-CH, NH₂), 4.95 (1H, br. s, CHOH), 4.65 (1H,

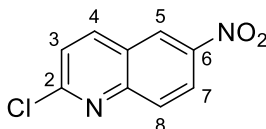
br. s, CH₂OH), 4.09 (1H, m, OCHH), 3.95 (1H, m, OCHH), 3.82 (1H, m, CHOH), 3.47 (2H, d, *J* = 5 Hz, CH₂OH); ¹³C NMR (126 MHz, DMSO-*d*₆) δ_C/ppm: 187.5 (C), 161.1 (d, ¹*J*_{CF} = 244 Hz, 4'-C), 158.7 (3''-C), 151.2 (5-C), 141.4 (3-CH), 140.9 (1''-C), 133.7 (d, ⁴*J*_{CF} = 3 Hz, 1'-C), 129.6 (5''-CH), 126.4 (d, ³*J*_{CF} = 9 Hz, 2', 6'-CH), 120.1 (6''-CH), 117.8 (4''-CH), 116.3 (d, ²*J*_{CF} = 23 Hz, 3', 5'-CH), 113.3 (2''-CH), 103.5 (4-C), 69.9 (CHOH), 69.8 (CH₂O), 62.6 (CH₂OH); *m/z* (EI⁺): 371 (M^{•+}, 10), 325 (33), 160 (100).

6.1.6.1. Procedure for isolation of [5-Amino-1-(4-fluorophenyl)-1*H*-pyrazo-4-yl]{3-[(*R*)-2,2-dimethyl-1,3-dioxolan-4-yl]methoxy}phenyl} ketone (136).

(*S*)-2,2-Dimethyl-1,3-dioxolan-4-ylmethyl *p*-toluenesulfonate (0.15 mL, 0.64 mmol) and anhydrous K₂CO₃ (0.11 g, 0.80 mmol) were added to a solution of [5-amino-1-(4-fluorophenyl)-1*H*-pyrazol-4-yl]-3-hydroxyphenyl ketone (**126**) (0.095 g, 0.32 mmol) in dry DMSO (5 mL) under argon and heated at 100 °C for 25 h. Once cooled the solution was diluted with water (15 mL) and extracted with EtOAc (3 x 20 mL), washed with brine, dried (MgSO₄), filtered and evaporated *in vacuo*. Purification by flash column chromatography on SiO₂ (dry-load), gradient eluting with EtOAc-hexanes (25:75) to (50:50), followed by crystallisation from hot EtOAc and hexane gave the *title compound* (0.056 g, 42%) as a colourless powder, mp 53.7-58.3 °C (EtOAc) (lit³⁴⁷ 58-61) (Found [ESI⁺]: 412.1657. C₂₂H₂₃N₃O₄F [*MH*] requires 412.1667); [α]_D²¹ -20 (*c* 0.6, EtOAc); IR (neat) ν_{max}/cm⁻¹: 3457 (N-H str), 3319 (N-H str), 2987 (C-H str), 1613 (C=O str), 1593 (NH₂), 1535 (C=N str), 1217 (C-O-C str), 1155 (C-F str), 1055 (C-O-C str), 829 (NH₂ wag); ¹H NMR (500 MHz, CDCl₃) δ_H/ppm: 7.80 (1H, s, 3-CH), 7.56 (2H, pdd, ³*J*_{HH} = 9, ⁴*J*_{HF} = 5 Hz, 2', 6'-CH), 7.45-7.39 (2H, m, 5'', 6''-CH), 7.36 (1H, m, 2''-CH), 7.25 (2H, pt, ³*J*_{HH}, ³*J*_{HF} = 9 Hz, 3', 5'-CH), 7.13 (1H, m, *J* = 7 Hz, 4''-CH), 6.03 (2H, br. s, NH₂), 4.52 (1H, q, *J* = 6 Hz, CH), 4.19 (1H, m, CHH), 4.14 (1H, dd, *J* = 9, 6 Hz, CHH), 4.03 (1H, dd, *J* = 9, 6 Hz, CHH), 3.93 (1H, dd, *J* = 8, 6 Hz, CHH), 1.48 (3H, s, Me), 1.42 (3H, s, Me); ¹³C NMR (126 MHz, CDCl₃) δ_C/ppm: 189.2 (C), 162.2 (d, ¹*J*_{CF} = 250 Hz, 4'-CF), 158.8 (3''-C), 150.6 (5-C), 142.0 (3-CH), 141.1 (1''-C), 133.2 (1'-C), 129.6 (5''-CH), 126.2 (d, ³*J*_{CF} = 9 Hz, 2', 6'-CH), 121.1 (6''-CH), 118.4 (4''-CH), 116.9 (d, ²*J*_{CF} = 24 Hz, 3', 5'-CH), 113.6 (2''-CH), 109.9 (CMe₂), 104.8 (4-C), 74.0 (CH), 69.1 (CH₂), 66.8 (CH₂), 26.8 (Me), 25.4 (Me); *m/z* (EI⁺): 411 (M^{•+}, 68), 310 (42), 204 (58).

6.2. Chapter 3.

6.2.1. 2-Chloro-6-nitroquinoline (151)



Chemical Formula: $C_9H_5N_2O_2Cl$

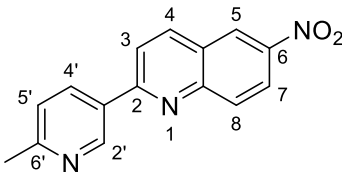
Mr: 208.60

$POCl_3$ (1.2 mL, 13.0 mmol) was added drop-wise to a stirred solution of 3,4-dihydro-6-nitroquinolin-2(1H)-one (1.00 g, 5.2 mmol) and DDQ (1.30 g, 5.7 mmol) in DMF (20 mL) and stirred at RT for 1 h. The reaction mixture was then poured into iced water and the precipitate formed collected by vacuum filtration, washed with water and dried in air to give the *title compound* (1.05 g, 97%) as an orange solid, mp 226.8-227.9 °C (lit.³⁴⁸ 230-230.5 °C) (Found [ESI⁺]: 209.0112. $C_9H_6^{35}ClN_2O_2$ [MH^+] requires 209.0112); IR (neat) ν_{max}/cm^{-1} : 3068 (C-H str), 1619 (C=C str), 1523 (N-O str), 1485 (C=C str), 1337 (N-O str), 1105 (C-N str); 1H NMR (500 MHz, $DMSO-d_6$) δ_H/ppm : 9.13 (1H, d, $J = 2$ Hz, 5-CH), 8.78 (1H, d, $J = 9$ Hz, 4-CH), 8.52 (1H, dd, $J = 9, 3$ Hz, 7-CH), 8.18 (1H, $J = 9$ Hz, 8-CH), 7.84 (1H, d, $J = 9$ Hz, 3-CH); ^{13}C NMR (126 MHz, $DMSO-d_6$) δ_C/ppm : 153.6 (C), 149.2 (C), 145.3 (C), 141.9 (4-CH), 129.7 (8-CH), 125.9 (C), 125.0 (5-CH), 124.4 (3-CH), 124.1 (7-CH); m/z (EI⁺): 208 ($M^{+35}Cl$, 100), 162 (48), 150 (49), 127 (81).

6.2.2. General procedure for Suzuki coupling

According to a modified procedure,³⁴⁹ a solution of 2-chloro-6-nitroquinoline (**151**), boronic acid (1.5-1.6 equiv.), aqueous Na_2CO_3 (2 equiv.) and $PdCl_2(PPh_3)_2$ (10 mol%) in MeCN (0.2 M) was irradiated at 140 °C for 15 min in a pressure-rated glass vial (35 mL) using a CEM Discover microwave synthesizer by moderating the initial power (200 W). After cooling in a flow of compressed air, volatiles were removed *in vacuo* and the residues triturated with water. Purification by flash column chromatography on SiO_2 gave the desired 2-pyridinyl-6-nitroquinoline.

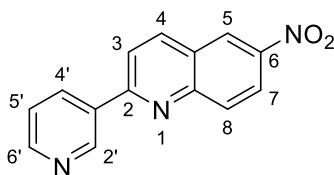
6.2.2.1. 2-(6-Methylpyridin-3-yl)-6-nitroquinoline (153)



Chemical Formula: $C_{15}H_{11}N_3O_2$

Mr: 265.27

Biaryl **153** was prepared according to the general synthetic procedure using 2-chloro-6-nitroquinoline (**151**) (0.45 g, 2.20 mmol), 6-methyl-3-pyridinylboronic acid (0.44 g, 3.20 mmol), aqueous Na_2CO_3 (1.5 M; 3 mL) and $PdCl_2(PPh_3)_2$ (0.15 g, 0.21 mmol) in MeCN (12 mL). Purification by flash column chromatography on SiO_2 (dry-load), gradient eluting with CH_2Cl_2 to CH_2Cl_2 -MeOH (90:10), gave the *title compound* as an orange solid (0.39 g, 69%), mp 237.5-239.1 °C (Found [ESI⁺]: 266.0923. $C_{15}H_{12}N_3O_2$ [MH] requires 266.0924); IR (neat) ν_{max}/cm^{-1} : 3070 (C-H str), 2921 (C-H str), 1596 (C-C str), 1534 (N-O str), 1327 (N-O str); 1H NMR (500 MHz, $CDCl_3$) δ_H/ppm : 9.30 (1H, d, $J=1$ Hz, 2'-CH), 8.82 (1H, d, $J=2$ Hz, 5-CH), 8.50 (2H, 4'-CH and 7-CH), 8.43 (1H, d, $J=9$ Hz, 4-CH), 8.28 (1H, d, $J=9$ Hz, 8-CH), 8.05 (1H, d, $J=9$ Hz, 3-CH), 7.36 (1H, d, $J=8$ Hz, 5'-CH), 2.68 (3H, s, Me); ^{13}C NMR (126 MHz, $CDCl_3$) δ_C/ppm : 160.6 (C), 158.2 (C), 150.4 (C), 148.4 (2'-CH), 145.5 (C), 138.7 (4-CH), 135.4 (4'-CH), 131.4 (8-CH), 131.3 (C), 126.0 (C), 124.3 (5-CH), 123.4 (7-CH), 123.4 (5'-CH), 120.0 (3-CH), 24.5 (Me).



6.2.2.2. 6-Nitro-2-(pyridin-3-yl)quinoline (152)

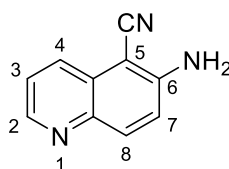
Chemical Formula: $C_{14}H_{13}N_3O_2$

Mr: 251.24

Biaryl **152** was prepared according to the general procedure using 2-chloro-6-nitroquinoline (**151**) (0.15 g, 0.71 mmol), 3-pyridinylboronic acid (0.10 g, 1.14 mmol), aqueous Na_2CO_3 (1.4 M, 1 mL) and $PdCl_2(PPh_3)_2$ (0.05 g, 0.07 mmol) in MeCN (3.6 mL). Purification by flash column chromatography on SiO_2 (dry-load), gradient eluting with EtOAc: CH_2Cl_2 (30:70), gave the *title*

compound (0.11 g, 62%) as a yellow solid, (Found [ESI⁺]: 252.0776. C₁₄H₁₀N₃O₂ [MH] requires 252.0768); IR (neat) $\nu_{\text{max}}/\text{cm}^{-1}$: 3081 (C-H str), 1607 (C=C str), 1528 (N-O str), 1337 (N-O str); ¹H NMR (500 MHz, CDCl₃) $\delta_{\text{H}}/\text{ppm}$: 9.43 (1H, br. s, 2'-CH), 8.84 (1H, d, *J* = 2 Hz, 5-CH), 8.78 (1H, d, *J* = 3 Hz, 6'-CH), 8.58 (1H, d, *J* = 8 Hz, 4'-CH), 8.53 (1H, dd, *J* = 9, 2 Hz, 7-CH), 8.48 (1H, d, *J* = 8 Hz, 4-CH), 8.31 (1H, d, *J* = 9 Hz, 8-CH), 8.08 (1H, d, *J* = 9 Hz, 3-CH), 7.52 (1H, m, 5'-CH); ¹³C NMR (126 MHz, CDCl₃) $\delta_{\text{C}}/\text{ppm}$: 158.0 (C), 151.2 (6'-CH), 150.4 (C), 149.0 (2'-CH), 138.9 (4-CH), 135.2 (4'-CH), 131.6 (8-CH), 128.5 (C), 128.4 (C), 126.1 (C), 124.3 (5-CH), 123.8 (C), 123.5 (7-CH), 120.2 (3-CH); *m/z* (EI⁺): 251 (*M*⁺, 100), 205 (35).

6.2.3. 6-Amino-5-cyanoquinoline (144)

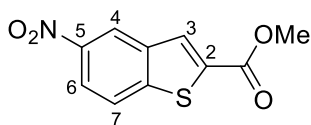


Chemical Formula: C₁₀H₇N₃

Mr: 169.06

According to a modified procedure,^{268,269} 6-nitroquinoline (0.50 g, 2.85 mmol) was added to a solution of ethyl cyanoacetate (0.91 mL, 8.61 mmol) and KOH (0.97 g, 17.0 mmol) in DMF (8.7 mL) and stirred for 64 h. The volatiles were then removed *in vacuo* and the residues taken up in aqueous NaOH solution (5%; 12 mL) and heated to reflux for 3 h. Once cooled, the reaction mixture was extracted into CHCl₃ (3 x 15 mL), the organic extracts combined, dried (MgSO₄), filtered and evaporated. Purification by flash column chromatography on SiO₂, eluting with CH₂Cl₂ to CH₂Cl₂-MeOH (9:1), gave the *title compound* (0.35 g, 72%) as an orange solid, mp 181.2-182.8 °C (lit.²⁶⁸ 181 °C) (Found [ESI⁺]: 170.0711. C₁₀H₈N₃ [MH] requires 170.0713); IR (neat) $\nu_{\text{max}}/\text{cm}^{-1}$: 3391 (N-H str), 3337 (N-H str), 3159 (C-H str), 2199 (C≡N str), 1635 (N-H bend), 1615 (C=C str), 1337 (C-N str); ¹H NMR (500 MHz, CDCl₃) $\delta_{\text{H}}/\text{ppm}$: 8.74 (1H, d, *J* = 3 Hz, 2-CH), 8.24 (1H, d, *J* = 8 Hz, 4-CH), 8.06 (1H, d, *J* = 9 Hz, 8-CH), 7.47 (1H, m, 3-CH), 7.15 (1H, d, *J* = 9 Hz, 7-CH), 4.88 (2H, br. s, NH₂); ¹³C NMR (126 MHz, CDCl₃) $\delta_{\text{C}}/\text{ppm}$: 150.3 (C), 147.7 (2-CH), 142.4 (C), 136.0 (8-CH), 131.2 (4-CH), 128.9 (C), 123.4 (3-CH), 120.3 (7-CH), 116.1 (CN), 86.9 (5-C); *m/z* (EI⁺): 169 (*M*⁺, 100).

6.2.4. Methyl 5-nitrobenzo[*b*]thiophene-2-carboxylate (162)



Chemical Formula: C₁₀H₇NO₄S

Mr: 237.23

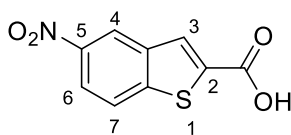
6.2.4.1. Conductive synthesis.

Based upon the procedure by Deng *et al.*,³⁵⁰ methyl thioglycolate (0.48 mL, 5.4 mmol) and K₂CO₃ (0.89 g, 6.5 mmol) were added sequentially to a solution of 2-chloro-5-nitrobenzaldehyde (1.01 g, 5.4 mmol) in DMF (6.5 mL), and stirred at RT for 17 h. The reaction was then quenched with iced water and the precipitate was isolated by vacuum filtration and dried in air to give the *title compound* (1.22 g, 95%) as an off-white solid, mp 213.3-217.6 °C (lit.³⁵¹ mp 213-215) (Found [FTMS⁺]: 255.0435. C₁₀H₁₁O₄N₂S [MNH₄⁺] requires 255.0434); IR (neat) ν_{max} /cm⁻¹: 3093 (C-H str), 1701 (C=O str), 1528 (N-O str), 1439 (C-C str), 1342 (N-O str), 1302 (C-O str); ¹H NMR (500 MHz, CDCl₃) δ_{H} /ppm: 8.79 (1H, d, *J* = 2 Hz, 4-CH), 8.32 (1H, dd, *J* = 9, 2 Hz, 6-CH), 8.20 (1H, s, 3-CH), 8.01 (1H, d, *J* = 9 Hz, 7-CH), 4.00 (3H, s, Me); ¹³C NMR (125 MHz, CDCl₃) δ_{C} /ppm: 162.2 (C), 147.4 (C), 145.9 (C), 138.3 (C), 137.2 (C), 130.7 (3-CH), 123.6 (7-CH), 121.2 (9-CH), 120.9 (7-CH), 52.9 (Me); *m/z* (EI⁺): 237 (*M*⁺, 100), 206 (64), 160 (27).

6.2.4.2. Microwave-assisted synthesis.

A mixture of 2-chloro-5-nitrobenzaldehyde (0.75 g, 4.0 mmol), methyl thioglycolate (0.45 mL, 5 mmol) and K₂CO₃ (0.67 g, 4.8 mmol) in DMF (4.5 mL) was irradiated at 90 °C for 15 min in a pressure-rated glass vial (35 mL) using a CEM Discover microwave synthesizer by moderating the initial power (100 W). After cooling in a flow of compressed air, the crystallised solid was poured into water and the solid filtered off under reduced pressure, washed with water and dried in air to give the *title compound* (0.84 g, 88%) as an off-white solid, mp 216.8-218.5 °C (lit.³⁵¹ 211-212), with identical spectroscopic data.

6.2.5. 5-Nitrobenzo[*b*]thiophene-2-carboxylic acid (**167**)



Chemical Formula: C₉H₅NO₄S

Mr: 223.21

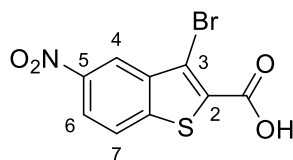
6.2.5.1. Conductive synthesis.

According to a modified procedure,³⁵² a solution of aqueous NaOH (1 M; 5 mL, 5 mmol) was added to a solution of methyl 5-nitrobenzo[*b*]thiophene-2-carboxylate (**162**) (0.40 g, 1.7 mmol) in MeOH (5.5 mL) and heated to reflux for 3 h. After cooling to RT the solution was acidified with 1 M HCl, the solid isolated by vacuum filtration and dried in air to give the *title compound* (0.36 g, 95%) as an off-white powder, mp 241.4-242.7 °C (lit.³⁵³ 239-241), (Found [TOF MS ASAP+]: 224.0020. C₉H₅NO₄S [MH] requires 224.0018); IR (neat) $\nu_{\text{max}}/\text{cm}^{-1}$: 2844 (br. O-H str), 1670 (C=O str), 1600 (C-C str), 1511 (N-O str), 1344 (N-O str), 1313 (C-O str); ¹H NMR (500 MHz, MeOH-*d*₄) $\delta_{\text{H}}/\text{ppm}$: 8.87 (1H, d, *J* = 2 Hz, 4-CH), 8.30 (1H, dd, *J* = 9, 2 Hz, 6-CH), 8.24 (1H, s, 3-CH), 8.15 (1H, d, *J* = 9 Hz, 7-CH); ¹³C NMR (125 MHz, MeOH-*d*₄) $\delta_{\text{C}}/\text{ppm}$: 164.8 (C), 148.9 (5-C), 147.7 (C), 140.3 (C), 140.0 (C), 132.0 (3-CH), 125.1 (7-CH), 122.3 (4-CH), 121.9 (6-CH); *m/z* (EI+): 223 (*M*⁺, 100), 195 (38), 149 (37).

6.2.5.2. Microwave-assisted synthesis.

A mixture of methyl 5-nitrobenzo[*b*]thiophene-2-carboxylate (**162**) (0.20 g, 0.84 mmol), aqueous NaOH solution (1M; 2.5 mL) and MeOH (3.5 mL) was irradiated at 100 °C for 3 min in a pressure-rated glass vial (10 mL) using a CEM Discover microwave synthesizer by moderating the initial power (100 W). After cooling in a flow of compressed air, the crystallised reaction mixture was diluted with water, acidified with 1 M HCl and the solid filtered under reduced pressure, washed with water and dried in air to give the *title compound* (0.16 g, 94 %) as an off-white powder, mp 241.3-242.1 °C, with identical spectroscopic data.

6.2.6. 3-Bromo-5-nitrobenzo[*b*]thiophene-2-carboxylic acid (**168**)

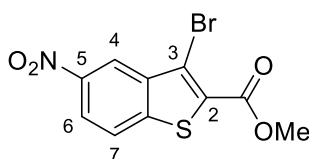


Chemical Formula: $C_9H_4BrNO_4S$

Mr: 302.10

According to a modified procedure,¹⁶⁰ bromine (1.4 mL, 27 mmol) was added portion-wise to a solution of 5-nitrobenzo[*b*]thiophene-2-carboxylic acid (**167**) (1.0 g, 4.5 mmol) and anhydrous NaOAc (1.13 g, 13 mmol) in glacial AcOH (28 mL) under N_2 . A reflux condenser was fitted and the solution heated at 55 °C for 27 h. Once cooled to RT the solution was poured into iced water, the solid isolated by vacuum filtration and dried in air to give the *title compound* (1.02 g, 75%) as a yellow powder, mp 309.5-316.8 (lit.¹⁵² 307-309) (Found [TOF MS ASAP+]: 303.9126. $C_9H_5NO_4S^{79}Br$ [MH] requires 301.9123); IR (neat) ν_{max}/cm^{-1} : 2961 (br, O-H str), 1701 (C=O str), 1600 (C-C str), 1511 (N=O str), 1347 (N=O str), 1270 (C-O str), 620 (C-Br str); 1H NMR (500 MHz, MeOH- d_4) δ_H/ppm : 8.83 (1H, d, $J = 2$ Hz, 4-CH), 8.39 (1H, dd, $J = 9, 2$ Hz, 6-CH), 8.21 (1H, d, $J = 9$ Hz, 7-CH); m/z (EI+): 303 ($M^{81}Br^{*+}$, 98), 301 ($M^{79}Br^{*+}$, 96), 293 (17), 291 (13).

6.2.7. Methyl 3-bromo-5-nitrobenzo[*b*]thiophene-2-carboxylate (**164**)



Chemical Formula: $C_{10}H_6BrNO_4S$

Mr: 316.13

6.2.7.1. From 3-bromo-5-nitrobenzo[*b*]thiophene-2-carboxylic acid (**168**)

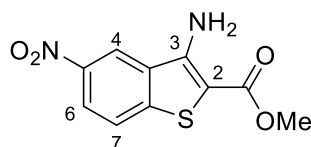
According to a modified method,^{160,354} iodomethane (0.46 mL, 7.4 mmol) was added to a solution of 3-bromo-5-nitrobenzo[*b*]thiophene-2-carboxylic acid (**168**) (1.12 g, 3.7 mmol) and K_2CO_3 (1.28 g, 9.2 mmol) in DMF (15 mL) and stirred at RT for 3 h. The reaction mixture was then

quenched with saturated aqueous NH_4Cl solution, poured into water and filtered under reduced pressure. The solid collected was washed with water and dried in air to give the *title compound* (1.09 g, 93%) as an off-white powder, mp 211.5-212.5 °C (lit.¹⁵² 211-212) (Found [TOF MS ASAP+]: 315.9279. $\text{C}_{10}\text{H}_7\text{NO}_4\text{S}^{79}\text{Br}$ [MH] requires 315.9279); IR (neat) $\nu_{\text{max}}/\text{cm}^{-1}$: 3101 (C-H str), 1691 (C=O str), 1600 (C-C str), 1514 (N-O str), 1347 (N-O str), 1089 (C-O str), 1052 (C-O str), 617 (C-Br str); ^1H NMR (500 MHz, CDCl_3) $\delta_{\text{H}}/\text{ppm}$: 8.89 (1H, d, $J = 2$ Hz, 4-CH), 8.37 (1H, dd, $J = 9, 2$ Hz, 6-CH), 7.99 (1H, d, $J = 9$ Hz, 7-CH), 4.02 (3H, s, Me); ^{13}C NMR (500 MHz, CDCl_3) $\delta_{\text{C}}/\text{ppm}$: 161.0 (C), 146.5 (5-C), 144.6 (C), 138.9 (C), 131.0 (C), 123.8 (7-CH), 122.2 (6-CH), 121.3 (4-CH), 115.6 (3-CH), 53.0 (Me); m/z (EI+): 317 ($M^{81}\text{Br}^{*+}$, 100), 315 ($M^{79}\text{Br}^{*+}$, 94), 286 (58), 284 (55).

6.2.7.2. From methyl 3-amino-5-nitrobenzothiophene-2-carboxylate (170).

Following the procedure of Iaroshenko *et al.*,²⁷⁰ CuBr_2 (0.94 g, 4.2 mmol) was added to a solution of *tert*-butyl nitrite (0.45 mL, 3.8 mmol) in dry MeCN (11 mL) cooled to 0 °C under argon. Methyl 3-amino-5-nitrobenzo[*b*]thiophene-2-carboxylate (**170**) (0.69 g, 2.7 mmol) was then added portion-wise and the solution kept at 0 °C until N_2 evolution stopped, at this point the reaction mixture was allowed to warm to RT and stirred for 2h. The reaction mixture was then poured into dilute HCl (10%, 25 mL). The aqueous mixture was then extracted with EtOAc (3 x 30 mL), dried (Na_2SO_4), filtered and evaporated *in vacuo* to give the *title compound* (0.86 g, 99%) as an orange solid, mp 212.3-213.0 °C (acetone) (lit.¹⁵² mp 211-212 °C), with identical spectroscopic data.

6.2.8. Methyl 3-amino-5-nitrobenzothiophene-2-carboxylate (170)



Chemical Formula: $\text{C}_{10}\text{H}_8\text{N}_2\text{O}_4\text{S}$

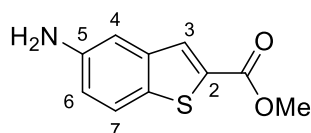
Mr: 252.25

6.2.8.1. Conductive method.

Based upon the procedure of Bridges *et al.*,³⁵⁵ NEt₃ (3.8 mL, 26 mmol) was added to a solution of 2-fluoro-5-nitro-benzonitrile (1.5 g, 9.0 mmol) and methyl thioglycolate (0.85 mL, 9.5 mmol) in DMSO (4.5 mL) under N₂ and heated to 100 °C for 2 h. With reaction completion confirmed by TLC analysis (hexanes:CH₂Cl₂ [50:50]), the reaction mixture was allowed to cool to RT, poured into iced water and the solid filtered off under reduced pressure and dried in air to give the *title compound* (2.16g, 95%) as an orange solid, mp 241.7-242.2 °C (lit.³⁵⁶ 244-246 °C), (Found [FTMS + p NSI full ms [120.00 – 2000.00]]: 253.0280. C₁₀H₉N₂O₄S [MH] requires 253.0278); IR (neat) $\nu_{\max}/\text{cm}^{-1}$: 3445 (N-H str), 3342 (N-H str), 3052 (C-H str aryl), 1681 (C=O str), 1572 (N-O str), 1432 (C-C str) 1328 (N-O str), 1276 (C-O str), 1093 (C-O str); ¹H NMR (DMSO-*d*₆, 500 MHz) $\delta_{\text{H}}/\text{ppm}$: 9.24 (1H, d, *J* = 2 Hz, 4-CH), 8.29 (1H, dd, *J* = 9, 2 Hz, 6-CH), 8.12 (1H, d, *J* = 9 Hz, 7-CH), 7.47 (2H, br. s., NH₂), 3.82 (3H, s, Me); ¹³C NMR (DMSO-*d*₆, 100 MHz) $\delta_{\text{C}}/\text{ppm}$: 164.3 (C), 149.6 (C), 144.9 (C), 144.5 (C), 131.4 (C), 124.3 (7-CH), 122.0 (6-CH), 119.4 (4-CH), 96.8 (3-C), 51.5 (Me); *m/z* (EI+): 252 (*M*⁺, 100), 219 (72).

6.2.8.2. Microwave-assisted synthesis. A mixture of 2-fluoro-5-nitro-benzonitrile (0.50g, 3.0 mmol), methyl thioglycolate (0.3 mL, 3.3 mmol) and NEt₃ (1.3 mL, 9.3 mmol) in DMSO (1.5 mL) under N₂ was irradiated at 130 °C for 11 min in a pressure-rated glass vial (10 mL) using a CEM Discover microwave synthesizer by moderating the initial power (200 W). After cooling in a flow of compressed air, the crystallised reaction mixture was poured into water and the solid filtered off under reduced pressure, washed with water and dried in air to give the *title compound* (0.71 g, 94%) as an orange solid, mp 243.4-244.1 °C (acetone), with identical spectroscopic data.

6.2.9. Methyl 5-aminobenzo[*b*]thiophene-2-carboxylate (158)

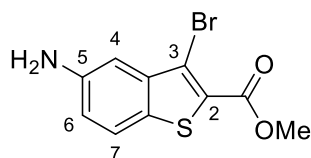


Chemical Formula: C₁₀H₉NO₂S

Mr: 207.25 According to a modified procedure,³⁵⁷ SnCl₂·2H₂O (7.18 g, 32 mmol) in EtOH (31 mL) and conc. HCl (10 M; 31 mL) was added to a solution of methyl 5-nitrobenzo[*b*]thiophene-2-

carboxylate (**162**) (1.50 g, 6.3 mmol) in EtOH (47 mL) and heated to reflux for 3 h. Once cooled to RT, the reaction mixture was diluted with water, slowly basified with saturated aqueous NaHCO₃ solution, extracted with Et₂O (3 x 40 mL). The organic extracts were combined, dried (Na₂SO₄), filtered and evaporated *in vacuo* to give the *title compound* (1.22g, 93%) as a yellow solid, mp 172.8-174.4 °C (Found [ESI⁺]: 208.0428. C₁₀H₁₀NO₂S [MH] requires 208.0427); IR (neat) $\nu_{\max}/\text{cm}^{-1}$: 1658 (C=O str), 1589 (N-H bend), 1449 (C-C str), 1252 (C-N str), 1018 (C-O str), 919 (N-H wag); ¹H NMR (500 MHz, DMSO-*d*₆) δ_{H} /ppm: 7.92 (1H, s, 3-CH), 7.65 (1H, d, *J* = 9 Hz, 7-CH), 7.06 (1H, d, *J* = 1 Hz 4-CH), 6.90 (1H, dd, *J* = 9, 1 Hz, 6-CH), 5.25 (2H, s, NH₂), 3.85 (3H, s, Me); ¹³C NMR (126 MHz, DMSO-*d*₆) δ_{C} /ppm: 162.6 (C), 146.7 (C), 139.8 (C), 132.1 (2-C), 130.0 (3-CH), 129.5 (5-C), 122.9 (7-CH), 117.9 (6-CH), 107.3 (4-CH), 52.3 (Me); *m/z* (EI⁺): 207 (*M*⁺, 100), 176 (45), 148 (30).

6.2.10. Methyl 5-amino-3-bromobenzo[b]thiophene-2-carboxylate (**165**)



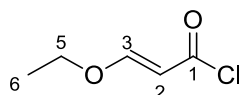
Chemical Formula: C₁₀H₈BrNO₂S

Mr: 286.15

According to a modified method,³⁵⁷ SnCl₂.2H₂O (3.36 g, 14.9 mmol) was taken up in EtOH (14 mL) and conc. HCl (10 M; 13 mL) and added to a solution of methyl 3-bromo-5-nitrobenzo[b]thiophene-2-carboxylate (**164**) (0.94 g, 3.0 mmol) in EtOH (15 mL), and heated to reflux for 3.5 h. Once cooled the solution was diluted with water, slowly basified with saturated aqueous Na₂CO₃ solution and extracted with Et₂O (3 x 40 mL). The organic extracts were combined, dried (Na₂SO₄), filtered and evaporated *in vacuo* to give the *title compound* (0.83 g, 97%) as a yellow solid, mp 147.8-150.7 °C (lit.¹⁵² 211-212) (Found [ESI⁺]: 285.9529. C₁₀H₁₀⁷⁹BrNO₂S [MH] requires 285.9532); IR (neat) $\nu_{\max}/\text{cm}^{-1}$: 3419 (N-H str), 3328 (N-H str), 1693 (C=O str), 1604 (N-H bend), 1506 (C-C str), 1286 (C-N str), 1087 (C-O str), 804 (N-H bend), 623 (C-Br str); ¹H NMR (500 MHz, DMSO-*d*₆): 7.70 (1H, d, *J* = 9 Hz, 7-CH), 7.04 (1H, d, *J* = 1 Hz, 4-CH),

6.97 (1H, dd, $J = 9, 1$ Hz, 6-CH), 5.33 (2H, br. s, NH₂), 3.87 (3H, s, Me); ¹³C NMR (126 MHz, DMSO-*d*₆): 161.2 (C), 147.8 (C), 139.3 (C), 126.3 (5-C), 123.4 (7-CH), 119.1 (6-CH), 112.9 (3-C), 105.7 (4-CH), 52.5 (Me) one signal not observed; m/z (EI⁺): 287 ($M^{81}\text{Br}^{*+}$, 100), 285 ($M^{79}\text{Br}^{*+}$, 99), 256 (34), 254 (35).

6.2.11. (2*E*)-3-Ethoxyprop-2-enoyl chloride

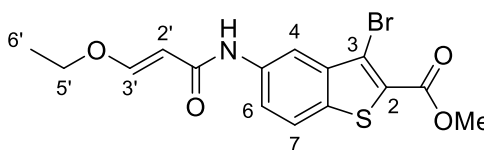


Chemical Formula: C₅H₇ClO₂

Mr: 134.01

Oxalyl chloride (0.25 mL, 2.9 mmol) was added dropwise to a solution of (2*E*)-3-ethoxyprop-2-enoic acid (0.15 g, 1.3 mmol) and catalytic DMF in dry CH₂Cl₂ (3.3 mL) at 0 °C, and the solution allowed to warm to RT over 2.5 h. Volatiles were removed *in vacuo* to give the title compound (0.17 g, 98%) and used crude in the next step. ¹H NMR (500 MHz, CDCl₃) δ_H/ppm: 7.79 (1H, d, $J = 12$ Hz, 2-CH), 5.52 (1H, d, $J = 12$ Hz, 3-CH), 4.06 (2H, q, $J = 7$ Hz, 5-CH₂), 1.41 (3H, t, $J = 7$ Hz, 6-CH₃) matches literature spectral data.³⁵⁸

6.2.12. Methyl 3-bromo-5-{[(2*E*)-3-ethoxyprop-2-enoyl]amino} benzo[*b*]thiophene-2-carboxylate (171)



Molecular Formula: C₁₅H₁₄BrNO₄S

Mr: 384.24

6.2.12.1. Table 2, entry 1.

(2*E*)-3-Ethoxyprop-2-enoic acid (30 mg, 0.26 mmol) was added to a solution of methyl 5-amino-3-bromobenzo[*b*]thiophene-2-carboxylate (**165**) (70 mg, 0.24 mmol), HOBT.H₂O (40 mg, 0.29

mmol), EDCI.HCl (56 mg, 0.29 mmol) and DIEA (0.1 mL, 0.61 mmol) in DMF (2.2 mL) under N₂, and the solution was stirred at RT for 24 h. Volatiles were then removed *in vacuo* and residues taken up the CH₂Cl₂ and washed with brine (3 x 15 mL), dried (Na₂SO₄), filtered and evaporated. Purification by flash column chromatography on SiO₂ (dry-load), gradient eluting with CH₂Cl₂ to EtOAc-CH₂Cl₂ (10:90), gave the *title compound* (38 mg, 40%) as a brown solid, mp 205.7-206.8 °C (Found [ESI+]: 383.9885. C₁₅H₁₅⁸¹BrNO₄S [MH] requires 385.9885); IR (neat) ν_{max} /cm⁻¹: 3263 (N-H str), 2956 (C-H str), 1719 (C=O str), 1672 (C=C str), 1598 (C-C str), 1202 (C-O str), 1138 (C-O str); ¹H NMR (500 MHz, DMSO-*d*₆) δ_{H} /ppm: 10.07 (1H, s, NH), 8.48 (1H, s, 4-CH), 8.02 (1H, d, *J* = 9 Hz, 7-CH), 7.73 (1H, d, *J* = 8 Hz, 6-CH), 7.54 (1H, d, *J* = 12 Hz, 2'-CH), 5.56 (1H, d, *J* = 12 Hz, 3'-CH), 3.98 (2H, q, *J* = 7 Hz, 5'-CH₂), 3.90 (3H, s, Me), 1.29 (3H, t, *J* = 7 Hz, 6'-CH₃); *m/z* (EI+): 385 (*M*⁸¹Br⁺⁺, 35), 383 (*M*⁷⁹Br⁺⁺, 34), 287 (96), 285 (95), 99 (100), 71 (90).

6.2.12.2. Table 2, Entry 2.

According to a modified procedure,²⁷³ catalytic DMAP was added to a solution of methyl 5-amino-3-bromobenzo[*b*]thiophene-2-carboxylate (**165**) (69 mg, 0.24 mmol), (2*E*)-3-ethoxyprop-2-enoic acid (31 mg, 0.26 mmol) and EDCI.HCl (95 mg, 0.5 mmol) in pyridine (0.05 mL) and DMF (0.1 mL) and stirred at RT for 17 h. Solution was then diluted with EtOAc (50 mL), washed with aqueous HCl solution (10%; 3 x 40 mL), saturated aqueous NaHCO₃ solution (3 x 40 mL) and brine (2 x 40 mL), dried (Na₂SO₄), filtered and evaporated *in vacuo*. Purification by flash column chromatography on SiO₂ (dry-load), gradient eluting with Et₂O-light petroleum (50:50) to (20:80) to give the *title compound* (9.4 mg, 10%) as a brown solid, with identical spectroscopic data.

6.2.12.3. Table 2, Entry 3. Following the procedure of Boger *et al.*,²⁷³ (2*E*)-3-ethoxyprop-2-enoic acid (41 mg, 0.35 mmol) was added to a solution of methyl 5-amino-3-bromobenzo[*b*]thiophene-2-carboxylate (**165**) (71 mg, 0.24 mmol), EDCI.HCl (94 mg, 0.49 mmol), pyridine (50 μ L, 0.62 mmol), DMAP (60 mg, 0.40 mmol) in DMF (1.25 mL) and stirred at room temperature for 22 h. Purification by the above procedure gave the *title compound* (1.0 mg, 10%) with identical spectroscopic data.

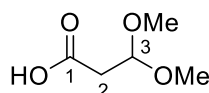
6.2.12.4. Table 2, Entry 4.

(2*E*)-3-ethoxyprop-2-enoic acid (35 mg, 0.29 mmol) was added to a solution of methyl 5-amino-3-bromobenzo[*b*]thiophene-2-carboxylate (**165**) (70 mg, 0.24 mmol), EDCI.HCl (92 mg, 0.48 mmol) and DMAP (33 mg, 0.27 mmol) in pyridine (1.25 mL, 16 mmol), and stirred at RT for 22 h. Purification by the above methods gave the *title compound* (14 mg, 15%) with identical spectroscopic data.

6.2.12.5. Table 2, entry 5.

Catalytic DMAP was added to a solution of methyl 5-amino-3-bromobenzo[*b*]thiophene-2-carboxylate (**165**) (50 mg, 0.17 mmol) in pyridine (0.25 mL) cooled to 0 °C, to this (2*E*)-3-ethoxyprop-2-enoyl chloride (34 mg, 0.25 mmol) in dry CH₂Cl₂ was added. The solution was allowed to warm to RT and stirred for 65 h. Volatiles were removed *in vacuo* and the residues taken up in CH₂Cl₂, washed with aqueous HCl solution (1 M, 10 mL), saturated aqueous NaHCO₃ solution (1 x 10 mL) and brine (1 x 10 mL), dried (MgSO₄), filtered and evaporated *in vacuo*. Purification by flash column chromatography on SiO₂ (dry-load), gradient eluting with CH₂Cl₂ to EtOAc-CH₂Cl₂ (20:80). No discernible product formation.

6.2.13. 3,3-Dimethoxypropanoic acid (**172**)

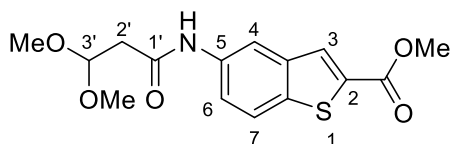


Chemical Formula: C₅H₁₀O₄

Mr: 134.13

Following the procedure of Edwankar *et al.*,³⁵⁹ methyl 3,3-dimethoxypropnaoate (**173**) (0.53 g, 3.6 mmol) in a solution of NaOH (3.9 M; 0.18 g in 1.14 mL H₂O) was stirred at 110 °C for 30 min, with reaction completion confirmed by TLC analysis (EtOAc-hexanes [50:50]). The solution was allowed to come to RT, cooled to 0 °C and carefully neutralized with cold 6 M HCl, then acidified to pH 3-4 at RT. The solution was then extracted with EtOAc (2 x 10 mL) and CH₂Cl₂ (1 x 10 mL), acidifying the aqueous phase after each extraction. The organic extracts were combined, dried (MgSO₄), filtered and evaporated *in vacuo* to give the title compound (0.36 g, 79%) as a clear, colourless oil, IR (neat) $\nu_{\text{max}}/\text{cm}^{-1}$: 2940 (O-H str) 1714 (C=O str), 1118 (C-O str acid), 1046 (C-O str, ether); ¹H NMR (500 MHz, CDCl₃) $\delta_{\text{H}}/\text{ppm}$: 4.84 (1H, t, *J* = 6 Hz, 3-CH), 3.40 (6H, s, OMe), 2.72 (2H, d, *J* = 6 Hz, 2-CH₂); ¹³C NMR (126 MHz, CDCl₃) $\delta_{\text{C}}/\text{ppm}$: 175.0 (1-C), 101.0 (3-CH), 53.6 (OMe), 38.7 (2-CH₂); *m/z* (EI⁺): 133 ([*M*⁺-H], 25) 103 ([*M*⁺-OMe], 65), 75 (100), 61 (97). Data matches literature.³⁶⁰

6.2.14. Methyl 5-(3,3-dimethoxypropanamido)benzo[*b*]thiophene-2-carboxylate (174)



Chemical Formula: C₁₅H₁₇NO₅S

Mr: 323.36

6.2.14.1. Conductive synthesis

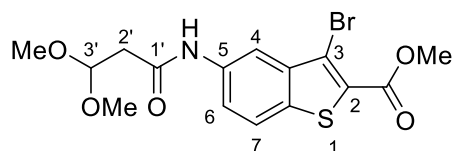
EDCI.HCl (0.12 g, 0.64 mmol), HOBt.H₂O (0.09 g, 0.64 mmol) and DIEA (0.22 mL, 1.3 mmol) were added to a solution of methyl 5-aminobenzo[*b*]thiophene-2-carboxylate (**158**) (0.11 g, 0.53 mmol) and 3,3-dimethoxypropanoic acid (**172**) (0.08 g, 0.41 mmol) in DMF (4.6 mL) under N₂, and stirred at RT for 24 h. Volatiles were removed under reduced pressure and the residues dissolved in CH₂Cl₂ (15 mL) and washed with brine (3 x 15 mL), dried (MgSO₄), filtered and evaporated *in vacuo*. Purification by flash column chromatography on SiO₂ (dry-load), gradient eluting with CH₂Cl₂ to EtOAc-CH₂Cl₂ (50:50), gave the *title compound* (0.10 g, 59%) as a pale brown solid, (Found [ESI⁺]: 346.0686. C₁₅H₁₇NNaO₅S [MNa] requires 346.0720); IR (neat) ν_{max} /cm⁻¹: 3262 (N-H str), 2948 (C-H str) 1723 (C=O str), 1651 (C=O str), 1252 (C-N str), 1053 (C-O str); ¹H NMR (500 MHz, CDCl₃) δ_{H} /ppm: 8.25 (1H, d, *J* = 1 Hz, 4-CH), 8.22 (1H, br. s, NH), 8.01 (1H, s, 3-CH), 7.78 (1H, d, *J* = 8 Hz, 7-CH), 7.44 (1H, dd, *J* = 8, 1 Hz, 6-CH), 4.78 (1H, t, *J* = 5 Hz, 3'-CH), 3.95 (3H, s, OMe), 3.48 (6H, s, 3'-OMe), 2.77 (2H, d, *J* = 5 Hz, 2'-CH₂); ¹³C NMR (126 MHz, CDCl₃) δ_{C} /ppm: 167.3 (1'-C), 163.1 (C), 139.3 (C), 137.9 (C), 135.3 (C), 134.5 (C), 130.5 (3-CH), 123.0 (4-CH), 120.4 (6-CH), 115.9 (7-CH), 102.1 (3'-CH), 54.4 (C(OMe)₂), 52.5 (OMe), 42.0 (2'-CH₂).

6.2.14.2. Microwave-assisted synthesis.

EDCI.HCl (73 mg, 0.38 mmol), HOBt.H₂O (53 mg, 0.39 mmol) and DIEA (0.1 mL, 0.61 mmol) were added to a solution of 3,3-dimethoxypropanoic acid (**172**) (41 mg, 0.30 mmol) and methyl 5-aminobenzo[*b*]thiophene-2-carboxylate (**158**) (50 mg, 0.24 mmol) in DMF (2.5 mL) under N₂ and irradiated at 78 °C for 1 h in a pressure-rated glass vial (10 mL) at using a CEM Discover

microwave synthesizer by moderating the initial power (200 W). After cooling in a flow of compressed air, the volatiles were removed and the residues dissolved in EtOAc and CH₂Cl₂ (20 mL) and washed with water (3 x 15 mL), brine (2 x 15 mL), dried (MgSO₄), filtered and evaporated *in vacuo*. Purification by flash column chromatography on SiO₂ (dry-load), gradient eluting with EtOAc-CH₂Cl₂ (5:95) to (50:50), gave the *title compound* (56 mg, 72%) as a pale brown solid, with identical spectroscopic data.

6.2.15. Methyl 3-bromo-5-(3,3-dimethoxypropanamido)benzo[*b*]thiophene-2-carboxylate (175)



Chemical Formula: C₁₅H₁₆BrNO₅S

Mr: 402.26

6.2.15.1. Conductive synthesis.

EDCI.HCl (1.58 g, 8.2 mmol), HOBT.H₂O (1.06 g, 7.8 mmol) and DIEA (2.2 mL, 13.4 mmol) were added to a solution of 3,3-dimethoxypropanoic acid (**172**) (0.74 g, 5.5 mmol) and methyl 5-amino-3-bromobenzo[*b*]thiophene-2-carboxylate (**165**) (1.49 g, 5.21 mmol) in DMF (50 mL) under N₂ and the solution was stirred at 25 °C for 26 h. Volatiles were removed and the residues taken up in EtOAc, washed with brine (5 x 15 mL), dried (Na₂SO₄), filtered and evaporated *in vacuo*. Purification by flash column chromatography on SiO₂ (dry-load), gradient eluting with EtOAc-CH₂Cl₂ (5:95) to (15:75), gave the *title compound* (1.24 g, 59%) as a pale brown solid, mp 161.9-162.9 °C (Found [ESI⁺]: 425.9808. C₁₅H₁₆⁸¹BrNNaO₅S [MNa] requires 425.9810); IR (neat) ν_{max} /cm⁻¹: 3369 (N-H str), 2950 (C-H str), 1705 (C=O str), 1572 (N-H str), 1508 (C-C str), 1233 (C-O str), 1066 (C-O str), 981 (C-H bend); ¹H NMR (500 MHz, DMSO-*d*₆) δ_{H} /ppm: 10.31 (1H, s, NH), 8.47 (1H, s, 4-CH), 8.04 (1H, d, *J* = 8 Hz, 7-CH), 7.71 (1H, d, *J* = 8 Hz, 6-CH), 4.83 (1H, t, *J* = 6 Hz, 3'-CH), 3.90 (3H, s, OMe), 3.30 (6H, s, OMe), 2.69 (2H, d, *J* = 6 Hz, 2'-CH₂); ¹³C NMR (125 MHz,

DMSO-*d*₆) δ_c /ppm: 167.7 (1'-C), 160.9 (C), 138.4 (C), 137.7 (C), 133.1 (C), 127.7 (C), 123.7 (7-CH), 121.2 (6-CH), 114.0 (5-C), 113.4 (4-CH), 101.8 (3'-CH), 53.2 (C(OMe)₂), 52.7 (OMe), 41.4 (2'-CH₂).

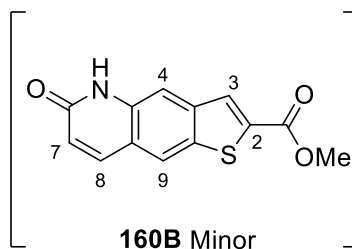
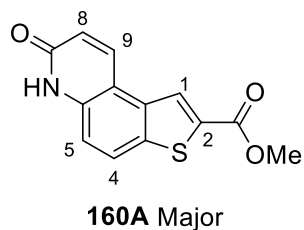
6.2.15.2. Microwave-assisted synthesis.

EDCI.HCl (107 mg, 0.56 mmol), HOBt.H₂O (70 mg, 0.52 mmol) and DIEA (0.15 mL, 0.92 mmol) were added to a solution of 3,3-dimethoxypropanoic acid (**172**) (57 mg, 0.42 mmol) and methyl 5-amino-3-bromobenzo[*b*]thiophene-2-carboxylate (**165**) (105 mg, 0.37 mmol) in DMF (3.5 mL) under N₂, and irradiated at 80 °C for 1 h in a pressure-rated glass vial (10 mL) using a CEM Discover microwave synthesizer by moderating the initial power (100 W). After cooling in a flow of compressed air, the volatiles were removed *in vacuo* and the residue was taken up in EtOAc and CH₂Cl₂ (20 mL) and washed with water (3 x 15 mL) and brine (2 x 15 mL), dried (Na₂SO₄), filtered and evaporated *in vacuo*. Purification by flash column chromatography on SiO₂ (dry-load), gradient eluting with EtOAc-CH₂Cl₂ (10:90) to (50:50), gave the title compound (79 mg, 56%) as an off-white solid, with identical spectroscopic data.

6.2.15.3. Microwave synthesis, using COMU reagent

DIEA (0.20 mL, 1.22 mmol) was added to a solution of methyl 5-amino-3-bromobenzo[*b*]thiophene-2-carboxylate (**165**) (0.15 g, 0.60 mmol), COMU (0.39 g, 0.92 mmol) and 3,3-dimethoxypropanoic acid (**172**) (0.11 g, 0.80 mmol) in DMF (4 mL) under N₂, and irradiated at 120 °C for 30 min in a pressure-rated glass vial (10 mL) using a CEM Discover microwave synthesizer through modulation of the initial power (120 W). After cooling in a flow of compressed air, the volatiles were removed *in vacuo* and the residue was taken up in EtOAc (20 mL) and washed with water (1 x 20 mL) and brine (3 x 30 mL), dried (Na₂SO₄), filtered and evaporated *in vacuo*. Purification by flash column chromatography on SiO₂ (dry-load), gradient eluting with CH₂Cl₂ to EtOAc-CH₂Cl₂ (50:50), to give the *title compound* (0.22 g, 89%) as a brown solid, with identical spectroscopic data.

6.2.16. Methyl 7-oxo-6,7-dihydrothieno[3,2-*f*]quinoline-2-carboxylate (**160A** and **160B**)

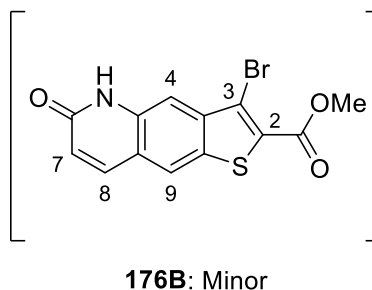
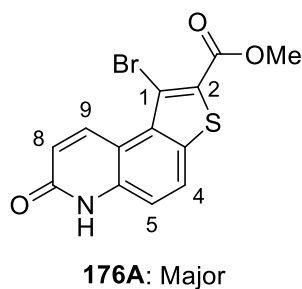


Chemical Formula: $C_{13}H_9NO_3S$

Mr: 259.28

Conc. H_2SO_4 (1.4 mL) was cooled to 0 °C and added to methyl 5-(3,3-dimethoxypropanamido)benzo[*b*]thiophene-2-carboxylate (**174**) (90 mg, 0.28 mmol) and stirred at RT for 3 h. The solution was then poured into iced water and the precipitate isolated by vacuum filtration, washed with water and dried in air to give a white solid (105 mg, >100%, wet). The 1H NMR spectrum confirmed a mixture of two regioisomers; the title compound (88%) and a side product (12%). This product was used crude in the next step. (Found [ESI⁺]: 260.0373. $C_{13}H_{10}NO_3S$ [MH] requires 260.0376); IR (neat) ν_{max}/cm^{-1} : 2842 (OH str), 1723 (C=O str), 1651 (C=O str), 1514 (C-C str), 1221 (C-O str), 1071 (N-H str); 1H NMR (500 MHz, $DMSO-d_6$) δ_H/ppm : (**160A**) 8.75 (1H, s, 1-CH), 8.64 (1H, d, $J = 9$ Hz, 9-CH), 8.16 (1H, d, $J = 9$, 4-CH), 7.51 (1H, d, $J = 9$ Hz, 5-CH), 6.63 (1H, d, $J = 9$ Hz, 8-CH), 3.91 (3H, br. s, Me); (**160B**): 8.38 (1H, s, 3-CH), 8.26 (1H, s, 4-CH), 7.99 (1H, d, $J = 10$ Hz, 8-CH), 7.87 (1H, s, 9-CH), 6.58 (1H, d, $J = 9$, 7-CH), 3.91 (3H, br. s, Me).

6.2.17. Methyl 1-bromo-7-oxo-6,7-dihydrothieno[3,2-*f*]quinoline-2-carboxylate (**176A** and **176B**)



Chemical Formula: $C_{13}H_8BrNO_3S$

Mr: 336.94

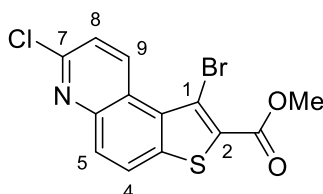
6.2.17.1. Using Methyl 3-bromo-5-{[(2*E*)-3-ethoxyprop-2-enoyl]amino} benzo[*b*]thiophene-2-carboxylate (**171**).

Conc. H₂SO₄ (2 mL) cooled to 0 °C was added to methyl 3-bromo-5-{[(2*E*)-3-ethoxyprop-2-enoyl]amino}benzo[*b*]thiophene-2-carboxylate (**171**) (72 mg, 0.19 mmol) and the solution allowed to warm to RT and stirred for 3 h. The solution was poured into iced water and the precipitate isolated by vacuum filtration, washed with water and dried in air to give a white solid (44 mg, 70%). The proton NMR indicated the presence of two regioisomers; the title compound (75%) and a side product (25%). Carried forward into next step with no purification. IR (neat) $\nu_{\text{max}}/\text{cm}^{-1}$: 1727 (C=O str), 1652 (C=O str), 1549 (C-C str), 1207 (C-O str), 1069 (C-) str; ¹H NMR (500 MHz, DMSO-*d*₆) $\delta_{\text{H}}/\text{ppm}$: (**176A**) 12.21 (1H, s, NH), 9.67 (1H, d, *J* = 10 Hz, 9-CH), 8.25 (1H, d, *J* = 9 Hz, 5-CH), 7.62 (1H, d, *J* = 9 Hz, 4-CH), 6.72 (1H, d, *J* = 10 Hz, 8-CH), 3.92 (3H, s, Me); (**176B**): 11.90 (1H, s, 5-NH), 8.45 (1H, s, 4-CH), 8.03 (1H, d, *J* = 10 Hz, 8-CH), 7.88 (1H, s, 9-CH), 6.63 (1H, d, *J* = 10 Hz, 7-CH), 3.92 (3H, s, Me); *m/z* (EI⁺): 339 (*M*⁸¹Br⁺⁺, 97), 337 (*M*⁷⁹Br⁺⁺, 93), 308 (46), 306 (43).

6.2.17.2. Using Methyl 3-bromo-5-(3,3-dimethoxypropanamido)benzo[*b*]thiophene-2-carboxylate (**174**).

Following the above method, **174** (75 mg, 0.19 mmol) was stirred with cooled conc. H₂SO₄ (2 mL), to give an off-white solid (55 mg, 87%). A mixture of products by ¹H NMR, title compound **176A** (65%), minor regioisomer **176B** (35%), ¹H NMR data matches above. Crude carried forward.

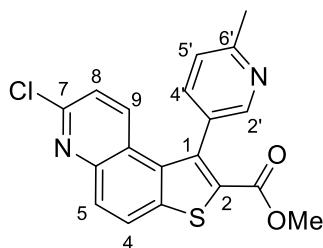
6.2.18. Methyl 1-bromo-7-chlorothieno[3,2-*f*]quinoline-2-carboxylate (**166**)



Chemical Formula: C₁₃H₇BrClNO₂S

Mr: 356.62 The crude mixture of methyl 1-bromo-7-oxo-6,7-dihydrothieno[3,2-*f*]quinoline-2-carboxylate (**176A**) and its regioisomer (**176B**) (40 mg, 0.12 mmol) was heated to reflux in POCl₃ (0.6 mL) for 2.5 h and then poured carefully into iced water, filtered, washed with water and dried in air. Purification by flash column chromatography on SiO₂ (dry-load), gradient eluting with light petroleum to Et₂O-light petroleum (10:90), gave the title compound (18 mg, 42%) as an off white solid, mp 211.8-223.6 °C (dec.) (Found [ESI⁺]: 357.9126. C₁₃H₈⁸¹Br³⁵ClNO₂S [MH] requires 357.9127); IR (neat) ν_{max} /cm⁻¹: 2922 (C-H str), 2853 (C-H str), 1731 (C=O str), 1490 (C-C str), 1212 (C-O str), 813 (C-Cl str); ¹H NMR (500 MHz, CDCl₃) δ_{H} /ppm: 10.18 (1H, d, *J* = 9 Hz, 9-CH), 8.09 (2H, m, 5-CH and 4-CH), 7.60 (1H, d, *J* = 9 Hz, 8-CH), 4.02 (3H, s, Me); ¹³C NMR (125 MHz, CDCl₃) δ_{C} /ppm: 161.4 (C), 150.2 (C), 147.9 (C), 139.8 (C), 133.5 (9-CH), 130.9 (C), 129.6 (CH), 128.6 (C), 124.9 (CH), 124.4 (C), 122.2 (8-CH), 113.5 (C), 52.8 (CH₃).

6.2.19. Methyl 7-chloro-1-(6-methylpyridin-3-yl)thieno[3,2-*f*]quinoline-2-carboxylate (**177**)



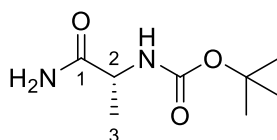
Chemical Formula: C₁₉H₁₃ClN₂O₂S

Mr: 368.84

According to a modified procedure,³⁶¹ a mixture of **166** (70 mg, 0.20 mmol), 6-methylpyridine-3-boronic acid (31 mg, 0.23 mmol), CsF (96 mg, 0.63 mmol) and PdCl₂(PPh₃)₂ (15 mg, 0.021 mmol) in anhydrous 1,4-dioxane (1.4 mL) under N₂ was irradiated at 140 °C for 30 min in a pressure-rated glass vial (10 mL) using a CEM Discover microwave synthesizer by moderating the initial power (200 W). After cooling in a flow of compressed air, the reaction mixture was poured into water, the solid filtered off under reduced pressure, washed with water and dried in air. Purification by flash column chromatography on SiO₂ (dry-load), gradient eluting with CH₂Cl₂ to EtOAc-CH₂Cl₂ (10:90), gave the *title compound* (13 mg, 18%) as an off white solid, mp 119.7-125.5 °C (Found [ESI⁺]: 369.0448. C₁₉H₁₄³⁵ClN₂O₂S [MH] requires 369.0465); IR (neat)

$\nu_{\max}/\text{cm}^{-1}$: 3295 (C-H str), 2925 (C-H str), 1720 (C=O str), 1554 (C-C str), 1050 (C-O str), 815 (C-Cl str); ^1H NMR (500 MHz, CDCl_3) $\delta_{\text{H}}/\text{ppm}$: 8.54 (1H, s, 2'-CH), 8.14 (1H, d, $J = 9$ Hz, 4-CH), 8.07 (1H, d, $J = 9$ Hz, 5-CH), 7.68 (1H, d, $J = 9$ Hz, 9-CH), 7.63 (1H, dd, $J = 8, 2$ Hz, 4'-CH), 7.40 (1H, d, $J = 8$ Hz, 5'-CH), 7.18 (1H, d, $J = 9$ Hz, 8-CH), 3.80 (3H, s, OMe), 2.75 (3H, s, Me); ^{13}C NMR (126 MHz, CDCl_3) $\delta_{\text{C}}/\text{ppm}$: 162.1 (C), 158.8 (6'-C), 149.8 (7-C), 148.7 (2'-CH), 147.9 (C), 141.3 (C), 140.2 (C), 136.9 (4'-CH), 133.6 (9-CH), 133.4 (C), 131.2 (C), 129.8 (C), 129.0 (5-CH), 125.1 (4-CH), 124.4 (C), 123.4 (5'-CH), 122.2 (8-CH), 52.5 (OMe), 24.5 (Me).

6.2.20. (*R*)-*tert*-Butyl-(1-amino-1-oxopropan-2-yl)carbamate (182)



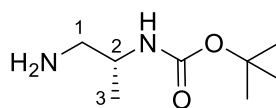
Chemical Formula: $\text{C}_8\text{H}_{16}\text{N}_2\text{O}_2$

Mr: 188.22

Method 1:³⁶²

Under N_2 , ethyl chloroformate (0.55 mL, 5.8 mmol) was added drop-wise to a stirred solution of Boc-D-alanine (1.0 g, 5.3 mmol) and NEt_3 (0.80 mL, 5.8 mmol) in dry THF (8.8 mL) at 0 °C. The reaction mixture was stirred at 0 °C for 45 min before addition of a solution of aqueous NH_3 (35%; 4 mL) in THF (1 mL). The resultant solution was stirred at 0 °C for 45 min, and then partitioned between water (20 mL) and EtOAc (30 mL) and the aqueous layer was further extracted with EtOAc (2 x 30 mL). The organic extracts were combined, washed with saturated aqueous NaHCO_3 solution (1 x 30 mL), brine (1 x 30 mL), aqueous HCl solution (1 M; 1 x 30 mL) and brine (2 x 30 mL), dried (Na_2SO_4), filtered and evaporated *in vacuo*. Purification by recrystallization from EtOAc and light petroleum gave the *title compound* (0.41 g, 41%) as colourless crystals, mp 125.8-126.9 °C (EtOAc) (lit.³⁶³ mp 120-121) (Found [ESI⁺]: 211.1060. $\text{C}_8\text{H}_{16}\text{N}_2\text{NaO}_3$ [MNa] requires 211.1053); IR (neat) $\nu_{\max}/\text{cm}^{-1}$: 3387 (N-H str), 3351 (N-H str), 3190 (N-H str), 2980 (C-H str), 1678 (C=O str), 1643 (C=O str), 1517 (N-H bend), 1320 (C-N str), 1244 (C-O str), 1164 (C-N str), 864 (N-H wag); ^1H NMR (500 MHz, CDCl_3) $\delta_{\text{H}}/\text{ppm}$: 6.25 (1H, br s, exch. D_2O , 1-NHH), 5.66 (1H, br s., exch. D_2O , 1-NHH), 5.09 (1H, br s, exch. D_2O , NH), 4.21 (1H, m, 2-CH), 1.45 (9H, s, CMe_3), 1.38 (3H, d, $J = 6$ Hz, 3-Me); ^{13}C NMR (126 MHz, CDCl_3) $\delta_{\text{C}}/\text{ppm}$: 175.5 (CONH_2), 155.5 (C), 80.1 (CMe_3), 49.7 (2-CH), 28.3 (CMe_3), 18.4 (3-Me).

6.2.21. *tert*-Butyl ([2*R*]-1-aminopropan-2-yl)carbamate (**137**)



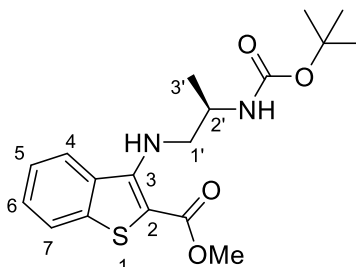
Chemical Formula: C₈H₁₈N₂O₂

Mr: 174.24

According to a modified method,³⁶⁴ a solution of Boc-D-Ala-OH (0.50 g, 2.64 mmol) and HOBT.H₂O (0.41 g, 3.0 mmol) in CH₂Cl₂ (20 mL) was cooled to 0 °C and EDCI.HCl (0.58 g, 3.0 mmol) added, the solution was allowed to warm to RT and stirred for 30 min. The solution was then cooled to 0 °C, aqueous NH₃ solution (18.1 M; 0.6 mL) was added drop-wise, stirred for 30 min at RT and the solids removed by filtration under reduced pressure. The filtrate was washed with water (1 x 20 mL) and brine (2 x 20 mL), dried (MgSO₄), filtered and evaporated *in vacuo*. Purification by flash column chromatography on SiO₂, gradient eluting with MeOH (3-7%) in CH₂Cl₂, gave the intermediate (*R*)-*tert*-butyl-(1-amino-1-oxopropan-2-yl)carbamate (**182**) (0.37g, 75%) as a white crystalline solid, mp 127.5-128.2 °C (lit.³⁶³ 120-121); with identical spectroscopic data.

According to a modified method,³⁶⁵ a solution of BH₃•SMe₂ in THF (2 M; 13.5 mL, 27 mmol) was added portion-wise to a solution of (*R*)-*tert*-butyl-(1-amino-1-oxopropan-2-yl)carbamate (**182**) (0.5 g, 2.7 mmol) in dry THF (9 mL) under N₂ at 0 °C. The reaction mixture was then allowed to warm to RT and stirred for 18 h, with reaction completion determined by TLC. The reaction mixture was concentrated *in vacuo* and the residue treated with MeOH (3 x 15 mL), stirring and concentrating to dryness *in vacuo*. Purification by SCX-2 ion exchange chromatography, gradient eluting with MeOH to 2 M NH₃ in MeOH, gave the *title compound* (0.39 g, 84%) as a colourless oil, (*R_f* 0.3; MeOH-CH₂Cl₂ [10:90]) (Found [ESI⁺]: 175.1443. C₈H₁₉N₂O₂ [*MH*] requires 175.1441); [α]_D²⁴ -5.7 (c 1.1, MeOH); IR (neat) ν_{max}/cm⁻¹: 2973 (C-H str), 1685 (C=O str), 1521 (N-H bend), 1247 (C-O str), 1165 (C-N str), 1045 (C-O str), 872 (N-H wag); ¹H NMR (500 MHz, CDCl₃) δ_H/ppm: 4.78 (1H, d, *J* = 7 Hz, *NHBoc*), 3.60 (1H, m, 2-CH), 2.70 (1H, m, 1-CHH), 2.59 (1H, m, 1-CHH), 1.40 (9H, s, CMe₃), 1.08 (3H, d, *J* = 7 Hz, 3-Me); ¹³C NMR (126 MHz, CDCl₃) δ_C/ppm: 155.7 (C), 79.1 (CMe₃), 48.6 (2-CH), 47.4 (1-CH₂), 28.4 (CMe₃), 18.5 (Me).

6.2.22. (R)-Methyl 3-((2-((tert-butoxycarbonyl)amino)propyl)amino)-benzo[*b*]thiophene-2-carboxylate (184)



Chemical Formula: C₁₈H₂₄N₂O₄S

Mr: 364.46

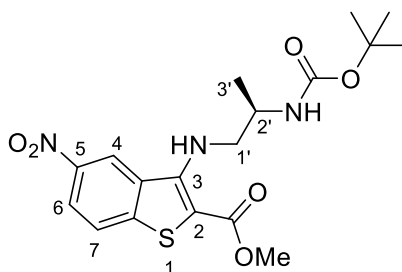
6.2.22.1. Conductive synthesis.

Under N₂, *tert*-butyl ([2*R*]-1-aminopropan-2-yl)carbamate (**137**) (70 mg, 0.37 mmol) was added to a stirred solution of methyl 3-bromobenzo[*b*]thiophene-2-carboxylate (100 mg, 0.37 mmol), Cs₂CO₃ (240 mg, 0.74 mmol), (±)-BINAP (23 mg, 0.037 mmol) and Pd(OAc)₂ (5 mg, 0.02 mmol) in dry toluene (1.2 mL) and heated to reflux for 22 h. Once cooled to RT, the reaction mixture was partitioned between water (15 mL) and Et₂O (15 mL) and the aqueous layer extracted with Et₂O (2 x 15 mL). The organic extracts were combined, dried (MgSO₄), filtered and evaporated *in vacuo*. Purification by flash column chromatography on SiO₂ (dry-load), gradient eluting with light petroleum to Et₂O-petroleum (75:25) gave the *title compound* (37 mg, 27%) as a gummy solid, IR (neat) $\nu_{\text{max}}/\text{cm}^{-1}$: 3368 (N-H str), 2957 (C-H str), 1704 (C=O str), 1652 (C=O str), 1516 (C-C str), 1286 (C-N str), 1235 (C-N str), 1165 (C-O str), 756 (N-H wag); ¹H NMR (500 MHz, CDCl₃) $\delta_{\text{H}}/\text{ppm}$: 8.09 (1H, d, *J* = 8 Hz, 4-CH), 7.71 (1H, d, *J* = 8 Hz, 7-CH), 7.42 (1H, t, *J* = 8 Hz, 6-CH), 7.31 (1H, t, *J* = 8 Hz, 5-CH), 4.66 (1H, br. s, NH), 3.99 (1H, m, 2'-CH), 3.88 (3H, s, OMe), 3.80 (1H, m, 1'-CHH), 3.72 (1H, m, 1'-CHH), 1.42 (9H, s, CMe₃), 1.28 (3H, d, *J* = 6 Hz, 3'-Me); ¹³C NMR (CDCl₃, 126 MHz) $\delta_{\text{C}}/\text{ppm}$: 166.2 (C), 155.3 (C), 152.0 (C), 140.6 (C), 136.9 (C), 131.9 (C), 127.7 (6-CH), 124.9 (4-CH), 123.7 (5-CH), 123.5 (7-CH), 121.2 (CMe₃), 51.5 (OMe), 47.0 (2'-CH), 29.7 (1'-CH₂), 28.3 (CMe₃), 18.5 (3'-Me); *m/z* (EI⁺): 364 (*M*⁺, 62), 220 (85), 188 (100).

6.2.22.2. Microwave-assisted synthesis.

Under N₂, *tert*-butyl ([2*R*]-1-aminopropan-2-yl)carbamate (**137**) in dry toluene (55 mg, 0.6 mL, 0.32 mmol) was added to a stirred solution of methyl 3-bromobenzo[*b*]thiophene-2-carboxylate (86 mg, 0.32 mmol), Cs₂CO₃ (145 mg, 0.44 mmol), (±)-BINAP (20 mg, 0.032 mmol) and Pd(OAc)₂ (3.5 mg, 0.02 mmol) in dry toluene (1.1 mL) was irradiated at 150 °C for 75 min in a pressure-rated glass vial (10 mL) using a CEM Discover microwave synthesizer by moderating the initial power (200 W). After cooling in a flow of compressed air, the reaction mixture was partitioned between water (10 mL) and Et₂O (10 mL) and the aqueous layer extracted with Et₂O (3 x 15 mL). The organic extracts were combined, dried (MgSO₄), filtered and evaporated *in vacuo*. Purification by flash column chromatography on SiO₂ (dry-load), gradient eluting with light petroleum to Et₂O, gave the *title compound* (45 mg, 60%) as a gummy colourless solid, with identical spectroscopic data.

6.2.23. (R)-Methyl 3-((2-((*tert*-butoxycarbonyl)amino)propyl)amino)-5-nitrobenzo[*b*]thiophene-2-carboxylate (**185**)



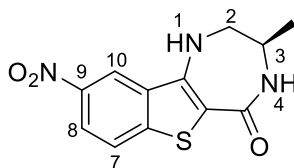
Chemical Formula: C₁₈H₂₃N₃O₆S

Mr: 409.46

According to a modified procedure,²⁷⁶ *tert*-butyl ([2*R*]-1-aminopropan-2-yl)carbamate (**137**) (35 mg, 0.20 mmol) was added to a mixture of methyl 3-bromo-5-nitrobenzo[*b*]thiophene-2-carboxyaldehyde (**164**) (50 mg, 0.16 mmol), Cs₂CO₃ (73 mg, 0.22 mmol), (±)-BINAP (13 mg, 0.02 mmol) and Pd(OAc)₂ (2.0 mg, 2.0 μmol) in dry toluene (1.0 mL) under N₂ and irradiated at 150 °C for 75 min in a pressure-rated glass vial (10 mL) using a CEM Discover microwave synthesizer by moderating the initial power (200 W). After cooling in a flow of compressed air, the reaction mixture was taken up in water (20 mL) and extracted with EtOAc (3 x 30 mL). The organic extracts were combined, washed with brine (1 x 30 mL), dried (Na₂SO₄), filtered and evaporated *in vacuo*.

Purification by flash column chromatography on SiO₂ (dry-load), gradient eluting with light petroleum to Et₂O-light petroleum (50:50), gave the *title compound* (50 mg, 76%) as a red solid, mp 182.9-184.0 °C, (Found [ESI⁺]: 410.1378. C₁₈H₂₄N₃O₆S [MH] requires 410.1380); [α]_D²⁴ +55.3 (c 0.11, MeOH); IR (neat) ν_{max}/cm⁻¹: 3355 (N-H str), 2954 (C-H str), 1672 (C=O str), 1588 (N-O str), 1508 (C-C str), 1325 (N-O str), 1230 (C-O str), 1060 (C-N str); ¹H NMR (500 MHz, DMSO-*d*₆) δ_H/ppm: 8.94 (1H, m, 4-CH), 8.27 (1H, d, *J* = 9 Hz, 6-CH), 8.15 (1H, d, *J* = 9 Hz, 7-CH), 7.54 (1H, m, 3-NH), 6.87 (1H, d, *J* = 6 Hz, 2'-NH), 3.81 (4H, 1'-CHH and OMe), 3.76 (1H, m, 2'-CH), 3.57 (1H, m, 1'-CHH), 1.32 (9H, s, CMe₃), 1.12 (1H, d, *J* = 6 Hz, 3'-Me); ¹³C NMR (126 MHz, DMSO-*d*₆) δ_C/ppm: 164.0 (C), 155.1 (C), 150.3 (3-C), 145.2 (C), 144.3 (C), 131.1 (C), 124.7 (7-CH), 121.6 (6-CH), 120.5 (4-CH), 99.5 (2-C), 77.6 (CMe₃), 51.7 (OMe), 50.5 (1'-CH₂), 46.2 (2'-CH), 28.1 (CMe₃), 18.3 (3'-Me); *m/z* (EI⁺): 410 (MH⁺, 100), 409 (M^{•+}, 70).

6.2.24. (3*R*)-3-Methyl-9-nitro-1,2,3,4-tetrahydro-5*H*-[1]benzothieno[3,2-*e*][1,4]diazepin-5-one (178)



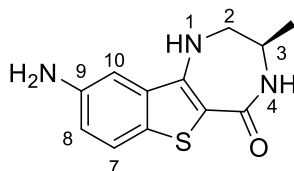
Chemical Formula: C₁₂H₁₁N₃O₃S

Mr: 277.30

According to a modified procedure,^{277,366} a solution of (*R*)-methyl 3-((2-((*tert*-butoxycarbonyl)amino)propyl)amino)-5-nitrobenzo[*b*]thiophene-2-carboxylate (**185**) (0.30 g, 0.73 mmol) in TFA (10% v/v in CH₂Cl₂) (5.7 mL, 7.3 mmol) was stirred at RT until salt formation was confirmed by TLC analysis (*R*_f 0.3; MeOH-CH₂Cl₂ [10:90]) and the volatiles removed *in vacuo*. The residue was dissolved in a solution of NaOMe (25 wt. % in MeOH; 1 mL, 4.4 mmol) in MeOH (5 mL) and warmed to 50 °C for 2 h before heating to reflux for 2 h. The reaction mixture was then allowed to cool to RT, cooled in an ice bath and neutralized by the addition of aqueous HCl solution (1 M) and stirred at 0 °C for 30 min. The solid was then isolated by vacuum filtration, washed with water and dried in air to give the *title compound* (0.18 g, 100%) as a red powder, mp 337.4-342.4 (dec.) (Found [ESI⁺]: 278.0590. C₁₂H₁₁N₃O₃S [MH] requires 278.0594); [α]_D²⁴ +110.6 (c 0.04, MeOH); IR (neat) ν_{max}/cm⁻¹: 3307 (N-H str), 1598 (C=O str), 1501 (N-O str), 1438

(C-C str), 1318 (N-O str), 1102 (C-N str), 736 (N-H wag); ^1H NMR (500 MHz, DMSO- d_6) δ_{H} /ppm: 9.03 (1H, d, $J = 2$ Hz, 10-CH), 8.22 (1H, dd, $J = 9, 2$ Hz, 8-CH), 8.05 (1H, d, $J = 9$ Hz, 7-CH), 8.02 (1H, m, 1-NH), 7.95 (1H, d, $J = 3$ Hz, 4-NH), 3.60 (1H, m, 3-CH), 3.39 (2H, m, 2-CH₂), 1.16 (3H, d, $J = 7$ Hz, Me); ^{13}C NMR (126 MHz, DMSO- d_6) δ_{C} /ppm: 164.2 (C), 145.3 (C), 144.2 (C), 141.8 (C), 132.9 (C), 123.8 (7-CH), 120.8 (8-CH), 118.6 (10-CH), 108.6 (C), 50.6 (2-CH₂), 47.6 (3-CH), 18.6 (Me); m/z (EI⁺): 277 ($M^{\bullet+}$, 87), 262 (M-CH₃, 24), 234 (29), 206 (30).

6.2.25. (3R)-9-Amino-3-methyl-1,2,3,4-tetrahydro-5H-[1]benzothieno[3,2-*e*][1,4]diaepin-5-one (179)

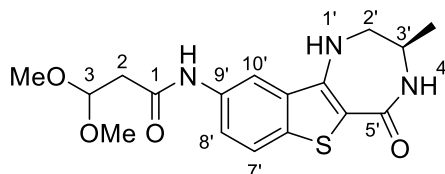


Chemical Formula: C₁₂H₁₃N₃OS

Mr: 247.32

Following the procedure of Spencer *et al.*,²⁷⁹ DBU (0.3 mL, 2.1 mmol) was added to a solution of **178** (0.19 g, 0.69 mmol) and Mo(CO)₆ (0.18 g, 0.69 mmol) in EtOH (7 mL) in a pressure-rated glass vial (35 mL) and irradiated at 150 °C for 30 min using a CEM Discover microwave synthesizer by moderating the initial power (300 W). After cooling in a flow of compressed air the volatiles were removed *in vacuo*. Purification by flash column chromatography on SiO₂ (dry-load), gradient eluting with CH₂Cl₂ to MeOH-CH₂Cl₂ (10:90), gave the *title compound* (0.16 g, 96%) as a brown solid, mp 154.1-160.4 °C (dec.) (Found [ESI⁺]: 248.0851. C₁₂H₁₄N₃OS [M^+] requires 248.0852); $[\alpha]_{\text{D}}^{24} + 48.7$ (c 0.11 MeOH); IR (neat) ν_{max} /cm⁻¹: 3238 (NH str), 1596 (N-H str), 1419 (C-C str), 1324 (C-N str), 1244 (C-N str); ^1H NMR (500 MHz, DMSO- d_6) δ_{H} /ppm: 7.60 (1H, d, $J = 2$ Hz, 4-NH), 7.37 (1H, d, $J = 8$ Hz, 7-CH), 7.14 (1H, m, 1-NH), 6.98 (1H, m, 10-CH), 6.79 (1H, d, $J = 8$ Hz, 8-CH), 5.04 (2H, br. s, 9-NH₂), 3.54 (1H, m, 3-CH), 3.30 (2H, m, 2-CH₂), 1.13 (3H, d, $J = 7$ Hz, Me); ^{13}C NMR (126 MHz, DMSO- d_6) δ_{C} /ppm: 164.8 (C), 145.4 (C), 141.2 (C), 134.1 (C), 126.7 (9-C), 122.7 (7-CH), 117.1 (8-CH), 106.6 (C), 104.9 (10-CH), 51.0 (2-CH₂), 47.7 (3-CH), 18.6 (Me).

6.2.26. 3,3-Dimethoxy-*N*-((3*R*)-3-methyl-5-oxo-2,3,4,5-tetrahydro-1*H*-[1]benzo[4,5]thieno[3,2-*e*][1,4]diazepin-9-yl)propanamide (186)



Chemical Formula: C₁₇H₂₁N₃O₄S

Mr: 363.43

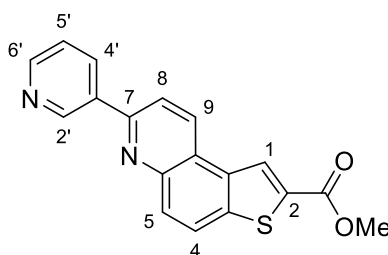
6.2.26.1. EDCI-HOBt mediated microwave-assisted synthesis

DIEA (0.2 mL, 1.2 mmol) was added to a solution of (*R*)-9-amino-3-methyl-1,2,3,4-tetrahydro-5*H*-[1]benzothieno[3,2-*e*][1,4]diazepin-5-one (**179**) (96 mg, 0.39 mmol), 3,3-dimethoxypropanoic acid (**172**) (65 mg, 0.48 mmol), HOBt.H₂O (87 mg, 0.64 mmol), and EDCI.HCl (120 mg, 0.60 mmol) in DMF (6 mL) under N₂, and irradiated at 120 °C for 15 min in a pressure-rated glass vial (10 mL) using a CEM Discover microwave synthesizer by modulating the initial power (200 W). After cooling in a flow of compressed air, the volatiles were removed *in vacuo* and the residue was taken up in CH₂Cl₂ and washed with water (3 x 30 mL) and brine (2 x 30 mL), dried (Na₂SO₄), filtered and evaporated *in vacuo*. Purification by flash column chromatography on SiO₂ (dry-load), gradient eluting with CH₂Cl₂ to MeOH in CH₂Cl₂ (10:90), gave the *title compound* (51 mg, 36%) as a brown solid, mp 299.5 °C (dec.) (Found [ESI⁺]: 364.1327. C₁₇H₂₂N₃O₄S [MH] requires 364.1326); IR (neat) ν_{\max} /cm⁻¹: 3253 (N-H str), 1668 (C=O str), 1590 (N-H bend), 1420 (C-C str), 1117 (C-N str), 1075 (C-O str); ¹H NMR (600 MHz, DMSO-*d*₆) δ_{H} /ppm: 10.06 (1H, s, NH), 8.30 (1H, s, 10'-CH), 7.76 (1H, d, *J* = 4 Hz, 4'-NH), 7.68 (1H, d, *J* = 9 Hz, 7'-CH), 7.47-7.43 (1H, m, 1'-NH), 7.37 (1H, dd, *J* = 9, 1, Hz, 8'-CH), 4.82 (1H, t, *J* = 6 Hz, 3-CH), 3.58-3.52 (1H, m, 3'-CH), 3.35-3.33 (2H, m, 2'-CH₂), 3.29 (6H, s, OMe), 2.67 (2H, d, *J* = 6 Hz, 2-CH₂), 1.13 (3H, d, *J* = 6.5 Hz, Me); ¹³C NMR (151 MHz, DMSO-*d*₆) δ_{C} /ppm: 167.2 (1-C), 164.7 (5'-C), 141.6 (C), 135.1 (9'-C), 133.9 (C), 133.2 (C), 122.8 (7'-CH), 120.4 (8'-CH), 112.8 (10'-CH), 107.2 (C), 102.0 (3-CH), 53.1 (OMe), 50.9 (2'-CH₂), 47.7 (3'-CH), 40.9 (2-CH₂), 18.6 (Me).

6.2.26.2. COMU mediated microwave-assisted synthesis.

(*R*)-9-Amino-3-methyl-1,2,3,4-tetrahydro-5*H*-[1]benzothieno[3,2-*e*][1,4]diaepin-5-one (**179**) (93 mg, 0.38 mmol) was added to a solution of 3,3-dimethoxypropanoic acid (**172**) (81 mg, 0.60 mmol), COMU (270 mg, 0.62 mmol), EDCI.HCl (120 mg, 0.62 mmol) and DIEA (0.13 mL, 0.80 mmol) in DMF (2.5 mL) under Ar and irradiated at 120 °C for 1 h in a pressure-rated glass vial (10 mL) using a CEM Discover microwave synthesizer by modulating the initial power (120 W). After cooling in a flow of compressed air, the volatiles were removed *in vacuo*. Purification by SCX-2 chromatography, gradient eluting with MeCN to MeOH, to give the *title compound* (110 mg, 83%) as a brown solid, with identical spectroscopic data. LCMS purity: 84% (UV), Ret. Time = 4.22 min.

6.2.27. Methyl 7-(pyridin-3-yl)thieno[3,2-*f*]quinoline-2-carboxylate (**195A**)



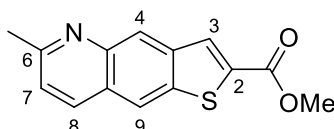
Chemical Formula: C₁₈H₁₂N₂O₂S

Mr: 320.65

Methyl 5-aminobenzothiophenen-2-carboxylate (**158**) (120 mg, 0.58 mmol) and 3-pyridinecarboxaldehyde (62 mg, 0.58 mmol) were stirred in MeCN (2 mL) for 1 h at RT. Iodine (62 mg, 0.24 mmol) and *n*-BVE (77 mg, 0.77 mmol) were then added and the solution irradiated at 100 °C for 3 h in a pressure-rated vial (10 mL) using a CEM Discover microwave synthesizer through modulation of the initial power (120 W). The solution was then diluted with EtOAc (30 mL), washed with aqueous Na₂S₂O₃ solution (1 M; 1 x 20 mL) and brine (1 x 20 mL), dried (Na₂SO₄), filtered and evaporated *in vacuo*. Purification by flash column chromatography on SiO₂ (dry-load), gradient eluting with hexanes-EtOAc (50:50) to (25:75) gave the *title compound* (49 mg, 27%) as a brown solid, mp 224.2 °C (dec.) (Found [ESI⁺]: 321.0676. C₂₁H₉N₂O₂ [MH] requires 321.0692); IR (neat) ν_{max} /cm⁻¹: 2922 (C-H str), 1718 (C=O str), 1569 (C-C str), 1266 (C-N str), 1018 (C-O str); ¹H NMR (500 MHz, CDCl₃) δ_{H} /ppm: 9.41 (1H, s, 2'-CH), 8.74 (2H, m, 9-CH and 6'-CH),

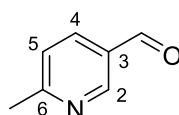
8.70 (1H, s, 1-CH), 8.55 (1H, d, $J = 8$ Hz, 4'-CH), 8.20-8.16 (1H, m, 4-CH), 8.14-8.10 (1H, m, 5-CH), 8.06 (1H, d, $J = 9$ Hz, 8-CH), 7.49 (1H, dd, $J = 5, 2$ Hz, 5'-CH), 4.02 (3H, s, Me); ^{13}C NMR (100 MHz, CDCl_3) δ_{C} /ppm: 162.9 (C), 154.1 (C), 150.3 (6'-CH), 148.7 (2'-CH), 147.2 (C), 141.2 (C), 134.8 (4'-CH), 134.3 (C), 132.5 (9-CH), 129.5 (5-CH), 127.9 (1-CH), 124.6 (4-CH), 124.1 (C), 123.7 (5'-CH), 119.1 (8-CH), one quaternary carbon not observed; m/z (EI+): 320 (M^{+} , 100), 289 (M-OMe, 26).

Side product data: Methyl 6-methylthieno[2,3-g]quinoline-2-carboxylate (**196**)



(Found [ESI+]: 258.0578. $\text{C}_{14}\text{H}_{12}\text{NO}_2\text{S}$ [MH] requires 258.0583); ^1H NMR (500 MHz, CDCl_3) δ_{H} /ppm: 8.63 (1H, s, 3-CH), 8.51 (1H, d, $J = 8$ Hz, 8-CH), 8.03 (2H, m, 4-CH and 9-CH), 7.44 (1H, d, $J = 9$ Hz, 7-CH), 4.00 (3H, s, OMe), 2.79 (3H, s, Me); ^{13}C NMR (126 MHz, CDCl_3) δ_{C} /ppm: 162.9 (C), 158.4 (C), 146.5 (C), 140.3 (C), 134.9 (C), 133.8 (C), 131.6 (8-CH), 128.8 (4- or 9-CH), 127.9 (4- or 9-CH), 123.8 (4- or 9-CH), 122.5 (7-CH), 52.5 (OMe), 25.1 (Me); m/z (EI+): 257 (M^{+} , 100), 226 (M-OMe).

6.2.28. 6-Methylpyridine-3-carboxaldehyde (**190**)



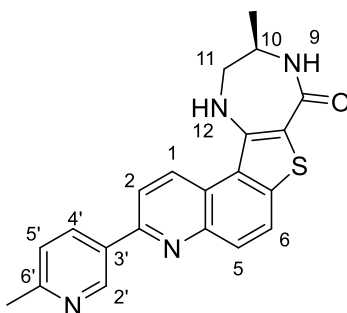
Chemical Formula: $\text{C}_7\text{H}_7\text{NO}$

Mr: 121.14

DMSO (1.05 mL, 15.0 mmol) in dry CH_2Cl_2 (7 mL) was added drop-wise over 20 min to a solution of $(\text{COCl})_2$ (2 M in CH_2Cl_2 ; 3.5 mL, 7.0 mmol) in dry CH_2Cl_2 (12 mL), cooled to -78°C under Ar, and the solution stirred for 20 min. To this solution, (6-methylpyridin-3-yl)methanol (**197**) (0.75 g, 6.1 mmol) in dry CH_2Cl_2 (3 mL) was added drop-wise over 20 min and the reaction mixture stirred for 20 min. Then NEt_3 (5 mL, 36 mmol) was added drop-wise over 10 min, and the solution allowed to warm to RT over 30 min. The solution was then poured into water (30 mL), extracted with CH_2Cl_2 (2 x 30 mL), the organic extracts were combined, washed with brine (1 x 30 mL),

dried (Na₂SO₄), filtered and evaporated *in vacuo*. Purification by flash column chromatography on SiO₂ (dry-load), gradient eluting with EtOAc in hexanes (50:50) to (70:30), gave the *title compound* (0.55 g, 75%) as a brown oil, (Found [ESI⁺]: 122.0602. C₇H₈NO [MH] requires 122.0600); ¹H NMR (500 MHz, CDCl₃) δ_H/ppm: 10.08 (1H, s, CHO), 8.97 (1H, d, *J* = 1 Hz, 2-CH), 8.08 (1H, dd, *J* = 8, 1.5 Hz, 4-CH), 7.34 (1H, d, *J* = 8 Hz, 5-CH), 2.67 (3H, s, Me); ¹³C NMR (126 MHz, CDCl₃) δ_C/ppm: 190.4 (CHO), 164.9 (6-C), 151.9 (2-CH), 135.9 (4-CH), 129.4 (3-C), 123.8 (5-CH), 24.9 (Me); *m/z* (EI⁺): 137 (*M*+OH, 62), 121 (*M*^{•+}, 100), 120 (90), 92 (84). Data matches literature values.^{367,368}

6.2.29. (R)-10-Methyl-3-(6-methylpyridin-3-yl)-9-10-11-12-tetrahydro-8H-[1,4]diazepino[5',6':4,5]thieno[3,2-*f*]quinoline-8-one. PF-3644022 (25)



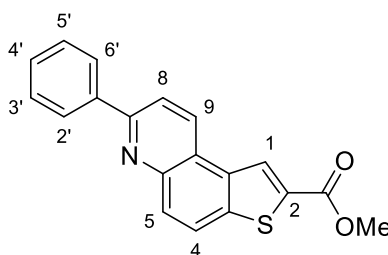
Chemical Formula: C₂₁H₁₈N₄OS

Mr: 374.12

6-Methylpyridine-3-carboxaldehyde (**190**) (100 mg, 0.86 mmol) and (*R*)-9-amino-3-methyl-3,4-dihydro-1*H*-benzo[4,5]thieno[3,2-*e*][1,4]diazepin-5(2*H*)-one (**179**) (150 mg, 0.61 mmol) were stirred in MeCN (2 mL) for 1 h at RT, and then *n*-BVE (100 mg, 1.0 mmol) and iodine (80 mg, 0.31 mmol) were added and the solution irradiated at 100 °C for 3 h in a pressure-rated glass vial (10 mL) using a CEM Discover microwave synthesizer through modulation of the initial power (120 W). After cooling in a flow of compressed air, the reaction mixture was diluted with EtOAc (20 mL) and then washed with aqueous Na₂S₂O₃ solution (1M; 1 x 20 mL) and brine (1 x 20 mL), dried (Na₂SO₄), filtered and evaporated *in vacuo*. Purification by flash column chromatography on SiO₂ (dry-load), gradient eluting with MeOH (4-12%) in EtOAc, gave the *title compound* (13 mg, 6%) as a brown solid, (Found [ESI⁺]: 375.1282. C₂₁H₁₉N₄OS [MH] requires 375.1274); [α]_D²⁴ + 32.0 (c

0.026, MeOH); IR (neat) $\nu_{\max}/\text{cm}^{-1}$: 2969 (C-H str), 1598 (broad, C=O str, N-H str), 1364 (C-N str), 1199 (C-N str), 1033 (C-O str); ^1H NMR (500 MHz, CDCl_3) $\delta_{\text{H}}/\text{ppm}$: 9.25 (1H, br. s, 2'-CH), 8.92 (1H, d, $J = 9$ Hz, 1-CH), 8.48 (1H, dd, $J = 8, 2$ Hz, 4'-CH), 8.11 (1H, d, $J = 9$ Hz, 6-CH), 7.99 (1H, d, $J = 9$ Hz, 5-CH), 7.96 (1H, d, $J = 9$ Hz, 2-CH), 7.34 (1H, d, $J = 8$ Hz, 5'-CH), 6.40 (1H, br. s, 9-NH), 5.42 (1H, br. s, 12-NH), 3.83 (1H, m, 10-CH), 3.75 (1H, m, 11-CHH), 3.68 (1H, m, 11-CHH), 2.66 (3H, s, Me), 1.41, (3H, d, $J = 7$ Hz, Me); ^{13}C NMR (100 MHz, CDCl_3) $\delta_{\text{C}}/\text{ppm}$: 165.3 (C), 159.3 (C), 152.6 (C), 147.7 (2'-CH), 145.0 (C), 140.4 (C), 135.1 (4'-CH), 131.8 (C), 129.8 (1-CH), 129.7 (6-CH), 125.6 (C), 125.2 (5-CH), 124.3 (C), 123.4 (5'-CH), 117.9 (2-CH), 114.0 (C), 52.9 (11-CH₂), 49.3 (10-CH), 24.3 (Me), 19.4 (Me), one quaternary carbon not observed; m/z (EI⁺): 374 (M^{+} , 100), 331 (70), 302 (38).

6.2.30. Methyl 7-phenylthieno[3,2-f]quinoline-2-carboxylate (199)



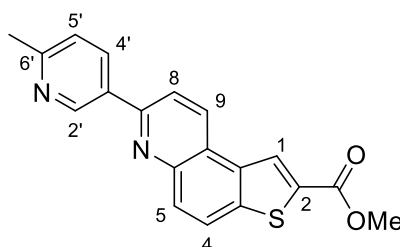
Chemical Formula: $\text{C}_{19}\text{H}_{13}\text{NO}_2\text{S}$

Mr: 319.38

Benzaldehyde (55 mg, 0.52 mmol) and methyl 3-aminobenzothiophene-2-carboxylate (**158**) (106 mg, 0.51 mmol) were stirred in MeCN (2 mL) for 1 h at RT, and then *n*-BVE (76 mg, 0.76 mmol) and iodine (71 mg, 0.28 mmol) were added and the solution irradiated at 100 °C for 3 h in a pressure-rated glass vial (10 mL) using a CEM Discover microwave synthesizer by modulation of the initial power (120 W). After cooling in a flow of compressed air, the reaction mixture was diluted with EtOAc (20 mL) and washed with aqueous $\text{Na}_2\text{S}_2\text{O}_3$ solution (1 M; 1 x 20 mL) and brine (1 x 20 mL), dried (Na_2SO_4), filtered and evaporated *in vacuo*. Purification by flash column chromatography on SiO_2 (dry-load), gradient eluting with hexanes to EtOAc-hexanes (25:75), gave the *title compound* (49 mg, 30%) as a brown solid, mp 175.1-177.8 °C (Found [ESI⁺]: 320.0750. $\text{C}_{19}\text{H}_{14}\text{NO}_2\text{S}$ [MH] requires 320.0740); IR (neat) $\nu_{\max}/\text{cm}^{-1}$: 3076 (C-H), 1713 (C=O str),

1570 (C-C str), 1244 (C-N str), 1068 (C-O str); ^1H NMR (500 MHz, CDCl_3) $\delta_{\text{H}}/\text{ppm}$: 8.66-8.61 (2H, 1-CH and 9-CH), 8.20 (2H, d, $J = 7.5$ Hz, 2', 6'-CH), 8.16 (1H, d, $J = 9$ Hz, 4-CH), 8.06 (1H, d, $J = 9$ Hz, 5-CH), 8.01 (1H, d, $J = 8$ Hz, 8-CH), 7.55 (2H, m, 3', 5'-CH), 7.49 (1H, m, 4'-CH), 4.00 (3H, s, Me); ^{13}C NMR (126 MHz, CDCl_3) $\delta_{\text{C}}/\text{ppm}$: 162.9 (C), 156.6 (C), 146.8 (C), 140.7 (C), 139.2 (C), 134.7 (C), 133.9 (C), 132.0 (9-CH), 129.6 (4-CH), 129.3 (4'-CH), 128.8 (3', 5'-CH), 127.9 (1-CH), 127.4 (2', 6'-CH), 124.0 (5-CH), 123.6 (C), 119.3 (8-CH), 52.5 (Me); m/z (EI $^{+}$): 319 (M^{++} , 100), 288 (40), 260 (19).

6.2.31. Methyl 7-(6-methylpyridin-3-yl)thieno[3,2-*f*]quinoline-2-carboxylate (200)



Chemical Formula: $\text{C}_{19}\text{H}_{14}\text{N}_2\text{O}_2\text{S}$

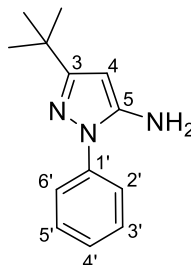
Mr: 334.39

6-Methylpyridine-3-carboxaldehyde (**190**) (59 mg, 0.49 mmol) and methyl 5-aminobenzo[*b*]thiophene-2-carboxylate (**158**) (99 mg, 0.48 mmol) were stirred in MeCN (2 mL) for 1 h at RT, and then *n*-BVE (72 mg, 72 mmol) and iodine (75 mg, 0.30 mmol) were then added and the solution irradiated at 100 °C for 3 h in a pressure-rated glass vial (10 mL) using a CEM Discover microwave synthesizer through modulation of the initial power (120 W). After cooling in a flow of compressed air, the solution was poured into EtOAc (20 mL), washed with aqueous $\text{Na}_2\text{S}_2\text{O}_3$ solution (1 M; 1 x 10 mL) and brine (1 x 10 mL), dried (Na_2SO_4), filtered and evaporated *in vacuo*. Purification by flash column chromatography on SiO_2 (dry-load), gradient eluting with EtOAc in hexanes (55:45) to (70:30), gave the *title compound* (7 mg, 4%) as a brown solid; (Found [ESI $^{+}$]: 355.0855. $\text{C}_{19}\text{H}_{15}\text{N}_2\text{O}_2\text{S}$ [$M\text{H}$] requires 335.0849); IR (neat) $\nu_{\text{max}}/\text{cm}^{-1}$: 2921 (C-H str), 1721 (C=O), 1570 (C-C str), 1258 (C-N str), 1070 (C-O str); ^1H NMR (500 MHz, CDCl_3) $\delta_{\text{H}}/\text{ppm}$: 9.27 (1H, br. s, 2'-CH), 8.71 (1H, d, $J = 8$ Hz, 9-CH), 8.69 (1H, s, 1-CH), 8.45 (1H, dd, $J = 8, 2$ Hz, 4'-CH), 8.17 (1H, d, $J = 9$ Hz, 4- or 5-CH), 8.10 (1H, d, $J = 9$ Hz, 4- or 5-CH), 8.03 (1H, d, $J = 9$ Hz, 8-CH), 7.34

(1H, d, $J = 8$ Hz, 5'-CH), 4.02 (3H, s, OMe), 2.67 (3H, s, Me); ^{13}C NMR (126 MHz, CDCl_3) δ_{C} /ppm: 162.9 (C), 159.4 (C), 154.3 (C), 148.0 (2'-CH), 147.1 (C), 141.1 (C), 135.1 (4'-CH), 134.8 (C), 134.2 (C), 132.4 (9-CH), 132.0 (C), 129.6 (4- or 5-CH), 128.0 (1-CH), 124.4 (4- or 5-CH), 124.0 (5'-CH), 123.3 (C), 119.0 (8-CH), 52.6 (OMe), 24.4 (Me); m/z (EI): 334 (M^{*+} , 100).

6.3. Chapter 4.

6.3.1. 3-*tert*-Butyl-1-phenyl-1*H*-pyrazole-5-amine (215)

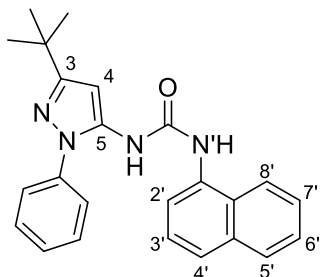


Chemical Formula C₁₃H₁₇N₃

Mr: 215.29

Phenyl hydrazine (0.43 mL, 4.4 mmol) was added to a solution of 4,4-dimethyl-3-oxopentanenitrile (0.50 g, 4.0 mmol) in toluene:glacial AcOH solution ([5:1]; 1.5 mL) and irradiated at 120 °C for 40 min in a pressure-rated glass vial (10 mL) using a CEM Discover microwave synthesizer by moderating the initial power (100 W). After cooling in a flow of compressed air, the volatiles were removed *in vacuo*. Purification by flash column chromatography on SiO₂ (dry-load), eluting with hexanes to EtOAc-hexanes (30:70) gave the *title compound* (0.78 g, 91%) as a crystalline brown solid, mp 63.6-64.6 °C (lit.⁵² 64-66 °C) (Found [ESI⁺]: 216.1495. C₁₃H₁₈N₃ [MH] requires 216.1495); IR (neat) $\nu_{\max}/\text{cm}^{-1}$: 2961 (C-H str), 1596 (N-H bend), 1554 (C=C str), 1506 (C=C str), 1375 (C-H bend), 1241 (C-N str), 988 (N-H wag.); ¹H NMR (500 MHz, DMSO-*d*₆) $\delta_{\text{H}}/\text{ppm}$: 7.57 (2H, d, *J* = 8 Hz, 2'-CH, 6'-CH), 7.44 (2H, t, *J* = 7 Hz, 3'-CH, 5'-CH), 7.25 (1H, t, *J* = 7 Hz, 4'-CH), 5.39 (1H, s, 4-CH), 5.16 (2H, s, NH₂), 1.22 (9H, s, CMe₃); ¹³C NMR (126 MHz, DMSO-*d*₆) $\delta_{\text{C}}/\text{ppm}$: 160.7 (3-C), 146.9 (5-C), 139.6 (1'-C), 128.8 (3'-CH, 5'-CH), 125.4 (4'-CH), 122.3 (2'-CH, 6'-CH), 86.9 (4-CH), 31.7 (3-CMe₃), 30.1 (CMe₃); *m/z* (EI⁺): 215 (*M*^{•+}, 75), 200 (*M* - Me, 100).

6.3.2. *N*-(3-(*tert*-Butyl)-1-phenyl-1*H*-pyrazol-5-yl)-*N'*-(naphthalene-1-yl)urea (215A**)**

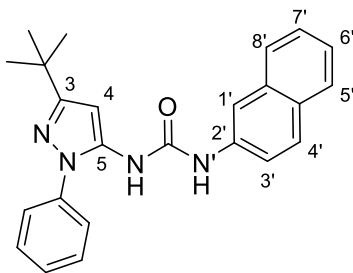


Chemical Formula: C₂₄H₂₄N₄O

Mr: 384.47

According to a modified procedure,⁵² 1-naphthyl isocyanate (0.15 mL, 1.60 mmol) was added to a solution of 3-*tert*-butyl-1-phenyl-1*H*-pyrazole-5-amine (**215**) (0.20 g, 0.93 mmol) in CH₂Cl₂ (1.8 mL) and stirred for 40 min at RT. Volatiles were removed *in vacuo* and the residue triturated with light petroleum. Purification by recrystallization from hot MeOH gave the *title compound* (0.23 g, 65%) as a colourless solid, mp 168.1-169.4 °C (MeOH) (Found [TOF MS EI⁺]: 385.2035. C₂₄H₂₅N₄O [MH] requires 385.2028); IR (neat) ν_{max} /cm⁻¹: 3261 (N-H str), 2957 (C-H str), 1644 (C=O str), 1547 (N-H bend), 1502 (N-H bend), 1018 (C-N str); ¹H NMR (500 MHz, DMSO-*d*₆) δ_{H} /ppm: 9.03 (1H, s, N'H), 8.79 (1H, s, NH), 8.01 (1H, d, *J* = 8 Hz, aryl-CH), 7.92 (2H, t, *J* = 7 Hz, aryl-CH), 7.65 (1H, d, *J* = 8 Hz, aryl-CH), 7.56-7.51 (6H, aryl-CH), 7.45 (2H, aryl-CH), 6.43 (1H, s, 4-CH), 1.29 (9H, s, CMe₃); ¹³C NMR (126 MHz, DMSO-*d*₆) δ_{C} /ppm: 160.7 (3-C), 152.1 (C), 138.61 (C), 137.2 (C), 133.9 (C), 133.6 (C), 129.2 (3,4-PhCH), 128.2 (CH), 127.1 (CH), 126.2 (C), 125.8 (CH), 125.7 (CH), 125.6 (CH), 124.2 (2, 6-PhCH), 123.3 (CH), 121.4 (CH), 118.0 (CH), 95.4 (4-CH), 31.9 (CMe₃), 30.1 (CMe₃).

6.3.3. *N*-(3-(*tert*-Butyl)-1-phenyl-1*H*-pyrazol-5-yl)-*N'*-(naphthalene-2-yl)urea (**215B**)

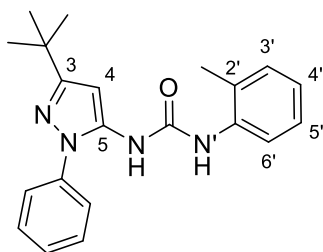


Chemical Formula: $C_{24}H_{24}N_4O$

Mr: $C_{24}H_{24}N_4O$

Following the procedure of Bagley *et al.*, 2-naphthalene isocyanate (0.16 g, 0.93 mmol) was added to a solution of 3-*tert*-butyl-1-phenyl-1*H*-pyrazole-5-amine (**215**) (0.20 g, 0.92 mmol) in CH_2Cl_2 (1.8 mL) and stirred at RT for 20 min. The volatiles were removed *in vacuo* and the residue triturated with EtOAc-light petroleum to give the *title compound* (0.29 g, 81%) as a colourless solid, mp 200.7–206.3 °C, (Found [TOF MS EI⁺]: 385.2021. $C_{24}H_{25}N_4O$ [MH] requires 385.2028); IR (neat) ν_{max}/cm^{-1} : 3285 (N-H str), 2958 (C-H str), 1654 (C=O str), 1550 (N-H bend), 1500 (N-H bend), 1033 (C-N str); 1H NMR (500 MHz, DMSO- d_6) δ_H/ppm : 9.22 (1H, s, N'H), 8.48 (1H, s, NH), 8.09 (1H, s, 1'-CH), 7.86–7.73 (3H, m, naphthyl-CH), 7.56 (4H, m, 2, 3, 5, 6-PhCH), 7.46–7.41 (3H, 4-PhCH and naphthyl-CH), 7.38–7.32 (1H, m, naphthyl-CH), 6.43 (1H, s, 4-CH), 1.30 (9H, s, CMe₃); ^{13}C NMR (126 MHz, DMSO- d_6) δ_C/ppm : 160.7 (3-C), 151.6 (C), 138.5 (1-PhC), 137.1 (5-C), 136.9 (2'-C), 133.6 (C), 129.2 (3, 5-PhCH), 129.1 (C), 128.3 (CH), 127.3 (CH), 127.1 (CH), 126.9 (CH), 126.3 (CH), 124.2 (2, 6-PhCH), 124.0 (CH), 119.4 (3'-CH), 113.5 (1'-CH), 95.3 (4-CH), 31.9 (CMe₃), 30.1 (CMe₃);

6.3.4. *N*-(3-(*tert*-Butyl)-1-phenyl-1*H*-pyrazol-5-yl)-*N'*-(*o*-tolyl)urea (**215C**)

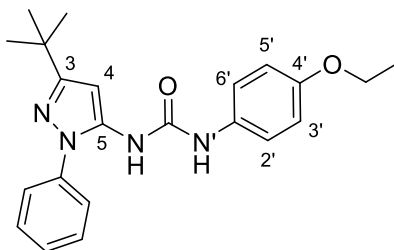


Chemical Formula: C₂₁H₂₄N₄O

Mr: 348.44

Following the procedure of Bagley *et al.*,⁵² *o*-tolyl isocyanate (0.12 mL, 0.97 mmol) was added to a solution of 3-*tert*-butyl-1-phenyl-1*H*-pyrazole-5-amine (**A**) (0.20 g, 0.93 mmol) in CH₂Cl₂ (1.8 mL) and stirred at RT for 20 min. The volatiles were removed *in vacuo* and the residue triturated with EtOAc-light petroleum (1:1) to give the *title compound* (0.17 g, 53%) as a colourless solid, mp 166.6-168.0 °C (MeOH) (Found [TOF MS EI⁺]: 349.2032. C₂₁H₂₅N₄O [MH] requires 349.2028); IR (neat) ν_{\max} /cm⁻¹: 3291 (N-H str), 2967 (C-H str), 1643 (C=O str), 1551 (N-H bend), 1502 (N-H bend), 1033 (C-N str); ¹H NMR (500 MHz, DMSO-*d*₆) δ_{H} /ppm: 8.71 (1H, s, NH), 8.19 (1H, s, N'H), 7.69 (1H, d, *J* = 8 Hz, *o*-tolyl-CH), 7.54 (4H, m, 2, 3, 5, 6-PhCH), 7.40 (1H, m, 4-PhCH), 7.14 (2H, m, *o*-tolyl-CH), 6.96 (1H, t, *J* = 7 Hz, *o*-tolyl-CH), 6.36 (1H, s, 4-CH), 2.17 (3H, s, Me), 1.28 (9H, s, CMe₃); ¹³C NMR (126 MHz, DMSO-*d*₆) δ_{C} /ppm: 160.7 (3-C), 152.0 (C), 138.7 (1-PhC), 137.2 (5-C), 136.9 (1'-C), 130.1 (CH), 129.2 (3, 5-PhCH), 128.3 (2'-C), 127.0 (4-PhCH), 126.0 (CH), 124.0 (2, 6-PhCH), 123.2 (CH), 121.8 (CH), 95.8 (4-CH), 32.0 (CMe₃), 30.1 (CMe₃), 17.8 (Me).

6.3.5. *N*-(3-(*tert*-Butyl)-1-phenyl-1*H*-pyrazol-5-yl)-*N'*-(4-ethoxyphenyl)urea (**215D**)



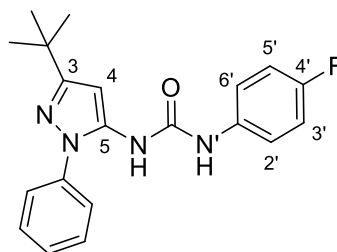
Chemical Formula: C₂₂H₂₆N₄O₂

Mr: 378.47

Following the procedure of Bagley *et al.*, 4-ethoxyphenyl isocyanate (0.15 mL, 0.93 mmol) was added to a solution of 3-*tert*-butyl-1-phenyl-1*H*-pyrazole-5-amine (**215**) (0.20 g, 0.93 mmol) in CH₂Cl₂ (1.8 mL) and stirred at RT for 20 min. Volatiles were then removed *in vacuo* and the residue triturated with ethyl acetate: light petroleum (1:1) to give the *title compound* (0.30 g, 86%) as a colourless solid, mp 215.7-219.3 °C (MeOH), (Found [TOF MS EI⁺]: 379.2130. [MH] requires 379.2134); IR (neat) ν_{\max} /cm⁻¹: 3291 (N-H str), 2966 (C-H str), 1656 (C=O str), 1543 (N-H

bend), 1510 (N-H bend), 1445 (C-H bend), 1245 (C-N str), 1050 (C-N str), 1033 (C-N str); ^1H NMR (500 MHz, $\text{DMSO-}d_6$) $\delta_{\text{H}}/\text{ppm}$: 8.78 (1H, s, NH), 8.27 (1H, s, N'H), 7.56-7.50 (4H, m, 2, 3, 5, 6-PhCH), 7.41 (1H, m, 4-PhCH), 7.28 (2H, d, $J = 9$ Hz, 2', 6'-CH), 6.83 (2H, d, $J = 9$ Hz, 3', 5'-CH), 6.35 (1H, s, 4-CH), 3.96 (2H, q, $J = 7$ Hz, CH_2), 1.34-1.24 (12H, Me and CMe_3); ^{13}C NMR (126 MHz, $\text{DMSO-}d_6$) $\delta_{\text{C}}/\text{ppm}$: 160.6 (3-C), 153.8 (4'-C), 151.7 (C), 138.6 (1-PhC), 137.3 (5-C), 132.2 (1'-C), 129.1 (3, 4-PhCH), 127.0 (4-PhCH), 124.1 (2, 6-PhCH), 119.9 (2', 6'-CH), 114.5 (3', 5'-CH), 95.3 (4-CH), 63.0 (CH_2), 31.9 (CMe_3), 30.1 (CMe_3), 14.6 (Me).

6.3.6. *N*-(3-(*tert*-Butyl)-1-phenyl-1*H*-pyrazol-5-yl)-*N'*-(4-fluorophenyl)urea (215E)

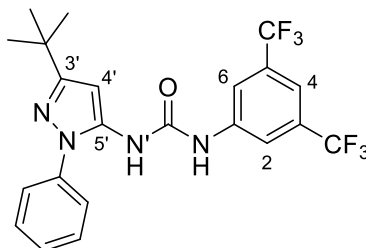


Chemical Formula: $\text{C}_{20}\text{H}_{21}\text{FN}_4\text{O}$

Mr: 352.40

Following the procedure of Bagley *et al.*, 4-fluorophenyl isocyanate (0.15 mL, 1.30 mmol) was added to a solution of 3-*tert*-butyl-1-phenyl-1*H*-pyrazole-5-amine (**215**) (0.20 g, 0.93 mmol) in CH_2Cl_2 (1.8 mL) and stirred at 20 °C for 20 min. Volatiles were removed *in vacuo* and the residue triturated with EtOAc-light petroleum (1:5) to give the *title compound* (0.28 g, 87%) as a colourless solid, mp 194.0-201.0 °C (MeOH) (Found [TOF MS EI⁺]: 353.1772. $\text{C}_{20}\text{H}_{22}\text{FN}_4\text{O}$ [MH] requires 353.1778); IR (neat) $\nu_{\text{max}}/\text{cm}^{-1}$: 3294 (N-H str), 2954 (C-H str), 1661 (C=O str), 1544 (N-H bend), 1509 (N-H bend), 1251 (C-N str), 1033 (C-N str); ^1H NMR (500 MHz, $\text{DMSO-}d_6$) $\delta_{\text{H}}/\text{ppm}$: 9.01 (1H, s, N'H), 8.36 (1H, s, NH), 7.53 (4H, m, 2, 3, 5, 6-PhCH), 7.41 (3H, 4-PhCH and 2', 6'-CH), 7.10 (2H, pt, $^3J_{\text{HH}}$, $^3J_{\text{FH}} = 9$ Hz, 3', 5'-CH), 6.36 (1H, s, 4-CH), 1.28 (9H, s, CMe_3); ^{13}C NMR (126 MHz, $\text{DMSO-}d_6$) $\delta_{\text{H}}/\text{ppm}$: 160.7 (3-C), 157.4 (d, $^1J_{\text{FC}} = 238$ Hz, 4'-CF), 151.7 (C), 138.5 (1-PhC), 137.0 (5-CH), 135.6 (d, $^4J_{\text{FC}} = 2$ Hz, 1'-C), 129.1 (3, 5-PhCH), 127.1 (4-PhCH), 124.1 (2, 6-PhCH), 119.9 (d, $^3J_{\text{FC}} = 8$ Hz, 2', 6'-CH), 115.2 (d, $^2J_{\text{FC}} = 22$ Hz, 3', 5'-CH), 95.6 (4-CH), 31.9 (CMe_3), 30.1 (CMe_3).

6.3.7. *N*-(3,5-Bis(trifluoromethyl)phenyl)-*N'*-(3-(*tert*-butyl)-1-phenyl-1*H*-pyrazol-5-yl)urea (**215F**)

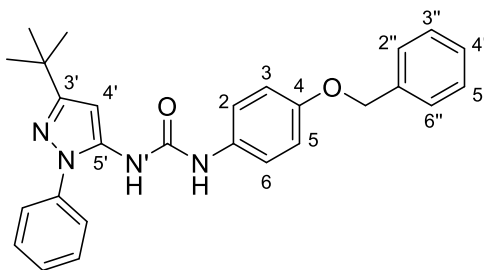


Chemical Formula: C₂₂H₂₀F₆N₄O

Mr: 470.41

Following the procedure of Bagley *et al.*, 3,5-bis(trifluoromethyl)phenyl isocyanate (0.18 mL, 1.04 mmol) was added to a solution of 3-*tert*-butyl-1-phenyl-1*H*-pyrazole-5-amine (**215**) (0.20 g, 0.93 mmol) in CH₂Cl₂ (1.8 mL) and stirred at 20 °C for 20 min. Volatiles were then removed *in vacuo* and the residue triturated with light petroleum to give the *title compound* (0.39 g, 88%) as a colourless solid, mp 175.7-177.8 °C (MeOH) (Found [TOF MS EI⁺]: 471.1617. C₂₂H₂₁N₄OF₆ [MH] requires 471.1620); IR (neat) ν_{max} /cm⁻¹: 3287 (N-H str), 2967 (C-H str), 1662 (C=O str), 1549 (N-H bend), 1502 (N-H bend), 1276 (C-N str), 1129 (C-F str), 1033 (C-N str); ¹H NMR (500 MHz, DMSO-*d*₆) δ_{H} /ppm: 9.70 (1H, s, NH), 8.67 (1H, s, N'H), 8.07 (2H, s, 2, 6-CH), 7.64 (1H, s, 4-CH), 7.56-7.49 (4H, m, 2, 3, 5, 6-PhCH), 7.40 (1H, t, ³J_{HH} = 6 Hz, 4-PhCH), 6.40 (1H, s, 4'-CH), 1.29 (9H, s, CMe₃); ¹³C NMR (100 MHz, DMSO-*d*₆) δ_{H} /ppm: 160.8 (3'-C), 151.9 (C), 141.5 (1-C), 138.5 (1-PhC), 136.3 (5'-C), 130.7 (q, ²J_{FC} = 37 Hz, 3, 5-C), 129.2 (3, 4-PhCH), 127.2 (4-PhCH), 124.0 (2, 6-PhCH), 124.0 (q, ¹J_{FC} = 272 Hz, CF₃), 117.9 (2, 6-CH), 114.6 (4-CH), 97.1 (4'-CH), 32.0 (CMe₃), 30.1 (CMe₃); *m/z* (EI⁺): 471 (*M*⁺, 100), 455 (*M* - Me, 45).

6.3.8. *N*-(4-(Benzyloxy)phenyl)-*N'*-(3-(*tert*-butyl)-1-phenyl-1*H*-pyrazol-5-yl)urea (**215G**)

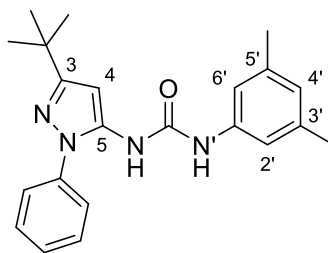


Chemical Formula: $C_{27}H_{28}N_4O_2$

Mr: 440.54

Following the procedure of Bagley *et al.*, 4-(benzyloxy)phenyl isocyanate (0.21 g, 0.94 mmol) was added to a solution of 3-*tert*-butyl-1-phenyl-1*H*-pyrazole-5-amine (**215**) (0.20 g, 0.92 mmol) in CH_2Cl_2 (1.8 mL) and stirred at RT for 20 min. Volatiles were then removed *in vacuo* and the residue triturated with EtOAc-light petroleum (1:5) to give the *title product* (0.33 g, 82%) as a colourless solid, mp 185.6-186.6 °C (MeOH) (Found [TOF MS EI⁺]: 441.2288. $C_{27}H_{29}N_4O_2$ [MH] requires 441.2291); IR (neat) ν_{max}/cm^{-1} : 3297 (N-H str), 2957 (C-H str), 1656 (C=O str), 1542 (N-H bend), 1509 (N-H bend), 1242 (C-N str), 1214 (C-O str), 1005 (C-N str); 1H NMR (500 MHz, $DMSO-d_6$) δ_H/ppm : 8.80 (1H, s, NH), 8.28 (1H, s, N'H), 7.54–7.49 (4H, m, 2, 3, 5, 6-PhCH), 7.35–7.44 (5H, m, Ar-CH), 7.31 (3H, m, Ar-CH), 6.92 (2H, d, $J = 9$ Hz, 3,5-CH), 6.35 (1H, s, 4''-CH), 5.04 (2H, s, CH_2), 1.27 (9H, s, CMe_3); ^{13}C NMR (126 MHz, $DMSO-d_6$) δ_C/ppm : 160.7 (3''-C), 153.6 (4-C), 151.7 (C), 138.6 (1-PhC), 137.3 (5''-C), 137.2 (1''-C), 132.6 (1-C), 129.1 (3, 5-PhCH), 128.3 (3', 5'-CH), 127.6 (4'-CH), 127.5 (2', 6'-CH), 127.1 (4-PhCH), 124.2 (2, 6-PhCH), 119.8 (2, 6-CH), 115.0 (3, 5-CH), 95.3 (4''-CH), 69.4 (CH_2), 31.9 (CMe_3), 30.1 (CMe_3).

6.3.9. *N*-(3-(*tert*-Butyl)-1-phenyl-1*H*-pyrazol-5-yl)-*N'*-(3,5-dimethylphenyl) urea (**215H**)

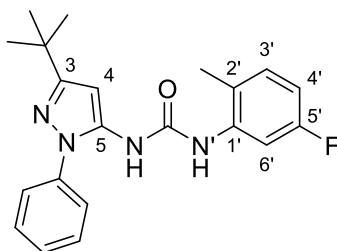


Chemical Formula: $C_{22}H_{26}N_4O$

Mr: 362.47

Following the procedure of Bagley *et al.*, 3,5-dimethylphenyl isocyanate (0.13 mL, 0.93 mmol) was added to a solution of 3-*tert*-butyl-1-phenyl-1*H*-pyrazole-5-amine (**215**) (0.18 g, 0.84 mmol) in CH₂Cl₂ (1.8 mL) and stirred at 20 °C for 20 min. Volatiles were removed *in vacuo* and the residue triturated with EtOAc-light petroleum (1:1) to give the *title compound* (0.27 g, 89%) as a colourless solid, mp 196.7-199.5 °C (MeOH) (Found [TOF MS EI⁺]: 363.2193. C₂₂H₂₇N₄O [MH] requires 363.2185); IR (neat) $\nu_{\max}/\text{cm}^{-1}$: 3001 (N-H str), 2957 (C-H str), 1657 (C=O str), 1543 (N-H bend), 1502 (N-H bend), 1372 (C-H bend), 1214 (C-N str), 1005 (C-N str); ¹H NMR (500 MHz, DMSO-*d*₆) $\delta_{\text{H}}/\text{ppm}$: 8.84 (1H, s, N'H), 8.34 (1H, s, NH), 7.52 (4H, m, 2, 3, 5, 6-PhCH), 7.41 (1H, m, 4-PhCH), 7.03 (2H, s, 2', 6'-CH), 6.61 (1H, s, 4'-CH), 6.38 (1H, s, 4-CH), 2.21 (6H, s, Me), 1.28 (9H, s, CMe₃); ¹³C NMR (126 MHz, DMSO-*d*₆) $\delta_{\text{C}}/\text{ppm}$: 160.7 (3-C), 151.4 (C), 139.1 (1'-C), 138.5 (1-PhC), 137.7 (3', 5'-C), 137.2 (5-C), 129.2 (3, 5-PhCH), 127.1 (4-PhCH), 124.2 (2, 6-PhCH), 123.6 (4'-CH), 115.8 (2', 6'-CH), 95.2 (4-CH), 31.9 (CMe₃), 30.1 (CMe₃), 21.0 (Me).

6.3.10. *N*-(3-(*tert*-Butyl)-1-phenyl-1*H*-pyrazol-5-yl)-*N'*-(5-fluoro-2-methylphenyl)urea (**215I**)



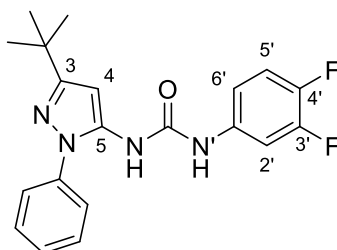
Chemical Formula: C₂₁H₂₃FN₄O

Mr: 366.43

Following the procedure of Bagley *et al.*, 5-fluoro-2-methylphenyl isocyanate (0.12 mL, 0.93 mmol) was added to a solution of 3-*tert*-butyl-1-phenyl-1*H*-pyrazole-5-amine (**215**) (0.20 g, 0.91 mmol) in CH₂Cl₂ (1.8 mL) and stirred at 20 °C for 20 min. Volatiles were then removed *in vacuo* and the residue triturated with EtOAc-light petroleum (1:5) to give the *title compound* (0.22 g, 67%) as a colourless solid, mp 164.9-166.4 °C (MeOH) (Found [TOF MS EI⁺]: 367.1937. C₂₁H₂₄N₄OF [MH] requires 367.1934); IR (neat) $\nu_{\max}/\text{cm}^{-1}$: 3284 (N-H str), 2958 (C-H str), 1654 (C=O str), 1546 (N-H bend), 1503 (N-H bend), 1236 (C-N str), 1004 (C-N bend); ¹H NMR (500 MHz,

DMSO-*d*₆) δ_{H} /ppm: 8.91 (1H, s, NH), 8.31 (1H, s, N'H), 7.73 (1H, dd, $^3J_{\text{FH}} = 12$ Hz, $^4J_{\text{HH}} = 2$ Hz, 6'-CH), 7.54 (4H, m, 2, 3, 5, 6-PhCH), 7.42 (1H, m, 4-PhCH), 7.17 (1H, pt, $^3J_{\text{HH}}$, $^4J_{\text{FH}} = 7$ Hz, 3'-CH), 6.76 (1H, ptd, $^3J_{\text{HH}}$, $^3J_{\text{FH}} = 8$, $^4J_{\text{HH}} = 2$ Hz, 4'-CH), 6.38 (1H, s, 4-CH), 2.15 (3H, s, Me), 1.28 (9H, s, CMe₃); ^{13}C NMR (126 MHz, DMSO-*d*₆) δ_{C} /ppm: 161.0 (3-C), 160.5 (d, $^1J_{\text{FC}} = 240$ Hz, 5'-CF), 151.9 (C), 138.7 (1-PhC), 138.5 (d, $^3J_{\text{FC}} = 11$ Hz, 1'-C), 137.0 (5-CH), 131.2 (d, $^3J_{\text{FC}} = 10$ Hz, 3'-CH), 129.4 (3, 5-PhCH), 127.3 (4-PhCH), 124.2 (2, 6-PhCH), 122.9 (d, $^4J_{\text{FC}} = 3$ Hz, 2'-C), 109.0 (d, $^2J_{\text{FC}} = 21$ Hz, 4'-CH), 107.3 (d, $^2J_{\text{FC}} = 26$ Hz, 6'-CH), 96.1 (4-CH), 32.1 (CMe₃), 30.2 (CMe₃), 17.2 (Me).

6.3.11. *N*-(3-(*tert*-Butyl)-1-phenyl-1*H*-pyrazol-5-yl)-*N'*-(3,4-difluorophenyl) urea (**215J**)



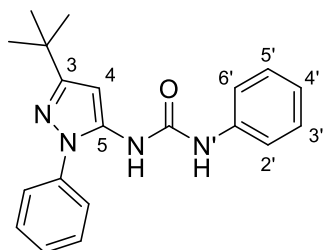
Chemical Formula: C₂₀H₂₀F₂N₄O

Mr: 370.39

Following the procedure of Bagley *et al.*, 3,4-difluorophenyl isocyanate (0.11 mL, 0.94 mmol) was added to a solution of 3-*tert*-butyl-1-phenyl-1*H*-pyrazole-5-amine (**215**) (0.20 g, 0.92 mmol) in CH₂Cl₂ (1.8 mL) and stirred at 20 °C for 20 min. Volatiles were then removed *in vacuo* and the residue triturated with EtOAc-light petroleum (1:5) to give the *title compound* (0.23 g, 67%) as a colourless solid, mp 154.1-156.4 °C (MeOH) (Found [TOF MS EI⁺]: 371.1681. C₂₀H₂₁N₄OF₂ [MH] requires 371.1683); IR (neat) ν_{max} /cm⁻¹: 3332 (N-H str), 2957 (C-H str), 1660 (C=O str), 1571 (N-H bend), 1513 (N-H bend), 1226 (C-N str), 1136 (C-N str); ^1H NMR (500 MHz, DMSO-*d*₆) δ_{H} /ppm: 9.20 (1H, s, N'H), 8.44 (1H, s, NH), 7.61 (1H, pddd, $^3J_{\text{FH}} = 13$, $^4J_{\text{HF}} = 7$, $^4J_{\text{HH}} = 2$ Hz, 2'CH), 7.52 (4H, m, 2, 3, 5, 6-PhCH), 7.41 (1H, m, 4-PhCH), 7.31 (1H, pq, $^3J_{\text{FH}}$, $^3J_{\text{HH}} = 10$ Hz, 5'-CH), 7.07 (1H, d, $^3J_{\text{HH}} = 9$ Hz, 6'-CH), 6.37 (1H, s, 4-CH), 1.28 (9H, s, CMe₃); ^{13}C NMR (126 MHz, DMSO-*d*₆) δ_{C} /ppm: 160.7 (3-C), 151.6 (C), 149.0 (dd, $^1J_{\text{FC}} = 243$, $^2J_{\text{FC}} = 13$ Hz, 3' or 4'-CF), 144.5 (dd, $^1J_{\text{FC}} = 240$, $^2J_{\text{FC}} = 12$ Hz, 4' or 3'-CF), 138.5 (1-PhC), 136.7 (5-C), 136.4 (dd, $^3J_{\text{FC}} = 9$, $^4J_{\text{FC}} = 2$ Hz, 1'-C), 129.2 (3, 5-PhCH),

127.1 (4-PhCH), 124.1 (2, 6-PhCH), 117.3 (d, $^2J_{\text{FC}} = 17$ Hz, 5'-CH), 114.3 (dd, $^3J_{\text{FC}} = 6$, $^4J_{\text{FC}} = 3$ Hz, 6'-CH), 107.1 (d, $^2J_{\text{FC}} = 22$ Hz, 2'-CH), 96.0 (4-CH), 31.9 (CMe₃), 30.1 (CMe₃).

6.3.12. *N*-(3-(*tert*-Butyl)-1-phenyl-1*H*-pyrazol-5-yl)-*N'*-phenylurea (215K)

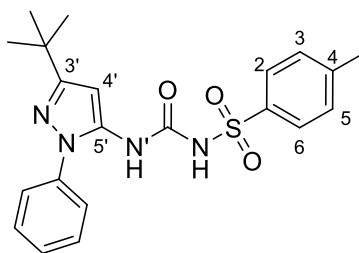


Chemical Formula: C₂₀H₂₂N₄O

Mr: 334.41

Following the procedure of Bagley *et al.*, phenyl isocyanate (0.11 mL, 1.01 mmol) was added to a solution of 3-*tert*-butyl-1-phenyl-1*H*-pyrazole-5-amine (**215**) (0.20 g, 0.92 mmol) in CH₂Cl₂ (1.8 mL) and stirred at 20 °C for 20 min. Volatiles were then removed *in vacuo*, and the residue triturated with EtOAc-light petroleum (1:5), and recrystallization with hot MeOH gave the *title compound* (0.26 g, 85%) as colourless crystals, mp 188.7-190.9 °C (Found [TOF MS EI⁺]: 335.1875. C₂₀H₂₃N₄O [MH] requires 335.1872); IR (neat) $\nu_{\text{max}}/\text{cm}^{-1}$: 3276 (N-H str), 2957 (C-H str), 1664 (C=O str), 1548 (N-H bend), 1498 (N-H bend), 1229 (C-N str), 1054 (C-N str); ¹H NMR (500 MHz, DMSO-*d*₆) $\delta_{\text{H}}/\text{ppm}$: 8.98 (1H, s, N'H), 8.37 (1H, s, NH), 7.56 - 7.51 (4H, m, 2, 3, 5, 6-PhCH), 7.41 (3H, 4-PhCH and 2', 6'-CH), 7.26 (2H, t, $J = 8$ Hz, 3', 5'-CH), 6.97 (1H, t, $J = 7$ Hz, 4'-CH), 6.38 (1H, s, 4-CH), 1.28 (9H, s, CMe₃); ¹³C NMR (126 MHz, DMSO-*d*₆) $\delta_{\text{C}}/\text{ppm}$: 160.7 (3-C), 151.5 (C), 139.3 (1'-C), 138.5 (1-PhC), 137.1 (5-C), 129.2 (3, 5-PhCH), 128.7 (3', 5'-CH), 127.1 (4-PhCH), 124.2 (2, 6-PhCH), 122.0 (4'-CH), 118.1 (2', 6'-CH), 95.4 (4-CH), 31.9 (CMe₃), 30.1 (CMe₃).

6.3.13. *N*-((3-(*tert*-Butyl)-1-phenyl-1*H*-pyrazol-5-yl)carbamoyl)-4-methylbenzenesulfonamide (215L)

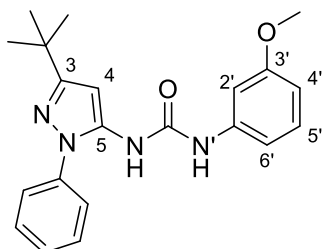


Chemical Formula: $C_{21}H_{24}N_4O_3S$

Mr: 412.50

Following the procedure of Bagley *et al.*, *p*-tolylsulfonyl isocyanate (0.15 mL, 1.10 mmol) was added to a solution of 3-*tert*-butyl-1-phenyl-1*H*-pyrazole-5-amine (**215**) (0.20 g, 0.91 mmol) in CH_2Cl_2 (1.8 mL) and stirred at 20 °C for 20 min. Volatiles were then removed *in vacuo* and the residue triturated with EtOAc-light petroleum (1:1) to give the *title compound* (0.28 g, 75%) as a colourless solid, mp 166.3-170.6 °C (Found [TOF MS EI⁺]: 413.1655. $C_{21}H_{25}N_4O_3S$ [MH] requires 413.1647); IR (neat) ν_{max}/cm^{-1} : 3290 (N-H str), 2957 (C-H str), 1657 (C=O str), 1541 (N-H bend), 1502 (N-H bend), 1212 (C-N str), 989 (S=O str); 1H NMR (500 MHz, DMSO- d_6) δ_H/ppm : 11.09 (1H, br. s, NH), 8.55 (1H, s, N'H), 7.77 (2H, d, J = 8 Hz, 2, 6-CH), 7.47 - 7.35 (7H, 3, 5-CH and 2-6-PhCH), 6.26 (1H, s, 4'-CH), 2.40 (3H, s, Me), 1.23 (9H, s, CMe₃); ^{13}C NMR (126 MHz, DMSO- d_6) δ_C/ppm : 160.7 (3'-C), 148.8 (C), 143.9 (4-C), 138.1 (1-PhC or 1-C), 136.7 (1-C or 1-PhC), 135.3 (5'-C), 129.4 (3, 5-CH), 129.1 (3, 5-PhCH), 127.3 (2, 6-CH), 127.3 (4-PhCH), 124.0 (2, 6-PhCH), 96.8 (4'-CH), 32.0 (CMe₃), 30.0 (CMe₃), 21.0 (Me).

6.3.14. *N*-(3-(*tert*-Butyl)-1-phenyl-1*H*-pyrazol-5-yl)-*N'*-(3-methoxyphenyl)urea (**215M**)

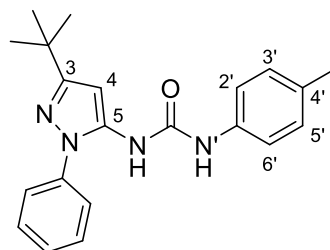


Chemical Formula: $C_{21}H_{24}N_4O_2$

Mr: 364.19

Following the procedure of Bagley *et al.*, 3-methoxyphenyl isocyanate (0.13 mL, 1.00 mmol) was added to a solution of 3-*tert*-butyl-1-phenyl-1*H*-pyrazole-5-amine (**215**) (0.20 g, 0.93 mmol) in CH₂Cl₂ (1.8 mL) and stirred at 20 °C for 20 min. Volatiles were then removed *in vacuo* and the residue triturated with EtOAc-light petroleum (1:2) to give the *title compound* (0.22 g, 65%) as a colourless solid, mp 177.1-179.2 °C (MeOH) (Found [TOF MS EI⁺]: 365.1980. C₂₁H₂₅N₄O₂ [MH] requires 365.1978); IR (neat) $\nu_{\max}/\text{cm}^{-1}$: 3285 (N-H str), 2958 (C-H str), 1661 (C=O str), 1599 (N-H str), 1549 (N-H str), 1045 (C-O str); ¹H NMR (500 MHz, DMSO-*d*₆) $\delta_{\text{H}}/\text{ppm}$: 9.00 (1H, s, N'H), 8.35 (1H, s, NH), 7.56 - 7.49 (4H, m, 2, 3, 5, 6-PhCH), 7.41 (1H, m, 4-PhCH), 7.14 (2H, 2', 5'-CH), 6.88 (1H, d, *J* = 8 Hz, 6'-CH), 6.55 (1H, dd, *J* = 8, 2 Hz, 4'-CH), 6.38 (1H, s, 4-CH), 3.71 (3H, s, Me), 1.28 (9H, s, CMe₃); ¹³C NMR (126 MHz, DMSO-*d*₆) $\delta_{\text{C}}/\text{ppm}$: 160.7 (3-C), 159.6 (3'-C), 151.4 (C), 140.5 (1'-C), 138.5 (1-PhC), 137.0 (5-C), 129.4 (5'-CH), 129.2 (3, 5-PhCH), 127.1 (4-PhCH), 124.2 (2, 6-PhCH), 110.3 (6'-CH), 107.6 (4'-CH), 103.8 (2'-CH), 95.4 (4-CH), 54.8 (OMe), 31.9 (CMe₃), 30.1 (CMe₃).

6.3.15. *N*-(3-(*tert*-Butyl)-1-phenyl-1*H*-pyrazol-5-yl)-*N'*-(*p*-tolyl)urea (**215N**)



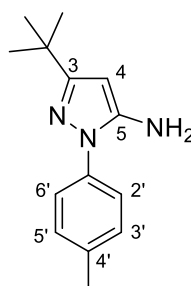
Chemical Formula: C₂₁H₂₄N₄O

Mr: 348.44

Following the procedure of Bagley *et al.*, *p*-tolyl isocyanate (0.13 mL, 1.03 mmol) was added to a solution of 3-*tert*-butyl-1-phenyl-1*H*-pyrazole-5-amine (**215**) (0.20 g, 0.92 mmol) in CH₂Cl₂ and stirred at 20 °C for 20 min. Volatiles were then removed *in vacuo* and the residue triturated with EtOAc-light petroleum (1:1) and recrystallization from hot MeOH gave the *title compound* (0.20 g, 62%) as a colourless solid, mp 197.8-199.2 °C (Found [TOF MS EI⁺]: 349.2041. C₂₁H₂₅N₄O [MH] requires 349.2028); IR (neat) $\nu_{\max}/\text{cm}^{-1}$: 3267 (N-H str), 2955 (C-H str), 1659 (C=O str), 1538 (N-H bend), 1362 (C-H rock), 1140 (C-N str); ¹H NMR (500 MHz, DMSO-*d*₆) $\delta_{\text{H}}/\text{ppm}$: 8.88 (1H, s, N'H),

8.32 (1H, s, NH), 7.56 - 7.50 (4H, m, 2, 3, 5, 6-PhCH), 7.41 (1H, m, 4-PhCH), 7.28 (2H, d, $J = 8$ Hz, 3', 5'-CH), 7.06 (2H, d, $J = 8$ Hz, 2', 6'-CH), 6.37 (1H, s, 4-CH), 2.23 (3H, s, CH₃), 1.28 (9H, s, CMe₃); ¹³C NMR (126 MHz, DMSO-*d*₆) δ_c /ppm: 160.7 (3-C), 151.5 (C), 138.5 (1-PhC), 137.2 (5-C), 136.7 (1'-C), 130.8 (4'-C), 129.2 (3, 5-PhCH), 129.1 (3', 4'-CH), 127.1 (4-PhCH), 124.2 (2, 6-PhCH), 118.2 (2', 6'-CH), 95.2 (4-CH), 31.9 (CMe₃), 30.1 (CMe₃), 20.1 (Me).

6.3.16. 3-(*tert*-Butyl)-1-(*p*-tolyl)-1*H*-pyrazol-5-amine (217)

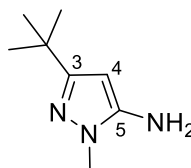


Chemical Formula: C₁₄H₁₉N₃

Mr: 229.32

According to a modified procedure,⁵⁰ *p*-tolylhydrazine hydrochloride (0.71 g, 0.44 mmol), 4,4-dimethyl-3-oxopentanitrile (0.50 g, 0.40 mmol) and a catalytic amount of conc. HCl in EtOH (20 mL) was irradiated at 130 °C for 20 min in a pressure-rated glass vial (35 mL) using a CEM Discover microwave synthesizer by modulating the initial power (200 W). After cooling in a flow of compressed air, the reaction mixture was basified with aqueous NaOH solution (10%) to pH 12 and extracted with EtOAc (3 x 20 mL). The organic extracts were combined, washed with brine (1 x 30 mL), dried (MgSO₄), filtered and evaporated *in vacuo*. Purification by flash column chromatography on SiO₂ (dry-load), gradient eluting with hexanes to CH₂Cl₂, gave the *title compound* (0.77 g, 83%) as a light orange crystalline solid, mp 115.4-118.4 °C, (Found [ESI⁺]: 230.1650. C₁₄H₂₀N₃ [MH] requires 230.1652); IR (neat) ν_{\max} /cm⁻¹: 3470 (N-H str), 2958 (C-H str), 1633 (N-H bend), 1558 (C=N str), 1516 (C-C str), 1245 (C-N str), 819 (N-H wag); ¹H NMR (500 MHz, CDCl₃) δ_H /ppm: 7.43 (2H, d, $J = 8$ Hz, 2', 6'-CH), 7.25 (2H, d, $J = 8$ Hz, 3', 5'-CH), 5.51 (1H, s, 4-CH), 3.69 (2H, br. s, NH₂), 2.38 (3H, s, Me), 1.32 (9H, s, CMe₃); ¹³C NMR (126 MHz, CDCl₃) δ_c /ppm: 162.1 (C), 144.6 (5-C), 136.8 (4'-C), 136.5 (1'-C), 129.9 (3', 5'-CH), 124.0 (2', 6'-CH), 87.4 (4-CH), 32.2 (CMe₃), 30.4 (CMe₃), 21.0 (Me).

6.3.17. 3-(*tert*-Butyl)-1-methyl-1*H*-pyrazol-5-amine (226)

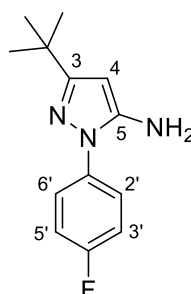


Chemical Formula: C₈H₁₅N₃

Mr: 153.22

Methyl hydrazine (0.09 mL, 1.70 mmol) and 4,4-dimethyl-3-oxopentanitrile (0.20 g, 1.60 mmol) in a toluene: glacial AcOH solution ([5:1]; 0.8 mL) was irradiated at 120 °C for 40 min in a pressure-rated glass vial (10 mL) using a CEM Discover microwave synthesizer by modulating the initial power (100 W). After cooling in a flow of compressed air the volatiles were removed *in vacuo*. Purification by flash column chromatography on SiO₂, gradient eluting with CH₂Cl₂ to EtOAc, gave the *title compound* (0.24 g, 95%) as an off white crystalline solid, mp 151.4-155.0 °C (lit.⁵² 156-157 (light petroleum)) (Found [ESI⁺]: 154.1339. C₈H₁₆N₃ [MH] requires 154.1339); IR (neat) $\nu_{\max}/\text{cm}^{-1}$: 3392 (N-H str), 2956 (C-H str), 1627 (N-H bend), 1567 (C=N str), 1360 (C-H bend); ¹H NMR (500 MHz, CDCl₃) $\delta_{\text{H}}/\text{ppm}$: 5.42 (1H, br. s, 4-CH), 3.62 (3H, s, Me), 1.26 (9H, s, CMe₃); ¹³C NMR (126 MHz, CDCl₃) $\delta_{\text{C}}/\text{ppm}$: 160.6 (3-C), 144.4 (5-C), 88.0 (4-CH), 33.9 (Me), 32.0 (CMe₃), 30.4 (CMe₃).

6.3.18. 3-(*tert*-Butyl)-1-(4-fluorophenyl)-1*H*-pyrazole-5-amine (227)

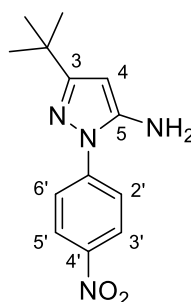


Chemical Formula: C₁₃H₁₆FN₃

Mr: 233.28

According to a modified procedure,⁵⁰ 4-fluorophenylhydrazine hydrochloride (0.26 g, 1.60 mmol), 4,4-dimethyl-3-oxopentanitrile (0.20 g, 1.57 mmol) and a catalytic amount of conc. HCl in EtOH (9 mL) was irradiated at 130 °C for 30 min in a pressure-rated glass vial (35 mL) using a CEM Discover microwave synthesizer by modulating the initial power (200 W). After cooling in a flow of compressed air, the reaction mixture was basified with aqueous NaOH solution (10%) to pH 12 and extracted with EtOAc (3 x 20 mL). The organic extracts were then combined, washed with brine (1 x 20 mL), dried (MgSO₄), filtered and evaporated *in vacuo*. The residues were then triturated with light petroleum to give the *title compound* (0.32 g, 88%) as a red crystalline solid, mp 101.0-105.2 °C (Found [ESI⁺]: 234.1399. C₁₃H₁₇N₃F [MH] requires 234.1401); IR (neat) ν_{max} /cm⁻¹: 3319 (N-H str), 2969 (C-H str), 1633 (N-H bend), 1510 (C=N str), 1216 (C-N str); ¹H NMR (500 MHz, CDCl₃) δ_{H} /ppm: 7.55 (2H, pdd, ³J_{HH} = 9 Hz, ⁴J_{FH} = 5 Hz 2', 6'-CH), 7.14 (2H, pt, ³J_{FH}, ³J_{HH} = 9 Hz, 3', 5'-CH), 5.53 (1H, s, 4-CH), 3.65 (2H, br. s, NH₂), 1.32 (9H, s, CMe₃); ¹³C NMR (126 MHz, CDCl₃) δ_{C} /ppm: 162.4 (3-C), 161.4 (d, ¹J_{FC} = 246 Hz, 4'-C), 144.7 (5-C), 135.2 (1'-C), 125.9 (d, ³J_{CF} = 9 Hz, 2', 6'-CH), 116.1 (d, ²J_{CF} = 23 Hz, 3', 5'-CH), 87.9 (4-CH), 32.2 (CMe₃), 30.1 (CMe₃).

6.3.19. 3-(*tert*-Butyl)-1-(4-nitrophenyl)-1*H*-pyrazol-5-amine (228)



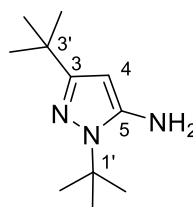
Chemical Formula: C₁₃H₁₆N₄O₂

Mr: 260.29

According to a modified procedure, 4-nitrophenyl hydrazine (0.25 g, 1.63 mmol) and 4,4-dimethyl-3-oxopentanitrile (0.20 g, 1.63 mmol) in a toluene: glacial AcOH solution ([5:1]; 0.8 mL) was irradiated at 120 °C for 40 min in a pressure-rated glass vial (10 mL) using a CEM Discover microwave synthesizer by modulating the initial power (100 W). After cooling in a flow

of compressed air the volatiles were removed *in vacuo*. Purification by flash column chromatography on SiO₂ (dry-load), gradient eluting with CH₂Cl₂-hexanes (50:50) to CH₂Cl₂, gave the *title compound* (0.21 g, 48%) as an off white crystalline solid, mp 162.1-164.8 °C (lit.³⁶⁹ 172) (Found [ESI+]: 261.1348. C₁₃H₁₇N₄O₂ [MH] requires 261.1346); IR (neat) $\nu_{\max}/\text{cm}^{-1}$: 3395 (N-H str), 2961 (C-H str), 1644 (N-H bend), 1592 (C=N str), 1504 (N-O str), 1331 (N-O str), 1241 (C-N str), 1108 (C-N str); ¹H NMR (500 MHz, CDCl₃) $\delta_{\text{H}}/\text{ppm}$: 8.29 (2H, d, *J* = 9 Hz, 3', 5'-CH), 7.90 (2H, d, *J* = 9 Hz, 2', 6'-CH), 5.62 (1H, s, 4-CH), 3.82 (2H, br. s, NH₂), 1.31 (9H, s, CMe₃); ¹³C NMR (126 MHz, CDCl₃) $\delta_{\text{C}}/\text{ppm}$: 164.0 (3-C), 145.4 (5-C), 145.0 (C), 144.8 (C), 124.9 (3', 5'-CH), 122.1 (2', 6'-CH), 90.6 (4-CH), 32.4 (CMe₃), 30.0 (CMe₃).

6.3.20. 1,3-Di-*tert*-butyl-1*H*-pyrazol-5-amine (229)

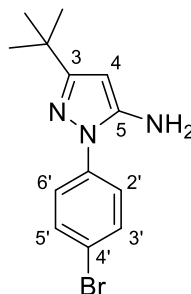


Chemical Formula: C₁₁H₂₁N₃

Mr: 195.30

4,4-Dimethyl-3-oxopentanitrile (0.50 g, 4.0 mmol) and *tert*-butyl hydrazine hydrochloride (0.66 g, 5.3 mmol) were taken up in EtOH (10 mL), a catalytic amount of concentrated HCl was added, and the solution was heated to reflux for 18 h. Once cooled to RT, the solution was basified with aqueous NaOH solution (10 w%) to pH 12 and extracted with EtOAc (3 x 30 mL). The organic extracts were combined, washed with brine (1 x 40 mL), dried (Na₂SO₄), filtered and evaporated *in vacuo*. Purification by flash column chromatography on SiO₂ (dry-load), gradient eluting with hexanes to EtOAc in hexanes (15:85), to give the *title compound* (0.47 g, 61%) as brown crystals, mp 68.7-70.4 °C (lit.³⁷⁰ 67-69 °C) (Found [ESI+]: 196.1800 C₁₁H₂₂N₃ [MH] requires 196.1808); IR (neat) $\nu_{\max}/\text{cm}^{-1}$: 3355 (N-H str), 2962 (C-H str), 1629 (N-H bend), 1544 (C=N str), 1359 (C-H bend), 1232 (CH₃ bend); ¹H NMR (500 MHz, DMSO-*d*₆) $\delta_{\text{H}}/\text{ppm}$: 5.24 (1H, s, 4-CH), 4.60 (2H, br. s, NH₂), 1.49 (9H, s, 1'-CMe₃), 1.14 (9H, s, 3'-CMe₃); ¹³C NMR (126 MHz, DMSO-*d*₆) $\delta_{\text{C}}/\text{ppm}$: 155.9 (3-C), 146.1 (5-C), 88.2 (4-CH), 56.9 (1'-CMe₃), 31.5 (3'-CMe₃), 30.4 (3'-CMe₃), 29.0 (1'-CMe₃); *m/z* (EI+): 195 (*M*⁺, 35), 139 (M-CMe₃, 74), 124 (100).

6.3.21. 1-(4-Bromophenyl)-3-(*tert*-butyl)-1*H*-pyrazol-5-amine (230)

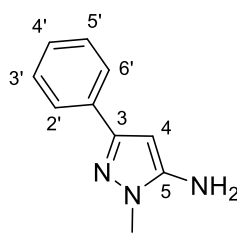


Chemical Formula: C₁₃H₁₆BrN₃

Mr: 294.20

4,4-Dimethyl-3-oxopentanitrile (0.20 g, 1.64 mmol) and 4-bromophenylhydrazine hydrochloride (0.35 g, 1.56 mmol) in a solution of EtOH (8 mL) and a catalytic amount of concentrated HCl was irradiated at 130 °C for 25 min in a pressure-rated glass vial (35 mL) using a CEM Discover microwave synthesizer by moderating the initial power (200 W). After cooling in a flow of compressed air, the solution was basified with aqueous NaOH solution (10 w%) to pH 12, partitioned between EtOAc (20 mL) and water (10 mL) and the aqueous layer extracted with EtOAc (2 x 20 mL). The organic extracts were combined, washed with brine (1 x 30 mL), dried (Na₂SO₄), filtered and evaporated *in vacuo*. Purification by flash column chromatography on SiO₂ (dry-load), gradient eluting with hexanes to EtOAc in hexanes (25:75) gave the *title compound* (0.27 g, 58%) as a brown solid, mp 133.7-136.4 °C (Found [ESI⁺]: 294.0601. C₁₃H₁₇N₃⁷⁹Br [MH] requires 294.0600); IR (neat) ν_{max} /cm⁻¹: 3437 (N-H str), 2957 (C-H str), 1635 (N-H bend), 1557 (C=N str), 1500 (C-C str), 1244 (C-N str), 1065 (C-N str); ¹H NMR (500 MHz, DMSO-*d*₆) δ_{H} /ppm: 7.62 (2H, d, *J* = 9 Hz, 2', 6'-CH), 7.56 (2H, d, *J* = 9 Hz, 3', 5'-CH), 5.40 (1H, s, 4-CH), 5.25 (2H, br. s, NH₂), 1.21 (9H, s, CMe₃); ¹³C NMR (126 MHz, DMSO-*d*₆) δ_{C} /ppm: 161.2 (3-C), 147.2 (5-C), 138.9 (1'-C), 131.7 (2', 6'-CH), 124.0 (3', 5'-CH), 117.6 (4'-C), 87.4 (4-CH), 31.7 (CMe₃), 30.0 (CMe₃); *m/z* (EI⁺): 295 (M⁸¹Br⁺⁺, 45), 293 (M⁷⁹Br⁺⁺, 48), 280 (M⁸¹Br – Me, 97), 278 (M⁷⁹Br-Me, 100).

6.3.22. 1-Methyl-3-phenyl-1*H*-pyrazol-5-amine (231)

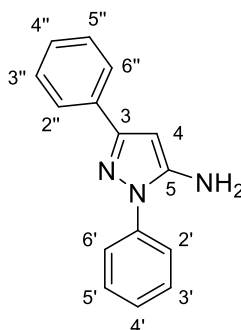


Chemical formula: $C_{10}H_{11}N_3$

Mr: 173.2

Methyl hydrazine (0.27g, 5.82 mmol) and benzoylacetonitrile (0.35 g, 2.40 mmol) in a toluene-glacial AcOH solution ([5:1]; 2 mL) was irradiated at 120 °C for 40 min in a pressure-rated glass vial (10 mL) using a CEM Discover microwave synthesizer by moderating the initial power (100 W). After cooling in a flow of compressed air, the volatiles were removed *in vacuo*. Purification by flash column chromatography on SiO_2 , gradient eluting with CH_2Cl_2 to MeOH- CH_2Cl_2 (5:95), and recrystallization from hot EtOAc gave the *title compound* (0.21 g, 50%), as a purple crystalline solid, mp 124.1-128.1 °C (lit.³⁷¹ 124-126) (Found [ESI+]: 174.1021. $C_{10}H_{10}N_3$ [MH] requires 174.1026); IR (neat) ν_{max}/cm^{-1} : 3425 (C-N str), 3145 (C-H str), 1623 (N-H bend), 1560 (C=N str), 1511 (C-C str), 1271 (C-N str); 1H NMR (500 MHz, DMSO- d_6) δ_H/ppm : 7.65 (1H, d, J = 8 Hz, 2', 6'-CH), 7.32 (2H, t, J = 7.5 Hz, 3', 5'-CH), 7.21 (1H, t, J = 7.5 Hz, 4'-CH), 5.68 (1H, s, 4-CH), 5.23 (2H, br. s, NH_2), 3.56 (3H, s, Me); ^{13}C NMR (126 MHz, DMSO- d_6) δ_C/ppm : 148.0 (5-C), 147.7 (3-C), 134.3 (1'-C), 128.2 (3', 5'-CH), 126.7 (4'-CH), 124.5 (2', 6'-CH), 85.2 (4-CH), 34.2 (Me); m/z (EI+): 173 (M^{*+} , 100), 130 (14), 102 (10), 77 (10).

6.3.23. 1,3-Diphenyl-1H-pyrazol-5-amine (232)

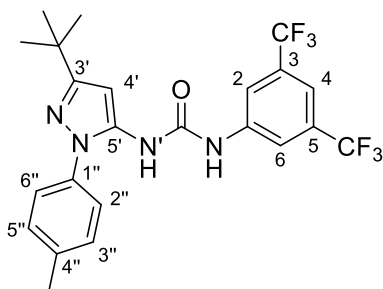


Chemical Formula: $C_{15}H_{13}N_3$

Mr: 235.28

Benzoylacetonitrile (0.34 g, 2.37 mmol) and phenylhydrazine (0.26 g, 2.43 mmol) in a toluene-glacial AcOH solution ([5:1]; 2 mL) was irradiated at 120 °C for 40 min in a pressure-rated glass vial (10 mL) using a CEM Discover microwave synthesizer, through modulation of the initial power (100 W). After cooling in a flow of compressed air, the volatiles were removed *in vacuo*. Purification by flash column chromatography on SiO₂ (dry-load), gradient eluting with hexanes to EtOAc-hexanes (30:70), gave the *title compound* (0.51 g, 91%) as a yellow solid, mp 129.1-130.2 °C (lit.³⁷² 129 -130 (CHCl₃)) (Found [ESI⁺]: 236.1176. C₁₅H₁₄N₃ [MH] requires 236.1182); IR (neat) $\nu_{\max}/\text{cm}^{-1}$: 3305 (N-H str), 1627 (N-H bend), 1598 (C=N str), 1505 (C-C str), 1377 (C-N str); ¹H NMR (500 MHz, DMSO-*d*₆) $\delta_{\text{H}}/\text{ppm}$: 7.74 (2H, d, *J* = 7.5 Hz, 2'', 6''-CH) 7.65 (2H, d, *J* = 8 Hz, 2', 6'-CH), 7.49 (2H, t, *J* = 8 Hz, 3', 5'-CH), 7.37 (2H, t, *J* = 7.5 Hz, 3'', 5''-CH), 7.32 (1H, t, *J* = 7.5 Hz, 4'-CH), 7.28 (1H, t, *J* = 7.5 Hz, 4''-CH), 5.90 (1H, s, 4-CH), 5.40 (2H, br. s, NH₂); ¹³C NMR (126 MHz, DMSO-*d*₆) $\delta_{\text{C}}/\text{ppm}$: 149.9 (3-C), 148.1 (5-C), 139.2 (1'-C), 133.6 (1''-C), 129.0 (3', 5'-CH), 128.4 (3'', 5''-CH), 127.4 (4''-CH), 126.2 (4'-CH), 125.0 (2'', 6''-CH), 122.8 (2', 6'-CH), 87.1 (4-CH); *m/z* (EI⁺): 235 (*M*⁺, 100), 234 (21), 207 (13).

6.3.24. *N*-(3,5-Bis(trifluoromethyl)phenyl)-*N'*-(3-(*tert*-butyl)-1-(*p*-tolyl)-1*H*-pyrazol-5-yl)urea (217F)



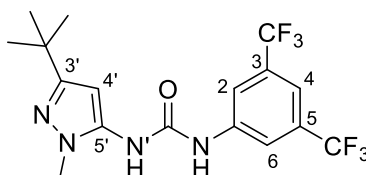
Chemical Formula: C₂₃H₂₂F₆N₄O

Mr: 484.44

3-(*tert*-Butyl)-1-(*p*-tolyl)-1*H*-pyrazol-5-amine (**217**) (0.21 g, 0.90 mmol) was added to a solution of 3,3-bis(trifluoromethyl)phenyl isocyanate (0.19 g, 0.76 mmol) in CH₂Cl₂ (1 mL) and stirred at RT for 20 min. Volatiles were then removed *in vacuo* and residue triturated with light petroleum and recrystallized from hot MeOH to give the *title compound* (0.155 g, 42%) as colourless

crystals, mp 155.3-158.3 °C (MeOH) (Found [ESI⁺]: 485.1749 C₂₃H₂₃N₄O₆ [MH] requires 485.1771); IR (neat) $\nu_{\text{max}}/\text{cm}^{-1}$: 3322 (N-H str), 2959 (C-H str), 1660 (C=O str), 1561 (N-H bend), 1383 (C-H str), 1271 (C-N str), 1172 (C-O str), 1139 (C-F str); ¹H NMR (500 MHz, DMSO-*d*₆) $\delta_{\text{H}}/\text{ppm}$: 9.70 (1H, br. s, NH), 8.60 (1H, br. s, N'H), 8.06 (2H, s, 2, 6-CH), 7.64 (1H, s, 4-CH), 7.40 (2H, d, *J* = 8 Hz, 2'', 6''-CH), 7.32 (2H, d, *J* = 8 Hz, 3'', 5''-CH), 6.38 (1H, s, 4'-CH), 2.36 (3H, s, Me), 1.28 (9H, s, CMe₃); ¹³C NMR (100 MHz, DMSO-*d*₆) $\delta_{\text{C}}/\text{ppm}$: 160.5 (3'-C), 151.8 (C), 141.5 (1-C), 136.7 (4''-C), 136.2 (5'-C), 136.0 (1''-C), 130.7 (q, ²*J*_{CF} = 33 Hz, 3, 5-C), 129.6 (3'', 5''-CH), 124.1 (2'', 6''-CH), 123.4 (q, ¹*J*_{CF} = 273 Hz, CF₃), 117.9 (d, ³*J*_{CF} = 3 Hz, 2, 6-CH), 114.6 (m, ³*J*_{CF} = 3 Hz, 4-CH), 96.5 (4'-CH), 32.0 (CMe₃), 30.1 (CMe₃), 20.5 (Me); *m/z* (EI⁺): 484 (*M*⁺, 100), 469 (72), 240 (64), 214 (76).

6.3.25. *N*-(3,5-Bis(trifluoromethyl)phenyl)-*N'*-(3-*tert*-butyl-1-methyl-1*H*-pyrazol-5-yl)urea (**226F**)

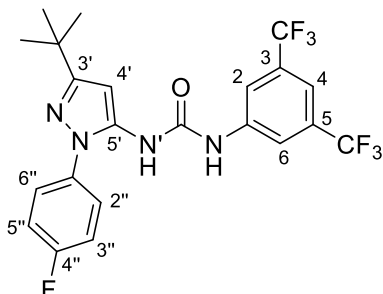


Chemical Formula: C₁₇H₁₈F₆N₄O

Mr: 408.34

3,5-Bis(trifluoromethyl)phenyl isocyanate (0.15 mL, 0.87 mmol) was added to a solution of 3-(*tert*-butyl)-1-methyl-1*H*-pyrazol-5-amine (**226**) (0.13 g, 0.84 mmol) in CH₂Cl₂ (1.7 mL) and stirred at RT for 20 min. Volatiles were then removed *in vacuo* and the residues triturated with light petroleum and recrystallized from hot MeOH to give the *title compound* (0.10 g, 30%) as an off-white powder, mp 155.7-159.7 °C (MeOH) (Found [ESI⁺]: 409.1454. C₁₇H₁₉N₄O₆ [MH] requires 409.1458); IR (neat) $\nu_{\text{max}}/\text{cm}^{-1}$: 3307 (N-H str), 2968 (C-H str), 1706 (C=O str), 1573 (N-H bend), 1386 (C-H str), 1276 (C-N str), 1166 (C-O str), 1130 (C-F str); ¹H NMR (500 MHz, DMSO-*d*₆) $\delta_{\text{H}}/\text{ppm}$: 9.61 (1H, s, NH), 8.74 (1H, s, N'H), 8.14 (2H, s, 2, 6-CH), 7.64 (1H, s, 4-CH), 6.07 (1H, s, 4'-CH), 3.61 (3H, s, Me), 1.22 (9H, s, CMe₃); ¹³C NMR (100 MHz, DMSO-*d*₆) $\delta_{\text{C}}/\text{ppm}$: 158.6 (3'-C), 152.1 (C), 141.7 (1'-C), 136.2 (5'-C), 130.7 (q, ²*J*_{CF} = 33 Hz, 3, 5-C), 123.3 (app. d, ¹*J*_{CF} = 274 Hz, CF₃), 118.0 (m, 2, 6-CH), 114.5 (4-C), 95.0 (4'-CH), 34.9 (Me), 31.8 (CMe₃), 30.3 (CMe₃).

6.3.26. *N*-(3,5-Bis(trifluoromethyl)phenyl)-*N'*-(3-*tert*-butyl-1-(4-fluorophenyl)-1*H*-pyrazol-5-yl)urea (**227F**)

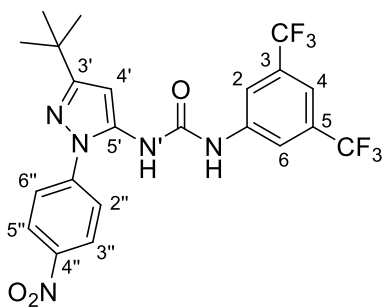


Chemical Formula: C₂₂H₁₉F₇N₄O

Mr: 488.40

3,5-Bis(trifluoromethyl)phenyl isocyanate (0.15 mL, 0.87 mmol) was added to a solution of 3-(*tert*-butyl)-1-(4-fluorophenyl)-1*H*-pyrazole-5-amine (**227**) (0.19 g, 0.82 mmol) in CH₂Cl₂ (1.7 mL) and stirred at RT for 20 min. Volatiles were then removed *in vacuo* and the residues triturated with light petroleum to give the *title compound* (0.30 g, 75%) as a yellow solid, mp 177.6-184.3 °C (Found [ESI⁺]: 489.1499. C₂₂H₂₀N₄OF₇ [MH] requires 489.1520); IR (neat) ν_{max} /cm⁻¹: 3350 (N-H str), 2962 (C-H str), 1664 (C=O str), 1569 (N-H bend), 1510 (N-H bend), 1383 (C-H str), 1271 (C-N str), 1140 (C-F str); ¹H NMR (500 MHz, DMSO-*d*₆) δ_{H} /ppm: 9.70 (1H, s, NH), 8.66 (1H, s, N'H), 8.07 (2H, s, 2, 6-CH), 7.63 (1H, s, 4-CH), 7.57 (2H, dd, ³*J*_{HH} = 9, ⁴*J*_{HF} = 5 Hz, 2'', 6''-CH), 7.35 (2H, pt, ³*J*_{HF} = 9, ³*J*_{HH} = 9 Hz, 3'', 5''-CH), 6.39 (1H, s, 4'-CH), 1.29 (9H, s, CMe₃); ¹³C NMR (100 MHz, DMSO-*d*₆) δ_{C} /ppm: 160.9 (d, ²*J*_{CF} = 245 Hz, 4''-C), 160.8 (3'-C), 151.9 (C), 141.5 (1-C), 136.4 (5'-C), 135.0 (d, ⁴*J*_{CF} = 3 Hz, 1''-C), 130.7 (q, ²*J*_{CF} = 32 Hz, 3, 5-C), 126.3 (d, ³*J*_{CF} = 9 Hz, 2'', 6''-CH), 123.2 (q, ¹*J*_{CF} = 273 Hz, CF₃), 117.9 (app. d, ³*J*_{CF} = 3 Hz, 2, 6-CH), 115.9 (d, ²*J*_{CF} = 23 Hz, 3'', 5''-CH), 114.6 (m, ³*J*_{CF} = 4 Hz, 4-CH), 97.2 (4'-CH), 32.0 (CMe₃), 30.1 (CMe₃); *m/z* (EI): 488 (*M*⁺, 100), 473 (55), 244 (60), 218 (75).

6.3.27. *N*-(3,5-Bis(trifluoromethyl)phenyl)-*N'*-(3-(*tert*-butyl)-1-(4-nitrophenyl)-1*H*-pyrazol-5-yl)urea (**228F**)

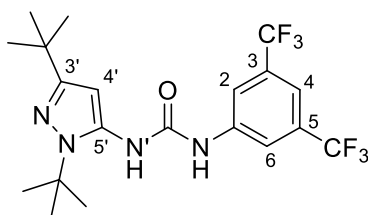


Chemical Formula: $C_{22}H_{19}F_6H_5O_3$

Mr: 515.41

3,5-Bis(trifluoromethyl)phenyl isocyanate (0.12g, 0.52 mmol) was added to a solution of 3-(*tert*-butyl)-1-(4-nitrophenyl)-1*H*-pyrazol-5-amine (**228**) (0.15 g, 0.58 mmol) in CH_2Cl_2 (1.2 mL) and stirred at RT for 20 min. Volatiles were then removed *in vacuo* and the residue triturated with light petroleum and recrystallized from hot MeOH to give the *title compound* (0.10 g, 35%) as orange crystals mp 215.1-217.8 °C (MeOH) (Found [ESI⁺]: 516.1442. $C_{22}H_{20}N_5O_3F_6$ [MH] requires 516.1465); IR (neat) ν_{max}/cm^{-1} : 3350 (N-H str), 2968 (C-H str), 1671 (C=O str), 1572 (N-H bend), 1504 (N-O str), 1340 (N-O str), 1272 (C-N str), 1175 (C-O str), 1135 (C-F str); 1H NMR (500 MHz, DMSO- d_6) δ_H/ppm : 9.79 (1H, br. s, NH), 8.92 (1H, br. s, N'H), 8.35 (2H, d, $J = 9$ Hz, 3'', 5''-CH), 8.09 (2H, s, 2, 6-CH), 7.88 (2H, d, $J = 9$ Hz, 2'', 6''-CH), 7.64 (1H, s, 4-CH), 6.48 (1H, s, 4'-CH), 1.31 (9H, s, CMe₃); ^{13}C NMR (100 MHz, DMSO- d_6) δ_C/ppm : 162.4 (3'-C), 152.2 (C), 145.0 (1''- or 4''-C), 143.9 (1''- or 4''-C), 141.5 (1-C), 137.1 (5'-C), 130.6 (q, $^2J_{CF} = 32$ Hz, 3, 5-C), 124.7 (3'', 5''-CH), 123.6 (q, $^1J_{CF} = 274$ Hz, CF₃), 123.0 (2'', 6''-CH), 118.1 (app. d, $^3J_{CF} = 3$ Hz, 2, 6-CH), 114.7 (m, $^3J_{CF} = 4$ Hz, 4-CH), 100.3 (4'-CH), 32.2 (CMe₃), 29.8 (CMe₃); m/z (EI⁺): 515 (M^{++} , 100), 286 (21), 271 (100).

6.3.28. ***N*-(3,5-Bis(trifluoromethyl)phenyl)-*N'*-((1,3-di-*tert*-butyl)-1*H*-pyrazol-5-yl)urea (229F)**

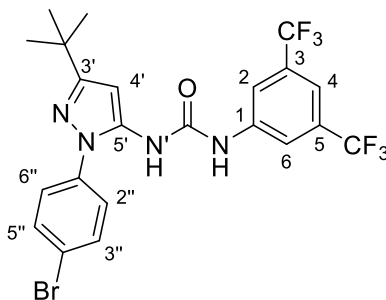


Chemical Formula: C₂₀H₂₄F₆N₄O

Mr: 450.43

1,3-Di-*tert*-butyl-1*H*-pyrazol-5-amine (**229**) (0.095 g, 0.49 mmol) was added to a solution of 3,5-bis(trifluoromethyl)phenyl isocyanate (0.11g, 0.43 mmol) in CH₂Cl₂ (1.5 mL) and stirred at RT for 30 min. Volatiles were then removed *in vacuo* and the residue triturated with light petroleum to give the *title compound* (0.14 g, 72%) as a colourless powder, mp 202.2-203.3 °C (Found [ESI⁺]: 451.1923. C₂₀H₂₅N₄OF₆ [MH] requires 451.1927); IR (neat) ν_{\max} /cm⁻¹: 3310 (N-H str), 2969 (C-H str), 1655 (C=O str), 1576 (N-H bend), 1384 (C-H str), 1272 (C-N str), 1184 (C-O str), 1133 (C-F str); ¹H NMR (500 MHz, DMSO-*d*₆) δ_{H} /ppm: 9.64 (1H, br. s, NH), 8.20 (1H, br. s, N'H), 8.15 (2H, s, 2, 6-CH), 7.62 (1H, s, 4-CH), 6.05 (1H, s, 4'-CH), 1.54 (9H, s, 1'-NCMe₃), 1.22 (9H, s, 3'-CMe₃); ¹³C NMR (100 MHz, DMSO-*d*₆) δ_{C} /ppm: 156.6 (3'-C), 153.0 (C), 141.9 (1-C), 134.5 (5'-C), 130.6 (q, ²J_{CF} = 32 Hz, 3, 5-C), 123.2 (q, ¹J_{CF} = 273 Hz, CF₃), 117.9 (app. d, ³J_{CF} = 3 Hz, 2, 6-CH), 114.4 (m, ³J_{CF} = 4 Hz, 4-CH), 100.7 (4'-CH), 58.8 (1'-NCMe₃), 31.8 (3'-CMe₃), 30.3 (3'-CMe₃), 29.6 (1'-NCMe₃); *m/z* (EI⁺):450 (*M*⁺, 30), 379 (34), 139 (100).

6.3.29. *N*-(3,5-Bis(trifluoromethyl)phenyl)-*N'*-(3-(*tert*-butyl)-1-(4-bromophenyl)-1*H*-pyrazol-5-yl)urea (**230F**)



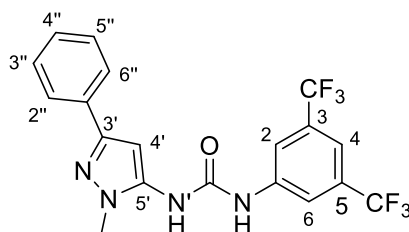
Chemical Formula: C₂₂H₁₉BrF₆N₄O

Mr: 549.06

1-(4-Bromophenyl)-3-(*tert*-butyl)-1*H*-pyrazol-5-amine (**230**) (0.16 g, 0.54 mmol) was added to a solution of 3,5-bis(trifluoromethyl)phenyl isocyanate (0.13g, 0.50 mmol) in CH₂Cl₂ (1 mL) and stirred at RT for 20 min. Volatiles were then removed *in vacuo* and the residue triturated with light petroleum to give the *title compound* (0.16 g, 59%) as a colourless powder, mp 196.5-198.2 °C (Found [ESI⁺]: 549.0715. C₂₂H₂₀N₄O⁷⁹BrF₆ [MH] requires 549.0719); IR (neat) ν_{\max} /cm⁻¹: 3286

(N-H str), 2962 (C-H str), 1664 (C=O str), 1564 (N-H bend), 1496 (C-C str), 1272 (C-N str), 1179 (C-O str), 1137 (C-F str); ^1H NMR (500 MHz, DMSO- d_6) δ_{H} /ppm: 9.70 (1H, br. s, NH), 8.71 (1H, br. s, N'H), 8.07 (2H, s, 2, 6-CH), 7.70 (2H, d, $J = 8$ Hz, 2'', 6''-CH), 7.65 (1H, s, 4-CH), 7.51 (2H, d, $J = 8$ Hz, 3'', 5''-CH), 6.40 (1H, br. s, 4'-CH), 1.29 (9H, s, CMe₃); ^{13}C NMR (100 MHz, DMSO- d_6) δ_{C} /ppm: 161.7 (3'-C), 152.4 (C), 142.0 (1-C), 138.3 (1-PhC), 136.9 (5'-C), 132.6 (2, 6-PhCH), 131.2 (q, $^2J_{\text{FC}} = 33$ Hz, 3, 5-C), 126.2 (3, 5-PhCH), 124.2 (q, $^1J_{\text{FC}} = 273$, CF₃), 120.3 (4-PhCBr), 118.5 (m, $^3J_{\text{FC}} = 3$ Hz, 2, 6-CH), 115.1 (m, $^3J_{\text{FC}} = 4$ Hz, 4-CH), 98.4 (4'-CH), 32.5 (CMe₃), 30.5 (CMe₃); m/z (EI⁺): 548 ($M^{79}\text{Br}^{++}$, 39), 535 (26), 306 (100), 278 (55), 228 (76).

6.3.30. *N*-(3,5-Bis(trifluoromethyl)phenyl)-*N'*-(1-methyl-3-phenyl-1*H*-pyrazol-5-yl)urea (**231F**)

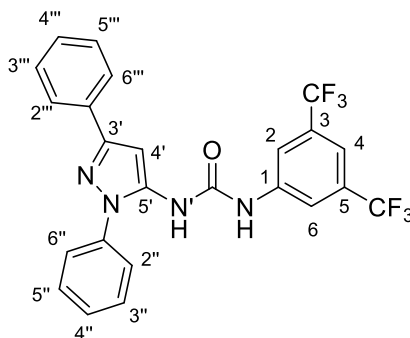


Chemical formula: C₁₉H₁₄F₆N₄O

Mr: 428.11

1-Methyl-3-phenyl-1*H*-pyrazol-5-amine (**231**) (0.15 g, 0.85 mmol) was added to a solution of 3,5-bis(trifluoromethyl)phenyl isocyanate (0.18 g, 0.71 mmol) in CH₂Cl₂ (2 mL) and stirred at RT for 20 min. Volatiles were then removed *in vacuo* and the residue triturated with light petroleum to give the *title compound* (0.22 g, 73%) as a colourless solid, mp 195.3-198.9 °C (MeOH) (Found [ESI⁺]: 429.1146. C₁₉H₁₅N₄OF₆ [M^+] requires 429.1144); IR (neat) ν_{max} /cm⁻¹: 3378 (N-H str), 2966 (C-H str), 1674 (C=O str), 1561 (N-H bend), 1472 (C-C str), 1276 (C-N str), 1125 (C-F str), 1054 (C-N str); ^1H NMR (500 MHz, DMSO- d_6) δ_{H} /ppm: 9.66 (1H, br. s, NH), 8.96 (1H, br. s, N'H), 8.18 (2H, s, 2, 6-CH), 7.77 (2H, d, $J = 8$ Hz, 2'', 6''-CH), 7.67 (1H, s, 4-CH), 7.39 (2H, t, $J = 8$ Hz, 3'', 5''-CH), 7.29 (1H, m, $J = 8$ Hz, 4''-CH), 6.67 (1H, s, 4'-CH), 3.74 (3H, s, Me); ^{13}C NMR (100 MHz, DMSO- d_6) δ_{C} /ppm: 152.1 (C), 148.1 (3'-C), 141.6 (1-C), 137.6 (5'-C), 133.4 (1''-C), 130.7 (q, $^2J_{\text{CF}} = 33$ Hz, 3,5-C), 128.5 (3'',5''-CH), 127.3 (4''-CH), 124.7 (2'',6''-CH), 123.2.0 (app d, $^1J_{\text{CF}} = 273$ Hz, CF₃), 118.2 (d, $^3J_{\text{CF}} = 4$ Hz, 2,6-CH), 114.7 (m, $^3J_{\text{CF}} = 5$ Hz, 4-CH), 96.2 (4'-CH), 35.4 (Me); m/z (EI⁺): 428 (M^{++} , 49), 173 (100).

6.3.31. *N*-(3,5-Bis(trifluoromethyl)phenyl)-*N'*-(1,3-diphenyl-1*H*-pyrazol-5-yl)urea (**232F**)

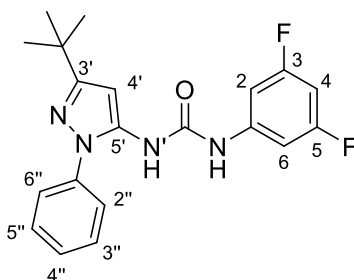


Chemical formula: C₂₄H₁₆F₆N₄O

Mr: 490.12

1,3-Diphenyl-1*H*-pyrazol-5-amine (**232**) (0.20 g, 0.86 mmol) was added to a solution of 3,5-bis(trifluoromethyl)phenyl isocyanate (0.19 g, 0.73 mmol) in CH₂Cl₂ (2 mL) and stirred at RT for 20 min. Volatiles were removed *in vacuo* and the residue triturated with light petroleum and recrystallized from hot MeOH to give the *title compound* (0.23 g, 65%) as colourless crystals, mp 205.7-206.9 °C (MeOH) (Found [ESI⁺]: 491.1288. C₂₄H₁₇F₆N₄O [*MH*] requires 491.1301); IR (neat) $\nu_{\text{max}}/\text{cm}^{-1}$: 3306 (N-H str), 2967 (C-H str), 1653 (C=O str), 1590 (N-H str), 1574 (N-H str), 1474 (C-C str), 1274 (C-N str), 1126 (C-F str), 1055 (C-N str); ¹H NMR (500 MHz, DMSO-*d*₆) $\delta_{\text{H}}/\text{ppm}$: 9.72 (1H, br. s, NH), 8.86 (1H, br. s, N'H), 8.10 (2H, s, 2, 6-CH), 7.88 (2H, d, *J* = 7 Hz, 2'', 6'''-CH), 7.65 (3H, 4-CH and 2'', 6''-CH), 7.58 (2H, t, *J* = 8 Hz, 3'', 5''-CH), 7.49-7.41 (3H, 4''-CH and 3''', 5'''-CH), 7.35 (1H, t, *J* = 7 Hz, 4'''-CH), 6.99 (1H, s, 4'-CH); ¹³C NMR (100 MHz, DMSO-*d*₆) $\delta_{\text{C}}/\text{ppm}$: 151.9 (C), 150.1 (3'-C), 141.4 (1-C), 138.3 (1''-C), 137.6 (5'-C), 132.9 (1'''-C), 130.7 (q, ²*J*_{CF} = 32 Hz, 3, 5-C), 129.3 (3'', 5''-CH), 128.6 (3''', 5'''-CH), 127.9 (4'' or 4'''-CH), 127.8 (4'' or 4'''-CH), 125.1 (2'', 6'''-CH), 124.3 (2'', 6''-CH), 123.7 (q, ¹*J*_{CF} = 273 Hz, CF₃), 118.1 (app d, ³*J*_{CF} = 3 Hz, 2, 6-CH), 114.8 (m, 4-CH), 98.0 (4'-CH); *m/z* (EI⁺): 490 (*M*⁺, 45), 384 (30), 261 (37), 235 (100).

6.3.32. *N*-(3,5-Difluorophenyl)-*N'*-(3-(*tert*-butyl)-1-(phenyl)-1*H*-pyrazol-5-yl)urea (**215O**)

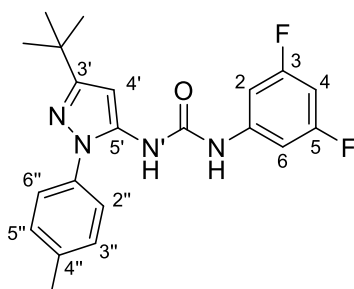


Chemical Formula: $C_{20}H_{20}F_2N_4O$

Mr: 370.40

3-(*tert*-Butyl)-1-phenyl-1*H*-pyrazol-5-amine (**215**) (0.16 g, 0.74 mmol) was added to 3,5-difluorophenyl isocyanate (0.12 g, 0.74 mmol) in CH_2Cl_2 (2 mL) and stirred at RT for 20 min. Volatiles were then removed *in vacuo* and the residue triturated with light petroleum to give the *title compound* (0.17 g, 61%) as a colourless solid, mp 171.0-173.0 °C (MeOH) (Found [ESI⁺]: 371.1673. $C_{20}H_{21}N_4OF_2$ [MH] requires 371.1678); IR (neat) ν_{max}/cm^{-1} : 3322 (N-H str), 2956 (N-H str), 1670 (C=O str), 1554 (N-H str), 1500 (C-C str), 1231 (C-N str), 1117 (C-F str); 1H NMR (500 MHz, DMSO- d_6) δ_H/ppm : 9.38 (1H, br. s, NH), 8.54 (1H, br. s, N'H), 7.53 (4H, m, 2'', 3'', 5'', 6''-CH), 7.44-7.36 (1H, m, 4''-CH), 7.14 (2H, d, $^3J_{HF}$ = 8.5 Hz, 2, 6-CH), 6.78 (1H, t, $^3J_{HF}$ = 9.5 Hz, 4-CH), 6.38 (1H, s, 4'-CH), 1.29 (9H, s, CMe₃); ^{13}C NMR (100 MHz, DMSO- d_6) δ_C/ppm : 162.5 (dd, $^1J_{CF}$ = 243, $^3J_{CF}$ = 15 Hz, 3, 5-CF), 160.7 (3'-C), 151.5 (C), 142.1 (t, $^3J_{CF}$ = 14 Hz, 1-C), 138.5 (1''-C), 136.5 (5'-C), 129.2 (3'', 5''-CH), 127.2 (4''-CH), 124.1 (2'', 6''-CH), 100.9 (dd, $^2J_{CF}$ = 21, $^4J_{CF}$ = 8 Hz, 2, 6-CH), 97.0 (t, $^2J_{CF}$ = 27 Hz, 4-CH), 96.3 (4'-CH), 32.0 (CMe₃), 30.1 (CMe₃); m/z (EI⁺): 370 (M^{*+} , 47), 350 (36), 226 (65), 200 (75), 139 (100).

6.3.33. *N*-(3,5-Difluorophenyl)-*N'*-(3-(*tert*-butyl)-1-(*p*-tolyl)-1*H*-pyrazol-5-yl)urea (**217O**)

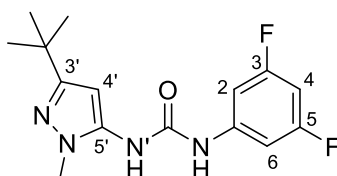


Chemical Formula: C₂₁H₂₂F₂N₄O

Mr: 384.18

3-(*tert*-Butyl)-1-(*p*-tolyl)-1*H*-pyrazol-5-amine (**B**) (0.16 g, 0.70 mmol) was added to a solution of 3,5-difluorophenyl isocyanate (0.11 g, 0.68 mmol) in CH₂Cl₂ (2 mL) and stirred at RT for 20 min. Volatiles were removed *in vacuo* and the residue triturated with light petroleum to give the *title compound* (0.17 g, 64%) as a colourless powder, mp 188.9-190.8 °C (MeOH) (Found [ESI⁺]: 385.1829. C₂₁H₂₃N₄OF₂ requires 385.1834); IR (neat) ν_{\max} /cm⁻¹: 3375 (N-H str), 2963 (C-H str), 1720 (C=O str), 1619 (N-H str), 1542 (N-H str), 1478 (C-C str), 1196 (C-N str), 1114 (C-F str); ¹H NMR (500 MHz, DMSO-*d*₆) δ_{H} /ppm: 9.37 (1H, br. s, NH), 8.47 (1H, br. s, N'H), 7.38 (2H, d, ³*J*_{HH} = 8 Hz, 2'', 6''-CH), 7.32 (2H, d, ³*J*_{HH} = 8 Hz, 3'', 5''-CH), 7.13 (2H, app d, ³*J*_{HF} = 9 Hz, 2, 6-CH), 6.79 (1H, t, ³*J*_{HF} = 9 Hz, 4-CH), 6.35 (1H, s, 4'-CH), 2.37 (3H, s, Me), 1.27 (9H, s, CMe₃); ¹³C NMR (100 MHz, DMSO-*d*₆) δ_{C} /ppm: 162.5 (dd, ¹*J*_{CF} = 243, ³*J*_{CF} = 16 Hz, 3, 5-CF), 160.5 (3'-C), 151.4 (C), 142.1 (t, ³*J*_{CF} = 14 Hz, 1-C), 136.8 (4''-C), 136.5 (5'-C), 136.0 (1''-C), 129.6 (3'', 5''-CH), 124.2 (2'', 6''-CH), 100.9 (dd, ²*J*_{CF} = 29, ⁴*J*_{CF} = 8 Hz, 2, 6-CH), 97.0 (app t, ²*J*_{CF} = 26 Hz, 4-CH), 95.7 (4'-CH), 32.0 (CMe₃), 30.2 (CMe₃), 20.5 (Me); *m/z* (EI⁺): 384 (*M*⁺, 52), 240 (71), 229 (46), 214 (100).

6.3.34. *N*-(3,5-Difluorophenyl)-*N'*-(3-*tert*-butyl-1-methyl-1*H*-pyrazol-5-yl)urea (**2260**)



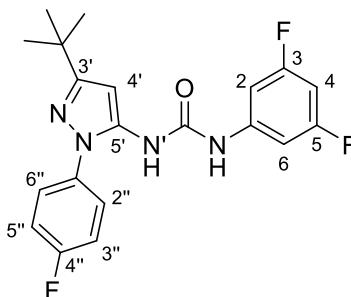
Chemical Formula: C₁₅H₁₈F₂N₄O

Mr: 308.33

1-Methyl-3-phenyl-1*H*-pyrazol-5-amine (**226**) (0.16 g, 1.01 mmol) was added to a solution of 3,5-difluorophenyl isocyanate (0.14 g, 0.93 mmol) in CH₂Cl₂ (2 mL) and stirred at RT for 20 min. Volatiles were then removed *in vacuo* and the residue triturated with light petroleum and recrystallized from hot MeOH to give the *title compound* (0.22 g, 78%) as colourless crystals, mp 189.0-191.1 °C (MeOH) (Found [ESI⁺]: 309.1517. C₁₅H₁₉N₄OF₂ [*MH*] requires 309.1521); IR (neat) ν_{\max} /cm⁻¹: 3322 (N-H str), 2964 (C-H str), 1711 (C=O str), 1610 (N-H bend), 1558 (N-H bend),

1478 (C-H bend), 1206 (C-N str), 1112 (C-F str); ^1H NMR (500 MHz, DMSO- d_6) δ_{H} /ppm: 9.27 (1H, br. s, NH), 8.61 (1H, br. s, N'H) 7.19 (2H, app d, $^3J_{\text{HF}} = 8$ Hz, 2, 6-CH), 6.80 (1H, t, $^3J_{\text{HF}} = 9$ Hz, 4-CH), 6.04 (1H, s, 4'-CH), 3.59 (3H, s, Me), 1.21 (9H, s, CMe₃); ^{13}C NMR (100 MHz, DMSO- d_6) δ_{C} /ppm: 162.5 (dd, $^1J_{\text{CF}} = 243$, $^3J_{\text{CF}} = 15$ Hz, 3, 5-CF), 158.5 (3'-CH), 151.7 (C), 142.2 (t, $^3J_{\text{CF}} = 14$ Hz, 1-C), 136.4 (5'-C), 101.0 (dd, $^2J_{\text{CF}} = 29$, $^4J_{\text{CF}} = 8$ Hz, 2, 6-CH), 96.9 (t, $^2J_{\text{CF}} = 26$ Hz, 4-CH), 94.4 (4'-CH), 34.9 (Me), 31.8 (CMe₃), 30.3 (CMe₃); m/z (EI⁺): 308 (M^{*+} , 56), 164 (71), 138 (100).

6.3.35. ***N*-(3,5-Difluorophenyl)-*N'*-(3-(*tert*-butyl)-1-(4-fluorophenyl)-1*H*-pyrazol-5-yl)urea (227O)**

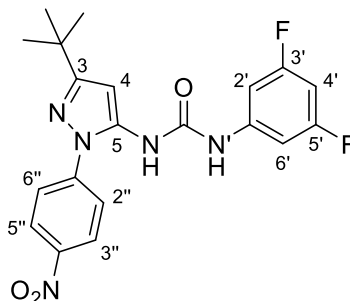


Chemical Formula: C₂₀H₁₉F₃N₄O

Mr: 388.15

3-(*tert*-Butyl)-1-(4-fluorophenyl)-1*H*-pyrazole-5-amine (**227**) (128 mg, 0.55 mmol) was added to a solution of 3,5-difluorophenyl isocyanate (80 mg, 0.52 mmol) in CH₂Cl₂ (2 mL) and stirred at RT for 20 min. Volatiles were then removed *in vacuo* and the residue triturated with light petroleum and recrystallized from hot MeOH to give the *title compound* (80 mg, 40%) as colourless crystals, mp 165.3-169.3 °C (MeOH) (Found [ESI⁺]: 389.1582. C₂₀H₂₀N₄OF₃ [MH] requires 389.1584); IR (neat) ν_{max} /cm⁻¹: 2966 (C-H str), 1728 (C=O str), 1612 (N-H bend), 1553 (N-H bend), 1226 (C-N str), 1113 (C-F str); ^1H NMR (500 MHz, DMSO- d_6) δ_{H} /ppm: 9.35 (1H, br. s, NH), 8.52 (1H, br. s, N'H), 7.55 (2H, dd, $^3J_{\text{HH}} = 8$, $^4J_{\text{HF}} = 5$ Hz, 2'', 6''-CH), 7.36 (2H, pt, $^3J_{\text{HH}} = 8.5$, $^3J_{\text{HF}} = 8.5$ Hz, 3'', 5''-CH), 7.13 (2H, app. d, $^3J_{\text{HF}} = 8$ Hz, 2, 6-CH), 6.79 (1H, t, $^3J_{\text{HF}} = 9$ Hz, 4-CH), 6.36 (1H, s, 4'-CH), 1.28 (9H, s, CMe₃); ^{13}C NMR (100 MHz, DMSO- d_6) δ_{C} /ppm: 161.2 (dd, $^1J_{\text{CF}} = 243$, $^3J_{\text{CF}} = 16$ Hz, 3, 5-CF), 160.9 (d, $^1J_{\text{CF}} = 245$, 4''-CF), 160.8 (3'-C), 151.5 (C), 142.0 (t, $^3J_{\text{CF}} = 14$ Hz, 1-C), 136.7 (5'-C), 134.9 (d, $^4J_{\text{CF}} = 3$ Hz, 1''-C), 126.5 (d, $^3J_{\text{HF}} = 8$ Hz, 2'', 6''-CH), 116.0 (d, $^2J_{\text{CF}} = 23$ Hz, 3'', 5''-CH), 100.9 (dd, $^2J_{\text{CF}} = 21$, $^4J_{\text{CF}} = 9$ Hz, 2, 6-CH), 97.0 (t, $^2J_{\text{CF}} = 26$ Hz, 4-CH), 96.4 (4'-CH), 32.0 (CMe₃), 30.1 (CMe₃); m/z (EI⁺): 389 (MH⁺, 72), 244 (65), 218 (100).

6.3.36. *N*-3-(*tert*-Butyl)-1-(4-nitrophenyl)-1*H*-pyrazol-5-yl)-*N'*-(3,5-difluorophenyl)urea (2280)

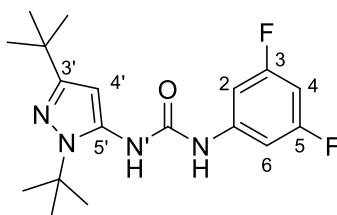


Chemical Formula: C₂₀H₁₉F₂N₅O₃

Mr: 415.15

3-(*tert*-Butyl)-1-(4-nitrophenyl)-1*H*-pyrazol-5-amine (**228**) (150 mg, 0.58 mmol) was added to a solution of 3,5-difluorophenylisocyanate (82 mg, 0.52 mmol) in CH₂Cl₂ (2 mL) and stirred at RT for 18 h. Volatiles were then removed *in vacuo* and the residue triturated with light petroleum and recrystallized from hot MeOH to give the *title compound* (54 mg, 25%) as yellow crystals, mp 178.6-182.0 °C (MeOH) (Found [ESI⁺]: 416.1534. C₂₀H₂₀N₅O₃F [MH] requires 416.1529); IR (neat) $\nu_{\max}/\text{cm}^{-1}$: 3298 (N-H str), 2963 (C-H str), 1662 (C=O str), 1610 (N-H bend), 1565 (N-H bend), 1503 (N-O str), 1334 (N-O str), 1234 (C-N str), 1116 (C-F str); ¹H NMR (500 MHz, DMSO-*d*₆) $\delta_{\text{H}}/\text{ppm}$: 9.45 (1H, br. s, N'H), 8.78 (1H, br. s, NH), 8.36 (2H, d, ³*J*_{HH} = 9 Hz, 3'', 5''-CH), 7.87 (2H, d, ³*J*_{HH} = 9 Hz, 2'', 6''-CH), 7.14 (2H, d, ³*J*_{HF} = 8 Hz, 2', 6'-CH), 6.79 (1H, t, ³*J*_{HF} = 9 Hz, 4'-CH), 6.45 (1H, s, 4-CH), 1.30 (9H, s, CMe₃); ¹³C NMR (100 MHz, DMSO-*d*₆) $\delta_{\text{C}}/\text{ppm}$: 162.5 (dd, ¹*J*_{CF} = 243, ³*J*_{CF} = 16 Hz, 3', 5'-CF), 162.4 (3-C), 151.8 (C), 145.0 (1'' or 4''-C), 143.9 (1'' or 4''-C), 142.0 (t, ³*J*_{CF} = 14 Hz, 1'-C), 137.4 (5-C), 124.8 (3'', 5''-CH), 123.1 (2'', 6''-CH), 101.1 (dd, ²*J*_{CF} = 21, ⁴*J*_{CF} = 9 Hz, 2', 6'-CH), 99.5 (4-CH), 97.4 (t, ²*J*_{CF} = 27 Hz, 4'-CH), 32.2 (CMe₃), 29.9 (CMe₃); *m/z* (EI⁺): 415 (*M*⁺, 30), 271 (100), 245 (88).

6.3.37. *N*-(3,5-Difluorophenyl)-*N'*-(1,3-(*tert*-butyl)-1*H*-pyrazol-5-yl)urea (2290)

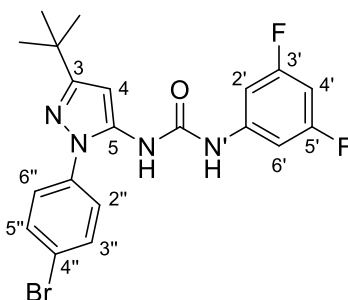


Chemical Formula: $C_{18}H_{24}F_2N_4O$

Mr: 350.19

1,3-Di-*tert*-butyl-1*H*-pyrazol-5-amine (**229**) (0.14 g, 0.72 mmol) was added to a solution of 3,5-difluorophenyl isocyanate (0.11 g, 0.68 mmol) in CH_2Cl_2 (2 mL) and stirred at RT for 20 min. Volatiles were then removed *in vacuo* and the residue triturated with light petroleum and recrystallized from hot MeOH to give the *title compound* (0.16 g, 69%) as colourless crystals, mp 212.9-214.5 °C (MeOH) (Found [ESI⁺]: 351.1987. $C_{18}H_{25}N_4OF_2$ [*MH*] requires 351.1991); IR (neat) ν_{max}/cm^{-1} : 3366 (N-H str), 2957 (C-H str), 1663 (C=O str), 1612 (N-H bend), 1566 (N-H bend), 1478 (C-H str), 1207 (C-N str), 1116 (C-F str); 1H NMR (500 MHz, DMSO- d_6) δ_H/ppm : 9.31 (1H, br. s, NH), 8.01 (1H, br. s, N'H), 7.18 (2H, app d, $^3J_{HF}$ = 8 Hz, 2, 6-CH), 6.77 (1H, t, $^3J_{HF}$ = 9 Hz, 4-CH), 6.02 (1H, s, 4'-CH), 1.53 (9H, s, 1'-CMe₃), 1.21 (9H, s, 3'-CMe₃); ^{13}C NMR (100 MHz, DMSO- d_6) δ_C/ppm : 162.5 (dd, $^1J_{CF}$ = 243, $^3J_{CF}$ = 15 Hz, 3, 5-CF), 156.5 (3'-C), 152.6 (C), 142.5 (t, $^3J_{CF}$ = 15 Hz, 1-C), 134.6 (5'-C), 100.9 (dd, $^2J_{CF}$ = 30, $^4J_{CF}$ = 9 Hz, 2, 6-CH), 100.4 (4'-CH), 96.7 (t, $^2J_{CF}$ = 27 Hz, 4-CH), 58.7 (1'-CMe₃), 31.8 (3'-CMe₃), 30.3 (3'-CMe₃), 29.5 (1'-CMe₃); m/z (EI⁺): 350 (M^{++} , 39), 150 (36), 139 (100).

6.3.38. *N*-(3-(*tert*-Butyl)-1-(4-bromophenyl)-1*H*-pyrazol-5-yl)-*N'*-(3,5-difluorophenyl)urea (**2300**)

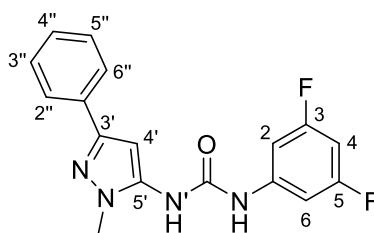


Chemical Formula: $C_{20}H_{19}BrF_2N_4O$

Mr: 448.07

1-(4-Bromophenyl)-3-(*tert*-butyl)-1*H*-pyrazol-5-amine (**230**) (0.21 g, 0.71 mmol) was added to a 3,5-difluorophenyl isocyanate (0.17 g, 1.01 mmol) in CH₂Cl₂ (2 mL) and stirred at RT for 20 min. Volatiles were then removed *in vacuo* and the residue triturated with light petroleum and recrystallized from hot MeOH to give the *title compound* (0.17 g, 54%) as colourless crystals, mp 158.0-159.4 °C (Found [ESI⁺]: 449.0782. C₂₀H₂₀N₄O⁷⁹BrF₂ [MH] requires 449.0783); IR (neat) ν_{max} /cm⁻¹: 3320 (N-H str), 2964 (C-H str), 1668 (C=O str), 1612 (N-H bend), 1552 (N-H bend), 1478 (C-C str), 1228 (C-N str), 1116 (C-F str), 670 (C-Br str); ¹H NMR (500 MHz, DMSO-*d*₆) δ_{H} /ppm: 9.37 (1H, br. s, N'H), 8.58 (1H, br. s, NH), 7.71 (2H, d, ³*J*_{HH} = 9 Hz, 3'', 5''-CH), 7.50 (2H, d, ³*J*_{HH} = 9 Hz, 2'', 6''-CH), 7.14 (2H, d, ³*J*_{HF} = 8 Hz, 2', 6'-CH), 6.78 (1H, t, ³*J*_{HF} = 9 Hz, 4'-CH), 6.38 (1H, s, 4-CH), 1.28 (9H, s, CMe₃); ¹³C NMR (100 MHz, DMSO-*d*₆) δ_{C} /ppm: 163.8 (dd, ¹*J*_{CF} = 243, ³*J*_{CF} = 16 Hz, 3', 6'-CF), 161.2 (3-C), 151.6 (C), 142.0 (t, ³*J*_{CF} = 14 Hz, 1'-C), 137.8 (1''-C), 136.7 (5-C), 132.1 (2'', 6''-CH), 125.9 (3'', 5''-CH), 119.8 (4''-C), 101.0 (dd, ²*J*_{CF} = 21, ⁴*J*_{CF} = 9 Hz, 2', 6'-CH), 97.0 (4'-CH and 4-CH), 32.0 (CMe₃), 30.0 (CMe₃); *m/z* (EI⁺): 449 (*M*⁷⁹Br⁺, 79), 305 (97), 279 (100).

6.3.39. *N*-(3,5-Difluorophenyl)-*N'*-(1-methyl-3-phenyl-1*H*-pyrazol-5-yl)urea (**2310**)



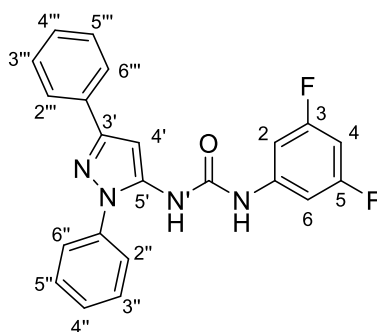
Chemical Formula: C₁₇H₁₄F₂N₄O

Mr: 328.11

1-Methyl-3-phenyl-1*H*-pyrazol-5-amine (**231**) (0.13 g, 0.73 mmol) was added to 3,5-difluorophenyl isocyanate (0.10 g, 0.66 mmol) in CH₂Cl₂ (3 mL) and stirred at RT for 20 min. Volatiles were then removed *in vacuo* and the residue triturated with light petroleum and recrystallized from hot MeOH to give the *title compound* (0.18 g, 85%) as clear colourless crystals, mp 205.6-206.7 °C (MeOH) (Found [ESI⁺]: 329.1204. C₁₇H₁₅N₄OF₂ [MH] requires

329.1208); IR (neat) $\nu_{\max}/\text{cm}^{-1}$: 3284 (N-H str), 2973 (C-H str), 1711 (C=O str), 1609 (N-H bend), 1558 (N-H bend), 1479 (C-H bend), 1235 (C-N str), 1114 (C-F str); ^1H NMR (500 MHz, DMSO- d_6) $\delta_{\text{H}}/\text{ppm}$: 9.34 (1H, br. s, NH), 8.82 (1H, br. s, N'H), 7.76 (2H, d, $^3J_{\text{HH}} = 7.5$ Hz, 2'', 6''-CH), 7.39 (2H, t, $^3J_{\text{HH}} = 7.5$ Hz, 3'', 5''-CH), 7.28 (1H, t, $^3J_{\text{HH}} = 7.5$ Hz, 4''-CH), 7.22 (2H, app d, $^3J_{\text{HF}} = 8.5$ Hz, 2, 6-CH), 6.81 (1H, t, $^3J_{\text{HF}} = 9$ Hz, 4-CH), 6.64 (1H, s, 4'-CH), 3.73 (3H, s, Me); ^{13}C NMR (100 MHz, DMSO- d_6) $\delta_{\text{C}}/\text{ppm}$: 163 (dd, $^1J_{\text{CF}} = 243$, $^3J_{\text{CF}} = 15$ Hz, 3, 5-CF), 151.7 (C), 148.1 (3'-C), 142.1 (t, $^3J_{\text{CF}} = 14$ Hz, 1-C), 137.8 (5'-C), 133.5 (1''-C), 128.5 (3'', 5''-CH), 127.3 (4''-CH), 124.7 (2'', 6''-CH), 101.1 (dd, $^2J_{\text{CF}} = 21$, $^4J_{\text{CF}} = 8$ Hz, 2, 6-CH), 96.8 (t, $^2J_{\text{CF}} = 26$ Hz, 4-CH), 95.5 (4'-CH), 35.4 (Me); m/z (EI+): 328 (M^{++} , 44), 199 (30), 173 (100).

6.3.40. *N*-(3,5-Difluorophenyl)-*N'*-(1,3-diphenyl-1*H*-pyrazol-5-yl)urea (**2320**)



Chemical Formula: $\text{C}_{22}\text{H}_{16}\text{F}_2\text{N}_4\text{O}$

Mr: 390.13

1,3-Diphenyl-1*H*-pyrazol-5-amine (**231**) (0.20 g, 0.85 mmol) was added to 3,5-difluorophenyl isocyanate (0.12 g, 0.75 mmol) in CH_2Cl_2 (2 mL) and stirred at RT for 20 min. Volatiles were then removed *in vacuo* and the residue triturated with light petroleum and recrystallized from hot MeOH to give the *title compound* (0.21 mg, 70%) as colourless crystals, mp 195.4-200.4 °C (MeOH) (Found [ESI+]: 391.1365. $\text{C}_{22}\text{H}_{17}\text{N}_4\text{OF}_2$ [M^+] requires 391.1365); IR (neat) $\nu_{\max}/\text{cm}^{-1}$: 3324 (N-H str), 2945 (C-H str), 1726 (C=O str), 1615 (N-H bend), 1544 (N-H bend), 1480 (C=C str), 1194 (C-N str), 1106 (C-F str); ^1H NMR (500 MHz, DMSO- d_6) $\delta_{\text{H}}/\text{ppm}$: 9.42 (1H, br. s, NH), 8.71 (1H, br. s, N'H), 7.86 (2H, d, $^3J_{\text{HH}} = 8$ Hz, 2''', 6'''-CH), 7.60 (4H, m, 2'', 3'', 5'', 6''-CH), 7.46 (3H, 4''-CH and 3''', 5'''-CH), 7.35 (1H, t, $^3J_{\text{HH}} = 7.5$ Hz, 4'''-CH), 7.16 (2H, app d, $^3J_{\text{HF}} = 8.5$ Hz, 2, 6-CH), 6.95 (1H, s, 4'-CH), 6.81 (1H, t, $^3J_{\text{HF}} = 9$ Hz, 4-CH); ^{13}C NMR (100 MHz, DMSO- d_6) $\delta_{\text{C}}/\text{ppm}$: 163.0

(dd, $^1J_{\text{CF}} = 243$, $^3J_{\text{CF}} = 17$ Hz, 3, 5-CF), 152.0 (C), 150.6 (3'-C), 142.5 (t, $^3J_{\text{CF}} = 14$ Hz, 1-C), 138.7 (1''-C), 138.4 (5'-C), 133.4 (1'''-C), 129.8 (3'', 5''-CH), 129.1 (3''', 5'''-CH), 128.4 (4'' or 4'''-CH), 128.3 (4' or 4'''-CH), 125.6 (2''', 6'''-CH), 124.9 (2'', 6''-CH), 101.5 (dd, $^2J_{\text{CF}} = 21$, $^4J_{\text{CF}} = 8$ Hz, 2, 6-CH), 97.6 (4-CH and 4'-CH); m/z (EI+): 390 (M^{*+} , 47), 261 (45), 235 (100).

7. References.

- 1 M. C. Bagley, J. E. Dwyer, M. Baashen, M. C. Dix, P. G. S. Murziani, M. J. Rokicki, D. Kipling and T. Davis, *Org. Biomol. Chem.*, 2016, **14**, 947–956.
- 2 M. C. Bagley, J. E. Dwyer, M. D. B. Molina, A. W. Rand, H. L. Rand and N. C. O. Tomkinson, *Org. Biomol. Chem.*, 2015, **13**, 6814–6824.
- 3 M. C. Bagley, M. Baashen, I. Chuckowree, J. E. Dwyer, D. Kipling and T. Davis, *Pharmaceuticals*, 2015, **8**, 257–276.
- 4 B. L. Strehler and A. S. Mildvan, *Science*, 1960, **132**, 14–21.
- 5 R. G. A. Faragher, A. N. Sheerin and E. L. Ostler, *Expert Rev. Mol. Med.*, 2009, **11**, e27.
- 6 I. Akushevich, J. Kravchenko, S. Ukraintseva, K. Arbeev, A. Kulminski and A. I. Yashin, *Exp. Gerontol.*, 2013, **48**, 1395–1401.
- 7 A. Krtolica, S. Parrinello, S. Lockett, P. Y. Desprez and J. Campisi, *Proc. Natl. Acad. Sci. U. S. A.*, 2001, **98**, 12072–12077.
- 8 E. L. Ostler, C. V Wallis, A. N. Sheerin and R. G. A. Faragher, *Exp. Gerontol.*, 2002, **37**, 285–292.
- 9 D. Kipling, T. Davis, E. L. Ostler and R. G. Faragher, *Science*, 2004, **305**, 1426–1431.
- 10 M. C. Bagley, T. Davis, P. G. S. Murziani, C. S. Widdowson and D. Kipling, *Pharmaceuticals*, 2010, **3**, 1842–1872.
- 11 C. J. Epstein, G. M. Martin, A. L. Schultz and A. G. Motulsky, *Werner's Syndrome: A Review of its Symptomatology, Natural History, Pathologic Features, Genetics and Relationship to the Natural Aging Process*, Springer US, 1985.
- 12 D. M. Baird, T. Davis, J. Rowson, C. J. Jones and D. Kipling, *Hum. Mol. Genet.*, 2004, **13**, 1515–1524.
- 13 C. Yu, J. Oshima, Y. Fu, E. M. Wijsman, F. Hisama, R. Alisch, S. Matthews, J. Nakura, T. Miki, S. Ouais, G. M. Martin, J. Mulligan and G. D. Schellenbergt, *Science*, 1996, **272**, 258–262.
- 14 T. Davis, D. M. Baird, M. F. Haughton, C. J. Jones and D. Kipling, *J. Gerontol., Ser. A*, 2005, **60**, 1386–1393.

- 15 R. G. Faragher, I. R. Kill, J. a Hunter, F. M. Pope, C. Tannock and S. Shall, *Proc. Natl. Acad. Sci. U. S. A.*, 1993, **90**, 12030–12034.
- 16 A. Rodríguez-López and D. Jackson, *Aging Cell*, 2002, **44**, 30–39.
- 17 D. Orren, S. Theodore and A. Machwe, *Biochemistry*, 2002, **80**, 13483–13488.
- 18 T. Davis, A. J. C. Brook, M. J. Rokicki, M. C. Bagley and D. Kipling, *Pharmaceuticals*, 2016, **9**, 23.
- 19 T. Davis, M. F. Haughton, C. J. Jones and D. Kipling, *Ann. N. Y. Acad. Sci.*, 2006, **1067**, 243–247.
- 20 T. Force, K. Kuida, M. Namchuk, K. Parang and J. M. Kyriakis, *Circulation*, 2004, **109**, 1196–1205.
- 21 J. M. Kyriakis and J. Avruch, *Physiol. Rev.*, 2001, **81**, 807–869.
- 22 A. Schlapbach and C. Huppertz, *Future Med. Chem.*, 2009, **1**, 1243–1257.
- 23 A. D. Bachstetter and L. J. Van Eldik, *Aging Dis.*, 2010, **1**, 199–211.
- 24 O. J. Broom, B. Widjaya, J. Troelsen, J. Olsen and O. H. Nielsen, *Clin. Exp. Immunol.*, 2009, **158**, 272–280.
- 25 Y. J. Feng and Y. Y. Li, *J. Dig. Dis.*, 2011, **12**, 327–332.
- 26 M. C. Genovese, *Arthritis Rheum.*, 2009, **60**, 317–320.
- 27 J. Lee, J. Laydon and P. McDonnell, *Nature*, 1994, **372**, 739–746.
- 28 K. Godl and H. Daub, *Cell Cycle*, 2004, **3**, 393–395.
- 29 T. F. Gallagher, S. M. Fler-Thompson, R. S. Garlgipatl, M. E. Sorenson, M. Juanita, D. Lee, P. E. Bendef, J. C. Lee, J. T. Laydon, D. E. Griswold, M. C. Chabot-Fletcher, J. J. Breton and J. L. Adams, *Bioorg. Med. Chem. Lett.*, 1995, **5**, 1171–1176.
- 30 J. C. Lee, D. E. Griswold, B. Votta and N. Hanna, *Int. J. Immunopharmacol.*, 1988, **10**, 835–843.
- 31 P. R. Young, M. M. McLaughlin, S. Kumar, S. Kassis, M. L. Doyle, D. McNulty, T. F. Gallagher, S. Fisher, P. C. McDonnell, S. A. Carr, M. J. Huddleston, G. Seibel, T. G. Porter, G. P. Livi, J. L. Adams and J. C. Lee, *J. Biol. Chem.*, 1997, **272**, 12116–12121.
- 32 J. Bain, L. Plater, M. Elliott, N. Shpiro, C. J. Hastie, H. McLauchlan, I. Klevernic, J. S. C.

- Arthur, D. R. Alessi and P. Cohen, *Biochem. J.*, 2007, **408**, 297–315.
- 33 A. Cuenda, J. Rouse, Y. N. Doza, R. Meier, P. Cohen, T. F. Gallagher, P. R. Young and J. C. Lee, *FEBS Lett*, 1995, **364**, 229–233.
- 34 K. P. Wilson, M. J. Fitzgibbon, P. R. Caron, J. P. Griffith, W. Chen, P. G. McCaffrey, S. P. Chambers and M. S. Su, *J. Biol. Chem.*, 1996, **271**, 27696–27700.
- 35 Z. Wang, B. J. Canagarajah, J. C. Boehm, S. Kassisà, M. H. Cobb, P. R. Young, S. Abdel-Meguid, J. L. Adams and E. J. Goldsmith, *Structure*, 1998, **6**, 1117–1128.
- 36 D. Hammaker and G. S. Firestein, *Ann. Rheum. Dis.*, 2010, **69**, 77–82.
- 37 D. M. Goldstein, A. Kuglstatter, Y. Lou and M. J. Soth, *J. Med. Chem.*, 2010, **53**, 2345–2353.
- 38 A. Trejo, H. Arzeno, M. Browner, S. Chanda, S. Cheng, D. D. Comer, S. a Dalrymple, P. Dunten, J. Lafargue, B. Lovejoy, J. Freire-Moar, J. Lim, J. McIntosh, J. Miller, E. Papp, D. Reuter, R. Roberts, F. Sanpablo, J. Saunders, K. Song, A. Villasenor, S. D. Warren, M. Welch, P. Weller, P. E. Whiteley, L. Zeng and D. M. Goldstein, *J. Med. Chem.*, 2003, **46**, 4702–4713.
- 39 R. Soliva, J. L. Gelpí, C. Almansa, M. Virgili and M. Orozco, *J. Med. Chem.*, 2007, **50**, 283–293.
- 40 M. C. Bagley, T. Davis, M. J. Rokicki, C. S. Widdowson and D. Kipling, *Future Med. Chem.*, 2010, **2**, 193–201.
- 41 K. Mihara, C. Almansa, R. L. Smeets, E. E. M. G. Loomans, J. Dulos, P. M. F. Vink, M. Rooseboom, H. Kreutzer, F. Cavalcanti, A. M. Boots and R. L. Nelissen, *Br. J. Pharmacol.*, 2008, **154**, 153–164.
- 42 A. de Dios, C. Shih, B. López de Uralde, C. Sánchez, M. del Prado, L. M. Martín Cabrejas, S. Pleite, J. Blanco-Urgoiti, M. J. Lorite, C. R. Nevill, R. Bonjouklian, J. York, M. Vieth, Y. Wang, N. Magnus, R. M. Campbell, B. D. Anderson, D. J. McCann, D. D. Giera, P. a Lee, R. M. Schultz, L. C. Li, L. M. Johnson and J. A. Wolos, *J. Med. Chem.*, 2005, **48**, 2270–2273.
- 43 K. F. McClure, Y. A. Abramov, E. R. Laird, J. T. Barberia, W. Cai, T. J. Carty, S. R. Cortina, D. E. Danley, A. J. Dipesa, K. M. Donahue, M. A. Dombroski, N. C. Elliott, C. A. Gabel, S. Han, T. R. Hynes, P. K. Lemotte, M. N. Mansour, E. S. Marr, M. A. Letavic, J. Pandit, D. B. Ripin, F. J. Sweeney, D. Tan and Y. Tao, *J. Med. Chem.*, 2005, **48**, 5728–5737.

- 44 C. Dominguez, N. Tamayo and D. Zhang, *Expert Opin. Ther. Pat.*, 2005, **15**, 801–816.
- 45 D. M. Goldstein, T. Alfredson, J. Bertrand, M. F. Browner, K. Clifford, S. a Dalrymple, J. Dunn, J. Freire-Moar, S. Harris, S. S. Labadie, J. La Fargue, J. M. Lapierre, S. Larrabee, F. Li, E. Papp, D. McWeeney, C. Ramesha, R. Roberts, D. Rotstein, B. San Pablo, E. B. Sjogren, O.-Y. So, F. X. Talamas, W. Tao, A. Trejo, A. Villasenor, M. Welch, T. Welch, P. Weller, P. E. Whiteley, K. Young and S. Zipfel, *J. Med. Chem.*, 2006, **49**, 1562–1575.
- 46 E. R. Ottosen, M. D. Sørensen, F. Björkling, T. Skak-Nielsen, M. S. Fjording, H. Aaes and L. Binderup, *J. Med. Chem.*, 2003, **46**, 5651–5662.
- 47 S. Natarajan and J. Doherty, *Curr. Top. Med. Chem.*, 2005, **5**, 987–1003.
- 48 M. C. Bagley, T. Davis, M. C. Dix, M. J. Rokicki and D. Kipling, *Bioorg. Med. Chem. Lett.*, 2007, **17**, 5107–5110.
- 49 C. Pargellis, L. Tong, L. Churchill, P. F. Cirillo, T. Gilmore, A. G. Graham, P. M. Grob, E. R. Hickey, N. Moss, S. Pav and J. Regan, *Nat. Struct. Biol.*, 2002, **9**, 268–272.
- 50 J. Regan, N. Moss, C. Pargellis, S. Pav, A. Proto, A. Swinamer, L. Tong, C. Torcellini, S. Breitfelder, P. Cirillo, T. Gilmore, A. G. Graham, E. Hickey, B. Klaus, J. Madwed and M. Moriak, *J. Med. Chem.*, 2002, **45**, 2994–3008.
- 51 J. Regan, C. a. Pargellis, P. F. Cirillo, T. Gilmore, E. R. Hickey, G. W. Peet, A. Proto, A. Swinamer and N. Moss, *Bioorg. Med. Chem. Lett.*, 2003, **13**, 3101–3104.
- 52 M. C. Bagley, T. Davis, M. C. Dix, C. S. Widdowson and D. Kipling, *Org. Biomol. Chem.*, 2006, **4**, 4158–4164.
- 53 K. Moffett, Z. Konteatis, D. Nguyen, R. Shetty, J. Ludington, T. Fujimoto, K. J. Lee, X. Chai, H. Namboodiri, M. Karpusas, B. Dorsey, F. Guarnieri, M. Bukhtiyarova, E. Springman and E. Michelotti, *Bioorg. Med. Chem. Lett.*, 2011, **21**, 7155–7165.
- 54 D. Zhu, X. Li, W. Zhong and D. Zhao, *Molecules*, 2015, **20**, 16604–16619.
- 55 M. Fiore, S. Forli and F. Manetti, *J. Med. Chem.*, 2016, **59**, 3609–3634.
- 56 P. Cohen, *Curr. Opin. Cell Biol.*, 2009, **21**, 317–324.
- 57 J. Guay, H. Lambert, G. Gingras-Breton, J. N. Lavoie, J. Huot and J. Landry, *J. Cell Sci.*, 1997, **110**, 357–368.
- 58 A. Kotlyarov, Y. Yannoni, S. Fritz, K. Laass, J.-B. Telliez, D. Pitman, L.-L. Lin and M. Gaestel,

Mol. Cell. Biol., 2002, **22**, 4827–4835.

- 59 D. R. Anderson, M. J. Meyers, W. F. Vernier, M. W. Mahoney, R. G. Kurumbail, N. Caspers, G. I. Poda, J. F. Schindler, D. B. Reitz and R. J. Mourey, *J. Med. Chem.*, 2007, **50**, 2647–2654.
- 60 T. Davis, M. J. Rokicki, M. C. Bagley and D. Kipling, *Chem. Cent. J.*, 2013, **7**, 18–21.
- 61 K. Underwood, K. Parris, E. Federico, L. Mosyak, R. Czerwinski, T. Shane, M. Taylor, K. Svenson, Y. Liu and C. Hsiao, *Structure*, 2003, **11**, 627–636.
- 62 D. R. Anderson, S. Hegde, E. Reinhard, L. Gomez, W. F. Vernier, L. Lee, S. Liu, A. Sambandam, P. A. Snider and L. Masih, *Bioorg. Med. Chem. Lett.*, 2005, **15**, 1587–1590.
- 63 T. Davis, M. C. Bagley, M. C. Dix, P. G. S. Murziani, M. J. Rokicki, C. S. Widdowson, J. M. Zayed, M. A. Bachler and D. Kipling, *Bioorg. Med. Chem. Lett.*, 2007, **17**, 6832–6835.
- 64 R. C. Hillig, U. Eberspaecher, F. Monteclaro, M. Huber, D. Nguyen, A. Mengel, B. Muller-Tiemann and U. Egner, *J. Mol. Biol.*, 2007, **369**, 735–745.
- 65 J. Velcicky, R. Feifel, S. Hawtin, R. Heng, C. Huppertz, G. Koch, M. Kroemer, H. Moebitz, L. Revesz, C. Scheufler and A. Schlapbach, *Bioorg. Med. Chem. Lett.*, 2010, **20**, 1293–1297.
- 66 J. I. Trujillo, M. J. Meyers, D. R. Anderson, S. Hegde, M. W. Mahoney, W. F. Vernier, I. P. Buchler, K. K. Wu, S. Yang, S. Yang, S. J. Hartmann and D. B. Reitz, *Bioorg. Med. Chem. Lett.*, 2007, **17**, 4657–4663.
- 67 D. R. Anderson, M. J. Meyers, R. G. Kurumbail, N. Caspers, G. I. Poda, S. A. Long, B. S. Pierce, M. W. Mahoney and R. J. Mourey, *Bioorg. Med. Chem. Lett.*, 2009, **19**, 4878–4881.
- 68 D. R. Anderson, M. J. Meyers, R. G. Kurumbail, N. Caspers, G. I. Poda, S. A. Long, B. S. Pierce, M. W. Mahoney, R. J. Mourey and M. D. Parikh, *Bioorg. Med. Chem. Lett.*, 2009, **19**, 4882–4884.
- 69 R. J. Mourey, B. L. Burnette, S. J. Brustkern, J. S. Daniels, J. L. Hirsch, W. F. Hood, M. J. Meyers, S. J. Mnich, B. S. Pierce, M. J. Saabye, J. F. Schindler, S. A. South, E. G. Webb, J. Zhang and A. D. R., *J. Pharmacol. Exp. Ther.*, 2010, **333**, 797–807.
- 70 X. Huang, G. W. Shipps, C. C. Cheng, P. Spacciapoli, X. Zhang, M. a. McCoy, D. F. Wyss, X. Yang, A. Achab, K. Soucy, D. K. Montavon, D. M. Murphy and C. E. Whitehurst, *ACS Med. Chem. Lett.*, 2011, **2**, 632–637.

- 71 D. Xiao, A. Palani, X. Huang, M. Sofolarides, W. Zhou, X. Chen, R. Aslanian, Z. Guo, J. Fossetta, F. Tian, P. Trivedi, P. Spacciapoli, C. E. Whitehurst and D. Lundell, *Bioorg. Med. Chem. Lett.*, 2013, **23**, 3262–3266.
- 72 S. Caddick and R. Fitzmaurice, *Tetrahedron*, 2009, **65**, 3325–3355.
- 73 P. Lidestrom, J. Tierney, B. Wathey and J. Westman, *Tetrahedron*, 2001, **57**, 9225–9283.
- 74 F. Mavandadi and Å. Pilotti, *Drug Discov. Today*, 2006, **11**, 165–174.
- 75 A. M. Jordan and S. D. Roughley, *Drug Discov. Today*, 2009, **14**, 731–744.
- 76 R. Aggarwal, V. Kumar, R. Kumar and S. P. Singh, *Beilstein J. Org. Chem.*, 2011, **7**, 179–197.
- 77 N. K. Terrett, A. S. Bell, D. Brown and P. Ellis, *Bioorg. Med. Chem. Lett.*, 1996, **6**, 1819–1824.
- 78 D. Hainzl, L. M. Cole and J. E. Casida, *Chem. Res. Toxicol.*, 1998, **11**, 1529–1535.
- 79 A. M. Vinggaard, U. Hass, M. Dalgaard, H. R. Andersen, E. Bonefeld-Jørgensen, S. Christiansen, P. Laier and M. E. Poulsen, *Int. J. Androl.*, 2006, **29**, 186–192.
- 80 P. Laier, S. B. Metzдорff, J. Borch, M. L. Hagen, U. Hass, S. Christiansen, M. Axelstad, T. Kledal, M. Dalgaard, C. McKinnell, L. J. S. Brokken and A. M. Vinggaard, *Toxicol. Appl. Pharmacol.*, 2006, **213**, 160–171.
- 81 J. A. Joule and K. Mills, *Heterocyclic Chemistry*, John Wiley & Sons Ltd, Chichester, West Sussex, 3rd edn., 2011.
- 82 S. Fustero, R. Román, J. F. Sanz-Cervera, A. Simón-Fuentes, A. C. Cuñat, S. Villanova and M. Murguía, *J. Org. Chem.*, 2008, **73**, 3523–3529.
- 83 A. R. Katritzky, M. Wang, S. Zhang, M. V. Voronkov and P. J. Steel, *J. Org. Chem.*, 2001, **66**, 6787–6791.
- 84 Y. R. Huang and J. A. Katzenellenbogen, *Org. Lett.*, 2000, **2**, 2833–2836.
- 85 V. K. Aggarwal, J. De Vicente and R. V. Bonnert, *J. Org. Chem.*, 2003, **68**, 5381–5383.
- 86 T. M. A. Elmaati and F. El-Taweel, *J. Heterocycl. Chem.*, 2004, **41**, 109–134.
- 87 P. D. Davis, J. M. Davis, D. F. C. Moffat, *WO Pat.*, 040 019 A1, 1997.
- 88 C. P. Kordik, C. Luo, B. C. Zanoni, T. W. Lovenberg, S. J. Wilson, A. H. Vaidya, J. J. Crooke,

- D. I. Rosenthal and A. B. Reitz, *Bioorg. Med. Chem. Lett.*, 2001, **11**, 2287–2290.
- 89 R. N. Daniels, K. Kim, E. P. Lebois, H. Muchalski, M. Hughes and C. W. Lindsley, *Tetrahedron Lett.*, 2008, **49**, 305–310.
- 90 F. A. Abu-Shanab, S. M. Sherif and S. A. S. Mousa, *J. Heterocycl. Chem.*, 2009, **46**, 801–827.
- 91 C. C. Cheng and R. K. Robins, *J. Org. Chem.*, 1956, **21**, 1240–1256.
- 92 N. Kaur, *J. Heterocycl. Chem.*, 2015, **52**, 953–973.
- 93 M. C. Bagley, M. Baashen, V. L. Paddock, D. Kipling and T. Davis, *Tetrahedron*, 2013, **69**, 8429–8438.
- 94 P. G. Baraldi, B. Cacciari, G. Spalluto, M. J. Pineda de Las Infanteas Y Villatro, C. Zocchi, S. Dionisotti and E. Ongini, *J. Med. Chem.*, 1996, **39**, 1164–1171.
- 95 D. Kennedy, *Nutrients*, 2016, **8**, 68–97.
- 96 G. D. Henry, *Tetrahedron*, 2004, **60**, 6043–6061.
- 97 S. D. Roughley and A. M. Jordan, *J. Med. Chem.*, 2011, **54**, 3451–3479.
- 98 G. S. Timmins, S. Master, F. Rusnak and V. Deretic, *Antimicrob. Agents Chemother.*, 2004, **48**, 3006–3009.
- 99 B. Vacher, B. Bonnaud, P. Funes, N. Jubault, W. Koek, M. B. Assié, C. Cosi and M. Kleven, *J. Med. Chem.*, 1999, **42**, 1648–1660.
- 100 A.-H. Li, S. Moro, N. Forsyth, N. Melman, X. Ji and K. A. Jacobson, *J. Med. Chem.*, 1999, **42**, 706–721.
- 101 J. Clayden, N. Greeves, S. Warren and P. Wothers, *Organic Chemistry*, Oxford University Press, 1st edn., 2001.
- 102 R. P. Mariella, *Org. Synth.*, 1952, **32**, 32–34.
- 103 J.-C. Jung, Y.-J. Jung and O.-S. Park, *Synth. Commun.*, 2001, **31**, 2507–2511.
- 104 J. P. Michael, *Nat. Prod. Rep.*, 2002, **19**, 742–760.
- 105 J. P. Michael, *Nat. Prod. Rep.*, 1997, **14**, 605–618.
- 106 M. Foley and L. Tilley, *Pharmacol. Ther.*, 1998, **79**, 55–87.

- 107 J. L. McCormick, T. C. McKee, J. H. Cardellina and M. R. Boyd, *J. Nat. Prod.*, 1996, **59**, 469–471.
- 108 S. Javanshir, S. Sharifi, A. Maleki, B. Sohrabi and M. Kiasadegh, *J. Phys. Org. Chem.*, 2014, **27**, 589–596.
- 109 U. Mävers, F. Berruex and M. Schlosser, *Tetrahedron*, 1996, **52**, 3223–3228.
- 110 W. M. Lauer and C. E. Kaslow, *Org. Synth.*, 1944, **24**, 68.
- 111 S. K. Anandan, J. S. Ward, R. D. Brokx, M. R. Bray, D. V. Patel and X. X. Xiao, *Bioorg. Med. Chem. Lett.*, 2005, **15**, 1969–1972.
- 112 H. T. Clarke and A. W. Davis, *Org. Synth.*, 1922, **2**, 79.
- 113 S. E. Denmark and S. Venkatraman, *J. Org. Chem.*, 2006, **71**, 1668–1676.
- 114 J. J. Eisch and T. Dluzniewski, *J. Org. Chem.*, 1989, **54**, 1269–1274.
- 115 O. Doebner, *Ber. Dtsch. Chem. Ges.*, 1887, **20**, 277–281.
- 116 J.-J. Li and E. J. Corey, Eds., *Name Reactions in Heterocyclic Chemistry*, John Wiley & Sons, Inc., Hoboken, New Jersey, 2005.
- 117 E. Lutz and F. Codington, *J. Am. Chem. Soc.*, 1946, **150**, 1813–1831.
- 118 X.-F. Lin, S.-L. Cui and Y.-G. Wang, *Tetrahedron Lett.*, 2006, **47**, 3127–3130.
- 119 X. Li, Z. Mao, Y. Wang, W. Chen and X. Lin, *Tetrahedron*, 2011, **67**, 3858–3862.
- 120 X.-S. Wang, Q. Li, J.-R. Wu, Y.-L. Li, C.-S. Yao and S.-J. Tu, *Synthesis*, 2008, **12**, 1902–1910.
- 121 X. S. Wang, Q. Li, C. S. Yao and S. J. Tu, *Eur. J. Org. Chem.*, 2008, 3513–3518.
- 122 X. S. Wang, Q. Li, J. R. Wu and S. J. Tu, *J. Comb. Chem.*, 2009, **11**, 433–437.
- 123 X. S. Wang, J. Zhou, M. Y. Yin, K. Yang and S. J. Tu, *J. Comb. Chem.*, 2010, **12**, 266–269.
- 124 H. Tondys, H. C. Vanderplas and M. Wozniak, *J. Heterocycl. Chem.*, 1985, **22**, 353–355.
- 125 M. Wozniak, A. Baranski and K. Nowak, *J. Org. Chem.*, 1987, **52**, 5643–5646.
- 126 M. Makosza and J. Winiarski, *Acc. Chem. Res.*, 1987, 282–289.
- 127 M. Makosza, *Pure Appl. Chem.*, 1997, **69**, 559–564.
- 128 M. Makosza and K. Wojciechowski, *Chem. Rev.*, 2004, **104**, 2631–2666.

- 129 A. R. Surrey and H. F. Hammer, *J. Am. Chem. Soc.*, 1946, **68**, 113–116.
- 130 K. Koike, Z. Jia, T. Nikaido, Y. Liu, Y. Zhao and D. Guo, *Org. Lett.*, 1999, **1**, 197–198.
- 131 S. Kim, N. Dahal and T. Kesharwani, *Tetrahedron Lett.*, 2013, **54**, 4373–4376.
- 132 J. Huang, H. Luo, L. Wang, Y. Guo, W. Zhang, H. Chen, M. Zhu, Y. Liu and G. Yu, *Org. Lett.*, 2012, **14**, 3300–3303.
- 133 K. Takimiya, I. Osaka, T. Mori and M. Nakano, *Acc. Chem. Res.*, 2014, **47**, 1493–1502.
- 134 A. M. Isloor, B. Kalluraya and K. Sridhar Pai, *Eur. J. Med. Chem.*, 2010, **45**, 825–830.
- 135 R. Romagnoli, P. G. Baraldi, M. Kimatrai Salvador, D. Preti, M. Aghazadeh Tabrizi, M. Bassetto, A. Brancale, E. Hamel, I. Castagliuolo, R. Bortolozzi, G. Basso and G. Viola, *J. Med. Chem.*, 2013, **56**, 2606–2618.
- 136 V. G. Vogel, J. P. Costantino, D. L. Wickerham, W. M. Cronin, R. S. Cecchini, J. N. Atkins, T. B. Bevers, L. Fehrenbacher, E. R. Pajon, J. L. Wade, A. Robidoux, R. G. Margolese, J. James, S. M. Lippman, C. D. Runowicz, P. A. Ganz, S. E. Reis, W. McCaskill-Stevens, L. G. Ford, V. C. Jordan and N. Wolmark, *JAMA, J. Am. Med. Assoc.*, 2006, **295**, 2727–2741.
- 137 K. C. Lee, B. S. Moon, J. H. Lee, K.-H. Chung, J. a Katzenellenbogen and D. Y. Chi, *Bioorg. Med. Chem.*, 2003, **11**, 3649–3658.
- 138 P. Lu, M. L. Schrag, D. E. Slaughter, C. E. Raab, M. Shou and A. D. Rodrigues, *Drug Metab. Distrib.*, 2003, **31**, 1352–1360.
- 139 E. Israel, R. Dermarkarian, M. Rosenberg, R. Sperling, G. Taylor, P. Rubin and J. M. Drazen, *N. Engl. J. Med.*, 1990, **323**, 1740–1744.
- 140 B. E. Sleebs, A. Levit, I. P. Street, H. Falk, T. Hammonds, A. C. Wong, M. D. Charles, M. F. Olson and J. B. Baell, *MedChemComm*, 2011, **2**, 977–981.
- 141 Z.-F. Tao, L. a Hasvold, J. D. Levenson, E. K. Han, R. Guan, E. F. Johnson, V. S. Stoll, K. D. Stewart, G. Stamper, N. Soni, J. J. Bouska, Y. Luo, T. J. Sowin, N.-H. Lin, V. S. Giranda, S. H. Rosenberg and T. D. Penning, *J. Med. Chem.*, 2009, **52**, 6621–6636.
- 142 C. Hou, Q. He and C. Yang, *Org. Lett.*, 2014, **16**, 5040–5043.
- 143 T. Aoyama, T. Takido and M. Kodomari, *Synlett*, 2005, 2739–2742.
- 144 T. Higa and A. Krubsack, *J. Org. Chem.*, 1975, **40**, 3037–3045.

- 145 S. Lee, H. Lee, Y. Y. Kyu, H. L. Byung, S. E. Yoo, K. Lee and S. C. Nam, *Bioorg. Med. Chem. Lett.*, 2005, **15**, 2998–3001.
- 146 A. J. Bridges, A. Lee, E. C. Maduakor and C. E. Schwartz, *Tetrahedron Lett.*, 1992, **33**, 7499–7502.
- 147 R. Beck, *J. Org. Chem.*, 1971, **37**, 3224–3226.
- 148 K. O. Hessian and B. L. Flynn, *Org. Lett.*, 2003, **5**, 4377–4380.
- 149 B. L. Flynn, P. Verdier-Pinard and E. Hamel, *Org. Lett.*, 2001, **3**, 651–654.
- 150 D. Yue and R. C. Larock, *J. Org. Chem.*, 2002, **67**, 1905–1909.
- 151 M. Martin-Smith and M. Gates, *J. Am. Chem. Soc.*, 1956, **78**, 6177–6180.
- 152 M. Martin-Smith and S. Reid, *J. Chem. Soc.*, 1960, 938–944.
- 153 J. F. D. Chabert, L. Joucla, E. David and M. Lemaire, *Tetrahedron*, 2004, **60**, 3221–3230.
- 154 A. Martinez, M.-V. Vazquez, J. L. Carreon-Macedo, L. E. Sansores and R. Salcedo, *Tetrahedron*, 2003, **59**, 6415–6422.
- 155 F. G. Bordwell and C. J. Albisetti, *J. Am. Chem. Soc.*, 1948, **70**, 1955–1958.
- 156 Y. Kutsunugi, S. Kawai, T. Nakashima and T. Kawai, *New J. Chem.*, 2009, **33**, 1368–1373.
- 157 R. P. Dickinson and B. Iddon, *J. Chem. Soc. C Org.*, 1971, **123**, 182–185.
- 158 W. Davies and Q. N. Porter, *J. Chem. Soc.*, 1957, 459–463.
- 159 A. Heynderickx, A. Samat and R. Guglielmetti, *Synthesis*, 2002, **2002**, 213–216.
- 160 J. M. Mbere, J. B. Bremner, B. W. Skelton and A. H. White, *Tetrahedron*, 2011, **67**, 6895–6900.
- 161 F. G. Bordwell and H. Stange, *J. Am. Chem. Soc.*, 1955, **77**, 5939–5944.
- 162 C. A. G. N. Montalbetti and V. Falque, *Tetrahedron*, 2005, **61**, 10827–10852.
- 163 J. S. Carey, D. Laffan, C. Thomson and M. T. Williams, *Org. Biomol. Chem.*, 2006, **4**, 2337–2347.
- 164 H. Lundberg, F. Tinnis, N. Selander and H. Adolfsson, *Chem. Soc. Rev.*, 2014, **43**, 2714–2742.
- 165 R. M. Lanigan and T. D. Sheppard, *Eur. J. Org. Chem.*, 2013, **2013**, 7453–7465.

- 166 T. J. Deming, *Prog. Polym. Sci.*, 2007, **32**, 858–875.
- 167 Z. Liu, Y. Jiao, Y. Wang, C. Zhou and Z. Zhang, *Adv. Drug Deliv. Rev.*, 2008, **60**, 1650–1662.
- 168 V. R. Pattabiraman and J. W. Bode, *Nature*, 2011, **480**, 471–479.
- 169 E. Valeur and M. Bradley, *Chem. Soc. Rev.*, 2009, **38**, 606–631.
- 170 J. C. Sheehan and G. P. Hess, *J. Am. Chem. Soc.*, 1955, **77**, 1067–1068.
- 171 W. König and R. Geiger, *Chem. Ber.*, 1970, **103**, 788–798.
- 172 L. A. Carpino, *J. Am. Chem. Soc.*, 1993, **115**, 4397–4398.
- 173 L. A. Carpino, H. Imazumi, A. El-Faham, F. J. Ferrer, C. Zhang, Y. Lee, B. M. Foxman, P. Henklein, C. Hanay, C. Mügge, H. Wenschuh, J. Klose, M. Beyermann and M. Bienert, *Angew. Chem. Int. Ed.*, 2002, **41**, 441–445.
- 174 F. Albericio, J. Bofill, A. El-Faham and S. A. Kates, *J. Org. Chem.*, 1998, **63**, 9678–9683.
- 175 K. D. Wehrstedt, P. a Wandrey and D. Heitkamp, *J. Hazard. Mater.*, 2005, **126**, 1–7.
- 176 A. El-Faham, R. Subirós Funosas, R. Prohens and F. Albericio, *Chem. - Eur. J.*, 2009, **15**, 9404–9416.
- 177 R. Subirós-Funosas, R. Prohens, R. Barbas, A. El-Faham and F. Albericio, *Chem. - Eur. J.*, 2009, **15**, 9394–9403.
- 178 R. Subirós-Funosas, L. Nieto-Rodriguez, K. J. Jensen and F. Albericio, *J. Pept. Sci.*, 2013, **19**, 408–414.
- 179 A. El-Faham and F. Albericio, *J. Org. Chem.*, 2008, **73**, 2731–2737.
- 180 B. Belleau and G. Malek, *J. Am. Chem. Soc.*, 1968, **90**, 1651–1652.
- 181 D. Cremin, A. Hegarty and M. Begley, *J. Chem. Soc., Perkin Trans. 2*, 1980, 412–420.
- 182 R. Merrifield, *J. Am. Chem. Soc.*, 1963, **85**, 2149–2154.
- 183 S. Wang, *J. Am. Chem. Soc.*, 1973, **95**, 1328–1333.
- 184 F. Ullmann and J. Bielecki, *Ber. Dtsch. Chem. Ges.*, 1901, **34**, 2174–2185.
- 185 C. Glaser, *Ber. Dtsch. Chem. Ges.*, 1869, **2**, 422–424.
- 186 C. C. C. Johansson Seechurn, M. O. Kitching, T. J. Colacot and V. Snieckus, *Angew. Chem. Int. Ed.*, 2012, **51**, 5062–5085.

- 187 X. F. Wu, P. Anbarasan, H. Neumann and M. Beller, *Angew. Chem. Int. Ed.*, 2010, **49**, 9047–9050.
- 188 P. J. Stang, M. H. Kowalski, M. D. Schiavelli and D. Longford, *J. Am. Chem. Soc.*, 1989, **111**, 3347–3356.
- 189 E. Negishi, *Acc. Chem. Res.*, 1982, **15**, 340–348.
- 190 I. P. Beletskaya and A. V. Cheprakov, *Chem. Rev.*, 2000, **100**, 3009–3066.
- 191 T. Mizoroki, K. Mori and A. Ozaki, *Bull. Chem. Soc. Jpn.*, 1971, **44**, 581–581.
- 192 R. F. Heck and J. P. Nolley, *J. Org. Chem.*, 1972, **37**, 2320–2322.
- 193 Q. Yao, E. P. Kinney and Z. Yang, *J. Org. Chem.*, 2003, **68**, 7528–7531.
- 194 A. F. Littke and G. C. Fu, *J. Am. Chem. Soc.*, 2001, **123**, 6989–7000.
- 195 S. Brase and A. de Meijere, *Palladium-catalyzed coupling of organyl halides to alkenes - The Heck reaction*, Wiley-VCH, Inc, New York, NY USA, 1998.
- 196 A. Battace, T. Zair, H. Doucet and M. Santelli, *Tetrahedron Lett.*, 2006, **47**, 459–462.
- 197 H. Zhao, M.-Z. Cai and C.-Y. Peng, *Synth. Commun.*, 2002, **32**, 3419–3423.
- 198 C. Deraedt and D. Astruc, *Acc. Chem. Res.*, 2014, **47**, 494–503.
- 199 J. G. de Vries, *Dalton Trans.*, 2006, 421–429.
- 200 H. A. Dieck and R. F. Heck, *J. Am. Chem. Soc.*, 1974, **96**, 1133–1136.
- 201 A. Battace, M. Feuerstein, M. Lemhadri, T. Zair, H. Doucet and M. Santelli, *Eur. J. Org. Chem.*, 2007, **4**, 3122–3132.
- 202 D. Laurenti, M. Feuerstein, G. Pèpe, H. Doucet and M. Santelli, *J. Org. Chem.*, 2001, **66**, 1633–1637.
- 203 D. Guest, V. H. Menezes da Silva, A. P. de Lima Batista, S. M. Roe, A. A. C. Braga and O. Navarro, *Organometallics*, 2015, **34**, 2463–2470.
- 204 C. Gallop, C. Zinser, D. Guest and O. Navarro, *Synlett*, 2014, **25**, 2225–2228.
- 205 M. T. Reetz and J. G. de Vries, *Chem. Commun.*, 2004, 1559.
- 206 A. Jutand, in *The Mizoroki – Heck Reaction*, ed. M. Oestereich, John Wiley & Sons Ltd, Chichester, West Sussex, 2009, pp. 1–50.

- 207 C. Amatore and A. Jutand, *J. Organomet. Chem.*, 1999, **576**, 254–278.
- 208 C. Amatore, A. Jutand and A. Suarez, *J. Am. Chem. Soc.*, 1993, **115**, 9531–9541.
- 209 C. Amatore, E. Came, A. Jutand, M. A. M'Barki and G. Meyer, *Organometallics*, 1995, **14**, 5605–5614.
- 210 T. Jeffery, *J. Chem. Soc., Chem. Commun.*, 1984, 1287–1289.
- 211 T. Jeffery, *Tetrahedron*, 1996, **52**, 10113–10130.
- 212 M. T. Reetz and E. Westermann, *Angew. Chem. Int. Ed.*, 2000, **39**, 165–168.
- 213 W. Cabri and I. Candiani, *Acc. Chem. Res.*, 1995, **28**, 2–7.
- 214 R. F. Heck, *Acc. Chem. Res.*, 1979, **12**, 146–151.
- 215 C. M. Andersson, A. Hallberg and G. D. Daves, *J. Org. Chem.*, 1987, **52**, 3529–3536.
- 216 H. Von Schenck, B. Åkermark and M. Svensson, *J. Am. Chem. Soc.*, 2003, **125**, 3503–3508.
- 217 N. A. Cortese, C. B. Ziegler, B. J. Hrnjez and R. F. Heck, *J. Org. Chem.*, 1978, **43**, 2952–2958.
- 218 J. Masllorens, M. Moreno-Mañas, A. Pla-Quintana, R. Pleixats and A. Roglans, *Synthesis*, 2002, **2002**, 1903–1911.
- 219 J. Wu, S. Xiang, J. Zeng, M. Leow and X. W. Liu, *Org. Lett.*, 2015, **17**, 222–225.
- 220 J. Lubkoll, A. Millemaggi, A. Perry and R. J. K. Taylor, *Tetrahedron*, 2010, **66**, 6606–6612.
- 221 A. Suzuki, *Angew. Chem. Int. Ed.*, 2011, **50**, 6723–6733.
- 222 N. Miyaura and A. Suzuki, *J. Chem. Soc., Chem. Commun.*, 1979, 866–867.
- 223 N. Miyaura, K. Yamada and A. Suzuki, *Tetrahedron Lett.*, 1979, 3437–3440.
- 224 N. Miyaura, T. Yanagi and A. Suzuki, *Synth. Commun.*, 1981, **11**, 513–519.
- 225 A. J. J. Lennox and G. C. Lloyd-Jones, *Angew. Chem. Int. Ed.*, 2013, **52**, 7362–7370.
- 226 N. Miyaura and A. Suzuki, *Chem. Rev.*, 1995, **95**, 2457–2483.
- 227 A. Suzuki, *Acc. Chem. Res.*, 1982, **15**, 178–184.
- 228 A. J. J. Lennox and G. C. Lloyd-Jones, *Chem. Soc. Rev.*, 2014, **43**, 412–443.
- 229 N. Miyaura, *J. Organomet. Chem.*, 2002, **653**, 54–57.

- 230 N. Miyaura, T. Ishiyama, H. Sasaki, M. Ishikawa, M. Satoh and A. Suzuki, *J. Am. Chem. Soc.*, 1989, **111**, 314–321.
- 231 N. Miyaura, Y. Tanabe and H. Suginome, *J. Organomet. Chem.*, 1982, **233**, C13–C16.
- 232 T. Moriya, N. Miyaura and A. Suzuki, *Synlett*, 1994, **2**, 149–151.
- 233 N. Miyaura, K. Yamada, H. Suginome and A. Suzuki, *J. Am. Chem. Soc.*, 1985, **107**, 972–980.
- 234 F. Sasaya, N. Miyaura and A. Suzuki, *Bull. Korean Chemical Soc.*, 1987, **8**, 329–332.
- 235 T. E. Barder, S. D. Walker, J. R. Martinelli and S. L. Buchwald, *J. Am. Chem. Soc.*, 2005, **127**, 4685–4696.
- 236 A. H. Cherney, N. T. Kadunce and S. E. Reisman, *Chem. Rev.*, 2015, **115**, 9587–9652.
- 237 M. N. Hopkinson and F. Glorius, *Nature*, 2014, **510**, 485–496.
- 238 D. Su, D. Meng, P. Bertinato, A. Balog, E. J. Sorensen, S. J. Danishefsky, Y. Zheng, T. Chou, L. He and S. B. Horwitz, *Angew. Chemie Int. Ed. English*, 1997, **36**, 757–759.
- 239 J. Lindley, *Tetrahedron*, 1984, **40**, 1433–1456.
- 240 J. F. Bunnett, *Acc. Chem. Res.*, 1978, **11**, 413–420.
- 241 L. D. Boger and J. S. Panek, *Tetrahedron Lett.*, 1984, **25**, 3175–3178.
- 242 M. Kosugi, M. Kameyama and T. Migita, *Chem. Lett.*, 1983, **12**, 927–928.
- 243 F. Paul, J. Patt and J. F. Hartwig, *J. Am. Chem. Soc.*, 1994, **116**, 5969–5970.
- 244 M. S. Driver and J. F. Hartwig, *J. Am. Chem. Soc.*, 1995, **117**, 4708–4709.
- 245 A. Guram and S. Buchwald, *J. Am. Chem. Soc.*, 1994, **116**, 7901–7902.
- 246 A. S. Guram, R. A. Rennels and S. L. Buchwald, *Angew. Chem. Int. Ed. Engl.*, 1995, **34**, 1348–1350.
- 247 J. Louie and J. F. Hartwig, *Tetrahedron Lett.*, 1995, **36**, 3609–3612.
- 248 J. F. Hartwig, *Nature*, 2008, **455**, 314–322.
- 249 J. P. Wolfe, S. Wagaw and S. L. Buchwald, *J. Am. Chem. Soc.*, 1996, **118**, 7215–7216.
- 250 R. A. Singer, M. Doré, J. E. Sieser and M. A. Berliner, *Tetrahedron Lett.*, 2006, **47**, 3727–3731.

- 251 D. S. Surry and S. L. Buchwald, *Angew. Chem. Int. Ed. Engl.*, 2008, **47**, 6338–6361.
- 252 Q. Shen, S. Shekhar, J. P. Stambuli and J. F. Hartwig, *Angew. Chem. Int. Ed. Engl.*, 2005, **44**, 1371–1375.
- 253 C. Fischer and B. Koenig, *Beilstein J. Org. Chem.*, 2011, **7**, 59–74.
- 254 T. Emoto, N. Kubosaki, Y. Yamagiwa and T. Kamikawa, *Tetrahedron Lett.*, 2000, **41**, 355–358.
- 255 M. H. Ali and S. L. Buchwald, *J. Org. Chem.*, 2001, **66**, 2560–2565.
- 256 T. J. Luker, H. G. Beaton, M. Whiting, A. Mete and D. R. Cheshire, *Tetrahedron Lett.*, 2000, **41**, 7731–7735.
- 257 J. Ji, W. H. Bunnelle, T. Li, J. M. Pace, M. R. Schrimpf, K. B. Sippy, D. J. Anderson and M. D. Meyer, *Pure Appl. Chem.*, 2005, **77**, 2041–2045.
- 258 M. C. Bagley, T. Davis, M. C. Dix, P. G. S. Murziani, M. J. Rokicki and D. Kipling, *Bioorg. Med. Chem. Lett.*, 2008, **18**, 3745–3748.
- 259 L. M. Gruenbaum, R. Schwartz, J. R. Woska, R. P. DeLeon, G. W. Peet, T. C. Warren, A. Capolino, L. Mara, M. M. Morelock, A. Shrutkowski, J. W. Jones and C. A. Pargellis, *Biochem. Pharmacol.*, 2009, **77**, 422–432.
- 260 M. C. Bagley, D. Terence, M. C. Dix, P. G. S. Murziani, M. J. Rokicki and D. Kipling, *Future Med. Chem.*, 2010, **2**, 203–213.
- 261 S. Cacchi, P. G. Ciattini, E. Morera and G. Ortar, *Tetrahedron Lett.*, 1987, **28**, 3039–3042.
- 262 M. Wuts, Peter, G and W. Greene, Theodora, *Greene's Protective Groups In Organic Synthesis*, John Wiley & Sons, Inc., Hoboken, New Jersey, 4th Ed., 2007.
- 263 C. Sousa and P. J. Silva, *Eur. J. Org. Chem.*, 2013, **2013**, 5195–5199.
- 264 T. Davis, F. S. Wyllie, M. J. Rokicki, M. C. Bagley and D. Kipling, *Ann. N. Y. Acad. Sci.*, 2007, **1100**, 455–469.
- 265 D. R. Goldberg, Y. Choi, D. Cogan, M. Corson, R. DeLeon, A. Gao, L. Gruenbaum, M. H. Hao, D. Joseph, M. a. Kashem, C. Miller, N. Moss, M. R. Netherton, C. P. Pargellis, J. Pelletier, R. Sellati, D. Skow, C. Torcellini, Y.-C. Tseng, J. Wang, R. Wasti, B. Werneburg, J. P. Wu and Z. Xiong, *Bioorg. Med. Chem. Lett.*, 2008, **18**, 938–941.
- 266 J.-P. Wu, J. Wang, A. Abeywardane, D. Andersen, M. Emmanuel, E. Gautschi, D. R.

- Goldberg, M. A. Kashem, S. Lukas, W. Mao, L. Martin, T. Morwick, N. Moss, C. Pargellis, U. R. Patel, L. Patnaude, G. W. Peet, D. Skow, R. J. Snow, Y. Ward, B. Werneburg and A. White, *Bioorg. Med. Chem. Lett.*, 2007, **17**, 4664–4669.
- 267 Z. Xiong, D. A. Gao, D. a Cogan, D. R. Goldberg, M.-H. Hao, N. Moss, E. Pack, C. Pargellis, D. Skow, T. Trieselmann, B. Werneburg and A. White, *Bioorg. Med. Chem. Lett.*, 2008, **18**, 1994–1999.
- 268 Y. Tomioka, A. Mochiike, J. Himeno and M. Yamazaki, *Chem. Pharm. Bull.*, 1981, **29**, 1286–1291.
- 269 Y. Tomioka, K. Ohkubo and M. Yamazaki, *Chem. Pharm. Bull.*, 1985, **33**, 1360–1366.
- 270 V. O. Iaroshenko, S. Ali, S. Mkrtchyan, A. Gevorgyan, T. M. Babar, V. Semeniuchenko, Z. Hassan, A. Villinger and P. Langer, *Tetrahedron Lett.*, 2012, **53**, 7135–7139.
- 271 I. Abdillahi and G. Kirsch, *Synthesis*, 2011, **9**, 1314–1318.
- 272 M. D. Meyer, R. J. Altenbach, F. Z. Basha, W. A. Carroll, S. Condon, S. W. Elmore, J. F. Kerwin, K. B. Sippy, K. Tietje, M. D. Wendt, A. A. Hancock, M. E. Brune, S. A. Buckner and I. Drizin, *J. Med. Chem.*, 2000, **43**, 1586–603.
- 273 D. L. Boger, B. E. Fink and M. P. Hedrick, *J. Am. Chem. Soc.*, 2000, **122**, 6382–6394.
- 274 M. C. Bagley, R. T. Buck, S. L. Hind and C. J. Moody, *J. Chem. Soc., Perkin Trans. 1*, 1998, 591–600.
- 275 H.-S. Chong, X. Sun, P. Dong and C. S. Kang, *Eur. J. Org. Chem.*, 2011, **2011**, 6641–6648.
- 276 M.-J. R. P. Queiroz, A. Begouin, I. C. F. R. Ferreira, G. Kirsch, R. C. Calhelha, S. Barbosa and L. M. Estevinho, *Eur. J. Org. Chem.*, 2004, 3679–3685.
- 277 S. S. Khatana, D. H. Boschelli, J. B. Kramer, D. T. Connor, H. Barth and P. Stoss, *J. Org. Chem.*, 1996, **61**, 6060–6062.
- 278 J. Spencer, R. P. Rathnam, H. Patel and N. Anjum, *Tetrahedron*, 2008, **64**, 10195–10200.
- 279 J. Spencer, N. Anjum, H. Patel, R. Rathnam and J. Verma, *Synlett*, 2007, **16**, 2557–2558.
- 280 S. Iyer and G. M. Kulkarni, *Synth. Commun.*, 2004, **34**, 721–725.
- 281 J. Wannberg and M. Larhed, *J. Org. Chem.*, 2003, **68**, 5750–5753.
- 282 M. Matsugi, F. Tabusa and J. Minamikawa, *Tetrahedron Lett.*, 2000, **41**, 8523–8525.

- 283 K. A. Reynolds, D. J. Young and W. A. Loughlin, *Synthesis*, 2010, 3645–3648.
- 284 X.-G. Li, X. Cheng and Q.-L. Zhou, *Synth. Commun.*, 2002, **32**, 2477–2481.
- 285 M. C. Bagley, C. Brace, J. W. Dale, M. Ohnesorge, N. G. Phillips, X. Xiong and J. Bower, *J. Chem. Soc. Perkin Trans. 1*, 2002, 1663–1671.
- 286 L. Kurti and B. Czako, *Strategic Applications of Named Reactions in Organic Synthesis*, Elsevier Academic Press, USA, 2005.
- 287 H. Fujiwara and K. Kitagawa, *Heterocycles*, 2000, **53**, 409–417.
- 288 J. S. Daniels, Y. Lai, S. South, P.-C. Chiang, D. Walker, B. Feng, R. Mireles, L. O. Whiteley, J. W. McKenzie, J. Stevens, R. Mourey, D. Anderson and J. W. Davis, *Drug Metab. Lett.*, 2013, **7**, 15–22.
- 289 J. M. Pedersen, P. Matsson, C. A. S. Bergström, U. Norinder, J. Hoogstraate and P. Artursson, *J. Med. Chem.*, 2008, **51**, 3275–3287.
- 290 P. D. Leeson, *Adv. Drug Deliv. Rev.*, 2016, **101**, 22–33.
- 291 X. Ge, P. Lyu, Y. Gu, L. Li, J. Li, Y. Wang, L. Zhang, C. Fu and Z. Cao, *Biochem. Biophys. Res. Commun.*, 2015, **464**, 862–868.
- 292 T. Davis, M. C. Bagley and J. E. Dwyer, *Unpublished results*, 2015.
- 293 D. C. Swinney, *Nat. Rev. Drug Discov.*, 2004, **3**, 801–808.
- 294 D. K. Treiber and N. P. Shah, *Chem. Biol.*, 2013, **20**, 745–746.
- 295 E. V Schneider, J. Böttcher, R. Huber, K. Maskos and L. Neumann, *Proc. Natl. Acad. Sci. U. S. A.*, 2013, **110**, 8081–8086.
- 296 K. P. Cusack, Y. Wang, M. Z. Hoemann, J. Marjanovic, R. G. Heym and A. Vasudevan, *Bioorg. Med. Chem. Lett.*, 2015, **25**, 2019–2027.
- 297 M. A. Fabian, W. H. Biggs, D. K. Treiber, C. E. Atteridge, M. D. Azimioara, M. G. Benedetti, T. A. Carter, P. Ciceri, P. T. Edeen, M. Floyd, J. M. Ford, M. Galvin, J. L. Gerlach, R. M. Grotzfeld, S. Herrgard, D. E. Insko, M. A. Insko, A. G. Lai, J.-M. Lélias, S. A. Mehta, Z. V Milanov, A. M. Velasco, L. M. Wodicka, H. K. Patel, P. P. Zarrinkar and D. J. Lockhart, *Nat. Biotechnol.*, 2005, **23**, 329–336.
- 298 G. Jin and S. T. C. Wong, *Drug Discov. Today*, 2014, **19**, 637–644.

- 299 D. B. Kastrinsky, J. Sangodkar, N. Zaware, S. Izadmehr, N. S. Dhawan, G. Narla and M. Ohlmeyer, *Bioorg. Med. Chem.*, 2015, **23**, 6528–6534.
- 300 F. Imperi, F. Massai, M. Facchini, E. Frangipani, D. Visaggio, L. Leoni, A. Bragonzi and P. Visca, *Proc. Natl. Acad. Sci. U. S. A.*, 2013, **110**, 7458–7463.
- 301 C. G. Wermuth, *Drug Discov. Today*, 2006, **11**, 160–164.
- 302 M. E. Bunnage, E. L. P. Chekler and L. H. Jones, *Nat. Chem. Biol.*, 2013, **9**, 195–199.
- 303 C. H. Arrowsmith, J. E. Audia, C. Austin, J. Baell, J. Bennett, J. Blagg, C. Bountra, P. E. Brennan, P. J. Brown, M. E. Bunnage, C. Buser-Doepner, R. M. Campbell, A. J. Carter, P. Cohen, R. A. Copeland, B. Cravatt, J. L. Dahlin, D. Dhanak, A. M. Edwards, S. V. Frye, N. Gray, C. E. Grimshaw, D. Hepworth, T. Howe, K. V. M. Huber, J. Jin, S. Knapp, J. D. Kotz, R. G. Kruger, D. Lowe, M. M. Mader, B. Marsden, A. Mueller-Fahrnow, S. Müller, R. C. O'Hagan, J. P. Overington, D. R. Owen, S. H. Rosenberg, B. Roth, R. Ross, M. Schapira, S. L. Schreiber, B. Shoichet, M. Sundström, G. Superti-Furga, J. Taunton, L. Toledo-Sherman, C. Walpole, M. A. Walters, T. M. Willson, P. Workman, R. N. Young and W. J. Zuercher, *Nat. Chem. Biol.*, 2015, **11**, 536–541.
- 304 J. Dumas, R. Sibley, B. Riedl, M. K. Monahan, W. Lee, T. B. Lowinger, A. M. Redman, J. S. Johnson, J. Kingery-Wood, W. J. Scott, R. A. Smith, M. Bobko, R. Schoenleber, G. E. Ranges, T. J. Housley, A. Bhargava, S. M. Wilhelm and A. Shrikhande, *Bioorg. Med. Chem. Lett.*, 2000, **10**, 2047–2050.
- 305 J. Dumas, H. Hatoum-Mokdad, R. Sibley, B. Riedl, W. J. Scott, M. K. Monahan, T. B. Lowinger, C. Brennan, R. Natero, T. Turner, J. S. Johnson, R. Schoenleber, A. Bhargava, S. M. Wilhelm, T. J. Housley, G. E. Ranges and A. Shrikhande, *Bioorg. Med. Chem. Lett.*, 2000, **10**, 2051–2054.
- 306 N. J. Liverton, J. W. Butcher, C. F. Claiborne, D. Claremon, B. E. Libby, K. T. Nguyen, S. M. Pitzenberger, H. G. Selnick, G. R. Smith, A. Tebben, J. P. Vacca, S. L. Varga, L. Agarwal, K. Dancheck, a J. Forsyth, D. S. Fletcher, B. Frantz, W. A. Hanlon, C. F. Harper, S. J. Hofsess, M. Kostura, J. Lin, S. Luell, E. A. O'Neill and S. J. O'Keefe, *J. Med. Chem.*, 1999, **42**, 2180–2190.
- 307 K. Bowden and E. R. H. Jones, *J. Chem. Soc.*, 1946, 953–954.
- 308 M. C. Bagley, M. C. Lubinu and C. Mason, *Synlett*, 2007, **5**, 704–708.
- 309 R. Harigae, K. Moriyama and H. Togo, *J. Org. Chem.*, 2014, **79**, 2049–2058.

- 310 M. Yoshimatsu, K. Ohta and N. Takahashi, *Chem. - Eur. J.*, 2012, **18**, 15602–15606.
- 311 S.-X. Xu, L. Hao, T. Wang, Z.-C. Ding and Z.-P. Zhan, *Org. Biomol. Chem.*, 2013, **11**, 294–298.
- 312 C. Raji Reddy, J. Vijaykumar and R. Grée, *Synthesis*, 2013, **45**, 830–836.
- 313 D. A. Nugiel, K. Jacobs, L. Cornelius, C. H. Chang, P. K. Jadhav, E. R. Holler, R. M. Klabe, L. T. Bacheler, B. Cordova, S. Garber, C. Reid, K. A. Logue, L. J. Gorey-Feret, G. N. Lam, S. Erickson-Viitanen and S. P. Seitz, *J. Med. Chem.*, 1997, **40**, 1465–74.
- 314 P. Y. Lam, P. K. Jadhav, C. J. Eyermann, C. N. Hodge, Y. Ru, L. T. Bacheler, J. L. Meek, M. J. Otto, M. M. Rayner, Y. N. Wong and A. Et, *Science*, 1994, **263**, 380–384.
- 315 C. N. Hodge, P. E. Aldrich, L. T. Bacheler, C. H. Chang, C. J. Eyermann, S. Garber, M. Grubb, D. a Jackson, P. K. Jadhav, B. Korant, P. Y. Lam, M. B. Maurin, J. L. Meek, M. J. Otto, M. M. Rayner, C. Reid, T. R. Sharpe, L. Shum, D. L. Winslow and S. Erickson-Viitanen, *Chem Biol*, 1996, **3**, 301–314.
- 316 H. Babad and A. G. Zeiler, *Chem. Rev.*, 1972, **73**, 75–91.
- 317 C. S. Widdowson, PhD Thesis, University of Cardiff, 2008.
- 318 O. Fedorov, F. H. Niesen and S. Knapp, in *Kinase Inhibitors: Methods and Protocols, Method in Molecular Biology*, eds. B. Kuster and J. M. Walker, Humana Press, c/o Springer Science+Buisness Media, New York, 796th edn., 2012, pp. 109–118.
- 319 M. Bachmann and T. Mörröy, *Int. J. Biochem. Cell Biol.*, 2005, **37**, 726–730.
- 320 N. A. Warfel and A. S. Kraft, *Pharmacol. Ther.*, 2015, **151**, 41–49.
- 321 F. M. Moeslein, M. P. Myers and G. E. Landreth, *J. Biol. Chem.*, 1999, **274**, 26697–26704.
- 322 H. J. Menegay, M. P. Myers, F. M. Moeslein and G. E. Landreth, *J. Cell Sci.*, 2000, **113**, 3241–3253.
- 323 M. Zu, C. Li, J. S. Fang, W. W. Lian, A. L. Liu, L. S. Zheng and G. H. Du, *Molecules*, 2015, **20**, 19735–19747.
- 324 K. Colwill, L. L. Feng, J. M. Yeakley, G. D. Gish and J. F. Ca, *J. Biol. Chem.*, 1996, **271**, 24569–24575.
- 325 C. Naro and C. Sette, *Int. J. Cell Biol.*, 2013, **2013**, 151839.

- 326 H. Daub, S. Blencke, P. Habenberger, A. Kurtenbach, J. Dennenmoser, J. Wissing, A. Ullrich, M. Cotten, S. H. B. V Core and P. Phosphorylation, *J. Virol.*, 2002, **76**, 8124–8137.
- 327 N. Janel, M. Sarazin, F. Corlier, H. Corne, L. C. de Souza, L. Hamelin, A. Aka, J. Lagarde, H. Blehaut, V. Hindié, J.-C. Rain, M. L. Arbones, B. Dubois, M. C. Potier, M. Bottlaender and J. M. Delabar, *Transl. Psychiatry*, 2014, **4**, e425.
- 328 J. C. Biffinger, H. W. Kim and S. G. DiMagno, *ChemBioChem*, 2004, **5**, 622–627.
- 329 D. O'Hagan, *Chem. Soc. Rev.*, 2008, **37**, 308–319.
- 330 W. K. Hagmann, *J. Med. Chem.*, 2008, **51**, 4359–4369.
- 331 C. W. Vose and R. M. J. Ings, in *The Handbook of Medicinal Chemistry: Principles and Practice*, eds. A. Davis and S. E. Ward, The Royal Society of Chemistry, Cambridge, 3rd edn., 2015, pp. 184–207.
- 332 F. P. Guengerich, *Chem. Res. Toxicol.*, 2008, **21**, 70–83.
- 333 A. F. Stepan, V. Mascitti, K. Beaumont and A. S. Kalgutkar, *MedChemComm*, 2013, **4**, 631–652.
- 334 Y. Zhou, J. Wang, Z. Gu, S. Wang, W. Zhu, J. Acen, V. A. Soloshonok, K. Izawa and H. Liu, *Chem. Rev.*, 2016, **116**, 422–518.
- 335 K. A. Menear, C. Adcock, R. Boulter, X. L. Cockcroft, L. Copsey, A. Cranston, K. J. Dillon, J. Drzewiecki, S. Garman, S. Gomez, H. Javaid, F. Kerrigan, C. Knights, A. Lau, V. M. Loh, I. T. W. Matthews, S. Moore, M. J. O'Connor, G. C. M. Smith and N. M. B. Martin, *J. Med. Chem.*, 2008, **51**, 6581–6591.
- 336 D. O'Hagan, *J. Fluor. Chem.*, 2010, **131**, 1071–1081.
- 337 W. R. Dolbier, *Guide to Fluorine NMR for Organic Chemists*, John Wiley & Sons, Inc., Hoboken, New Jersey, New Jersey, USA, 2009.
- 338 R. E. Hubbard, in *The Handbook of Medicinal Chemistry: Principles and Practice*, eds. A. Davis and S. E. Ward, The Royal Society of Chemistry, Cambridge, 3rd edn., 2015, pp. 122–153.
- 339 S. Morooka, M. Hoshina, I. Kii, T. Okabe, H. Kojima, N. Inoue, Y. Okuno, M. Denawa, S. Yoshida, J. Fukuhara, K. Ninomiya, T. Ikura, T. Furuya, T. Nagano, K. Noda, S. Ishida, T. Hosoya, N. Ito, N. Yoshimura and M. Hagiwara, *Mol. Pharmacol.*, 2015, **88**, 316–325.

- 340 I. Franc, A. Lipinski and P. J. Feeney, *Adv. Drug Deliv. Rev.*, 1997, **23**, 3–25.
- 341 M. P. Gleeson, P. D. Leeson and H. Van De Waterbeemd, in *The Handbook of Medicinal Chemistry: Principles and Practice*, eds. A. Davis and S. E. Ward, The Royal Society of Chemistry, Cambridge, 3rd edn., 2015, pp. 1–31.
- 342 P. Ertl, B. Rohde and P. Selzer, *J. Med. Chem.*, 2000, **43**, 3714–3717.
- 343 F. Lovering, J. Bikker and C. Humblet, *J. Med. Chem.*, 2009, **52**, 6752–6756.
- 344 F. Lovering, *Med. Chem. Commun.*, 2013, **4**, 515–519.
- 345 J. S. Arthur and S. C. Ley, *Nat. Rev. Immunol.*, 2013, **13**, 679–692.
- 346 C. Ota, S. Kumata, S. Kawaguchi, Nihon Nohyaku Co. Ltd., *Eur. Pat.*, 1 544 202 A1, 2005, 56–57.
- 347 M. A. M. Baashen, PhD Thesis, University of Sussex, 2013.
- 348 M. Hamana, *Yakugaku Zsshi*, 1967, **66**, 1090.
- 349 D. P. Sutherlin, D. Sampath, M. Berry, G. Castanedo, Z. Chang, I. Chuckowree, J. Dotson, A. Folkes, L. Friedman, R. Goldsmith, T. Heffron, L. Lee, J. Lesnick, C. Lewis, S. Mathieu, J. Nonomiya, A. Olivero, J. Pang, W. W. Prior, L. Salphati, S. Sideris, Q. Tian, V. Tsui, N. C. Wan, S. Wang, C. Wiesmann, S. Wong and B.-Y. Zhu, *J. Med. Chem.*, 2010, **53**, 1086–1097.
- 350 W. Deng, P. Lye, Y. H. Lim, S*Bio PTE Ltd., *WO Pat.*, 101 454 A1, 2006.
- 351 V. G. Matassa, F. J. Brown, P. R. Bernstein, H. S. Shapiro, T. P. J. Maduskuie, L. A. Cronk, E. P. Vacek, Y. K. Yee, D. W. Snyder, R. D. Krell, C. L. Lerman and J. J. Maloney, *J. Med. Chem.*, 1990, **61**, 2621–2629.
- 352 A. L. Smith, P. E. Brennan, F. E. Demorin, G. Liu, N. A. Paras, D. M. Retz, *WO Pat.*, 066 172 A1, 2006, 27.
- 353 L. Fieser and R. Kennelly, *J. Am. Chem. Soc.*, 1935, **57**, 1611–1616.
- 354 M. D. Carter, M. Hadden, D. F. Weaver, S. M. H. Jacobo, E. Lu, *WO Pat.*, 125 324 A1, 2006.
- 355 A. J. Bridges, W. A. Denny, D. Fry, A. Kraker, R. F. Meyer, G. W. Rewcastle, A. M. Thompson, H. D. H. Showalter, *US Pat.*, 5 679 683, 1997.
- 356 V. Bertolasi, K. Dudová, P. Šimůnek, J. Černý and V. Macháček, *J. Mol. Struct.*, 2003, **658**, 33–42.

- 357 H. D'Orchymont, L. van Hijfte, A. Zimmermann, *US Pat.*, 0 004 000 A1, 2006, 20–21.
- 358 T. J. Donohoe, C. R. Jones and L. C. A. Barbosa, *J. Am. Chem. Soc.*, 2011, **133**, 16418–16421.
- 359 R. V Edwankar, C. R. Edwankar, O. A. Namjoshi, J. R. Deschamps and J. M. Cook, *J. Nat. Prod.*, 2012, **75**, 181–8.
- 360 A.-G. Valade, D. Dugat, G. Jeminet, J. Royer and H. Husson, *Eur. J. Med. Chem.*, 2001, 2041–2053.
- 361 M. D. Chapell, S. E. Conner, V. I. C. Gonzalez, J. E. Lamar, J. Li, J. S. Moyers, R. A. Owens, A. E. Tripp, G. Zu, Eli Lilly Co., *WO Pat.* 118 542 A1, 2005.
- 362 M. C. Bagley, R. T. Buck, S. L. Hind and C. J. Moody, *J. Chem. Soc., Perkin Trans. 1*, 1998, 591–600.
- 363 Z. Xia and C. D. Smith, *J. Org. Chem.*, 2001, **66**, 3459–66.
- 364 W. Wu, Z. Li, G. Zhou and S. Jiang, *Tetrahedron Lett.*, 2011, **52**, 2488–2491.
- 365 A. Marquart and B. Podlogar, *J. Org. Chem.*, 1994, **59**, 2092–2100.
- 366 H. Liu, P. B. Phillip, IRM LLC., *WO Pat.*, 018 568 A2, 2005.
- 367 A. H. Davidson, D. F. C. Moffat, F. A. Day, A. D. G. Donald, Chroma Therapeutics Ltd, *WO Pat.*, 040 934 A1, 2008, 28.
- 368 E. P. Kyba, S. T. Liu, K. Chockalingam and B. R. Reddy, *J. Org. Chem.*, 1988, **53**, 3513–3521.
- 369 J. N. Low, J. Cobo, R. Abonia, J. Quiroga and C. Glidewell, *Acta Crystallogr. Sect. C Struct. Chem.*, 2004, **60**, 194–195.
- 370 M. Mackay, A. Nortcliffe, H. McNab and A. N. Hulme, *Synthesis*, 2015, **47**, 242–248.
- 371 L. R. Swett, J. D. Ratajczyk, P. R. Young, Abbott Laboratories, *US Pat.*, 3, 686, 171, 1972.
- 372 J. C. Antilla, J. M. Baskin, T. E. Barder and S. L. Buchwald, *J. Org. Chem.*, 2004, **69**, 5578–5587.
- 373 G. M. Sheldrick, *Acta Crystallogr. Sect. A Found. Crystallogr.*, 2008, **64**, 112–122.
- 374 B. P. Wu, M. L. Pang, T. F. Tan and J. Ben Meng, *J. Mol. Struct.*, 2013, **1032**, 126–132.

Supplementary Information

Article

Microwave-Assisted Synthesis of a MK2 Inhibitor by Suzuki-Miyaura Coupling for Study in Werner Syndrome Cells

Mark C. Bagley ^{1,*}, Mohammed Baashen ¹, Irina Chuckowree ¹, Jessica E. Dwyer ¹, David Kipling ² and Terence Davis ²

¹ Department of Chemistry, School of Life Sciences, University of Sussex, Falmer, Brighton, East Sussex, BN1 9QJ, UK; E-Mails: baashen2000@hotmail.com (M.B.); I.Chuckowree@sussex.ac.uk (I.C.); J.E.Dwyer@sussex.ac.uk (J.E.D.)

² Institute of Cancer and Genetics, Cardiff University School of Medicine, Heath Park, Cardiff, CF14 4XN, UK; E-Mails: KiplingD@cardiff.ac.uk (D.K.); davist2@cardiff.ac.uk (T.D.)

* Author to whom correspondence should be addressed; E-Mail: m.c.bagley@sussex.ac.uk; Tel.: +44-1273-873-170.

Academic Editor: Jean Jacques Vanden Eynde

Received: 2 April 2015 / Accepted: 1 June 2015 / Published: 3 June 2015

Abstract: Microwave-assisted Suzuki-Miyaura cross-coupling reactions have been employed towards the synthesis of three different MAPKAPK2 (MK2) inhibitors to study accelerated aging in Werner syndrome (WS) cells, including the cross-coupling of a 2-chloroquinoline with a 3-pyridinylboronic acid, the coupling of an aryl bromide with an indolylboronic acid and the reaction of a 3-amino-4-bromopyrazole with 4-carbamoylphenylboronic acid. In all of these processes, the Suzuki-Miyaura reaction was fast and relatively efficient using a palladium catalyst under microwave irradiation. The process was incorporated into a rapid 3-step microwave-assisted method for the synthesis of a MK2 inhibitor involving 3-aminopyrazole formation, pyrazole C-4 bromination using *N*-bromosuccinimide (NBS), and Suzuki-Miyaura cross-coupling of the pyrazolyl bromide with 4-carbamoylphenylboronic acid to give the target 4-arylpyrazole in 35% overall yield, suitable for study in WS cells.

Keywords: Suzuki-Miyaura; cross-coupling; MK2 inhibitor; Werner syndrome; cell aging; pyrazoles; heterocycles; microwave-assisted synthesis; boronic acid

1. Introduction

Werner syndrome (WS) is an example of a monogenic segmental progeroid syndrome—a rare human autosomal recessive genetic instability syndrome that mimics many, but not all, of the polygenic features of physiological aging [1,2]. It was first characterized by Dr. Otto Werner [3] and its modern diagnosis often relies upon knowledge of previous family incidence and/or presentation with a series of clinical symptoms, including juvenile bilateral cataracts, scleroderma-like skin and premature graying of the hair [4]. Patients manifest a characteristic premature aging phenotype in their twenties or thirties and exhibit an increased predisposition to a number of pro-inflammatory age-related diseases [1], including type II diabetes mellitus, osteoporosis, and atherosclerosis, with premature death occurring typically from cancer or cardiovascular disease. Patients typically have high levels of inflammatory cytokines and intercellular adhesion molecule-1 (ICAM-1) and the same phenomenon can be observed in cell-based studies, with WS fibroblasts showing pronounced activation of inflammatory signaling pathways [5–7]. As a result, WS is often classified as an example of “inflamm-aging” [5,7] to highlight its association with, and patient pre-disposition to, age-related inflammatory disease pathologies [8]. The genetic basis of WS is known, with WS resulting from mutations in the RecQ3 DNA helicase-encoding gene *WRN* that give rise to a pathology attributed for the most part to the key role of RecQ3 in cellular responses to specific types of DNA damage. Lack of RecQ3 leads to frequent DNA replication fork stalling and subsequently genomic instability [9] and WS is classified as a chromosome instability syndrome [10]. The replication fork stalling and an increased pro-oxidant state [11] could provide the trigger for replication stress in WS leading to a decreased ability for WS cells to undergo division [5]. This is supported by the observation that young WS cells show a much reduced division capability compared to cells from normal individuals and resemble fibroblasts that have undergone stress-induced premature senescence [12], which is known from many different stimuli to be transduced by the mitogen activated protein kinase (MAPK) p38 [13–15]. This implicates the involvement of p38 signaling in the premature cell cycle arrest in WS and the short replicative life span observed in WS cell cultures. This in turn implicates a reduced ability of WS cells to divide as an underlying cause of accelerated aging in WS [2].

1.1. Studies of P38 Inhibitors in WS Cells

The role of stress signaling in Werner syndrome cells has been investigated using a range of small molecule inhibitors (Figure 1) of p38 MAPK [16], including SB203580 [12,17,18], VX-745 [19–21], RO3201195 [22,23], UR-13756 [24], and BIRB 796 [25], to study the link between replicative senescence *in vitro* and *in vivo* pathophysiology. WS fibroblasts treated with a p38 inhibitor display an unexpected reversal of the accelerated aging phenotype [12] and, as such, this may provide a suitable model for future therapeutic interventions designed to combat the aging process itself [12,26].

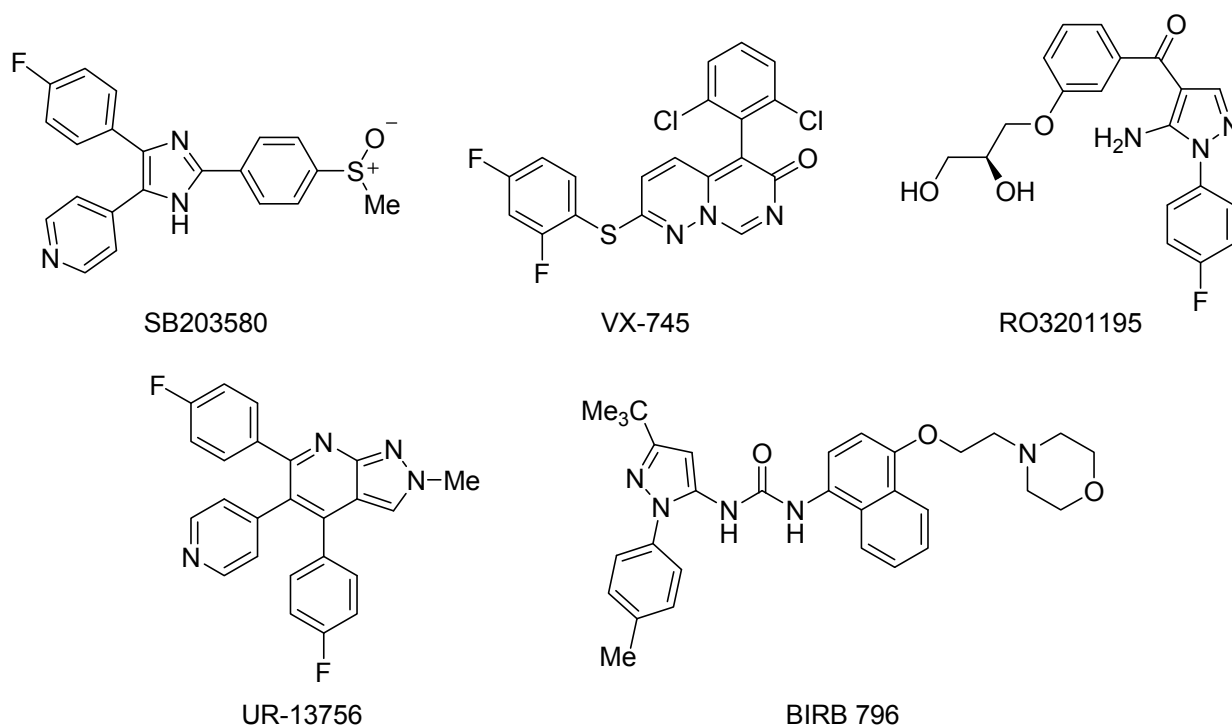


Figure 1. Inhibitors of p38 MAPK examined in WS cells.

1.2. Synthesis and Properties of MK2 Inhibitors

Although progress in the clinical development of successful p38 inhibitors for *in vivo* use is currently a considerable challenge [27], probably frustrated by toxicity issues, it may be possible to elicit a similar biological response by targeting the downstream kinase MAPKAPK2 (MK2) [16,28], which may itself be involved in the phenotypic characteristics seen in WS, including enlarged cellular morphology and prominent F-actin stress fibres [12]. MK2 activity up-regulates the expression of inflammatory pathways [29] and recent data suggest that MK2 acts as a checkpoint kinase that can lead to cell cycle arrest [30]. Furthermore MK2 knock-out mice exhibit normal, healthy phenotypes and are inflammation resistant [31], whereas p38 knock-out mice are lethal [32]. This could indicate that chemical inhibition of MK2 may be less problematic than inhibition of p38, whilst providing similar *in vivo* efficacy.

As a consequence of these observations, there has been considerable recent activity in drug discovery programs to develop small molecule inhibitors of MK2 [33]. A number of different chemotypes have been investigated [34], including a series of pyrrolopyridines **1** [35], pyrazinoindolone **2** [36], the benzo[4,5]thieno[3,2-*e*][1,4]diazepinone PF-3644022 [37] and recently tricyclic lactams **3** as a non-ATP-competitive inhibitor scaffold [38], yet issues of selectivity, potency and/or toxicity remain [34,39]. Many, but not all, of these approaches used Suzuki-Miyaura reactions to introduce diversity to an advanced intermediate for scaffold optimization (Figure 2). Since its initial discovery as a Pd-catalyzed stereospecific cross-coupling reaction of 1-alkenylboranes [40], the Suzuki-Miyaura reaction has become one of the most efficient methods for C–C bond formation, in particular for aryl-aryl coupling [41]. It offers many advantages over other methods, in that it is largely unaffected by the presence of water, produces non-toxic inorganic by-products that are easily removed, tolerates

a broad range of functional groups and proceeds generally with regio- and stereocontrol [42]. In a recent analysis of reactions used in the pursuit of drug candidates taken from a 2008 data set [43], biaryl linkages were present in 40% of the compounds that were analyzed and the Suzuki-Miyaura reaction occurred in over 4% of all reactions and in 40% of all C–C bond forming reactions. Given the amenability of transition-metal mediated processes to be accelerated under microwave dielectric heating [44], and thus readily automated to probe SAR, it is perhaps not surprising to observe so many uses of this reaction in the development of MK2 inhibitors [28] and such a high occurrence of this reaction in drug discovery programs in general [44].

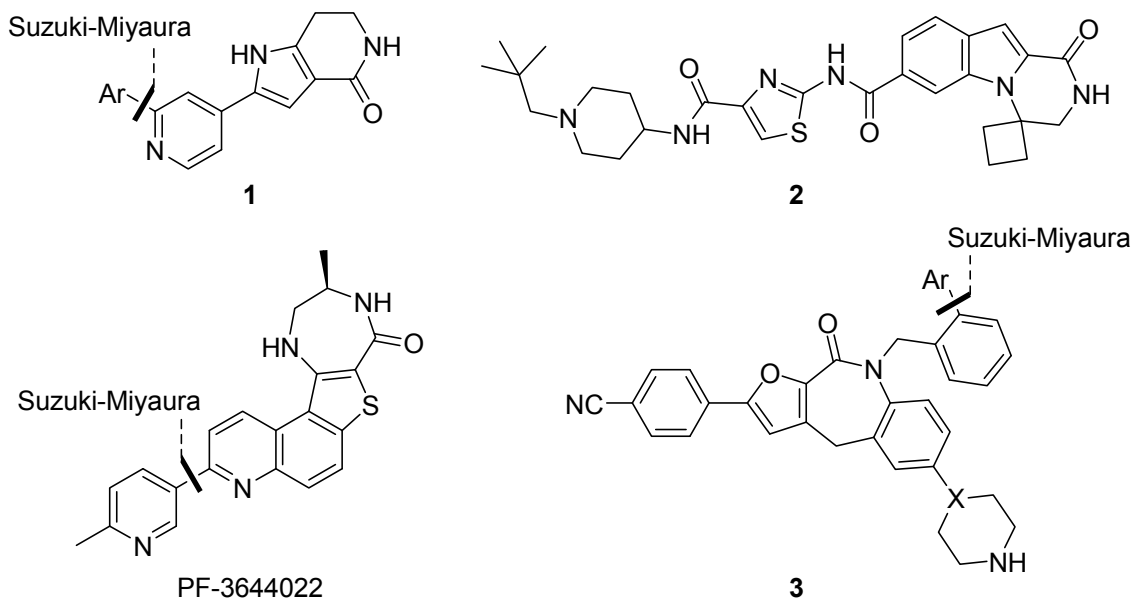


Figure 2. Examples of MK2 inhibitors from different drug discovery programs, showing the use of Suzuki-Miyaura aryl-aryl coupling for late-stage scaffold optimization.

Given the success of a p38 inhibitor in rescuing accelerated aging in WS cells, we carried out studies on a number of MK2 inhibitors (Figure 3) to establish their effect on cell aging phenotypes using fibroblasts from human WS [28,45,46]. Of these inhibitors, butyramide **4** was reported to act by blocking p38-MK2 docking, thus preventing the activation of MK2 by phospho-p38 [47] but in WS cells caused a stressed morphology and permanent cell cycle arrest [46] by a pathway that appeared not to involve MK2 inhibition [46]. A benzopyranopyridine inhibitor **5** [48] gave a similar cellular response at a concentration that inhibited MK2, but this was thought to be due to non-specific toxicity issues [46]. However, when primary WS fibroblasts were treated with a tetrahydropyrrolo[3,2-*c*]pyridin-4-one inhibitor **6**, the stressed cellular morphology and shortened replicative lifespan were both corrected, although the extension in life span was much smaller than the one seen upon treatment with SB203580 [45]. Given this promising indication, and the wide range of MK2 inhibitors investigated in other cellular models, a rapid route to another MK2 inhibitory chemotype was urgently required to provide added confirmation of the above findings.

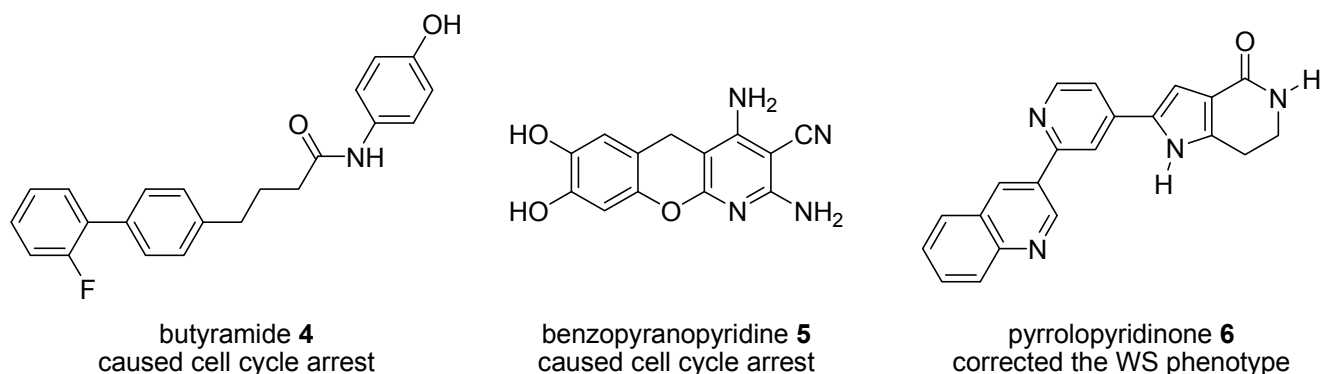


Figure 3. MK2 inhibitor chemotypes and their effect on WS cells.

2. Results and Discussion

Our first approach aimed to take advantage of the Suzuki-Miyaura coupling in a rapid route to the Pfizer MK2 inhibitor PF-3644022 [37,49,50]. Although this compound exhibits single digit nanomolar potency against MK2 (IC_{50} 5 nM), cellular activity below 500 nM (U937 TNF α release IC_{50} 150 nM) [50], good selectivity across 200 human kinases and projected human pharmacokinetics sufficient for oral dosing, it was found to lead to acute hepatotoxicity in dogs, probably by disrupting hepatobiliary transporters [39]. Nevertheless, for study in WS cells, its activity and selectivity profile made it a compelling target, with preliminary data using this inhibitor showing extension of cellular replicative capacity in WS fibroblasts and correction of the stressed morphology (Figure 4), a result similar in magnitude to that seen using the tetrahydropyrrolo[3,2-*c*]pyridin-4-one inhibitor **6** [45].

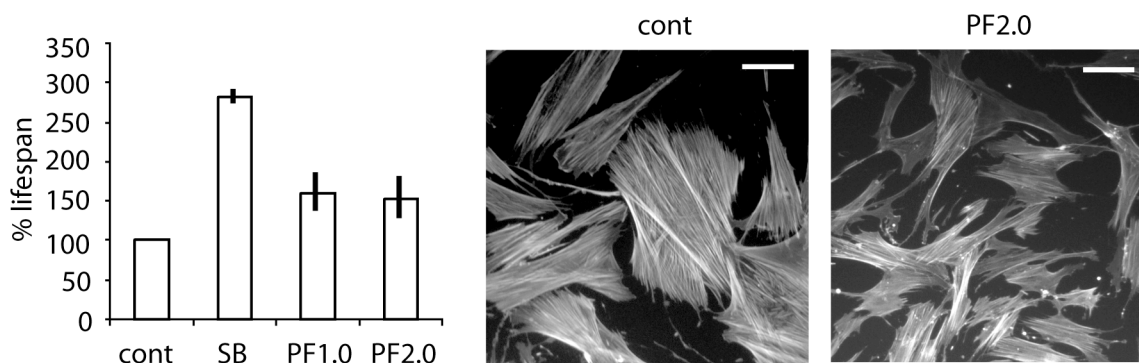


Figure 4. Increased replicative lifespan (\pm SD; $n = 3$) and improvement cellular morphology in WS cells using PF-3644022. Cont = control, SB = SB203580 at 2.5 μ M, PF1.0 and PF2.0 = PF-3644022 at 1.0 and 2.0 μ M respectively. White bar = 100 μ m (for methods see experimental section).

The development of this inhibitor utilized a late-stage Suzuki-Miyaura coupling to introduce diversity at C-7 of a thieno[3,2-*f*]quinoline ring (see Figure 2) [49], following initial identification of promising SAR studies and cellular potency with a benzo[4,5]thieno[3,2-*e*][1,4]diazepin-5(2*H*)-one scaffold [50]. Given that our goal was the introduction of a 6-methyl-3-pyridyl substituent at C-7, we set out to incorporate the Suzuki-Miyaura coupling of the pyridinylboronic acid **10a** and 2-chloroquinoline **11** into an early stage of the synthesis (Figure 5). Elaboration of the target inhibitor should then

proceed in a similar fashion to Anderson's route [49]: one-step formation of aminocyanoquinoline **8a** from nitroquinoline **9a**, followed by synthesis of aminobenzothiophene **7** by diazotization and subsequent reaction with methyl thioglycolate before the introduction of the diazepinone ring.

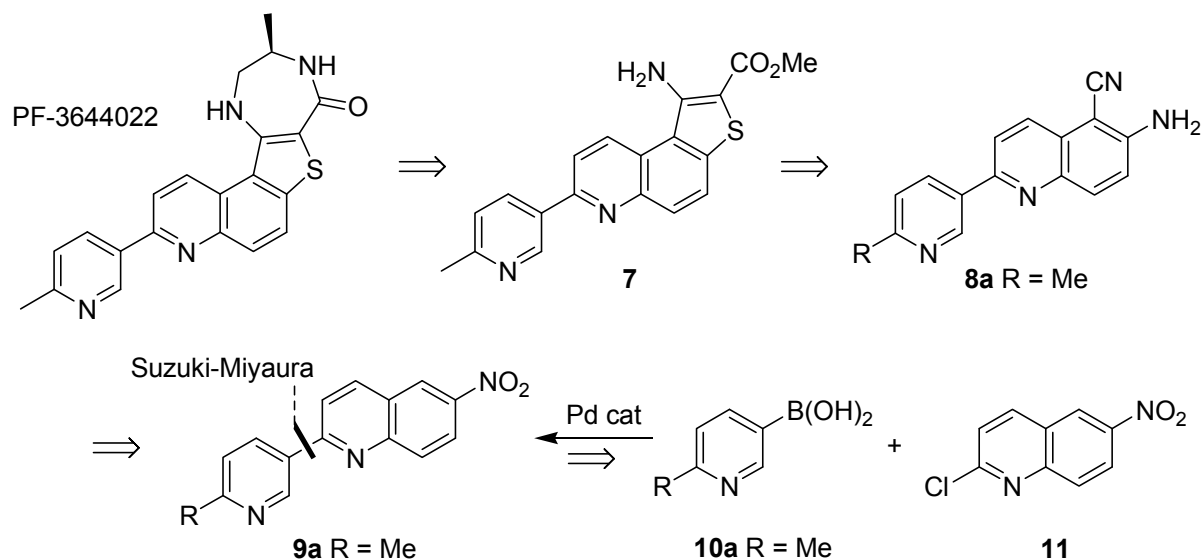


Figure 5. Disconnective approach to the synthesis of PF-3644022, utilizing an early-stage Suzuki-Miyaura cross-coupling reaction.

2.1. Early-Stage Suzuki-Miyaura Cross-Coupling Reactions for the Synthesis of PF-3644022

Starting with a known route to **11** [51], 3,4-dihydroquinolin-2(1*H*)-one (**12**) was nitrated using $\text{HNO}_3/\text{H}_2\text{SO}_4$ and then treated with phosphorus oxychloride in DMF in the presence of DDQ as oxidant to give 2-chloro-6-nitroquinoline (**11**) in 90% isolated yield over the two steps (Figure 5). Suzuki-Miyaura cross-coupling with 6-methyl-3-pyridinylboronic acid (**10a**) using Na_2CO_3 base and $\text{PdCl}_2(\text{PPh}_3)_2$ as catalyst in $\text{MeCN}-\text{H}_2\text{O}$ at 140 °C under microwave irradiation gave the cross-coupled product **9a** in reasonable yield. However, use of the Yamazaki method for the synthesis of *ortho*-aminoaroylnitriles [52], namely treating nitroquinoline **9a** with ethyl cyanoacetate and KOH in DMF at room temperature for up to 72 h, followed by hydrolysis using 5% NaOH (aq) at reflux for 3 h, in accordance with Anderson's approach, gave only a trace of the 6-amino-5-cyanoquinoline **8a**. Given the wide range of nitroquinolines compatible with this chemistry in Yamazaki's original report [52], and its previous use in a route to PF-3644022 by Anderson [49], this was unexpected. To probe whether the acidity of the pyridine 6-methyl group had been responsible for this observation, the Suzuki-Miyaura cross-coupling reaction was repeated using 3-pyridinylboronic acid (**10b**), to give the 2-pyridylquinoline **9b** in 62% isolated yield (Figure 6). When this substrate was investigated in the Yamazaki cyanation reaction under identical conditions it behaved in a very similar fashion and only a trace of the cyanoquinoline product **8b** was observed by ^1H NMR spectroscopic analysis of a complex mixture. Efforts to introduce the Yamazaki cyanation at an earlier stage in the process were similarly unsuccessful. Dihydroquinolone **13** was inert to treatment with ethyl cyanoacetate and KOH in DMF, either at room temperature for 24 h followed by treatment with aqueous base or under more forcing conditions, when heated to 50 °C for 64 h. In both cases only unreacted starting material **13** was

obtained. Alternatively, when chloroquinoline **11** was reacted with ethyl cyanoacetate in the presence of base at RT for 64 h (Figure 6) a complex mixture of products was obtained, rather than cyanoquinoline **8c**. It was apparent that either the lactam ring or an electrophilic chloroquinoline function interfered unfavorably with this cyanation reaction. For comparison, Yamazaki cyanation of 6-nitroquinoline (**14**) under identical conditions gave the expected product, 6-amino-5-cyanoquinoline (**15**) in good yield (72%) after basic hydrolysis. Thus it was concluded that an early-stage Suzuki-Miyaura cross-coupling strategy was efficient for biaryl C-C bond formation but the 2-pyridylquinoline products, as well as other quinoline-containing precursors, were incompatible with Yamazaki's aminoaroylnitrile synthesis and so could not be used for the rapid synthesis of the MK2 inhibitor, PF-3644022.

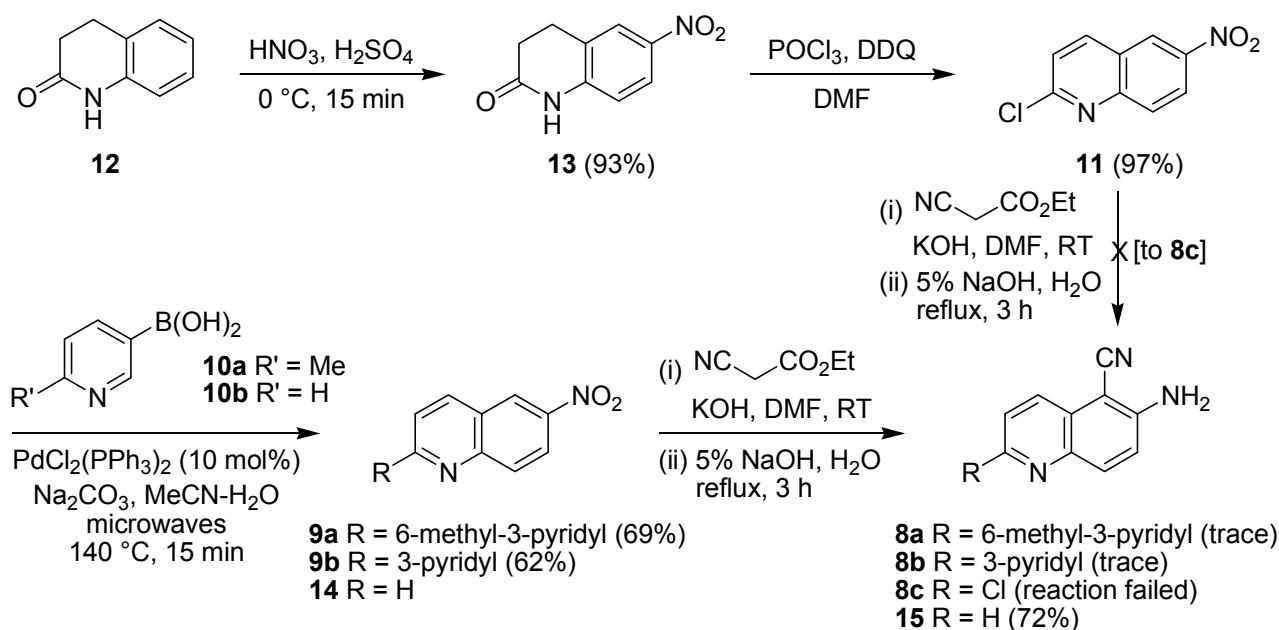


Figure 6. Synthesis of chloroquinoline **11** and subsequent Suzuki-Miyaura cross-coupling.

2.2. Suzuki-Miyaura Cross-Coupling Reactions for the Synthesis of (Indolyl)phenylpyrazole MK2 Inhibitor **18**

Given the success of pyrrolopyridinone **6** in correcting the WS phenotype, we next turned to the scaffold hopping strategy of Velcicky *et al.* [53] for rapid access to a MK2 inhibitor for study in WS cells. Velcicky found that replacing the pyrrolopyrimidinone pharmacophore **16**, which overlays well with pyrrolopyridinone **6**, with a series of benzamide derivatives **17** led to the development of a 3-aminopyrazole **18** that inhibited intracellular phosphorylation of HSP27, as well as LPS-induced TNF α release in cells (Figure 7) [53]. The synthesis of this inhibitor employed two successive Suzuki-Miyaura cross-coupling reactions to establish the biaryl bonds. Given our recent report on the regiocontrolled synthesis of 3-aminopyrazoles [54], this was a compelling scaffold to study.

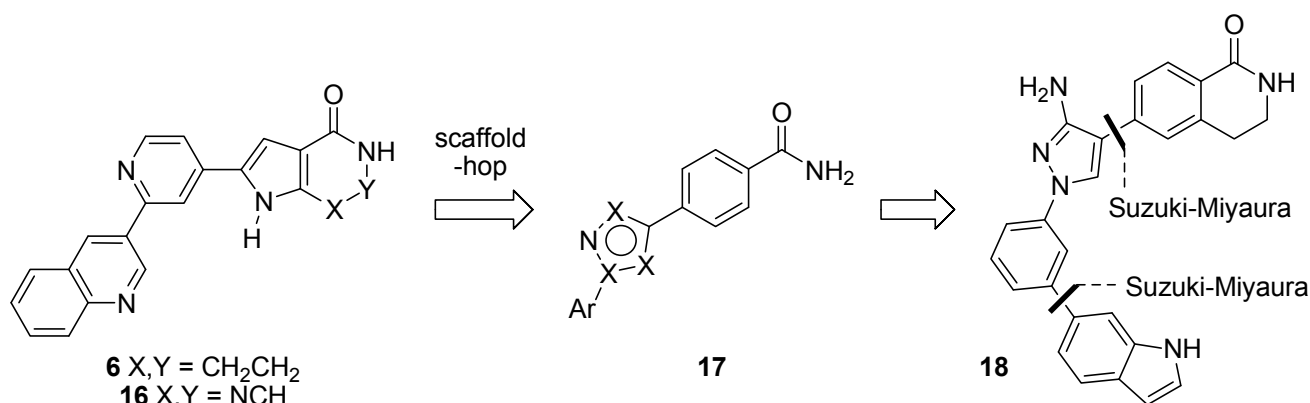


Figure 7. Scaffold-hopping strategy of Velcicky *et al.* [53], showing the use of Suzuki-Miyaura aryl-aryl coupling for scaffold optimization.

The hydrochloride salt of 3-bromophenylhydrazine (**19**) was reacted with 3-methoxyacrylonitrile (**20**) (2 equiv.) in the presence of a large excess of sodium ethoxide in ethanol at reflux for 20 h (Figure 8) to give 3-aminopyrazole **21** in excellent yield (90%), or more rapidly under microwave irradiation at 150 °C for 1 h in a sealed tube to give the same product in comparable yield (89%) [54]. Under the strongly basic conditions, no 5-aminopyrazole regioisomers were isolated or observed. Efforts to improve the microwave-assisted procedure, by switching to *tert*-butyl alcohol in the presence of *tert*-butoxide as base and irradiating at 150 °C for 2 h caused a significant reduction in yield (68%) and so the overnight conductive heating method was adopted as the procedure of choice as it could be readily carried out on gram scale. Suzuki-Miyaura cross-coupling of the arylbromide **21** with 6-indolylboronic acid **22** under microwave irradiation at 150 °C for 2 h in DMF in the presence of cesium carbonate and tetrakis(triphenylphosphine)palladium(0) (10 mol%) gave the coupled product **23** in 84% isolated yield. Unfortunately, bromination at C-4 of aminopyrazole **23** using NBS failed to provide 4-bromopyrazole **24** and instead gave a complex mixture of products, presumably due to competing bromination of the indolyl ring. It was possible to install the C-4 bromo group prior to Suzuki-Miyaura coupling by treating the *N*-(bromophenyl)pyrazole **21** with NBS in THF at RT for 16 h to give dibromide **25** in 83% yield after purification by column chromatography. However, Suzuki-Miyaura cross-coupling of dibromide **25** with the 6-indolylboronic acid **22** under similar conditions did not provide the 4-bromopyrazole **24** and instead gave a complex mixture of products and could not differentiate between the two reactive sites. Although potentially this could be resolved through the use of different halogen moieties, given the difficulties or the need to use protecting group chemistries for the synthesis of the indole-containing inhibitor, we switched to a simpler pyrazole target, benzamide **26**, reported to possess reasonable potency (IC₅₀ 2.0 μM), as a more accessible inhibitor for evaluation in WS cells.

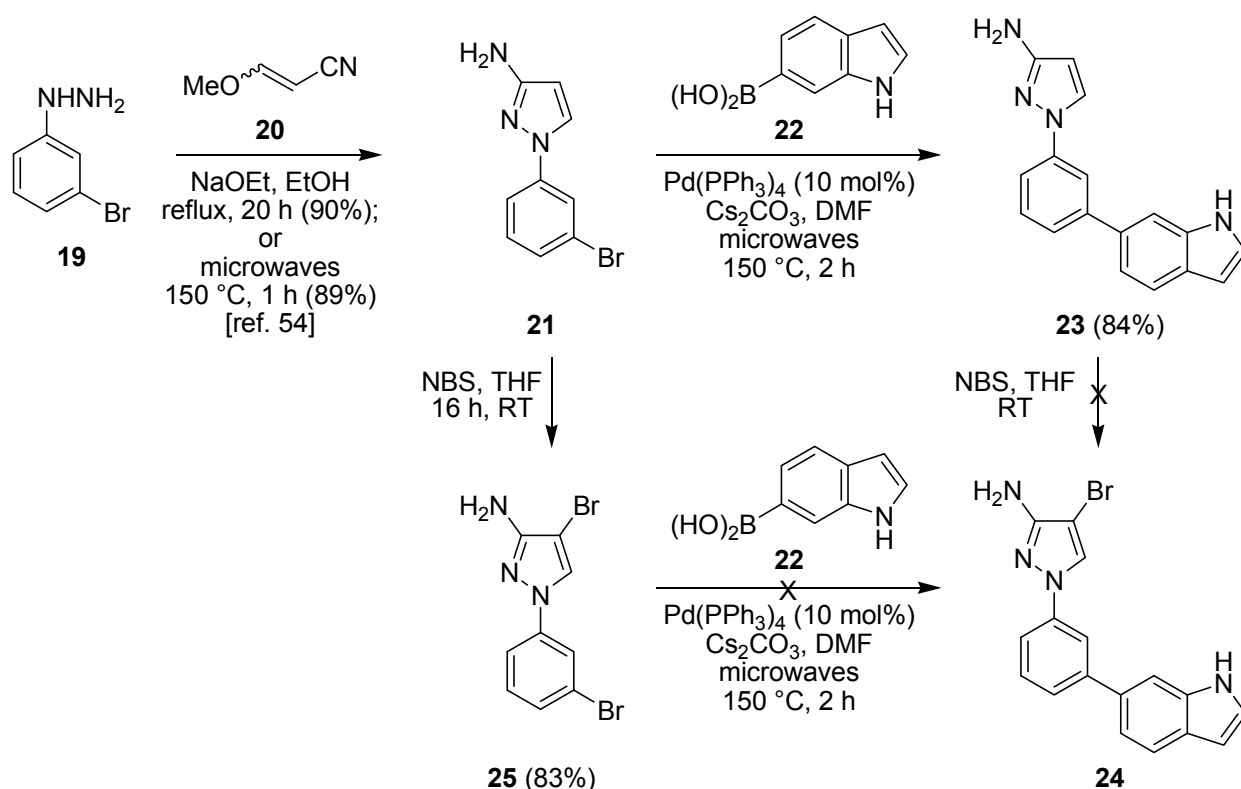


Figure 8. Suzuki-Miyaura cross-coupling for the synthesis of 6-indolyl scaffolds.

2.3. Suzuki-Miyaura Cross-Coupling Reactions for the Synthesis of Aminopyrazole MK2 Inhibitor **26**

Adopting a similar route, the hydrochloride salt of 4-methoxyphenylhydrazine (**27**) was reacted with 3-methoxyacrylonitrile (**20**) (2 equiv.) under basic conditions using sodium ethoxide in ethanol under microwave irradiation at 150 °C for 2 h to give 3-amino-1-(4-methoxyphenyl)pyrazole (**28**) as the only observed regioisomer in 85% yield (Figure 9). Bromination using NBS in THF under microwave irradiation at 150 °C for 2 h gave the C-4 brominated pyrazole **29** in 77% yield. This rapid microwave-assisted procedure was preferred over a method under ambient conditions, which required stirring with NBS in THF for 16 h but did give bromide **29** in slightly improved yield (82%). Suzuki-Miyaura coupling of the pyrazolylbromide **29** with 4-carbamoylphenylboronic acid (**30**) in *i*PrOH–H₂O in the presence of potassium carbonate and bis(triphenylphosphine)palladium(II) chloride (10 mol%) under microwave irradiation at 150 °C for 2 h using similar conditions to Velcicky *et al.* [53] gave the coupled product **26** in 54% yield after purification by column chromatography. This route to pyrazole **26** utilized three microwave-assisted steps, each of 2 h duration, starting from commercially-available materials and provided the target MK2 inhibitor in 35% overall yield, suitable for study in WS cells.

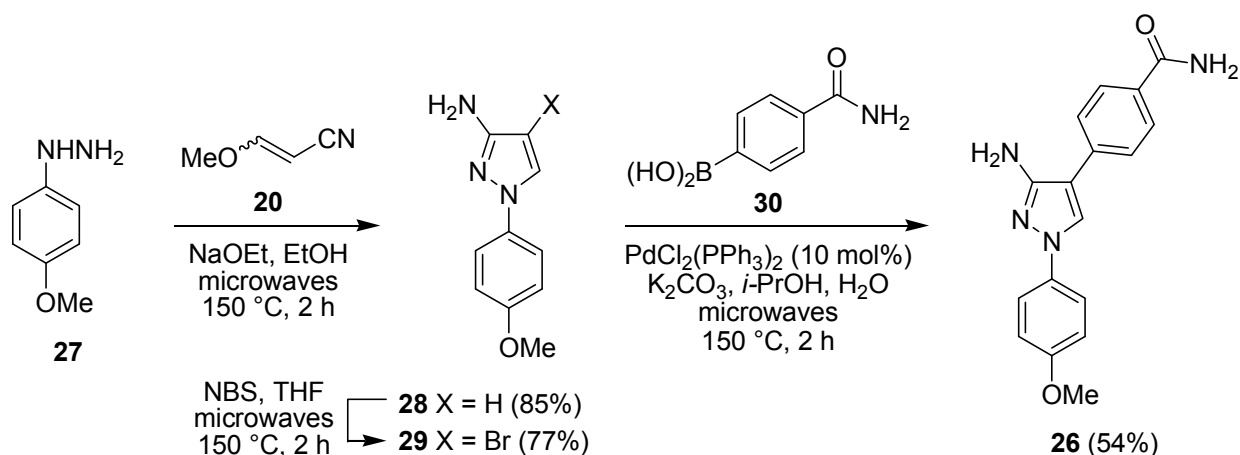


Figure 9. Microwave-assisted synthesis of the MK2 inhibitor **26** using a Suzuki-Miyaura cross-coupling.

2.4. Biological Evaluation of Aminopyrazole MK2 Inhibitor **26** in WS Cells

When WS fibroblasts were grown in the presence of inhibitor **26** at 25 μ M a small lifespan extension was noted, although it was difficult to ascertain if this was significant, especially as little inhibition of MK2 activity was seen at this concentration [28]. Treatment with inhibitor **26** did, however, show improvement in the cellular morphology of the WS cells at 25 μ M and 50 μ M. These results were encouraging for the further development of MK2 inhibitors in this and other inflammatory therapeutic areas.

2.5. The Role of MK2 in the WS Cell Phenotype and Its Modulation Using Chemical Inhibitors

Effects of MK2 inhibitors on the growth and morphology of WS cells have been ambiguous: inhibitors **4** and **5** resulted in growth inhibition that was not related to MK2 inhibition [46]; inhibitor **6** increased cellular replicative capacity at a concentration that maximally inhibited MK2 [45]; inhibitor **26** showed a small increase in replicative capacity and alleviated the stressed morphology [28]; and finally, PF-3644022 had an effect similar in magnitude to inhibitor **6** at a dose that fully inhibited MK2 (this work). Thus, three MK2 inhibitors with very different chemotypes gave similar results for WS fibroblasts on all cellular parameters tested. These data suggest a role for p38-activated MK2 in replicative senescence in WS fibroblasts, although this role appears to be much reduced compared to that of p38, as the p38 inhibitor SB203580 has much larger effects on the replicative capacity of WS fibroblasts [12]. Possible reasons for the reduced effects of MK2 inhibitors on replicative capacity are that MK2 may be only one of the downstream effectors of p38 responsible for cellular growth arrest [55], or that MK2 inhibitors have a narrow therapeutic window and become toxic to cell growth at levels close to the maximally effective dose [34]. This latter is seen with both PF-3644022 that is effective at 2.0 μ M but becomes toxic to cell growth at levels of 5.0 μ M and above (unpublished data), and with inhibitor **6** that is maximally effective at 5.0 μ M but toxic at 10.0 μ M [45]. These data also suggest that MK2 inhibitors may not be as useful therapeutically as p38 inhibitors if the accelerated cell aging seen in WS does underlie the accelerated whole body aging, as suggested [2], but may prove useful in the alleviation of the associated inflammatory conditions that are thought to be MK2 dependent [29].

As inflammatory conditions that may be due to MK2 activation are an increasing issue during the normal human aging process [56], such inhibitors may be of wider therapeutic benefit in the general population. This then provides a good rationale for the continued efforts to find suitable MK2 inhibitors for *in vivo* use.

3. Experimental Section

3.1. Synthetic Materials and Methods

Commercially available reagents were used without further purification; solvents were dried by standard procedures. Light petroleum refers to the fraction with bp 40–60 °C and ether (Et₂O) refers to diethyl ether. Column chromatography was carried out using Merck Kieselgel 60 H silica or Matrex silica 60. Analytical thin layer chromatography was carried out using aluminium-backed plates coated with Merck Kieselgel 60 GF₂₅₄ that were visualised under UV light (at 254 and/or 360 nm). Microwave irradiation experiments were performed in a sealed Pyrex tube using a self-tunable CEM Discover or CEM Explorer focused monomodal microwave synthesizer at the given temperature using the instrument's in-built IR temperature measuring device, by varying the irradiation power (initial power given in parentheses).

Fully characterized compounds were chromatographically homogeneous. Melting points (mp) were determined on a Kofler hot stage apparatus or Stanford Research Systems Optimelt and are uncorrected. Infra-red (IR) spectra were recorded in the range 4000–600 cm⁻¹ on a Perkin-Elmer 1600 series FTIR spectrometer using an ATR probe or as a KBr disk (KBr) and are reported in cm⁻¹. Nuclear magnetic resonance (NMR) spectra were recorded in CDCl₃ at 25 °C unless stated otherwise using a Varian VNMRs instrument operating at 400 or 500 MHz or a Bruker DPX 400 or 500 Avance instrument operating at 400 or 500 MHz for ¹H spectra and 100 or 126 MHz for ¹³C spectra and were reported in ppm; *J* values were recorded in Hz and multiplicities were expressed by the usual conventions (s = singlet, d = doublet, t = triplet, app = apparent, m = multiplet, br = broad). Mass spectra (MS) were determined with a Fisons VG Platform II Quadrupole instrument using atmospheric pressure chemical ionization (APCI), a Waters Q-TOF Ultima using electrospray positive ionization (ES), a Waters LCT premier XE using atmospheric pressure chemical ionization (APCI), an Agilent 6130 single quadrupole with an APCI/electrospray dual source, a Fisons Instrument VG Autospec using electron ionization (EI) at 70 eV (low resolution) or a ThermoQuest Finnigan LCQ DUO electrospray, unless otherwise stated. Some high-resolution mass spectra were obtained courtesy of the EPSRC Mass Spectrometry Service at Swansea, UK using the ionisation methods specified. *In vacuo* refers to evaporation at reduced pressure using a rotary evaporator and diaphragm pump, followed by the removal of trace volatiles using a vacuum (oil) pump.

3.2. General Synthetic Procedures

General Procedure for Suzuki-Miyaura Cross-Coupling

A solution of 2-chloro-6-nitroquinoline, boronic acid (1.5–1.6 equiv.), aqueous Na₂CO₃ solution (2 equiv.) and PdCl₂(PPh₃)₂ (10 mol%) in MeCN (0.2 M) was irradiated at 140 °C for 15 min in a

pressure-rated glass tube (35 mL) using a CEM Discover microwave synthesizer by moderating the initial power (200 W). After cooling in a flow of compressed air, the solvent was evaporated *in vacuo* and the residue was triturated with water. Purification by flash column chromatography on SiO₂ gave the desired 2-pyridinyl-6-nitroquinoline.

3.3. Synthetic Experimental Procedures

3.3.1. 3,4-Dihydro-6-nitroquinolin-2(1H)-one (**13**)

According to a known literature procedure [51], concentrated sulfuric acid (20 mL) was added to 3,4-dihydro-2-(1H)-quinoline (**12**) (1.00 g, 6.79 mmol) in a 100 mL round-bottom flask. The reaction was placed into an ice-acetone bath (−10 °C approx.) and stirred to dissolve the solid. Nitric acid (69%; 0.50 mL, 11.3 mmol, 1.7 equiv.) was added dropwise and the orange-red solution was stirred at −10 to 0 °C for 30 min. The reaction was quenched by pouring onto a stirred ice-water slush (300 mL). The ice was allowed to melt and the precipitate was collected by vacuum filtration, washed with water and air dried under suction to give a beige-coloured solid (1.21 g, 93%), with identical physical and spectroscopic properties to literature data [51].

3.3.2. 2-Chloro-6-nitroquinoline (**11**)

POCl₃ (1.2 mL, 13.0 mmol) was added dropwise to a stirred solution of **13** (1.00 g, 5.2 mmol) and DDQ (1.30 g, 5.7 mmol) in DMF (20 mL) and the reaction mixture was stirred at RT for 1 h. The reaction mixture was then poured into iced water and the resultant precipitate was collected by vacuum filtration, washed with water and dried in air to give the *title compound* (1.05 g, 97%) as an orange solid, mp 226.8–227.9 °C (lit. [51] mp 235.5–236.5 °C) (Found [ES]: MH⁺, 209.0112. C₉H₆ClN₂O₂ [MH] requires 209.0112); IR (neat) $\nu_{\max}/\text{cm}^{-1}$ 3068 (C-H), 1619 (C=C), 1523 (NO₂), 1485 (C=C), 1337 (NO₂), 1105 (C-N); ¹H-NMR (500 MHz, *d*₆-DMSO) $\delta_{\text{H}}/\text{ppm}$ 9.13 (1H, d, *J* 2.5, 5-CH), 8.78 (1H, d, *J* 9, 4-CH), 8.52 (1H, dd, *J* 9, 2.5, 7-CH), 8.18 (1H, d, *J* 9, 8-CH), 7.84 (1H, d, *J* 9, 3-CH); ¹³C-NMR (126 MHz, *d*₆-DMSO) $\delta_{\text{C}}/\text{ppm}$ 153.6 (C), 149.2 (C), 145.3 (C), 141.9 (4-CH), 129.7 (8-CH), 125.9 (C), 125.0 (5-CH), 124.4 (3-CH), 124.1 (7-CH); *m/z* (EI) 208 (M⁺, 100), 162 (48), 150 (49), 127 (81).

3.3.3. 2-(6-Methylpyridin-3-yl)-6-nitroquinoline (**9a**)

Biaryl **9a** was prepared according to general synthetic procedure 3.2.1 using 2-chloro-6-nitroquinoline (**11**) (0.45 g, 2.20 mmol), 6-methyl-3-pyridinylboronic acid (**10a**) (0.44 g, 3.20 mmol), aqueous Na₂CO₃ solution (1.5 M; 3 mL) and PdCl₂(PPh₃)₂ (0.15 g, 0.21 mmol) in MeCN (12 mL). Purification by column chromatography on SiO₂ gel, gradient eluting with CH₂Cl₂ to CH₂Cl₂–MeOH (9:1), gave the *title compound* (0.39 g, 69%) as an orange solid, mp 237.5–239.1 °C (Found [ES]: MH⁺, 266.0923. C₁₅H₁₂N₃O₂ [MH] requires 266.0924); IR (neat) $\nu_{\max}/\text{cm}^{-1}$ 3070 (C-H), 2921 (C-H), 1596 (C-C), 1534 (NO₂), 1327 (NO₂); ¹H-NMR (500 MHz, CDCl₃) $\delta_{\text{H}}/\text{ppm}$ 9.30 (1H, d, *J* 1, 2'-CH), 8.82 (1H, d, *J* 2, 5-CH), 8.50 (2H, 4'-CH and 7-CH), 8.43 (1H, d, *J* 9, 4-CH), 8.28 (1H, d, *J* 9, 8-CH), 8.05 (1H, d, *J* 9, 3-CH), 7.36 (1H, d, *J* 8, 5'-CH), 2.68 (3H, s, Me); ¹³C-NMR (126 MHz, CDCl₃) $\delta_{\text{C}}/\text{ppm}$ 160.6 (C), 158.2 (C), 150.4 (C), 148.4 (2'-CH), 145.5 (C), 138.7 (4-CH), 135.4 (4'-CH), 131.4 (8-CH), 131.3 (C), 126.0 (C), 124.3 (5-CH), 123.4 (7-CH), 123.4 (5'-CH), 120.0 (3-CH), 24.5 (Me).

3.3.4. 2-(Pyridin-3-yl)-6-nitroquinoline (**9b**)

Biaryl **9b** was prepared according to the general procedure 3.2.1 using 2-chloro-6-nitroquinoline (**11**) (0.15 g, 0.71 mmol), 3-pyridinylboronic acid (**10b**) (0.10 g, 1.14 mmol), aqueous Na₂CO₃ (1.4 M, 1 mL) and PdCl₂(PPh₃)₂ (0.05 g, 0.07 mmol) in MeCN (3.6 mL). Purification by column chromatography on SiO₂ gel, eluting with EtOAc–CH₂Cl₂ (3:7), gave the *title compound* (0.11 g, 62%) as a yellow solid (Found [ES]: MH⁺, 252.0776. C₁₄H₁₀N₃O₂ [MH] requires 252.0767); IR (neat) $\nu_{\max}/\text{cm}^{-1}$ 3081 (C-H), 1607 (C=C), 1528 (NO₂), 1337 (NO₂); ¹H-NMR (500 MHz, CDCl₃) $\delta_{\text{H}}/\text{ppm}$ 9.43 (1H, br s, 2'-CH), 8.84 (1H, d, *J* 2, 5-CH), 8.78 (1H, d, *J* 3, 6'-CH), 8.58 (1H, d, *J* 8, 4'-CH), 8.53 (1H, dd, *J* 9, 2, 7-CH), 8.48 (1H, d, *J* 8, 4-CH), 8.31 (1H, d, *J* 9, 8-CH), 8.08 (1H, d, *J* 9, 3-CH), 7.52 (1H, m, 5'-CH); ¹³C-NMR (126 MHz, CDCl₃) $\delta_{\text{C}}/\text{ppm}$ 158.0 (C), 151.2 (6'-CH), 150.4 (C), 149.0 (2'-CH), 138.9 (4-CH), 135.2 (4'-CH), 131.6 (8-CH), 128.5 (C), 128.4 (C), 126.1 (C), 124.3 (5-CH), 123.8 (C), 123.5 (7-CH), 120.2 (3-CH); *m/z* (EI) 251 (M⁺, 100), 205 (35).

3.3.5. 6-Amino-5-cyanoquinoline (**15**)

6-Nitroquinoline (0.50 g, 2.85 mmol) was added to a solution of ethyl cyanoacetate (0.91 mL, 8.61 mmol) and KOH (0.97 g, 17.0 mmol) in DMF (8.7 mL) and the mixture was stirred for 64 h. The solvent was evaporated *in vacuo* and the residue was dissolved in aqueous NaOH solution (5%; 12 mL) and heated at reflux for 3 h. The reaction mixture was allowed to cool and extracted with CHCl₃ (3 × 15 mL). The organic extracts were combined, dried (MgSO₄) and evaporated *in vacuo*. Purification by flash column chromatography on SiO₂ gel, gradient eluting with CH₂Cl₂ to CH₂Cl₂–MeOH (9:1), gave the *title compound* (0.35 g, 72%) as an orange solid, mp 181.2–182.8 °C (lit. [57] mp 181 °C) (Found [ES]: MH⁺, 170.0711. C₁₀H₈N₃ [MH] requires 170.0713); IR (neat) $\nu_{\max}/\text{cm}^{-1}$ 3391 (N-H), 3337 (N-H), 3159 (C-H), 2199 (C≡N), 1635 (N-H), 1615 (C=C), 1337 (C-N); ¹H-NMR (500 MHz, CDCl₃) $\delta_{\text{H}}/\text{ppm}$ 8.74 (1H, d, *J* 3, 2-CH), 8.24 (1H, d, *J* 8, 4-CH), 8.06 (1H, d, *J* 9, 8-CH), 7.47 (1H, m, 3-CH), 7.15 (1H, d, *J* 9, 7-CH), 4.93 (2H, br s, NH₂); ¹³C-NMR (126 MHz, CDCl₃) $\delta_{\text{C}}/\text{ppm}$ 150.3 (6-C), 147.7 (2-CH), 142.4 (C), 136.0 (8-CH), 131.2 (4-CH), 128.9 (C), 123.4 (3-CH), 120.2 (7-CH), 116.1 (CN), 86.9 (5-C).

3.3.6. 3-Amino-1-(3-bromophenyl)-1H-pyrazole (**21**)

A solution of 3-bromophenyl hydrazine hydrochloride (1.36 g, 6.00 mmol), 3-methoxyacrylonitrile (1.0 mL, 12.0 mmol) and NaOEt (1.77 g, 26.0 mmol) in dry EtOH (30 mL) was heated at reflux for 20 h. After cooling the mixture to room temperature, water was added and the resultant precipitate was filtered, washed with water and finally dissolved in CH₂Cl₂. The organic extract was washed successively with water and brine, dried (MgSO₄) and evaporated *in vacuo* to give the *title compound* (1.29 g, 90%) as a yellow solid, with identical physical and spectroscopic properties to literature data [54].

3.3.7. 3-Amino-1-[3-(1H-indol-6-yl)phenyl]-1H-pyrazole (**23**)

A mixture of 3-amino-1-(3-bromophenyl)-1H-pyrazole (**21**) (0.20 g, 0.84 mmol), 6-indolylboronic acid (**22**) (0.13 g, 0.25 mmol), caesium carbonate (0.55 g, 1.68 mmol) and Pd(PPh₃)₄ (0.10 g, 0.08 mmol) in DMF (4 mL) was irradiated at 150 °C for 2 h in a sealed pressure-rated glass tube (10 mL) using

a CEM Discover microwave synthesizer by moderating the initial power (150 W). The mixture was cooled by passing a stream of compressed air through the microwave cavity and water was added (10 mL). The aqueous layer was extracted with EtOAc (3×20 mL) and the organic extracts were combined, washed with brine, dried (MgSO_4) and evaporated *in vacuo*. Purification by column chromatography on silica gel, eluting with hexane–EtOAc (1:1 v/v) gave the *title compound* [53] (0.19 g, 84%) as a colorless solid, mp 97–99 °C (Found: M^{+} , 274.1218. $\text{C}_{17}\text{H}_{14}\text{N}_2$ [M] requires 274.1222); IR (KBr) $\nu_{\text{max}}/\text{cm}^{-1}$ 3411 (NH), 2922 (CH), 1626, 1604, 1586, 1479; ^1H -NMR (400 MHz; d_6 -DMSO) $\delta_{\text{H}}/\text{ppm}$ 11.18 (1H, s, exch. D_2O , NH), 8.26 (1H, d, J 2.6, H-5), 7.96 (1H, m, H-2'), 7.69 (1H, m, H-7''), 7.63 (1H, d, J 8.3, H-6'), 7.58 (1H, m, H-5'), 7.46–7.41 (3H, H-4', H-2'' and H-4''), 7.35 (1H, dd, J 8.3, 1.6, H-4''), 6.47 (1H, m, H-3''), 5.76 (1H, d, J 2.6, H-4), 5.17 (2H, s, exch. D_2O , NH_2); ^{13}C -NMR (100 MHz, d_6 -DMSO) $\delta_{\text{C}}/\text{ppm}$ 157.5 (C), 134.3 (C), 141.0 (C), 137.0 (C), 133.5 (C), 130.2 (C), 128.5 (CH), 127.9 (CH), 126.8 (CH), 122.7 (CH), 120.9 (CH), 118.8 (CH), 115.2 (CH), 114.9 (CH), 110.0 (CH), 101.5 (CH), 96.7 (CH); m/z (EI) 275 (MH^{+} , 100%), 274 (M^{+} , 100), 273 (19), 246 (7), 205 (6), 191 (9), 133 (14), 84 (21).

3.3.8. 3-Amino-4-bromo-1-(3-bromophenyl)-1H-pyrazole (25)

A solution of 3-amino-1-(3-bromophenyl)-1H-pyrazole (**21**) (0.16 g, 0.68 mmol) and NBS (0.120 g, 0.68 mmol) in THF (10 mL) was stirred at room temperature for 16 h and then the solvent was vaporated *in vacuo*. The residue was dissolved in EtOAc, filtered through Celite and evaporated *in vacuo*. Purification by column chromatography on silica gel, eluting with hexane–EtOAc (3:1 v/v), gave the *title compound* (0.18 g, 83%) as a brown solid, mp 93–95 °C (Found: M^{+} , 314.9005. $\text{C}_9\text{H}_7^{79}\text{Br}_2\text{N}_3$ [M] requires 314.9007); IR (KBr) $\nu_{\text{max}}/\text{cm}^{-1}$ 3415, 3312, 3213, 1629, 1594, 1556; ^1H -NMR (400 MHz; d_6 -DMSO) $\delta_{\text{H}}/\text{ppm}$ 8.55 (1H, s, H-5), 7.88 (1H, m, H-2'), 7.67 (1H, m, H-5'), 7.37–7.35 (2H, m, H-4' and H-6'), 5.38 (2H, s, exch. D_2O , NH_2); ^{13}C -NMR (100 MHz, d_6 -DMSO) $\delta_{\text{C}}/\text{ppm}$ 159.9 (C), 142.5 (C), 131.8 (CH), 128.6 (CH), 127.5 (CH), 122.7 (C), 119.3 (CH), 115.1 (CH), 85.2 (C); m/z (EI) 275 (MH^{+} , 100%); 319 ($\text{C}_9\text{H}_7^{81}\text{Br}_2\text{N}_3^{++}$, 61) 317 ($\text{C}_9\text{H}_7^{81}\text{Br}^{79}\text{BrN}_3^{++}$, 30), 315 ($\text{C}_9\text{H}_7^{79}\text{Br}_2\text{N}_3^{++}$, 17), 220 (42), 205 (100), 189 (8), 177 (14), 145 (15), 105 (12).

3.3.9. 3-Amino-1-(4-methoxyphenyl)-1H-pyrazole (28)

The *title compound* was prepared as a yellow solid, exactly in accordance with our previously published microwave-assisted procedure [54].

3.3.10. 3-Amino-4-bromo-1-(4-methoxyphenyl)-1H-pyrazole (29)

A solution of 3-amino-1-(4-methoxyphenyl)-1H-pyrazole (**28**) (0.13 g, 0.68 mmol) and NBS (0.12 g, 0.68 mmol) in THF (4 mL) was irradiated at 150 °C for 2 h in a sealed pressure-rated glass tube (10 mL) using a CEM Discover microwave synthesizer by moderating the initial power (150 W). The mixture was cooled by passing a stream of compressed air through the microwave cavity and evaporated *in vacuo*. The residue was dissolved in EtOAc, filtered through Celite and the solvent was evaporated *in vacuo*. Purification by column chromatography on silica gel, eluting with hexane–EtOAc (3:1 v/v), gave the *title compound* (0.14 g, 77%) as a brown solid, mp 93–96 °C (Found: M^{+} ,

267.0015. $C_{10}H_{10}^{79}BrN_3O$ [M] requires 267.0007) IR (KBr) ν_{max}/cm^{-1} 3353 (NH), 1548, 1516, 1403, 1245, 1084, 1041; 1H -NMR (400 MHz; d_6 -DMSO) δ_H/ppm 8.34 (1H, s, H-5), 7.57 (2H, d, J 9.0, H-2' and H-6'), 6.98 (2H, d, J 9.0, H-3' and H-5'), 5.15 (2H, s, exch. D_2O , NH_2), 3.76 (3H, s, OMe); ^{13}C -NMR (100 MHz, d_6 -DMSO) δ_C/ppm 157.0 (C), 155.5 (C), 134.2 (C), 127.8 (CH), 118.5 (CH), 114.9 (CH), 95.3 (C), 55.8 (Me); m/z (EI) 269 ($C_{10}H_{10}^{81}BrN_3O^+$, 97), 267 ($C_{10}H_{10}^{79}BrN_3O^+$, 100).

3.3.11. 3-Amino-4-(4-aminocarbonylphenyl)-1-(4-methoxyphenyl)-1H-pyrazole (26)

A mixture of 3-amino-4-bromo-1-(4-methoxyphenyl)-1H-pyrazole (**29**) (0.15 g, 0.55 mmol), 4-carbamoylphenylboronic acid (**30**) (90 mg, 0.54 mmol), K_2CO_3 (0.20 g, 1.44 mmol) and $PdCl_2(PPh_3)_2$ (40 mg, 0.05 mmol) in $iPrOH-H_2O$ (1:1 v/v) (5 mL) was irradiated at 150 °C for 2 h in a sealed pressure-rated glass tube (10 mL) using a CEM Discover microwave synthesizer by moderating the initial power (150 W). The mixture was cooled by passing a stream of compressed air through the microwave cavity and water was added (10 mL). The aqueous layer was extracted with EtOAc (2 × 20 mL) and the organic extracts were combined, washed with brine, dried ($MgSO_4$) and evaporated *in vacuo*. Purification by column chromatography on silica gel, eluting with hexane–EtOAc (1:3 v/v), gave the *title compound* (90 mg, 54%) as a cream solid, mp 251–253 °C (Found: M^+ , 308.1281. $C_{17}H_{16}N_4O_2$ [M] requires 308.1273); IR (KBr) ν_{max}/cm^{-1} 3389 (NH), 1653 (C=O), 1554, 1522, 1399, 1106; 1H -NMR (400 MHz; d_6 -DMSO) δ_H/ppm 8.59 (1H, s, H-5), 7.96 (1H, br s, exch. D_2O , NHH), 7.90 (2H, d, J 8.4, H-2' and H-6'), 7.69 (2H, d, J 7.6, H-3" and H-5"), 7.67 (2H, d, J 7.6, H-2" and H-6"), 7.31 (1H, br s, exch. D_2O , NHH), 7.02 (2H, d, J 8.4, H-3' and H-5'), 5.18 (2H, s, exch. D_2O , NH_2), 3.51 (3H, s, OMe); ^{13}C -NMR (100 MHz, d_6 -DMSO) δ_C/ppm 168.2 (C), 158.3 (C), 155.5 (C), 135.1 (C), 133.6 (C), 132.1 (C), 128.9 (CH), 126.5 (CH), 125.5 (CH), 119.5 (CH), 116.7 (CH), 56.0 (Me); m/z (EI) 308 (M^+ , 100).

3.4. Biological Procedures

Werner syndrome fibroblast strains AG03141F, AG05229C and AG05229D were obtained from the Coriell Cell Repository (Camden, NJ, USA). All cells were cultured and treated with p38 and MK2 inhibitors and grown to replicative senescence as described previously [45]. The replicative lifespan for inhibitor treated cells is measured as a percentage of the experimental lifespan seen in the respective control (non-inhibitor treated) cells for each cell strain. The results are plotted as mean ± standard deviation. The assay to detect F-actin stress fibres and cellular morphological changes using phalloidin-FITC is exactly as described previously [45].

4. Conclusions

Suzuki-Miyaura cross-coupling reactions have been investigated for the synthesis of three different MK2 inhibitors for study in WS cells. Towards the synthesis of PF-3644022, cross-coupling of a 2-chloroquinoline with a 3-pyridinylboronic acid provided the desired biaryl target but the pyridine moiety and the chloroquinoline precursor both proved incompatible with the subsequent Yamazaki cyanation of a 6-nitroquinoline, en route to the benzothiophene ring. Thus, although a relatively early-stage Suzuki-Miyaura coupling would appear incompatible with this cyanation method,

alternative strategies for the incorporation of the 3-aminobenzo[*b*]thiophene moiety could be envisaged and thus incorporated with this transformation [58]. Towards the synthesis of a 3-aminopyrazole MK2 inhibitor, bearing a 1-[(6-indolyl)phenyl] substituent, the Suzuki-Miyaura cross-coupling reaction established one biaryl linkage, but the unprotected indole group interfered with the subsequent NBS bromination required to set up the second Suzuki-Miyaura coupling. Use of a simpler 3-aminopyrazole circumvented this problem and provided an MK2 inhibitor for study in WS cells. In all cases with simple aryl bromides, the Suzuki-Miyaura cross-coupling reactions were reliable and relatively efficient. The synthesis of the 3-amino-1-(4-methoxyphenyl)pyrazole MK2 inhibitor proceeded in three steps and 35% overall yield from commercially-available materials, each step complete in 2 h under microwave irradiation. This constitutes an extremely rapid method for access to this chemical tool, of value in elucidating the role of MK2 in accelerated aging in this progeroid syndrome. Although MK2 inhibitors may not be as useful therapeutically as p38 inhibitors, if the accelerated cell aging seen in WS does underlie the accelerated whole body aging, they may prove useful in the alleviation of the associated inflammatory conditions that are thought to be MK2 dependent and have certainly helped to suggest a role for p38-activated MK2 in replicative senescence in WS fibroblasts.

Acknowledgments

We thank the EPSRC-BBSRC-MRC sponsored network SMS-Drug (EP/I037229/1; award to MCB), Saudi Cultural Bureau (support for MB), BBSRC (BB/D524140/1; award to DK, MCB and TD), SPARC (awards to MCB and TD), ESRC under the New Dynamics of Ageing Initiative (RES-356-25-0024; award to MCB, DK and TD), EPSRC (studentship award to JD) and the R M Phillips Trust (award to MCB) for support of this work and the EPSRC Mass Spectrometry Service at the University of Wales, Swansea UK for high-resolution mass spectra.

Author Contributions

MCB participated in study design and coordination, synthesis of MK2 inhibitors, manuscript preparation and helped conceive the study, TD participated in study design, manuscript preparation, growth experiments and phalloidin assays, and helped conceive the study, DK conceived the study, participated in its design and coordination and helped to draft the manuscript, MB and IC participated in the synthesis of MK2 inhibitors and JED participated in the synthesis of MK2 inhibitors and manuscript preparation. All authors read and approved the final manuscript.

Conflicts of Interest

The authors declare no conflict of interest.

References

1. Martin, G.M.; Oshima, J.; Gray, M.D.; Poot, M. What geriatricians should know about the werner syndrome. *J. Am. Geriatr. Soc.* **1999**, *47*, 1136–1144.
2. Kipling, D.; Davis, T.; Ostler, E.L.; Faragher, R.G. What can progeroid syndromes tell us about human aging? *Science* **2004**, *305*, 1426–1431.

3. Werner, O. On Cataract Associated in Conjunction with Scleroderma. Ph.D. Thesis, Kiel University, Schmidt and Klaunig, Kiel, Germany, 1904.
4. Thannhauser, S.J. Werner's syndrome (progeria of the adult) and rothmund's syndrome: Two types of closely related heredofamilial atrophic dermatosis with juvenile cataracts and endocrine features. A critical study of five new cases. *Ann. Int. Med.* **1945**, *23*, 559–625.
5. Davis, T.; Kipling, D. Werner syndrome as an example of inflamm-aging: Possible therapeutic opportunities for a progeroid syndrome? *Rejuvenation Res.* **2006**, *9*, 402–407.
6. Yokote, K.; Hara, K.; Mori, S.; Kadowaki, T.; Saito, Y.; Goto, M. Dysadipocytokinemia in werner syndrome and its recovery by treatment with pioglitazone. *Diabetes Care* **2004**, *27*, 2562–2563.
7. Franceschi, C.; Bonafe, M.; Valensin, S.; Olivieri, F.; De Luca, M.; Ottaviani, E.; de Benedictis, G. Inflamm-aging. An evolutionary perspective on immunosenescence. *Ann. N. Y. Acad. Sci.* **2000**, *908*, 244–254.
8. Vasto, S.; Candore, G.; Balistreri, C.R.; Caruso, M.; Colonna-Romano, G.; Grimaldi, M.P.; Listi, F.; Nuzzo, D.; Lio, D.; Caruso, C. Inflammatory networks in ageing, age-related diseases and longevity. *Mech. Ageing Dev.* **2007**, *128*, 83–91.
9. Rodriguez-Lopez, A.M.; Jackson, D.A.; Iborra, F.; Cox, L.S. Asymmetry of DNA replication fork progression in Werner's syndrome. *Aging Cell* **2002**, *1*, 30–39.
10. Meyn, M.S. Chromosome instability syndromes: Lessons for carcinogenesis. *Curr. Top. Microbiol. Immunol.* **1997**, *221*, 71–148.
11. Pagano, G.; Zatterale, A.; Degan, P.; d'Ischia, M.; Kelly, F.J.; Pallardo, F.V.; Kodama, S. Multiple involvement of oxidative stress in werner syndrome phenotype. *Biogerontology* **2005**, *6*, 233–243.
12. Davis, T.; Baird, D.M.; Haughton, M.F.; Jones, C.J.; Kipling, D. Prevention of accelerated cell aging in werner syndrome using a p38 mitogen-activated protein kinase inhibitor. *J. Gerontol. A Biol. Sci. Med. Sci.* **2005**, *60*, 1386–1393.
13. Huot, J.; Houle, F.; Marceau, F.; Landry, J. Oxidative stress-induced actin reorganization mediated by the p38 mitogen-activated protein kinase/heat shock protein 27 pathway in vascular endothelial cells. *Circ. Res.* **1997**, *80*, 383–392.
14. Kim, G.Y.; Mercer, S.E.; Ewton, D.Z.; Yan, Z.; Jin, K.; Friedman, E. The stress-activated protein kinases p38 alpha and JNK1 stabilize p21(cip1) by phosphorylation. *J. Biol. Chem.* **2002**, *277*, 29792–29802.
15. Wang, W.; Chen, J.X.; Liao, R.; Deng, Q.; Zhou, J.J.; Huang, S.; Sun, P. Sequential activation of the MEK-extracellular signal-regulated kinase and MKK3/6-p38 mitogen-activated protein kinase pathways mediates oncogenic ras-induced premature senescence. *Mol. Cell. Biol.* **2002**, *22*, 3389–3403.
16. Bagley, M.C.; Davis, T.; Murziani, P.G.S.; Widdowson, C.S.; Kipling, D. Use of p38 MAPK inhibitors for the treatment of werner syndrome. *Pharmaceuticals* **2010**, *3*, 1842–1872.
17. Davis, T.; Haughton, M.F.; Jones, C.J.; Kipling, D. Prevention of accelerated cell aging in the werner syndrome. *Ann. N. Y. Acad. Sci.* **2006**, *1067*, 243–247.
18. Davis, T.; Bachler, M.A.; Wyllie, F.S.; Bagley, M.C.; Kipling, D. Evaluating the role of p38 map kinase in growth of werner syndrome fibroblasts. *Ann. N. Y. Acad. Sci.* **2010**, *1197*, 45–48.

19. Bagley, M.C.; Davis, T.; Dix, M.C.; Rokicki, M.J.; Kipling, D. Rapid synthesis of VX-745: p38 map kinase inhibition in werner syndrome cells. *Bioorg. Med. Chem. Lett.* **2007**, *17*, 5107–5110.
20. Bagley, M.C.; Davis, T.; Dix, M.C.; Fusillo, V.; Pigeaux, M.; Rokicki, M.J.; Kipling, D. Microwave-assisted ullmann C-S bond formation: Synthesis of the p38alpha MAPK clinical candidate VX-745. *J. Org. Chem.* **2009**, *74*, 8336–8342.
21. Bagley, M.C.; Davis, T.; Dix, M.C.; Fusillo, V.; Pigeaux, M.; Rokicki, M.J.; Kipling, D. Gramme-scale synthesis of the p38 α MAPK inhibitor VX-745 for pre-clinical studies into werner syndrome. *Future Med. Chem.* **2010**, *2*, 1417–1427.
22. Bagley, M.C.; Davis, T.; Dix, M.C.; Murziani, P.G.; Rokicki, M.J.; Kipling, D. Microwave-assisted synthesis of 5-aminopyrazol-4-yl ketones and the p38(MAPK) inhibitor RO3201195 for study in werner syndrome cells. *Bioorg. Med. Chem. Lett.* **2008**, *18*, 3745–3748.
23. Bagley, M.C.; Davis, T.; Dix, M.C.; Murziani, P.G.; Rokicki, M.J.; Kipling, D. Microwave-assisted synthesis of a pyrazolyl ketone library for evaluation as p38 MAPK inhibitors in werner syndrome cells. *Future Med. Chem.* **2010**, *2*, 203–213.
24. Bagley, M.C.; Davis, T.; Rokicki, M.J.; Widdowson, C.S.; kipling, D. Synthesis of the highly selective p38 MAPK inhibitor UR-13756 for possible therapeutic use in werner syndrome. *Future Med. Chem.* **2010**, *2*, 193–201.
25. Bagley, M.C.; Davis, T.; Dix, M.C.; Widdowson, C.S.; Kipling, D. Microwave-assisted synthesis of N-pyrazole ureas and the p38alpha inhibitor BIRB 796 for study into accelerated cell ageing. *Org. Biomol. Chem.* **2006**, *4*, 4158–4164.
26. Davis, T.; Wyllie, F.S.; Rokicki, M.J.; Bagley, M.C.; Kipling, D. The role of cellular senescence in werner syndrome: Toward therapeutic intervention in human premature aging. *Ann. N. Y. Acad. Sci.* **2007**, *1100*, 455–469.
27. Genovese, M.C. Inhibition of p38: Has the fat lady sung? *Arthritis Rheum.* **2009**, *60*, 317–320.
28. Bagley, M.C.; Baashen, M.; Dwyer, J.; Milbeo, P.; Kipling, D.; Davis, T. Microwave-assisted synthesis of inhibitors of MK2 for targeting p38 map kinase signalling in werner syndrome cells. In *Microwaves in Drug Discovery and Development: Recent Advances*; Spencer, J., Bagley, M., Eds.; Future Sci Ltd.: London, UK, 2014; pp. 86–104.
29. Dean, J.L.; Sully, G.; Clark, A.R.; Saklatvala, J. The involvement of AU-rich element-binding proteins in p38 mitogen-activated protein kinase pathway-mediated mrna stabilisation. *Cell Signal.* **2004**, *16*, 1113–1121.
30. Manke, I.A.; Nguyen, A.; Lim, D.; Stewart, M.Q.; Elia, A.E.; Yaffe, M.B. Mapkap kinase-2 is a cell cycle checkpoint kinase that regulates the G2/M transition and S phase progression in response to UV irradiation. *Mol. Cell* **2005**, *17*, 37–48.
31. Hegen, M.; Gaestel, M.; Nickerson-Nutter, C.L.; Lin, L.L.; Telliez, J.B. MAPKAP kinase 2-deficient mice are resistant to collagen-induced arthritis. *J. Immunol.* **2006**, *177*, 1913–1917.
32. Ronkina, N.; Kotlyarov, A.; Gaestel, M. MK2 and MK3—A pair of isoenzymes? *Front. Biosci.* **2008**, *13*, 5511–5521.
33. Duraisamy, S.; Bajpai, M.; Bughani, U.; Dastidar, S.G.; Ray, A.; Chopra, P. MK2: A novel molecular target for anti-inflammatory therapy. *Expert Opin. Ther. Targets* **2008**, *12*, 921–936.
34. Schlappbach, A.; Huppertz, C. Low-molecular-weight MK2 inhibitors: A tough nut to crack! *Future Med. Chem.* **2009**, *1*, 1243–1257.

35. Anderson, D.R.; Meyers, M.J.; Vernier, W.F.; Mahoney, M.W.; Kurumbail, R.G.; Caspers, N.; Poda, G.I.; Schindler, J.F.; Reitz, D.B.; Mourey, R.J. Pyrrolopyridine inhibitors of mitogen-activated protein kinase-activated protein kinase 2 (MK-2). *J. Med. Chem.* **2007**, *50*, 2647–2654.
36. Goldberg, D.R.; Choi, Y.; Cogan, D.; Corson, M.; DeLeon, R.; Gao, A.; Gruenbaum, L.; Hao, M.H.; Joseph, D.; Kashem, M.A.; *et al.* Pyrazinoindolone inhibitors of MAPKAP-K2. *Bioorg. Med. Chem. Lett.* **2008**, *18*, 938–941.
37. Mourey, R.J.; Burnette, B.L.; Brustkern, S.J.; Daniels, J.S.; Hirsch, J.L.; Hood, W.F.; Meyers, M.J.; Mnich, S.J.; Pierce, B.S.; Saabye, M.J.; *et al.* A benzothiophene inhibitor of mitogen-activated protein kinase-activated protein kinase 2 inhibits tumor necrosis factor alpha production and has oral anti-inflammatory efficacy in acute and chronic models of inflammation. *J. Pharmacol. Exp. Ther.* **2010**, *333*, 797–807.
38. Xiao, D.; Palani, A.; Huang, X.; Sofolarides, M.; Zhou, W.; Chen, X.; Aslanian, R.; Guo, Z.; Fossetta, J.; Tian, F.; *et al.* Conformation constraint of anilides enabling the discovery of tricyclic lactams as potent MK2 non-ATP competitive inhibitors. *Bioorg. Med. Chem. Lett.* **2013**, *23*, 3262–3266.
39. Daniels, J.S.; Lai, Y.; South, S.; Chiang, P.C.; Walker, D.; Feng, B.; Mireles, R.; Whiteley, L.O.; McKenzie, J.W.; Stevens, J.; *et al.* Inhibition of hepatobiliary transporters by a novel kinase inhibitor contributes to hepatotoxicity in beagle dogs. *Drug Metab. Lett.* **2013**, *7*, 15–22.
40. Miyaura, N.; Lahiri, K.; Suzuki, A. A new stereospecific cross-coupling by the palladium catalyzed reaction of 1-alkenylboranes with 1-alkenyl or 1-alkynyl halides. *Tetrahedron Lett.* **1979**, *36*, 3437–3440.
41. Kotha, S.; Lahiri, K.; Kashinath, D. Recent applications of the suzuki-miyaura cross-coupling reaction in organic synthesis. *Tetrahedron* **2002**, *58*, 9633–9695.
42. Suzuki, A. Recent advances in the cross-coupling reactions of organoboron derivatives with organic electrophiles 1995–1998. *J. Organomet. Chem.* **1999**, *576*, 147–168.
43. Roughley, S.D.; Jordan, A.M. The medicinal chemist's toolbox: An analysis of reactions used in the pursuit of drug candidates. *J. Med. Chem.* **2011**, *54*, 3451–3479.
44. Mavandadi, F.; Pilotti, Å. The impact of microwave-assisted organic synthesis in drug discovery. *Drug Discov. Today* **2006**, *11*, 165–174.
45. Davis, T.; Rokicki, M.J.; Bagley, M.C.; Kipling, D. The effect of small-molecule inhibition of MAPKAPK2 on cell ageing phenotypes of fibroblasts from human werner syndrome. *Chem. Cent. J.* **2013**, *7*, 18.
46. Davis, T.; Bagley, M.C.; Dix, M.C.; Murziani, P.G.; Rokicki, M.J.; Widdowson, C.S.; Zayed, J.M.; Bachler, M.A.; Kipling, D. Synthesis and *in vivo* activity of MK2 and MK2 substrate-selective p38 α (MAPK) inhibitors in werner syndrome cells. *Bioorg. Med. Chem. Lett.* **2007**, *17*, 6832–6835.
47. Davidson, W.; Frego, L.; Peet, G.W.; Kroe, R.R.; Labadia, M.E.; Lukas, S.M.; Snow, R.J.; Jakes, S.; Grygon, C.A.; Pargellis, C.; *et al.* Discovery and characterization of a substrate selective p38 α inhibitor. *Biochemistry* **2004**, *43*, 11658–11671.
48. Anderson, D.R.; Hegde, S.; Reinhard, E.; Gomez, L.; Vernier, W.F.; Lee, L.; Liu, S.; Sambandam, A.; Snider, P.A.; Masih, L. Aminocyanopyridine inhibitors of mitogen activated protein kinase-activated protein kinase 2 (MK-2). *Bioorg. Med. Chem. Lett.* **2005**, *15*, 1587–1590.

49. Anderson, D.R.; Meyers, M.J.; Kurumbail, R.G.; Caspers, N.; Poda, G.I.; Long, S.A.; Pierce, B.S.; Mahoney, M.W.; Mourey, R.J. Benzothiophene inhibitors of MK2. Part 1: Structure-activity relationships, assessments of selectivity and cellular potency. *Bioorg. Med. Chem. Lett.* **2009**, *19*, 4878–4881.
50. Anderson, D.R.; Meyers, M.J.; Kurumbail, R.G.; Caspers, N.; Poda, G.I.; Long, S.A.; Pierce, B.S.; Mahoney, M.W.; Mourey, R.J.; Parikh, M.D. Benzothiophene inhibitors of MK2. Part 2: Improvements in kinase selectivity and cell potency. *Bioorg. Med. Chem. Lett.* **2009**, *19*, 4882–4884.
51. Lee, B.S.; Lee, B.C.; Jun, J.-G.; Chi, D.Y. A new efficient synthesis of 6-nitroquipazine. *Heterocycles* **1998**, *48*, 2637–2641.
52. Tomioka, Y.; Ohkubo, K.; Yamazaki, M. Studies on aromatic nitro compounds V. A simple one-pot preparation of *o*-aminoarylnitriles from some aromatic nitro compounds. *Chem. Pharm. Bull.* **1985**, *33*, 1360–1366.
53. Velcicky, J.; Feifel, R.; Hawtin, S.; Heng, R.; Huppertz, C.; Koch, G.; Kroemer, M.; Moebitz, H.; Revesz, L.; Scheufler, C.; *et al.* Novel 3-aminopyrazole inhibitors of MK-2 discovered by scaffold hopping strategy. *Bioorg. Med. Chem. Lett.* **2010**, *20*, 1293–1297.
54. Bagley, M.C.; Baashen, M.; Paddock, V.L.; Kipling, D.; Davis, T. Microwave-assisted synthesis of 3- and 5-aminopyrazole, pyrazolo[3,4-d]pyrimidine, pyrazolo[3,4-b]pyridine and pyrazolo[3,4-b]quinolin-4-one scaffolds for mapk inhibition. *Tetrahedron* **2013**, *68*, 8429–8438.
55. Kyriakis, J.M.; Avruch, J. Mammalian mitogen-activated protein kinase signal transduction pathways activated by stress and inflammation. *Physiol. Rev.* **2001**, *81*, 807–869.
56. van Deursen, J.M. The role of senescent cells in ageing. *Nature* **2014**, *509*, 439–446.
57. Tomioka, Y.; Mochiike, A.; Himeno, J.; Yamazaki, M. Studies on aromatic nitro compounds. I. Reaction of 6-nitroquinoline with active methylene compounds in the presence of bases. *Chem. Pharm. Bull.* **1981**, *29*, 1286–1291.
58. Bagley, M.C.; Dwyer, J.E.; Molina, M.D.B.; Rand, A.; Rand, H.L.; Tomkinson, N.C.O. Microwave-assisted synthesis of 3-aminobenzo[*b*]thiophene scaffolds for the preparation of kinase inhibitors. *Org. Biomol. Chem.* **2015**, doi:10.1039/C5OB00819K.



Cite this: *Org. Biomol. Chem.*, 2015, **13**, 6814

Microwave-assisted synthesis of 3-aminobenzo[*b*]-thiophene scaffolds for the preparation of kinase inhibitors†

Mark C. Bagley,^{*a} Jessica E. Dwyer,^a Maria D. Beltran Molina,^b Alexander W. Rand,^a Hayley L. Rand^a and Nicholas C. O. Tomkinson^b

Received 23rd April 2015,
Accepted 11th May 2015

DOI: 10.1039/c5ob00819k

www.rsc.org/obc

Microwave irradiation of 2-halobenzonitriles and methyl thioglycolate in the presence of triethylamine in DMSO at 130 °C provides rapid access to 3-aminobenzo[*b*]thiophenes in 58–96% yield. This transformation has been applied in the synthesis of the thieno[2,3-*b*]pyridine core motif of LIMK1 inhibitors, the benzo[4,5]thieno[3,2-*e*][1,4]diazepin-5(2*H*)-one scaffold of MK2 inhibitors and a benzo[4,5]thieno[3,2-*d*]pyrimidin-4-one inhibitor of the PIM kinases.

Introduction

Benzothiophenes are naturally-occurring heterocycles, found in petroleum deposits in their simplest form but also discovered recently as a motif in more complex glycosides isolated from the roots of *E. grijissii*.¹ Benzothiophenes are important components of organic semiconductors due to their potential for elongated and highly delocalised electronic structures.^{2,3} Substituted benzothiophenes have also found application in drug discovery as highly-privileged structures and valuable building blocks in medicinal chemistry, being incorporated into tubulin polymerisation inhibitors,^{4,5} acetyl-CoA carboxylase inhibitors,⁶ antidepressants,⁷ and as estrogen receptor modulators.^{8,9} Benzothiophenes are present in a number of clinical agents, including Raloxifene,¹⁰ a selective estrogen receptor modulator, Zileuton,¹¹ an inhibitor of 5-lipoxygenase and leukotriene biosynthesis used for the treatment of asthma, and the antifungal agent Sertaconazole, which inhibits the synthesis of ergosterol.¹²

Scaffolds based upon 2- or 3-aminobenzo[*b*]thiophenes have enormous potential for further derivatization and have shown great promise in fragment-based drug discovery and in hit identification or lead development, including approaches towards antimetabolic agents^{5,13} and in the development of inhibitors of kinase targets, such as the LIMK protein family,¹⁴ PIM-kinases¹⁵ and MAPK-2 kinase (MK2) (Fig. 1).^{16,17} A number of 3-aminothieno[2,3-*b*]pyridine-2-carboxamide hits,

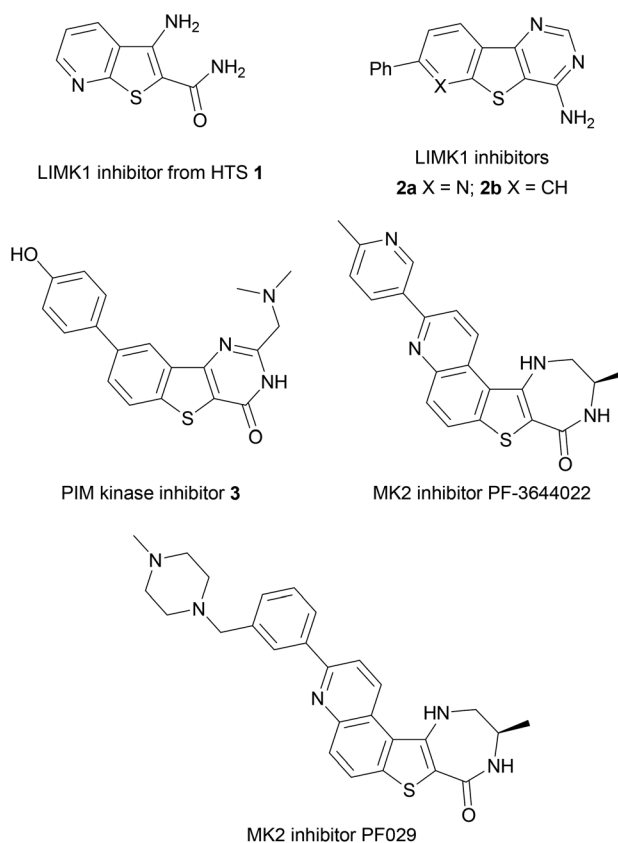


Fig. 1 Aminobenzothiophene scaffolds in drug discovery.

^aDepartment of Chemistry, School of Life Sciences, University of Sussex, Falmer, Brighton, East Sussex, BN1 9QJ, UK. E-mail: m.c.bagley@sussex.ac.uk

^bWestCHEM, Department of Pure and Applied Chemistry, University of Strathclyde, Glasgow, G1 1XL, UK

†Electronic supplementary information (ESI) available. See DOI: 10.1039/c5ob00819k

such as **1**, were identified from high throughput screening (HTS) as inhibitors of LIMK1, leading to the development of tricyclic derivatives such as **2a** and the benzothieno[3,2-*d*]pyri-

midine **2b** as a LIMK1 inhibitor lead candidate, to disrupt actin polymerisation and thus prevent the metastatic potential of tumour cells where LIMK is over-expressed.¹⁴

Benzothienopyrimidinones have been investigated as PIM kinase inhibitors.¹⁵ The PIM kinases (PIM1, PIM2 and PIM3) have been implicated in tumourigenesis and simultaneous targeting of all three isoforms has presented itself as a promising approach in cancer therapy, with PIM triple knockout mice found to be viable and fertile.¹⁸ The benzothiophene scaffold was again identified from an initial HTS hit,¹⁵ leading to the development of a range of potent and selective benzo[*b*]thiophene-derived inhibitors such as **3** with nM activity (K_i values of 2, 3 and 0.5 nM against PIM1, PIM2 and PIM3, respectively) with oral bioavailability in mouse models.

Examples of aminobenzothiophene derivatives are also found amongst inhibitors of the mitogen activated protein kinase (MAPK) family of enzymes. These enzymes are essential for inflammatory cell signalling events and contain historically popular drug targets for inflammatory diseases, including rheumatoid arthritis and Crohn's disease because of their involvement in the production of pro-inflammatory cytokines,¹⁹ as well as being implicated in accelerated cellular ageing in Werner syndrome (WS) *via* p38.^{20–23} MAPK-activated protein kinase (MK2) is a rate-limiting kinase downstream of p38 in the MAPK pathway and has been the subject of many studies in recent years,²⁴ as MK2 knock-out mice possess normal healthy phenotypes whereas p38 knock-out mice are lethal.²⁵ The aminobenzo[*b*]thiophene derivative PF-3644022 shows excellent kinase selectivity for MK2, *in vivo* potency on a nanomolar scale and projected ADME characteristics that suggested it was suitable for oral human dosing.^{17,26,27} However, PF-3644022 was found to result in hepatotoxicity in dogs²⁷ and so the analogue PF029 was developed and exhibited an improved toxicological profile with no loss of cellular potency. This was rationalized through installation of a metabolic shunt onto the reactive diazepinone ring and extension of the biaryl ring section to increase the compound's cationic character, thus reducing its molecular affinity for transporter proteins.

As part of our interest in the synthesis of MAPK inhibitors for the study of cellular ageing in Werner syndrome,^{20,28–33} the benzothiophene scaffold, and its selectivity and cellular activity profile for MK2 exemplified by PF-3644022, made it an attractive target for synthesis. We have shown that treating young WS cell cultures with p38 MAPK inhibitors can bring about a complete reversal of the ageing phenotype, giving increased replicative life-span, growth rates comparable to normal young cells and a reduction in levels of F-actin stress fibres.^{20,23} These findings suggested that WS could be amenable to therapeutic intervention, but with high toxicity and poor kinase selectivity exhibited *in vivo* by many p38 inhibitors,^{34–36} an inhibitor scaffold that targeted the downstream kinase MK2 would offer a promising alternative target.^{20,37}

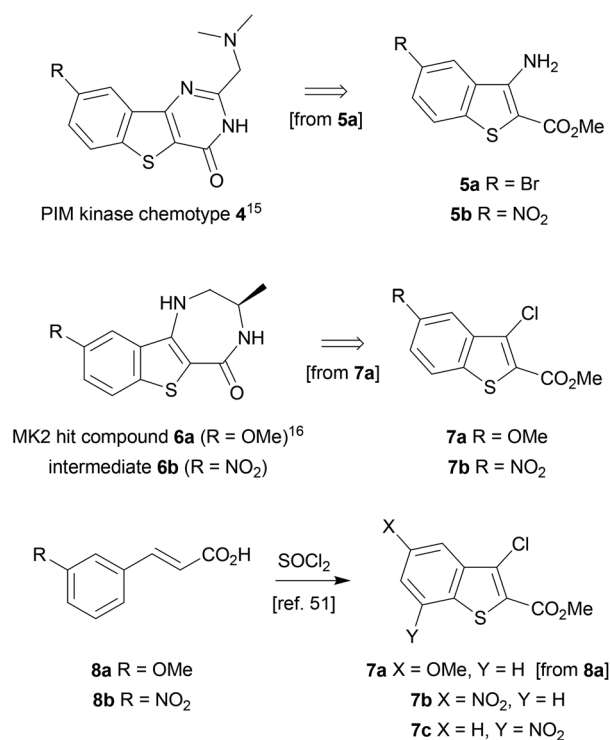
With such a range of biological properties, there is a continuing interest in the search for new methods to access substituted benzothiophenes.³⁸ One approach, with the potential to incorporate diversity into a target library, would be to employ

transition metal-mediated processes from the corresponding 3-halobenzo[*b*]thiophenes.³⁹ However, methods for the synthesis of 3-halobenzo[*b*]thiophenes are currently fairly limited. In particular, routes can be problematic when using ring halogenation due to the low reactivity of the heteroaryl unit and its functional group compatibility.^{40–43} The 5-*endo-dig* halocyclisation of *ortho*-alkynylaryl thiophenol derivatives offers an alternative approach,^{44–48} but this requires installation of an alkyne by metal-catalyzed cross-coupling followed by cyclisation, mediated by a halogen-containing electrophile, so can exhibit a number of inherent disadvantages.

Herein, we present an annulation-based method for the rapid preparation of 3-halo and 3-amino-2-substituted benzo[*b*]thiophenes suitable for elaboration to a range of kinase inhibitors.⁴⁹ It employs microwave irradiation as a convenient platform for fast reaction kinetics, and to improve reaction efficiency, and avoids the need for metal-catalyzed processes to establish the parent heterocycle. This method is shown to be suitable to access the pharmacophore of a range of biologically-active scaffolds for application in medicinal chemistry and drug discovery.

Results and discussion

The benzothiophene-containing chemotypes appearing in recent drug discovery programmes (Fig. 1) feature, or could in principle be derived from, electron-poor aminobenzothiophene intermediates or their 7-aza analogues (Scheme 1). For



Scheme 1 Benzothiophene precursors to kinase inhibitors.

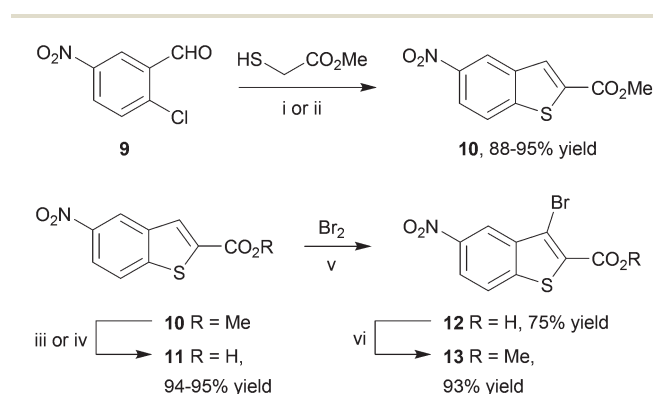
example, the PIM kinase inhibitor scaffold **4** has been accessed from 5-bromobenzothiophene **5a**, using the halogen as a handle for library diversification in a late-stage Suzuki coupling.¹⁵ Similarly, it could be hypothesized that inhibitors of MK2 for study in WS cells, such as PF-3644022 (Fig. 1), could be prepared from the same core motif **5**, using 5-nitrobenzothiophene **5b**, rather than by the functionalization of 6-nitroquinoline as reported by Anderson *et al.*¹⁷ This approach would enable the synthesis of a range of diverse chemical tools from a single common template. The original route to MK2 hit compound **6a**, prior to the development of PF-3644022,¹⁶ employed cinnamic acid **8a** in reaction with thionyl chloride in chlorobenzene at 120 °C to establish the 3-chlorobenzothiophene scaffold **7a** (Scheme 1).⁵⁰ Unfortunately this route would be wholly inappropriate for the synthesis of benzothiophene **7b** for elaboration to the desired intermediate **6b** on route to PF-3644022, as altering the substituent-directing effects to a nitro group results in poor yields and inseparable mixtures of **7b** and **7c** in the benzothiophene synthesis, as well as giving other side products, as reported by Higa.⁵¹ Hence an alternative route had to be sought.

Our first approach towards scaffold **6b** used an alternative and established method to access 3-halobenzothiophenes by halogenation of the corresponding benzothiophene.⁴⁰ The condensation of methyl thioglycolate with 2-chloro-5-nitrobenzaldehyde (**9**) under basic conditions gave methyl 5-nitrobenzo[*b*]-thiophene-2-carboxylate (**10**) in high yield (Scheme 2). We have shown in previous work how microwave dielectric heating can be used to dramatically reduce reaction times in the synthesis of inhibitor scaffolds.^{30,32,33,37,52} Given that elevated temperature has promoted this,^{53,54} and a closely-related process for the synthesis of 2-acetylbenzothiophenes,⁵⁵ we carried out this transformation under microwave irradiation at 90 °C to give the benzothiophene **10** in good yield, whilst shortening the reaction time from 17 h to 15 min. Selective halogenation at C-3 of **10** was facilitated in a convoluted sequence of reactions *via* the carboxylic acid **11** to overcome poor heterocycle reactivity.⁴⁰ Saponification, again conducted by microwave dielectric

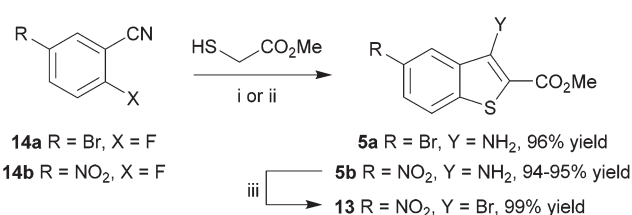
heating, under basic conditions was complete in 3 min at 100 °C and gave the carboxylic acid **11** in excellent yield. Subsequent heating with excess bromine and sodium acetate in glacial acetic acid did give 3-bromobenzothiophene **13** in good yield after esterification using methyl iodide on a number of occasions. However, the bromination was found to be highly variable and efforts to develop an alternative process using microwave heating were constantly frustrated⁵⁶ and so a more reliable and efficient route was sought. The poor yield of this bromination reaction is catalogued in a recent report.⁵⁷

In an alternative approach, our success in the microwave-assisted synthesis of **10** was adapted to incorporate an amino group at C-3, amenable by diazotization chemistry to provide efficient access to 3-bromobenzothiophene **13**. The cyclocondensation of methyl thioglycolate with 2-nitrobenzonitriles under basic conditions has been established by Beck,^{58–60} and adapted methods with halide displacement have also been reported.^{61–64} By switching the base from NaOMe⁶¹ to Et₃N⁶³ and heating either 5-bromo-2-fluorobenzonitrile (**14a**) or 2-fluoro-5-nitrobenzonitrile (**14b**) and methyl thioglycolate gave the corresponding 3-aminobenzothiophene **5a,b** in very high yield (Scheme 3), *e.g.* for **5b** either at 100 °C in DMSO for 2 h using conductive heating (95% yield) or under microwave irradiation at 130 °C for 11 min (94% yield), after simply pouring the reaction mixture into ice-water and collecting the product by filtration. Subsequent deaminative bromination⁶⁰ of aminobenzo[*b*]thiophene **5b** using *tert*-butyl nitrite in acetonitrile in the presence of copper(II) bromide gave the target bromobenzothiophene **13** in excellent yield by this much more direct route.

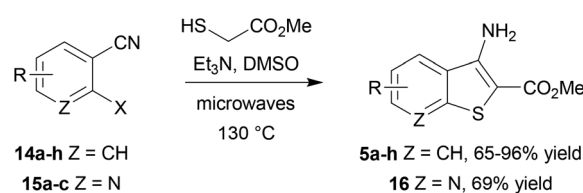
The scope of this method was further explored by investigating a number of substrates (Scheme 4, Table 1), suitable for



Scheme 2 Reagents and conditions: (i) K₂CO₃, DMF, RT, 17 h; (ii) K₂CO₃, DMF, microwaves, 90 °C, 15 min; (iii) NaOH, MeOH–H₂O, reflux, 3 h; (iv) NaOH, MeOH–H₂O, microwaves, 100 °C, 3 min; (v) Br₂, AcOH, NaOAc, 55 °C, 48 h; (vi) MeI, K₂CO₃, DMF, RT, 3 h.



Scheme 3 Reagents and conditions: (i) Et₃N, DMSO, 100 °C, 2 h; H₂O; (ii) Et₃N, DMSO, microwaves, 130 °C, 11 min; H₂O; (iii) *tert*-BuONO, CuBr₂, MeCN, 0 °C; RT, 2 h; HCl (aq.).



Scheme 4 Synthesis of benzothiophenes **5a–h** and 7-aza-**16**.

Table 1 Scope of the microwave-assisted synthesis of 3-amino benzothioophenes **5a–h** (Y = NH₂) and the 7-aza analogue **16**

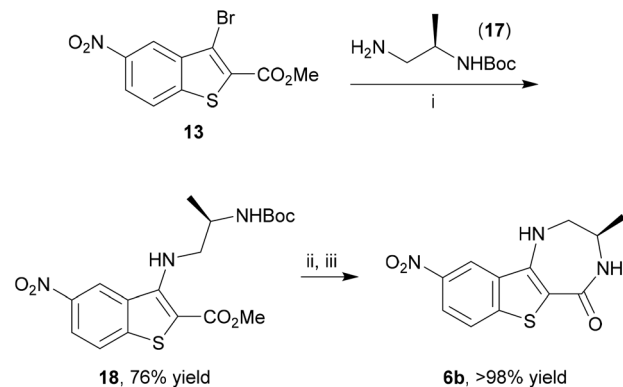
Entry	Substrate	R	X	Z	Time/ min ^a	Product	Yield ^b (%)
1	14a	5-Br	F	CH	11	5a	96
2	14b	5-NO ₂	F	CH	11	5b	94
3	14c	5-Cl	F	CH	11	5c	92
4	14d	4-CF ₃	F	CH	18	5d (R = 6-CF ₃)	80
5	14e	4-NO ₂	F	CH	35	5e (R = 6-NO ₂)	67
6 ^c	14f	5-Ph	F	CH	15	5f	85
7	14g	H	F	CH	15	5g	65
8	14g	H	Br	CH	15	5g	23
9	14g	H	I	CH	15	5g	47
10	14h	5-CF ₃	F	CH	20	5h	88
11	15a	H	F	N	15	16	66
12	15b	H	Cl	N	15	16	69
13	15c	H	Br	N	15	16	51

^a Hold time at the given temperature, as measured by the in-built IR sensor, by modulation of the initial microwave power. ^b Isolated yield of product **5** or **16** after reaction according to Scheme 4, cooling in a stream of compressed air and pouring the reaction mixture into iced water. ^c Product was isolated by aqueous work up, followed by purification by column chromatography on silica gel.

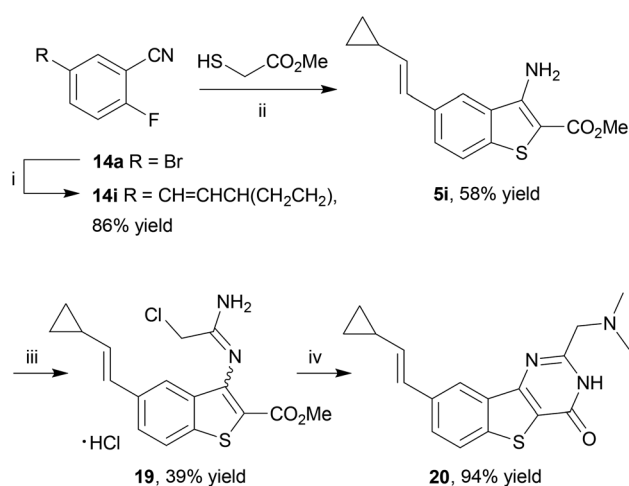
elaboration to a range of benzothioophene-containing scaffolds found in drug discovery (Fig. 1).

It was found that the process was most efficient for highly electron-poor precursors, such as **14a–d** (entries 1–4), and was generally most effective with 2-fluorides, but could also accommodate bromides and iodides albeit with reduced efficiency (Table 1, entries 8 and 9). In most cases a very simple work up procedure was effective, providing benzothioophenes **5a–h** in 65–96% yield in reaction times varying between 11 and 35 min, depending upon substrate. The efficiency compared well to other available methods (*cf.* Table 1, entry 7, with Beck synthesis of **5g**,⁵⁸ 52% yield after 20 h), and so this method was adopted as the route of choice to access the benzothioophene scaffold. Furthermore, it was possible to apply the procedure to the synthesis of 7-azabenzothioophene **16** using 2-halonicotinonitriles **15a–c**. Interestingly, the choice of halogen as substrate did not cause much variation in the yield of azabenzothioophene product **16** (entries 11–13), which represents the core heterocyclic motif of the 3-aminothieno[2,3-*b*]pyridine-2-carboxamide inhibitors¹⁴ of LIMK1.

Having developed this rapid microwave-assisted method to prepare benzothioophenes, the 5-nitro analogue **13** was further elaborated to the benzo[4,5]thieno[3,2-*e*][1,4]diazepin-5(2*H*)-one MK2 inhibitor scaffold **6b**. Buchwald–Hartwig coupling of (*R*)-*tert*-butyl (1-aminopropan-2-yl)carbamate (**17**) and bromobenzothioophene **13** gave a good yield of the *N*-arylated product **18** under microwave irradiation at 150 °C after 75 min (Scheme 5). Subsequent Boc-deprotection using TFA and lactamization by treatment with NaOMe using a modified procedure of Boschelli⁶⁵ under conductive heating gave the MK2 inhibitor scaffold **6b**, bearing suitable functionality for further elaboration, in essentially quantitative yield.

**Scheme 5** Reagents and conditions: (i) Pd(OAc)₂ (5 mol%), Cs₂CO₃, (±)-BINAP (13 mol%), PhMe, microwaves, 150 °C, 75 min; (ii) TFA, CH₂Cl₂, RT, 4.5 h; (iii) NaOMe, MeOH, 50 °C, 2 h; reflux, 2 h; HCl (aq.).

Finally, an application of our microwave-assisted method to access a pre-functionalized benzothioophene **5i** for direct transformation to a benzo[4,5]thieno[3,2-*d*]pyrimidin-4-one scaffold **21** as a chemical tool for PIM kinase inhibition^{15,66} was investigated. This inhibitor exhibits subnanomolar to single-digit nanomolar *K_i* values against all three PIM kinases and has been co-crystallised with PIM1, guiding subsequent SAR studies. It was postulated that rather than introducing the cyclopropylvinyl group by a late-stage Suzuki coupling, in accordance with the original diversification study, this group could be incorporated from the start in order to access **20** directly. To that end, 2-fluorobenzonitrile **14i** was prepared by the Pd-catalyzed Suzuki–Miyaura coupling of 5-bromo-2-fluorobenzonitrile (**14a**) and the corresponding boronate ester at 80 °C,¹⁵ and heated with methyl thioglycolate in the presence

**Scheme 6** Reagents and conditions: (i) *trans*-2-cyclopropylvinylboronic acid pinacol ester, Pd(Ph₃)₂Cl₂ (10 mol%), 1 M Na₂CO₃, DME/EtOH/H₂O, 80 °C, 16 h; (ii) Et₃N, DMSO, microwaves, 130 °C, 35 min; (iii) 2-chloroacetonitrile, HCl, dioxane, RT, 16 h; (iv) Me₂NH, EtOH, RT, 16 h; SCX column, MeOH/CH₂Cl₂; NH₃, MeOH.

of Et₃N in DMSO at 130 °C for 35 min under microwave irradiation to give the corresponding benzothiophene **5i** in reasonable yield after purification by column chromatography (Scheme 6). The cyclopropylvinyl group was found to be compatible with the subsequent chemistry: reaction of **5i** with chloroacetonitrile in 4 N HCl in dioxane gave chloromethyl derivative **19** which, on reaction with dimethylamine, underwent further cyclization to give the thienopyrimidinone scaffold **20** after purification by immobilization on an acidic resin. Thus the method delivered this known PIM kinase inhibitor by an extremely rapid route, suitable for biological study.

Experimental

Materials and methods

Commercially available reagents were used without further purification; solvents were dried by standard procedures. Light petroleum refers to the fraction with bp 40–60 °C and ether refers to diethyl ether. Unless otherwise stated, reactions were performed under an atmosphere of air. Flash chromatography was carried out using Merck Kieselgel 60 H silica or Matrex silica 60. Analytical thin layer chromatography was carried out using aluminium-backed plates coated with Merck Kieselgel 60 GF₂₅₄ that were visualised under UV light (at 254 and/or 360 nm). Microwave irradiation experiments were performed in a sealed Pyrex tube using a self-tunable CEM Discover, CEM Explorer or Biotage Initiator 2.5 EXP EU focused monomodal microwave synthesizer at the given temperature using the instrument's in-built IR temperature measuring device, by varying the irradiation power (initial power given in parentheses).

Fully characterized compounds were chromatographically homogeneous. Melting points were determined on a Kofler hot stage apparatus or Stanford Research Systems Optimelt and are uncorrected. Specific rotations were measured at the indicated temperature (in °C) using a ADP440 polarimeter (Bellingham + Stanley) at the sodium D line and are given in deg cm⁻³ g⁻¹ dm⁻¹ with concentration *c* in 10⁻² g cm⁻³. Infra-red spectra were recorded in the range 4000–600 cm⁻¹ on a Perkin-Elmer 1600 series FTIR spectrometer using an ATR probe or a Shimadzu IRAffinity-1 equipped with an ATR accessory and are reported in cm⁻¹. NMR spectra were recorded using a Varian VNMRs instrument operating at 400 or 500 MHz or a Bruker Avance III 400 MHz or Bruker Avance DRX 500 MHz for ¹H spectra and 100 or 126 MHz for ¹³C spectra; *J* values were recorded in Hz and multiplicities were expressed by the usual conventions. Low resolution mass spectra were determined using a Waters Q-TOF Ultima using electrospray positive ionization, A Waters LCT premier XE using atmospheric pressure chemical ionization (APCI), an Agilent 6130 single quadrupole with an APCI/electrospray dual source, a Fisons Instrument VG Autospec using electron ionization at 70 eV (low resolution) or a ThermoQuest Finnigan LCQ DUO electrospray, unless otherwise stated. TOFMS refers to time-of-flight mass spectrometry, ES refers to electrospray ionization, CI refers to chemical ionization (ammonia), FTMS refers to Fourier trans-

form mass spectrometry, NSI refers to nano-electrospray ionization and EI refers to electron ionization. A number of high resolution mass spectra were obtained courtesy of the EPSRC Mass Spectrometry Service at University College of Wales, Swansea, UK using the ionization methods specified.

Synthetic procedures

General procedure for synthesis of 3-aminobenzo[*b*]thiophenes **5 from benzonitriles **14**.** A mixture of the benzonitrile **14** (1.0 equiv.), methyl thioglycolate (1.05 equiv.) and triethylamine (3.1 equiv.) in dry DMSO (2 M) was irradiated in a Biotage Initiator 2.5 EXP EU or CEM Discover microwave synthesizer at 130 °C for the time specified (hold time) by modulating the initial microwave power. After cooling to room temperature in a stream of compressed air, the reaction mixture was poured into ice-water and the resulting solid collected, washed with water and dried *in vacuo* to give the desired product.

Methyl 3-amino-5-bromobenzo[*b*]thiophene-2-carboxylate (5a**).** 5-Bromo-2-fluorobenzonitrile (**14a**) (0.50 g, 2.50 mmol), methyl thioglycolate (0.22 mL, 2.60 mmol) and triethylamine (1.10 mL, 7.75 mmol) were reacted according to the above general procedure for 11 min to give the *title compound* (700 mg, 96%) as a brown solid, mp 170–171 °C (Found [ES⁺]: 285.9535. C₁₀H₉⁷⁹BrNO₂S [*MH*] requires 285.9532); IR (neat) $\nu_{\max}/\text{cm}^{-1}$ 3477 (N–H), 3363 (N–H), 2954 (C–H), 1681 (C=O); ¹H NMR (400 MHz, *d*₆-DMSO) $\delta_{\text{H}}/\text{ppm}$ 8.44 (1H, d, *J* = 1.9 Hz, 4-CH), 7.82 (1H, d, *J* = 8.6 Hz, 7-CH), 7.64 (1H, dd, *J* = 8.6, 1.9 Hz, 6-CH), 7.17 (2H, bs, NH₂), 3.79 (3H, s, Me); ¹³C NMR (101 MHz, *d*₆-DMSO) $\delta_{\text{C}}/\text{ppm}$ 164.6 (C), 148.6 (C), 137.7 (C), 133.2 (C), 131.0 (C), 125.7 (CH), 125.2 (CH), 117.1 (CH), 96.1 (C), 51.4 (Me); *m/z* (ES) 286 [M⁺Br]⁺, 100%.

Methyl 3-amino-5-nitrobenzo[*b*]thiophene-2-carboxylate (5b**).** 2-Fluoro-5-nitrobenzonitrile (**14b**) (0.50 g, 3.0 mmol), methyl thioglycolate (0.30 mL, 3.3 mmol) and triethylamine (1.3 mL, 9.3 mmol) were reacted according to the above general procedure for 11 min to give the *title compound* (0.71 g, 94%) as an orange solid, mp 243.4–244.1 °C (acetone) (lit.,⁶⁷ mp 244–246 °C) (Found [FTMS]: 253.0280. C₁₀H₉N₂O₅S [*MH*] requires 253.0278); IR (neat) $\nu_{\max}/\text{cm}^{-1}$ 3445 (N–H), 3342 (N–H), 1681 (C=O), 1572 (NO₂), 1432 (C–C), 1328 (NO₂), 1276 (C–O), 1093 (C–O); ¹H NMR (500 MHz, *d*₆-DMSO) $\delta_{\text{H}}/\text{ppm}$ 9.24 (1H, d, *J* = 2 Hz, 4-CH), 8.29 (1H, dd, *J* = 9, 2 Hz, 6-CH), 8.12 (1H, d, *J* = 9 Hz, 7-CH), 7.47 (2H, bs, NH₂), 3.82 (3H, s, Me); ¹³C NMR (100 MHz, *d*₆-DMSO) $\delta_{\text{C}}/\text{ppm}$ 164.2 (C), 149.6 (C), 144.9 (C), 144.5 (C), 131.4 (C), 124.3 (CH), 122.0 (CH), 119.4 (CH), 96.8 (C), 51.4 (Me); *m/z* (EI) 252 (M⁺, 100%), 219 (72). ¹H and ¹³C NMR spectroscopic analyses were in good agreement with literature data.⁶⁷

Methyl 3-amino-5-chlorobenzo[*b*]thiophene-2-carboxylate (5c**).** 5-Chloro-2-fluorobenzonitrile (**14c**) (0.50 g, 3.2 mmol), methyl thioglycolate (0.30 mL, 3.36 mmol) and triethylamine (1.38 mL, 9.92 mmol) were reacted according to the above general procedure for 11 min to give the *title compound* (710 mg, 92%) as a colourless solid, mp 170–172 °C (Found [ES⁺]: 242.0039. C₁₀H₉³⁵ClNO₂S [*MH*] requires 242.0037); IR (neat) $\nu_{\max}/\text{cm}^{-1}$ 3477 (N–H), 3365 (N–H), 1681 (C=O), 1278

(C–O); ^1H NMR (500 MHz, d_6 -DMSO) δ_{H} /ppm 8.30 (1H, d, J = 2.1 Hz, 4-CH), 7.88 (1H, d, J = 8.6 Hz, 7-CH), 7.53 (1H, dd, J = 8.6, 2.1 Hz, 6-CH), 7.17 (2H, bs, NH_2), 3.79 (3H, s, Me); ^{13}C NMR (126 MHz, d_6 -DMSO) δ_{C} /ppm 164.6 (C), 148.7 (C), 137.3 (C), 132.7 (C), 129.1 (C), 128.4 (CH), 125.0 (CH), 122.7 (CH), 96.2 (C), 51.4 (Me); m/z (ES) 242 ($[\text{M}^{35}\text{Cl}]\text{H}^+$, 100%). ^1H NMR spectroscopic analyses were in good agreement with literature data.¹⁵

Methyl 3-amino-6-(trifluoromethyl)benzo[*b*]thiophene-2-carboxylate (5d). 2-Fluoro-4-(trifluoromethyl)benzonitrile (**14d**) (0.50 g, 2.64 mmol), methyl thioglycolate (0.24 mL, 2.73 mmol) and triethylamine (1.14 mL, 8.20 mmol) were reacted according to the above general procedure for 20 min to give the *title compound* (580 mg, 80%) as a colourless solid, mp 159–161 °C (Found [ES⁺]: 298.0120. $\text{C}_{11}\text{H}_8\text{F}_3\text{NNaO}_2\text{S}$ [*MNa*] requires 298.0124); IR (neat) $\nu_{\text{max}}/\text{cm}^{-1}$ 3471 (N–H), 3344 (N–H), 2964 (C–H), 1664 (C=O); ^1H NMR (400 MHz, d_6 -DMSO) δ_{H} /ppm 8.38–8.32 (2H, 5-CH and 7-CH), 7.72 (1H, d, J = 8.7 Hz, 4-CH), 7.26 (2H, bs, NH_2), 3.82 (3H, s, Me); ^{13}C NMR (126 MHz, d_6 -DMSO) δ_{C} /ppm 164.5 (C), 148.8 (C), 138.9 (C), 134.1 (C), 128.4 (q, $^2J_{\text{C-F}}$ = 31.8 Hz, C), 124.2 (q, $^1J_{\text{C-F}}$ = 272.7 Hz, C), 124.1 (CH), 121.0–120.7 (m, CH), 120.3–120.0 (m, CH), 97.4 (C), 51.5 (Me); m/z (ES) 276 (MH^+ , 100%).

Methyl 3-amino-6-nitrobenzo[*b*]thiophene-2-carboxylate (5e). 2-Fluoro-4-nitrobenzonitrile (**14e**) (0.50 g, 3.00 mmol), methyl thioglycolate (0.28 mL, 3.15 mmol) and triethylamine (1.29 mL, 9.30 mmol) were reacted according to the above general procedure for 35 min to give the *title compound* (510 mg, 67%) as a colourless solid, mp 228–231 °C (lit.,⁵⁸ mp 229–231 °C) (Found [ES⁺]: 275.0101. $\text{C}_{10}\text{H}_8\text{N}_2\text{NaO}_4\text{S}$ [*MNa*] requires 275.0097); IR (neat) $\nu_{\text{max}}/\text{cm}^{-1}$ 3489 (N–H), 3367 (N–H), 1697 (C=O), 1624 (C–O); ^1H NMR (400 MHz, d_6 -DMSO) δ_{H} /ppm 8.90 (1H, d, J = 2.1 Hz, 7-CH), 8.37 (1H, d, J = 8.7 Hz, 4-CH), 8.19 (1H, dd, J = 8.7, 2.1 Hz, 5-CH), 7.30 (2H, bs, NH_2), 3.83 (3H, s, Me); ^{13}C NMR (101 MHz, d_6 -DMSO) δ_{C} /ppm 164.3 (C), 148.4 (C), 147.0 (C), 138.8 (C), 135.6 (C), 124.2 (CH), 119.8 (CH), 118.5 (CH), 99.8 (C), 51.7 (Me); m/z (ES) 253 (MH^+ , 20%), 252 (M^+ , 100). ^1H NMR spectroscopic analyses were in good agreement with literature data.⁶³

Methyl 3-amino-5-phenylbenzo[*b*]thiophene-2-carboxylate (5f). 4-Fluoro-[1,1'-biphenyl]-3-carbonitrile (**14f**) (0.30 g, 1.52 mmol), methyl thioglycolate (0.14 mL, 1.59 mmol) and triethylamine (0.65 mL, 4.74 mmol) were reacted according to a modified general procedure for 15 min. After cooling in a stream of compressed air, EtOAc (25 mL) was added and the solution was washed sequentially with water (3 × 25 mL) and brine (3 × 25 mL), dried over MgSO_4 and evaporated *in vacuo*. Purification by flash chromatography on silica gel, eluting with light petroleum–EtOAc (4 : 1), gave the *title compound* (380 mg, 85%) as a colourless solid, mp 96–97 °C (Found [ES⁺]: 284.0741. $\text{C}_{16}\text{H}_{14}\text{NO}_2\text{S}$ [*MH*] requires 284.0740); IR (neat) $\nu_{\text{max}}/\text{cm}^{-1}$ 3439 (N–H), 3338 (N–H), 2949 (C–H), 1658 (C=O); ^1H NMR (400 MHz, d_6 -DMSO) δ_{H} /ppm 8.54 (1H, s, 4-CH), 7.91 (1H, d, J = 8.5 Hz, 7-CH), 7.84 (1H, d, J = 8.5 Hz, 6-CH), 7.78 (2H, d, J = 7.5 Hz, 2',6'-PhH), 7.51 (2H, app t, J = 7.5 Hz, 3',5'-PhH), 7.39 (1H, t, J = 7.5 Hz, 4'-PhH), 7.26 (2H, bs, NH_2), 3.80 (3H, s, Me); ^{13}C NMR (101 MHz, d_6 -DMSO) δ_{C} /ppm 164.8 (C),

149.9 (C), 139.6 (C), 138.0 (C), 136.2 (C), 132.2 (C), 129.0 (CH), 127.5 (CH), 127.2 (CH), 126.7 (CH), 123.6 (CH), 121.0 (CH), 95.0 (C), 51.2 (Me); m/z (ES) 284 (MH^+ , 100%).

Methyl 3-aminobenzo[*b*]thiophene-2-carboxylate (5g). 2-Fluorobenzonitrile (**14g**) (0.16 mL, 1.5 mmol), methyl thioglycolate (0.135 mL, 1.5 mmol) and triethylamine (0.63 mL, 4.5 mmol) were reacted according to the above general procedure for 15 min to give the *title compound* (203 mg, 65%) as a purple solid, mp 107.6–107.8 °C (MeOH– H_2O) (lit.,⁵⁸ mp 110–111 °C) (Found [ES⁺]: 208.0434. $\text{C}_{10}\text{H}_{10}\text{NO}_2\text{S}$ [*MH*] requires 208.0432); IR (neat) $\nu_{\text{max}}/\text{cm}^{-1}$ 3434 (N–H), 3337 (N–H), 1659 (C=O), 1520, 1289 (C–O); ^1H NMR (500 MHz, d_6 -DMSO) δ_{H} /ppm 8.13 (1H, d, J = 8.1 Hz, 4-CH), 7.82 (1H, d, J = 8.1 Hz, 7-CH), 7.50 (1H, m, 6-CH), 7.39 (1H, m, 5-CH), 7.15 (2H, bs, NH_2), 3.78 (3H, s, Me); ^{13}C NMR (101 MHz, d_6 -DMSO) δ_{C} /ppm 164.8 (C=O), 149.8 (3-C), 138.8 (7 α -C), 131.4 (3 α -C), 128.5 (6-CH), 123.8 (5-CH), 123.1 (4-CH), 123.1 (7-CH), 94.4 (2-C), 51.2 (Me); m/z (ES) 207 (M^+ , 93%), 176 (30), 175 (100), 147 (34), 146 (37). NMR spectroscopic analyses were in good agreement with literature data.^{59,68}

Methyl 3-amino-5-(trifluoromethyl)benzo[*b*]thiophene-2-carboxylate (5h). 2-Fluoro-5-(trifluoromethyl)benzonitrile (**14h**) (0.50 g, 2.6 mmol), methyl thioglycolate (0.24 mL, 2.73 mmol) and triethylamine (1.14 mL, 8.20 mmol) were reacted according to the above general procedure for 20 min to give the *title compound* (640 mg, 88%) as a colourless solid, mp 140–141 °C (Found [ES⁺]: 298.0121. $\text{C}_{11}\text{H}_8\text{F}_3\text{NNaO}_2\text{S}$ [*MNa*] requires 298.0120); IR (neat) $\nu_{\text{max}}/\text{cm}^{-1}$ 3468 (N–H), 3335 (N–H), 1664 (C=O); ^1H NMR (400 MHz, d_6 -DMSO) δ_{H} /ppm 8.67 (1H, bs, 4-CH), 8.09 (1H, d, J = 8.5 Hz, 7-CH), 7.79 (1H, dd, J = 8.5, 1.5 Hz, 6-CH), 7.34 (2H, s, NH_2), 3.82 (3H, s, Me); ^{13}C NMR (101 MHz, d_6 -DMSO) δ_{C} /ppm 164.5 (C), 149.3 (C), 142.5 (C), 131.3 (C), 124.9 (q, $^2J_{\text{C-F}}$ = 32.7 Hz, C), 124.5 (q, $^1J_{\text{C-F}}$ = 272.1 Hz, C), 124.4 (C–H), 124.1 (m, C–H), 120.7 (m, C–H), 96.2 (C), 51.4 (Me); m/z (ES) 276 (MH^+ , 100%).

Methyl (*E*)-3-amino-5-(2-cyclopropylvinyl)benzo[*b*]thiophene-2-carboxylate (5i). (*E*)-5-(2-Cyclopropylvinyl)-2-fluorobenzonitrile (**14i**) (0.25 g, 1.33 mmol), methyl thioglycolate (0.12 mL, 1.39 mmol) and triethylamine (0.57 mL, 4.12 mmol) were reacted according to a modified general procedure for 35 min. After cooling in a stream of compressed air, EtOAc (25 mL) was added and the solution was washed sequentially with water (3 × 25 mL) and brine (3 × 25 mL), dried over MgSO_4 and evaporated *in vacuo*. Purification by flash chromatography on silica gel, eluting with light petroleum–EtOAc (4 : 1), gave the *title compound* (210 mg, 58%) as a colourless solid, mp 131–132 °C (Found [ES⁺]: 274.0899. $\text{C}_{15}\text{H}_{16}\text{NO}_2\text{S}$ [*M*] requires 274.0896); IR (neat) $\nu_{\text{max}}/\text{cm}^{-1}$ 3481 (N–H), 3365 (N–H), 1672 (C=O); ^1H NMR (400 MHz, d_6 -DMSO) δ_{H} /ppm 8.12 (1H, d, J = 1.6 Hz, 4-CH), 7.71 (1H, d, J = 8.5 Hz, 7-CH), 7.50 (1H, dd, J = 8.5, 1.6 Hz, 6-CH), 7.12 (2H, bs, NH_2), 6.53 (1H, d, J = 15.8 Hz, CH), 5.93 (1H, dd, J = 15.8, 9.1 Hz, CH), 3.78 (3H, s, Me), 1.69–1.55 (1H, m, CH), 0.86–0.80 (2H, m, CHH), 0.56–0.49 (2H, m, CHH); ^{13}C NMR (101 MHz, d_6 -DMSO) δ_{C} /ppm 164.8 (C), 149.7 (C), 136.9 (C), 135.2 (C), 133.7 (CH), 131.9 (C), 126.4 (CH), 126.4 (CH), 123.1 (CH), 119.4 (CH),

94.9 (C), 51.2 (Me), 14.4 (CH), 7.1 (CH₂); *m/z* (ES) 274 (MH⁺, 100%).

(3*R*)-3-Methyl-9-nitro-1,2,3,4-tetrahydro-5*H*-[1]benzothieno-[3,2-*e*][1,4]diazepin-5-one (6b). A solution of (*R*)-methyl 3-((2-((*tert*-butoxycarbonyl)amino)propyl)amino)-5-nitrobenzo[*b*]-thiophene-2-carboxylate (**18**) (0.30 g, 0.73 mmol) in TFA (10% *v/v* in CH₂Cl₂) (5.7 mL, 7.3 mmol) was stirred at room temperature for 4.5 h. When salt formation was confirmed by TLC analysis [*R*_f 0.3 in MeOH–CH₂Cl₂ (1:9)] the mixture was evaporated *in vacuo*. The residue was dissolved in a mixture of MeOH (5 mL) and NaOMe (25 wt% in MeOH; 1 mL, 4.4 mmol) and warmed to 50 °C for 2 h before heating at reflux for 2 h. The reaction mixture was then allowed to cool to room temperature, cooled in an ice bath, neutralized by the addition of hydrochloric acid (1 M) and stirred at 0 °C for 30 min. The resulting solid was isolated by filtration under reduced pressure, washed with water and dried in air to give the *title compound* (0.18 g, 100%) as a red powder, mp 337.4–342.4 °C (dec.) (Found [ES⁺]: 278.0590. C₁₂H₁₅N₃O₃S [*MH*⁺] requires 278.0594); [α]_D²⁴ +110.6 (*c* 0.04, MeOH); IR (neat) $\nu_{\max}/\text{cm}^{-1}$ 3307 (N–H), 1598 (C=O), 1501 (NO₂), 1438 (C–C), 1318 (NO₂), 1102 (C–N), 736 (N–H); ¹H NMR (500 MHz, *d*₆-DMSO) $\delta_{\text{H}}/\text{ppm}$ 9.03 (1H, d, *J* = 2 Hz, 10-CH), 8.22 (1H, dd, *J* = 9, 2 Hz, 8-CH), 8.05 (1H, d, *J* = 9 Hz, 7-CH), 8.02 (1H, m, 1-NH), 7.95 (1H, d, *J* = 3 Hz, 4-NH), 3.60 (1H, m, 3-CH), 3.39 (2H, m, 2-CH₂), 1.16 (3H, d, *J* = 7 Hz, Me); ¹³C NMR (125 MHz, *d*₆-DMSO) $\delta_{\text{C}}/\text{ppm}$ 164.2 (5-C), 145.3 (C), 144.2 (C), 141.8 (C), 132.9 (C), 123.8 (7-CH), 120.8 (8-CH), 118.6 (10-CH), 108.6 (C), 50.6 (2-CH₂), 47.6 (3-CH), 18.6 (Me); *m/z* (ES) 277 (M⁺, 87%), 262 (24), 234 (29), 206 (30).

Methyl 5-nitrobenzo[*b*]thiophene-2-carboxylate (10), prepared under ambient conditions. Methyl thioglycolate (0.48 mL, 5.4 mmol) and K₂CO₃ (0.89 g, 6.5 mmol) were added sequentially to a solution of 2-chloro-5-nitrobenzaldehyde (1.01 g, 5.4 mmol) in DMF (6.5 mL) and the mixture was stirred at room temperature for 17 h. The reaction was then quenched in ice-water and the resulting solid collected, washed with water and dried *in vacuo* to give the *title compound* (1.22 g, 95%) as an off-white solid, mp 213.3–217.6 °C (lit.,⁶⁹ mp 213–215 °C) (Found [FTMS + *p* NSI]: 255.0435. C₁₀H₁₁N₂O₄S [*MNH*₄⁺] requires 255.0434); IR (neat) $\nu_{\max}/\text{cm}^{-1}$ 3093 (C–H), 1701 (C=O), 1528 (NO₂), 1439 (C–C), 1342 (NO₂), 1302 (C–O); ¹H NMR (500 MHz, CDCl₃) $\delta_{\text{H}}/\text{ppm}$ 8.80 (1H, d, *J* = 2 Hz, 4-CH), 8.32 (1H, dd, *J* = 9, 2 Hz, 6-CH), 8.20 (1H, s, 3-CH), 8.01 (1H, d, *J* = 9 Hz, 7-CH), 4.00 (3H, s, Me); ¹³C NMR (125 MHz, CDCl₃) $\delta_{\text{C}}/\text{ppm}$ 162.2 (C), 147.4 (C), 145.9 (C), 138.3 (C), 137.2 (C), 130.7 (3-CH), 123.6 (7-CH), 121.2 (9-CH), 120.9 (7-CH), 52.9 (Me); *m/z* (EI) 237 (M⁺, 100%), 206 (63), 160 (25). ¹H NMR spectroscopic analyses were in good agreement with literature data.^{53,70}

Methyl 5-nitrobenzo[*b*]thiophene-2-carboxylate (10), using microwave-assisted conditions. A mixture of 2-chloro-5-nitrobenzaldehyde (0.75 g, 4.0 mmol), methyl thioglycolate (0.45 mL, 5 mmol) and K₂CO₃ (0.67 g, 4.8 mmol) in DMF (4.5 mL) was irradiated at 90 °C for 15 min (hold time) in a pressure-rated glass tube (35 mL) using a CEM Discover microwave synthesizer by moderating the initial power (100 W). After cooling in a flow

of compressed air, the reaction mixture was poured into water and the resulting solid filtered under reduced pressure, washed with water and dried in air to give the *title compound* (0.84 g, 88%) as an off-white solid, mp 216.8–218.5 °C (lit.,⁶⁹ mp 213–215 °C), with identical spectroscopic properties.

5-Nitrobenzo[*b*]thiophene-2-carboxylic acid (11), using conductive heating. A solution of aqueous NaOH (1 M; 5 mL, 5 mmol) was added to a solution of methyl 5-nitrobenzo[*b*]thiophene-2-carboxylate (**10**) (0.40 g, 1.7 mmol) in MeOH (5.5 mL) and the mixture was heated at reflux for 3 h. After cooling to room temperature, the solution was acidified with 1 M HCl (aq.) and the resulting solid filtered under reduced pressure and dried in air to give the *title compound* (0.36 g, 95%) as an off-white powder, mp 241.4–242.7 °C (lit.,⁷¹ mp 239–241 °C) (Found [TOFMS]: 224.0020. C₉H₆NO₄S [*MH*⁺] requires 224.0018); IR (neat) $\nu_{\max}/\text{cm}^{-1}$ 2844 (br, O–H), 1670 (C=O), 1600 (C–C), 1511 (NO₂), 1344 (NO₂), 1313 (C–O); ¹H NMR (500 MHz, CD₃OD) $\delta_{\text{H}}/\text{ppm}$ 8.87 (1H, d, *J* = 2 Hz, 4-CH), 8.30 (1H, dd, *J* = 9, 2 Hz, 6-CH), 8.24 (1H, s, 3-CH), 8.15 (1H, d, *J* = 9 Hz, 7-CH); ¹³C NMR (125 MHz, CD₃OD) $\delta_{\text{C}}/\text{ppm}$ 164.8 (C), 148.9 (5-C), 147.5 (C), 140.3 (C), 140.0 (C), 132.0 (3-CH), 125.1 (7-CH), 122.3 (4-CH), 121.9 (6-CH); *m/z* (EI) 223 (M⁺, 100%), 195 (38), 149 (37). ¹H NMR spectroscopic analyses were in good agreement with literature data.⁵³

5-Nitrobenzo[*b*]thiophene-2-carboxylic acid (11), using microwave-assisted heating. A mixture of methyl 5-nitrobenzo[*b*]thiophene-2-carboxylate (**10**) (0.20 g, 0.84 mmol), aqueous NaOH solution (1 M; 2.5 mL) and MeOH (3.5 mL) was irradiated at 100 °C for 3 min (hold time) in a pressure-rated glass tube (10 mL) using a CEM Discover microwave synthesizer by moderating the initial power (100 W). After cooling in a flow of compressed air, the reaction mixture was diluted with water, acidified with 1 M HCl and the resulting solid was filtered under reduced pressure, washed with water and dried in air to give the *title compound* (0.16 g, 94%) as an off-white powder, mp 241.3–242.1 °C (lit.,⁷¹ mp 239–241 °C), with identical spectroscopic properties.

3-Bromo-5-nitrobenzo[*b*]thiophene-2-carboxylic acid (12). According to a modified literature procedure,⁵⁷ bromine (1.4 mL, 27 mmol) was added portion-wise to a solution of 5-nitrobenzo[*b*]thiophene-2-carboxylic acid (**11**) (1.0 g, 4.5 mmol) and anhydrous sodium acetate (1.13 g, 13 mmol) in glacial acetic acid (28 mL) under N₂. A reflux condenser was fitted and the solution heated at 55 °C for 27 h. After cooling to room temperature, the solution was poured into ice-water and the resulting solid isolated by vacuum filtration and dried in air to give the *title compound* (1.02 g, 75%) as a yellow powder, mp 309.5–316.8 °C (lit.,⁴⁰ mp 307–309 °C) (Found [TOF MS]: 301.9126. C₉H₅⁷⁹BrNO₄S [*MH*⁺] requires 301.9123); IR (neat) $\nu_{\max}/\text{cm}^{-1}$ 2961 (br, O–H), 1701 (C=O), 1600 (C–C), 1511 (NO₂), 1347 (NO₂), 1270 (C–O), 620 (C–Br); ¹H NMR (500 MHz, CD₃OD) $\delta_{\text{H}}/\text{ppm}$ 8.83 (1H, d, *J* = 2 Hz, 4-CH), 8.39 (1H, dd, *J* = 9, 2 Hz, 6-CH), 8.21 (1H, d, *J* = 9 Hz, 7-CH); *m/z* (EI) 303 (M⁺[⁸¹Br]⁺, 98%), 301 (M⁺[⁷⁹Br]⁺, 96), 293 (17), 291 (13).

Methyl 3-bromo-5-nitrobenzo[*b*]thiophene-2-carboxylate (13), from acid 12. According to a modified literature pro-

cedure,⁵⁷ iodomethane (0.46 mL, 7.4 mmol) was added to a solution of 3-bromo-5-nitrobenzo[*b*]thiophene-2-carboxylic acid (**12**) (1.12 g, 3.7 mmol) and K₂CO₃ (1.28 g, 9.2 mmol) in DMF (15 mL). After stirring at room temperature for 3 h, the reaction mixture was quenched with saturated aqueous NH₄Cl solution, poured into excess water and filtered under reduced pressure. The collected solid was washed with water and dried in air to give the *title compound* (1.09 g, 93%) as an off-white powder, mp 211.5–212.5 °C (lit.,⁴⁰ mp 211–212 °C) (Found [TOF MS]: 315.9279. C₁₀H₇⁷⁹BrNO₄S [*MH*] requires 315.9279); IR (neat) $\nu_{\max}/\text{cm}^{-1}$ 3101 (C–H), 1691 (C=O), 1600 (C–C), 1514 (NO₂), 1347 (NO₂), 1089 (C–O), 1052 (C–O), 617 (C–Br); ¹H NMR (500 MHz, CDCl₃) $\delta_{\text{H}}/\text{ppm}$ 8.90 (1H, d, *J* = 2 Hz, 4-CH), 8.38 (1H, dd, *J* = 9, 2 Hz, 6-CH), 8.00 (1H, d, *J* = 9 Hz, 7-CH), 4.02 (3H, s, Me); ¹³C NMR (125 MHz, CDCl₃) $\delta_{\text{C}}/\text{ppm}$ 161.0 (C), 146.5 (5-C), 144.6 (C), 138.9 (C), 131.0 (3 α -C), 123.8 (7-CH), 122.2 (6-CH), 121.3 (4-CH), 115.6 (3-CH), 53.0 (Me); *m/z* (EI) 317 (M⁺[⁸¹Br]⁺, 100%), 315 (M⁺[⁷⁹Br]⁺, 94), 286 (58), 284 (55).

Methyl 3-bromo-5-nitrobenzo[*b*]thiophene-2-carboxylate (13), from 3-aminobenzothiophene 5b. Following the procedure of Iaroshenko *et al.*,⁶⁰ CuBr₂ (0.94 g, 4.2 mmol) was added to a solution of *tert*-butyl nitrite (0.45 mL, 3.8 mmol) in dry MeCN (11 mL) at 0 °C under argon. Methyl 3-amino-4-nitrobenzo[*b*]thiophene-2-carboxylate (**5b**) (0.69 g, 2.7 mmol) was then added portion-wise and the solution kept at 0 °C until nitrogen evolution ceased. The reaction mixture was allowed to warm to room temperature, stirred for 2 h and then poured into dilute hydrochloric acid (10%; 25 mL). The aqueous mixture was extracted with EtOAc (3 \times 30 mL) and the organic extracts were combined, dried (Na₂SO₄) and evaporated *in vacuo* to give the *title compound* (0.86 g, 99%) as an orange solid, mp 212.3–213.0 °C (acetone) (lit.,⁴⁰ mp 211–212 °C), with identical spectroscopic and spectrometric properties.

(*E*)-5-(2-Cyclopropylvinyl)-2-fluorobenzonitrile (14i). To a solution containing 5-bromo-2-fluorobenzonitrile (**14a**) (3.0 g, 15.0 mmol), Pd(PPh₃)₂Cl₂ (1.0 g, 1.5 mmol) and *trans*-2-cyclopropylvinylboronic acid pinacol ester (3.7 mL, 18 mmol) in DME/EtOH/H₂O (7 : 2 : 3) (50 mL) was added aqueous Na₂CO₃ solution (1 M; 27 mL). The resulting mixture was placed under an atmosphere of nitrogen and heated at 80 °C for 16 h after which time the reaction was cooled to room temperature and filtered through Celite. Purification by flash column chromatography on silica gel, eluting with light petroleum–EtOAc (9 : 1), gave the *title compound* (2.4 g, 86%) as a yellow oil (Found [ES⁺]: 188.0868. C₁₂H₁₁NF [*MH*] requires 188.0870); IR (neat) $\nu_{\max}/\text{cm}^{-1}$ 3007 (C–H), 2496 (CN), 1672 (C=C); ¹H NMR (400 MHz, CDCl₃) $\delta_{\text{H}}/\text{ppm}$ 7.53–7.46 (2H, m), 7.16–7.08 (1H, m), 6.39 (1H, d, *J* = 15.7 Hz), 5.71 (1H, dd, *J* = 15.7, 9.0 Hz), 1.65–1.53 (1H, m), 0.92–0.84 (2H, m), 0.59–0.52 (2H, m); ¹³C NMR (101 MHz, CDCl₃) $\delta_{\text{C}}/\text{ppm}$ 161.7 (d, *J* = 258.2 Hz), 137.9, 135.3 (d, *J* = 3.5 Hz), 131.8 (d, *J* = 7.9 Hz), 130.0, 124.2, 116.5 (d, *J* = 20.3 Hz), 101.5 (d, *J* = 15.7 Hz), 77.2, 14.7, 7.6; *m/z* (ES) 188 (MH⁺, 100%).

Methyl 3-aminothieno[2,3-*b*]pyridine-2-carboxylate (16). 2-Chloro-3-pyridinecarbonitrile (**15b**) (35 mg, 0.25 mmol), methyl thioglycolate (0.22 mL, 0.25 mmol) and triethylamine (0.10 mL, 0.72 mmol) were reacted according to the above

general procedure for 15 min to give the *title compound* (36 mg, 69%) as a yellow solid, mp 191 °C (dec.) (lit.,¹³ mp 194–196 °C) (Found [ES⁺]: 209.0380. C₉H₉N₂O₂S [*MH*] requires 209.0385); IR (neat) $\nu_{\max}/\text{cm}^{-1}$ 3417 (N–H), 3314, 3202, 2943, 1679 (C=O), 1291 (C–O), 1127 (C–O); ¹H NMR (500 MHz, *d*₆-DMSO) $\delta_{\text{H}}/\text{ppm}$ 8.68 (1H, dd, *J* = 4.6, 1.6 Hz, 6-CH), 8.54 (1H, dd, *J* = 8.1, 1.6 Hz, 4-CH), 7.46 (1H, dd, *J* = 8.1, 4.6 Hz, 5-CH), 7.30 (2H, bs, NH₂), 3.80 (3H, s, Me); ¹³C NMR (101 MHz, *d*₆-DMSO) $\delta_{\text{C}}/\text{ppm}$ 164.7 (C=O), 159.7 (7 α -C), 150.7 (6-CH), 147.7 (3-C), 131.4 (4-CH), 125.5 (3 α -C), 119.4 (5-CH), 93.2 (2-C), 51.4 (Me); *m/z* (EI) 208 (M⁺, 100%), 177 (28), 176 (93), 148 (60). ¹H NMR spectroscopic analyses were in good agreement with literature data.¹³

***tert*-Butyl [(2*R*)-1-aminopropan-2-yl]carbamate (17).** According to a modified literature procedure,⁷² a solution of Boc-D-Ala-OH (0.50 g, 2.64 mmol) and HOBt·H₂O (0.41 g, 3.0 mmol) in CH₂Cl₂ (20 mL) was cooled to 0 °C and EDCI·HCl (0.58 g, 3.0 mmol) was added. The solution was allowed to warm to room temperature and stirred for 30 min. The solution was then cooled to 0 °C, aqueous NH₃ (18.1 M; 0.6 mL) was added drop-wise and the mixture was stirred at room temperature for 30 min. Any solid residue was removed by filtration and the filtrate was washed sequentially with water (20 mL) and brine (2 \times 20 mL), dried (MgSO₄) and evaporated *in vacuo*. Purification by flash column chromatography on SiO₂, gradient eluting with MeOH–CH₂Cl₂ (from 3–7% MeOH), gave Boc-D-Ala-NH₂ (0.37 g, 75%) as colourless crystals, mp 127.5–128.2 °C (lit.,⁷³ mp 120–121 °C). According to a modified literature procedure,⁷⁴ BH₃·SMe₂ (2 M in THF; 13.5 mL, 27 mmol) was added portion-wise to a solution Boc-D-Ala-NH₂ (0.5 g, 2.7 mmol) in dry THF (9 mL) under N₂ at 0 °C. The reaction mixture was allowed to warm to room temperature, stirred for 18 h, evaporated *in vacuo* and treated with MeOH (3 \times 15 mL), stirring and evaporating *in vacuo* each time. Purification by ion exchange chromatography using an Isolute SPE SCX-2 flash column, eluting first with MeOH and then with a solution of NH₃ in MeOH (2 M), gave the *title compound* (0.39 g, 84%) as a colourless oil [*R*_f 0.3 in MeOH–CH₂Cl₂ (1 : 9)] (Found [ES⁺]: 175.1443. C₈H₁₉N₂O₂ [*MH*] requires 175.1441); [α]_D²⁴ –5.7 (*c* 1.1, MeOH); IR (neat) $\nu_{\max}/\text{cm}^{-1}$ 2973 (C–H), 1685 (C=O), 1521 (N–H), 1364 (CH₃ deformation), 1247 (C–O), 1165 (C–N), 1045 (C–O), 872 (N–H); ¹H NMR (500 MHz, CDCl₃) $\delta_{\text{H}}/\text{ppm}$ 4.78 (1H, m, NHBoc), 3.60 (1H, m, 2-CH), 2.70 (1H, m, 1-CHH), 2.59 (1H, m, 1-CHH), 1.40 (9H, s, CMe₃), 1.08 (3H, d, *J* = 7 Hz, 3-Me); ¹³C NMR (125 MHz, CDCl₃) $\delta_{\text{C}}/\text{ppm}$ 155.7 (C), 79.1 (C), 48.6 (2-CH), 47.4 (4-CH₂), 28.4 (CMe₃), 18.5 (Me). ¹H NMR spectroscopic analyses were in good agreement with literature data.⁷⁵

(*R*)-Methyl 3-((2-((*tert*-butoxycarbonyl)amino)propyl)amino)-5-nitrobenzo[*b*]thiophene-2-carboxylate (18). According to a modified literature procedure,⁷⁶ (*R*)-*tert*-butyl (1-aminopropan-2-yl)carbamate (**17**) (35 mg, 0.20 mmol) was added to a stirred mixture of methyl 3-bromo-5-nitrobenzo[*b*]thiophene-2-carboxylate (**13**) (50 mg, 0.16 mmol), Cs₂CO₃ (73 mg, 0.22 mmol), (±)-BINAP (13 mg, 0.02 mmol) and Pd(OAc)₂ (2.0 mg, 8.0 μ mol) in dry toluene (1.0 mL) under N₂ and the mixture was irra-

diated at 150 °C for 75 min (hold time) in a pressure-rated glass tube (10 mL) using a CEM Discover microwave synthesizer by moderating the initial power (200 W). After cooling in a flow of compressed air, the reaction mixture was partitioned between water (20 mL) and EtOAc (30 mL). The aqueous layer was further extracted with EtOAc (2 × 30 mL) and the organic extracts were combined, washed with brine (30 mL), dried (Na₂SO₄) and evaporated. Purification by flash column chromatography on SiO₂ (dry load), gradient eluting with light petroleum to Et₂O–light petroleum (1 : 1), gave the *title compound* (50 mg, 76%) as a red solid, mp 182.9–184.0 °C (Found [ES⁺]: 410.1378. C₁₈H₂₄N₃O₆S [MH] requires 410.1380); [α]_D²⁴ +55.3 (c 0.1, MeOH); IR (neat) $\nu_{\max}/\text{cm}^{-1}$ 3355 (N–H), 2954 (C–H), 1672 (C=O), 1588 (NO₂), 1508 (C–C), 1325 (NO₂), 1230 (C–O), 1060 (C–N); ¹H NMR (500 MHz, d₆-DMSO) $\delta_{\text{H}}/\text{ppm}$ 8.94 (1H, m, 4-CH), 8.27 (1H, d, *J* = 9 Hz, 6-CH), 8.15 (1H, d, *J* = 9 Hz, 7-CH), 7.54 (1H, m, 3-NH), 6.87 (1H, d, *J* = 6 Hz, 2'-NH), 3.81 (4H, m, 1'-CHH and OMe), 3.76 (1H, m, 2'-CH), 3.57 (1H, m, 1'-CHH), 1.32 (9H, s, CMe₃), 1.12 (1H, d, *J* = 6 Hz, 3'-Me); ¹³C NMR (125 MHz, d₆-DMSO) $\delta_{\text{C}}/\text{ppm}$ 164.0 (C), 155.1 (C), 150.3 (3-C), 145.2 (C), 144.3 (C), 131.1 (3 α -C), 124.7 (7-CH), 121.6 (6-CH), 120.5 (4-CH), 99.5 (2-C), 77.6 (CMe₃), 51.7 (OMe), 50.5 (1'-CH₂), 46.2 (2'-CH), 28.1 (CMe₃), 18.3 (3'-Me); *m/z* (EI) 410 (MH⁺, 100%), 409 (M⁺, 70).

Methyl 3-((1-amino-2-chloroethylidene)amino)-5-((*E*)-2-cyclopropylvinyl)benzo[*b*]thiophene-2-carboxylate hydrochloride (19). Methyl (*E*)-3-amino-5-(2-cyclopropylvinyl)benzo[*b*]thiophene-2-carboxylate (**5i**) (200 mg, 0.73 mmol) was suspended in a solution of HCl in 1,4-dioxane (4 M; 3 mL) and chloroacetonitrile (91 μL , 1.43 mmol) was added drop-wise. The reaction mixture was stirred at room temperature for 16 h and the suspension was filtered under reduced pressure, washed with light petroleum (60 mL) and dried *in vacuo* for 6 h to give the *title compound* (110 mg, 39%) as a colourless solid, mp 195–197 °C (dec.) (Found [ES⁺]: 317.0512. C₁₆H₁₄³⁵ClN₂OS [MH – MeOH] requires 317.0515); IR (neat) $\nu_{\max}/\text{cm}^{-1}$ 3332 (br, N–H), 3001 (C–H), 2675 (C–H), 1676 (C=O), 1620 (C=C); ¹H NMR (400 MHz, CD₃OD) $\delta_{\text{H}}/\text{ppm}$ 7.91 (1H, d, *J* = 8.6 Hz, 7-CH), 7.72 (1H, d, *J* = 1.5 Hz, 4-CH), 7.67 (1H, dd, *J* = 8.6, 1.5 Hz, 6-CH), 6.60 (1H, d, *J* = 15.8 Hz, CH), 5.96 (1H, dd, *J* = 15.8, 9.1 Hz, CH), 4.73 (2H, s, CH₂), 3.94 (3H, s, Me), 1.65–1.55 (1H, m, CH), 0.87–0.79 (2H, m, CHH), 0.59–0.48 (2H, m, CHH); ¹³C NMR (101 MHz, CD₃OD) $\delta_{\text{C}}/\text{ppm}$ 166.3 (C), 162.4 (C), 138.9 (C), 138.3 (CH), 138.0 (C), 135.8 (C), 130.5 (C), 130.4 (C), 127.7 (CH), 127.3 (CH), 124.6 (CH), 119.6 (CH), 53.4 (Me), 40.1 (CH), 15.5 (CH), 7.8 (CH₂, CH₂); *m/z* (ES) 349 (M [³⁵Cl]⁺H⁺, 100%).

(*E*)-8-(2-Cyclopropylvinyl)-2-((dimethylamino)methyl)benzo[4,5]thieno[3,2-*d*]pyrimidin-4(3*H*)-one (20). Compound **19** (70 mg, 0.18 mmol) was added to a solution of dimethylamine in ethanol (33%; 3 mL) and the reaction mixture was stirred at room temperature for 16 h. The solvent was evaporated *in vacuo* and the resulting colourless solid was dissolved in MeOH–CH₂Cl₂ (1 : 1; 5 mL) and loaded onto an SCX cartridge (1 g). The cartridge was flushed with MeOH (3 × 5 mL) and then eluted with a solution of NH₃ in MeOH (2 M; 8 mL) to

give the *title compound* as a colourless solid (55 mg, 94%), mp 202–203 °C (dec.) (Found [ES⁺]: 326.1324 C₁₈H₂₀N₃OS [MH] requires 326.1322); IR (neat) $\nu_{\max}/\text{cm}^{-1}$ 2873 (br, C–H), 1672 (C=O), 1587 (C=C); ¹H NMR (400 MHz, d₆-DMSO) $\delta_{\text{H}}/\text{ppm}$ 12.41 (1H, bs, NH), 8.09 (1H, d, *J* = 1.5 Hz, 4-CH), 8.03 (1H, d, *J* = 8.5 Hz, 7-CH), 7.69 (1H, dd, *J* = 8.5, 1.5 Hz, 6-CH), 6.68 (1H, d, *J* = 15.8 Hz, CH), 6.01 (1H, dd, *J* = 15.8, 9.2 Hz, CH), 3.52 (2H, s, CH₂), 2.29 (6H, s, Me), 1.66–1.56 (1H, m, CH), 0.85–0.78 (2H, m, CHH), 0.61–0.54 (2H, m, CHH); ¹³C NMR (101 MHz, d₆-DMSO) $\delta_{\text{C}}/\text{ppm}$ 158.5 (C), 157.2 (C), 152.7 (C), 138.3 (C), 136.2 (CH), 135.2 (CH), 134.6 (C), 126.5 (C), 126.2 (CH), 123.9 (CH), 122.0 (C), 119.7 (CH), 61.3 (CH₂), 45.1 (Me, Me), 14.7 (CH), 7.2 (CH₂, CH₂); *m/z* (ES) 326 (MH⁺, 100%). ¹H NMR spectroscopic analyses were in good agreement with literature data for the corresponding HCl salt.¹⁵

Conclusions

This method for the microwave-assisted synthesis of 3-amino-benzo[*b*]thiophenes is rapid, simple to carry out and generally high yielding. It has been applied in the synthesis of a range of functional benzothiophenes and their 7-aza analogues and constitutes a very efficient route to the corresponding 3-halo-benzothiophenes using diazonium chemistry. Applications of this process have been shown in the synthesis of the thieno-[2,3-*b*]pyridine core motif of LIMK1 inhibitors using 2-halopyridine-3-carbonitriles, the benzo[4,5]thieno[3,2-*e*][1,4]diazepin-5(2*H*)-one scaffold of MK2 inhibitors with functionality suitable for subsequent modification using Buchwald–Hartwig chemistry, and a benzo[4,5]thieno[3,2-*d*]pyrimidin-4-one target as a chemical tool for inhibition of PIM kinases. In the case of inhibitors of MK2, the use of this approach has been shown to be superior to traditional bromination chemistry using the parent benzothiophene heterocycle. Given the speed, efficiency and reliability of these methods, and their ability to incorporate a wide range of functionality, these approaches are likely to find application in providing chemical tools, rapidly, reliably and efficiently, for advancing studies in chemical biology, as well as to access targets in medicinal chemistry.

Acknowledgements

We thank the EPSRC-BBSRC-MRC sponsored network SMS-Drug (EP/I037229/1; award to MCB and NCOT), EPSRC (studentship awards to JED and HLR) and the R M Phillips Trust (award to MCB) for support of this work and Dr Alaa Abdul-Sada at the University of Sussex and the EPSRC Mass Spectrometry Service at the University of Wales, Swansea UK for mass spectra.

Notes and references

- 1 K. Koike, Z. Jia, T. Nikaido, Y. Liu, Y. Zhao and D. Guo, *Org. Lett.*, 1999, **1**, 197.

- 2 J. Huang, H. Luo, L. Wang, Y. Guo, W. Zhang, H. Chen, M. Zhu, Y. Liu and G. Yu, *Org. Lett.*, 2012, **14**, 3300.
- 3 Y. Ni, K. Nakajima, K. Kanno and T. Takahashi, *Org. Lett.*, 2009, **11**, 3702.
- 4 K. G. Pinney, a. D. Bounds, K. M. Dingeman, V. P. Mocharla, G. R. Pettit, R. Bai and E. Hamel, *Bioorg. Med. Chem. Lett.*, 1999, **9**, 1081.
- 5 R. Romagnoli, P. G. Baraldi, M. D. Carrion, C. L. Cara, D. Preti, F. Fruttarolo, M. G. Pavani, M. A. Tabrizi, M. Tolomeo, S. Grimaudo, A. Di Cristina, J. Balzarini, J. A. Hadfield, A. Brancale and E. Hamel, *J. Med. Chem.*, 2007, **50**, 2273.
- 6 T. Chonan, D. Wakasugi, D. Yamamoto, M. Yashiro, T. Oi, H. Tanaka, A. Ohoka-Sugita, F. Io, H. Koretsune and A. Hiratate, *Bioorg. Med. Chem.*, 2011, **19**, 1580.
- 7 L. Berrade, B. Aisa, M. J. Ramirez, S. Galiano, S. Guccione, L. R. Moltzau, F. O. Levy, F. Nicoletti, G. Battaglia, G. Molinaro, I. Aldana, A. Monge and S. Perez-Silanes, *J. Med. Chem.*, 2011, **54**, 3086.
- 8 K. C. Lee, B. S. Moon, J. H. Lee, K.-H. Chung, J. A. Katzenellenbogen and D. Y. Chi, *Bioorg. Med. Chem.*, 2003, **11**, 3649.
- 9 C. D. Jones, M. G. Jevnikar, A. J. Pike, M. K. Peters, L. J. Black, A. R. Thompson, J. F. Falcone and J. A. Clemens, *J. Med. Chem.*, 1984, **27**, 1057.
- 10 Editorial, *Lancet Oncol.*, 2006, **7**, 443; V. G. Vogel, J. P. Costantino, D. L. Wickerham, W. M. Cronin, R. S. Cecchini, J. N. Atkins, T. B. Bevers, L. Fehrenbacher, E. R. Pajon, J. L. Wade, A. Robidoux, R. G. Margolese, J. James, S. M. Lippman, C. D. Runowicz, P. A. Ganz, S. E. Reis, W. McCaskill-Stevens, L. G. Ford, V. C. Jordan and N. Wolmark, *JAMA*, 2006, **295**, 2727.
- 11 P. Lu, M. L. Schrag, D. E. Slaughter, C. E. Raab, M. Shou and A. D. Rodrigues, *Drug Metab. Dispos.*, 2003, **31**, 1352.
- 12 J. D. Croxtall and G. L. Plosker, *Drugs*, 2009, **69**, 339.
- 13 R. Romagnoli, P. G. Baraldi, M. K. Salvador, D. Preti, M. A. Tabrizi, M. Bassetto, A. Brancale, E. Hamel, I. Castagliuolo, R. Bortolozzi, G. Basso and G. Viola, *J. Med. Chem.*, 2013, **56**, 2606.
- 14 B. E. Sleebs, A. Levit, I. P. Street, H. Falk, T. Hammonds, A. C. Wong, M. D. Charles, M. F. Olson and J. B. Baell, *Med. Chem. Commun.*, 2011, **2**, 977.
- 15 Z.-F. Tao, L. A. Hasvold, J. D. Levenson, E. K. Han, R. Guan, E. F. Johnson, V. S. Stoll, K. D. Stewart, G. Stamper, N. Soni, J. J. Bouska, Y. Luo, T. J. Sowin, N.-H. Lin, V. S. Giranda, S. H. Rosenberg and T. D. Penning, *J. Med. Chem.*, 2009, **52**, 6621.
- 16 D. R. Anderson, M. J. Meyers, R. G. Kurumbail, N. Caspers, G. I. Poda, S. A. Long, B. S. Pierce, M. W. Mahoney and R. J. Mourey, *Bioorg. Med. Chem. Lett.*, 2009, **19**, 4878.
- 17 D. R. Anderson, M. J. Meyers, R. G. Kurumbail, N. Caspers, G. I. Poda, S. A. Long, B. S. Pierce, M. W. Mahoney, R. J. Mourey and M. D. Parikh, *Bioorg. Med. Chem. Lett.*, 2009, **19**, 4882.
- 18 H. Mikkers, M. Nawijn, J. Allen, C. Brouwers, E. Verhoeven, J. Jonkers and A. Berns, *Mol. Cell. Biol.*, 2004, **24**, 6104.
- 19 S. Kumar, J. Boehm and J. C. Lee, *Nat. Rev. Drug Discovery*, 2003, **2**, 717.
- 20 M. C. Bagley, T. Davis, P. G. S. Murziani, C. S. Widdowson and D. Kipling, *Pharmaceuticals*, 2010, **3**, 1842.
- 21 D. Kipling, T. Davis, E. L. Ostler and R. G. Faragher, *Science*, 2004, **305**, 1426.
- 22 T. Davis, M. F. Haughton, C. J. Jones and D. Kipling, *Ann. N. Y. Acad. Sci.*, 2006, **1067**, 243.
- 23 T. Davis, D. M. Baird, M. F. Haughton, C. J. Jones and D. Kipling, *J. Gerontol., Ser. A*, 2005, **60**, 1386.
- 24 A. Schlappbach and C. Huppertz, *Future Med. Chem.*, 2009, **1**, 1243.
- 25 N. Ronkina, A. Kotlyarov and M. Gaestel, *Front. Biosci.*, 2008, **13**, 5511.
- 26 R. J. Mourey, B. L. Burnette, S. J. Brustkern, J. S. Daniels, J. L. Hirsch, W. F. Hood, M. J. Meyers, S. J. Mnich, B. S. Pierce, M. J. Saabye, J. F. Schindler, S. A. South, E. G. Webb, J. Zhang and D. R. Anderson, *J. Pharmacol. Exp. Ther.*, 2010, **333**, 797.
- 27 J. S. Daniels, Y. Lai, S. South, P.-C. Chiang, D. Walker, B. Feng, R. Mireles, L. O. Whiteley, J. W. McKenzie, J. Stevens, R. Mourey, D. Anderson and J. W. Davis II, *Drug Metab. Lett.*, 2013, **7**, 15.
- 28 T. Davis, M. J. Rokicki, M. C. Bagley and D. Kipling, *Chem. Cent. J.*, 2013, **7**, 18.
- 29 M. C. Bagley, M. Baashen, J. Dwyer, P. Milbeo, D. Kipling and T. Davis, in *Microwaves in Drug Discovery and Development: Recent Advances*, ed. J. Spencer and M. C. Bagley, Future Science Ltd., 2014, ch. 5, pp. 86–104.
- 30 M. C. Bagley, M. Baashen, V. L. Paddock, D. Kipling and T. Davis, *Tetrahedron*, 2013, **69**, 8429.
- 31 T. Davis, M. C. Dix, M. J. Rokicki, C. S. Widdowson, A. J. C. Brook, D. Kipling and M. C. Bagley, *Chem. Cent. J.*, 2011, **5**, 83.
- 32 M. C. Bagley, T. Davis, M. C. Dix, V. Fusillo, M. Pigeaux, M. J. Rokicki and D. Kipling, *J. Org. Chem.*, 2009, **74**, 8336.
- 33 M. C. Bagley, T. Davis, M. C. Dix, C. S. Widdowson and D. Kipling, *Org. Biomol. Chem.*, 2006, **4**, 4158.
- 34 T. Force, K. Kuida, M. Namchuk, K. Parang and J. M. Kyriakis, *Circulation*, 2004, **109**, 1196.
- 35 D. M. Goldstein, A. Kuglstatter, Y. Lou and M. J. Soth, *J. Med. Chem.*, 2010, **53**, 2345.
- 36 M. C. Genovese, *Arthritis Rheum.*, 2009, **60**, 317.
- 37 T. Davis, M. C. Bagley, M. C. Dix, P. G. S. Murziani, M. J. Rokicki, C. S. Widdowson, J. M. Zayed, M. A. Bachler and D. Kipling, *Bioorg. Med. Chem. Lett.*, 2007, **17**, 6832.
- 38 C. Hou, Q. He and C. Yang, *Org. Lett.*, 2014, **16**, 5040.
- 39 E. David, J. Perrin, S. Pellet-Rostaing, J. Fournier dit Chabert and M. Lemaire, *J. Org. Chem.*, 2005, **70**, 3569.
- 40 M. Martin-Smith and S. Reid, *J. Chem. Soc.*, 1960, 938.
- 41 M. Martin-Smith and M. Gates, *J. Am. Chem. Soc.*, 1956, **78**, 5351.
- 42 M. Martin-Smith and M. Gates, *J. Am. Chem. Soc.*, 1956, **78**, 6177.
- 43 J. Fournier Dit Chabert, L. Joucla, E. David and M. Lemaire, *Tetrahedron*, 2004, **60**, 3221.

- 44 K. O. Hessian and B. L. Flynn, *Org. Lett.*, 2003, **5**, 4377.
- 45 B. L. Flynn, P. Verdier-Pinard and E. Hamel, *Org. Lett.*, 2001, **3**, 651.
- 46 D. Yue and R. C. Larock, *J. Org. Chem.*, 2002, **67**, 1905.
- 47 S. Kim, N. Dahal and T. Kesharwani, *Tetrahedron Lett.*, 2013, **54**, 4373.
- 48 V. Guilarte, M. A. Fernández-Rodriguez, P. García-García, E. Hernando and R. Sanz, *Org. Lett.*, 2011, **13**, 5100.
- 49 S. Knapp, P. Arruda, J. Blagg, S. Burley, D. H. Drewry, A. Edwards, D. Fabbro, P. Gillespie, N. S. Gray, B. Kuster, K. E. Lackey, P. Mazzafera, N. C. O. Tomkinson, T. M. Willson, P. Workman and W. J. Zuercher, *Nat. Chem. Biol.*, 2013, **9**, 3.
- 50 T. Higa and A. J. Krubsack, *J. Org. Chem.*, 1976, **41**, 3399.
- 51 T. Higa and A. J. Krubsack, *J. Org. Chem.*, 1975, **40**, 3037.
- 52 M. C. Bagley, T. Davis, M. C. Dix, P. G. S. Murziani, M. J. Rokicki and D. Kipling, *Bioorg. Med. Chem. Lett.*, 2008, **18**, 3745.
- 53 R. A. Zambias and M. L. Hammond, *Synth. Commun.*, 1991, **21**, 959.
- 54 J. Cai, S. Zhang, M. Zheng, X. Wu, J. Chen and M. Ji, *Bioorg. Med. Chem. Lett.*, 2012, **22**, 806.
- 55 J. Debray, M. Lemaire and F. Popowycz, *Synlett*, 2013, 37.
- 56 M. C. Bagley, J. E. Dwyer and P. Milbeo, unpublished work.
- 57 J. M. Mbere, J. B. Bremner, B. W. Skelton and A. H. White, *Tetrahedron*, 2011, **67**, 6895.
- 58 J. R. Beck, *J. Org. Chem.*, 1972, **37**, 3224.
- 59 M. H. Norman, F. Navas III, J. B. Thompson and G. C. Rigdon, *J. Med. Chem.*, 1996, **39**, 4692.
- 60 V. O. Iaroshenko, S. Ali, S. Mkrtchyan, A. Gevorgyan, T. M. Babar, V. Semeniuchenko, Z. Hassan, A. Villinger and P. Langer, *Tetrahedron Lett.*, 2012, **53**, 7135.
- 61 I. Abdillahi and G. Kirsch, *Synthesis*, 2011, 1314.
- 62 I. Abdillahi and G. Kirsch, *Synthesis*, 2010, 1428.
- 63 A. J. Bridges and H. Zhou, *J. Heterocycl. Chem.*, 1997, **34**, 1163.
- 64 M. D. Meyer, R. J. Altenbach, F. Z. Basha, W. A. Carroll, S. Condon, S. W. Elmore, J. F. Kerwin Jr., K. B. Sippy, K. Tietje, M. D. Wendt, A. A. Hancock, M. E. Brune, S. A. Buckner and I. Drizin, *J. Med. Chem.*, 2000, **43**, 1586.
- 65 S. S. Khatana, D. H. Boschelli, J. B. Kramer, D. T. Connor, H. Barth and P. Stoss, *J. Org. Chem.*, 1996, **61**, 6060.
- 66 R. Ekambaram, E. Enkvist, A. Vaasa, M. Kasari, G. Raidaru, S. Knapp and A. Uri, *ChemMedChem*, 2013, **8**, 909.
- 67 V. Bertolasi, K. Dudová, P. Šimůnek, J. Černý and V. Macháček, *J. Mol. Struct.*, 2003, **658**, 33.
- 68 L. N. Tumey, Y. Bennani and D. C. Bom, *WO Pat.*, 014 647 A2, 2006.
- 69 V. G. Matassa, F. J. Brown, P. R. Bernstein, H. S. Shapiro, T. P. Maduskuie Jr., L. A. Cronk, E. P. Vacek, Y. K. Yee, D. W. Snyder, R. D. Krell, C. L. Lerman and J. J. Maloney, *J. Med. Chem.*, 1990, **61**, 2621.
- 70 D. L. Boger, B. E. Fink and M. P. Hedrick, *J. Am. Chem. Soc.*, 2000, **122**, 6382.
- 71 L. Fieser and R. Kennelly, *J. Am. Chem. Soc.*, 1935, **57**, 1611.
- 72 W. Wu, Z. Li, G. Zhou and S. Jiang, *Tetrahedron Lett.*, 2011, **52**, 2488.
- 73 Z. Xia and C. D. Smith, *J. Org. Chem.*, 2001, **66**, 3459.
- 74 A. Marquart and B. Podlogar, *J. Org. Chem.*, 1994, **59**, 2092.
- 75 Z. Huang, J. Jin, T. D. Machajewski, W. R. Antonios-McCrea, M. McKenna, D. Poon, P. A. Renhowe, M. Sendzik, C. M. Shafer, A. Smith, Y. Xu and Q. Zhang, *WO Pat.*, 115 572 A2, 2009.
- 76 M.-J. R. P. Queiroz, A. Begouin, I. C. F. R. Ferreira, G. Kirsch, R. C. Calhelha, S. Barbosa and L. M. Estevinho, *Eur. J. Org. Chem.*, 2004, 3679.



Cite this: *Org. Biomol. Chem.*, 2016, **14**, 947

The effect of RO3201195 and a pyrazolyl ketone P38 MAPK inhibitor library on the proliferation of Werner syndrome cells†

Mark C. Bagley,^{*a} Jessica E. Dwyer,^a Mohammed Baashen,^{‡a} Matthew C. Dix,^b Paola G. S. Murziani,^b Michal J. Rokicki,^c David Kipling^c and Terence Davis^{*c}

Received 28th October 2015,
Accepted 11th November 2015

DOI: 10.1039/c5ob02229k

www.rsc.org/obc

Microwave-assisted synthesis of the pyrazolyl ketone p38 MAPK inhibitor RO3201195 in 7 steps and 15% overall yield, and the comparison of its effect upon the proliferation of Werner Syndrome cells with a library of pyrazolyl ketones, strengthens the evidence that p38 MAPK inhibition plays a critical role in modulating premature cellular senescence in this progeroid syndrome and the reversal of accelerated ageing observed *in vitro* on treatment with SB203580.

Introduction

P38 α is one isoform of the mitogen-activated protein kinase (MAPK) intracellular enzymes which are central to the regulation of cytokine biosynthesis and inflammatory cell signalling.^{1,2} The reduction of pro-inflammatory cytokine levels offers a means for the treatment of inflammatory disorders such as rheumatoid arthritis and atherosclerosis.^{3,4} In addition to inflammatory disorders, p38 α is known to play a role in the resistance of various cancers to chemotherapy, cancer proliferation and metastasis.^{5,6} This makes p38 α a compelling therapeutic target for the design of safe and efficacious inhibitors suitable for clinical investigation.^{2,7} Following the discovery that pyridinylimidazole p38 α inhibitors such as SB203580 mediate multiple cellular responses,¹ including the production of inflammatory cytokines, a wide variety of structurally-distinct chemotypes^{8,9} have been discovered to inhibit this enzyme with notable differences in binding motif.¹⁰ Many of these have been used in stage II or III clinical trials.¹¹

Werner syndrome (WS) is a rare autosomal recessive disorder.¹² The mutated gene (WRN) encodes for a RecQ helicase involved in DNA replication, recombination and repair. Individuals living with the syndrome display the premature onset

of many of the clinical features of old age, show early susceptibility to a number of major age-related diseases and have an abbreviated median life expectancy (47 years). Consequently, WS is widely used as a model disease to investigate the mechanisms underlying normal human ageing. Associated with these aged features, fibroblasts from WS individuals have a much-reduced replicative capacity when compared with fibroblasts from normal individuals, and have a stressed, aged, morphology and high levels of activated p38 α .^{13–15} This accelerated cellular senescence is thought to underlie whole body ageing in this syndrome. As part of our interest in mechanisms of premature cell senescence, we showed that administering the p38 α inhibitor SB203580 to WS cells rescues all of the features of accelerated replicative decline.¹³ This observation suggested that the abbreviated life span of WS cells is due to stress-induced growth arrest mediated by p38 α MAPK, which we speculate is transduced from the frequently stalled DNA replication forks observed in these cells.¹⁶ It also offers a means to clinically regulate this process and, by therapeutic means, intervene in a premature ageing syndrome.¹⁶

However, it has been shown that SB203580 is not specific for p38 α , but also inhibits the related N-terminal c-Jun kinases (JNKs) that may play a role in cellular senescence.^{17–19} Thus more work is needed using inhibitors that do not target the JNKs to verify the role played by p38 α in WS cells. In addition, SB203580 is not suitable for possible *in vivo* use.¹¹

This manuscript describes a rapid route to one such inhibitor, RO3201195 (1),²⁰ the study of this inhibitor in WS cells, and its comparison with the canonical p38 α inhibitor SB203580 to investigate the role of p38 α MAPK signal transduction in replicative senescence. This pyrazolyl ketone p38 α MAPK inhibitor progressed to clinical trials, is orally bio-available, exhibits high kinase selectivity, and inhibited the

^aDepartment of Chemistry, School of Life Sciences, University of Sussex, Falmer, Brighton, East Sussex, BN1 9QJ, UK. E-mail: m.c.bagley@sussex.ac.uk

^bSchool of Chemistry, Main Building, Cardiff University, Park Place, Cardiff, CF10 3AT, UK

^cInstitute of Cancer and Genetics, Cardiff University School of Medicine, Heath Park, Cardiff, CF14 4XN, UK

†Electronic supplementary information (ESI) available. See DOI: 10.1039/c5ob02229k

‡Current address: Department of Chemistry, College of Science and Humanities, Shaqra University, Kingdom of Saudi Arabia.



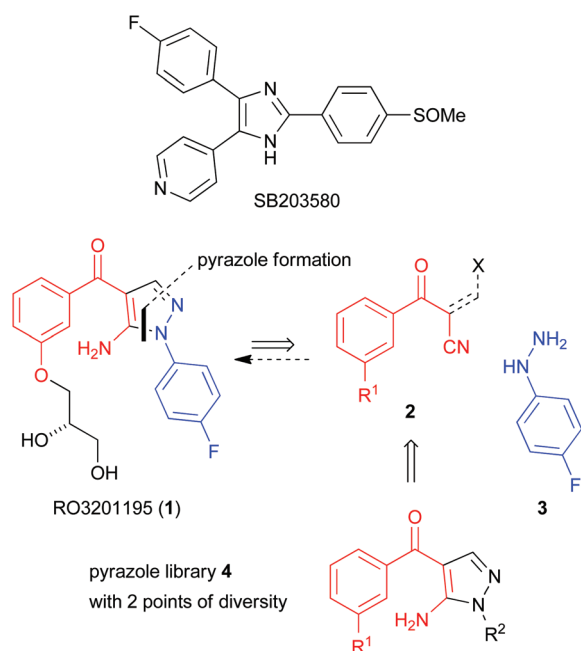
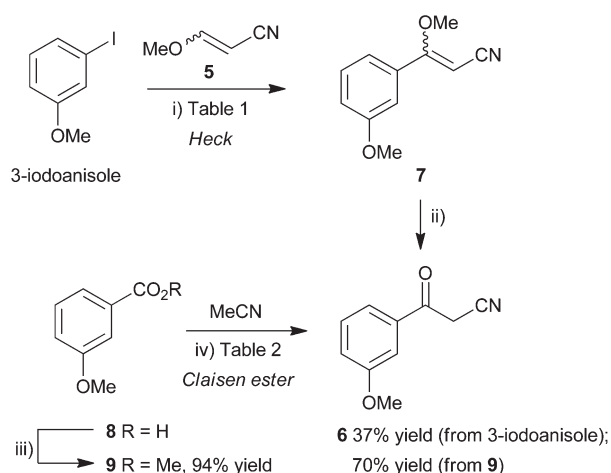


Fig. 1 P38 MAPK inhibitors SB203580 and RO3201195 (1), a pyrazolyl ketone library 4 and disconnection approach to 1.

production of the cytokines IL-6 and TNF α upon lipopolysaccharide (LPS) challenge in rats.²⁰ Thus, RO3201195 could be a valuable chemical tool in dissecting the accelerated ageing pathophysiology seen in WS cells and its rescue *in vitro* using small molecule inhibitors of this stress signalling pathway.^{13,21} Our rapid approach to the inhibitor employs microwave irradiation to accelerate a number of steps, preparing the central pyrazole motif through cyclocondensation of hydrazine 3 and a suitably protected benzoylnitrile 2, derivatized by homologation prior to heterocycle formation (Fig. 1). This approach had been successful for the synthesis of a pyrazolyl ketone library (4)²² and so should be suitable for rapid production of the target inhibitor under microwave-assisted conditions.

Results and discussion

The synthesis of a suitably functionalized β -ketonitrile derivative 2, as a precursor for pyrazole formation, was first investigated using the Pd-catalyzed Heck reaction^{23,24} of 3-iodoanisole and 3-methoxyacrylonitrile (5). This approach had the advantage that, potentially, it could access 3-methoxybenzoylacetonitrile (6) directly from commercially-available materials, upon acid hydrolysis of the coupled product, methyl vinyl ether 7 (Scheme 1, top), providing a very rapid route into the pyrazole skeleton. Heck reactions of α - or β -substituted enol ethers are known and have been shown to provide efficient access to 1-arylpropanone derivatives.²⁵ However, although there are numerous examples of Heck reactions of α,β -disubstituted alkenes such as methylacrylates,²⁶ 3-ethoxy-



Scheme 1 Synthesis of 3-methoxybenzoylacetonitrile (6) by Heck coupling (top) or Claisen ester condensation (bottom). Reagents and conditions: (i) see Table 1; (ii) CHCl₃-MeOH (1 : 4), microwaves, 110 °C, 30 min; (iii) MeOH, H₂SO₄, reflux, 2.5 h (90%); or MeOH, H₂SO₄, microwaves, 110 °C, 10 min (94%); (iv) see Table 2; HCl (aq).

acrylates,²⁷ cinnamates,²⁸ crotonates²⁹ and alkoxypropenes,³⁰ there are very few examples of β -alkoxyacrylonitriles in these and related processes. Enol ethers are less reactive than electron-poor alkenes in Heck transformations and so these slow reactions often require high catalyst loadings, more reactive aryl iodides as substrates and the use of certain additives, particularly when performed under solid-liquid phase transfer conditions.³¹ Furthermore, α,β -disubstituted alkenes may suffer from steric constraints and so, although direct, this approach for the synthesis of benzoylacetonitriles was untested. Ortay *et al.*³² did describe the arylation of an α -methoxyacrylate back in 1987 using aryl iodides, palladium acetate (3 mol%), NaHCO₃ base and tetrabutylammonium chloride as additive. Using Jeffery's conditions for Heck-type processes as a starting point,³³ methods related to the conditions for arylation of acrylonitrile with aryl iodides³⁴ were investigated in the Heck reaction of 3-iodoanisole and 3-methoxyacrylonitrile (5). The use of Pd(OAc)₂ (10 mol%) as catalyst in MeCN-H₂O (3 : 1) (Table 1) under microwave-assisted heating at 130 °C for 1.5 h (entry 4) with K₂CO₃ as base and tetrabutylammonium bromide (TBAB) as additive gave, following aqueous work up, the α -aryl enol ether 7 as a mixture of (*E*)- and (*Z*)-diastereoisomers, in a 2 : 1 ratio, as determined by ¹H NMR spectroscopic analysis. The diastereoisomers could be separated by column chromatography, albeit in variable and poor yield. Low conversions and poor diastereocontrol has been observed before in Heck reactions of β -alkoxyacrylonitriles²⁵ but, in our case, separation would not be required if the mixture could be converted directly to the target benzoylacetonitrile 6.

Surprisingly the hydrolysis of the enol ether diastereoisomeric mixture 7 required very forcing conditions. Simple treatment of the Heck reaction mixture with acid under ambient conditions failed to provide β -ketonitrile 6. The hydrolysis of related alkoxyacrylonitriles were notable, by their absence,



Table 1 Investigating conditions for Heck reaction of 3-iodoanisole and 3-methoxyacrylonitrile (**5**) to give benzoylacetone nitrile **6**

Entry	Base	Additive	Conditions ^a	Yield ^b (%)
1	K ₂ CO ₃	TBAB	Conductive heating, 90 °C, 24 h	36
2	NaHCO ₃	TBAB	Conductive heating, 90 °C, 24 h	34
3	K ₂ CO ₃	TBAB	Microwaves, ^c 130 °C, 1 h	26
4	K ₂ CO ₃	TBAB	Microwaves, ^c 130 °C, 1.5 h	20
5	NaHCO ₃	TBAB	Microwaves, ^c 130 °C, 1.5 h	37
6	NaHCO ₃	TBAB	Microwaves, ^c 140 °C, 1 h	19
7	K ₂ CO ₃	DPPP	Microwaves, ^c 150 °C, 1.5 h	31

^a Isolated yield of benzoylacetone nitrile **6**. ^b Reaction of 3-iodoanisole (1 equiv.), 3-methoxyacrylonitrile (**5**) (4 equiv.), Pd(OAc)₂ (10 mol%), base (2 equiv.) and additive (10 mol%) in MeCN–H₂O (3 : 1) under the given conditions, followed by aqueous work up, microwave irradiation in *c*HCl–MeOH (1 : 4) at 110 °C (hold time) for 30 min (by moderation of initial power, 150 W) and aqueous work up, followed by purification by column chromatography on silica. ^c Microwave irradiation in a sealed tube at the given temperature, as measured by the instrument's in-built IR sensor, for the given time (hold time) by moderation of the initial power (150 W).

from the study of Doucet and Santelli following Heck reaction of 3-ethoxyacrylonitrile, catalyzed by a tetraphosphane/palladium complex.²⁵ However, by resorting to more forcing conditions, gratifyingly, microwave irradiation of the isolated diastereoisomeric mixture **7** in *c*HCl–MeOH (1 : 4) at 110 °C for 30 min finally provided benzoylacetone nitrile **6** after purification by column chromatography but only in modest isolated yield over the two steps (Table 1, entry 1, 36%).

Efforts to improve the overall yield of this process by changing the base from K₂CO₃ to NaHCO₃, in accordance with Heck methods for the synthesis of cinnamionitriles,³⁴ carrying out the hydrolysis in *c*HCl–MeOH (1 : 4) under microwave irradiation as before (Table 1, entry 2), gave no improvement in yield (34%). Similarly, carrying out the Heck reaction in a sealed tube under microwave irradiation using K₂CO₃ at 130 °C for 1 h (entry 3) or 1.5 h (entry 4) was poorly efficient. The microwave-assisted reaction using NaHCO₃ at 130 °C for 1.5 h (entry 5) did give a modest yield of product (37%), similar to the longer conductive heating processes, but this was not improved further by raising the temperature of reaction to 140 °C (entry 6) or to 150 °C in the presence of an alternative additive DPPP (10 mol%) (entry 7). Although the route had been successful for the preparation of ketonitrile **6**, the need to isolate enol ether **7**, in order to carry out the hydrolysis under high-temperature conditions, and the modest yield for the overall process (entry 5 gave the best yield, at 37%) meant that an alternative route had to be sought.

Considering the original approach to RO3201195 (**1**) by Roche,²⁰ efforts were made to access ketonitrile **6** by a more traditional Claisen ester approach. Fischer esterification of 3-methoxybenzoic acid (**8**) in methanol using sulfuric acid as catalyst at reflux for 3 h gave methyl ester **9** in good yield (90%). This was improved further by carrying out the process in a sealed tube under microwave irradiation at 110 °C for 10 min to give methyl ester **9** in 94% yield (Scheme 1, bottom).

Table 2 Investigating conditions for base-mediated Claisen condensation of methyl benzoate **9** and acetonitrile to give benzoylacetone nitrile **6**

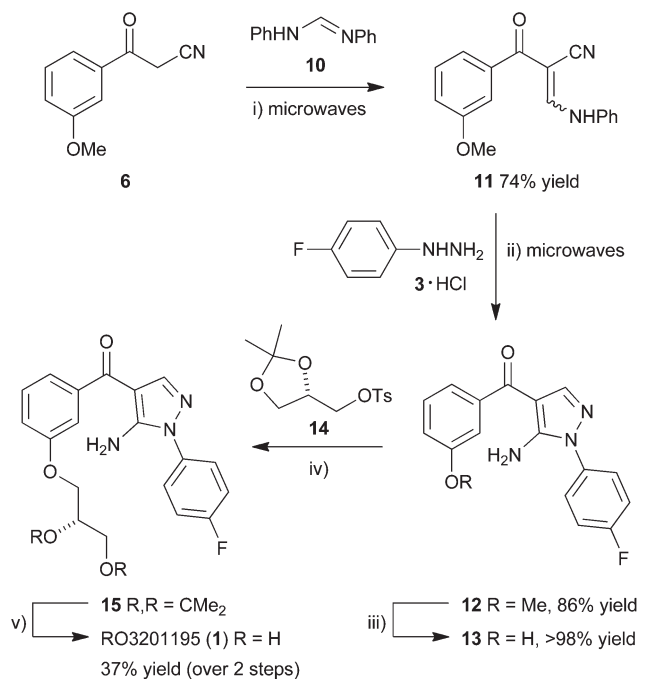
Entry	Base	Conditions	Yield ^a (%)
1	NaOEt	MeCN, RT; reflux, 24 h	9
2	NaOMe	MeCN, RT; reflux, 24 h	9
3	NaH	THF, reflux, 1 h	15
4 ^b	NaH	THF, microwaves, 150 °C, 1 h	35
5	NaH	PhMe, 90 °C, 16 h	34
6	LDA	THF, –78 °C, 1.5 h	18
7	LDA	THF, –50 °C, 3 h	70

^a Isolated yield of benzoylacetone nitrile **6** from methyl benzoate **9** after purification by column chromatography on silica. ^b Microwave irradiation in a sealed tube at the given temperature, as measured by the instrument's in-built IR sensor, for the given time (hold time) by moderation of the initial power.

A well-established method³⁵ for Claisen condensation using sodium ethoxide or sodium methoxide as base was frustrated by the almost immediate formation of a homogenous gelatinous mass and so a range of conditions were investigated (Table 2). Heating this mixture in acetonitrile at reflux for 24 h gave only a very low yield (9% in both cases) of the benzoylacetone nitrile **6** (entries 1 and 2) and significant return of unreacted ester and so alternative methods were employed. Carrying out the reaction using NaH in THF at reflux for 1.5 h gave an immediate improvement in efficiency and provided the condensation product **6** in 15% yield (entry 3), 35% yield if heated at 150 °C for 1 h in a sealed tube under microwave irradiation (entry 4). Changing the solvent to toluene and heating the mixture at 90 °C for 16 h gave a similar yield (entry 5, 34%). However, the use of freshly-prepared LDA as base at –50 °C in THF (entry 7) gave the Claisen condensation product **6** in good yield (70%), whereas at lower temperatures was inefficient (entry 6). Given the high yield and speed of the microwave-assisted esterification, this route now represented the quickest and most efficient means to access this key intermediate.

Considering our previous success in the use of microwave irradiation in cyclocondensation reactions for the preparation of pyrazoles,^{17,36,37} the aminopyrazole core motif of BIRB 796,³⁸ and pyrazolyl ketone libraries,^{22,39} benzoylacetone nitrile **6** was homologated in a microwave-assisted Knoevenagel condensation using *N,N'*-diphenylformamidinium (**10**) in xylenes at 180 °C for 20 min to give enaminone **11** in good yield (74%) (Scheme 2). Cyclocondensation by microwave irradiation with the hydrochloride salt of 4-fluorophenylhydrazine (**3**) in the presence of Et₃N in EtOH at 140 °C for 1 h gave 5-aminopyrazole **12** in superior yield (86%) to a range of other methods,³⁹ after purification by column chromatography. Protodemethylation using BBr₃ in CH₂Cl₂ (1 M) at RT overnight gave the corresponding phenol **13** in quantitative yield, which was reacted in a S_N2 displacement reaction with ketal-protected tosyl glycerate **14** under basic conditions. The reaction in DMF in the presence of K₂CO₃ at 80 °C for 24 h gave only a very low yield of product **15** (9%)³⁹ but switching to DMSO and carrying





Scheme 2 Microwave-assisted synthesis of RO3201195. Reagents and conditions: (i) xylenes, microwaves, 180 °C, 20 min; (ii) Et₃N, EtOH, 140 °C, 1 h; (iii) BBr₃ in CH₂Cl₂ (1 M), 0 °C–RT, 18 h; (iv) K₂CO₃, DMSO, 100 °C, 40 h; (v) TsOH, MeOH–H₂O, 50 °C, 18 h.

out the S_N2 displacement at a slightly higher temperature (100 °C) for prolonged period (40 h) gave phenyl ether 15 in improved yield (42%) after purification by column chromatography, followed by recrystallization. Submitting the product of tosylate displacement 15 to ketal deprotection directly, prior to recrystallization, under acid-catalyzed aqueous conditions at 50 °C for 18 h gave RO3201195 (1) in 37% yield over the two steps, after purification by column chromatography and recrystallization. The target inhibitor exhibited spectroscopic data that matched literature values.^{22,39} It was prepared in 15% overall yield in 7 separate steps from commercially-available material, three of them employing microwave irradiation, to provide rapid access to material suitable for examination in WS cells.

Due to limited supplies of primary WS fibroblasts, initial experiments to determine the effects of novel kinase inhibitors on cellular proliferation were performed using WS^{tert} cells (see materials and methods for a description of these cells). Despite being immortal, these telomerized cells retain the slow proliferation rate typical of primary WS cells and show a similar response to SB203580 treatment.¹⁴ Thus, these cells can be used to test the effects of modulators of the p38-signaling pathway prior to their use on primary cells.

WS^{tert} cells were grown in standard medium supplemented with SB203580 at a final concentration ranging from 10 nM to 50 μM (Fig. 2a). SB203580 inhibited p38α even at the lowest doses used of 10 nM with maximum inhibition seen at 1.0 μM and above (Fig. 2c), and has an IC₅₀ for p38α of approximately

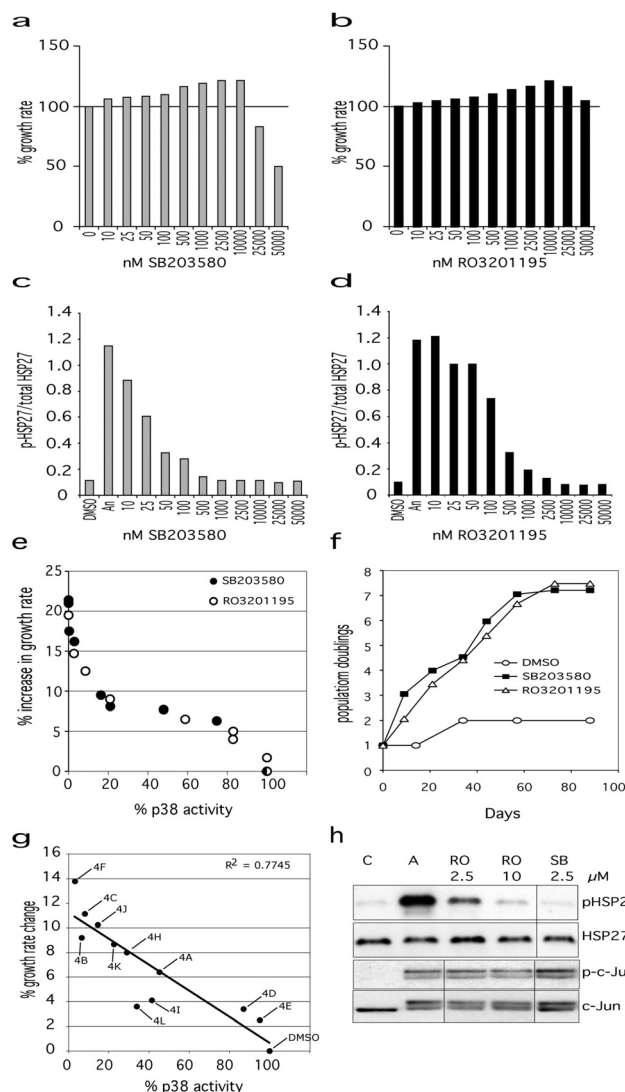


Fig. 2 Effects of p38α inhibitors on Werner syndrome cells. Effects of SB203580 (a) and RO3201195 (b) on the proliferation rate of WS^{tert} cells, with 100% representing the DMSO control. Titration curves for inhibition of p38α activity for SB203580 (c) and RO3201195 (d) measured as the ratio of phosphorylated HSP27 to total HSP27 (measured by ELISA). For (a) to (d) DMSO are control cells, 'An' are cells treated with anisomycin to activate p38α, 10 to 50 000 are cells treated with p38 inhibitors at the indicated concentration. (e) Plot of % p38α activity versus % increase in WS^{tert} cell proliferation rate for both SB203580 and RO3201195. (f) Proliferation of Werner syndrome AG05229 primary fibroblasts in the presence of SB203580 (2.5 μM) or RO3201195 (10 μM) measured as population doublings versus days. (g) Plot of % increase in proliferation rate of WS^{tert} cells against % p38α activity using pyrazolyl ketone library 4. See Table 3 for compound identities. (h) Immunoblot showing that neither SB203580 nor RO3201195 inhibit JNK at the optimal concentrations for their effects on cellular proliferation rates. C = DMSO control, A = cells treated with anisomycin to activate p38α and JNK, and the other three lanes show the effect of the given inhibitor concentrations in anisomycin-treated cells.

30 nM as measured by us, and others.^{40,41} SB203580 treatment resulted in an increased proliferation rate of the WS^{tert} cells compared to DMSO-treated control cells even at the lowest con-



centration used, with the effect on proliferation rate increasing steadily with increasing SB203580 concentration and reaching a maximum between 2.5 μM and 10 μM . When the level of p38 α activity was plotted against the effects upon proliferation rate a sigmoid curve was found (Fig. 2e). At 2.5 μM SB203580 resulted in an increase in proliferation rate of approximately 22% compared to DMSO controls (Fig. 2a and e).

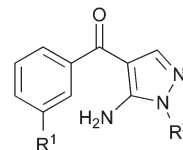
RO3201195 has an IC_{50} of approximately 190 nM with maximal inhibition between 2.5 and 10 μM .³⁹ In this work, RO3201195 inhibited p38 α at a minimum concentration of 25 nM, with the maximal effect seen at 10.0 μM (Fig. 2d). RO3201195 had an increasing effect on the proliferation rate of WS^{tert} cells up to 10.0 μM concentration, thereafter becoming inhibitory (Fig. 2b). As seen for SB203580, when the level of p38 α activity was plotted against the effects of RO3201195 upon proliferation rate a sigmoid curve was found (Fig. 2e); indeed the curve was essentially identical with the curve obtained using SB203580. The maximal increase seen in the proliferation rate of WS^{tert} cells was 19% at 10.0 μM (Fig. 2b and e).

The above data show that the optimal concentration of these inhibitors for the maximal effects on WS^{tert} cells are 2.5 μM for SB203580 and 10.0 μM for RO3201195. The inhibitors completely inhibited p38 α but did not inhibit total JNK activity in WS^{tert} cells at these concentrations as measured by analyzing the phosphorylation of their downstream targets HSP27 and c-Jun by immunoblot (Fig. 2h). WS^{tert} cells are stimulated with anisomycin that activates p38 α and JNKs as shown by the increased presence of the band in the A lane of the p-HSP27 panel, and the appearance of the doublet in the p-c-Jun and c-Jun panels (Fig. 2h). RO3201195 at 10.0 μM and SB203580 at 2.5 μM concentration reduced the p-HSP27 band to the level seen in the unstimulated control (C lane), but had no effect on the doublet seen in p-c-Jun and c-Jun.

We next used the p38 α inhibitors on the primary Werner syndrome fibroblast strain WAG05229 that was close to replicative senescence to determine their effects on cellular senescence. For SB203580 a concentration of 2.5 μM was used, whereas for RO3201195 10.0 μM concentration was employed, as these were the lowest concentrations that resulted in maximal proliferation rate and 100% p38 α inhibition (see Fig. 2). The cells were re-fed with DMEM containing the inhibitors as described previously.¹⁵ DMSO-treated fibroblasts proliferated very slowly and only achieved a single population doubling in the 88 days of the experiment (Fig. 2f). Inhibitor treated cells, however, had a much elevated proliferation rate, and managed approximately 7.5 population doublings prior to growth arrest (Fig. 2f). There was essentially no difference whichever inhibitor was used. Thus, as the effects of these inhibitors on WS cells are essentially identical and yet they show very different kinase specificity profiles at the concentrations used (the only common denominator being p38), the conclusion is that the effects on proliferation seen in both WS^{tert} cells and primary WS fibroblasts result from the inhibition of p38 α .

Table 3 Pyrazolyl ketone library 4 studied in WS^{tert} cells^a

4	R ¹	R ²
A	OMe	4-Iodophenyl
B ^b	OMe	4-Fluorophenyl
C	H	4-Fluorophenyl
D	H	4-Bromophenyl
E	H	2,6-Dichlorophenyl
F	H	2,4-Difluorophenyl
H	H	Phenyl
I	OMe	4-Tolyl
J	OMe	Methyl
K	H	4-Chloromethyl
L	OMe	4-Chloromethyl



^a See ref. 22 for preparation. ^b Corresponds with compound 12 from Scheme 2.

Finally, we used a pyrazolyl ketone library 4 (Table 3) of compounds related to RO3201195²² for their effects on the proliferation of WS^{tert} cells (Fig. 2g). These were used at a concentration of 1.5 μM that resulted in a varied degree of p38 α inhibition from approximately 5% to greater than 95% (Fig. 2g and ref. 22). When the effect on the proliferation rate of WS^{tert} cells by this pyrazolyl ketone library were plotted against the % p38 α activity (as assessed by ELISA²²), a linear response was seen (Fig. 2g), providing further support that these effects on cellular proliferation are due to p38 α inhibition.

The data presented in this paper showing that RO3201195 has essentially identical effects on the proliferation of WS cells as SB203580, and that the proliferation rate is dependent on p38 activity, provide very strong support that the prevention of premature senescence seen in WS fibroblasts by SB203580 reported previously¹³ is *via* p38 α signalling. If premature cellular senescence does underlie the accelerated ageing seen in WS individuals, these data also provide further support that the use of p38 inhibitors *in vivo* may alleviate this accelerated ageing.¹⁶ Finally, RO3201195 is shown to be a useful tool for the dissection of signalling pathways in human cells, as it is efficacious, relatively potent and is more kinase selective than SB203580.²⁰ In addition, it has shown therapeutic efficacy *in vivo* in rats in regulating cytokine production upon LPS challenge,²⁰ so may prove useful for future *in vivo* use.

Experimental

Materials and methods

Commercially available reagents were used without further purification; solvents were dried by standard procedures. Light petroleum refers to the fraction with bp 40–60 °C and ether refers to diethyl ether. Unless otherwise stated, reactions were performed under an atmosphere of air. Flash chromatography was carried out using Merck Kieselgel 60 H silica or Matrex silica 60. Analytical thin layer chromatography was carried out using aluminium-backed plates coated with Merck Kieselgel



60 GF₂₅₄ that were visualised under UV light (at 254 and/or 360 nm). Microwave irradiation experiments were performed in a sealed Pyrex tube using a self-tunable CEM Discover or CEM Explorer focused monomodal microwave synthesizer at the given temperature using the instrument's in-built IR temperature measuring device, by varying the irradiation power (initial power given in parentheses).

Fully characterized compounds were chromatographically homogeneous. Melting points were determined on a Kofler hot stage apparatus or Stanford Research Systems Optimelt and are uncorrected. Specific rotations were measured at the indicated temperature (in °C) using a ADP440 polarimeter (Bellingham + Stanley) at the sodium D line and are given in deg cm³ g⁻¹ dm⁻¹ with concentration *c* in 10⁻² g cm⁻³. Infrared spectra were recorded in the range 4000–600 cm⁻¹ on a Perkin-Elmer 1600 series FTIR spectrometer using an ATR probe or using KBr disks or as a nujol mull for solid samples and thin films between NaCl plates for liquid samples and are reported in cm⁻¹. NMR spectra were recorded using a Varian VNMRs instrument operating at 400 or 500 MHz or a Bruker Avance III 400 MHz for ¹H spectra and 101 or 126 MHz for ¹³C spectra; *J* values were recorded in Hz and multiplicities were expressed by the usual conventions. Low resolution mass spectra were determined using a Waters Q-TOF Ultima using electrospray positive ionization, a Waters LCT premier XE using atmospheric pressure chemical ionization (APCI), an Agilent 6130 single quadrupole with an APCI/electrospray dual source, a Fisons Instrument VG Autospec using electron ionization at 70 eV (low resolution) or a ThermoQuest Finnigan LCQ DUO electrospray, unless otherwise stated. TOFMS refers to time-of-flight mass spectrometry, ES refers to electrospray ionization, CI refers to chemical ionization (ammonia), FTMS refers to Fourier transform mass spectrometry, NSI refers to nano-electrospray ionization and EI refers to electron ionization. A number of high resolution mass spectra were obtained courtesy of the EPSRC Mass Spectrometry Service at University College of Wales, Swansea, UK using the ionization methods specified.

Synthetic procedures

3-Methoxybenzoylacetonitrile (6) by Claisen ester condensation using LDA as base (Table 2, entry 6). *n*-BuLi (2.5 M in hexanes; 5.3 mL, 13.2 mmol) was added dropwise to a stirred solution of DIPA (1.9 mL, 13.6 mmol) in dry THF (2 mL) at 0 °C under Ar, and the mixture was stirred at 0 °C for 10 min. In a separate flask, a solution of methyl 3-methoxybenzoate (9) (1.1 g, 6.6 mmol) and dry acetonitrile (0.5 mL, 9.5 mmol) in dry THF (5 mL) was cooled to –50 °C. The cold LDA solution was added dropwise and the reaction mixture was stirred at –50 °C for 3 h. Saturated aqueous NH₄Cl solution (10 mL) was then added. The solution was allowed to warm to room temperature, extracted with EtOAc (3 × 20 mL), washed with aqueous HCl solution (1 M; 20 mL) and brine (20 mL), dried (MgSO₄) and evaporated *in vacuo*. Purification by column chromatography on silica gel (dry load), gradient eluting with hexanes to EtOAc–hexanes (2:3), gave the *title compound*

(0.82 g, 70%) as a yellow solid, mp 86.3–87.4 °C (MeOH) (lit.,⁴² mp 87–88 °C) (Found [ES]: 198.0523. C₁₀H₉NO₂Na [MNa] requires 198.0525); IR (neat) ν_{max} /cm⁻¹ 2948 (CH str.), 2252 (C≡N str.), 1694 (C=O str.), 1580 (CC), 1451 (CH), 1258 (C–O), 1012 (C–O); ¹H NMR (500 MHz, CDCl₃) δ_{H} /ppm 7.49–7.41 (3H, 2-, 5- and 6-CH), 7.21 (1H, d, *J* = 8, 4-CH), 4.07 (2H, s, CH₂), 3.88 (3H, s, Me); ¹³C NMR (126 MHz, CDCl₃) δ_{C} /ppm 186.9 (C), 160.2 (3-C), 135.7 (1-C), 130.1 (5-CH), 121.2 (4-CH), 120.9 (6-CH), 113.6 (CN), 112.8 (2-CH), 55.6 (Me), 29.4 (CH₂); *m/z* (EI) 175 (M⁺, 36%), 135 ([M – CH₂CN]⁺, 100).

3-Methoxybenzoylacetonitrile (6) by Claisen ester condensation using NaH as base (Table 2, entry 5). NaH (60% dispersion in mineral oil; 0.49 g, 12.0 mmol) was added portionwise to a stirred solution of dry MeCN (0.65 mL, 20.3 mmol) in dry toluene (5 mL) at 0 °C under Ar, and the mixture was warmed to room temperature and stirred for 2 h. The reaction mixture was then cooled to 0 °C before dropwise addition of a solution of methyl 3-methoxybenzoate (9) (1.05 g, 6.3 mmol) in dry toluene (5 mL). Once complete, the solution was allowed to warm to room temperature and stirred at 90 °C for 16 h. After cooling, the reaction mixture was filtered and the filtrate was extracted with water (20 mL). The isolated solids were then dissolved in the aqueous extract, acidified to pH 3–4 using aqueous HCl solution (1 M), extracted with EtOAc (3 × 20 mL), dried (Na₂SO₄) and evaporated *in vacuo*. Purification by column chromatography on silica gel (dry load), gradient eluting with hexanes to EtOAc–hexanes (2:3), and recrystallization (EtOAc–hexanes) gave the *title compound* (0.36 g, 34%) as a colourless solid, mp 87.3–88.2 °C (EtOAc) (lit.,⁴² mp 87–88 °C), with identical spectroscopic properties.

3-Methoxybenzoylacetonitrile (6) by Heck coupling, followed by enol ether hydrolysis (Table 1). 3-Methoxyacrylonitrile (5) (0.28 g, 3.40 mmol) was added to a stirred solution of 3-iodoanisole (0.20 g, 0.86 mmol), base (1.71 mmol), tetrabutylammonium bromide (27 mg, 86 μ mol) and Pd(OAc)₂ (19 mg, 86 μ mol) in water–MeCN (3:1) (3 mL) under Ar and the mixture was heated at 90 °C for 20 h (entries 1 and 2) or irradiated at 130 °C or 140 °C for 1–1.5 h in a pressure-rated glass vial (10 mL) using a CEM Discover microwave synthesizer (entries 3–6) by moderating the initial power (150 W). After cooling, the solution was partitioned between water and EtOAc and the aqueous layer was further extracted with EtOAc (2 × 10 mL). The organic extracts were combined, washed with brine (20 mL), dried (Na₂SO₄) and evaporated *in vacuo*. The crude residue was dissolved in MeOH (2 mL) in air and concentrated HCl was added (10.2 M; 0.5 mL). The mixture was irradiated at 110 °C for 1 h in a pressure-rated glass vial (10 mL) using a CEM Discover microwave synthesiser by moderating the initial power (150 W). After cooling in a flow of compressed air, the solution was partitioned between water and EtOAc, and the aqueous layer was further extracted with EtOAc (2 × 10 mL). The organic extracts were combined, washed with brine (20 mL), dried and evaporated *in vacuo*. Purification by column chromatography on silica gel (dry load), gradient eluting with hexanes to EtOAc–hexanes (2:3), gave the *title compound* as a yellow solid, mp 87.0–87.6 °C



(MeOH) (lit.,⁴² mp 87–88 °C), with identical spectroscopic properties.

(E)- and (Z)-3-Methoxy-3-(3-methoxyphenyl)prop-2-enitrile (7) by Heck coupling. 3-Methoxyacrylonitrile (**5**) (0.72 g, 8.7 mmol) was added to a stirred solution of potassium carbonate (0.63 g, 4.5 mmol), tetrabutylammonium bromide (80 mg, 0.24 mmol), 3-iodoanisole (0.47 g, 2.0 mmol) and palladium acetate (50 mg, 0.20 mmol) in water–MeCN (4 : 1) (12 mL) under Ar and the solution was stirred at 90 °C for 24 h. After cooling, the solution was partitioned between water and EtOAc and the aqueous layer was further extracted with EtOAc (2 × 20 mL). The organic extracts were combined, washed with brine (20 mL), dried (Na₂SO₄) and evaporated *in vacuo*. Purification by column chromatography on silica gel (dry load), gradient eluting with hexanes to EtOAc–hexanes (15 : 85), gave the *title compounds* (0.26 g, 68%; Z : E (1 : 2)) as yellow oils [*R*_f 0.5 (Z)-7 and 0.3 (E)-7 in EtOAc–light petroleum (1 : 4)] (Found [ES]: 212.0679. C₁₁H₁₁NO₂Na [MNa] requires 212.0682; IR (neat) $\nu_{\max}/\text{cm}^{-1}$ 3069 (C–H str.), 2950 (C–H str.), 2198 (C≡N str.), 1605 (C=C str.), 1579 (C–C str.), 1437 (C–H bend), 1215 (C–O str.), 1117 (C–O str.), 1047 (C–O str.); ¹H NMR (500 MHz, CDCl₃) $\delta_{\text{H}}/\text{ppm}$ [(Z)-7] 7.31 (1H, t, *J* = 8, 5'-CH), 7.11 (1H, d, *J* = 8, 6'-CH), 7.06 (1H, s, 2'-CH), 7.00 (1H, d, *J* = 8, 3'-CH), 4.96 (1H, s, 2-CH), 4.24 (3H, s, 3-OMe), 3.84 (3H, s, 3'-OMe); $\delta_{\text{H}}/\text{ppm}$ [(E)-7] 7.40–7.33 (2H, 5',6'-CH), 7.30 (1H, s, 2'-CH), 7.03 (1H, d, *J* = 7, 4'-CH), 4.65 (1H, s, 2-CH), 3.85 (6H, app s, 3- and 3'-OMe); ¹³C NMR (126 MHz, CDCl₃) $\delta_{\text{C}}/\text{ppm}$ [(Z)-7] 170.9 (3-C), 159.7 (3'-C), 135.3 (1'-C), 129.7 (5'-CH), 118.9 (6'-CH), 117.3 (CN), 116.7 (4'-CH), 112.2 (2'-CH), 71.2 (2-CH), 59.6 (3-OMe), 55.4 (3'-OMe); $\delta_{\text{C}}/\text{ppm}$ [(E)-7] 173.0 (3-C), 159.4 (3'-C), 134.1 (1'-C), 129.5 (5'-CH), 120.3 (6'-CH), 118.4 (CN), 117.4 (4'-CH), 112.9 (2'-CH), 69.9 (2-CH), 56.8 (3-OMe), 55.4 (3'-OMe); *m/z* (EI) 189 (M⁺, 100%), 132 (29), 69 (39).

Methyl 3-methoxybenzoate (9) using conductive heating. A catalytic amount of concentrated H₂SO₄ (0.01 mL, 0.20 mmol) was added to a stirred solution of 3-methoxybenzoic acid (**8**) (1.48 g, 9.7 mmol) in MeOH (10 mL) and the mixture was stirred at reflux for 3 h. After cooling to room temperature, the solvent was evaporated *in vacuo* and the residue was partitioned between water and Et₂O. The ethereal solution was washed with saturated aqueous NaHCO₃ solution, dried (Na₂SO₄) and evaporated *in vacuo* to give the *title compound* (1.45 g, 90%) as a colourless oil (Found [ES]: 189.0520. C₉H₁₀O₃Na [MNa] requires 189.0522; IR (neat) $\nu_{\max}/\text{cm}^{-1}$ 2953 (C–H str.), 1718 (C=O str.), 1601 (CC str.), 1276 (C–O str.), 1221 (C–O str.); ¹H NMR (500 MHz, CDCl₃) $\delta_{\text{H}}/\text{ppm}$ 7.64 (1H, d, *J* = 8, 6-CH), 7.57 (1H, br. s, 2-CH), 7.35 (1H, t, *J* = 8, 5-CH), 7.11 (1H, dd, *J* = 8, 2, 4-CH), 3.92 (3H, s, CO₂Me), 3.86 (3H, s, OMe); ¹³C NMR (126 MHz, CDCl₃) $\delta_{\text{C}}/\text{ppm}$ 166.9 (C), 159.6 (3-C), 131.5 (1-C), 129.3 (5-CH), 122.0 (6-CH), 199.5 (4-CH), 144.0 (2-CH), 55.4 (OMe), 52.1 (CO₂Me); *m/z* (EI): 166 (M⁺, 14%), 135 ([M – OMe]⁺, 39), 93 (100).

Methyl 3-methoxybenzoate (9) using microwave irradiation. A catalytic amount of concentrated H₂SO₄ (0.01 mL, 0.20 mmol) was added to a stirred solution of 3-methoxy-

benzoic acid (**8**) (1.48 g, 9.7 mmol) in MeOH (10 mL) and the mixture was irradiated at 110 °C for 10 min in a pressure-rated glass tube (35 mL) using a CEM Discover microwave synthesizer by moderating the initial power (200 W). After cooling in a flow of compressed air, the solvent was evaporated *in vacuo* and the residue was partitioned between water and Et₂O. The ethereal solution was washed with saturated aqueous NaHCO₃ solution, dried (Na₂SO₄) and evaporated *in vacuo* to give the *title compound* (1.52 g, 94%) as a colourless oil, with identical physical and spectroscopic properties.

2-(3-Methoxybenzoyl)-3-(phenylamino)acrylonitrile (11). A solution of 3-methoxybenzoylacetonitrile (**6**) (0.20 g, 1.1 mmol) and *N,N'*-diphenylformamidine (**10**) (0.24 g, 1.2 mmol) in dry xylenes (7.5 mL) was irradiated at 180 °C under Ar for 20 min in a pressure-rated glass tube (35 mL) using a CEM Discover microwave synthesizer by moderating the initial power (200 W). After cooling in a stream of compressed air, the solution was diluted with hexanes to give a precipitate. Isolation by gravity filtration gave the *title compound* (0.23 g, 74%) as a colourless solid, mp 107.4–108.8 °C (lit.,²² mp 105 °C) (Found [ES]: 279.1126. C₁₇H₁₅N₂O₂ [MH] requires 279.1128; IR (neat) $\nu_{\max}/\text{cm}^{-1}$ 3062 (C–H str.), 2921 (C–H str.), 2204 (C≡N str.), 1634 (C=O str.), 1596 (N–H bend), 1571 (C–C str.), 1392 (C–C str.), 1313 (C–N str.), 1225 (C–O str.), 1044 (C–O str.), 990 (C–H bend), 867 (N–H wag); ¹H NMR (500 MHz, CDCl₃) $\delta_{\text{H}}/\text{ppm}$ 12.76 (1H, d, *J* = 12, NH), 8.06 (1H, d, *J* = 12, 3-CH), 7.57 (1H, d, *J* = 8, 6'-CH), 7.46 (3H, m, 2', 3", and 5"-CH), 7.40 (1H, t, *J* = 8, 5'-CH), 7.30 (1H, m, 4"-CH), 7.23 (2H, d, *J* = 8, 2"- and 6"-CH), 7.11 (1H, d, *J* = 8, 6'-CH), 3.89 (3H, s, Me); ¹³C NMR (126 MHz, CDCl₃) $\delta_{\text{C}}/\text{ppm}$ 192.1 (C), 159.6 (3'-C), 154.1 (3-CH), 139.2 (1'-C), 138.1 (1"-C), 130.2 (3", 5"-CH), 129.4 (5'-CH), 126.6 (4"-CH), 120.5 (6'-CH), 120.3 (1-CN), 118.9 (4'-CH), 117.9 (2", 6"-CH), 112.7 (2'-CH), 83.5 (2-C), 55.5 (Me); *m/z* (EI): 278 (M⁺, 49%), 277 ([M – H]⁺, 100), 135 (52).

[5-Amino-1-(4-fluorophenyl)-1H-pyrazol-4-yl]-3-methoxyphenyl ketone (12). A mixture of 2-(3-methoxybenzoyl)-3-(phenylamino)acrylonitrile (**11**) (0.13 g, 0.46 mmol), 4-fluorophenylhydrazine hydrochloride (3-HCl) (73 mg, 0.47 mmol) and triethylamine (20 μL , 140 μmol) in ethanol (3 mL) was irradiated at 140 °C for 1 h in a pressure-rated glass vial (10 mL) using a CEM Discover microwave synthesizer by moderating the initial power (150 W). After cooling in a stream of compressed air, the solvent was evaporated *in vacuo*. Purification by column chromatography on silica gel (dry load), gradient eluting with hexanes to EtOAc–hexanes (3 : 7), gave the *title compound* (0.11 g, 86%) as a pink solid, mp 130.1–132.0 °C (Found [ES]: 312.1138. C₁₇H₁₅FN₃O₂ [MH] requires 312.1143; IR (neat) $\nu_{\max}/\text{cm}^{-1}$ 3318 (N–H str.), 2925 (C–H str.), 1610 (C=O str.), 1595 (N–H bend), 1539 (C–C str.), 1286 (C–N str.), 1223 (C–O str.), 1051 (C–O str.), 838 (N–H wag); ¹H NMR (400 MHz, CDCl₃) $\delta_{\text{H}}/\text{ppm}$ 7.81 (1H, s, 3-CH), 7.56 (2H, m, 2', 6'-CH), 7.42 (2H, m, 5", 6"-CH), 7.35 (1H, s, 2"-CH), 7.25 (2H, m, 3', 5'-CH), 7.11 (1H, m, 4"-CH), 6.04 (2H, bs, exch. D₂O, NH₂), 3.89 (3H, s, Me); ¹³C NMR (101 MHz, CDCl₃) $\delta_{\text{C}}/\text{ppm}$ 189.4 (C), 162.2 (d, ¹*J*_{CF} = 250, 4'-CF), 159.8 (3"-C), 150.6 (5-C), 142.0 (3-CH), 141.1 (1"-C), 133.3 (d, ⁴*J*_{CF} = 4, 1'-C), 129.5



(5''-CH), 126.1 (d, $^3J_{CF}$ = 9, 2', 6'-CH), 120.7 (6''-CH), 117.8 (4''-CH), 116.9 (d, $^2J_{CF}$ = 23, 3', 5'-CH), 113.0 (2''-CH), 104.8 (4-C), 55.4 (OMe); m/z (APCI) 312 (MH^+ , 100%).

[5-Amino-1-(4-fluorophenyl)-1H-pyrazol-4-yl]-3-hydroxyphenyl ketone (13). Boron tribromide solution (1 M in CH_2Cl_2 ; 1.7 mL, 1.70 mmol) was added dropwise to a solution of [5-amino-1-(4-fluorophenyl)-1H-pyrazol-4-yl]-3-methoxyphenyl ketone (12) (0.10 g, 0.34 mmol) in dry CH_2Cl_2 (1 mL) at 0 °C under Ar. The mixture was allowed to warm to room temperature and stirred for 20 h. Water (15 mL) was then added cautiously and the mixture was extracted with EtOAc (3 × 15 mL). The organic extracts were combined, washed with brine, dried ($MgSO_4$) and evaporated *in vacuo* to give the *title compound* (0.10 g, quant.) as a brown solid, mp 192.2–194.9 °C (Found [ES]: 298.0984. $C_{16}H_{13}FN_3O_2$ [MH] requires 298.0986); IR (neat) ν_{max}/cm^{-1} 3320 (N–H str.), 3204 (br. O–H), 3072 (C–H str.), 1610 (C=O str.), 1592 (N–H bend), 1538 (C–C str.), 1310 (C–N str.), 1126 (C–O str.), 841 (N–H wag); 1H NMR (500 MHz, CD_3OD) δ_H/ppm 7.78 (1H, s, 3-CH), 7.59 (2H, m, 2', 6'-CH), 7.37–7.29 (3H, 3', 5'- and 5''-CH), 7.23 (1H, d, J = 7, 6''-CH), 7.18 (1H, s, 2''-CH), 7.00 (1H, dd, J = 7, 1, 4''-CH); ^{13}C NMR (100 MHz, CD_3OD) δ_C/ppm 191.6 (C), 164.1 (d, $^1J_{CF}$ = 247, 4'-CF), 159.2 (3''-C), 153.4 (5-C), 143.6 (3-CH), 142.7 (1''-C), 135.0 (d, $^4J_{CF}$ = 3, 1'-C), 131.1 (5''-CH), 128.5 (d, $^3J_{CF}$ = 9, 2', 6'-CH), 120.6 (6''-CH), 120.1 (4''-CH), 118.0 (d, $^3J_{CF}$ = 24, 3', 5'-CH), 116.0 (2''-CH), 105.7 (4-C); m/z (EI) 297 (M^+ , 91%), 296 ($[M - H]^+$, 100), 204 (31).

5-Amino-1-(4-fluorophenyl)-4-{3-[2(S)-3-dihydroxypropoxy]-benzoyl}pyrazole (RO3201195) (1). (S)-2,2-Dimethyl-1,3-dioxolan-4-ylmethyl *p*-toluenesulfonate (14) (0.60 mL, 2.5 mmol) and anhydrous K_2CO_3 (0.59 g, 4.25 mmol) were added to a solution of [5-amino-1-(4-fluorophenyl)-1H-pyrazol-4-yl]-3-hydroxyphenyl ketone (13) (0.48 g, 1.61 mmol) in dry DMSO (15 mL) under argon and the mixture was heated at 100 °C for 40 h. After cooling, the solution was diluted with water (25 mL) and extracted with EtOAc (3 × 20 mL). The organic extracts were combined, washed with brine, dried ($MgSO_4$) and evaporated *in vacuo*. Purification by column chromatography on silica gel (dry load), gradient eluting with light petroleum to EtOAc–light petroleum (2:3), gave [5-amino-1-(4-fluorophenyl)-1H-pyrazol-4-yl] {3-[(R)-2,2-dimethyl-1,3-dioxolan-4-yl]-methoxy}phenyl ketone (15), which was dissolved in MeOH–water (4:1) (4 mL). *p*-Toluene sulfonic acid monohydrate (40 mg, 0.21 mmol) was added and the solution was heated at 50 °C for 18 h. After cooling, the solvent was evaporated *in vacuo*. The residue was dissolved in EtOAc, washed with saturated aqueous $NaHCO_3$ solution, dried ($MgSO_4$) and evaporated *in vacuo*. Purification by column chromatography on silica gel (dry load), gradient eluting with light petroleum to EtOAc, followed by recrystallization (EtOAc–hexanes) gave the *title compound* (0.22 g, 37%) as a colourless solid, mp 154.1–154.6 °C (EtOAc) (Found [ES]: 372.1353. $C_{19}H_{19}FN_3O_4$ [MH] requires 372.1354); $[\alpha]_D^{21}$ –28 (c 0.2, EtOAc); $[\alpha]_D^{22}$ + 6.5 (c 0.6, MeOH); IR (neat) ν_{max}/cm^{-1} 3440 (N–H str.), 3330 (O–H str.), 3229 (O–H str.), 2896 (C–H str.), 1633 (C=O str.), 1597 (NH₂ str.), 1540 (C=N str.), 1498 (C–C str.), 1292 (C–O str.),

1222 (C–F str.), 1053 (C–O str.), 839 (NH₂ wag.); 1H NMR (500 MHz, d_6 -DMSO) δ_H/ppm 7.80 (1H, s, 3H), 7.61 (2H, m, 2', 6'-CH), 7.47–7.37 (3H, 3', 4'- and 5''-CH), 7.33 (1H, d, J = 7, 6''-CH), 7.25 (1H, m, 2''-CH), 7.14 (3H, 4''-CH and NH₂), 4.95 (1H, bs, CHOH), 4.65 (1H, bs, CH₂OH), 4.09 (1H, m, OCHH), 3.95 (1H, m, OCHH), 3.82 (1H, m, CHOH), 3.47 (2H, d, J = 5, CH₂OH); ^{13}C NMR (126 MHz, d_6 -DMSO) δ_C/ppm 187.5 (C), 161.1 (d, $^1J_{CF}$ = 244, 4'-C), 158.7 (3''-C), 151.2 (5-C), 141.4 (3-CH), 140.9 (1''-C), 133.7 (d, $^4J_{CF}$ = 3, 1'-C), 129.6 (5''-CH), 126.4 (d, $^3J_{CF}$ = 9, 2', 6'-CH), 120.1 (6''-CH), 117.8 (4''-CH), 116.3 (d, $^2J_{CF}$ = 23, 3', 5'-CH), 113.3 (2''-CH), 103.5 (4-C), 69.9 (CHOH), 69.8 (CH₂O), 62.6 (CH₂OH); m/z (EI) 371 (M^+ , 10%), 325 (33), 160 (100).

Cells and cell growth

Human adult dermal primary Werner syndrome AG05229 and AG03141 fibroblasts were obtained from the Coriell Cell Repositories (Camden, NJ, USA). WS^{tert} cells are AG03141 fibroblasts that have been immortalised by the ectopic expression of human enzyme telomerase and have been described previously.¹⁴

Cells were grown in DMEM growth medium as previously described.¹⁵ Cell proliferation rates for the WS^{tert} cells were measured as cumulated population doublings (CPDs) divided by the number of days of the experiment concerned and expressed as a percentage of the proliferation rate of control cells (with the control being 100%). The number of CPDs achieved at each passage of the cells was calculated according to the formula: PDs = $\log(N_t/N_0)/\log 2$, where N_t is number of cells counted and N_0 is number of cells seeded. For primary cells the CPDs were plotted *versus* days in culture. For assessing the effects of the various kinase inhibitors the culture medium was supplemented with the inhibitor dissolved in DMSO, with the medium being replaced daily. For controls an equivalent volume of the inhibitor solvent (DMSO) was added to the medium.

P38 inhibitor assay

The ability of SB203580 and RO3201195 to inhibit the p38 α signalling pathway was tested in human immortalised HCA2 cells using an ELISA system (obtained from Cell Signalling, NEB, UK) as previously described.³⁹ Kinase activity was detected using antibodies specific for HSP27 and its phosphorylated form, the degree of activation being measured as the ratio of phospho-protein/total protein (Fig. 2d and e). In this system activation of p38 α by anisomycin activates the kinase MK2 that then phosphorylates the small heat shock protein HSP27. As MK2 is the major HSP27 kinase,⁴³ the activity of p38 α can be assessed by the phosphorylation status of HSP27.

Immunoblot assays for stress kinase activity in WS cells

The ability of SB203580 and RO3201195 to inhibit the p38 α and JNK signalling pathways in WS^{tert} cells was tested by immunoblot detection of the phosphorylated versions of their



downstream targets HSP27 (pHSP27) and c-Jun (p-c-Jun) as previously described.^{15,44}

EPSRC Mass Spectrometry Service at the University of Wales, Swansea UK for mass spectra.

Conclusions

This manuscript describes the chemical synthesis and biological evaluation of a p38 α MAPK inhibitor, RO3201195 (**1**), in WS cells. Two complementary routes for the chemical synthesis of a key intermediate, benzoylacetone nitrile **6**, are described, both of them involving the use of microwave dielectric heating for rapid reaction kinetics. Of these two routes, a classical approach based upon a Claisen ester condensation was found to be the most efficient. The benzoylacetone nitrile intermediate **6** was transformed by Knoevenagel condensation, followed by cyclocondensation with a hydrazine, both under microwave irradiation, to give the core pyrazole motif. Phenoxide alkylation by S_N2 displacement of tosylate, followed by ketal deprotection, gave the target inhibitor in a sequence of 7 steps and 15% overall yield.

The effects of RO3201195 (**1**) on cellular proliferation were first examined using WS^{tert} cells, where it was found that the inhibitor elicited a very similar response to the prototypical p38 MAPK inhibitor SB203580. The maximal increase seen in the proliferation rate of WS^{tert} cells was 19% at 10.0 μ M concentration of RO3201195 (**1**). At this concentration, the inhibitor completely inhibited p38 α but did not inhibit total JNK activity in WS^{tert} cells, as determined by immunoblot assay. Following these findings, the cellular senescence of primary Werner syndrome fibroblast strain WAG05229 was investigated on treatment with SB203580 or RO3201195 (**1**). Despite the fact that these inhibitors showed very different kinase specificity profiles at the concentrations used, the effects on WS cells were essentially identical. Thus, we concluded that the effects on proliferation of treating WS^{tert} cells or primary WS fibroblasts with SB203580 or RO3201195 (**1**) resulted from inhibition of p38 α . This was further supported by studying the effects of a pyrazolyl ketone library on WS^{tert} cells at a given concentration, which showed a linear relationship between the proliferation rate and % p38 α activity. Thus, we conclude RO3201195 (**1**) is a useful chemical tool for dissecting signalling pathways in human cells in order to understand the effect of p38 MAPK signalling upon cell proliferation in this human progeroid syndrome.

Acknowledgements

We thank the EPSRC-BBSRC-MRC sponsored network SMS-Drug (EP/I037229/1; award to MCB), EPSRC (studentship award to JED), Saudi Cultural Bureau (support for MB), BBSRC (BB/D524140/1; award to DK, MCB and TD), SPARC (awards to MCB and TD), ESRC under the New Dynamics of Ageing Initiative (RES-356-25-0024; award to MCB, DK and TD) and the R M Phillips Trust (award to MCB) for support of this work and Dr Alaa Abdul-Sada at the University of Sussex and the

Notes and references

- J. C. Lee, J. T. Laydon, P. C. McDonnell, T. F. Gallagher, S. Kumar, D. Green, D. McNulty, M. J. Blumenthal, J. R. Heys, S. W. Landvatter, *et al.*, *Nature*, 1994, **372**, 739.
- G. L. Schieven, *Curr. Top. Med. Chem.*, 2005, **5**, 921.
- E. Salgado, J. R. Maneiro, L. Carmona and J. J. Gomez-Reino, *Ann. Rheum. Dis.*, 2014, **73**, 871.
- M. Back and G. K. Hansson, *Nat. Rev. Cardiol.*, 2015, **12**, 199–211.
- V. Grossi, A. Peserico, T. Tezil and C. Simone, *World J. Gastroenterol.*, 2014, **20**, 9744.
- K. Yumoto, M. R. Eber, J. E. Berry, R. S. Taichman and Y. Shiozawa, *Clin. Cancer Res.*, 2014, **20**, 3384.
- C. Dominguez, D. A. Powers and N. Tamayo, *Curr. Opin. Drug Discovery Dev.*, 2005, **8**, 421.
- D. J. Diller, T. H. Lin and A. Metzger, *Curr. Top. Med. Chem.*, 2005, **5**, 953.
- D. M. Goldstein and T. Gabriel, *Curr. Top. Med. Chem.*, 2005, **5**, 1017.
- S. T. Wroblewski and A. M. Doweyko, *Curr. Top. Med. Chem.*, 2005, **5**, 1005.
- J. Saklatvala, *Curr. Opin. Pharmacol.*, 2004, **4**, 372.
- D. Kipling, T. Davis, E. L. Ostler and R. G. Faragher, *Science*, 2004, **305**, 1426.
- T. Davis, D. M. Baird, M. F. Haughton, C. J. Jones and D. Kipling, *J. Gerontol., Ser. A*, 2005, **60**, 1386.
- T. Davis, M. F. Haughton, C. J. Jones and D. Kipling, *Ann. N. Y. Acad. Sci.*, 2006, **1067**, 243.
- T. Davis and D. Kipling, *Biogerontology*, 2009, **10**, 253.
- T. Davis and D. Kipling, *Rejuvenation Res.*, 2006, **9**, 402.
- M. C. Bagley, T. Davis, M. J. Rokicki, C. S. Widdowson and D. Kipling, *Future Med. Chem.*, 2010, **2**, 193.
- J. Bain, L. Plater, M. Elliott, N. Shpiro, C. J. Hastie, H. McLauchlan, I. Klevernic, J. S. Arthur, D. R. Alessi and P. Cohen, *Biochem. J.*, 2007, **408**, 297.
- K. Godl and H. Daub, *Cell Cycle*, 2004, **3**, 393.
- D. M. Goldstein, T. Alfredson, J. Bertrand, M. F. Browner, K. Clifford, S. A. Dalrymple, J. Dunn, J. Freire-Moar, S. Harris, S. S. Labadie, J. La Fargue, J. M. Lapierre, S. Larrabee, F. Li, E. Papp, D. McWeeney, C. Ramesha, R. Roberts, D. Rotstein, B. San Pablo, E. B. Sjogren, O. Y. So, F. X. Talamas, W. Tao, A. Trejo, A. Villasenor, M. Welch, T. Welch, P. Weller, P. E. Whiteley, K. Young and S. Zipfel, *J. Med. Chem.*, 2006, **49**, 1562.
- M. C. Bagley, T. Davis, P. G. S. Murziani, C. S. Widdowson and D. Kipling, *Pharmaceuticals*, 2010, **3**, 1842.
- M. C. Bagley, T. Davis, M. C. Dix, P. G. Murziani, M. J. Rokicki and D. Kipling, *Future Med. Chem.*, 2010, **2**, 203.
- T. Mizoroki, K. Mori and A. Ozaki, *Bull. Chem. Soc. Jpn.*, 1971, **44**, 581.

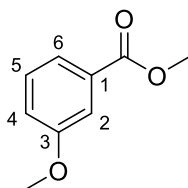


- 24 R. F. Heck and J. P. Nolley, *J. Org. Chem.*, 1972, **37**, 2320.
- 25 A. Battace, M. Feuerstein, M. Lemhadri, T. Zair, H. Doucet and M. Santelli, *Eur. J. Org. Chem.*, 2007, 3122.
- 26 M. Beller and T. H. Riermeier, *Tetrahedron Lett.*, 1996, **37**, 6535.
- 27 T. Sakamoto, Y. Kondo, Y. Kashiwagi and H. Yamanaka, *Heterocycles*, 1988, **27**, 257.
- 28 N. A. Cortese, C. B. Ziegler, B. J. Hrncic and R. F. Heck, *J. Org. Chem.*, 1978, **43**, 2952.
- 29 A. F. Littke and G. C. Fu, *J. Am. Chem. Soc.*, 2001, **123**, 6989.
- 30 C. M. Andersson, A. Hallberg and G. D. Daves, *J. Org. Chem.*, 1987, **52**, 3529.
- 31 T. Jeffery, *J. Chem. Soc., Chem. Commun.*, 1984, 1287.
- 32 S. Cacchi, P. G. Ciattini, E. Morera and G. Ortari, *Tetrahedron Lett.*, 1987, **28**, 3039.
- 33 T. Jeffery, *Tetrahedron*, 1996, **52**, 10113.
- 34 H. Zhao, M.-Z. Cai and C.-Y. Peng, *Synth. Commun.*, 2002, **32**, 3419.
- 35 J. B. Dorsch and S. M. McElvain, *J. Am. Chem. Soc.*, 1932, **54**, 2960.
- 36 M. C. Bagley, M. C. Lubinu and C. Mason, *Synlett*, 2007, 704.
- 37 M. C. Bagley, M. Baashen, V. L. Paddock, D. Kipling and T. Davis, *Tetrahedron*, 2013, **68**, 8429.
- 38 M. C. Bagley, T. Davis, M. C. Dix, C. S. Widdowson and D. Kipling, *Org. Biomol. Chem.*, 2006, **4**, 4158.
- 39 M. C. Bagley, T. Davis, M. C. Dix, P. G. Murziani, M. J. Rokicki and D. Kipling, *Bioorg. Med. Chem. Lett.*, 2008, **18**, 3745.
- 40 S. P. Davies, H. Reddy, M. Caivano and P. Cohen, *Biochem. J.*, 2000, **351**, 95.
- 41 K. Godl, J. Wissing, A. Kurtenbach, P. Habenberger, S. Blencke, H. Gutbrod, K. Salassidis, M. Stein-Gerlach, A. Missio, M. Cotten and H. Daub, *Proc. Natl. Acad. Sci. U. S. A.*, 2003, **100**, 15434.
- 42 C. Ota, S. Kumata and S. Kawaguchi, *EP 1544202A1*, 2005, 56–57.
- 43 J. X. Shi, X. Su, J. Xu, W. Y. Zhang and Y. Shi, *Am. J. Physiol.: Lung Cell. Mol. Physiol.*, 2012, **302**, L793.
- 44 T. Davis, M. C. Dix, M. J. Rokicki, A. J. C. Brook, C. S. Widdowson, D. Kipling and M. C. Bagley, *Chem. Cent. J.*, 2011, **5**, 83.



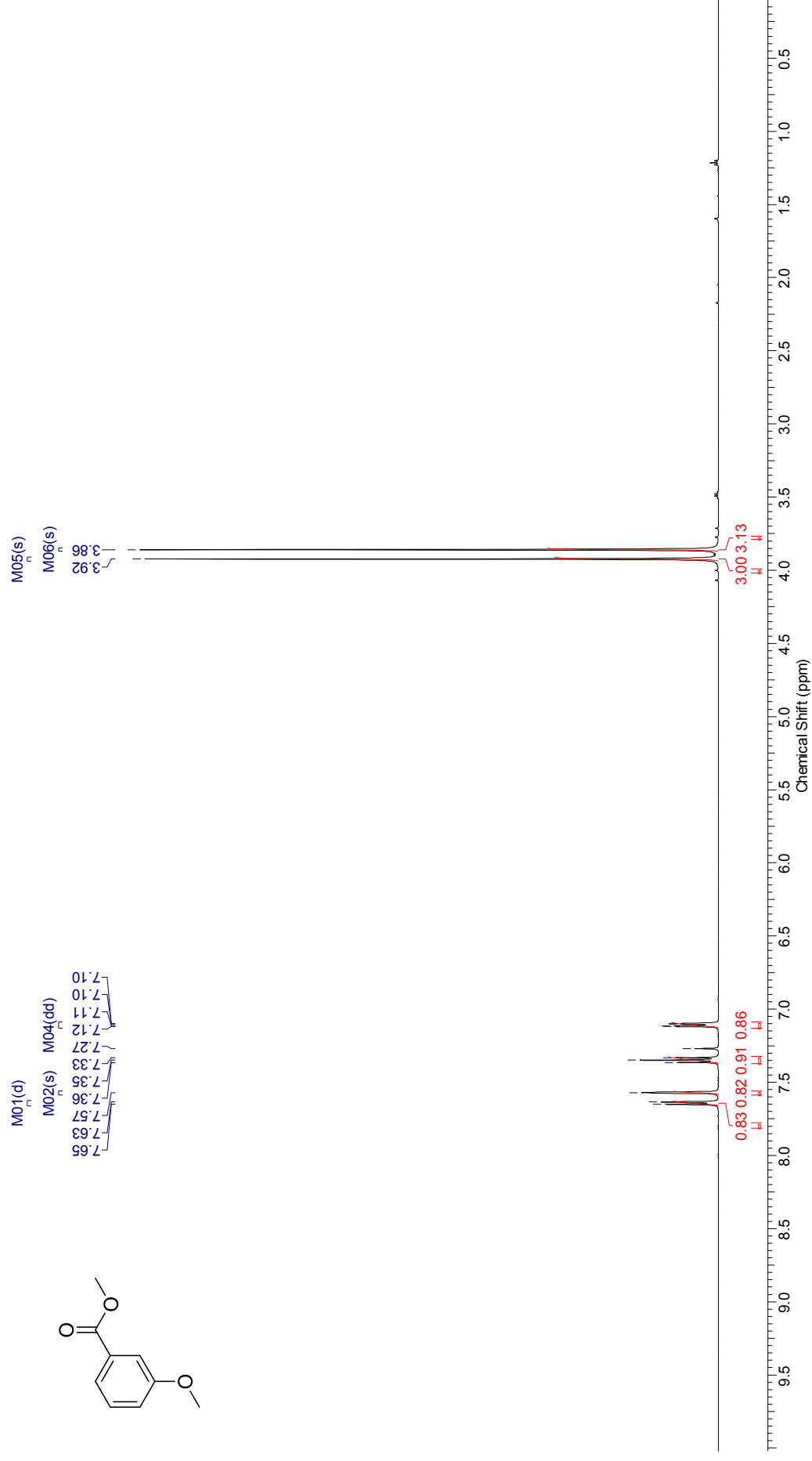
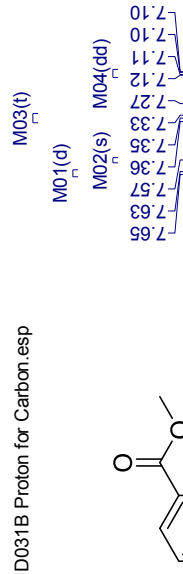
Chapter 2: ^1H NMR, ^{13}C NMR, IR and Mass spectra

Methyl 3-methoxybenzoate (123)



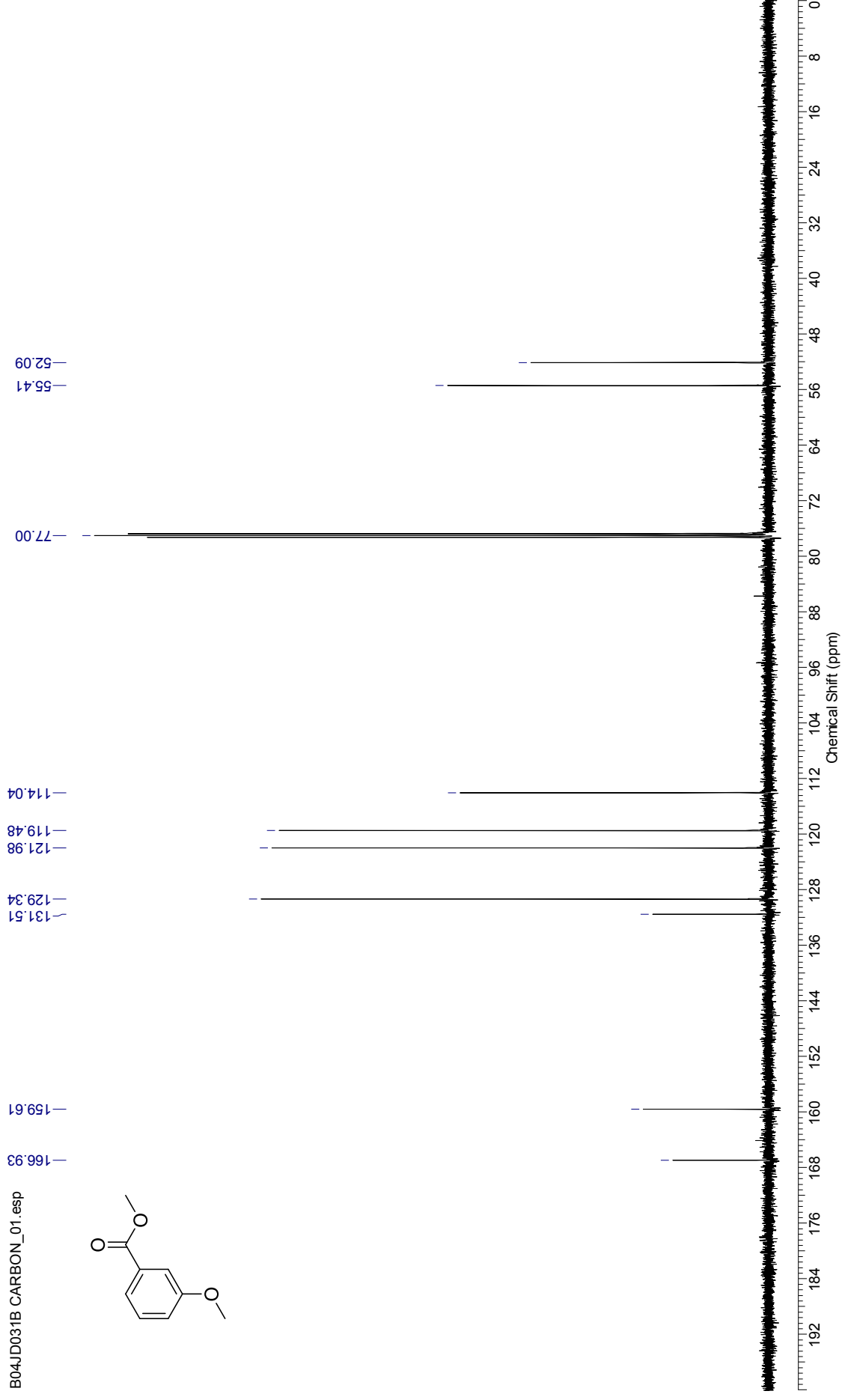
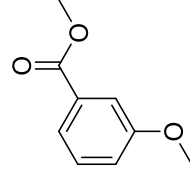
¹H NMR Spectrum (500 MHz, CDCl₃) for methyl 3-methoxybenzoate

B04JD031B Proton for Carbon.esp



¹³C NMR spectrum (126 MHz, CDCl₃) for methyl 3-methoxybenzoate

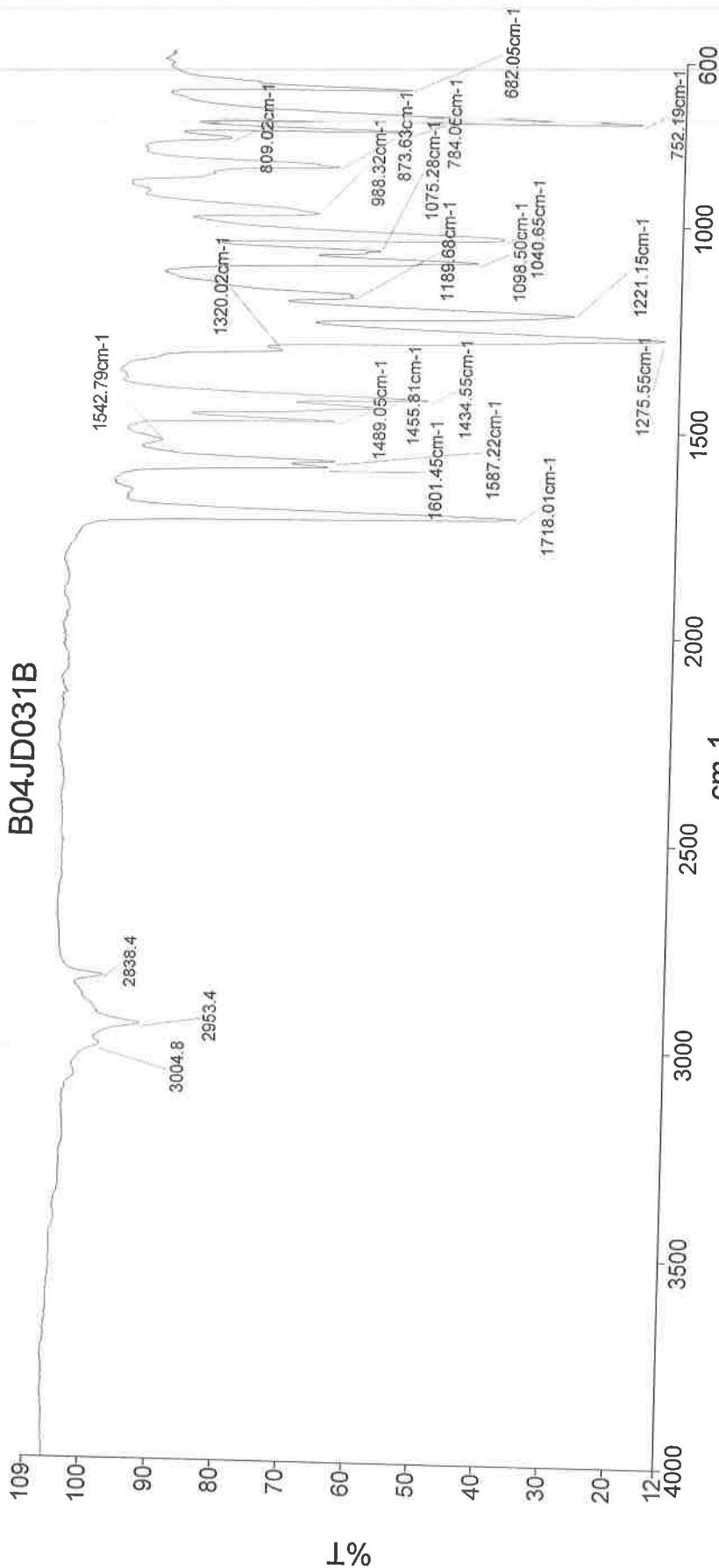
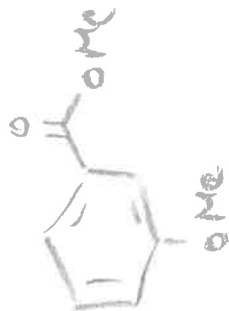
B04JD031B CARBON_01.esp



Analyst
Date

Administrator
28 May 2015 14:39

B04JD031B

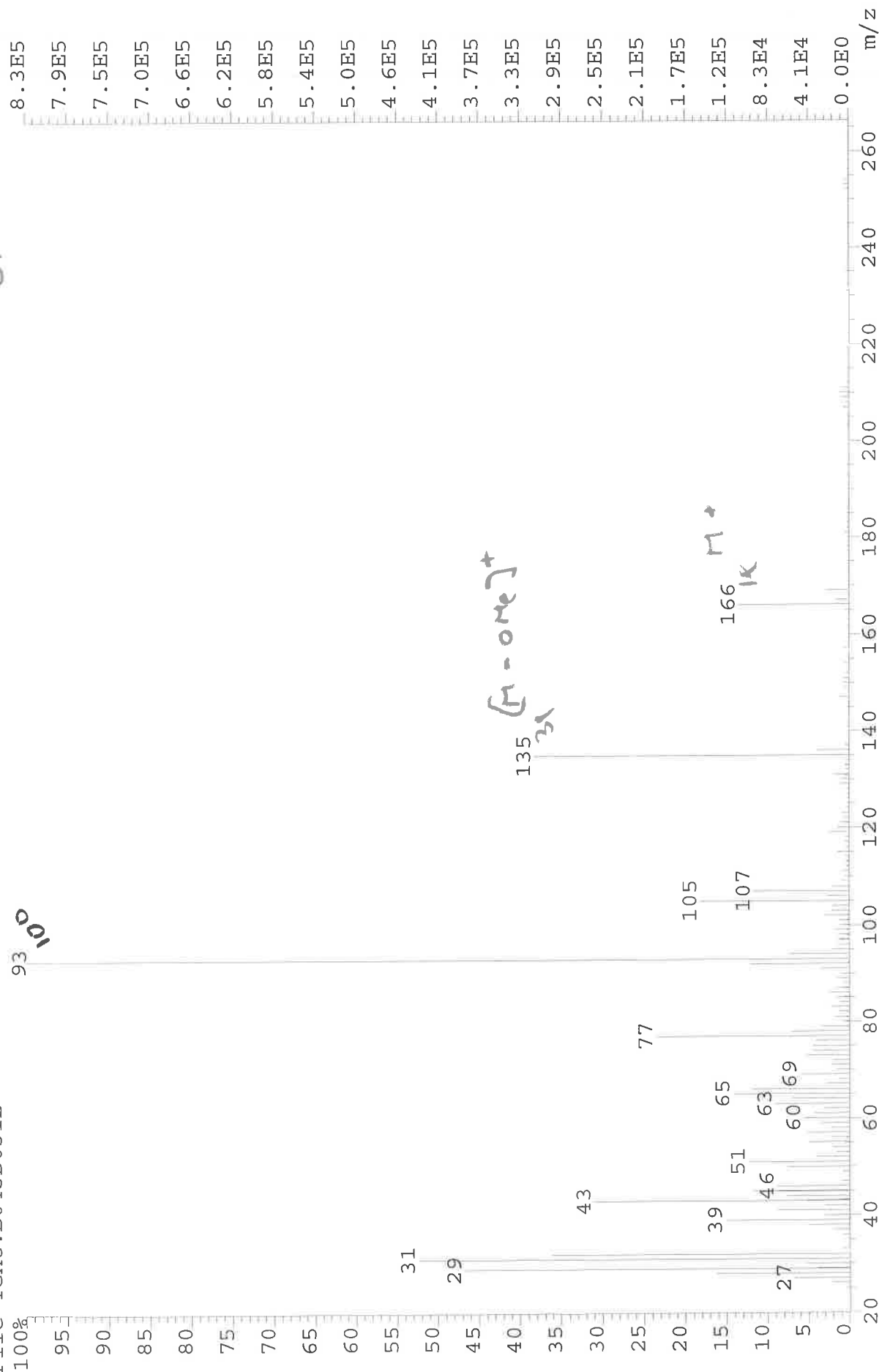
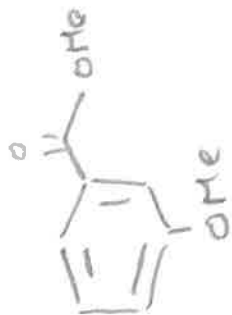


Absorption

2953
1718
1601 (1587)
1555 (1434)
1276
1228
1040
752

Administrator 20 Sample 020 By Administrator Date Thursday, May 28 2015

File: JESS5159 Ident: 2 Acq: 28-MAY-2015 15:44:28 +0:11 Cal: CAL1
AutospecE EI+ Magnet BpI: 828210 TIC: 6492152 Flags: HALL
File Text: B04JD031B



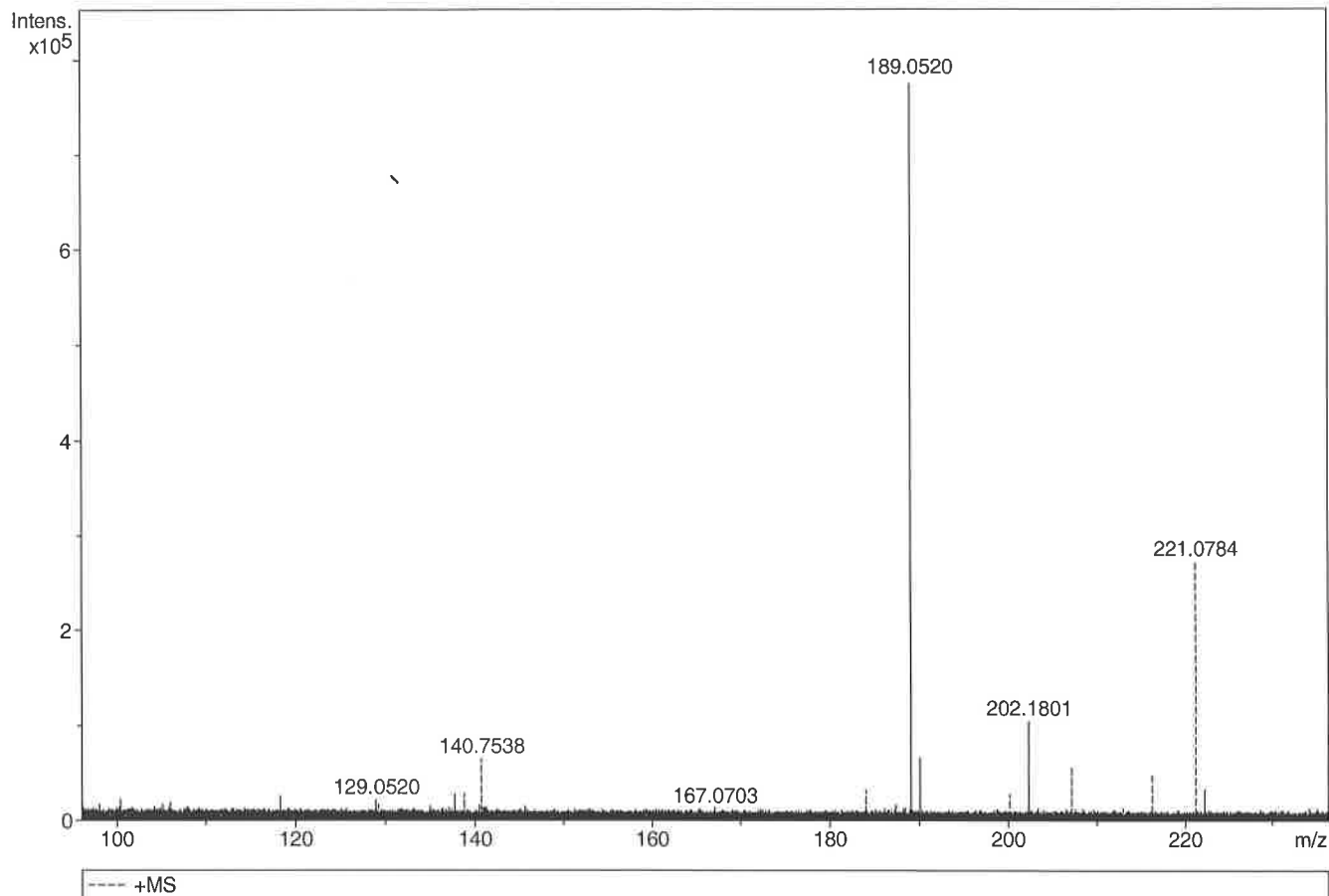
Generic Display Report

Analysis Info

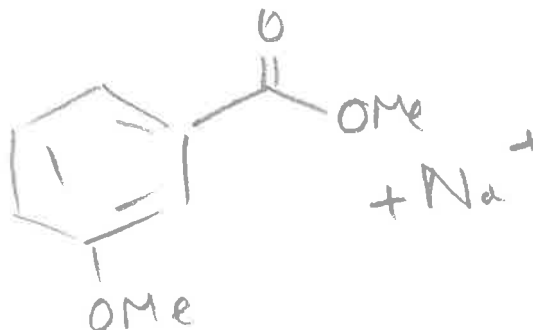
Analysis Name D:\Data\Alinanopos\JESS6113_000002.d
Method pos20090608esi
Sample Name POS ESI B04JD062A
Comment

Acquisition Date 10/09/2015 13:58:46

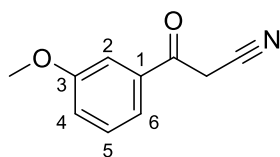
Operator Administrator
Instrument apex-III



Sum Formula	Sigma	m/z	Err [ppm]	Mean Err [ppm]	Err [mDa]	rdB	N Rule	e ⁻
C 9 H 10 Na 1 O 3	0.014	189.0522	1.02	0.70	0.13	4.50	ok	even

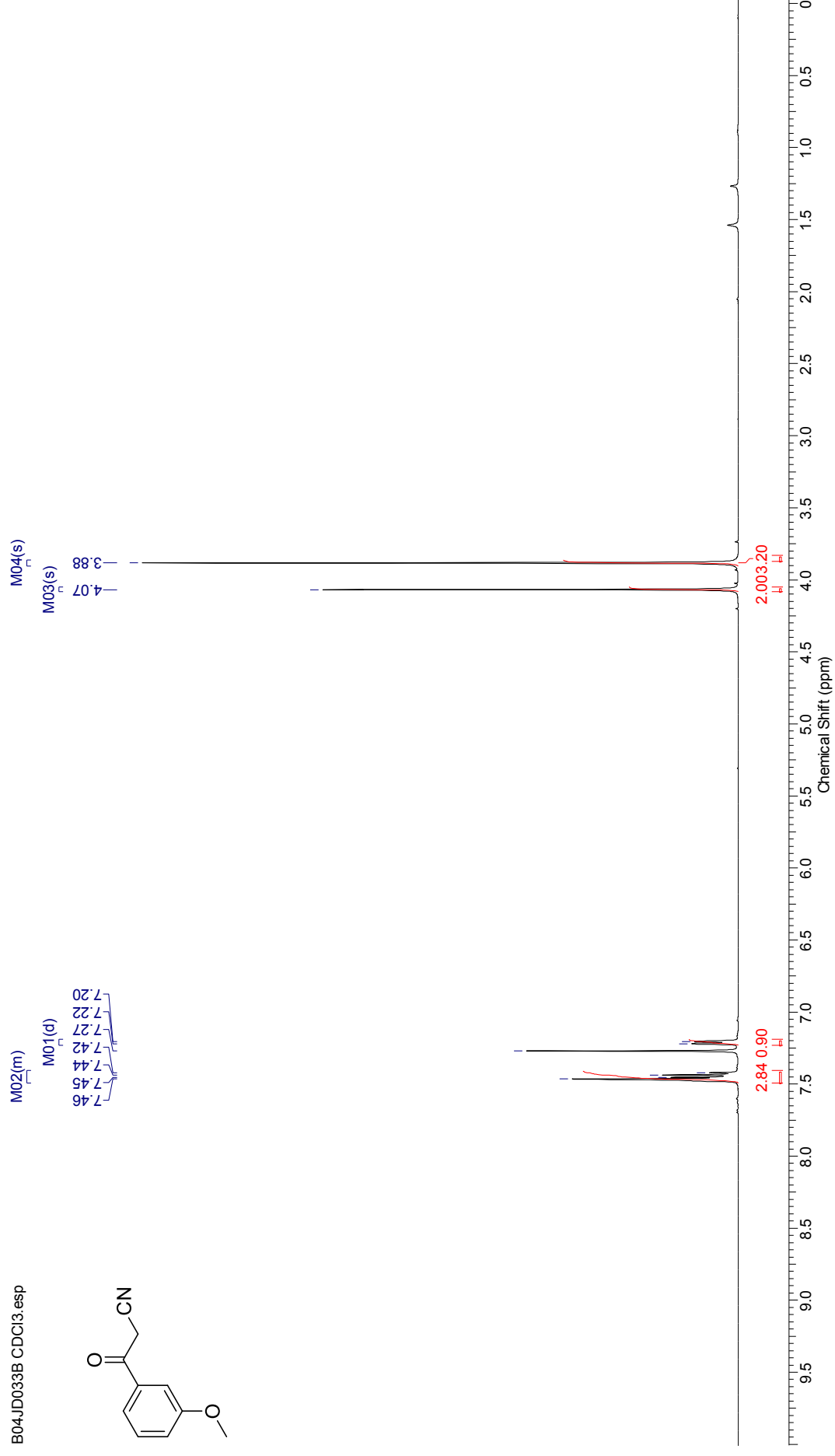
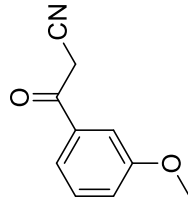


3-Methoxybenzoylacetonitrile (107)



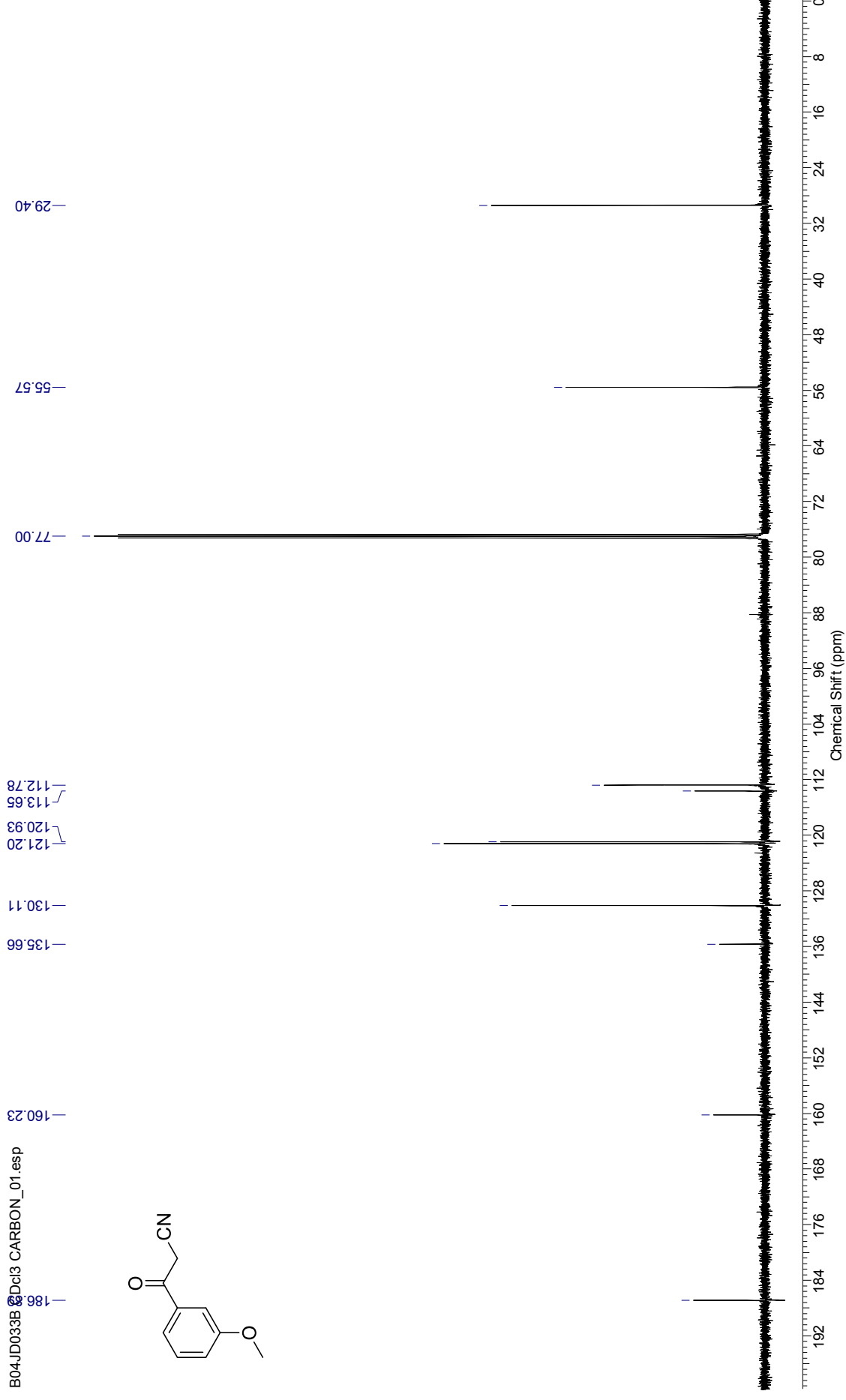
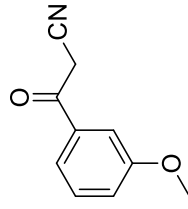
¹H NMR Spectrum (500 MHz, CDCl₃) for methyl 3-methoxybenzoylacetonitrile

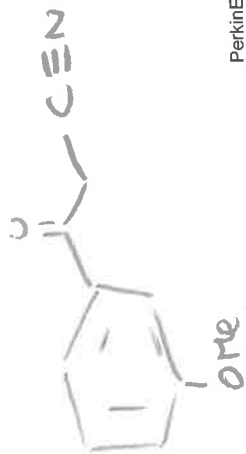
B04JD033B CDCl₃.esp



¹³C NMR Spectrum (126 MHz, CDCl₃) for methyl 3-methoxybenzoylacetonitrile

B04JD033B 2DCl3 CARBON_01.esp





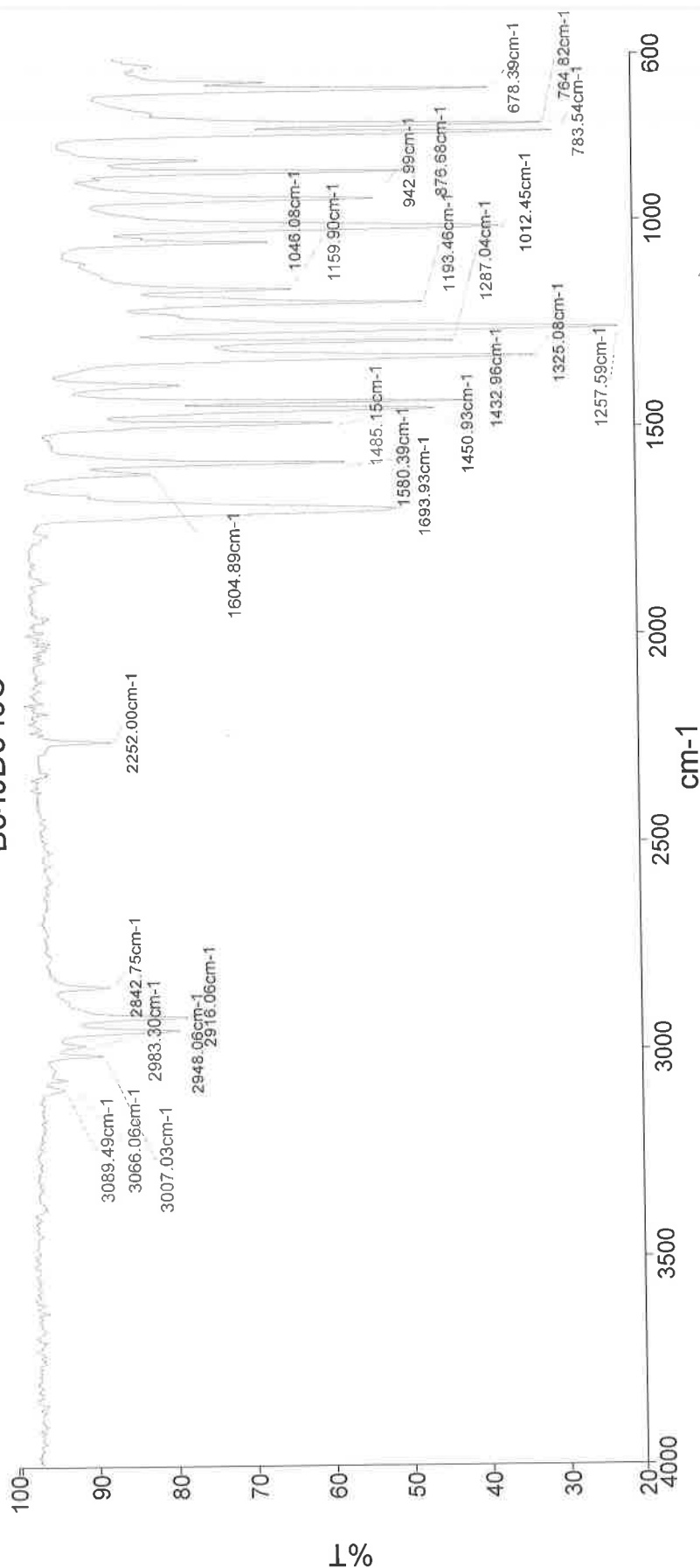
PerkinElmer Spectrum Version 10.03.06
09 September 2015 13:21

Analyst

Date

Administrator
09 September 2015 13:21

B04JD049C



2948 - C-H str.

2252 - C≡N str.

1694 - C=O str.

1580 - C-C in ring str.

1451 C-13 bend

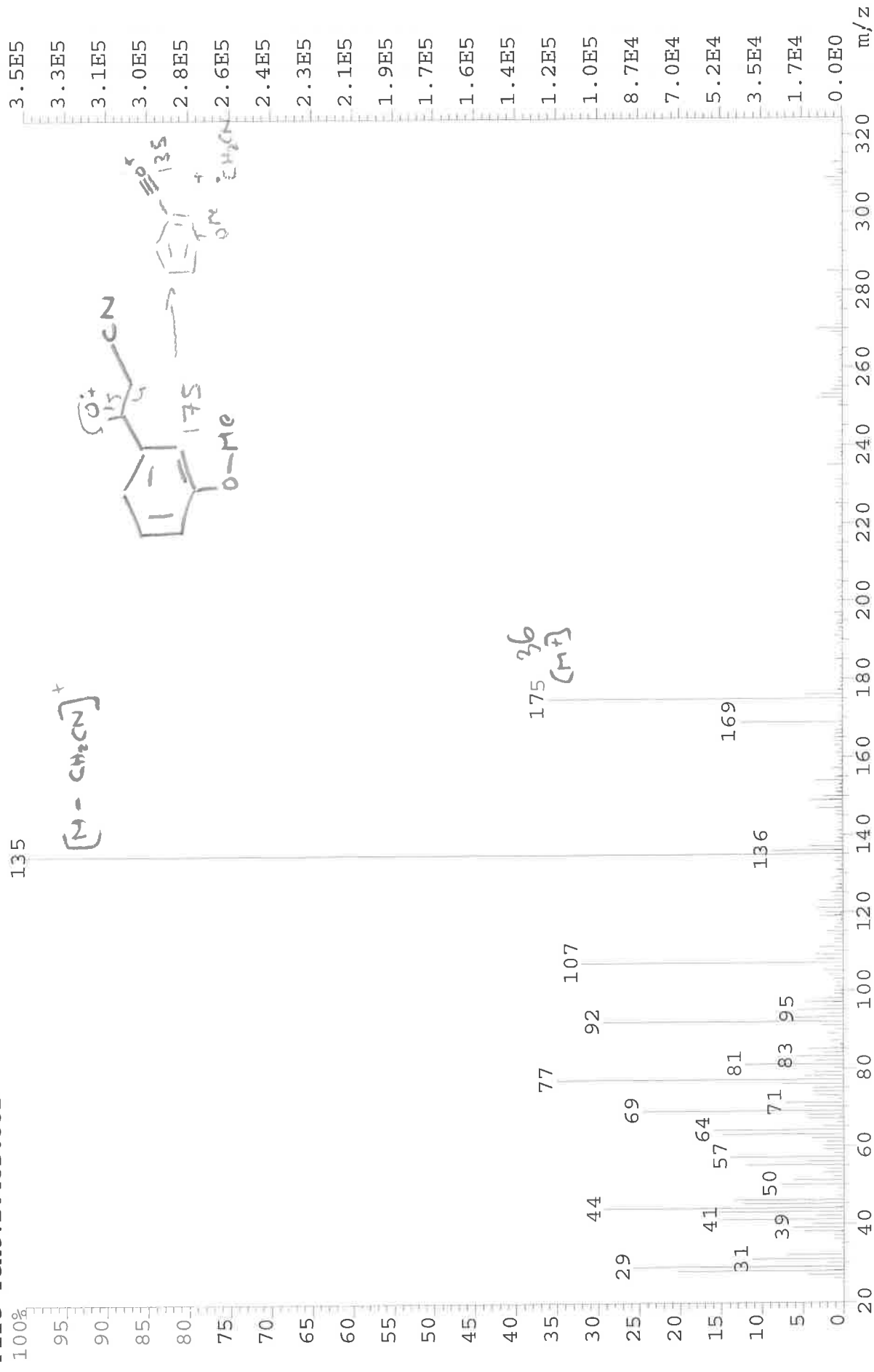
1258 C-O str.

1012 C-O str.

249-012 Sample 012 By Administrator Date Wednesday, September 09 2015

B04JD033B

File:JESS5806 Ident:48 Acq:11-JUN-2015 11:31:11 +3:00 Cal:CAL1
AutoSpecE EI+ Magnet BpI:348689 TIC:3086609 Flags:HALI
File Text:B04JD033B



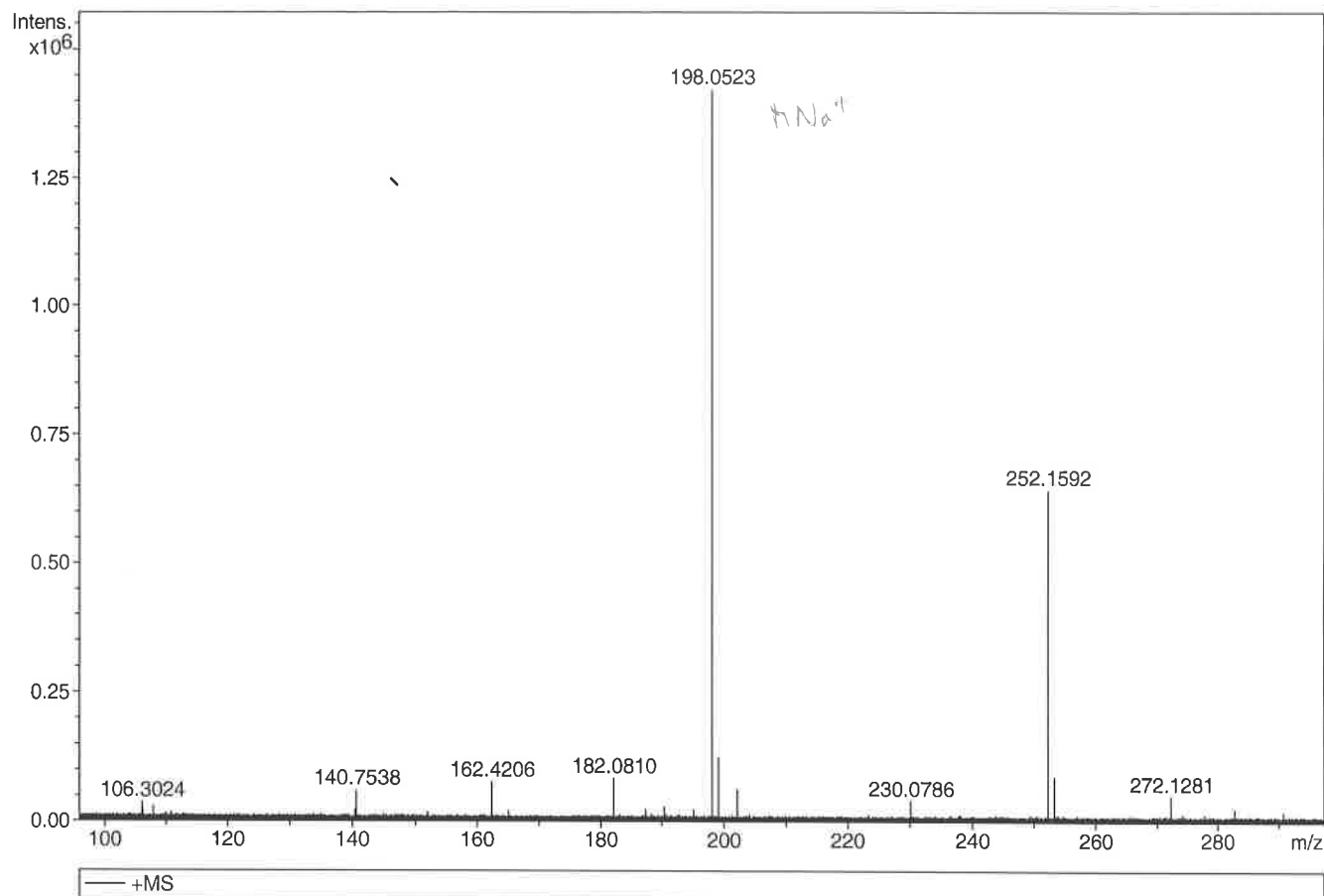
Generic Display Report

Analysis Info

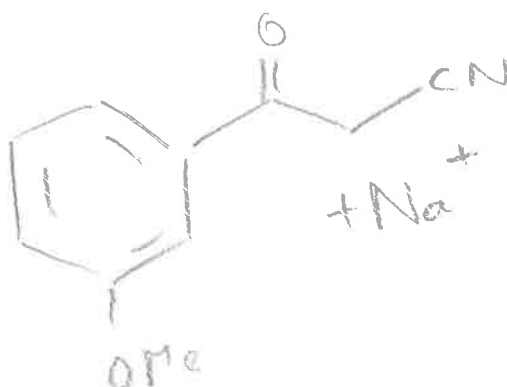
Analysis Name D:\Data\Alinanopos\JESS6114_000001.d
Method pos20090608esi
Sample Name POS ESI BO4JD040C
Comment

Acquisition Date 10/09/2015 15:09:20

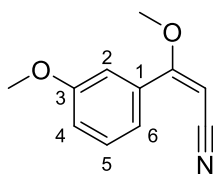
Operator Administrator
Instrument apex-III



Sum Formula	Sigma	m/z	Err [ppm]	Mean Err [ppm]	Err [mDa]	rdB	N Rule	e ⁻
C ₁₀ H ₉ N ₁ Na ₁ O ₂	0.025	198.0525	1.28	0.10	0.02	6.50	ok	even

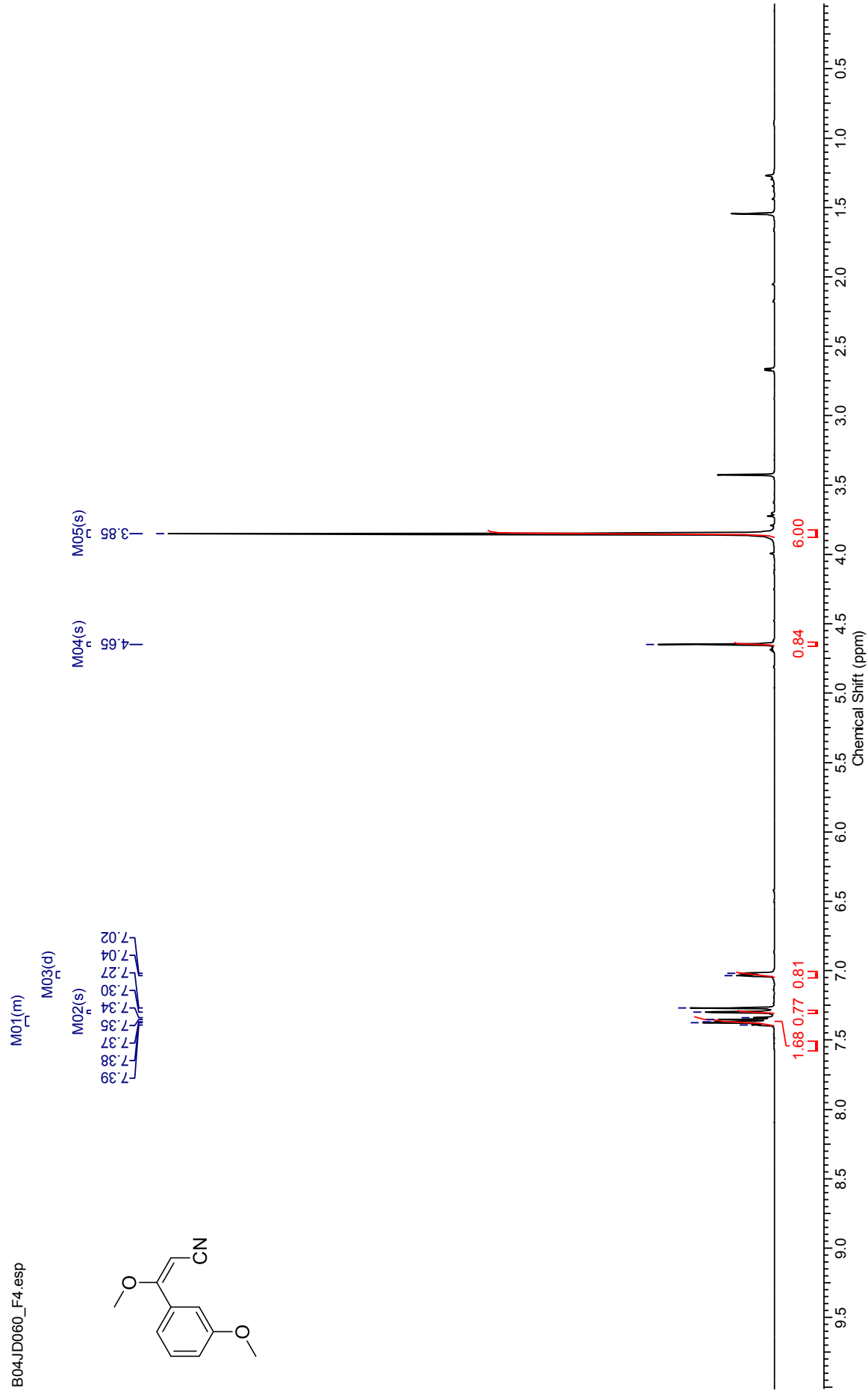


(*E*)-3-Methoxy-3-(3-methoxyphenyl)prop-2-enitrile (129-*E*)



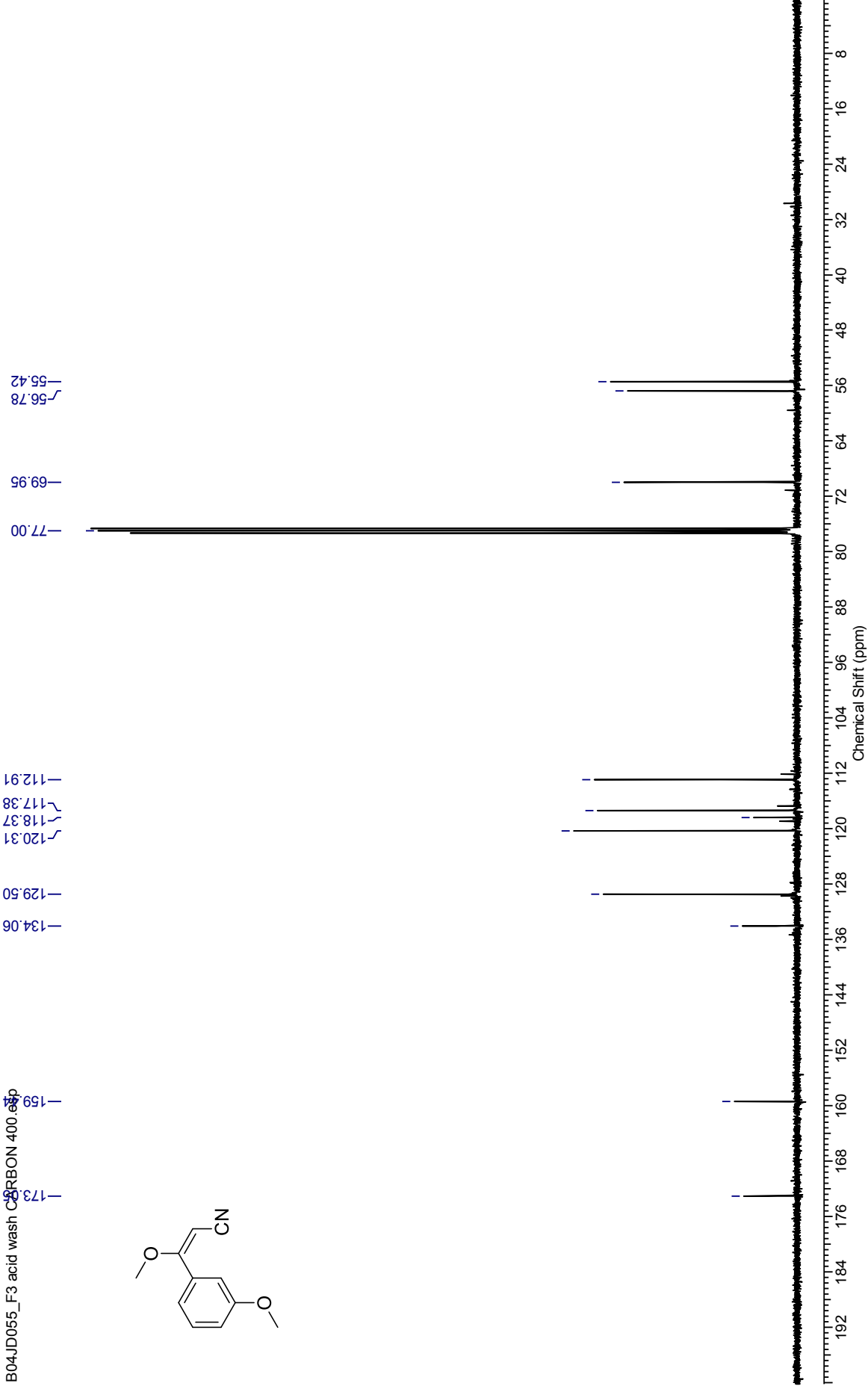
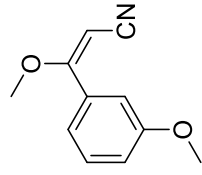
¹H NMR Spectrum (500 MHz, CDCl₃) for (E)-3-methoxy-3-(3-methoxyphenyl)prop-2-enenitrile

B04JD060_F4.esp

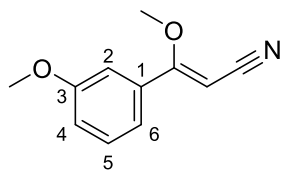


¹³C NMR Spectrum (126 MHz, CDCl₃) for (E)-3-methoxy-3-(3-methoxyphenyl)prop-2-enitrile

B04JD055_F3 acid wash CD₃CO₂RBON 400.08ppm

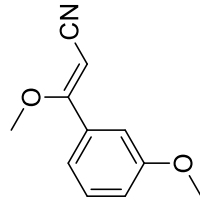


(Z)-3-Methoxy-3-(3-methoxyphenyl)prop-2-enitrile (129-Z)

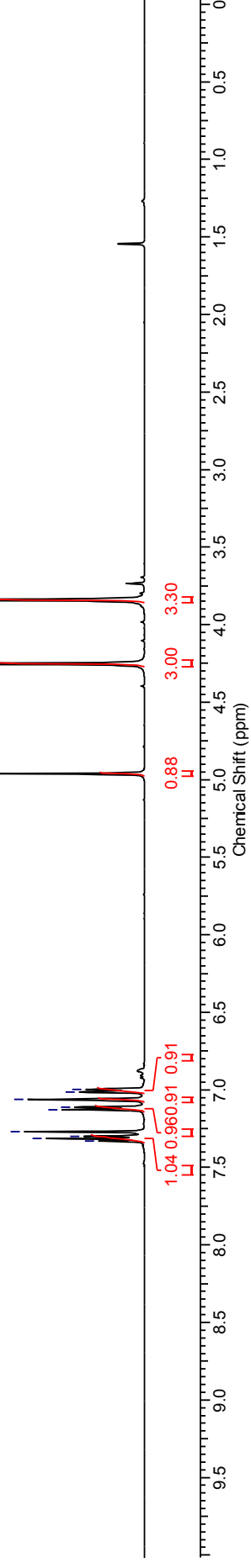


¹H NMR Spectrum (500 MHz, CDCl₃) for (Z)-3-methoxy-3-(3-methoxyphenyl)prop-2-enitrile

B04JD059_F1 .esp

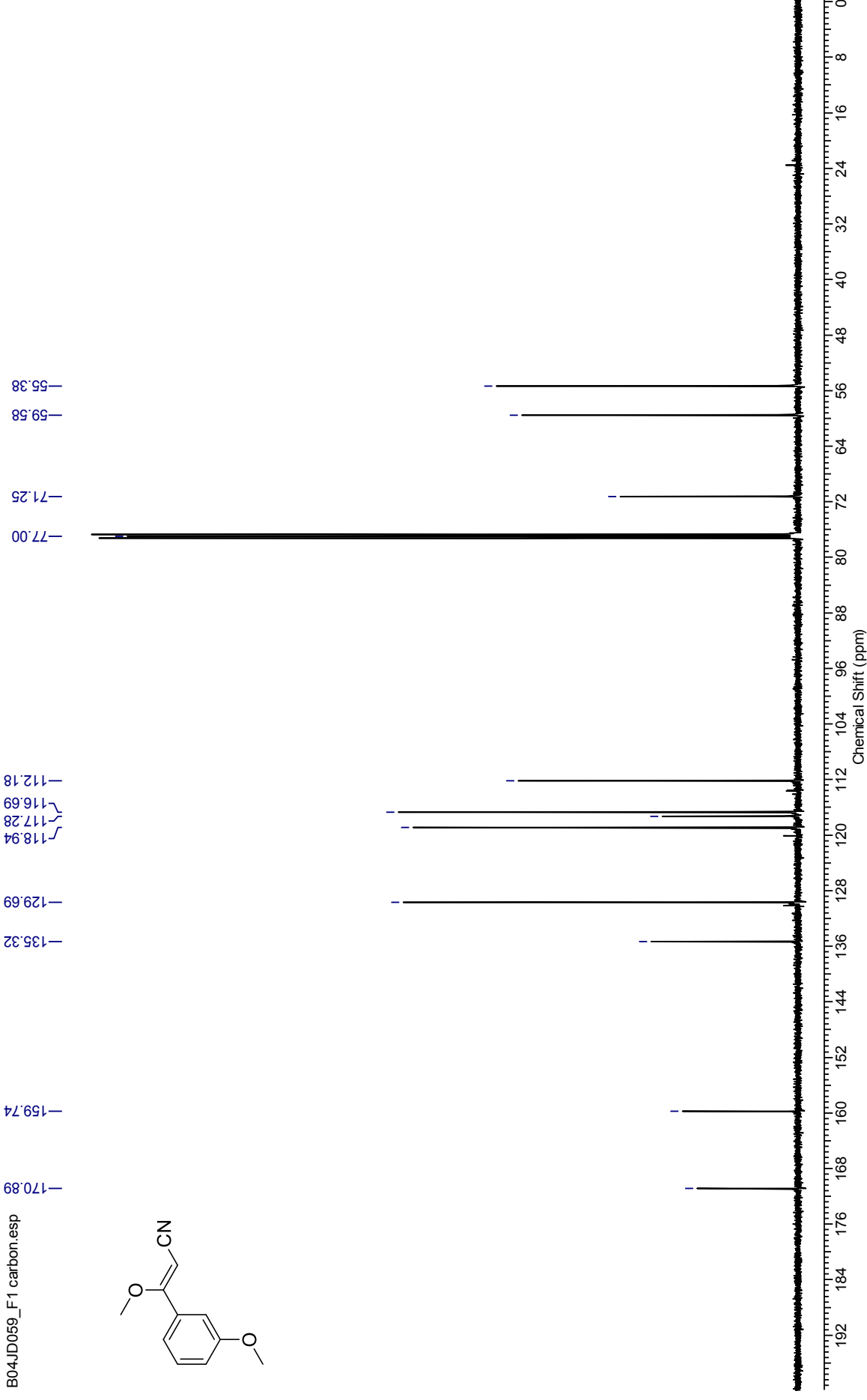
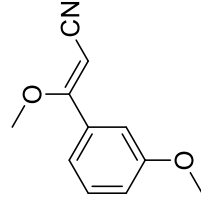


M01(m)
7.33
7.32
7.30
7.27
M02(d)
7.13
7.11
7.06
7.01
7.00
M03(s)
M04(d)
M05(s)
4.96
M06(s)
4.25
M07(s)
3.84

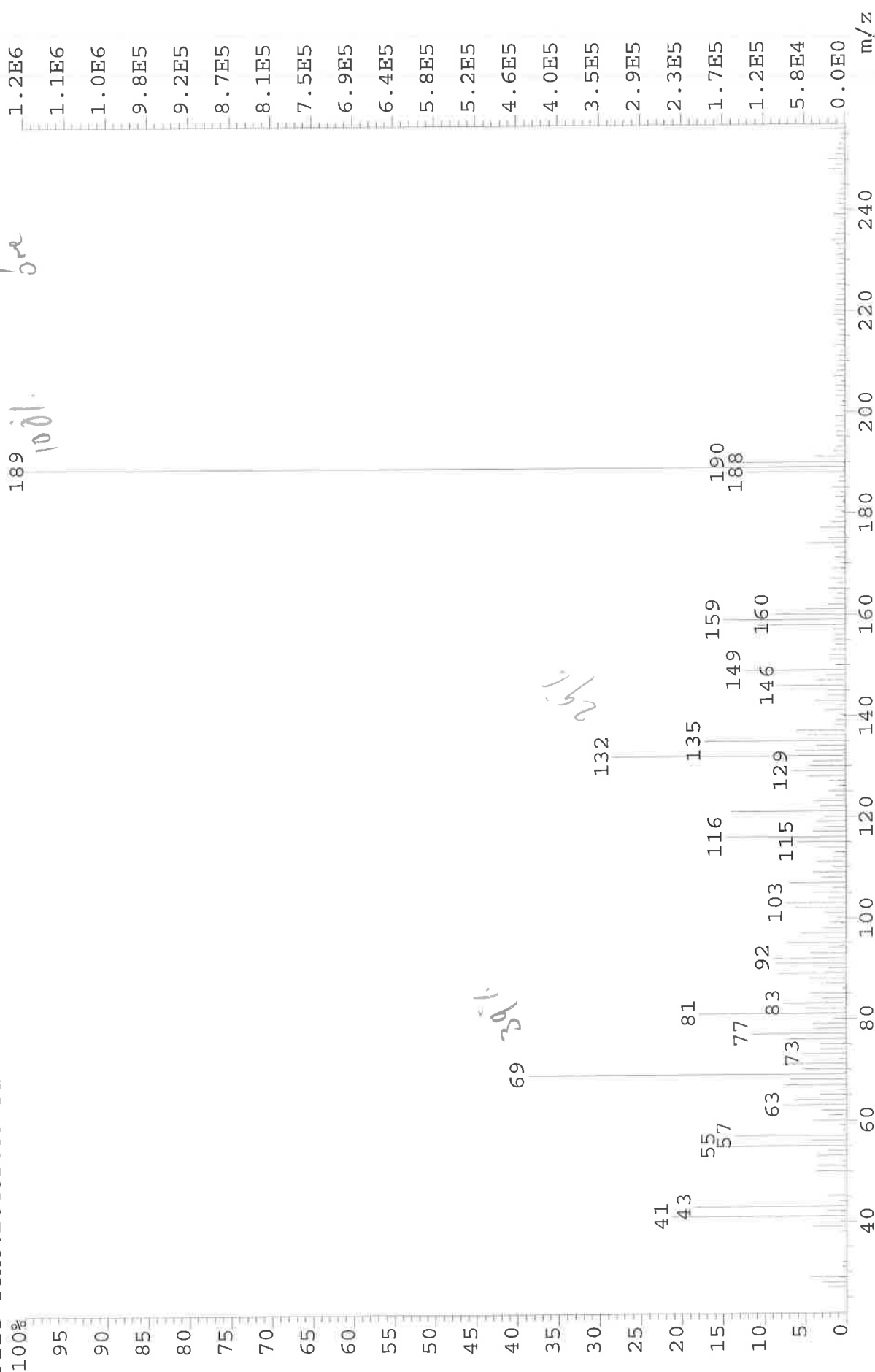


¹³C NMR Spectrum (126 MHz, CDCl₃) for (Z)-3-methoxy-3-(3-methoxyphenyl)prop-2-enitrile

B04JD059_F1 carbon.esp



File: JESS6098 Ident: 5 Acq: 1-SEP-2015 15:05:38 +0:17 Cal: LO
AutoSpecE EI+ Magnet BpI: 1156320 TIC: 10972372 Flags: HALL
File Text: BO4JD059-F1



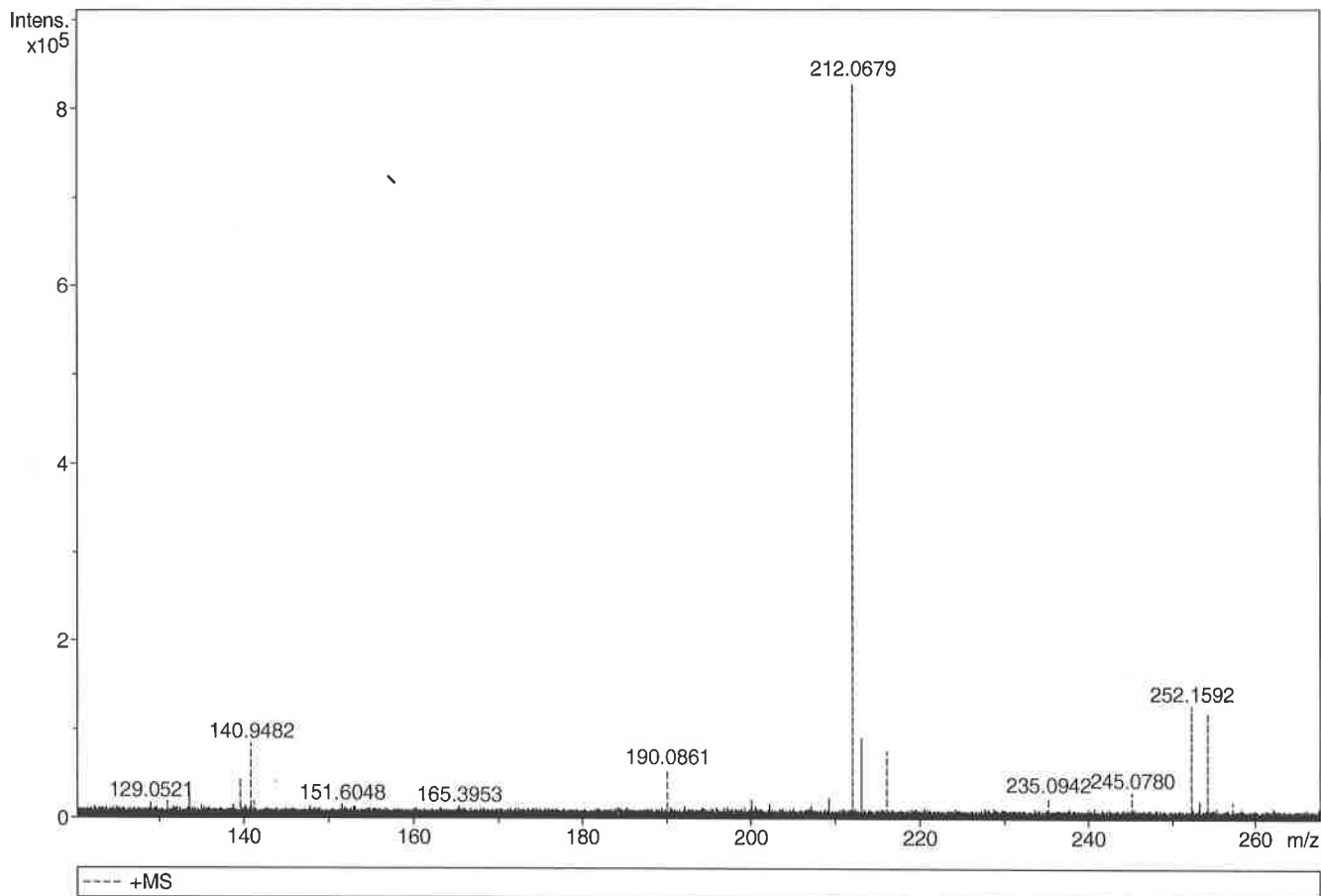
Generic Display Report

Analysis Info

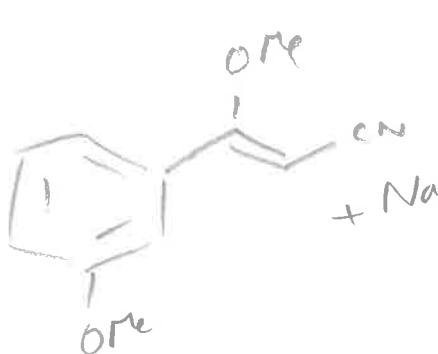
Analysis Name D:\Data\Alinanopos\JESS6098_000001.d
Method pos20090608esi
Sample Name POS ESI BO4JD059-F1
Comment

Acquisition Date 01/09/2015 14:57:44

Operator Administrator
Instrument apex-III

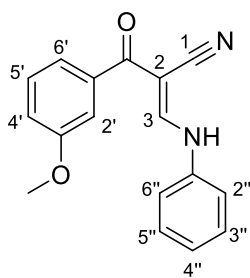


Sum Formula	Sigma	m/z	Err [ppm]	Mean Err [ppm]	Err [mDa]	rdb	N Rule	e ⁻
C 11 H 11 N 1 Na 1 O 2	0.018	212.0682	1.19	13.31	2.82	6.50	ok	even



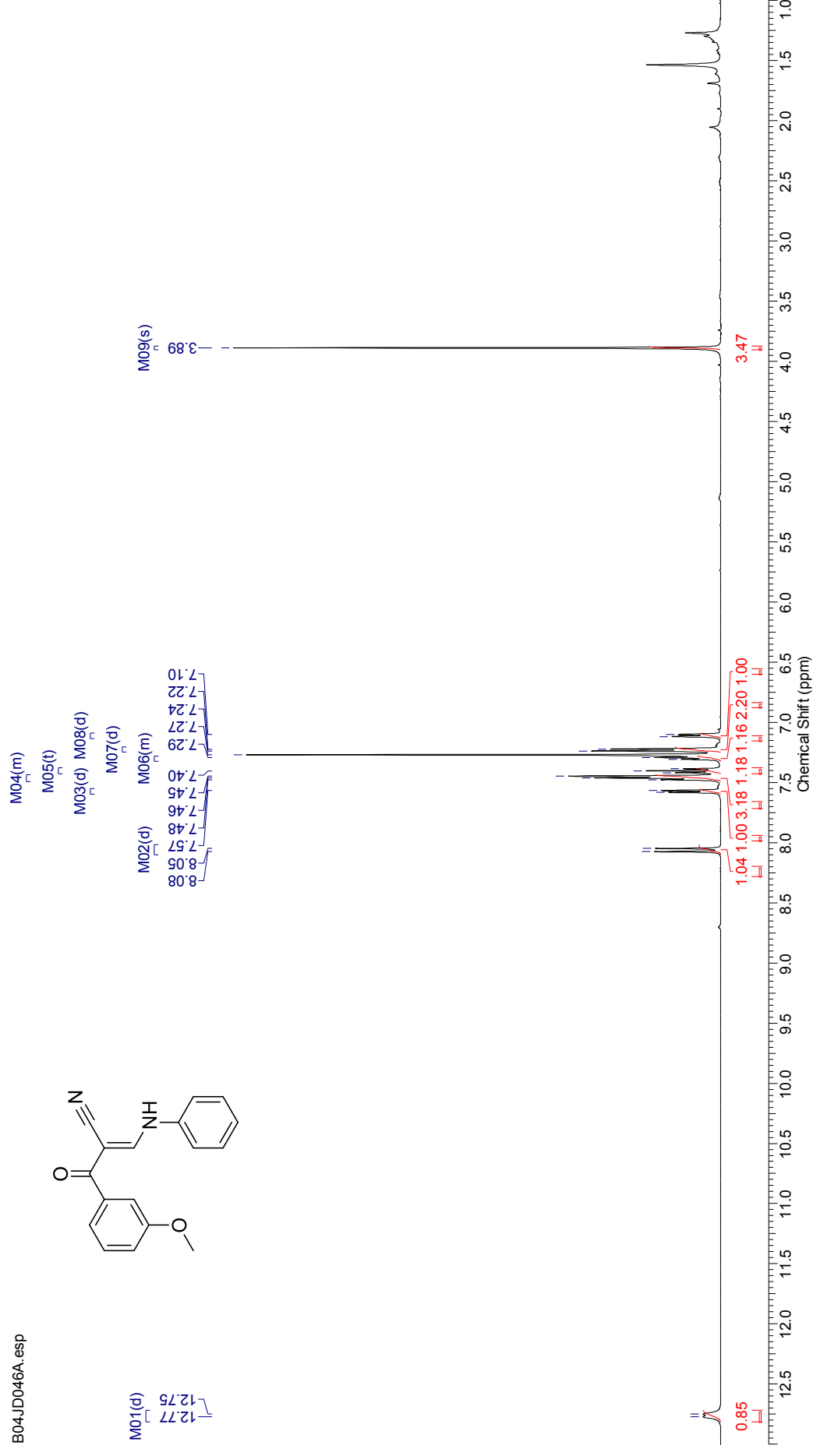
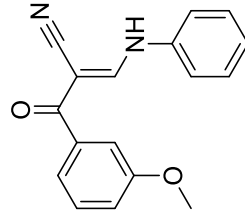
Z-isomer

2-(3-Methoxybenzoyl)-3-(phenylamino)prop-2-enitrile (124)



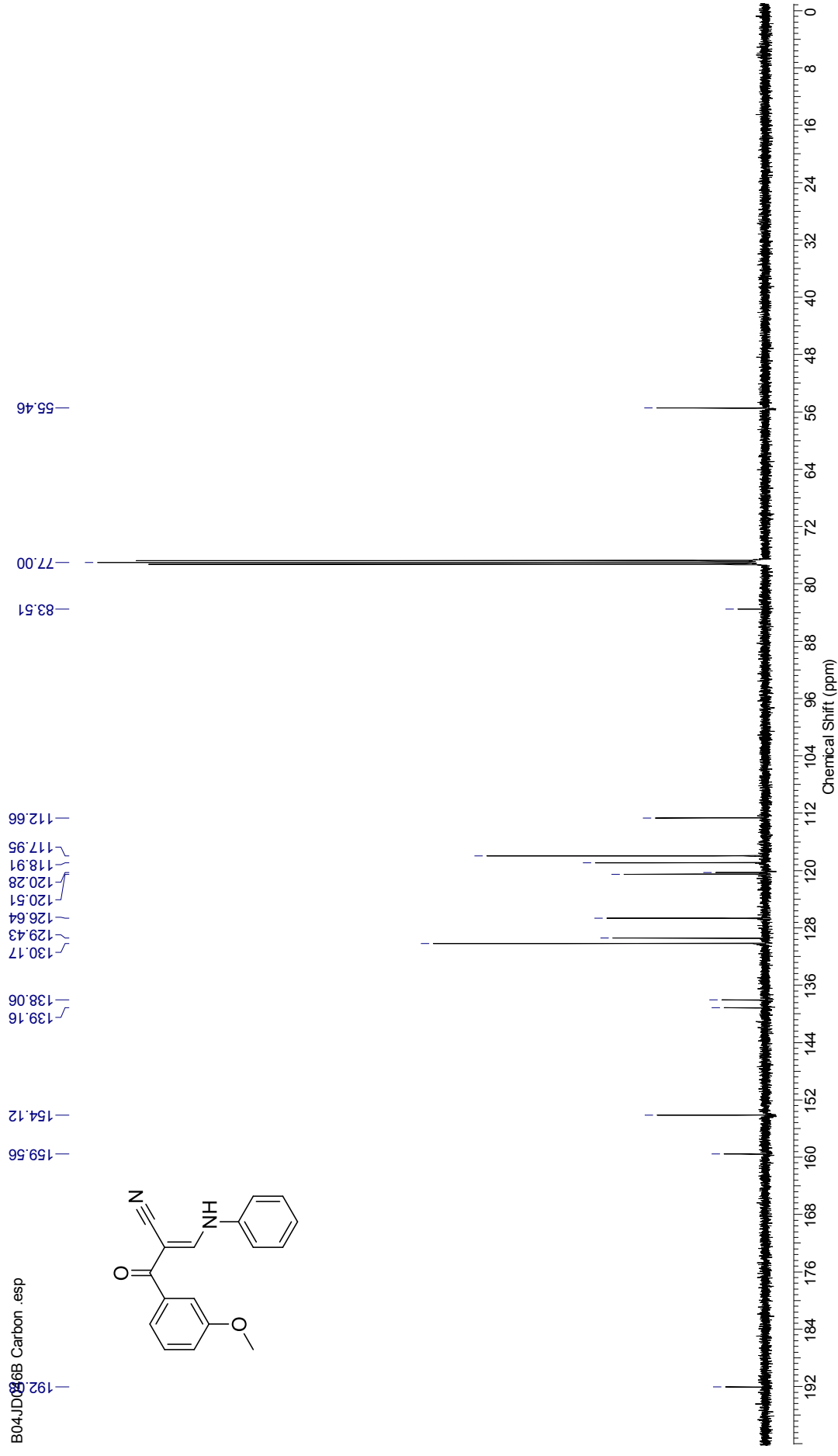
¹H NMR Spectrum (500 MHz, CDCl₃) for 2-(3-methoxybenzoyl)-3-(phenylamino)prop-2-enitrile

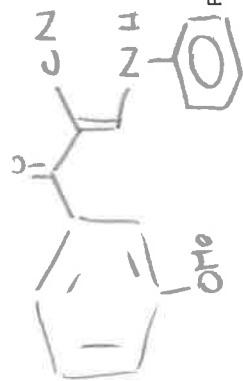
B04JD046A.esp



¹³C NMR Spectrum (126 MHz, CDCl₃) for 2-(3-methoxybenzoyl)-3-(phenylamino)prop-2-enitrile

B04JD086B Carbon .esp



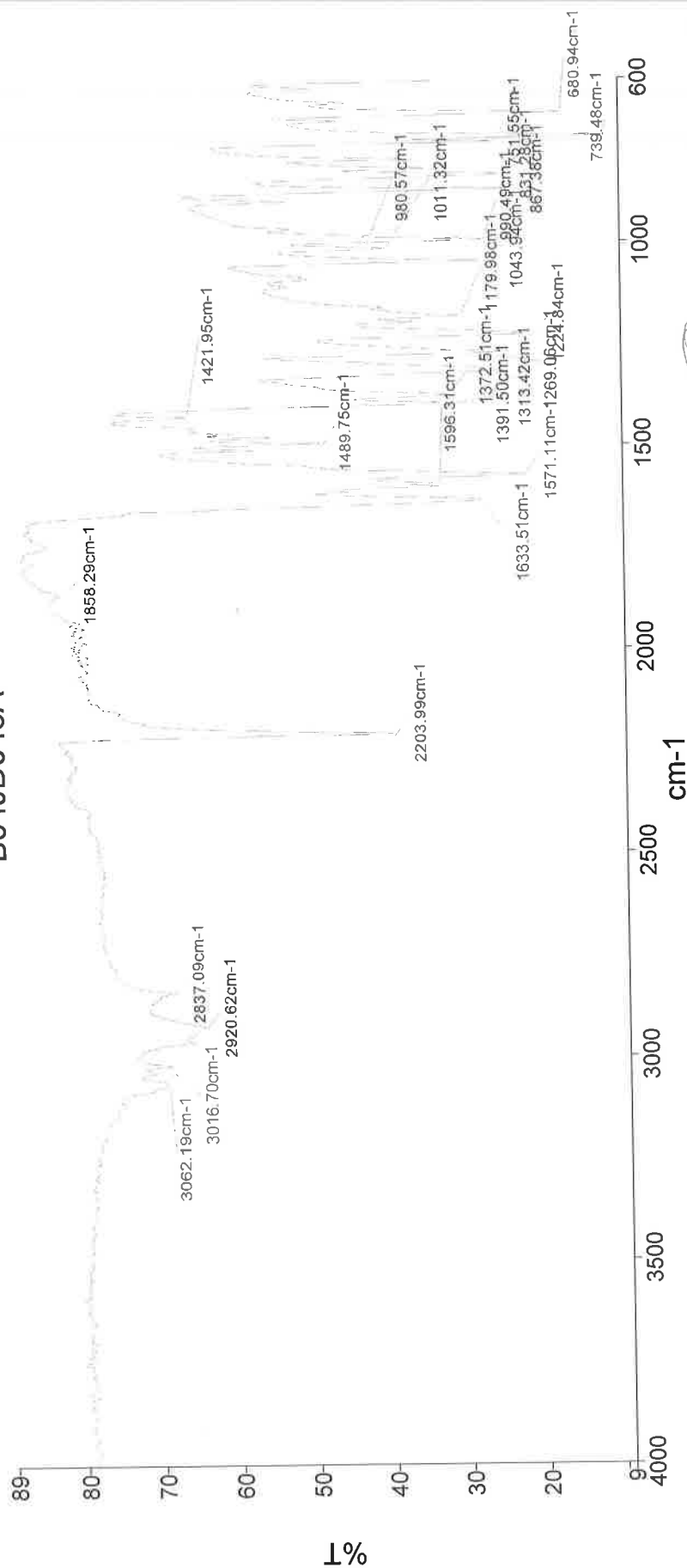


PerkinElmer Spectrum Version 10.03.06
09 September 2015 13:09

Analyst
Date

Administrator
09 September 2015 13:09

B04JD046A

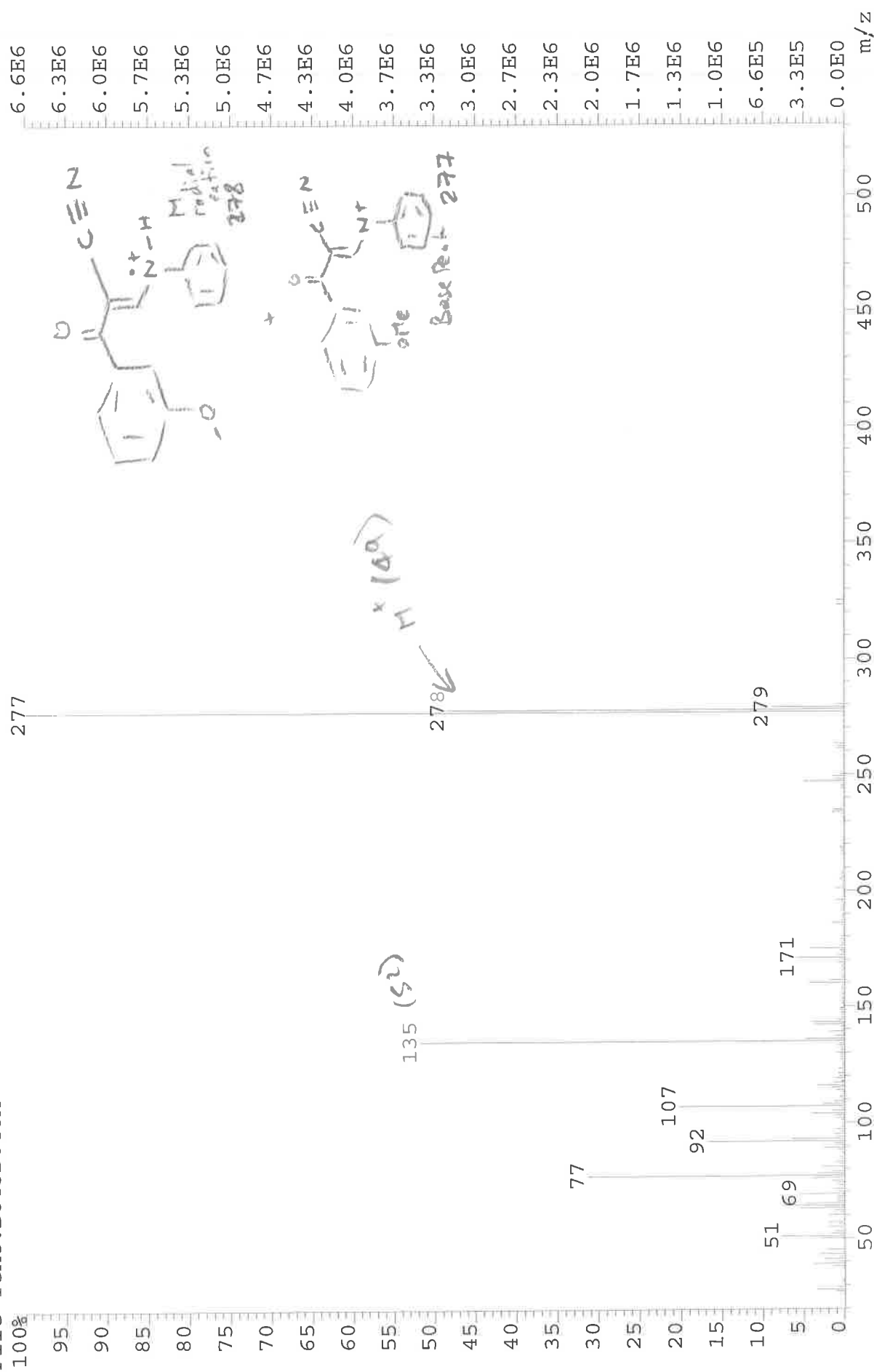


3062 - C-H
 2921 - C-H str.
 2204 - C≡N str.
 1634 - C=O str.
 1571 - C=C str.
 1392 - C-N str.
 1313 - C-N str.

1225 - C-O
 1044 - C-O
 990 - C-H alkene bend
 867 - C-H wag

249- 009 Sample 009 By Administrator Date Wednesday, September 09 2015

File: JESS5952 Ident: 10 Acq: 20-JUL-2015 14:52:28 +0:40 Cal: CAL1
 AutoSpecE EI+ Magnet BpI: 6651454 TIC: 33905552 Flags: HALL
 File Text: BO4JD048A



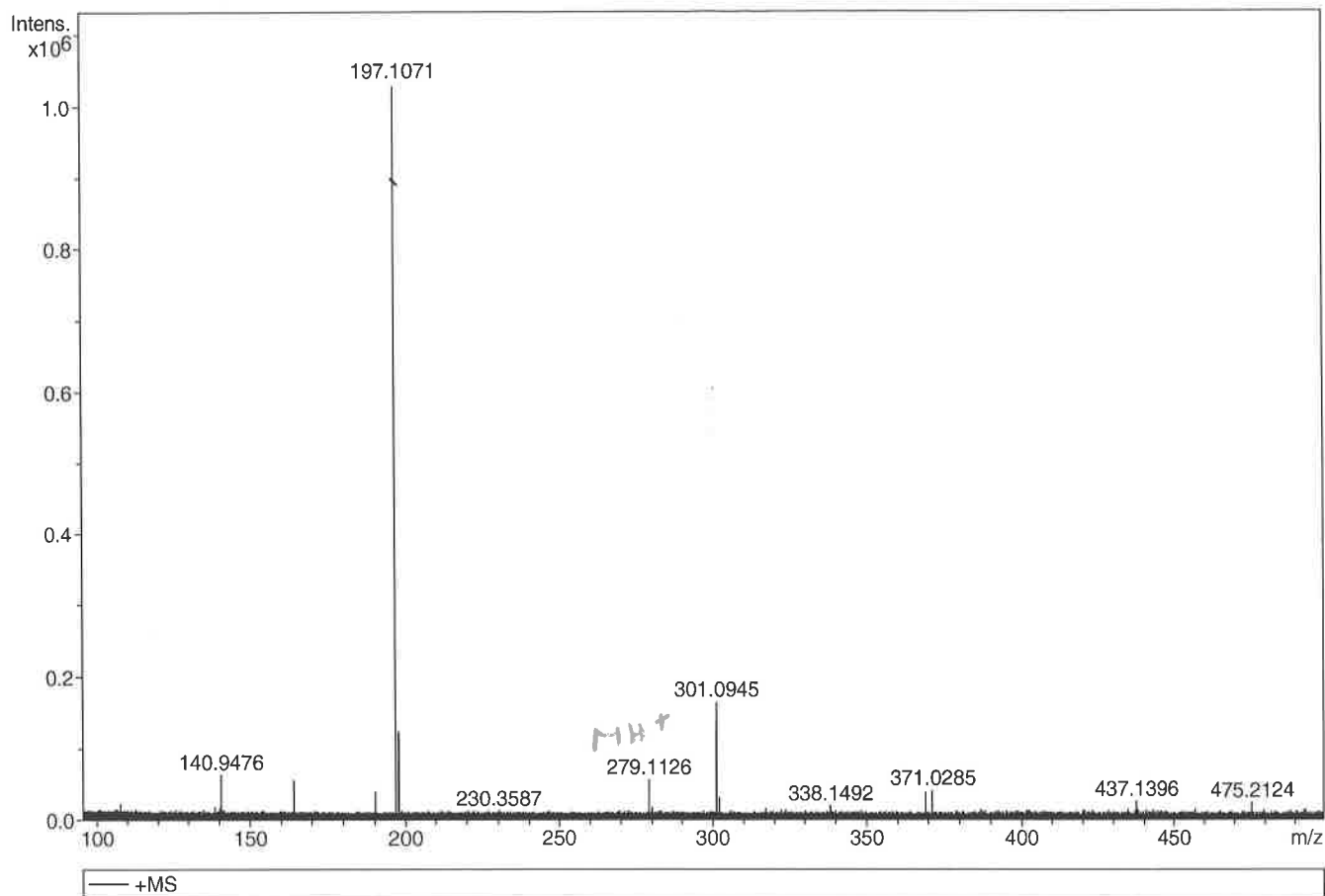
Generic Display Report

Analysis Info

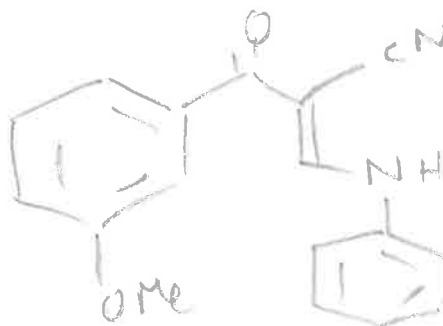
Analysis Name D:\Data\Alinanopos\JESS5952_000001.d
 Method pos20090608esi
 Sample Name POS ESI BO4JD048A
 Comment

Acquisition Date 20/07/2015 15:04:19

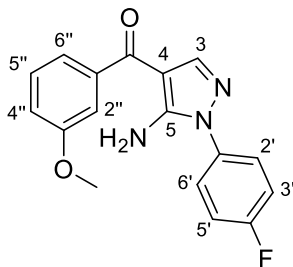
Operator Administrator
 Instrument apex-III



Sum Formula	Sigma	m/z	Err [ppm]	Mean Err [ppm]	Err [mDa]	rdB	N Rule	e ⁻
C 17 H 15 N 2 O 2	0.066	279.1128	0.66	1.37	0.38	11.50	ok	even

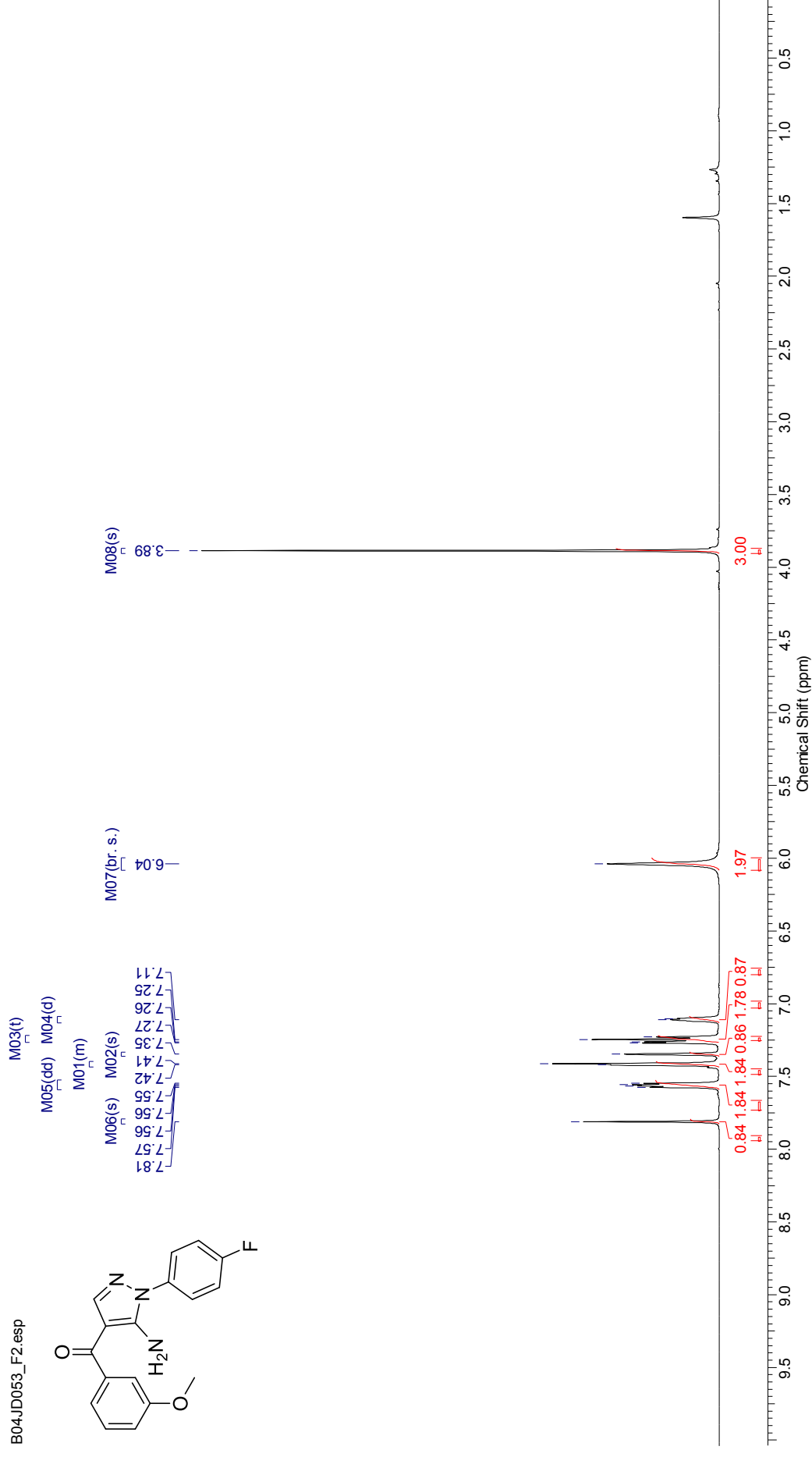
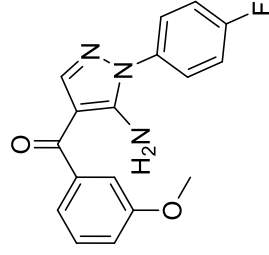


[5-Amino-1-(4-fluorophenyl)-1*H*-pyrazol-4-yl]-3-methoxyphenyl ketone (125)



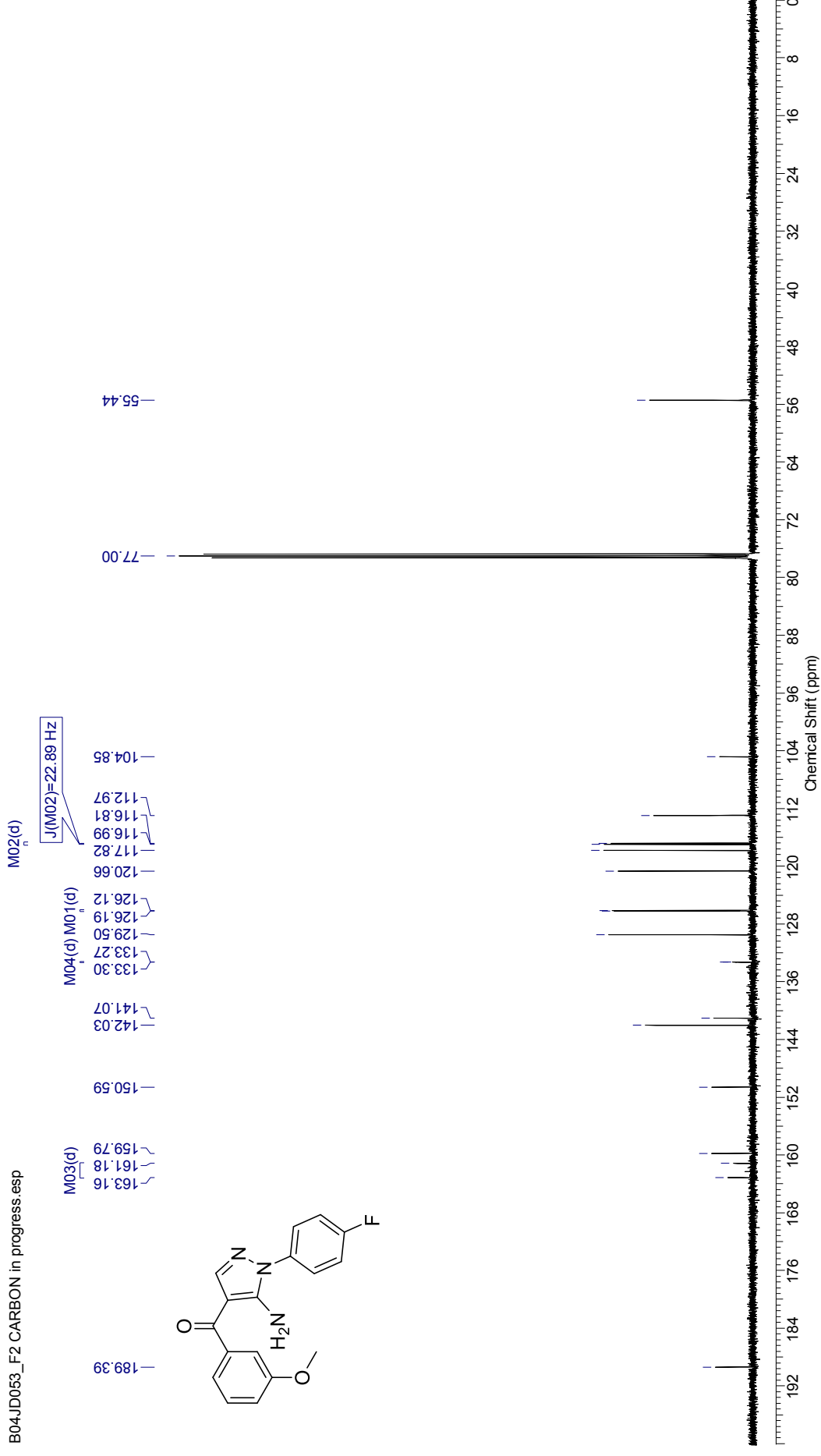
¹H NMR spectrum (500 MHz, CDCl₃) for [5-amino-1-(4-fluorophenyl)-1H-pyrazol-4-yl]-3-methoxyphenyl ketone

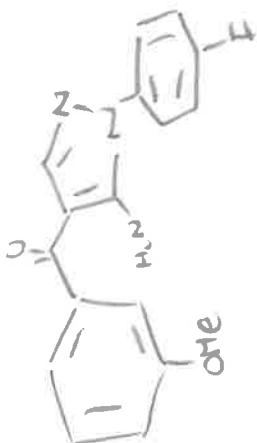
B04JD053_F2.esp



¹³C NMR spectrum (126 MHz, CDCl₃) for [5-amino-1-(4-fluorophenyl)-1*H*-pyrazol-4-yl]-3-methoxyphenyl ketone

B04JD053_F2 CARBON in progress.esp



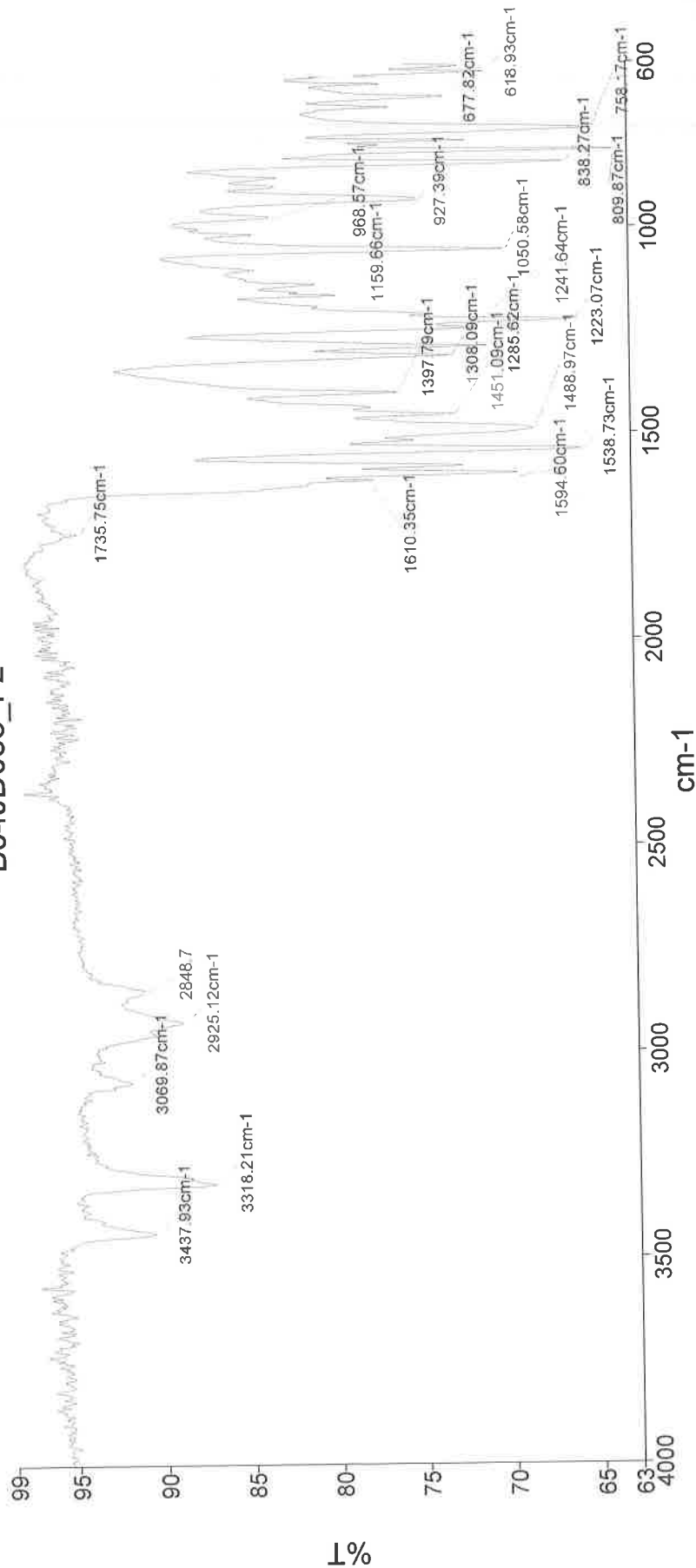


Analyst
Date

Administrator

09 September 2015 13:14

B04JD053_F2



249-010 Sample 010 By Administrator Date Wednesday, September 09 2015

3318 - N-H str
2925 - C-H str
1610 - C=O
1595 - N-H bend
1539 - C-C str
1286 - C-N str
1223 - C-O str
1051 - C-O
838 - N-H bend
838 - C-H bend

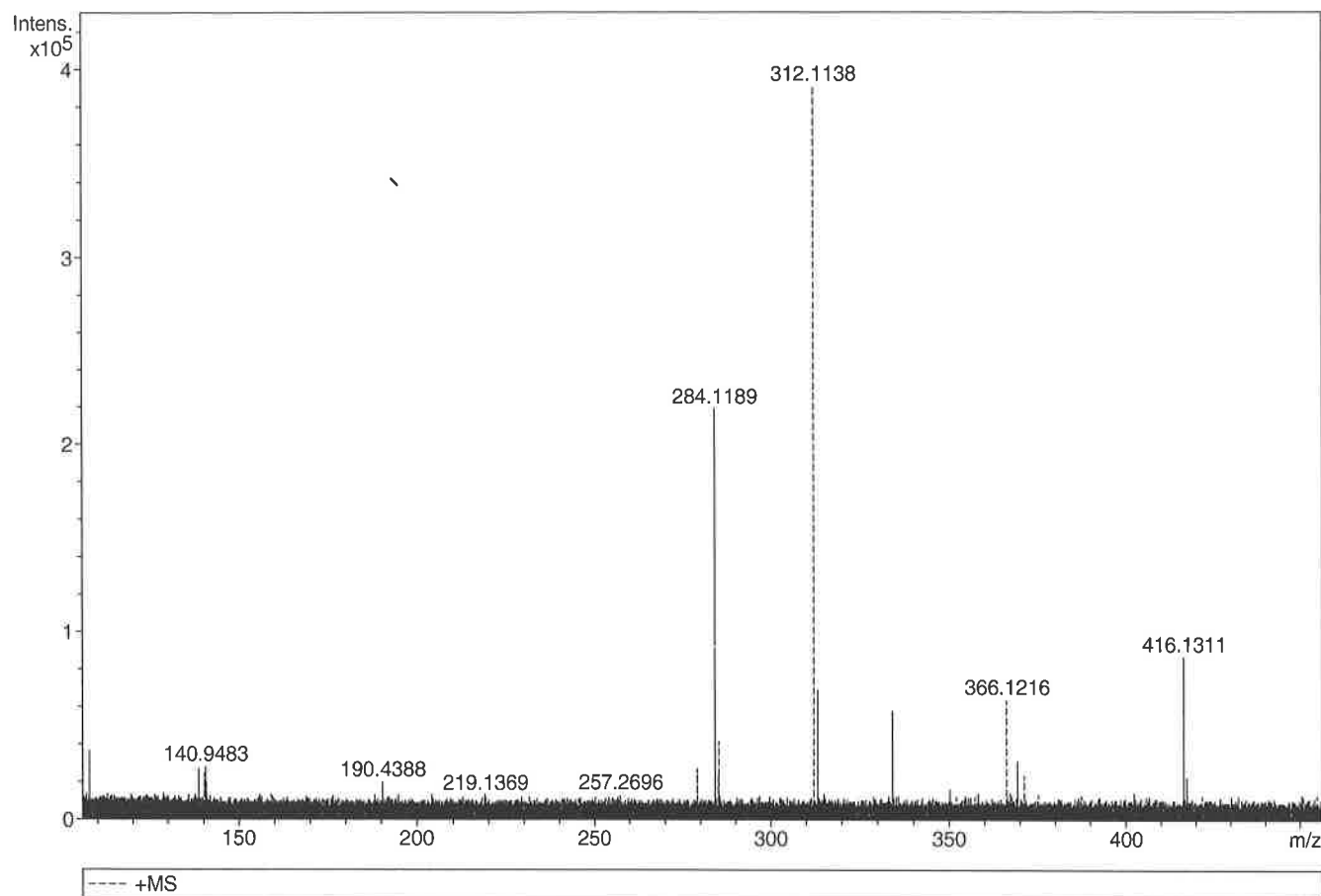
Generic Display Report

Analysis Info

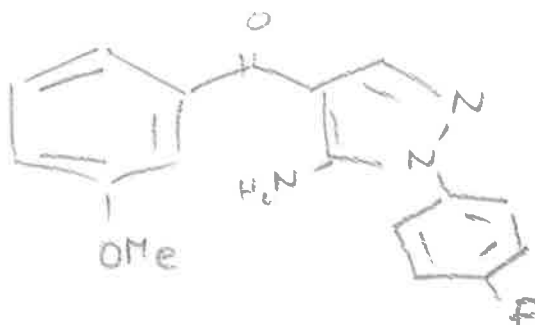
Analysis Name D:\Data\Alinanopos\JESS5972_000001.d
 Method pos20090608esi
 Sample Name POS ESI BO4JD053-F2
 Comment

Acquisition Date 27/07/2015 14:17:54

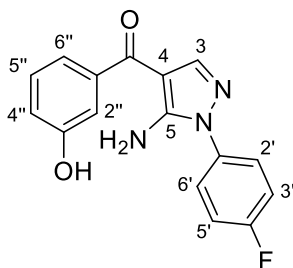
Operator Administrator
 Instrument apex-III



Sum Formula	Sigma	m/z	Err [ppm]	Mean Err [ppm]	Err [mDa]	rdb	N Rule	e ⁻
C ₁₇ H ₁₅ F ₁ N ₃ O ₂	0.007	312.1143	1.50	-7.39	-2.31	11.50	ok	even

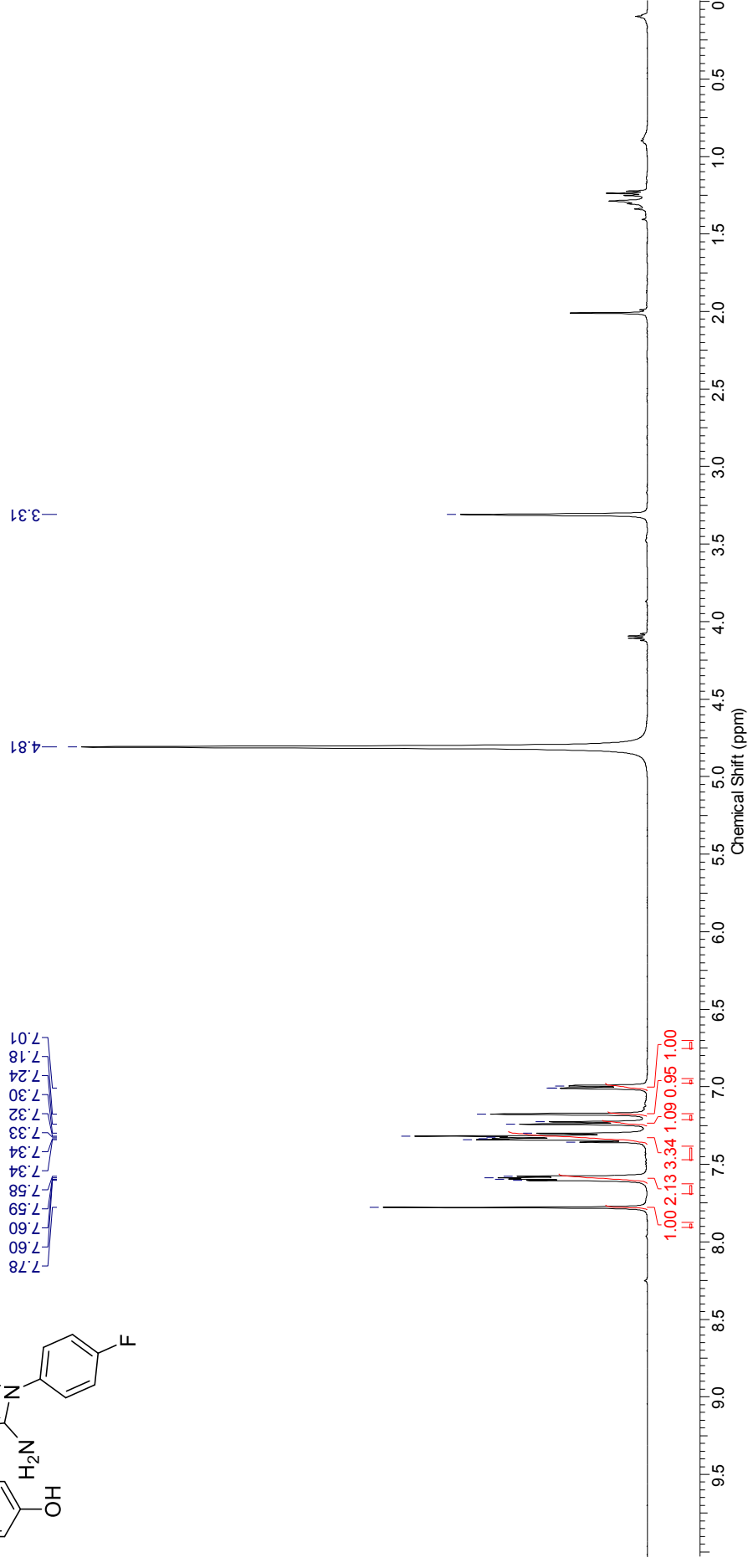
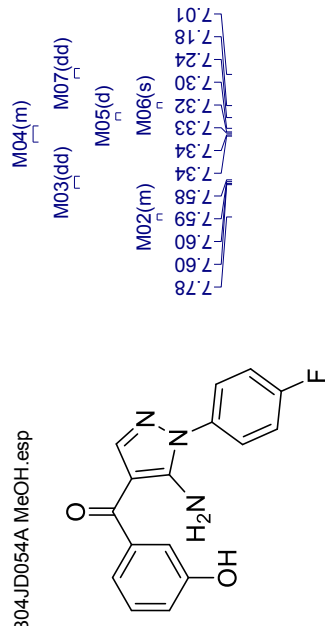


**[5-Amino-1-(4-fluorophenyl)-1*H*-pyrazol-4-yl]-3-hydroxyphenyl
ketone (126)**



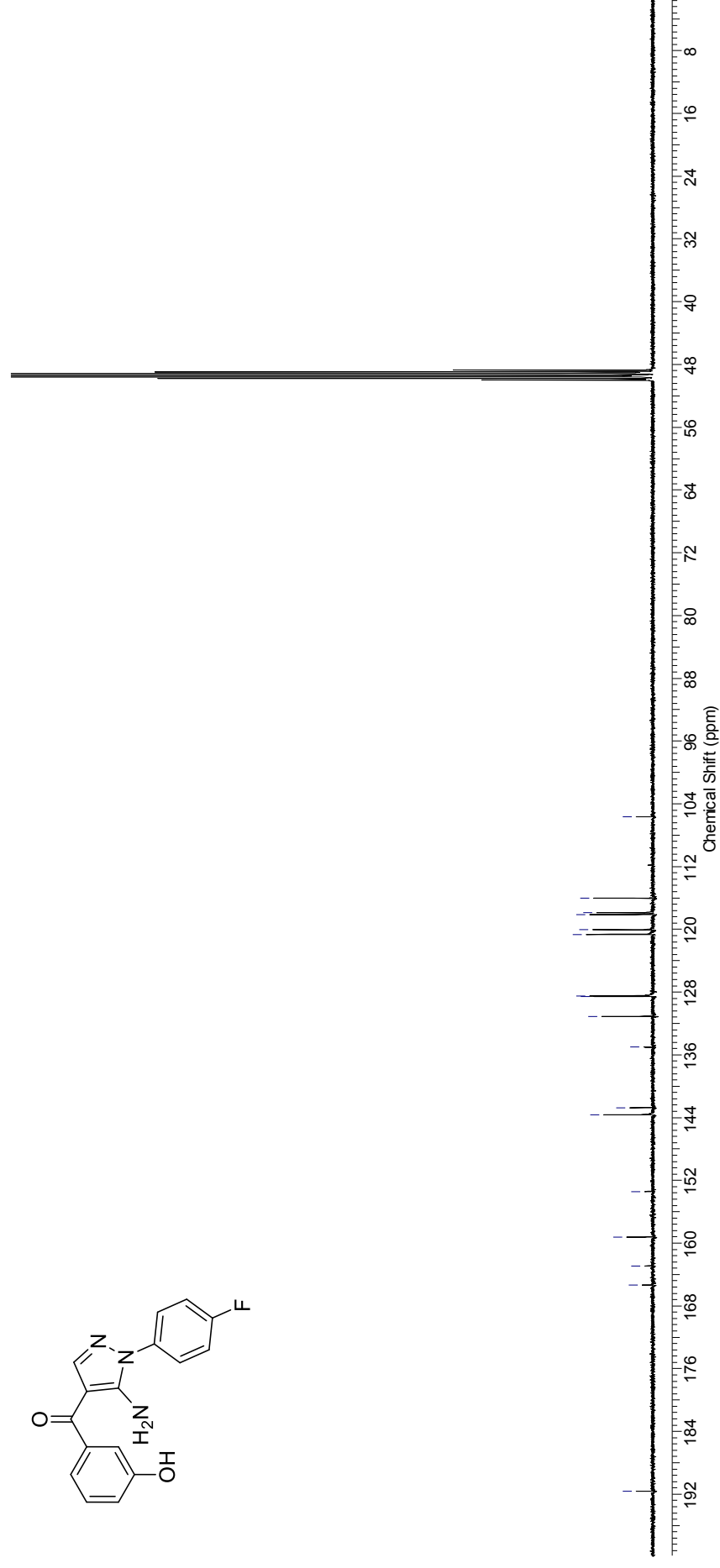
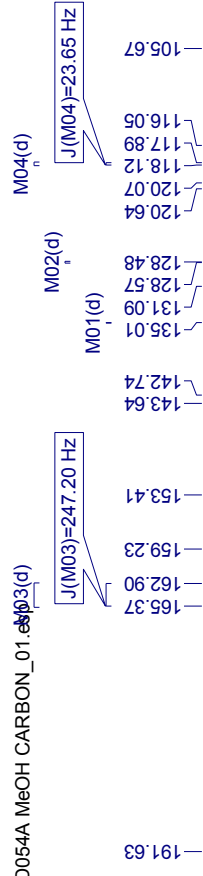
¹H NMR spectrum (500 MHz, MeOH-*d*₄) for [5-amino-1-(4-fluorophenyl)-1*H*-pyrazol-4-yl]-3-hydroxyphenyl ketone

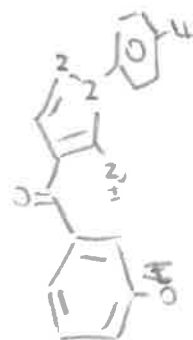
B04JD054A MeOH.esp



¹³C NMR spectrum (100 MHz, MeOH-*d*₄) for [5-amino-1-(4-fluorophenyl)-1*H*-pyrazol-4-yl]-3-hydroxyphenyl ketone

B04JD054A MeOH CARBON_01: 1003(d)



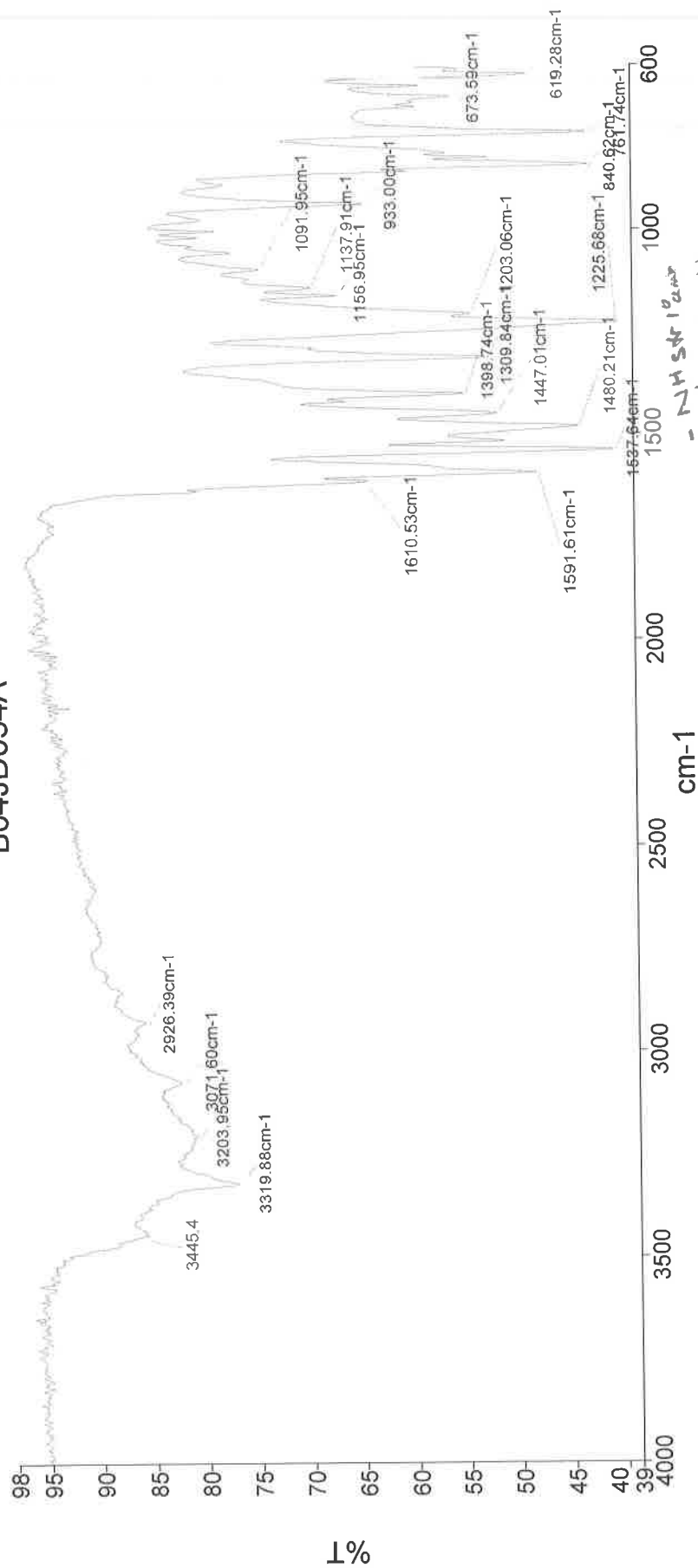


Analyst
Date

Administrator

09 September 2015 13:18

B04JD054A

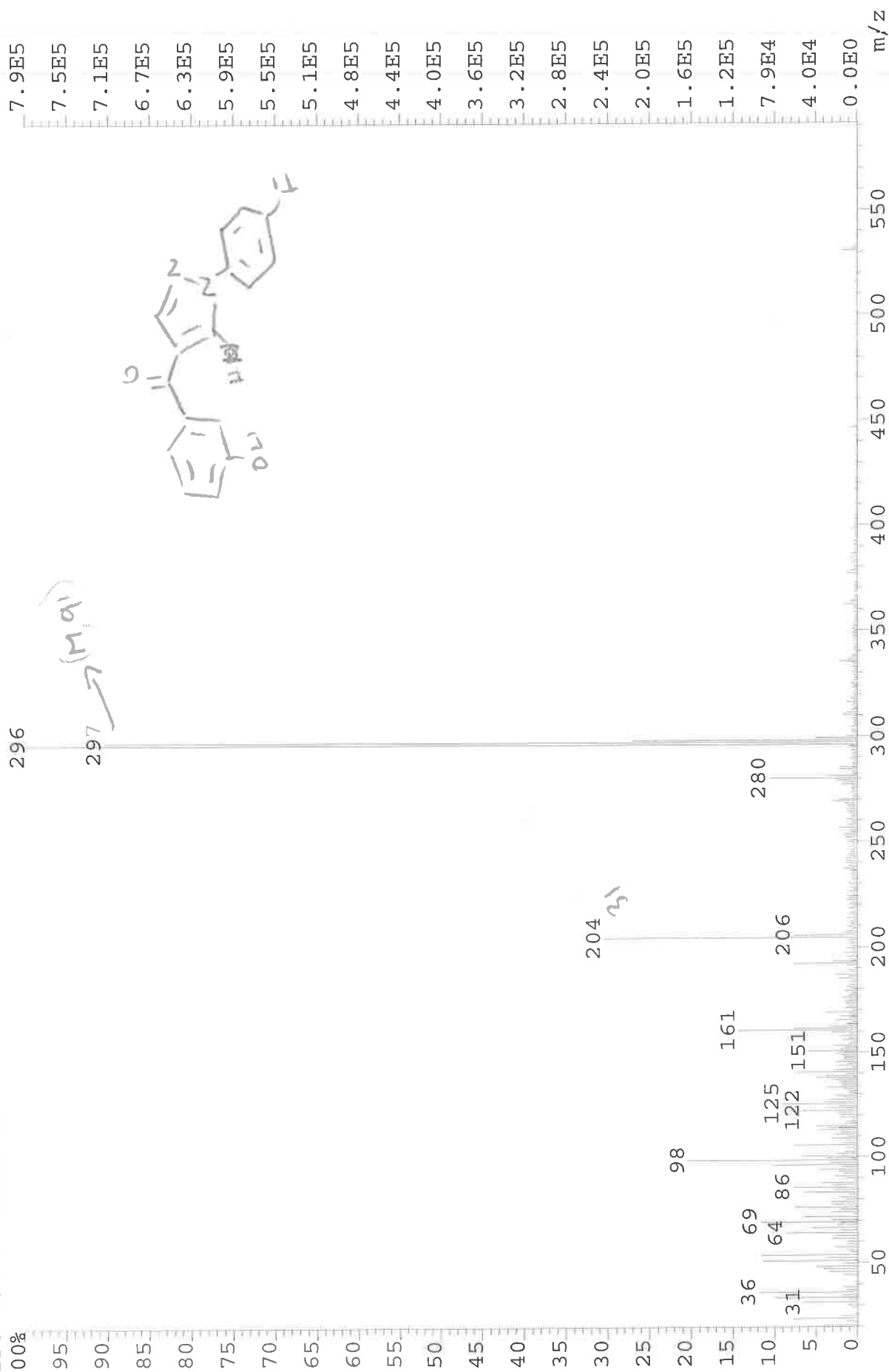


cm⁻¹

249-011 Sample 011 By Administrator Date Wednesday, September 09 2015

3320 - NH str 12 str
3204 - br. O-H
3072 - C-H str.
1610 - C=O
1592 - N-H bend
1538 - C-C str.
1310 - C-N str
1226 - C-O str
840 - N-H wag

File: JESS6049 Ident: 18 Acq: 18-AUG-2015 15:55:28 +1:10 Cal: CAL1
AutoSpecE EI+ Magnet BpI: 791896 TIC: 7767468 Flags: HALL
File Text: B04JDO54A



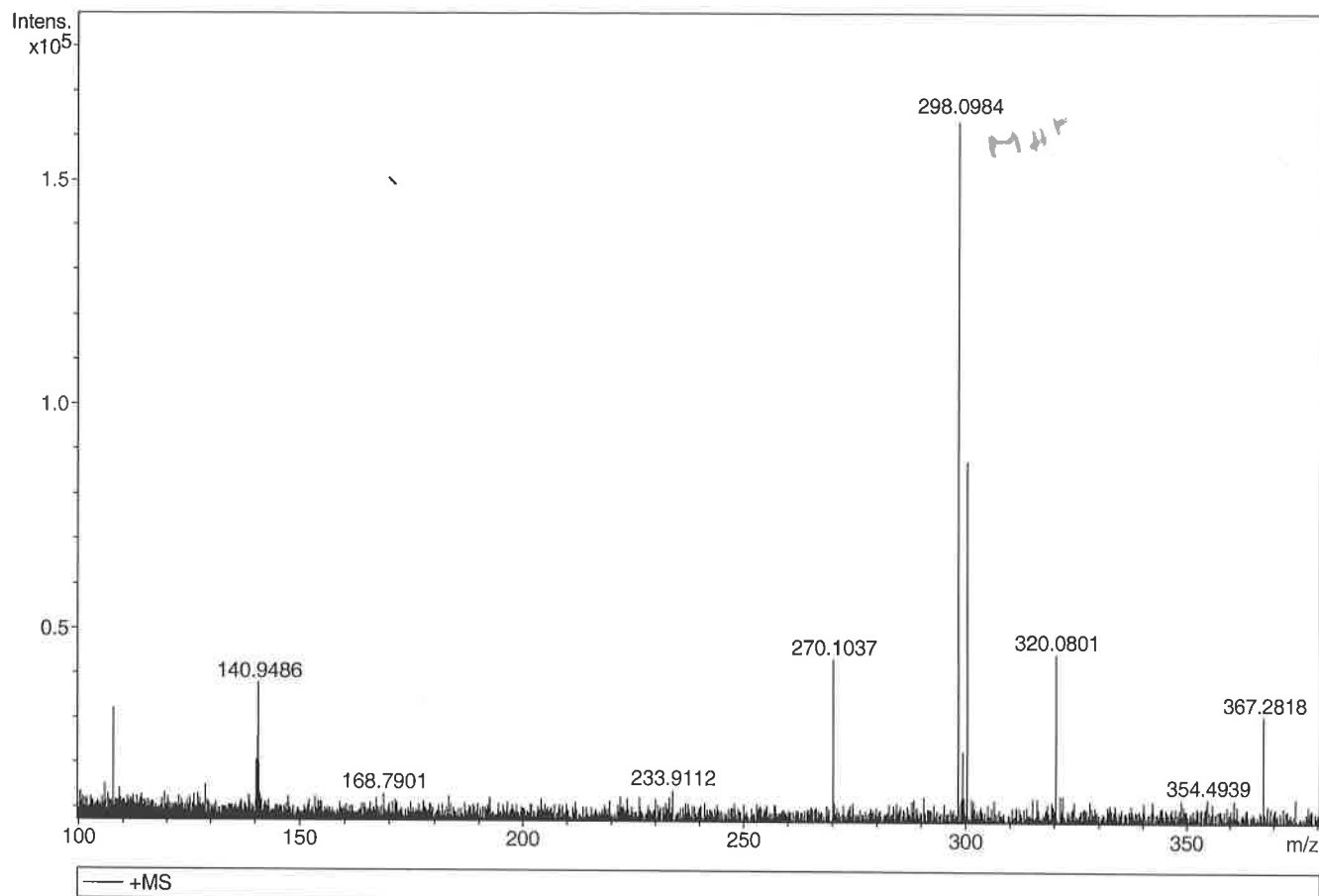
Generic Display Report

Analysis Info

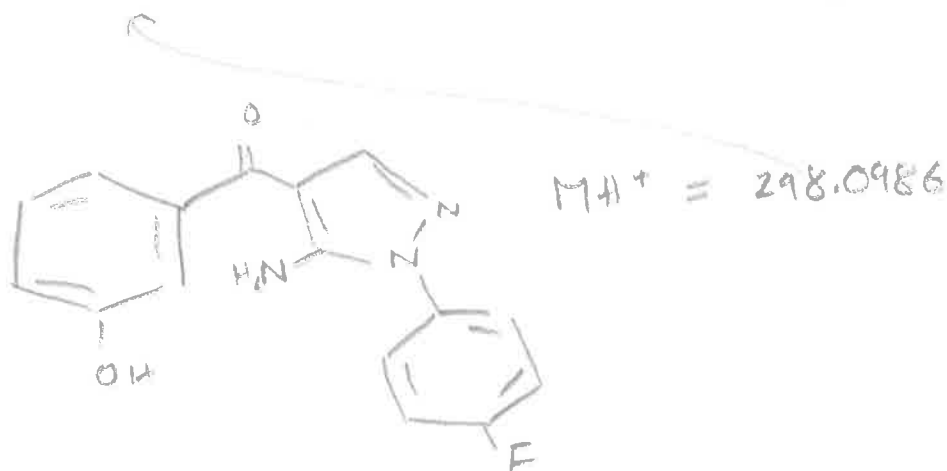
Analysis Name D:\Data\Alinanopos\JESS6049_000001.d
Method pos20090608esi
Sample Name POS ESI BO4JD054A
Comment

Acquisition Date 18/08/2015 15:38:24

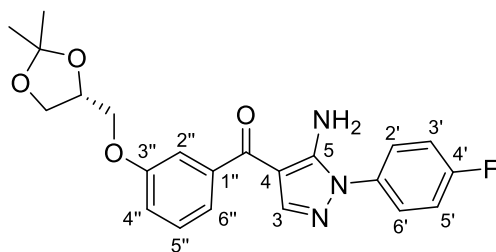
Operator Administrator
Instrument apex-III



Sum Formula	Sigma	m/z	Err [ppm]	Mean Err [ppm]	Err [mDa]	rdb	N Rule	e ⁻
C 16 H 13 F 1 N 3 O 2	0.299	298.0986	0.86	2.02	0.60	11.50	ok	even



[5-Amino-1-(4-fluorophenyl)-1*H*-pyrazo-4-yl]{3-[(*R*)-2,2-dimethyl-1,3-dioxolan-4-yl)methoxy]phenyl} ketone (136)



136

¹H NMR spectrum (500 MHz, CDCl₃) for [5-amino-1-(4-fluorophenyl)-1*H*-pyrazo-4-yl]{3-[(*R*)-2,2-dimethyl-1,3-dioxolan-4-yl)methoxy}phenyl} ketone

B04JD036C Proton for Carbon CDCl₃.esp

M03(m) M05(t)
M02(dd) M06(d)
M01(s) M04(m)

7.80
7.57
7.56
7.56
7.55
7.43
7.41
7.36
7.27
7.26
7.25
7.13

M07(br. s.)

6.03

M11(dd)

M10(dd)

M09(dd)

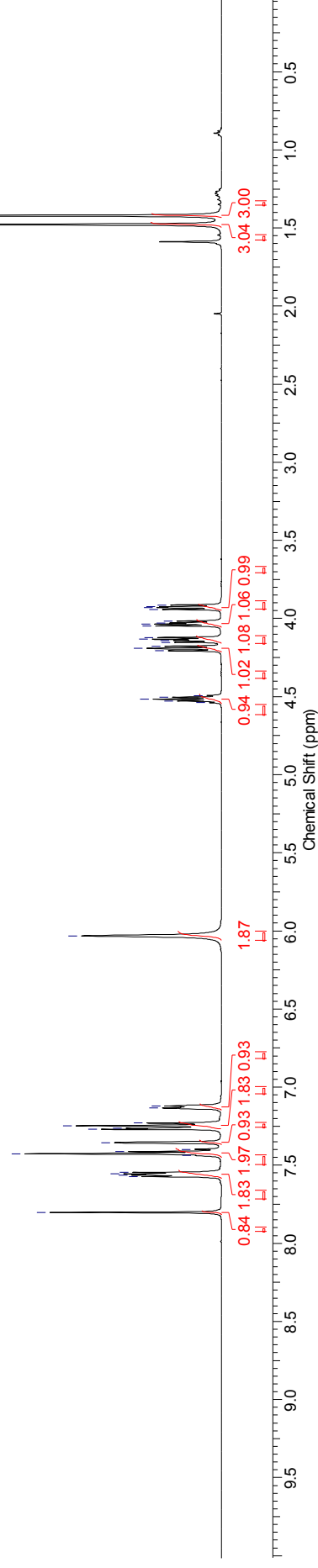
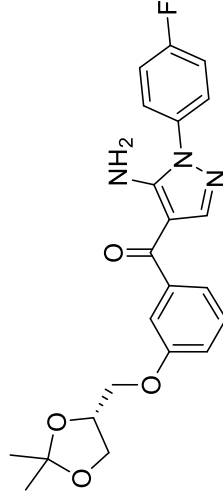
M08(quin) M12(dd)

4.53
4.52
4.50
4.21
4.19
4.15
4.13
4.12
4.05
3.94
3.92

M13(s)

M14(s)

1.48
1.42



¹³C NMR spectrum (126 MHz, CDCl₃) for [5-amino-1-(4-fluorophenyl)-1*H*-pyrazo-4-yl][3-[(*R*)-2,2-dimethyl-1,3-dioxolan-4-yl)methoxy]phenyl} ketone

B04JD036C CARBON_01.esp

M03(d)

M02(d)

J(M03)=249.87 Hz

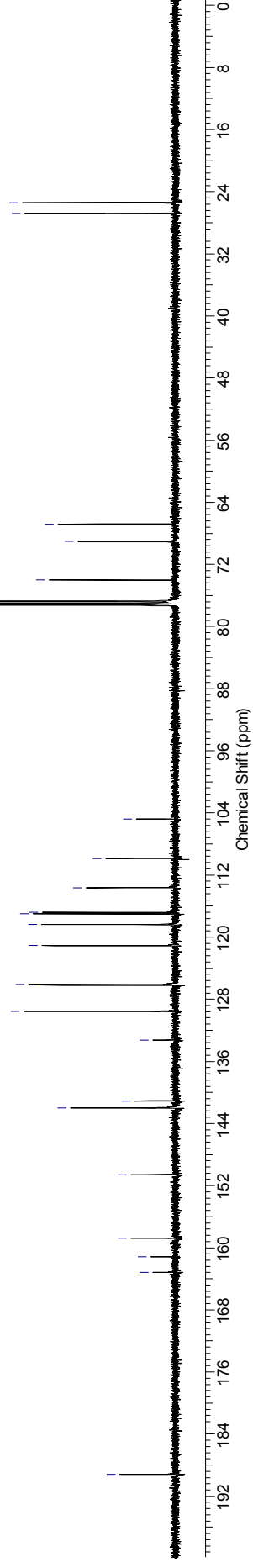
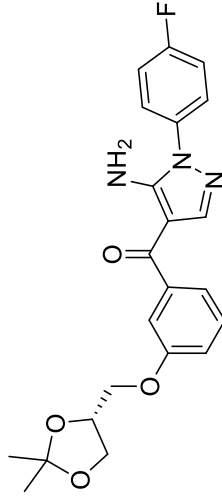
J(M02)=23.84 Hz

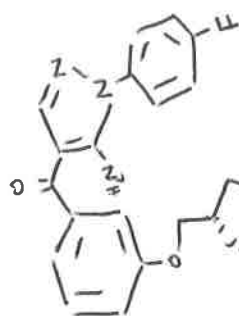
189.18
163.16
161.18
158.78
150.59
141.99
141.09

M01(d)

133.25
129.56
126.19
126.12
121.10
118.38
117.01
116.82
113.64
109.86
104.80

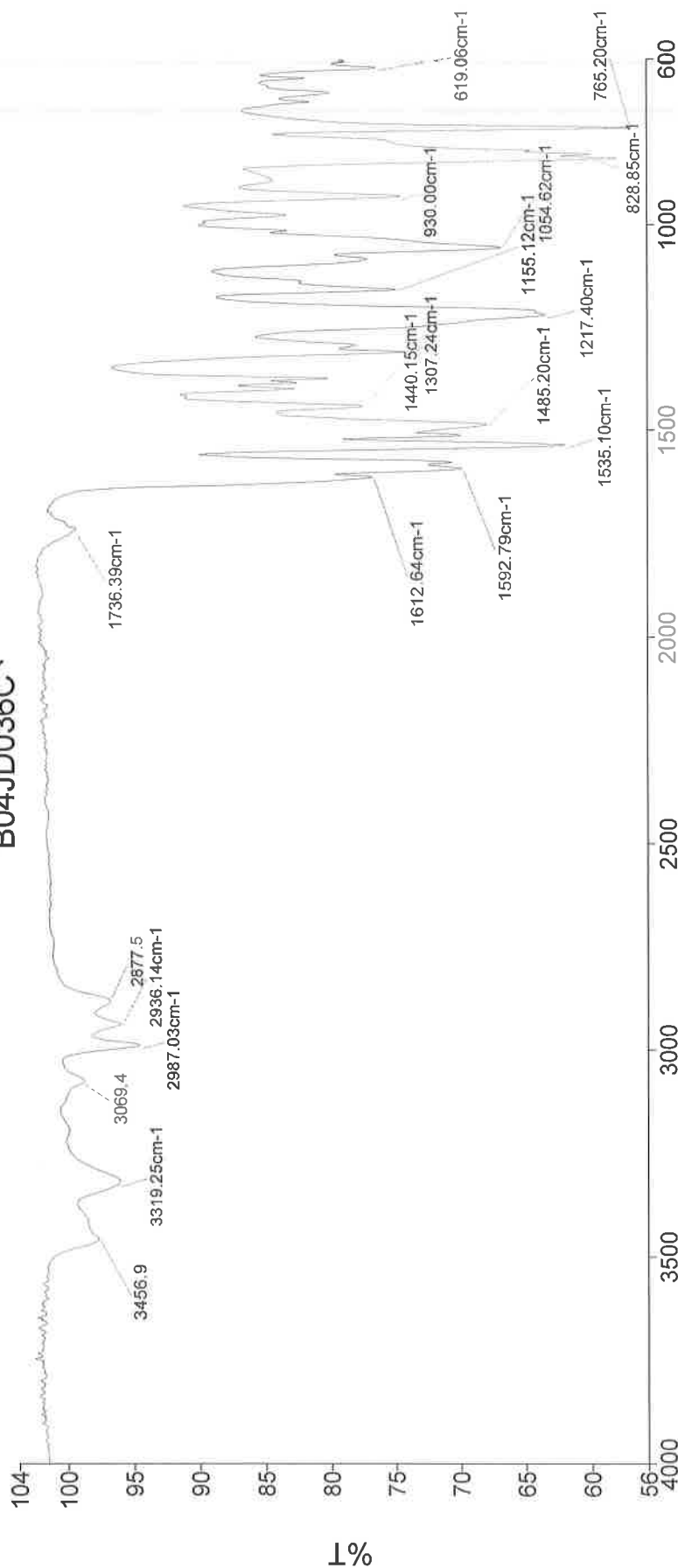
77.00
74.01
69.06
66.81
26.79
25.40





Analyst
Date

B04JD036C

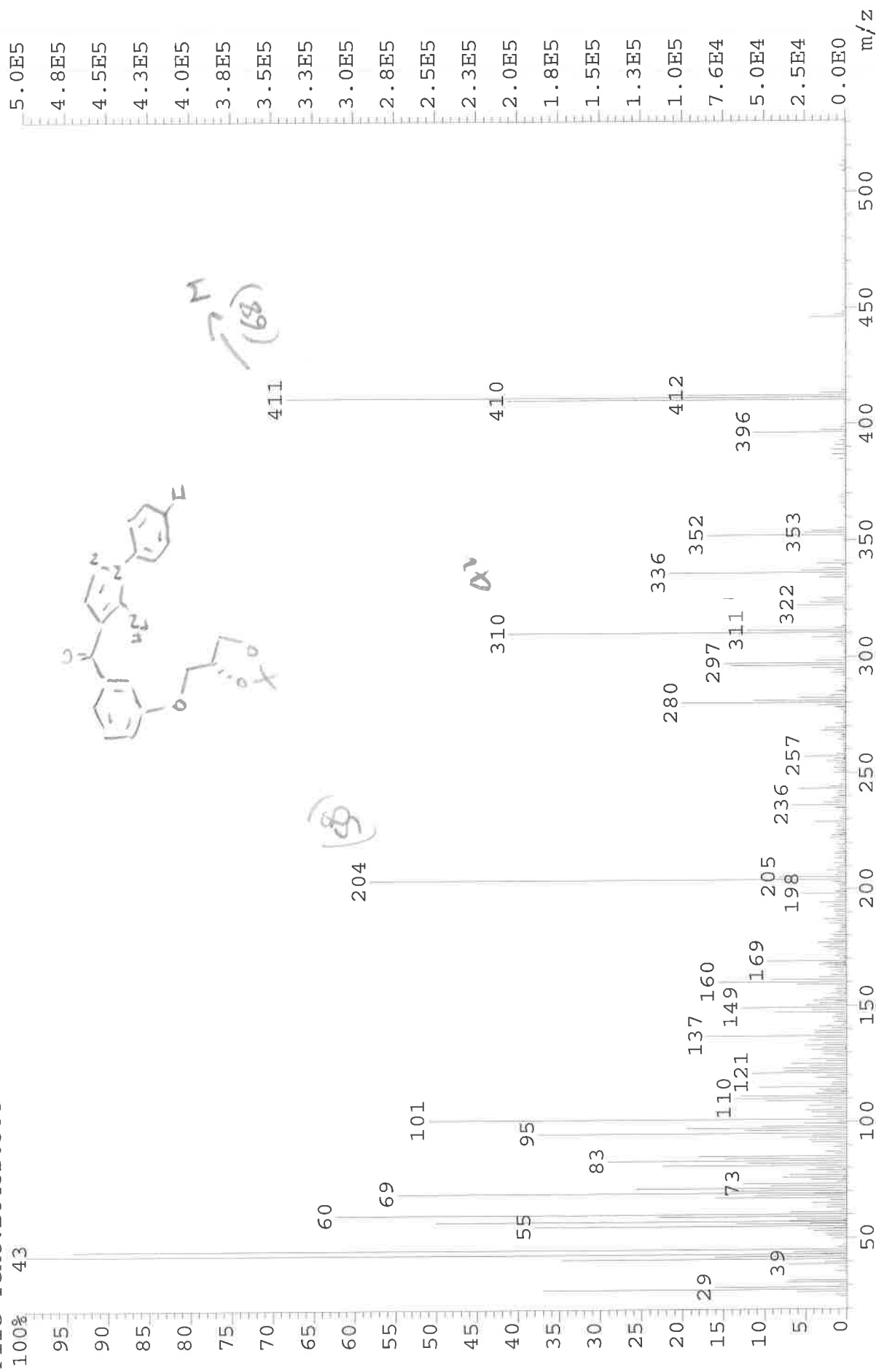


cm-1

Administrator 23 Sample 023 By Administrator Date Thursday, June 25 2015

3457 N-H
3319 N-H st.
2987 C-H st.
1613 C=O
1593 NH2
1535 C=O
1485 C-O-C
1217 C-O-C
1055 C-O-C
828.85 -NH2
→ 1155 -ArCF

File: JESS5953 Ident: 10 Acq: 20-JUL-2015 13:50:19 +0:40 Cal: CAL1
AutoSpecE EI+ Magnet BpI: 504875 TIC: 10986791 Flags: HALL
File Text: BO4JD036C



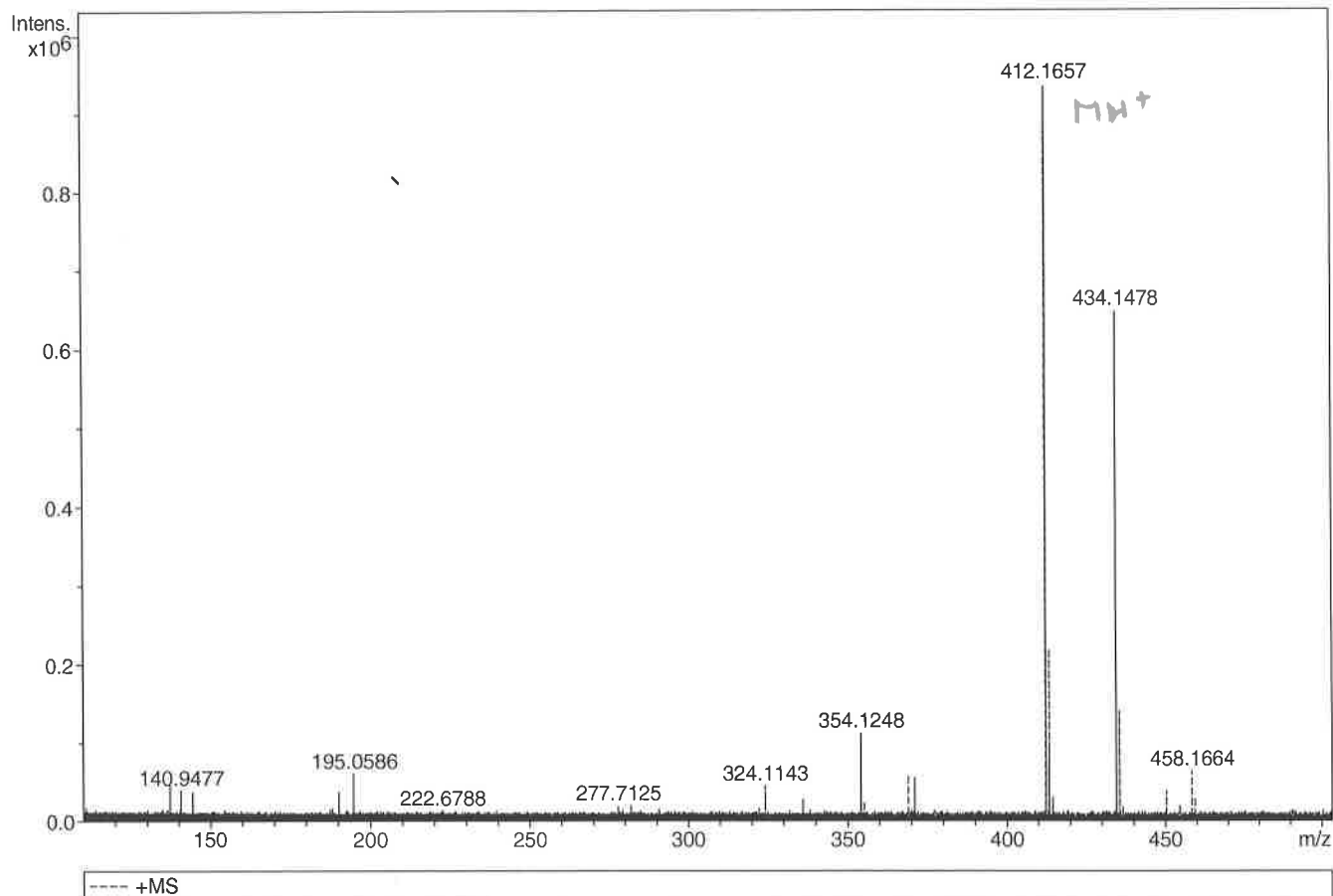
Generic Display Report

Analysis Info

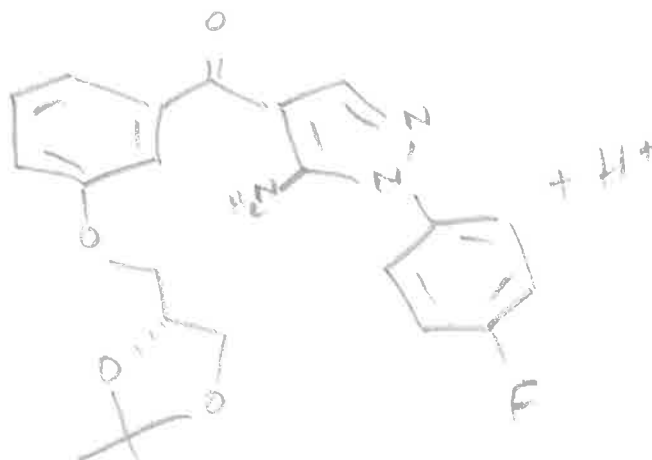
Analysis Name D:\Data\Alinanopos\JESS5953_000001.d
Method pos20090608esi
Sample Name POS ESI BO4JD036C
Comment

Acquisition Date 20/07/2015 13:05:10

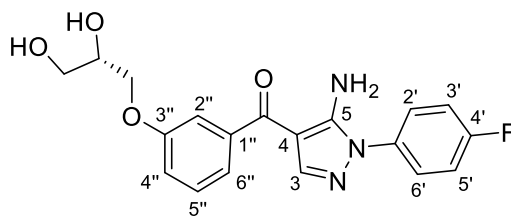
Operator Administrator
Instrument apex-III



Sum Formula	Sigma	m/z	Err [ppm]	Mean Err [ppm]	Err [mDa]	rdB	N Rule	e ⁻
C 22 H 23 F 1 N 3 O 4	0.021	412.1667	2.43	0.19	0.08	12.50	ok	even



5-Amino-1-(4-fluorophenyl)-4-{3-[2(S)-3-dihydroxypropoxy]benzoyl} pyrazole (RO3201195) (10)



RO3201195 (10)

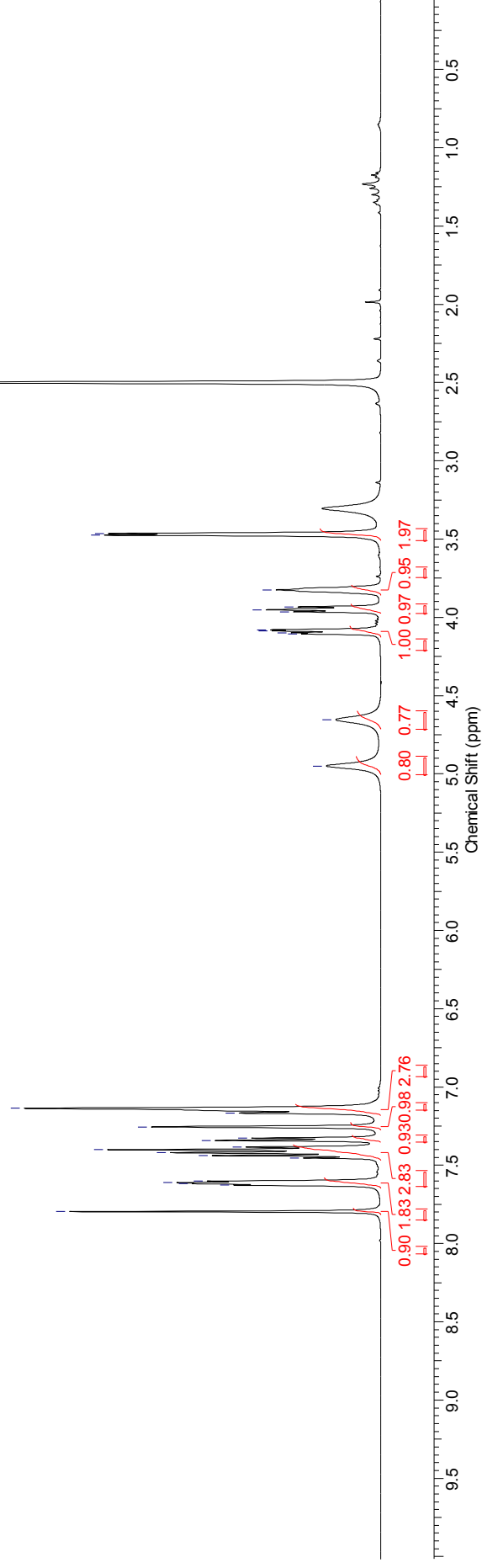
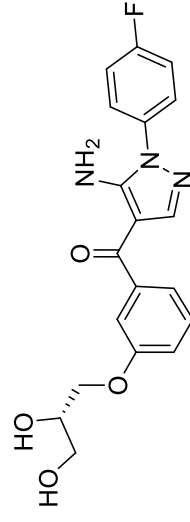
¹H NMR (500 MHz, DMSO-*d*₆) for 5-amino-1-(4-fluorophenyl)-4-{3-[2(*S*)-3-dihydroxypropoxy]benzoyl}pyrazole (RO3201195)

B04JD043A DMSO Proton for carbon.esp

M03(m) 7.80, 7.63, 7.62, 7.61, 7.44, 7.42, 7.40, 7.34, 7.26, 7.17, 7.14
M02(dd) M06(m)
M05(br. s.)
M01(s) M04(d)

M08(br. s.) 4.95, 4.66, 4.11, 4.10, 4.09, 4.08, 3.96, 3.95, 3.93, 3.82
M11(br. s.)
M10(m) M12(d) 3.47, 3.46

DMSO



¹³C NMR (126 MHz, DMSO-*d*₆) for 5-amino-1-(4-fluorophenyl)-4-{3-[2(*S*)-3-dihydroxypropoxy]benzoyl}pyrazole (RO3201195)

B04JD043A DMSO CARBON .esp

M04(d)

M03(d) M02(d)

M01(d)

J(M04)=244.15 Hz

J(M03)=2.86 Hz

J(M01)=22.89 Hz

187.54

162.04
160.09
158.73

151.17

141.38
140.90

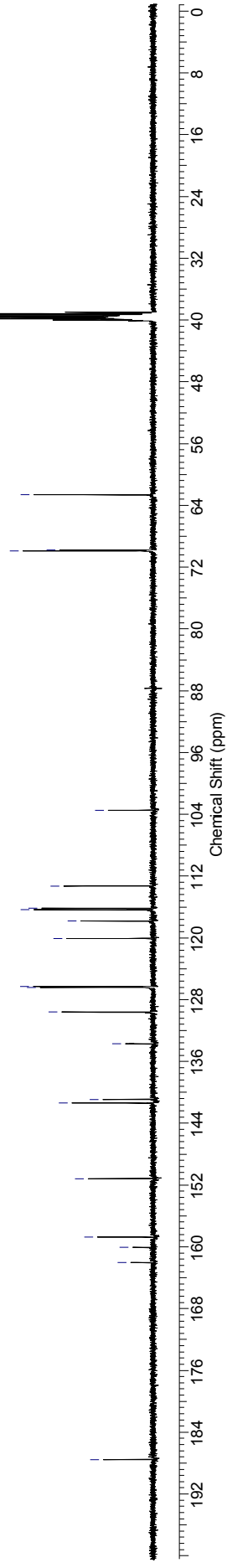
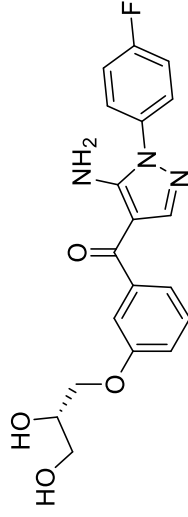
133.72
129.61
126.39
126.32

120.07
117.83
116.37
116.18
113.27

103.46

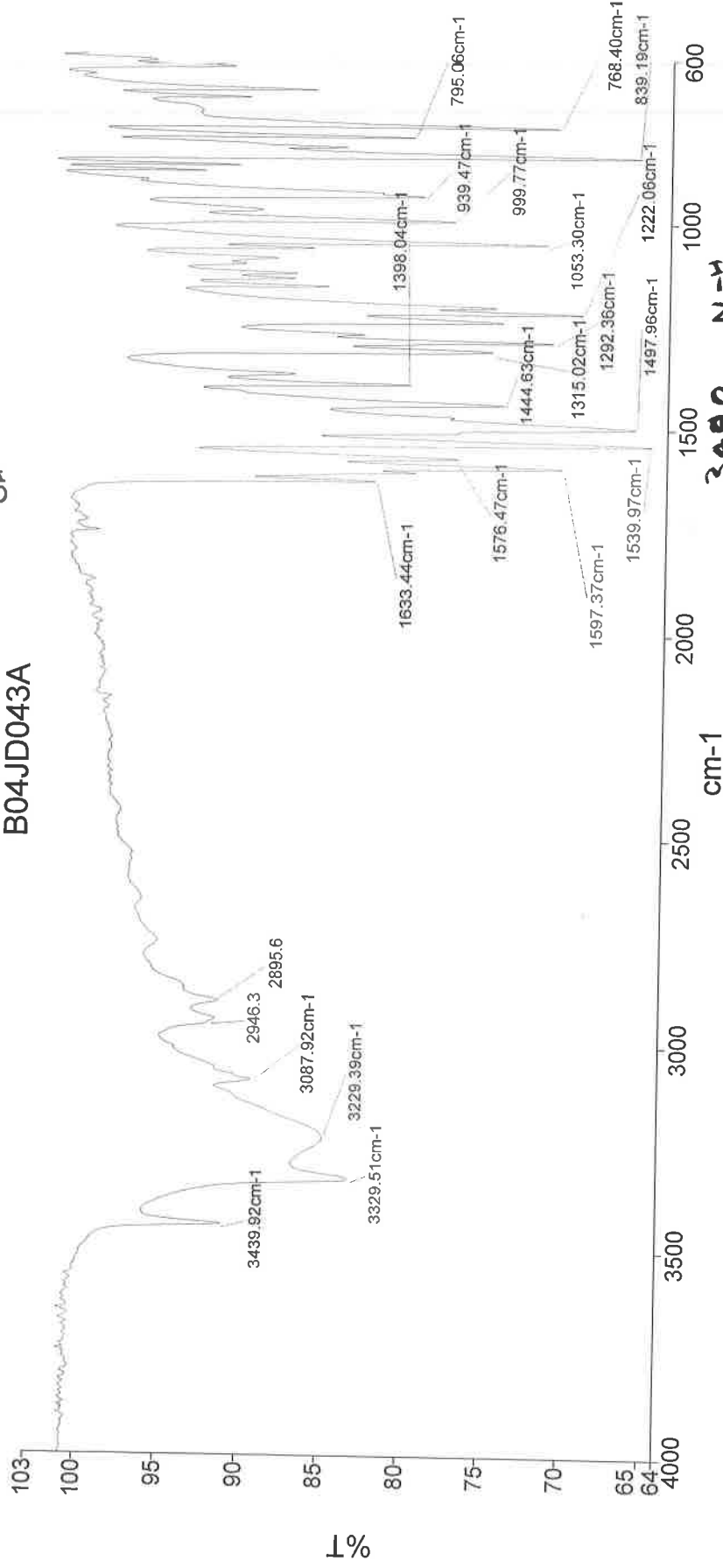
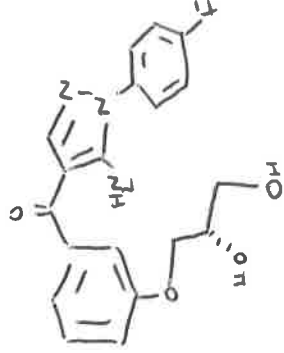
69.89
69.79
62.63

39.51



Analyst
Date
Administrator
25 June 2015 10:33

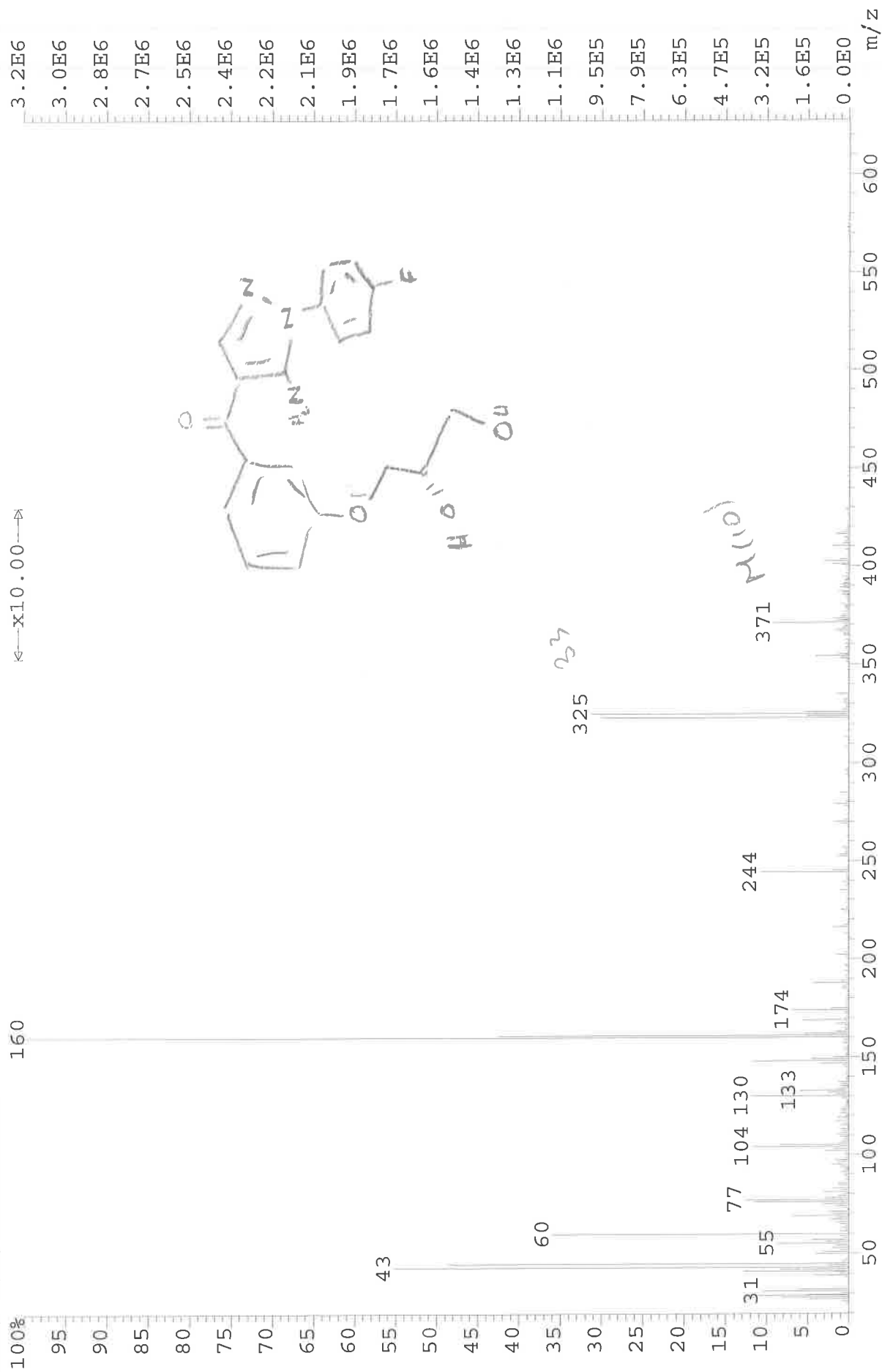
B04JD043A



1292 C-O-C
1222 Aromatic
1053 C-O-C
839 N-H

3490 N-H
3330 O-H
3229 O-H
2896 C-H
1633 C=O
1597 NH₂
1540 C=N
1498 C-C

File: JESS5951 Ident: 11 Acq: 20-JUL-2015 12:27:19 +0:44 Cal: CAL1
 AutoSpecE EI+ Magnet BpI: 3157384 TIC: 24076982 Flags: HALI
 File Text: BO4JD043B



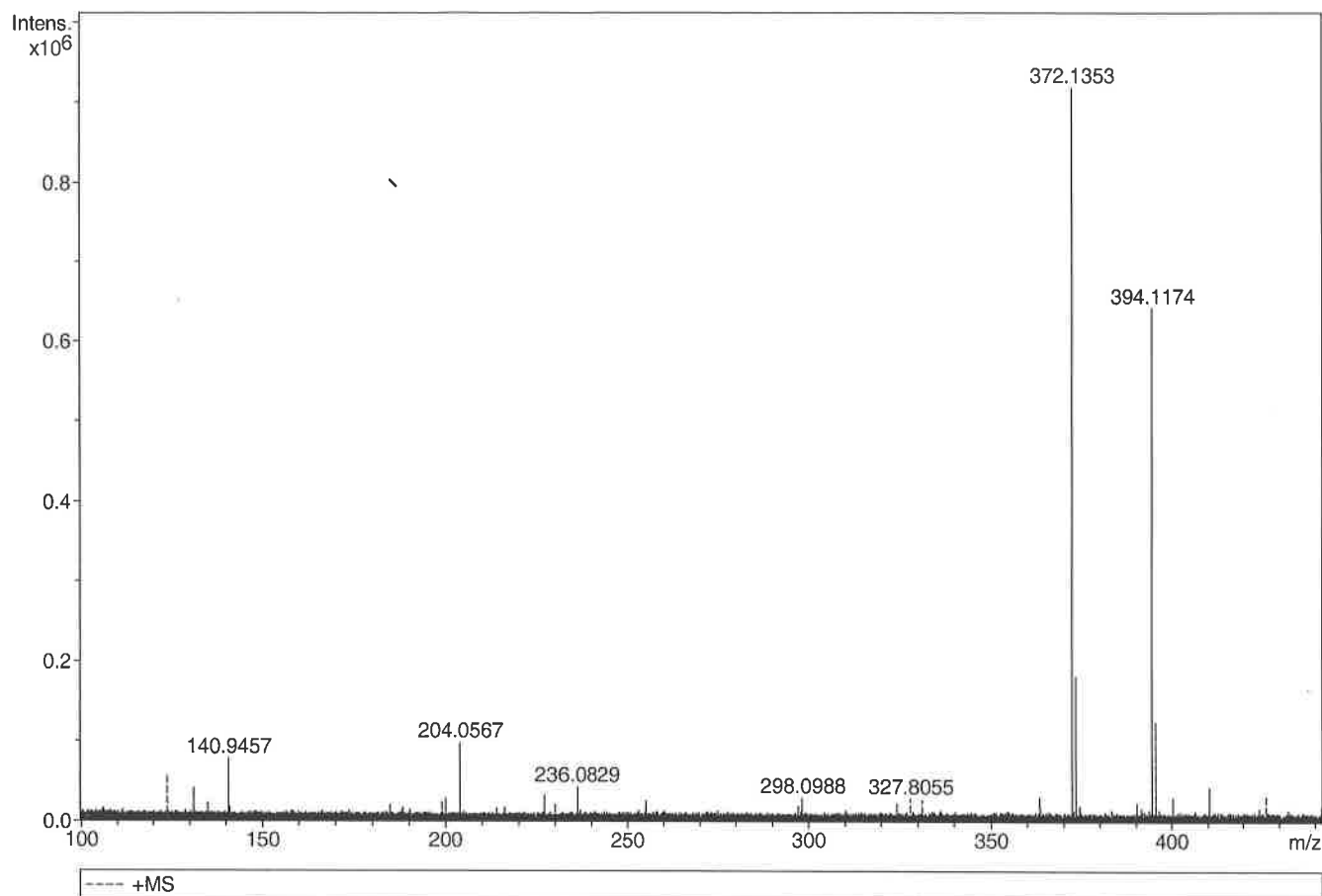
Generic Display Report

Analysis Info

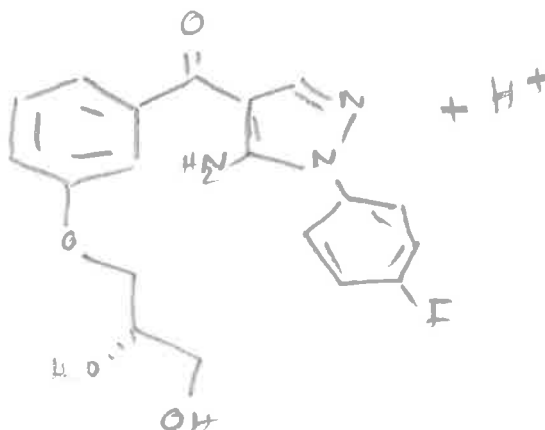
Analysis Name D:\Data\Alinanopos\JESS5871_000001.d
Method pos20090608esi
Sample Name POS ESI B04JD043A
Comment

Acquisition Date 25/06/2015 10:42:49

Operator Administrator
Instrument apex-III

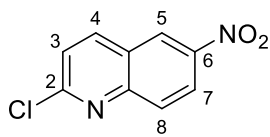


Sum Formula	Sigma	m/z	Err [ppm]	Mean Err [ppm]	Err [mDa]	rdB	N Rule	e ⁻
C 19 H 19 F 1 N 3 O 4	0.024	372.1354	0.23	0.15	0.06	11.50	ok	even



Chapter 3: ^1H NMR, ^{13}C NMR, IR and Mass spectra

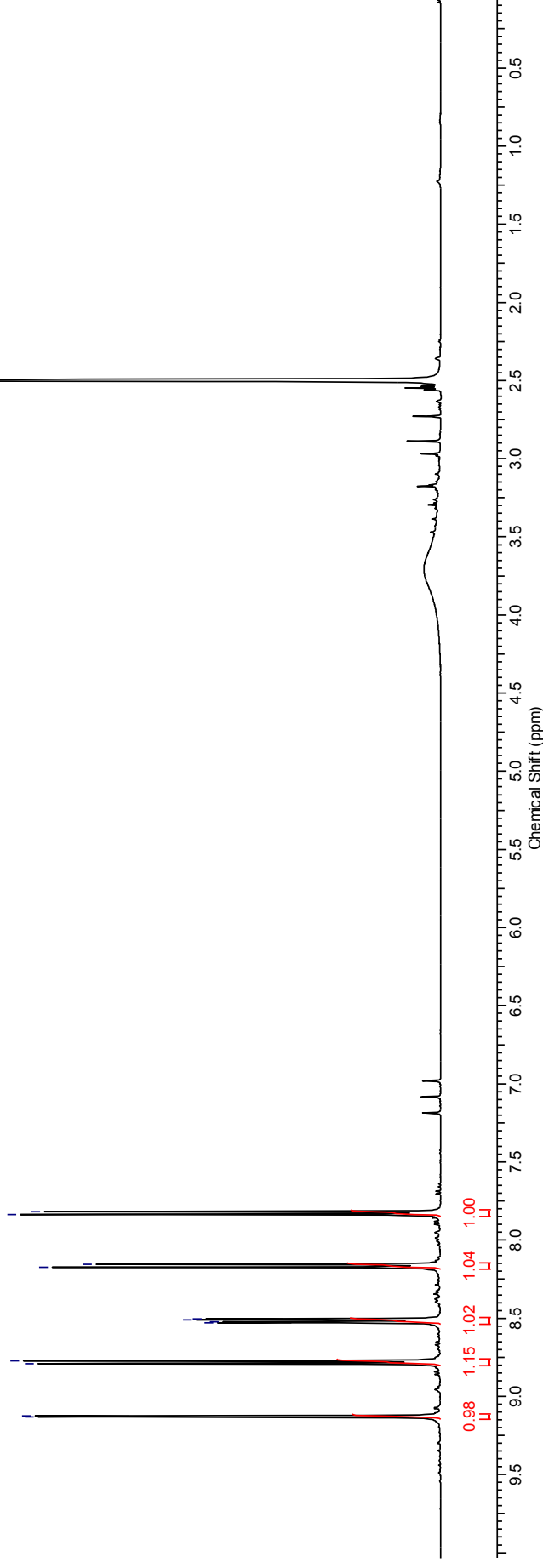
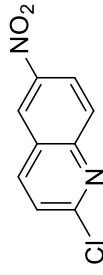
2-Chloro-6-nitroquinoline (151)



¹H NMR (500 MHz, DMSO-*d*₆) for 2-Chloro-6-nitroquinoline

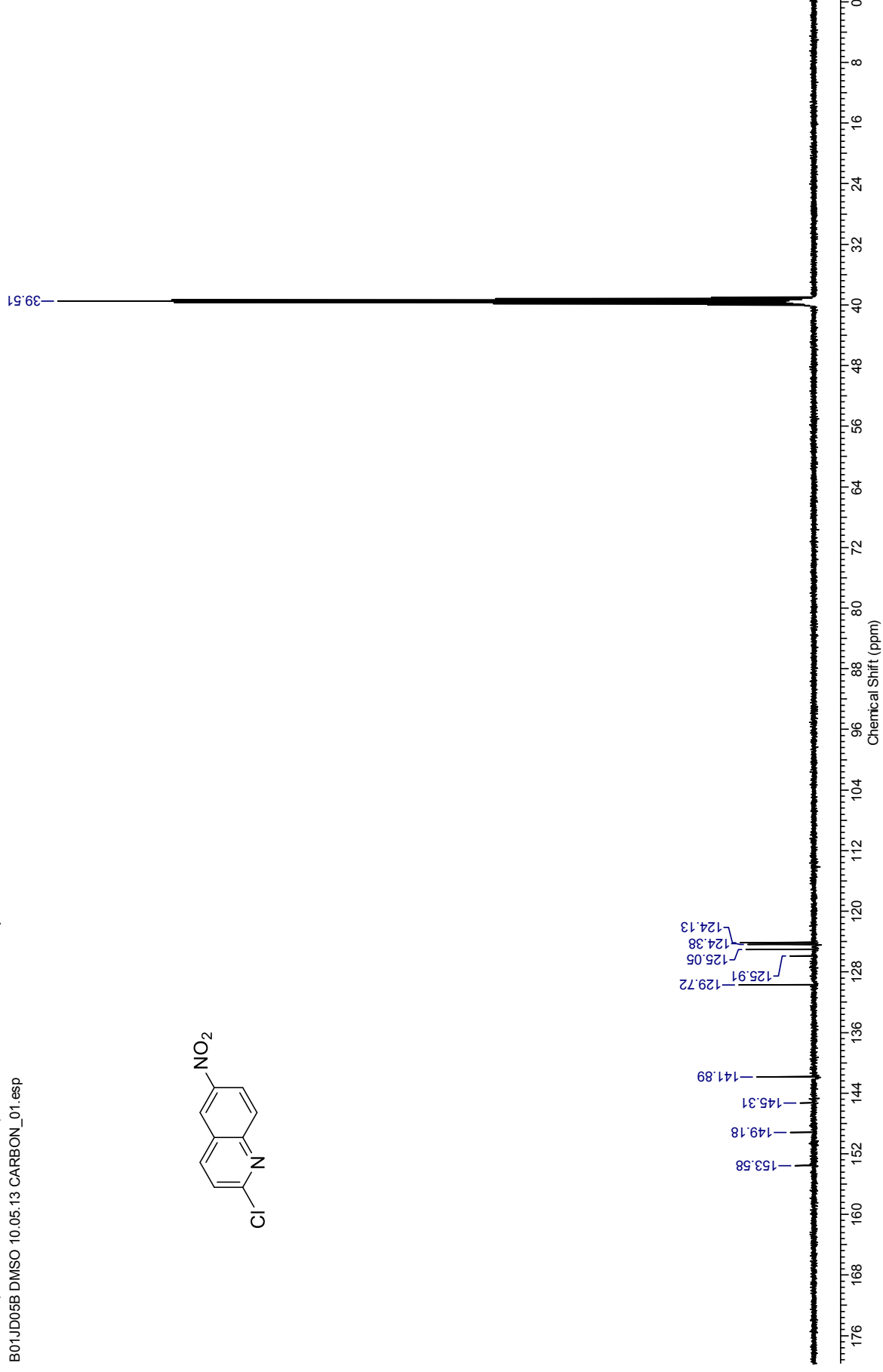
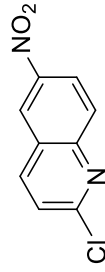
B01JD05B DMSO 10.05M PROTON_01.esp

9.13	M01(d)	8.79	M03(dd)	8.51	M05(d)
9.13		8.77		8.52	
		8.53		8.17	
				8.16	
				7.84	
				7.82	



¹³C NMR (126 MHz, DMSO-*d*₆) for 2-Chloro-6-nitroquinoline

B01JD05B DMSO 10.05.13 CARBON_01.esp

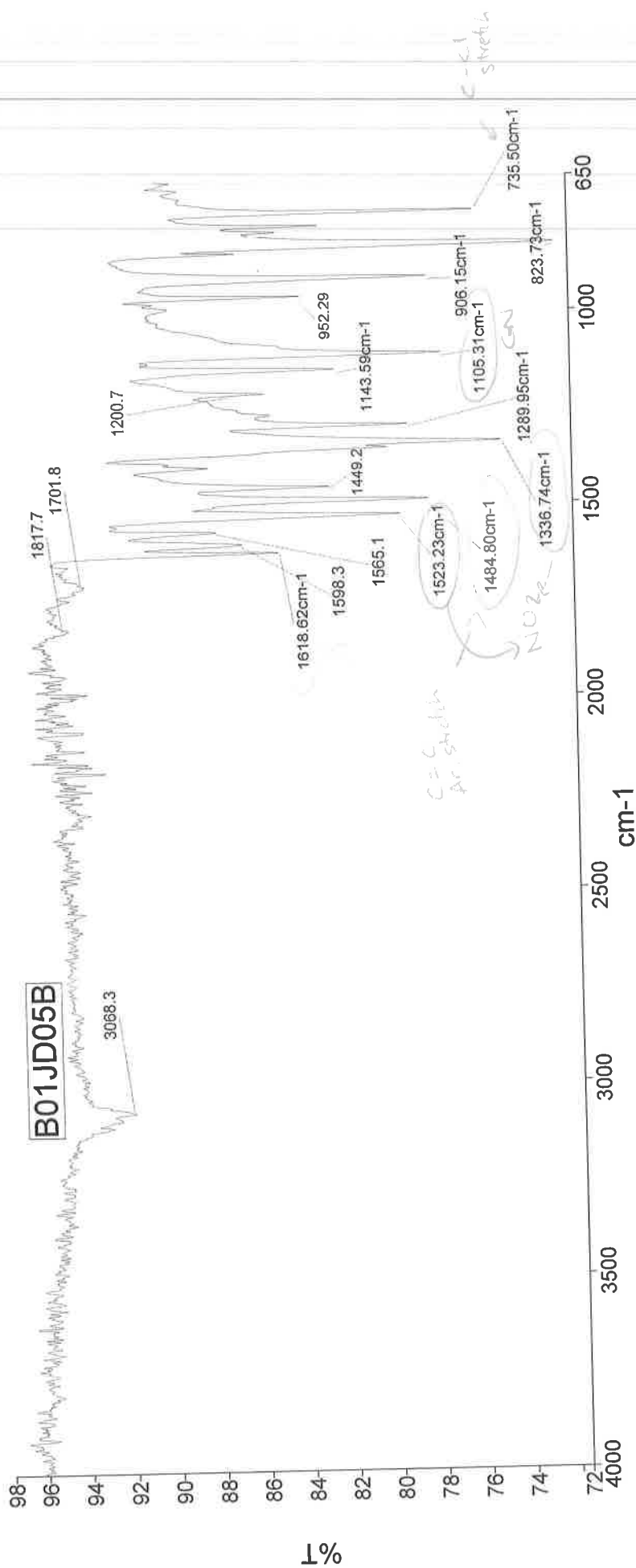




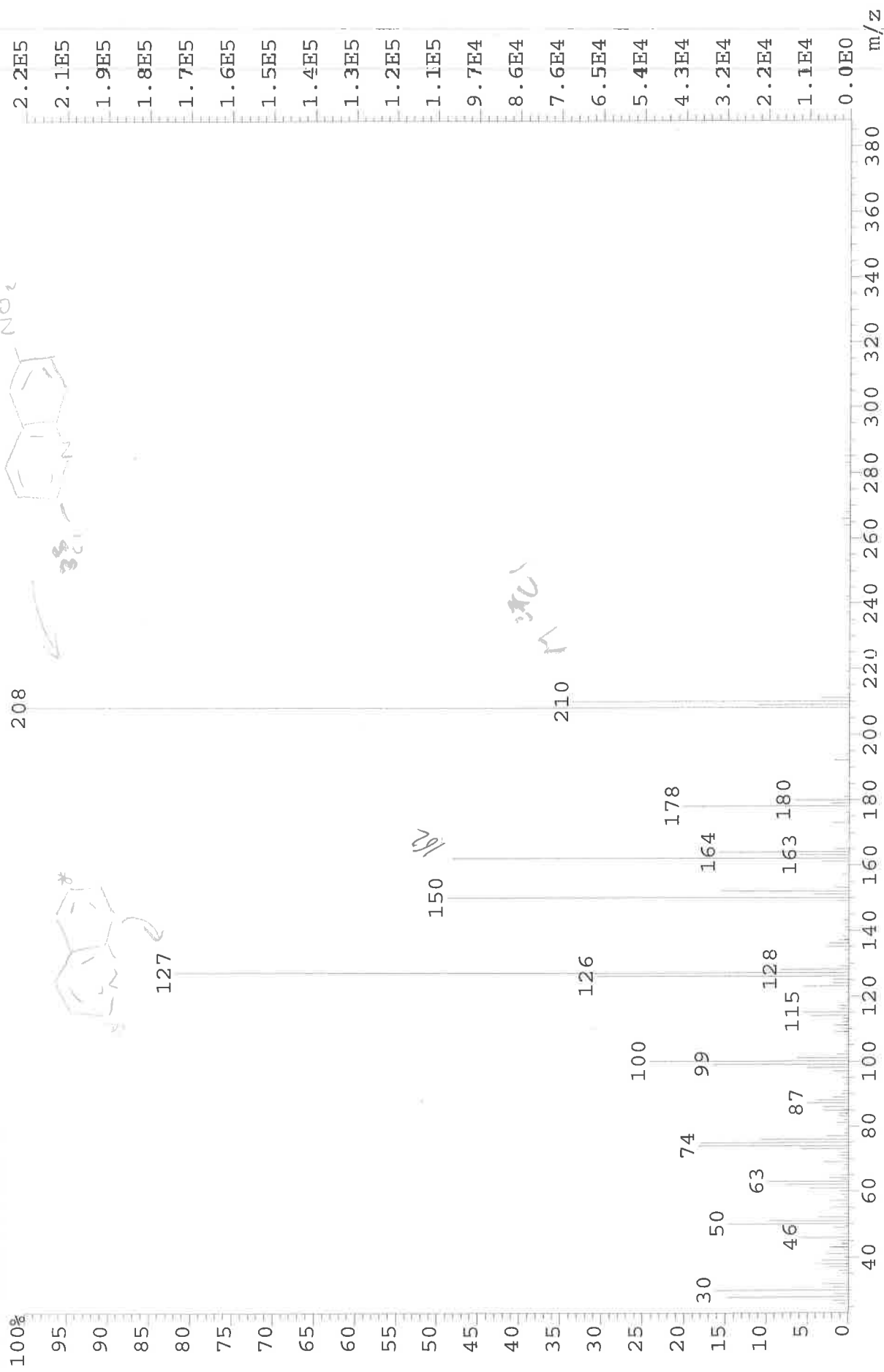
Analyst
Date

Administrator

07 November 2012 15:58



File: JESSICA8717 Ident: 78 Acq: 26-OCT-2012 10:12:57 +4:50 Cal: CAL1
AutoSpec EI+ Magnet BpI: 216102 TIC: 1698832 Flags: HALL
File Text: B01JD05B



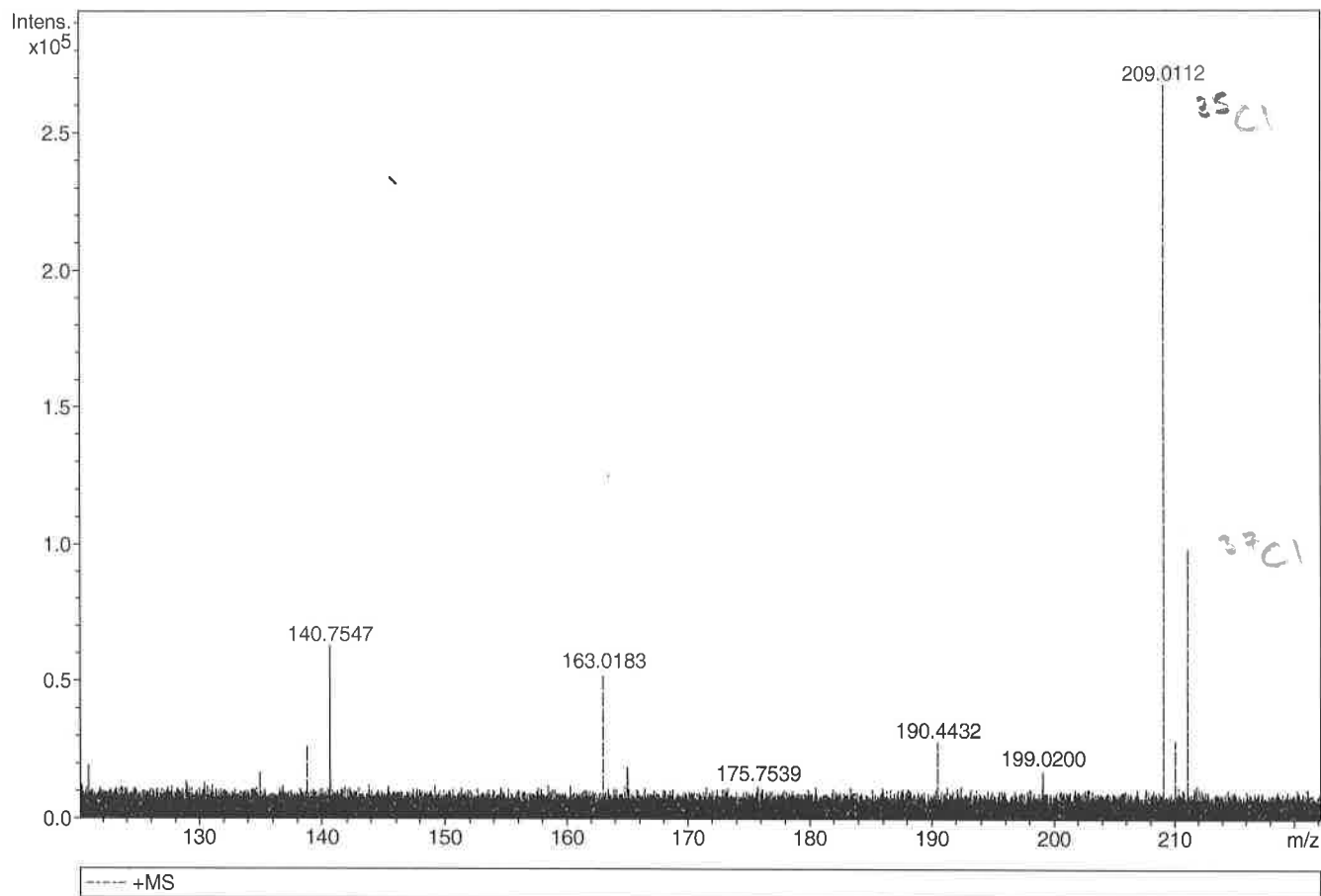
Generic Display Report

Analysis Info

Analysis Name D:\Data\Alinanopos\JESS4931_000003.d
 Method pos20090608esi
 Sample Name POS ESI BO3JD005B
 Comment

Acquisition Date 23/03/2015 11:16:58

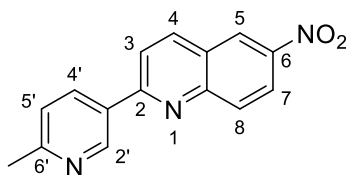
Operator Administrator
 Instrument apex-III



Sum Formula	Sigma	m/z	Err [ppm]	Mean Err [ppm]	Err [mDa]	rdb	N Rule	e ⁻
C ₉ H ₆ ClN ₂ O ₂	0.021	209.0112	0.13	0.13	0.03	7.50	ok	even



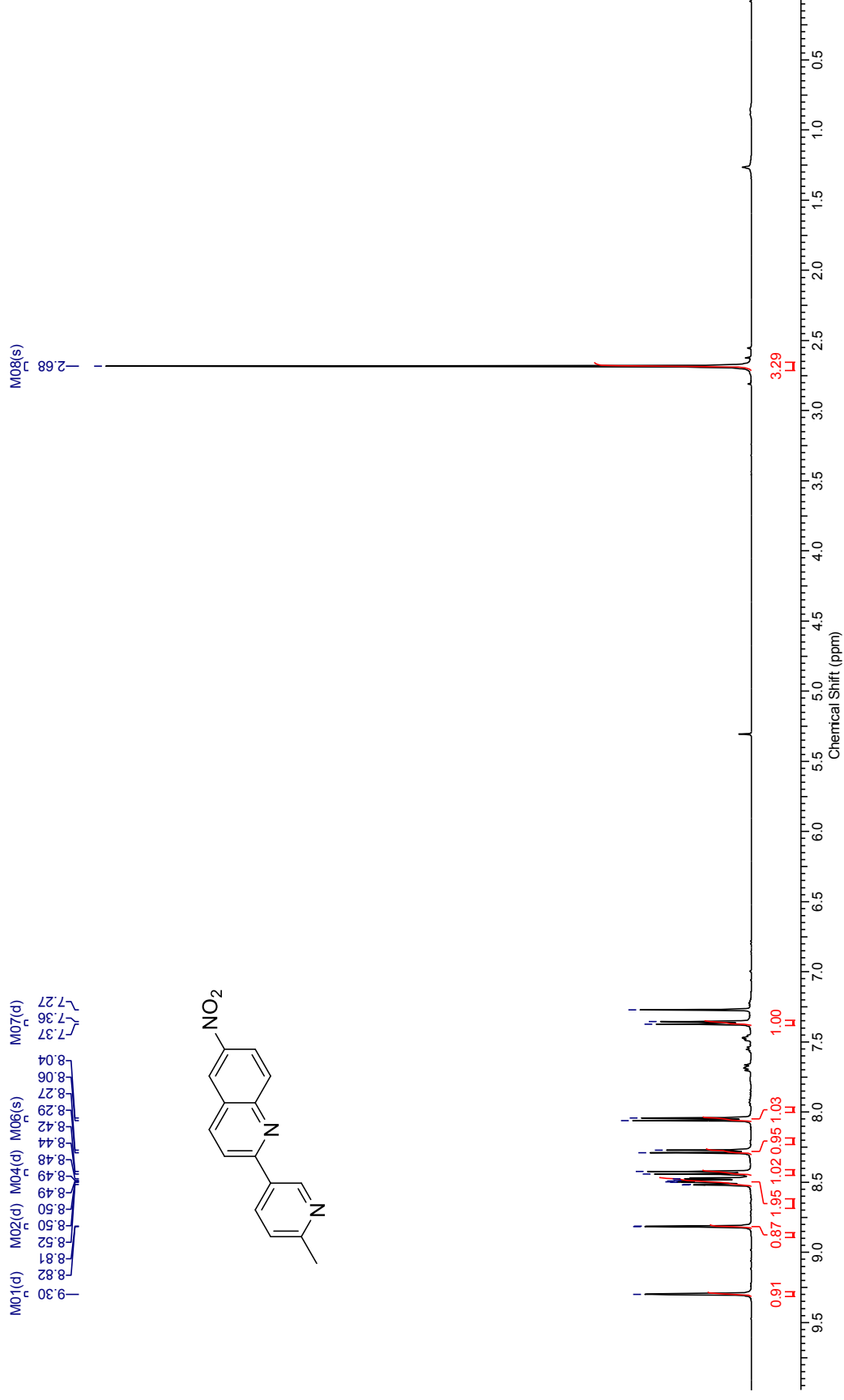
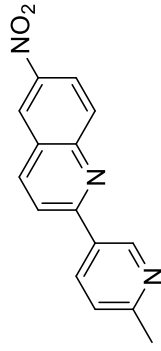
2-(6-Methylpyridin-3-yl)-6-nitroquinoline (153)



¹H NMR (500 MHz, CDCl₃) for 2-(6-Methylpyridin-3-yl)-6-nitroquinoline

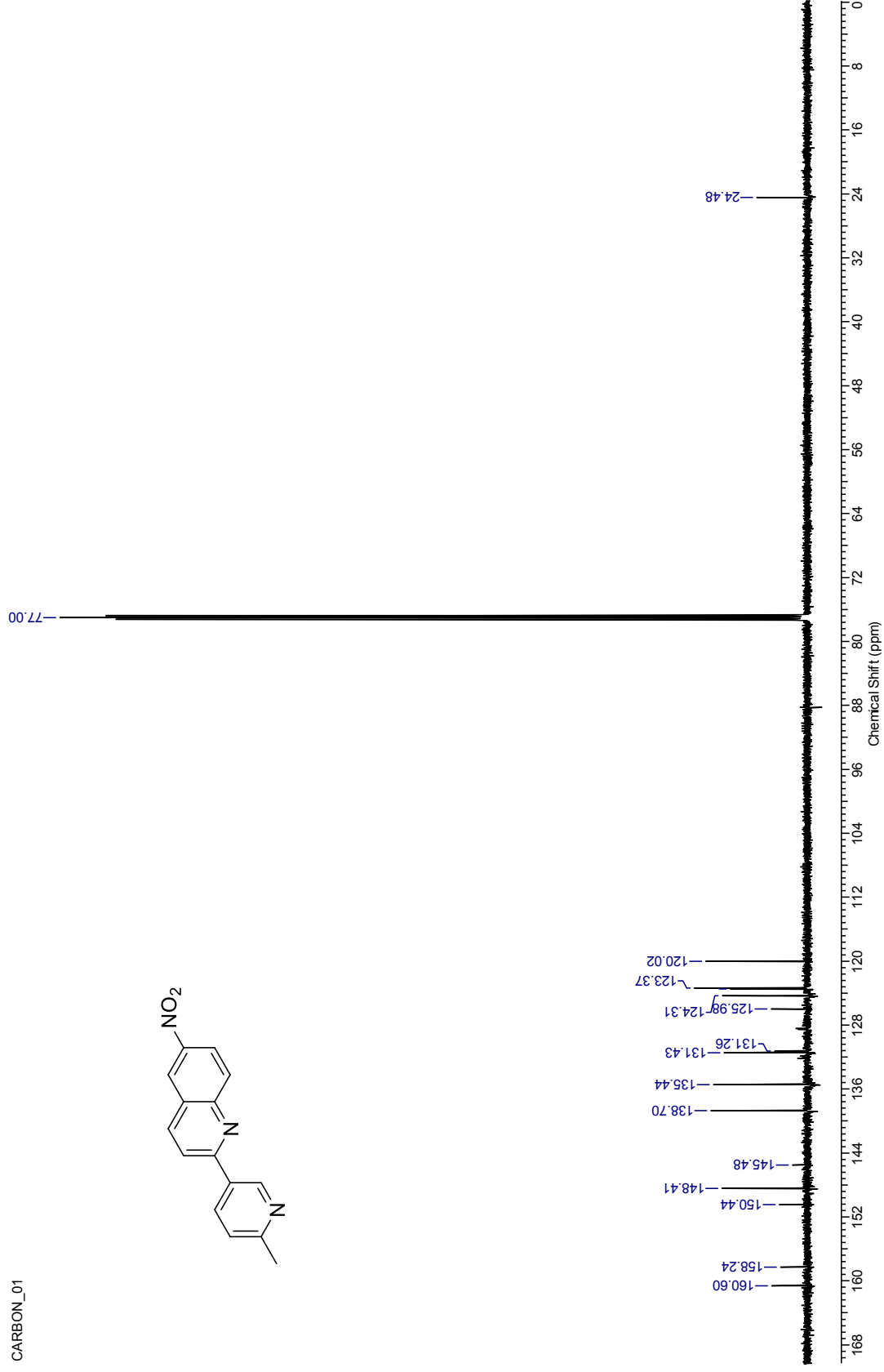
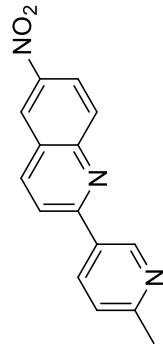
B03JD041A CDCl₃ Proton NMR

M05(d)			
M01(d)	M02(d)	M04(d)	M06(s)
9.30	8.82	8.81	8.52
8.82	8.50	8.49	8.48
8.49	8.44	8.42	8.29
8.27	8.06	8.04	7.37
7.36			7.27



¹³C NMR (126 MHz, CDCl₃) for 2-(6-Methylpyridin-3-yl)-6-nitroquinoline

CARBON_01

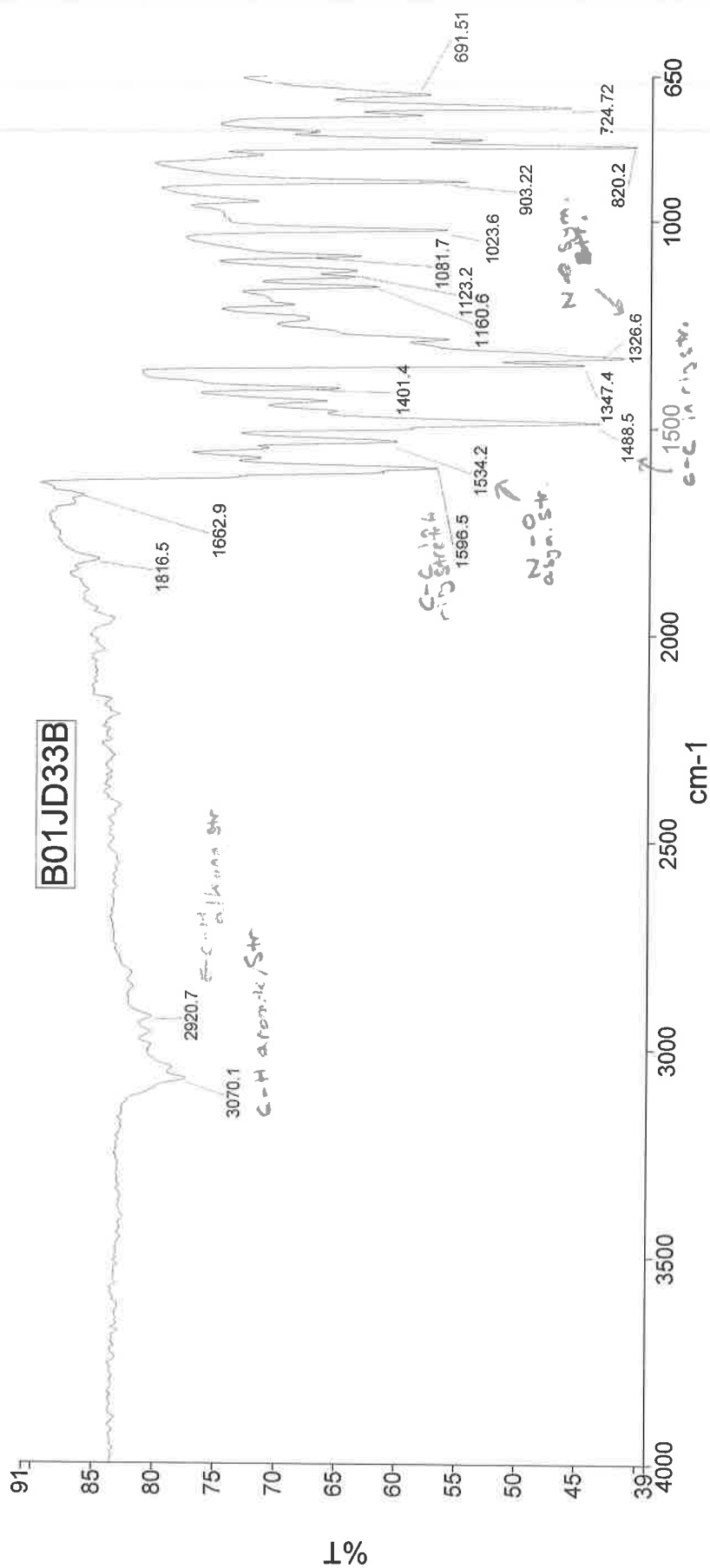




PerkinElmer Spectrum Version 10.03.06
26 November 2012 09:42

Analyst
Date

Administrator
26 November 2012 09:42



Administrator 625 Sample 625 By Administrator Date Monday, November 26 2012

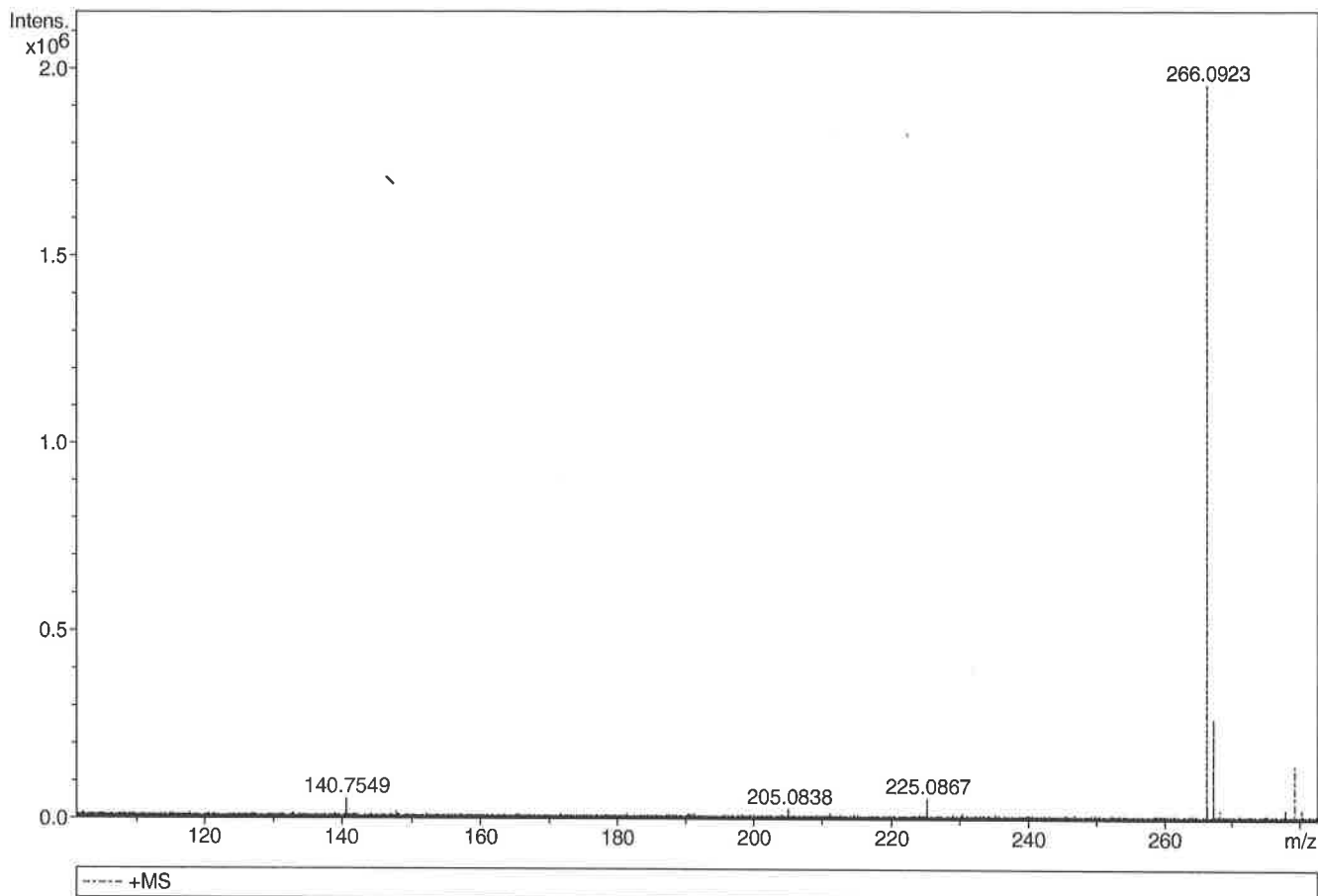
Generic Display Report

Analysis Info

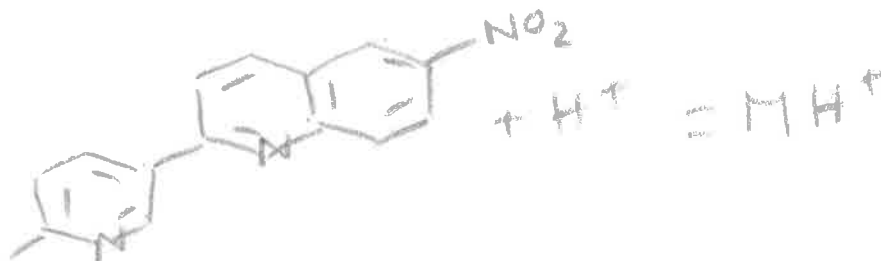
Analysis Name D:\Data\Alinanopos\JESS8817_000001.d
Method pos20090608esi
Sample Name POS ESI B01JD41B
Comment

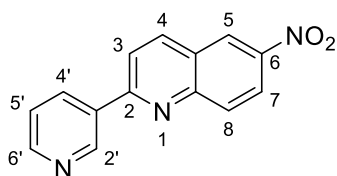
Acquisition Date 03/12/2012 12:56:14

Operator Administrator
Instrument apex-III



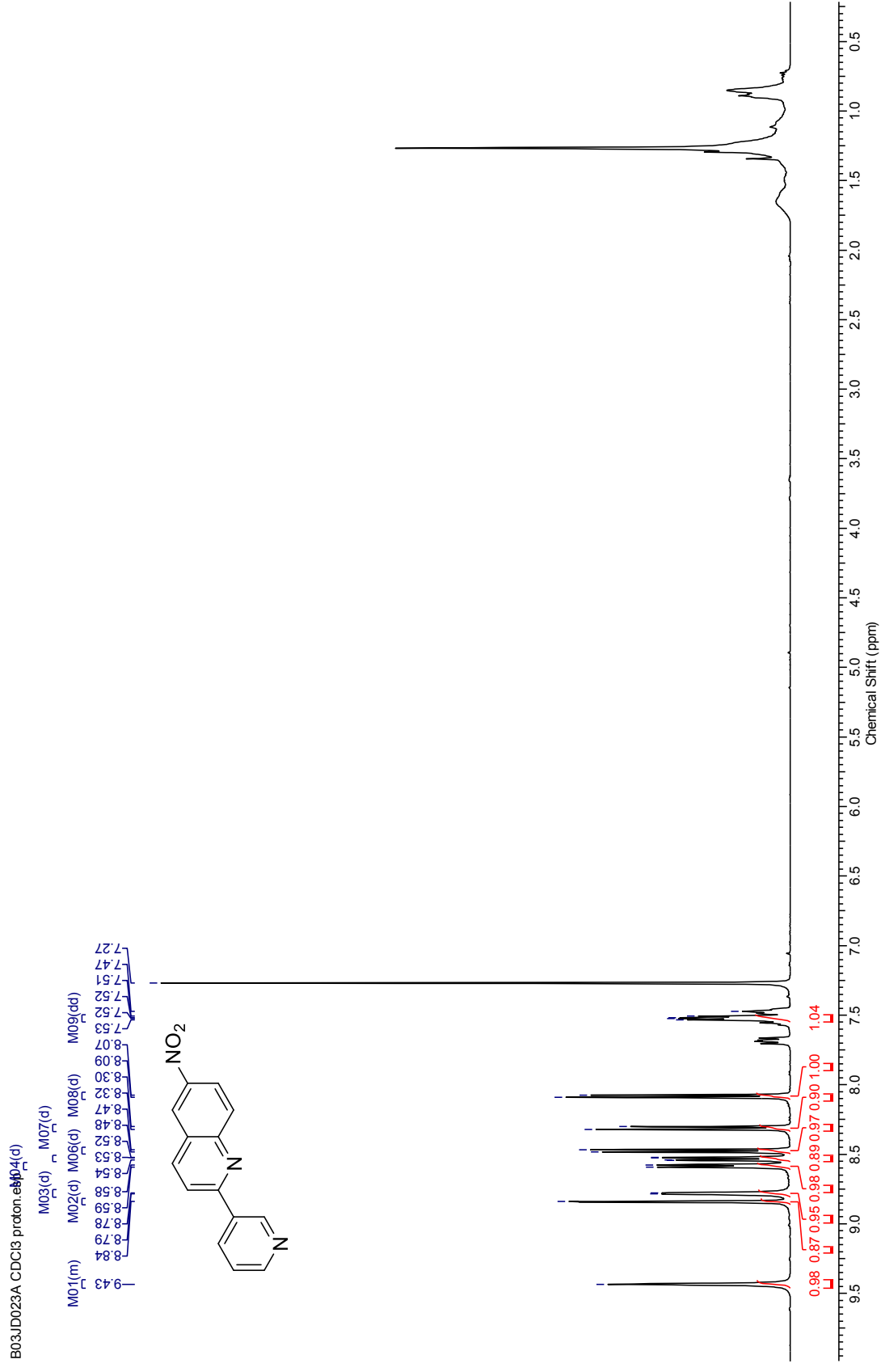
Sum Formula	Sigma	m/z	Err [ppm]	Mean Err [ppm]	Err [mDa]	rdB	N Rule	e ⁻
C 15 H 12 N 3 O 2	0.038	266.0924	0.55	0.72	0.19	11.50	ok	even





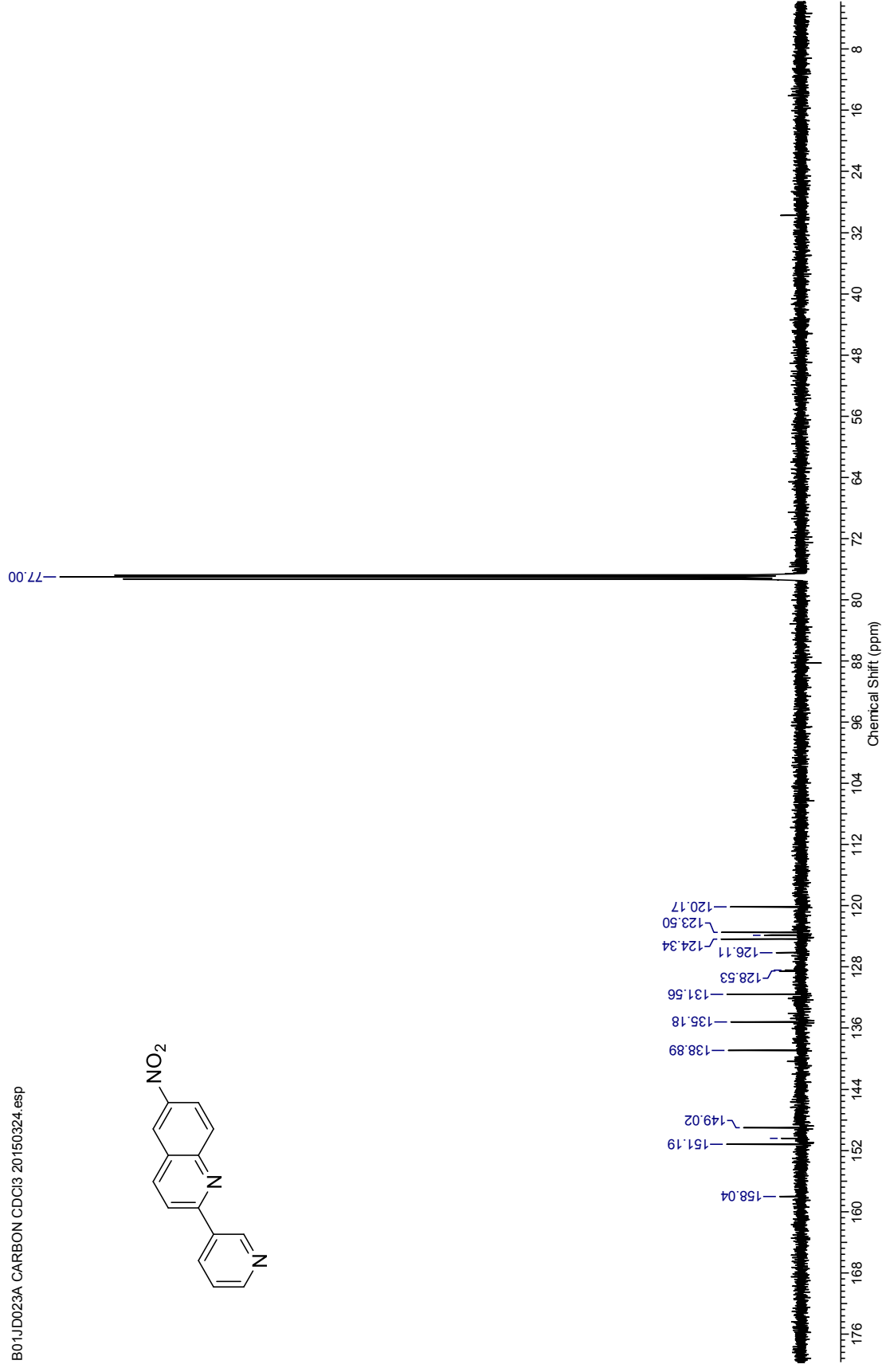
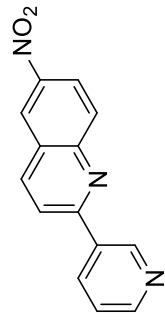
6-Nitro-2-(pyridin-3-yl)quinoline (152)

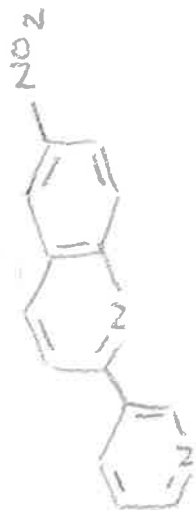
¹H NMR (500 MHz, CDCl₃) for 6-Nitro-2-(pyridin-3-yl)quinoline



¹³C NMR (126 MHz, CDCl₃) for 6-Nitro-2-(pyridin-3-yl)quinoline

B01JD023A CARBON CDCl₃ 20150324.esp



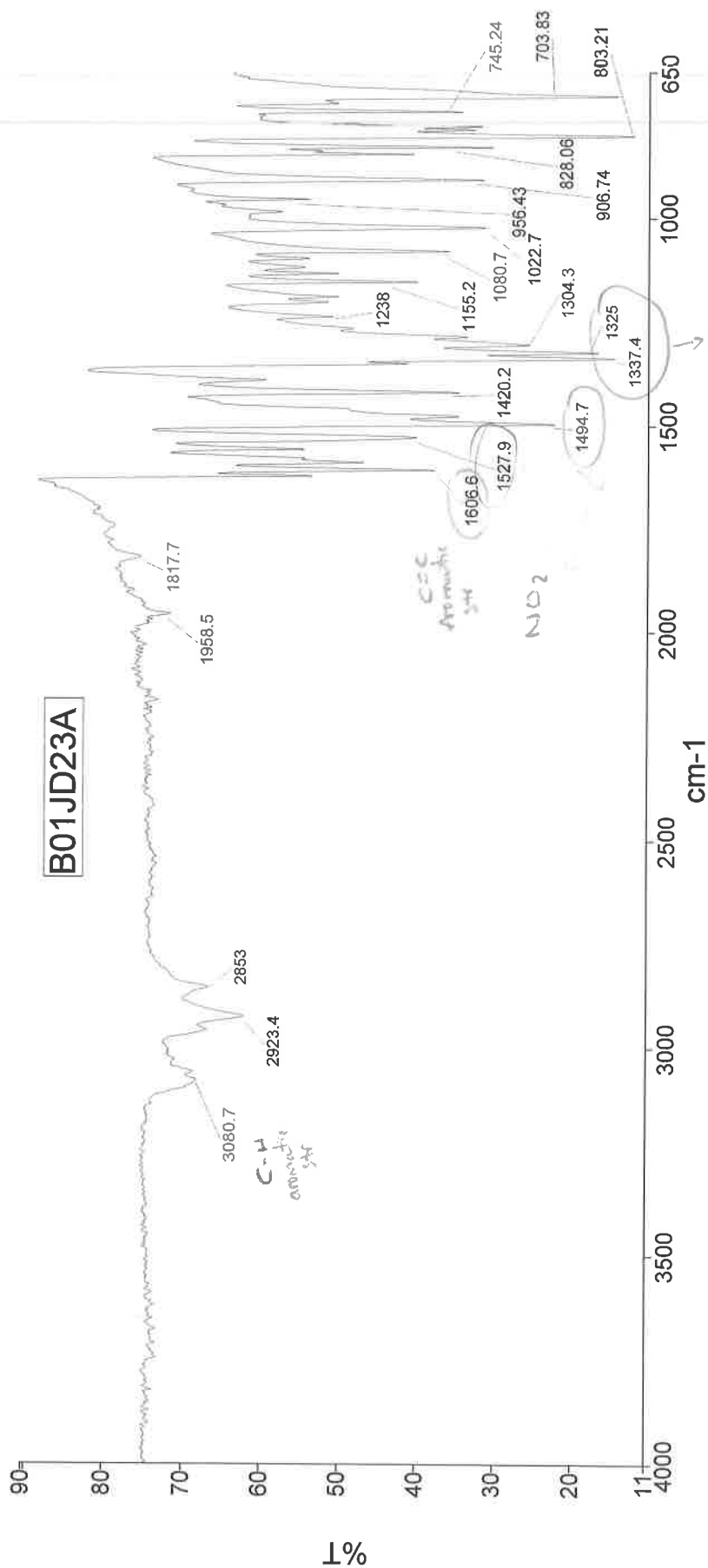


PerkinElmer Spectrum Version 10.03.06
14 November 2012 09:43

Analyst
Date

Administrator

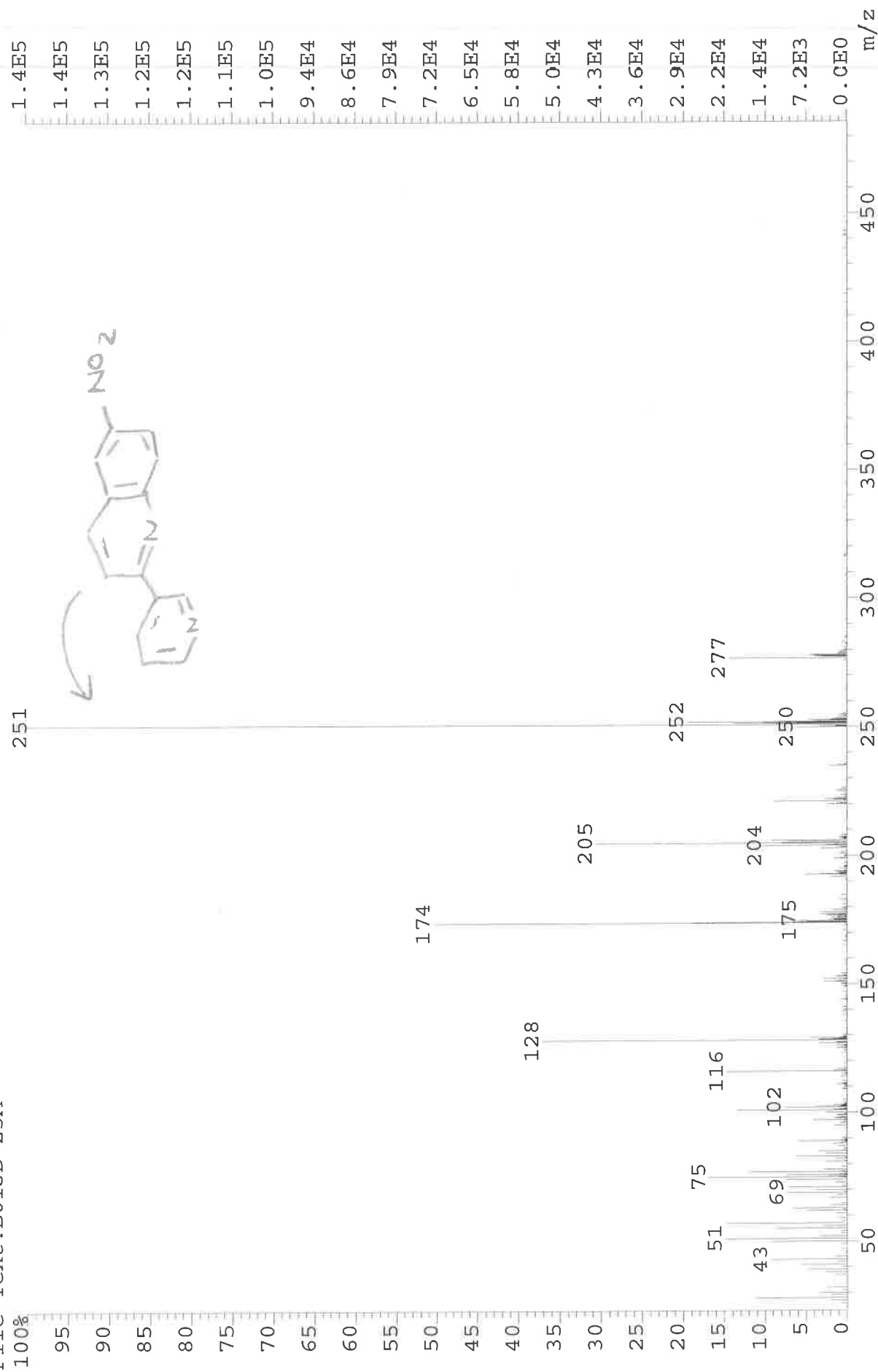
14 November 2012 09:43



Administrator 478 Sample 478 By Administrator Date Wednesday, November 14 2012

1580-1490
1350-1315
NO₂
Aromatic

File: JESSICA8760 Ident: 34 Acq: 14-NOV-2012 11:32:10 +2:08 Cal: CAL1
AutoSpecE EI+ Magnet BpI: 143900 TIC: 1343577 Flags: HALL
File Text: B01JD 23A



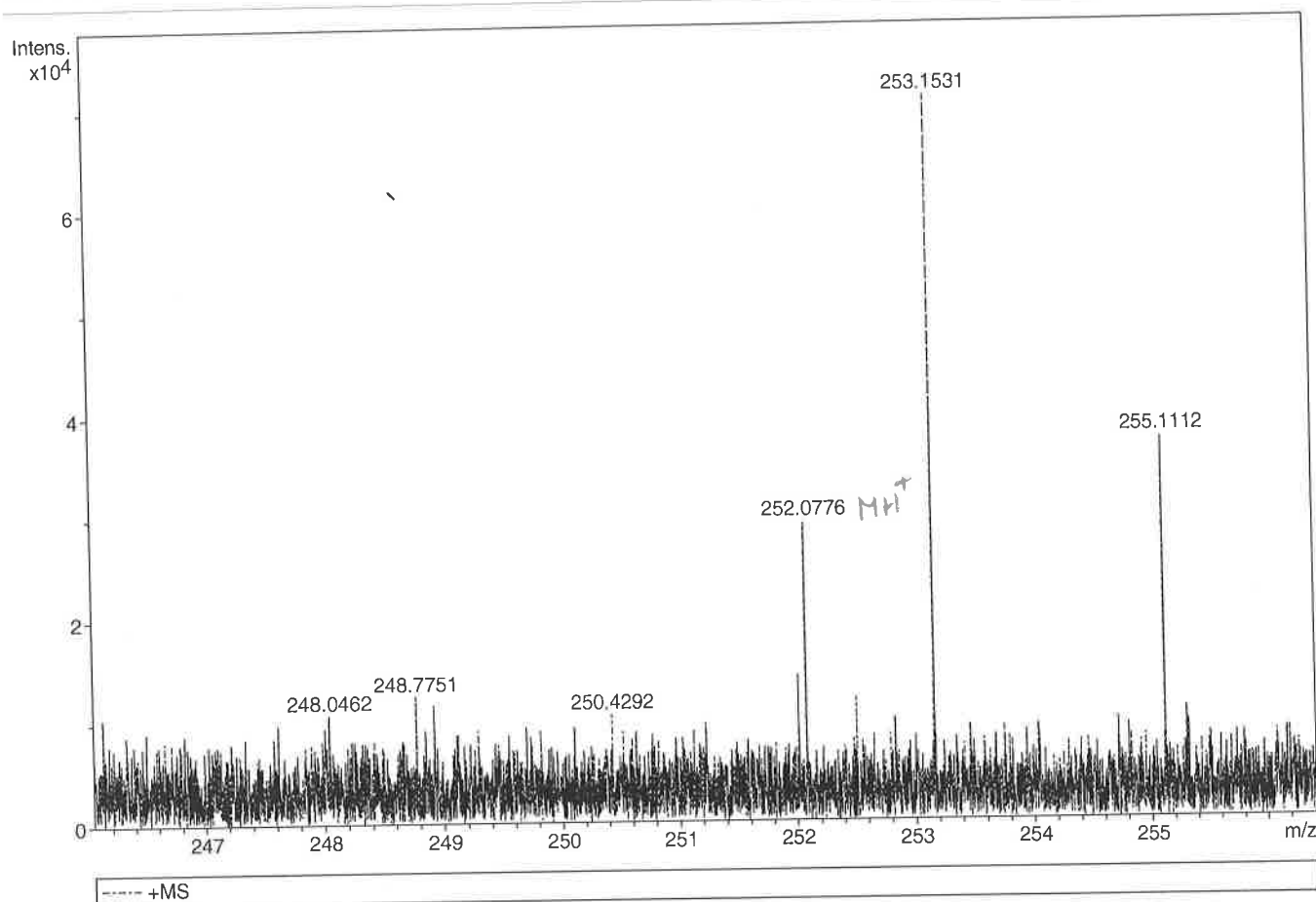
Generic Display Report

Analysis Info

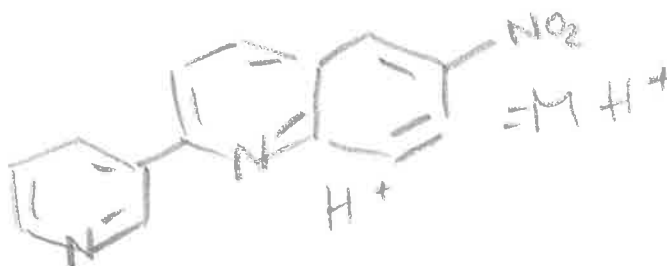
Analysis Name D:\Data\Alinanopos\JESS4955_000001.d
 Method pos20090608esi
 Sample Name PQS ESI B01JD023C
 Comment

Acquisition Date 31/03/2015 15:20:45

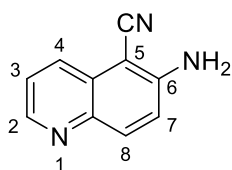
Operator Administrator
 Instrument apex-III



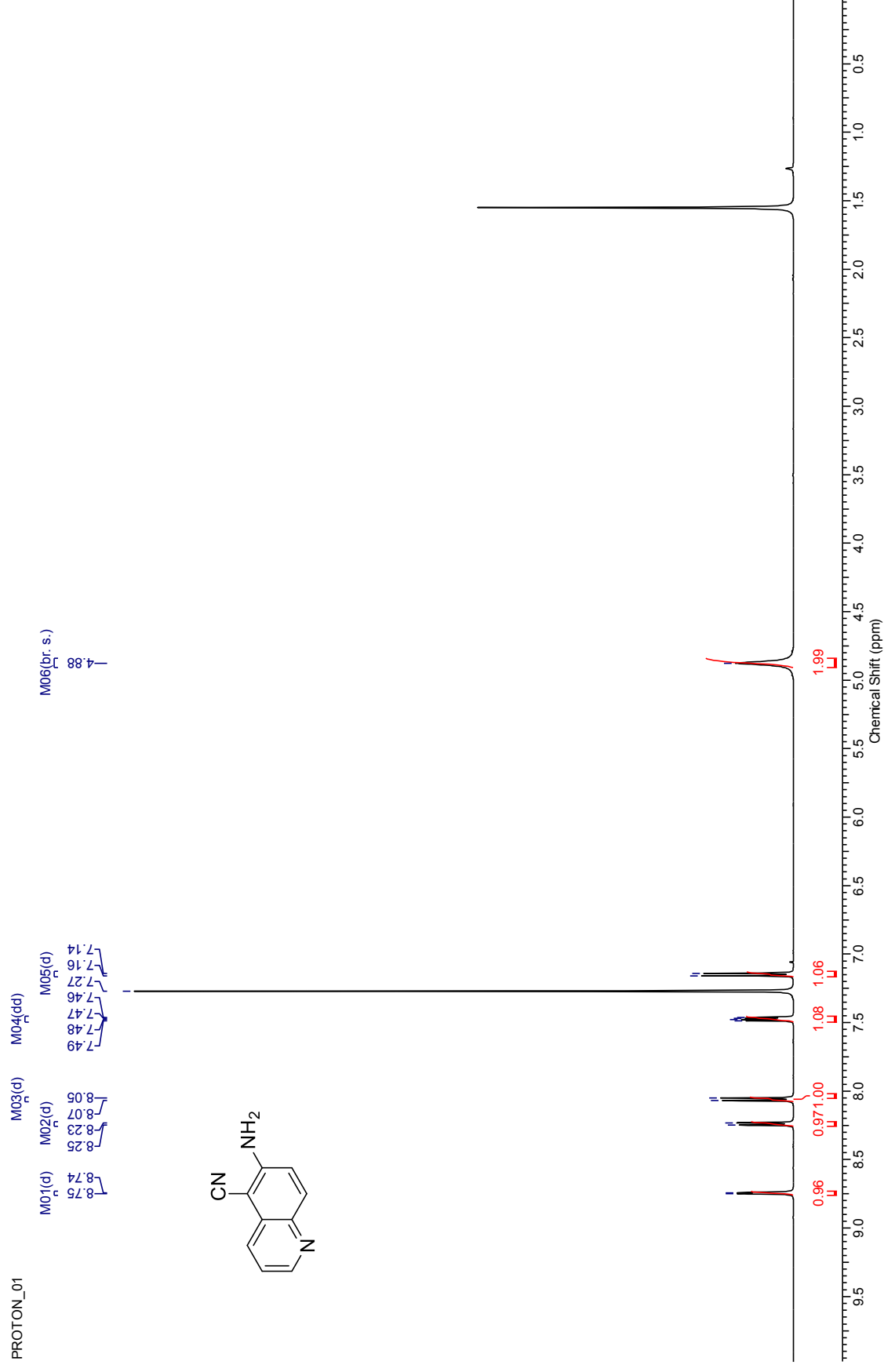
Sum Formula	Sigma	m/z	Err [ppm]	Mean Err [ppm]	Err [mDa]	rdb	N Rule	e ⁻
C ₁₄ H ₁₀ N ₃ O ₂	0.590	252.0768	-3.17	-206.38	-52.18	11.50	ok	even



6-Amino-5-cyanoquinoline (144)

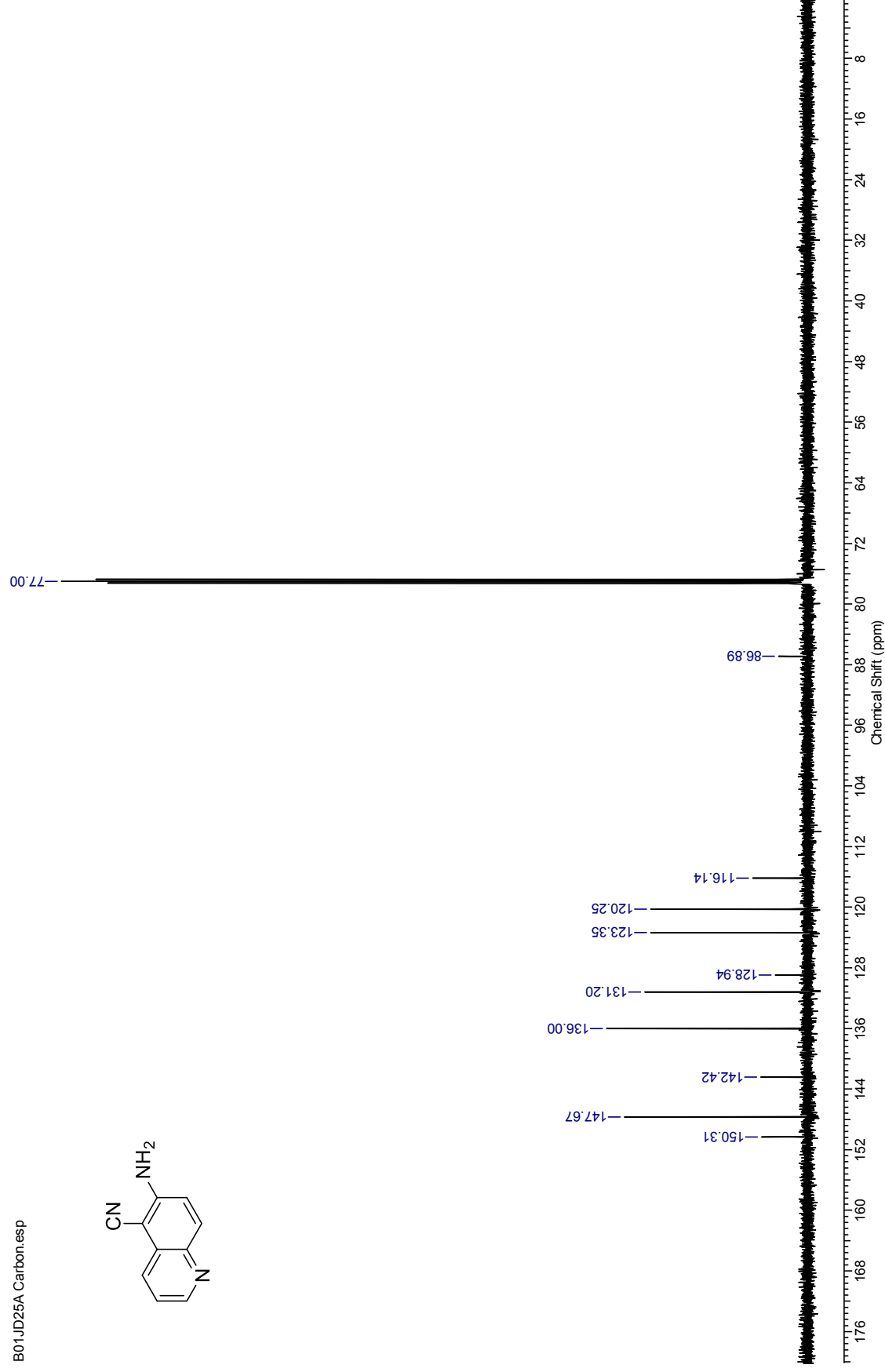
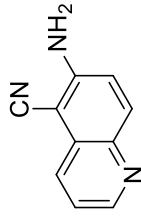


¹H NMR (500 MHz, CDCl₃) for 6-Amino-5-cyanoquinoline



¹³C NMR (126 MHz, CDCl₃) for 6-Amino-5-cyanoquinoline

B01JD25A Carbon.esp

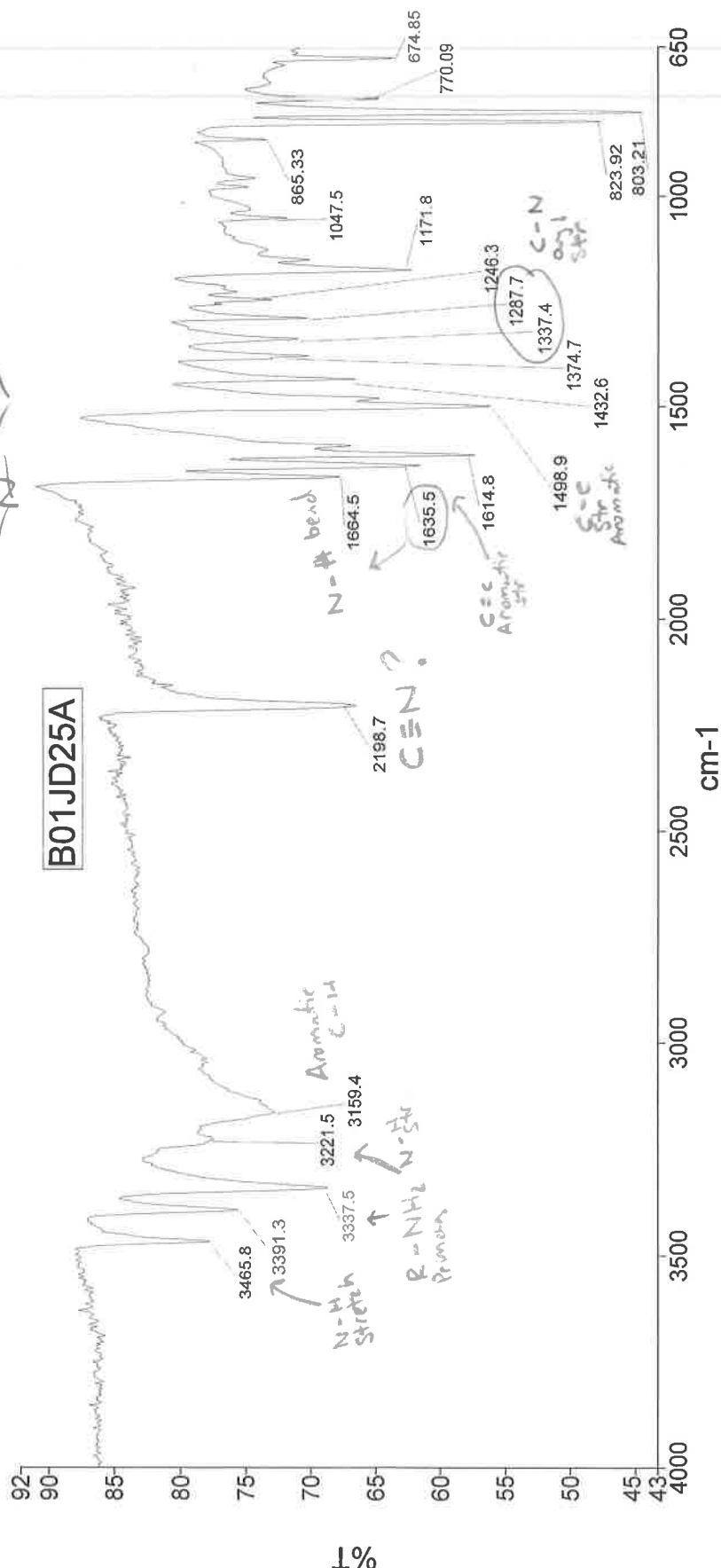




Analyst
Date

Administrator

14 November 2012 09:38



Ar-NH₂

C-NH₂ 1360-1250

Sample 477 By Administrator Date Wednesday, November 14 2012

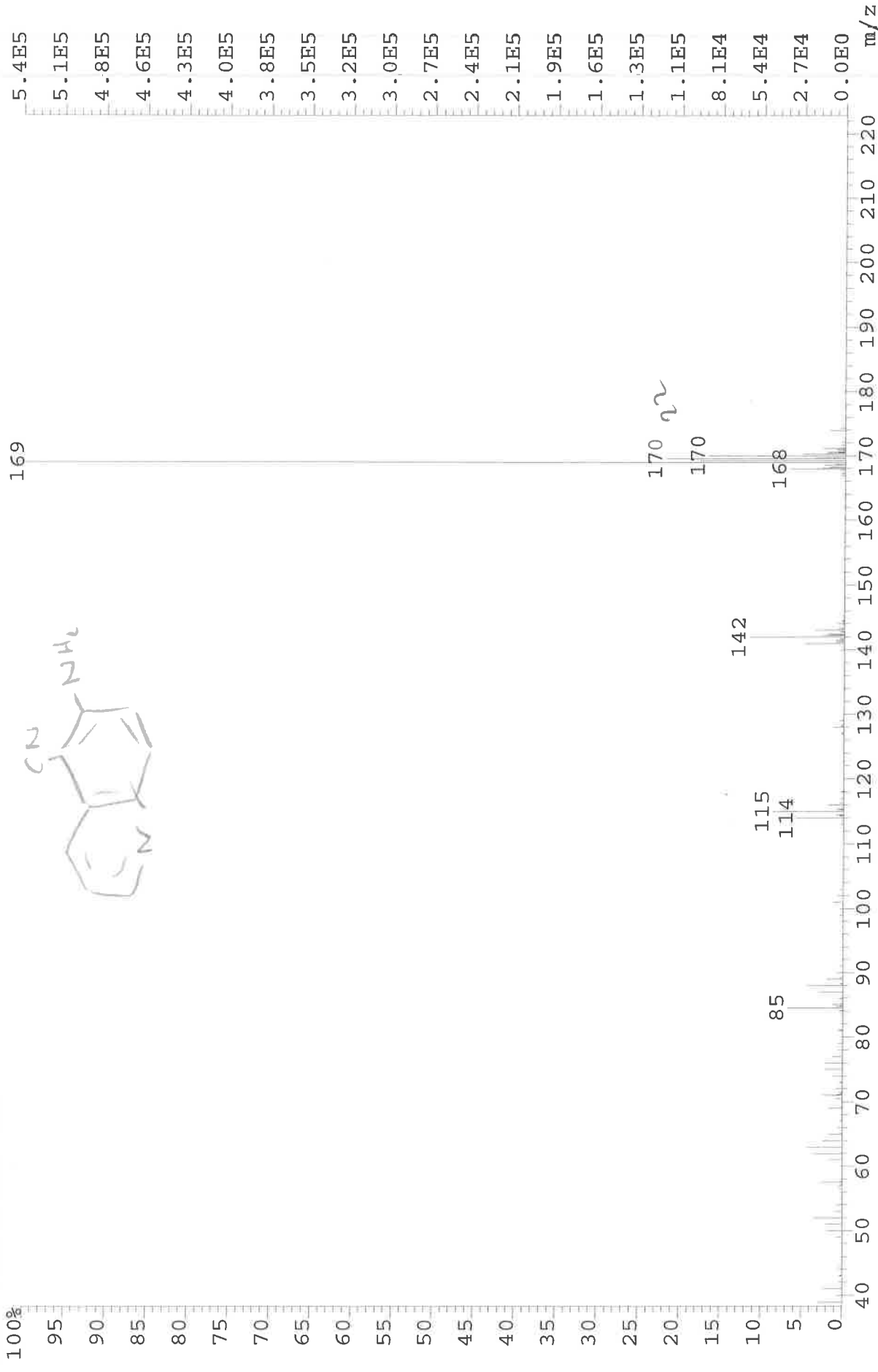
Administrator 477

N-H str = 3500-3300

N-H bend = 1600-1500

C≡N ~2250 [2210-2200 [but Aromatic!]]

File: JESSICA8762 Ident: 43 Acq: 14-NOV-2012 11:38:16 +2:41 Cal: CAL1
AutoSpecE EI+ Magnet BpI: 537357 TIC: 1894243 Flags: HALL
File Text: B01JD 25A



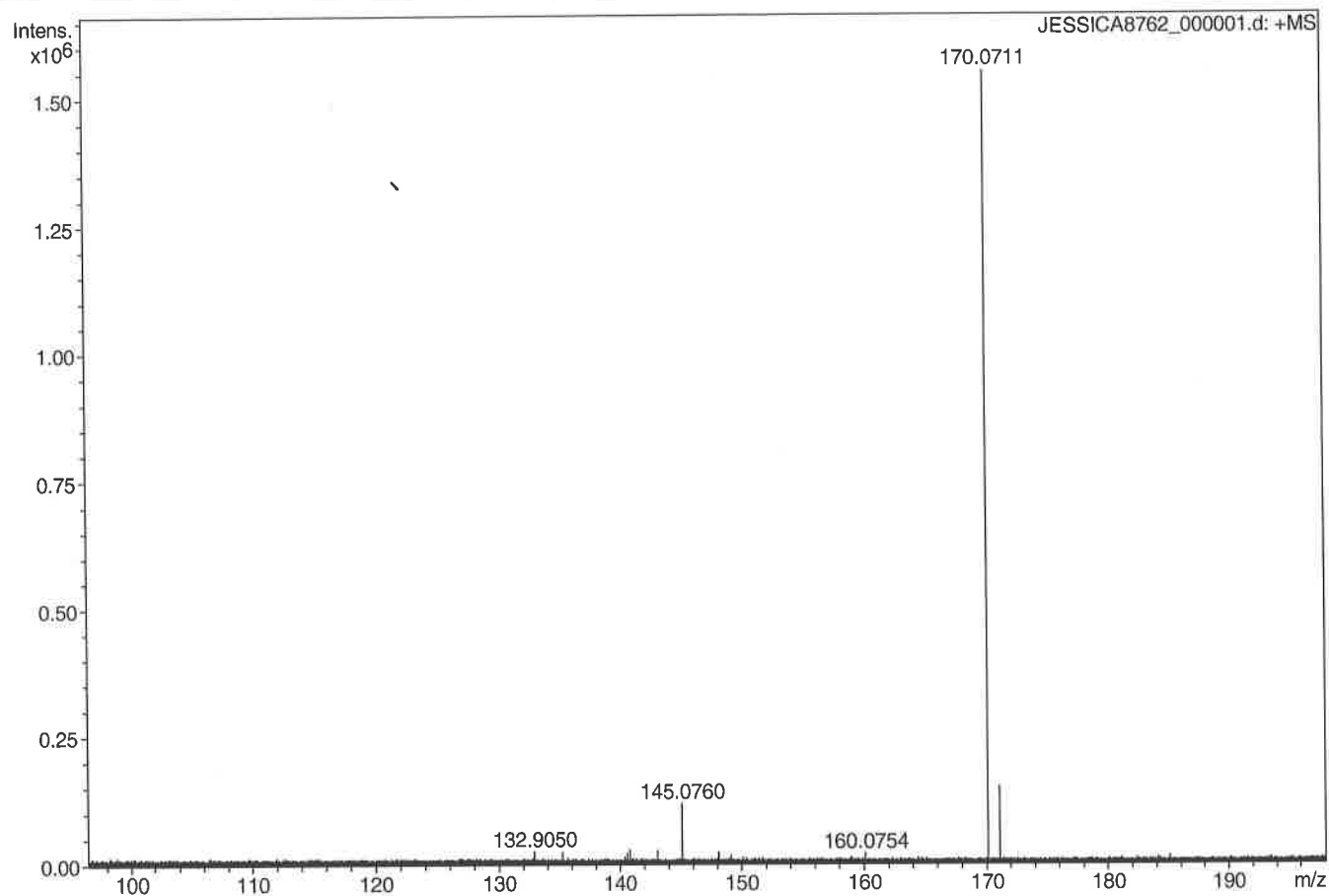
Generic Display Report

Analysis Info

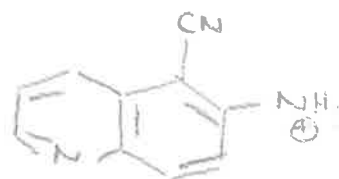
Analysis Name D:\Data\Allnanopos\JESSICA8762_000001.d
Method pos20090608esi
Sample Name POS ESI B01JD 25 A
Comment

Acquisition Date 14/11/2012 10:54:38

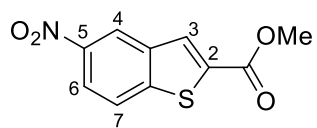
Operator Administrator
Instrument apex-III



Sum Formula	Sigma	m/z	Err [ppm]	Mean Err [ppm]	Err [mDa]	rdB	N Rule	e ⁻
C ₁₀ H ₈ N ₃	0.020	170.0713	1.24	-0.01	-0.00	8.50	ok	even



Methyl 5-nitrobenzo[*b*]thiophene-2-carboxylate (162)



¹H NMR (500 MHz, CDCl₃) for Methyl 5-nitrobenzo[b]thiophene-2-carboxylate

B02JD072A.esp

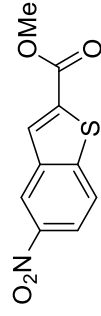
M04(d)

M02(dd)

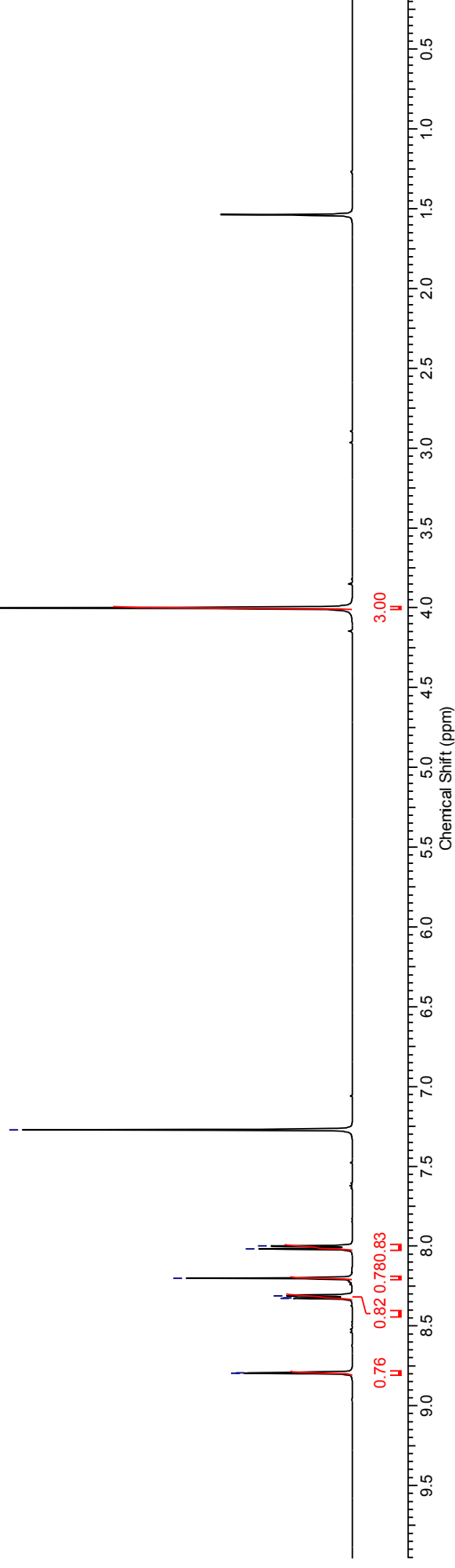
M01(d) M03(s)

8.80
8.79
8.33
8.33
8.31
8.20
8.02
8.00

-7.27

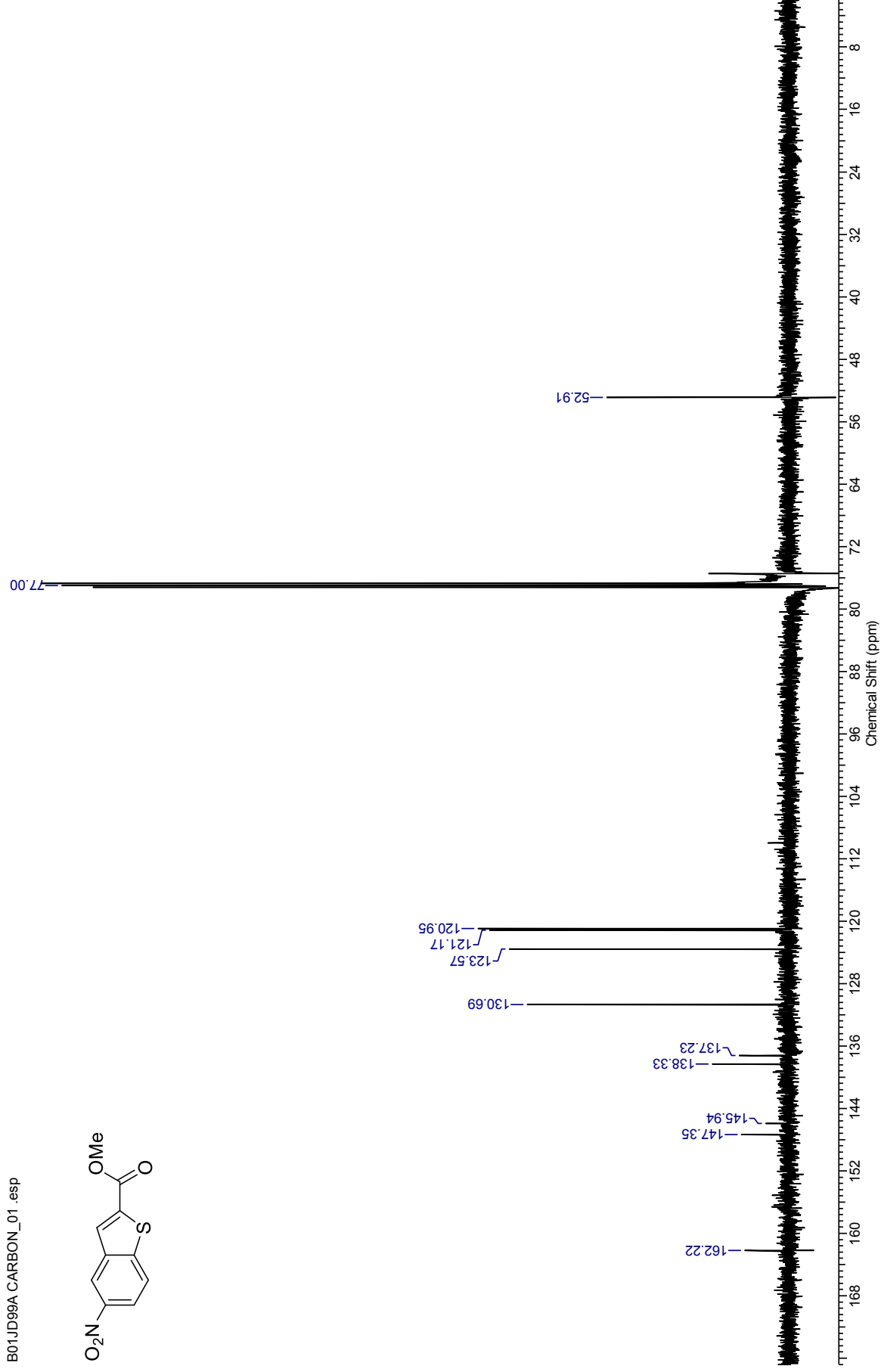
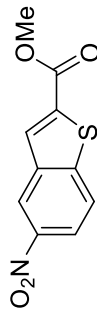


M05(s)



¹³C NMR (126 MHz, CDCl₃) for Methyl 5-nitrobenzo[b]thiophene-2-carboxylate

B01JD99A CARBON_01 .esp



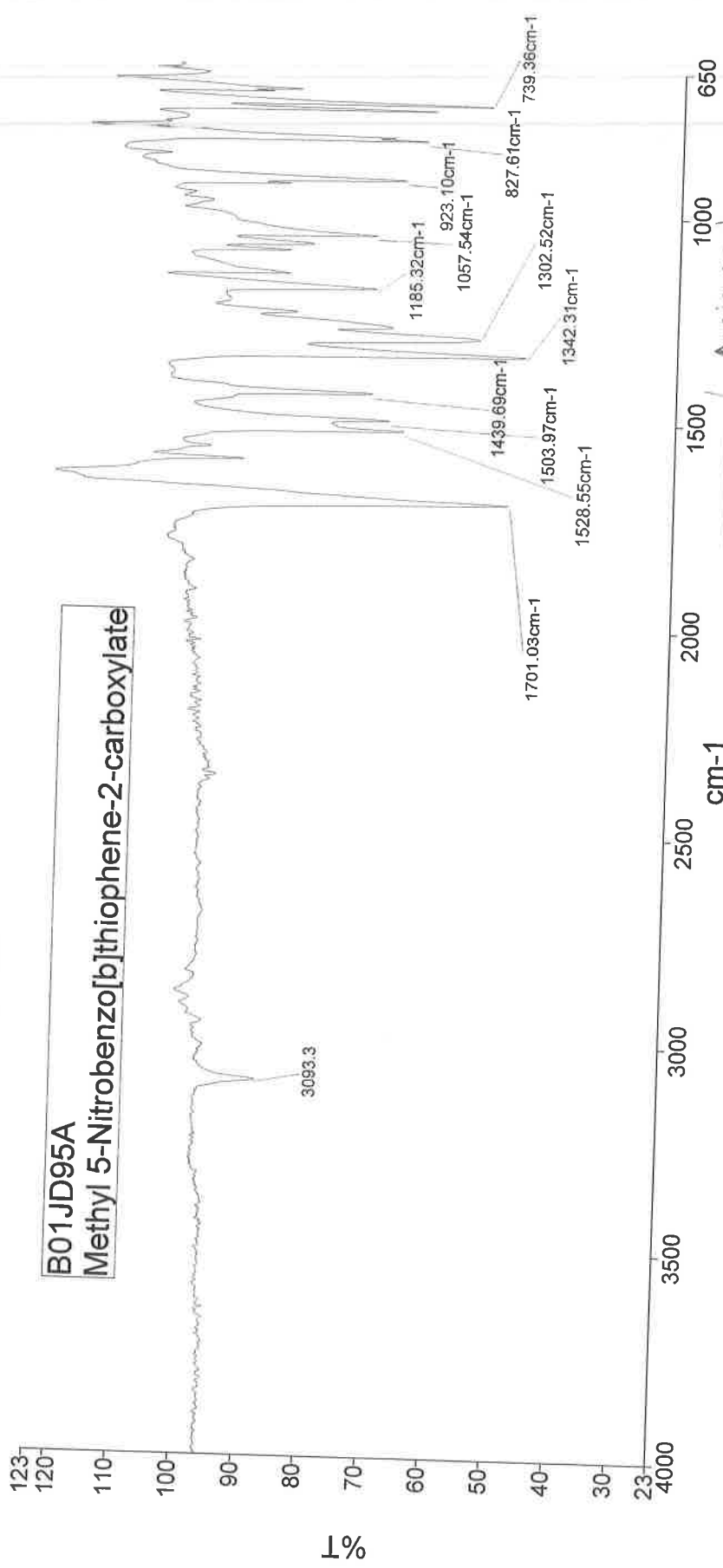
Analyst
Date

Administrator
28 February 2013 13:36

PerkinElmer Spectrum Version 10.03.06
28 February 2013 13:36



B01JD95A
Methyl 5-Nitrobenzo[b]thiophene-2-carboxylate

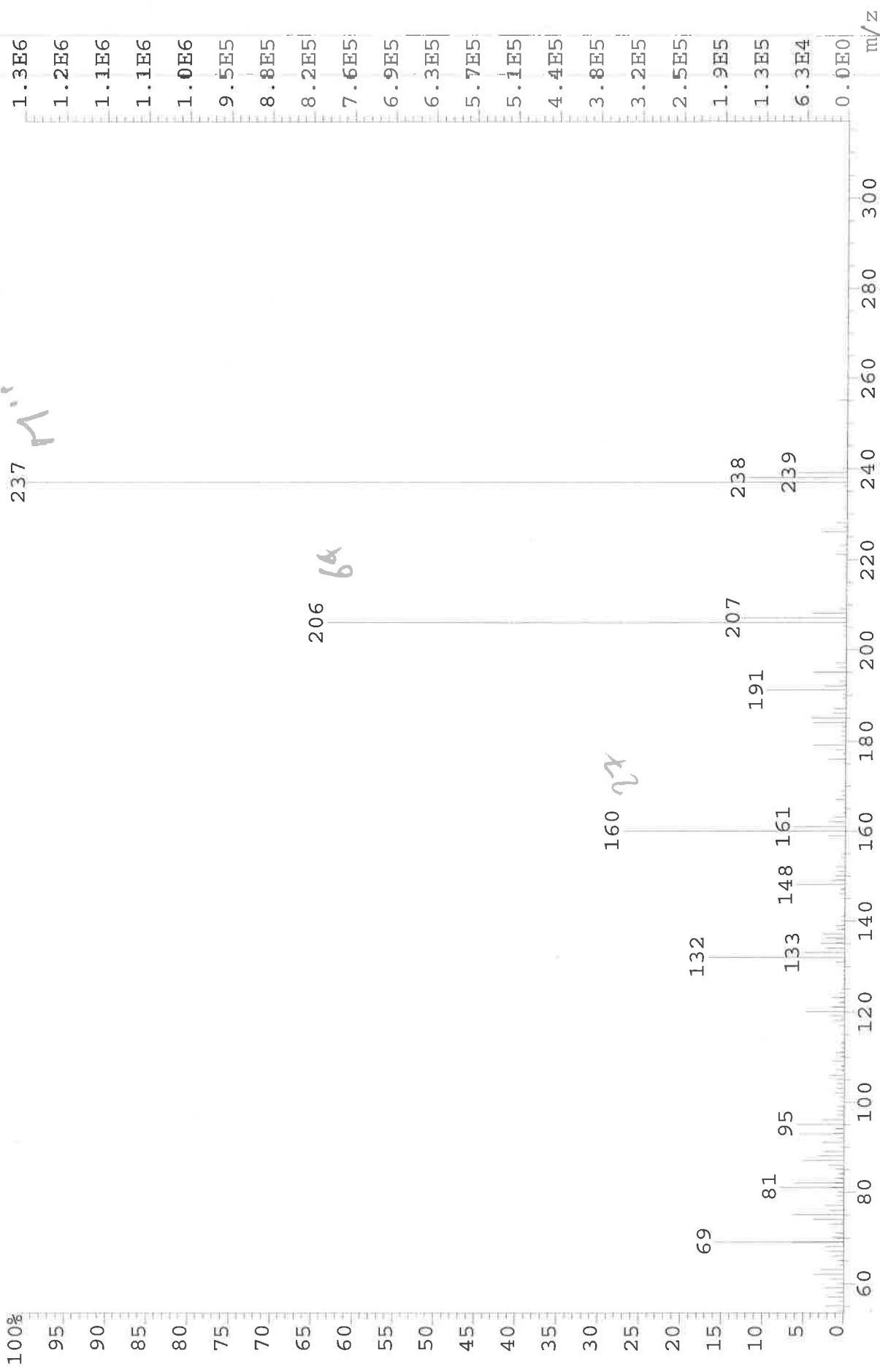


Wavenumber (cm ⁻¹)	Assignment
3093	C-H aromatic str.
1701	C=O str. ester
1528 (d)	NO ₂ aromatic str.
1439	C-C in-ring str.
1342	NO ₂ - aromatic str.
1302	C-O ester
1185	C-O str. ester
923	C-H bend / ring puckering

Administrator 1034 Sample 1034 By Administrator Date Thursday, February 28 2013
Administrator 1034_1 Sample 1034 By Administrator Date Thursday, February 28 2013



File: JESSICA9022 Ident: 7 Acq: 14-FEB-2013 18:59:46 +0:29 Cal: CAL1
AutoSpecE EI+ Magnet BpI: 1262992 TIC: 8095339 Flags: HALL
File Text: B01JD99A

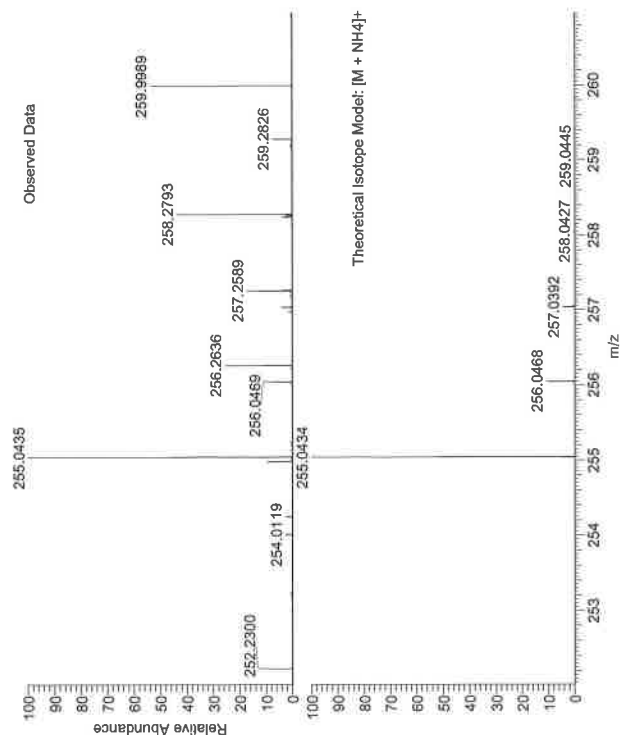




A.Rand BT MW=2377
(MeOH/MeOH + NH4OAc)

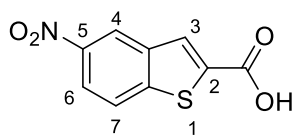
EPSRC National Facility Swansea
LTO Orbitrap XL

Rhannon
09/03/2015 10:44:52



Isotope(s)	Mass	Relative Abundance (%)	Composition
14 N	14.003074	1.1	C ₁₀ H ₁₁ N ₂ O ₄ S ₁
15 N	15.003069	0.4	C ₁₀ H ₁₁ N ₂ O ₄ S ₁
16 O	15.994915	1.1	C ₁₀ H ₁₁ N ₂ O ₄ S ₁
17 O	16.999131	0.04	C ₁₀ H ₁₁ N ₂ O ₄ S ₁
18 O	17.999161	0.01	C ₁₀ H ₁₁ N ₂ O ₄ S ₁
19 F	18.998403	0.01	C ₁₀ H ₁₁ N ₂ O ₄ S ₁
20 Ne	19.992435	0.005	C ₁₀ H ₁₁ N ₂ O ₄ S ₁
21 Ne	20.993833	0.001	C ₁₀ H ₁₁ N ₂ O ₄ S ₁
22 Ne	21.991363	0.001	C ₁₀ H ₁₁ N ₂ O ₄ S ₁
23 Na	22.989769	0.001	C ₁₀ H ₁₁ N ₂ O ₄ S ₁
24 Mg	23.985042	0.001	C ₁₀ H ₁₁ N ₂ O ₄ S ₁
25 Mg	24.985839	0.001	C ₁₀ H ₁₁ N ₂ O ₄ S ₁
26 Mg	25.982593	0.001	C ₁₀ H ₁₁ N ₂ O ₄ S ₁
27 Al	26.981538	0.001	C ₁₀ H ₁₁ N ₂ O ₄ S ₁
28 Si	27.976927	0.001	C ₁₀ H ₁₁ N ₂ O ₄ S ₁
29 Si	28.976495	0.001	C ₁₀ H ₁₁ N ₂ O ₄ S ₁
30 Si	29.973762	0.001	C ₁₀ H ₁₁ N ₂ O ₄ S ₁
31 P	30.973762	0.001	C ₁₀ H ₁₁ N ₂ O ₄ S ₁
32 S	31.972071	0.001	C ₁₀ H ₁₁ N ₂ O ₄ S ₁
33 S	32.971755	0.001	C ₁₀ H ₁₁ N ₂ O ₄ S ₁
34 S	33.970337	0.001	C ₁₀ H ₁₁ N ₂ O ₄ S ₁
35 S	34.969032	0.001	C ₁₀ H ₁₁ N ₂ O ₄ S ₁
36 S	35.967081	0.001	C ₁₀ H ₁₁ N ₂ O ₄ S ₁
37 Cl	36.965903	0.001	C ₁₀ H ₁₁ N ₂ O ₄ S ₁
38 Cl	37.966472	0.001	C ₁₀ H ₁₁ N ₂ O ₄ S ₁
39 K	38.963707	0.001	C ₁₀ H ₁₁ N ₂ O ₄ S ₁
40 K	39.964034	0.001	C ₁₀ H ₁₁ N ₂ O ₄ S ₁
41 K	40.961825	0.001	C ₁₀ H ₁₁ N ₂ O ₄ S ₁
42 Ca	41.958618	0.001	C ₁₀ H ₁₁ N ₂ O ₄ S ₁
43 Ca	42.959446	0.001	C ₁₀ H ₁₁ N ₂ O ₄ S ₁
44 Ca	43.959441	0.001	C ₁₀ H ₁₁ N ₂ O ₄ S ₁
45 Ca	44.956135	0.001	C ₁₀ H ₁₁ N ₂ O ₄ S ₁
46 Ca	45.953629	0.001	C ₁₀ H ₁₁ N ₂ O ₄ S ₁
47 Ca	46.952416	0.001	C ₁₀ H ₁₁ N ₂ O ₄ S ₁
48 Ca	47.952534	0.001	C ₁₀ H ₁₁ N ₂ O ₄ S ₁
49 Ti	47.944643	0.001	C ₁₀ H ₁₁ N ₂ O ₄ S ₁
50 Ti	48.946129	0.001	C ₁₀ H ₁₁ N ₂ O ₄ S ₁
51 V	50.943959	0.001	C ₁₀ H ₁₁ N ₂ O ₄ S ₁
52 V	51.944736	0.001	C ₁₀ H ₁₁ N ₂ O ₄ S ₁
53 Cr	52.940651	0.001	C ₁₀ H ₁₁ N ₂ O ₄ S ₁
54 Cr	53.940357	0.001	C ₁₀ H ₁₁ N ₂ O ₄ S ₁
55 Mn	54.938045	0.001	C ₁₀ H ₁₁ N ₂ O ₄ S ₁
56 Fe	55.934936	0.001	C ₁₀ H ₁₁ N ₂ O ₄ S ₁
57 Fe	56.937009	0.001	C ₁₀ H ₁₁ N ₂ O ₄ S ₁
58 Fe	57.935347	0.001	C ₁₀ H ₁₁ N ₂ O ₄ S ₁
59 Co	58.933195	0.001	C ₁₀ H ₁₁ N ₂ O ₄ S ₁
60 Ni	59.930786	0.001	C ₁₀ H ₁₁ N ₂ O ₄ S ₁
61 Ni	60.931060	0.001	C ₁₀ H ₁₁ N ₂ O ₄ S ₁
62 Ni	61.929142	0.001	C ₁₀ H ₁₁ N ₂ O ₄ S ₁
63 Cu	62.929598	0.001	C ₁₀ H ₁₁ N ₂ O ₄ S ₁
64 Cu	63.929764	0.001	C ₁₀ H ₁₁ N ₂ O ₄ S ₁
65 Cu	64.927789	0.001	C ₁₀ H ₁₁ N ₂ O ₄ S ₁
66 Zn	65.926430	0.001	C ₁₀ H ₁₁ N ₂ O ₄ S ₁
67 Zn	66.924248	0.001	C ₁₀ H ₁₁ N ₂ O ₄ S ₁
68 Zn	67.924847	0.001	C ₁₀ H ₁₁ N ₂ O ₄ S ₁
69 Ga	68.925573	0.001	C ₁₀ H ₁₁ N ₂ O ₄ S ₁
70 Ga	69.924070	0.001	C ₁₀ H ₁₁ N ₂ O ₄ S ₁
71 Ga	70.924701	0.001	C ₁₀ H ₁₁ N ₂ O ₄ S ₁
72 Ge	71.922146	0.001	C ₁₀ H ₁₁ N ₂ O ₄ S ₁
73 Ge	72.923439	0.001	C ₁₀ H ₁₁ N ₂ O ₄ S ₁
74 Ge	73.924207	0.001	C ₁₀ H ₁₁ N ₂ O ₄ S ₁
75 As	74.921595	0.001	C ₁₀ H ₁₁ N ₂ O ₄ S ₁
76 As	75.922272	0.001	C ₁₀ H ₁₁ N ₂ O ₄ S ₁
77 Se	76.920053	0.001	C ₁₀ H ₁₁ N ₂ O ₄ S ₁
78 Se	77.921636	0.001	C ₁₀ H ₁₁ N ₂ O ₄ S ₁
79 Br	78.918337	0.001	C ₁₀ H ₁₁ N ₂ O ₄ S ₁
80 Br	79.916291	0.001	C ₁₀ H ₁₁ N ₂ O ₄ S ₁
81 Br	80.916291	0.001	C ₁₀ H ₁₁ N ₂ O ₄ S ₁
82 Kr	81.912612	0.001	C ₁₀ H ₁₁ N ₂ O ₄ S ₁
83 Kr	82.914311	0.001	C ₁₀ H ₁₁ N ₂ O ₄ S ₁
84 Kr	83.914398	0.001	C ₁₀ H ₁₁ N ₂ O ₄ S ₁
85 Rb	84.912574	0.001	C ₁₀ H ₁₁ N ₂ O ₄ S ₁
86 Rb	85.914619	0.001	C ₁₀ H ₁₁ N ₂ O ₄ S ₁
87 Rb	86.915139	0.001	C ₁₀ H ₁₁ N ₂ O ₄ S ₁
88 Sr	87.905612	0.001	C ₁₀ H ₁₁ N ₂ O ₄ S ₁
89 Y	88.905848	0.001	C ₁₀ H ₁₁ N ₂ O ₄ S ₁
90 Zr	89.904684	0.001	C ₁₀ H ₁₁ N ₂ O ₄ S ₁
91 Zr	90.905441	0.001	C ₁₀ H ₁₁ N ₂ O ₄ S ₁
92 Zr	91.906377	0.001	C ₁₀ H ₁₁ N ₂ O ₄ S ₁
93 Nb	92.906377	0.001	C ₁₀ H ₁₁ N ₂ O ₄ S ₁
94 Nb	93.907830	0.001	C ₁₀ H ₁₁ N ₂ O ₄ S ₁
95 Mo	94.905884	0.001	C ₁₀ H ₁₁ N ₂ O ₄ S ₁
96 Mo	95.906377	0.001	C ₁₀ H ₁₁ N ₂ O ₄ S ₁
97 Mo	96.906377	0.001	C ₁₀ H ₁₁ N ₂ O ₄ S ₁
98 Mo	97.906377	0.001	C ₁₀ H ₁₁ N ₂ O ₄ S ₁
99 Tc	98.906377	0.001	C ₁₀ H ₁₁ N ₂ O ₄ S ₁
100 Ru	99.906377	0.001	C ₁₀ H ₁₁ N ₂ O ₄ S ₁
101 Ru	100.906377	0.001	C ₁₀ H ₁₁ N ₂ O ₄ S ₁
102 Ru	101.906377	0.001	C ₁₀ H ₁₁ N ₂ O ₄ S ₁
103 Rh	102.906377	0.001	C ₁₀ H ₁₁ N ₂ O ₄ S ₁
104 Rh	103.906377	0.001	C ₁₀ H ₁₁ N ₂ O ₄ S ₁
105 Pd	104.906377	0.001	C ₁₀ H ₁₁ N ₂ O ₄ S ₁
106 Pd	105.906377	0.001	C ₁₀ H ₁₁ N ₂ O ₄ S ₁
107 Pd	106.906377	0.001	C ₁₀ H ₁₁ N ₂ O ₄ S ₁
108 Pd	107.906377	0.001	C ₁₀ H ₁₁ N ₂ O ₄ S ₁
109 Ag	108.906377	0.001	C ₁₀ H ₁₁ N ₂ O ₄ S ₁
110 Ag	109.906377	0.001	C ₁₀ H ₁₁ N ₂ O ₄ S ₁
111 Cd	110.906377	0.001	C ₁₀ H ₁₁ N ₂ O ₄ S ₁
112 Cd	111.906377	0.001	C ₁₀ H ₁₁ N ₂ O ₄ S ₁
113 Cd	112.906377	0.001	C ₁₀ H ₁₁ N ₂ O ₄ S ₁
114 Cd	113.906377	0.001	C ₁₀ H ₁₁ N ₂ O ₄ S ₁
115 In	114.906377	0.001	C ₁₀ H ₁₁ N ₂ O ₄ S ₁
116 In	115.906377	0.001	C ₁₀ H ₁₁ N ₂ O ₄ S ₁
117 Sn	116.906377	0.001	C ₁₀ H ₁₁ N ₂ O ₄ S ₁
118 Sn	117.906377	0.001	C ₁₀ H ₁₁ N ₂ O ₄ S ₁
119 Sn	118.906377	0.001	C ₁₀ H ₁₁ N ₂ O ₄ S ₁
120 Sn	119.906377	0.001	C ₁₀ H ₁₁ N ₂ O ₄ S ₁
121 Pb	120.906377	0.001	C ₁₀ H ₁₁ N ₂ O ₄ S ₁
122 Pb	121.906377	0.001	C ₁₀ H ₁₁ N ₂ O ₄ S ₁
123 Pb	122.906377	0.001	C ₁₀ H ₁₁ N ₂ O ₄ S ₁
124 Pb	123.906377	0.001	C ₁₀ H ₁₁ N ₂ O ₄ S ₁
125 Pb	124.906377	0.001	C ₁₀ H ₁₁ N ₂ O ₄ S ₁
126 Pb	125.906377	0.001	C ₁₀ H ₁₁ N ₂ O ₄ S ₁
127 Pb	126.906377	0.001	C ₁₀ H ₁₁ N ₂ O ₄ S ₁
128 Pb	127.906377	0.001	C ₁₀ H ₁₁ N ₂ O ₄ S ₁
129 Pb	128.906377	0.001	C ₁₀ H ₁₁ N ₂ O ₄ S ₁
130 Pb	129.906377	0.001	C ₁₀ H ₁₁ N ₂ O ₄ S ₁
131 Bi	130.906377	0.001	C ₁₀ H ₁₁ N ₂ O ₄ S ₁
132 Bi	131.906377	0.001	C ₁₀ H ₁₁ N ₂ O ₄ S ₁
133 Bi	132.906377	0.001	C ₁₀ H ₁₁ N ₂ O ₄ S ₁
134 Bi	133.906377	0.001	C ₁₀ H ₁₁ N ₂ O ₄ S ₁
135 Bi	134.906377	0.001	C ₁₀ H ₁₁ N ₂ O ₄ S ₁
136 Bi	135.906377	0.001	C ₁₀ H ₁₁ N ₂ O ₄ S ₁
137 Bi	136.906377	0.001	C ₁₀ H ₁₁ N ₂ O ₄ S ₁
138 Bi	137.906377	0.001	C ₁₀ H ₁₁ N ₂ O ₄ S ₁

5-Nitrobenzo[*b*]thiophene-2-carboxylic acid (167)



¹H NMR (500 MHz, CDCl₃) for 5-Nitrobenzo[b]thiophene-2-carboxylic acid

B02JD097A MeOH!!i. esp

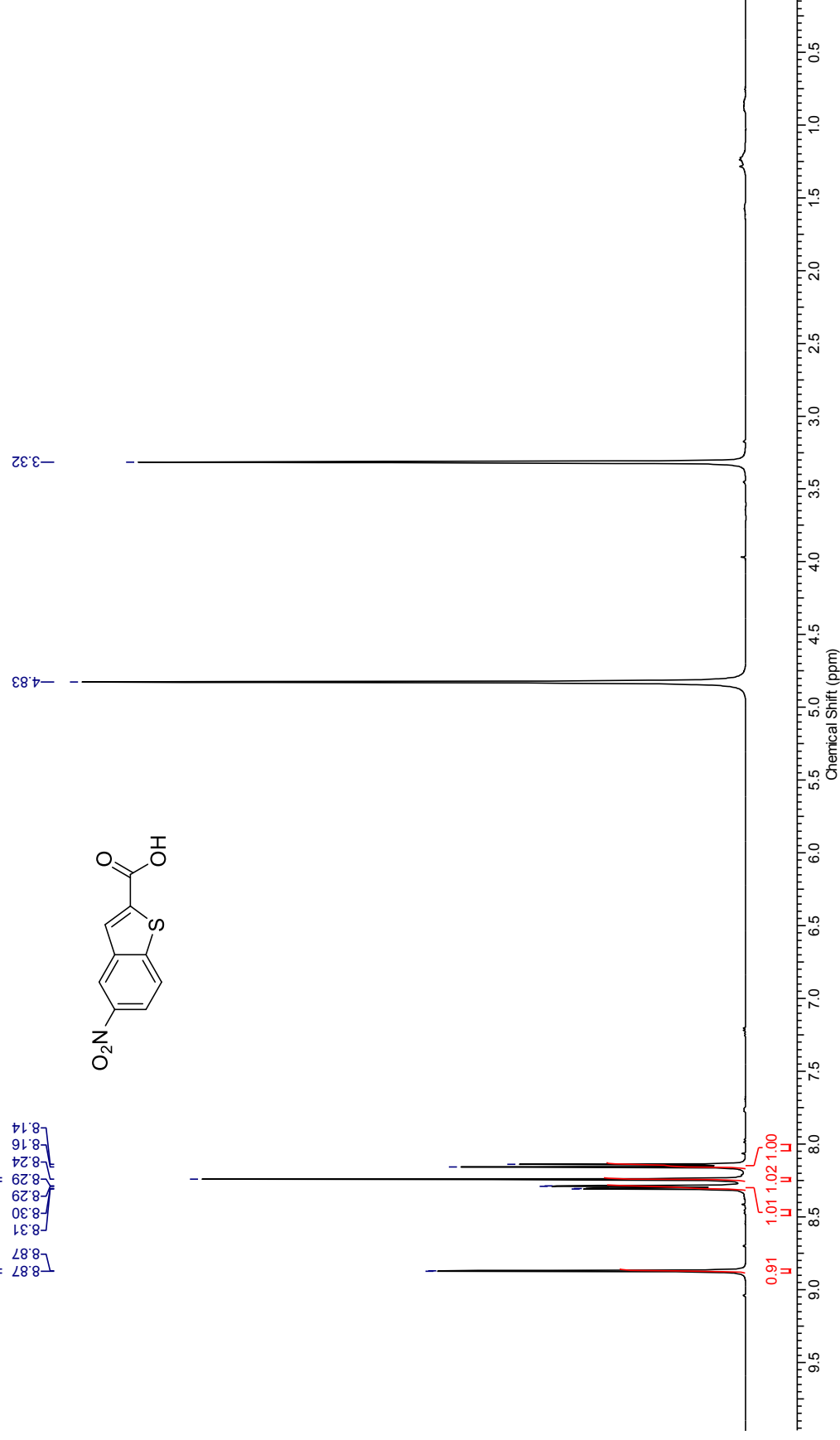
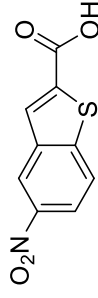
M04(d)

M02(dd)

M01(d)

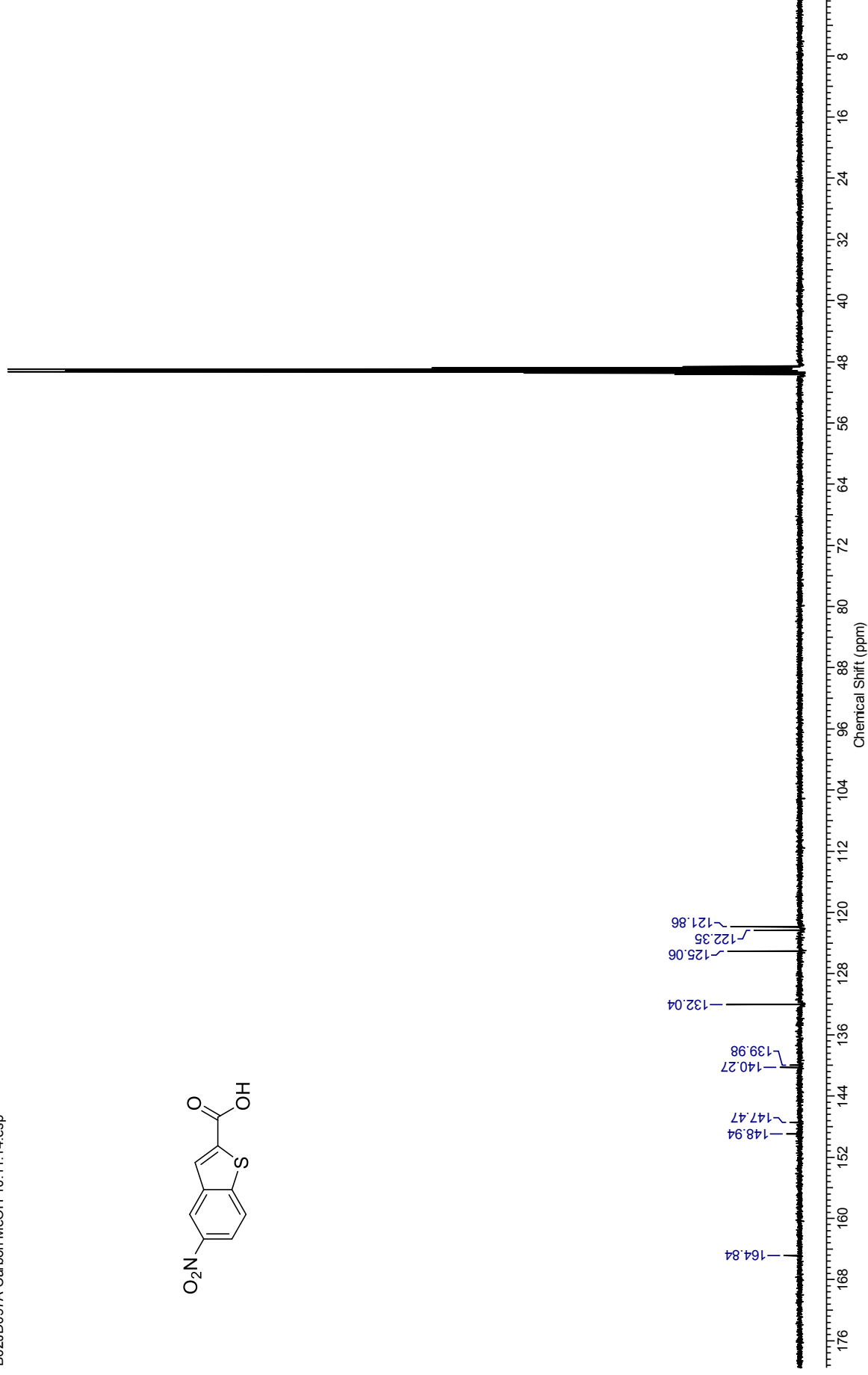
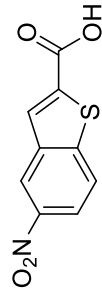
M03(s)

8.87
8.87
8.31
8.30
8.29
8.29
8.24
8.16
8.14



¹³C NMR (126 MHz, CDCl₃) for 5-Nitrobenzo[b]thiophene-2-carboxylic acid

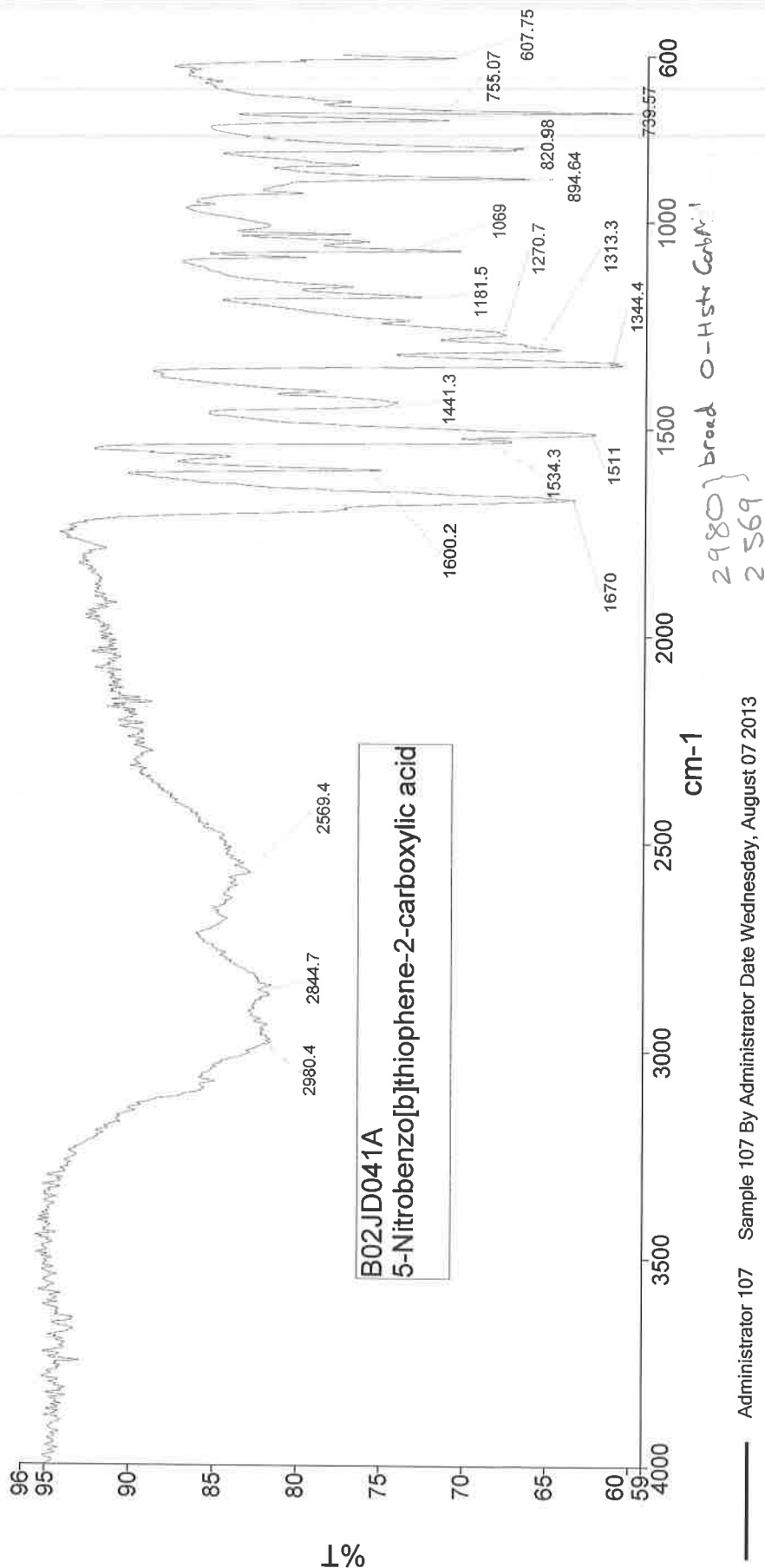
B02JD097A Carbon MeOH 10.11.14 esp





Analyst
Date

Administrator
07 August 2013 13:51



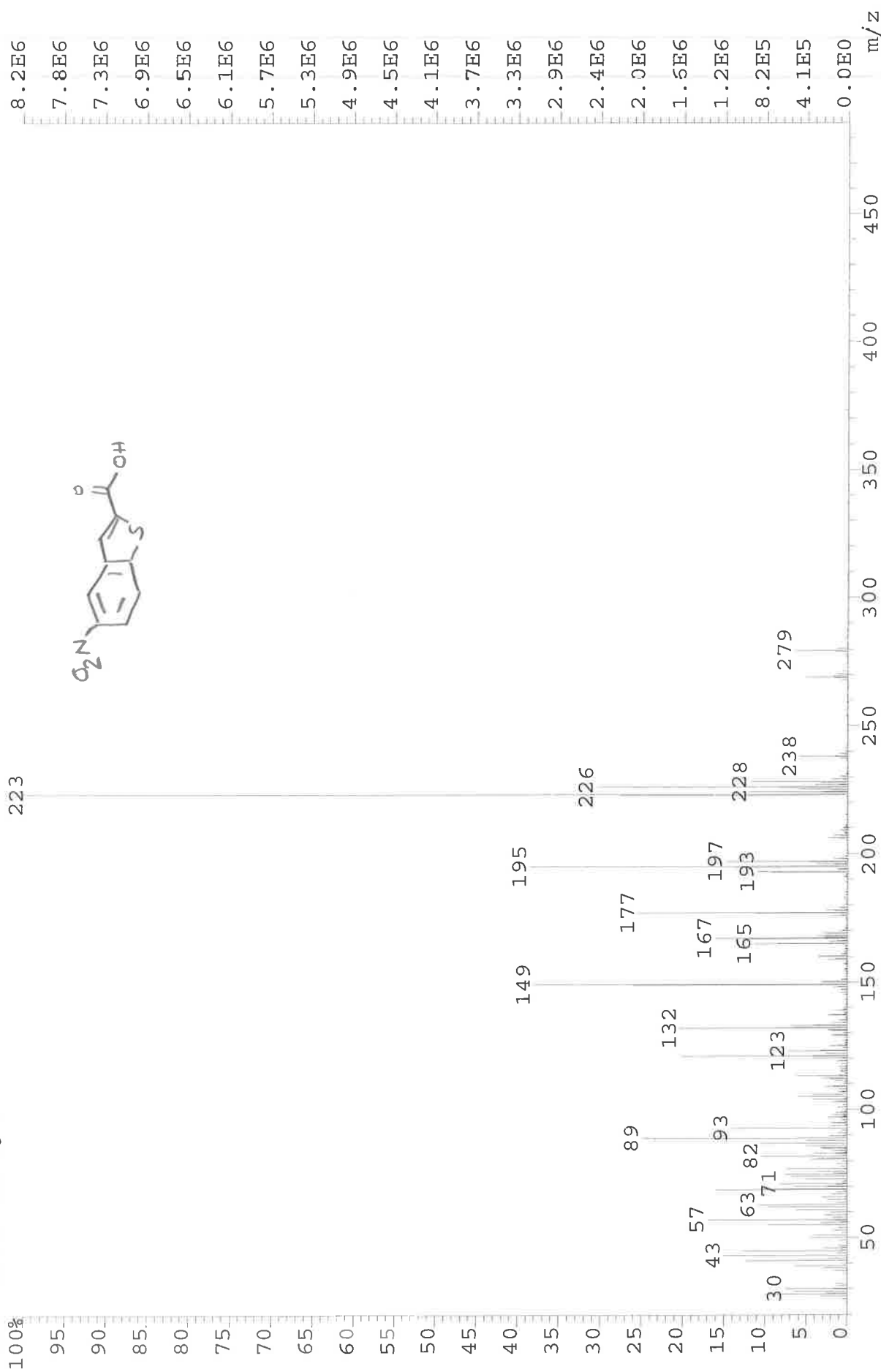
Administrator 107 Sample 107 By Administrator Date Wednesday, August 07 2013

2980 } broad O-H str Carb
2869 }

1670 C=O str Carb Acid
1600 C-C (in ring) str.
1511 N=O str.
1441 C-C (in ring) str.
1344 N=O str
1313 C-O str Carb Acid

894 O-H bend
739 C-H bend aromatic

File: JESSICA3027 Ident: 40 Acq: 6-JUN-2013 16:45:33 +2:31 Cal: CAL1
AutoSpecE EI+ Magnet BpI: 8162175 TIC: 97920176 Flags: HALL
File Text: B01JD187A



B02JD097A MW=223?
SOLID

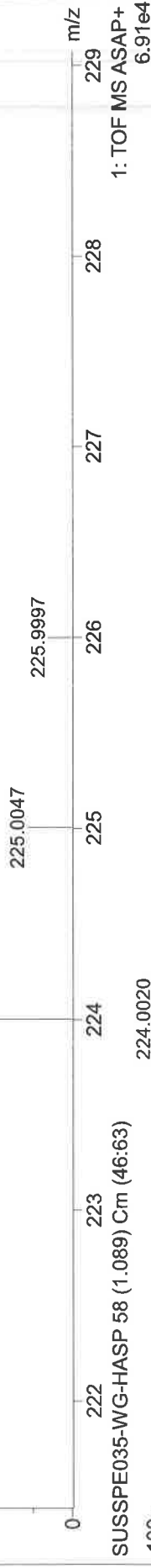
National Mass Spectrometry Facility, Swansea
Waters Xevo G2-S

Rhiannon
13-Oct-2014

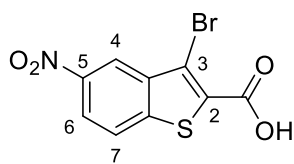
SUSSPE035-WG-HASP (0.045) Is (1.00,1.00) C₉H₅NO₄SH
224.0018

1: TOF MS ASAP+
8.50e12

Theoretical Isotope Pattern (M+H)



3-Bromo-5-nitrobenzo[b]thiophene-2-carboxylic acid (168)



¹H NMR (500 MHz, CDCl₃) for 3-Bromo-5-nitrobenzo[b]thiophene-2-carboxylic acid

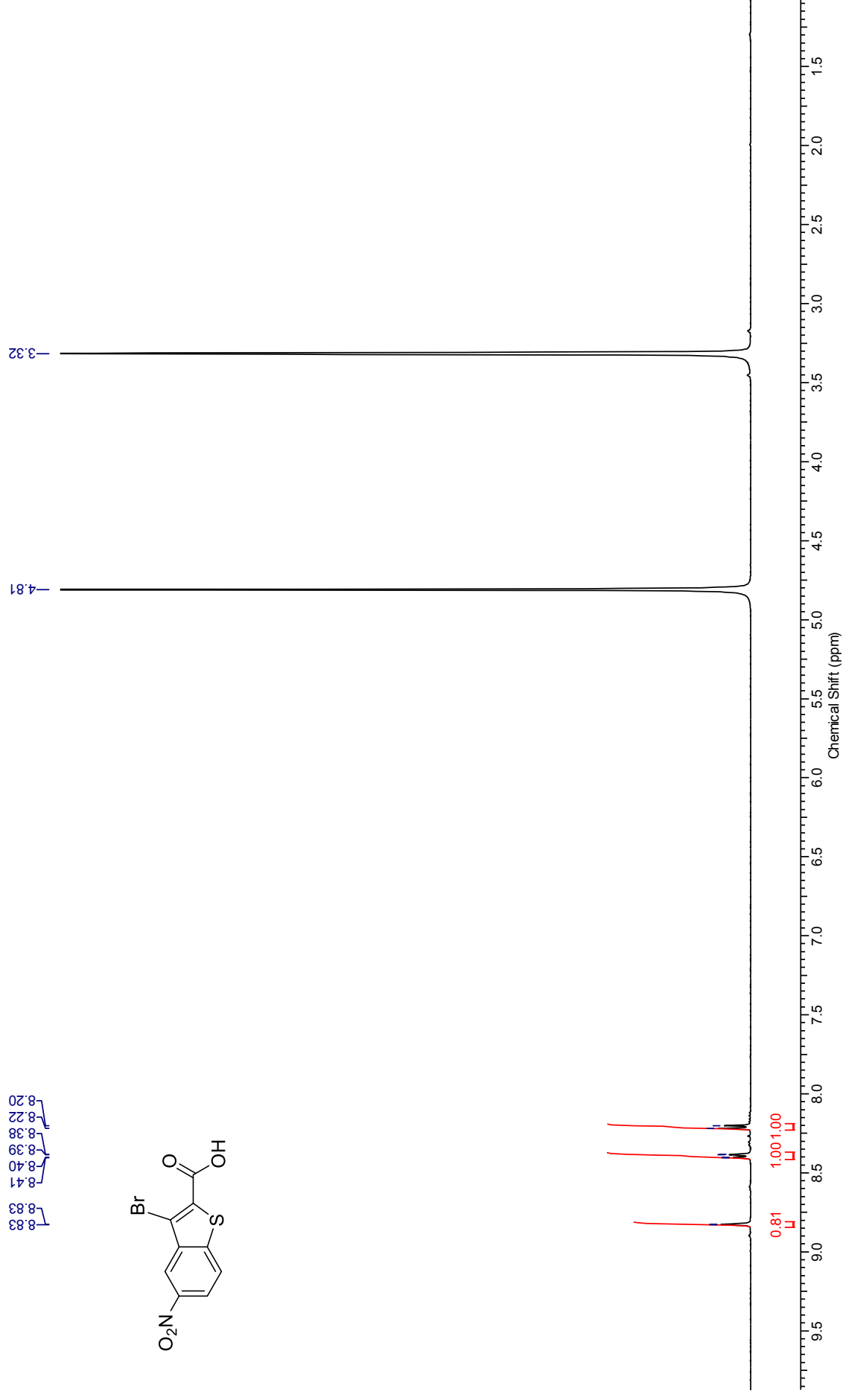
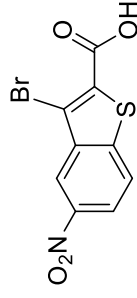
B02JD036A MeOH:esp

M02(dd)

M01(d)

M03(d)

8.83
8.83
8.83
8.41
8.40
8.39
8.38
8.22
8.20

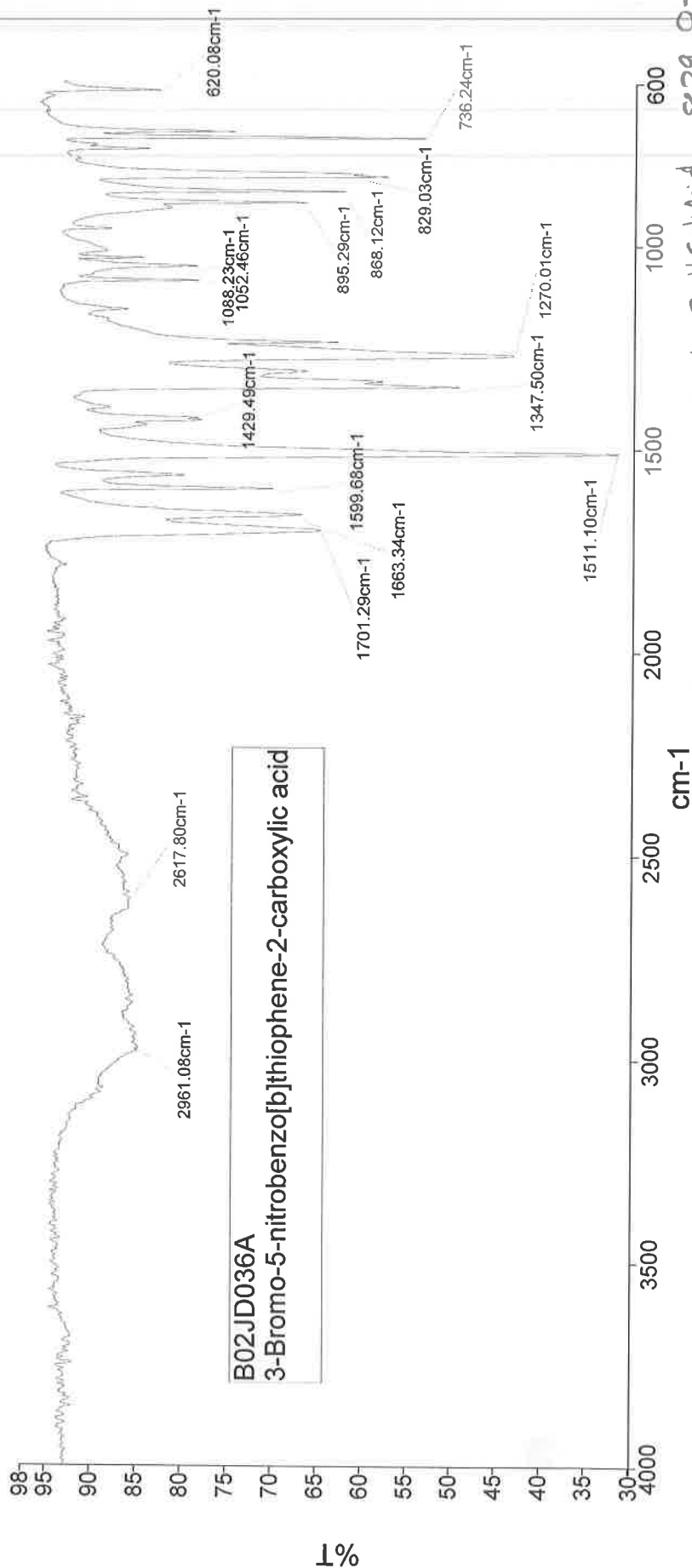




PerkinElmer Spectrum Version 10.03.06
07 August 2013 13:46

Administrator
07 August 2013 13:46

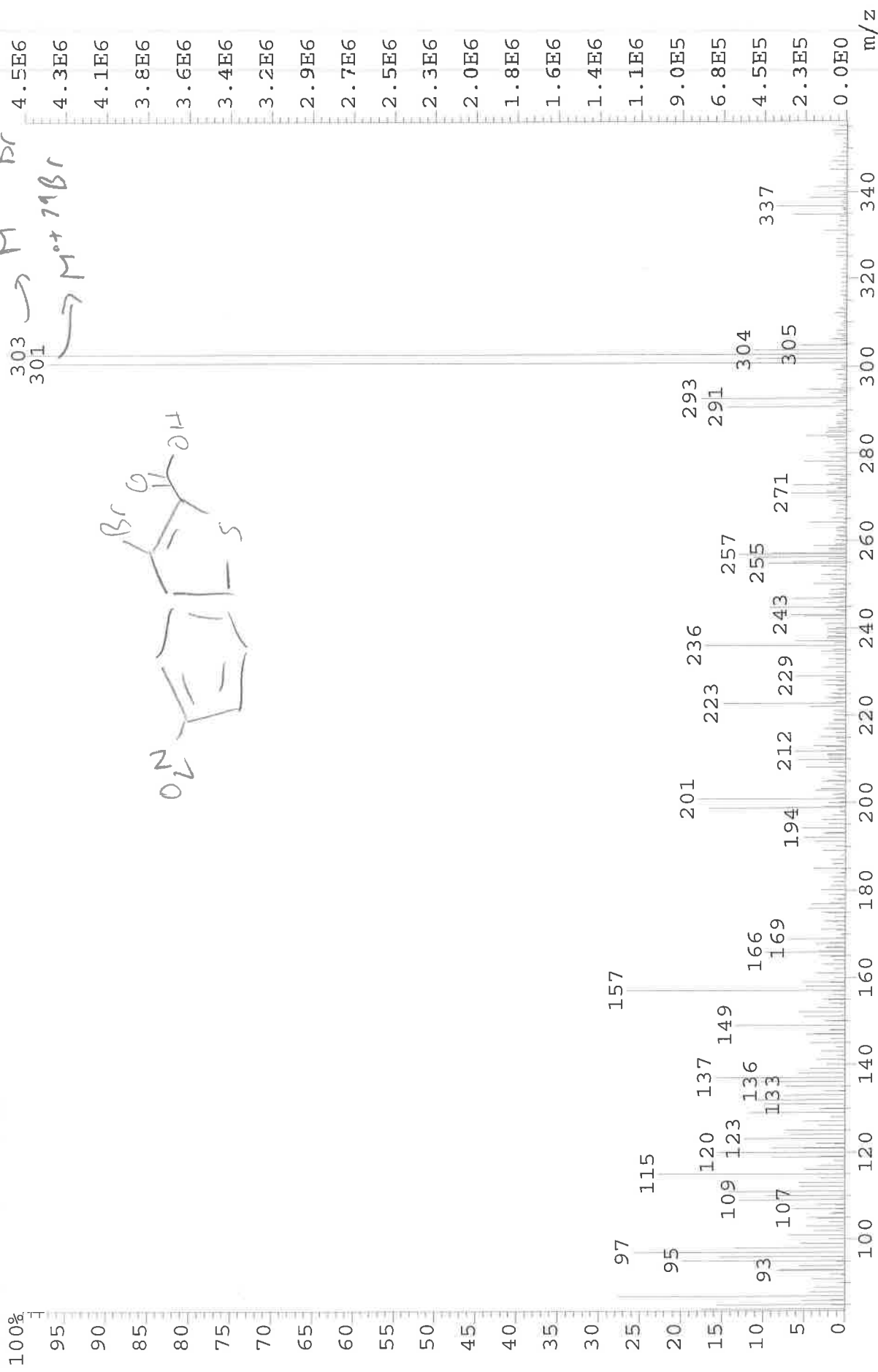
Analyst
Date



Administrator 106 Sample 106 By Administrator Date Wednesday, August 07 2013

2961 - 2618 br. O-H Carb Acid
1701 C=O Carb Acid
1600 C=C in ring str.
1511 N=O str.
1347 N=O str.
1270 C-O str. Carb Acid
829 O-H bend
736 C-H bend
620 C-Br str.

File: JESS3139 Ident: 50 Acq: 1-AUG-2013 12:56:31 +3:07 Cal: CAL1
AutoSpecE EI+ Magnet BpI: 4504462 TIC: 116767688 Flags: HALL
File Text: BO2JD036A



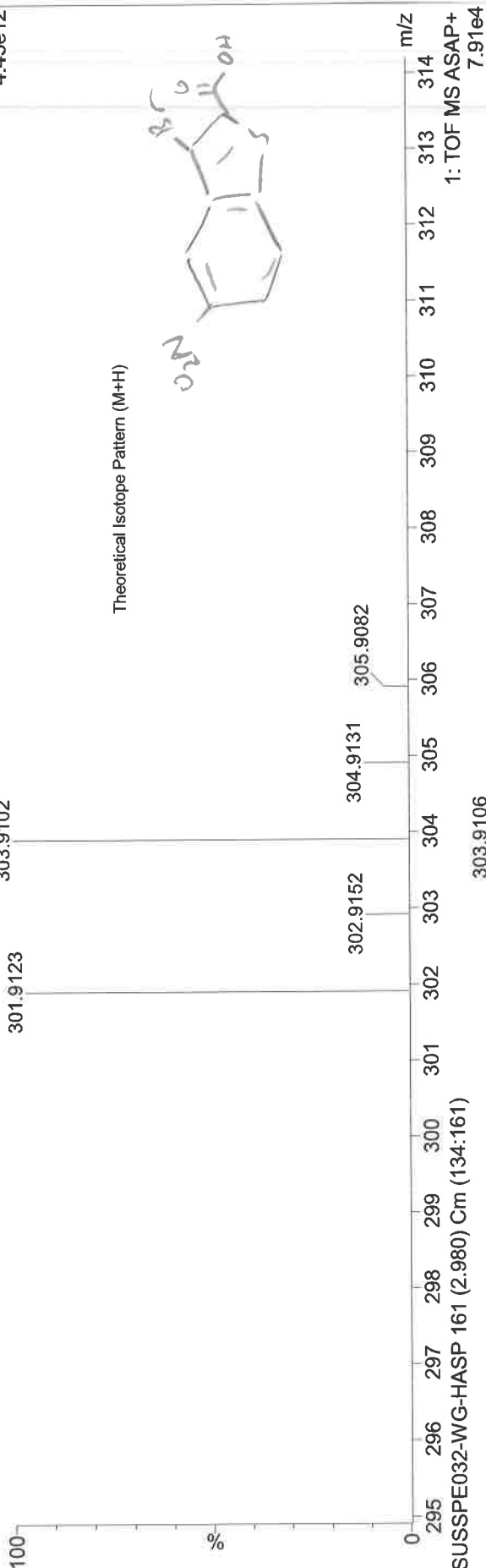
B02JD114A MW=302?
SOLID

National Mass Spectrometry Facility, Swansea
Waters Xevo G2-S

Rhiannon
13-Oct-2014

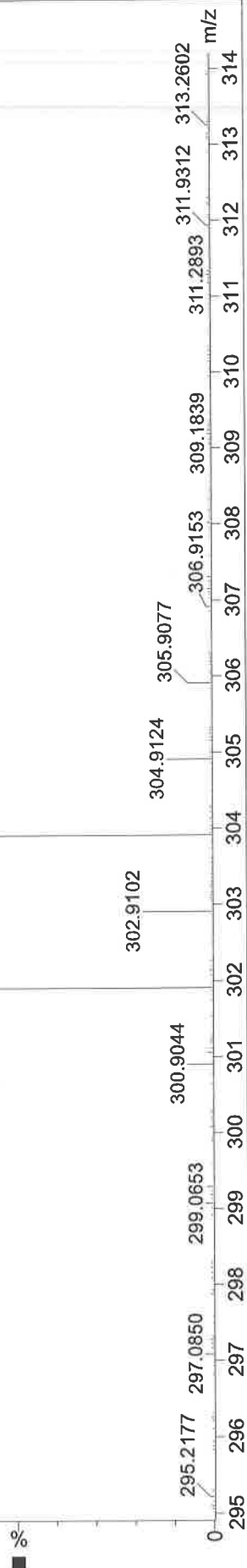
SUSSPE032-WG-HASP (0.045) Is (1.00,1.00) C₉H₄BrNO₄SH

1: TOF MS ASAP+
4.45e12

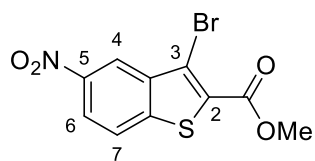


SUSSPE032-WG-HASP 161 (2.980) Cm (134:161)

Observed Data



Methyl 3-bromo-5-nitrobenzo[b]thiophene-2-carboxylate (164)



^1H NMR (500 MHz, CDCl_3) for Methyl 3-bromo-5-nitrobenzo[b]thiophene-2-carboxylate

B02JD033A .esp

M01(d)

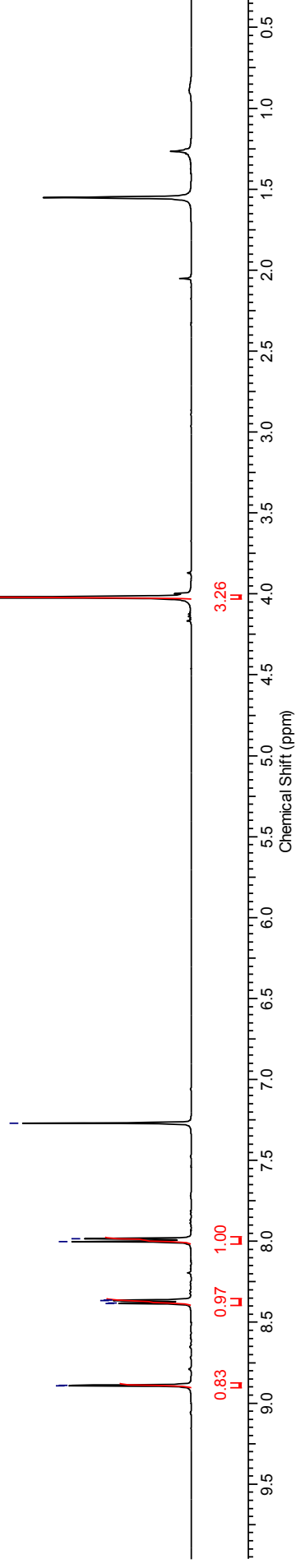
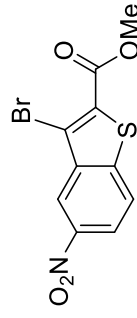
M02(dd) M03(s)

8.89 8.89 8.38 8.38 8.37 8.36 8.00 7.98

-7.27

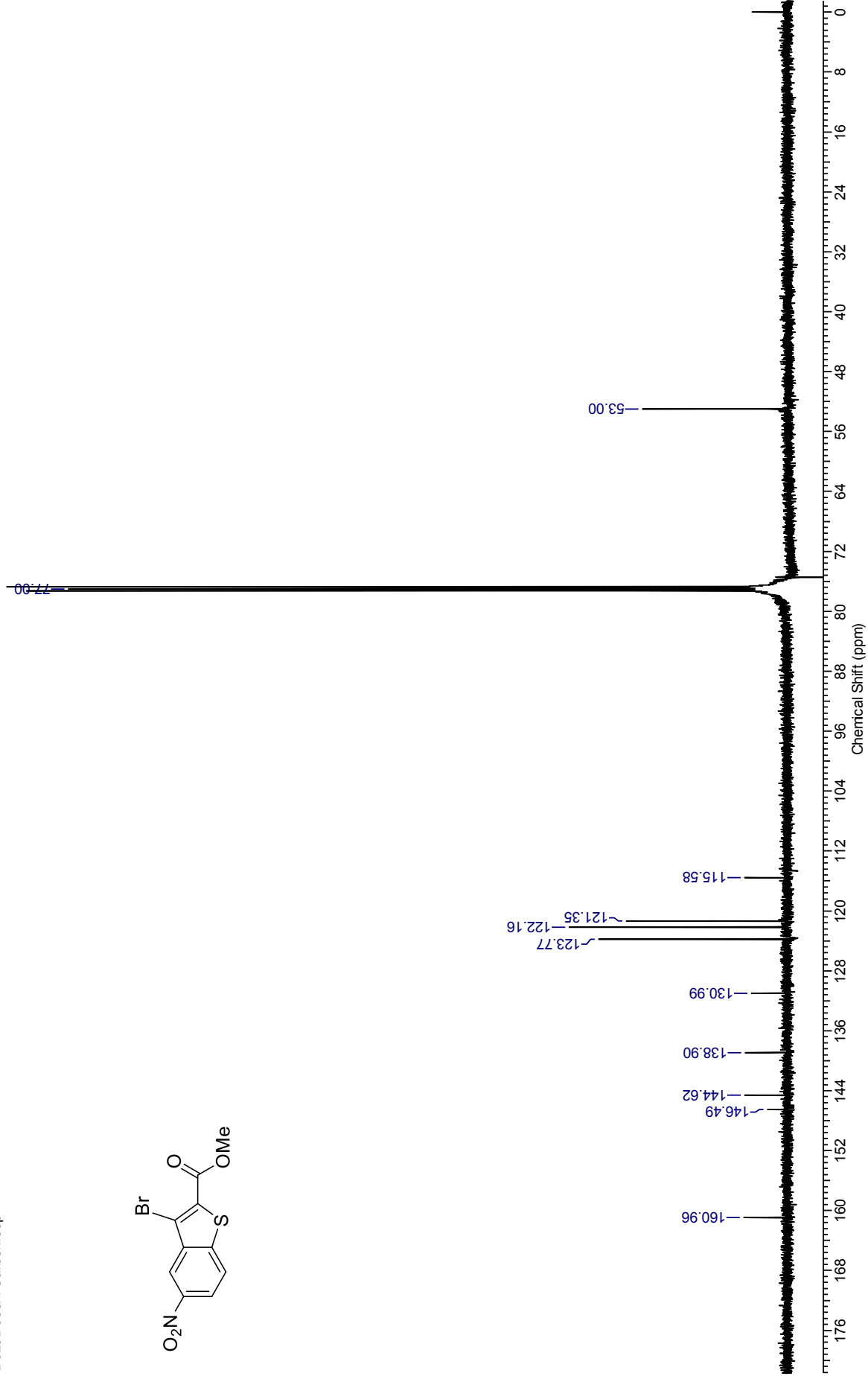
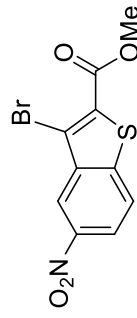
M04(s)

-4.02



¹³C NMR (126 MHz, CDCl₃) for Methyl 3-bromo-5-nitrobenzo[b]thiophene-2-carboxylate

B02JD033A Carbon.esp

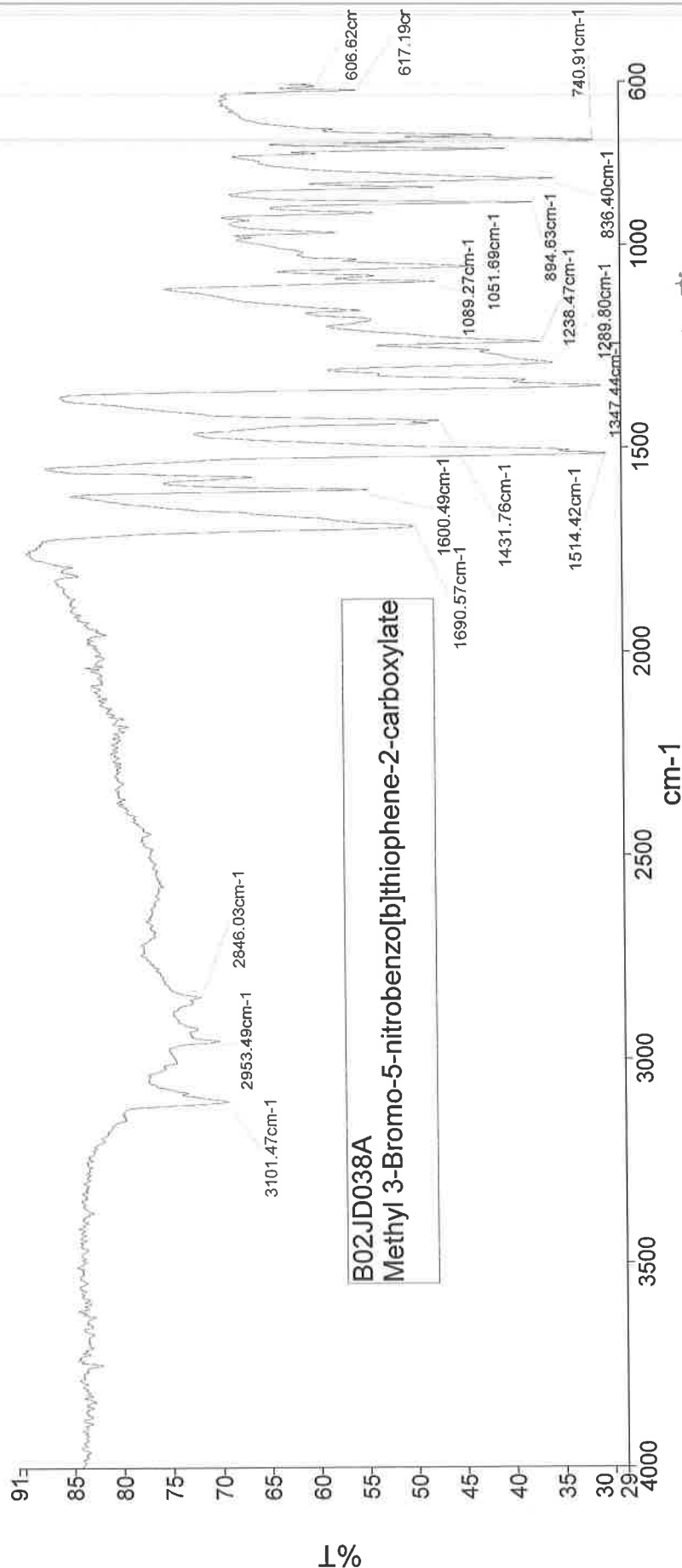




PerkinElmer Spectrum Version 10.03.06
07 August 2013 13:55

Analyst
Date

Administrator
07 August 2013 13:55



3101 C-H aromatic str.

Administrator 108 Sample 108 By Administrator Date Wednesday, August 07 2013

1691 C=O str Carb Acid

1600 C-C in ring str.

1514 N=O str.

1431 C-C in ring str.

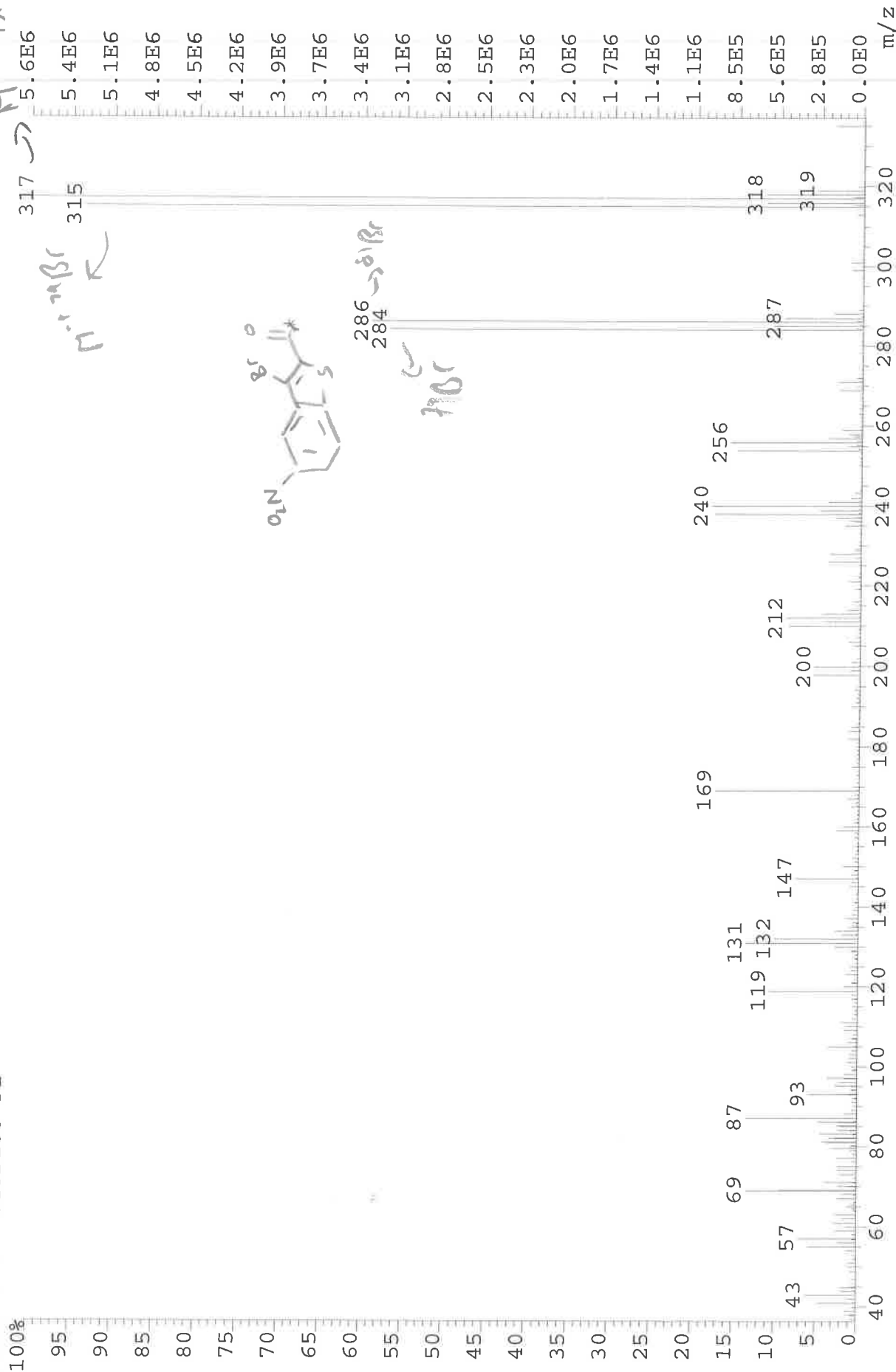
1347 N=O str.

1089 C=O str.

1052 C-O str.

741, C-H bend aromat
617 C-Br str

File: JESS92224 Ident: 40 Acq: 15-APR-2013 14:43:32 +2:30 Cal: CAL1
 AutoSpecE EI+ Magnet BpI: 5641742 TIC: 53442964 Flags: HALL
 File Text: B01JD153-F1



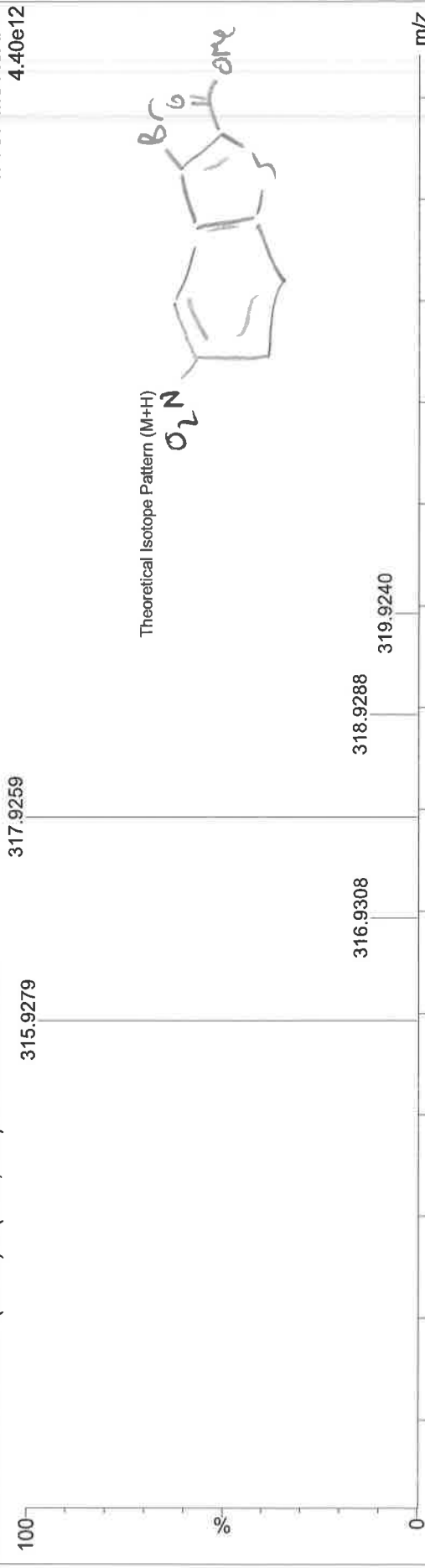
B03JD043A MW=316?
SOLID

National Mass Spectrometry Facility, Swansea
Waters Xevo G2-S

Rhiannon
13-Oct-2014

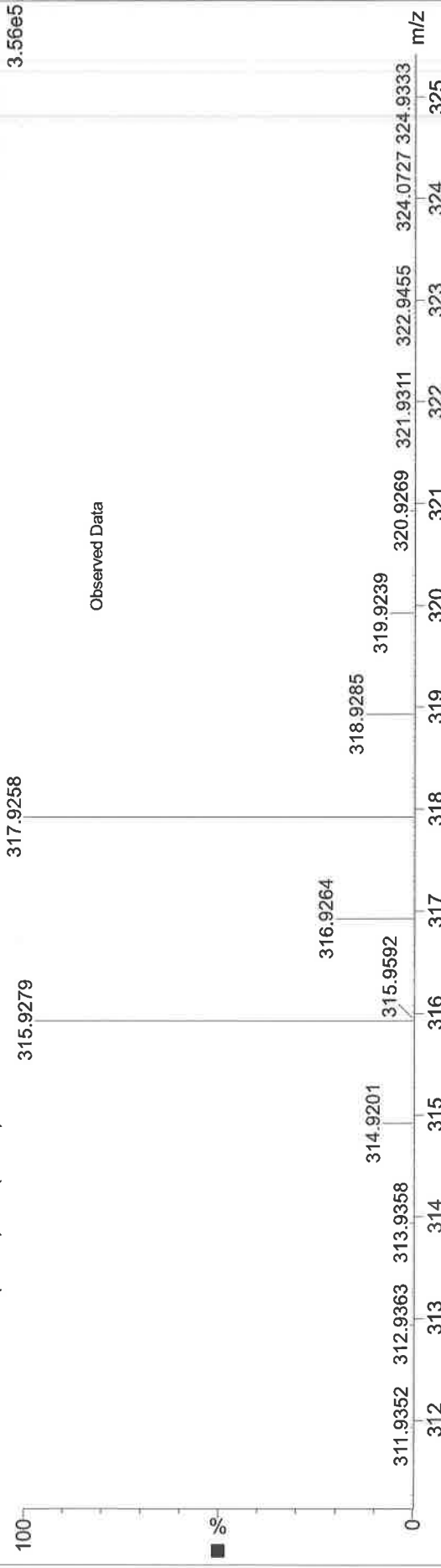
SUSSPE036-WG-HASP (0.045) Is (1.00, 1.00) C₁₀H₆BrNO₄SH

1: TOF MS ASAP+
4.40e12

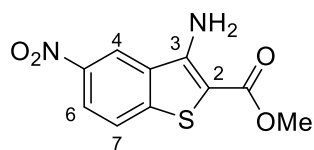


SUSSPE036-WG-HASP 37 (0.700) Cm (35:69)

1: TOF MS ASAP+
3.56e5



Methyl 3-amino-5-nitrobenzothiophene-2-carboxylate (170)



¹H NMR (500 MHz, DMSO-*d*₆) for Methyl 3-amino-5-nitrobenzo[*b*]thiophene-2-carboxylate

B03JD118A DMSO proton:esp

M02(dd)

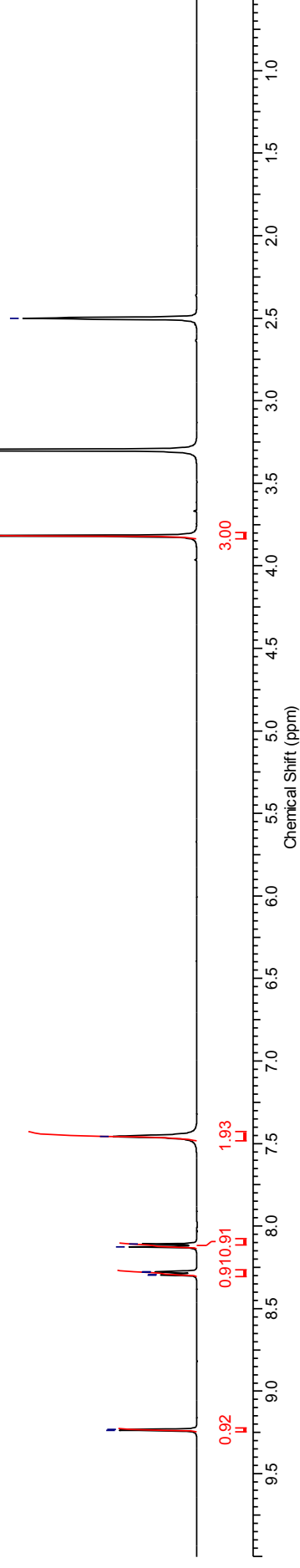
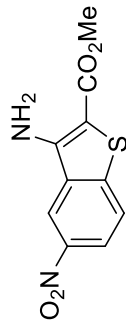
M01(d)
9.24
9.23

M03(d)
8.30
8.29
8.28
8.28
8.13
8.11

M04(br. s.)
7.46

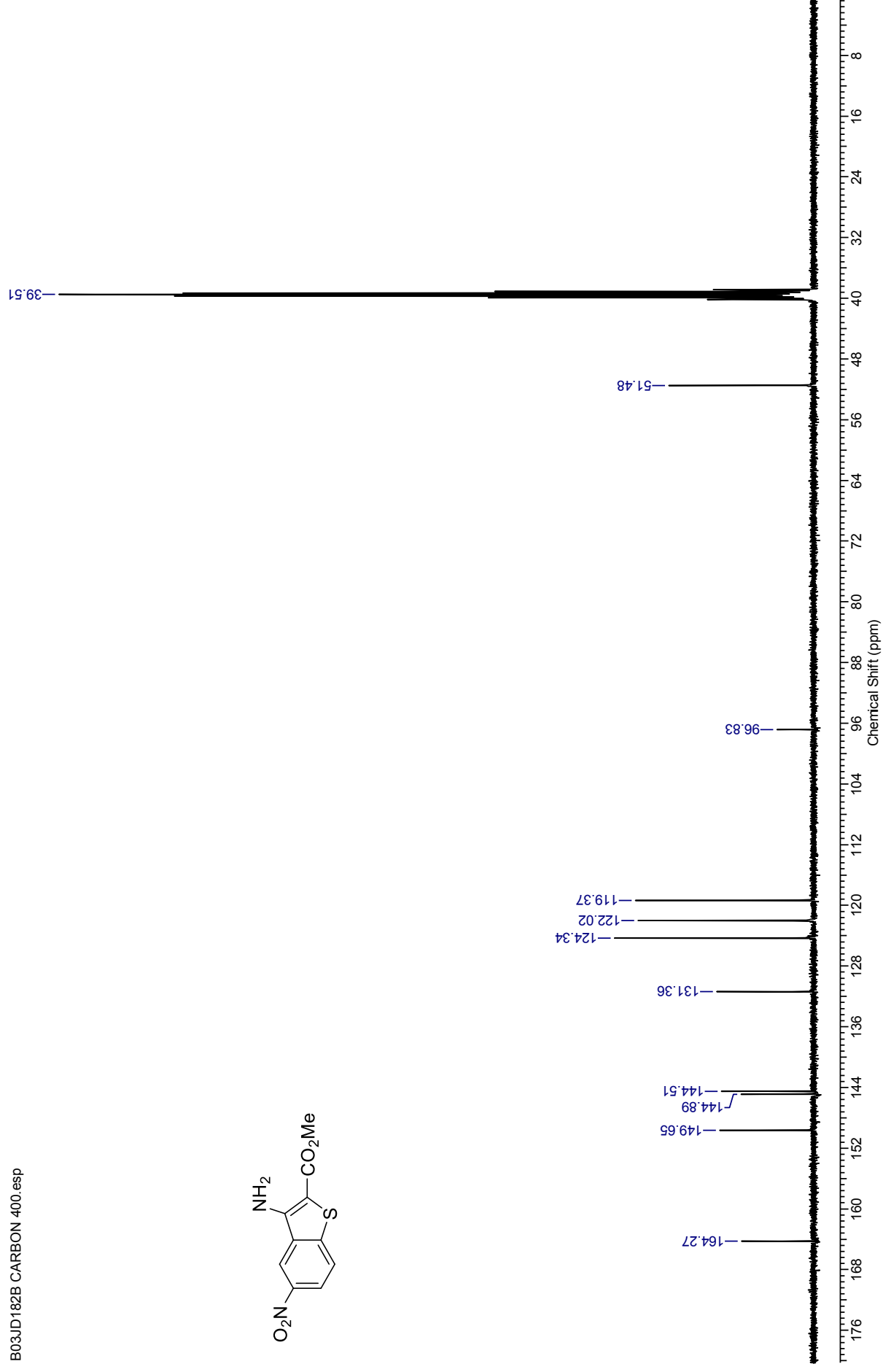
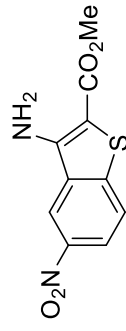
M05(s)
3.82

2.50



¹³C NMR (100 MHz, DMSO-*d*₆) for Methyl 3-amino-5-nitrobenzo[*b*]thiophene-2-carboxylate

B03JD182B CARBON 400.esp

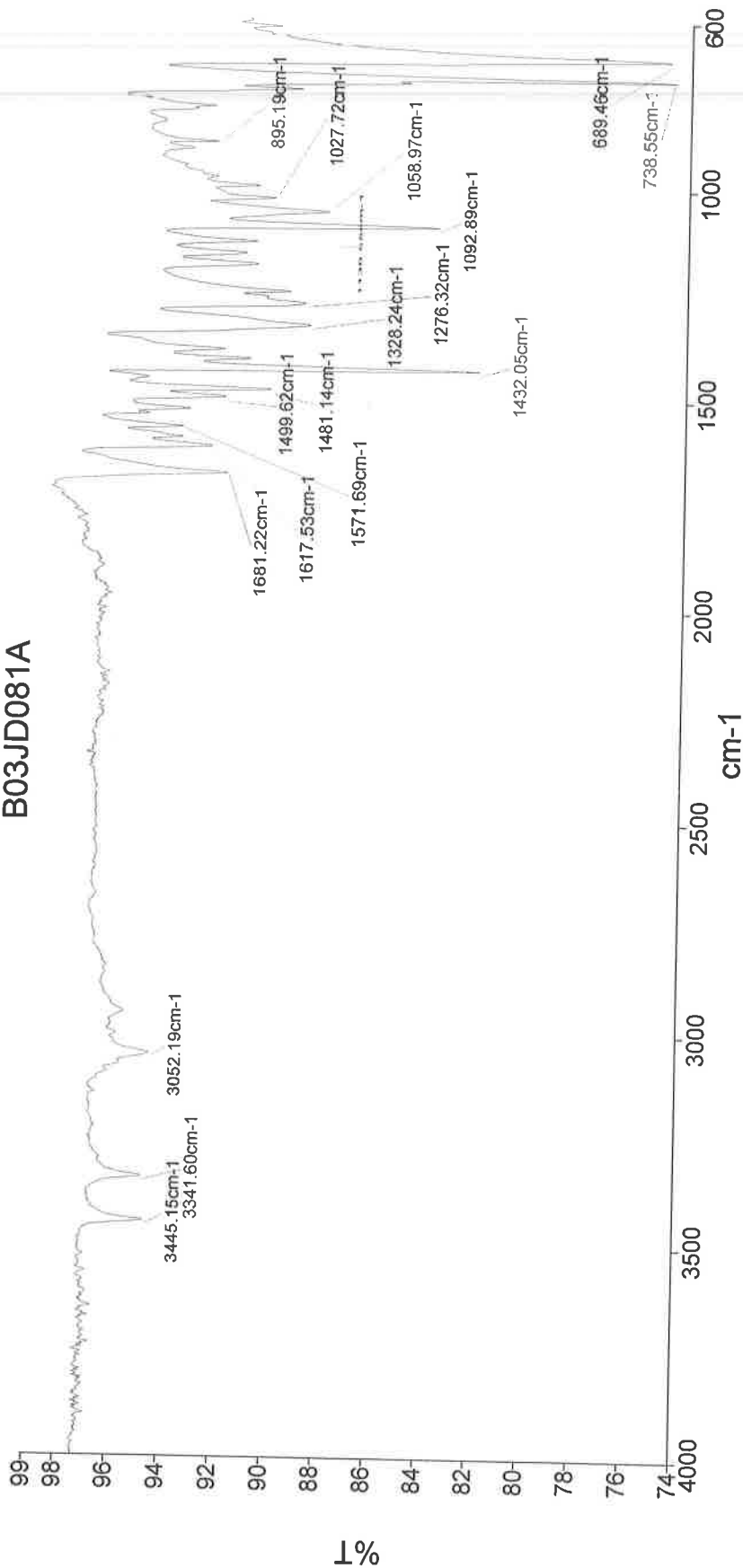




PerkinElmer Spectrum Version 10.03.06
23 February 2015 15:48

Analyst
Date
Administrator
23 February 2015 15:48

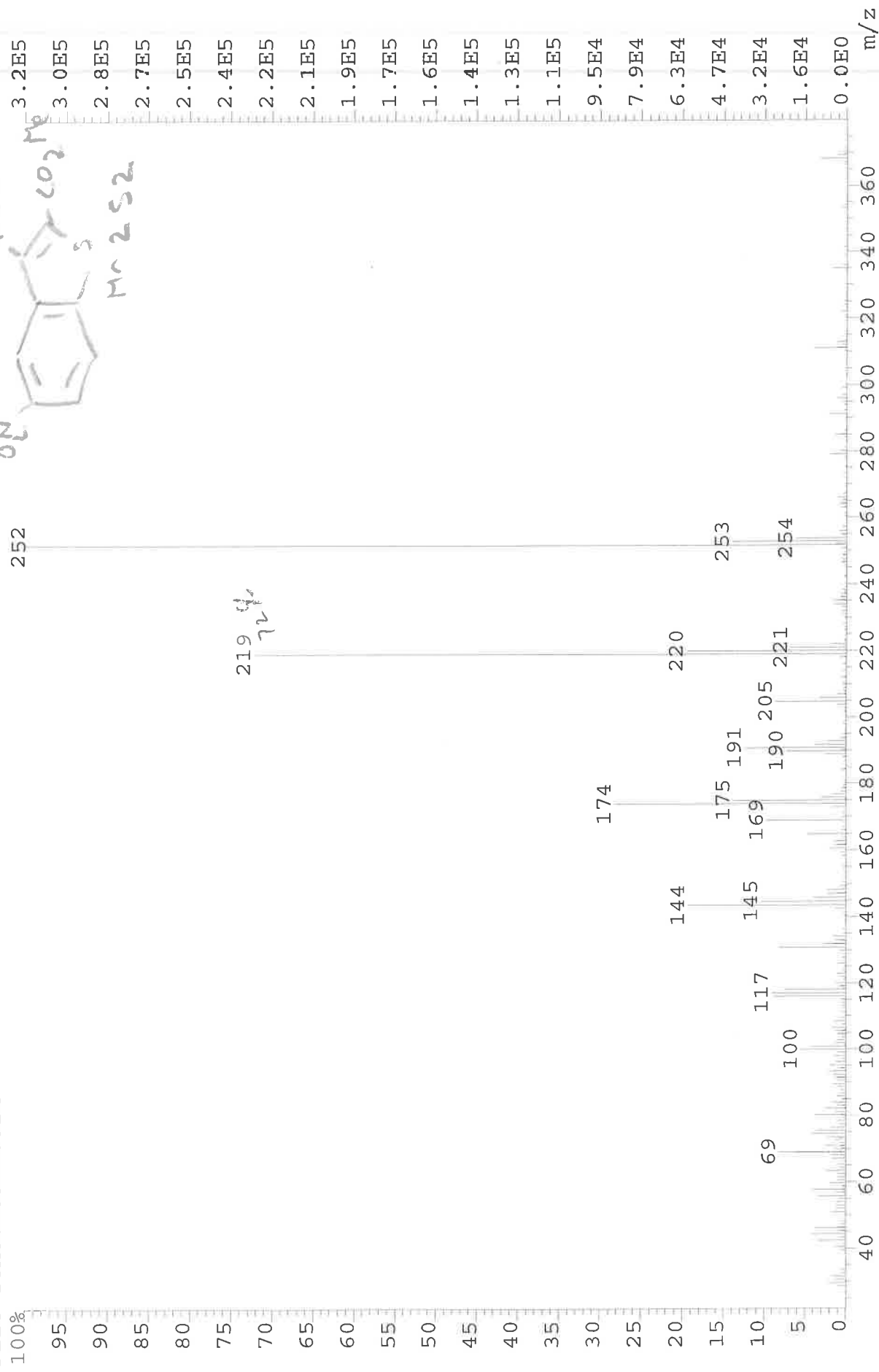
B03JD081A



3445 N-H str.
3342 N-H str.
3052 C-H str. arom.
1681 C=O str.
1572 N-O str. asym.
1432 C-N str.
1328 N-O str. sym.
1276 C=O
1093 C=O

Administrator 14 Sample 014 By Administrator Date Friday, February 20 2015

File: JESS4485A Ident: 33 Acq: 8-JUL-2014 12:32:48 +2:05 Cal: CAL1
AutoSpecE EI+ Magnet BpI: 315735 TIC: 2143522 Flags: HALL
File Text: BO3TD081A



B03JD090A MW=252?
(DCM)/MeOH + NH4OAc
C10H8N2O4S

EPSRC National Facility Swansea
LTQ Orbitrap XL

Rhiannon Jones
15/10/2014 13:15:08

SM: 7G

253.0280

NL:

3.46E6

SUSSPE034-OE-HNESP-2#30-
50 RT: 0.72-1.28 AV: 20 T:
FTMS + p NSI Full ms
[120.00-2000.00]

Relative Abundance

Observed Data



254.0311

255.0236

253.0278

NL:

1.96E4

C₁₀ H₈ N₂ O₄ SH:
C₁₀ H₉ N₂ O₄ S₁
p (gss, s /p:40) Chrg 1
R: 100000 Res .Pwr . @FWHM

Theoretical Isotope Model: [M + H]⁺

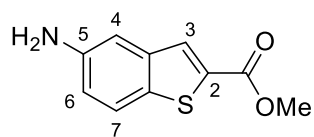
254.0311

255.0236

256.0270

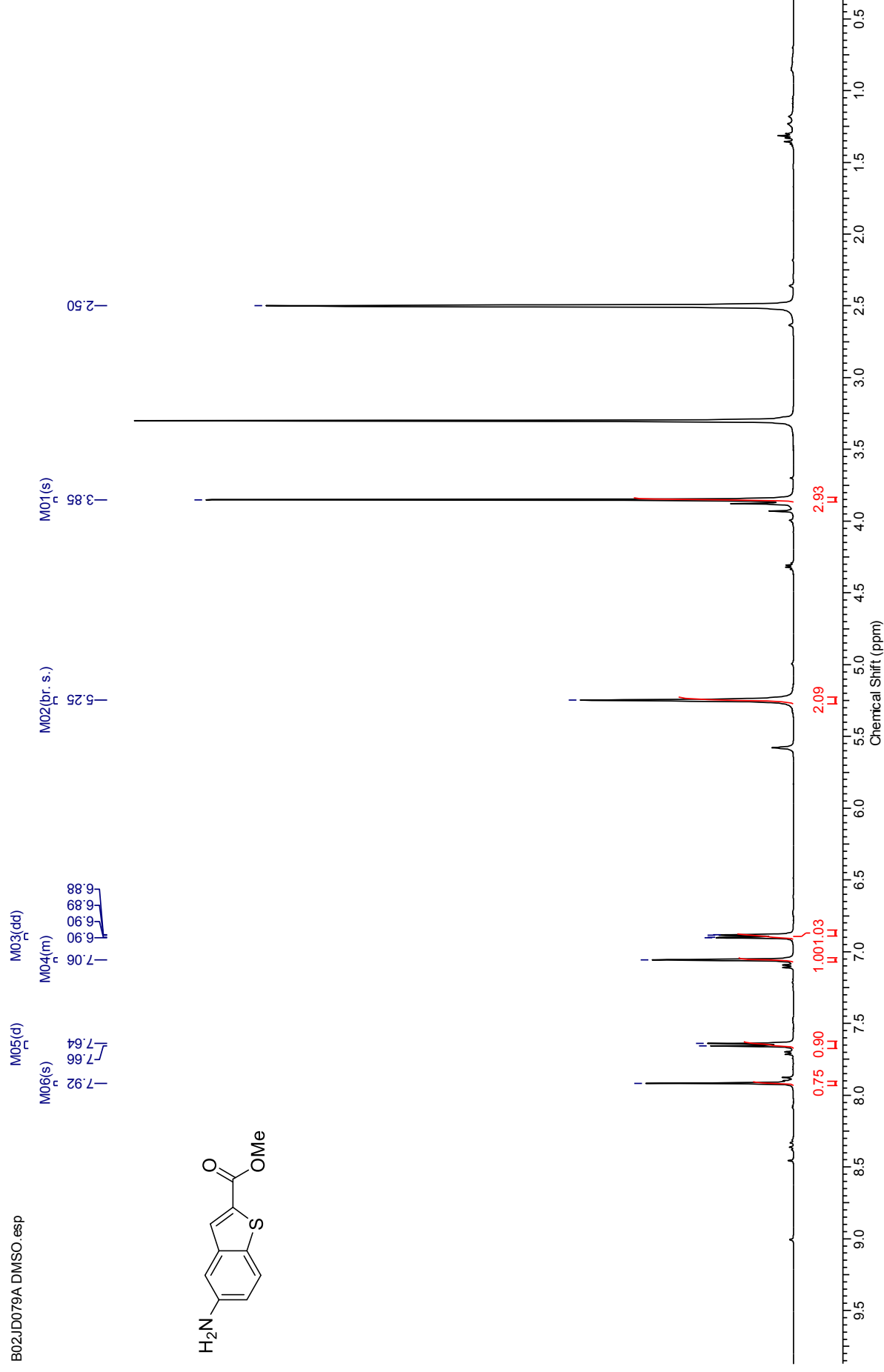
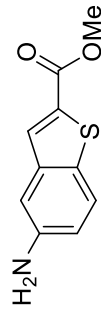
m/z

Methyl 5-aminobenzo[*b*]thiophene-2-carboxylate (158)



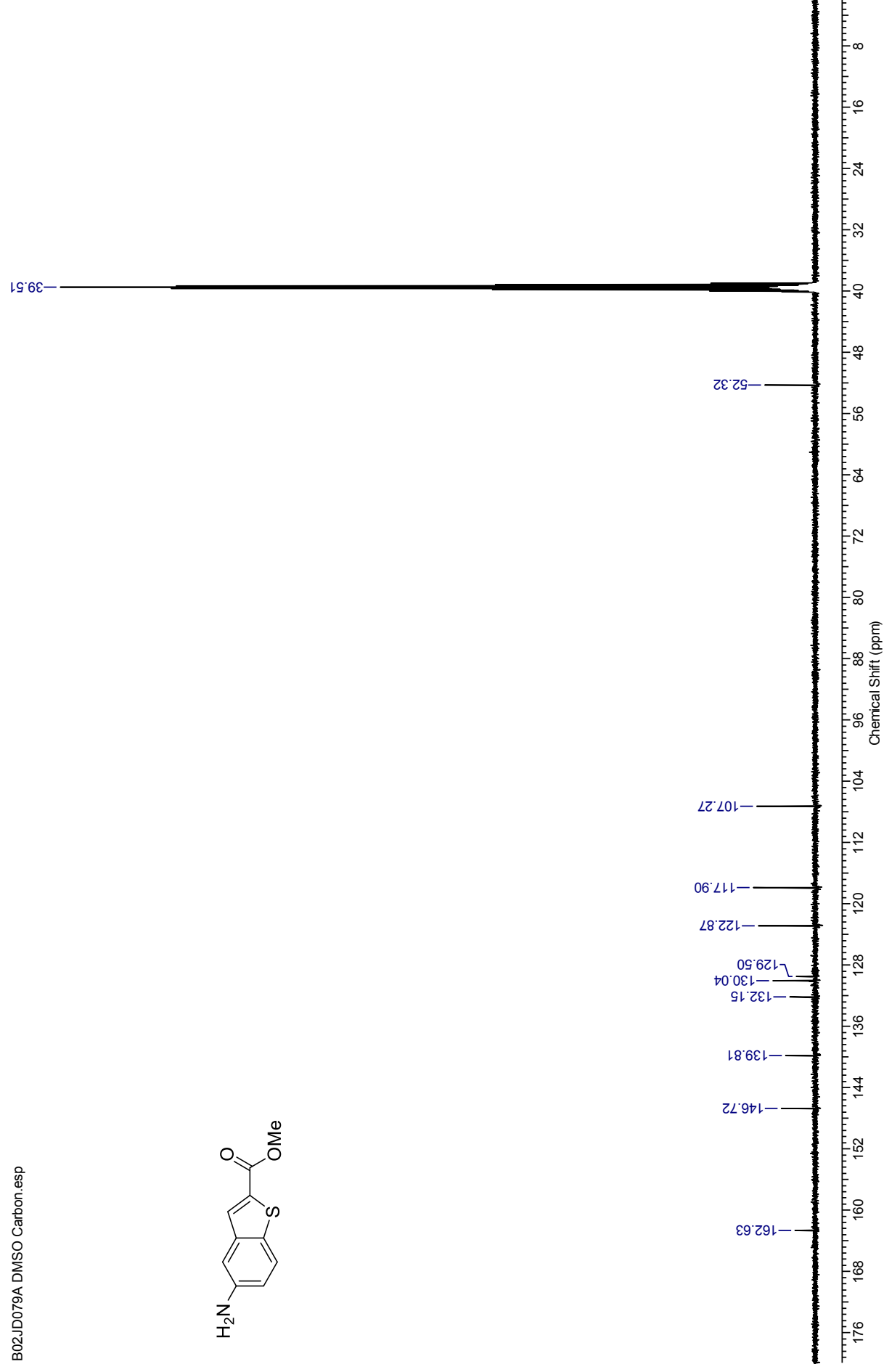
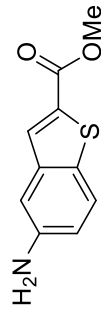
¹H NMR (500 MHz, DMSO-*d*₆) for Methyl 5-aminobenzo[*b*]thiophene-2-carboxylate

B02JD079A.DMSO.esp



¹³C NMR (126 MHz, DMSO-*d*₆) for Methyl 5-aminobenzo[*b*]thiophene-2-carboxylate

B02JD079A DMSO Carbon.esp



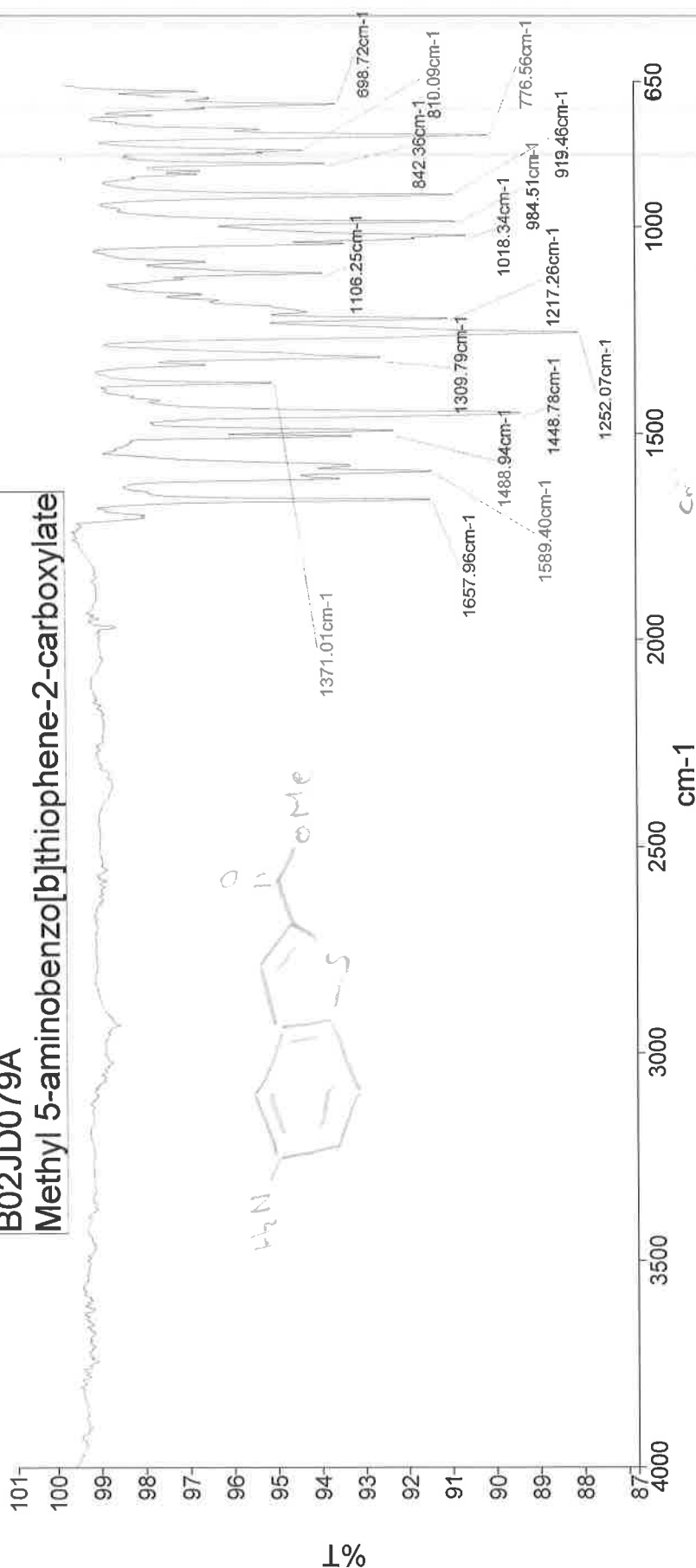
Administrator

16 October 2013 15:20

Analyst
Date

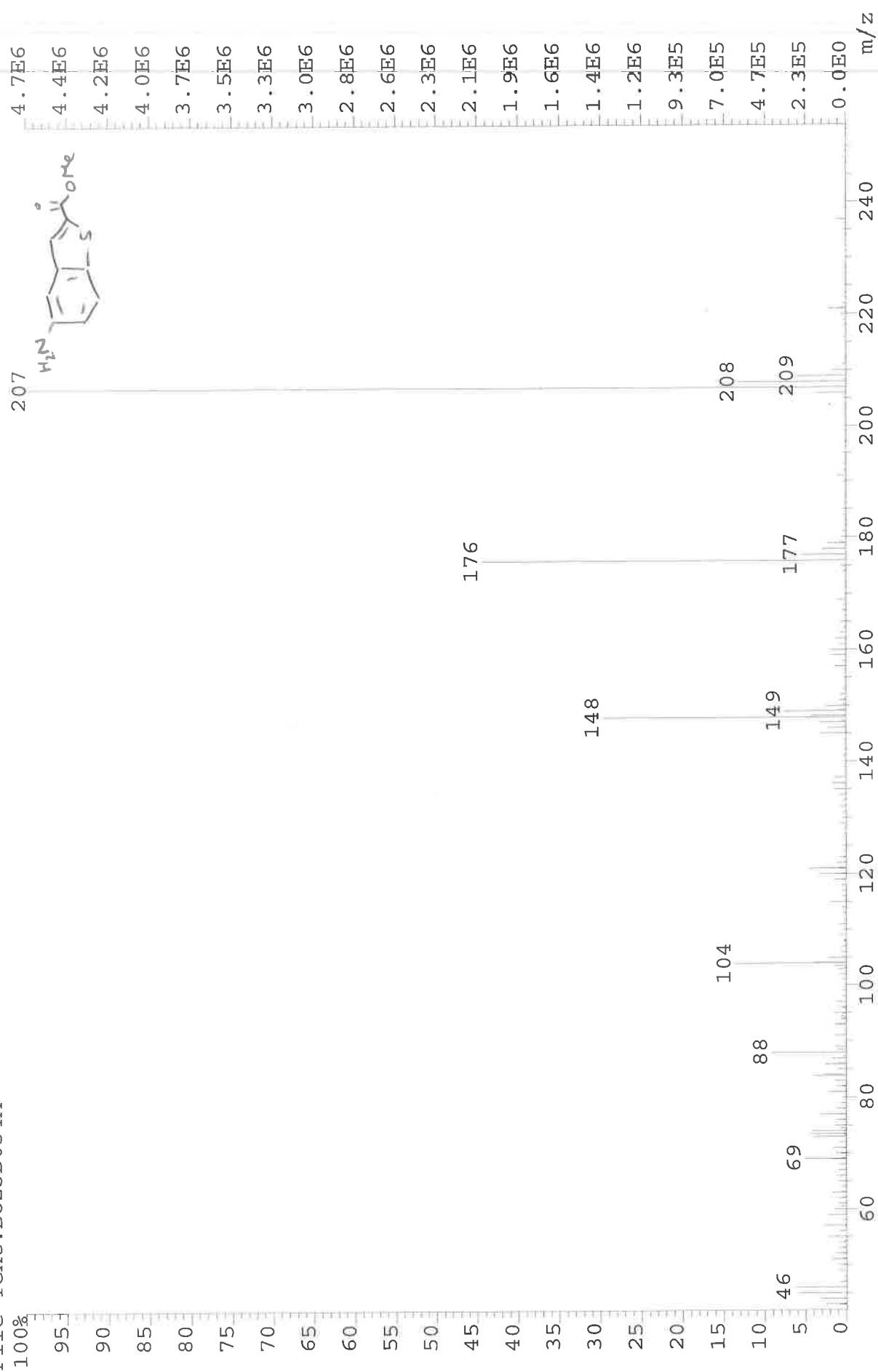
B02JD079A

Methyl 5-aminobenzo[b]thiophene-2-carboxylate



Administrator 205_1_1 Sample 205 By Administrator Date Wednesday, October 16 2013

File: JESS3113 Ident: 6 Acq: 17-JUL-2013 15:21:38 +0:26 Cal: CAL1
AutoSpecE EI+ Magnet BpI: 9629965 TIC: 51441392 Flags: HALL
File Text: B02JD034A



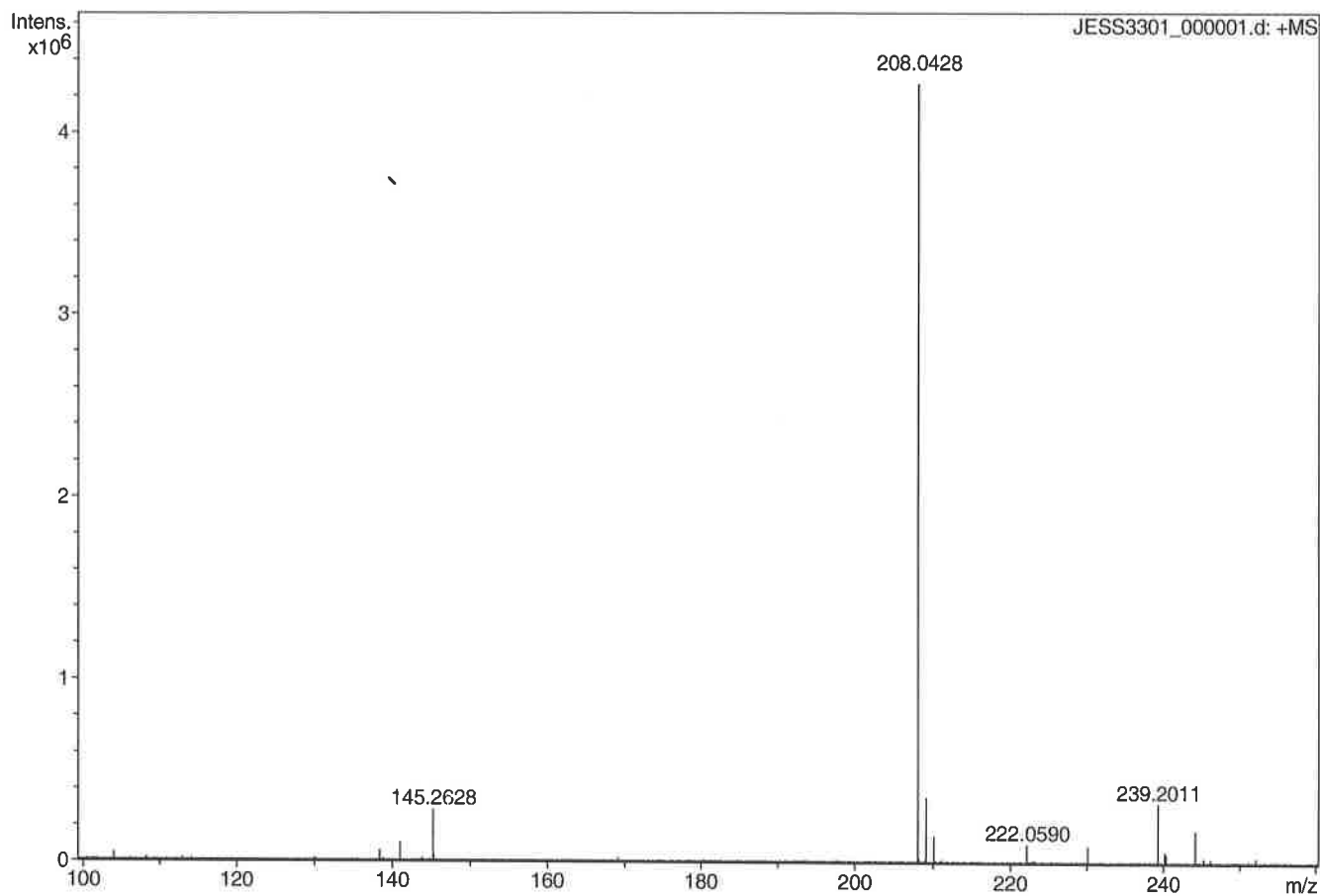
Generic Display Report

Analysis Info

Analysis Name D:\Data\Alinanopos\JESS3301_000001.d
Method pos20090608esi
Sample Name POSIVE ESI BO2JD079A
Comment

Acquisition Date 17/10/2013 16:19:30

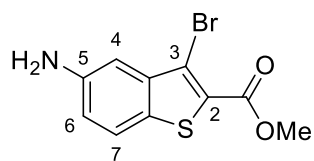
Operator Administrator
Instrument apex-III



Sum Formula	Sigma	m/z	Err [ppm]	Mean Err [ppm]	Err [mDa]	rdB	N Rule	e ⁻
C ₁₀ H ₁₀ N ₁ O ₂ S ₁	0.035	208.0427	-0.51	-1.08	-0.22	6.50	ok	even

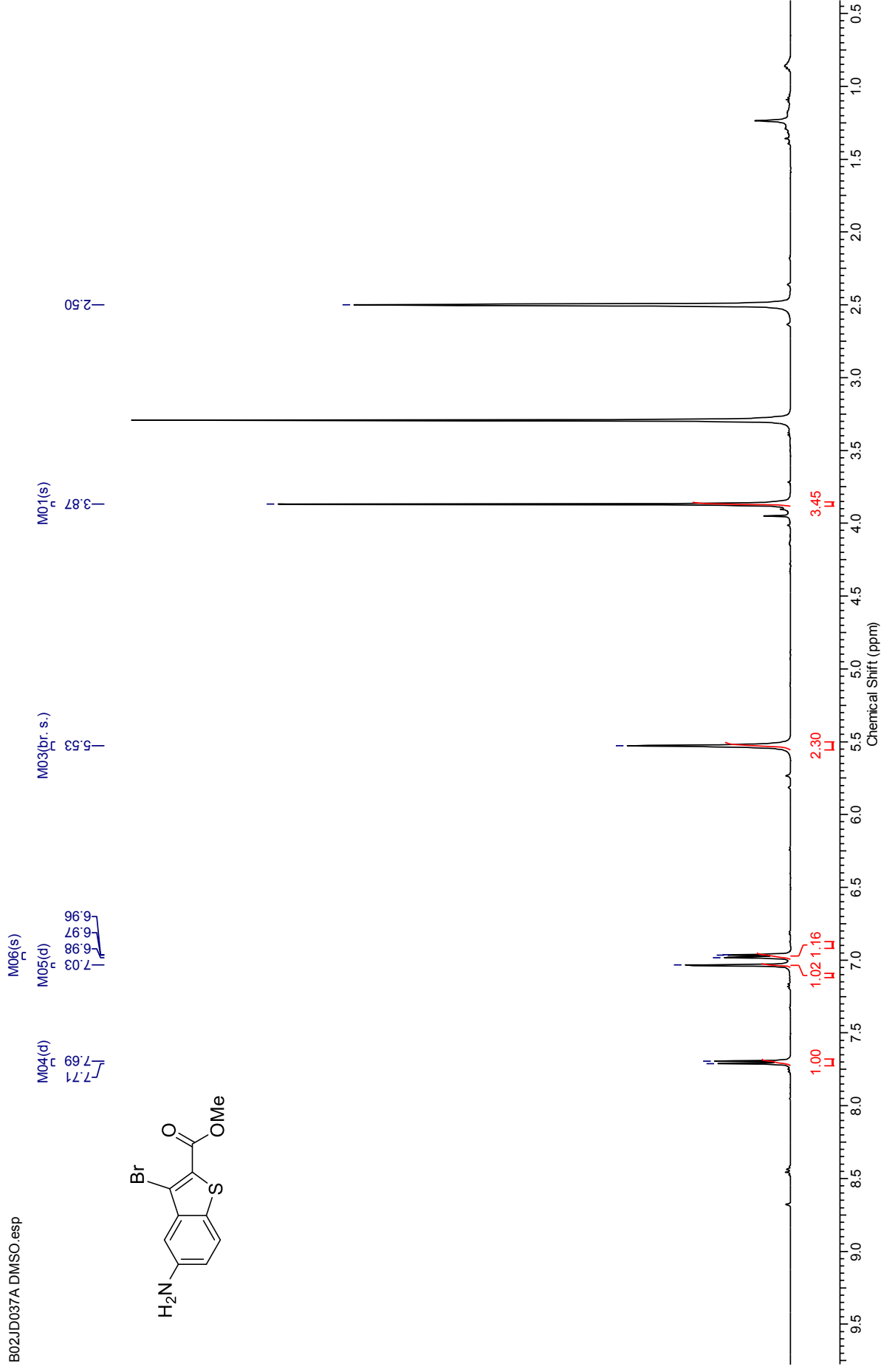


Methyl 5-amino-3-bromobenzo[b]thiophene-2-carboxylate (165)



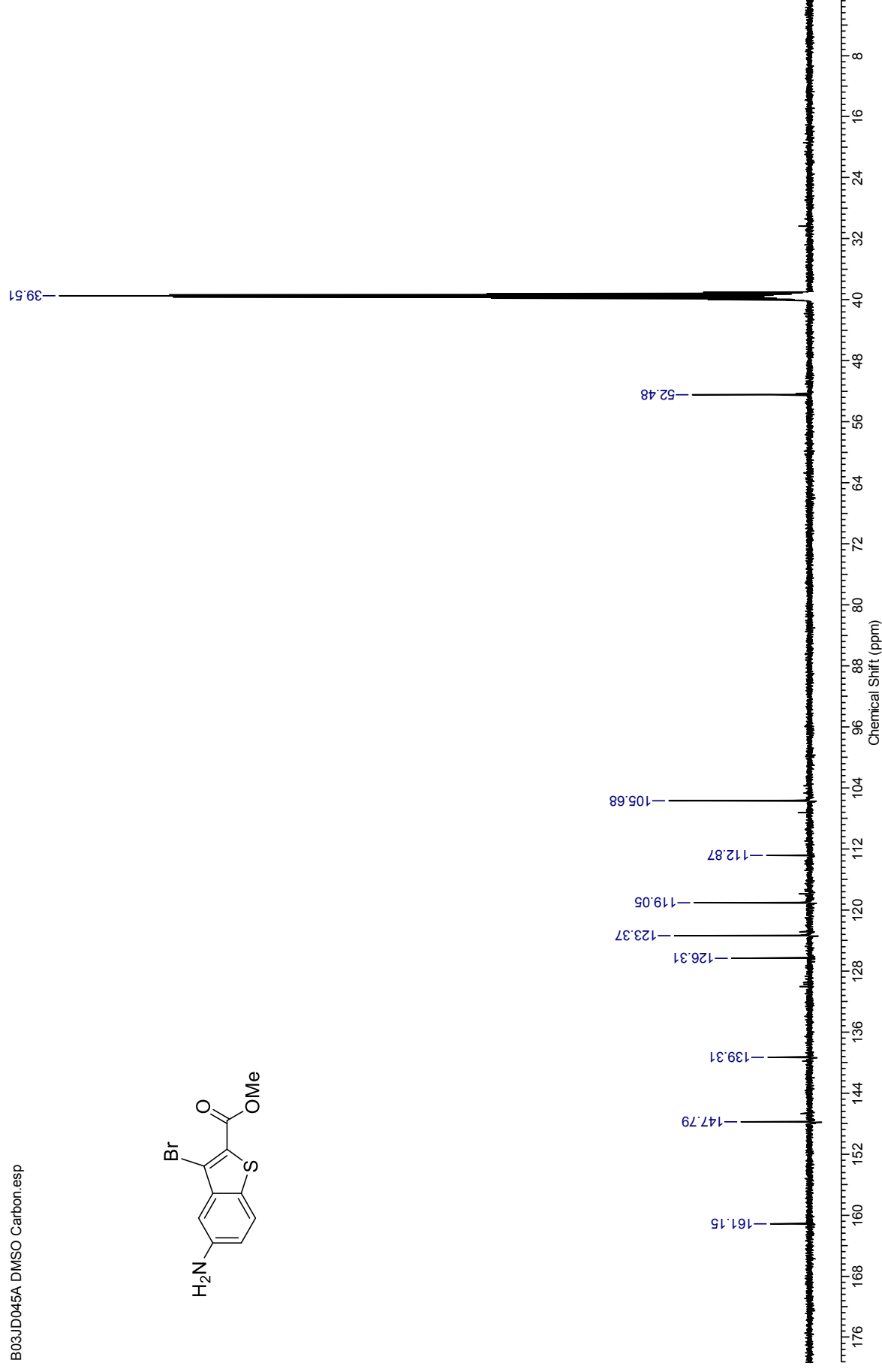
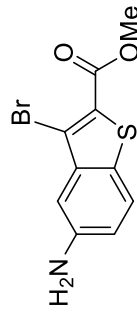
¹H NMR (500 MHz, DMSO-*d*₆) for Methyl 5-amino-3-bromobenzo[*b*]thiophene-2-carboxylate

B02JD037A DMSO.esp



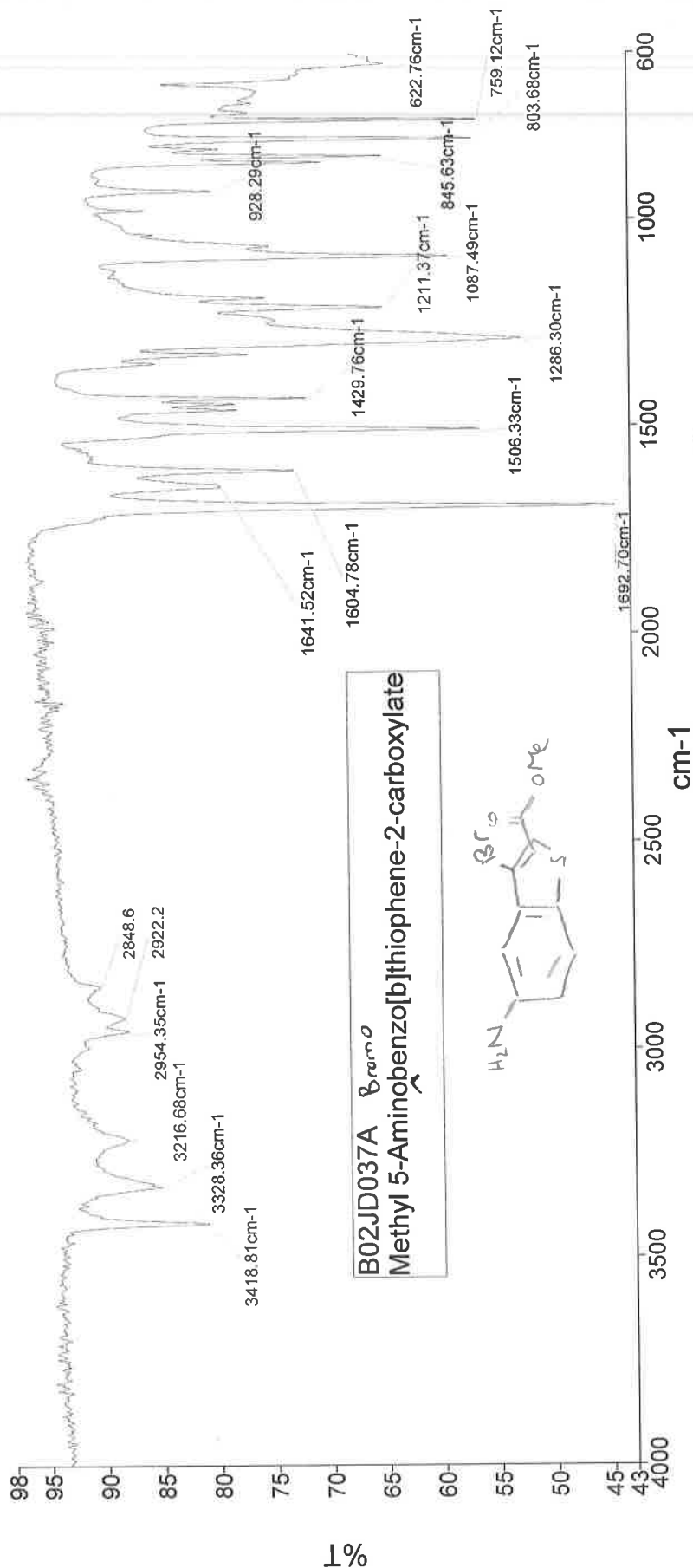
¹³C NMR (126 MHz, DMSO-*d*₆) for Methyl 5-amino-3-bromobenzo[*b*]thiophene-2-carboxylate

B03JD045A DMSO Carbon.esp



Analyst
Date

Administrator
07 August 2013 14:03

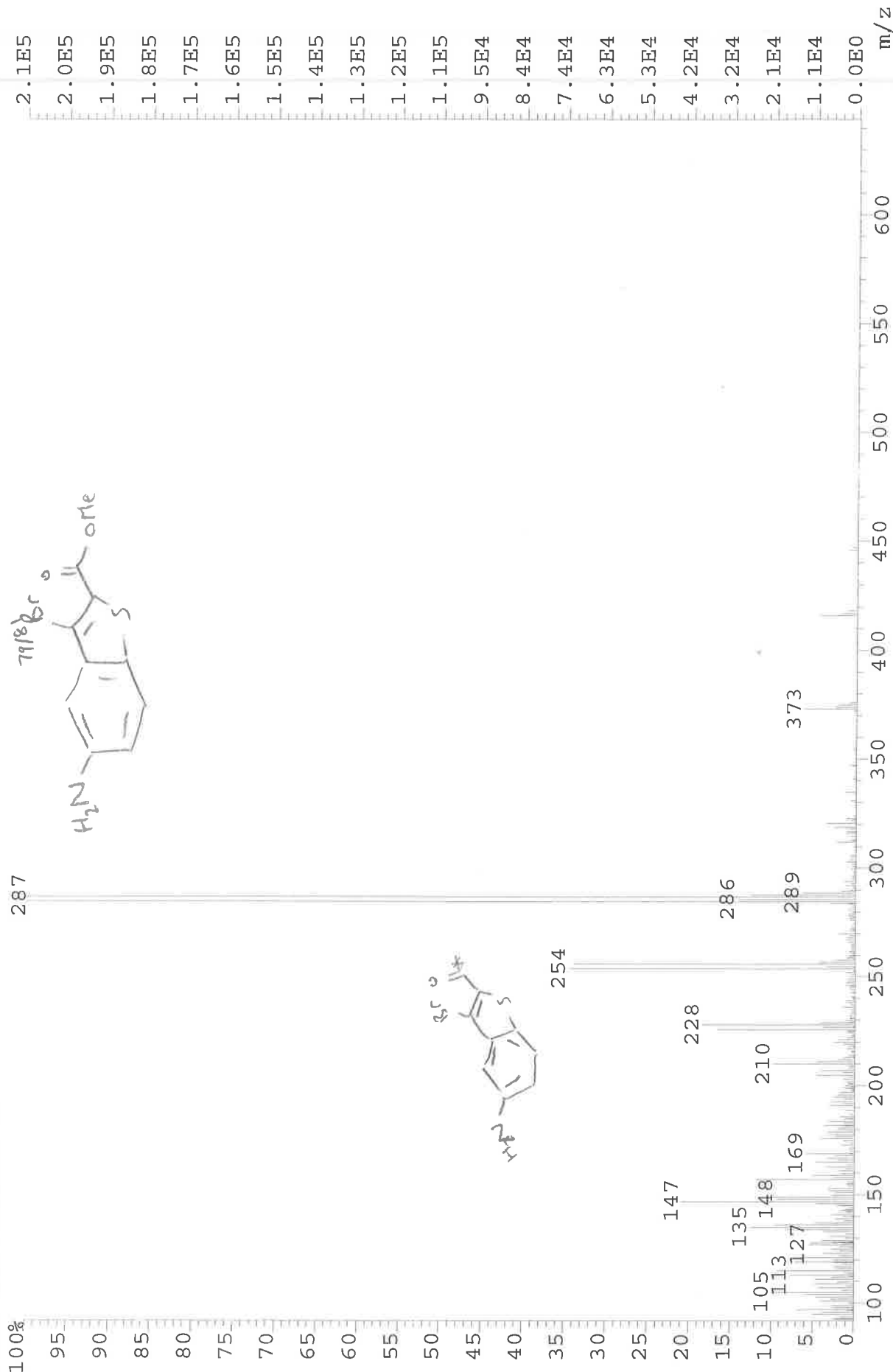


804 N-H amine bend
759 C-H bend aromatic
622 C-Br str.

3419 } N-H str.
3328 }

1693 C=O ester
1604 N-H bend
1506 C=C in ring str.
1286 C-N aromatic
1087 C-O ester str.

File: JESS3125 Ident: 63 Acq: 26-JUL-2013 10:09:39 +3:55 Cal: CAL1
 AutoSpecE EI+ Magnet BpI: 2890279 TIC: 6733926 Flags: HALL
 File Text: BO2JD037A



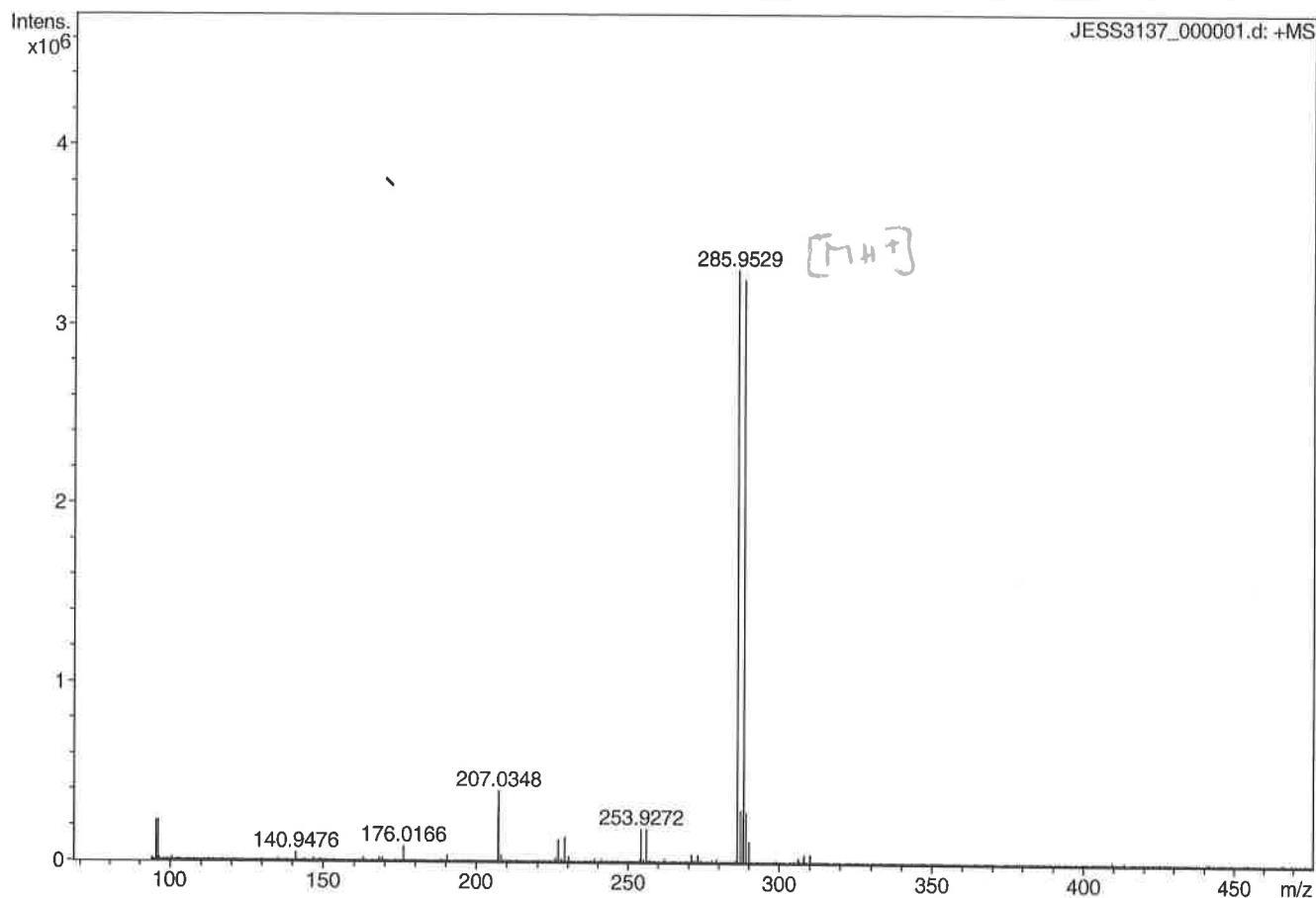
Generic Display Report

Analysis Info

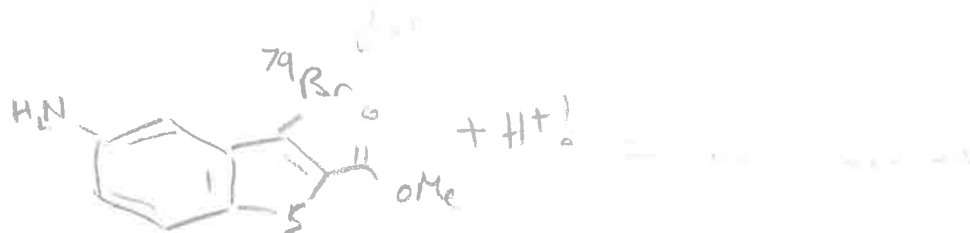
Analysis Name D:\Data\Alinanopos\JESS3137_000001.d
Method pos20090608esi
Sample Name POS ESI BO2JD040B
Comment

Acquisition Date 01/08/2013 14:54:26

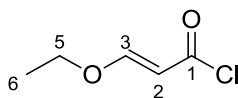
Operator Administrator
Instrument apex-III



Sum Formula	Sigma	m/z	Err [ppm]	Mean Err [ppm]	Err [mDa]	rdb	N Rule	e ⁻
C 10 H 9 Br 1 N 1 O 2 S 1	0.030	285.9532	0.99	1.78	0.51	6.50	ok	even

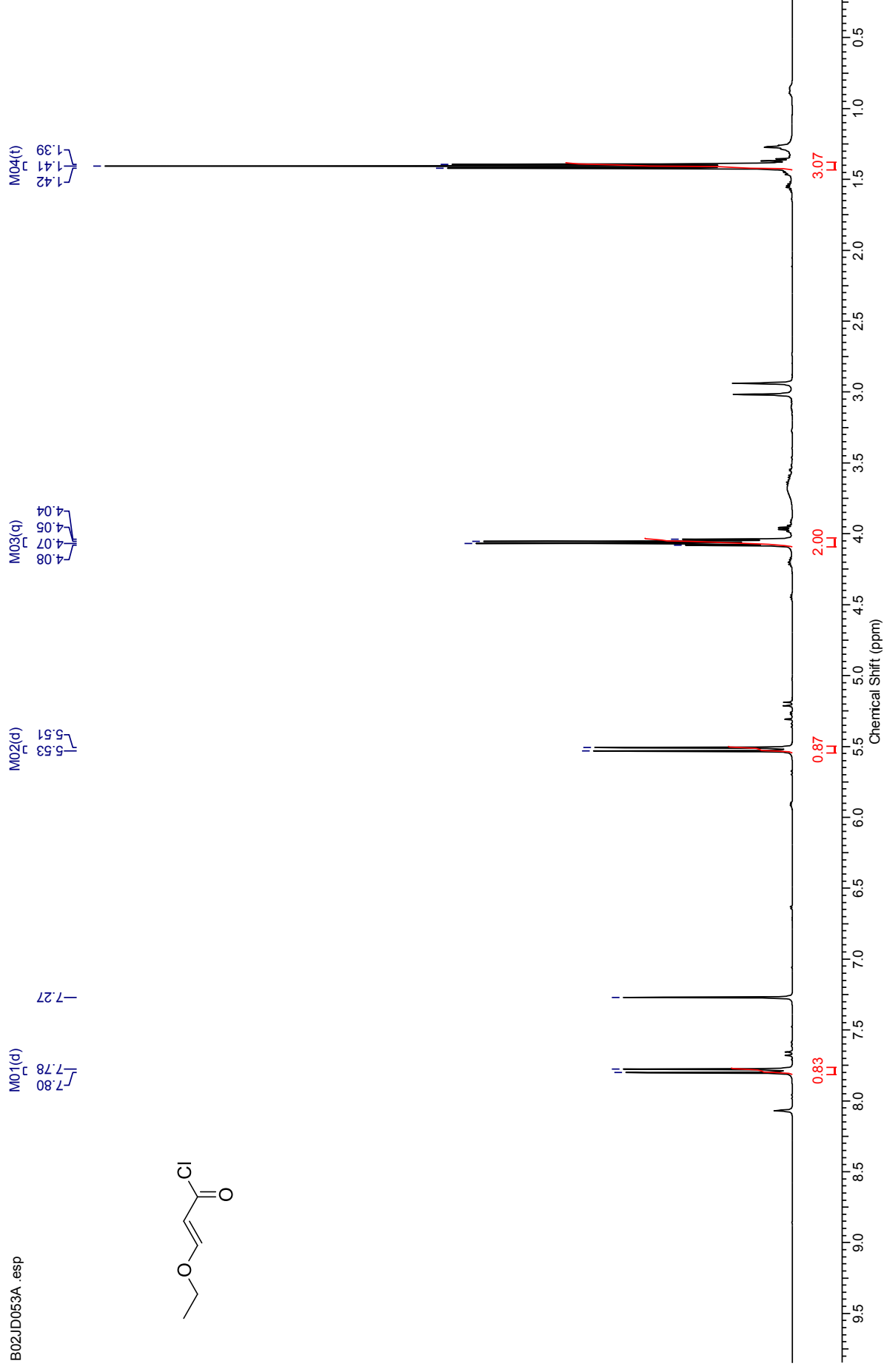
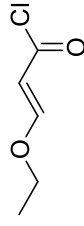


(2E)-3-Ethoxyprop-2-enoyl chloride

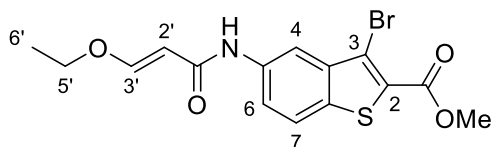


¹H NMR (500 MHz, CDCl₃) for (2*E*)-3-Ethoxyprop-2-enoyl chloride

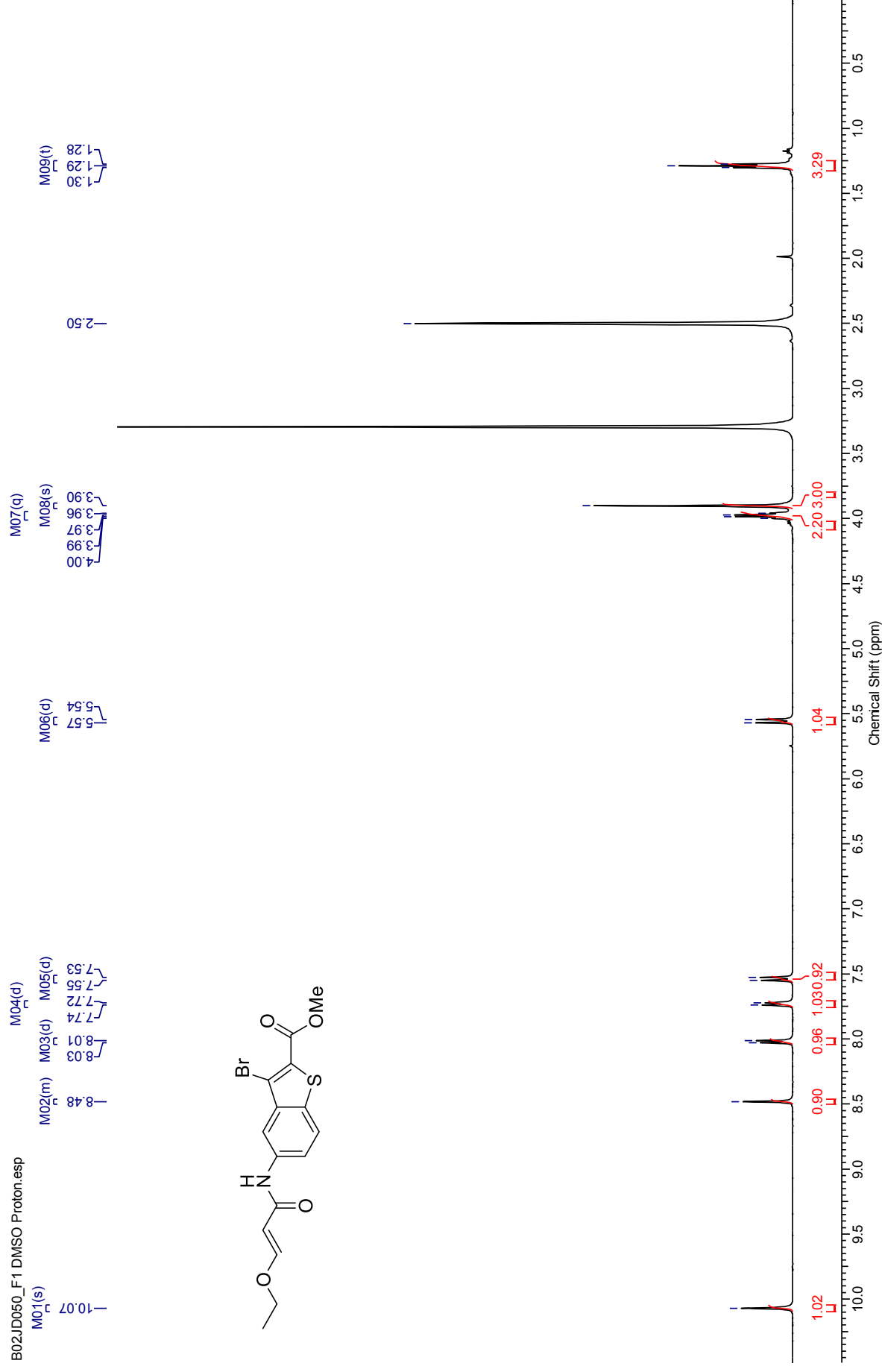
B02JD053A .esp



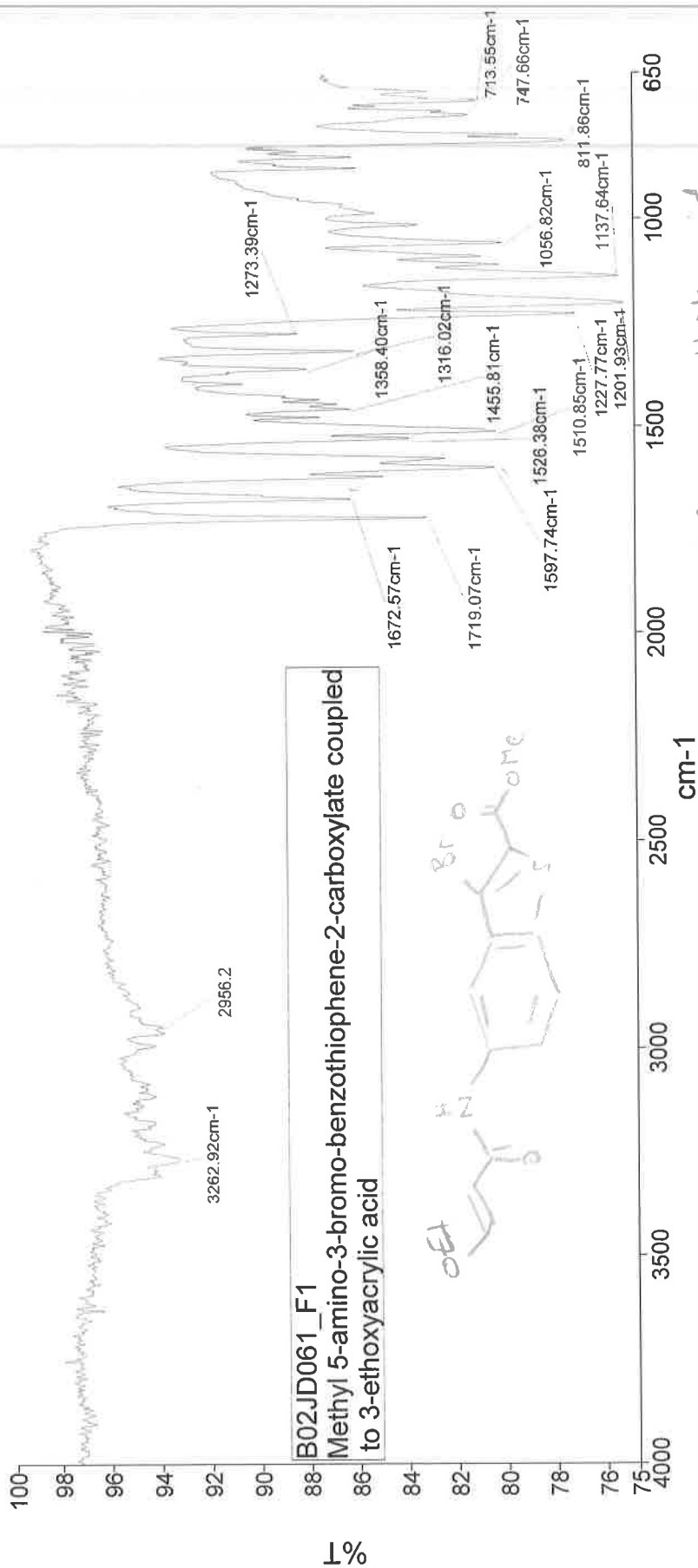
Methyl 3-bromo-5-[[*(2E)*-3-ethoxyprop-2-enoyl]amino]benzo[*b*]thiophene-2-carboxylate (171)



¹H NMR (500 MHz, DMSO-*d*₆) for Methyl 3-bromo-5-([(2*E*)-3-ethoxyprop-2-enyl]amino)benzo[*b*]thiophene-2-carboxylate

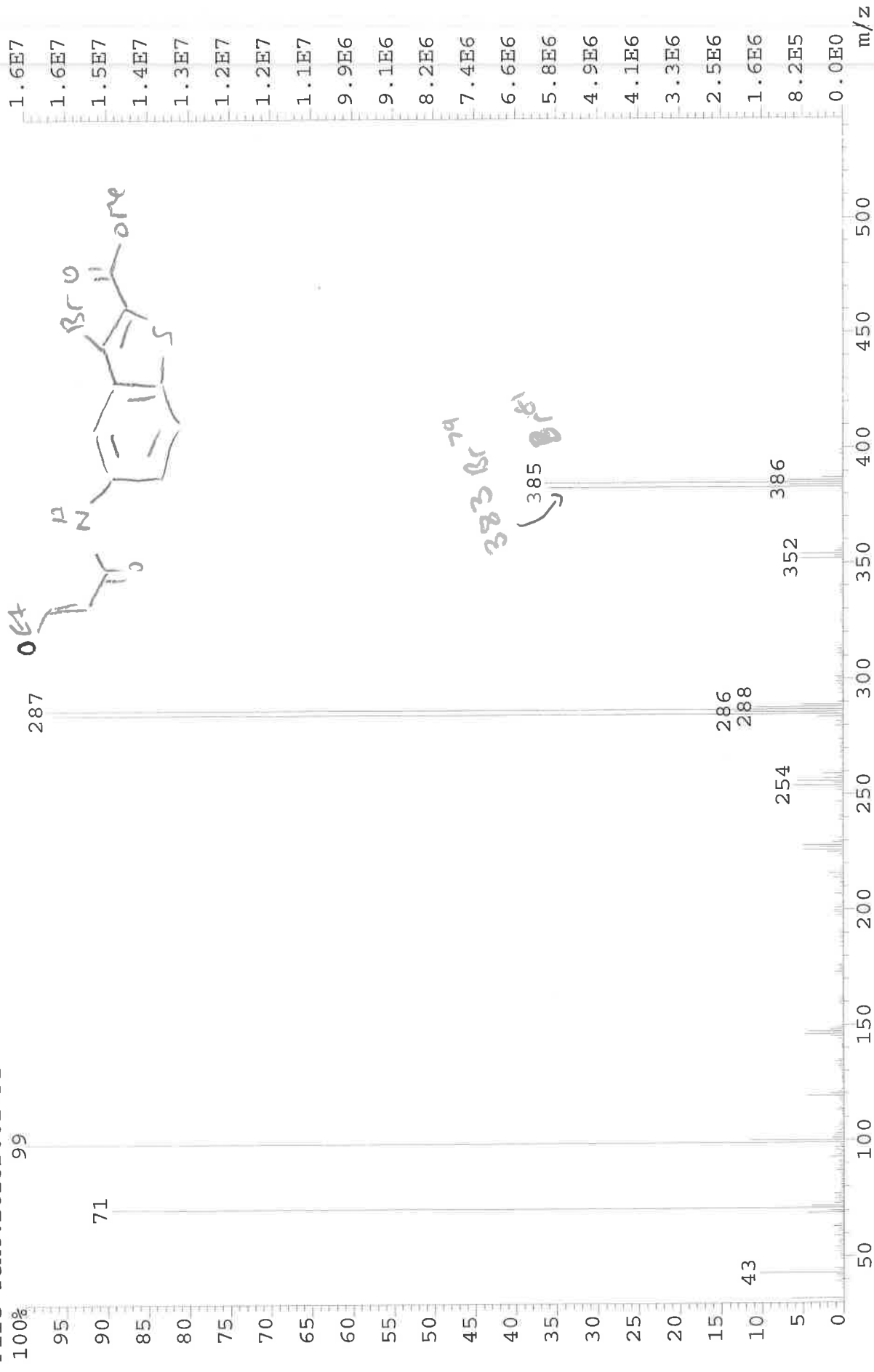


Analyst
Date
Administrator
16 October 2013 15:35



3263 N-H str, amide
2956 C-H str, alkane
1719 C=O str, ester
1672 C=C str, alkene
1598 C-C in ring str.
1202 C-O str, ester
1138 C-O str, ether
812 C-H bend, aromatic

File: JESS3217 Ident: 34 Acq: 29-AUG-2013 16:39:52 +2:08 Cal: CAL1
 AutoSpecE EI+ Magnet BpI: 16464525 TIC: 125396296 Flags: HALL
 File Text: BO2JD061-F1



Generic Display Report

Analysis Info

Analysis Name D:\Data\Alinanopos\JESS3186_000001.d
Method pos20090608esi
Sample Name POS ESI B02JDO57-F3
Comment

Acquisition Date 20/08/2013 16:50:25

Operator Administrator
Instrument apex-III

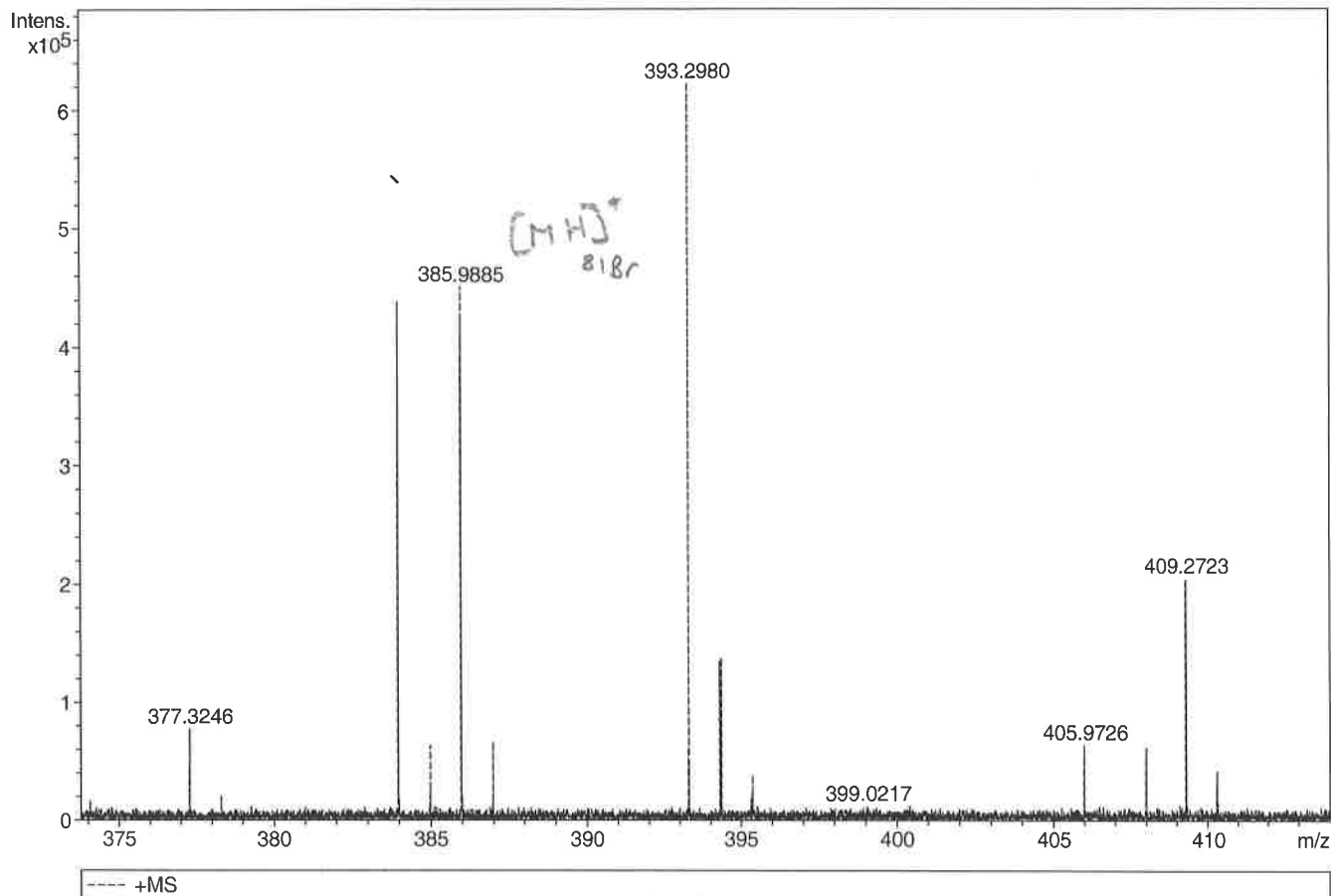
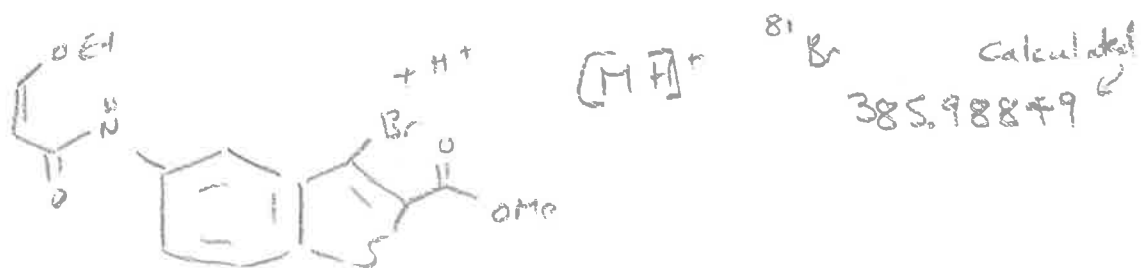
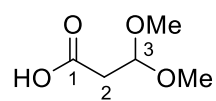


Table 'GenFormulaResults' could not be found in this analysis

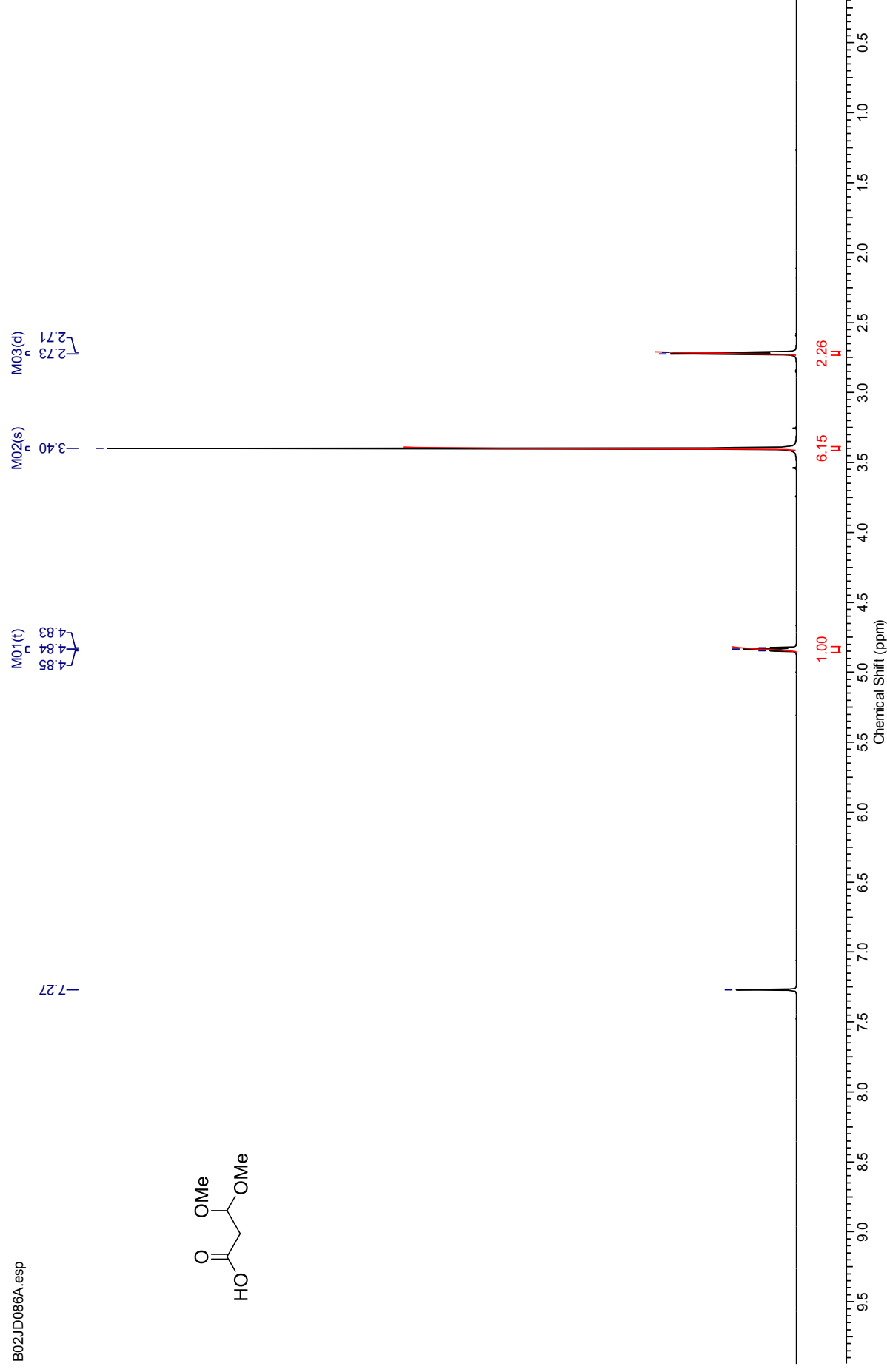
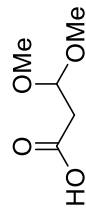


3,3-Dimethoxypropanoic acid (172)



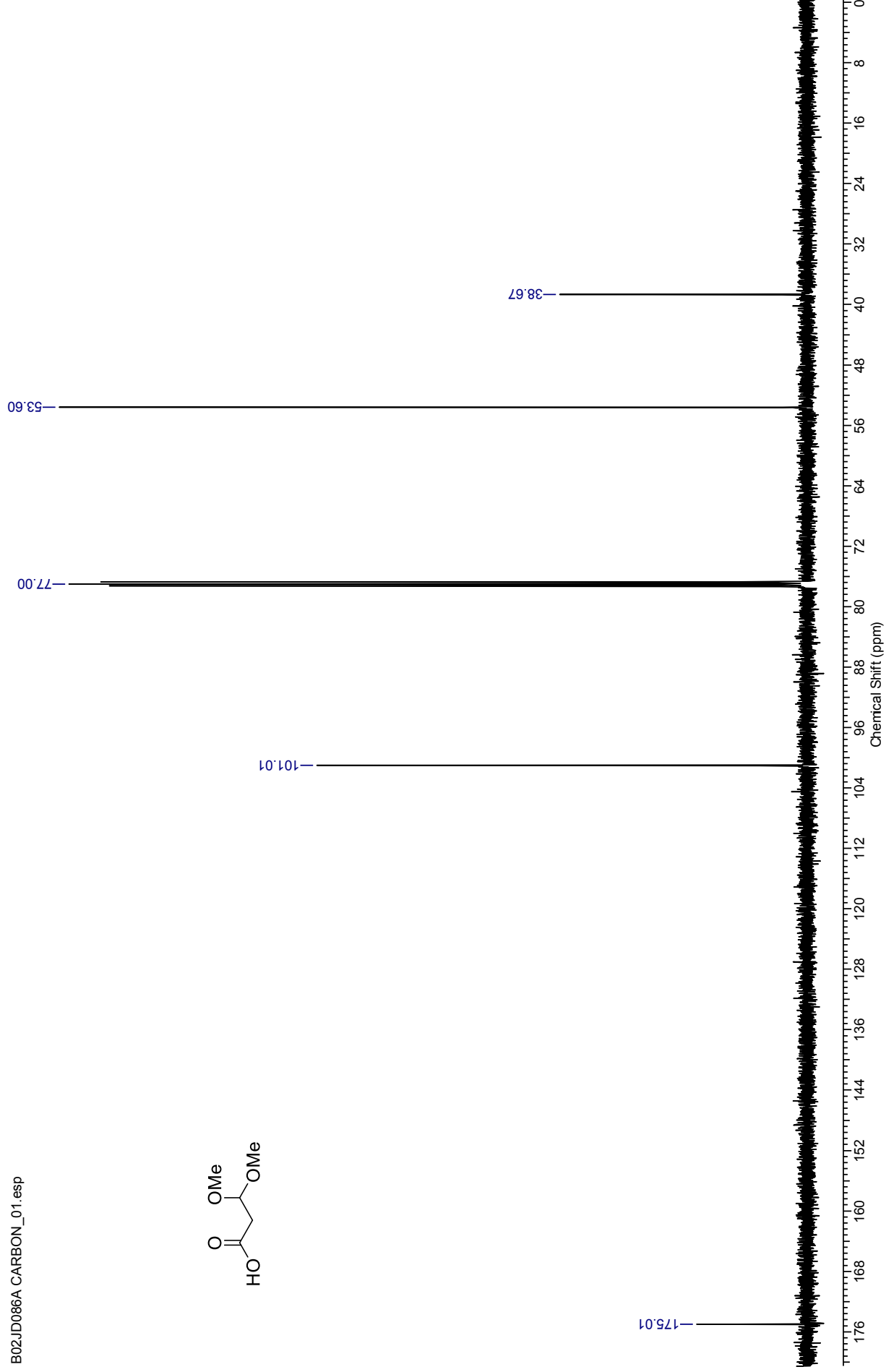
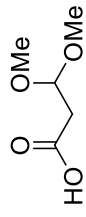
¹H NMR (500 MHz, CDCl₃) for 3,3-Dimethoxypropanoic acid

B02JD086A.esp



¹³C NMR (126 MHz, CDCl₃) for 3,3-Dimethoxypropanoic acid

B02JD086A CARBON_01.esp

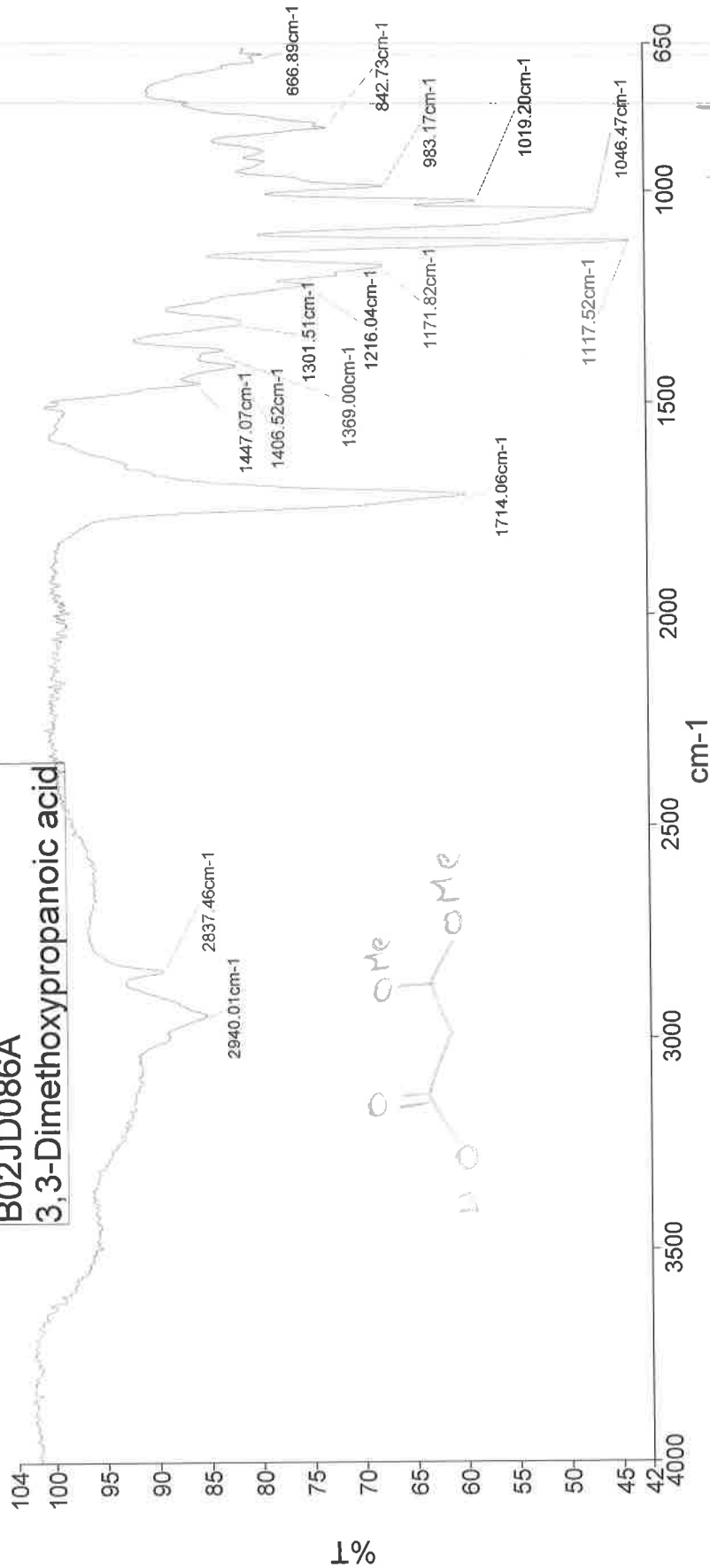


Analyst
Date

Administrator
16 October 2013 15:24

B02JD086A

3,3-Dimethoxypropanoic acid



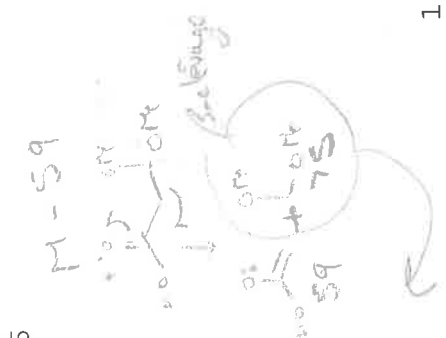
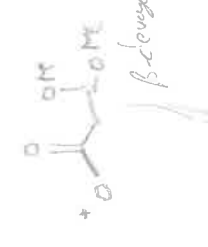
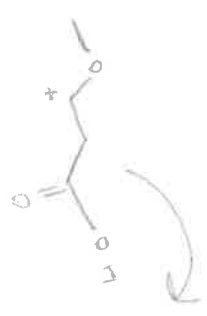
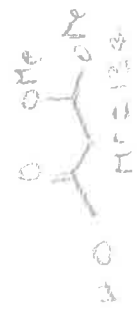
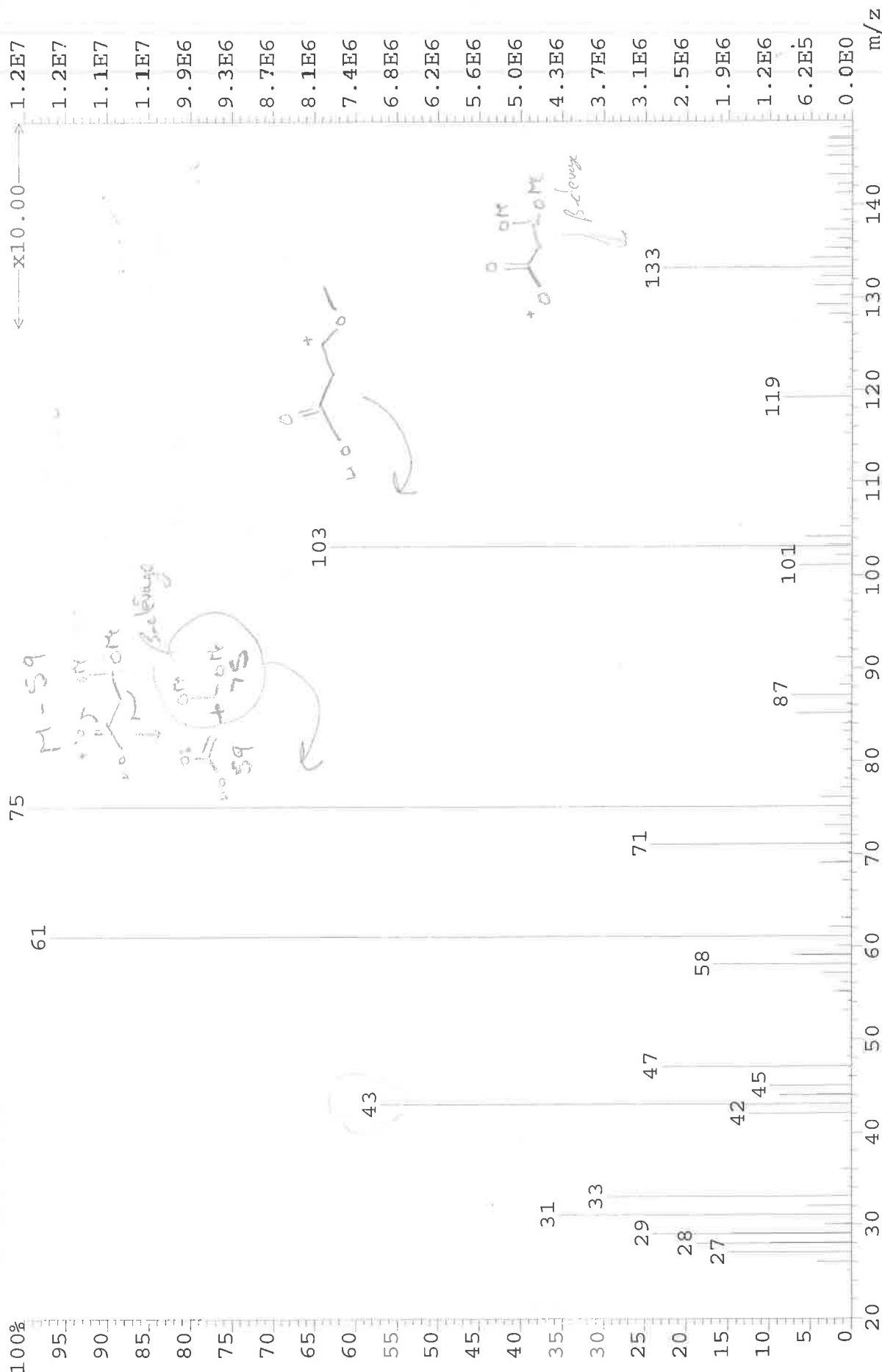
Administrator 206 Sample 206 By Administrator Date Wednesday, October 16 2013

Compare to

2940
2837
1714
1118
1046
983

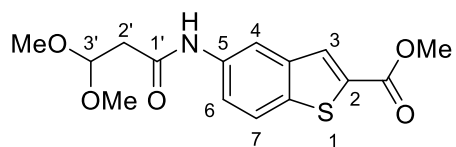
O-H str, carb acid
C-H alkane str.
C=O str, carb acid
C-O str, acid
C-O str, ether
O-H bend, carb acid

File: JESS3277 Ident: 21 Acq: 14-OCT-2013 10:02:44 +1:21 Cal: CALL1
 AutospecE EI+ Magnet BpI: 12389349 TIC: 91267960 Flags: HALL
 File Text: B02JD086A



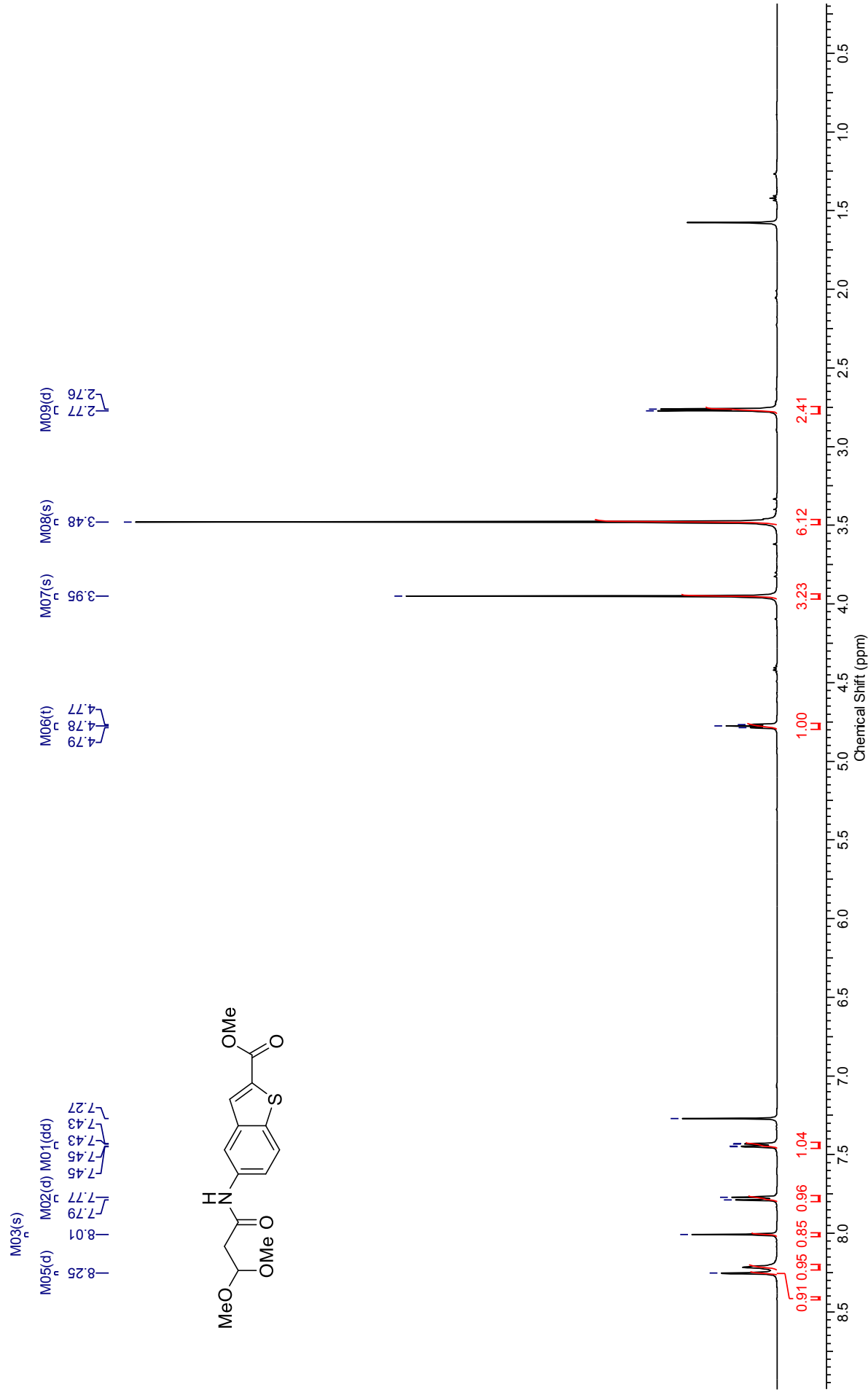
Correlates with data
 Valdego
 Eur S
 chem
 20021
 07041.2053

Methyl 5-(3,3-dimethoxypropanamido)benzo[*b*]thiophene-2-carboxylate (174)



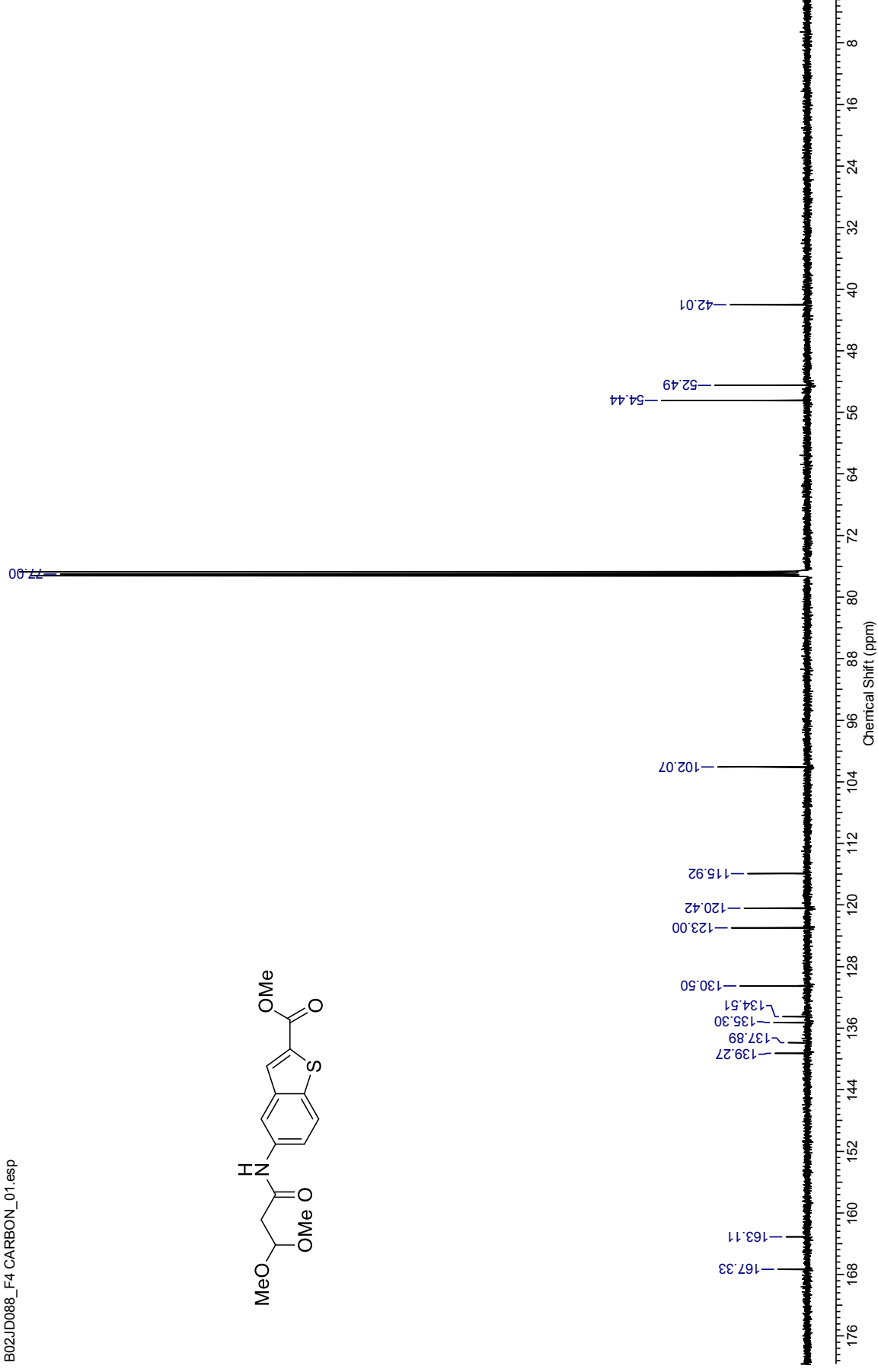
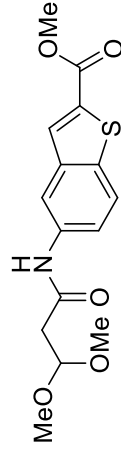
¹H NMR (500 MHz, CDCl₃) for Methyl 5-(3,3-dimethoxypropanamido)benzo[b]thiophene-2-carboxylate

B02JD088_F4 00000131esp

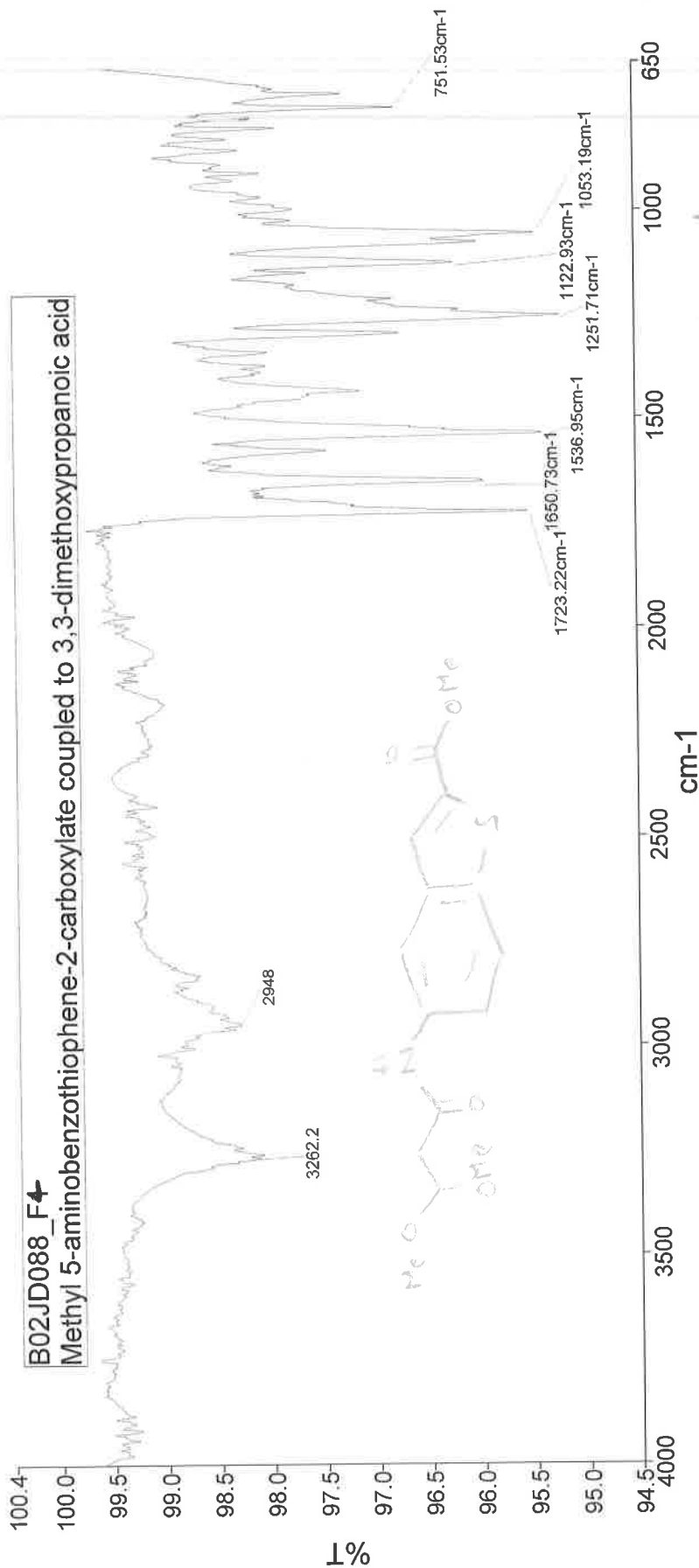


¹³C NMR (126 MHz, CDCl₃) for Methyl 5-(3,3-dimethoxypropanamido)benzo[*b*]thiophene-2-carboxylate

B02JD088_F4 CARBON_01.esp



Analyst
Date
Administrator
16 October 2013 15:30



3262
2948
1723
1651
1537
1252
1053
752

N-H str, amide
C-H str, alkane
C=O str, ester
C=O str, amide
C=C in ring str.
C-N str, amide
C-O str, ester
C-H oop, aromatic

Administrator 208_1 Sample 208 By Administrator Date Wednesday, October 16 2013

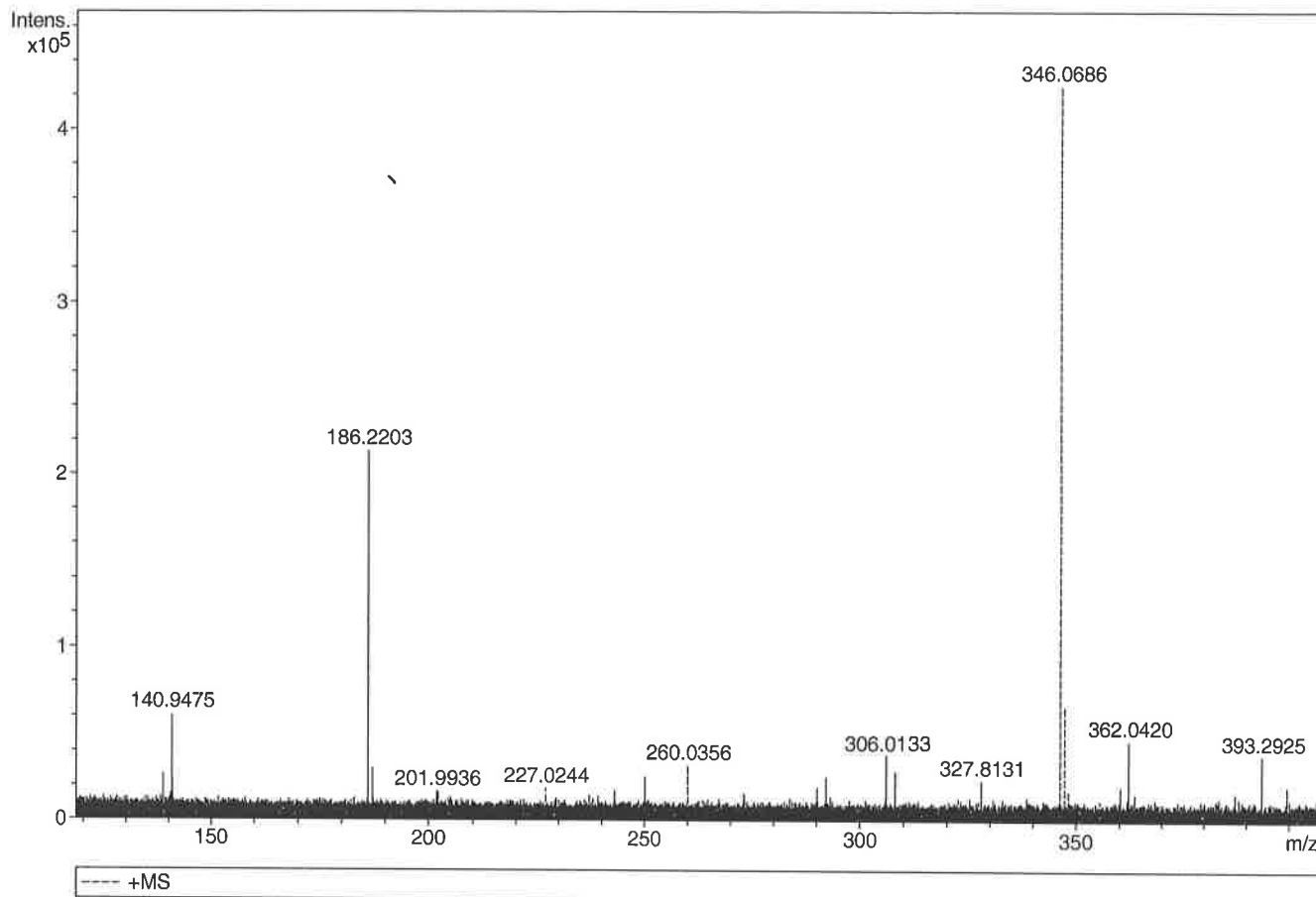
Generic Display Report

Analysis Info

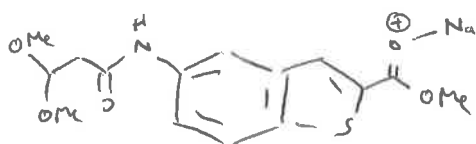
Analysis Name D:\Data\Alinanopos\JESSICA3251_000003.d
 Method pos20090608esi
 Sample Name POS ESI BO2JD088-F4
 Comment

Acquisition Date 03/10/2013 13:41:11

Operator Administrator
 Instrument apex-III

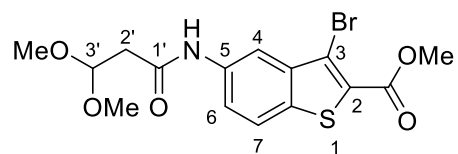


Sum Formula	Sigma	m/z	Err [ppm]	Mean Err [ppm]	Err [mDa]	rdb	N Rule	e ⁻
C 15 H 17 N 1 Na 1 O 5 S 1	0.018	346.0720	9.85	9.82	3.40	7.50	ok	even



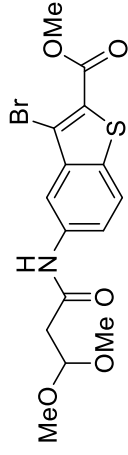
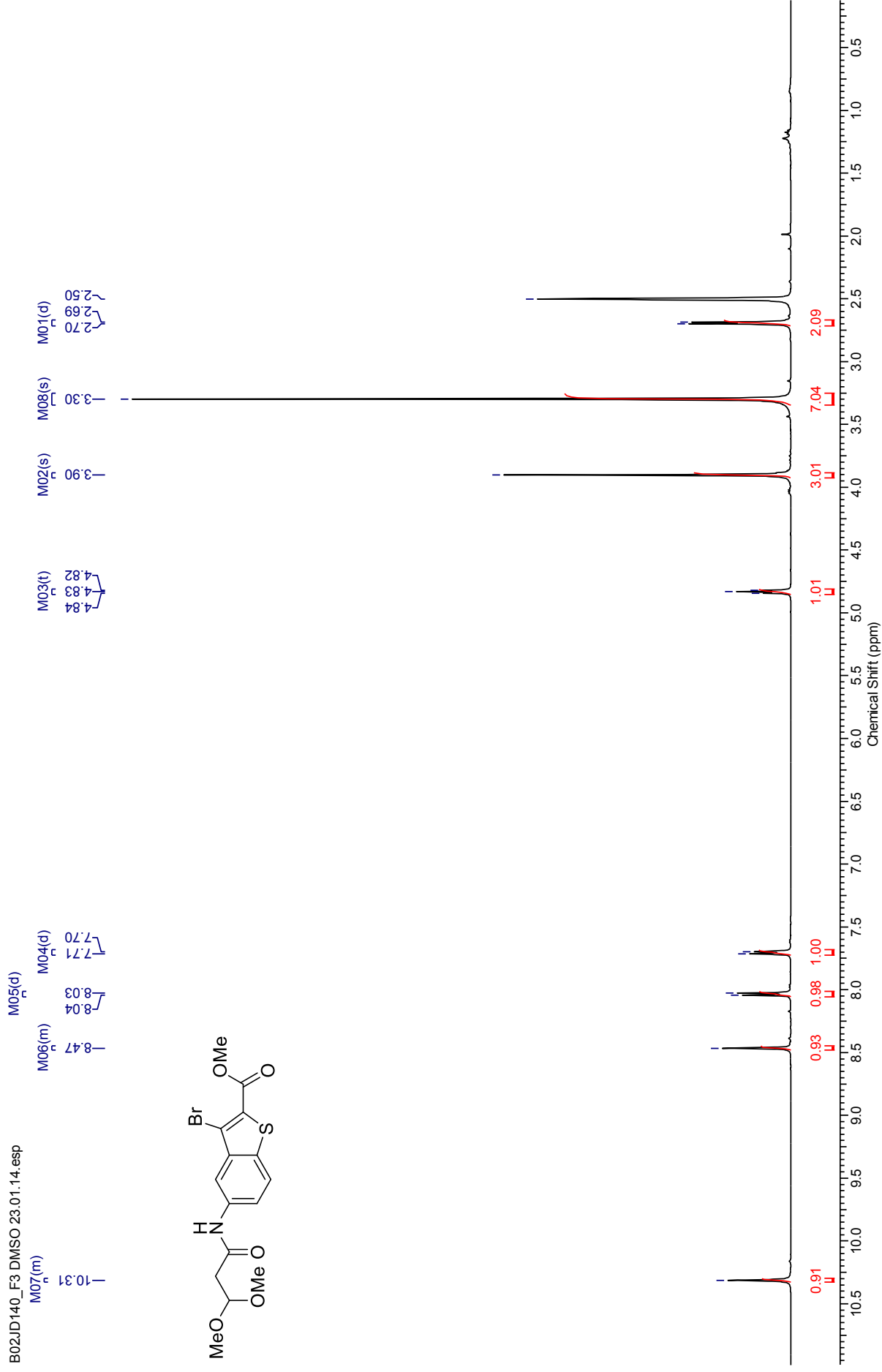
$[MNa]^+ = 346.0714$

**Methyl 3-bromo-5-(3,3-dimethoxypropanamido)benzo[b]
thiophene-2-carboxylate (175)**



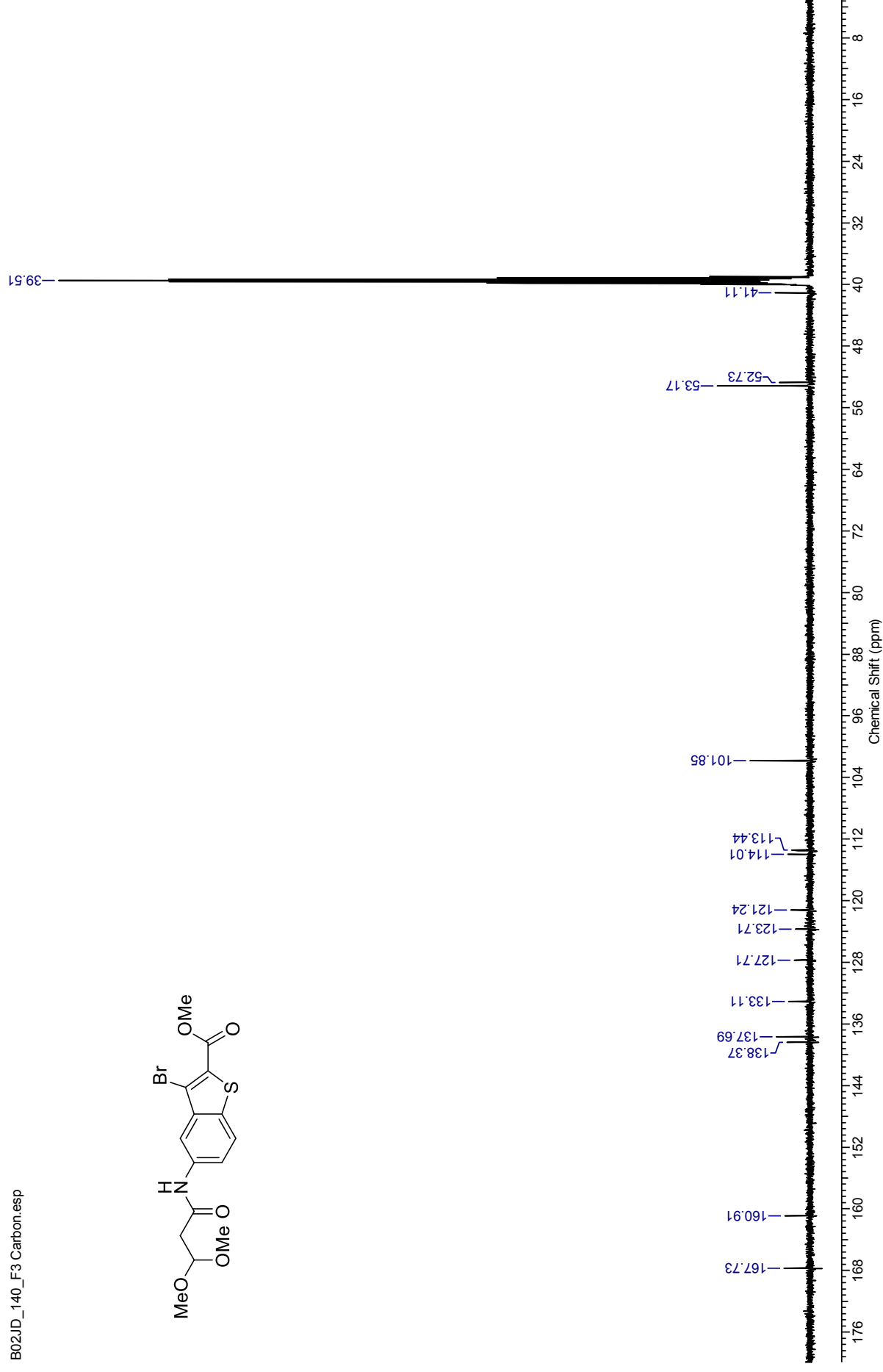
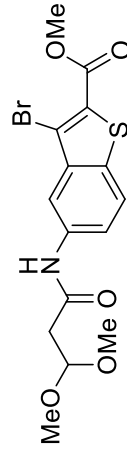
¹H NMR (500 MHz, DMSO-*d*₆) for Methyl 3-bromo-5-(3,3-dimethoxypropanamido)benzo[b]thiophene-2-carboxylate

B02JD140_F3 DMSO 23.01.14.esp



¹³C NMR (126 MHz, DMSO-*d*₆) for Methyl 3-bromo-5-(3,3-dimethoxypropanamido)benzo[*b*]thiophene-2-carboxylate

B02JD_140_F3 Carbon.esp





PerkinElmer Spectrum Version 10.03.06
25 March 2014 15:55

Analyst
Date

Administrator
25 March 2014 15:55

B02JD099_F1



3369 - N-H str, amide
2950 - C-H alkanes
1705 - C=O str, ester
1572 - N-H
1508 - C-C str. (in ring)
1233 - C-O str, ester
1066 - C-O str, ether
981 - C-H bend (aromatic)

Administrator 23 Sample 023 By Administrator Date Tuesday, March 25 2014

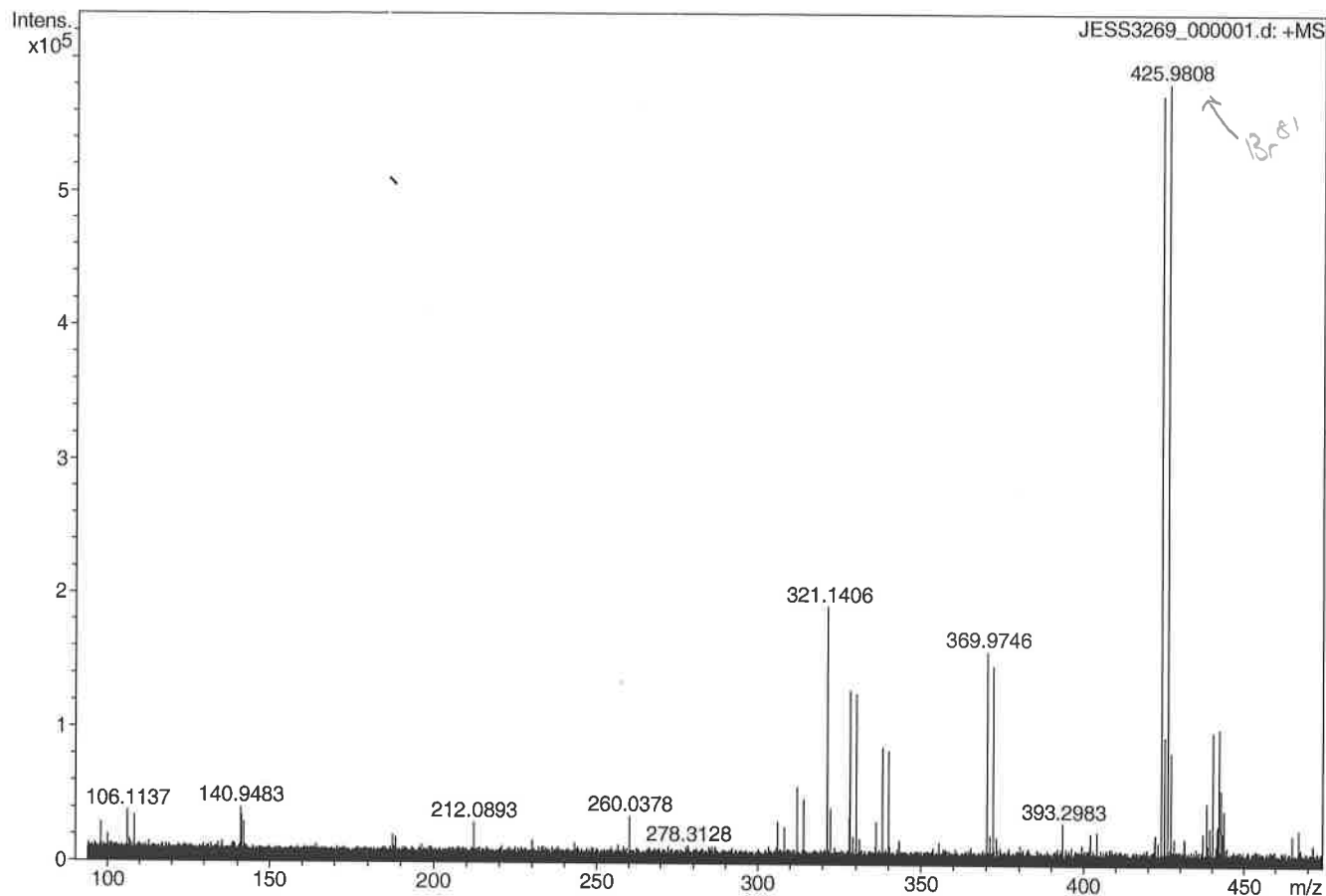
Generic Display Report

Analysis Info

Analysis Name D:\Data\Alinanopos\JESS3269_000001.d
 Method pos20090608esi
 Sample Name POS ESI B02JD092-F2
 Comment

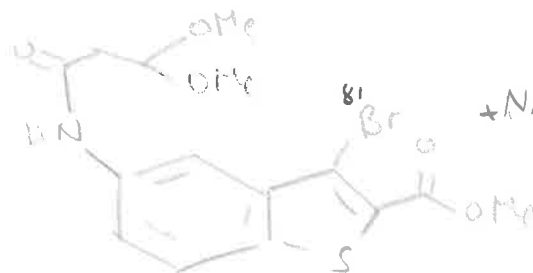
Acquisition Date 11/10/2013 11:16:19

Operator Administrator
 Instrument apex-III

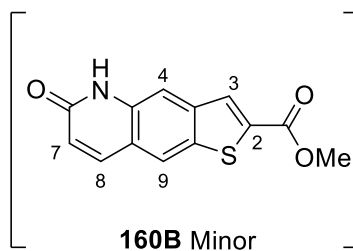
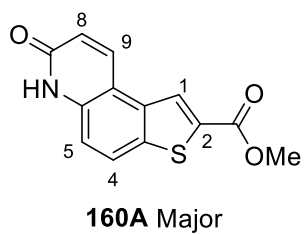


Sum Formula	Sigma	m/z	Err [ppm]	Mean Err [ppm]	Err [mDa]	rdb	N Rule	e ⁻
C 15 H 16 Br 1 N 1 Na 1 O 5 S 1	0.020	423.9825	0.10	-0.46	-0.20	7.50	ok	even

↑
 79
 Br



Methyl 7-oxo-6,7-dihydrothieno[3,2-*f*]quinoline-2-carboxylate
(160A and 160B)



¹H NMR (500 MHz, DMSO-*d*₆) for Mixture of regioisomers Methyl 7-oxo-6,7-dihydrothieno[3,2-*f*]quinoline-2-carboxylate and methyl 6-oxo-5,6-dihydrothieno[2,3-*g*]quinoline-2-carboxylate

B02JD094A DMSO.esp

M03(d)

Model	Model
M02(d)	M06(d)

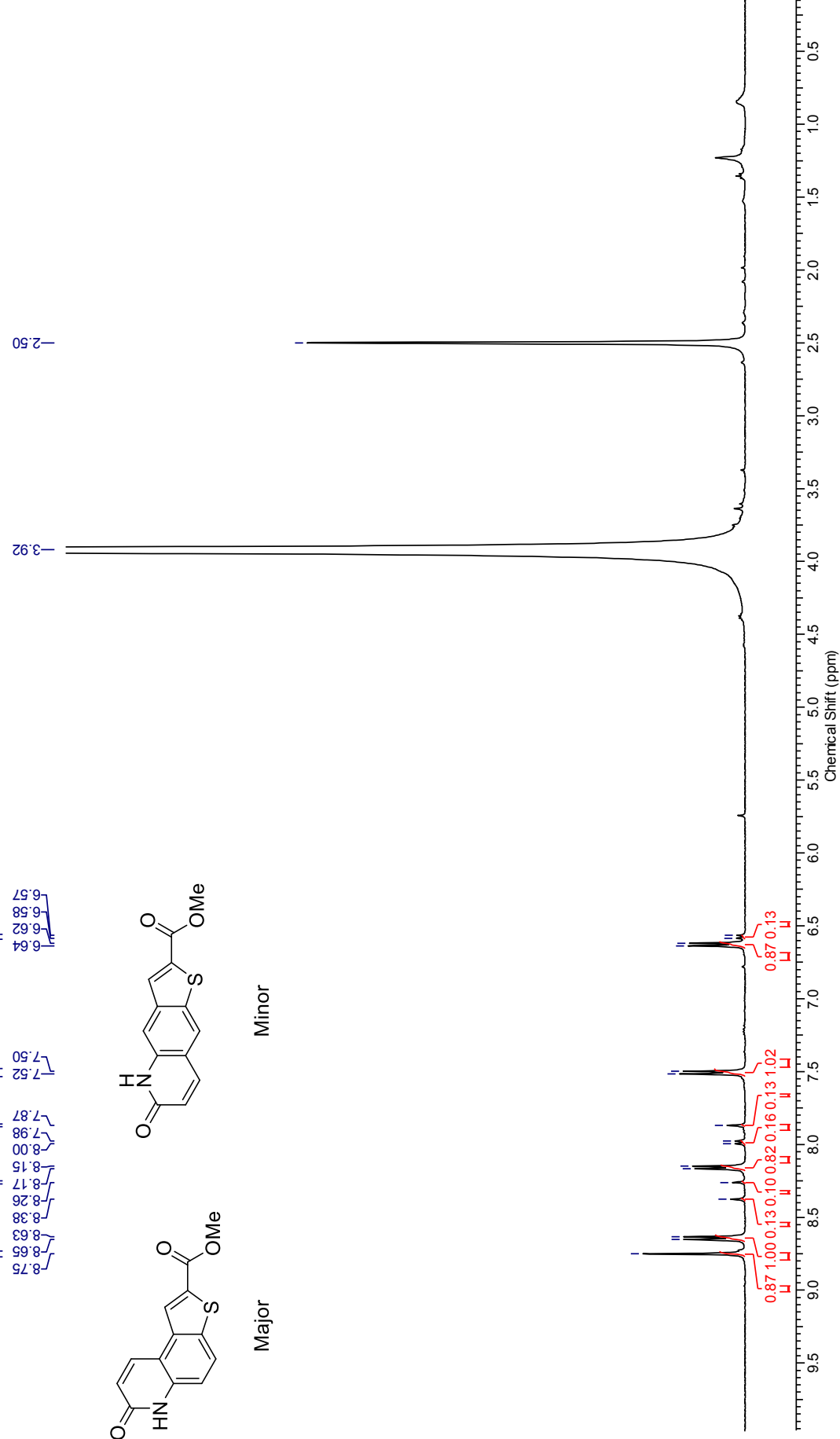
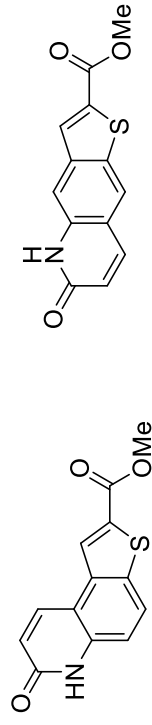
M09(d)

M01(m) M07(s) M05(r)

M10(d)

8.75
8.65
8.63
8.38
8.26
8.17
8.15
8.00
7.98
7.87
7.52
7.50
6.64
6.62
6.58
6.57

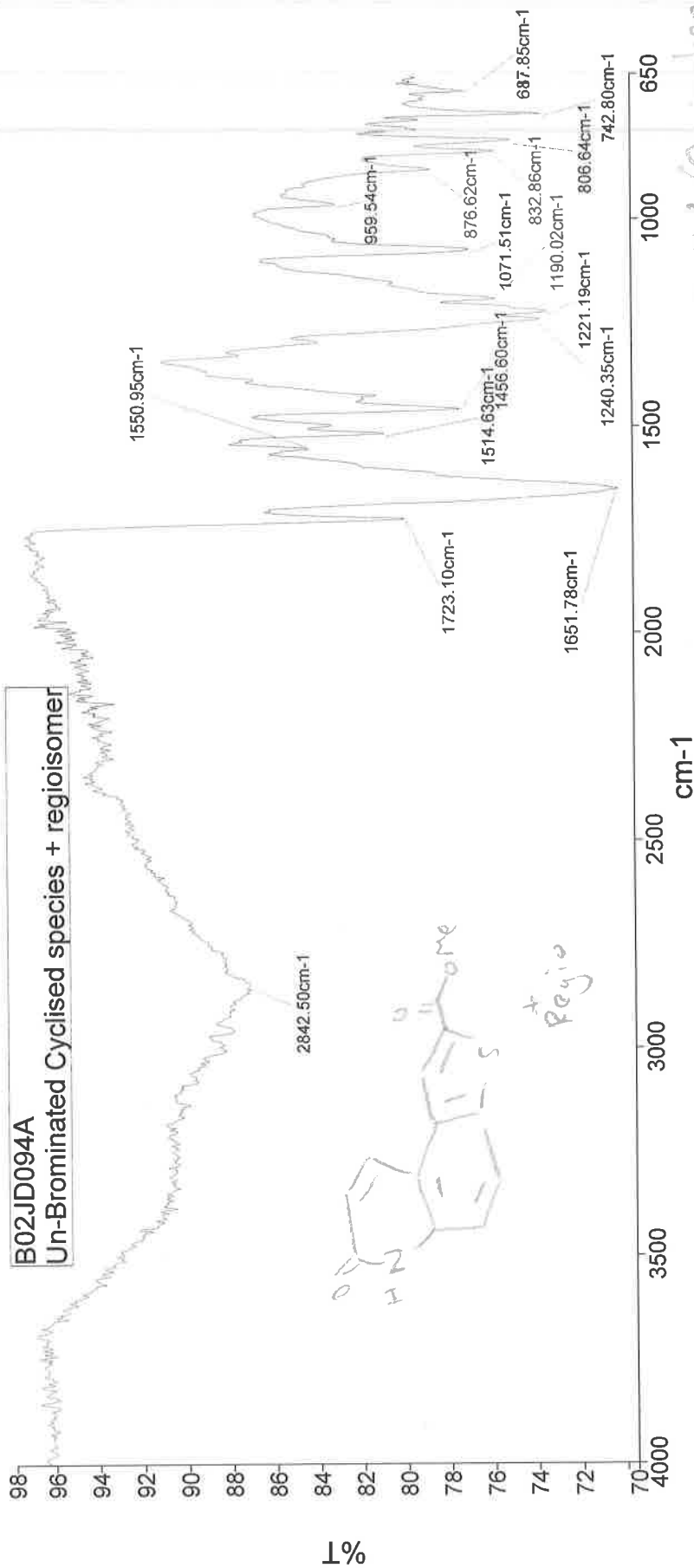
6.64
6.62
6.58
6.57



Analyst
Date

Administrator
16 October 2013 15:45

B02JD094A
Un-Brominated Cyclised species + regioisomer



2842.5

1723.1

1651.8

1514.6

1456.6

1221.2

1071.5

806.6

O-H? (Quinoline?)
+ amine?

C=O str.

C=O str.

C-C str, in ring

C-C str, in ring

C-O str, ester

C-N str, amine

C-H 'oop', aromatic

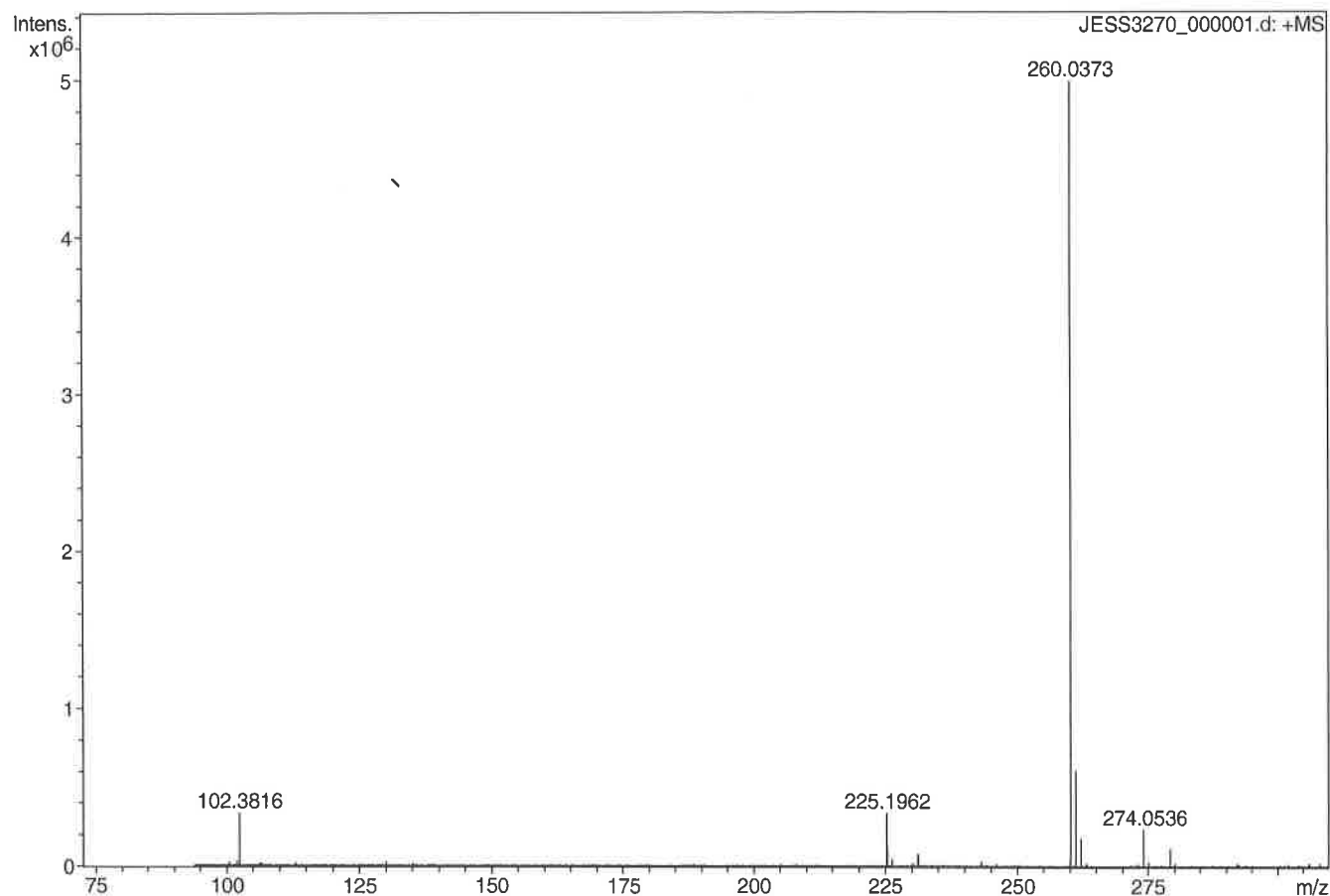
Generic Display Report

Analysis Info

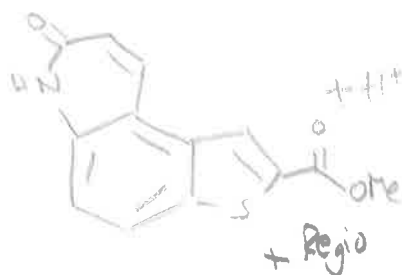
Analysis Name D:\Data\Alinanopos\JESS3270_000001.d
Method pos20090608esi
Sample Name POS ESI B02JD094A
Comment

Acquisition Date 11/10/2013 11:13:15

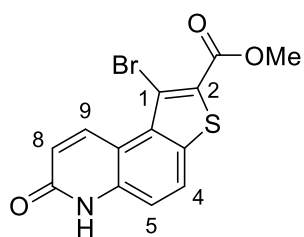
Operator Administrator
Instrument apex-III



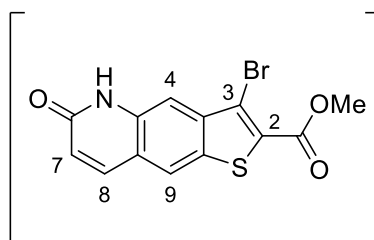
Sum Formula	Sigma	m/z	Err [ppm]	Mean Err [ppm]	Err [mDa]	rdB	N Rule	e ⁻
C 13 H 10 N 1 O 3 S 1	0.033	260.0376	1.10	-0.20	-0.05	9.50	ok	even



Methyl 1-bromo-7-oxo-6,7-dihydrothieno[3,2-*f*]quinoline-2-carboxylate (176A and 176B)

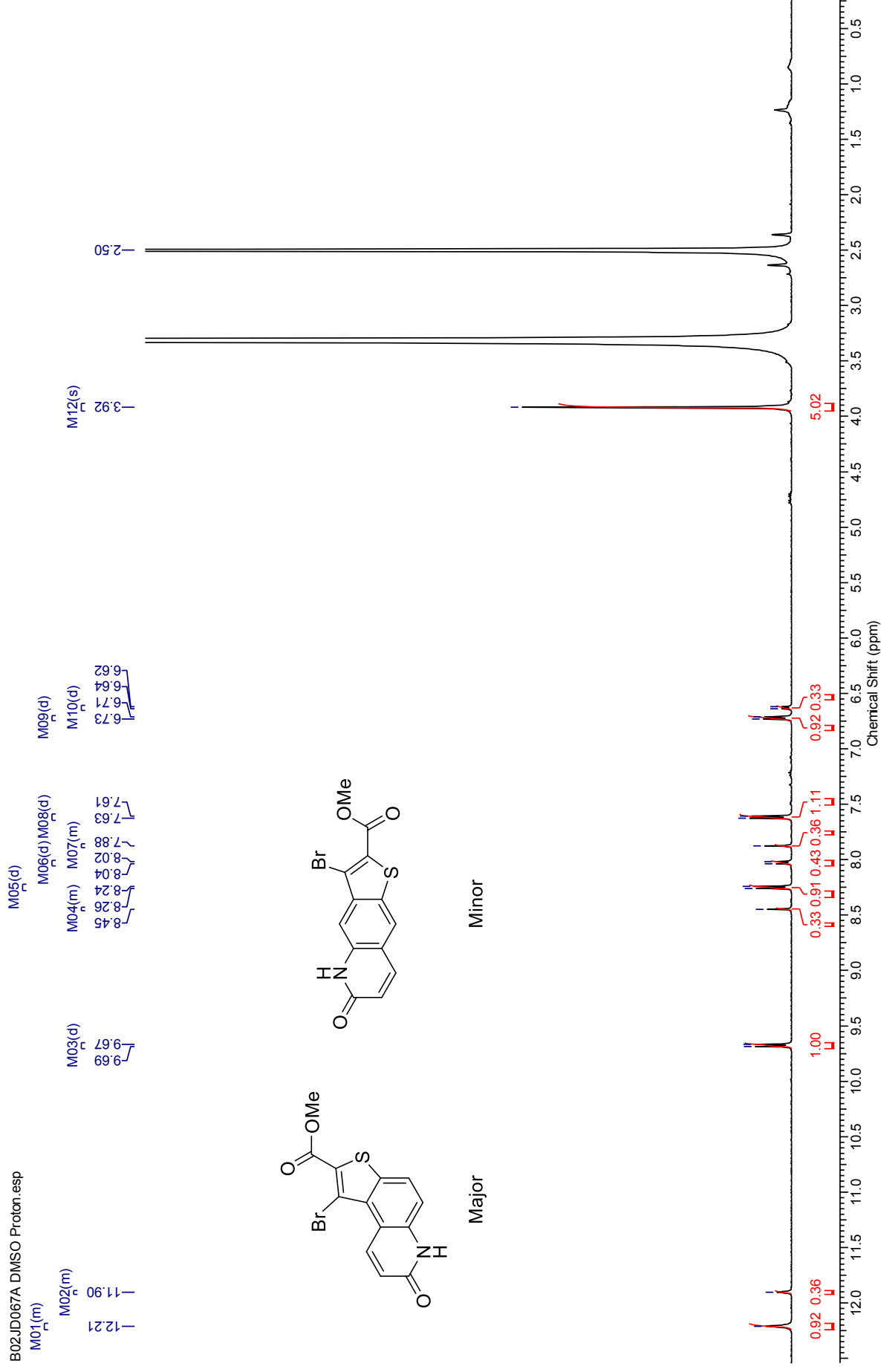


176A: Major



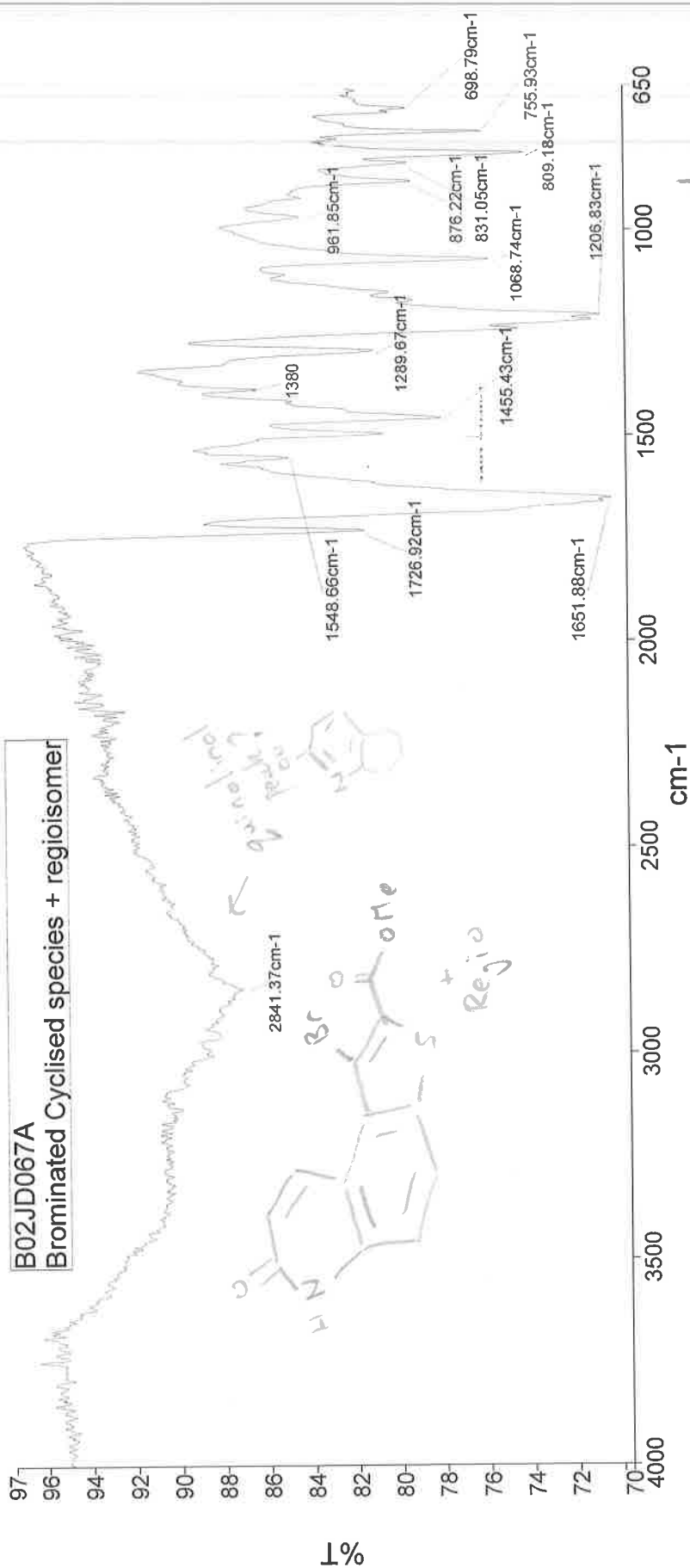
176B: Minor

^1H NMR (500 MHz, DMSO- d_6) for mixture of regioisomers Methyl 1-bromo-7-oxo-6,7-dihydrothieno[3,2-*f*]quinoline-2-carboxylate and methyl 3-bromo-6-oxo-5,6-dihydrothieno[2,3-*g*]quinoline-2-carboxylate



Analyst
Date

Administrator
16 October 2013 15:40



2841.4 N-H str, amide

1726.9 C=O str

1651.9 C=O str

1548.7 C-C in ring str.

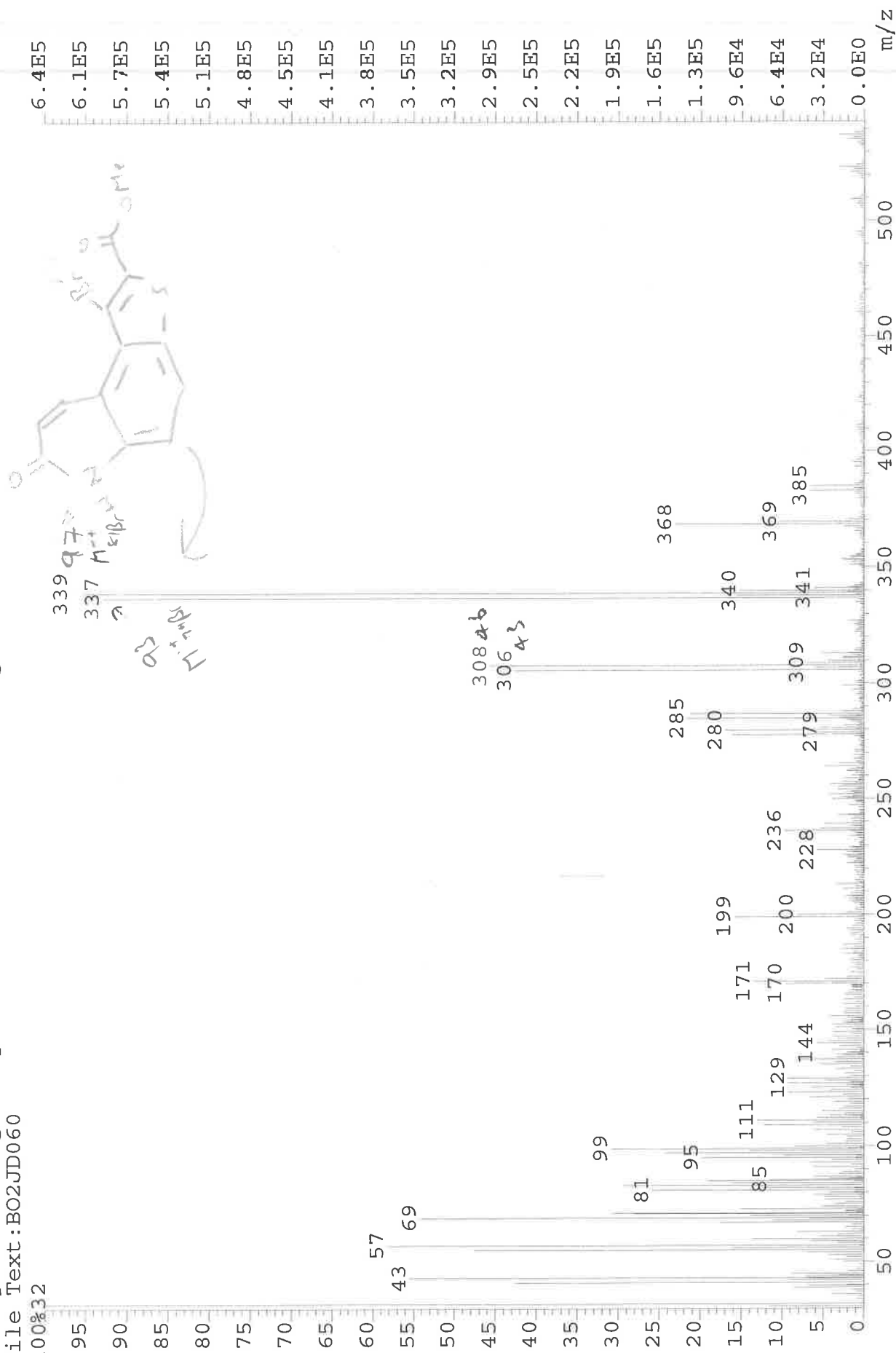
1455.4 C-H bend alkane

1289.7 C-N str, amide

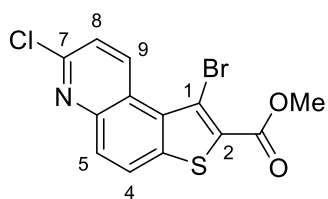
1068.7 C-O str, ester

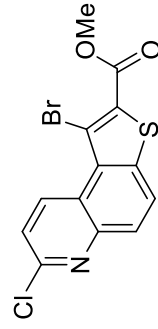
809.2 N-H wag

File: JESS3218 Ident: 16 Acq: 29-AUG-2013 16:47:49 +1:02 Cal: CAL1
 AutoSpecE EI+ Magnet BpI: 2811783 TIC: 17849976 Flags: HALL
 File Text: BO2JD060
 100%32



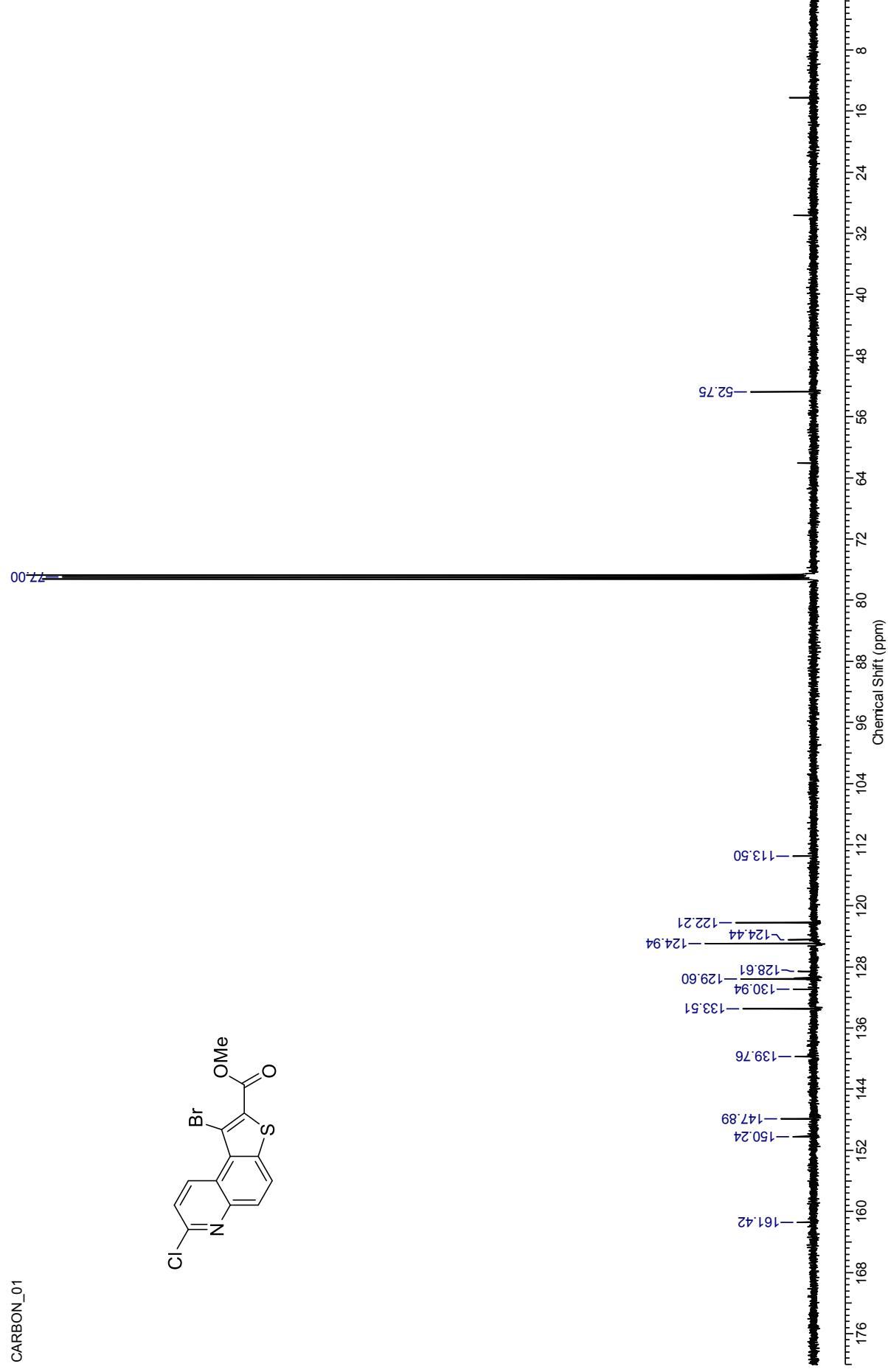
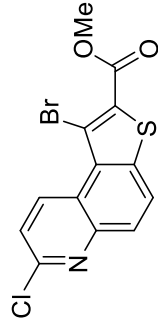
Methyl 1-bromo-7-chlorothieno[3,2-*f*]quinoline-2-carboxylate (166)



¹H NMR (500 MHz, CDCl₃) for Methyl 1-bromo-7-chlorothieno[3,2-*f*]quinoline-2-carboxylate

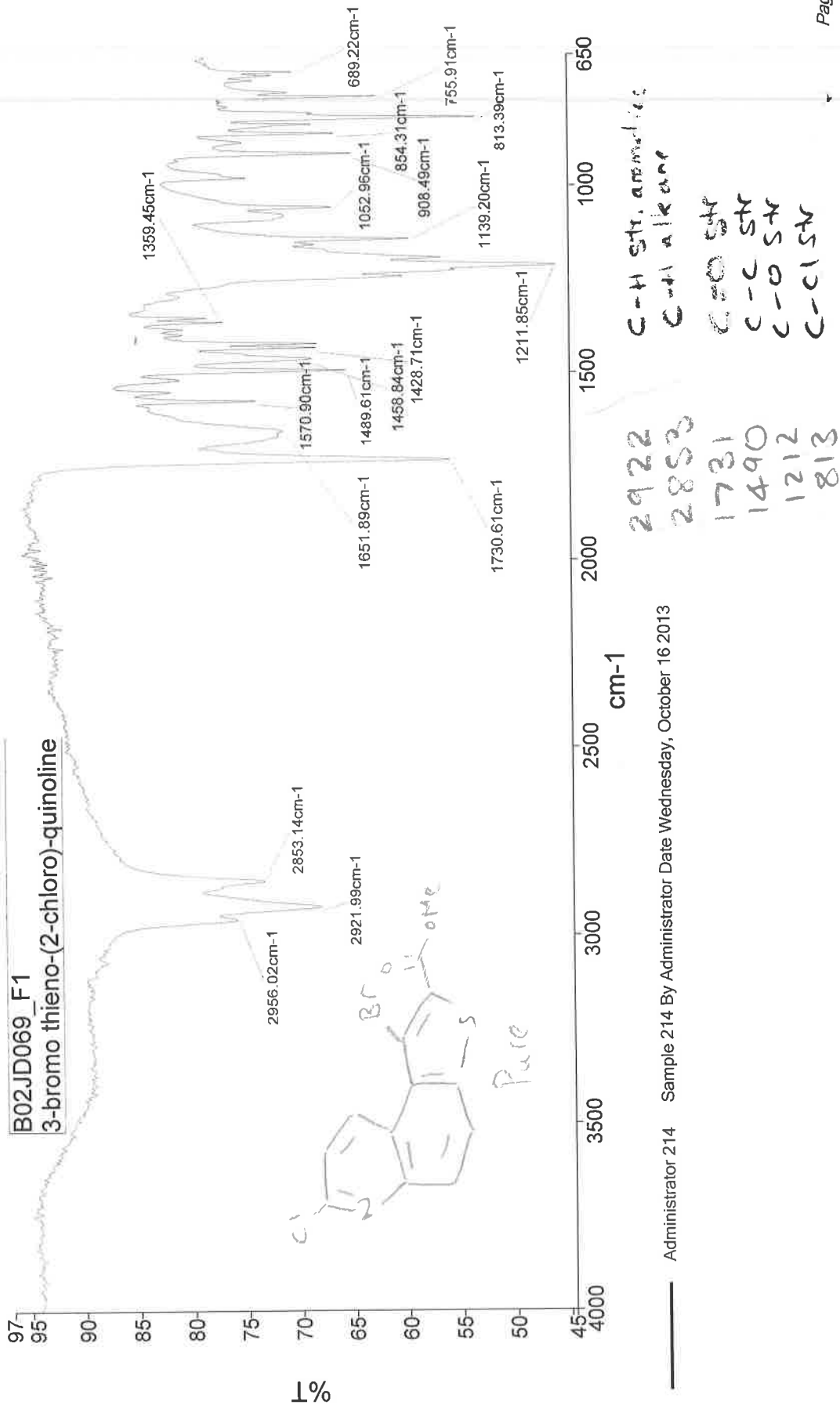
¹³C NMR (126 MHz, CDCl₃) for Methyl 1-bromo-7-chloro-2-thienopyrido[3,2-f]quinoline-2-carboxylate

CARBON_01



Analyst
Date

Administrator
16 October 2013 15:51



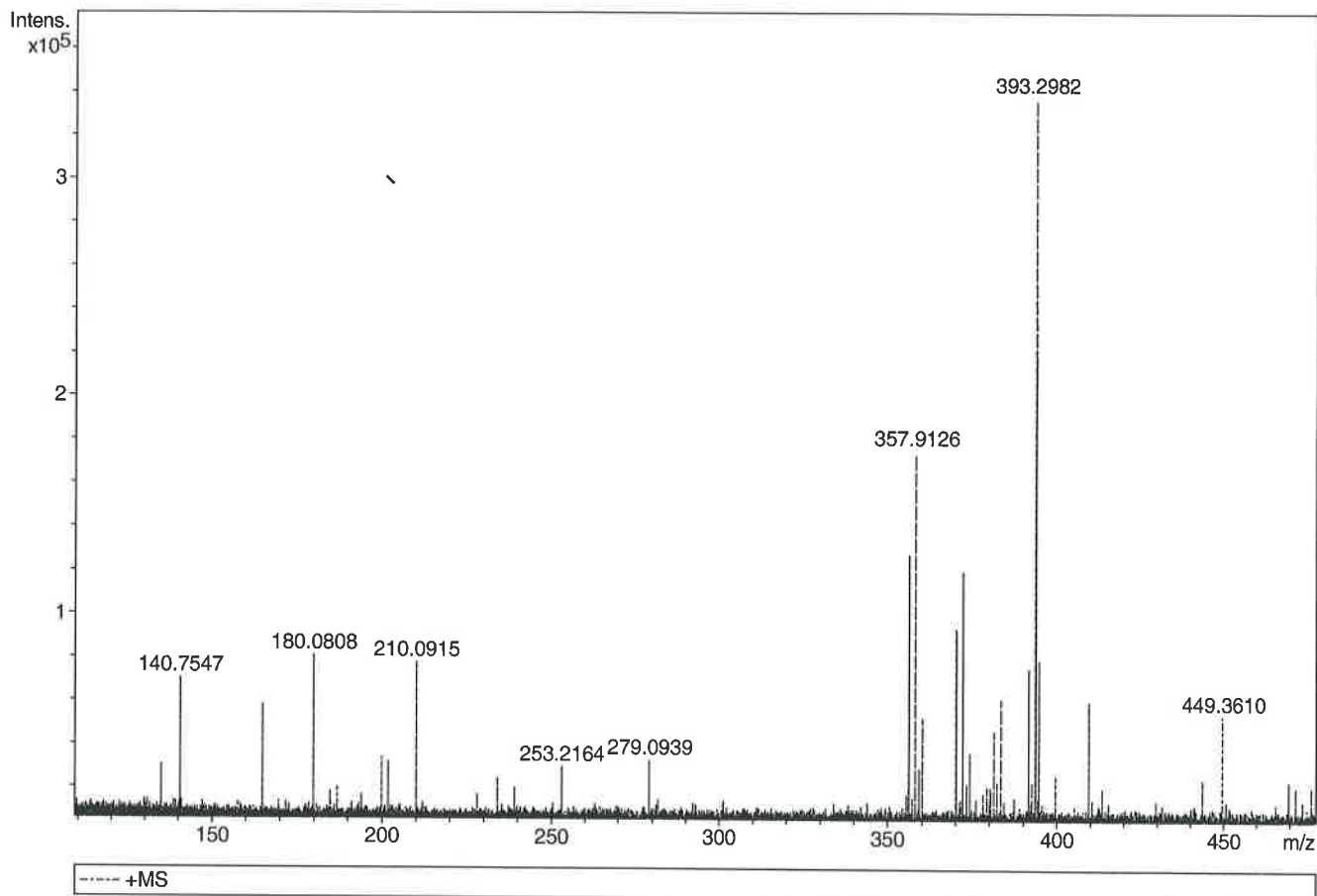
Generic Display Report

Analysis Info

Analysis Name D:\Data\Alinanopos\JESS4353_000001.d
 Method pos20090608esi
 Sample Name POS ESI BO2JD126-F3
 Comment

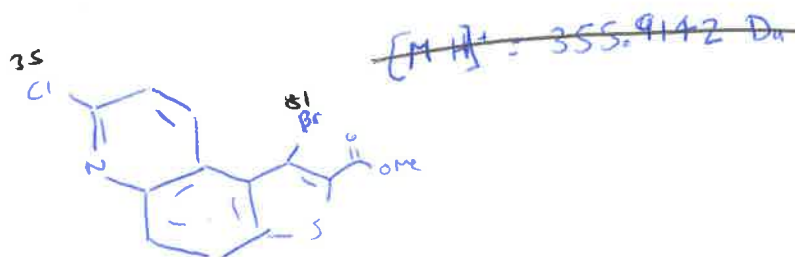
Acquisition Date 07/05/2014 11:44:32

Operator Administrator
 Instrument apex-III

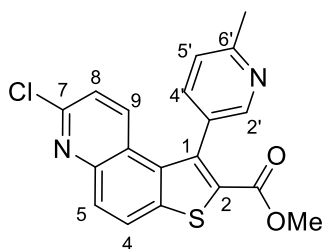


Sum Formula	Sigma	m/z	Err [ppm]	Mean Err [ppm]	Err [mDa]	rdb	N Rule	e ⁻
C ₁₃ H ₈ BrClN ₁ O ₂ S ₁	0.027	355.9142	-1.68	-0.49	-0.18	9.50	ok	even

$C_{13}H_8Br^{81}Cl^{35}NO_2S$ 357.9127



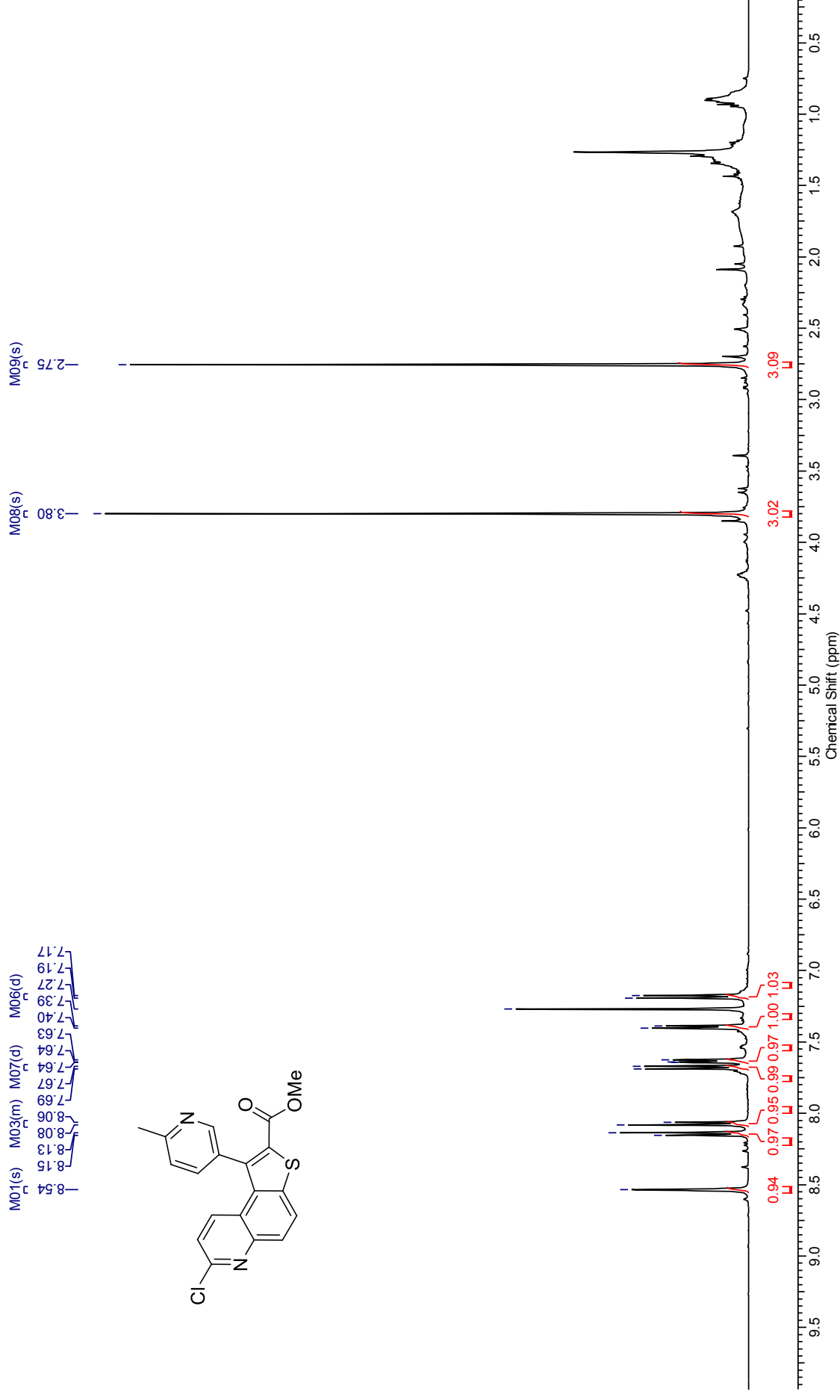
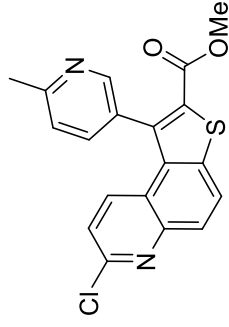
Methyl 7-chloro-1-(6-methylpyridin-3-yl)thieno[3,2-*f*]quinoline-2-carboxylate (177)



¹H NMR (500 MHz, CDCl₃) for Methyl 7-chloro-1-(6-methylpyridin-3-yl)thieno[3,2-*f*]quinoline-2-carboxylate

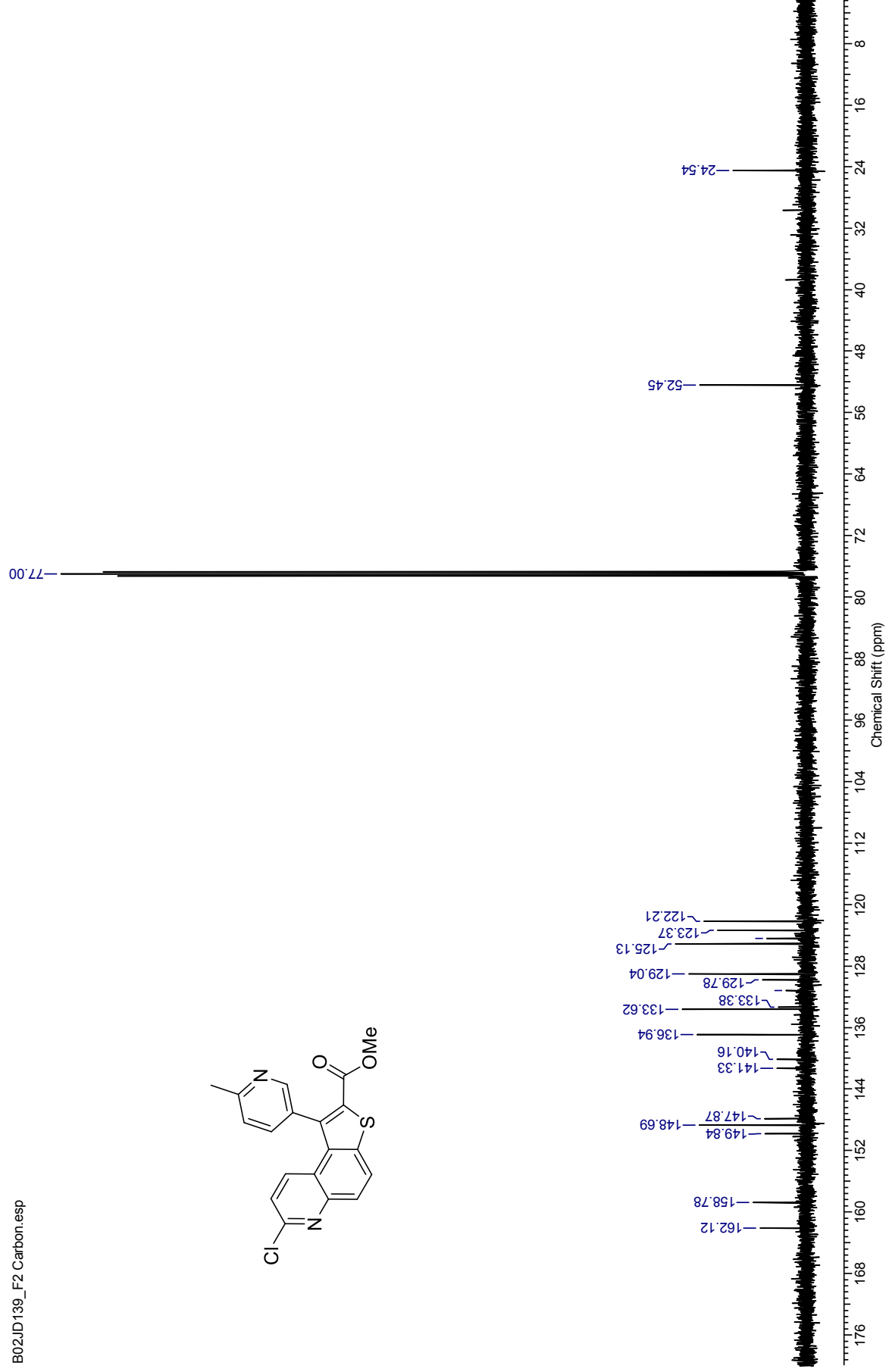
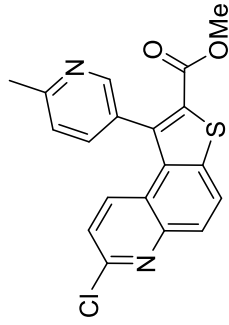
B02JD139_F2.esp

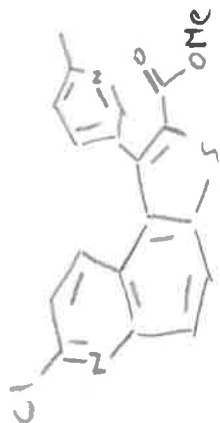
M04(dd)			M05(d)		
M01(s)	M02(m)	M03(m)	M07(d)	M06(d)	M05(d)
8.54	8.15	8.13	7.69	7.67	7.64
8.06	8.08	8.06	7.64	7.63	7.40
7.89	7.67	7.64	7.39	7.27	7.19
7.17					



¹³C NMR (126 MHz, CDCl₃) for Methyl 7-chloro-1-(6-methylpyridin-3-yl)thieno[3,2-*f*]quinoline-2-carboxylate

B02JD139_F2 Carbon.esp

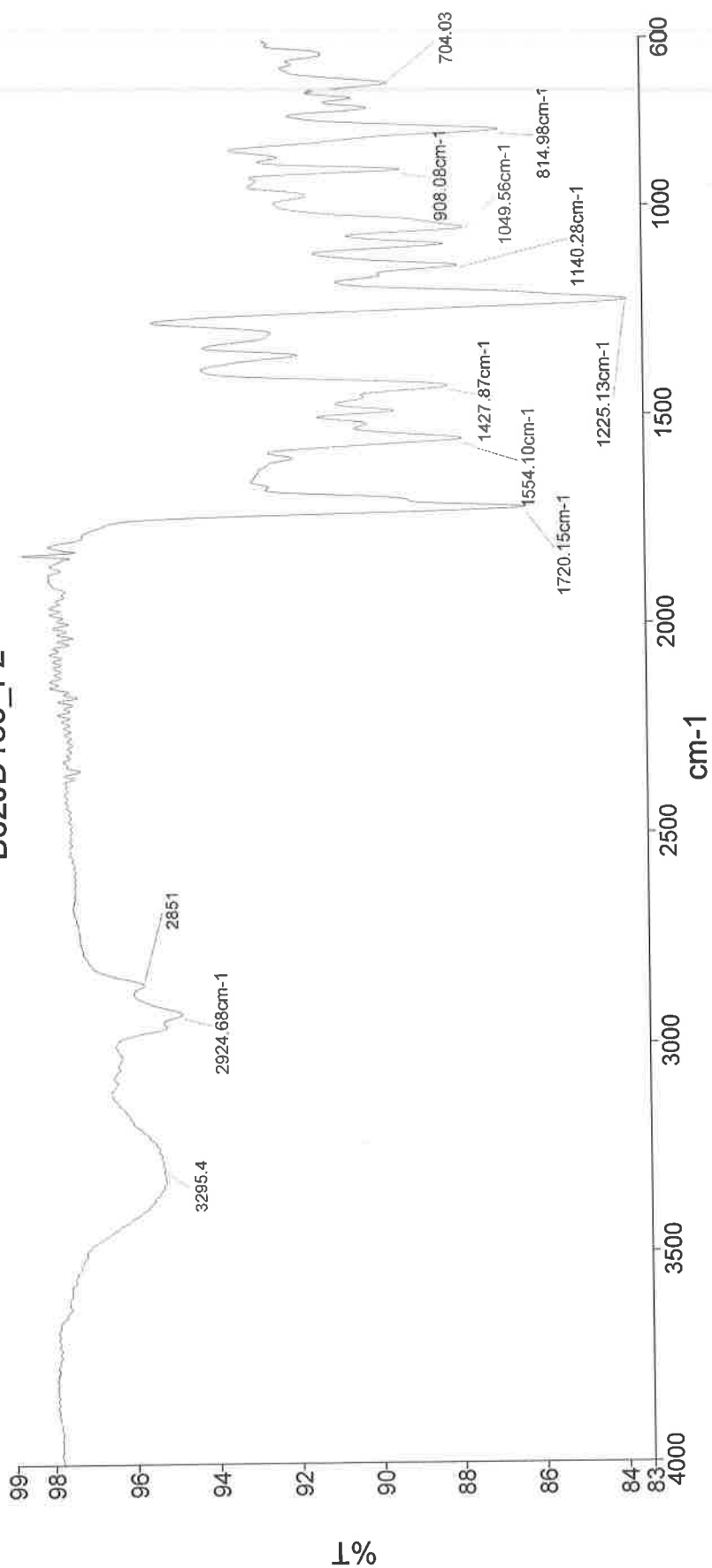




Administrator
25 March 2014 16:19

Analyst
Date

B02JD139_F2



3295 - C-H arene str.
2925 - C-H alkanes str.
1720 - C=O estr str.
1554 - C=C str. (in ring)
1225 - C-O estr str.
1049 - C-O str.
815 - C-Cl str.

Administrator 31 Sample 031 By Administrator Date Tuesday, March 25 2014

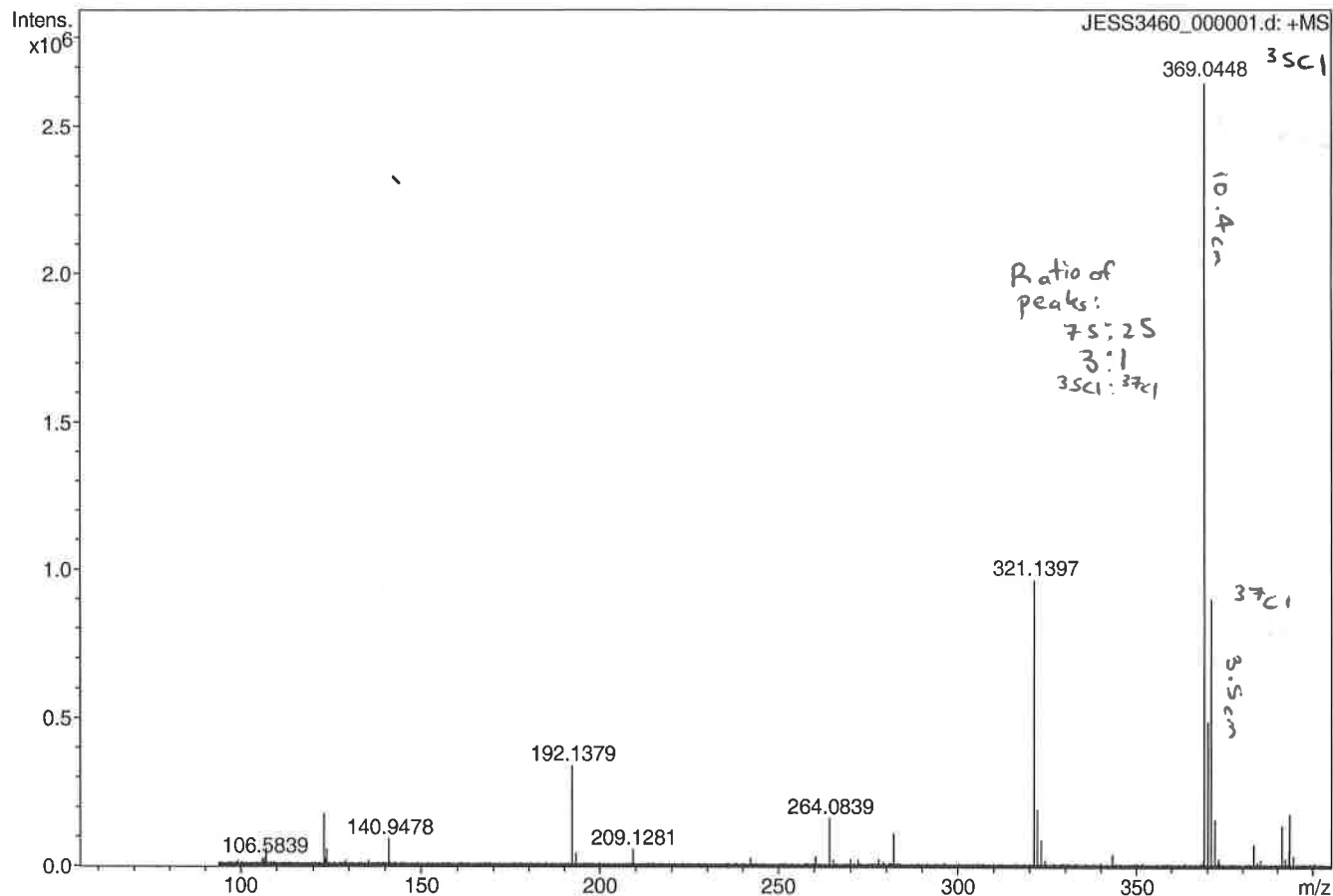
Generic Display Report

Analysis Info

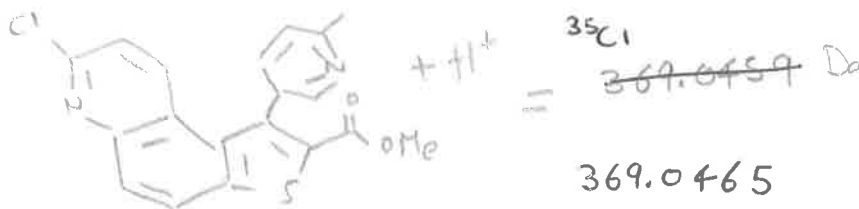
Analysis Name D:\Data\Alinanopos\JESS3460_000001.d
 Method pos20090608esi
 Sample Name POS ESI BO2JD139-F2
 Comment

Acquisition Date 16/12/2013 12:24:12

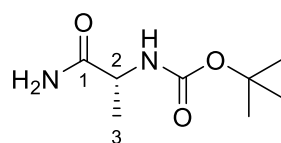
Operator Administrator
 Instrument apex-III



Sum Formula	Sigma	m/z	Err [ppm]	Mean Err [ppm]	Err [mDa]	rdB	N Rule	e ⁻
C 19 H 14 Cl 1 N 2 O 2 S 1	0.043	369.0459	3.10	3.93	1.46	13.50	ok	even

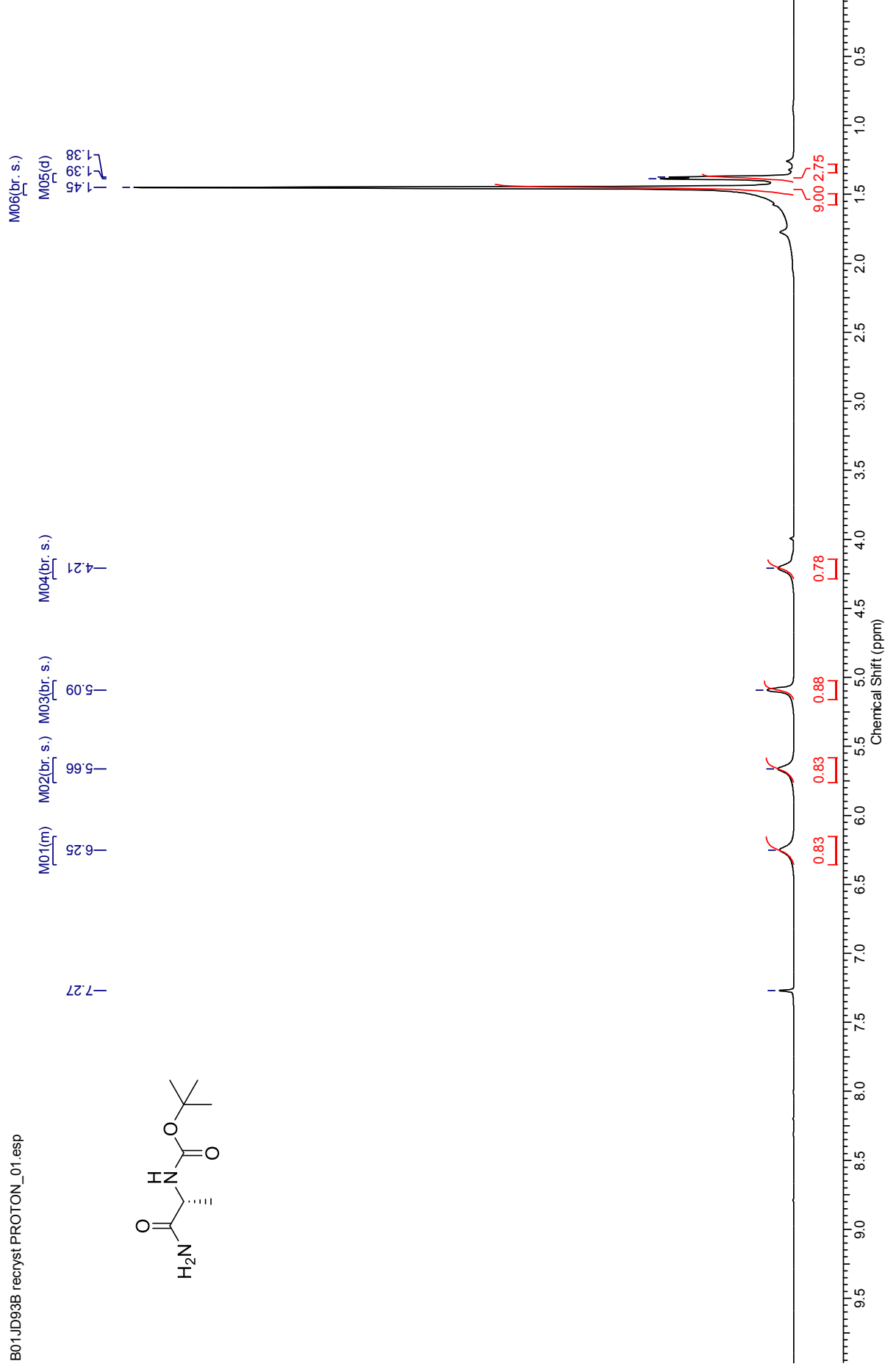
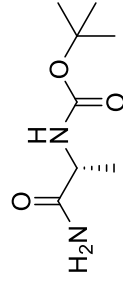


(*R*)-*tert*-Butyl-(1-amino-1-oxopropan-2-yl)carbamate (182)



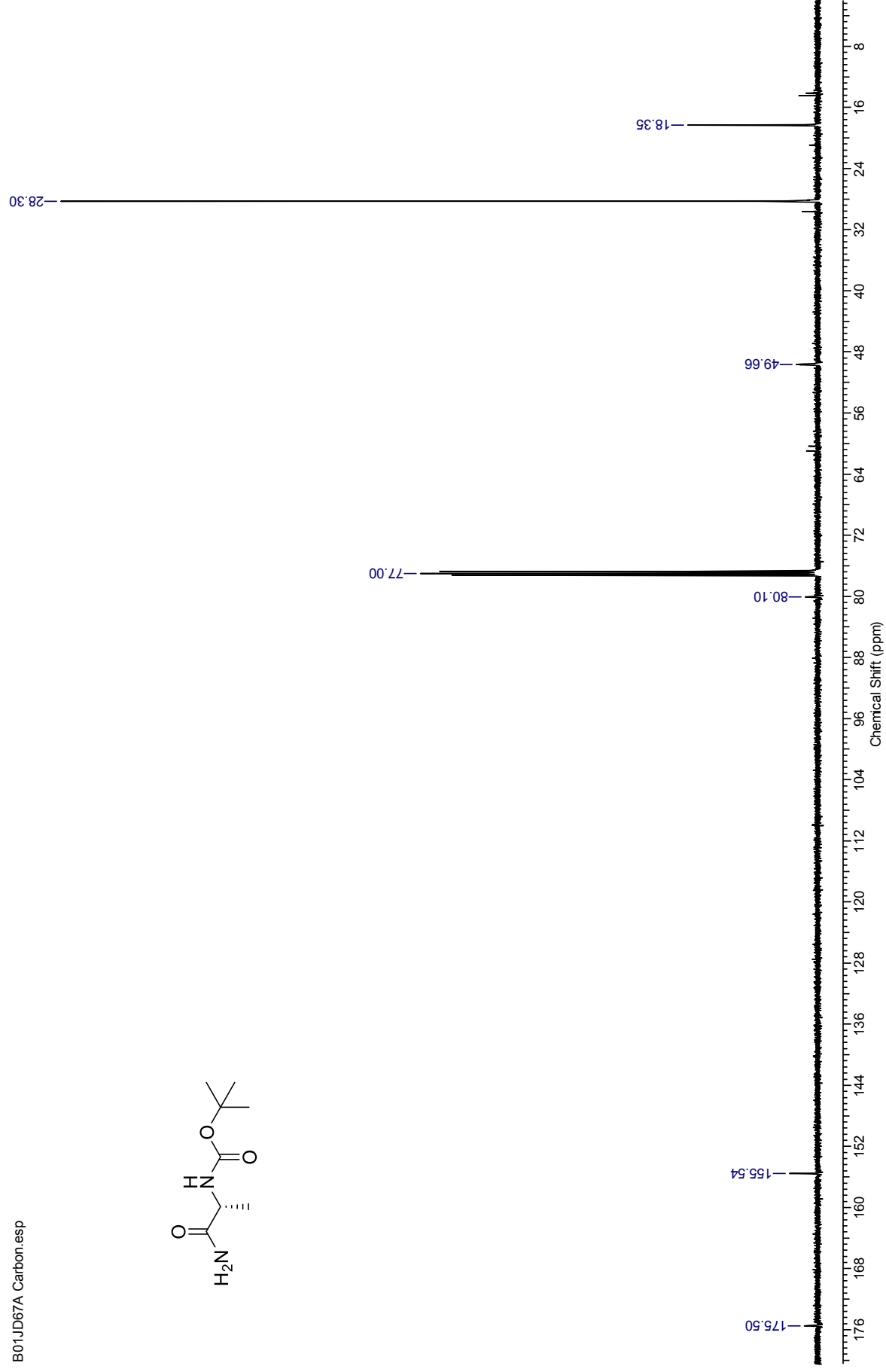
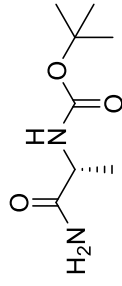
¹H NMR (500 MHz, CDCl₃) for (R)-tert-Butyl-(1-amino-1-oxopropan-2-yl)carbamate

B01JD93B recryst PROTON_01.esp



¹³C NMR (126 MHz, CDCl₃) for for (R)-*tert*-Butyl-(1-amino-1-oxopropan-2-yl)carbamate

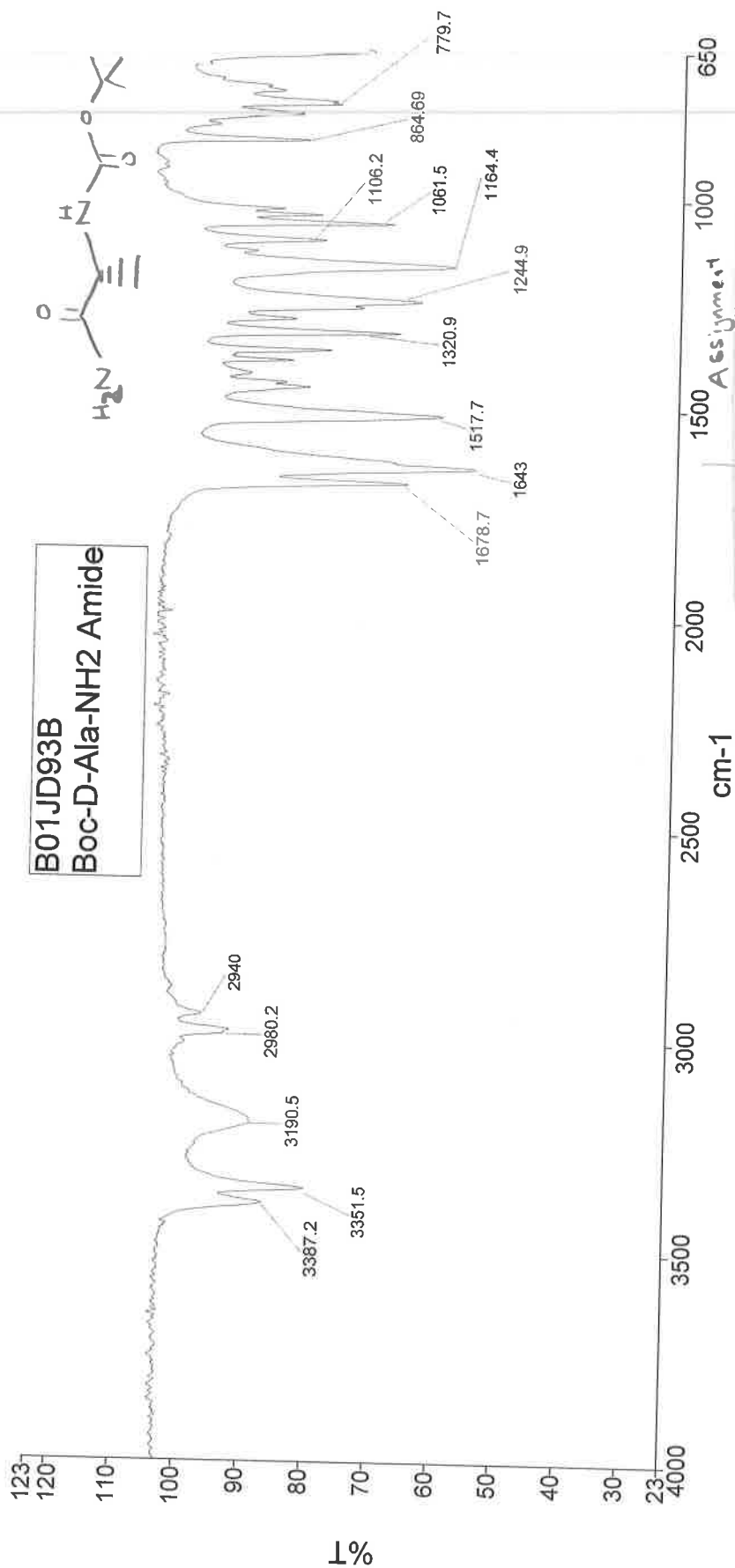
B01JD67A Carbon.esp



Analyst
Date

Administrator
28 February 2013 13:24

PerkinElmer Spectrum Version 10.03.06
28 February 2013 13:24



3387
3351
2980
2940
1678
1643
1517
1320
1244
1164
864

Administrator 1024 Sample 1024 By Administrator Date Thursday, February 28 2013

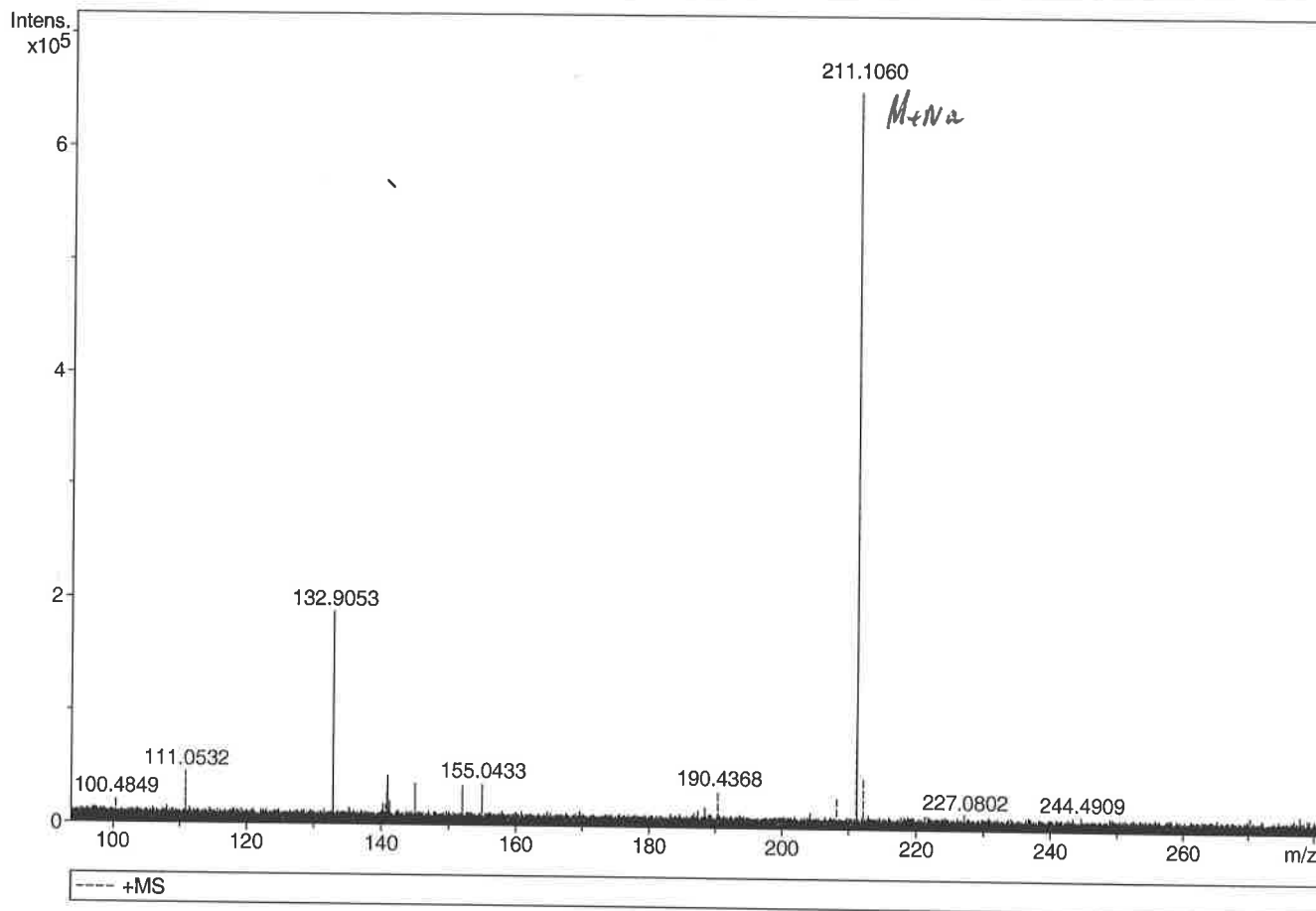
Generic Display Report

Analysis Info

Analysis Name D:\Data\Alinanopos\JESSICA8996_000001.d
Method pos20090608esi
Sample Name POS ESI B01JD77B
Comment

Acquisition Date 08/02/2013 09:53:45

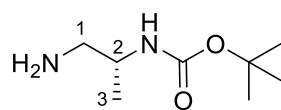
Operator Administrator
Instrument apex-III



Sum Formula	Sigma	m/z	Err [ppm]	Mean Err [ppm]	Err [mDa]	rdb	N Rule	e ⁻
C ₈ H ₁₆ N ₂ NaO ₃	0.024	211.1053	-3.11	-11.93	-2.52	1.50	ok	even

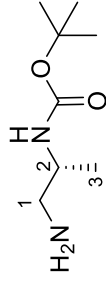
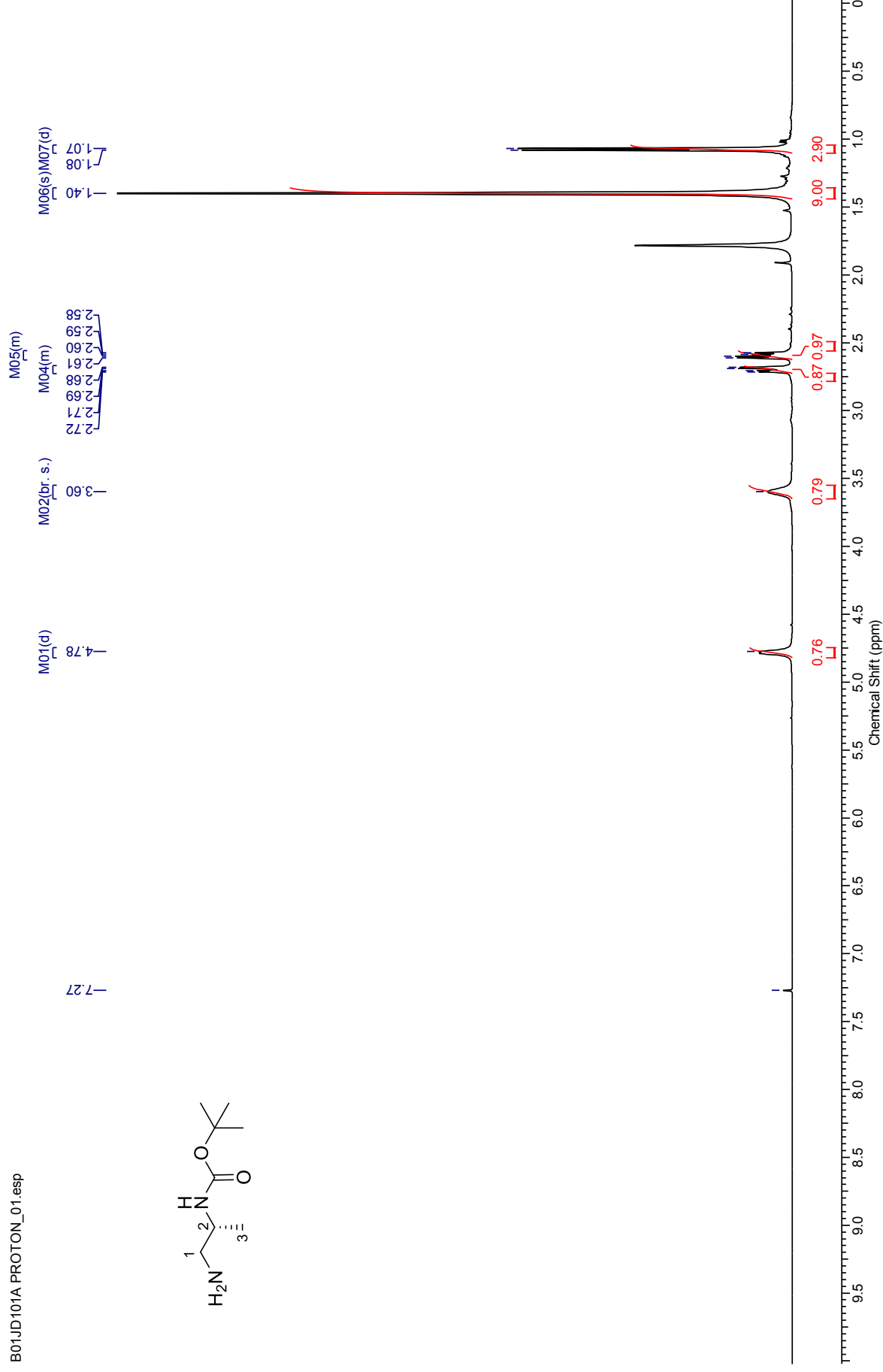


***tert*-Butyl ([2*R*]-1-aminopropan-2-yl)carbamate (137)**



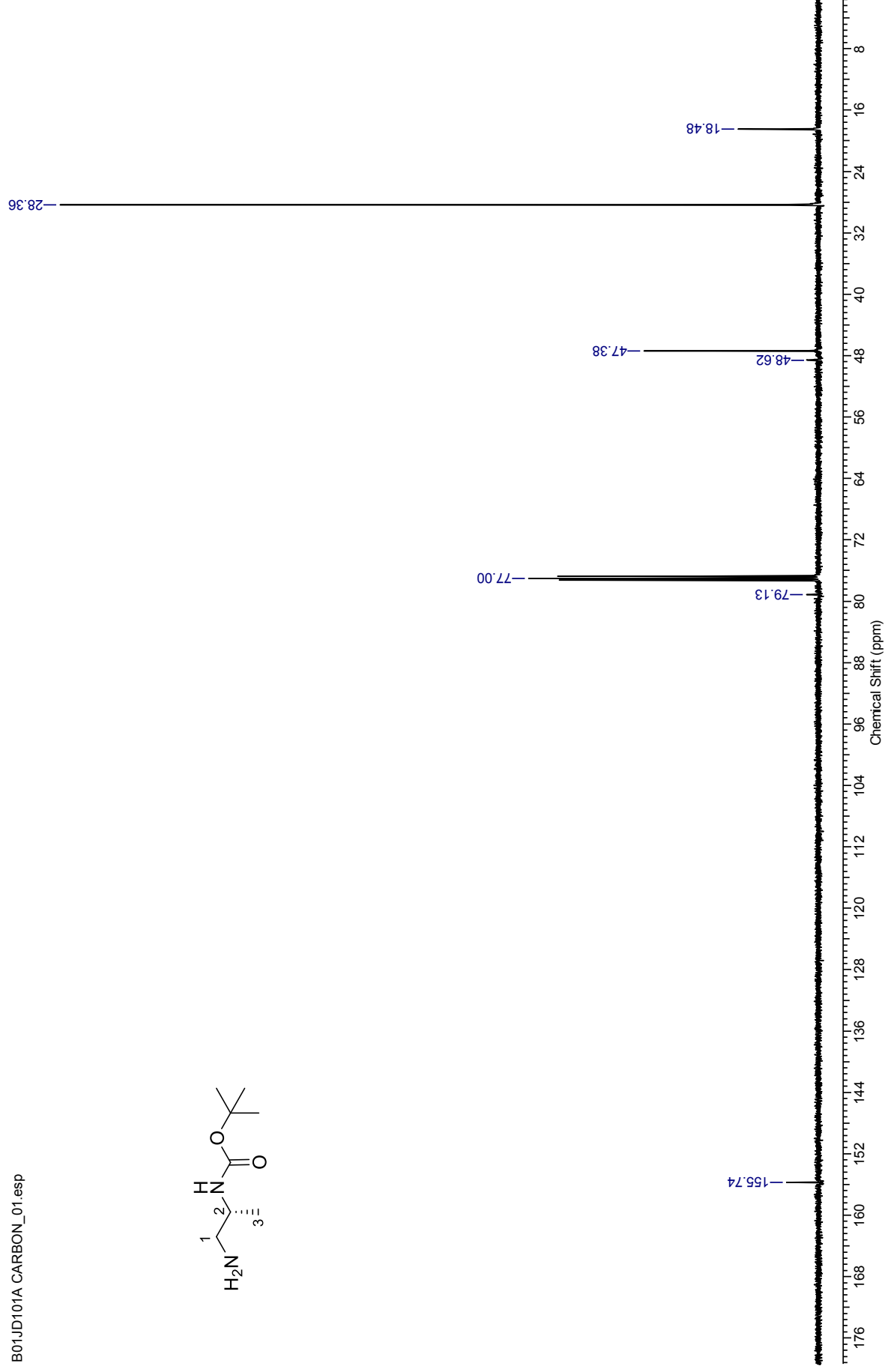
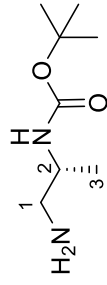
¹H NMR (500 MHz, CDCl₃) for *tert*-Butyl [(2*R*)-1-aminopropan-2-yl]carbamate

B01JD101A PROTON_01.esp



¹³C NMR (126 MHz, CDCl₃) for *tert*-Butyl [(2*R*)-1-aminopropan-2-yl]carbamate

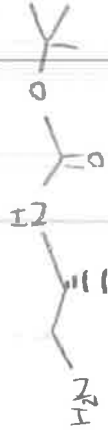
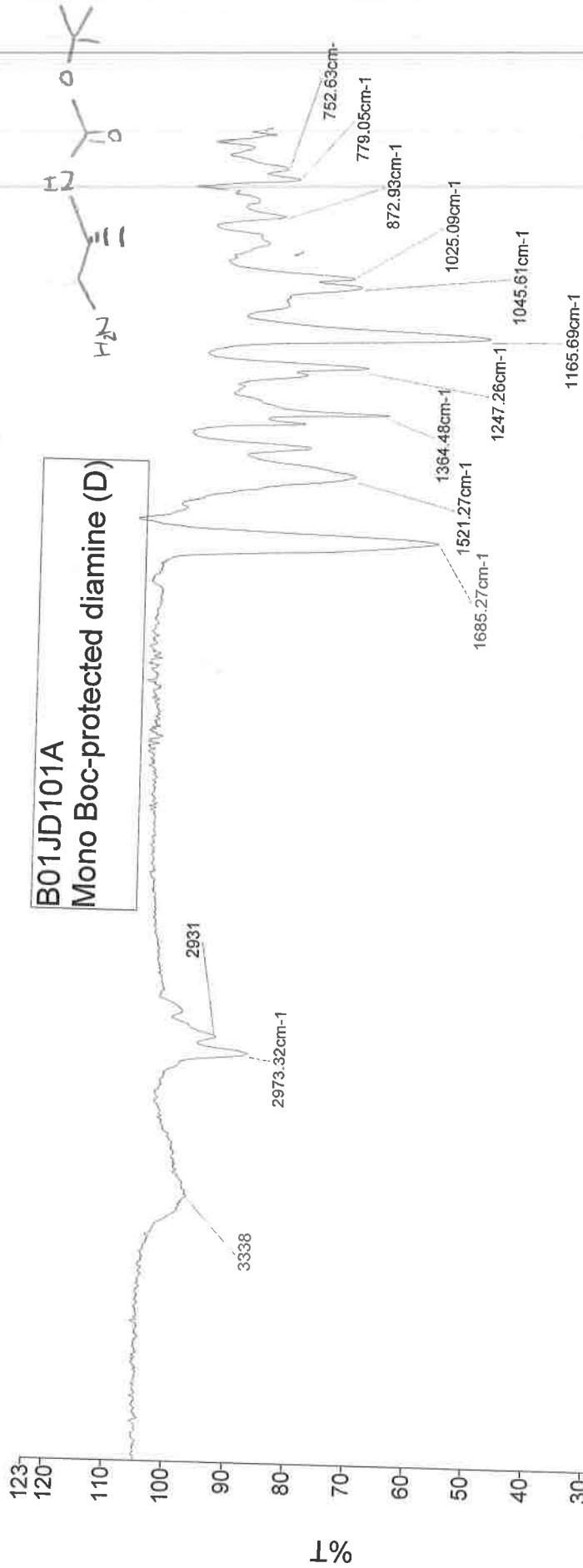
B01JD101A CARBON_01.esp



Analyst
Date

Administrator
28 February 2013 13:30

PerkinElmer Spectrum Version 10.03.06
28 February 2013 13:30



cm⁻¹	Assignment
2973	C-H str. alkane
1685	C=O Carbamate str
1521	N-H bend
1364	CH₃ deformation (umbrella)
1247	C-O Ester str
1165	C-N str aliphatic amine
1045	C-O ether str.
872	N-H wag 1° amine

Administrator 1027 Sample 1027 By Administrator Date Thursday, February 28 2013

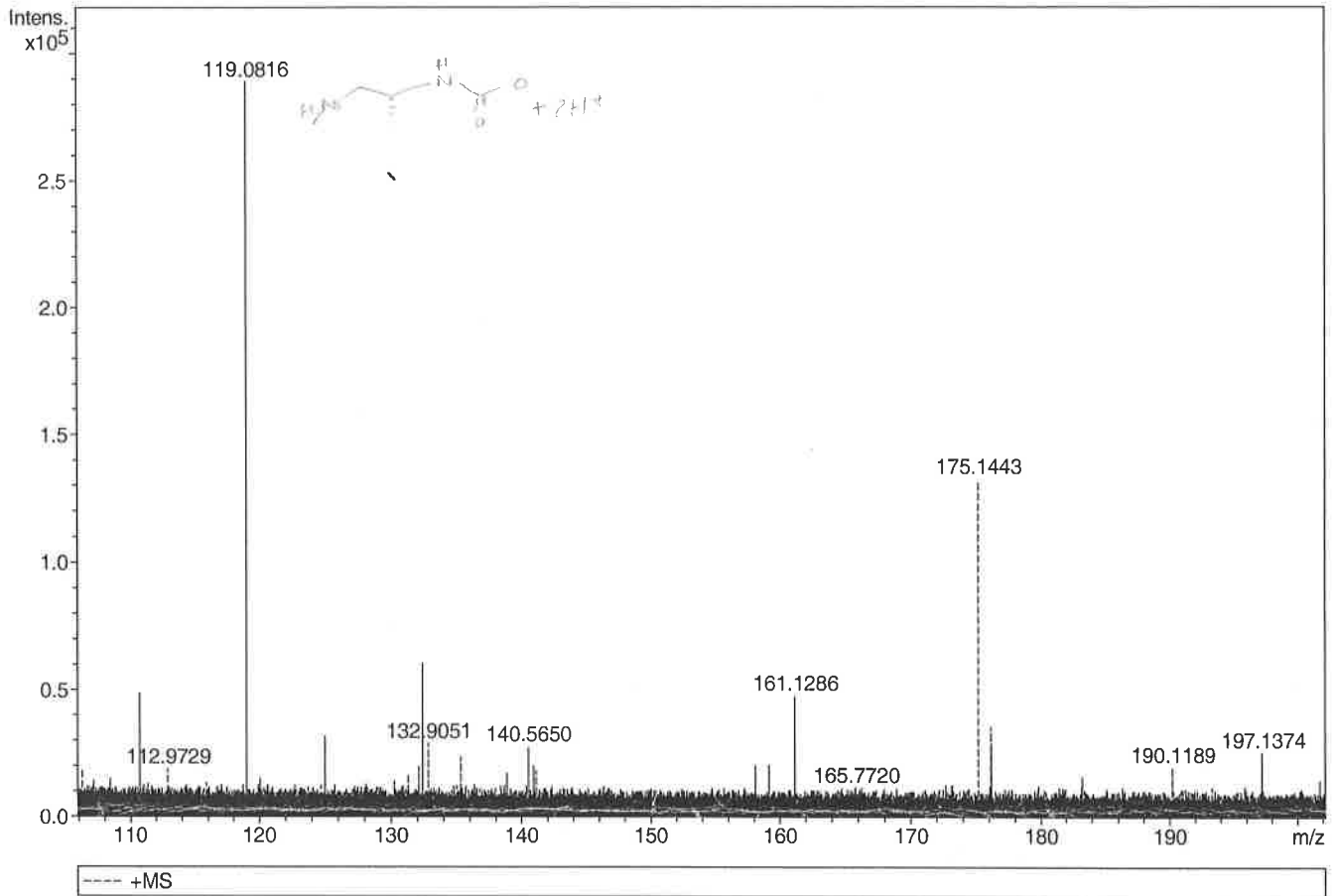
Generic Display Report

Analysis Info

Analysis Name D:\Data\Alinanopos\JESS8945_000002.d
Method pos20090608esi
Sample Name POS ESI BO1JD87A
Comment

Acquisition Date 30/01/2013 18:26:23

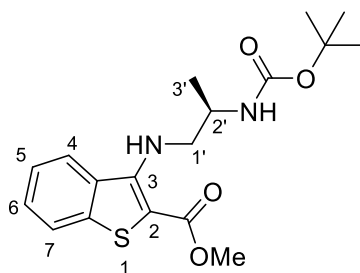
Operator Administrator
Instrument apex-III



Sum	Formula	Sigma	m/z	Err [ppm]	Mean Err [ppm]	Err [mDa]	rdB	N Rule	e ⁻
C 8 H 19 N 2 O 2		0.086	175.1441	-1.09	-16.36	-2.87	0.50	ok	even

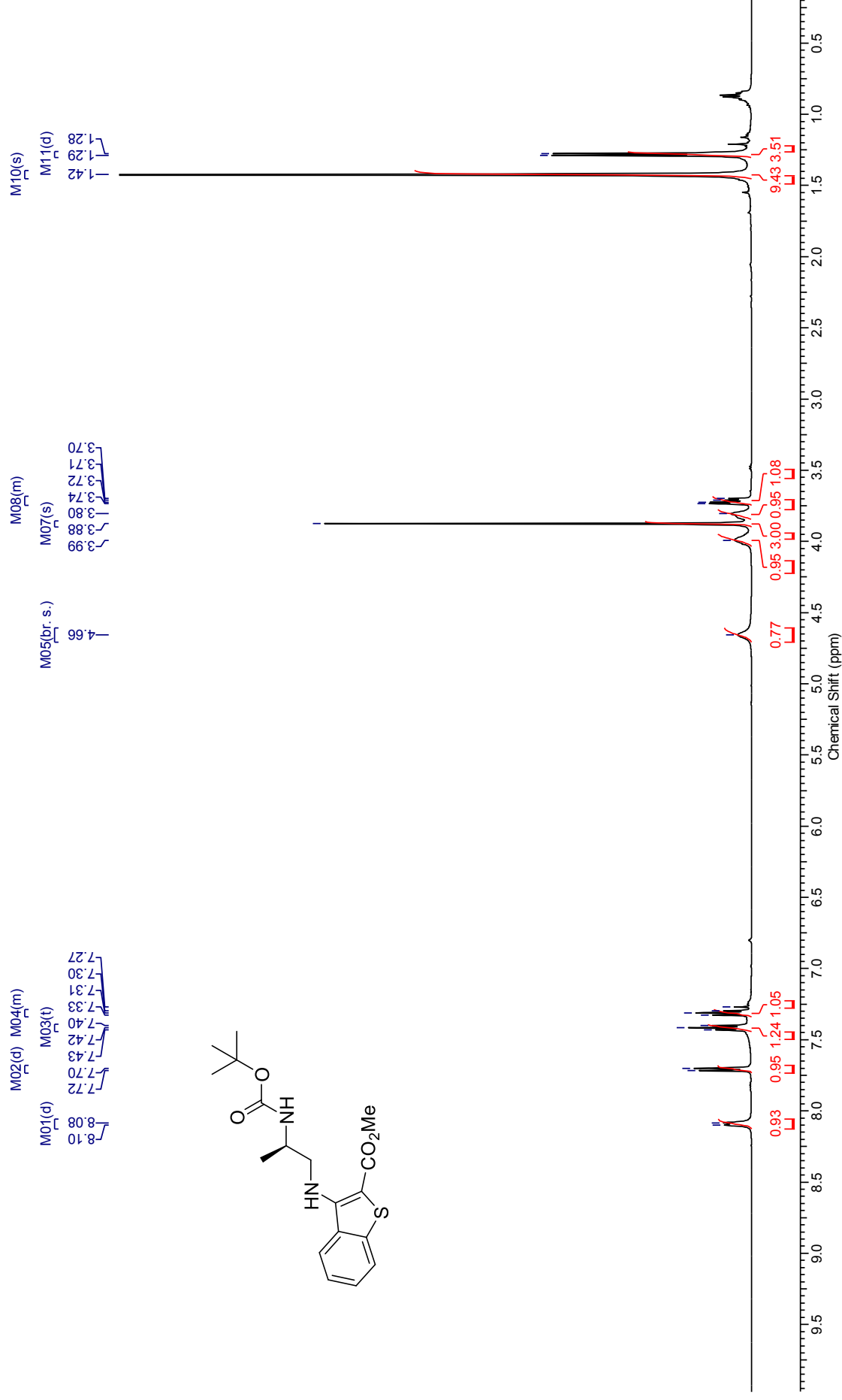


(R)-Methyl 3-((2-((*tert*-butoxycarbonyl)amino)propyl)amino)-benzo[*b*]thiophene-2-carboxylate (184)



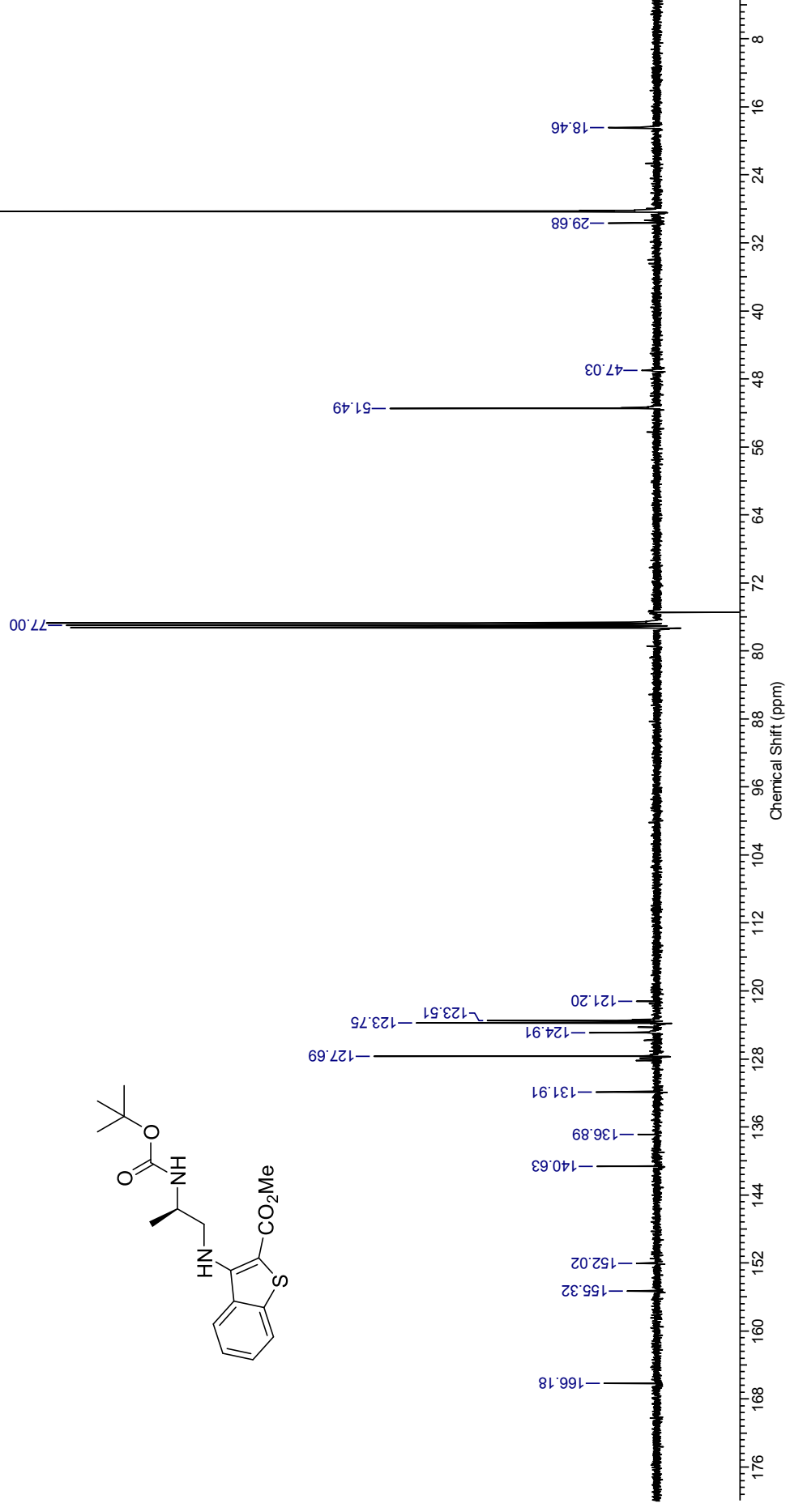
¹H NMR (500 MHz, CDCl₃) for (R)-Methyl 3-((2-((*tert*-butoxycarbonyl)amino)propyl)amino)-benzo[*b*]thiophene-2-carboxylate

B01JD157B PROTON_01.esp



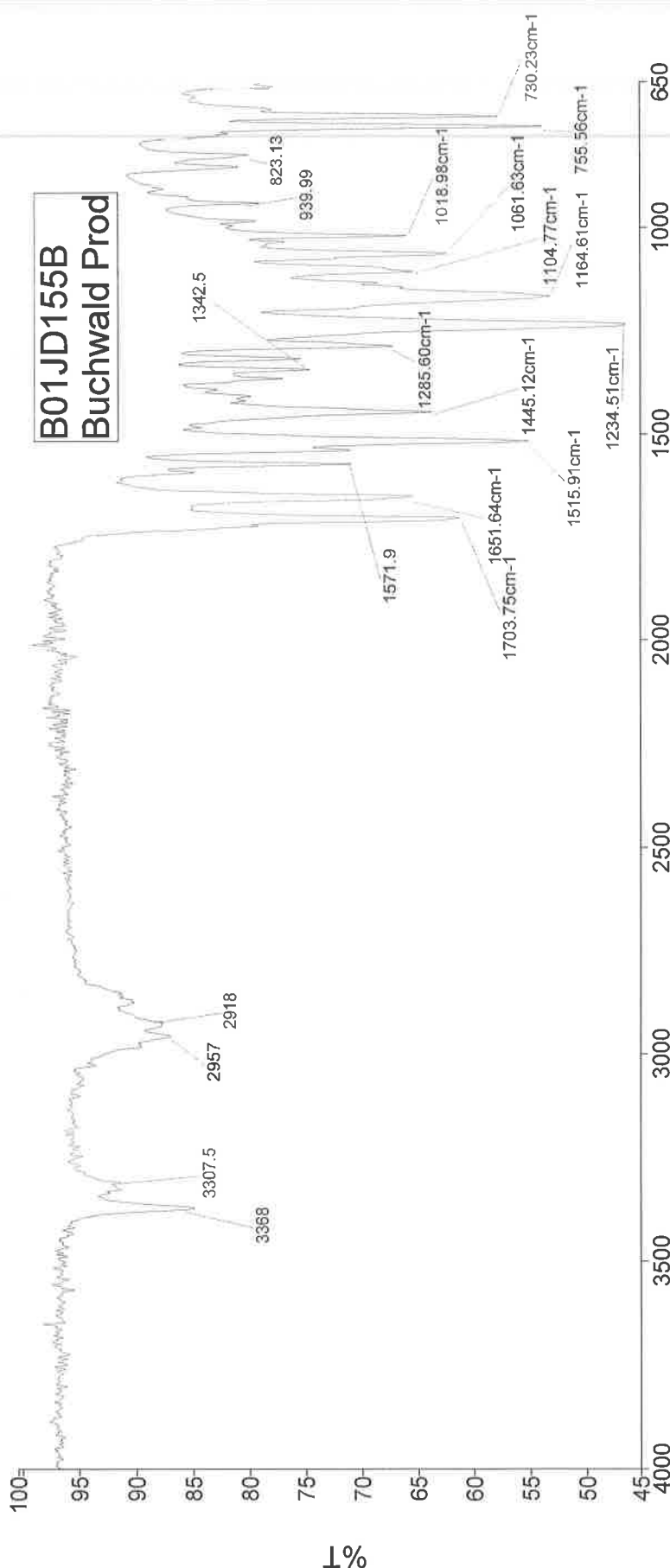
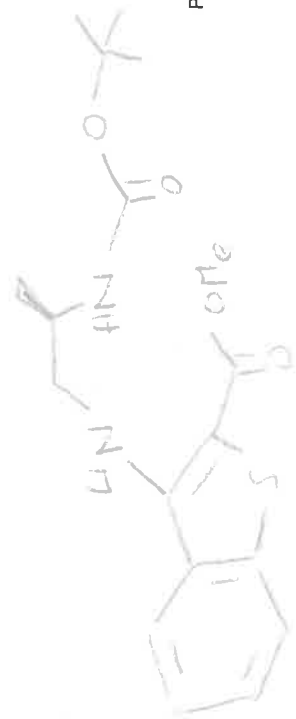
¹³C NMR (126 MHz, CDCl₃) for (R)-Methyl 3-((2-((*tert*-butoxycarbonyl)amino)propyl)amino)-benzo[*b*]thiophene-2-carboxylate

B01JD155B CARBON_01.esp



Analyst
Date

Administrator
14 May 2013 10:14

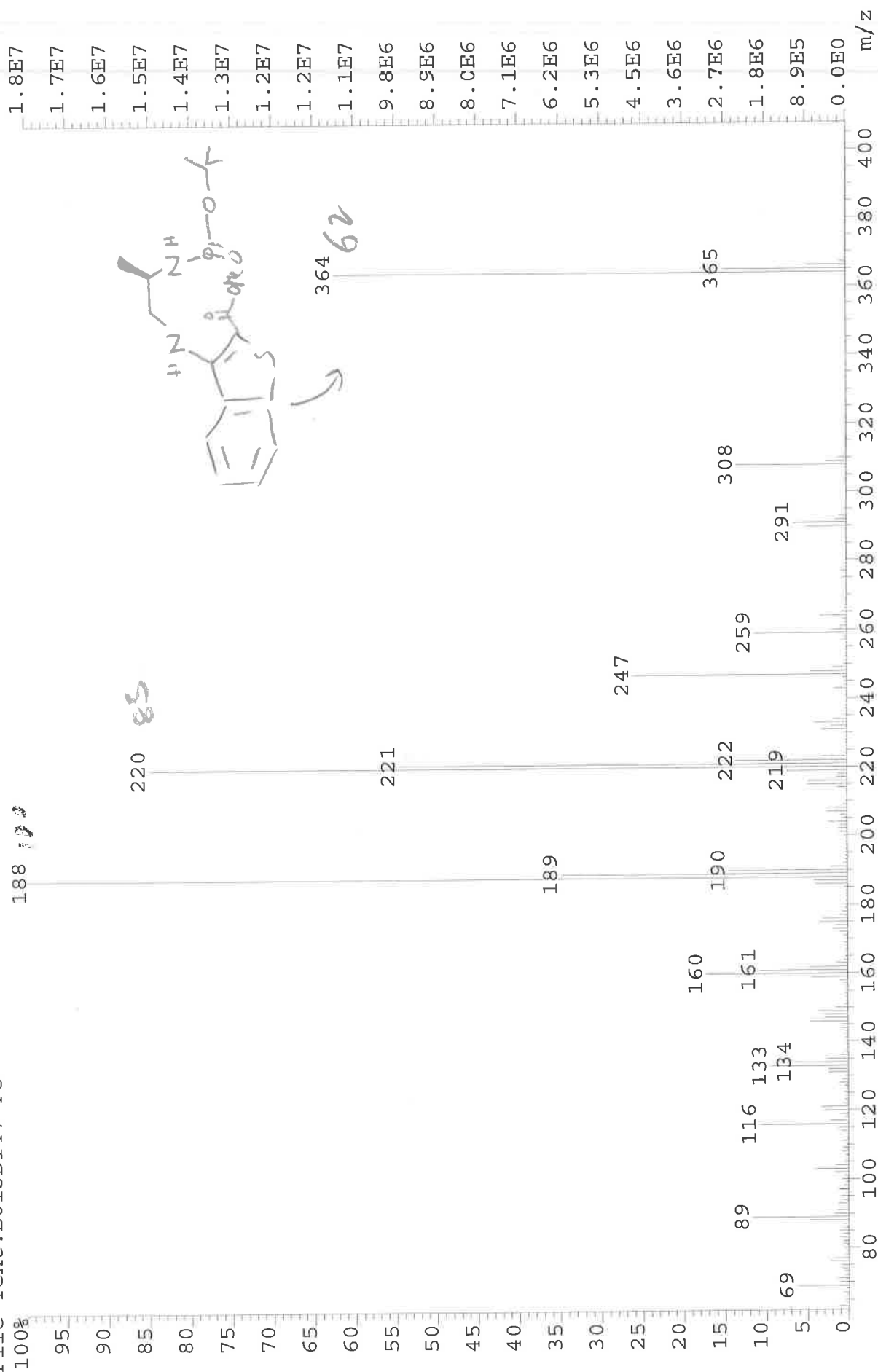


cm⁻¹

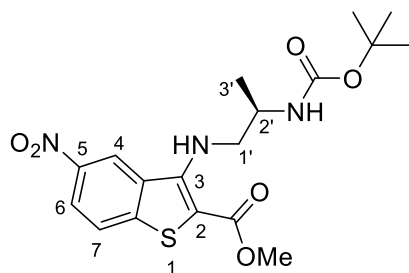
3368 N-H str
2957 C-H alk str
1704 C=O str
1652 C=O str
1516 C=C bend
1445 C-H2 bend
1286 C-N str
1235 C-N str
1165 C-O str
756 C-H2 bend

Administrator 41 Sample 041 By Administrator Date Tuesday, May 14 2013

File: JESS9147 Ident: 46 Acq: 20-MAR-2013 19:04:35 +2:52 Cal: CAL1
AutoSpecE EI+ Magnet BpI: 17805388 TIC: 170024336 Flags: HALL
File Text: B01JD147-F3

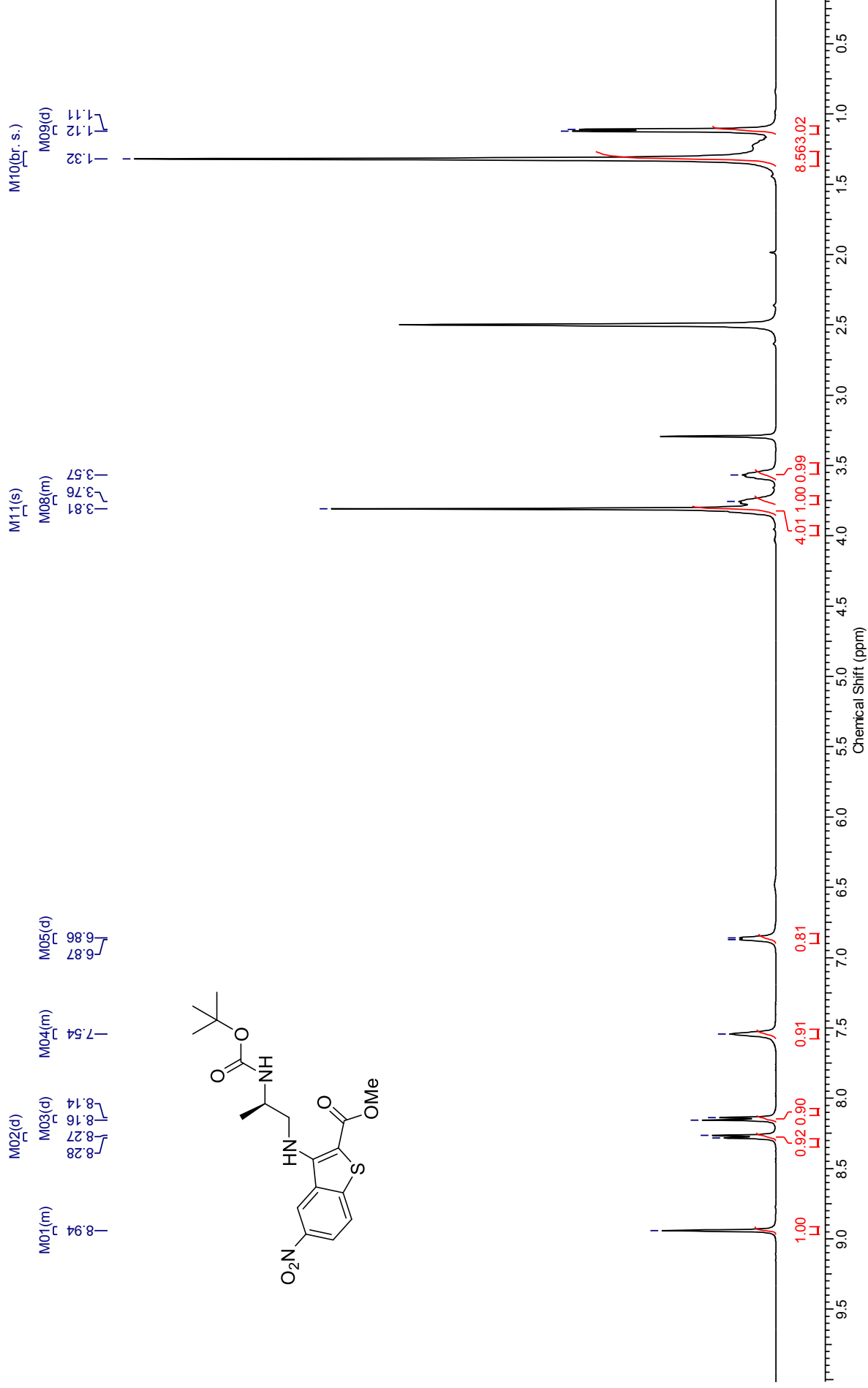


(R)-Methyl 3-((2-((*tert*-butoxycarbonyl)amino)propyl)amino)-5-nitrobenzo[*b*]thiophene-2-carboxylate (185)



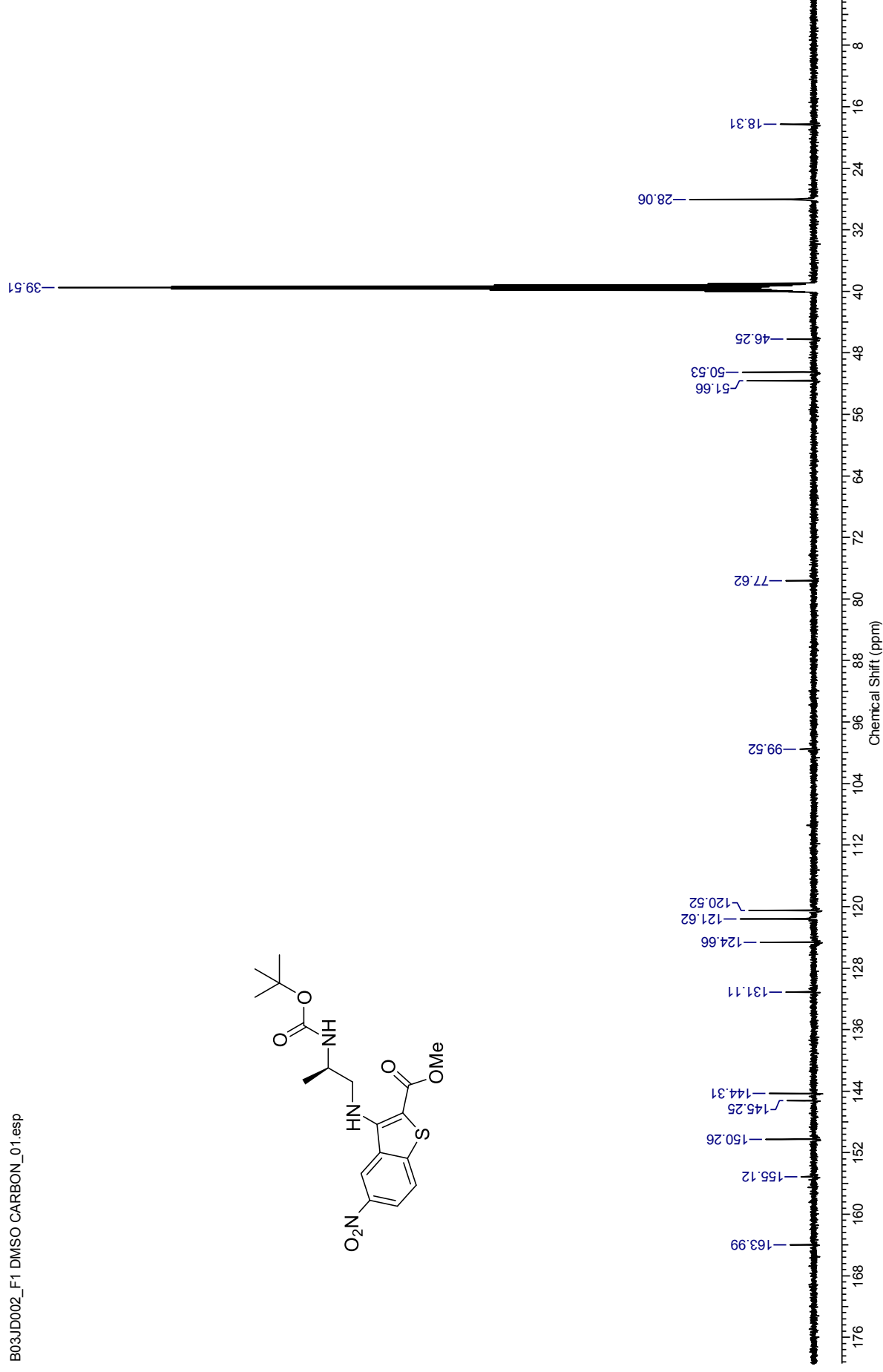
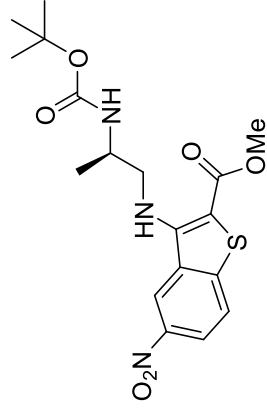
¹H NMR (500 MHz, DMSO-*d*₆) for (R)-Methyl 3-((2-((*tert*-butoxycarbonyl)amino)propyl)amino)-5-nitrobenzo[b]thiophene-2-carboxylate

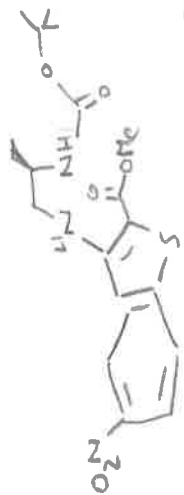
B03JD002_F1 DMSO Proton 4 carbon.esp



¹³C NMR (126 MHz, DMSO-*d*₆) for for (*R*)-Methyl 3-(2-((*tert*-butoxycarbonyl)amino)propyl)amino-5-nitrobenzo[*b*]thiophene-2-carboxylate

B03JD002_F1 DMSO CARBON_01.esp



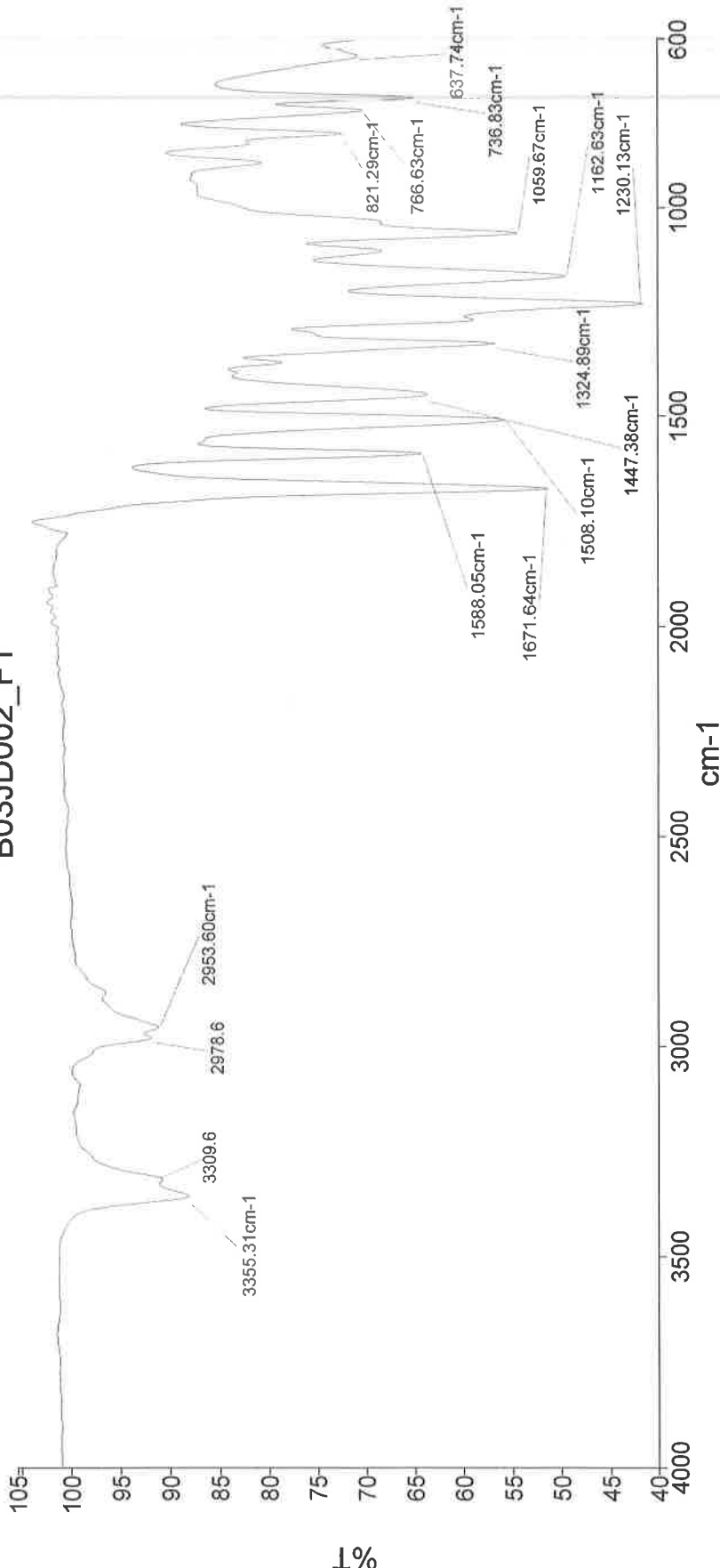


PerkinElmer Spectrum Version 10.03.06
25 March 2014 15:58

Analyst
Date

Administrator
25 March 2014 15:58

B03JD002_F1

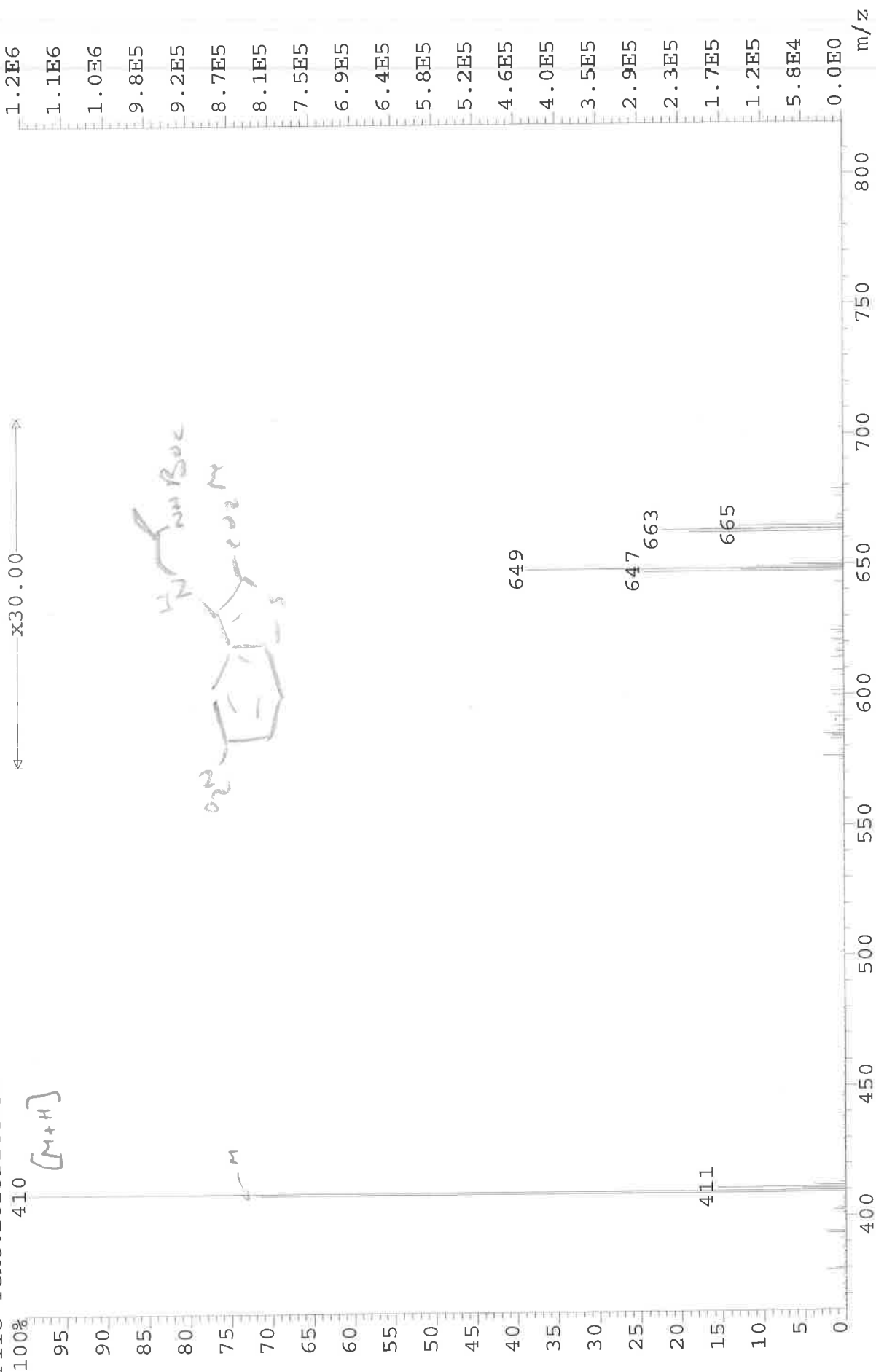


- 3355** - 2° N-H str.
2954 - C-H str. alkane
1672 - C=O amide str.
1588 - N=O asym str.
1508 - C-C (ring) str.
1447 - C-H asym str
1325 - N=O Sym str
1230 - C-O str ester str
1162 - C-O str. carbamate (?)
1060 - C-N aliphatic amine
737 - N-H wag 2° amine

Administrator 24 Sample 024 By Administrator Date Tuesday, March 25 2014

Page 1

File: JESS3474 Ident: 34 Acq: 10-JAN-2014 12:58:06 +2:08 Cal: CALL
AutoSpecE EI+ Magnet BpI: 12845118 TIC: 133789160 Flags: HALL
File Text: B02JD144-F2



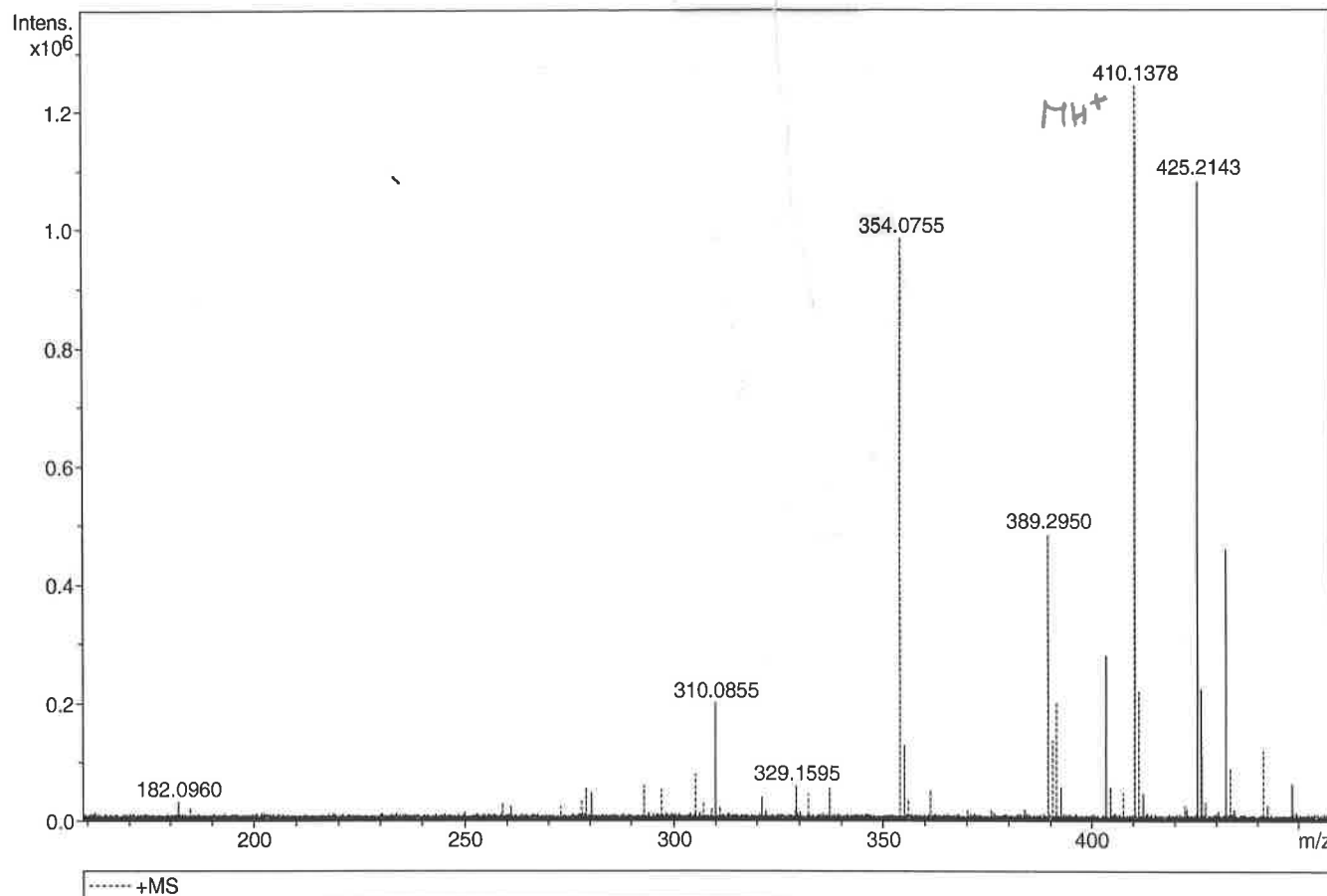
Generic Display Report

Analysis Info

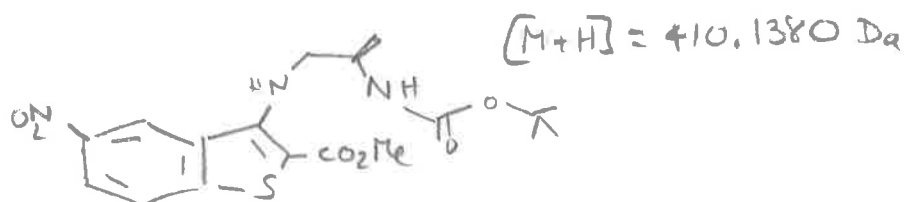
Analysis Name D:\Data\Alinanopos\JESS4094_000001.d
 Method pos20090608esi
 Sample Name POS ESI BO2JD183-F2
 Comment

Acquisition Date 03/03/2014 11:11:37

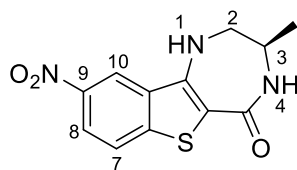
Operator Administrator
 Instrument apex-III



Sum Formula	Sigma	m/z	Err [ppm]	Mean Err [ppm]	Err [mDa]	rdB	N Rule	e ⁻
C 18 H 24 N 3 O 6 S 1	0.033	410.1380	0.54	-0.19	-0.08	8.50	ok	even



(3*R*)-3-Methyl-9-nitro-1,2,3,4-tetrahydro-5*H*-[1]benzothieno[3,2-*e*][1,4]diazepin-5-one (178)



¹H NMR (500 MHz, DMSO-*d*₆) for (3*R*)-3-Methyl-9-nitro-1,2,3,4-tetrahydro-5*H*-[1,4]diazepin-5-one

B03JD004A DMSO. esp

M05(dd)

M07(d)

M06(d)

M08(m)

M04(d)

M01(m)

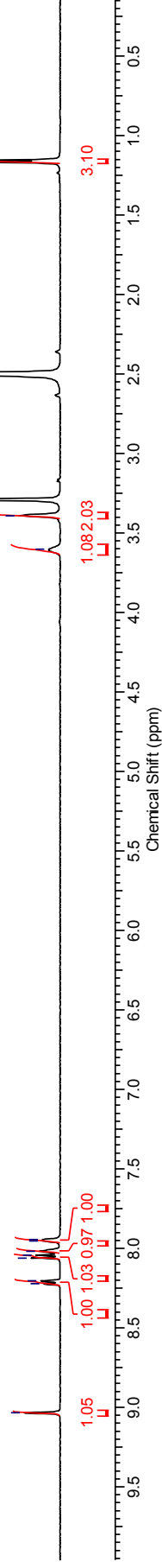
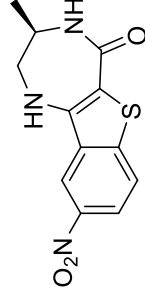
M02(m)

M03(d)

9.03
8.22
8.20
8.06
8.04
8.02
7.95
7.95

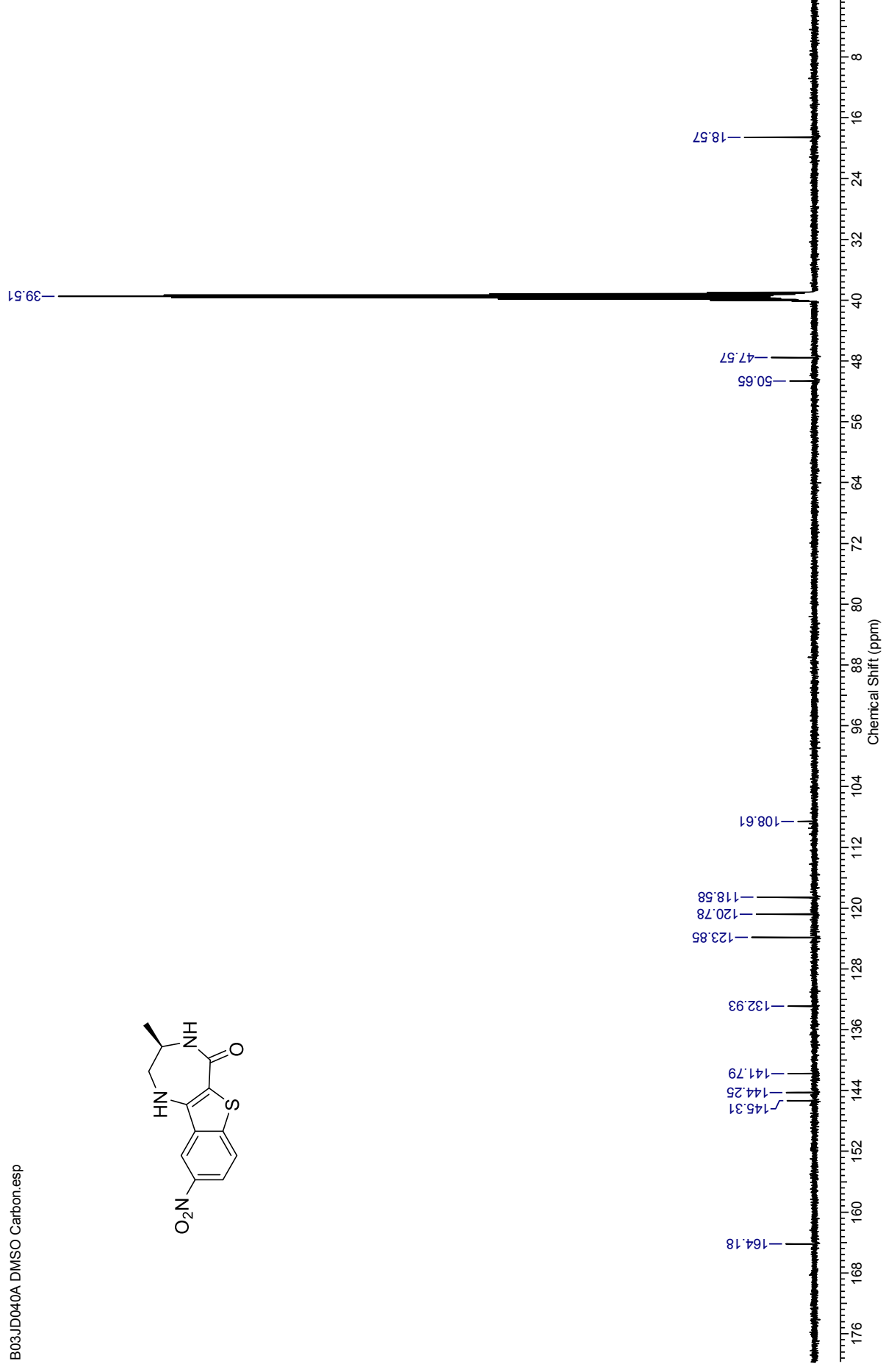
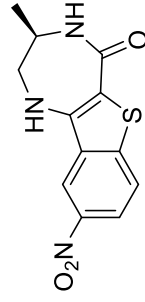
2.50

1.17
1.16



¹³C NMR (126 MHz, DMSO-*d*₆) for (3*R*)-3-Methyl-9-nitro-1,2,3,4-tetrahydro-5*H*-[1]benzothieno[3,2-*e*][1,4]diazepin-5-one

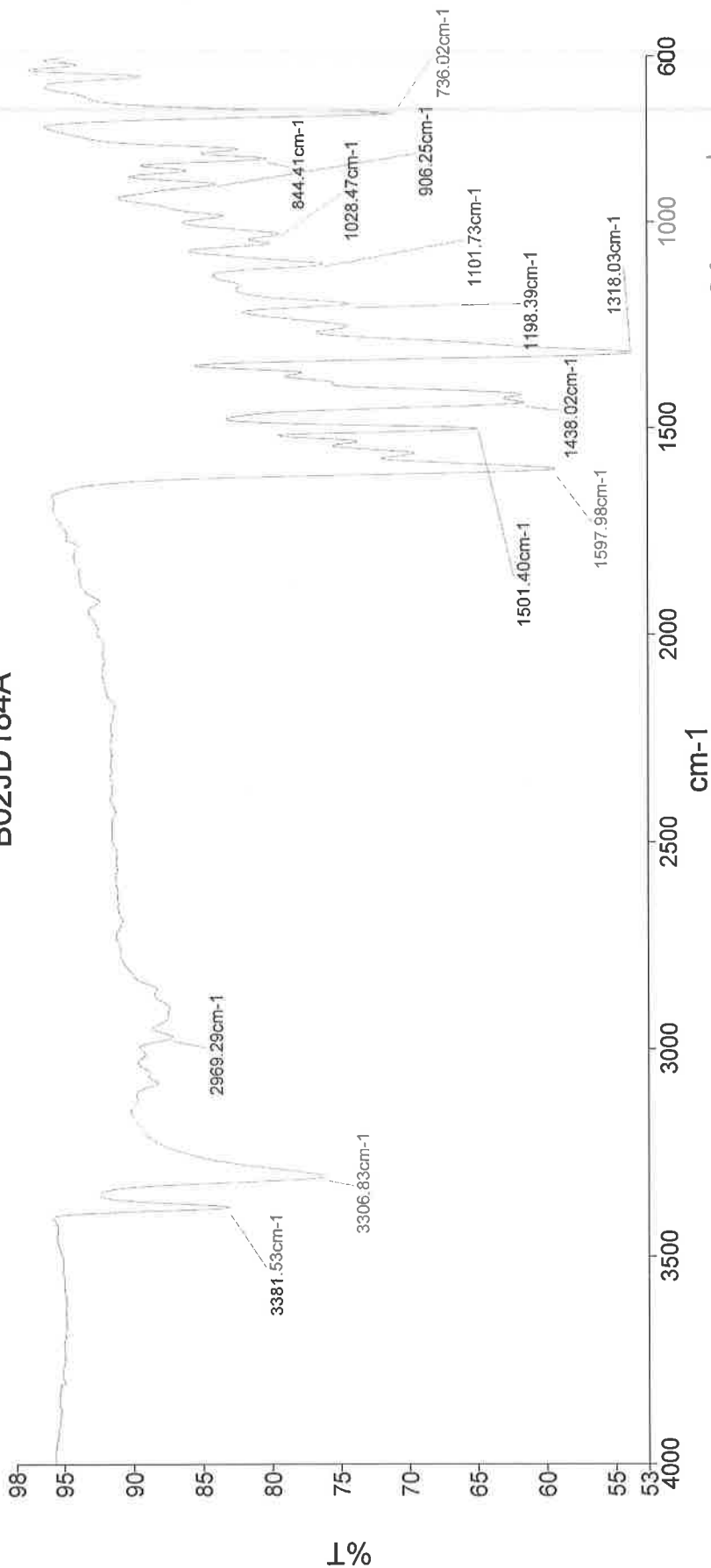
B03JD040A DMSO Carbon.esp



Analyst
Date

Administrator
25 March 2014 16:05

B02JD184A



3382 - N-H 2° amine str.
3307 - N-H 2° amine/amide str.
1598 - C=O amide str.
1501 - NO₂ str. asym.
1438 - C-C str. (in ring)
1318 - NO₂ str. sym.
1102 - C-N aliphatic amine
736 - N-H wag 2° amine

File: JESS4832 Ident: 21 Acq: 25-FEB-2015 10:16:26 +1:21 Cal: CAL1
 AutoSpecE EI+ Magnet BpI: 96010 TIC: 876328 Flags: HALL
 File Text: BO3JD179A



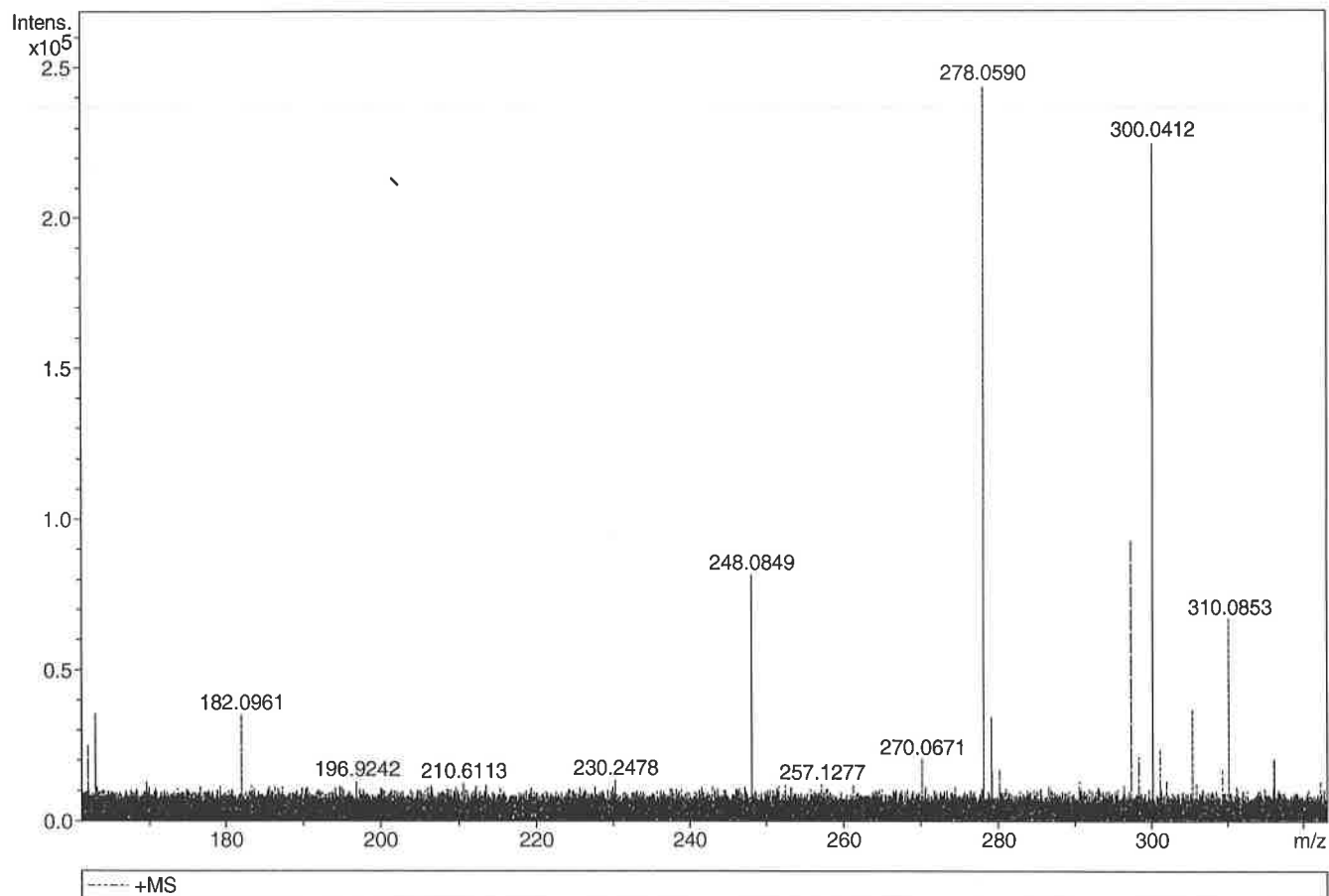
Generic Display Report

Analysis Info

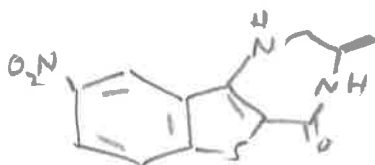
Analysis Name D:\Data\Alinanopos\JESS4092_000001.d
Method pos20090608esi
Sample Name POS ESI BO2JD181A
Comment

Acquisition Date 03/03/2014 11:17:52

Operator Administrator
Instrument apex-III

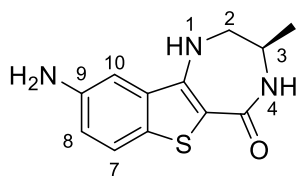


Sum	Formula	Sigma	m/z	Err [ppm]	Mean Err [ppm]	Err [mDa]	rdb	N Rule	e ⁻
C 12 H 12 N 3 O 3 S 1		0.011	278.0594	1.25	-8.98	-2.50	8.50	ok	even



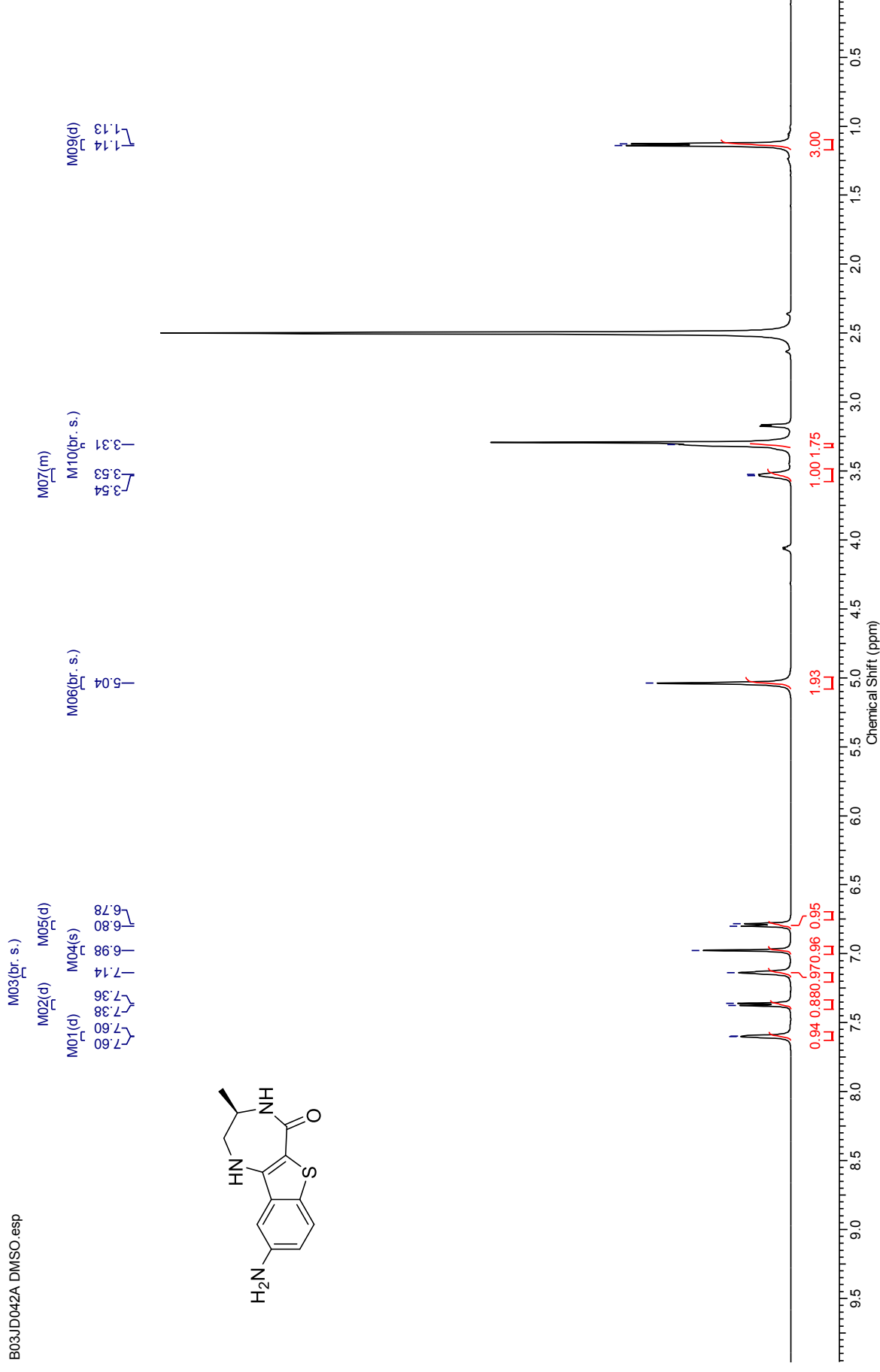
$[M+H]^+ = 278.0594 \text{ Da}$

(3*R*)-9-Amino-3-methyl-1,2,3,4-tetrahydro-5*H*-[1]benzothieno[3,2-*e*][1,4]diaepin-5-one (179)



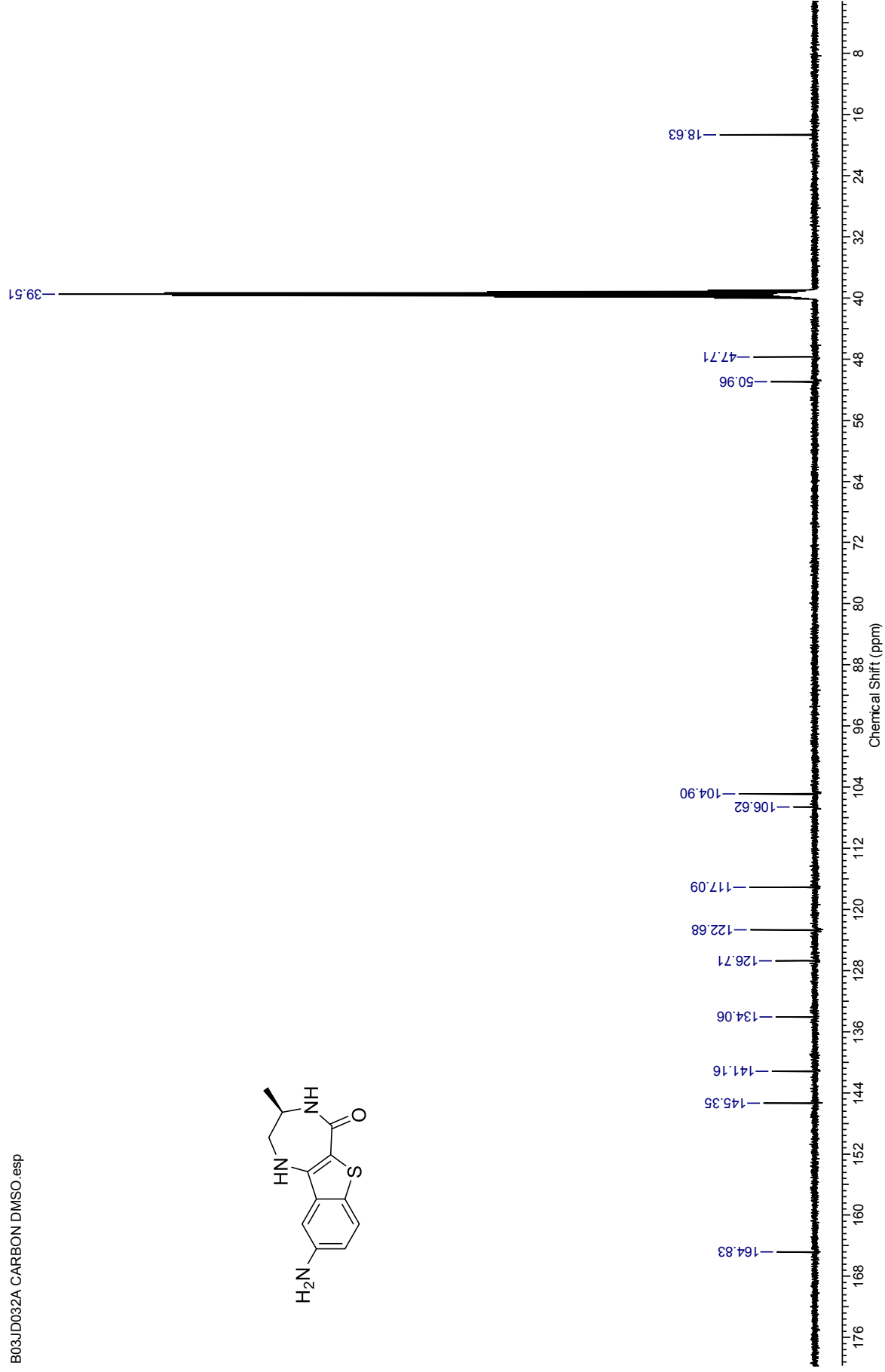
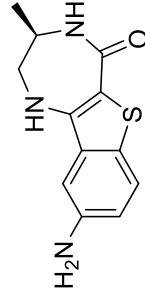
¹H NMR (500 MHz, DMSO-*d*₆) for (3*R*)-9-Amino-3-methyl-1,2,3,4-tetrahydro-5*H*-[1]benzothieno[3,2-*e*][1,4]diaepin-5-one

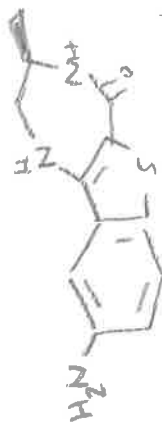
B03JD042A DMSO.esp



¹³C NMR (126 MHz, DMSO-*d*₆) for (3*R*)-9-Amino-3-methyl-1,2,3,4-tetrahydro-5*H*-[1]benzothieno[3,2-*e*][1,4]diaepin-5-one

B03JD032A CARBON DMSO esp



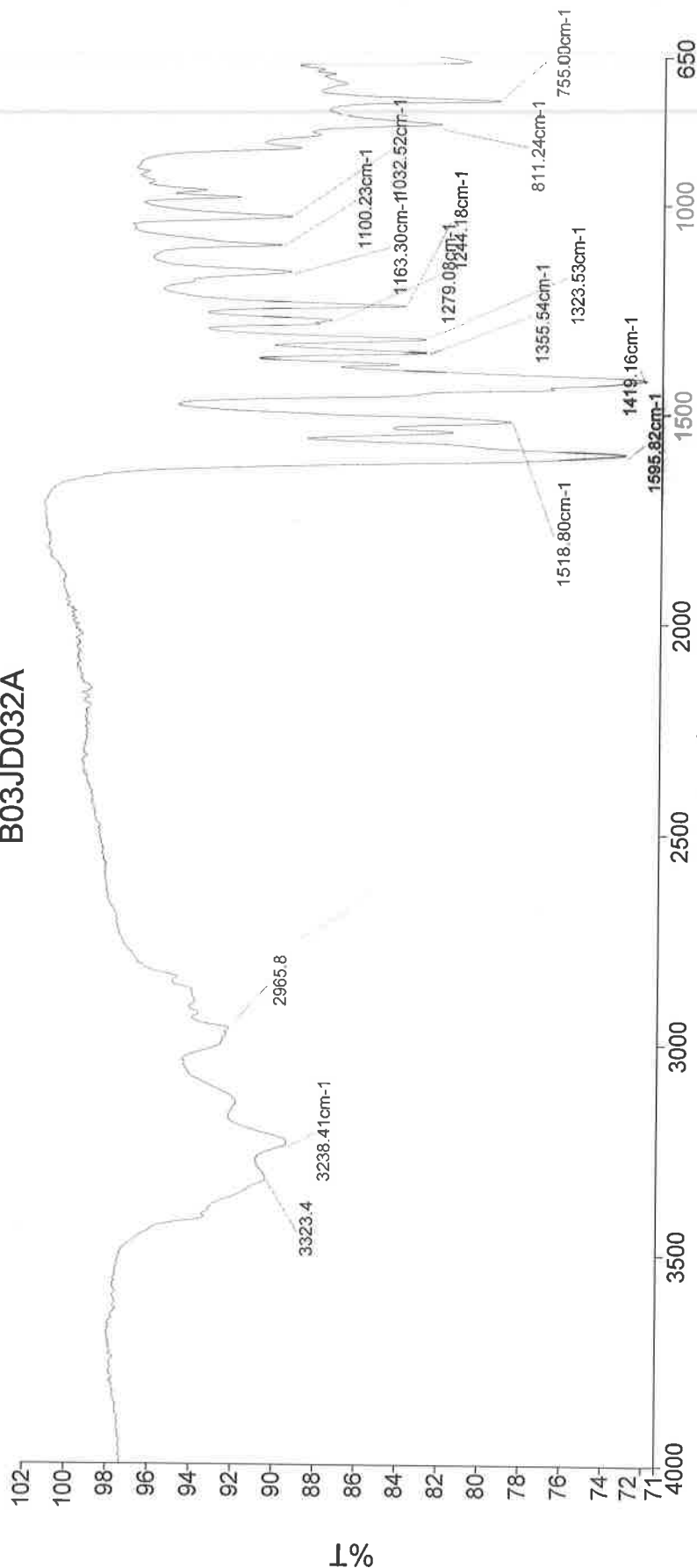


(R)-4-Amino-3-methyl-2,3,4-tetrahydro-1H-benzothieno[3,2-b]pyridine-5-one

Analyst
Date

PerkinElmer Spectrum Version 10.03.06
22 May 2014 11:56

B03JD032A



3238 N-H stretch Amide

Administrator 223 Sample 223 By Administrator Date Thursday, May 22 2014

1596 N-H str. 1° amine
1419 C=C in ring (aromatic)
1324 C-N str. aromatic amine
1244 C-N aliphatic amine

Generic Display Report

Analysis Info

Analysis Name D:\Data\Alinanopos\JESS4185_000001.d
Method pos20090608esi
Sample Name POS ESI BO3JD013-F2
Comment

Acquisition Date 20/03/2014 09:37:36

Operator Administrator
Instrument apex-III

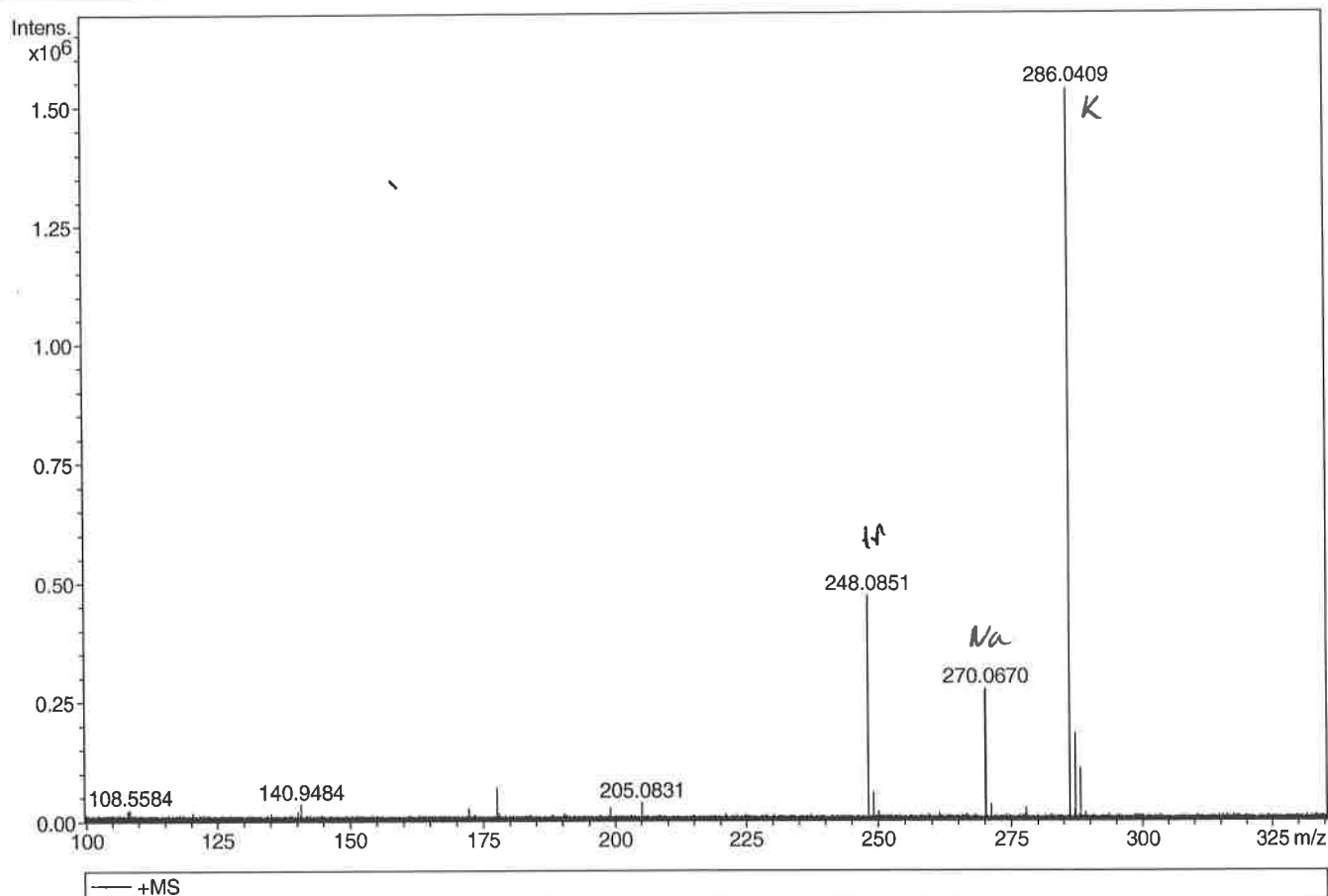
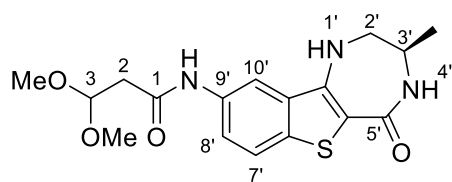


Table 'GenFormulaResults' could not be found in this analysis



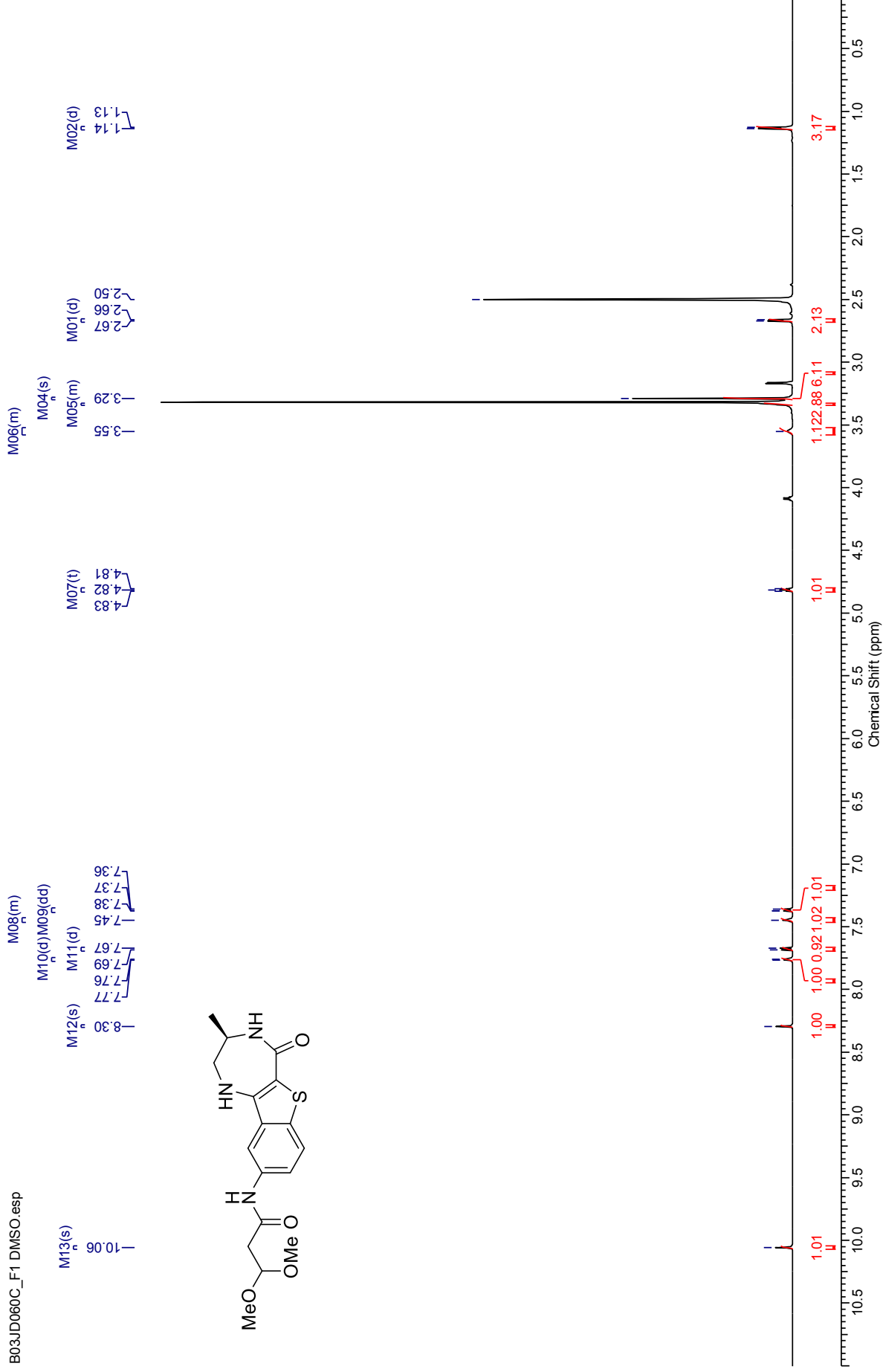
$[M+H]^+ = 248.0852 \text{ Da}$
 $[M+Na]^+ = 270.0666 \text{ Da}$
 $[M+K]^+ = 286.0405 \text{ Da}$

**3,3-Dimethoxy-*N*-((3*R*)-3-methyl-5-oxo-2,3,4,5-tetrahydro-1*H*-
[1]benzo[4,5]thieno[3,2-*e*][1,4]diazepin-9-yl)propanamide (186)**



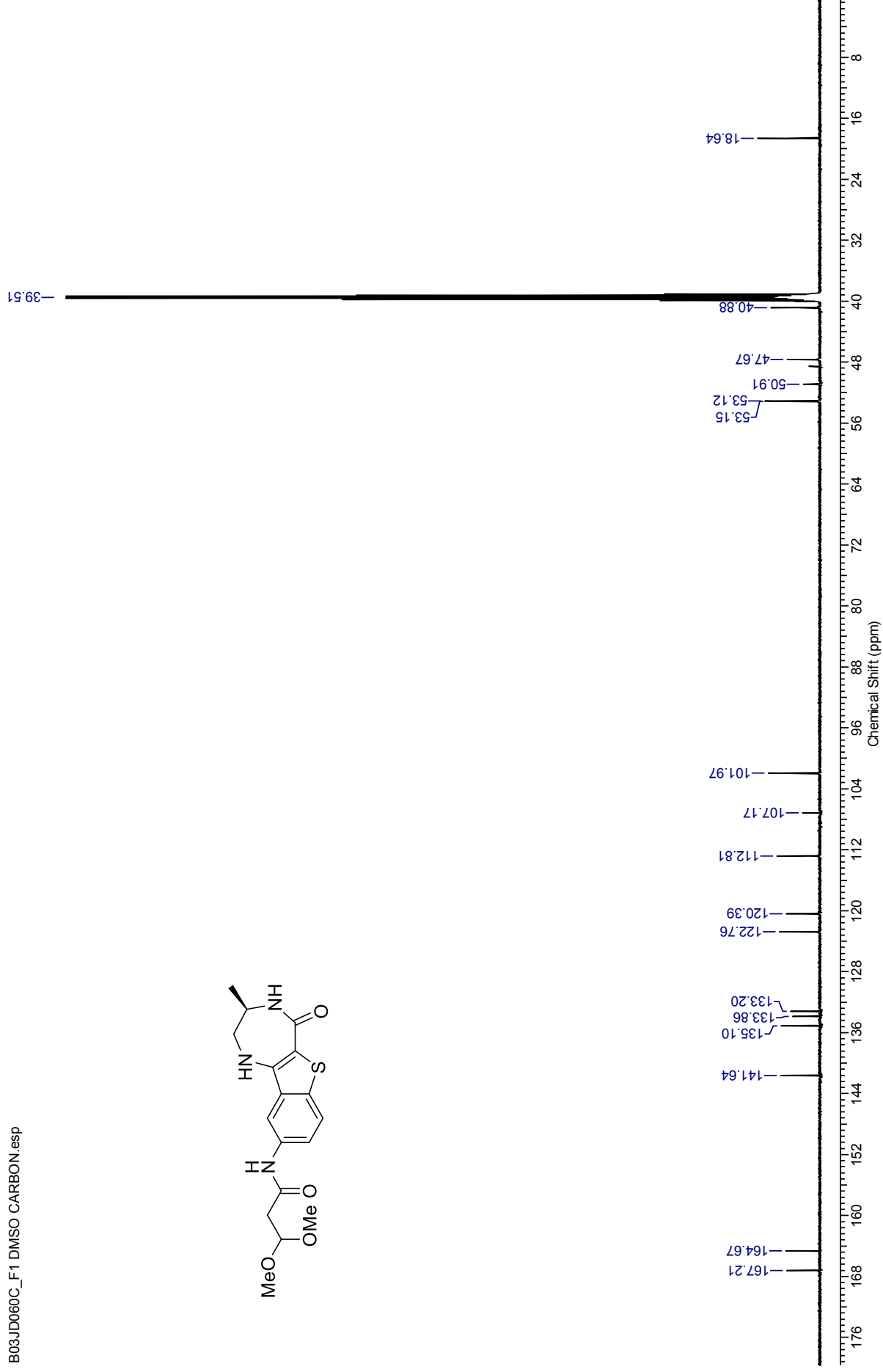
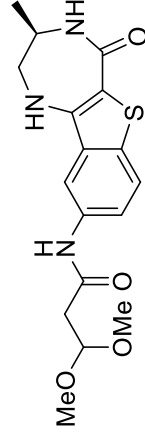
¹H NMR (600 MHz, DMSO-d₆) for 3,3-Dimethoxy-N-((3*R*)-3-methyl-5-oxo-2,3,4,5-tetrahydro-1*H*-[1]benzo[4,5]thieno[3,2-*e*][1,4]diazepin-9-yl)propanamide

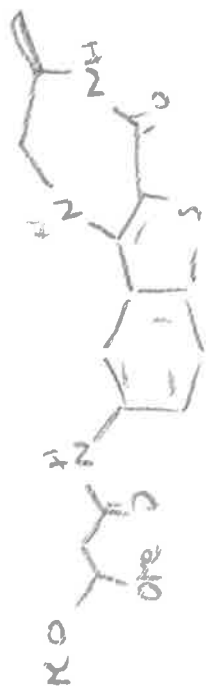
B03JD060C_F1 DMSO.esp



¹³C NMR (151 MHz, DMSO-*d*₆) for 3,3-Dimethoxy-*N*-((3*R*)-3-methyl-5-oxo-2,3,4,5-tetrahydro-1*H*-[1,4]diazepin-9-yl)propanamide

B03JD060C_F1 DMSO CARBON.esp

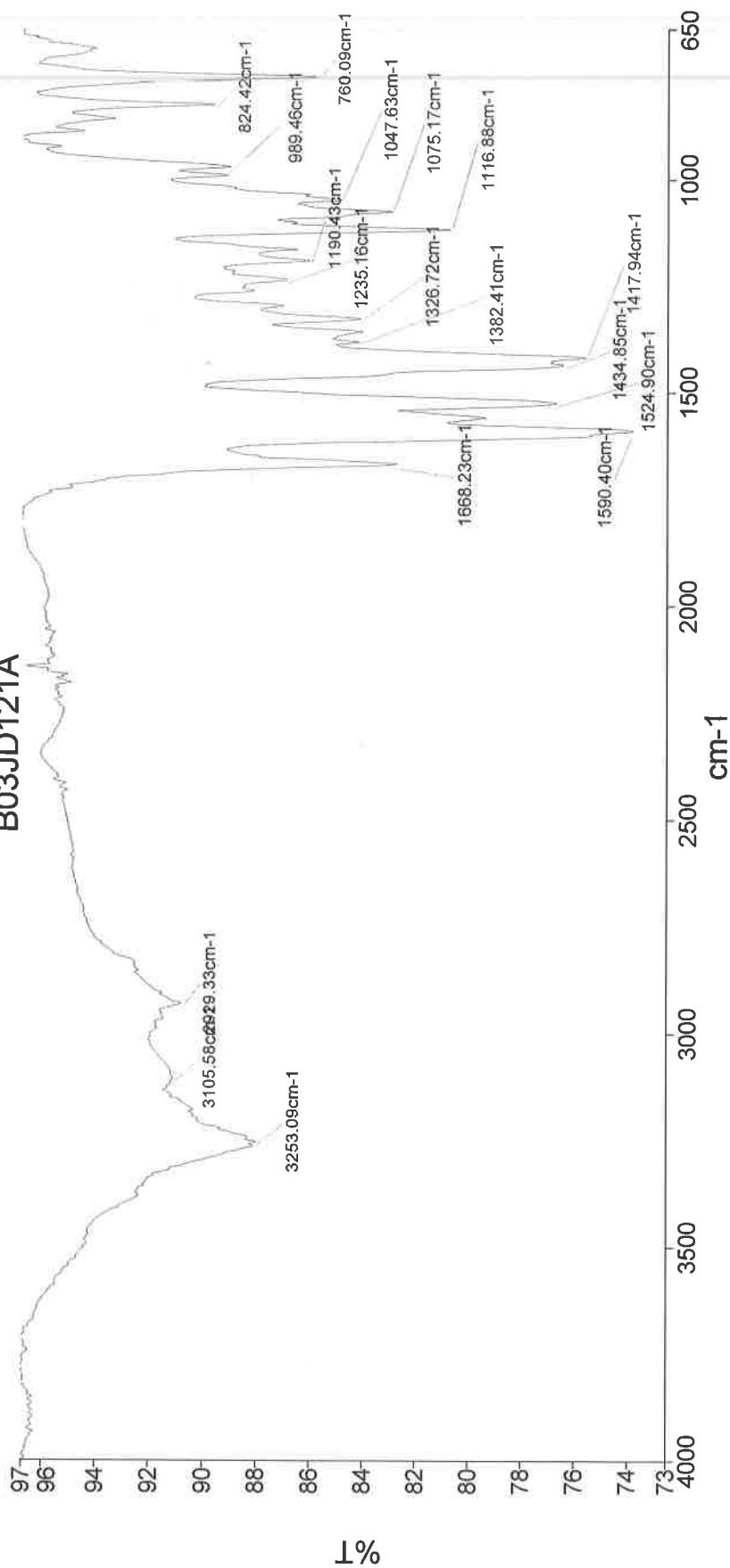




PerkinElmer Spectrum Version 10.03.06
02 June 2016 13:02

Analyst
Date
Administrator
02 June 2016 13:02

B03JD121A



3253 N-H str
1668 C=O str
1590 N-H bend

1420 C-C str
1117 C-N str
1075 C-O str

249-011_1 Sample 011 By Administrator Date Thursday, June 02 2016

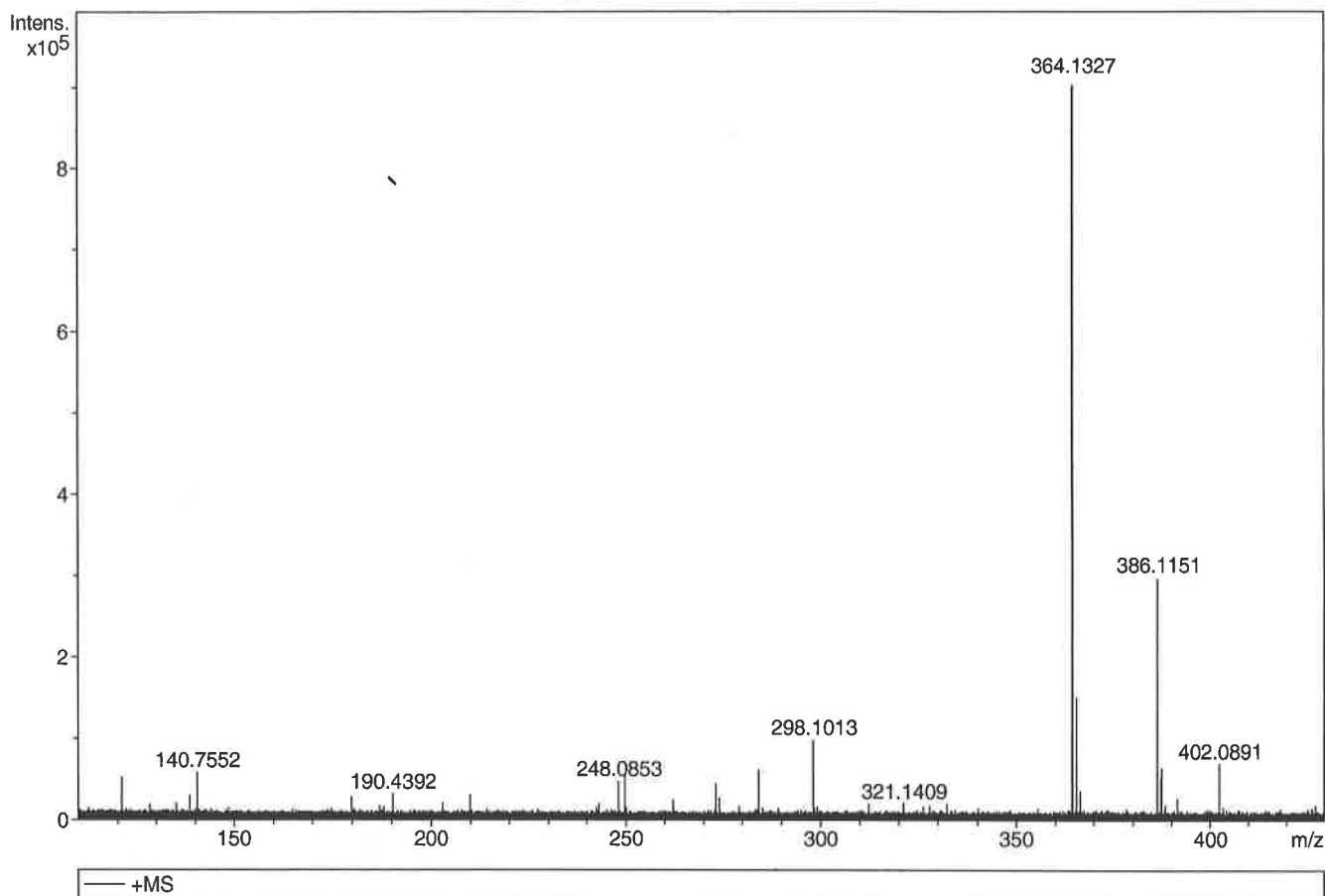
Generic Display Report

Analysis Info

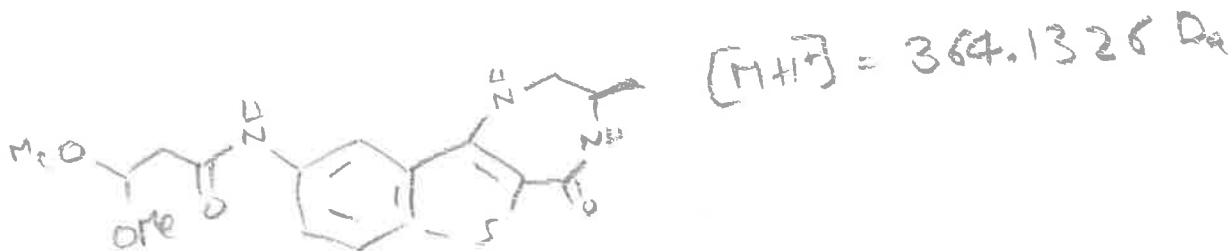
Analysis Name D:\Data\Alinanopos\JESS4409_000001.d
Method pos20090608esi
Sample Name POS ESI BO3JD026-F1
Comment

Acquisition Date 16/05/2014 15:48:23

Operator Administrator
Instrument apex-III



Sum Formula	Sigma	m/z	Err [ppm]	Mean Err [ppm]	Err [mDa]	rdb	N Rule	e ⁻
C 17 H 22 N 3 O 4 S 1	0.035	364.1326	-0.41	-2.54	-0.92	8.50	ok	even



File Name: W:\Lcms\B03JD121

Sample ID: 42

Comment: Crude 10 min MeOH-DMF

9/3/2014 2:07:46 PM

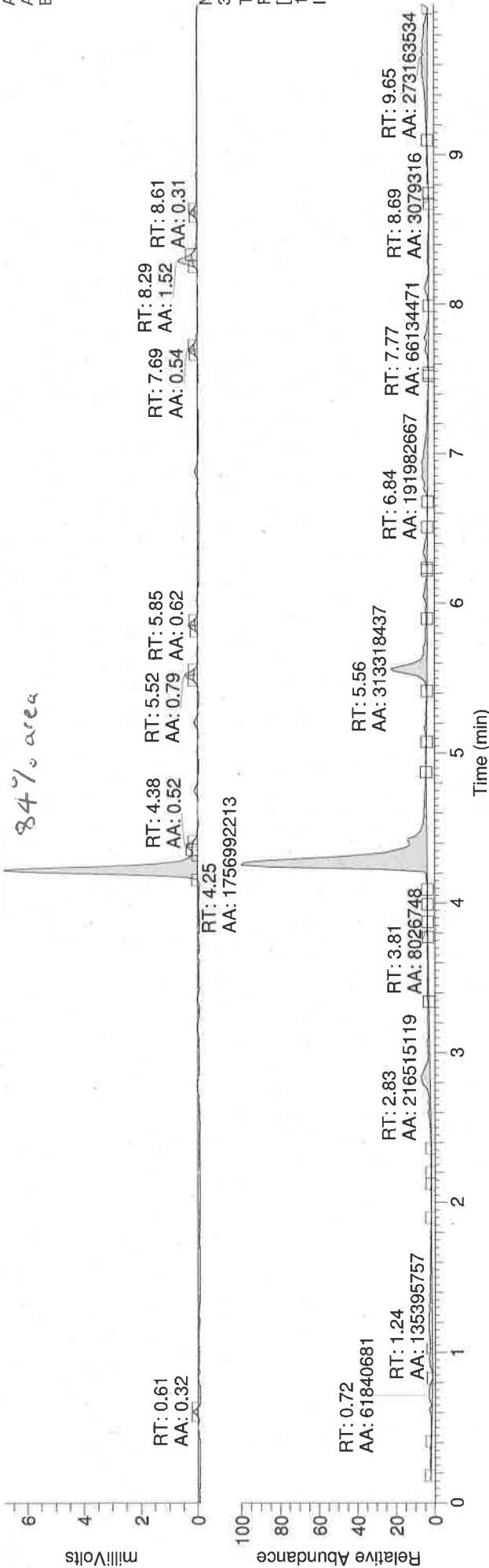
Vial position: 26

Sample Name: CC1=CC=C(C=C1)C2=CC=CC=C2
Vial: 4
CCH44
E DC1
Mr = 363.43

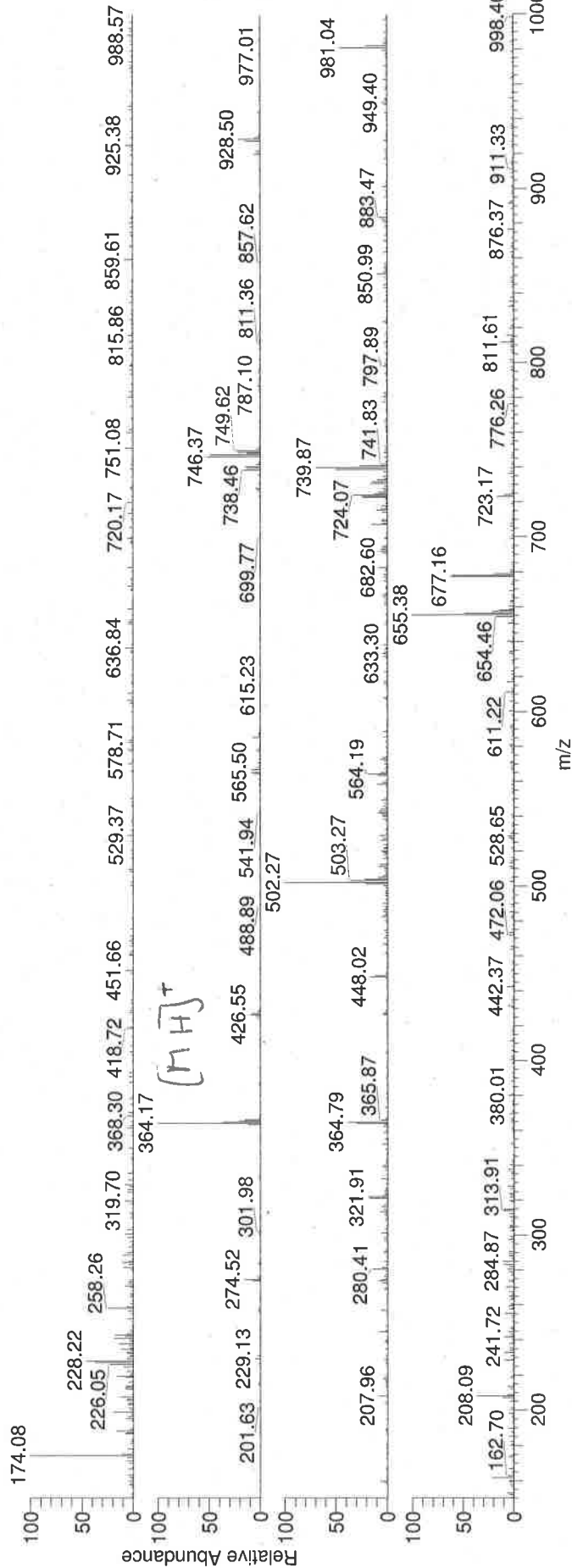
RT: 0.00 - 10.00

RT: 4.22
MA: 24.10

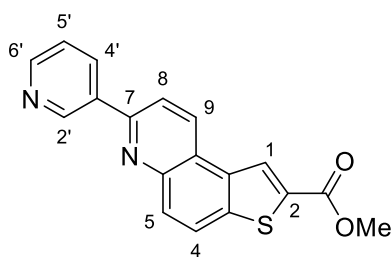
84% area



NL: 3.09E8
TIC F: + c ESI
Full ms
[150.00-
1000.00] MS
ICIS B03JD121



Methyl 7-(pyridin-3-yl)thieno[3,2-f]quinoline-2-carboxylate (195A)



¹H NMR (500 MHz, CDCl₃) for Methyl 7-(pyridin-3-yl)thieno[3,2-f]quinoline-2-carboxylate

B04JD133_F2.esp

M04(d) M06(d)

M02(d) M05(m)

M01(br. s.)

M03(s)

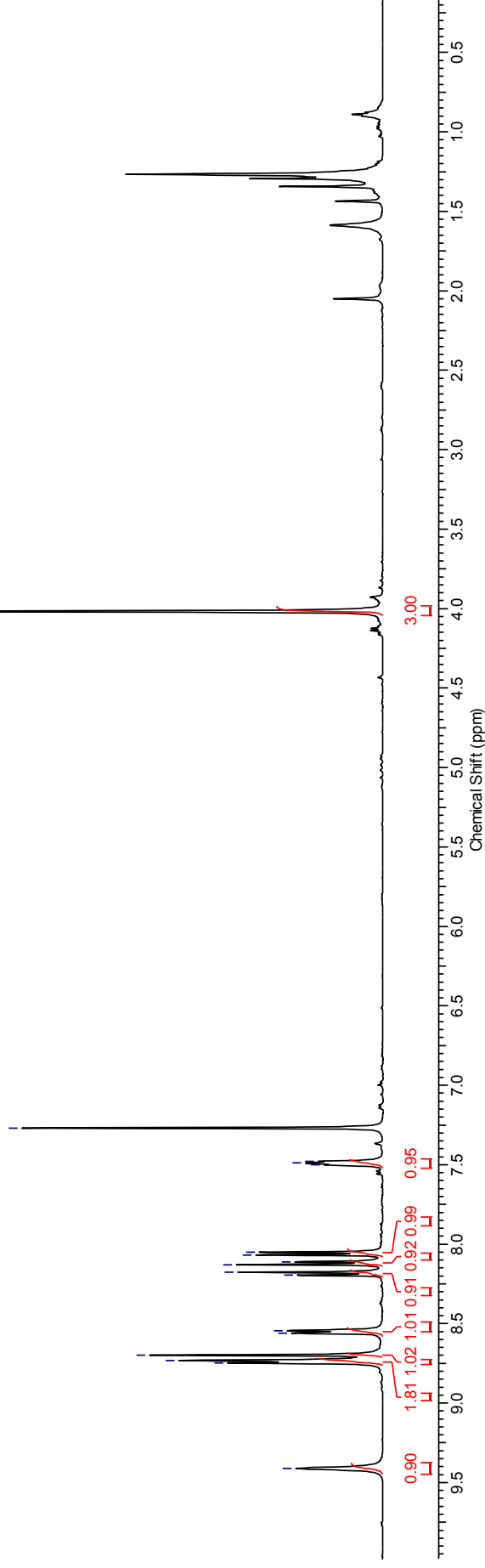
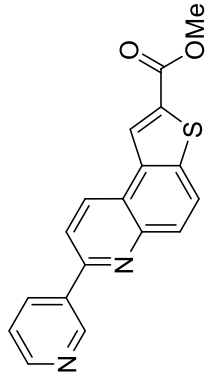
M07(m)

M08(dd)

8.75
8.73
8.70
8.56
8.54
8.20
8.18
8.13
8.11
8.07
8.05
7.50
7.49
7.48
7.27

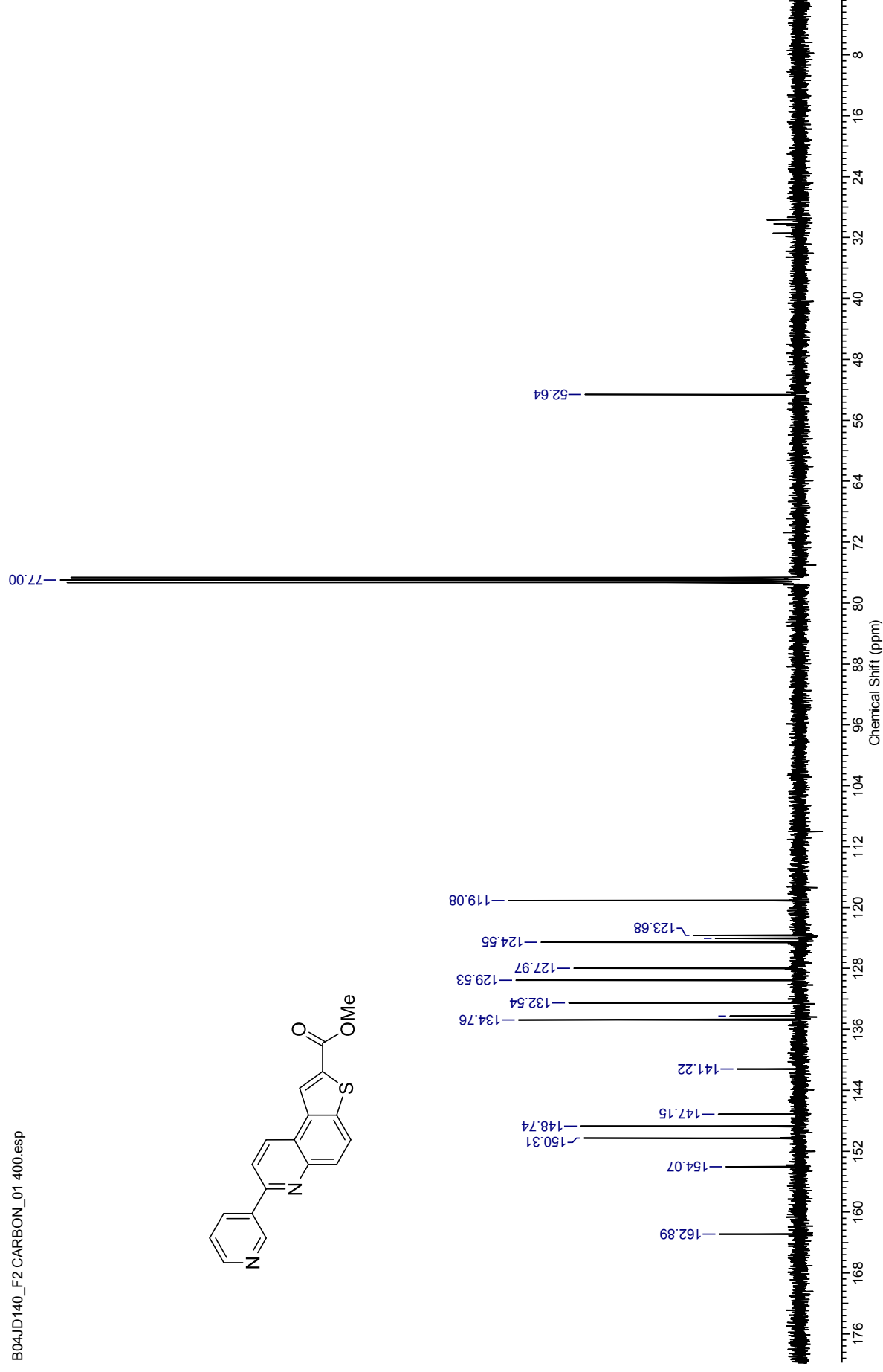
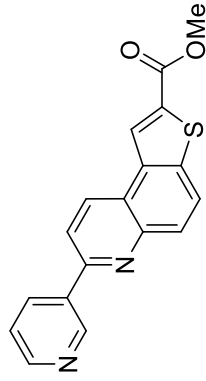
M09(s)

4.02



¹³C NMR (100 MHz, CDCl₃) for Methyl 7-(pyridin-3-yl)thieno[3,2-*f*]quinoline-2-carboxylate

B04JD140_F2 CARBON_01 400.esp

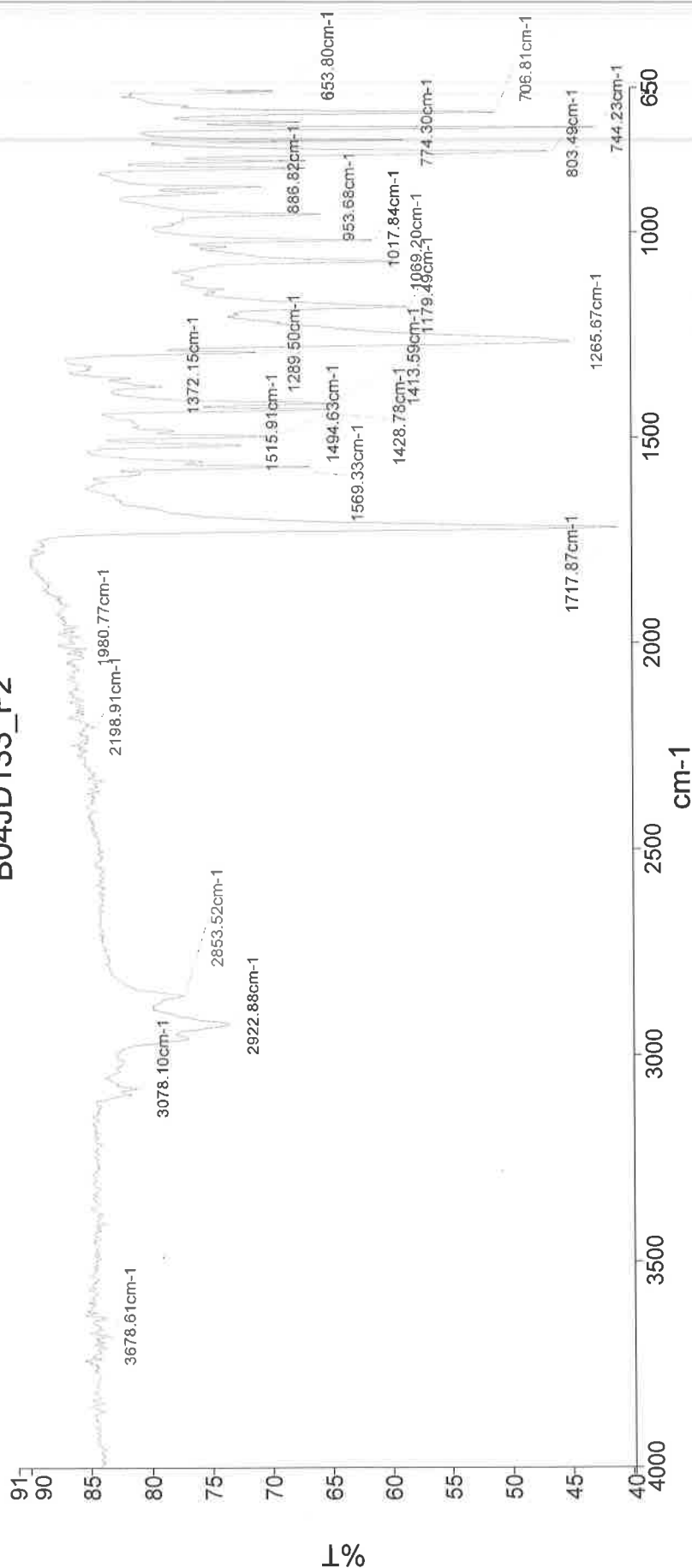




PerkinElmer Spectrum Version 10.03.06
05 April 2016 10:43

Analyst
Date
Administrator
05 April 2016 10:43

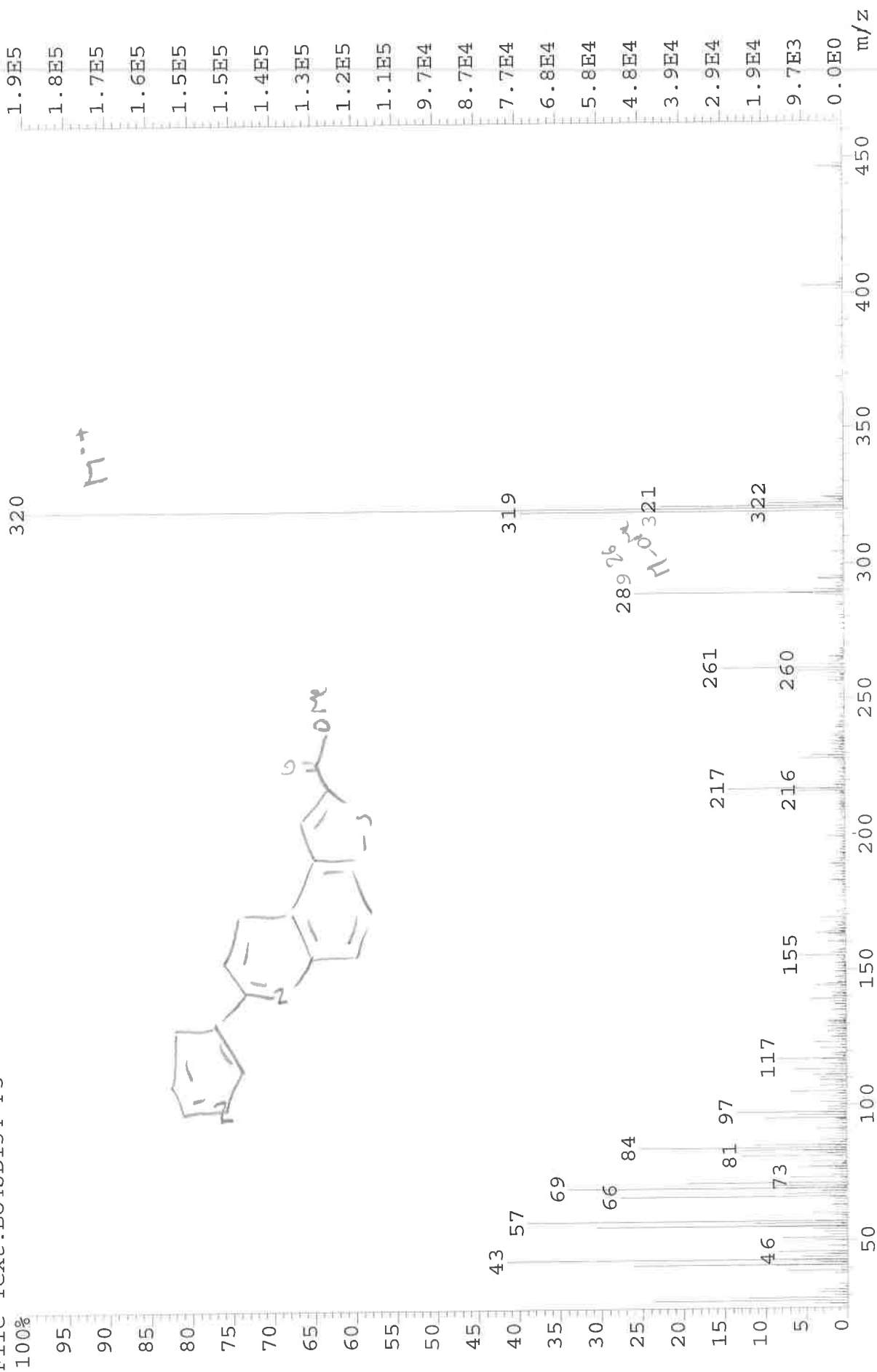
B04JD133_F2



2922 C-H str.
1718 C=O str.
1569 C-C str.
1266 C-N str.
1179 C-H str.
1018 C-O str.
803 C-H

249-006 Sample 006 By Administrator Date Tuesday, April 05 2016

File: JESS6504 Ident: 42 Acq: 15-JAN-2016 16:22:27 +2:02 Cal: LO
 AutoSpecE EI+ Magnet BpI: 193355 TIC: 3036332 Flags: HALL
 File Text: B04JD134-F3



Generic Display Report

Analysis Info

Analysis Name D:\Data\Alinanopos\JESS6504_000002.d
Method pos20090608esi
Sample Name POS ESI POSATIVE BO4JD134-F3
Comment

Acquisition Date 15/01/2016 15:14:21

Operator Administrator
Instrument apex-III

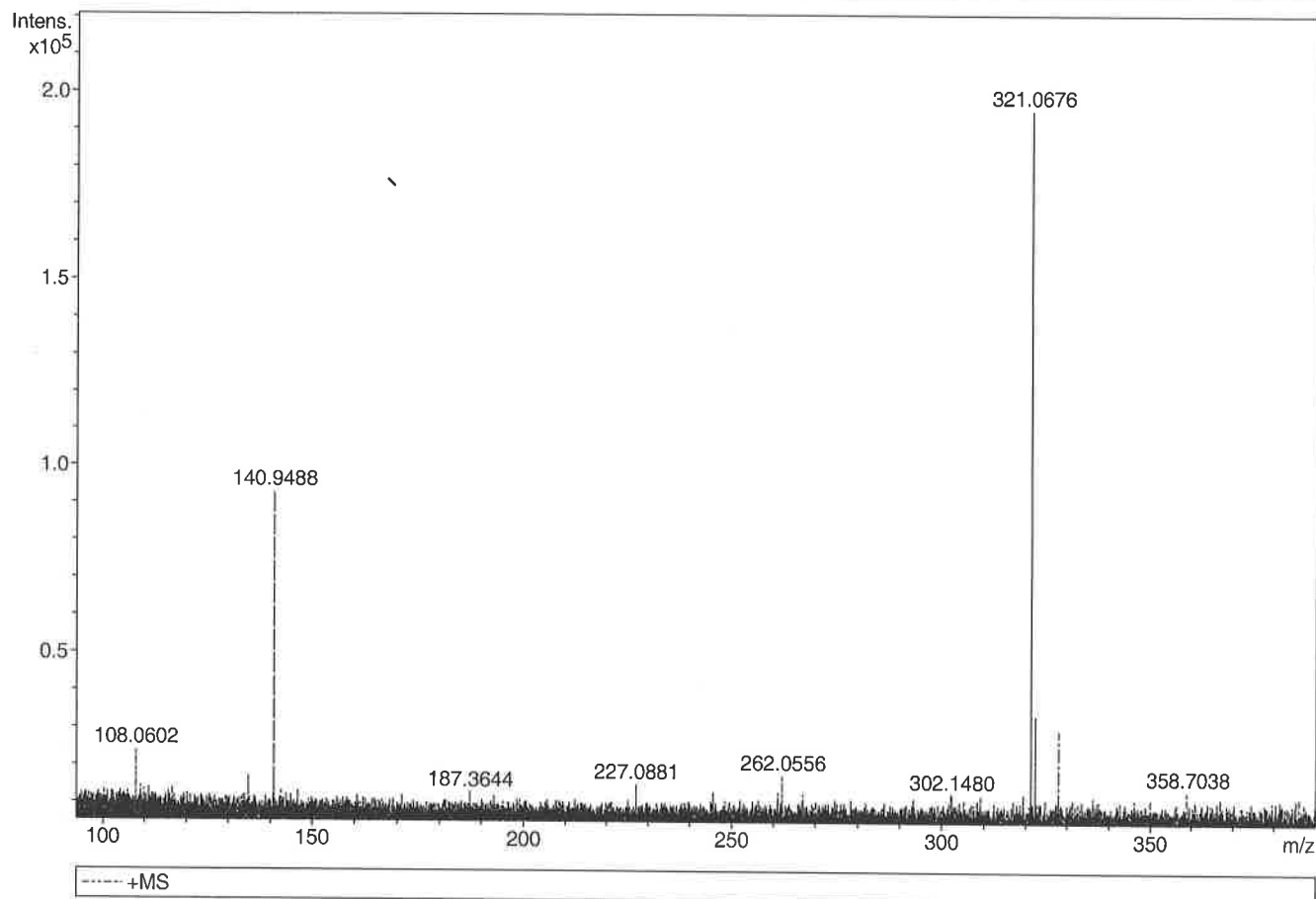
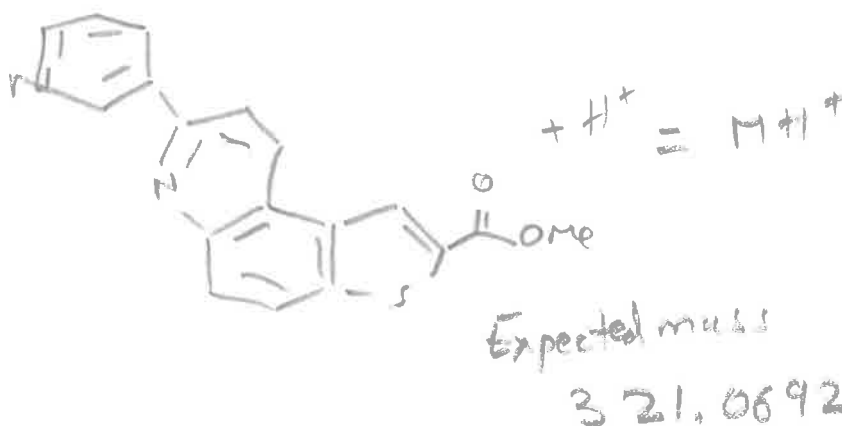
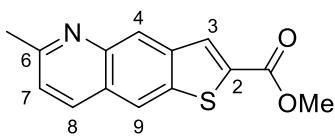


Table 'GenFormulaResults' could not be found in this analysis



Methyl 6-methylthieno[2,3-g]quinoline-2-carboxylate (196)



¹H NMR (500 MHz, CDCl₃) for Methyl 6-methylthieno[2,3-*g*]quinoline-2-carboxylate

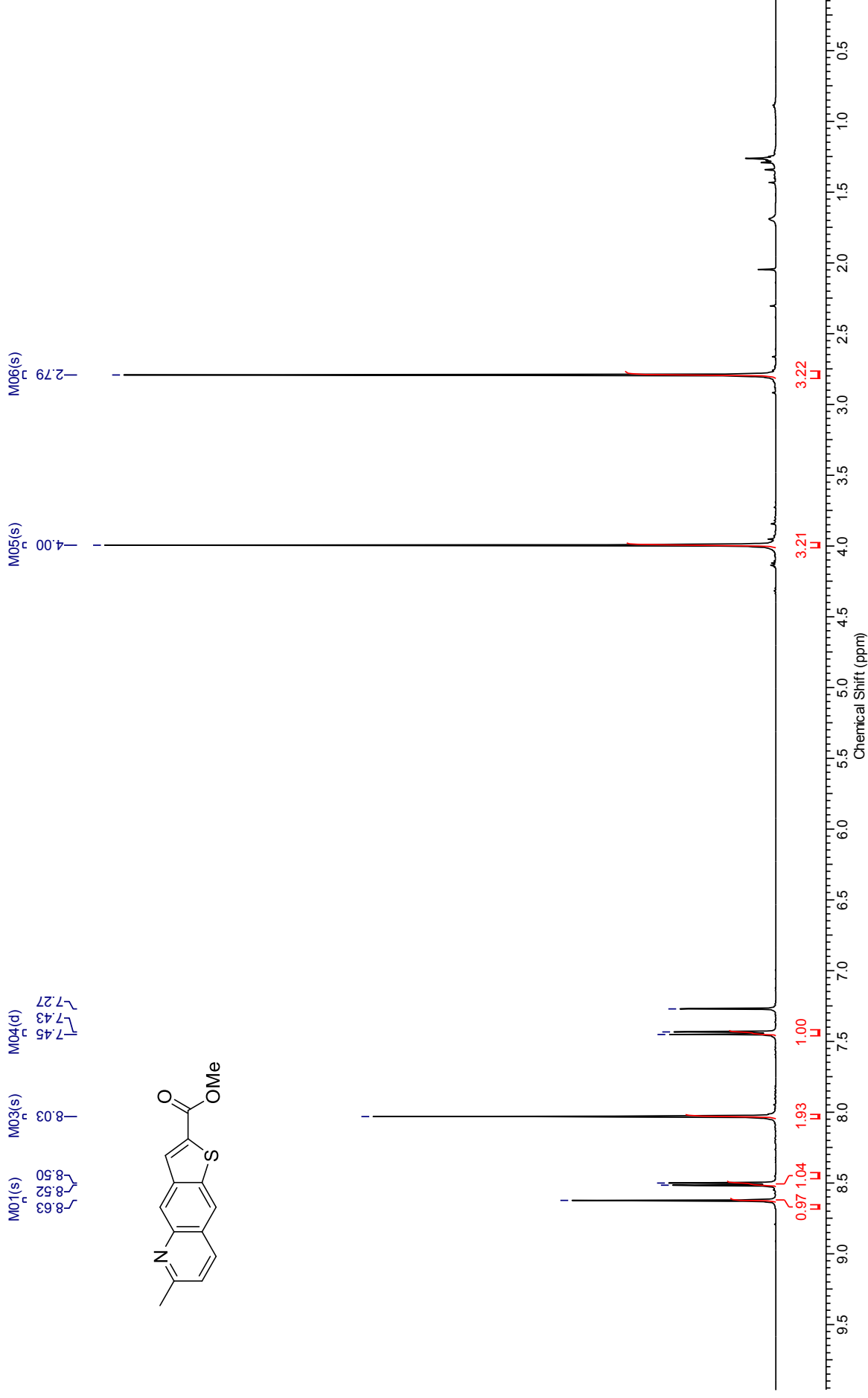
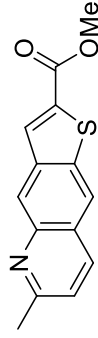
B04JD140_F1.esp

M02(d)

M01(s)
8.63
8.52
8.50

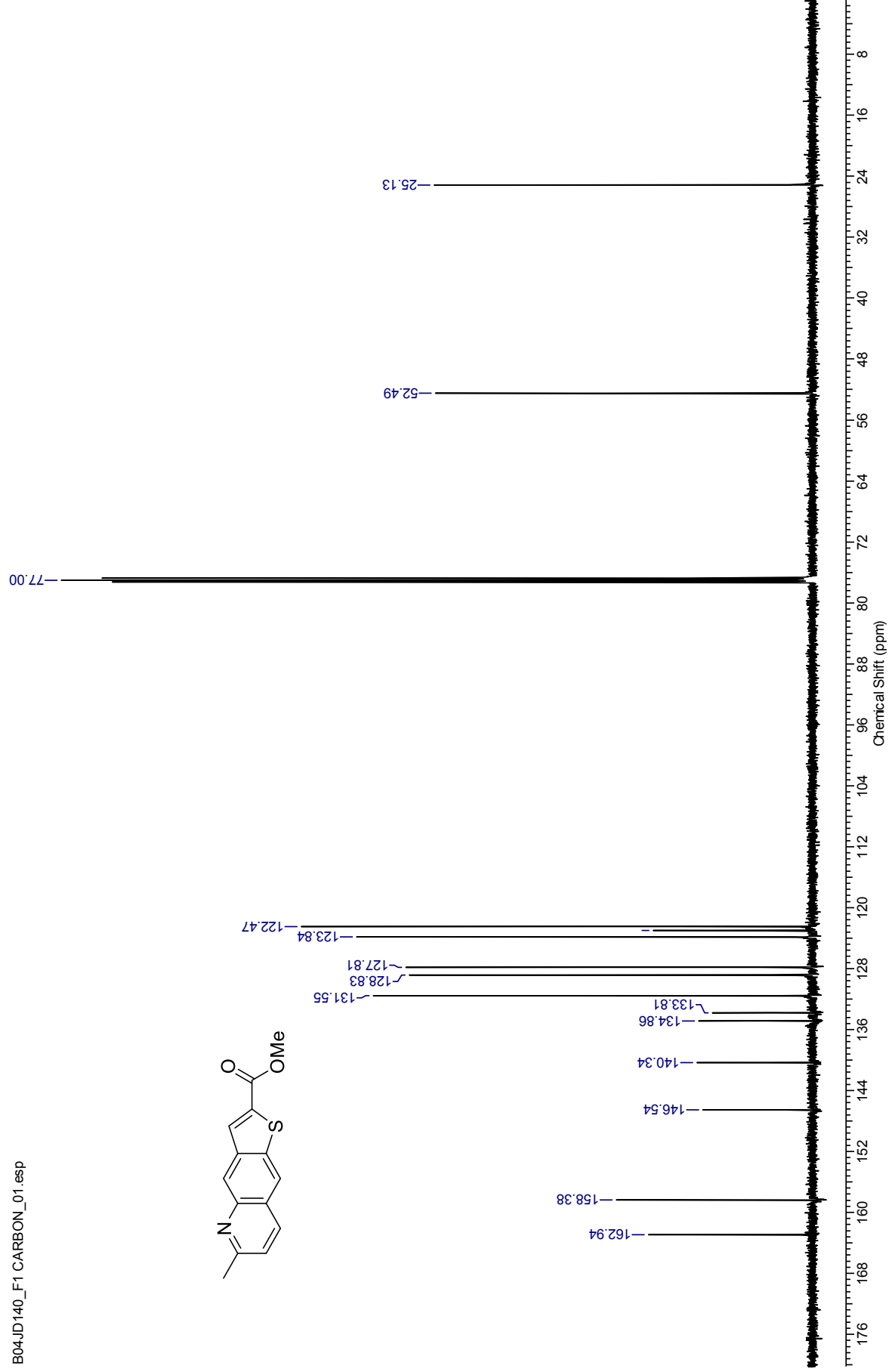
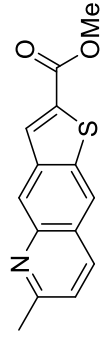
M03(s)
8.03

M04(d)
7.45
7.43
7.27

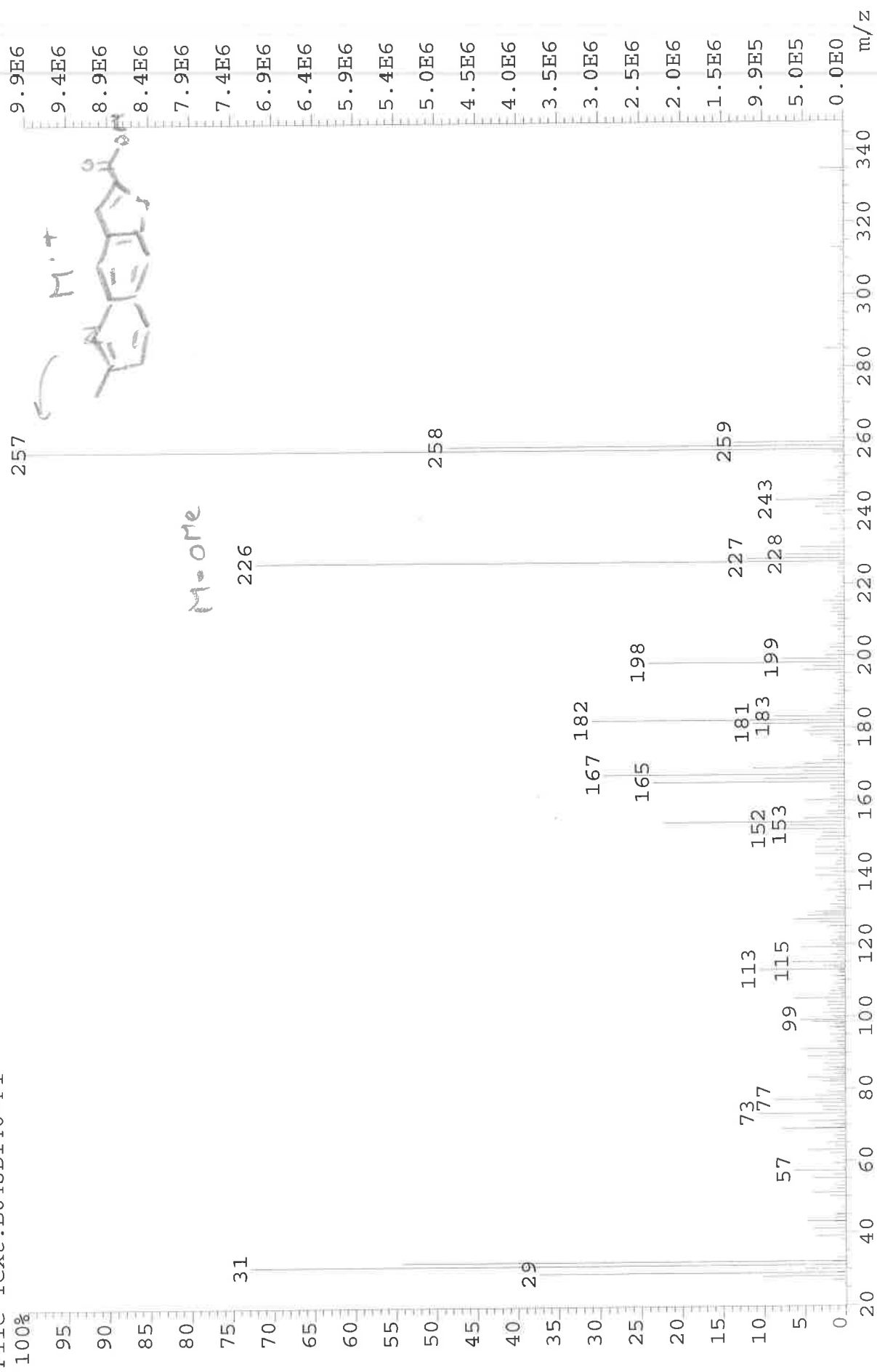


¹³C NMR (126 MHz, CDCl₃) for Methyl 6-methylthieno[2,3-*g*]quinoline-2-carboxylate

B04JD140_F1 CARBON_01.esp



File: JESS6614 Ident: 20 Acq: 10-FEB-2016 16:58:35 +1:17 Cal: CAL1
AutoSpecE EI+ Magnet BpI: 9911362 TIC: 112181592 Flags: HALL
File Text: B04JD140-F1



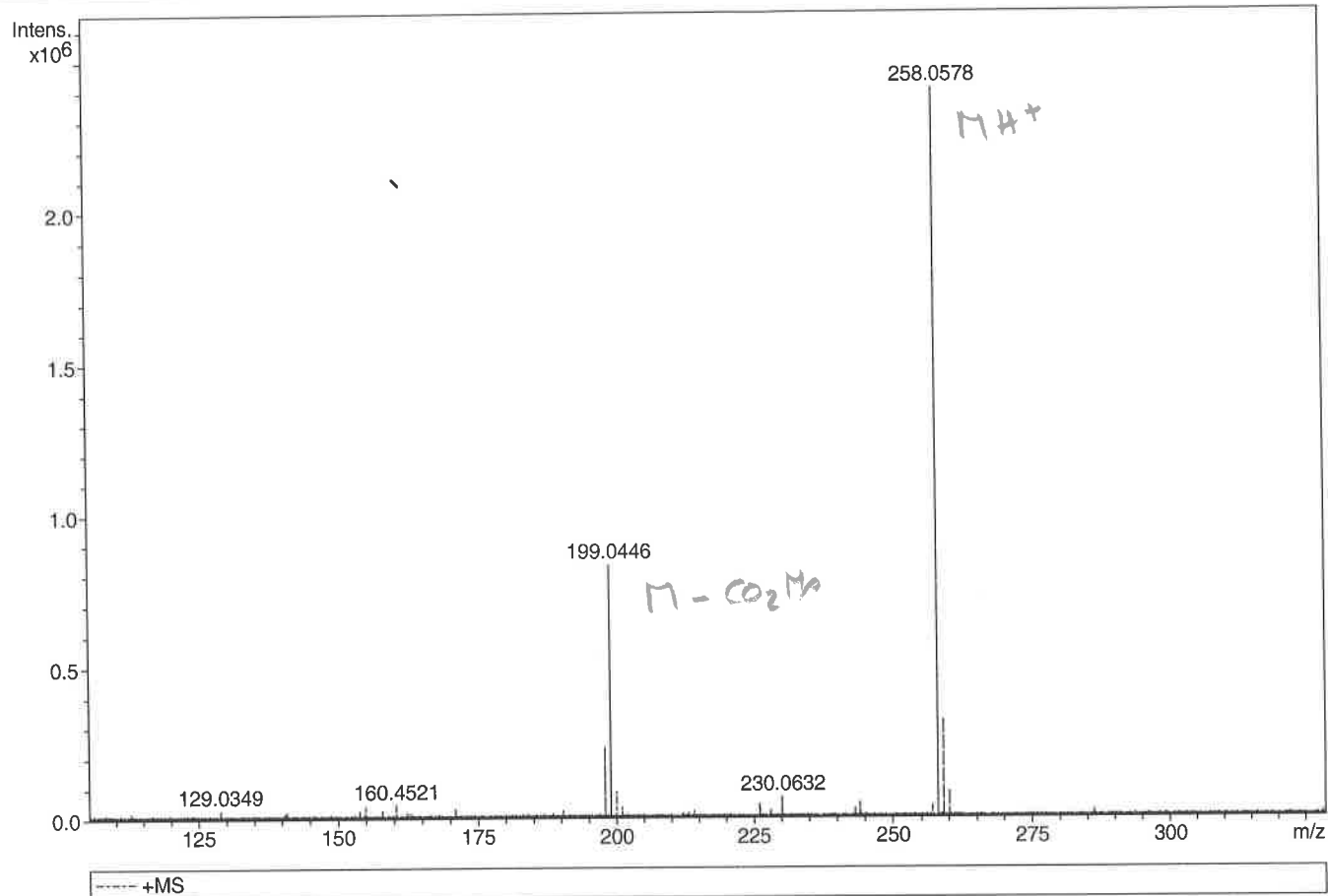
Generic Display Report

Analysis Info

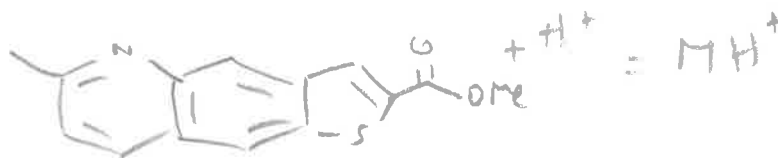
Analysis Name D:\Data\Alinanopos\JESS_6614_000001.d
 Method pos20090608esi
 Sample Name POT ESI B04JD140-F1
 Comment

Acquisition Date 10/02/2016 16:13:27

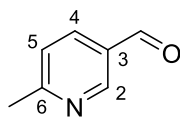
Operator Administrator
 Instrument apex-III



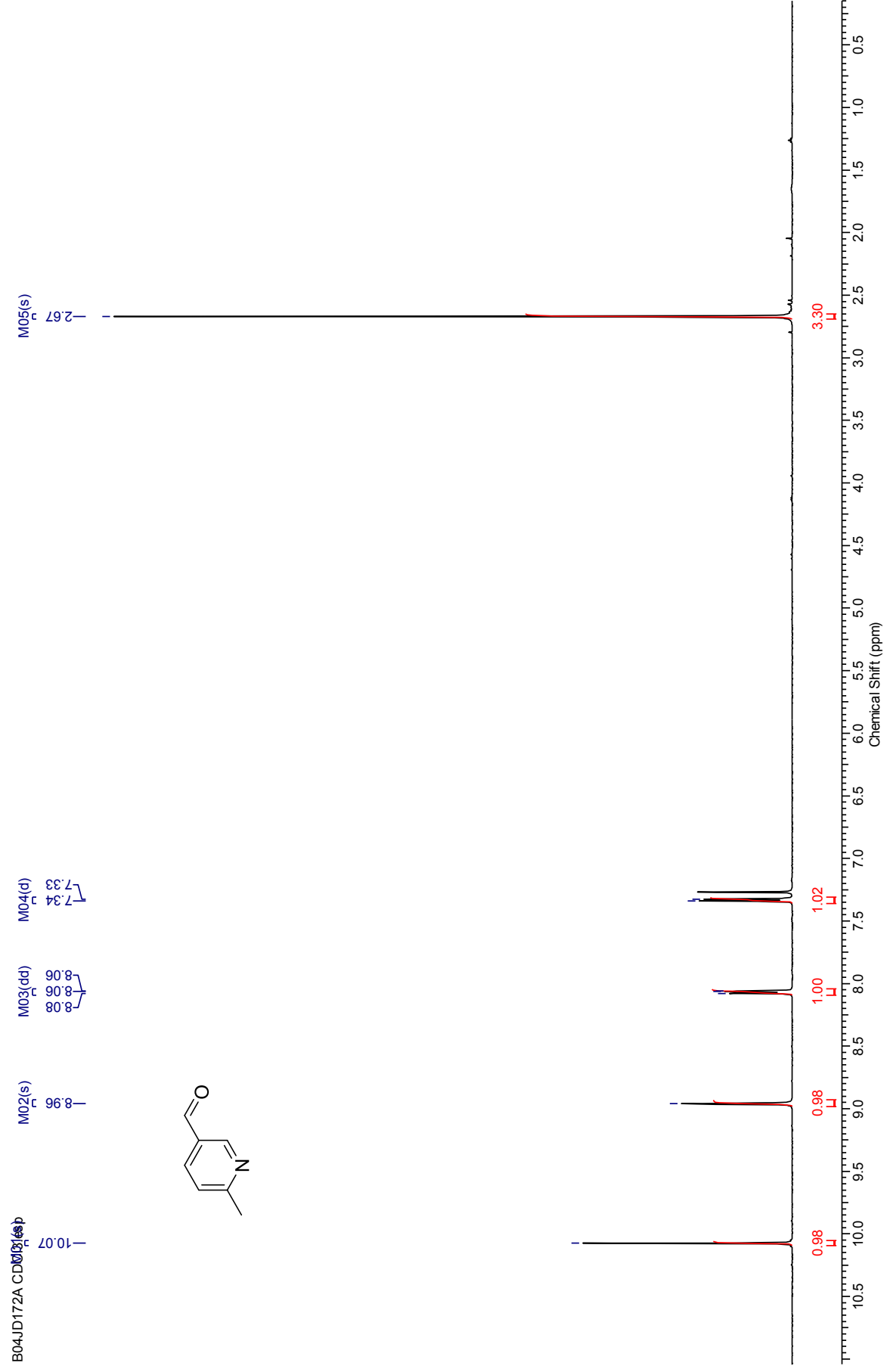
Sum Formula	Sigma	m/z	Err [ppm]	Mean Err [ppm]	Err [mDa]	rdb	N Rule	e ⁻
C ₁₄ H ₁₂ N ₁ O ₂ S ₁	0.029	258.0583	2.12	1.86	0.48	9.50	ok	even



6-Methylpyridine-3-carboxaldehyde (190)

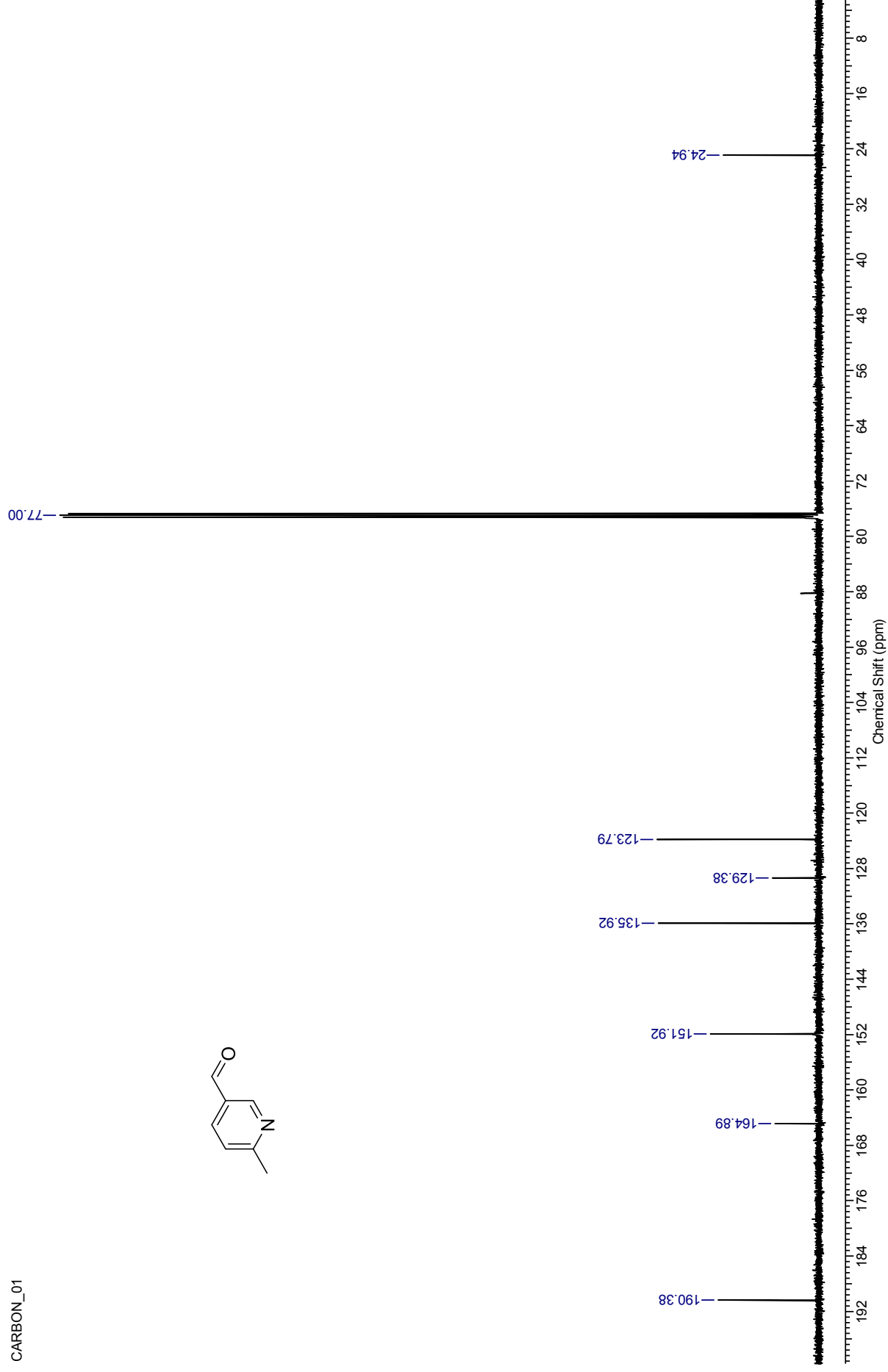
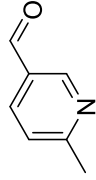


¹H NMR (500 MHz, CDCl₃) for 6-Methylpyridine-3-carboxaldehyde

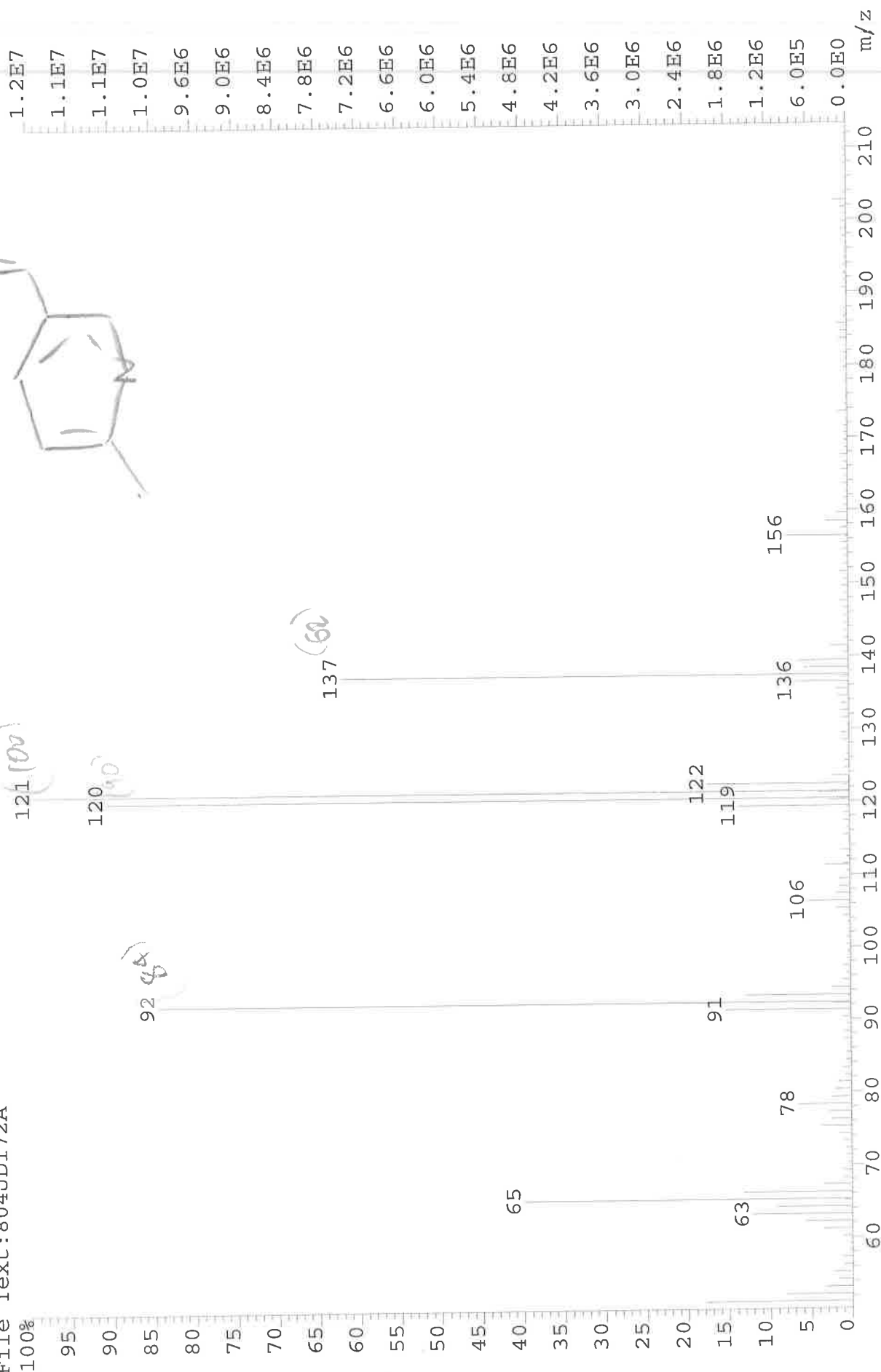


¹³C NMR (126 MHz, CDCl₃) for 6-Methylpyridine-3-carboxaldehyde

CARBON_01



File: JESS6645 Ident: 35 Acq: 29-FEB-2016 11:54:34 +2:12 Cal: CAL1
AutoSpecE EI+ Magnet BpI: 11996711 TIC: 97060856 Flags: HALL
File Text: 804JD172A



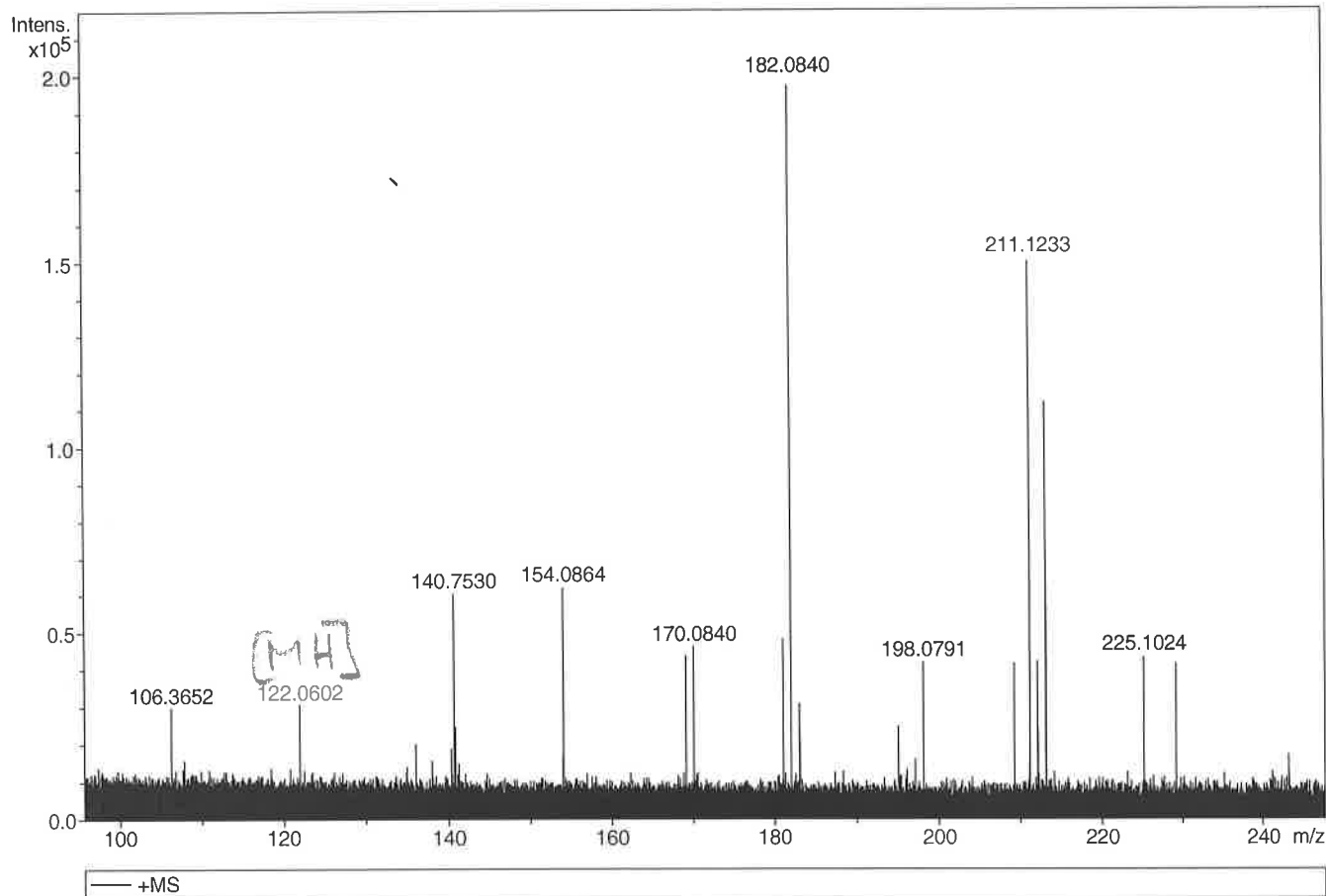
Generic Display Report

Analysis Info

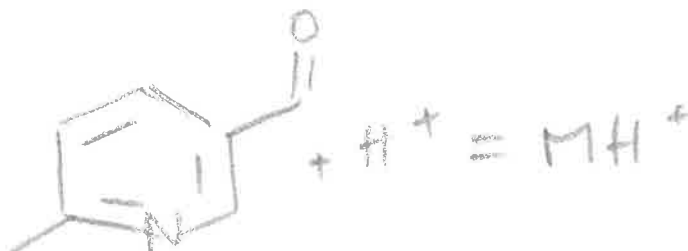
Analysis Name D:\Data\Alinanopos\JESS_6645_000001.d
 Method pos20090608esi
 Sample Name POT ESI 804JD172A
 Comment

Acquisition Date 29/02/2016 11:20:25

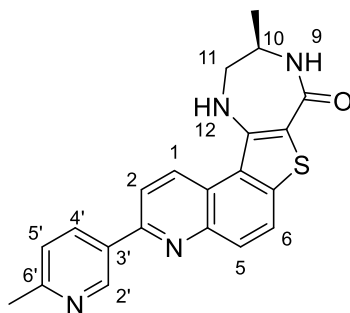
Operator Administrator
 Instrument apex-III



Sum Formula	Sigma	m/z	Err [ppm]	Mean Err [ppm]	Err [mDa]	rdB	N Rule	e ⁻
C ₇ H ₈ N ₁ O ₁	0.397	122.0600	-1.46	24.77	3.03	4.50	ok	even

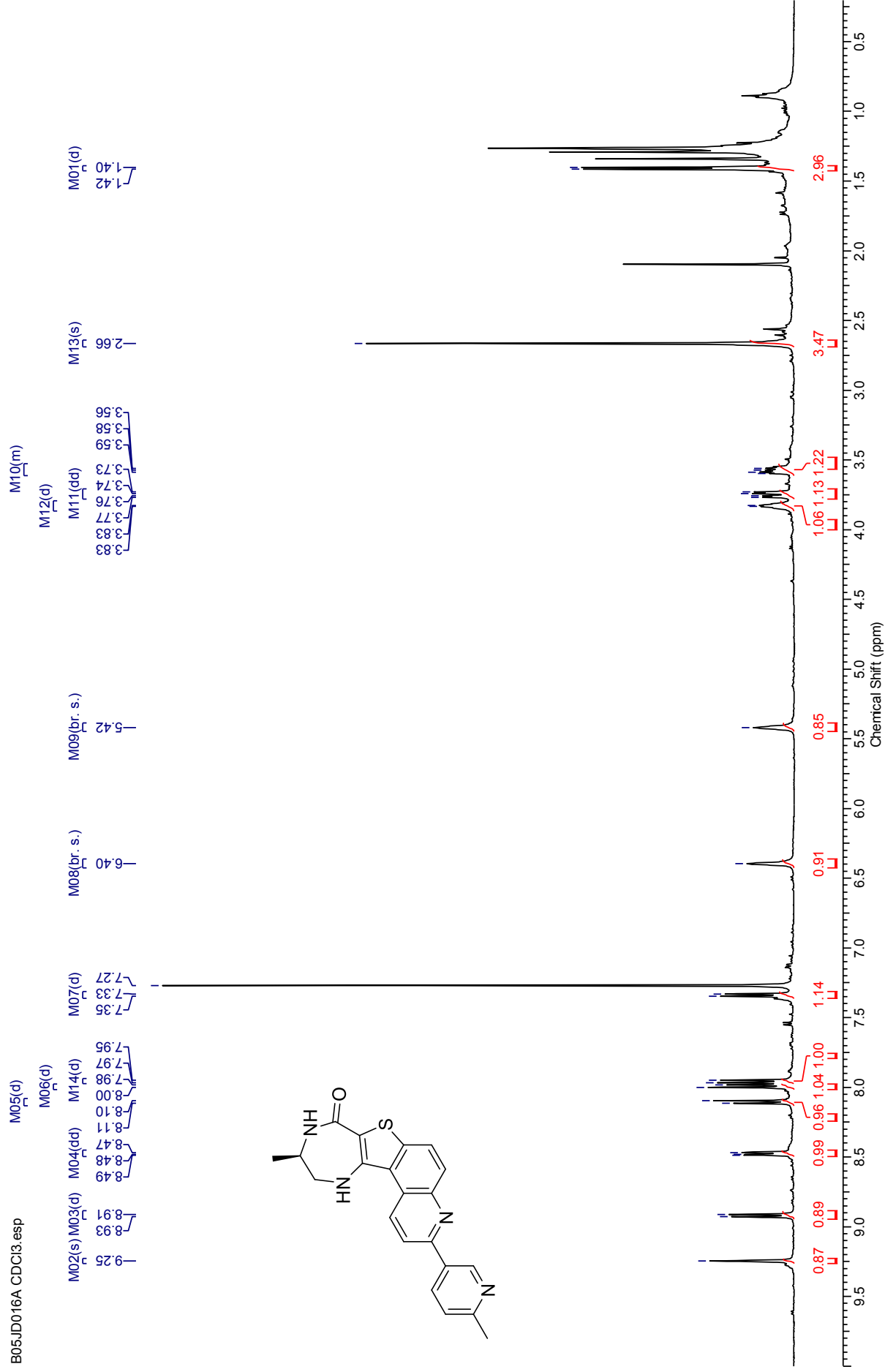


(R)-10-Methyl-3-(6-methylpyridin-3-yl)-9-10-11-12-tetrahydro-8H-[1,4]diazepino[5',6':4,5]thieno[3,2-f]quinoline-8-one. PF-3644022
(25)



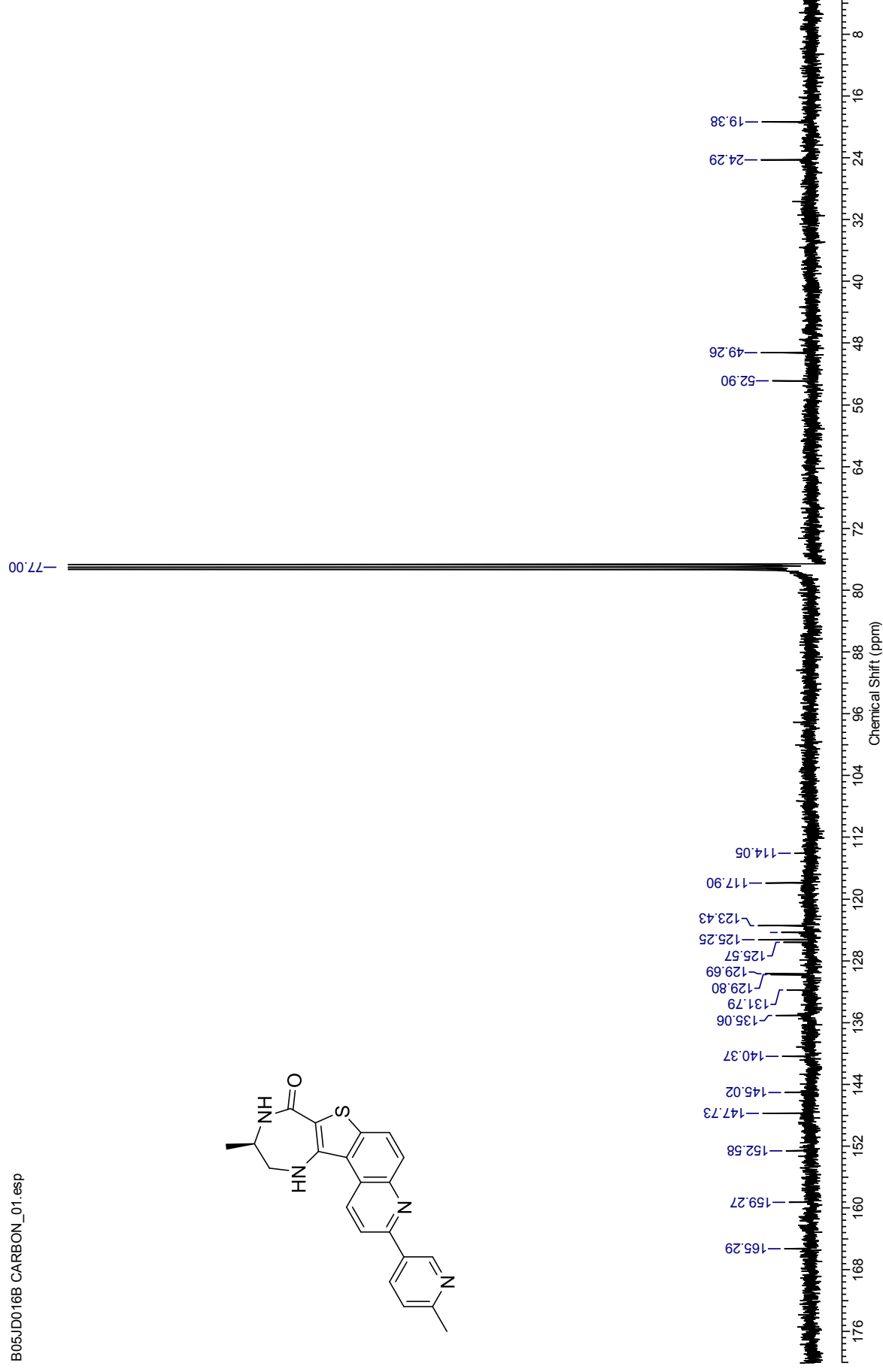
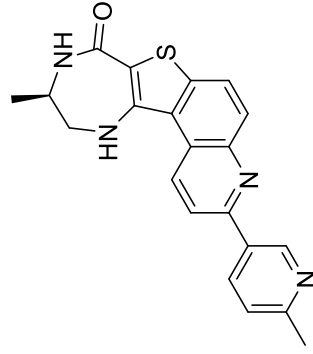
¹H NMR (500 MHz, CDCl₃) for (R)-10-Methyl-3-(6-methylpyridin-3-yl)-9-10-11-12-tetrahydro-8H-[1,4]diazepino[5',6':4,5]thieno[3,2-f]quinoline-8-one

B05JD016A CDCl₃.esp



¹³C NMR (100 MHz, CDCl₃) for (R)-10-Methyl-3-(6-methylpyridin-3-yl)-9-10-11-12-tetrahydro-8H-[1,4]diazepino[5',6':4,5]thieno[3,2-f]quinoline-8-one

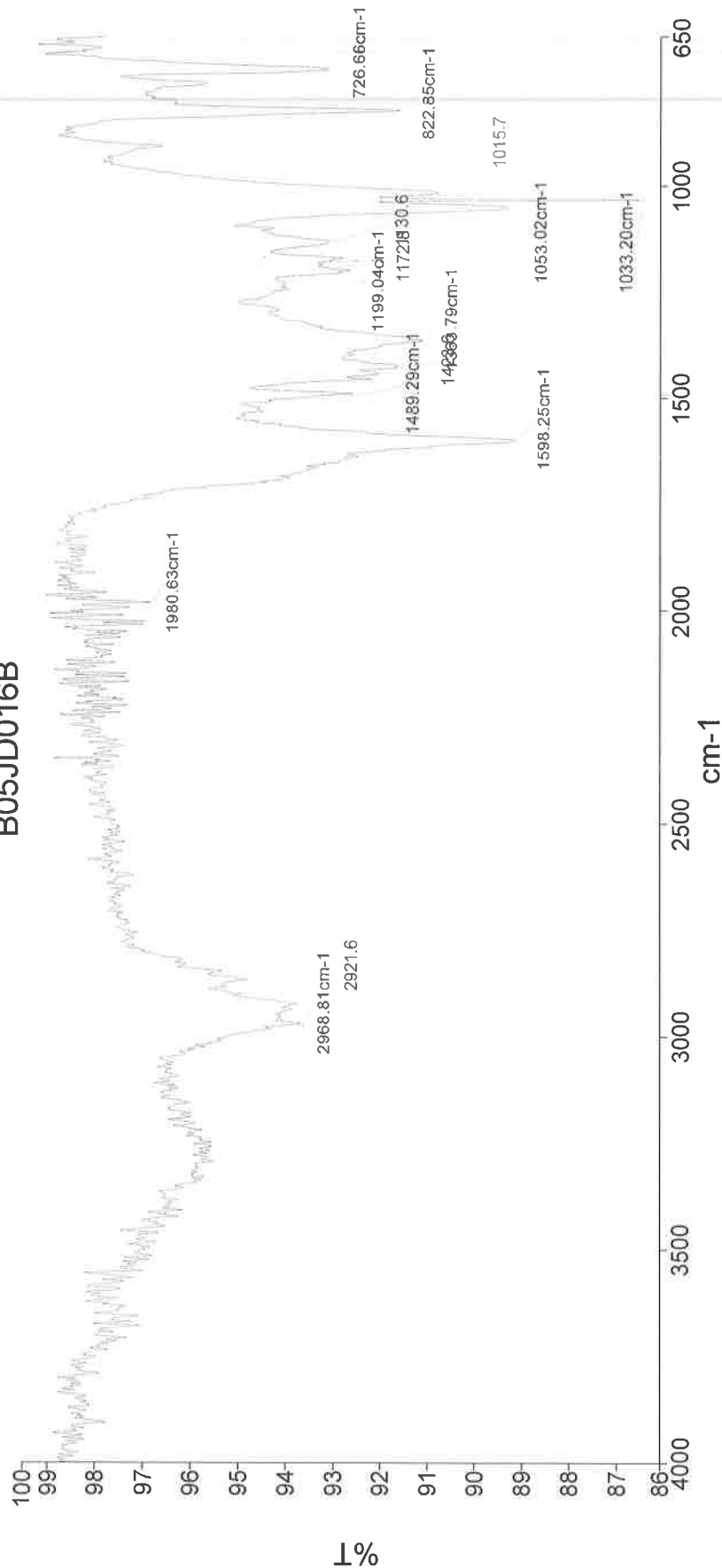
B05JD016B CARBON_01.esp



Analyst
Date

Administrator
05 April 2016 10:55

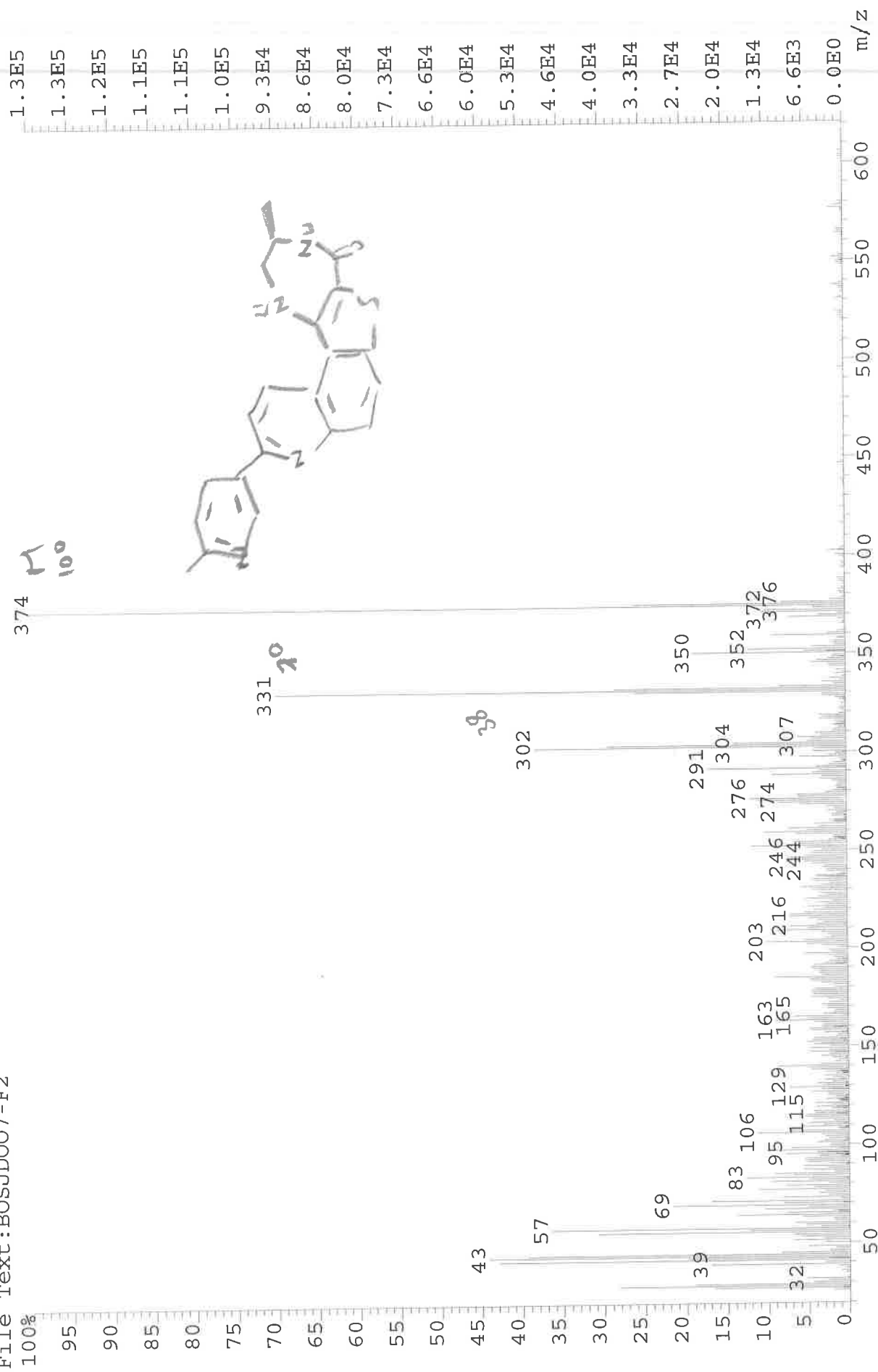
B05JD016B



2969 C-H str.
1598 N-H str. + C=O broad!
1489 C-C str.
1364 C-N str. Ar.
1199 C-N str. Alk.
1053 C-N str.
1033 C-O str.
823 C-H str.

249-013_1 Sample 013 By Administrator Date Tuesday, April 05 2016

File: JESS6496 Ident: 25 Acq: 14-MAR-2016 12:43:17 +1:35 Cal: CAL1
AutoSpecE EI+ Magnet BpI: 132862 TIC: 2836681 Flags: HALL
File Text: BOSJDO07-F2



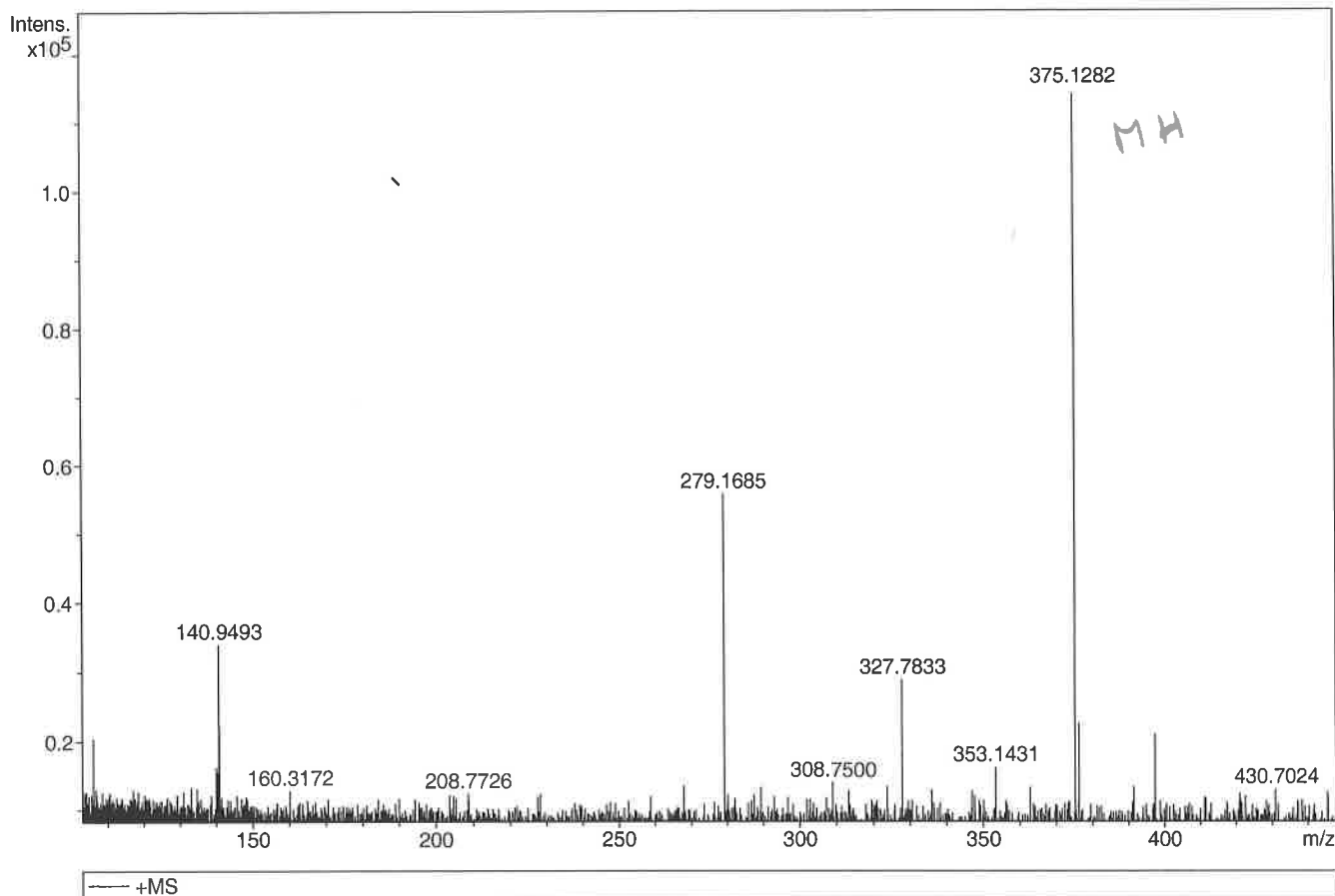
Generic Display Report

Analysis Info

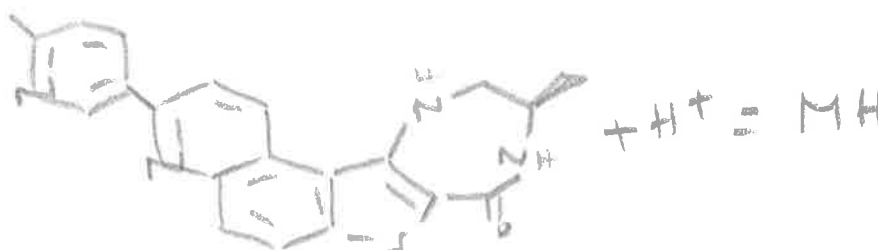
Analysis Name D:\Data\Alinanopos\JESS6496_000001.d
 Method pos20090608esi
 Sample Name POS ESI BOSJD007-F2
 Comment

Acquisition Date 14/03/2016 12:18:03

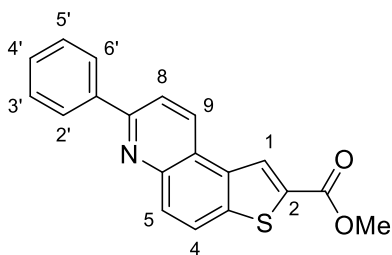
Operator Administrator
 Instrument apex-III



Sum Formula	Sigma	m/z	Err [ppm]	Mean Err [ppm]	Err [mDa]	rdB	N Rule	e ⁻
C 21 H 19 N 4 O 1 S 1	0.049	375.1274	-2.22	-2.10	-0.79	14.50	ok	even



Methyl 7-phenylthieno[3,2-f]quinoline-2-carboxylate (199)



¹H NMR (500 MHz, CDCl₃) for Methyl 7-phenylthieno[3,2-f]quinoline-2-carboxylate

B05JD008_F1.esp

M05(d)

M06(d)

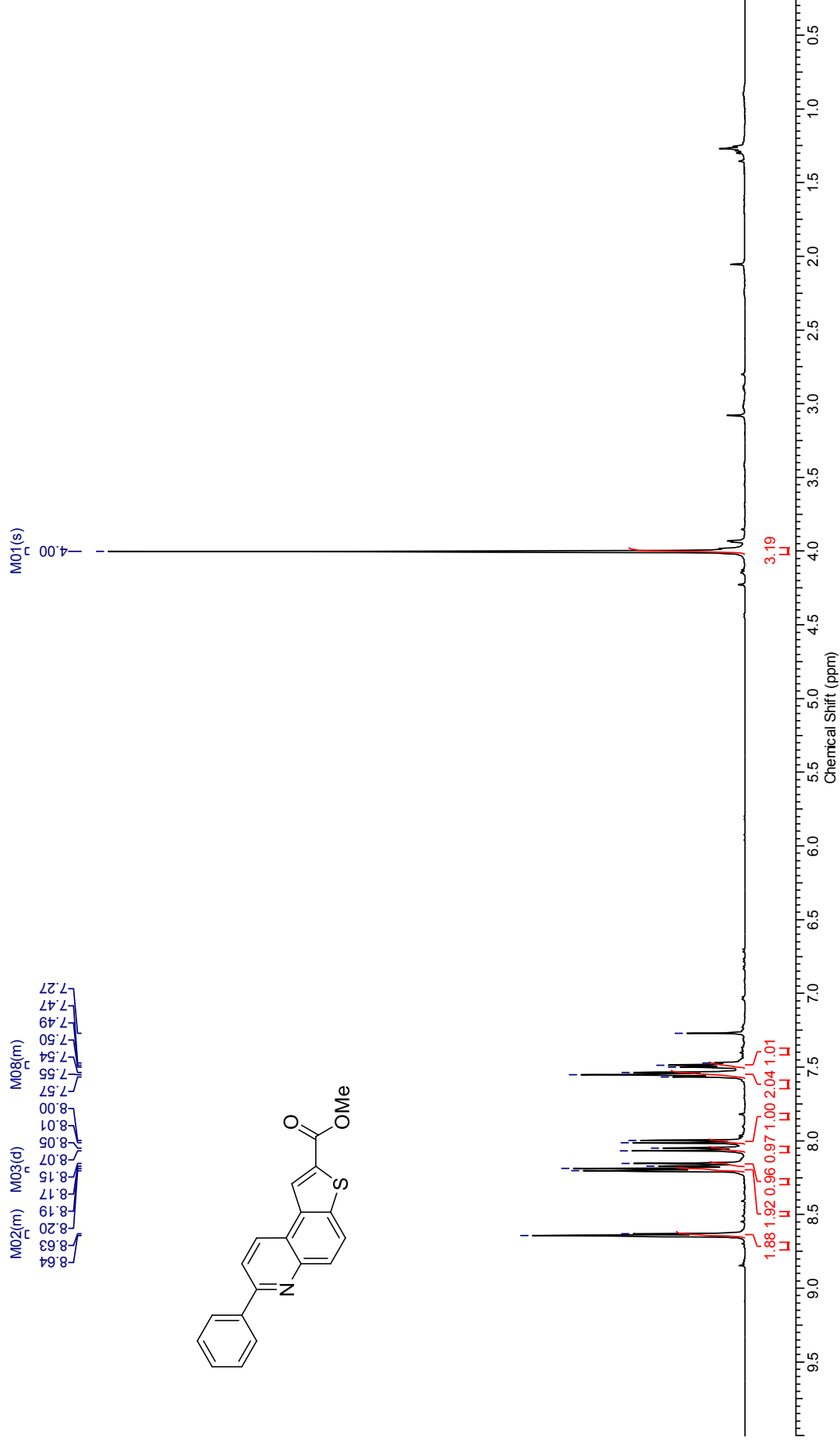
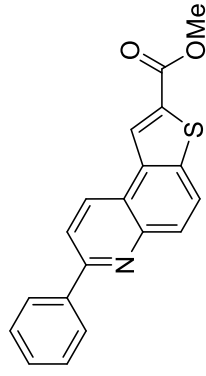
M04(d)

M07(m)

M03(d)

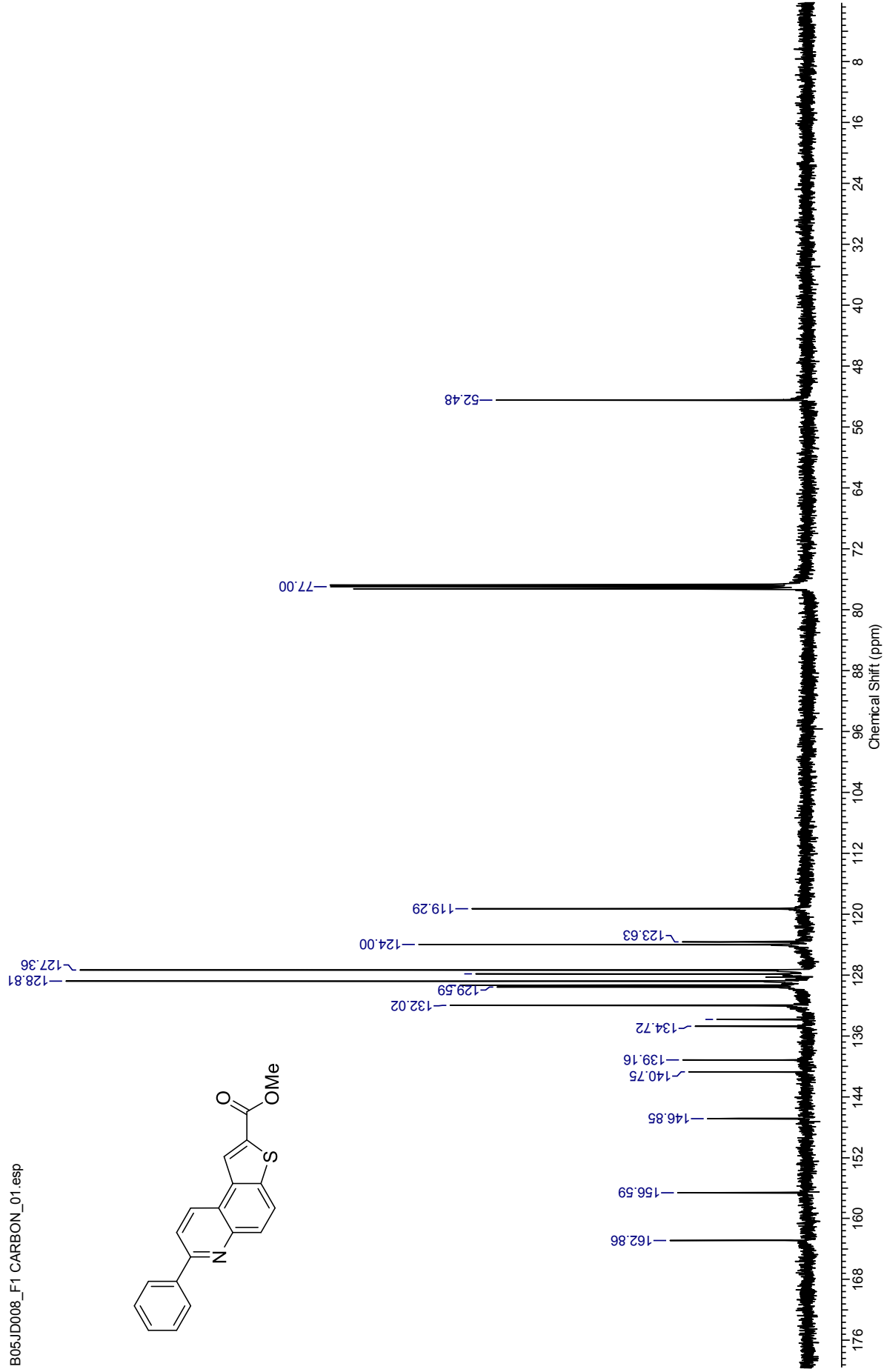
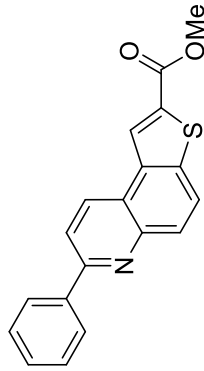
M08(m)

8.64
8.63
8.20
8.19
8.17
8.15
8.07
8.05
8.01
7.57
7.55
7.54
7.50
7.49
7.47
7.27



¹³C NMR (126 MHz, CDCl₃) for Methyl 7-phenylthieno[3,2-f]quinoline-2-carboxylate

B05JD008_F1 CARBON_01.esp



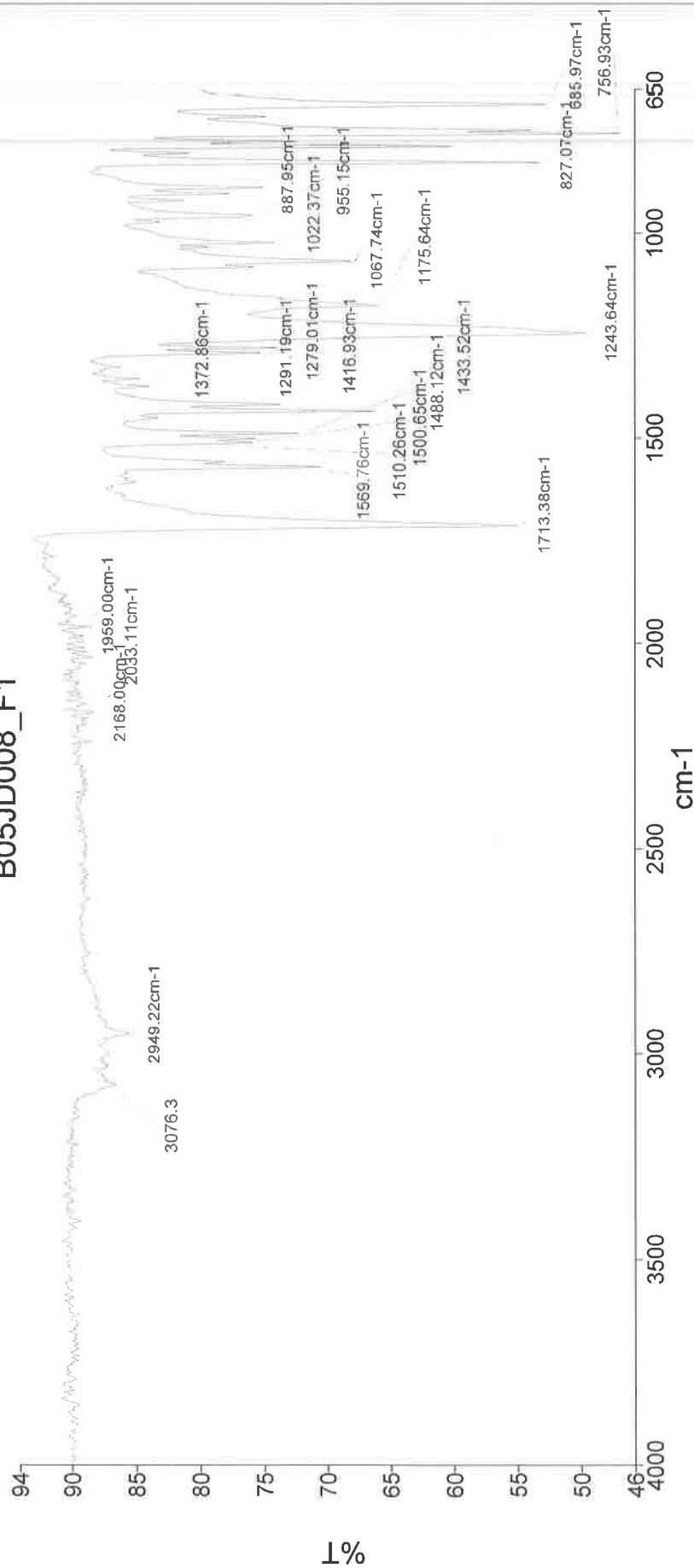


PerkinElmer Spectrum Version 10.03.06
05 April 2016 10:47

Analyst
Date

Administrator
05 April 2016 10:47

B05JD008_F1

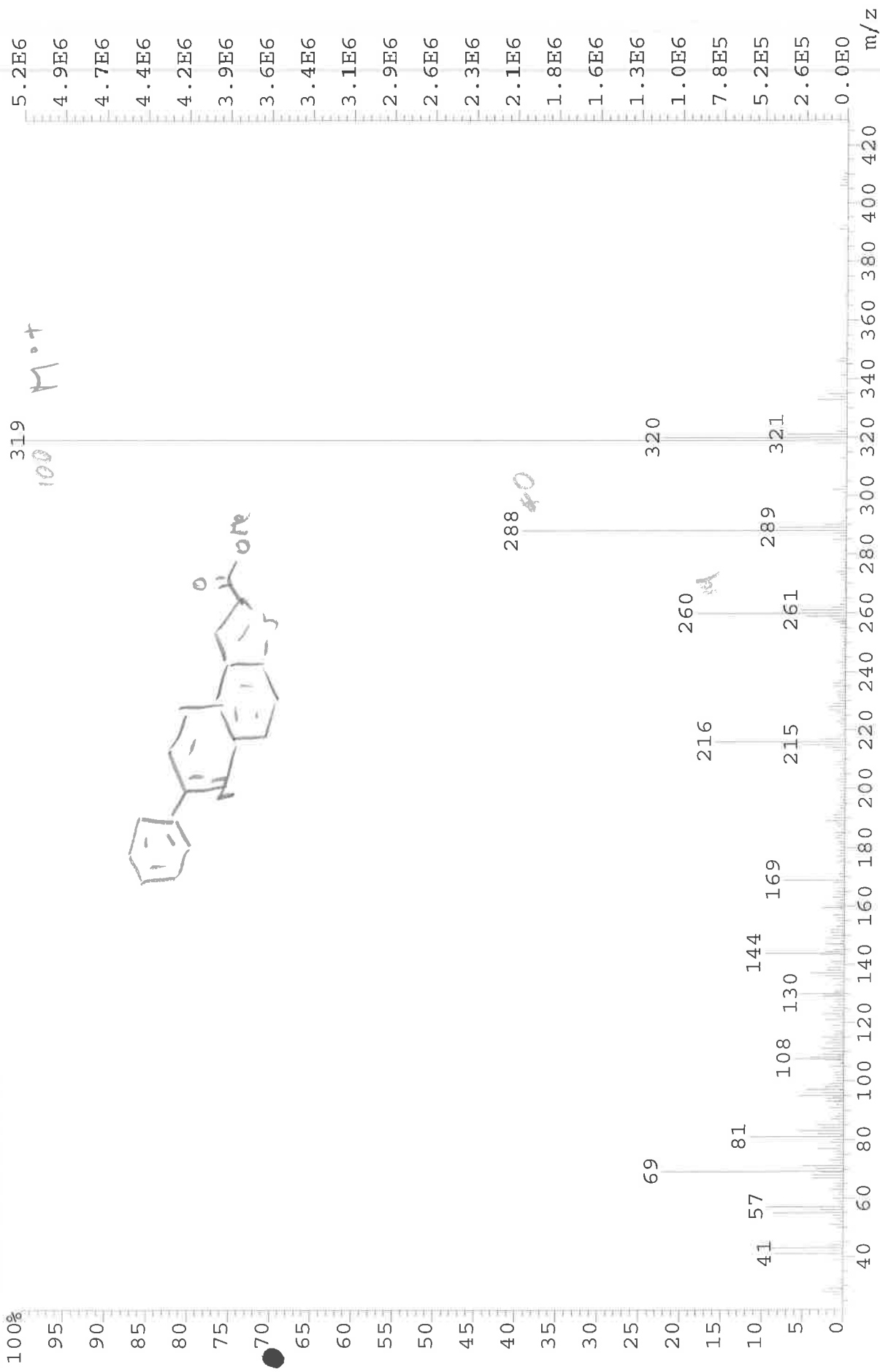


3076
1713
1570

1434
1244
1176
1068
827

249-007 Sample 007 By Administrator Date Tuesday, April 05 2016

File: JESS_6859 Ident: 9 Acq: 1-APR-2016 11:32:59 +0:37 Cal: CAL1
AutoSpecE- EI+ Magnet BpI: 5200947 TIC: 35246132 Flags: HALL
File Text: BOSJD008-F1



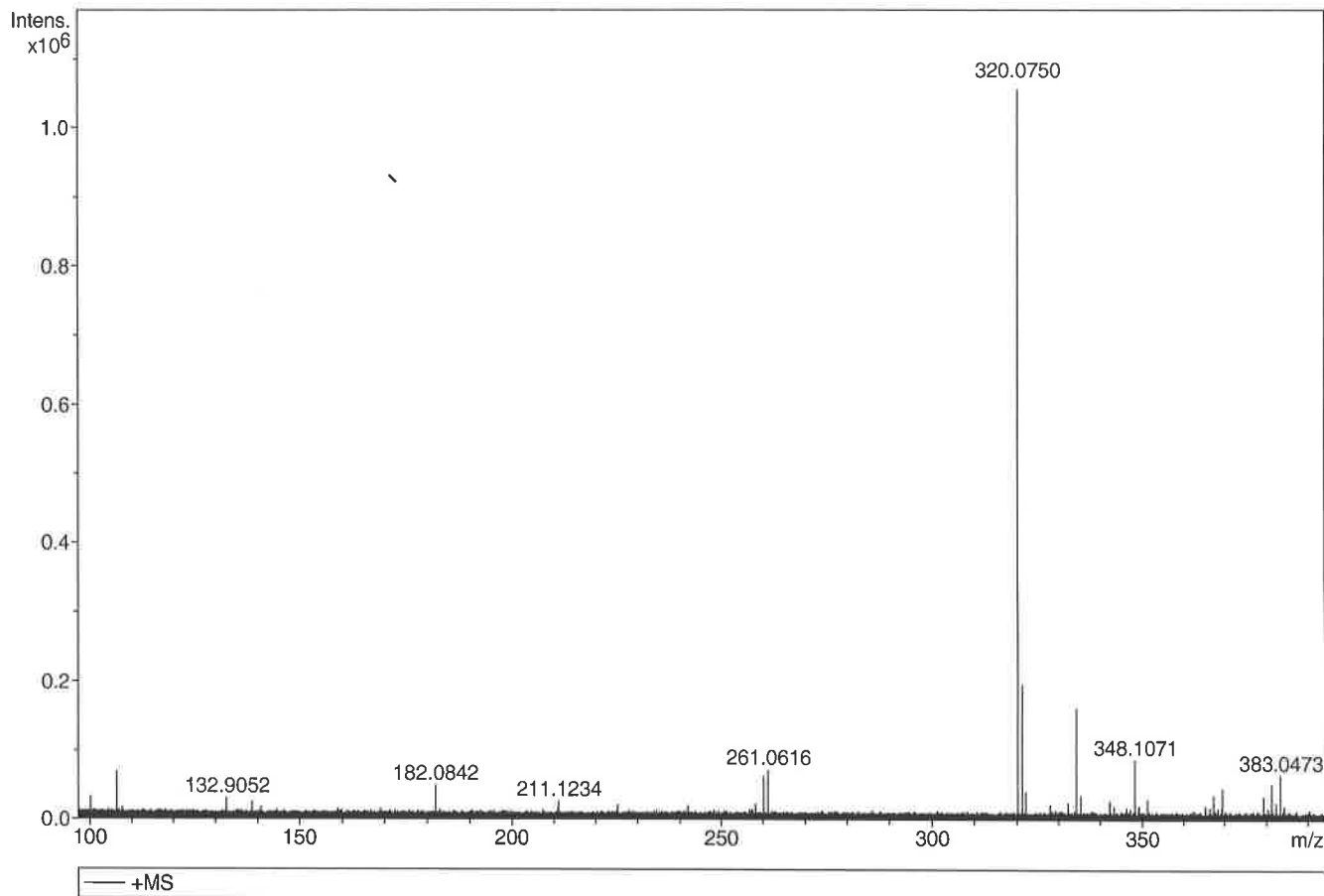
Generic Display Report

Analysis Info

Analysis Name D:\Data\Alinanopos\JESS_6859_000002.d
Method pos20090608esi
Sample Name POS ESI BOSJD008-F1
Comment

Acquisition Date 01/04/2016 11:49:09

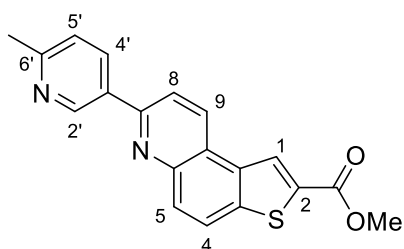
Operator Administrator
Instrument apex-III



Sum	Formula	Sigma	m/z	Err [ppm]	Mean Err [ppm]	Err [mDa]	rdb	N Rule	e ⁻
C 19 H 14 N 1 O 2 S 1		0.043	320.0740	-3.34	-3.03	-0.97	13.50	ok	even

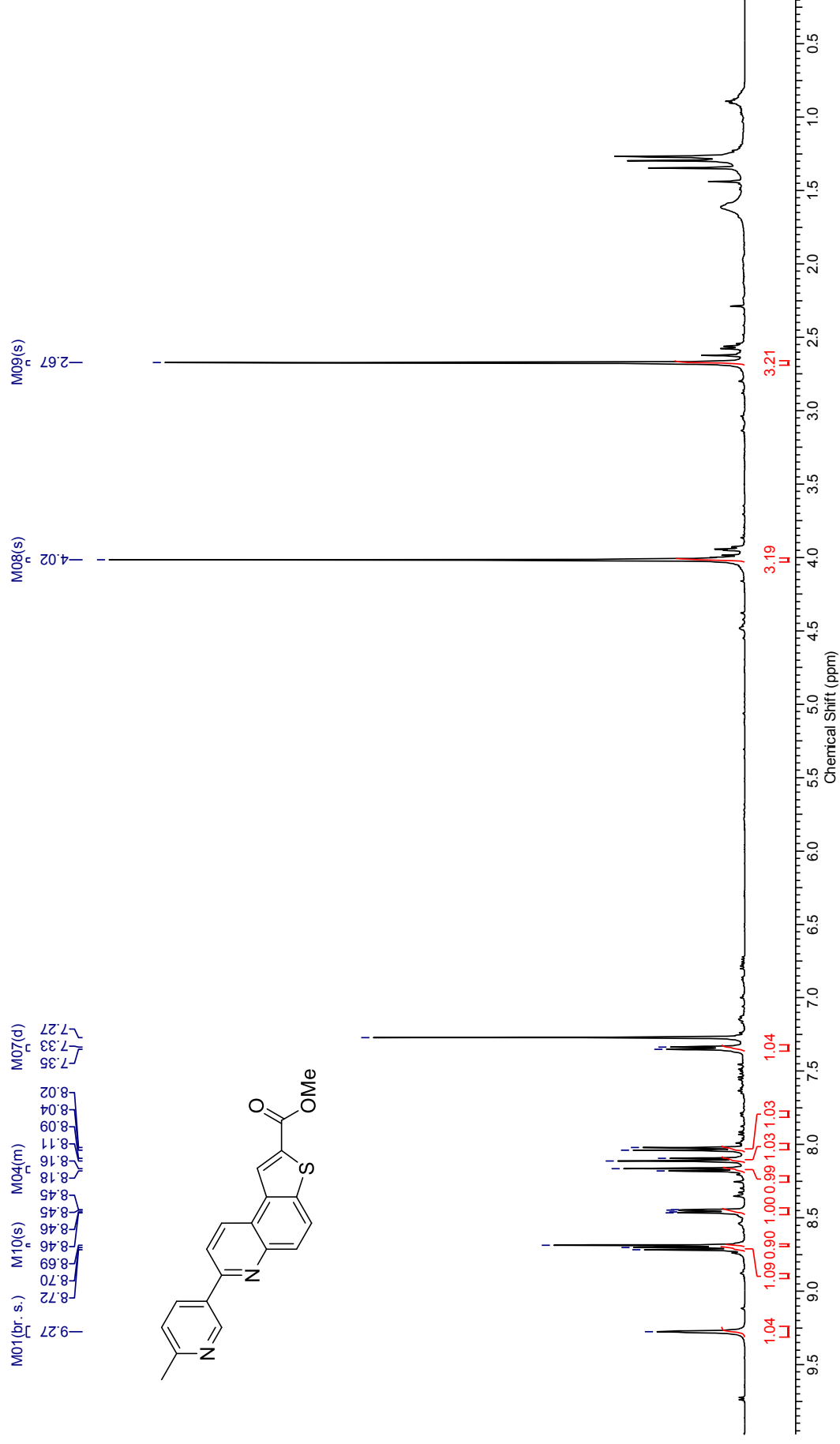
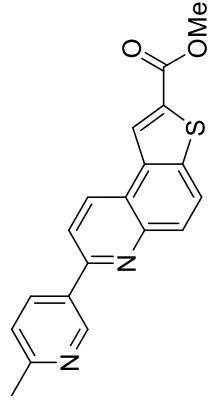
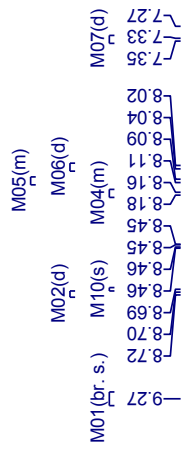


Methyl 7-(6-methylpyridin-3-yl)thieno[3,2-*f*]quinoline-2-carboxylate (200)



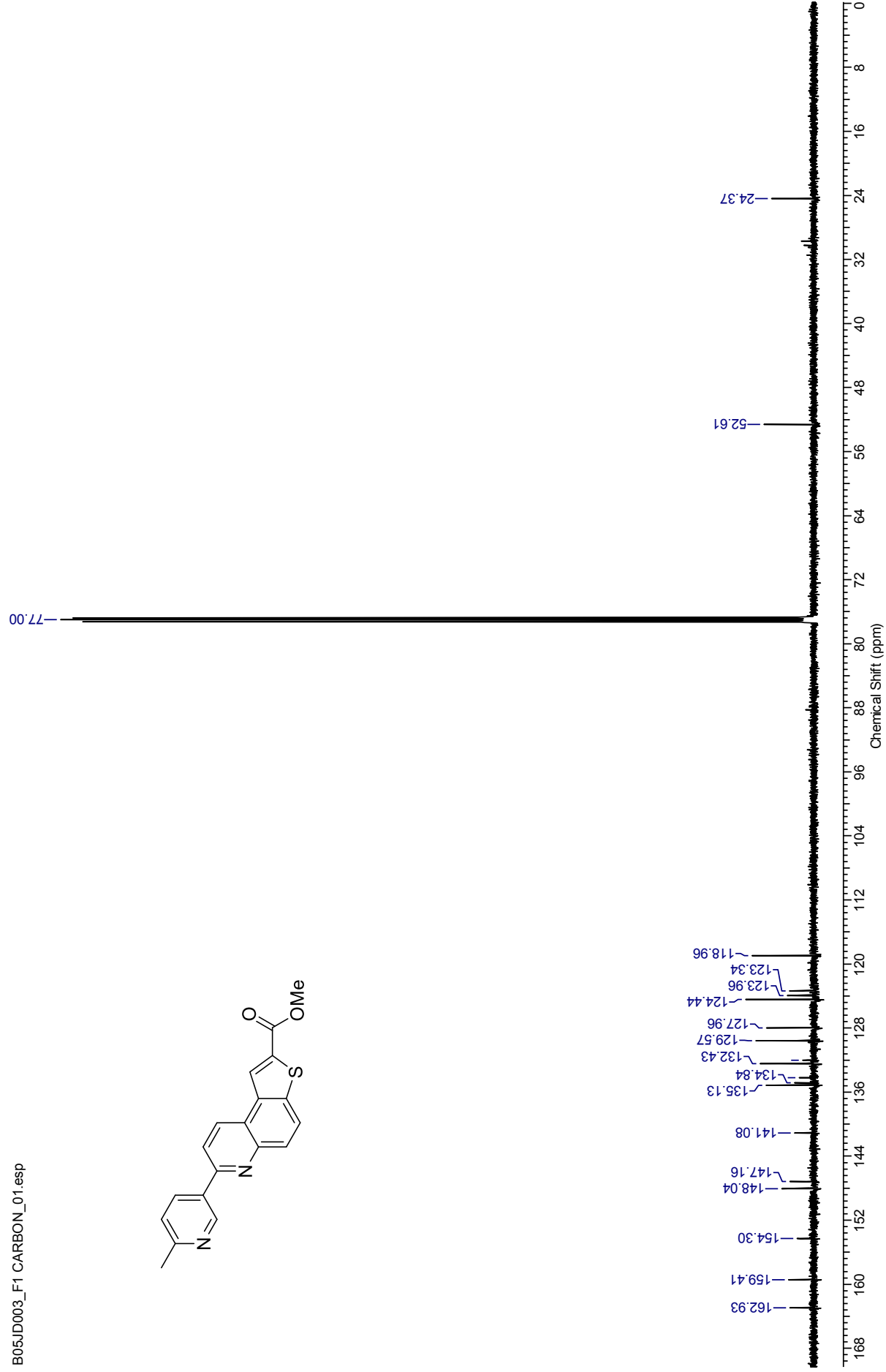
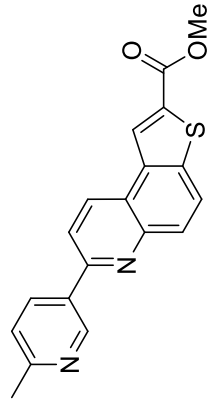
¹H NMR (500 MHz, CDCl₃) for Methyl 7-(6-methylpyridin-3-yl)thieno[3,2-f]quinoline-2-carboxylate

B04JD003_F1 CDCl₃.esp M03(dd)



¹³C NMR (126 MHz, CDCl₃) for Methyl 7-(6-methylpyridin-3-yl)thieno[3,2-f]quinoline-2-carboxylate

B05JD003_F1 CARBON_01.esp

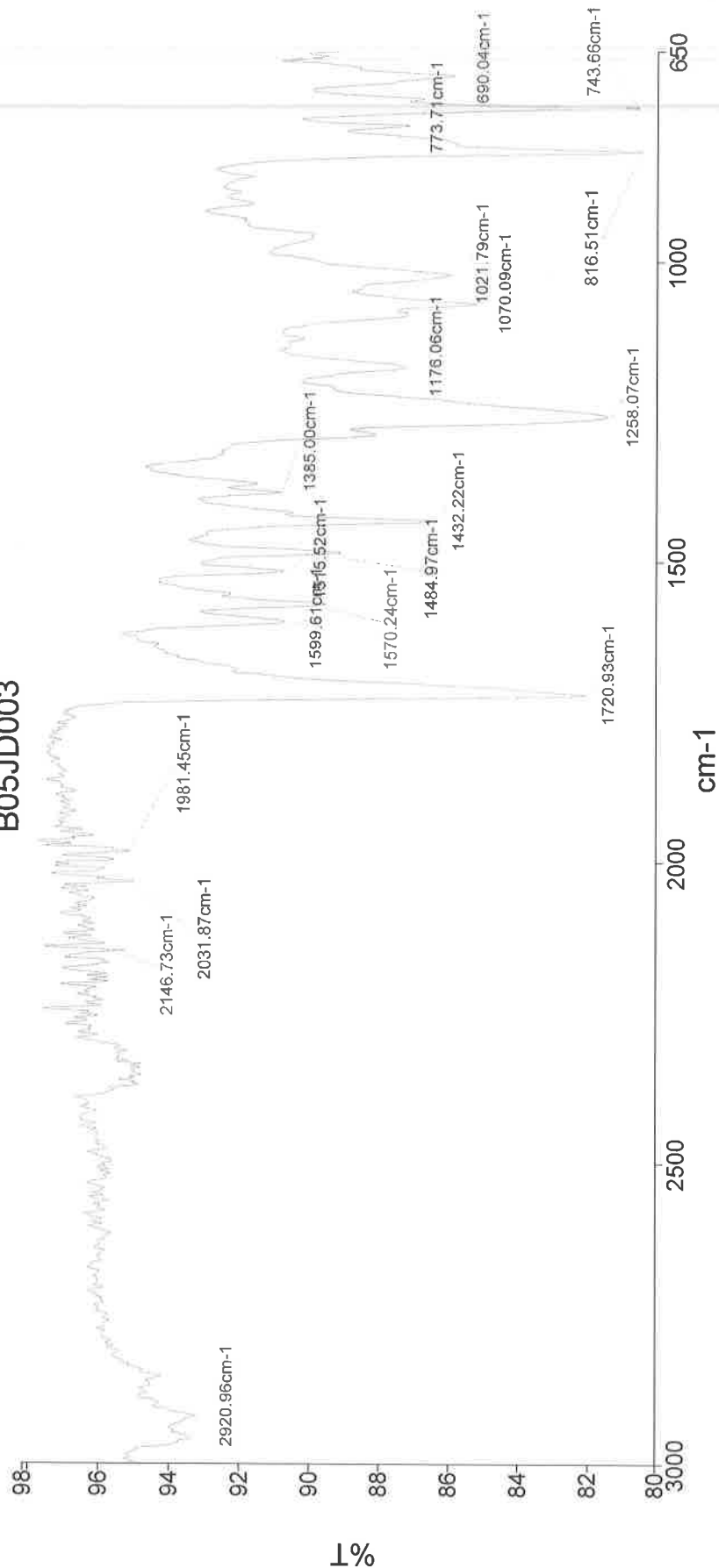




PerkinElmer Spectrum Version 10.03.06
05 April 2016 10:39

Analyst
Date
Administrator
05 April 2016 10:39

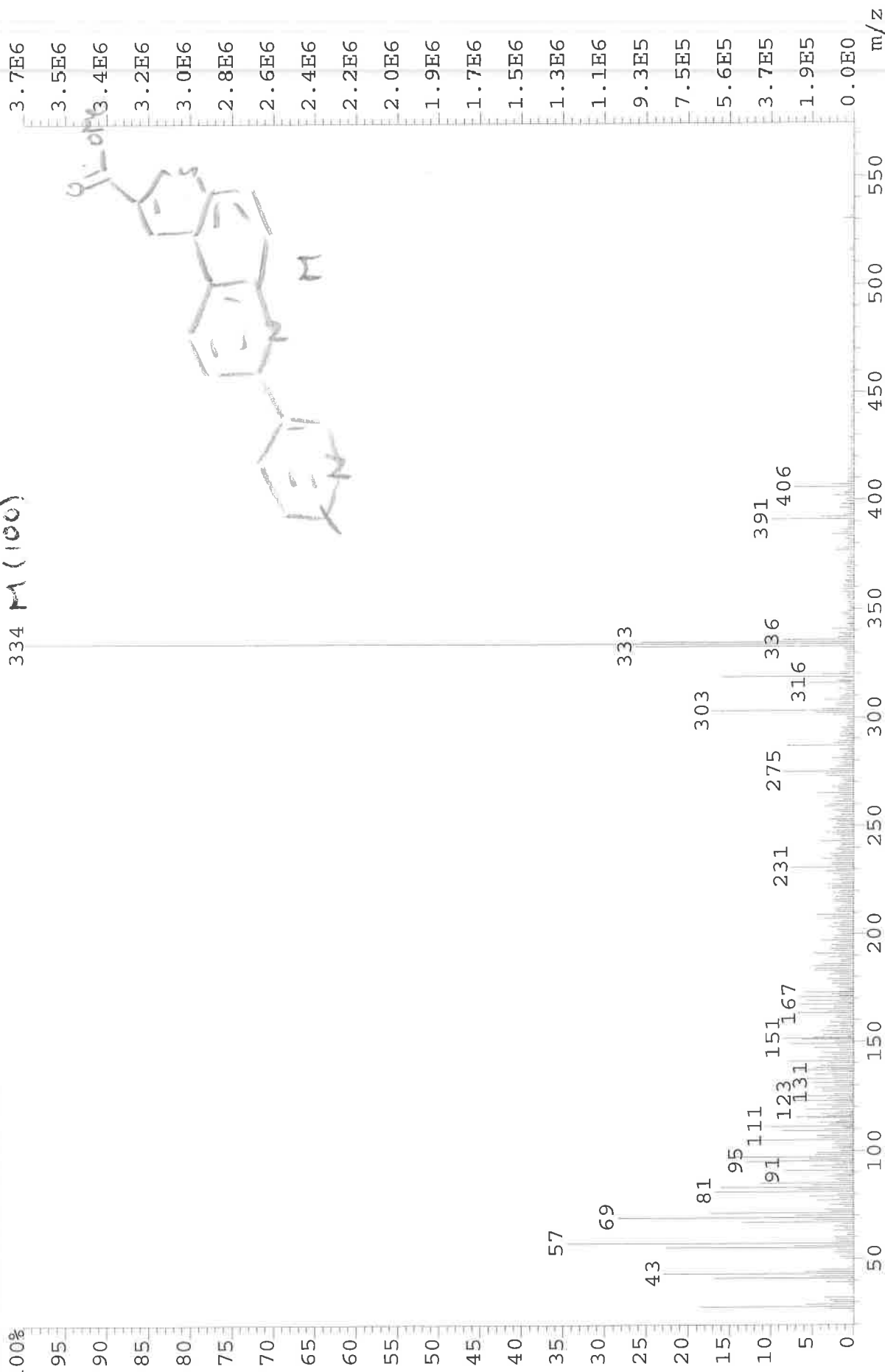
B05JD003



2921 C-H str.
1721 C=O str.
1570 C-C in ring str.
1432 C-C str.
1258 C-N str.
1070 C-O str.
816 C-H

249-003 Sample 003 By Administrator Date Tuesday, April 05 2016

File: JESS6754 Ident: 97 Acq: 8-MAR-2016 12:57:01 +5:58 Cal: CAL1
AutoSpecE EI+ Magnet BpI: 3726676 TIC: 54165184 Flags: HALL
File Text: B05JD003-F1
100% 334 M (100)



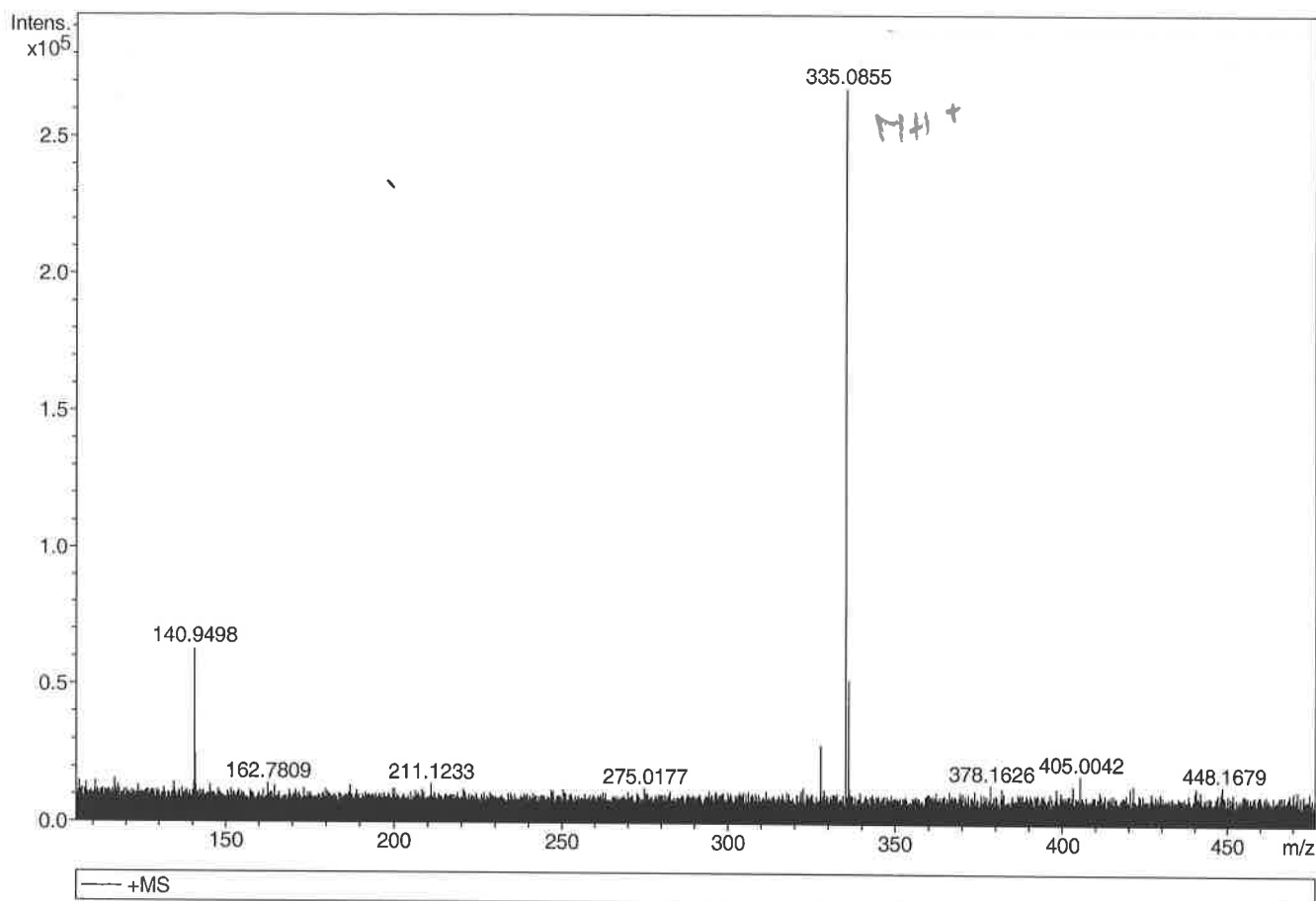
Generic Display Report

Analysis Info

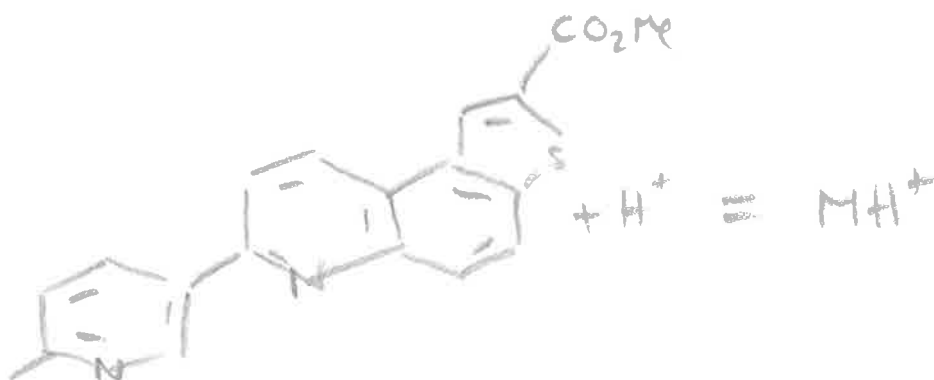
Analysis Name D:\Data\Alinanopos\JESS_6748_000001.d
 Method pos20090608esi
 Sample Name POS ESI B05JD003-F1
 Comment

Acquisition Date 07/03/2016 17:25:49

Operator Administrator
 Instrument apex-III

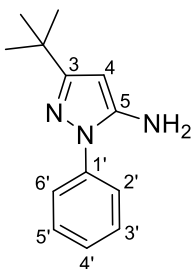


Sum Formula	Sigma	m/z	Err [ppm]	Mean Err [ppm]	Err [mDa]	rdb	N Rule	e ⁻
C 19 H 15 N 2 O 2 S 1	0.029	335.0849	-2.01	-20.47	-6.87	13.50	ok	even



Chapter 4: ^1H NMR, ^{13}C NMR, IR and Mass spectra and DSF results

3-*tert*-Butyl-1-phenyl-1*H*-pyrazole-5-amine (215)

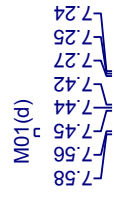
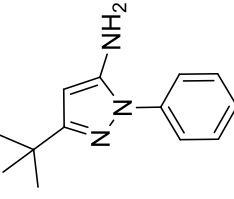


¹H NMR spectrum (500 MHz, DMSO-*d*₆) for 3-*tert*-butyl-1-phenyl-1H-pyrazole-5-amine

B03JD132A Proton 4 Carbon DMSO.esp

M03(m)

M02(t)

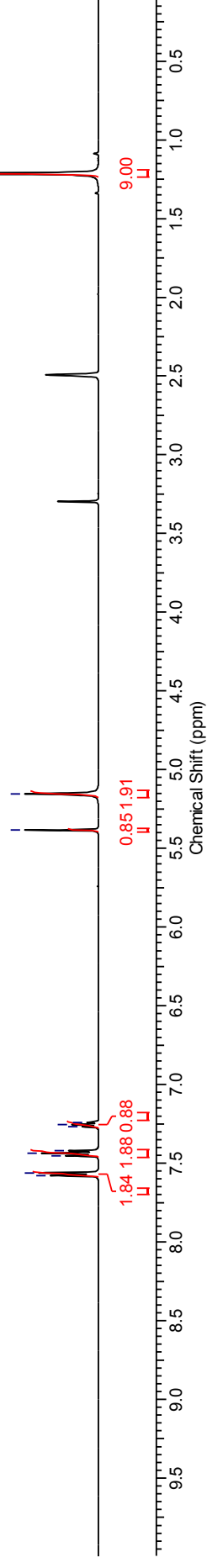


M05(s)

M04(m)

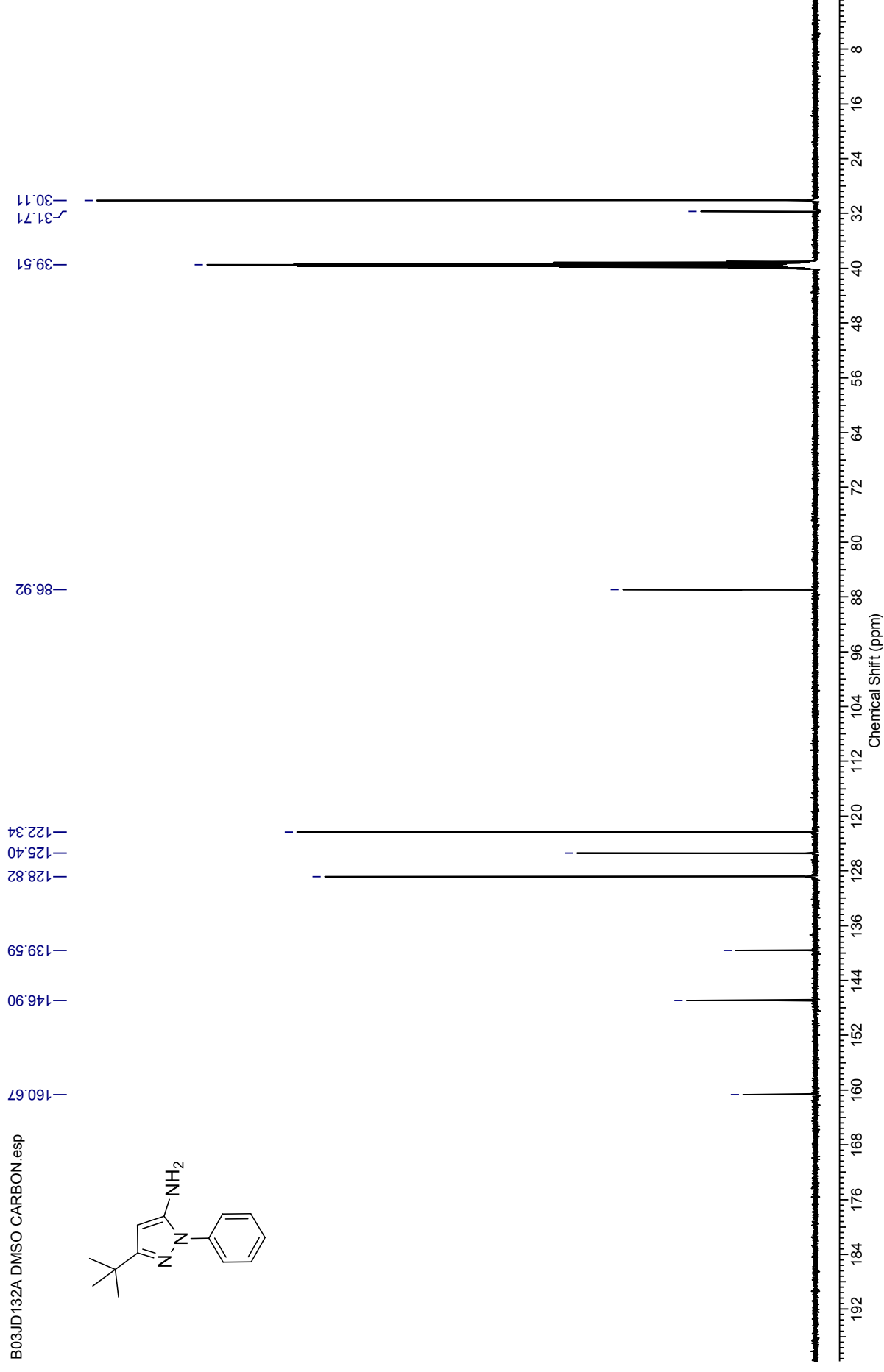
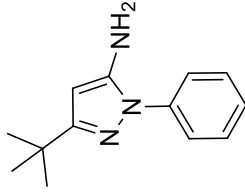


M06(s)



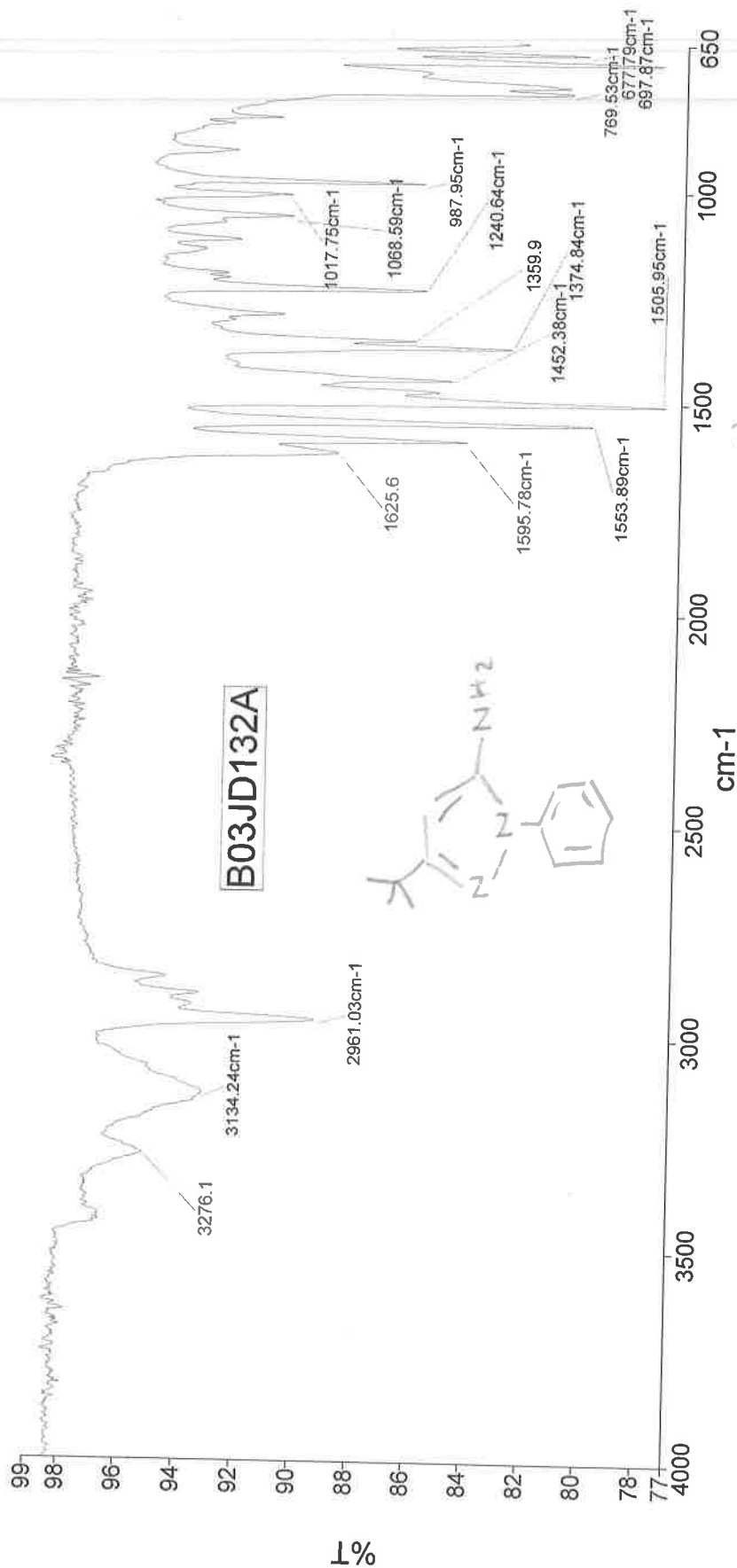
¹³C NMR spectrum (125 MHz, DMSO-*d*₆) for 3-*tert*-butyl-1-phenyl-1*H*-pyrazole-5-amine

B03JD132A DMSO CARBON.esp



Analyst
Date

Administrator
26 November 2014 14:56

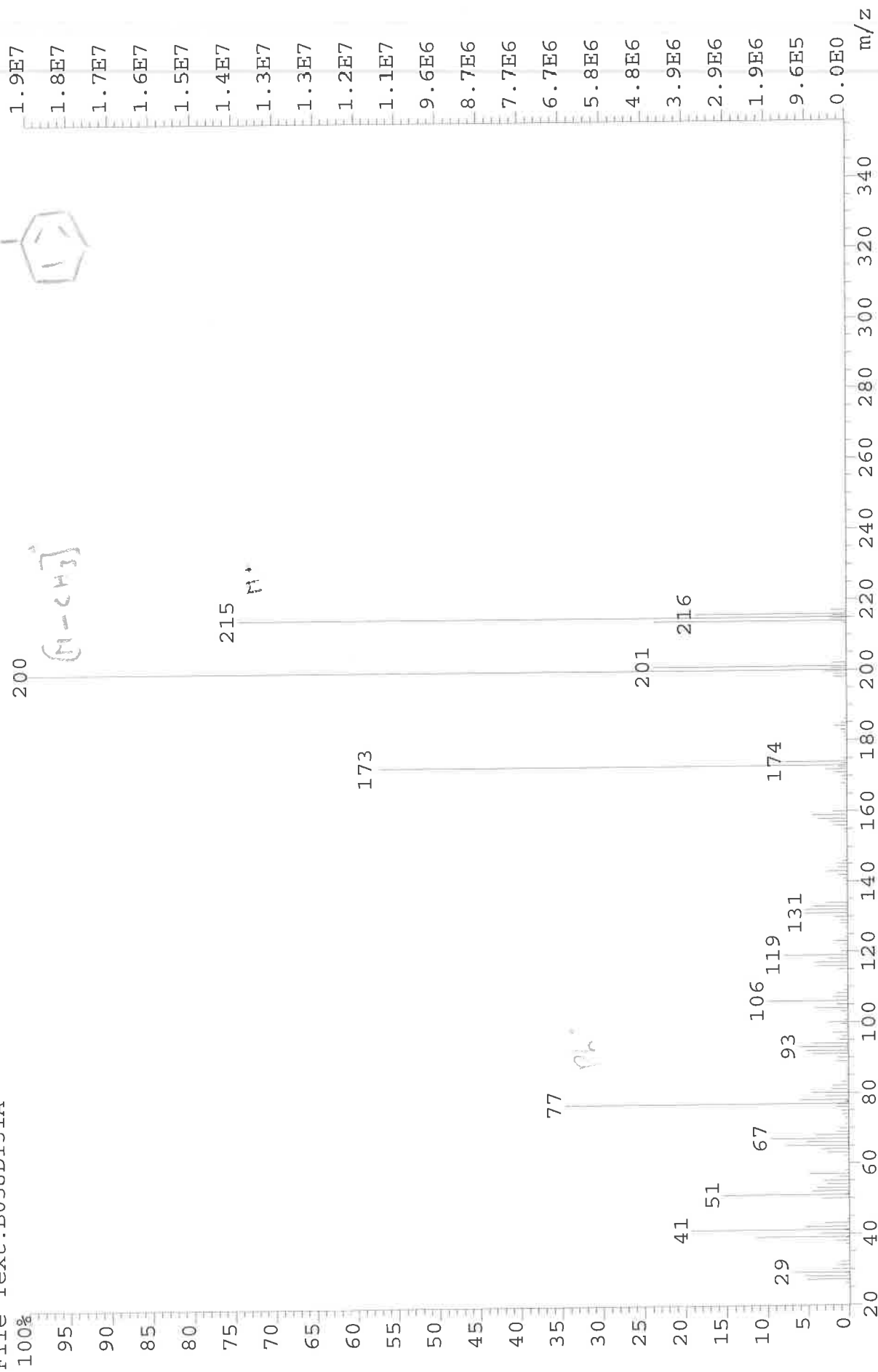
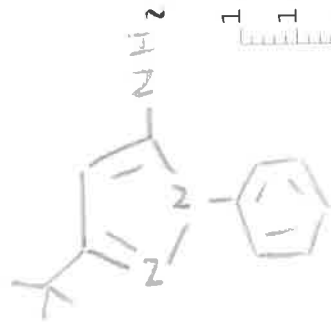


Administrator 34 Sample 034 By Administrator Date Tuesday, November 25 2014

cm⁻¹

- 2961 - C-H Strong alkene
- 1596 - N-H bend primary
- 1554 - C=C in ring str
- 1506 - C=C in ring
- 1375 - C-H rock alkene
- 1241 - 3° amine C-N
- 988 - N-H wag primary

File: JESSICA4448 Ident: 106 Acq: 23-OCT-2014 12:05:09 +6:32 Cal: CAL1
AutospecE EI+ Magnet BpI: 19264090 TIC: 129114512 Flags: HALL
File Text: B03JD131A



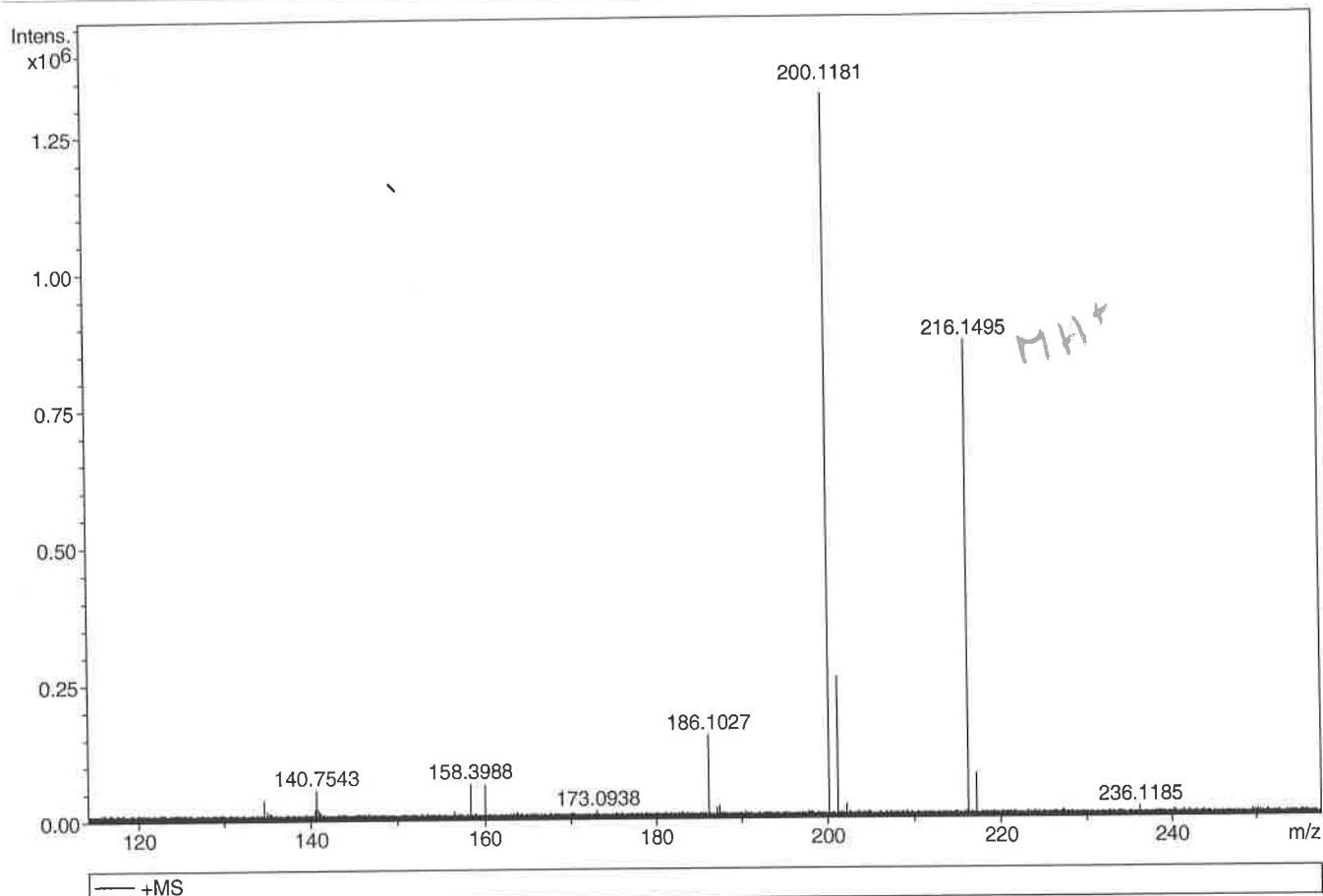
Generic Display Report

Analysis Info

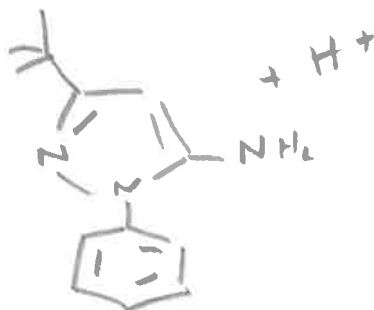
Analysis Name D:\Data\Alinanopos\JESS5155_000001.d
Method pos20090608esi
Sample Name POS ESI BO3JD150-F2
Comment

Acquisition Date 28/05/2015 16:22:30

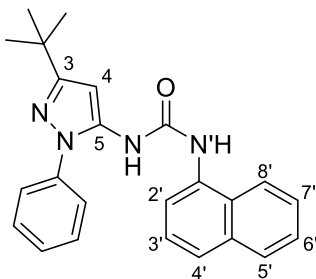
Operator Administrator
Instrument apex-III



Sum Formula	Sigma	m/z	Err [ppm]	Mean Err [ppm]	Err [mDa]	rdB	N Rule	e ⁻
C 13 H 18 N 3	0.023	216.1495	0.22	-11.56	-2.50	6.50	ok	even



***N*-(3-(*tert*-Butyl)-1-phenyl-1*H*-pyrazol-5-yl)-*N'*-(naphthalene-1-yl)urea (215A)**



¹H NMR spectrum (500 MHz, DMSO-*d*₆) for *N*-(3-(*tert*-butyl)-1*H*-pyrazol-5-yl)-1-phenyl-1*H*-pyrazol-5-yl)-*N*'-(naphthalene-2-yl)urea

B03JD138A DMSO Proton from Carbon. esy104(m)

M05(br. s.)

M07(m)

M01(br. s.)

M02(s)

M03(m)

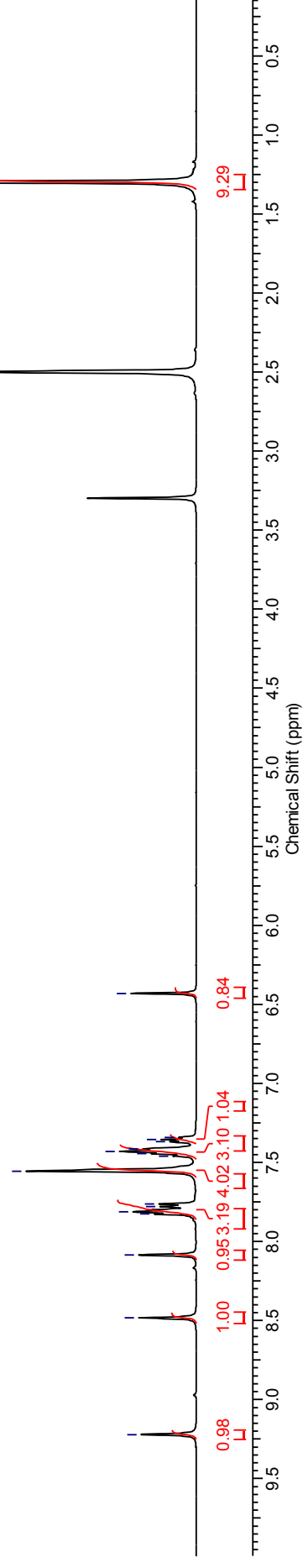
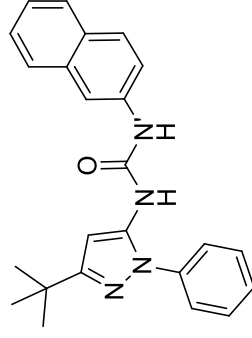
M06(m)

M08(s)

M09(s)

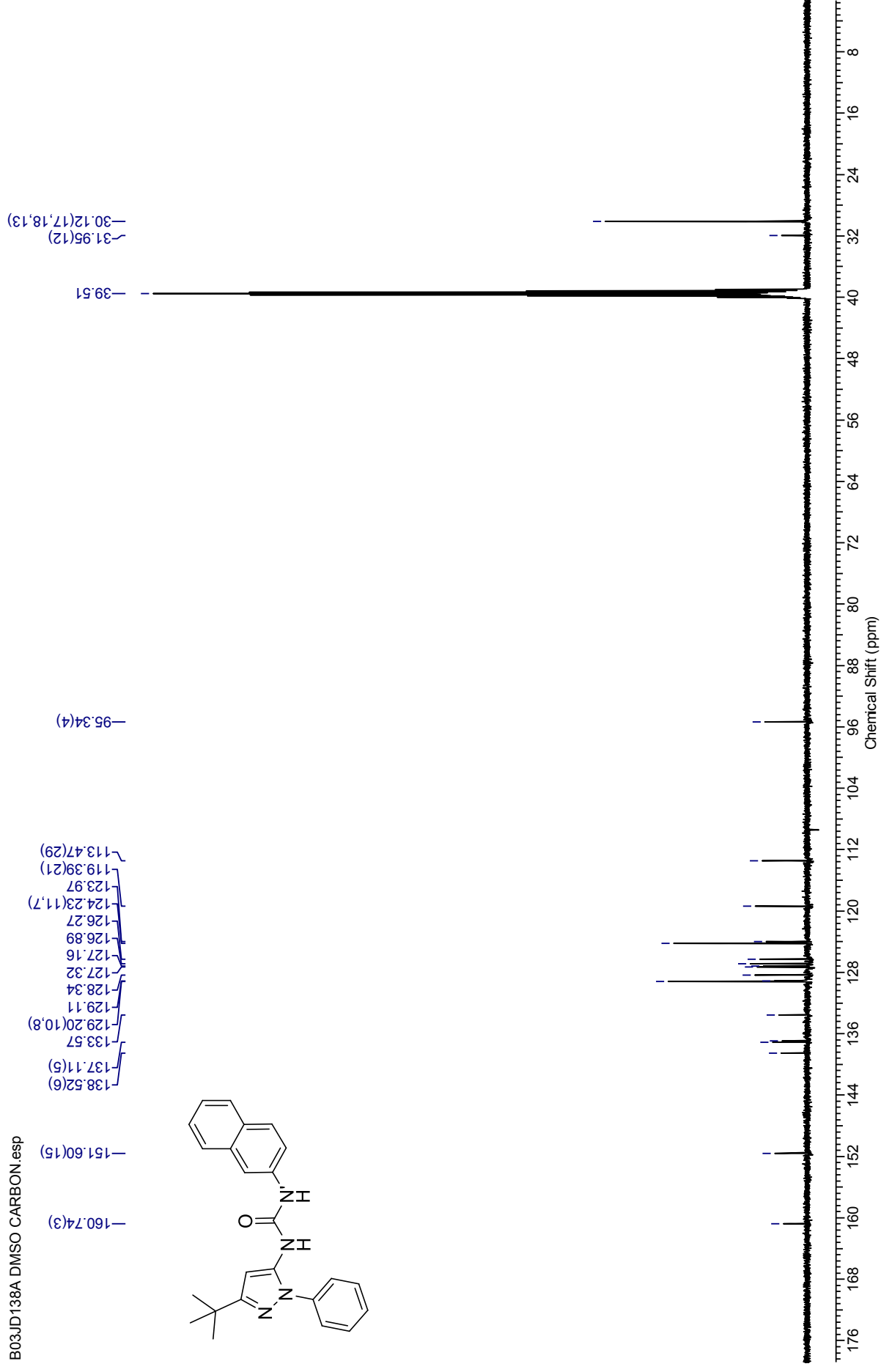
8.09
8.03
7.83
7.81
7.78
7.76
7.56
7.44
7.43
7.41
7.37
7.36

1.30



¹³C NMR spectrum (126 MHz, DMSO-*d*₆) for *N*-(3-(*tert*-butyl)-1-phenyl-1*H*-pyrazol-5-yl)-1-phenyl-1*H*-pyrazol-5-yl)-*N'*-(naphthalene-2-yl)urea

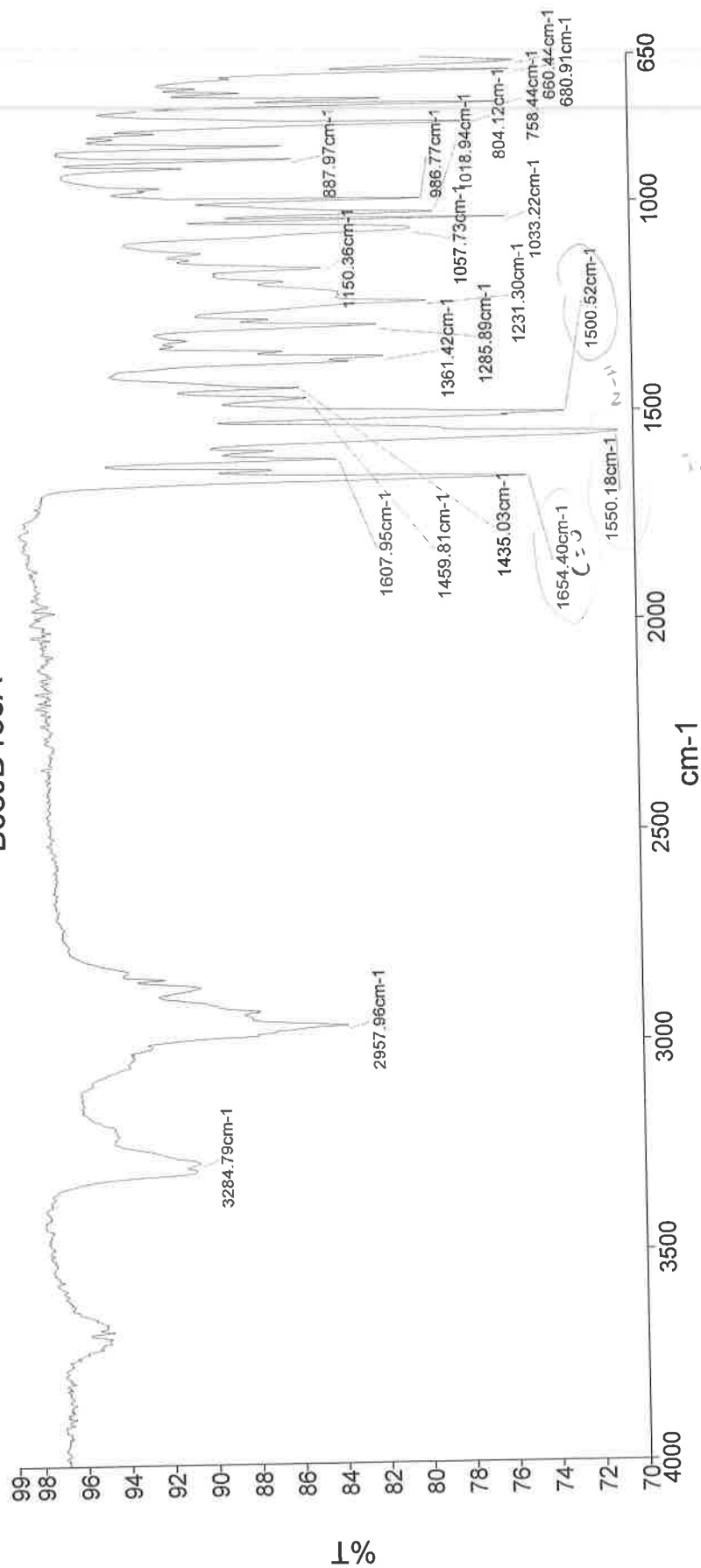
B03JD138A DMSO CARBON.esp



Analyst
Date

Administrator
26 November 2014 15:16

B03JD138A



cm⁻¹

- 3285 - N-H str. urea
- 2958 - C-H str. alk.
- 1654 - C=O str.
- 1550 - N-H bend
- 1500 - N-H bend
- 1231 - C-N aromatic
- 1033 - C-N str.
- 758 - C-H alkyl

Administrator 07 Sample 007 By Administrator Date Wednesday, November 26 2014

Single Mass Analysis

Tolerance = 100.0 PPM / DBE: min = -1.5, max = 50.0

Element prediction: Off

Number of isotope peaks used for i-FIT = 3

Monoisotopic Mass, Even Electron Ions

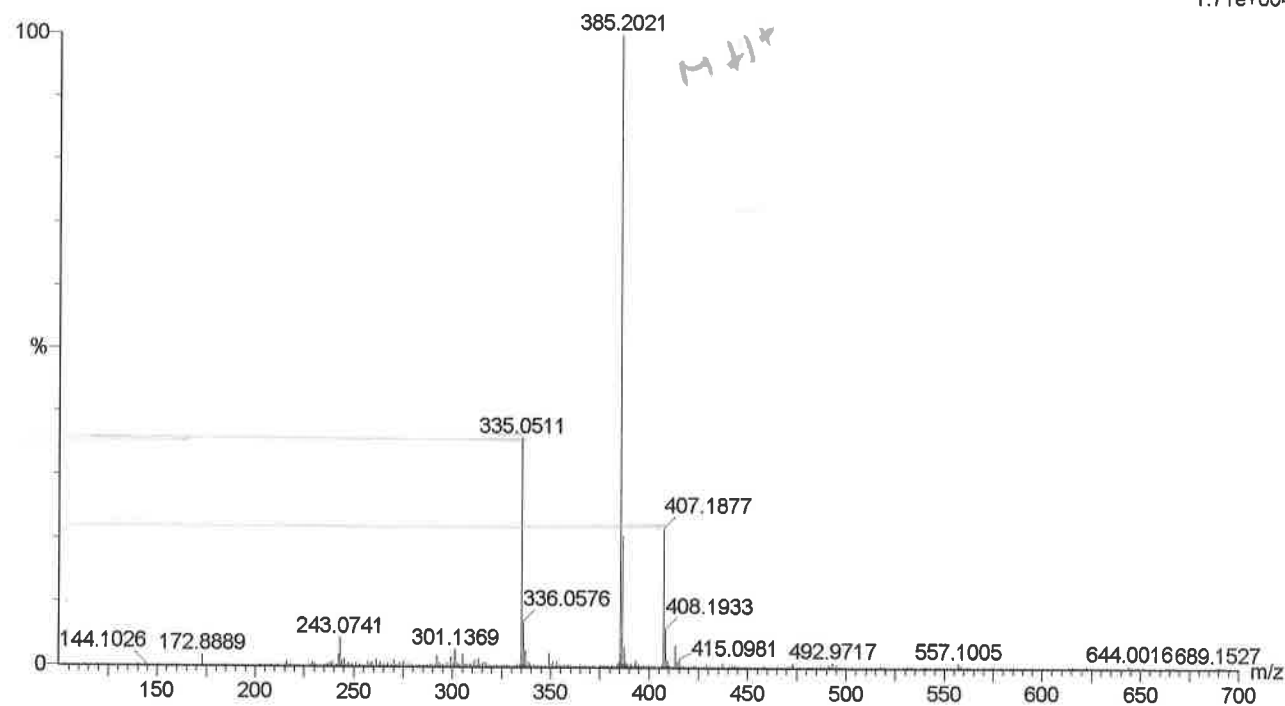
2 formula(e) evaluated with 1 results within limits (all results (up to 1000) for each mass)

Elements Used:

C: 24-24 H: 13-50 11B: 0-1 N: 4-4 O: 1-1

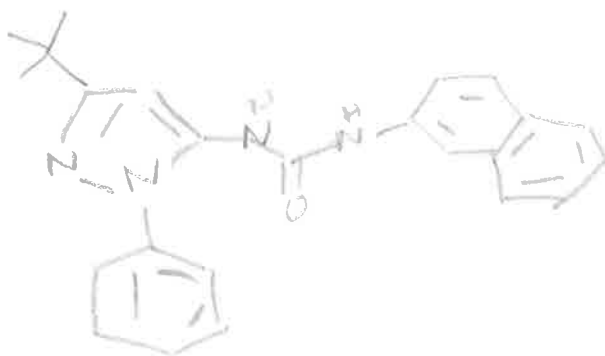
BO3JD138A

JESS4474 192 (2.582) Cm (192)

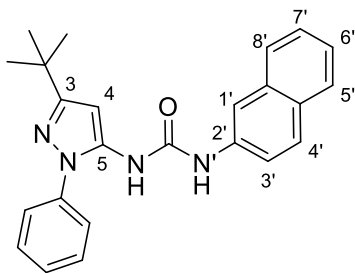
1: TOF MS ES+
1.71e+004

Minimum: -1.5
Maximum: 5.0 100.0 50.0

Mass	Calc. Mass	mDa	PPM	DBE	i-FIT	Formula
385.2021	385.2028	-0.7	-1.8	14.5	205.4	C ₂₄ H ₂₅ N ₄ O

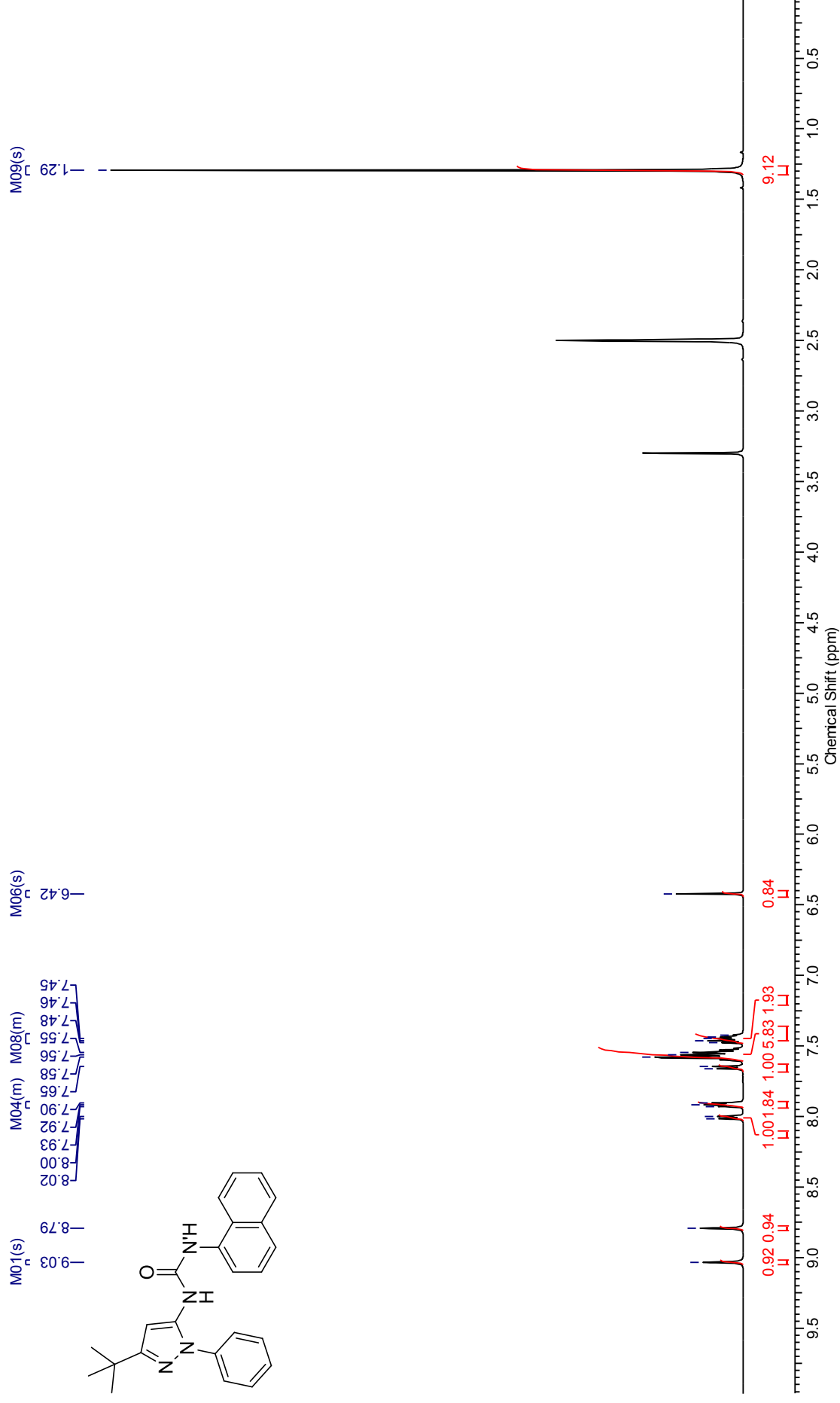
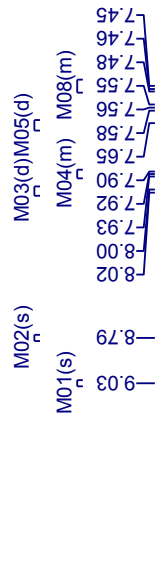


***N*-(3-(*tert*-Butyl)-1-phenyl-1*H*-pyrazol-5-yl)-*N'*-(naphthalene-2-yl)urea (215B)**



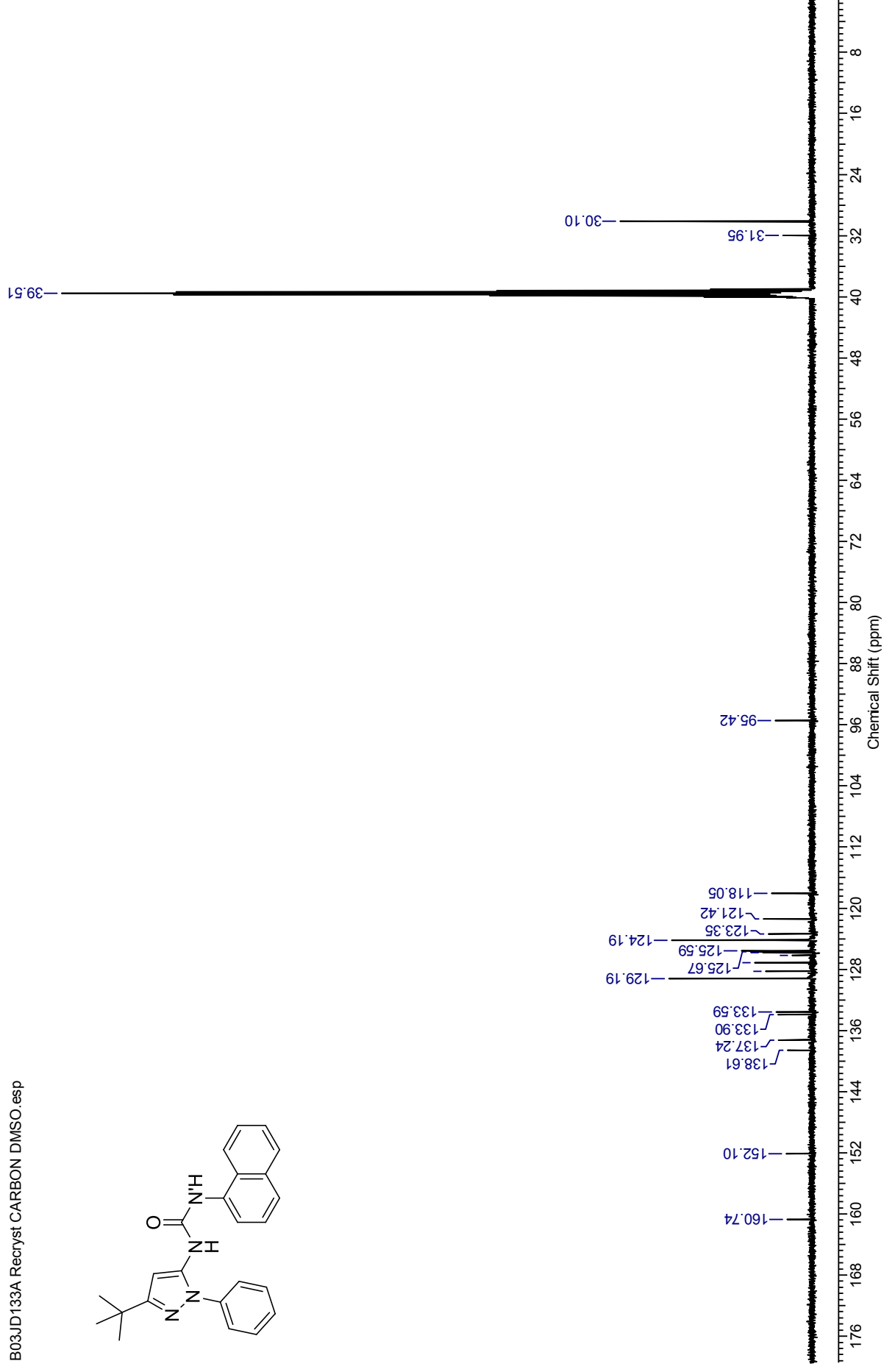
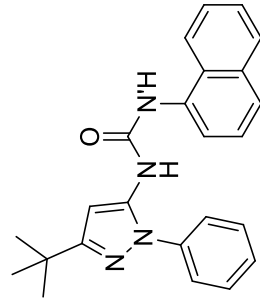
¹H NMR spectrum (500 MHz, DMSO-*d*₆) for *N*-(3-(*tert*-butyl)-1-phenyl-1*H*-pyrazol-5-yl)-1-phenyl-1*H*-pyrazol-5-yl)-*N'*-(naphthalene-1-yl)urea

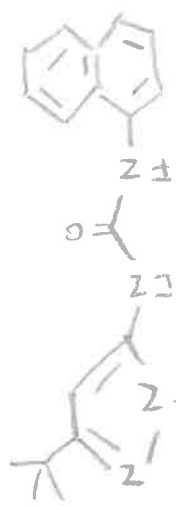
B03JD133A Recryst Proton 4 carbon DMSO-*d*₆ 400.13 MHz



¹³C NMR spectrum (126 MHz, DMSO-*d*₆) for *N*-(3-(*tert*-butyl)-1-phenyl-1*H*-pyrazol-5-yl)-1-phenyl-1*H*-pyrazol-5-yl)-*N'*-(naphthalene-1-yl)urea

B03JD133A Recryst CARBON DMSO.esp



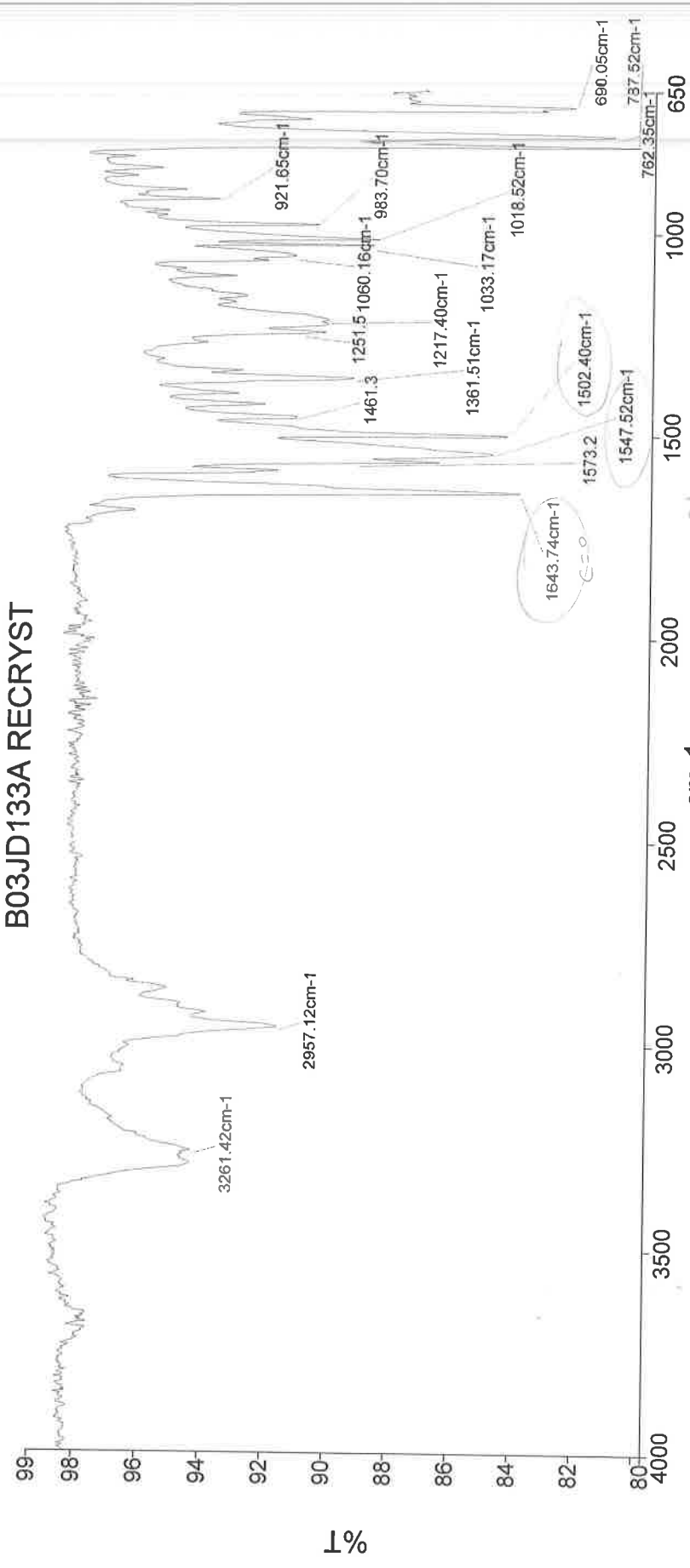


Analyst
Date

Administrator
26 November 2014 15:11

PerkinElmer Spectrum Version 10.03.06
26 November 2014 15:11

B03JD133A RECRYST



cm-1

3261	N-H urea, str.
2957	C-H alk str
1644	C=O - amide str
1547	N-H amide bend
1502	N-H amide bend
1573	C-N str
1018	C-H rock
762	C-H rock

Administrator 05 Sample 005 By Administrator Date Wednesday, November 26 2014

Single Mass Analysis

Tolerance = 100.0 PPM / DBE: min = -1.5, max = 50.0

Element prediction: Off

Number of isotope peaks used for i-FIT = 3

Monoisotopic Mass, Even Electron Ions

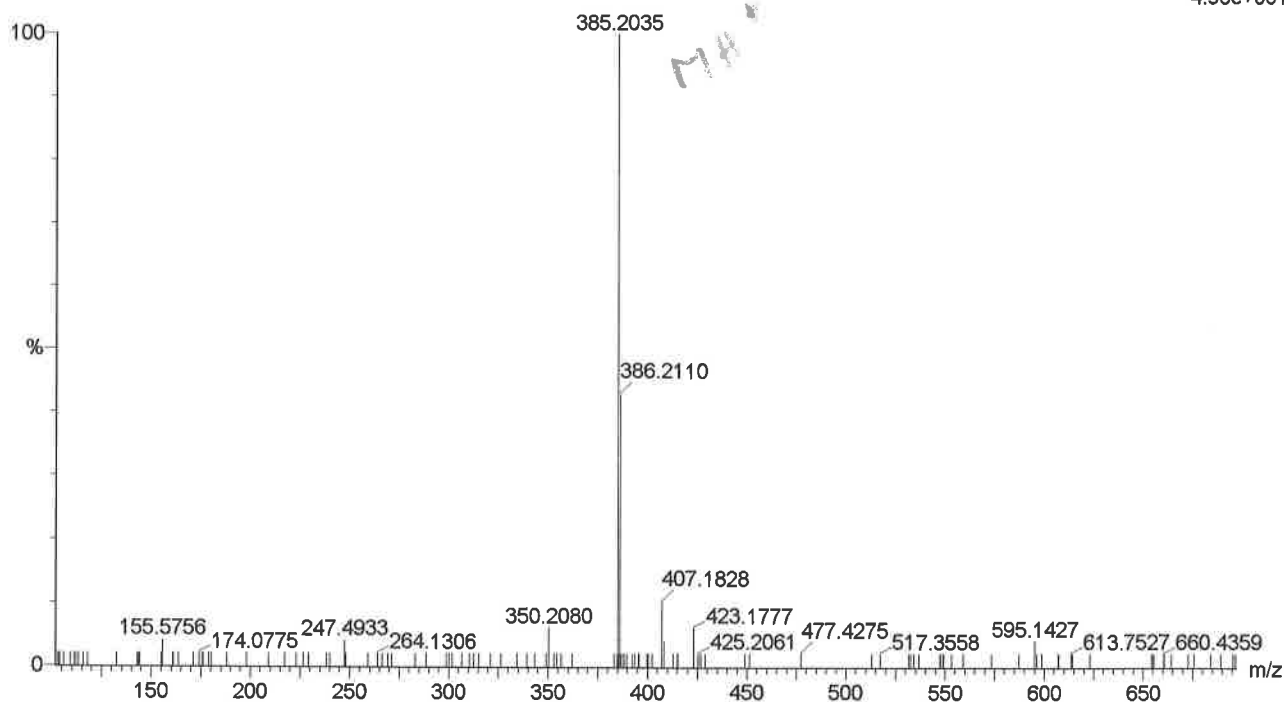
2 formula(e) evaluated with 1 results within limits (all results (up to 1000) for each mass)

Elements Used:

C: 24-24 H: 13-50 11B: 0-1 N: 4-4 O: 1-1

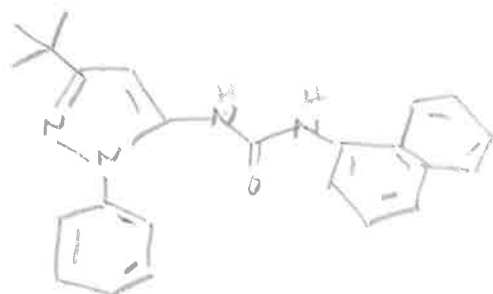
BO3JD136B

JESS4476 48 (0.652)

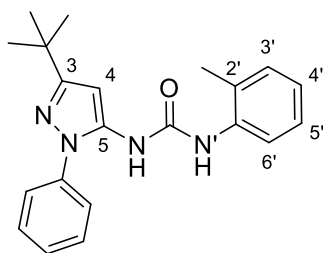
1: TOF MS ES+
4.96e+001

Minimum: -1.5
Maximum: 5.0 100.0 50.0

Mass	Calc. Mass	mDa	PPM	DBE	i-FIT	Formula
385.2035	385.2028	0.7	1.8	14.5	1.7	C ₂₄ H ₂₅ N ₄ O

MH⁺ = 385.2023

***N*-(3-(*tert*-Butyl)-1-phenyl-1*H*-pyrazol-5-yl)-*N'*-(*o*-tolyl)urea (215C)**



¹H NMR spectrum (500 MHz, DMSO-*d*₆) for *N*-(3-(*tert*-butyl)-1*H*-pyrazol-5-yl)-1-phenyl-1*H*-pyrazol-5-yl)-*N*'-(*o*-tolyl)urea

B03JD137A Proton 4 carbonDMSO.esp

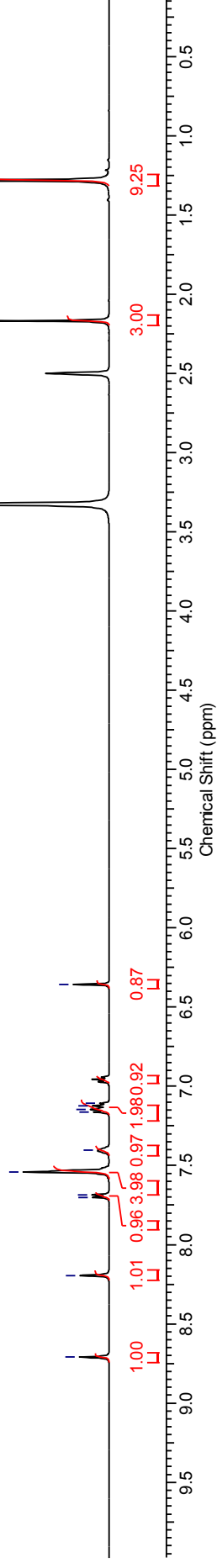
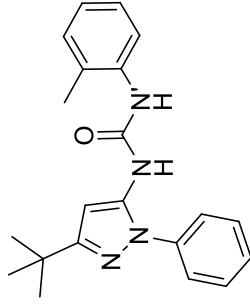
M06(m)

M04(br. s.)

M05(m)

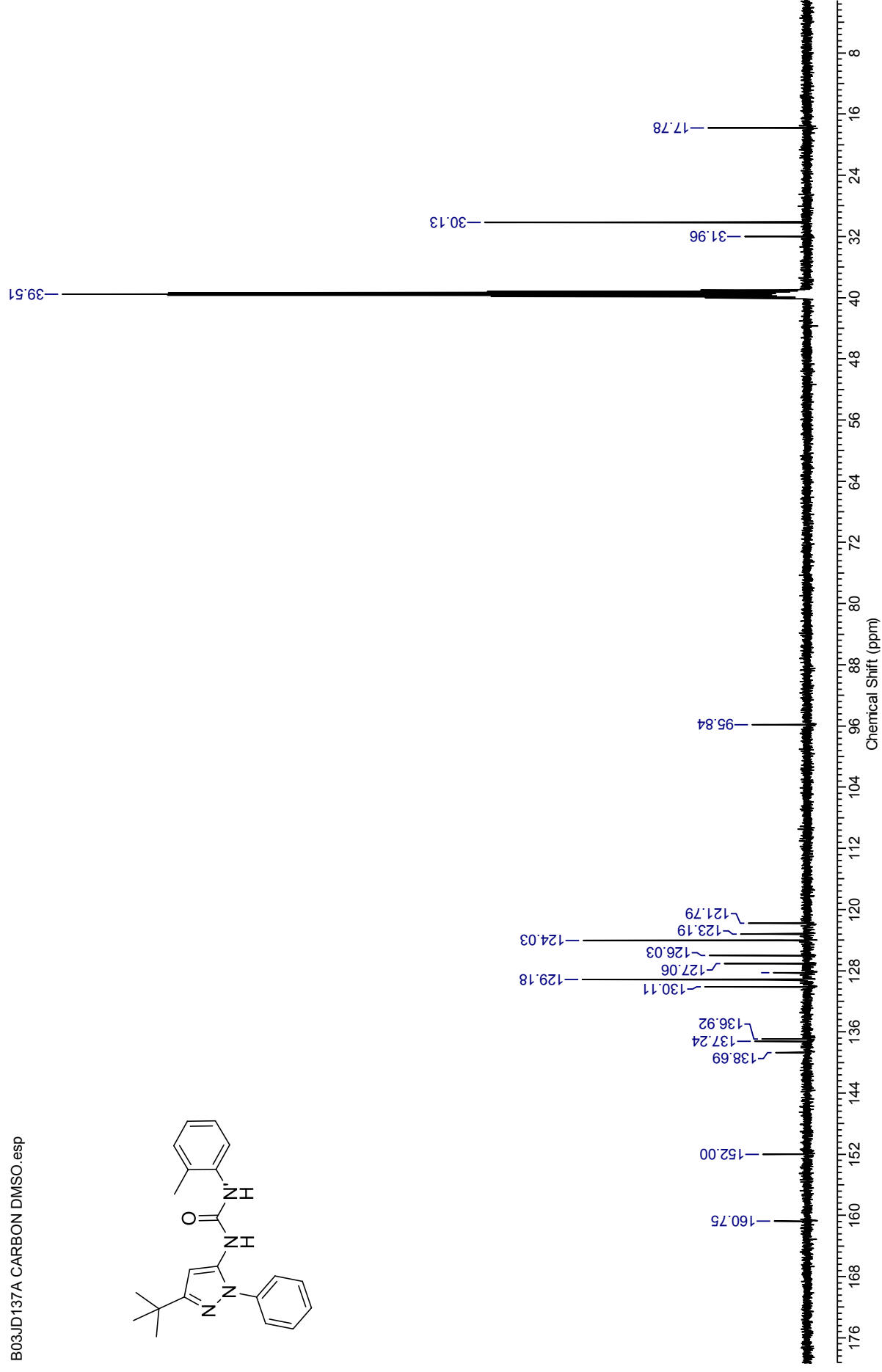
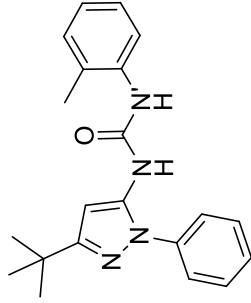
M01(s) 8.71 M02(s) 8.19 M03(d) 7.70 7.68 7.54 M04(br. s.) 7.40 7.16 7.15 7.12 7.11 M05(m) 7.08 6.92 6.87 M06(m) 6.36 M07(m) 6.36 M08(s) 6.36

M09(s) 2.17 M10(s) 1.28



¹³C NMR spectrum (126 MHz, DMSO-*d*₆) for *N*-(3-(*tert*-butyl)-1-phenyl-1*H*-pyrazol-5-yl)-1-phenyl-1*H*-pyrazol-5-yl)-*N'*-(*o*-tolyl)urea

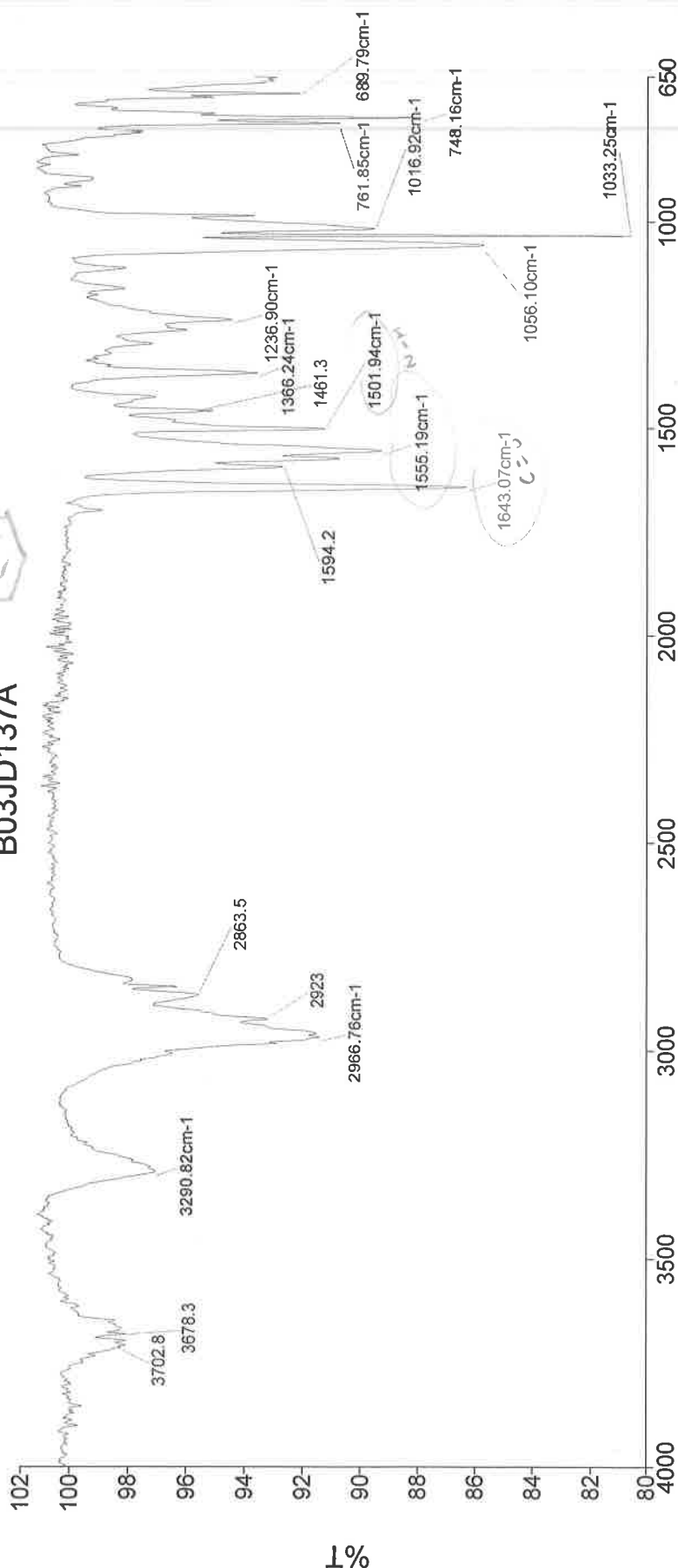
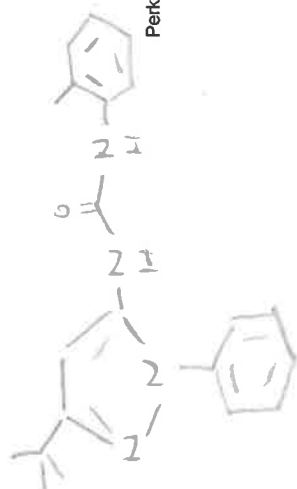
B03JD137A CARBON DMSO.esp



Analyst
Date

Administrator
26 November 2014 15:13

B03JD137A



cm⁻¹

- 3291 - N-H str. Amide
- 2967 - C-H alk. str.
- 1643 - C=O amide bond
- 1551 - N-H amide bond
- 1502 - "
- 1033 - C-N str.
- 748 - C-H rocky

Administrator 06 Sample 006 By Administrator Date Wednesday, November 26 2014

Single Mass Analysis

Tolerance = 100.0 PPM / DBE: min = -1.5, max = 50.0

Element prediction: Off

Number of isotope peaks used for i-FIT = 3

Monoisotopic Mass, Even Electron Ions

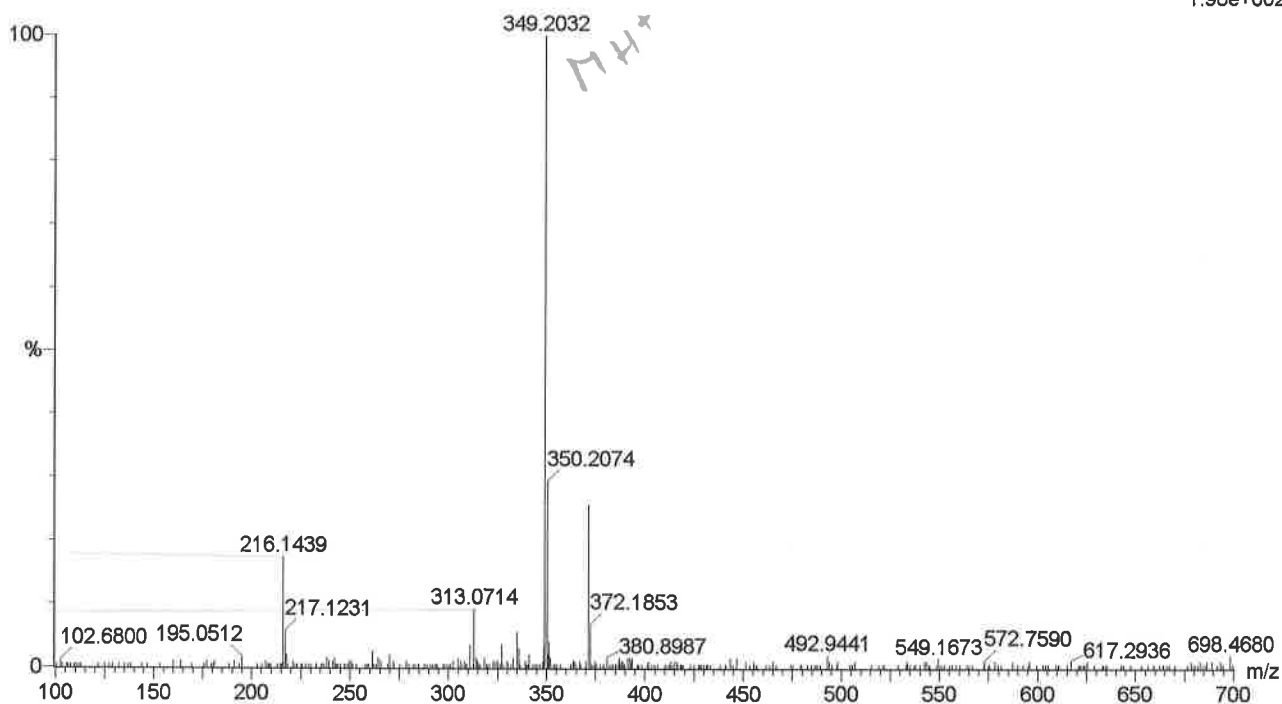
2 formula(e) evaluated with 1 results within limits (all results (up to 1000) for each mass)

Elements Used:

C: 21-21 H: 13-50 11B: 0-1 N: 4-4 O: 1-1

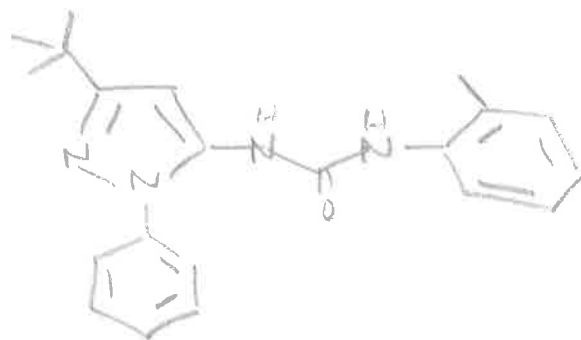
BO3JD137A

JESS4473 117 (1.587) Cm (115:117)

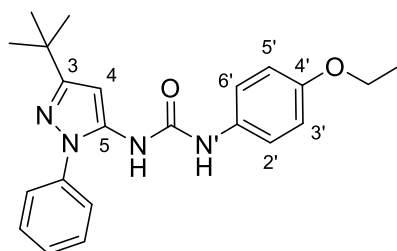
1: TOF MS ES+
1.98e+002

Minimum: -1.5
Maximum: 5.0 100.0 50.0

Mass	Calc. Mass	mDa	PPM	DBE	i-FIT	Formula
349.2032	349.2028	0.4	1.1	11.5	0.6	C ₂₁ H ₂₅ N ₄ O



***N*-(3-(*tert*-Butyl)-1-phenyl-1*H*-pyrazol-5-yl)-*N'*-(4-ethoxyphenyl)urea**
(215D)



¹H NMR spectrum (500 MHz, DMSO-*d*₆) for *N*-(3-(*tert*-butyl)-1-phenyl-1*H*-pyrazol-5-yl)-1-phenyl-1*H*-pyrazol-5-yl)-*N'*-(4-ethoxyphenyl)urea

B03JD139A DMSO. esp

M03(m)

M07(m)

M01(s)

M02(s)

7.53
7.52
7.41
7.41
7.40
7.29
7.27

M04(d)

M05(d)

M06(s)

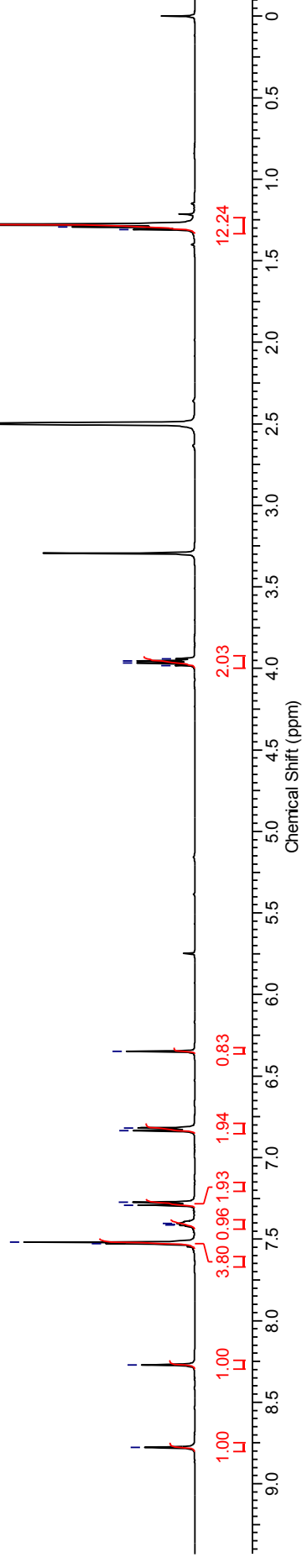
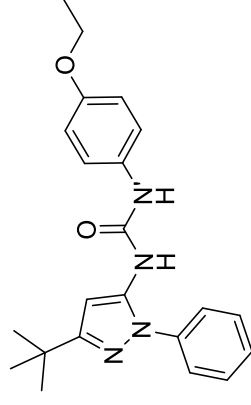
6.84
6.82

M08(q)

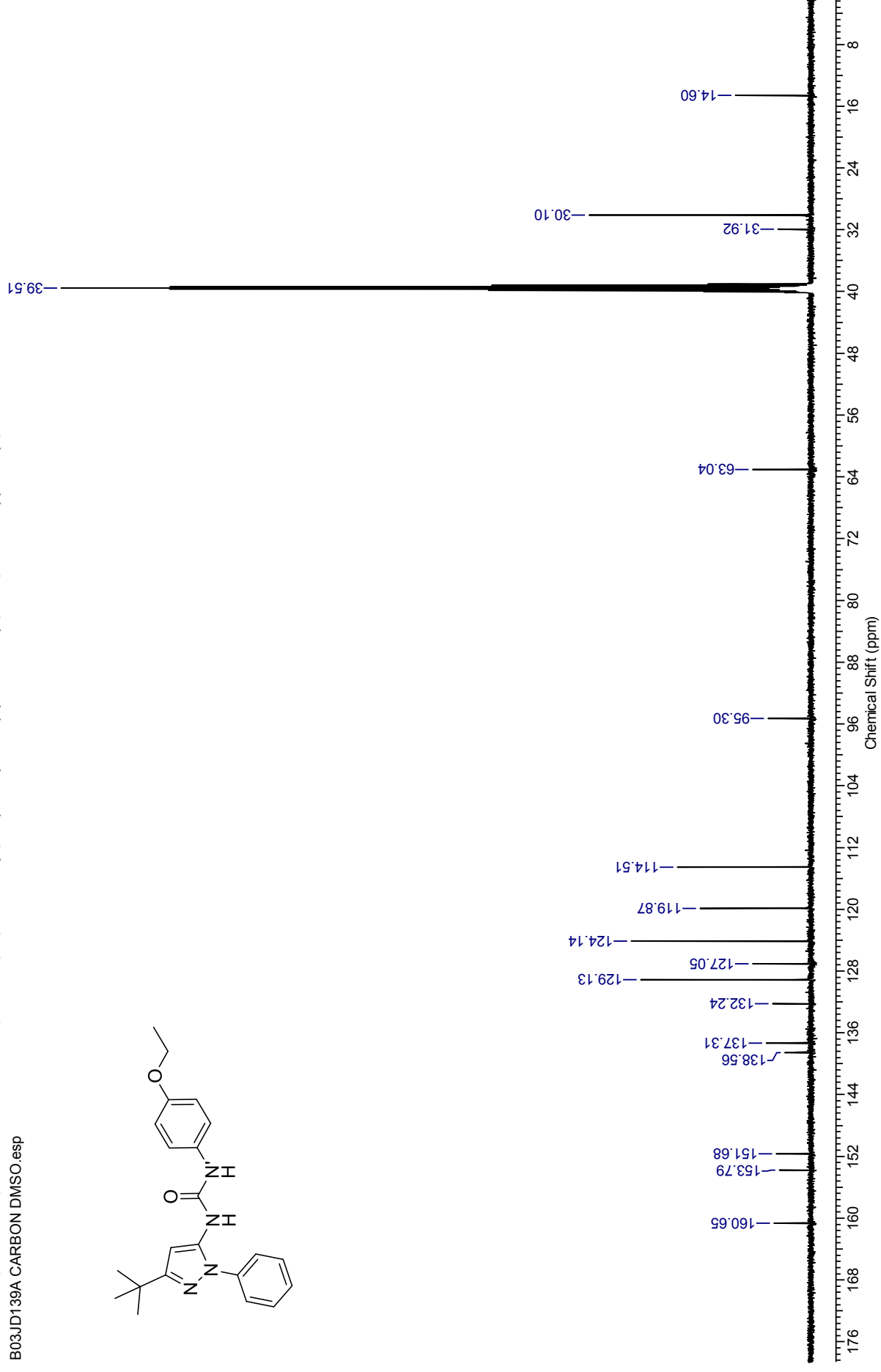
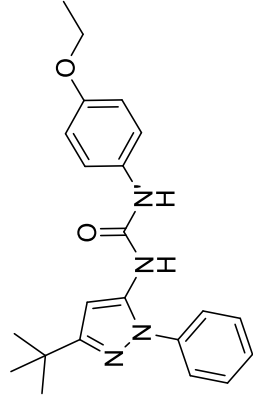
3.98
3.97
3.95
3.94

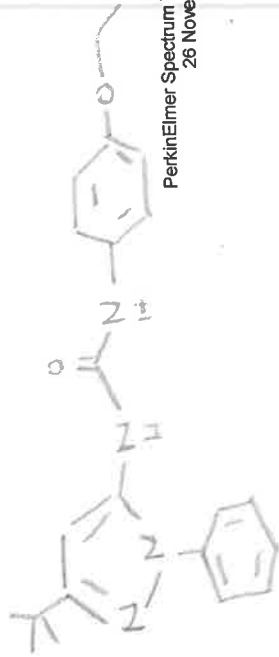
M11(m)

1.31
1.30
1.28



¹³C NMR spectrum (126 MHz, DMSO-*d*₆) for *N*-(3-(*tert*-butyl)-1-phenyl-1*H*-pyrazol-5-yl)-*N'*-(4-ethoxyphenyl)urea
B03JD139A CARBON DMSO.esp





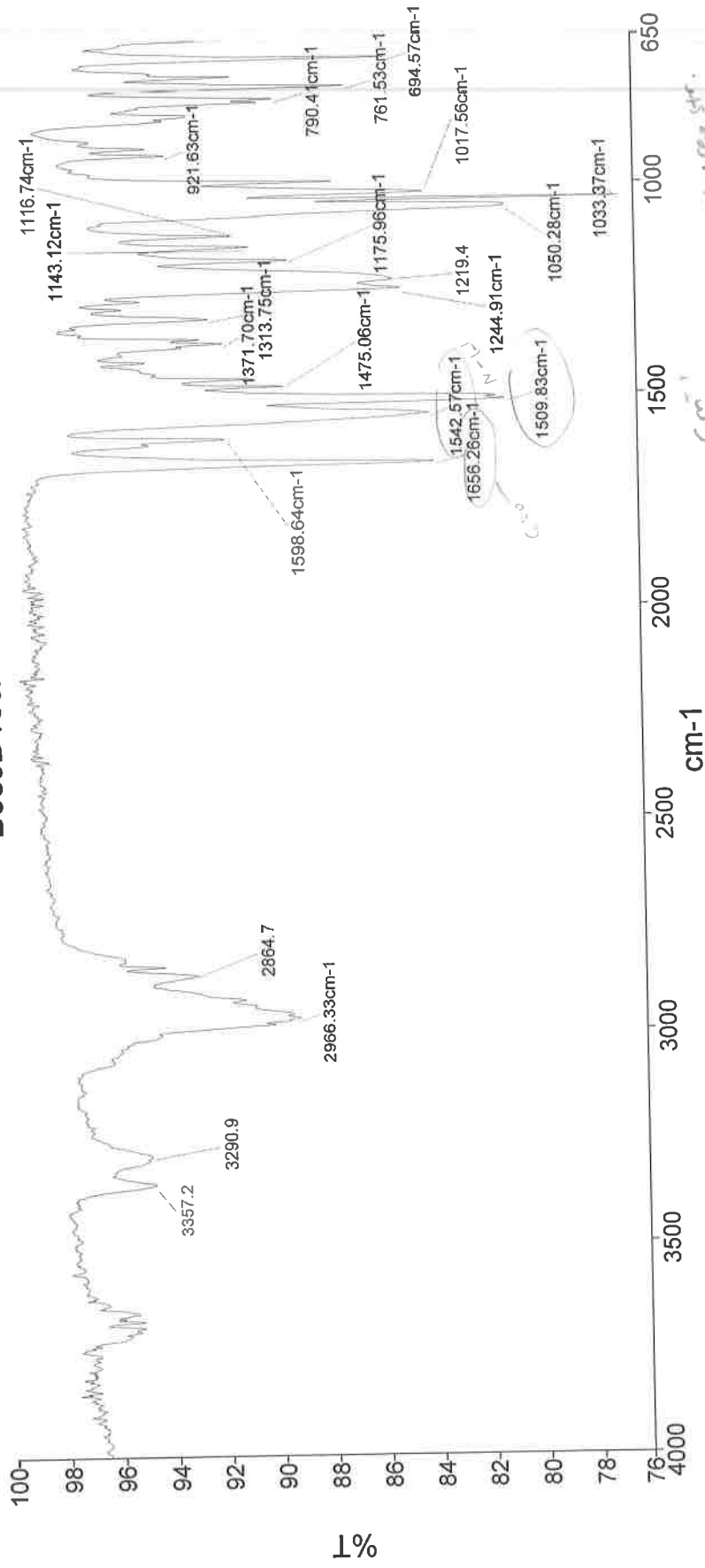
PerkinElmer Spectrum Version 10.03.06
26 November 2014 15:19

Analyst

Date

Administrator
26 November 2014 15:19

B03JD139A



cm⁻¹

- 3291 - N-H stretch
- 2966 - C-H alk. str.
- 2966 - C-H alk. str.
- 1656 - C=O amide stretch
- 1656 - N-H stretch
- 1543 - N-H str.
- 1510 - CH alk bend
- 1445 - C-N amide str.
- 1430 - C-O str. ether
- 1033 - C-N str.

Single Mass Analysis

Tolerance = 100.0 PPM / DBE: min = -1.5, max = 50.0

Element prediction: Off

Number of isotope peaks used for i-FIT = 3

Monoisotopic Mass, Even Electron Ions

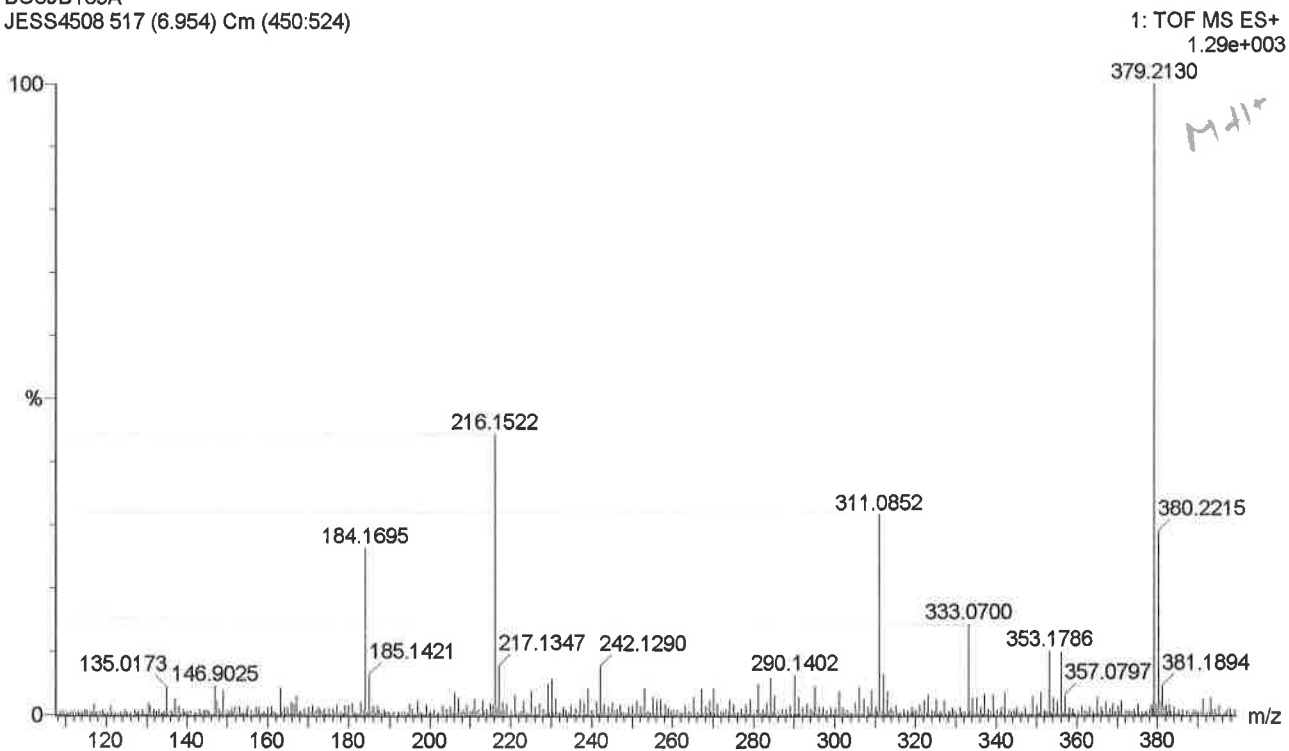
2 formula(e) evaluated with 1 results within limits (all results (up to 1000) for each mass)

Elements Used:

C: 22-22 H: 0-50 N: 4-4 O: 1-2

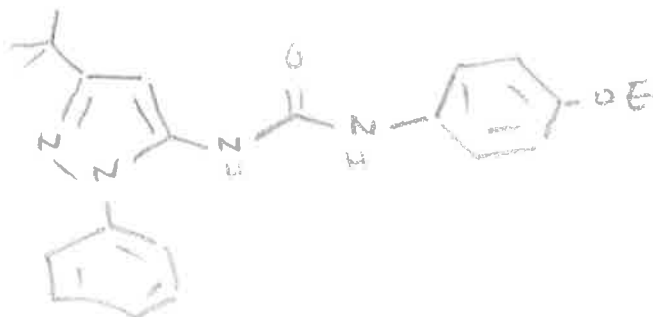
BO3JD139A

JESS4508 517 (6.954) Cm (450:524)

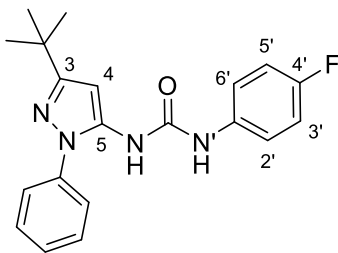


Minimum: -1.5
Maximum: 5.0 100.0 50.0

Mass	Calc. Mass	mDa	PPM	DBE	i-FIT	Formula
379.2130	379.2134	-0.4	-1.1	11.5	2.9	C22 H27 N4 O2

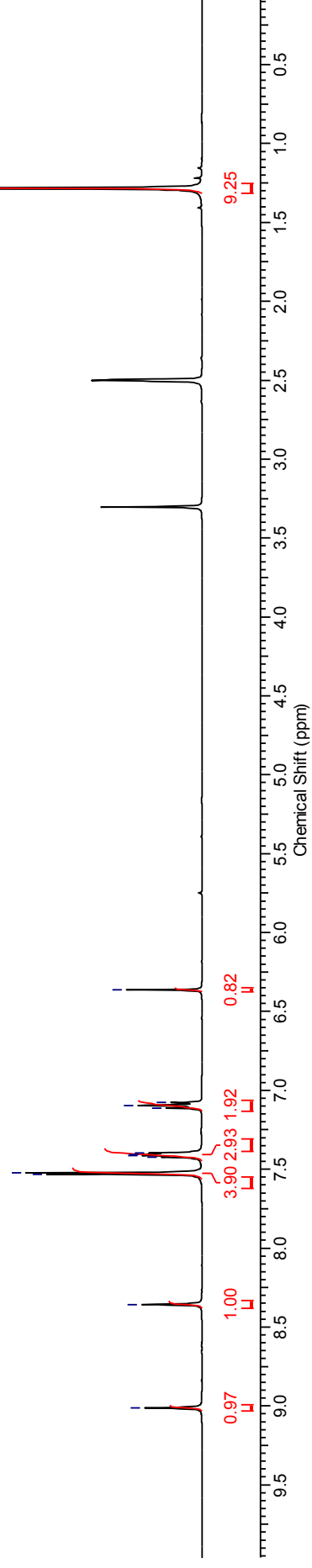
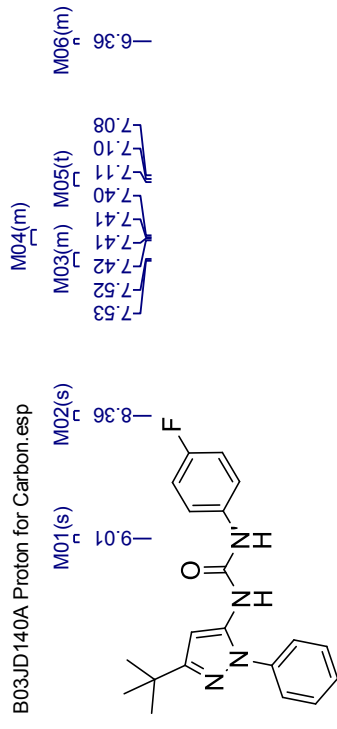


***N*-(3-(*tert*-Butyl)-1-phenyl-1*H*-pyrazol-5-yl)-*N'*-(4-fluorophenyl)urea**
(215E)



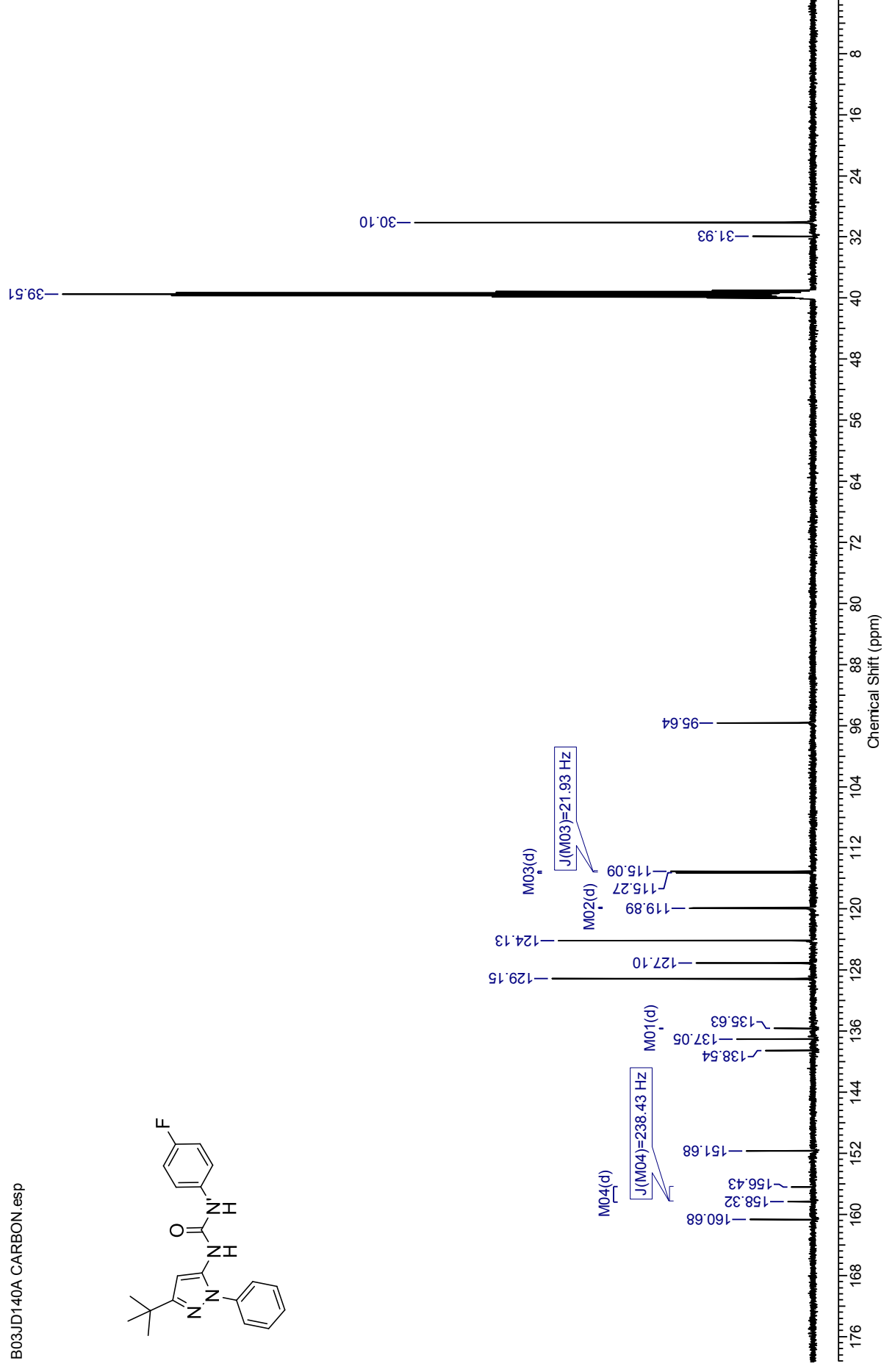
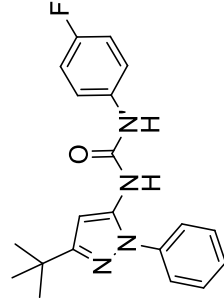
¹H NMR spectrum (500 MHz, DMSO-*d*₆) for *N*-(3-(*tert*-butyl)-1*H*-pyrazol-5-yl)-1-phenyl-1*H*-pyrazol-5-yl)-*N'*-(4-fluorophenyl)urea

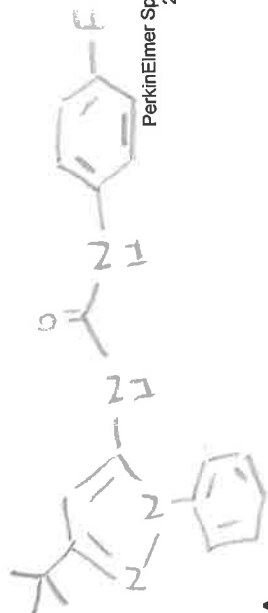
B03JD140A Proton for Carbon. esp



¹³C NMR spectrum (126 MHz, DMSO-*d*₆) for *N*-(3-(*tert*-butyl)-1-phenyl-1*H*-pyrazol-5-yl)-*N'*-(4-fluorophenyl)urea

B03JD140A CARBON.esp



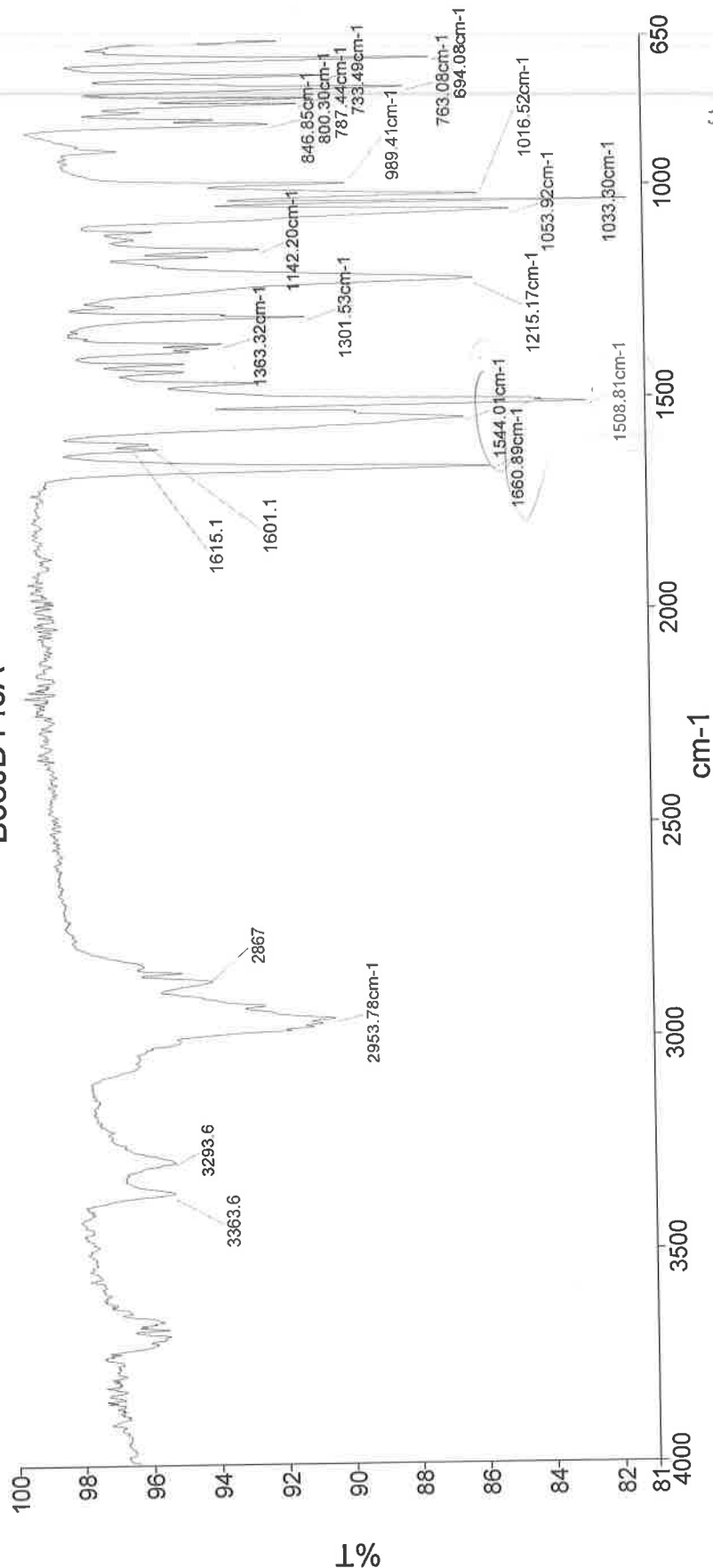


PerkinElmer Spectrum Version 10.03.06
26 November 2014 15:22

Analyst
Date

Administrator
26 November 2014 15:22

B03JD140A



3294 - N-H Urea str.
2954 - C-H alk. str.
1661 - C=O str. bend
1544 - N-H amide bend
1509 - N-H amide
1251 - C-N str. aromatic amide
1033 - C-N bend
763 - C-H rock

Single Mass Analysis

Tolerance = 100.0 PPM / DBE: min = -1.5, max = 50.0

Element prediction: Off

Number of isotope peaks used for i-FIT = 3

Monoisotopic Mass, Even Electron Ions

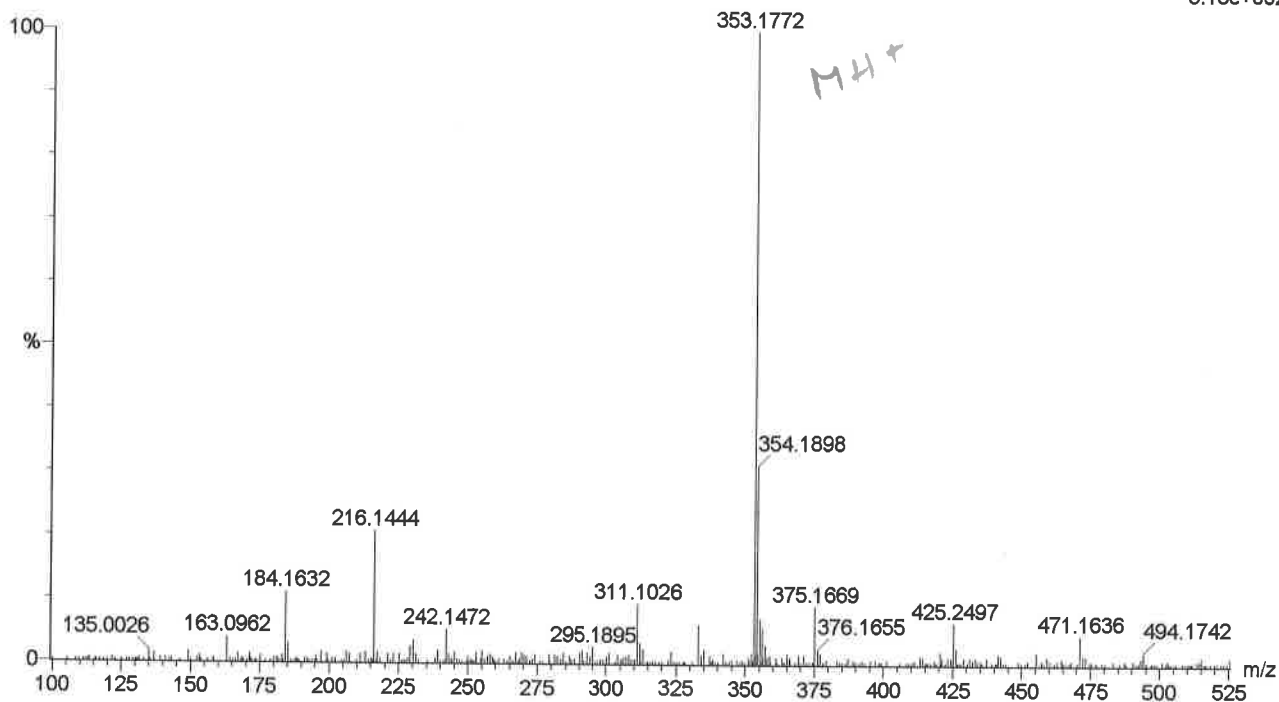
1 formula(e) evaluated with 1 results within limits (all results (up to 1000) for each mass)

Elements Used:

C: 20-20 H: 0-50 N: 4-4 O: 1-1 F: 1-1

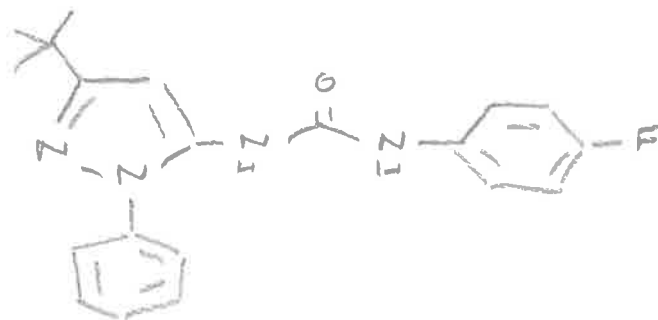
BO3JD140A

JESS4509 133 (1.801) Cm (127:136)

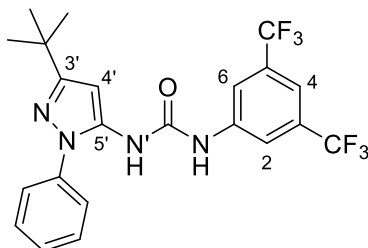
1: TOF MS ES+
3.13e+002

Minimum: -1.5
Maximum: 5.0 100.0 50.0

Mass	Calc. Mass	mDa	PPM	DBE	i-FIT	Formula
353.1772	353.1778	-0.6	-1.7	11.5	6.3	C20 H22 N4 O F



***N*-(3,5-Bis(trifluoromethyl)phenyl)-*N'*-(3-(*tert*-butyl)-1-phenyl-1*H*-pyrazol-5-yl)urea (215F)**



¹H NMR spectrum (500 MHz, DMSO-*d*₆) for *N*-(3,5-bis(trifluoromethyl)phenyl)-*N'*-(3-(*tert*-butyl)-1*H*-pyrazol-5-yl)urea

B03JD141A DMSO Proton for Carbon.esp

M08(m)

M07(m)

M03(br s.)
9.70

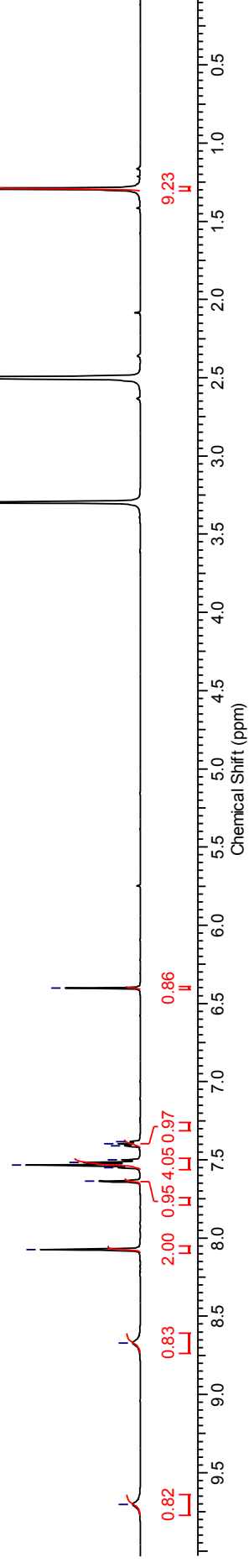
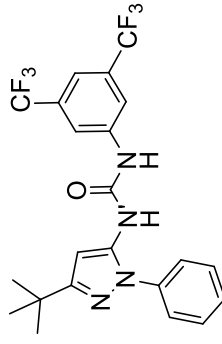
M04(br s.)
8.67

M05(s)
8.07

M06(s)
7.64
7.56
7.53
7.52
7.50
7.41
7.40
7.38

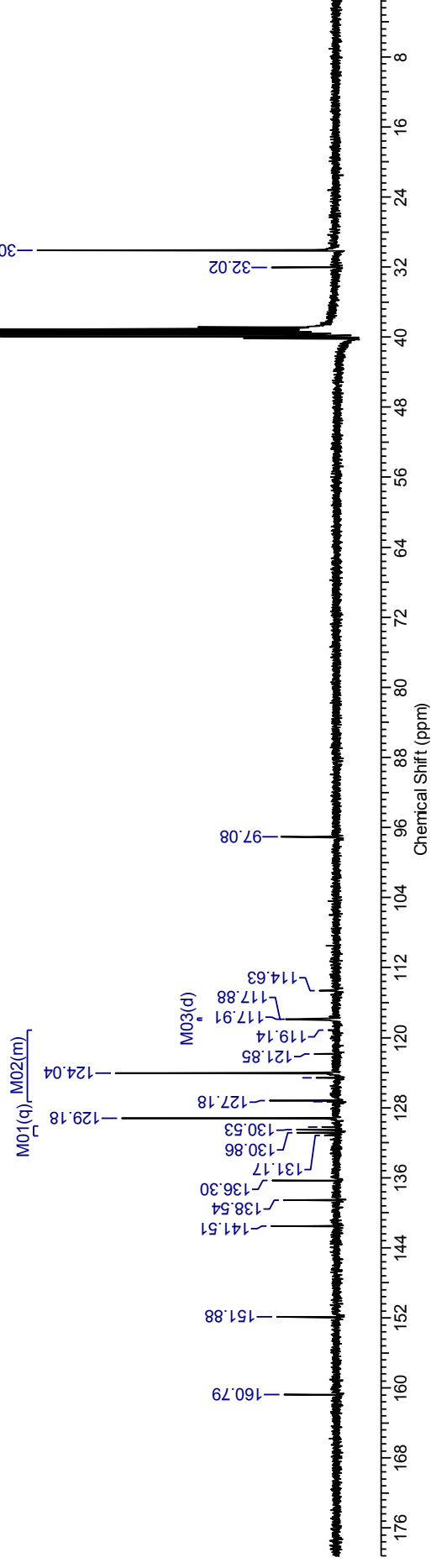
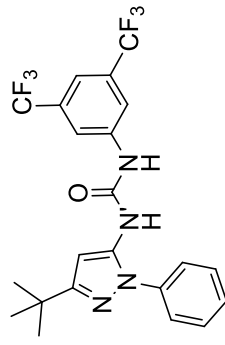
M02(s)
6.40

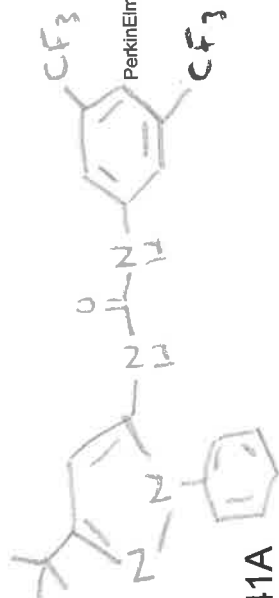
M01(s)
1.29



¹³C NMR spectrum (100 MHz, DMSO-*d*₆) for *N*-(3,5-bis(trifluoromethyl)phenyl)-*N'*-(3-(*tert*-butyl)-1-phenyl-1*H*-pyrazol-5-yl)urea

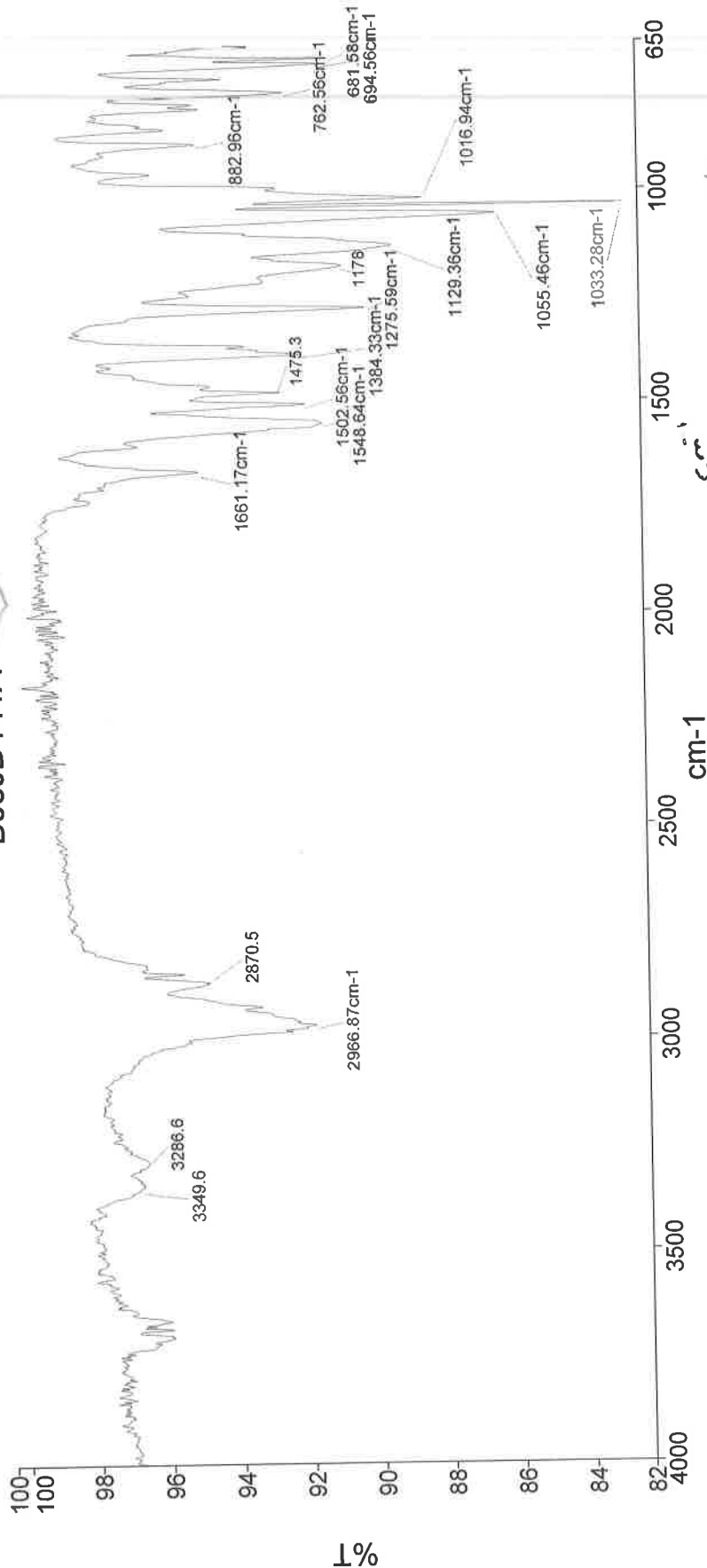
B03JD141A DMSO CARBON vNMR 400.esp





B03JD141A

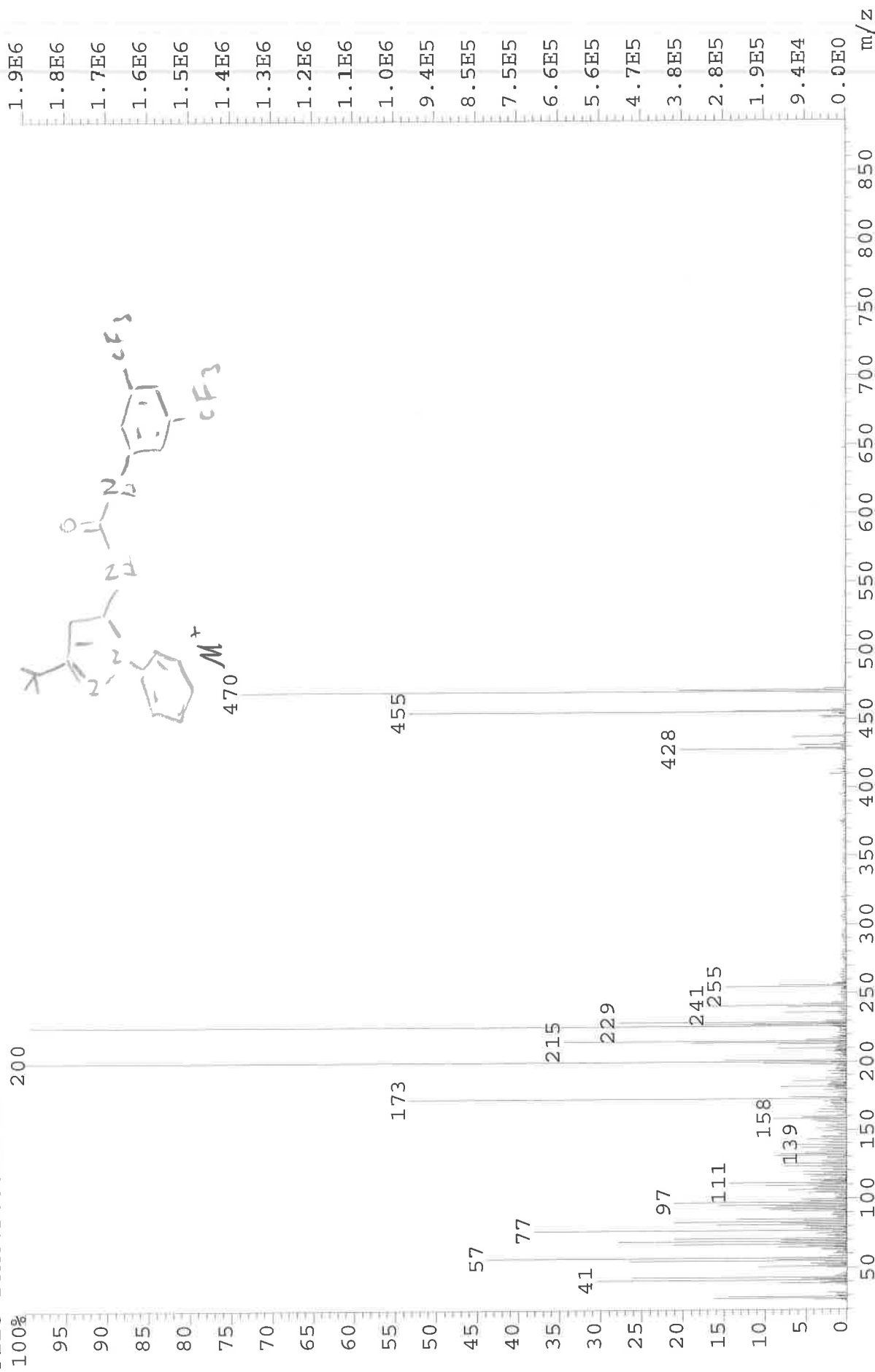
Analyst
Date
26 November 2014 15:24



Administrator 10 Sample 010 By Administrator Date Wednesday, November 26 2014

3287 - N-H urea str.
2967 - C-H str. alk
1662 - C=O str.
1549 - N-H bend
1502 - N-H bend
1276 - C-N str.
1129 - C-F
1033 - C-N str.
762 - C-F rock aryl

File: JESS4510 Ident: 22 Acq: 12-NOV-2014 13:49:43 +1:24 Cal: CAL1
AutoSpecE EI+ Magnet BpI: 1881008 TIC: 33837172 Flags: HALL
File Text: B03JD141A



Single Mass Analysis

Tolerance = 2000.0 PPM / DBE: min = -1.5, max = 50.0

Element prediction: Off

Number of isotope peaks used for i-FIT = 3

Monoisotopic Mass, Even Electron Ions

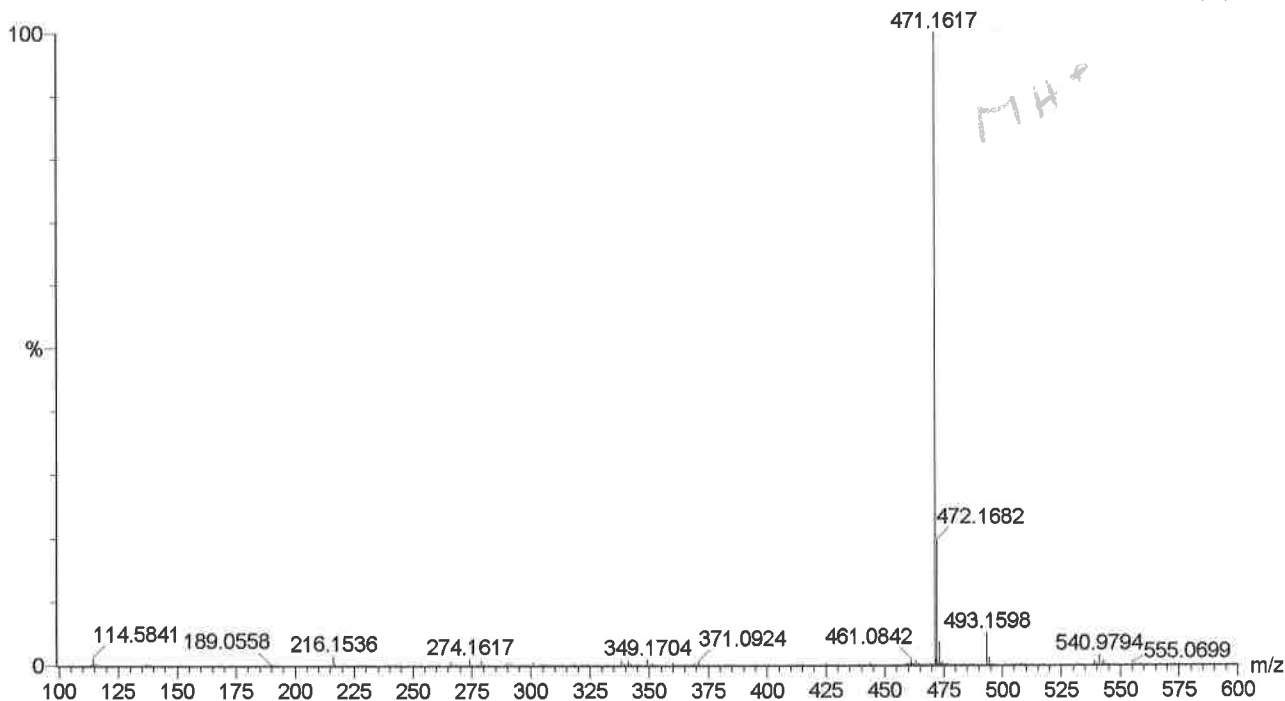
1 formula(e) evaluated with 1 results within limits (all results (up to 1000) for each mass)

Elements Used:

C: 22-22 H: 0-30 N: 4-4 O: 1-1 F: 6-6 ²³Na: 0-1

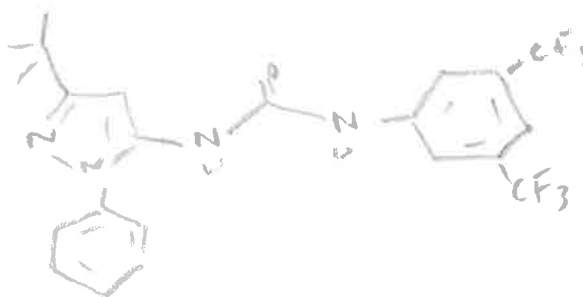
BO3JD141A

JESS4745 96 (1.296) Cm (91:96)

1: TOF MS ES+
5.84e+004

Minimum: -1.5
Maximum: 5.0 2000.0 50.0

Mass	Calc. Mass	mDa	PPM	DBE	i-FIT	Formula
471.1617	471.1620	-0.3	-0.6	11.5	895535.4	C22 H21 N4 O F6



BIRB_libhit1

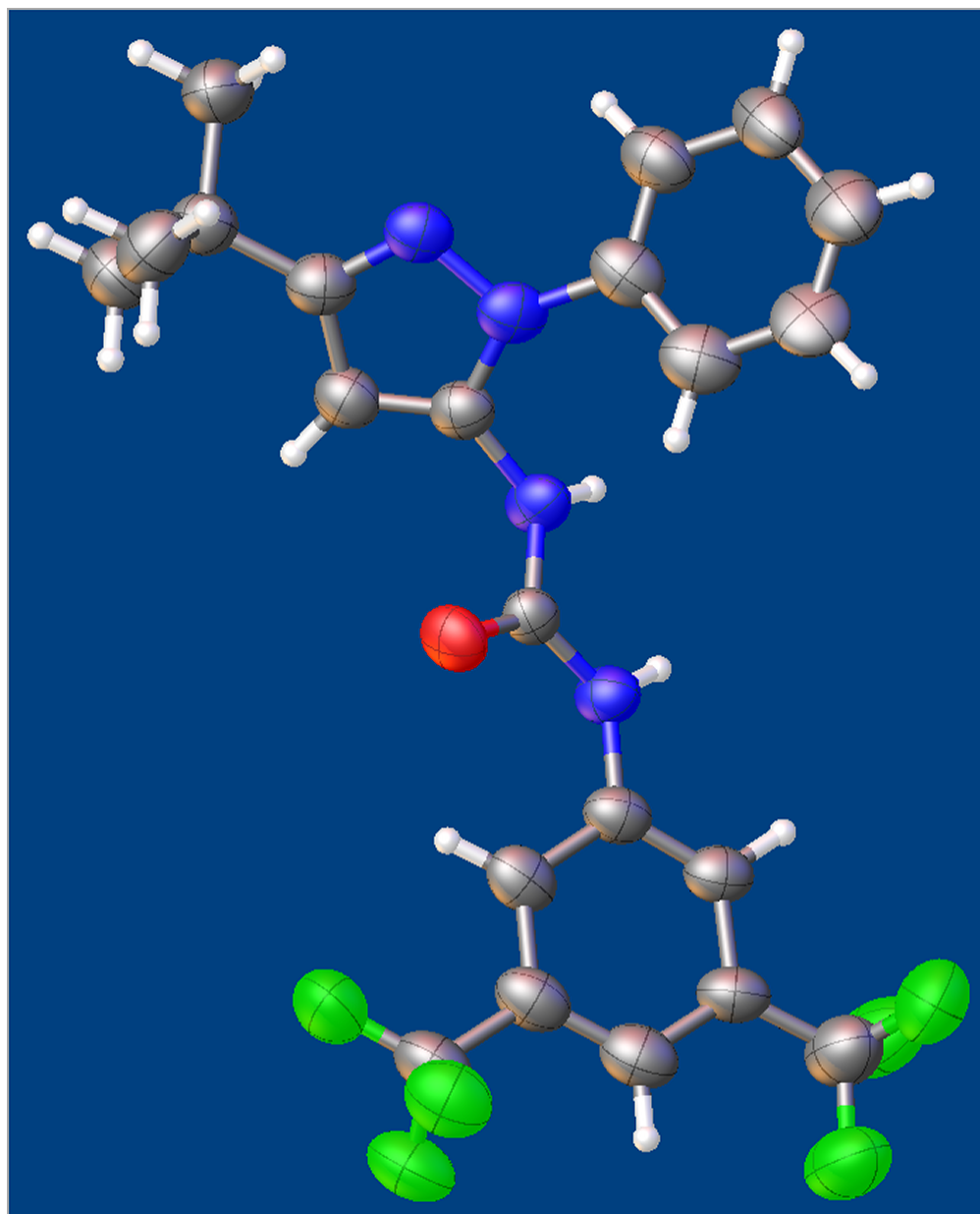


Table 1 Crystal data and structure refinement for BIRB_libhit1.

Identification code	BIRB_libhit1
Empirical formula	C ₂₂ H ₂₀ F ₆ N ₄ O
Formula weight	470.42
Temperature/K	173.0
Crystal system	monoclinic
Space group	P2 ₁ /c
a/Å	14.621(4)
b/Å	16.734(6)
c/Å	8.879(3)
α /°	90
β /°	100.61(3)
γ /°	90
Volume/Å ³	2135.4(12)
Z	4
ρ _{calc} /cm ³	1.463

μ/mm^{-1}	1.119
F(000)	968.0
Crystal size/ mm^3	$0.2 \times 0.04 \times 0.02$
Radiation	$\text{CuK}\alpha$ ($\lambda = 1.54184$)
2Θ range for data collection/ $^\circ$	8.11 to 79.926
Index ranges	$-12 \leq h \leq 12$, $-13 \leq k \leq 13$, $-7 \leq l \leq 5$
Reflections collected	2308
Independent reflections	1271 [$R_{\text{int}} = 0.0540$, $R_{\text{sigma}} = 0.1074$]
Data/restraints/parameters	1271/267/302
Goodness-of-fit on F^2	1.056
Final R indexes [$I \geq 2\sigma(I)$]	$R_1 = 0.0848$, $wR_2 = 0.2201$
Final R indexes [all data]	$R_1 = 0.1342$, $wR_2 = 0.2902$
Largest diff. peak/hole / $e \text{ \AA}^{-3}$	0.27/-0.30

Table 2 Fractional Atomic Coordinates ($\times 10^4$) and Equivalent Isotropic Displacement Parameters ($\text{\AA}^2 \times 10^3$) for BIRB_libhit1. U_{eq} is defined as 1/3 of the trace of the orthogonalised U_{IJ} tensor.

Atom	<i>x</i>	<i>y</i>	<i>z</i>	<i>U</i> (eq)
F1	9182 (6)	615 (7)	4684 (11)	106 (4)
F2	9676 (6)	1788 (7)	5096 (11)	103 (3)
F3	10234 (6)	877 (7)	6629 (10)	103 (4)
F4	7556 (6)	1271 (6)	11324 (10)	92 (3)
F5	8692 (6)	500 (5)	11145 (9)	84 (3)
F6	8918 (6)	1741 (5)	11492 (10)	87 (3)
O1	5687 (6)	2615 (5)	7743 (10)	61 (3)
N1	2990 (8)	3912 (7)	5520 (13)	55 (3)
N2	3804 (8)	3679 (7)	5005 (13)	57 (3)
N3	4836 (7)	2560 (7)	5355 (12)	56 (4)
N4	6304 (7)	2001 (7)	5873 (12)	54 (3)
C1	2814 (10)	3372 (9)	6517 (17)	59 (4)
C2	3490 (10)	2760 (9)	6659 (16)	57 (4)
C3	4059 (10)	2966 (9)	5733 (16)	52 (4)
C4	5640 (10)	2401 (8)	6399 (17)	44 (4)
C5	7169 (10)	1751 (8)	6694 (17)	54 (4)
C6	7867 (10)	1570 (8)	5946 (17)	55 (4)
C7	8738 (10)	1297 (9)	6687 (18)	58 (4)
C8	8876 (11)	1180 (9)	8248 (18)	67 (4)
C9	8172 (11)	1343 (9)	9053 (17)	63 (4)
C10	7302 (10)	1604 (8)	8255 (16)	58 (4)
C11	9451 (13)	1127 (13)	5820 (20)	84 (4)
C12	8315 (13)	1217 (11)	10695 (19)	73 (4)
C13	2016 (10)	3470 (9)	7334 (16)	61 (4)
C14	1196 (10)	3854 (10)	6277 (17)	75 (5)
C15	1720 (10)	2666 (9)	7862 (18)	76 (5)
C16	2322 (10)	3996 (10)	8758 (17)	78 (5)
C17	4102 (12)	4168 (9)	3875 (18)	64 (4)
C18	3491 (11)	4556 (9)	2833 (16)	68 (5)
C19	3811 (12)	5064 (10)	1812 (17)	73 (5)
C20	4763 (13)	5123 (10)	1890 (18)	81 (5)
C21	5350 (12)	4719 (9)	2946 (18)	71 (4)
C22	5051 (11)	4217 (9)	3995 (18)	69 (4)

Table 3 Anisotropic Displacement Parameters ($\text{\AA}^2 \times 10^3$) for BIRB_libhit1. The Anisotropic displacement factor exponent takes the form:

$$-2\pi^2[h^2a^{*2}U_{11}+2hka^*b^*U_{12}+...].$$

Atom	U_{11}	U_{22}	U_{33}	U_{23}	U_{13}	U_{12}
F1	84 (7)	129 (8)	101 (7)	-36 (6)	9 (5)	22 (6)
F2	91 (7)	122 (8)	104 (7)	5 (6)	41 (6)	15 (6)
F3	75 (6)	140 (9)	92 (7)	-4 (6)	8 (5)	25 (6)
F4	86 (6)	117 (8)	70 (6)	22 (5)	9 (5)	7 (5)
F5	106 (7)	67 (6)	71 (6)	9 (4)	-6 (5)	9 (5)
F6	95 (7)	81 (7)	76 (6)	-6 (5)	-4 (5)	-5 (5)
O1	70 (7)	68 (7)	41 (6)	-5 (5)	2 (5)	2 (5)
N1	51 (6)	57 (7)	53 (7)	-4 (5)	-3 (5)	-5 (5)
N2	49 (6)	55 (7)	60 (7)	-3 (5)	-3 (5)	-7 (5)
N3	50 (6)	74 (8)	41 (7)	-9 (6)	0 (5)	6 (5)
N4	53 (6)	57 (8)	51 (7)	-5 (6)	6 (5)	7 (5)
C1	58 (7)	54 (8)	64 (8)	0 (6)	5 (6)	1 (5)
C2	60 (8)	56 (8)	51 (8)	0 (6)	3 (6)	0 (6)
C3	51 (7)	56 (7)	47 (8)	-4 (5)	1 (5)	2 (6)
C4	41 (7)	48 (9)	41 (7)	0 (6)	2 (5)	-7 (6)
C5	52 (7)	49 (9)	55 (7)	3 (6)	-2 (5)	-2 (6)
C6	53 (7)	47 (10)	62 (8)	3 (7)	1 (5)	2 (6)
C7	55 (7)	53 (9)	61 (7)	1 (6)	-4 (5)	6 (6)
C8	75 (8)	54 (11)	65 (7)	2 (6)	-3 (6)	2 (7)
C9	72 (7)	56 (9)	55 (6)	2 (5)	-7 (5)	-5 (7)
C10	64 (7)	49 (9)	57 (7)	2 (6)	0 (5)	-12 (6)
C11	71 (8)	104 (9)	74 (8)	-6 (6)	9 (6)	12 (6)
C12	85 (8)	71 (8)	57 (7)	8 (5)	-4 (6)	5 (6)
C13	58 (7)	64 (8)	60 (7)	5 (6)	5 (5)	3 (6)
C14	62 (8)	83 (11)	80 (9)	15 (8)	12 (7)	6 (7)
C15	78 (11)	76 (8)	72 (10)	10 (7)	13 (8)	2 (7)
C16	63 (10)	91 (11)	81 (9)	-13 (7)	16 (7)	3 (8)
C17	80 (7)	52 (9)	55 (8)	-3 (6)	-1 (6)	-7 (7)
C18	81 (8)	66 (10)	53 (8)	-1 (7)	2 (6)	7 (7)
C19	104 (9)	62 (10)	55 (9)	-1 (7)	20 (7)	20 (8)
C20	104 (9)	62 (11)	79 (11)	-8 (8)	27 (8)	19 (8)
C21	94 (9)	35 (10)	85 (10)	-16 (7)	19 (7)	9 (7)
C22	79 (8)	49 (10)	73 (9)	-9 (7)	0 (7)	-2 (7)

Table 4 Bond Lengths for BIRB_libhit1.

Atom	Atom	Length/Å	Atom	Atom	Length/Å
F1	C11	1.327 (19)	C5	C6	1.351 (18)
F2	C11	1.35 (2)	C5	C10	1.386 (18)
F3	C11	1.303 (18)	C6	C7	1.399 (18)
F4	C12	1.333 (19)	C7	C8	1.377 (19)
F5	C12	1.350 (17)	C7	C11	1.43 (2)
F6	C12	1.349 (17)	C8	C9	1.38 (2)
O1	C4	1.236 (14)	C9	C10	1.407 (19)
N1	N2	1.406 (15)	C9	C12	1.45 (2)
N1	C1	1.323 (17)	C13	C14	1.523 (19)
N2	C3	1.376 (17)	C13	C15	1.51 (2)
N2	C17	1.424 (19)	C13	C16	1.539 (19)
N3	C3	1.416 (17)	C17	C18	1.332 (19)
N3	C4	1.382 (16)	C17	C22	1.37 (2)
N4	C4	1.334 (16)	C18	C19	1.39 (2)
N4	C5	1.401 (16)	C19	C20	1.39 (2)
C1	C2	1.412 (19)	C20	C21	1.333 (19)
C1	C13	1.49 (2)	C21	C22	1.38 (2)
C2	C3	1.319 (18)			

Table 5 Bond Angles for BIRB_libhit1.

Atom	Atom	Atom	Angle/°	Atom	Atom	Atom	Angle/°
C1	N1	N2	107.9 (12)	C5	C10	C9	120.5 (15)
N1	N2	C17	117.2 (12)	F1	C11	F2	103.4 (15)
C3	N2	N1	105.1 (12)	F1	C11	C7	113.2 (16)
C3	N2	C17	137.5 (14)	F2	C11	C7	111.0 (16)
C4	N3	C3	123.6 (12)	F3	C11	F1	108.6 (16)
C4	N4	C5	127.8 (12)	F3	C11	F2	105.1 (16)
N1	C1	C2	109.7 (14)	F3	C11	C7	114.8 (16)
N1	C1	C13	121.1 (14)	F4	C12	F5	105.2 (14)
C2	C1	C13	129.2 (15)	F4	C12	F6	104.5 (14)
C3	C2	C1	105.5 (15)	F4	C12	C9	115.8 (14)
N2	C3	N3	117.7 (14)	F5	C12	C9	113.7 (14)
C2	C3	N2	111.8 (15)	F6	C12	F5	103.3 (13)
C2	C3	N3	130.5 (15)	F6	C12	C9	113.1 (15)
O1	C4	N3	118.8 (14)	C1	C13	C14	110.1 (12)
O1	C4	N4	124.7 (14)	C1	C13	C15	110.3 (13)
N4	C4	N3	116.5 (13)	C1	C13	C16	109.1 (12)
C6	C5	N4	120.2 (13)	C14	C13	C16	110.0 (13)
C6	C5	C10	118.1 (14)	C15	C13	C14	109.2 (12)
C10	C5	N4	121.4 (14)	C15	C13	C16	108.1 (13)
C5	C6	C7	123.2 (14)	C18	C17	N2	121.1 (15)
C6	C7	C11	120.1 (15)	C18	C17	C22	124.3 (16)
C8	C7	C6	118.1 (15)	C22	C17	N2	114.6 (15)
C8	C7	C11	121.8 (15)	C17	C18	C19	119.4 (16)
C7	C8	C9	120.5 (15)	C18	C19	C20	117.9 (16)
C8	C9	C10	119.3 (15)	C21	C20	C19	120.7 (18)
C8	C9	C12	120.6 (15)	C20	C21	C22	122.6 (17)
C10	C9	C12	120.1 (16)	C17	C22	C21	115.1 (16)

Table 6 Torsion Angles for BIRB_libhit1.

A	B	C	D	Angle/°	A	B	C	D	Angle/°
N1	N2	C3	N3	176.2 (11)	C5	C6	C7	C8	2 (2)
N1	N2	C3	C2	-1.4 (15)	C5	C6	C7	C11	-179.1 (16)
N1	N2	C17	C18	-32.1 (19)	C6	C5	C10	C9	6 (2)
N1	N2	C17	C22	146.0 (12)	C6	C7	C8	C9	-1 (2)
N1	C1	C2	C3	0.5 (16)	C6	C7	C11	F1	-55 (2)
N1	C1	C13	C14	36.0 (19)	C6	C7	C11	F2	61 (2)
N1	C1	C13	C15	156.6 (13)	C6	C7	C11	F3	180.0 (15)
N1	C1	C13	C16	-84.8 (16)	C7	C8	C9	C10	2 (2)
N2	N1	C1	C2	-1.4 (15)	C7	C8	C9	C12	179.8 (14)
N2	N1	C1	C13	177.0 (11)	C8	C7	C11	F1	123.7 (17)
N2	C17	C18	C19	176.1 (13)	C8	C7	C11	F2	-120.6 (16)
N2	C17	C22	C21	-177.2 (12)	C8	C7	C11	F3	-2 (3)
N4	C5	C6	C7	-178.2 (13)	C8	C9	C10	C5	-4 (2)
N4	C5	C10	C9	179.0 (13)	C8	C9	C12	F4	-170.0 (14)
C1	N1	N2	C3	1.7 (14)	C8	C9	C12	F5	-48 (2)
C1	N1	N2	C17	177.9 (11)	C8	C9	C12	F6	69 (2)
C1	C2	C3	N2	0.6 (16)	C10	C5	C6	C7	-5 (2)
C1	C2	C3	N3	-176.6 (13)	C10	C9	C12	F4	8 (2)
C2	C1	C13	C14	-145.9 (15)	C10	C9	C12	F5	129.8 (15)
C2	C1	C13	C15	-25 (2)	C10	C9	C12	F6	-112.8 (17)
C2	C1	C13	C16	93.3 (18)	C11	C7	C8	C9	-179.4 (16)
C3	N2	C17	C18	142.5 (16)	C12	C9	C10	C5	177.8 (14)
C3	N2	C17	C22	-39 (2)	C13	C1	C2	C3	-177.7 (14)
C3	N3	C4	O1	1 (2)	C17	N2	C3	N3	1 (2)
C3	N3	C4	N4	178.8 (13)	C17	N2	C3	C2	-176.4 (15)
C4	N3	C3	N2	118.2 (14)	C17	C18	C19	C20	2 (2)
C4	N3	C3	C2	-65 (2)	C18	C17	C22	C21	1 (2)
C4	N4	C5	C6	-160.1 (14)	C18	C19	C20	C21	-2 (2)
C4	N4	C5	C10	27 (2)	C19	C20	C21	C22	1 (2)
C5	N4	C4	O1	-1 (2)	C20	C21	C22	C17	0 (2)
C5	N4	C4	N3	-178.5 (12)	C22	C17	C18	C19	-2 (2)

Table 7 Hydrogen Atom Coordinates ($\text{\AA} \times 10^4$) and Isotropic Displacement Parameters ($\text{\AA}^2 \times 10^3$) for BIRB_libhit1.

Atom	x	y	z	U(eq)
H3	4805	2400	4403	67
H4	6186	1878	4893	65
H2	3526	2298	7289	68
H6	7761	1631	4864	66
H8	9458	987	8775	80
H10	6803	1681	8791	70
H14A	1382	4378	5943	113
H14B	678	3920	6828	113
H14C	999	3511	5381	113
H15A	1505	2326	6968	113
H15B	1215	2741	8435	113
H15C	2250	2411	8524	113
H16A	2859	3751	9421	117
H16B	1808	4045	9322	117
H16C	2494	4528	8440	117
H18	2842	4486	2790	82
H19	3390	5363	1081	87
H20	5001	5455	1184	97
H21	6000	4778	2980	85
H22	5471	3928	4743	83

Experimental

Single crystals of $\text{C}_{22}\text{H}_{20}\text{F}_6\text{N}_4\text{O}$ [BIRB_libhit1] were [1]. A suitable crystal was selected and [1] on a **Xcalibur, Eos, Gemini ultra** diffractometer. The crystal was kept at 173.0 K during data collection. Using Olex2 [1], the structure was solved with the ShelXT [2] structure solution program using Direct Methods and refined with the ShelXL [3] refinement package using Least Squares minimisation.

1. Dolomanov, O.V., Bourhis, L.J., Gildea, R.J., Howard, J.A.K. & Puschmann, H. (2009), J. Appl. Cryst. 42, 339-341.
2. Sheldrick, G.M. (2008). Acta Cryst. A64, 112-122.
3. Sheldrick, G.M. (2008). Acta Cryst. A64, 112-122.

Crystal structure determination of [BIRB_libhit1]

Crystal Data for $\text{C}_{22}\text{H}_{20}\text{F}_6\text{N}_4\text{O}$ ($M = 470.42$ g/mol): monoclinic, space group $P2_1/c$ (no. 14), $a = 14.621(4)$ Å, $b = 16.734(6)$ Å, $c = 8.879(3)$ Å, $\beta = 100.61(3)^\circ$, $V = 2135.4(12)$ Å³, $Z = 4$, $T = 173.0$ K, $\mu(\text{CuK}\alpha) = 1.119$ mm⁻¹, $D_{\text{calc}} = 1.463$ g/cm³, 2308 reflections measured ($8.11^\circ \leq 2\theta \leq 79.926^\circ$), 1271 unique ($R_{\text{int}} = 0.0540$, $R_{\text{sigma}} = 0.1074$) which were used in all calculations. The final R_1 was 0.0848 ($I > 2\sigma(I)$) and wR_2 was 0.2902 (all data).

Refinement model description

Number of restraints - 267, number of constraints - unknown.

Details:

1. Fixed Uiso

At 1.2 times of:

All C(H) groups, All N(H) groups

At 1.5 times of:

All C(H,H,H) groups

2. Rigid body (RIGU) restraints

C4, F5, C12, F6, F4, C9, C10, C8, C5, C7, N4, C6, C11, F3, F2, F1, O1, N3, C3, N2, C2, N1, C17, C1, C22, C18, C13, C21, C19, C14, C15, C16, C20

with sigma for 1-2 distances of 0.004 and sigma for 1-3 distances of 0.004

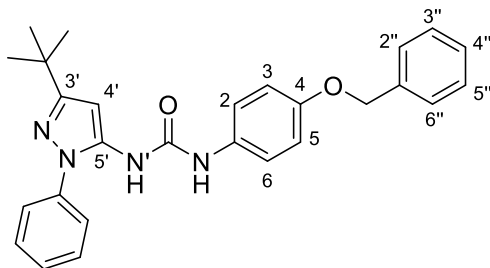
3.a Aromatic/amide H refined with riding coordinates:

N3(H3), N4(H4), C2(H2), C6(H6), C8(H8), C10(H10), C18(H18), C19(H19), C20(H20), C21(H21), C22(H22)

3.b Idealised Me refined as rotating group:

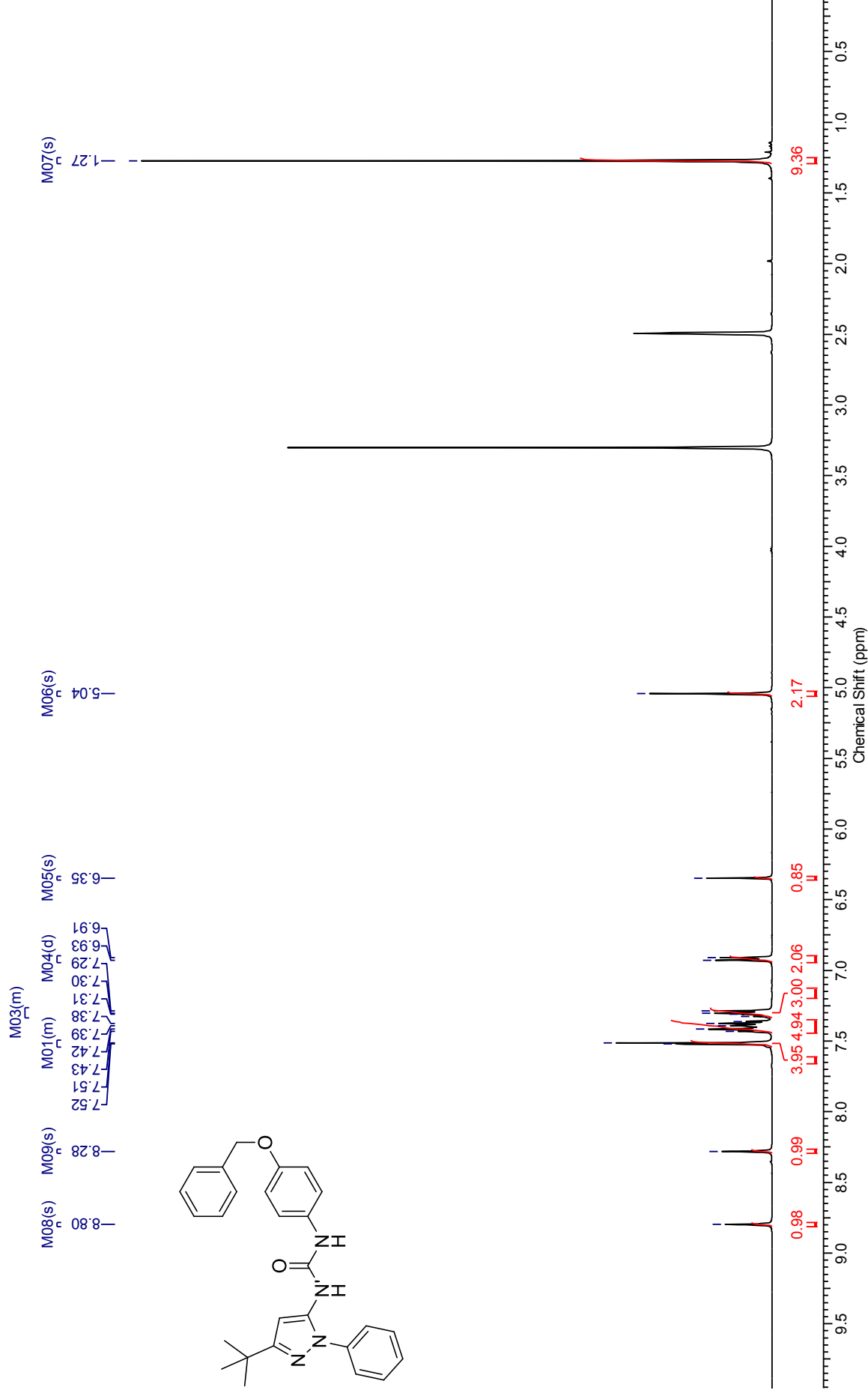
C14(H14A,H14B,H14C), C15(H15A,H15B,H15C), C16(H16A,H16B,H16C)

***N*-(4-(Benzyloxy)phenyl)-*N'*-(3-(*tert*-butyl)-1-phenyl-1*H*-pyrazol-5-yl)urea (215G)**



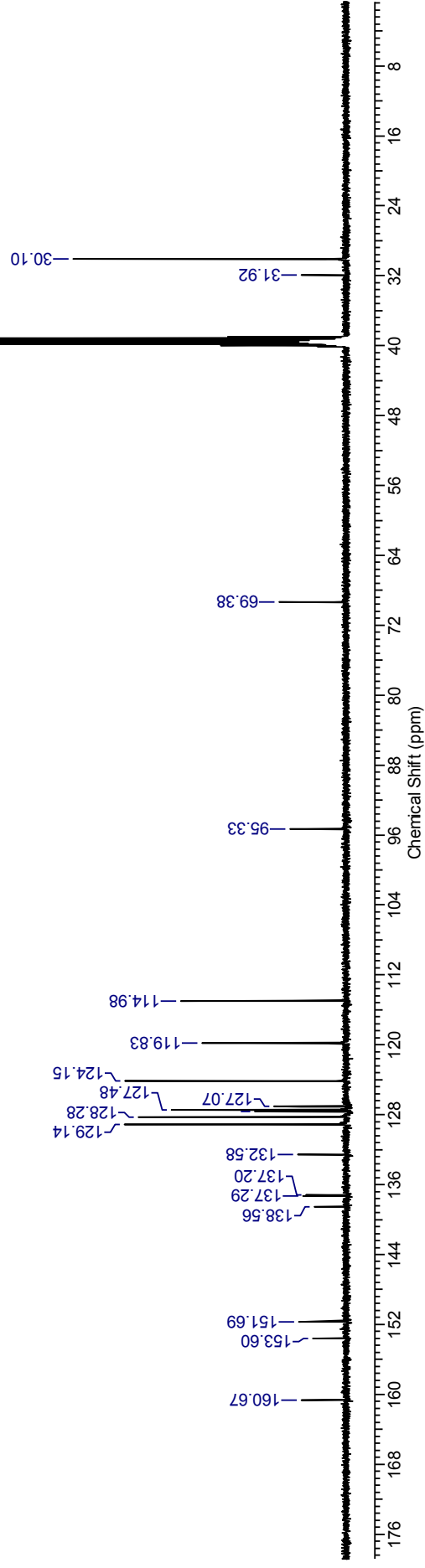
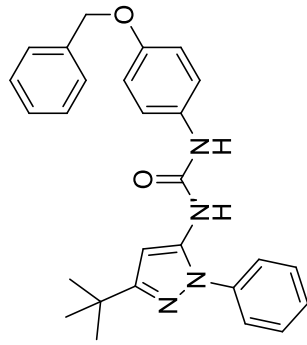
¹H NMR spectrum (500 MHz, DMSO-*d*₆) for *N*-(4-(benzyloxy)phenyl)-*N'*-(3-(*tert*-butyl)-1*H*-pyrazol-5-yl)urea

B03JD143A DMSO PROTON FOR CARBON.espM02(m)



¹³C NMR spectrum (126 MHz, DMSO-*d*₆) for *N*-(4-(benzyloxy)phenyl)-*N'*-(3-(*tert*-butyl)phenyl)-1*H*-pyrazol-5-yl)urea

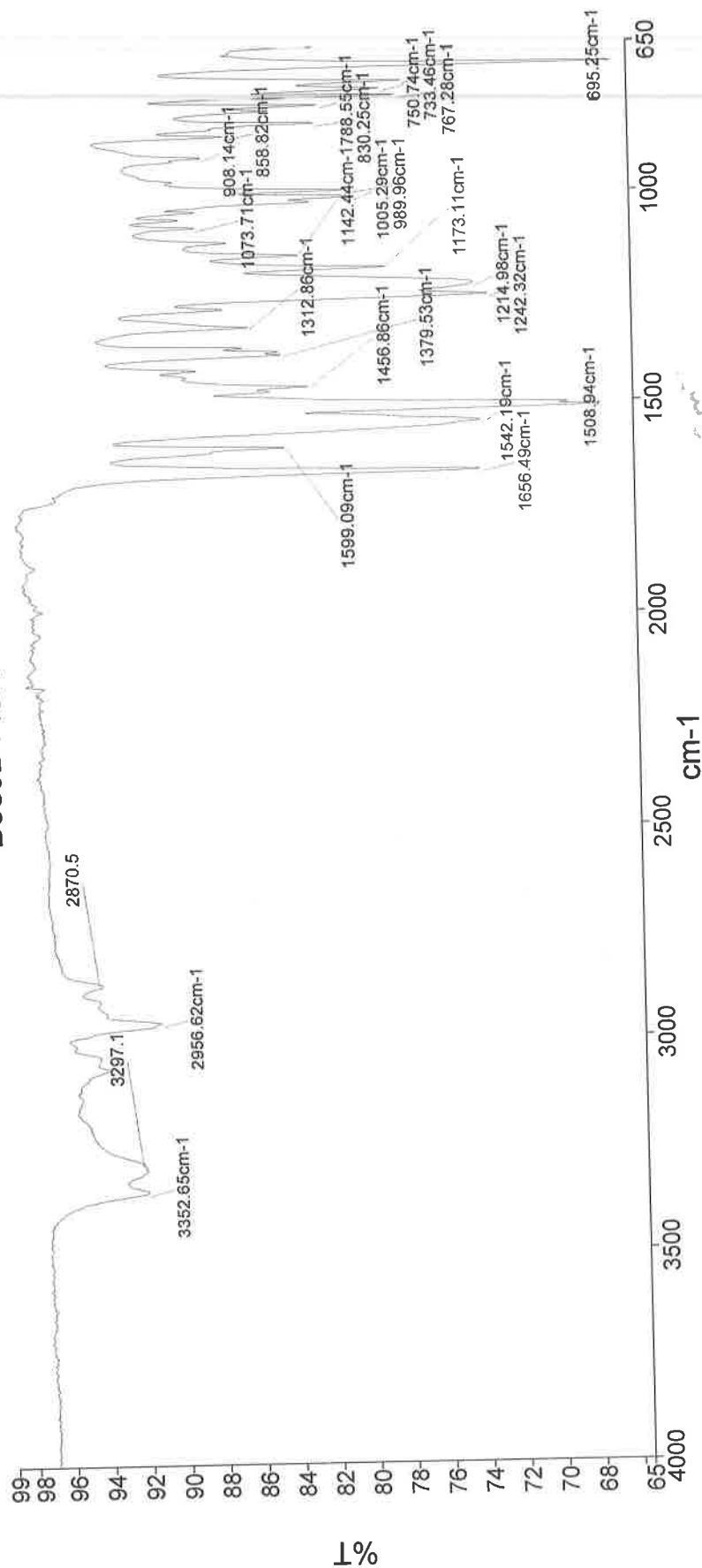
B03JD143A DMSO CARBON.esp



Analyst
Date

Administrator
26 November 2014 15:28

B03JD143A



Administrator 11 Sample 011 By Administrator Date Wednesday, November 26 2014

3297 - N-H urea str.
2957 - C-H alk. str.
1656 - C=O amide str.
1542 - N-H bend
1509 - N-H bend
1242 - C-N str.
1214 - C-O str.
1005 - C-H alk. str.
695 - C-H alk. str.

Single Mass Analysis

Tolerance = 100.0 PPM / DBE: min = -1.5, max = 50.0

Element prediction: Off

Number of isotope peaks used for i-FIT = 3

Monoisotopic Mass, Even Electron Ions

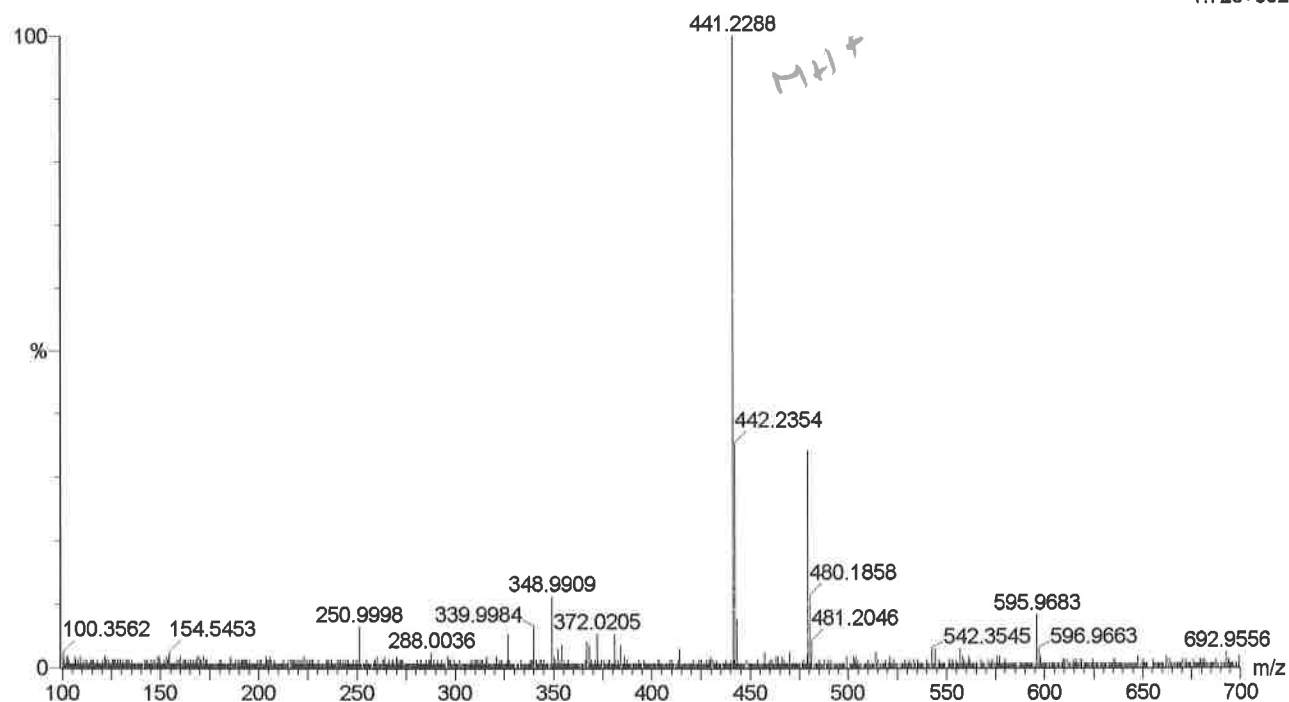
3 formula(e) evaluated with 1 results within limits (all results (up to 1000) for each mass)

Elements Used:

C: 27-27 H: 0-50 N: 4-4 O: 2-2 Na: 0-2

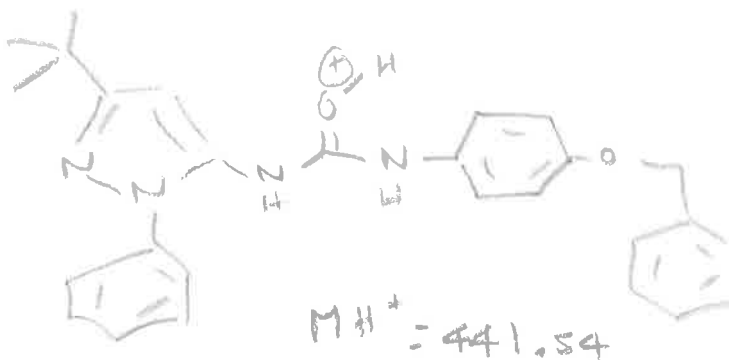
BO3JD143A

JESS4566 66 (0.899)

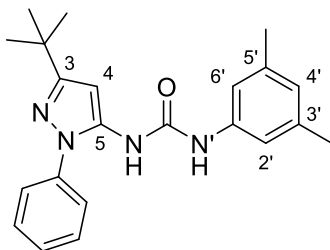
1: TOF MS ES+
1.72e+002

Minimum: -1.5
Maximum: 5.0 100.0 50.0

Mass	Calc. Mass	mDa	PPM	DBE	i-FIT	Formula
441.2288	441.2291	-0.3	-0.7	15.5	0.7	C27 H29 N4 O2



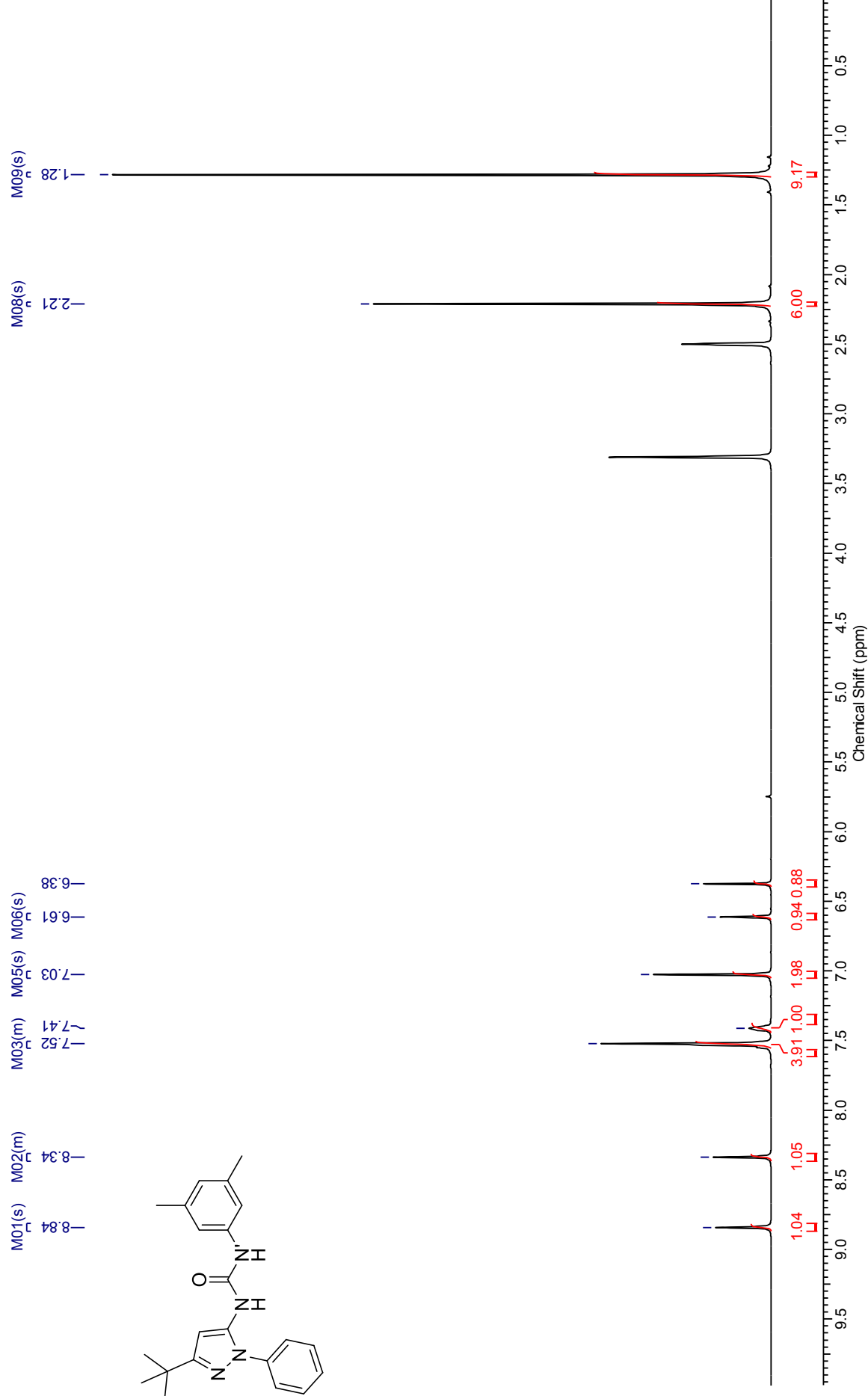
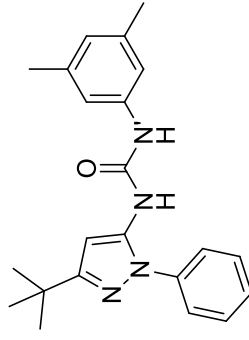
***N*-(3-(*tert*-Butyl)-1-phenyl-1*H*-pyrazol-5-yl)-*N'*-(3,5-dimethylphenyl)
urea (215H)**



¹H NMR spectrum (500 MHz, DMSO-*d*₆) for *N*-(3-(*tert*-butyl)-1*H*-pyrazol-5-yl)-1-phenyl-1*H*-pyrazol-5-yl)-*N'*-(3,5-dimethylphenyl)urea

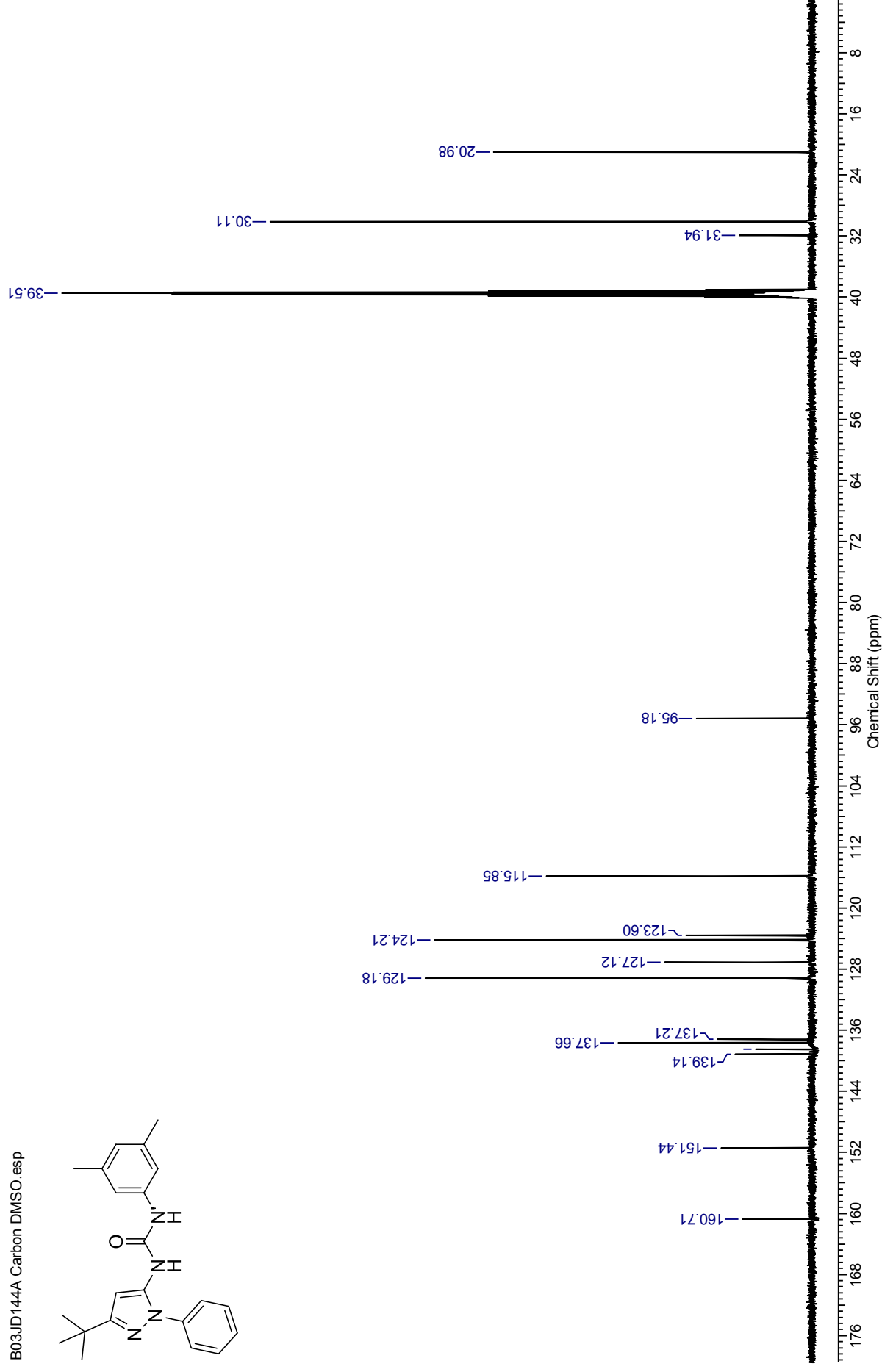
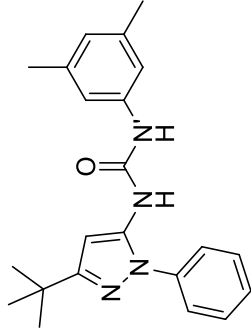
B03JD144A Proton for Carbon DMSO. esp

	M01(s)	M02(m)	M03(m)	M04(m)	M05(s)	M06(s)	M07(m)
	-8.84	-8.34	-7.52	-7.41	-7.03	-6.61	-6.38



¹³C NMR spectrum (126 MHz, DMSO-*d*₆) for *N*-(3-(*tert*-butyl)-1-phenyl-1*H*-pyrazol-5-yl)-1-phenyl-1*H*-pyrazol-5-yl)-*N'*-(3,5-dimethylphenyl)urea

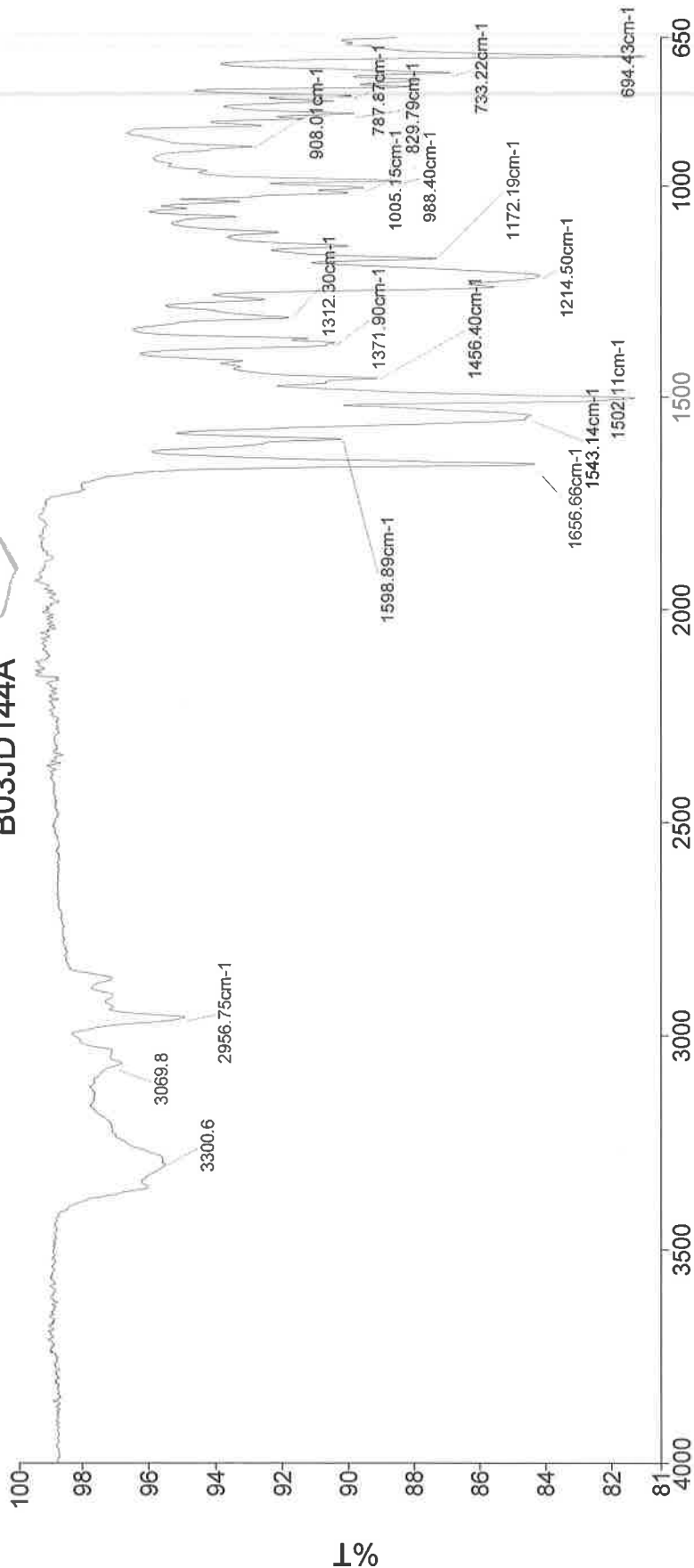
B03JD144A Carbon DMSO.esp



Analyst

Date 26 November 2014 15:34

B03JD144A



cm⁻¹	
3301	- N-H urea str.
2957	- C-H alk. str.
1657	- C=O str.
1543	- N-H bend
1502	- N-H bend
1372	- C-H alk. bend
1214	- C-N str. aromatic
1005	- C-N str.
694	- C-H rock

Administrator 13 Sample 013 By Administrator Date Wednesday, November 26 2014

Single Mass Analysis

Tolerance = 100.0 PPM / DBE: min = -1.5, max = 50.0

Element prediction: Off

Number of isotope peaks used for i-FIT = 3

Monoisotopic Mass, Even Electron Ions

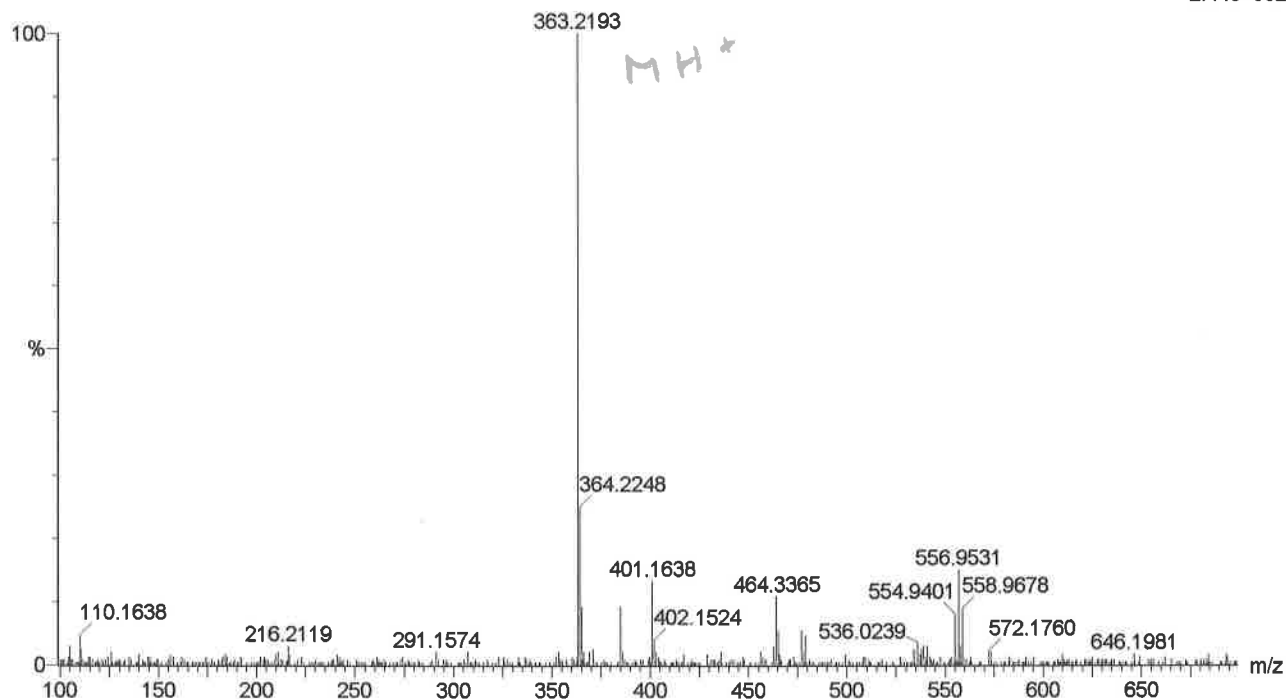
3 formula(e) evaluated with 1 results within limits (all results (up to 1000) for each mass)

Elements Used:

C: 22-22 H: 0-50 N: 4-4 O: 1-1 Na: 0-2

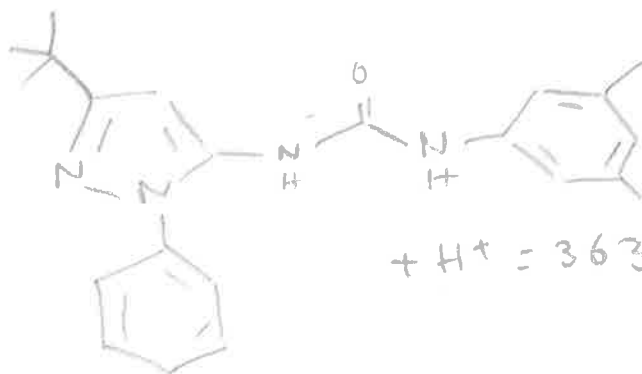
BO3JD144A

JESS4567 30 (0.416) Cm (28:30)

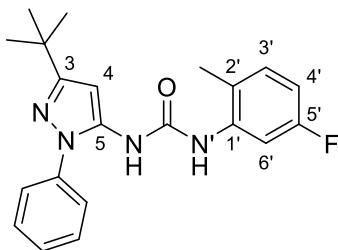
1: TOF MS ES+
2.44e+002

Minimum: -1.5
Maximum: 5.0 100.0 50.0

Mass	Calc. Mass	mDa	PPM	DBE	i-FIT	Formula
363.2193	363.2185	0.8	2.2	11.5	4.4	C22 H27 N4 O



***N*-(3-(*tert*-Butyl)-1-phenyl-1*H*-pyrazol-5-yl)-*N'*-(5-fluoro-2-methylphenyl)urea (215I)**



¹H NMR spectrum (500 MHz, DMSO-*d*₆) for *N*-(3-(*tert*-butyl)-1*H*-pyrazol-5-yl)-1-phenyl-1*H*-pyrazol-5-yl)-*N*'-(5-fluoro-2-methylphenyl)urea

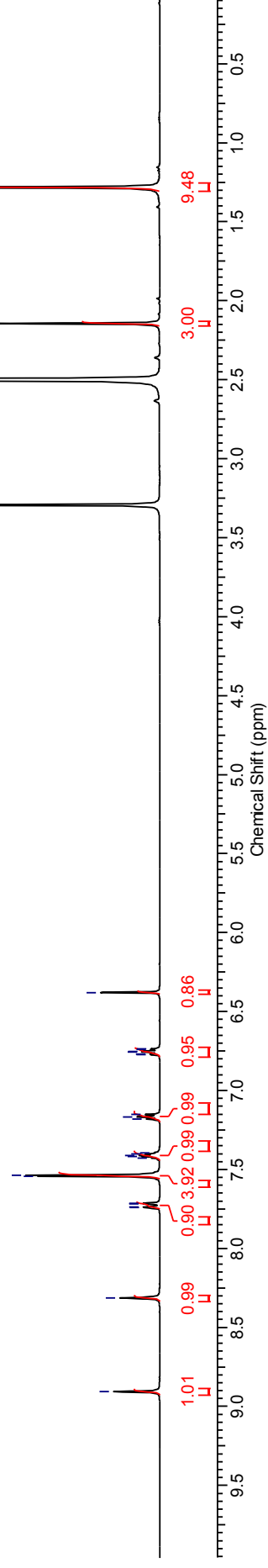
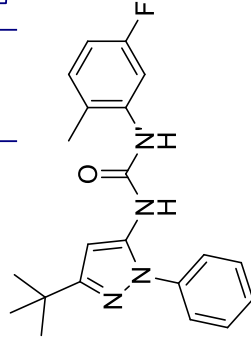
B03JD145A DMSO.esp

M05(m)

M03(dd)

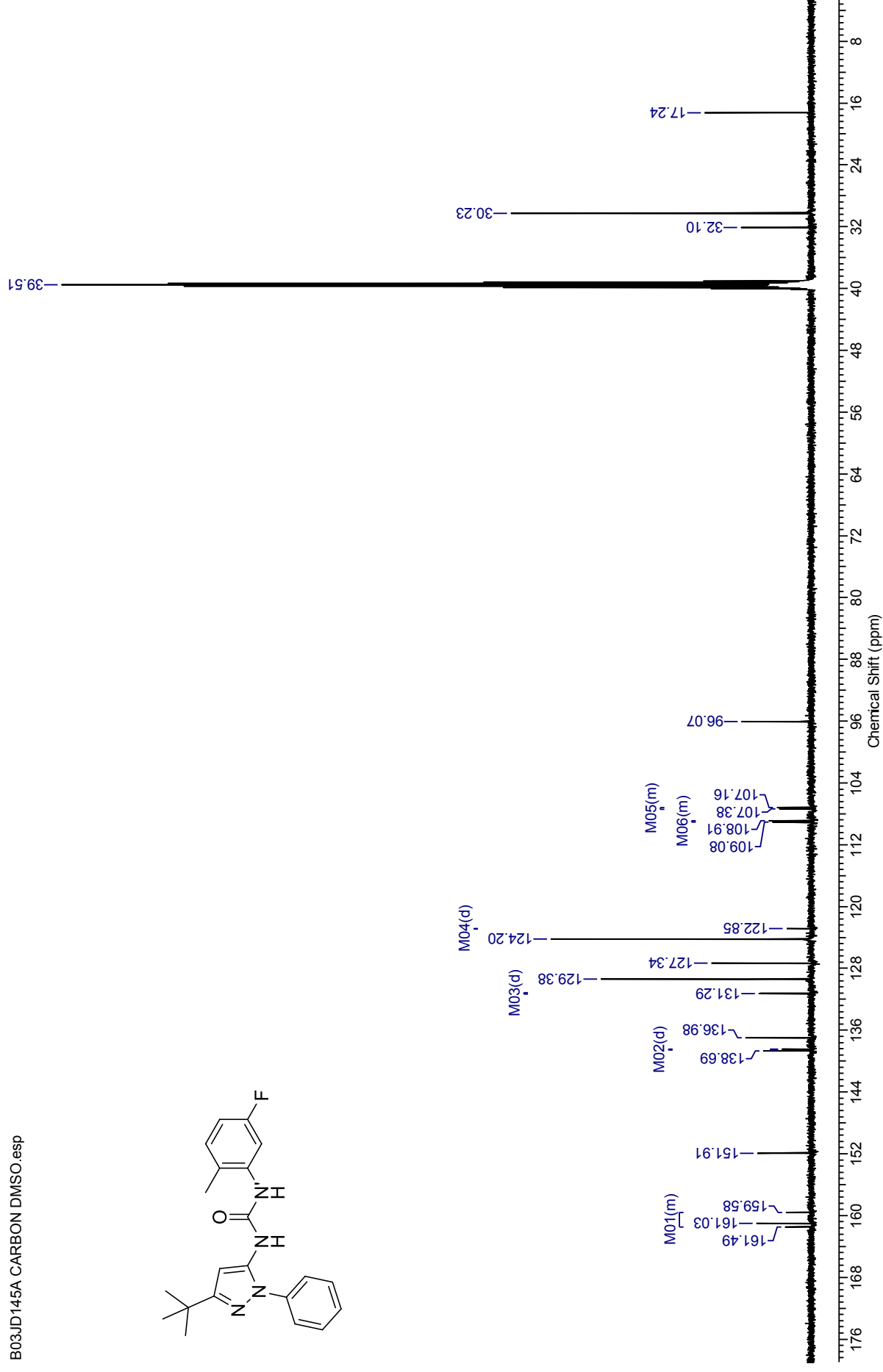
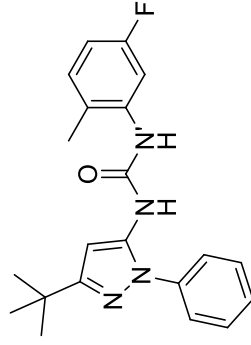
M01(m) M02(m) M04(m) M06(t) M07(td) M08(s)
8.91 8.31 7.74 7.74 7.72 7.71 7.54 7.54 7.42 7.41 7.18 7.17 7.15 6.77 6.76 6.75 6.38

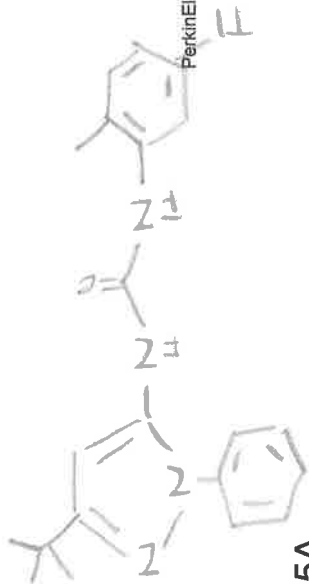
M09(s) M10(s)
2.15 1.28



¹³C NMR spectrum (126 MHz, DMSO-*d*₆) for *N*-(3-(*tert*-butyl)-1-phenyl-1*H*-pyrazol-5-yl)-*N'*-(5-fluoro-2-methylphenyl)urea

B03JD145A CARBON DMSO.esp



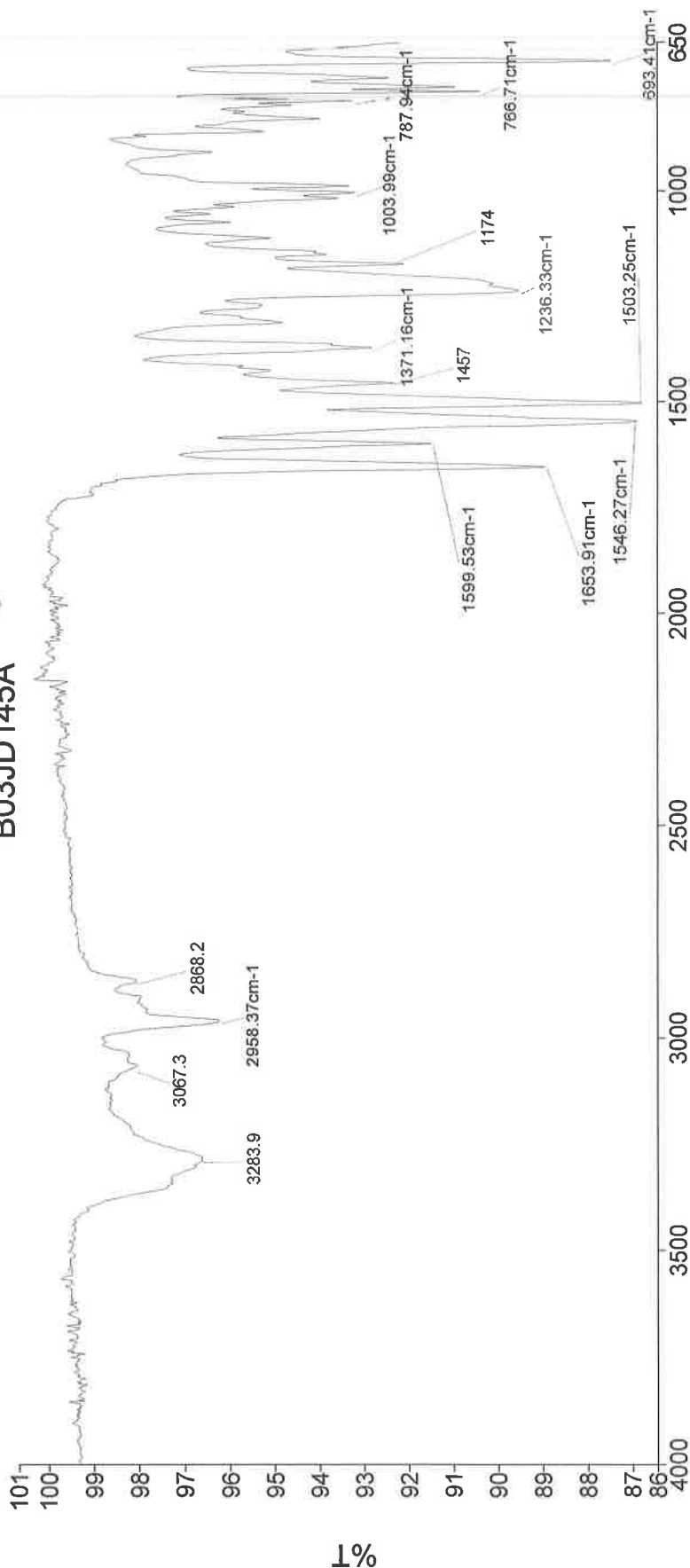


PerkinElmer Spectrum Version 10.03.06
26 November 2014 15:37

Analyst
Date

Administrator
26 November 2014 15:37

B03JD145A



cm⁻¹
3284 - N-H urea str.
2958 - C-H alk. str.
1654 - C=O str.
1546 - N-H bend
1503 - N-H bend
1457 - C-N str.
1371 - C-N bend
1236 - C-H rock
1174 -
1003 -
787 -
766 -
693 -

Administrator 14 Sample 014 By Administrator Date Wednesday, November 26 2014

Single Mass Analysis

Tolerance = 100.0 PPM / DBE: min = -1.5, max = 50.0

Element prediction: Off

Number of isotope peaks used for i-FIT = 3

Monoisotopic Mass, Even Electron Ions

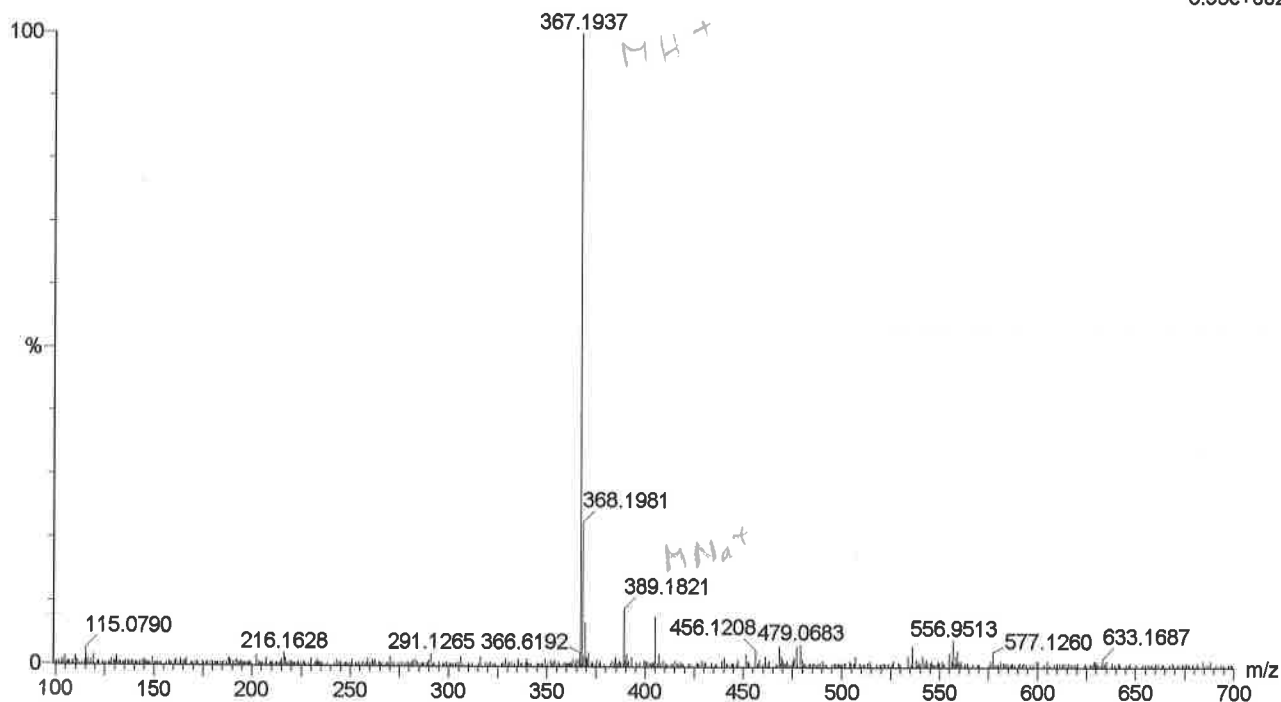
3 formula(e) evaluated with 1 results within limits (all results (up to 1000) for each mass)

Elements Used:

C: 21-21 H: 0-50 N: 4-4 O: 1-1 Na: 0-2 F: 1-1

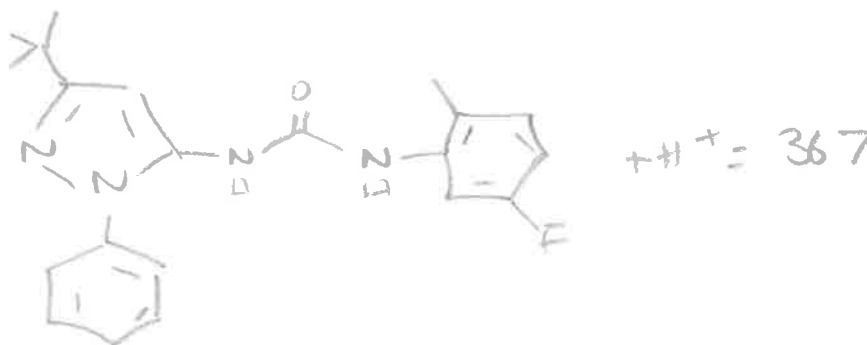
BO3JD145A

JESS4568 8 (0.115) Cm (7:8)

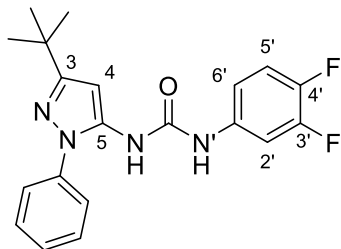
1: TOF MS ES+
3.95e+002

Minimum: -1.5
Maximum: 5.0 100.0 50.0

Mass	Calc. Mass	mDa	PPM	DBE	i-FIT	Formula
367.1937	367.1934	0.3	0.8	11.5	4.4	C21 H24 N4 O F



***N*-(3-(*tert*-Butyl)-1-phenyl-1*H*-pyrazol-5-yl)-*N'*-(3,4-difluorophenyl)
urea (215J)**



¹H NMR spectrum (500 MHz, DMSO-*d*₆) for *N*-(3-(*tert*-butyl)-1*H*-pyrazol-5-yl)-1-phenyl-1*H*-pyrazol-5-yl)-*N'*-(3,4-difluorophenyl)urea

B03JD146A Proton for carbon.esp

M05(q)

M07(m)

M06(m)

M08(d)

M04(d)

M03(s)

M02(s)

M01(s)

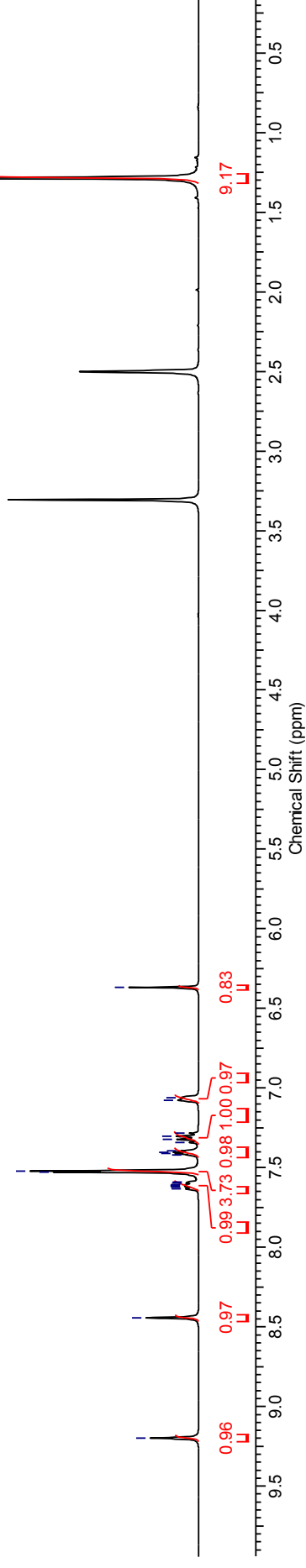
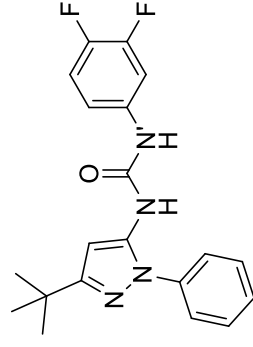
7.62
7.61
7.61
7.53
7.52
7.41
7.40
7.39
7.32
7.30
7.08
7.06

M09(s)

M03(s)

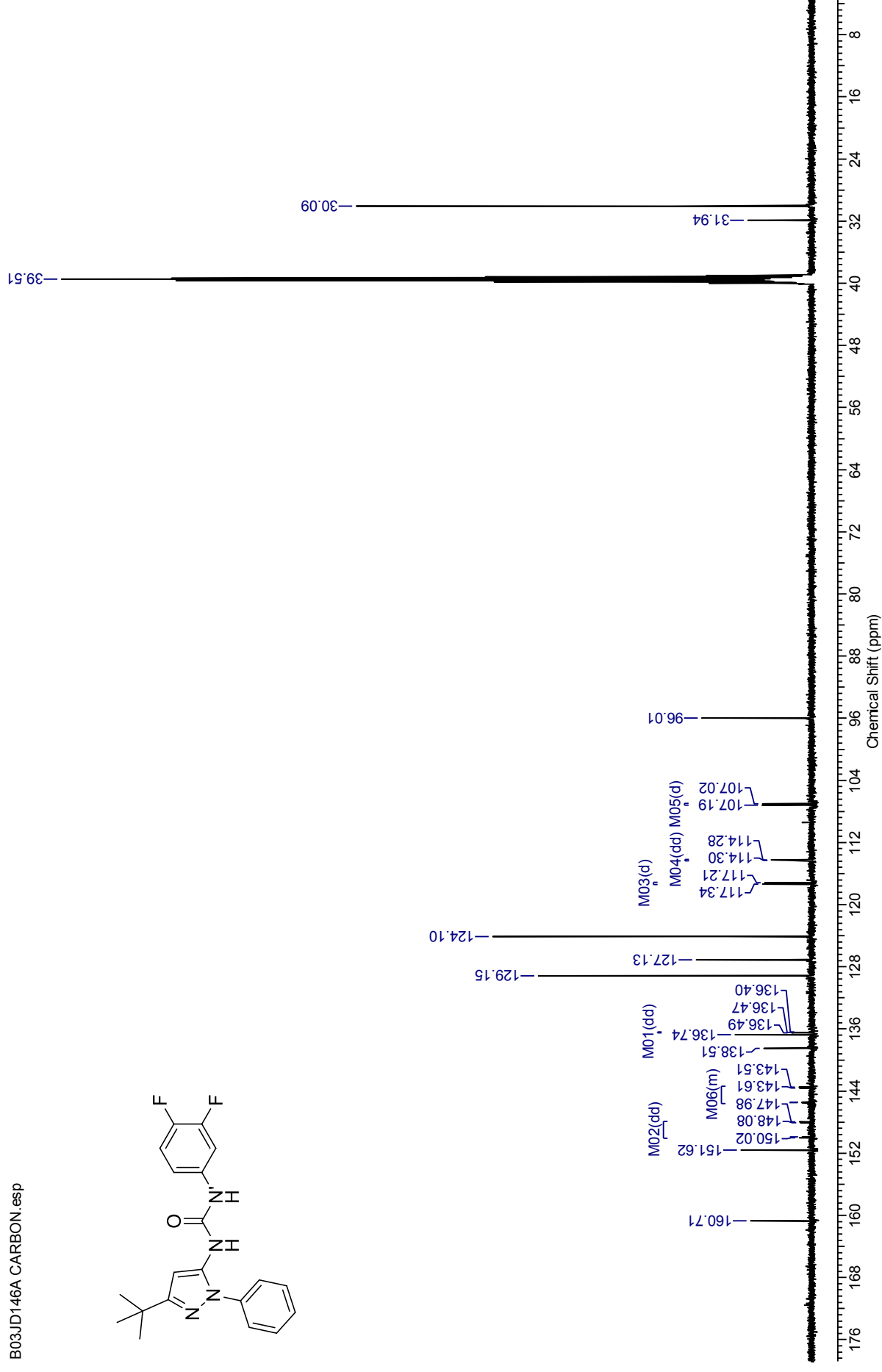
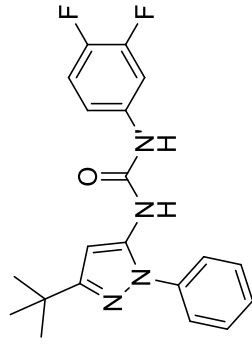
M02(s)

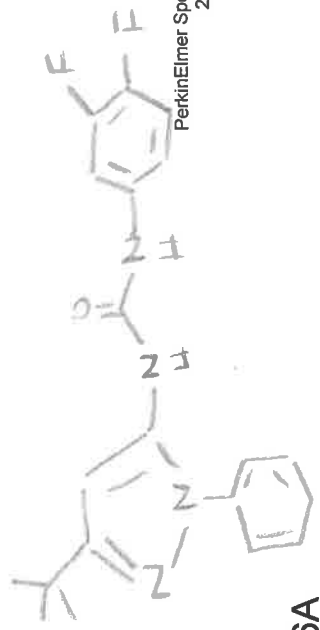
M01(s)



¹³C NMR spectrum (126 MHz, DMSO-*d*₆) for *N*-(3-(*tert*-butyl)-1-phenyl-1*H*-pyrazol-5-yl)-*N'*-(3,4-difluorophenyl)urea

B03JD146A CARBON.esp



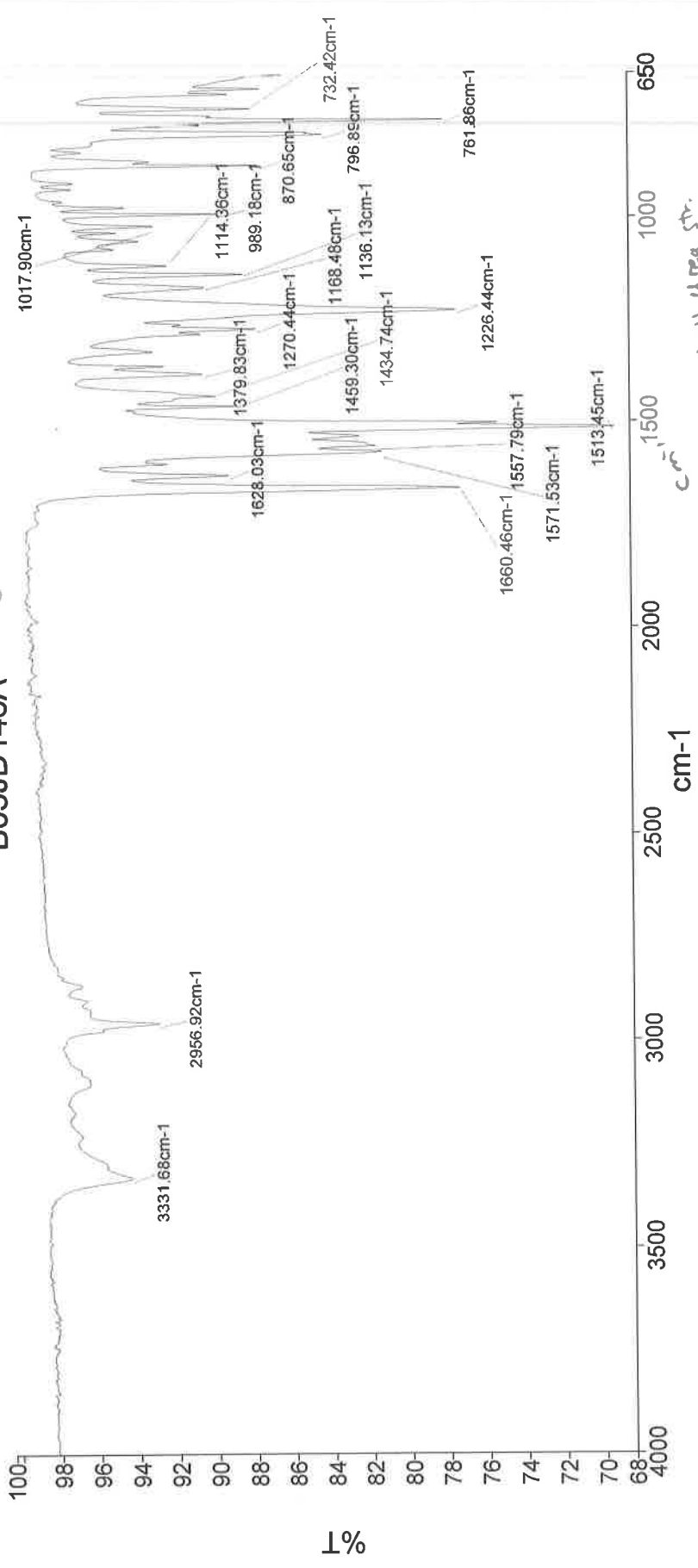


PerkinElmer Spectrum Version 10.03.06
26 November 2014 15:39

Analyst
Date

Administrator
26 November 2014 15:39

B03JD146A



- cm⁻¹
- 3332 - N-H urea str.
 - 2957 - C-H alk str
 - 1660 - C=O str.
 - 1571 - N-H bend
 - 1513 - C-N str.
 - 1226 - C-N str.
 - 1136 - C-N str.
 - 761 - C-H rock

Administrator 15 Sample 015 By Administrator Date Wednesday, November 26 2014

Single Mass Analysis

Tolerance = 100.0 PPM / DBE: min = -1.5, max = 50.0

Element prediction: Off

Number of isotope peaks used for i-FIT = 3

Monoisotopic Mass, Even Electron Ions

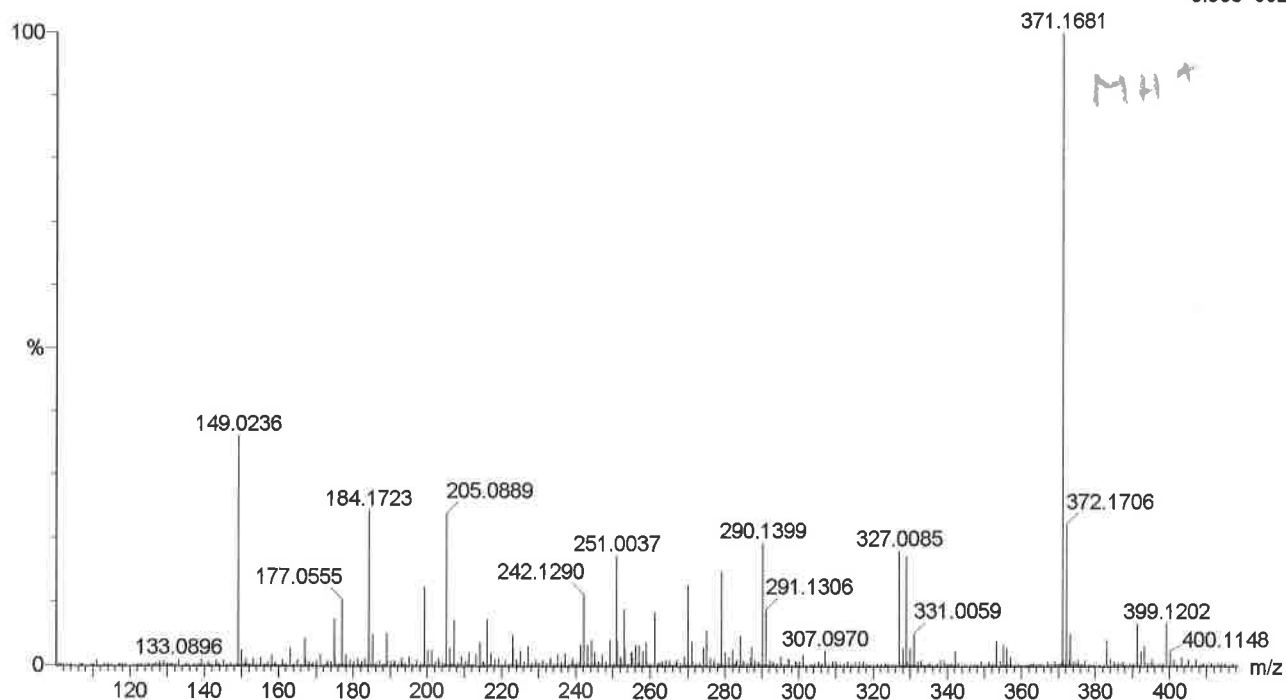
1 formula(e) evaluated with 1 results within limits (all results (up to 1000) for each mass)

Elements Used:

C: 20-20 H: 0-50 N: 4-4 O: 1-1 F: 2-2

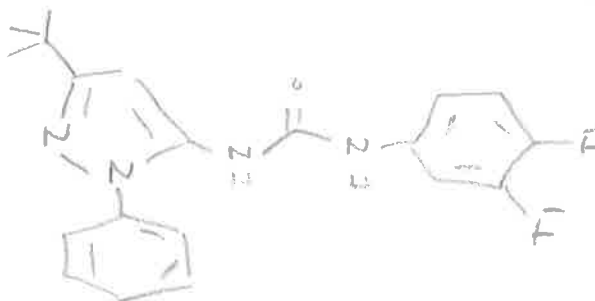
BO3JD146A

JESS4569 498 (6.686)

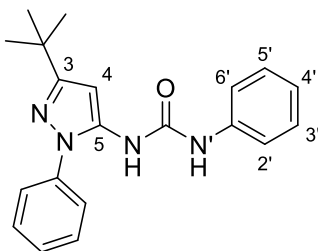
1: TOF MS ES+
8.93e+002

Minimum: -1.5
Maximum: 50.0

Mass	Calc. Mass	mDa	PPM	DBE	i-FIT	Formula
371.1681	371.1683	-0.2	-0.5	11.5	4.6	C20 H21 N4 O F2



***N*-(3-(*tert*-Butyl)-1-phenyl-1*H*-pyrazol-5-yl)-*N'*-phenylurea (215K)**



¹H NMR spectrum (500 MHz, DMSO-*d*₆) for *N*-(3-(*tert*-butyl)-1*H*-pyrazol-5-yl)-1-phenyl-1*H*-pyrazol-5-yl)-*N'*-phenylurea

B03JD147A Proton for Carbon DMSO.esp

M05(t)

M04(m)

M01(m)

M02(s)

M03(m)

M06(t)

M07(s)

8.98

8.37

6.38

6.96

6.97

6.98

7.24

7.26

7.28

7.39

7.41

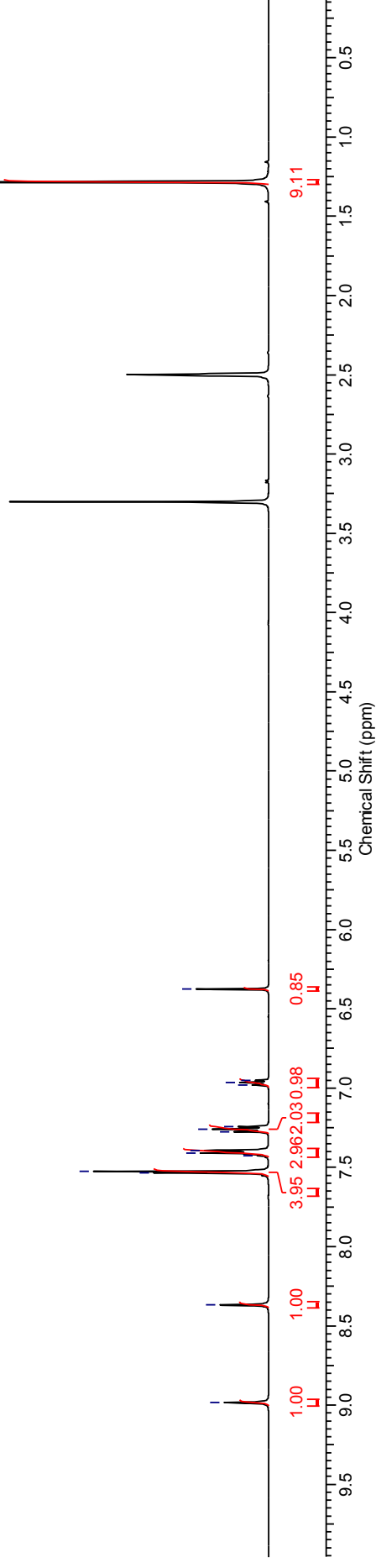
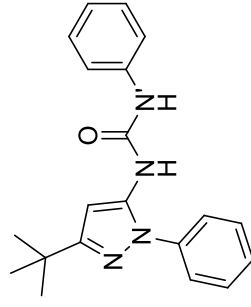
7.43

7.53

7.54

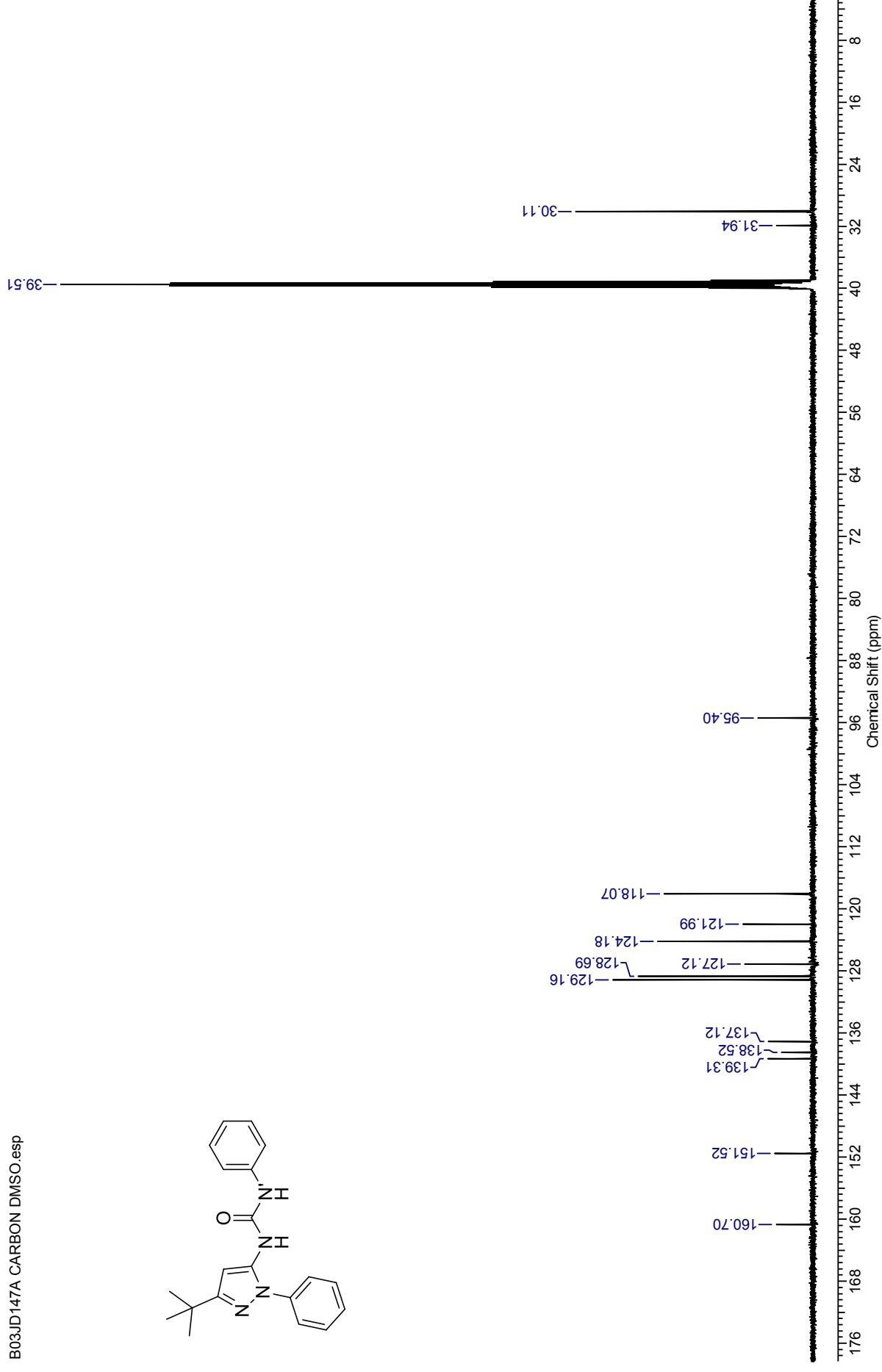
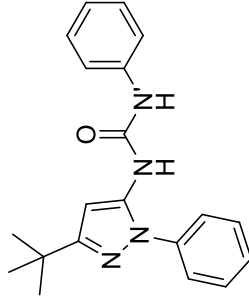
M08(s)

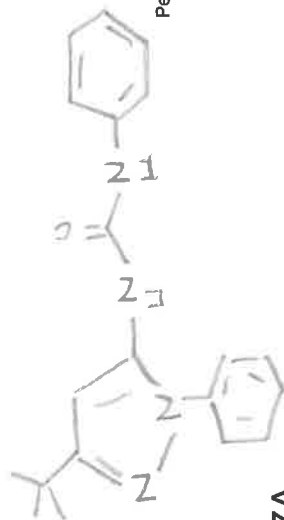
1.28



¹³C NMR spectrum (126 MHz, DMSO-*d*₆) for *N*-(3-(*tert*-butyl)-1-phenyl-1*H*-pyrazol-5-yl)-1-phenyl-1*H*-pyrazol-5-yl)-*N'*-phenylurea

B03JD147A CARBON DMSO.esp



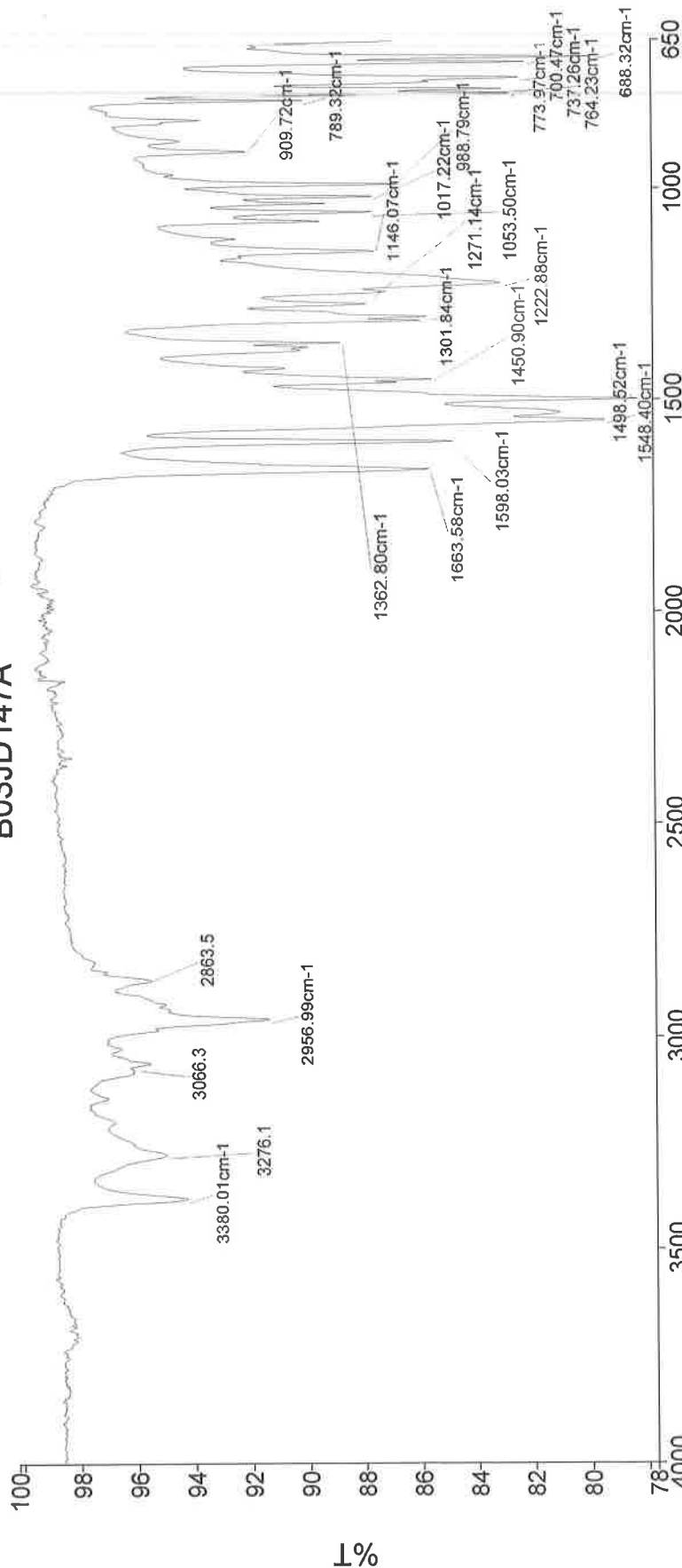


Analyst
Date

Administrator

26 November 2014 15:42

B03JD147A



Administrator 16 Sample 016 By Administrator Date Wednesday, November 26 2014

cm⁻¹
1054 - C-N str
774 C-H rock on

3276 - N-H urea, str.
2957 - C-H str, alk
1664 - C=O amide
1598 - C-N stretch
1548 - N-H amide bend
1498 - C-N stretch
1450 - C-N stretch
1362 - C-N stretch
1301 - C-N stretch
1271 - C-N stretch
1222 - C-N stretch
1063 - C-N stretch
1017 - C-N stretch
988 - C-N stretch
909 - C-N stretch
789 - C-N stretch
773 - C-N stretch
764 - C-N stretch
700 - C-N stretch
688 - C-N stretch

Single Mass Analysis

Tolerance = 100.0 PPM / DBE: min = -1.5, max = 50.0

Element prediction: Off

Number-of-isotope-peaks-used-for i-FIT = 3

Monoisotopic Mass, Even Electron Ions

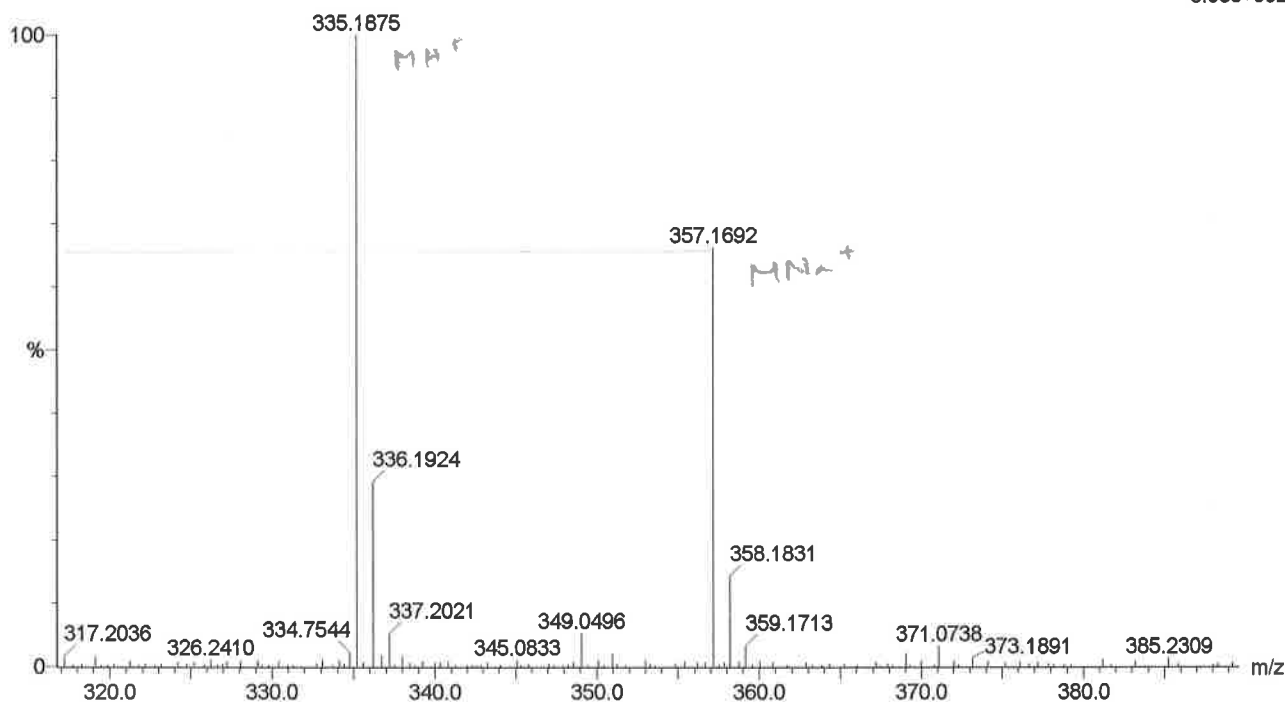
1 formula(e) evaluated with 1 results within limits (all results (up to 1000) for each mass)

Elements Used:

C: 20-20 H: 0-50 N: 4-4 O: 1-1

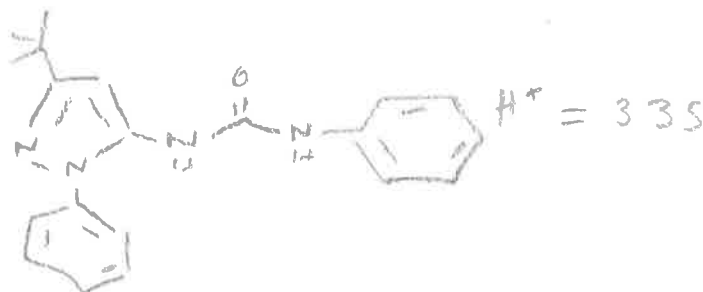
BO3JD147A

JESS4550a 44 (0.598) Cm (42:44)

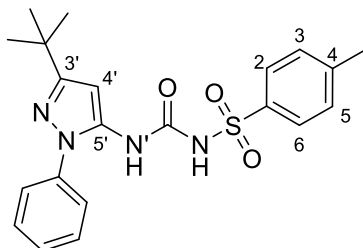
1: TOF MS ES+
5.05e+002

Minimum: -1.5
Maximum: 50.0

Mass	Calc. Mass	mDa	PPM	DBE	i-FIT	Formula
335.1875	335.1872	0.3	0.9	11.5	3.7	C20 H23 N4 O

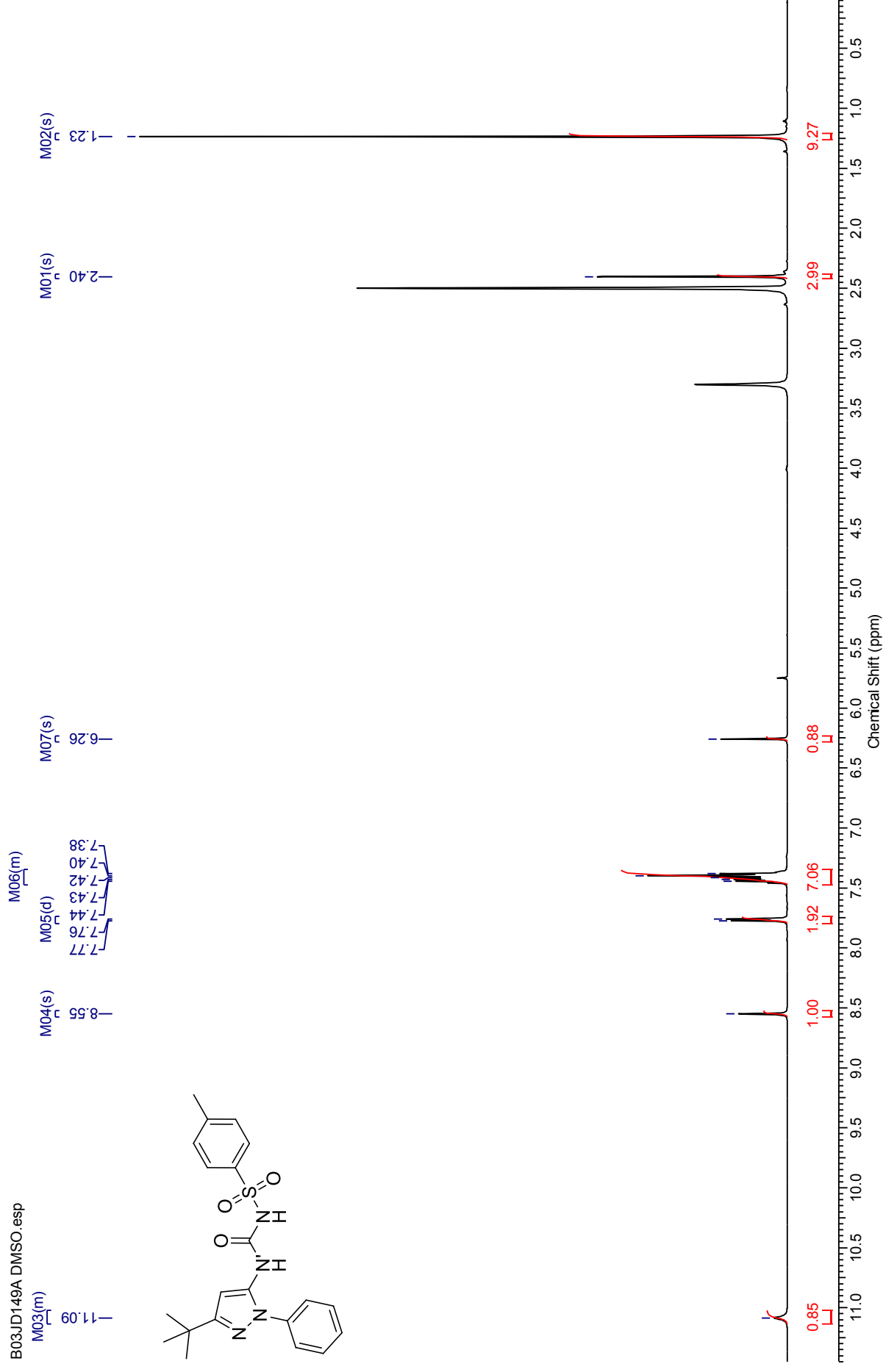


***N*-((3-(*tert*-Butyl)-1-phenyl-1*H*-pyrazol-5-yl)carbamoyl)-4-methylbenzenesulfonamide (215L)**



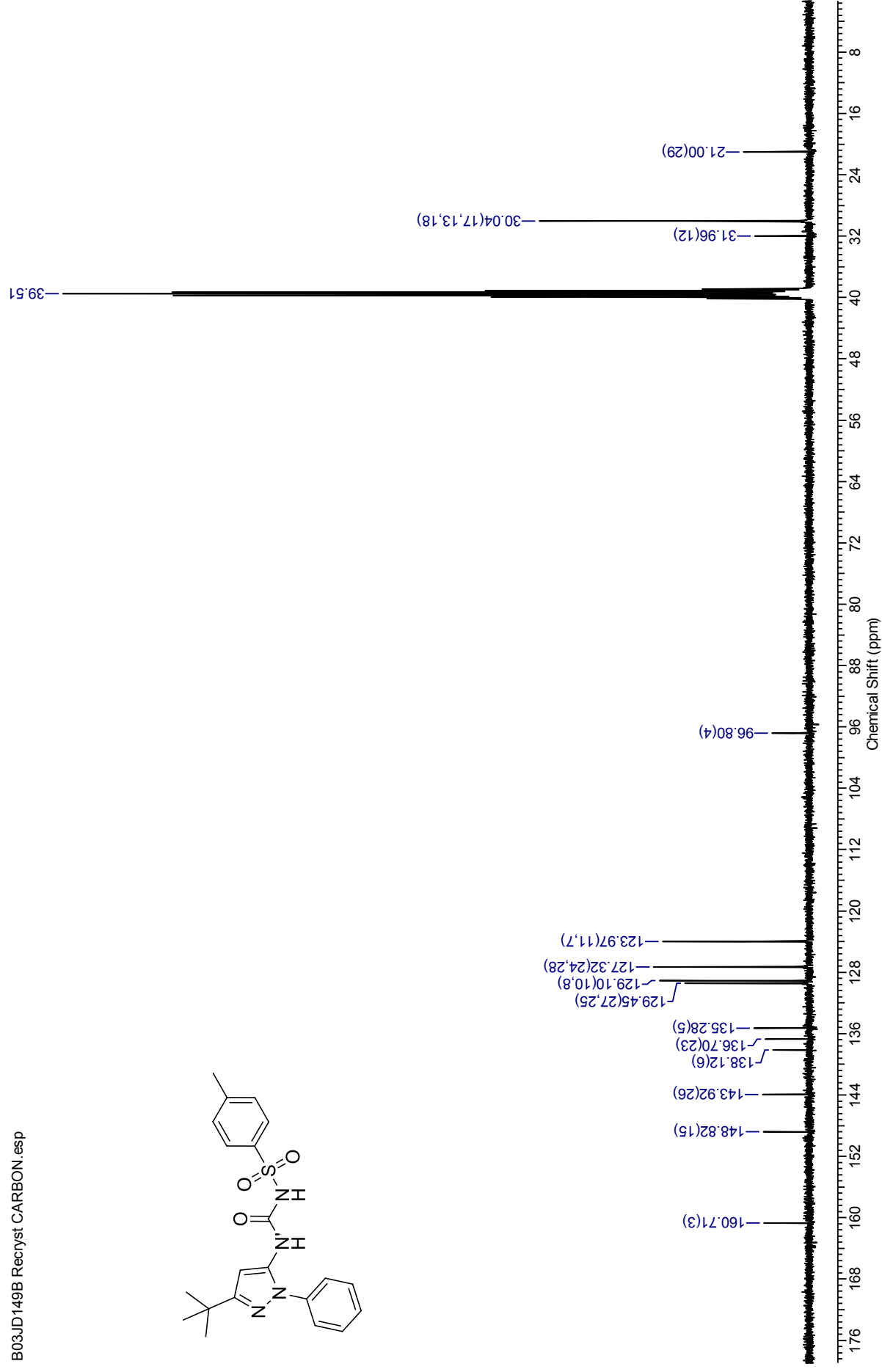
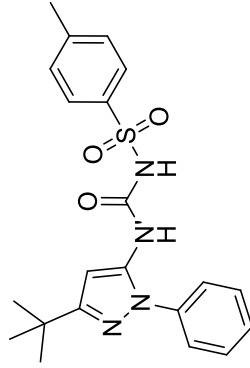
¹H NMR spectrum (500 MHz, DMSO-*d*₆) for *N*-((3-(*tert*-butyl)-1-phenyl-1*H*-pyrazol-5-yl)carbamoyl)-4-methylbenzenesulfonamide

B03JD149A.DMSO.esp



¹³C NMR spectrum (126 MHz, DMSO-*d*₆) for *N*-((3-(*tert*-butyl)-1*H*-pyrazol-5-yl)-1-phenyl-1*H*-pyrazol-5-yl)carbamoyl)-4-methylbenzenesulfonamide

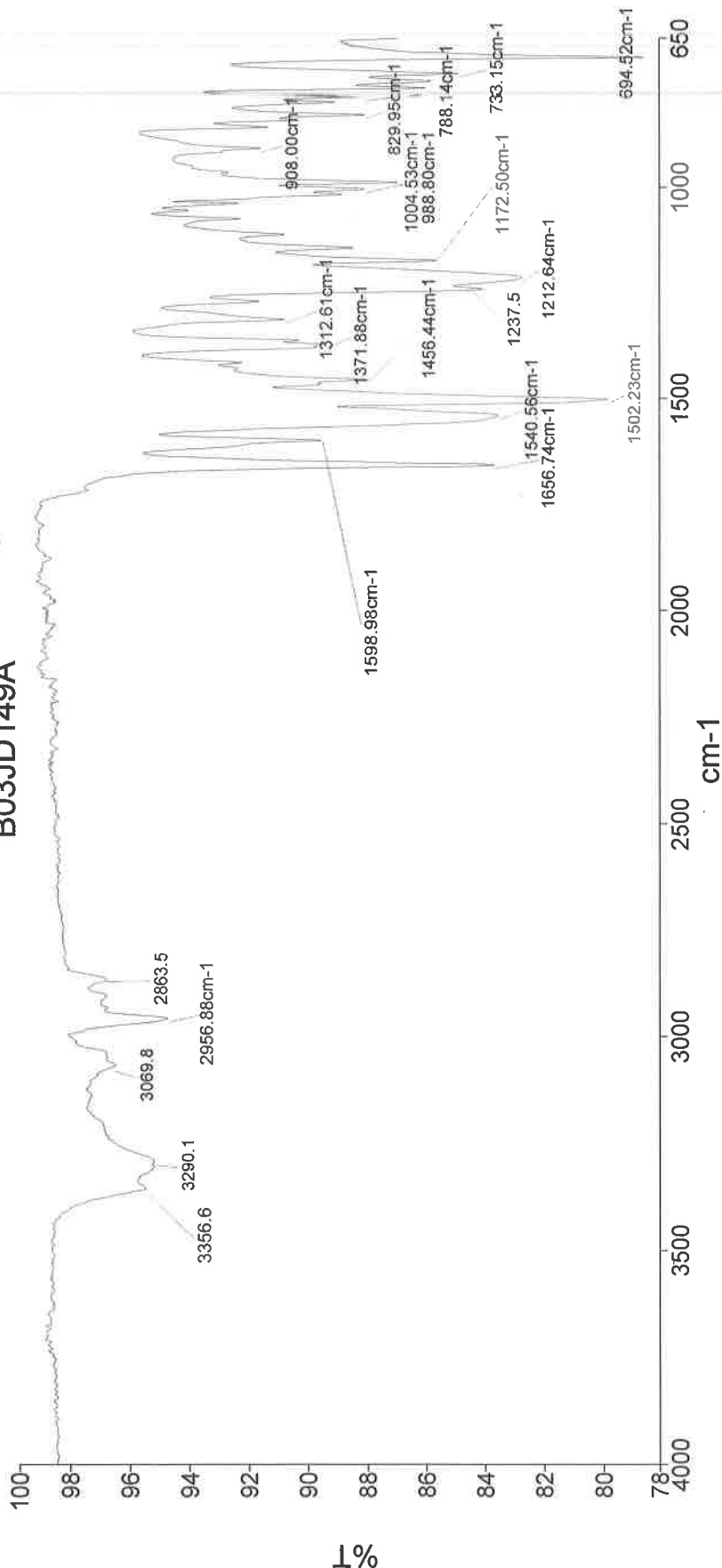
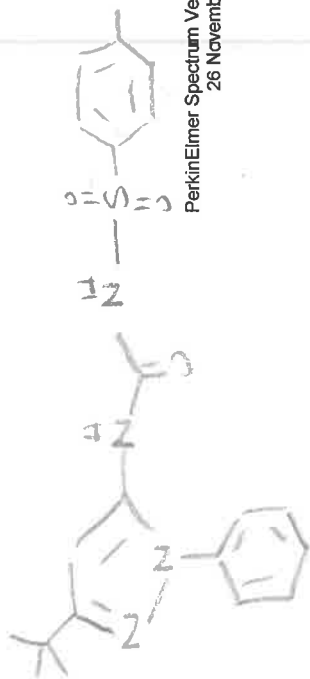
B03JD149B Recryst CARBON. esp



Analyst
Date

Administrator
26 November 2014 15:32

B03JD149A



3290 - N-H str.
2957 - C-H alk str.
1657 - C=O str
1541 - N-H bend
1502 - N-H bend
1212 - C-N str.
988 - S=O str.
694 - C-H rock

Administrator 12 Sample 012 By Administrator Date Wednesday, November 26 2014

Single Mass Analysis

Tolerance = 100.0 PPM / DBE: min = -1.5, max = 50.0

Element prediction: Off

Number of isotope peaks used for i-FIT = 3

Monoisotopic Mass, Even Electron Ions

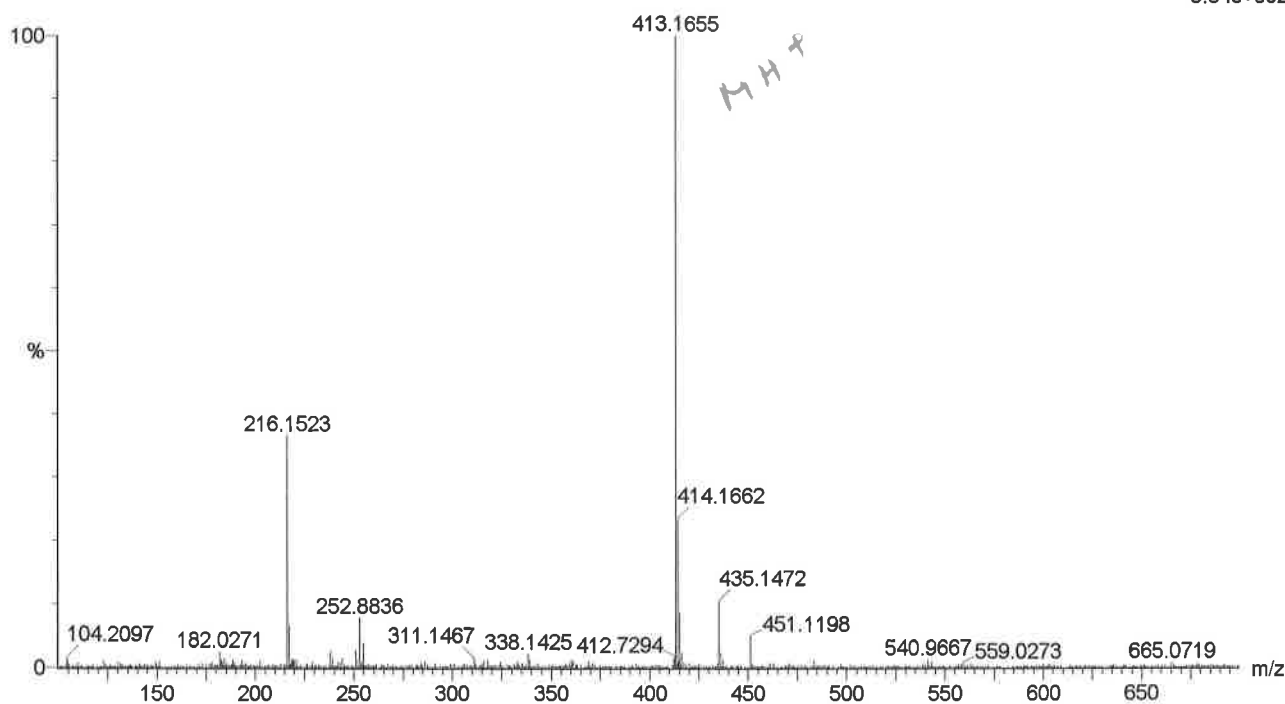
1 formula(e) evaluated with 1 results within limits (all results (up to 1000) for each mass)

Elements Used:

C: 21-21 H: 0-50 N: 4-4 O: 3-3 S: 1-1

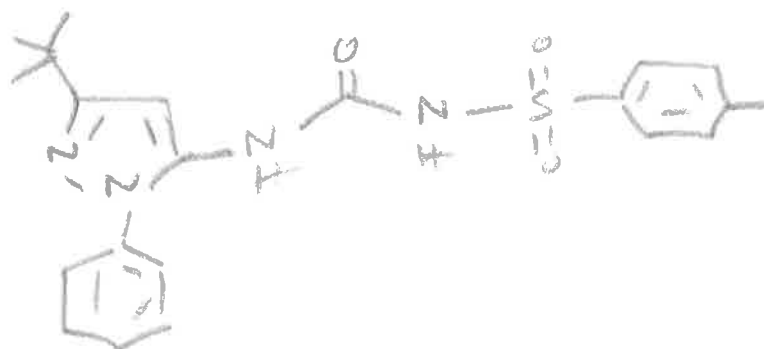
BO3JD152B

JESS4565 65 (0.889) Cm (65:68)

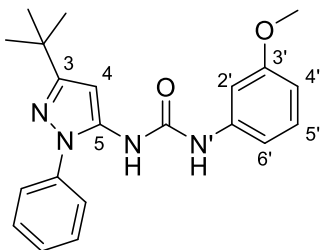
1: TOF MS ES+
9.34e+002

Minimum: -1.5
Maximum: 5.0 100.0 50.0

Mass	Calc. Mass	mDa	PPM	DBE	i-FIT	Formula
413.1655	413.1647	0.8	1.9	11.5	1.4	C21 H25 N4 O3 S

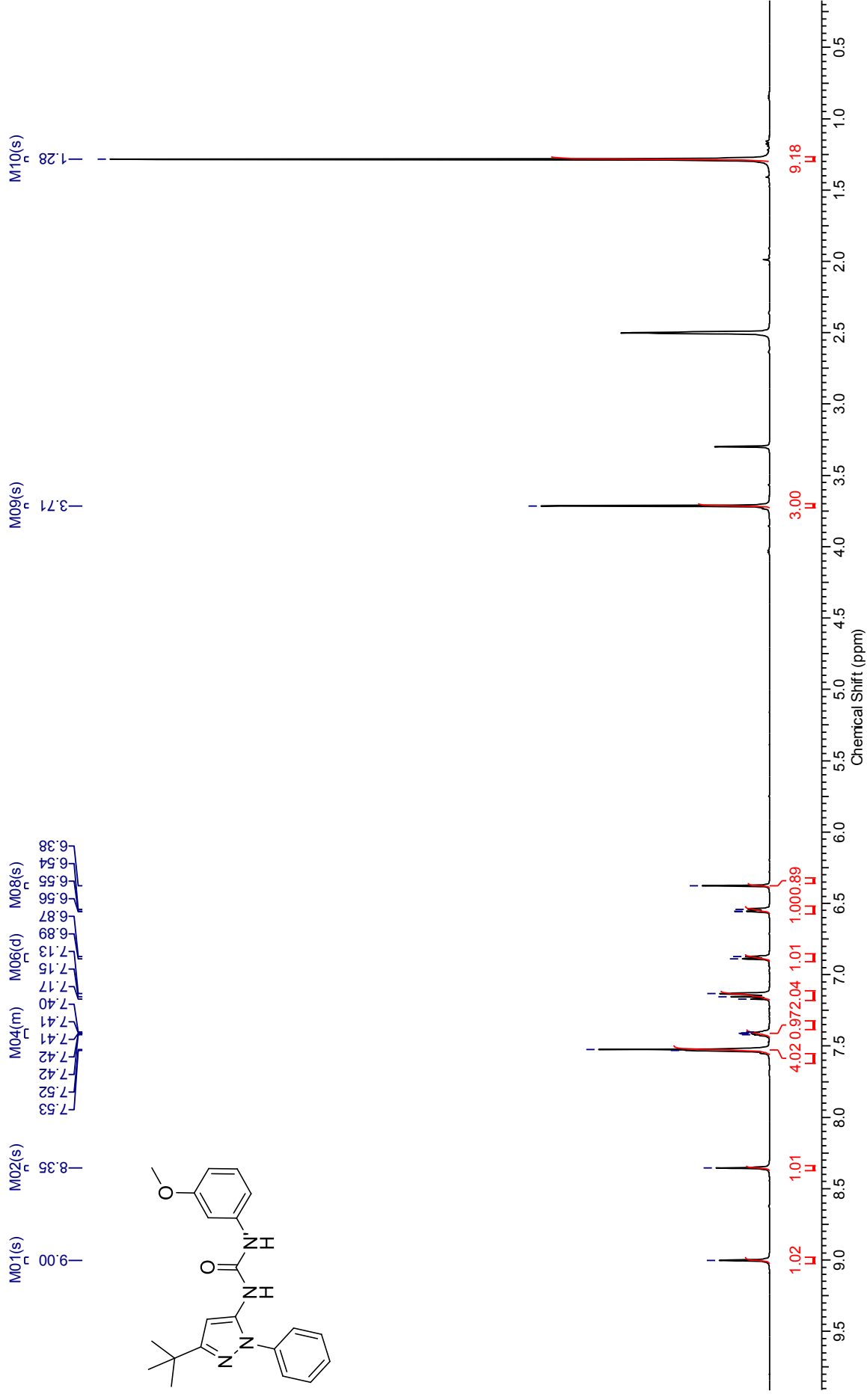
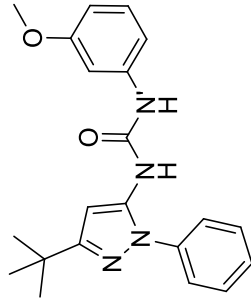
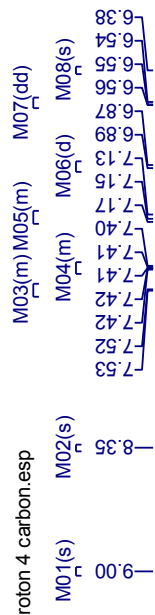


***N*-(3-(*tert*-Butyl)-1-phenyl-1*H*-pyrazol-5-yl)-*N'*-(3-methoxyphenyl)urea (215M)**



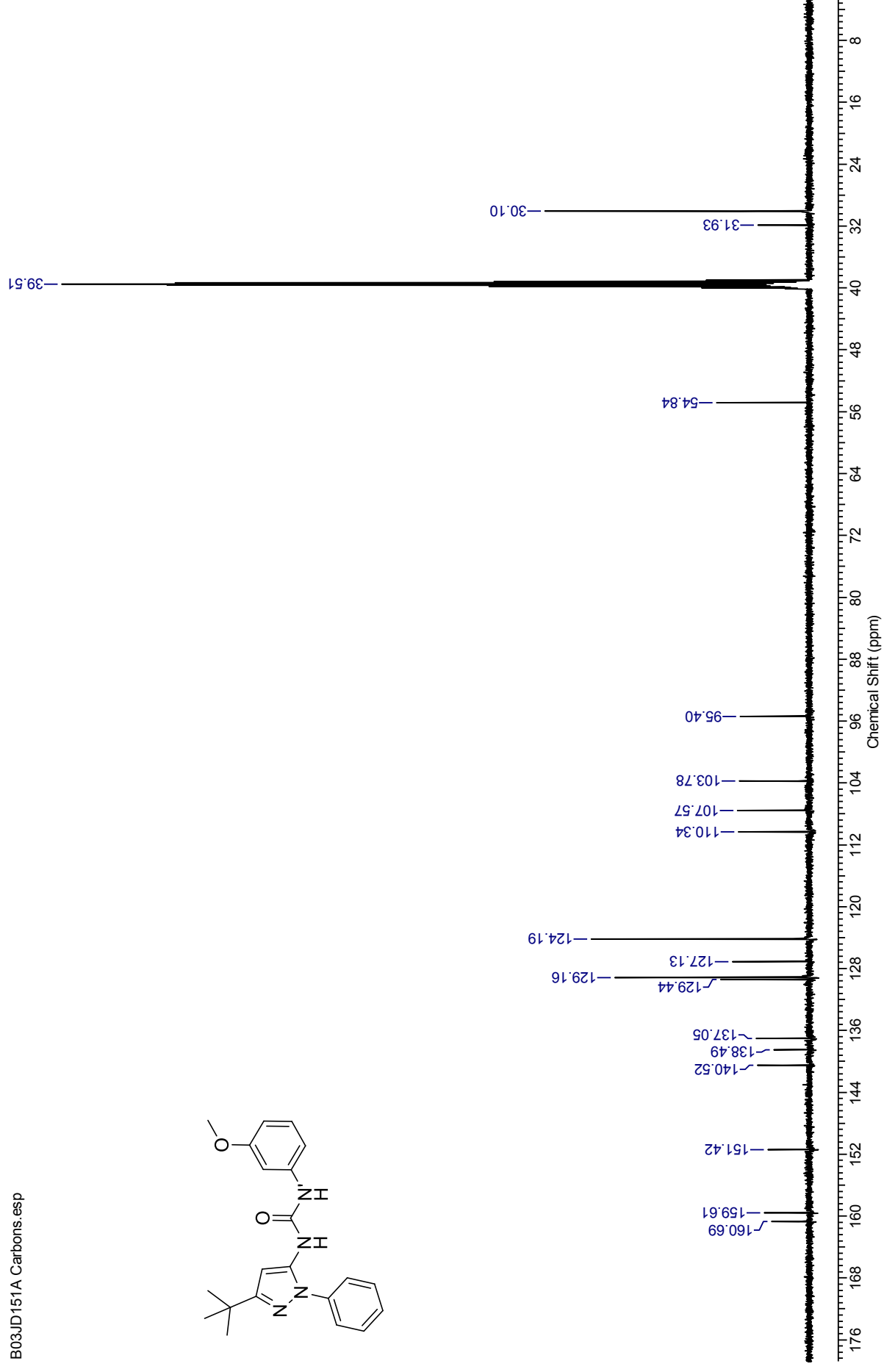
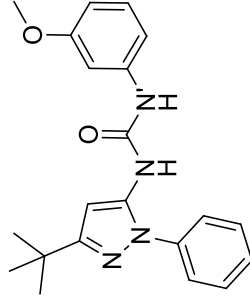
¹H NMR spectrum (500 MHz, DMSO-*d*₆) for *N*-(3-(*tert*-butyl)-1-phenyl-1*H*-pyrazol-5-yl)-*N'*-(3-methoxyphenyl)urea

B03JD151A Proton 4 carbon.esp



¹³C NMR spectrum (126 MHz, DMSO-*d*₆) for *N*-(3-(*tert*-butyl)-1*H*-pyrazol-5-yl)-1-phenyl-1*H*-pyrazol-5-yl)-*N'*-(3-methoxyphenyl)urea

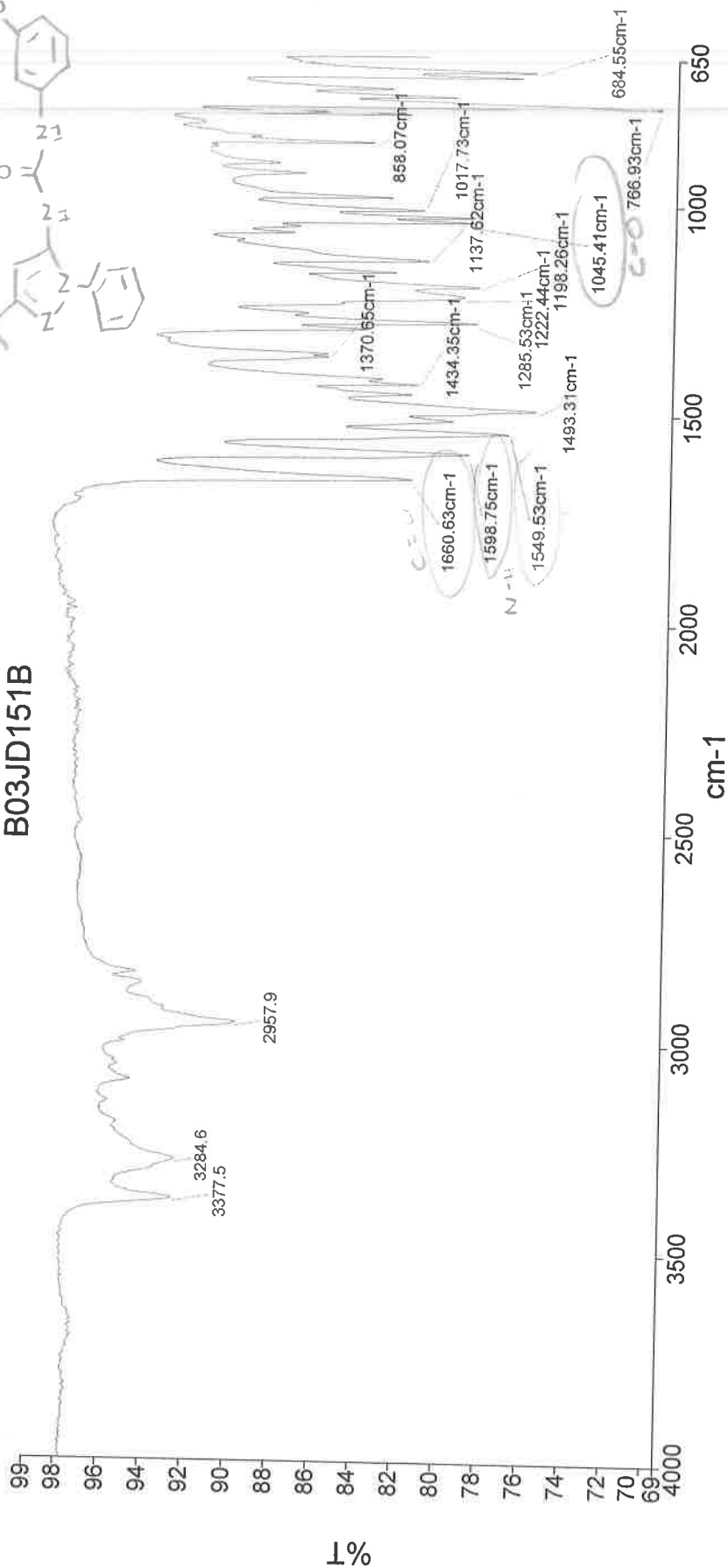
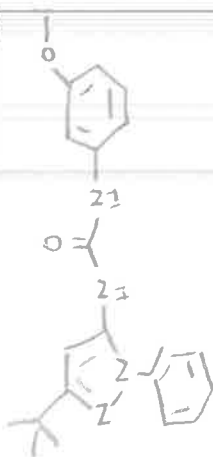
B03JD151A Carbons.esp



Administrator
03 February 2015 10:51

Analyst
Date

B03JD151B



3285 - N-H str.
2958 - C-H str.
1660 - C=O amide
1599 - N-H str.
1549 - N-H str.
1493 - C-C in ring str.
1045 - C-O str. ether

Administrator 46 Sample 046 By Administrator Date Tuesday, February 03 2015

Single Mass Analysis

Tolerance = 100.0 PPM / DBE: min = -1.5, max = 50.0

Element prediction: Off

Number of isotope peaks used for i-FIT = 3

Monoisotopic Mass, Even Electron Ions

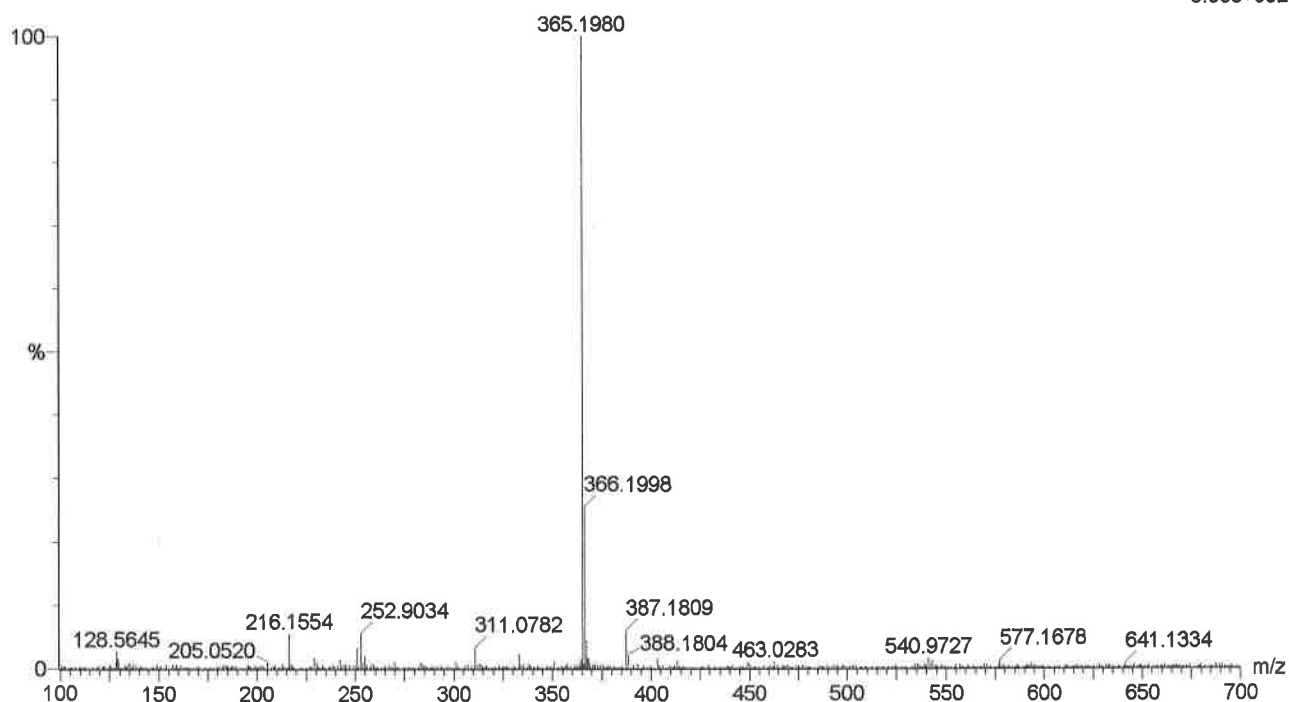
1 formula(e) evaluated with 1 results within limits (all results (up to 1000) for each mass)

Elements Used:

C: 21-21 H: 0-50 N: 4-4 O: 2-2

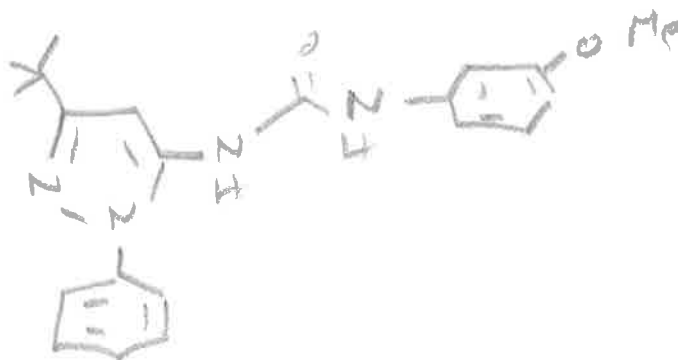
BO3JD151B

JESS4564 41 (0.567) Cm (41:46)

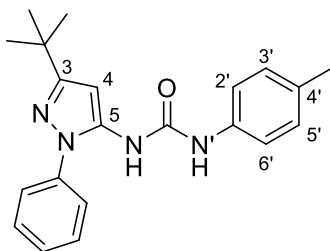
1: TOF MS ES+
8.06e+002

Minimum: -1.5
Maximum: 5.0 100.0 50.0

Mass	Calc. Mass	mDa	PPM	DBE	i-FIT	Formula
365.1980	365.1978	0.2	0.5	11.5	1.2	C21 H25 N4 O2



***N*-(3-(*tert*-Butyl)-1-phenyl-1*H*-pyrazol-5-yl)-*N'*-(*p*-tolyl)urea (215N)**



¹H NMR spectrum (500 MHz, DMSO-*d*₆) for *N*-(3-(*tert*-butyl)-1*H*-pyrazol-5-yl)-1-phenyl-1*H*-pyrazol-5-yl)-*N'*-(*p*-tolyl)urea

B03JD160A Proton DMSO.esp

M03(m,10,11,7,8)

M04(m,9)

M05(d,22,24)

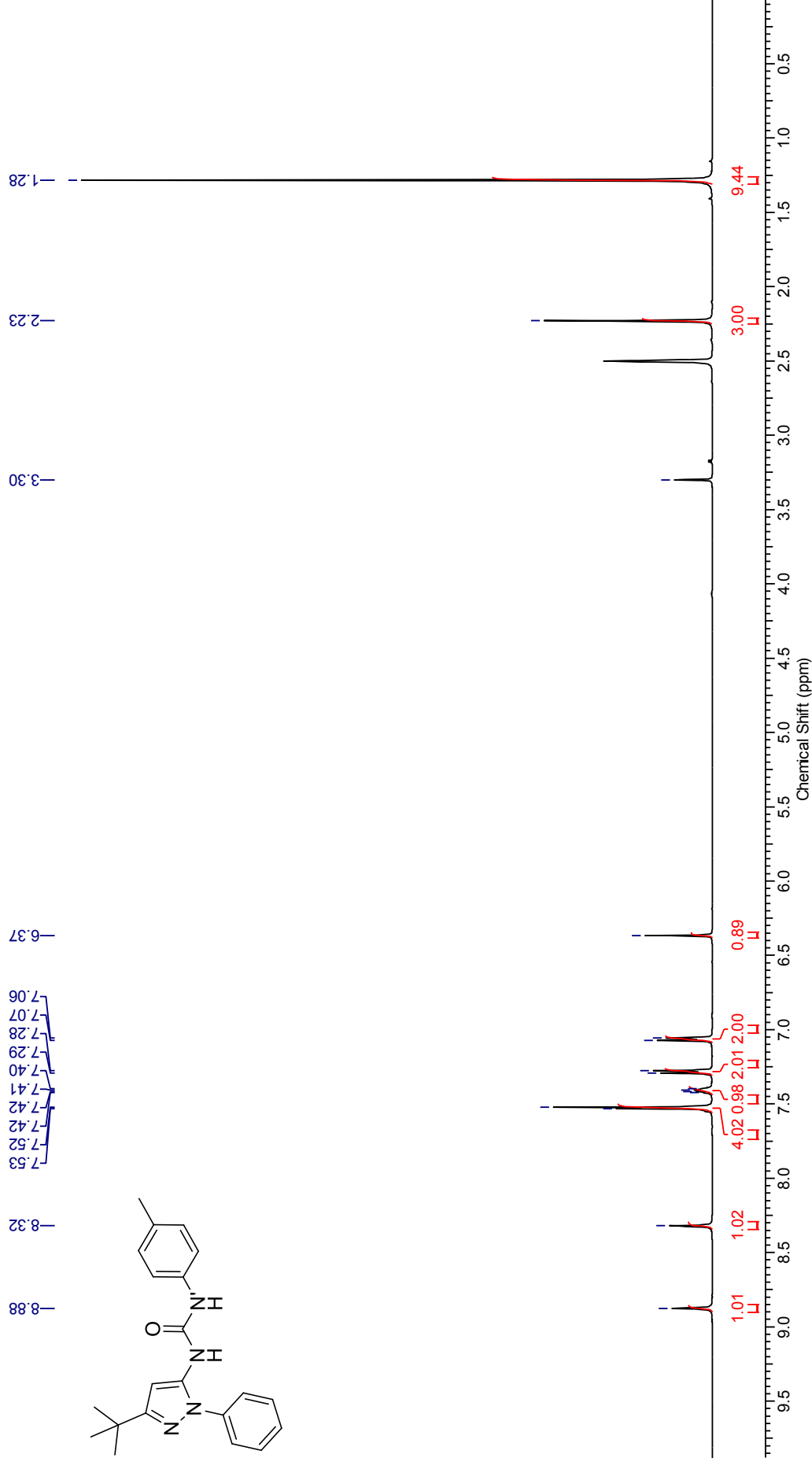
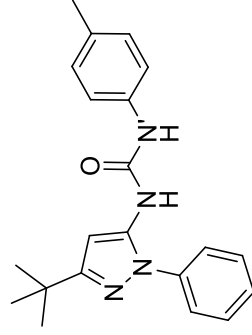
M01(s,19) M02(s,14)

M06(d,21,25)

M07(s,4)

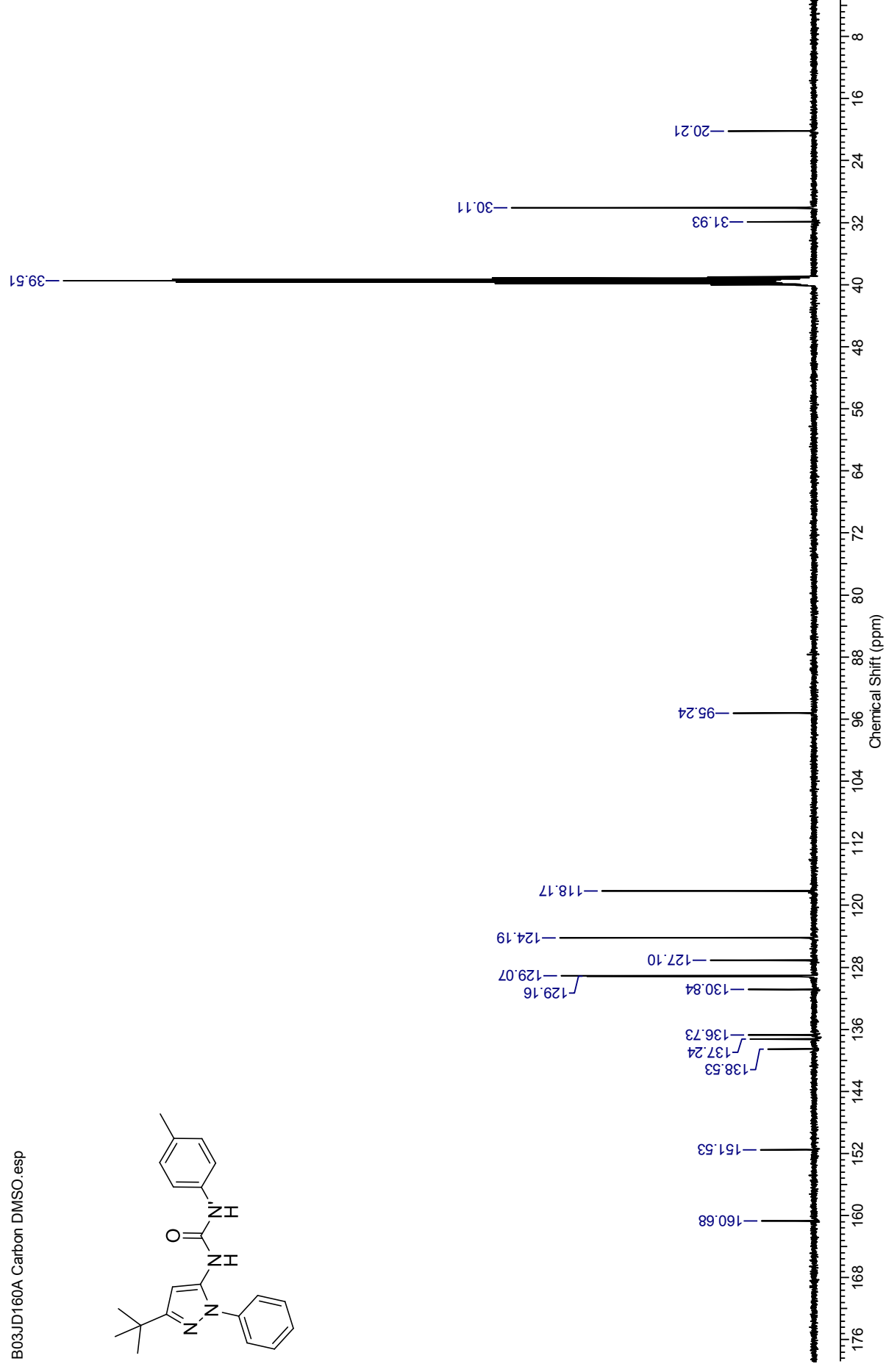
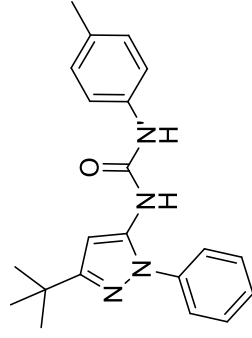
M09(m,26)

M08(s,17,18,13)



¹³C NMR spectrum (126 MHz, DMSO-*d*₆) for *N*-(3-(*tert*-butyl)-1-phenyl-1*H*-pyrazol-5-yl)-1-phenyl-1*H*-pyrazol-5-yl)-*N'*-(*p*-tolyl)urea

B03JD160A Carbon DMSO.esp

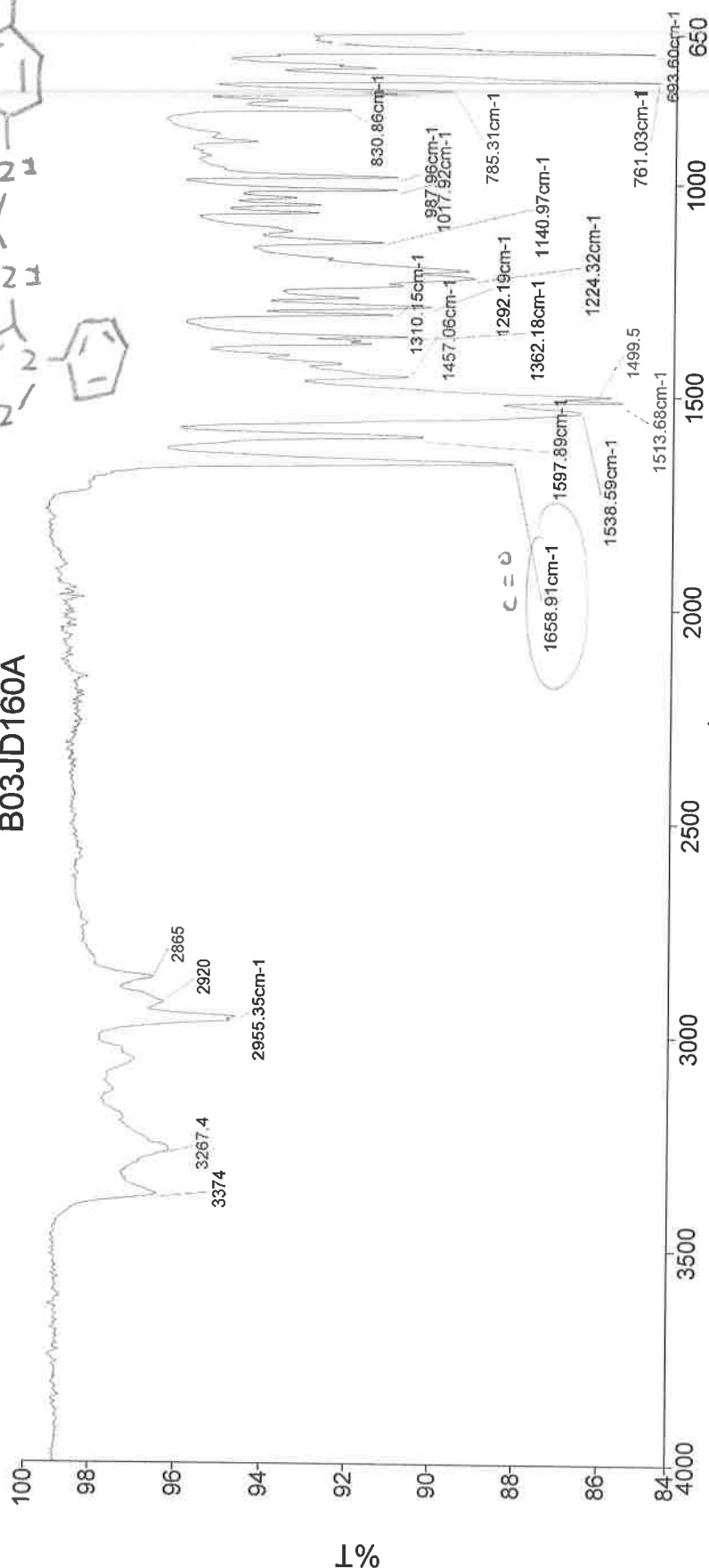
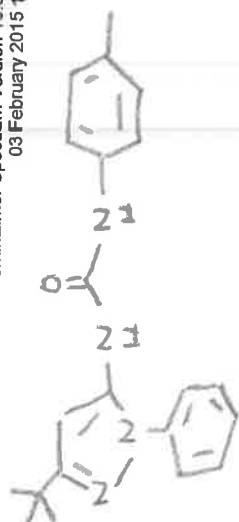


Analyst
Date

Administrator

03 February 2015 10:48

B03JD160A



- 3267 - N-H str. Amide
- 2955 - C-H alk. str.
- 1659 - C=O amide str.
- 1538 - N-H amide band
- 1362 - C-H rock, alkane
- 1140 - C-N str.
- 761 - C-H rock, aryl.

Administrator 45 Sample 045 By Administrator Date Tuesday, February 03 2015

Single Mass Analysis

Tolerance = 1000.0 PPM / DBE: min = -1.5, max = 50.0

Element prediction: Off

Number of isotope peaks used for i-FIT = 3

Monoisotopic Mass, Even Electron Ions

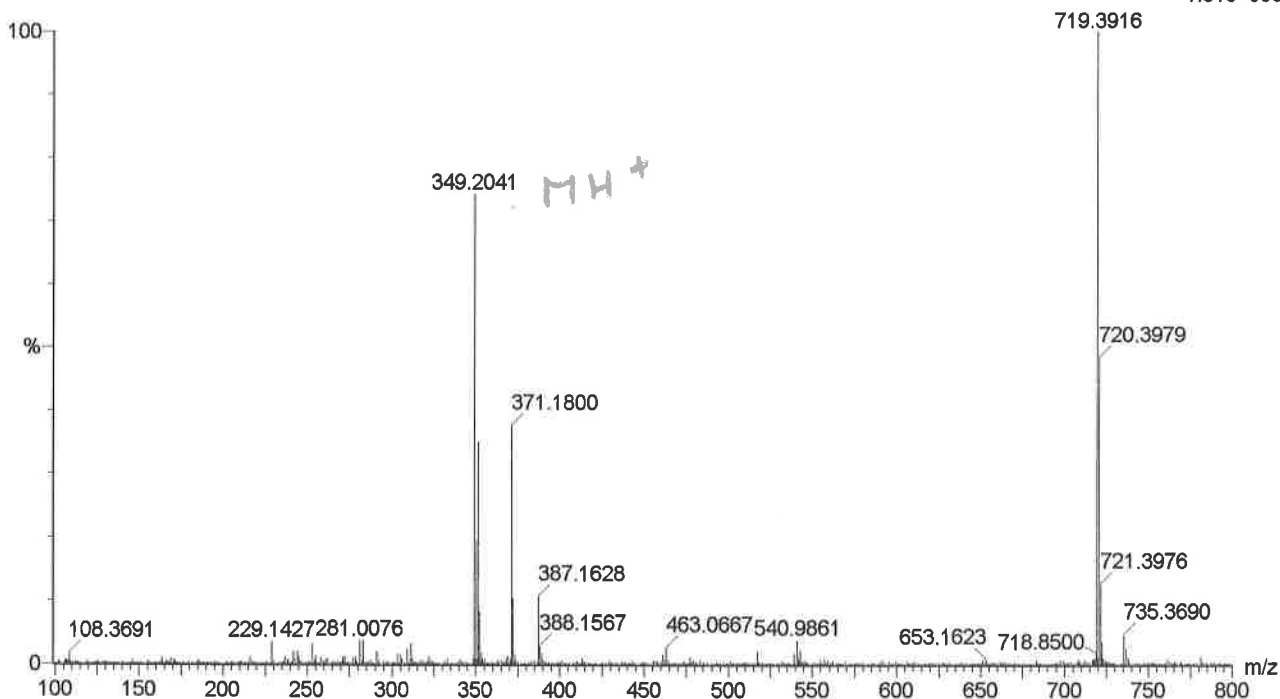
1 formula(e) evaluated with 1 results within limits (all results (up to 1000) for each mass)

Elements Used:

C: 21-21 H: 0-50 N: 4-4 O: 1-1

BO3JD160A

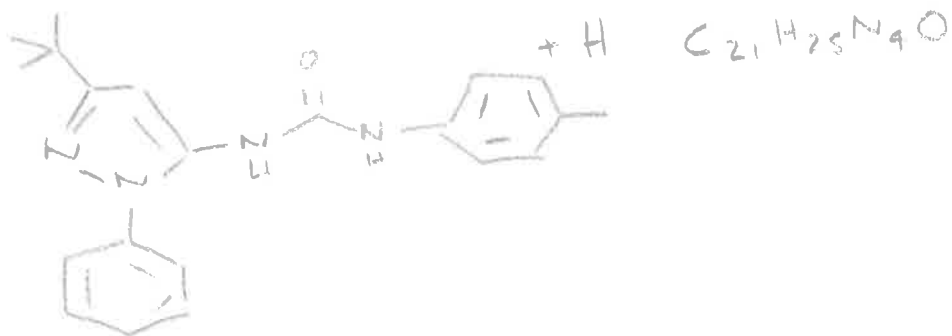
JESS4621 27 (0.373) Cm (24:27)

1: TOF MS ES+
1.51e+003

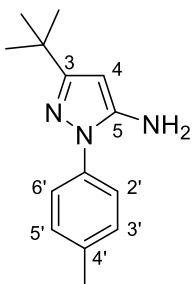
Minimum:

Maximum: 5.0 1000.0 -1.5 50.0

Mass	Calc. Mass	mDa	PPM	DBE	i-FIT	Formula
349.2041	349.2028	1.3	3.7	11.5	235.4	C21 H25 N4 O

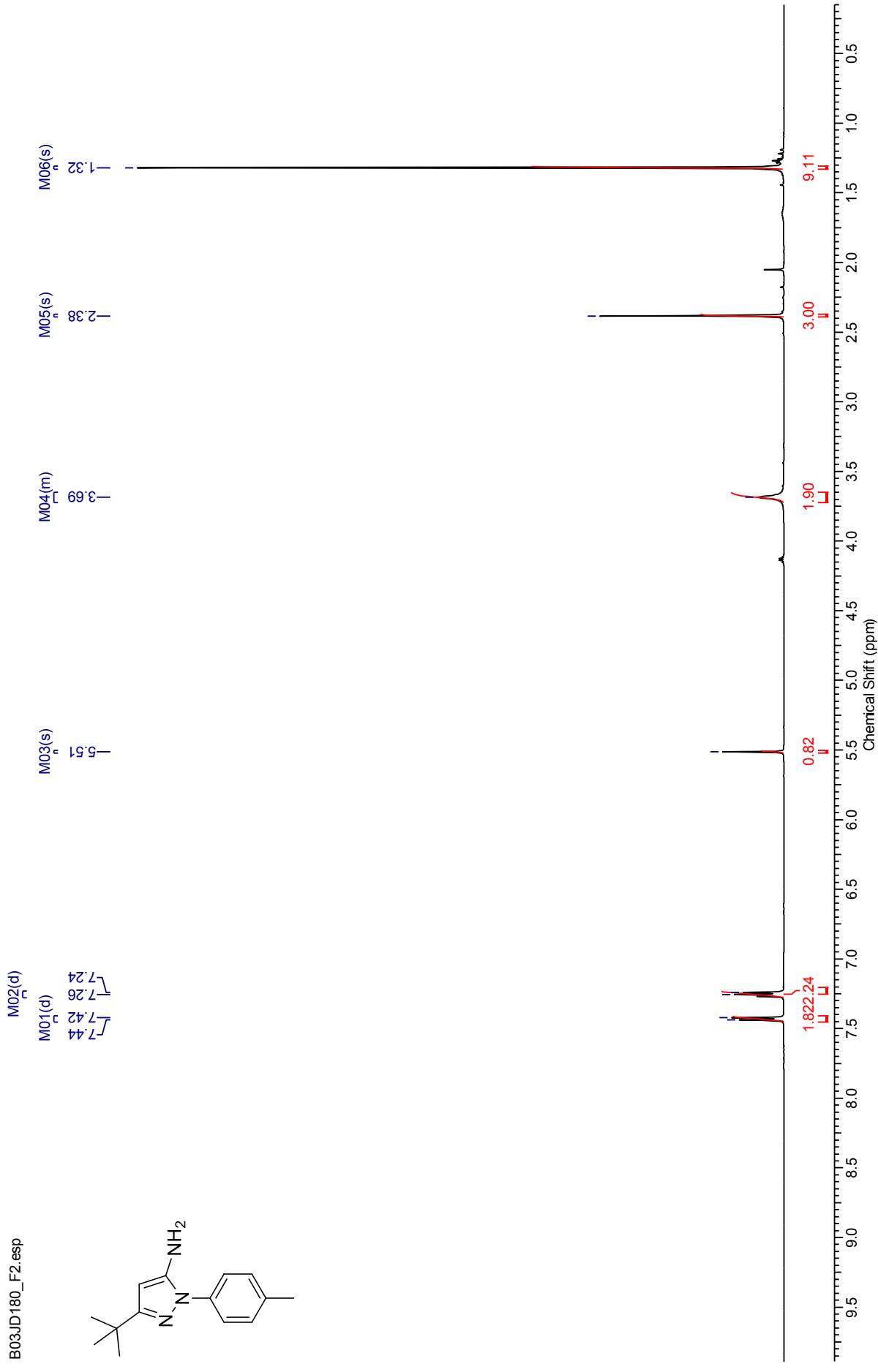


3-(*tert*-Butyl)-1-(*p*-tolyl)-1*H*-pyrazol-5-amine (217)



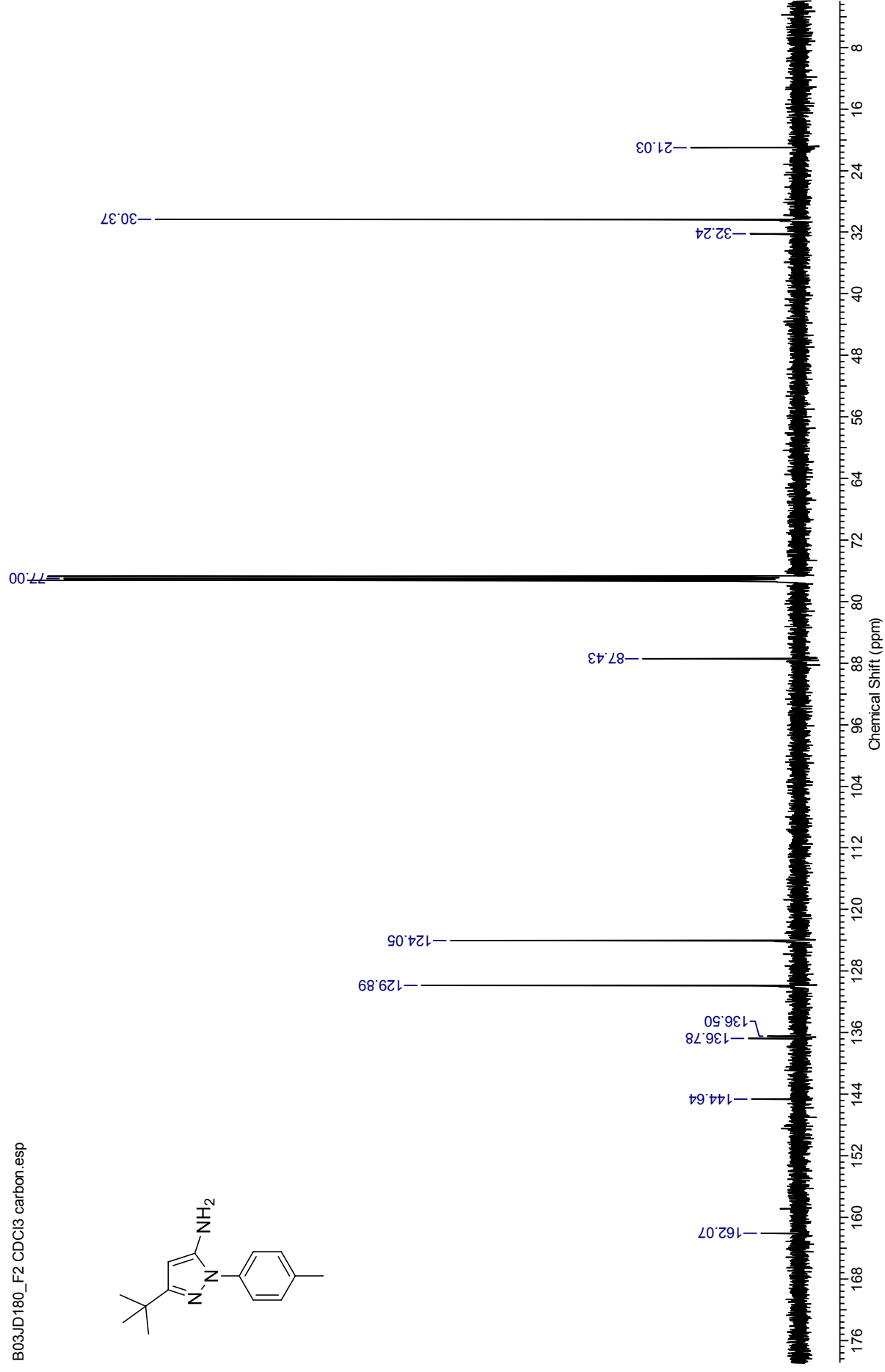
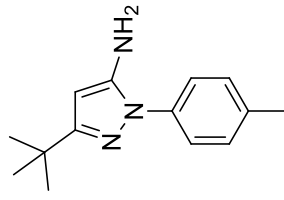
¹H NMR spectrum (500 MHz, CDCl₃) for 3-(*tert*-butyl)-1-(*p*-tolyl)-1*H*-pyrazol-5-amine

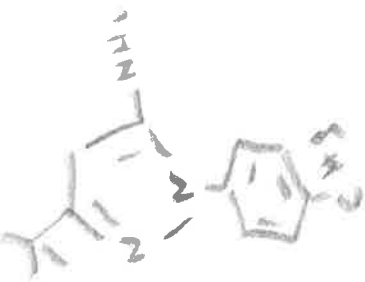
B03JD180_F2.esp



¹³C NMR spectrum (126 MHz, CDCl₃) for 3-(*tert*-Butyl)-1-(*p*-tolyl)-1*H*-pyrazol-5-amine

B03JD180_F2 CDCl3 carbon.esp

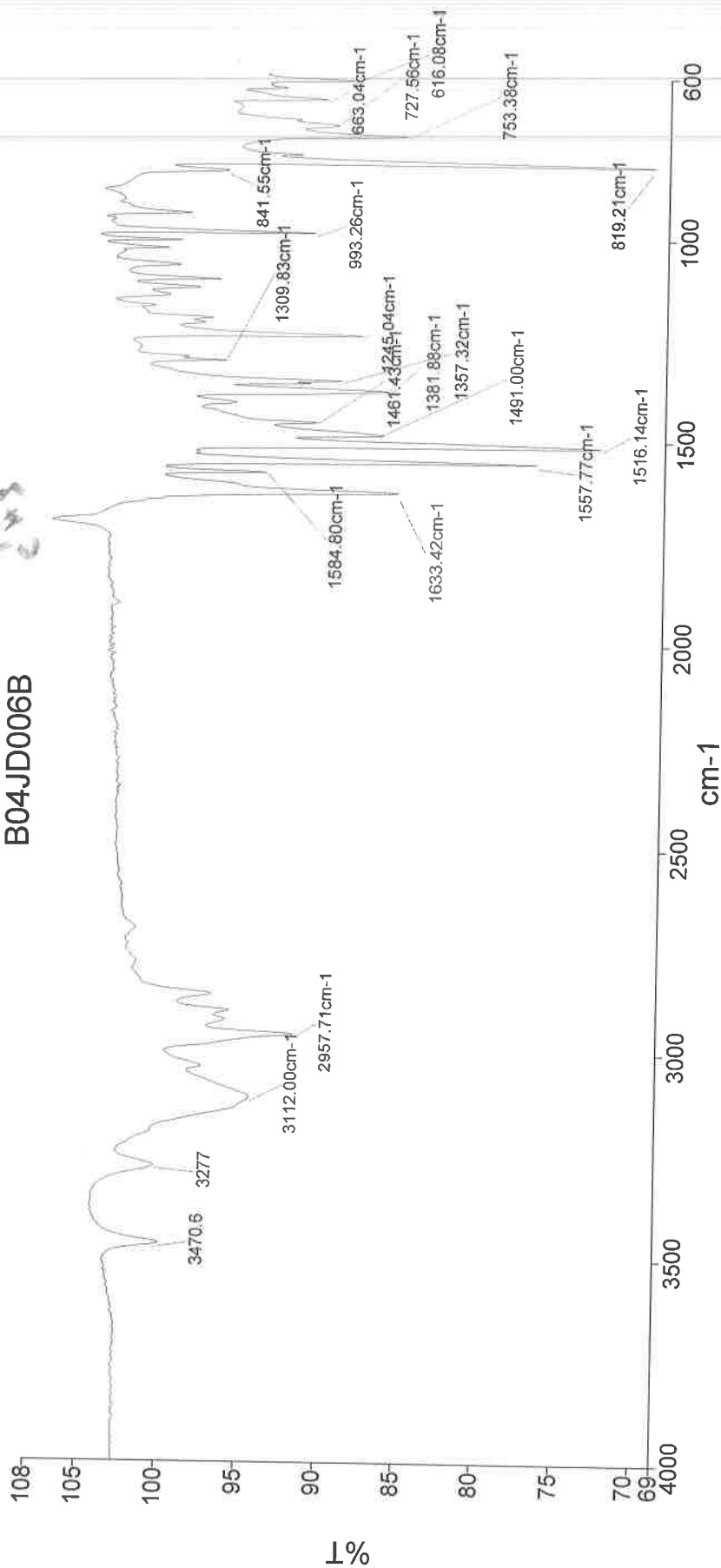




PerkinElmer Spectrum Version 10.03.06
28 May 2015 15:19

Analyst
Date
Administrator
28 May 2015 15:19

B04JD006B



Administrator 32 Sample 032 By Administrator Date Thursday, May 28 2015

3470 - N-H str.
3112 - C-H str.
2958 - C-H str.
1633 - N-H bend
1558 - C=N
1516 - C-C in ring
1382
1245 - C-N str.
993
819 - N-H wag

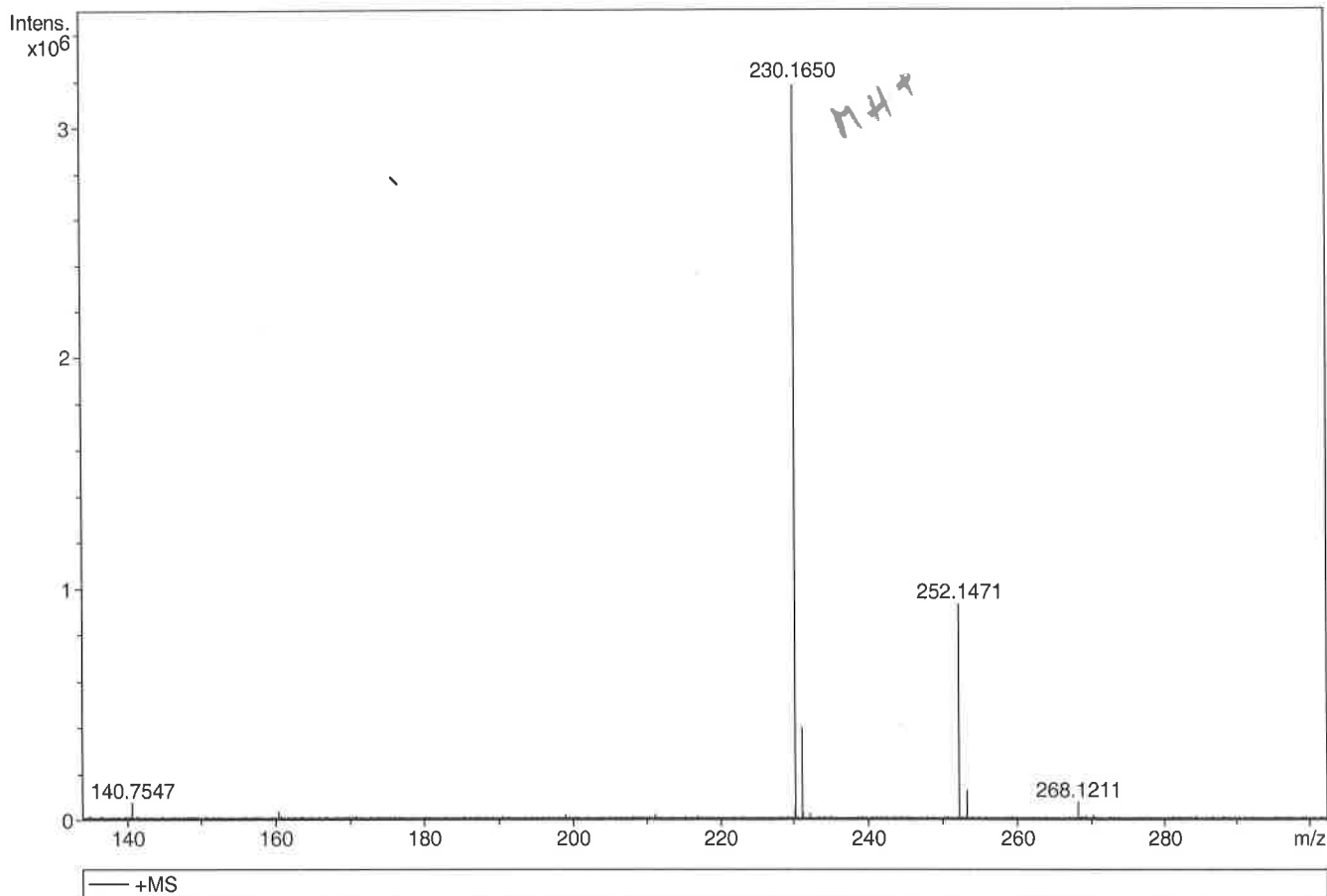
Generic Display Report

Analysis Info

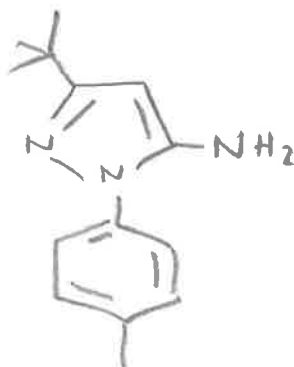
Analysis Name D:\Data\Alinanopos\JESS1929_000001.d
Method pos20090608esi
Sample Name POS ESI BO3JD180 F2
Comment

Acquisition Date 23/03/2015 11:05:55

Operator Administrator
Instrument apex-III

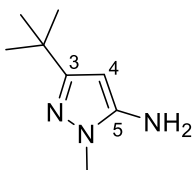


Sum	Formula	Sigma	m/z	Err [ppm]	Mean Err [ppm]	Err [mDa]	rdB	N Rule	e ⁻
C 14 H 20 N 3		0.034	230.1652	0.77	1.70	0.39	6.50	ok	even



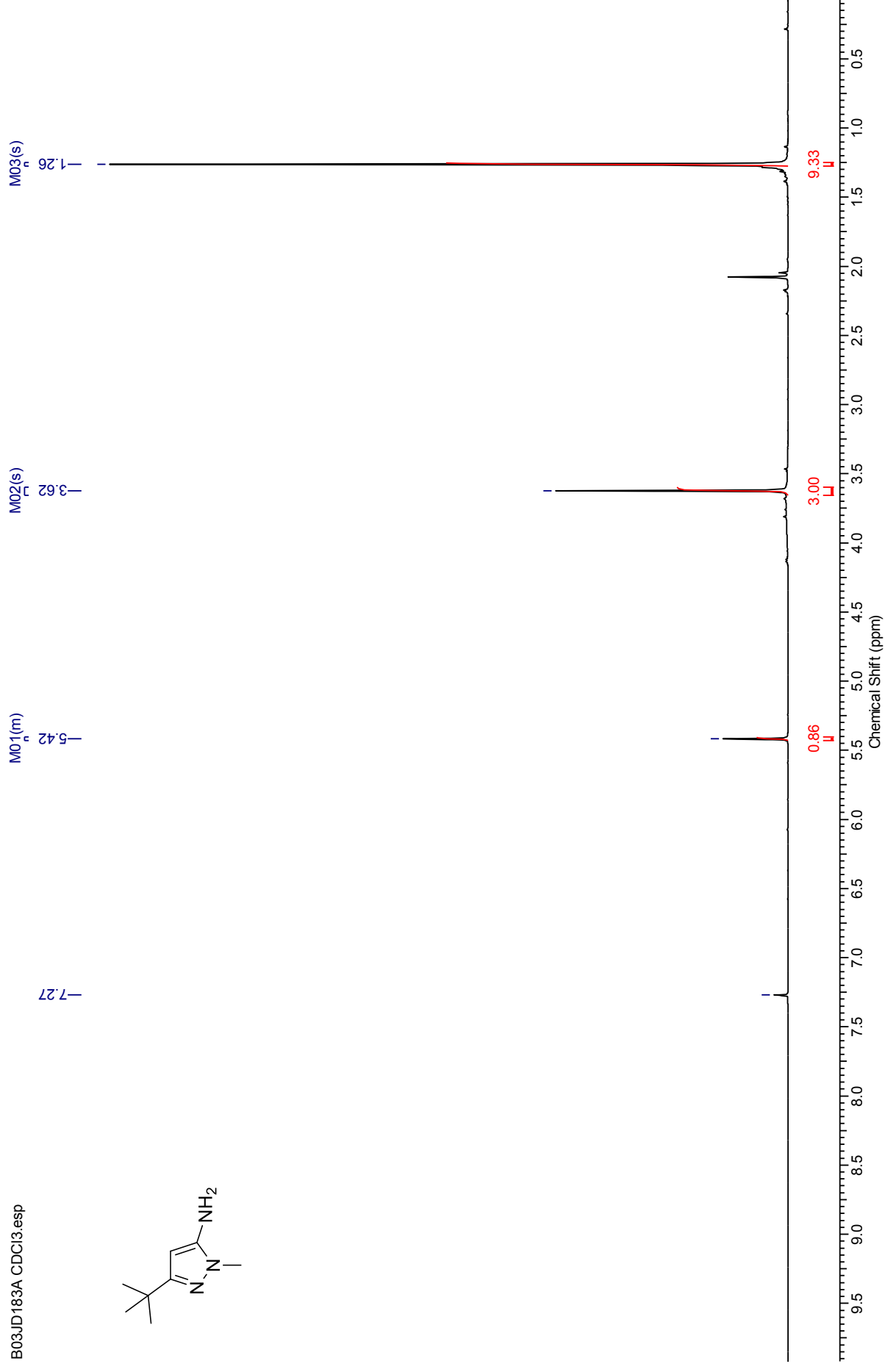
$[MH^+]$ requires 230.1652 Da

3-(*tert*-Butyl)-1-methyl-1*H*-pyrazol-5-amine (226)



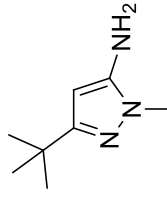
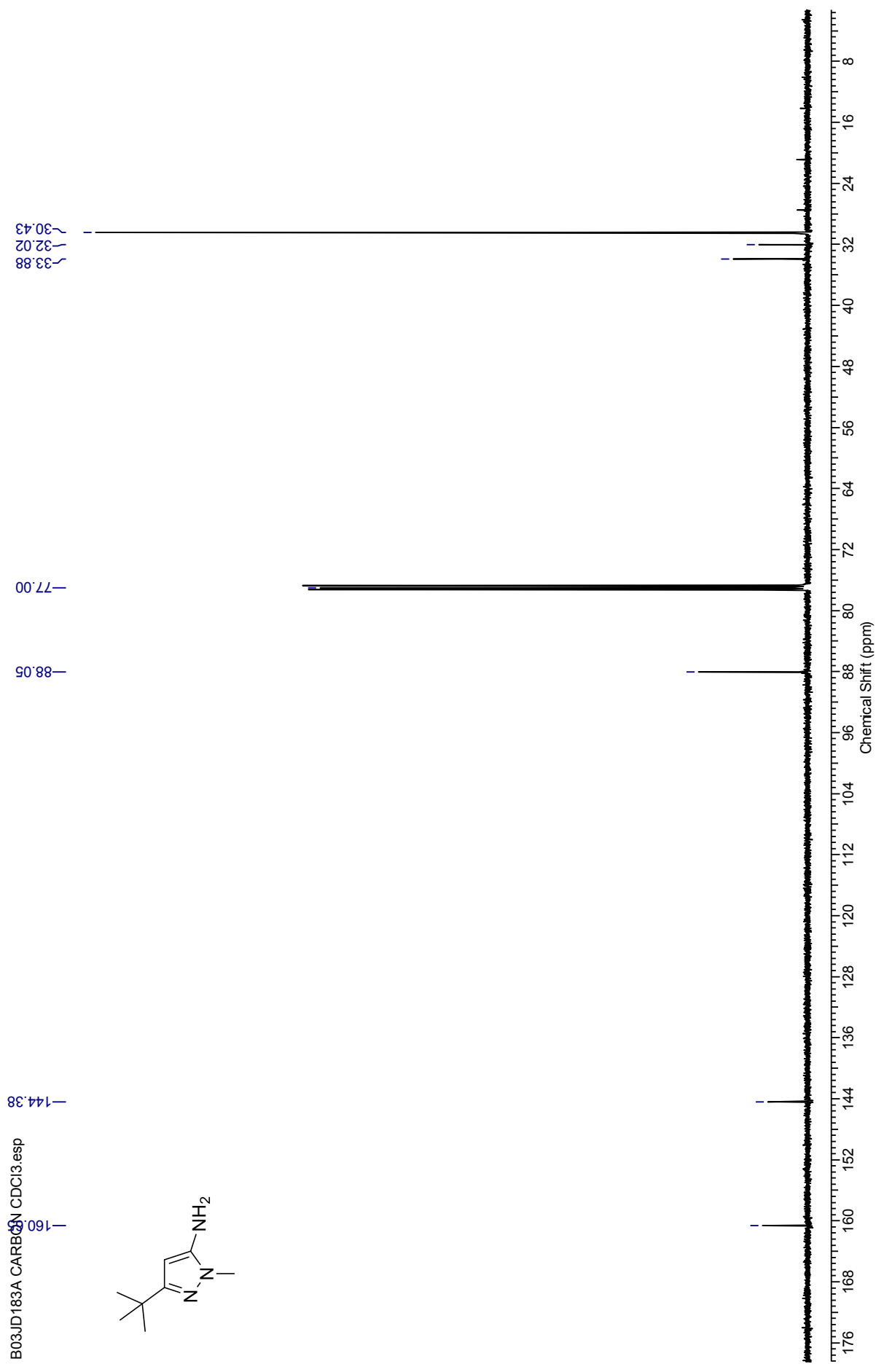
¹H NMR spectrum (500 MHz, CDCl₃) for 3-(*tert*-butyl)-1-methyl-1*H*-pyrazol-5-amine

B03JD183A CDCl3.esp



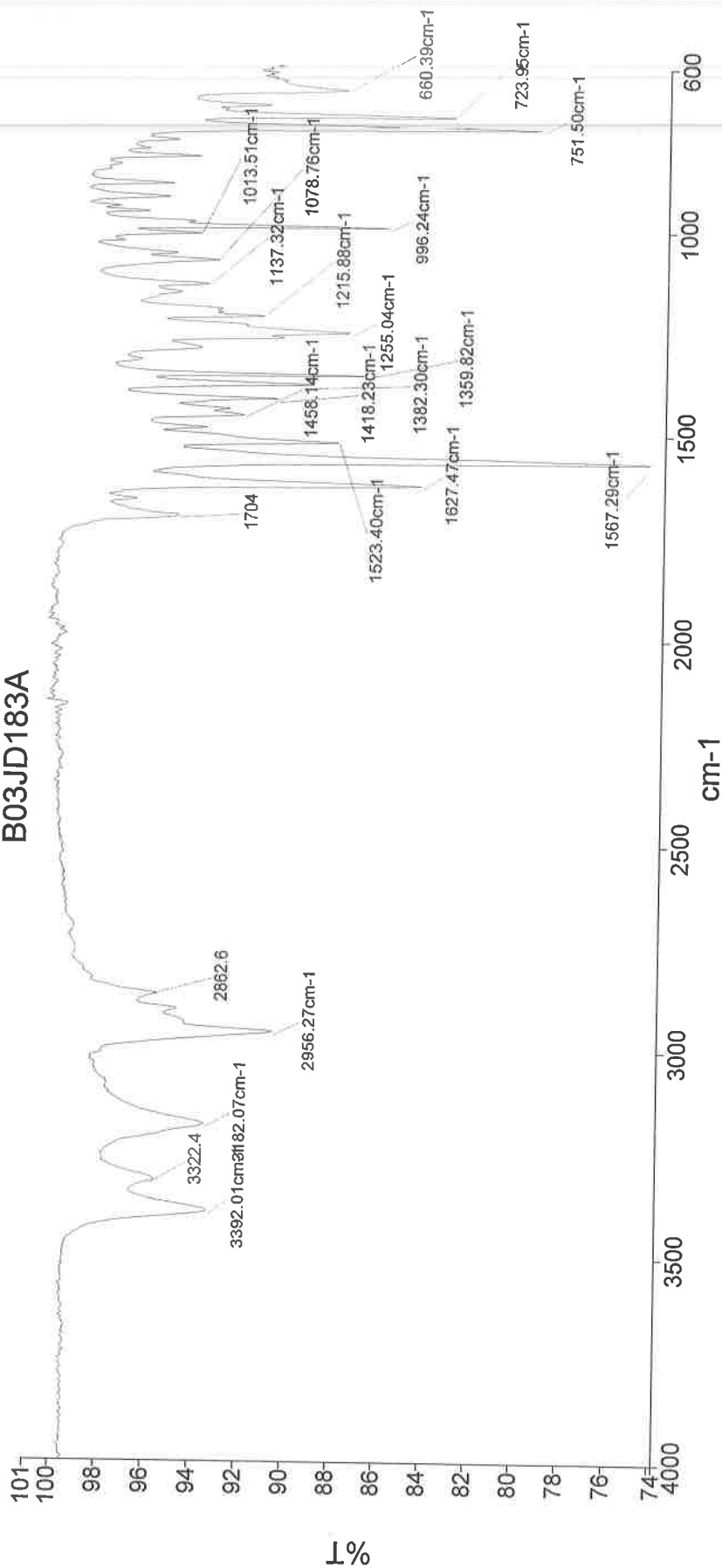
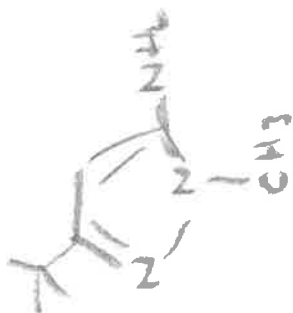
¹³C NMR spectrum (126 MHz, CDCl₃) for 3-(*tert*-butyl)-1-methyl-1*H*-pyrazol-5-amine

B03JD183A CARBON-13



Analyst
Date
Administrator
28 May 2015 14:48

B03JD183A



3392.01 N-H str.
3322.4 C-H str.
2956.27 N-H bend
2862.6 C-H str.
1704 C=O str.
1627.47 C=N str.
1567.29 C-N bend
1523.40 C-N str.
1458.14 C-H bend
1418.23 C-H bend
1382.30 C-H bend
1359.82 C-H bend
1255.04 C-N str.
1215.88 C-N str.
1137.32 C-N str.
1078.76 C-N str.
1013.51 C-N str.
996.24 C-N str.
751.50 C-N str.
723.95 C-N str.
660.39 C-N str.

Administrator 23 Sample 023 By Administrator Date Thursday, May 28 2015

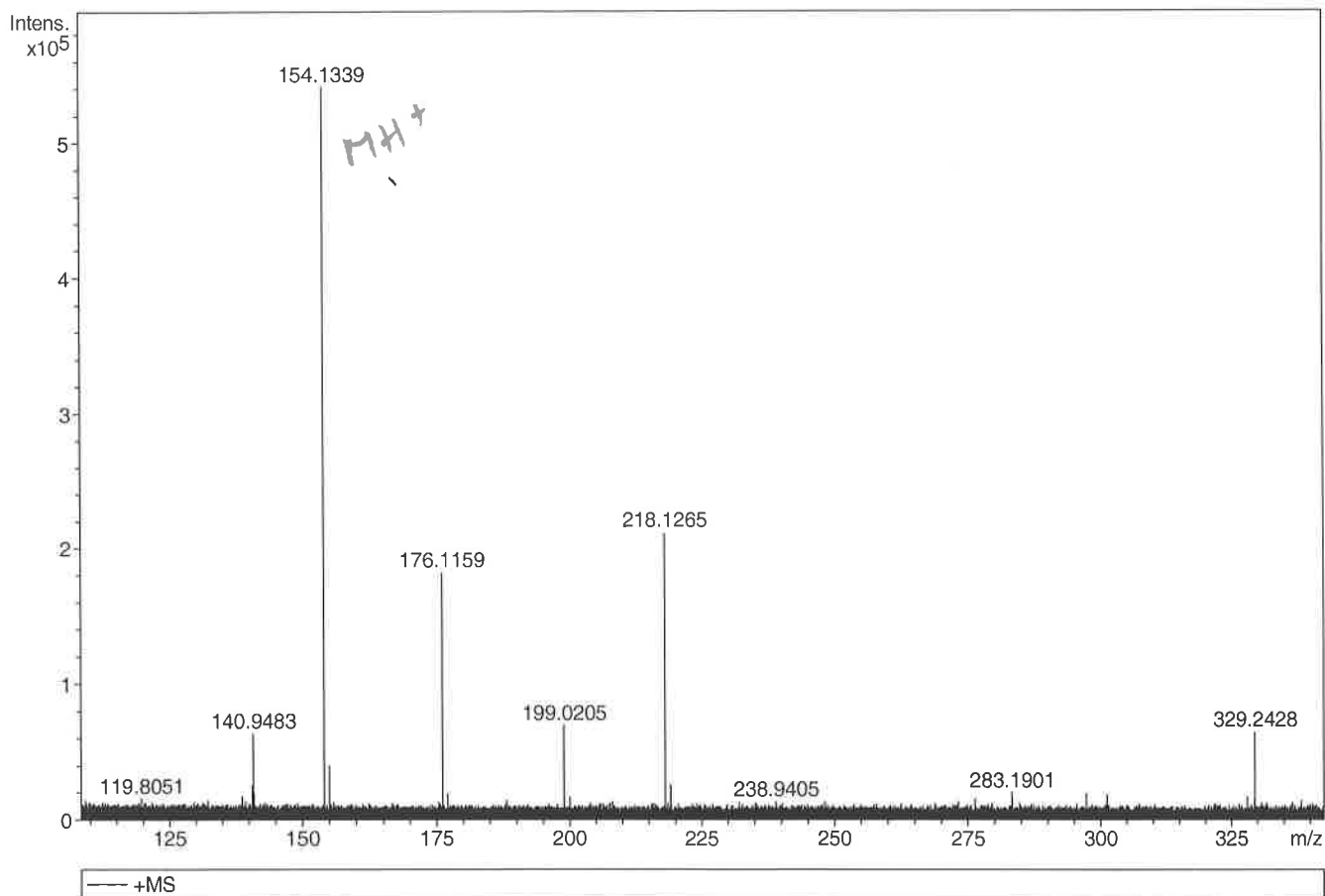
Generic Display Report

Analysis Info

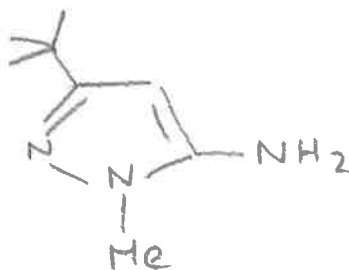
Analysis Name D:\Data\Alinanopos\JESS4930_000001.d
 Method pos20090608esi
 Sample Name POS ESI BO3JD183A
 Comment

Acquisition Date 20/03/2015 16:22:27

Operator Administrator
 Instrument apex-III

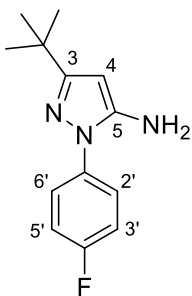


Sum	Formula	Sigma	m/z	Err [ppm]	Mean Err [ppm]	Err [mDa]	rdb	N Rule	e ⁻
C 8 H 16 N 3		0.020	154.1339	-0.13	0.79	0.12	2.50	ok	even



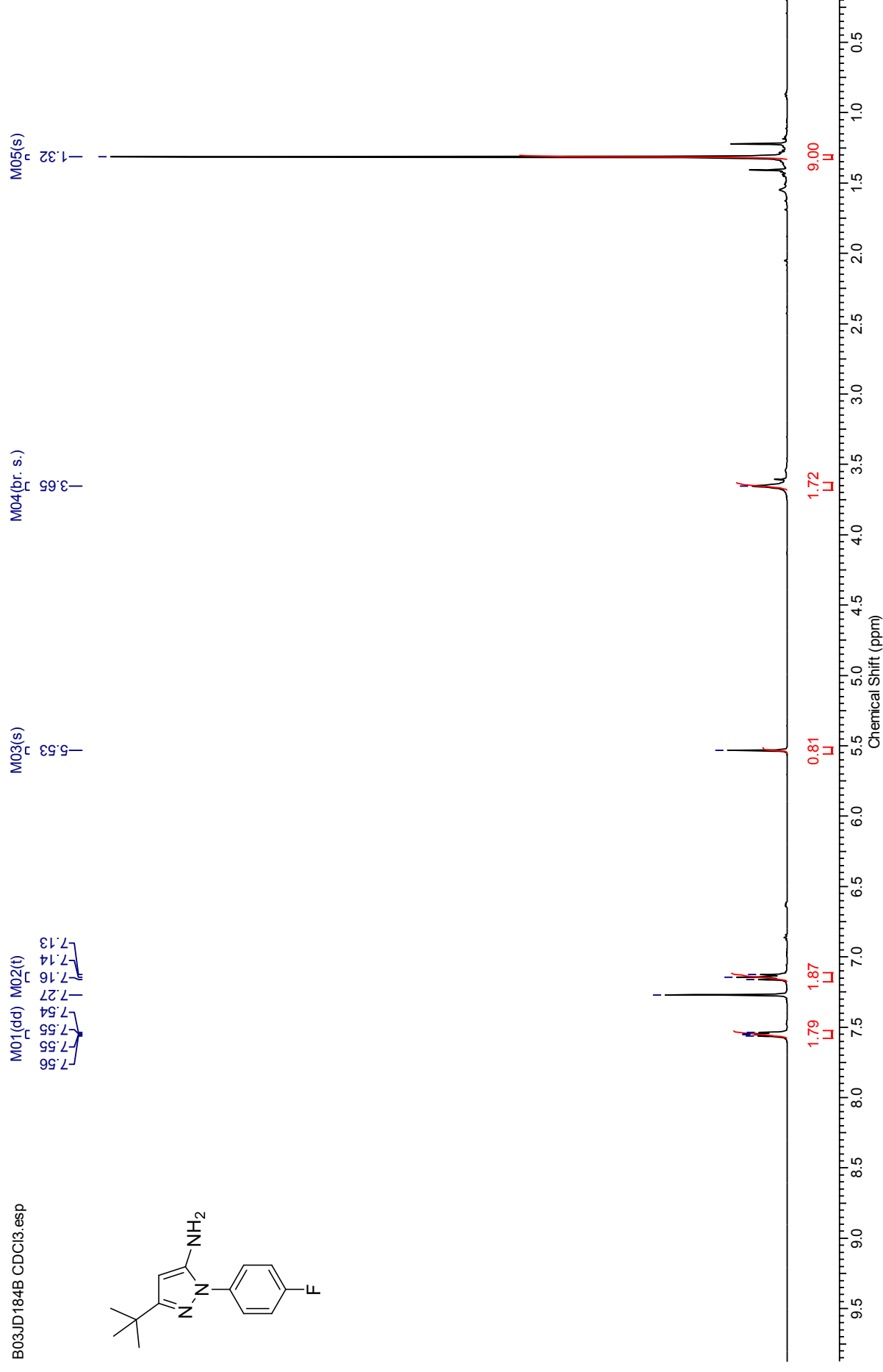
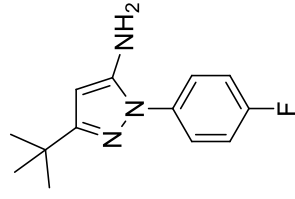
$[MH]^+$ requires
154.1339 Da

3-(*tert*-Butyl)-1-(4-fluorophenyl)-1*H*-pyrazole-5-amine (227)



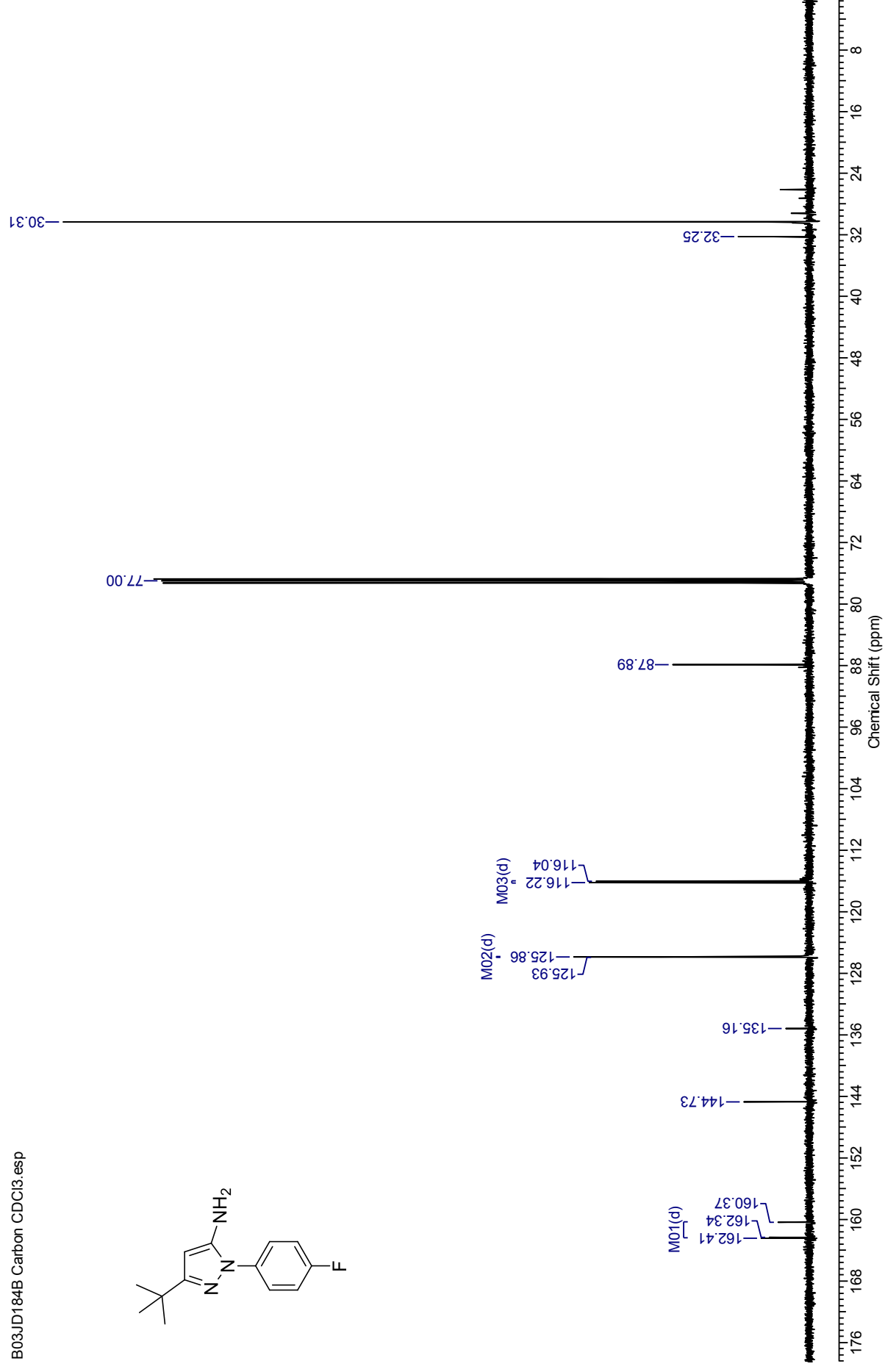
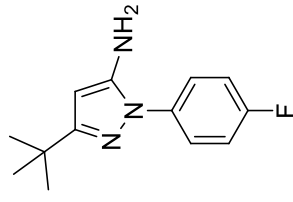
¹H NMR spectrum (500 MHz, CDCl₃) for 3-(*tert*-butyl)-1-(4-fluorophenyl)-1*H*-pyrazole-5-amine

B03JD184B CDCl₃.esp



¹³C NMR spectrum (126 MHz, CDCl₃) for 3-(*tert*-butyl)-1-(4-fluorophenyl)-1*H*-pyrazole-5-amine

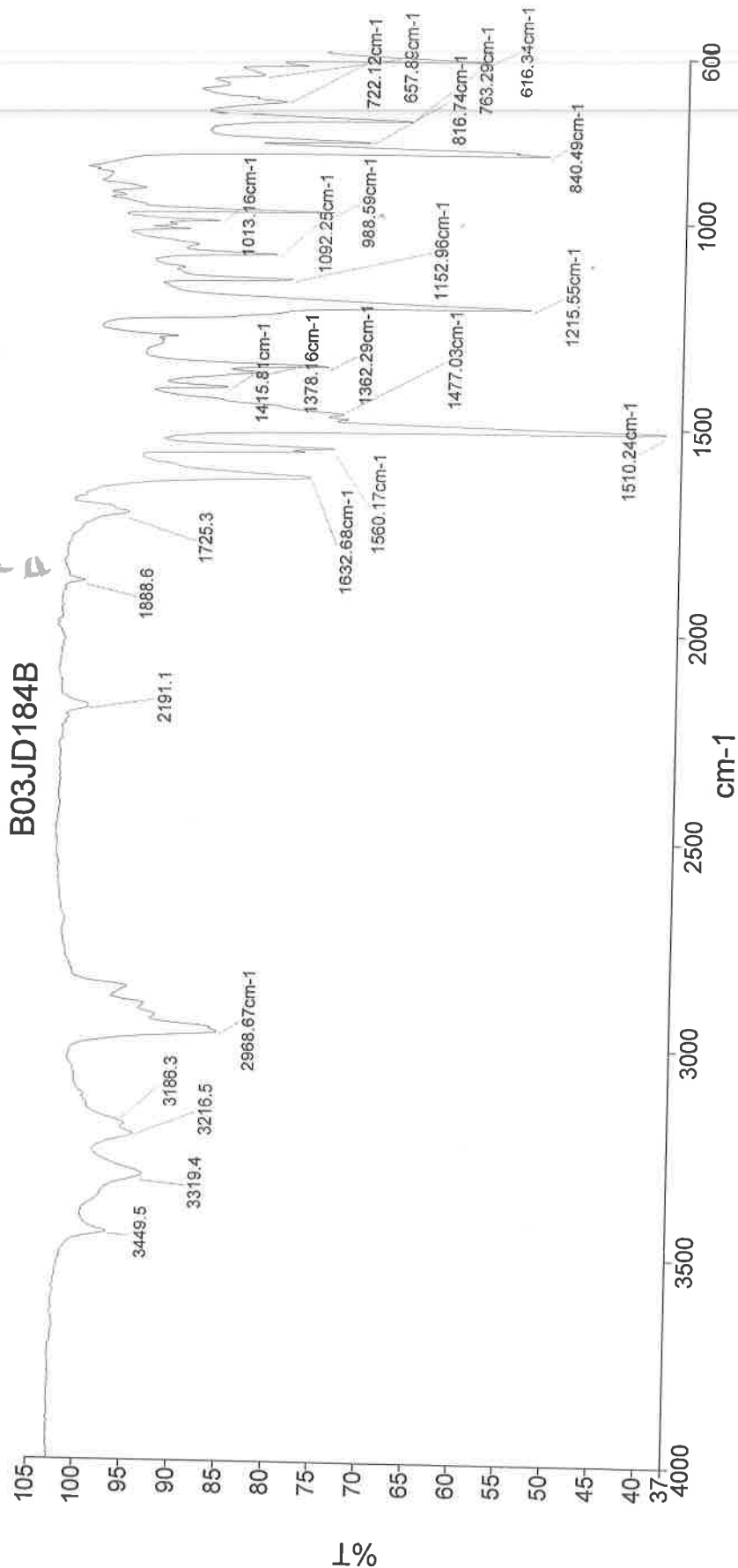
B03JD184B Carbon CDCl₃.esp



Analyst
Date

Administrator
28 May 2015 14:54

B03JD184B



Administrator 25 Sample 025 By Administrator Date Thursday, May 28 2015

3314 N-H str.
2969 C-H str.
1633 N-H str.
1510 C=N bond
1362 C-H str.
1216 C-N str.

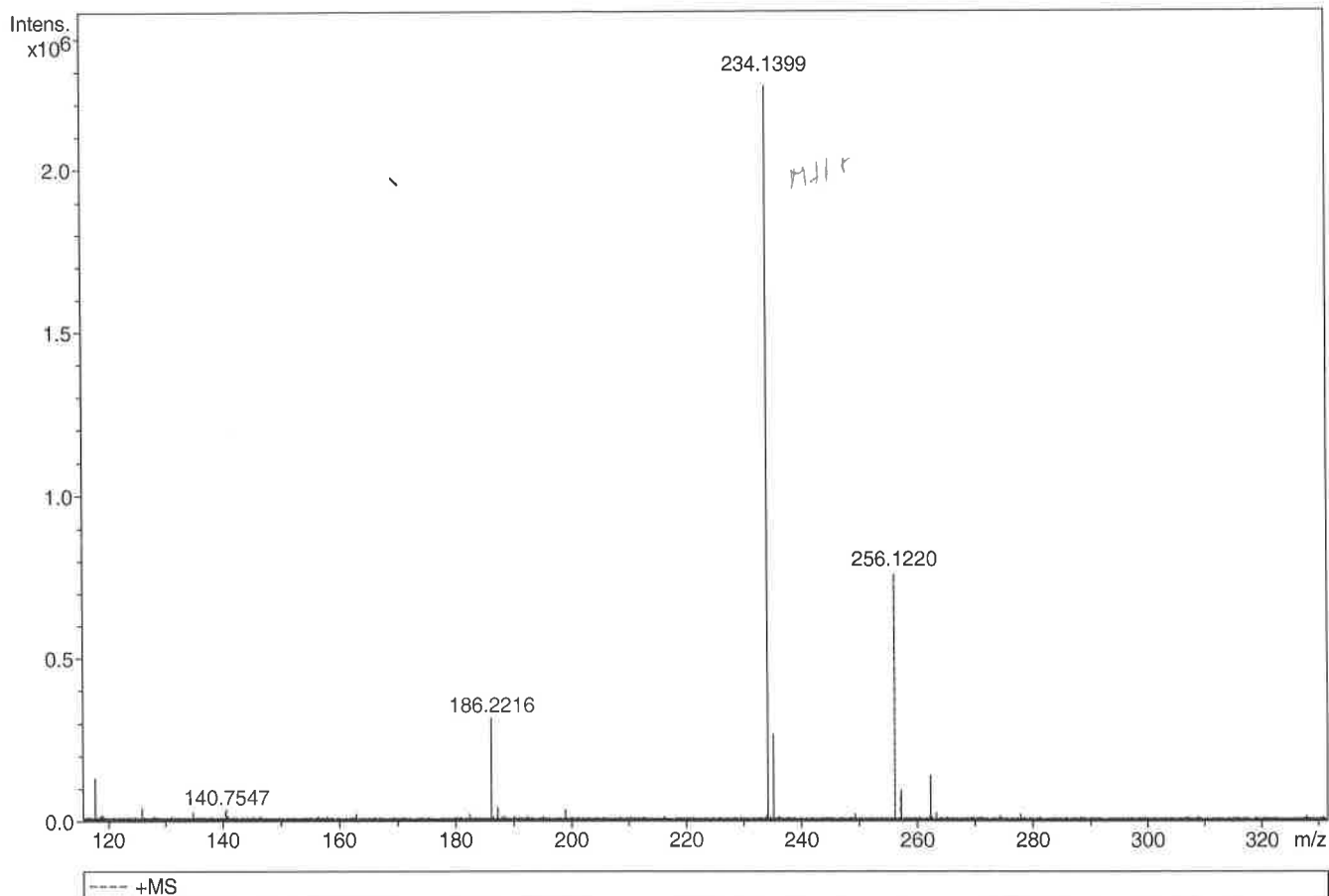
Generic Display Report

Analysis Info

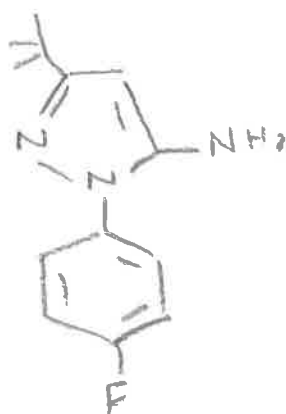
Analysis Name D:\Data\Alinanopos\JESS4932_000001.d
Method pos20090608esi
Sample Name POS ESI BO3JD184A
Comment

Acquisition Date 23/03/2015 11:47:28

Operator Administrator
Instrument apex-III

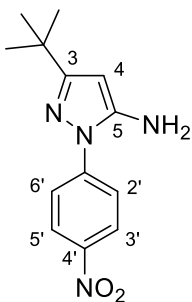


Sum	Formula	Sigma	m/z	Err [ppm]	Mean Err [ppm]	Err [mDa]	rdb	N Rule	e ⁻
C 13 H 17 F 1 N 3		0.040	234.1401	0.66	1.10	0.26	6.50	ok	even

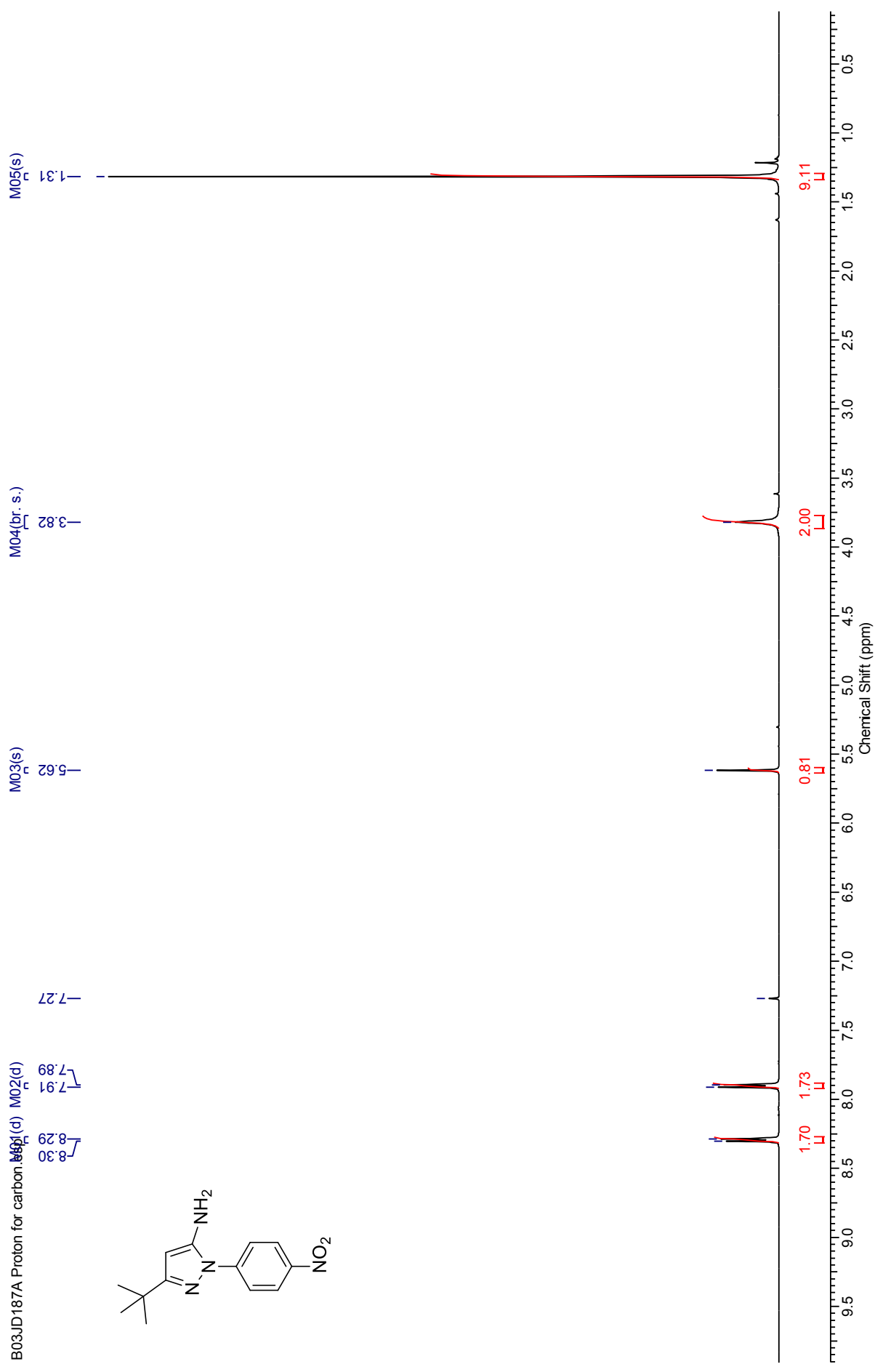


$[MH]^+$ requires 234.1401 Da

3-(*tert*-Butyl)-1-(4-nitrophenyl)-1*H*-pyrazol-5-amine (228)

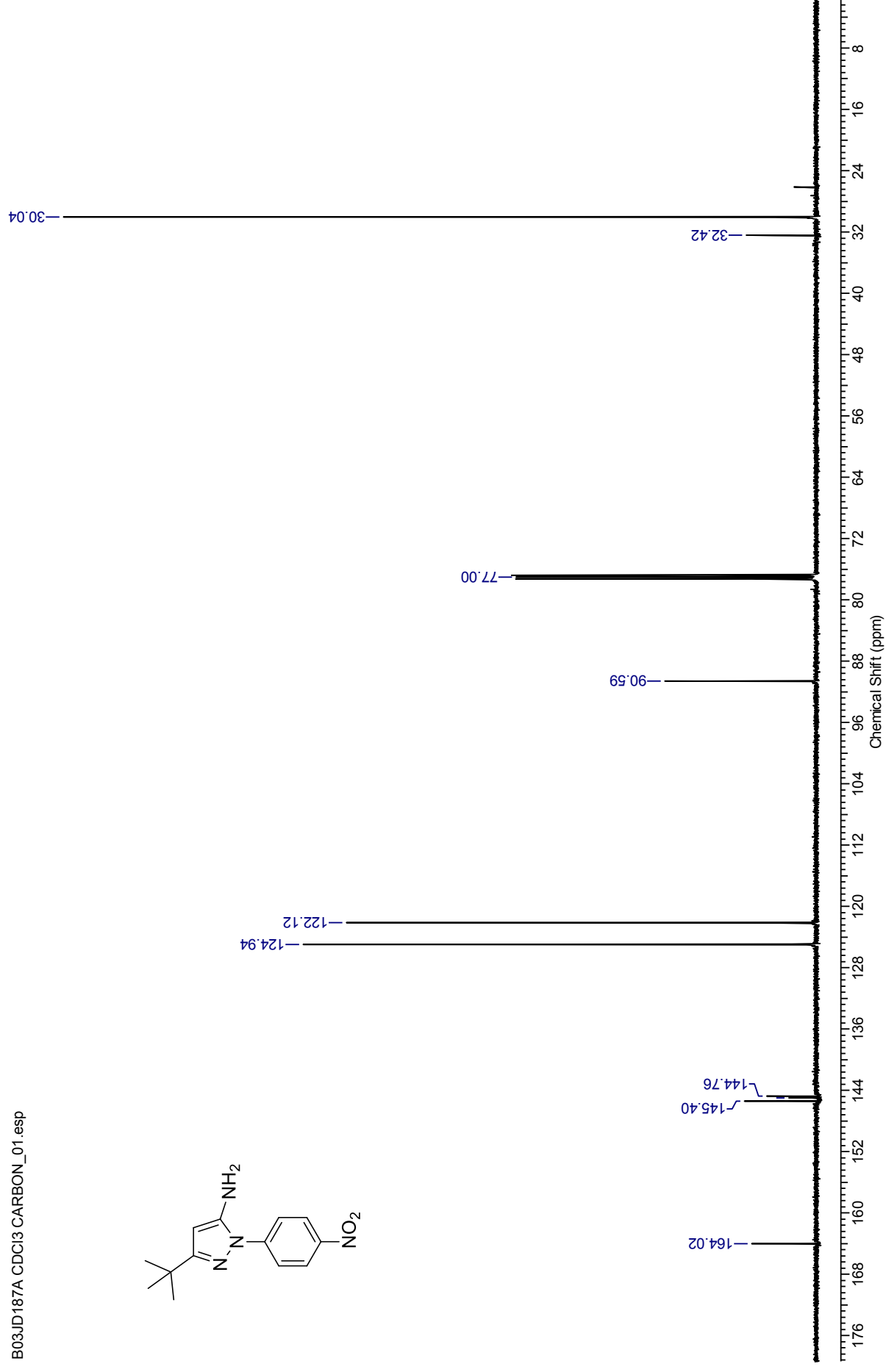
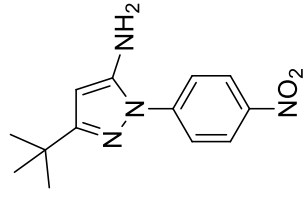


¹H NMR spectrum (500 MHz, CDCl₃) for 3-(*tert*-butyl)-1-(4-nitrophenyl)-1*H*-pyrazol-5-amine



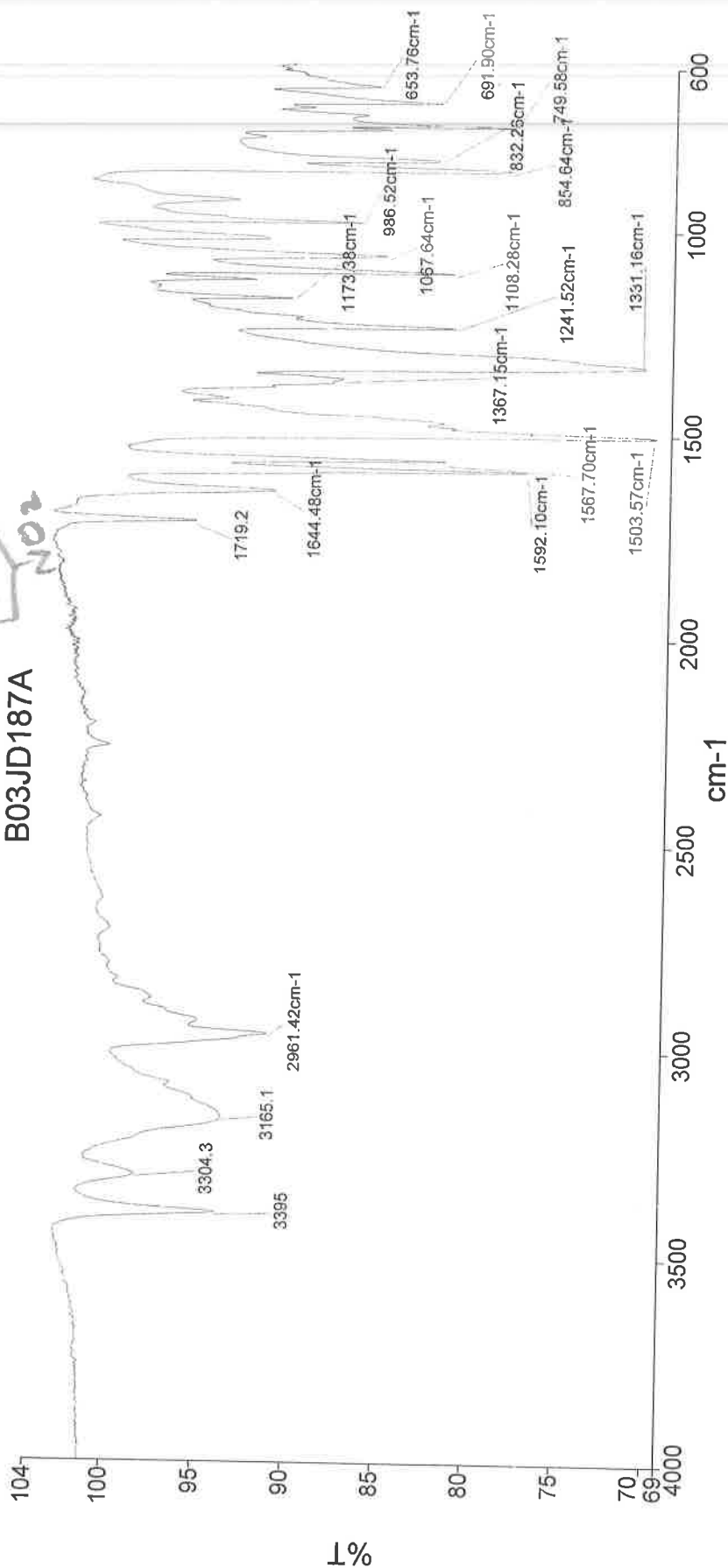
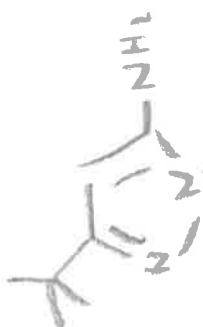
¹³C NMR spectrum (126 MHz, CDCl₃) for 3-(*tert*-butyl)-1-(4-nitrophenyl)-1*H*-pyrazol-5-amine

B03JD187A CDCl₃ CARBON_01.esp



Analyst
Date
Administrator
28 May 2015 15:03

B03JD187A



3395 - N-H str
2961 - C-H str
1644 - C=O str
1542 - C=N
1504 - NO2
1367 - NO2
1241 - C-N str
1108 - C-N str

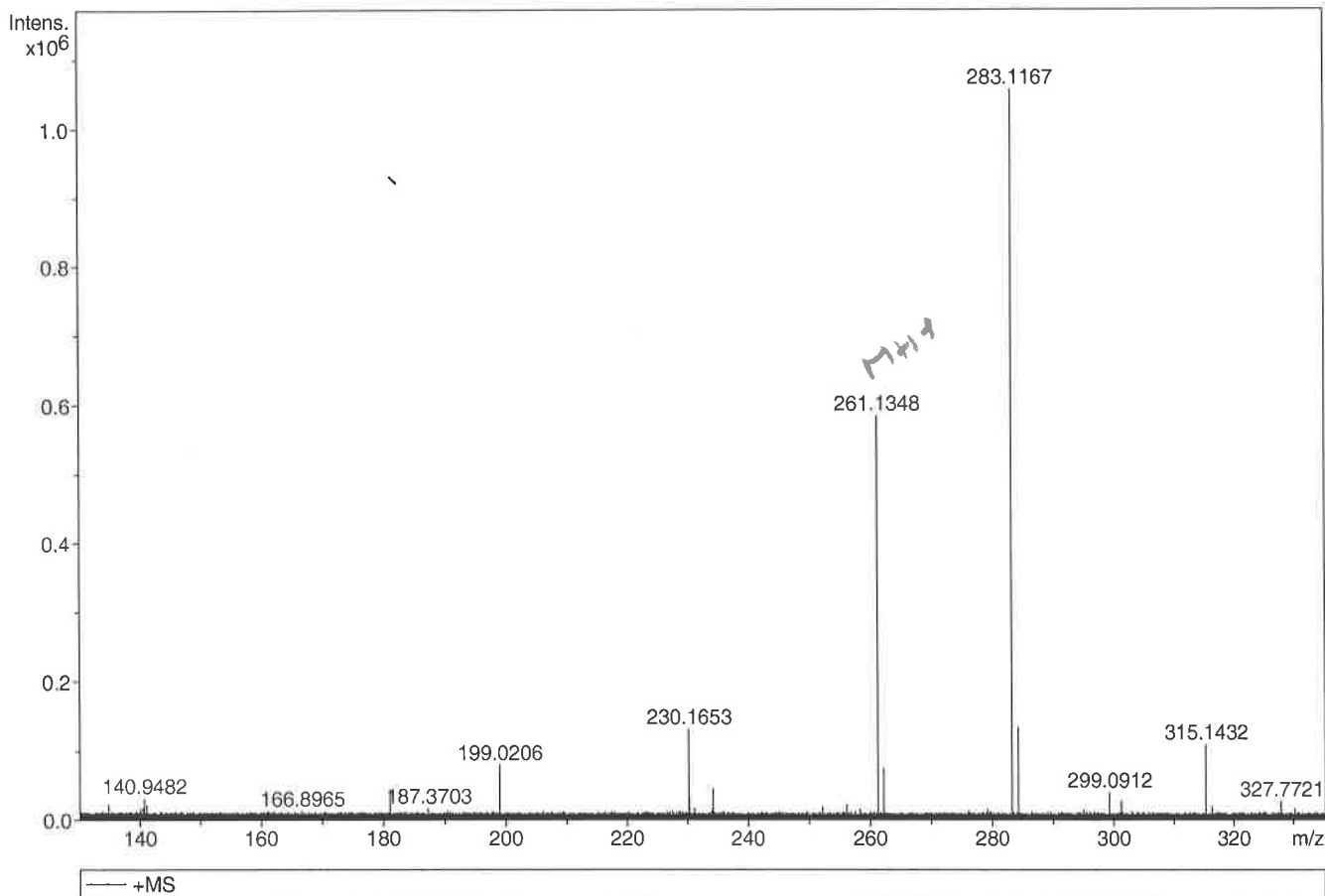
Generic Display Report

Analysis Info

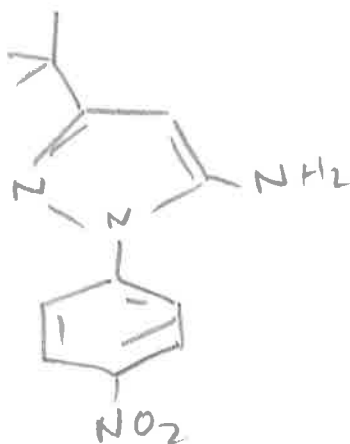
Analysis Name D:\Data\linanopos\JESS1836_000001.d
Method pos20090608esi
Sample Name POS ESI BO3JD187A
Comment

Acquisition Date 23/03/2015 15:15:06

Operator Administrator
Instrument apex-III

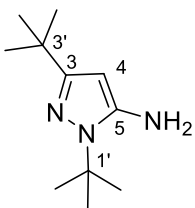


Sum Formula	Sigma	m/z	Err [ppm]	Mean Err [ppm]	Err [mDa]	rdb	N Rule	e ⁻
C 13 H 17 N 4 O 2	0.027	261.1346	-0.83	-2.50	-0.65	7.50	ok	even



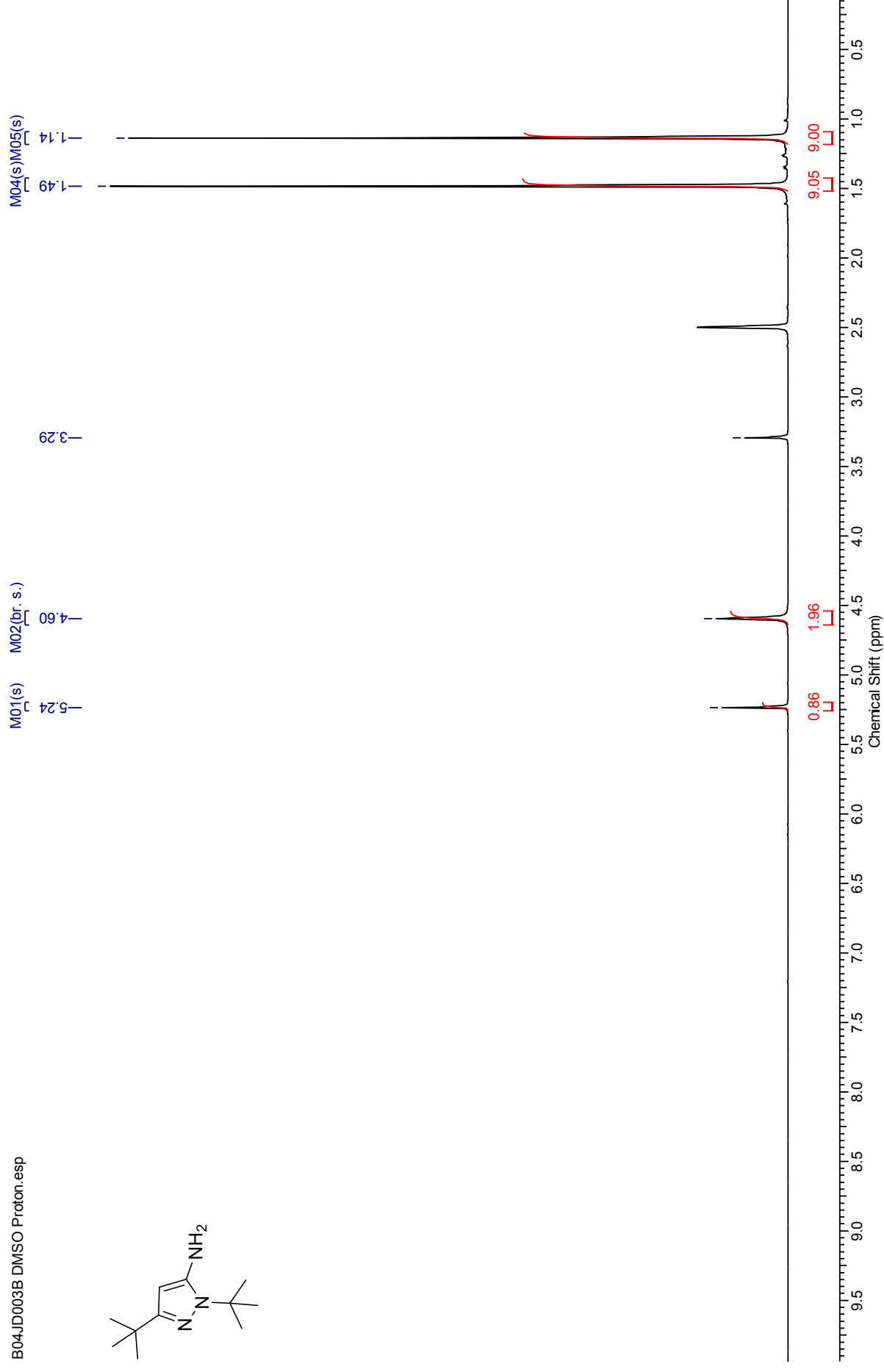
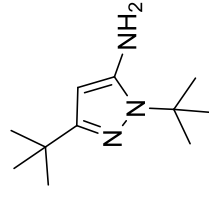
MH⁺ = 261.1346 Da

1,3-Di-*tert*-butyl-1*H*-pyrazol-5-amine (229)



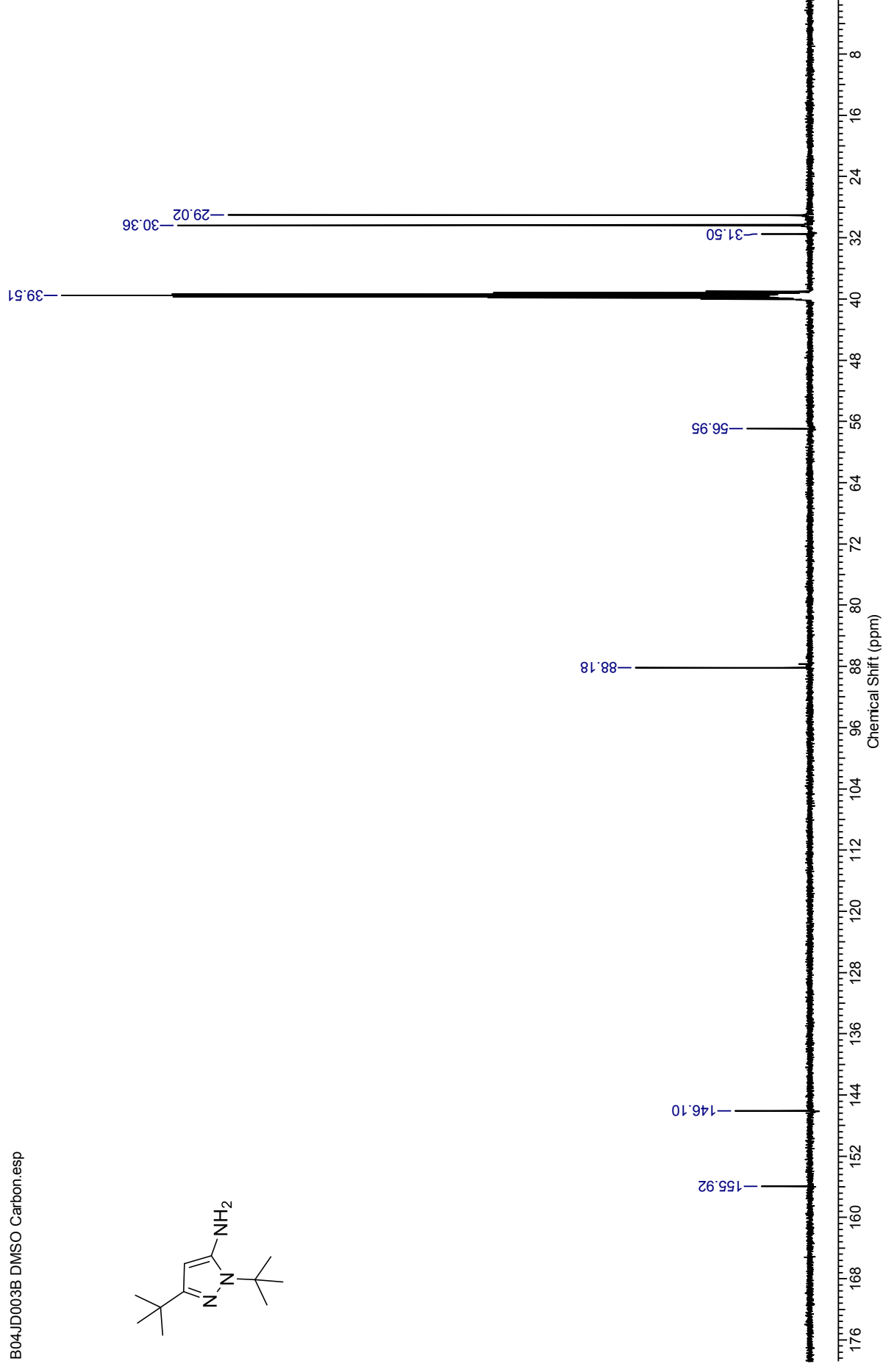
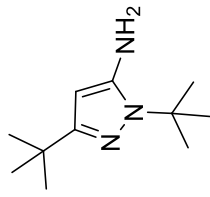
¹H NMR spectrum (500 MHz, DMSO-*d*₆) for 1,3-di-*tert*-butyl-1*H*-pyrazol-5-amine

B04JD003B DMSO Proton.esp



¹³C NMR spectrum (125 MHz, DMSO-*d*₆) for 1,3-Di-*tert*-butyl-1*H*-pyrazol-5-amine

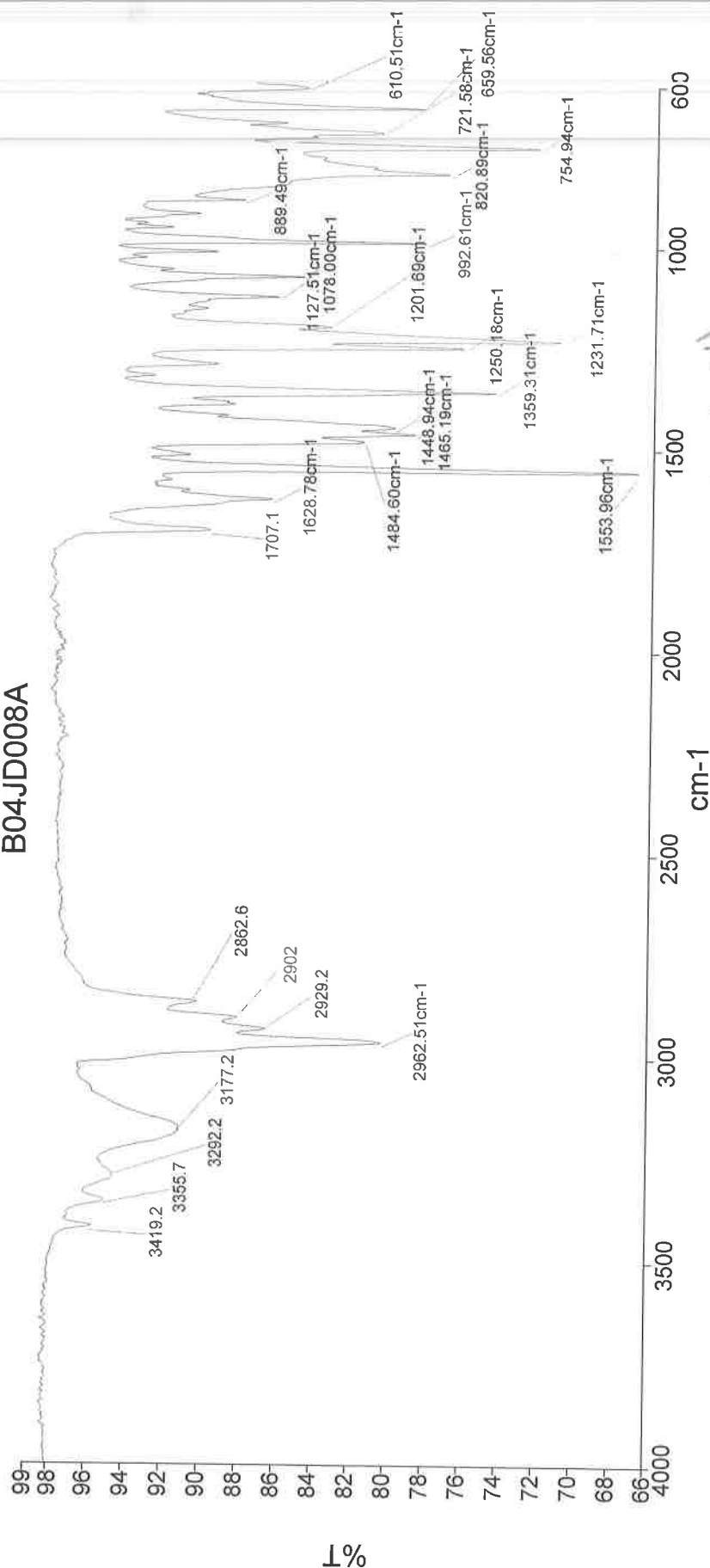
B04JD003B DMSO Carbon.esp



Analyst
Date

Administrator
28 May 2015 14:45

B04JD008A

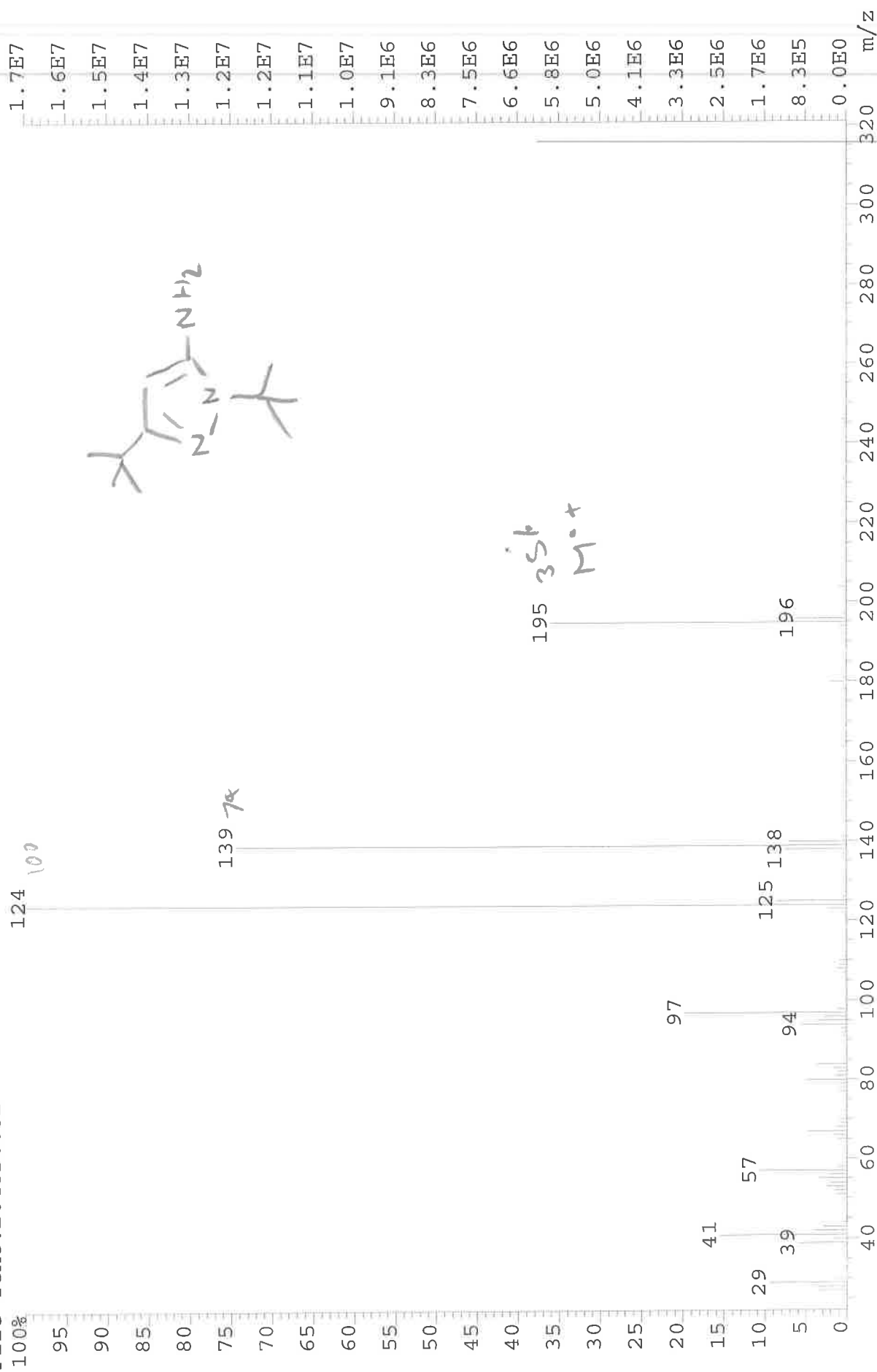


Absorption (cm⁻¹)
3355 - N-H str.
2962 - C-H str.

1629 - N-H bend
1554 - C=N str.
1465 - C-H bend
1359 - C-H bend
1222 - CH₃ bend

Administrator 22 Sample 022 By Administrator Date Thursday, May 28 2015

File: JESS4995 Ident: 5 Acq: 21-APR-2015 12:36:51 +0:22 Cal: CAL1
AutoSpecE EI+ Magnet BpI: 16599169 TIC: 66378032 Flags: HALL
File Text: B04JD003B



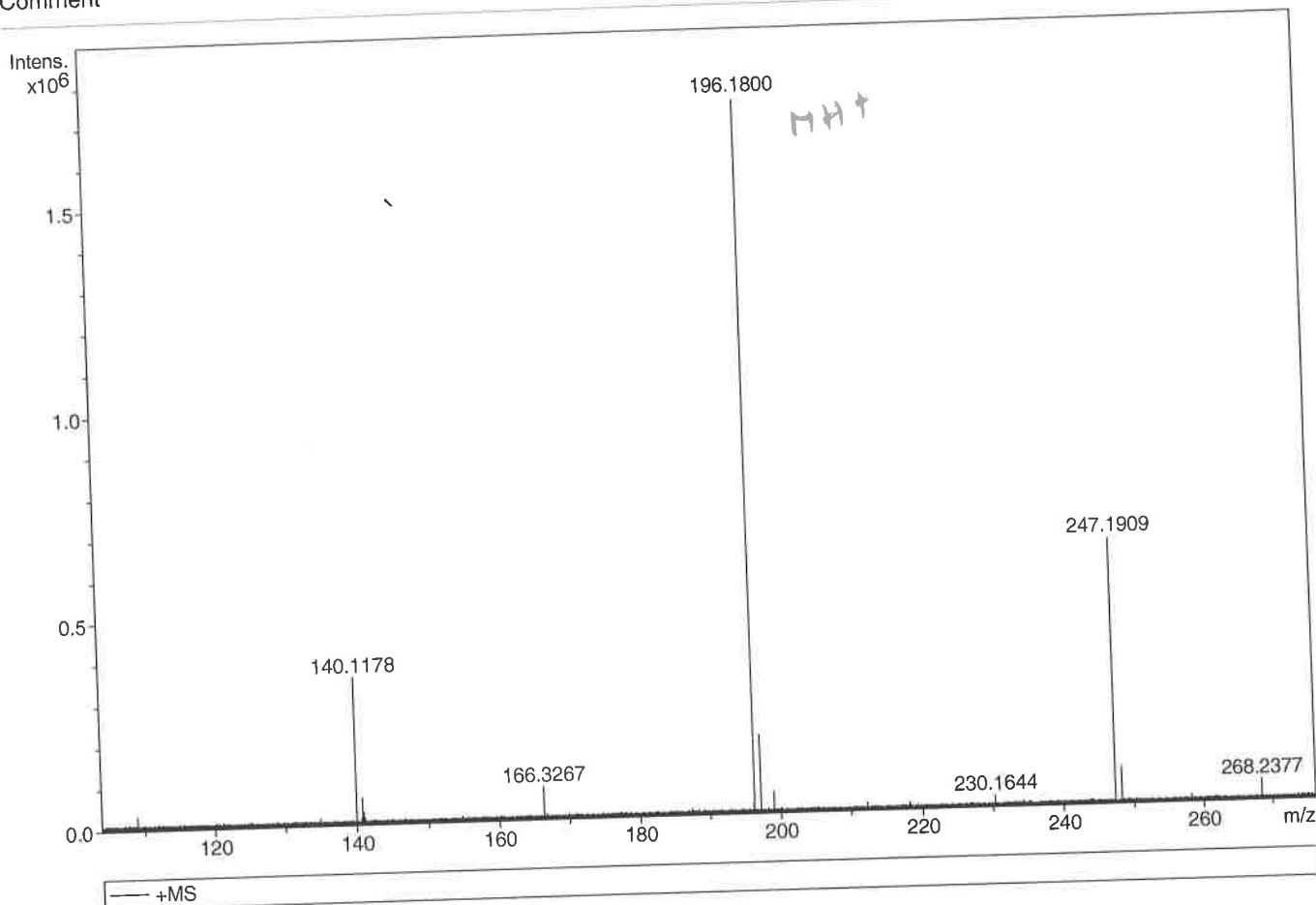
Generic Display Report

Analysis Info

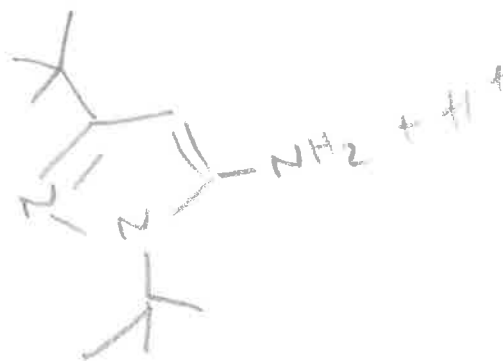
Analysis Name D:\Data\Alinanopos\JESS4995_000001.d
 Method pos20090608esi
 Sample Name POS ESI BO4JD003B
 Comment

Acquisition Date 21/04/2015 10:04:17

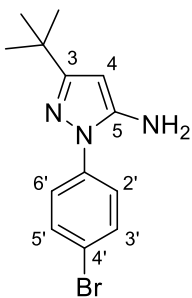
Operator Administrator
 Instrument apex-III



Sum Formula	Sigma	m/z	Err [ppm]	Mean Err [ppm]	Err [mDa]	rdb	N Rule	e ⁻
C 11 H 22 N 3	0.025	196.1808	4.08	3.36	0.66	2.50	ok	even



1-(4-Bromophenyl)-3-(*tert*-butyl)-1*H*-pyrazol-5-amine (230)



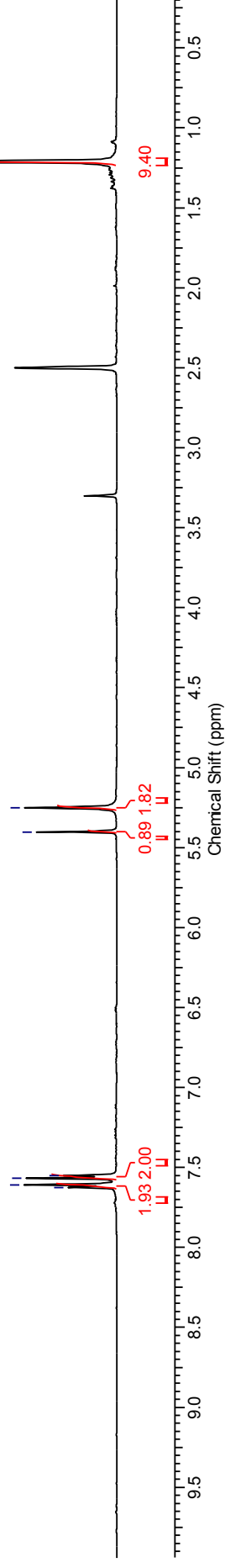
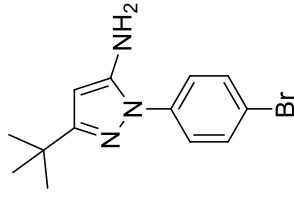
^1H NMR spectrum (500 MHz, $\text{DMSO-}d_6$) for 1-(4-bromophenyl)-3-(*tert*-butyl)-1*H*-pyrazol-5-amine

B04JD011A DMSO Proton for Carbon.esp

M05(m)
M04(m)
7.63
7.61
7.57
7.55

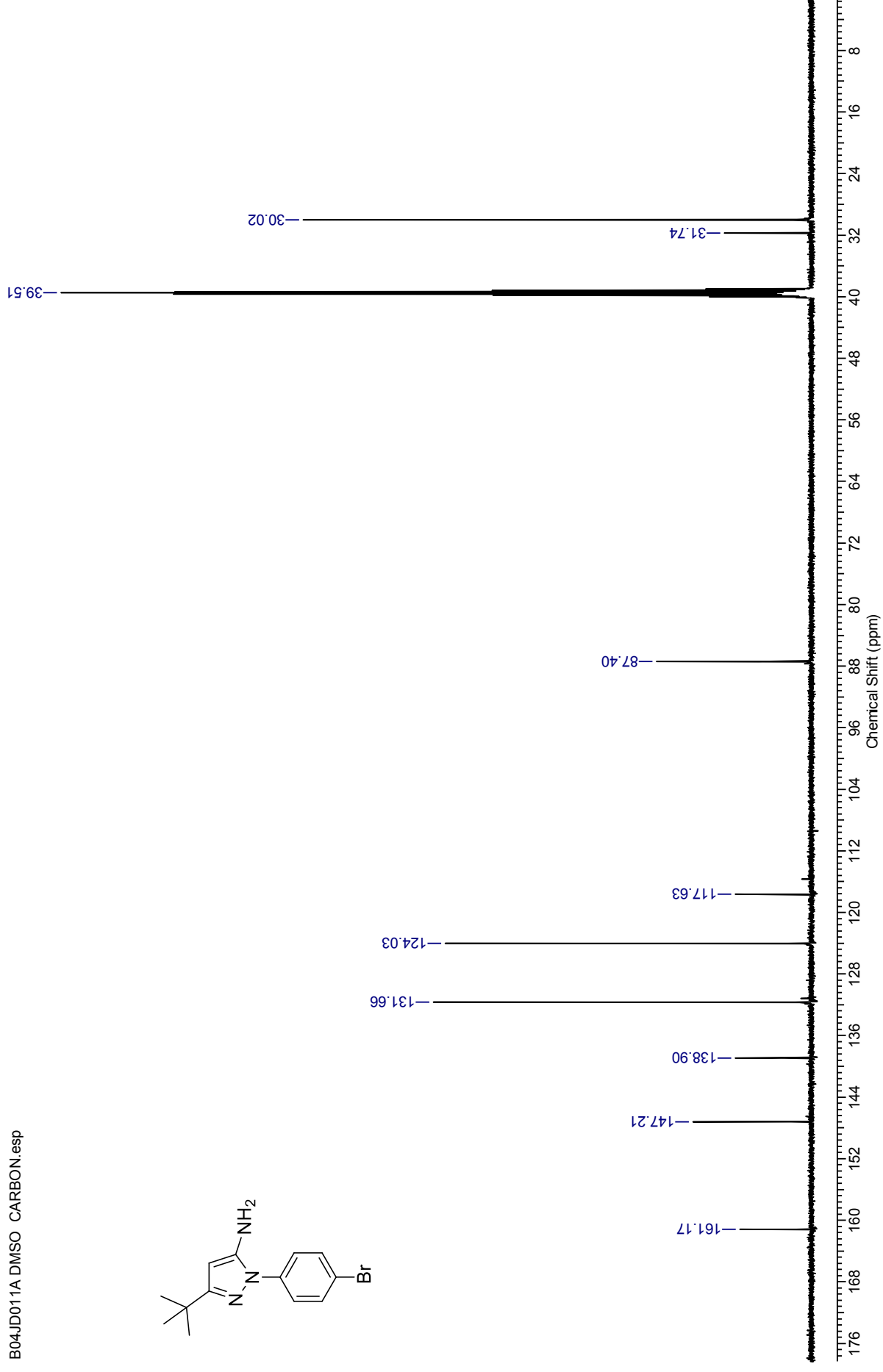
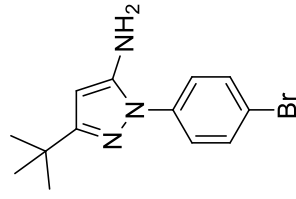
M03(s)
M02(s)
5.40
5.25

M01(s)
1.21



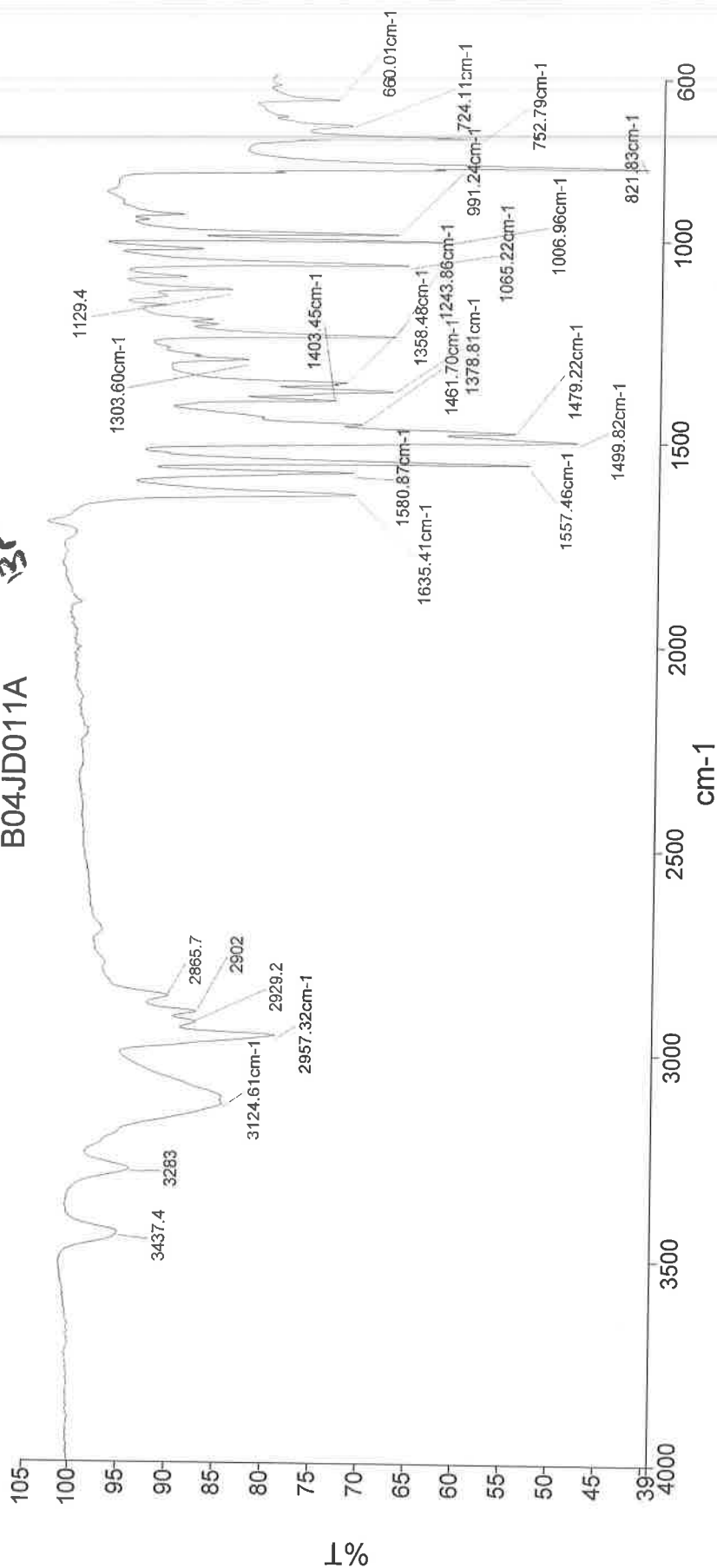
¹³C NMR spectrum (126 MHz, DMSO-*d*₆) for 1-(4-bromophenyl)-3-(*tert*-butyl)-1*H*-pyrazol-5-amine

B04JD011A DMSO CARBON.esp



Analyst
Date
Administrator
28 May 2015 15:25

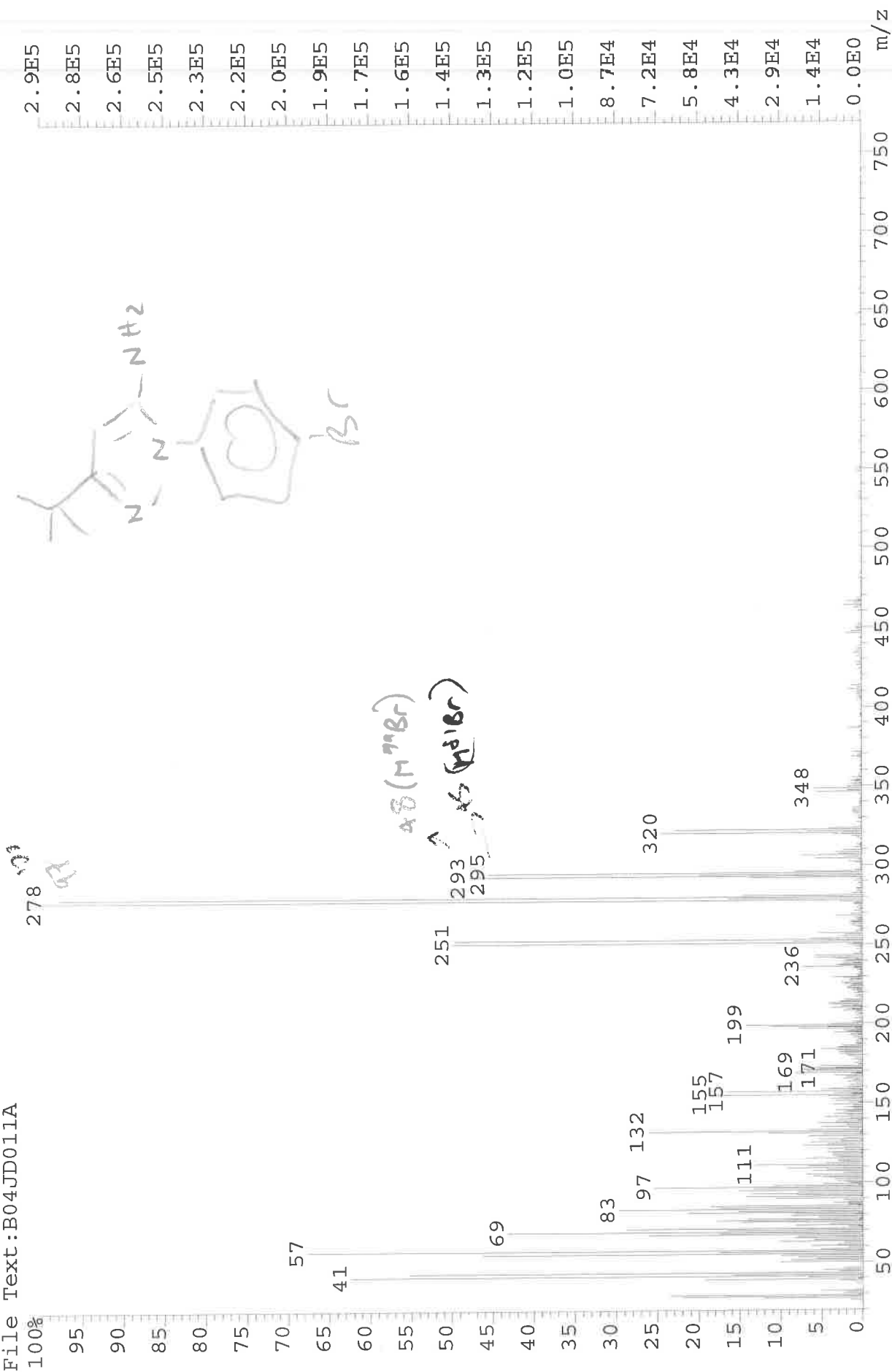
B04JD011A



3437 - N-H str.
3125 - C-H alk. str.
2957 - C-H bend
1635 - N-H bend
1557 - C=N in ring str.
1500 - C=C str.
1244 - C-N str.
1065 - C-N str.

Administrator 34 Sample 034 By Administrator Date Thursday, May 28 2015

File: JESS5156 Ident: 48 Acq: 28-MAY-2015 16:03:07 +3:00 Cal: CAL1
AutoSpecE EI+ Magnet BpI: 289962 TIC: 6589442 Flags: HALL
File Text: B04JD011A



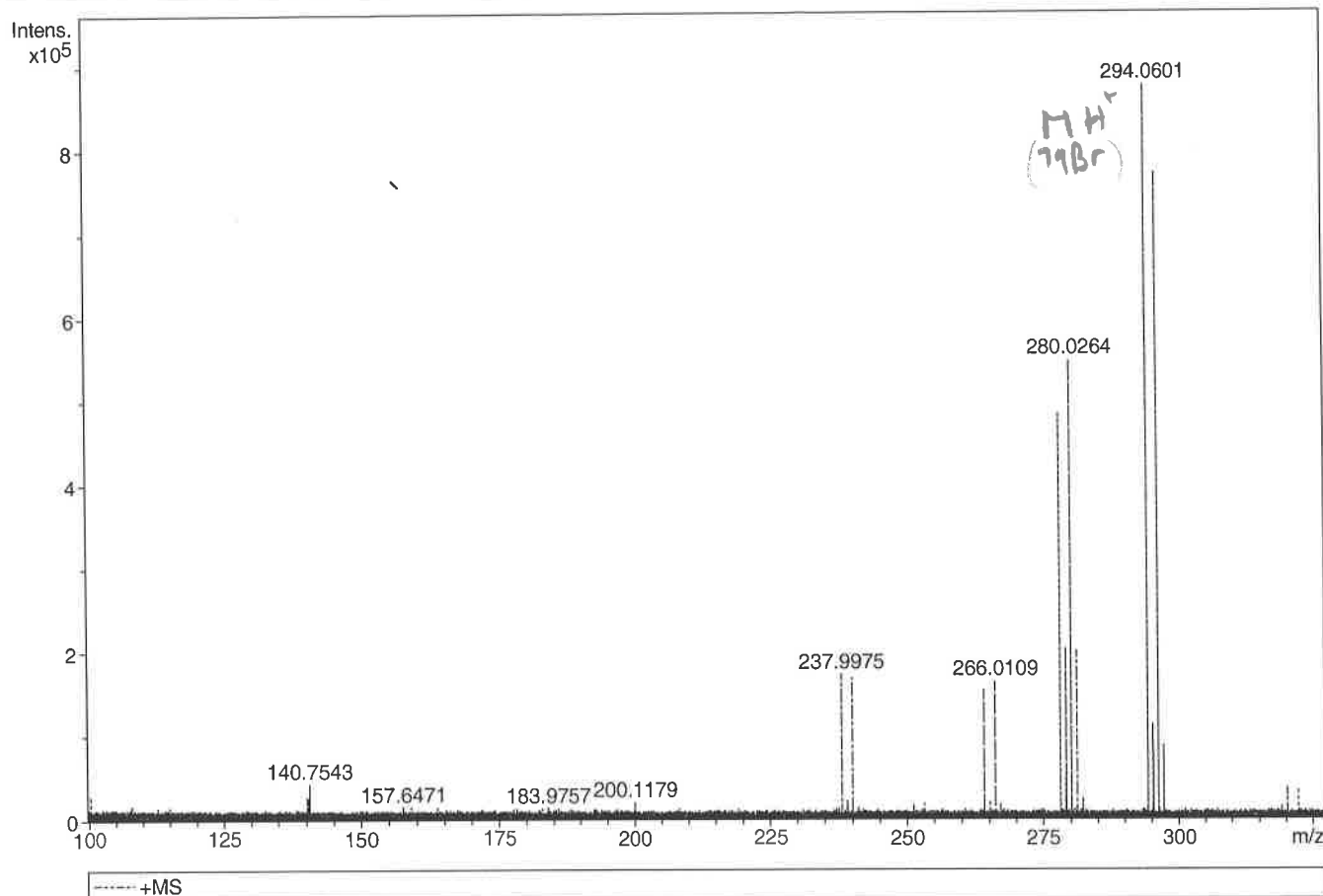
Generic Display Report

Analysis Info

Analysis Name D:\Data\Allnanopus\JESS5156_000001.d
 Method pos20090608esi
 Sample Name POS ESI BO4JD011A
 Comment

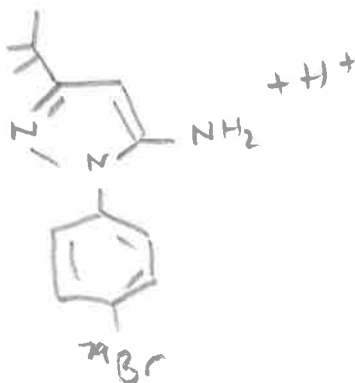
Acquisition Date 28/05/2015 16:18:49

Operator Administrator
 Instrument apex-III

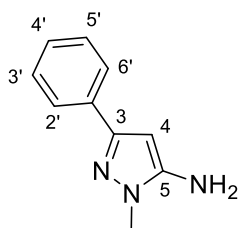


Sum Formula	Sigma	m/z	Err [ppm]	Mean Err [ppm]	Err [mDa]	rdB	N Rule	e ⁻
C 13 H 17 Br 1 N 3	0.043	294.0600	-0.27	2.20	0.65	6.50	ok	even

↑
79Br



1-Methyl-3-phenyl-1*H*-pyrazol-5-amine (231)



¹H NMR spectrum (500 MHz, DMSO-*d*₆) for 1-Methyl-3-phenyl-1*H*-pyrazol-5-amine

B04JD082C DMSO proton for carbon.esp

M05(t,9,11)

M04(m,10)

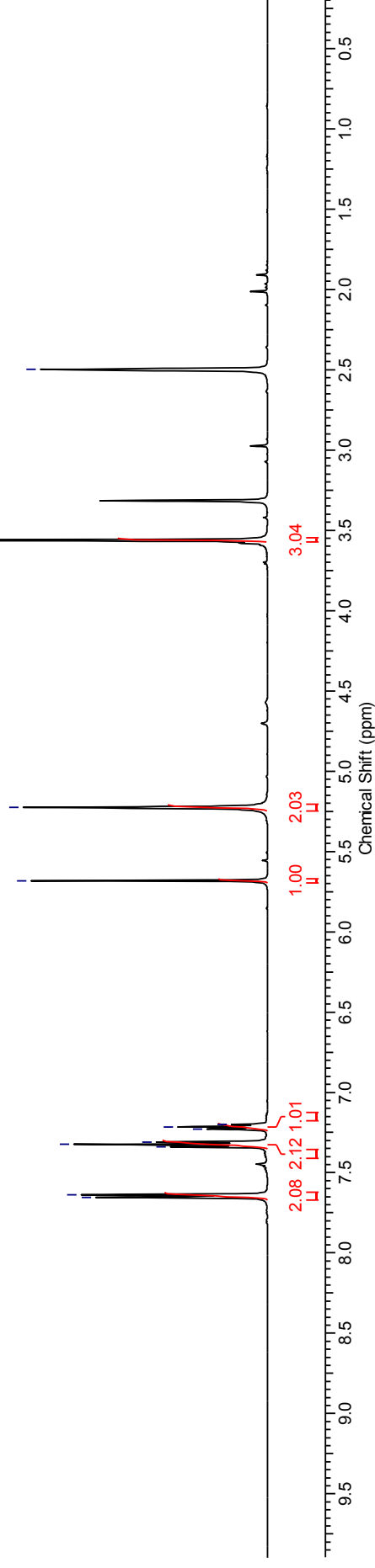
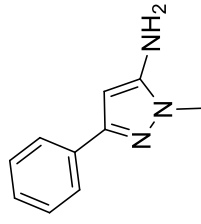
M06(d,12,8)

M03(s,4)M02(s,13)

M01(s,6)

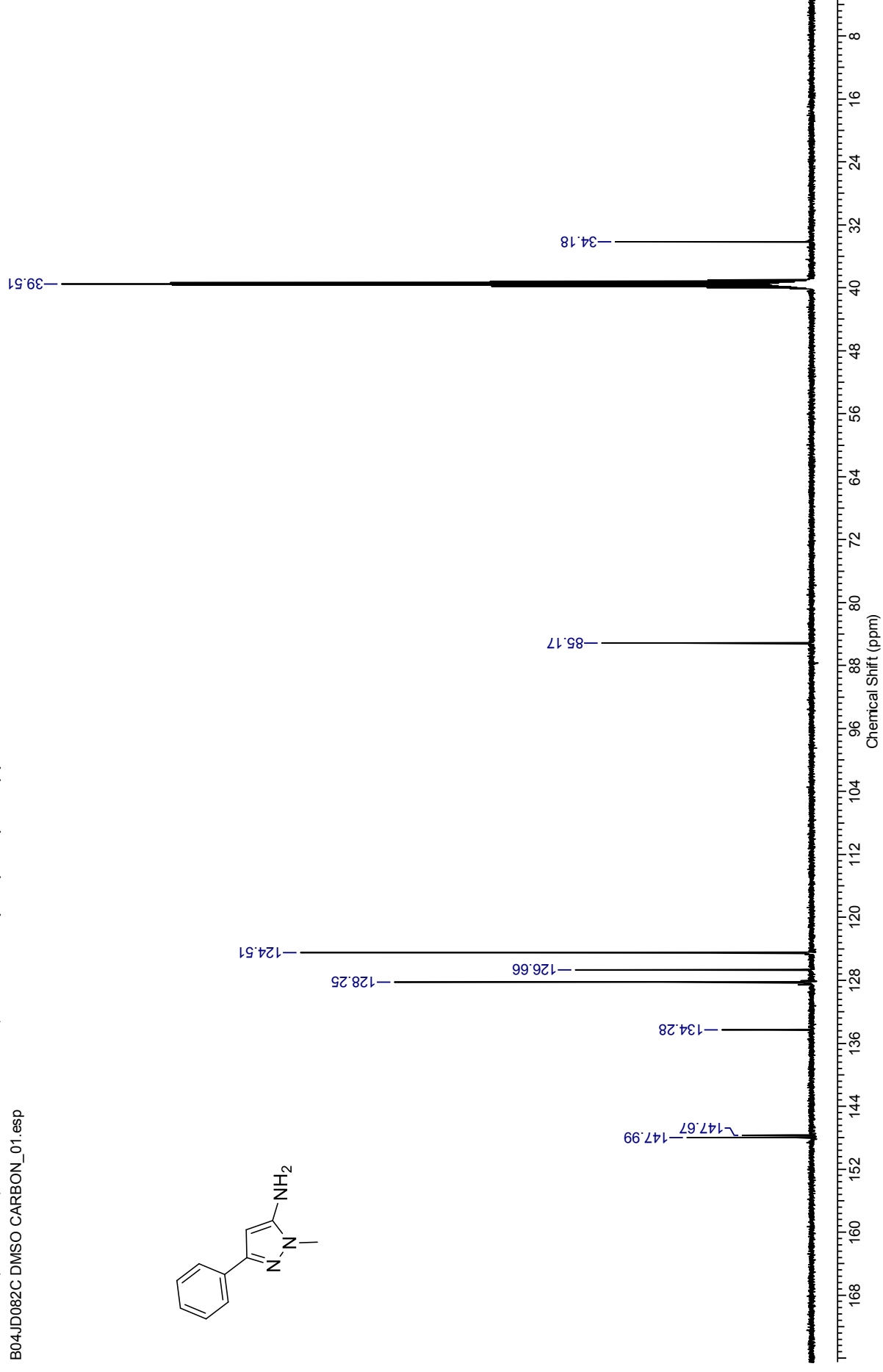
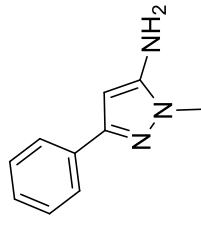
7.65
7.64
7.34
7.32
7.31
7.23
7.21
7.20

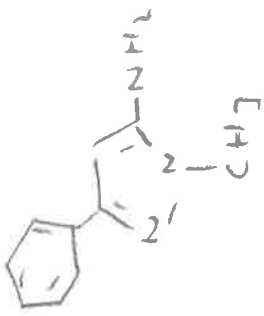
3.56
2.50



¹³C NMR spectrum (126 MHz, DMSO-*d*₆) for 1-Methyl-3-phenyl-1*H*-pyrazol-5-amine

B04JD082C DMSO CARBON_01.esp

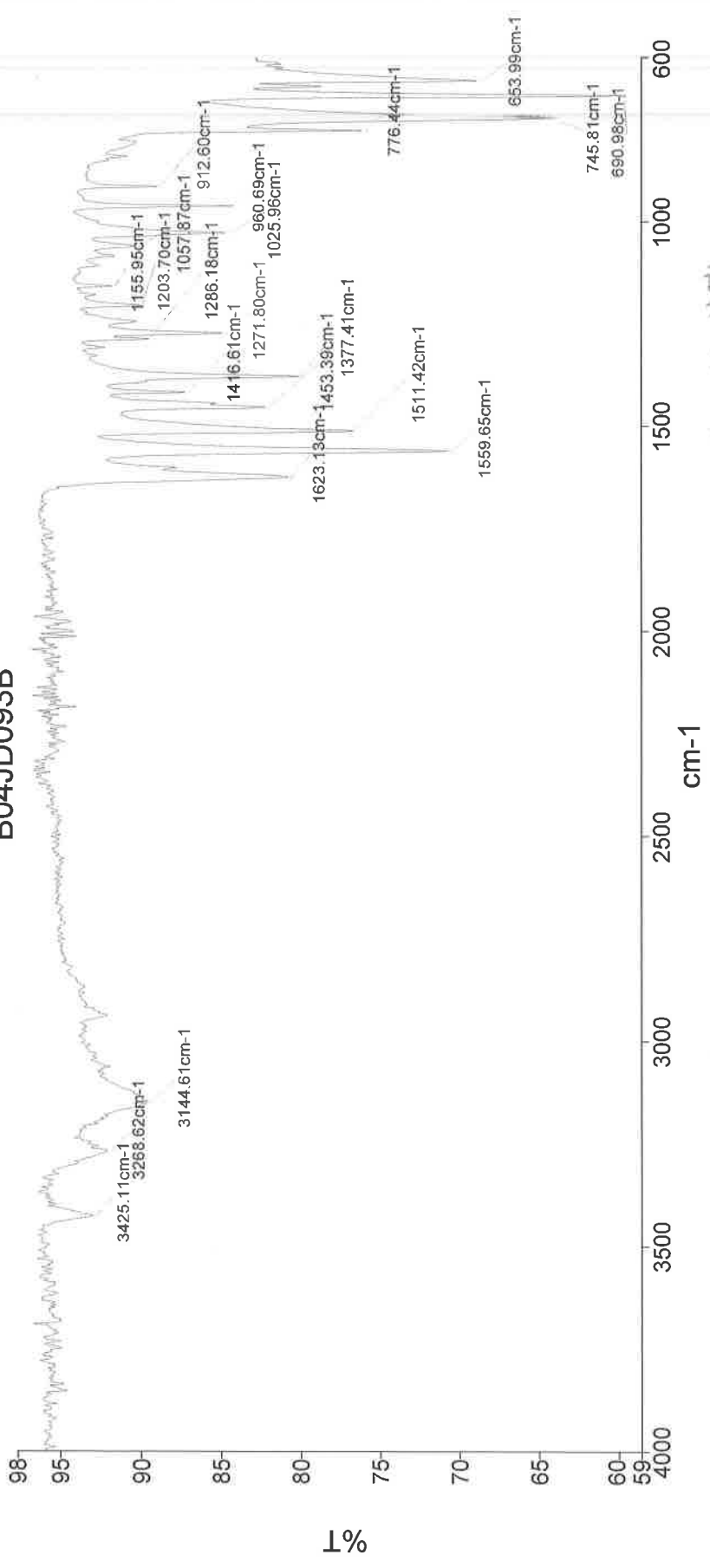




PerkinElmer Spectrum Version 10.03.06
11 November 2015 13:42

Analyst
Date
Administrator
11 November 2015 13:42

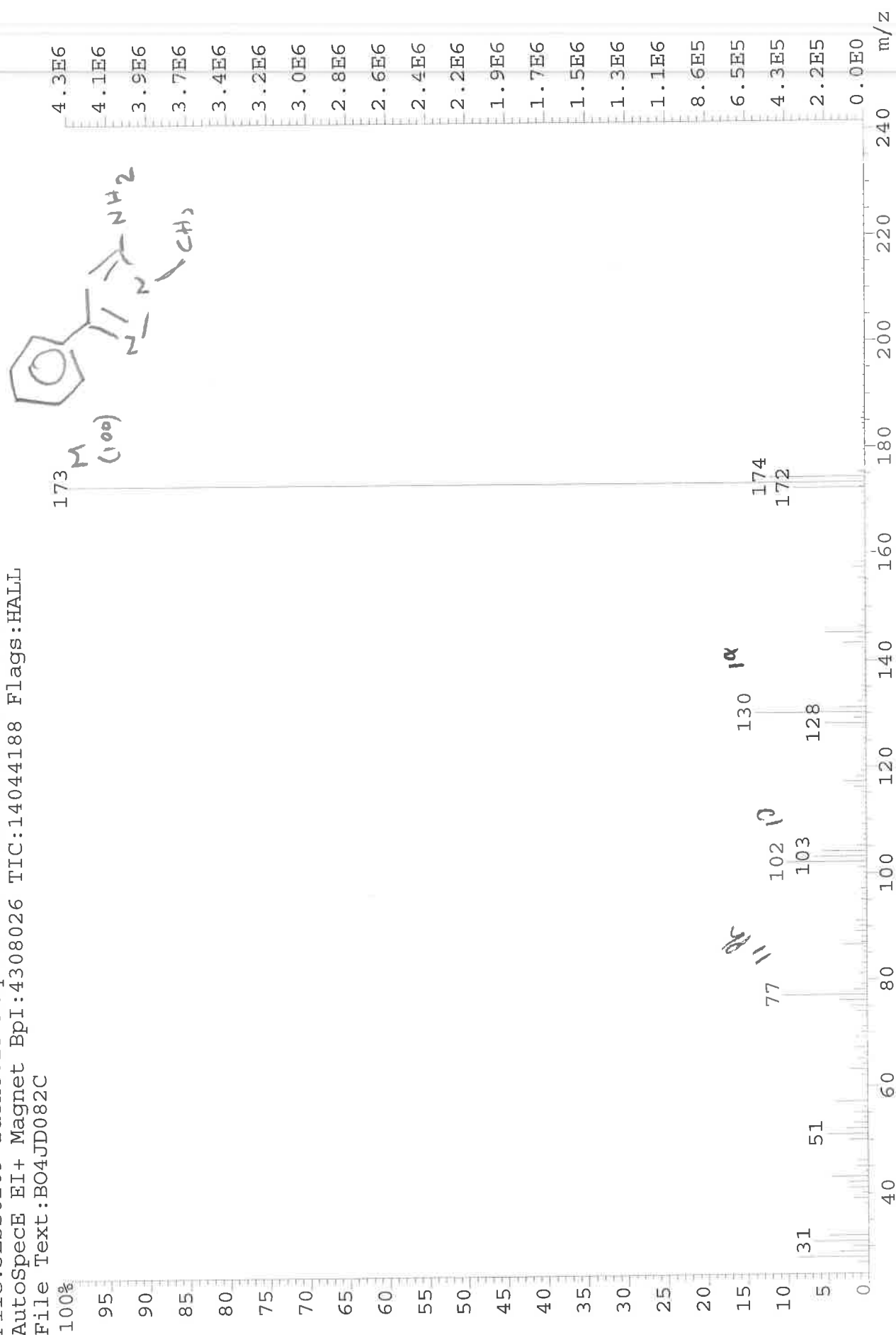
B04JD093B



3425 - N-H str
 3145 - C-H str
 1623 - N-H bend
 1560 - C=N str
 1511 - C-C in ring str
 1453 - C-C in ring
 1377 - C-H str
 1271 - C-N str

249- 070 Sample 070 By Administrator Date Wednesday, November 11 2015

File: JESS6209 Ident: 15 Acq: 21-OCT-2015 11:49:34 +0:59 Cal: CALL
AutoSpecE EI+ Magnet BpI: 4308026 TIC: 14044188 Flags: HALL
File Text: B04JD082C



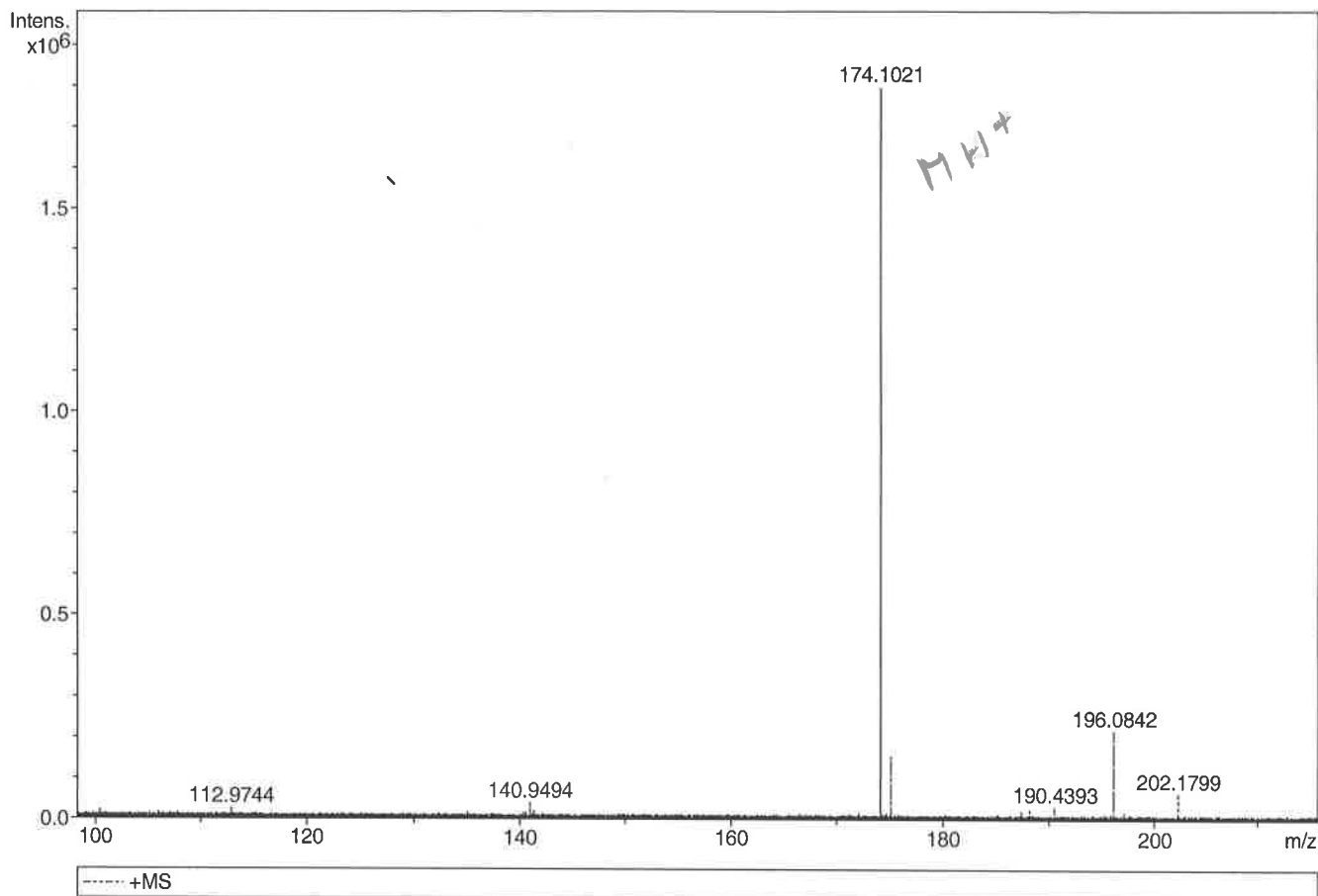
Generic Display Report

Analysis Info

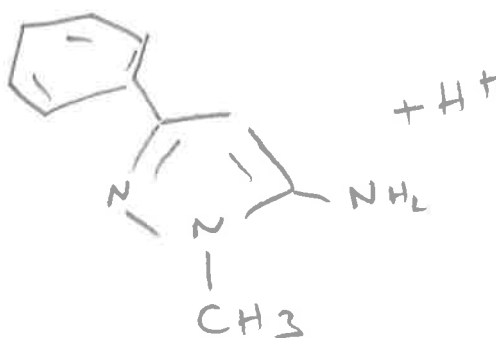
Analysis Name D:\Data\Alinanopos\JESS6209_000001.d
Method pos20090608esi
Sample Name POS FSI B04JD082G
Comment

Acquisition Date 21/10/2015 09:58:56

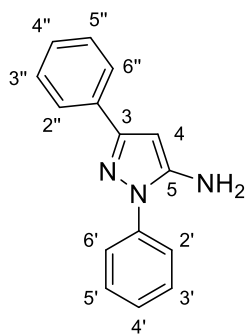
Operator Administrator
Instrument apex-III



Sum Formula	Sigma	m/z	Err [ppm]	Mean Err [ppm]	Err [mDa]	rdb	N Rule	e ⁻
C 10 H 12 N 3	0.027	174.1026	2.85	1.64	0.29	6.50	ok	even



1,3-Diphenyl-1*H*-pyrazol-5-amine (232)



¹H NMR spectrum (500 MHz, DMSO-*d*₆) for 1,3-diphenyl-1*H*-pyrazol-5-amine

B04JD085_F1 DMSO.esp

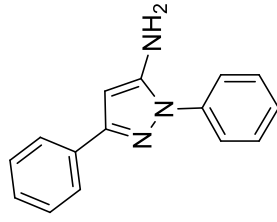
M05(t)

M06(t)

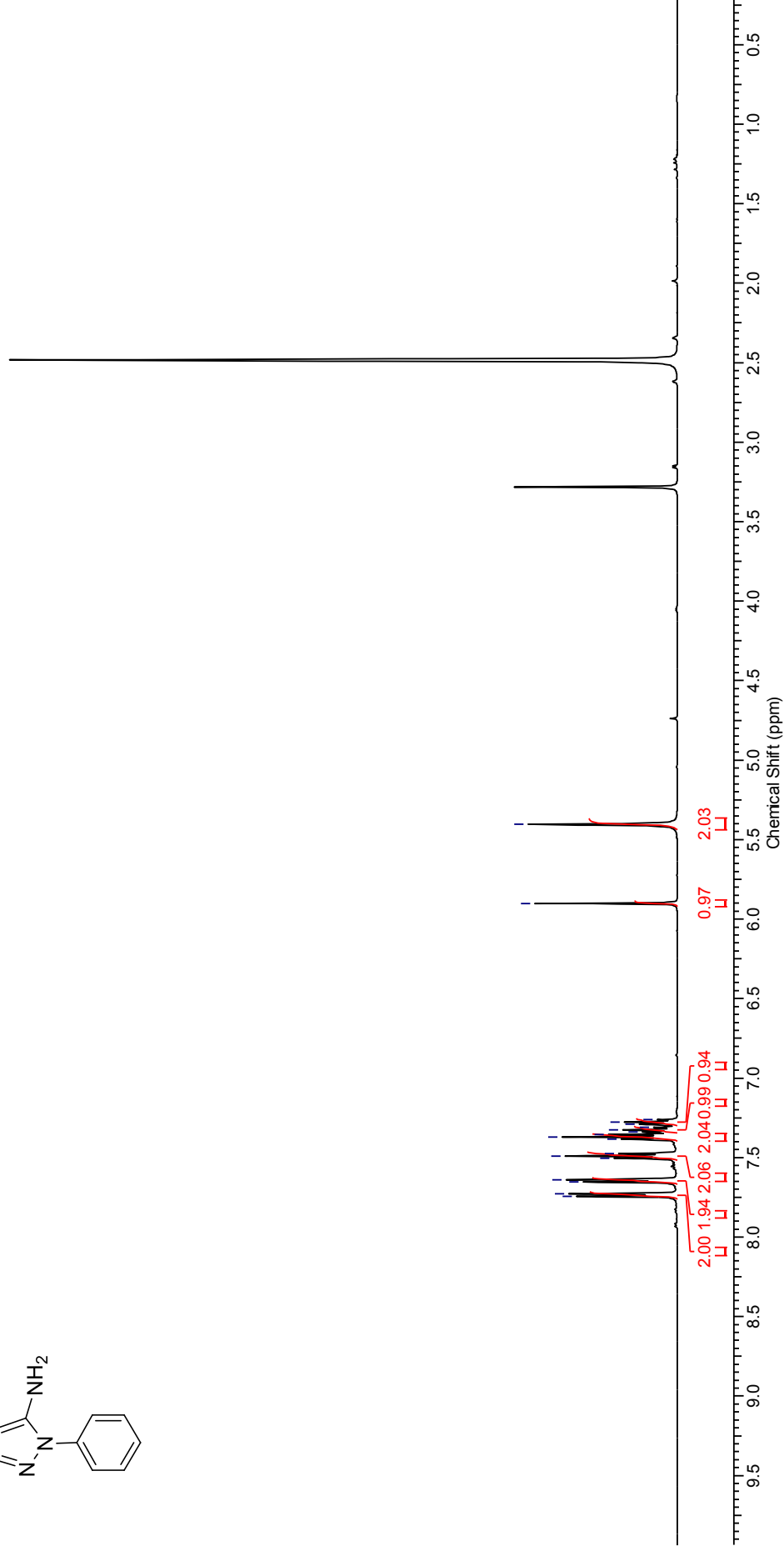
M03(d) M07(m)

M04(d) M08(m)

M01(s) M02(s)

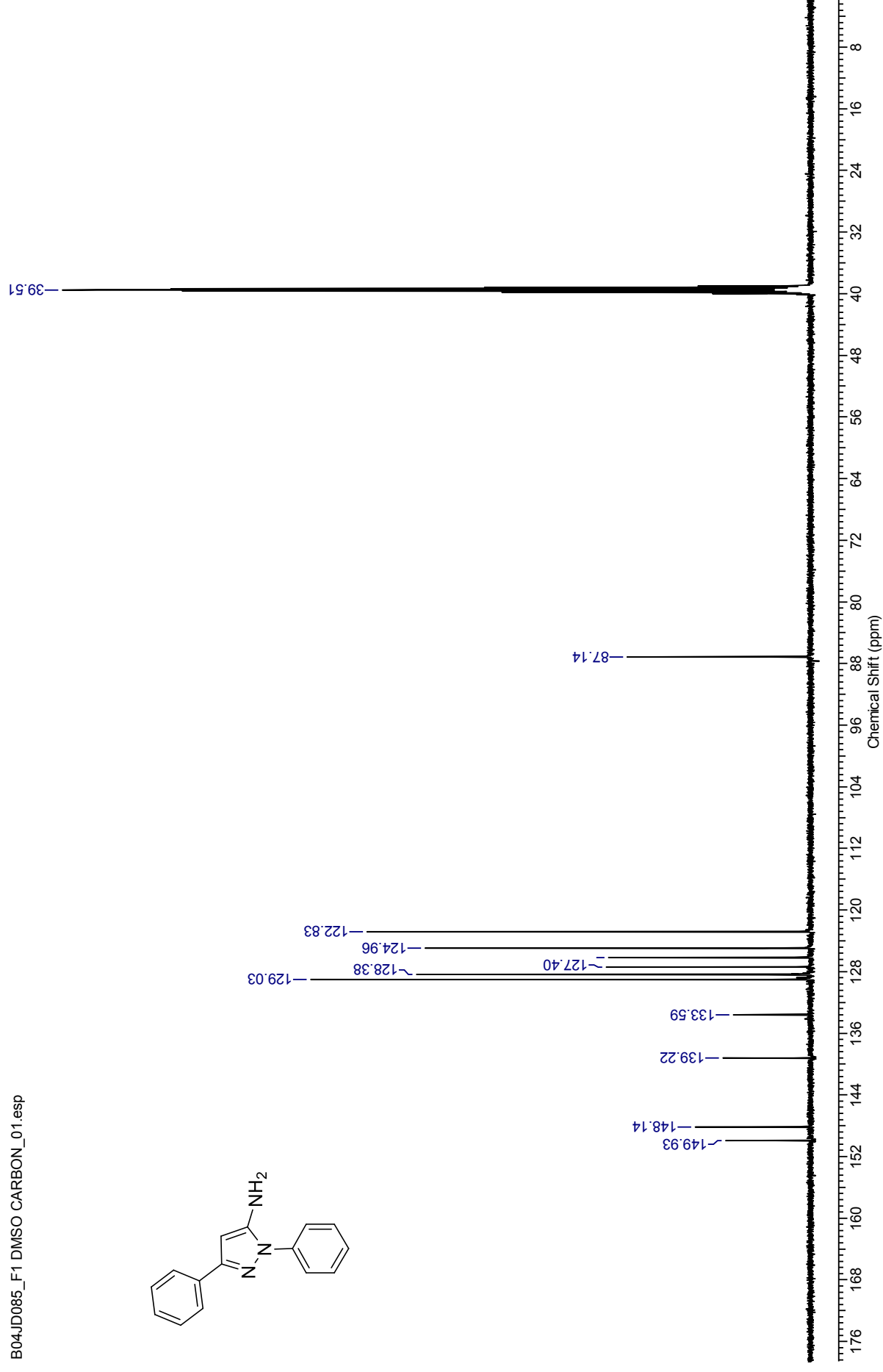
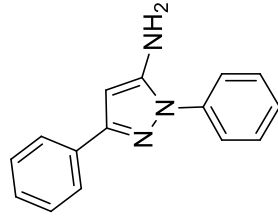


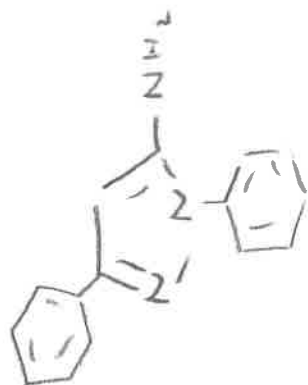
7.74
7.73
7.65
7.64
7.51
7.49
7.47
7.38
7.37
7.36
7.33



¹³C NMR spectrum (126 MHz, DMSO-*d*₆) for 1,3-diphenyl-1*H*-pyrazol-5-amine

B04JD085_F1 DMSO CARBON_01.esp

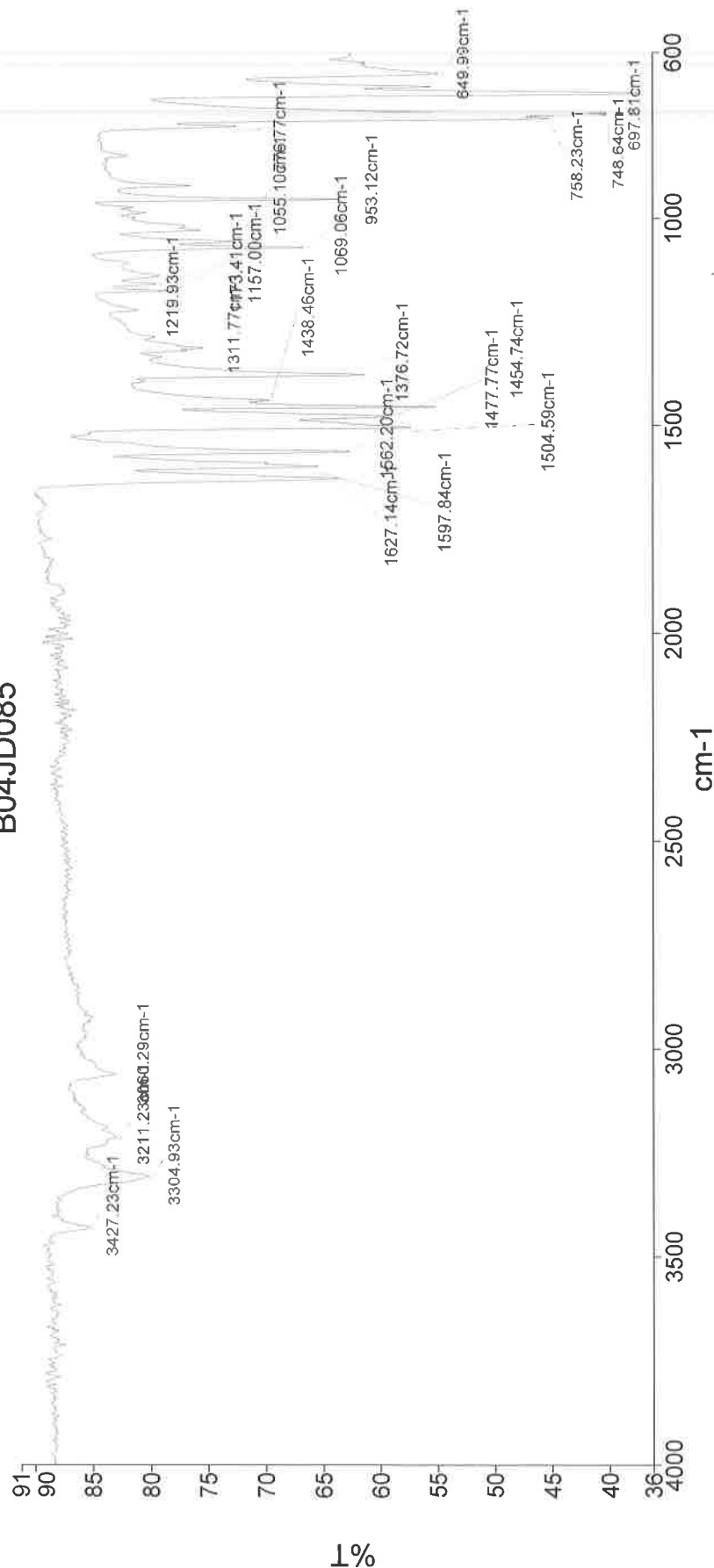




PerkinElmer Spectrum Version 10.03.06
11 November 2015 13:45

Analyst
Date
Administrator
11 November 2015 13:45

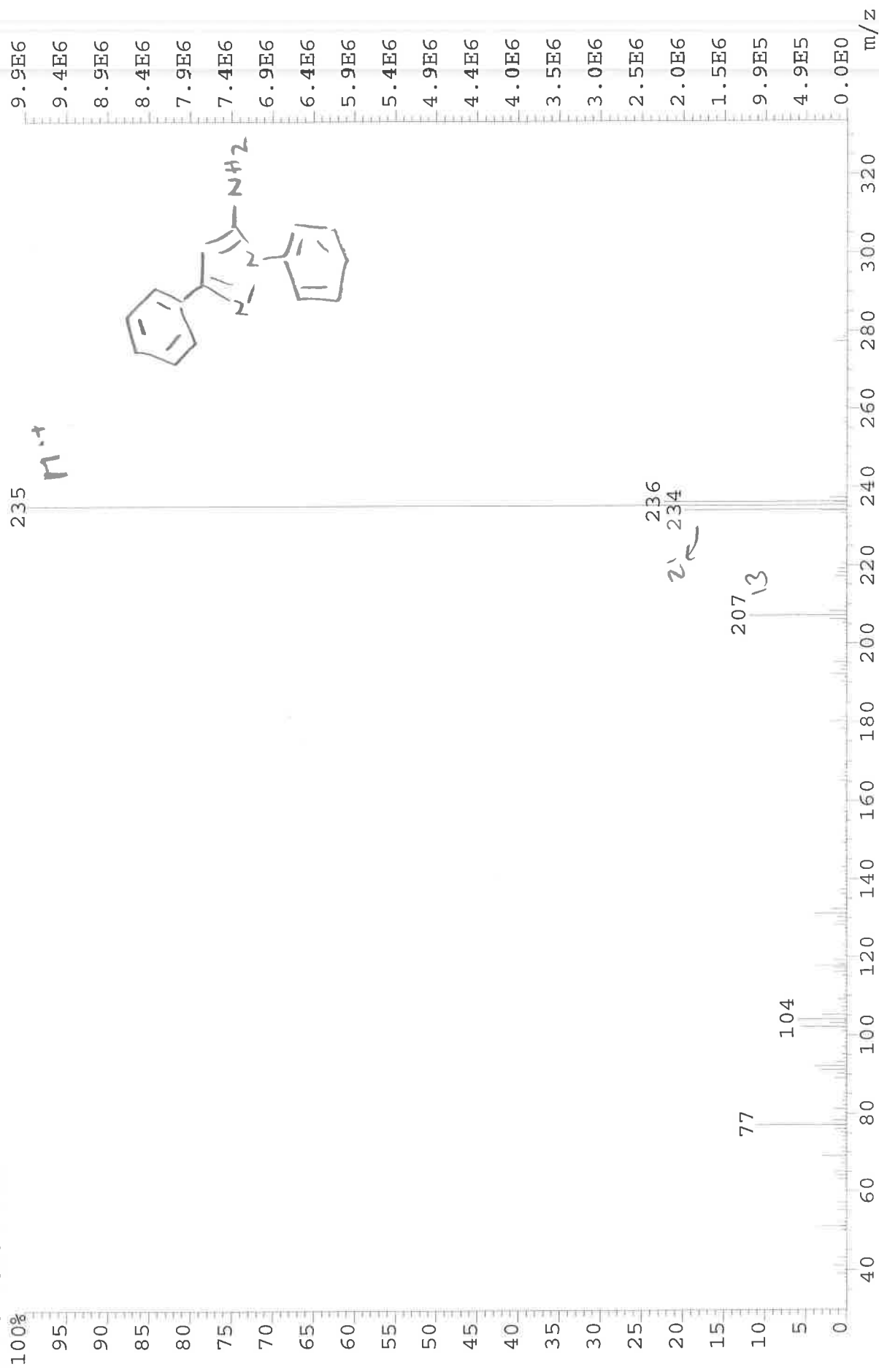
B04JD085



3427 - N-H str
3305
1627 - N-H bend
1598 - C-N str
1505 - C-C in ring
1455 - C-C in ring
1377 - C-N str
1069 - C-N str

249-071 Sample 071 By Administrator Date Wednesday, November 11 2015

File: JESS6235 Ident: 15 Acq: 26-OCT-2015 16:49:12 +0:59 Cal: CAL1
AutoSpecE EI+ Magnet BpI: 9881287 TIC: 30768424 Flags: HALL
File Text: B04JD085



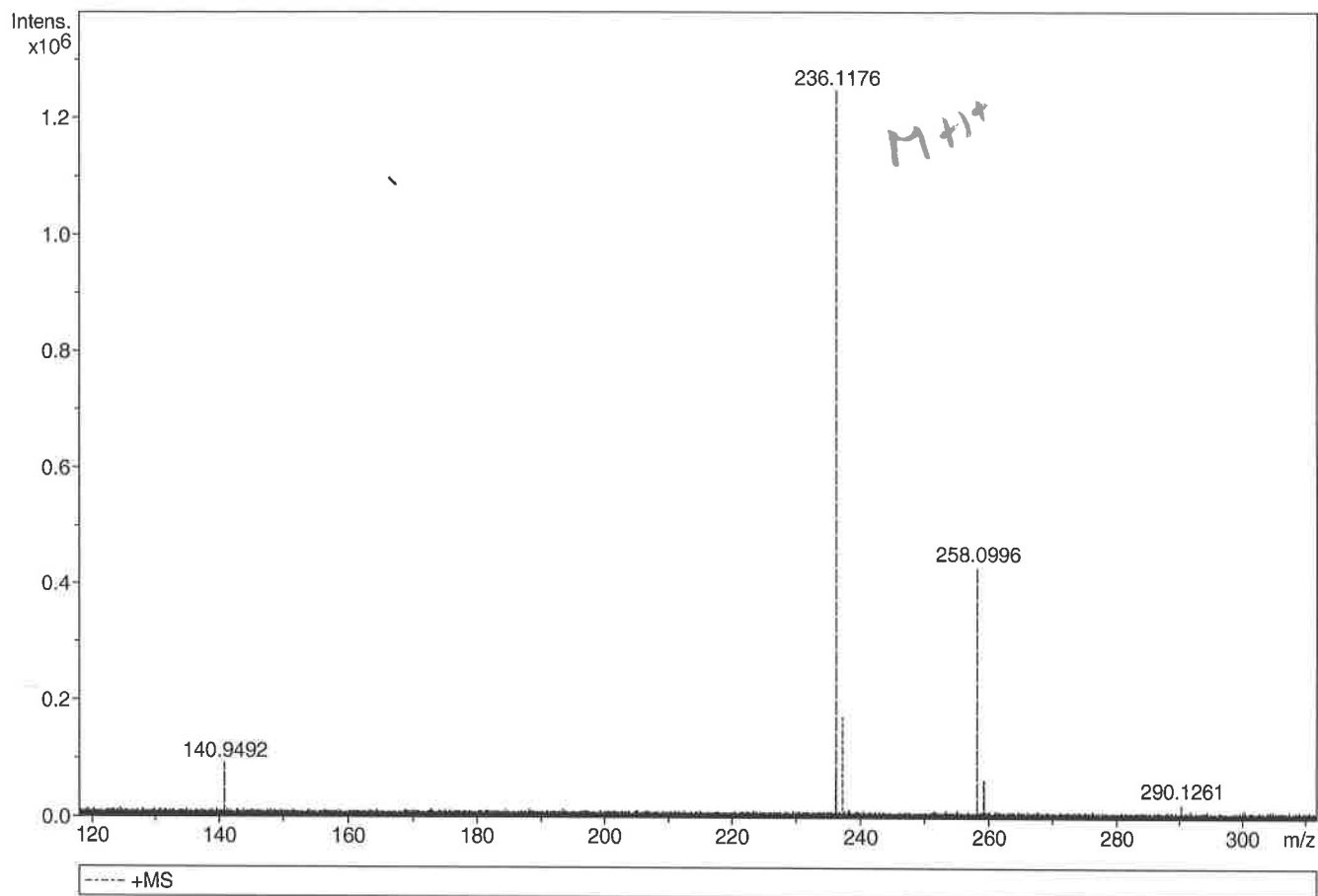
Generic Display Report

Analysis Info

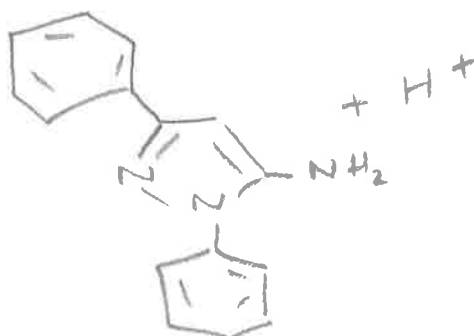
Analysis Name D:\Data\Alinanopos\JESS6235_000001.d
Method pos20090608esi
Sample Name POS ESI B04D085
Comment

Acquisition Date 26/10/2015 15:58:50

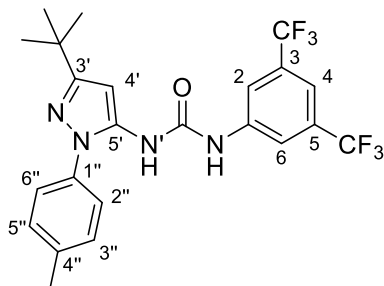
Operator Administrator
Instrument apex-III



Sum	Formula	Sigma	m/z	Err [ppm]	Mean Err [ppm]	Err [mDa]	rdB	N Rule	e ⁻
C 15 H 14 N 3		0.027	236.1182	2.53	0.86	0.20	10.50	ok	even

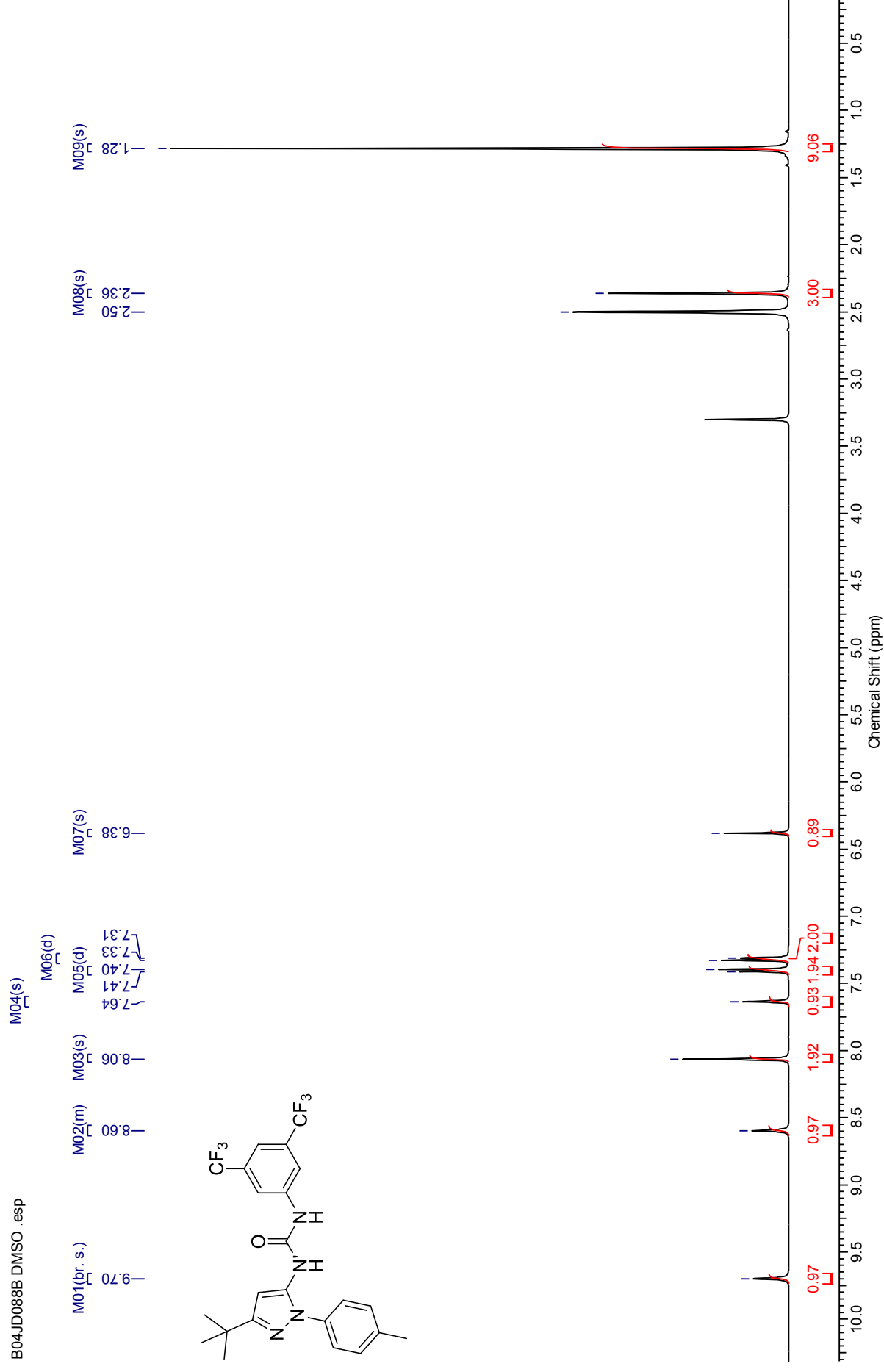


***N*-(3,5-Bis(trifluoromethyl)phenyl)-*N'*-(3-(*tert*-butyl)-1-(*p*-tolyl)-1*H*-pyrazol-5-yl)urea (217F)**



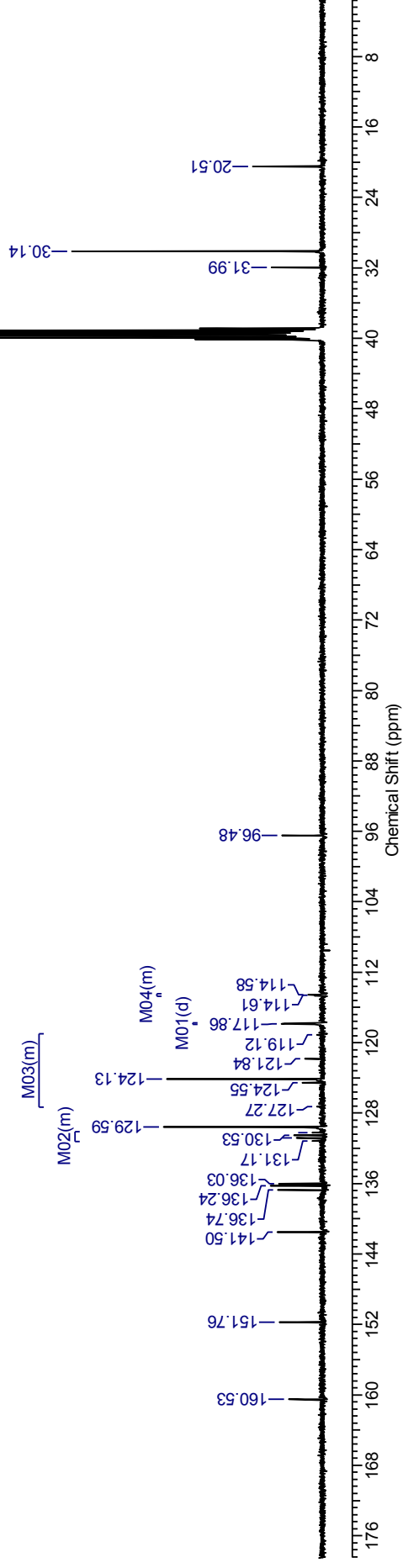
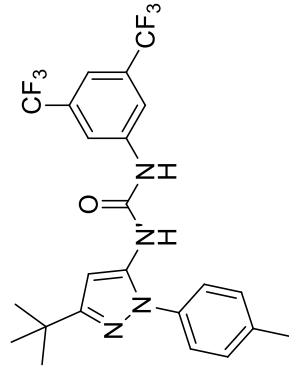
¹H NMR spectrum (500 MHz, DMSO-*d*₆) for *N*-(3,5-bis(trifluoromethyl)phenyl)-*N'*-(3-(*tert*-butyl)-1-*H*-pyrazol-5-yl)urea

B04JD088B DMSO .esp



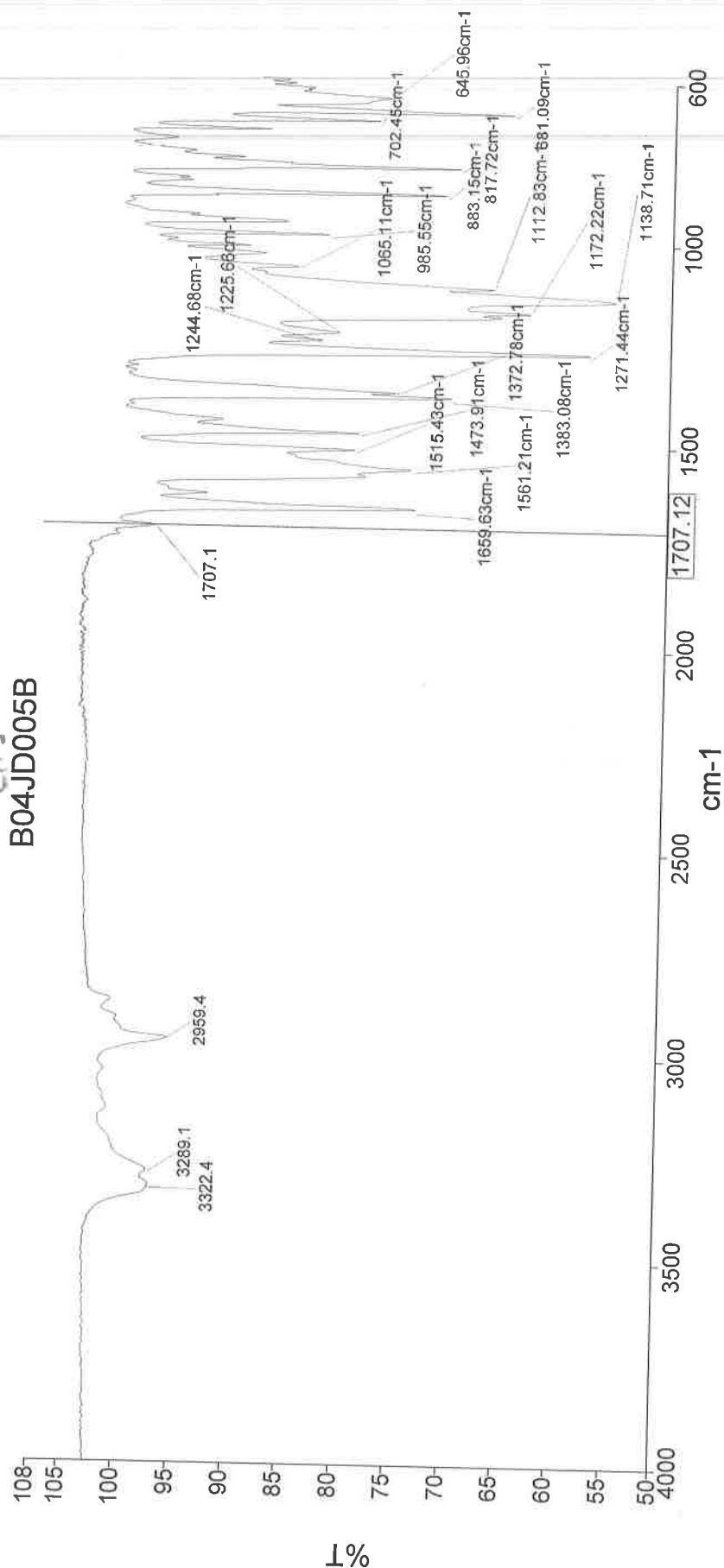
¹³C NMR spectrum (100 MHz, DMSO-*d*₆) for *N*-(3,5-bis(trifluoromethyl)phenyl)-*N'*-(3-(*tert*-butyl)-1-(*p*-tolyl)-1*H*-pyrazol-5-yl)urea

B04JD088B Carbon.esp



Analyst
Date
Administrator
28 May 2015 15:00

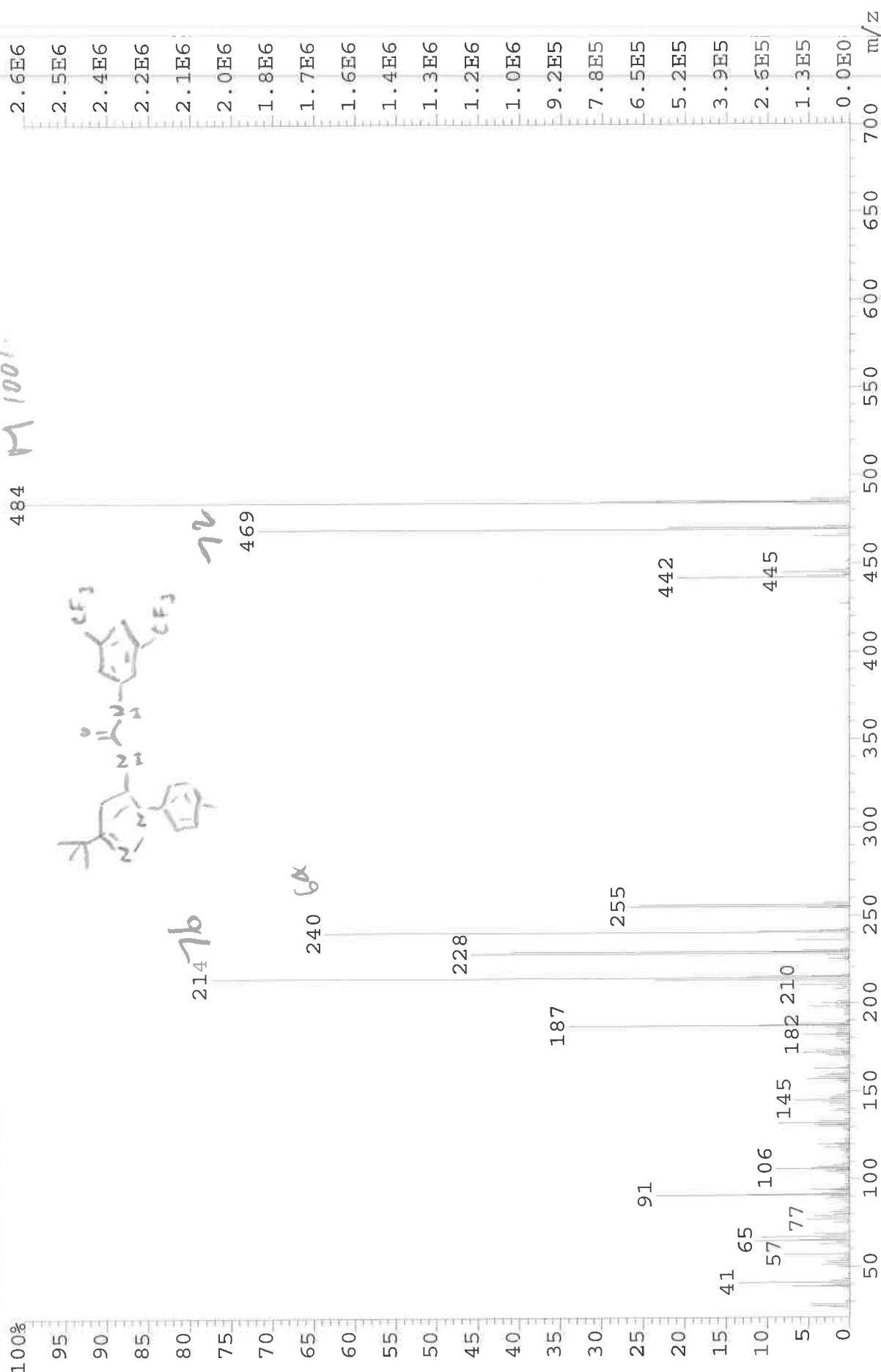
B04JD005B



Administrator 27 97.61 %T Sample 027 By Administrator Date Thursday, May 28 2015

3322 N-H str.
2959 C-H str.
1660 C=O str.
1561 N-H bend.
1383 C-H
1271 C-N str.
1172 C-O
1139 C-F str.
817 C-O bend

File: JESS4997A Ident: 50 Acq: 21-APR-2015 12:46:26 +2:24 Cal: LO
AutoSpecE EI+ Magnet BpI: 2617104 TIC: 34109576 Flags: HALL
File Text: B04JD005C



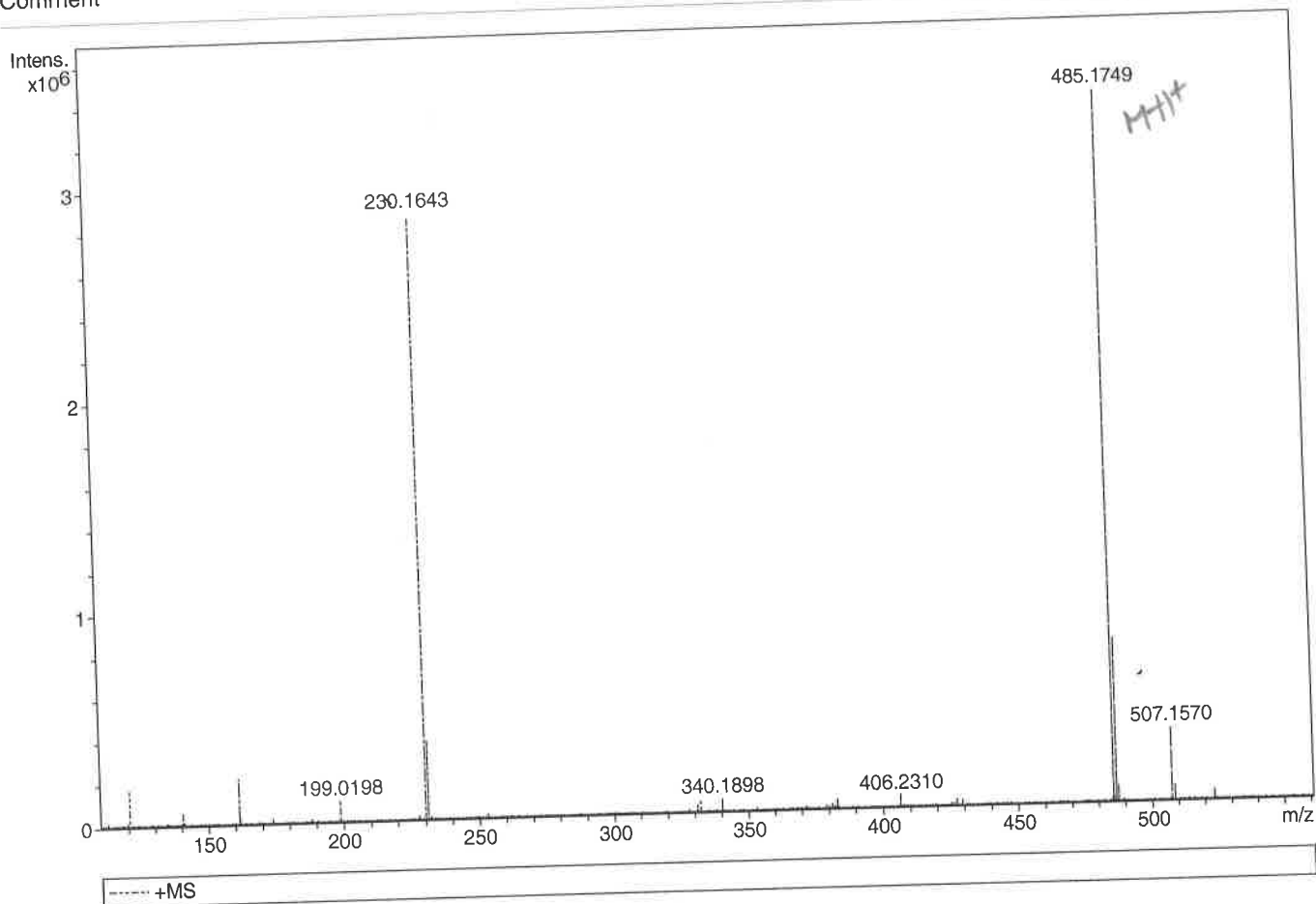
Generic Display Report

Analysis Info

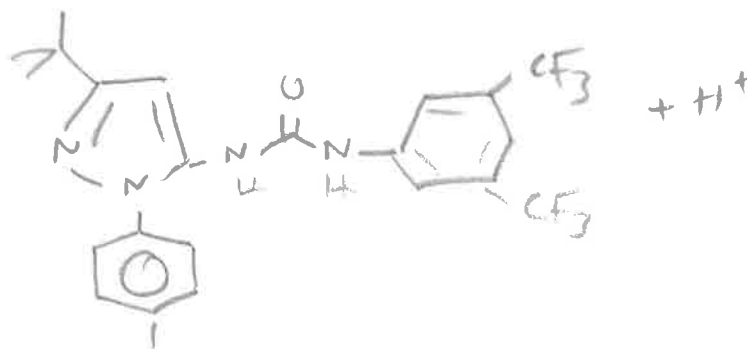
Analysis Name D:\Data\Alinanopos\JESS4997_000001.d
 Method pos20090608esi
 Sample Name POS ESI BO4JD00SC
 Comment

Acquisition Date 21/04/2015 09:54:11

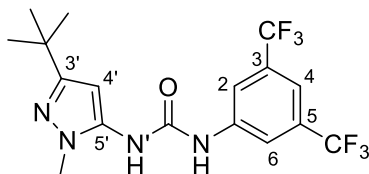
Operator Administrator
 Instrument apex-III



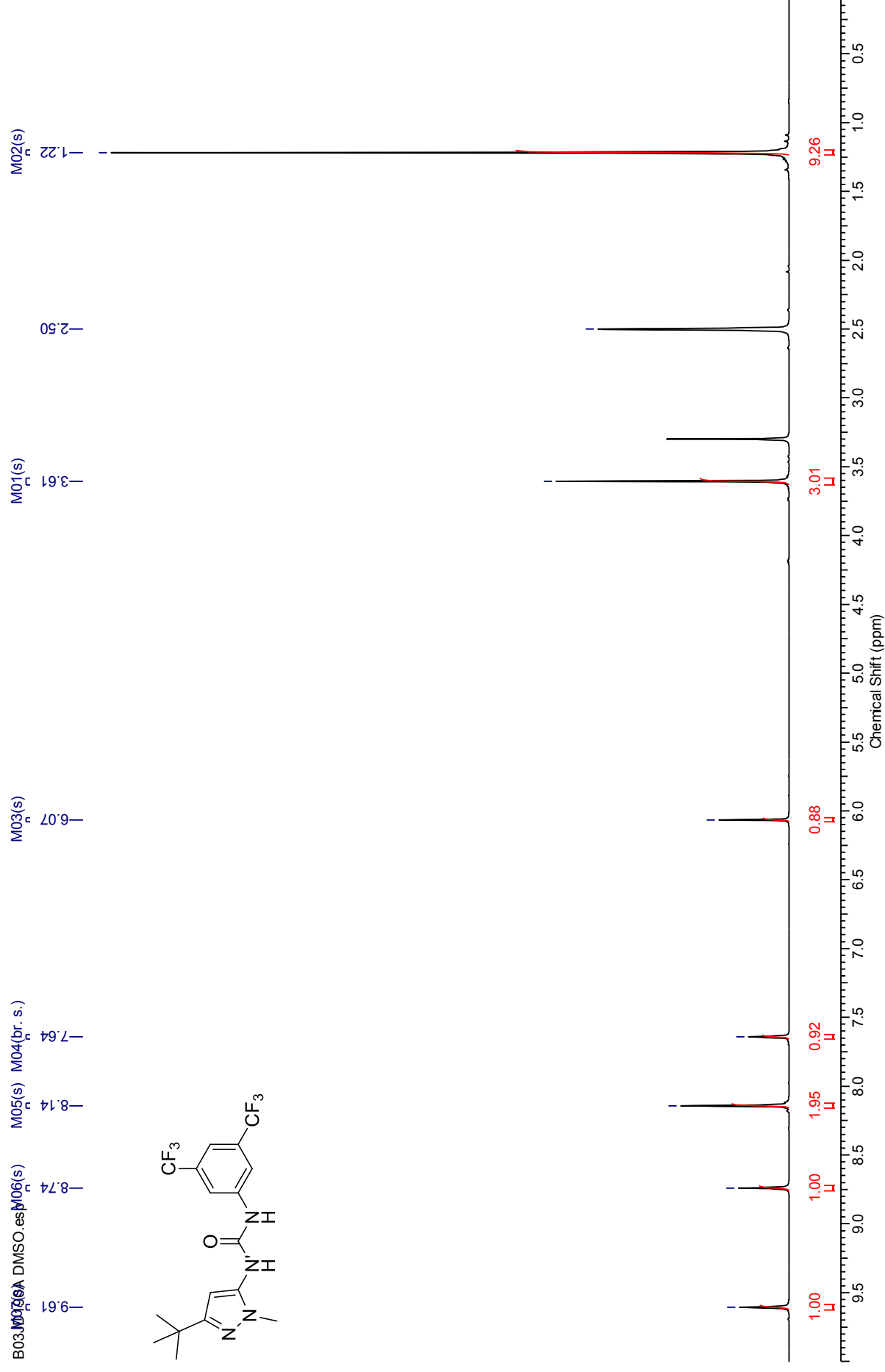
Sum Formula	Sigma	m/z	Err [ppm]	Mean Err [ppm]	Err [mDa]	rdB	N Rule	e ⁻
C ₂₃ H ₂₃ F ₆ N ₄ O ₁	0.029	485.1771	4.42	3.85	1.87	11.50	ok	even



***N*-(3,5-Bis(trifluoromethyl)phenyl)-*N'*-(3-*tert*-butyl-1-methyl-1*H*-pyrazol-5-yl)urea (226F)**

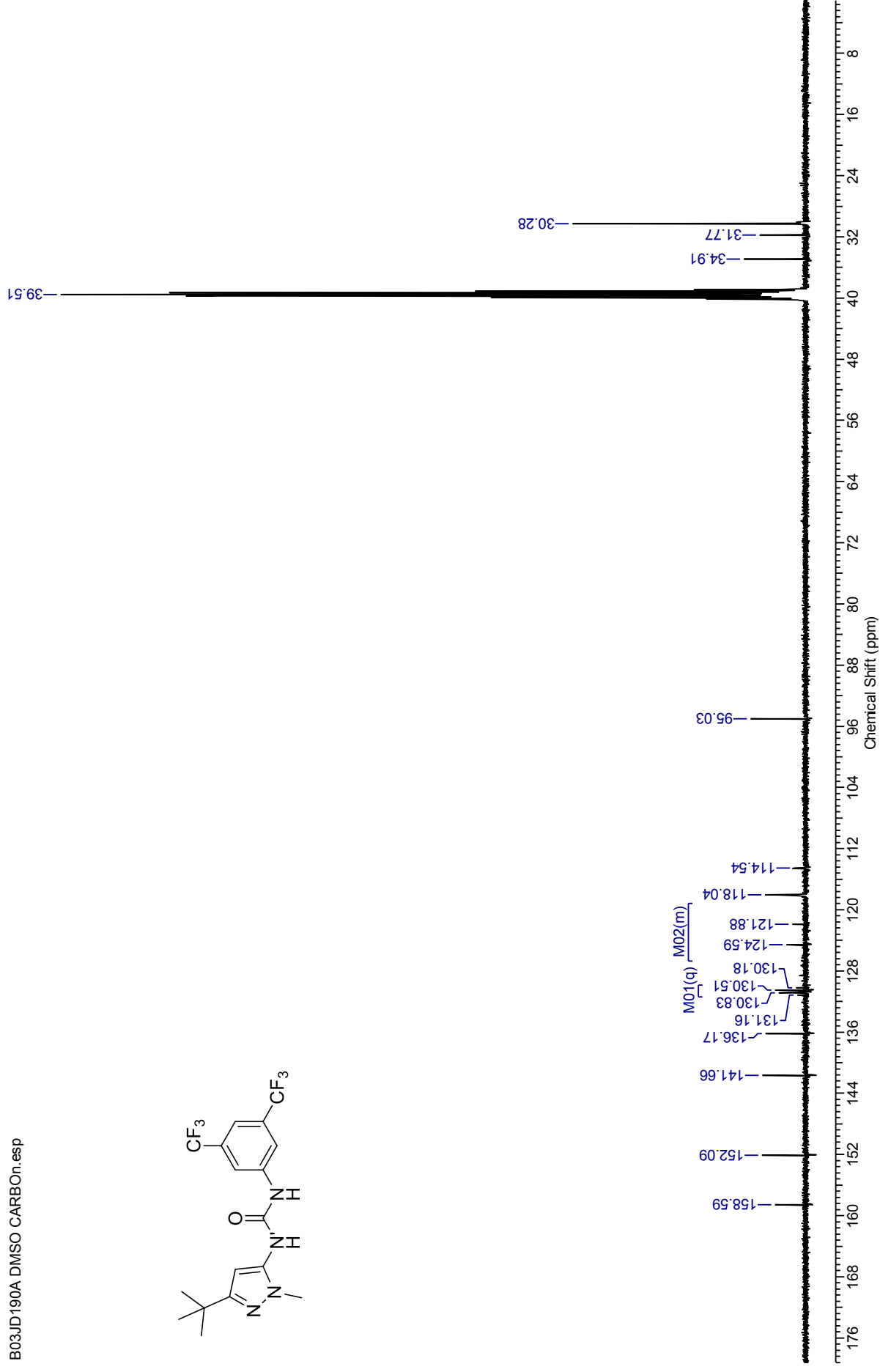
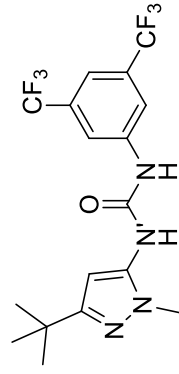


¹H NMR spectrum (500 MHz, DMSO-*d*₆) for *N*-(3,5-bis(trifluoromethyl)phenyl)-*N'*-(3-*tert*-butyl-1-methyl-1*H*-pyrazol-5-yl)urea



¹³C NMR spectrum (100 MHz, DMSO-*d*₆) for *N*-(3,5-bis(trifluoromethyl)phenyl)-*N'*-(3-*tert*-butyl-1-*H*-pyrazol-5-yl)urea

B03JD190A DMSO CARBOn.esp

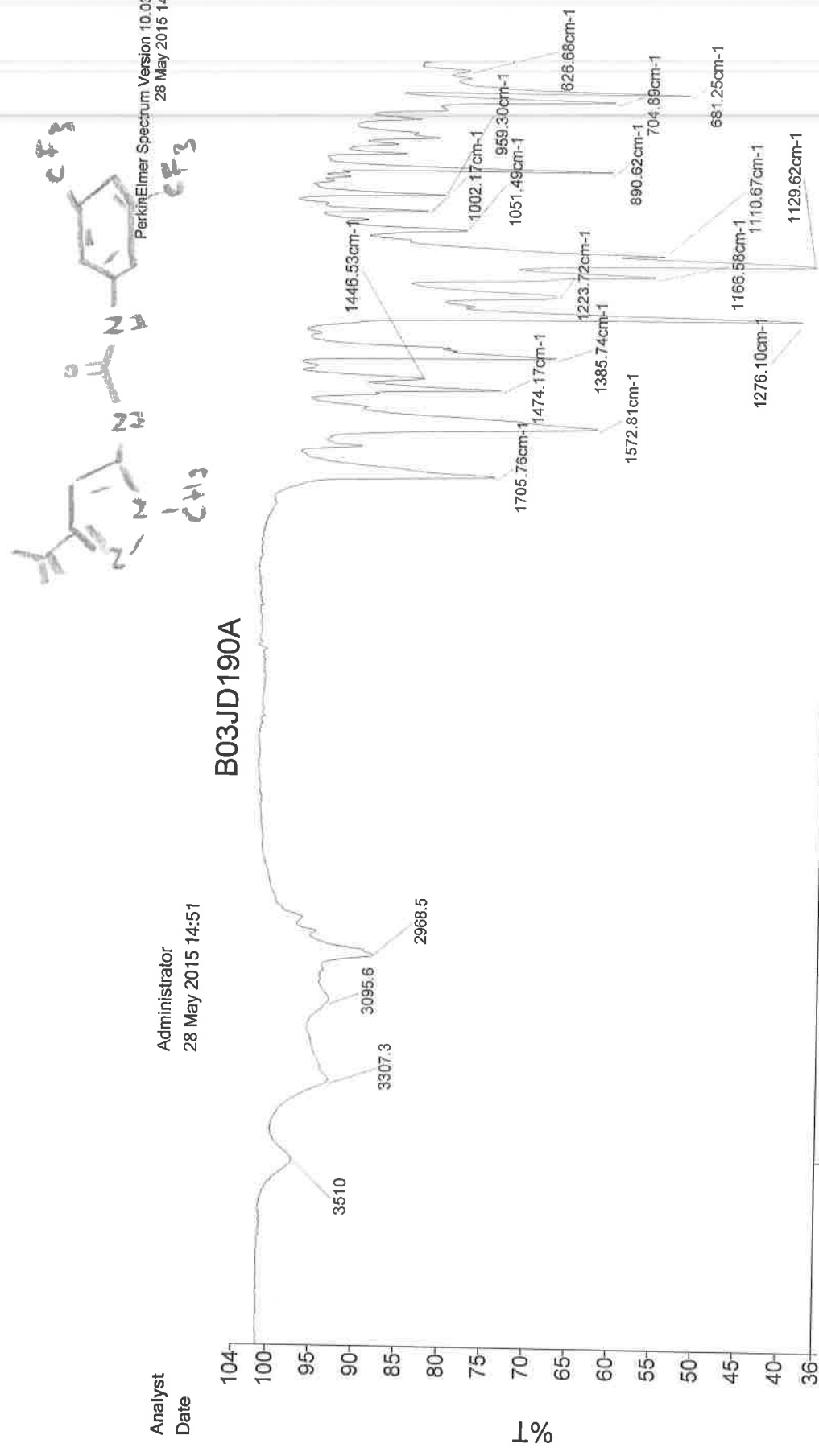


Analyst
Date

Administrator
28 May 2015 14:51

PerkinElmer Spectrum Version 10.03.06
28 May 2015 14:51

B03JD190A



- 3307 N-H str.
- 2968 C-H str.
- 1706 C=O str.
- 1573 N-H bend
- 1474 C-H
- 1386 C-H
- 1276 C-N str.
- 1166 C-O
- 1130 C-F str.

Administrator 24 Sample 024 By Administrator Date Thursday, May 28 2015

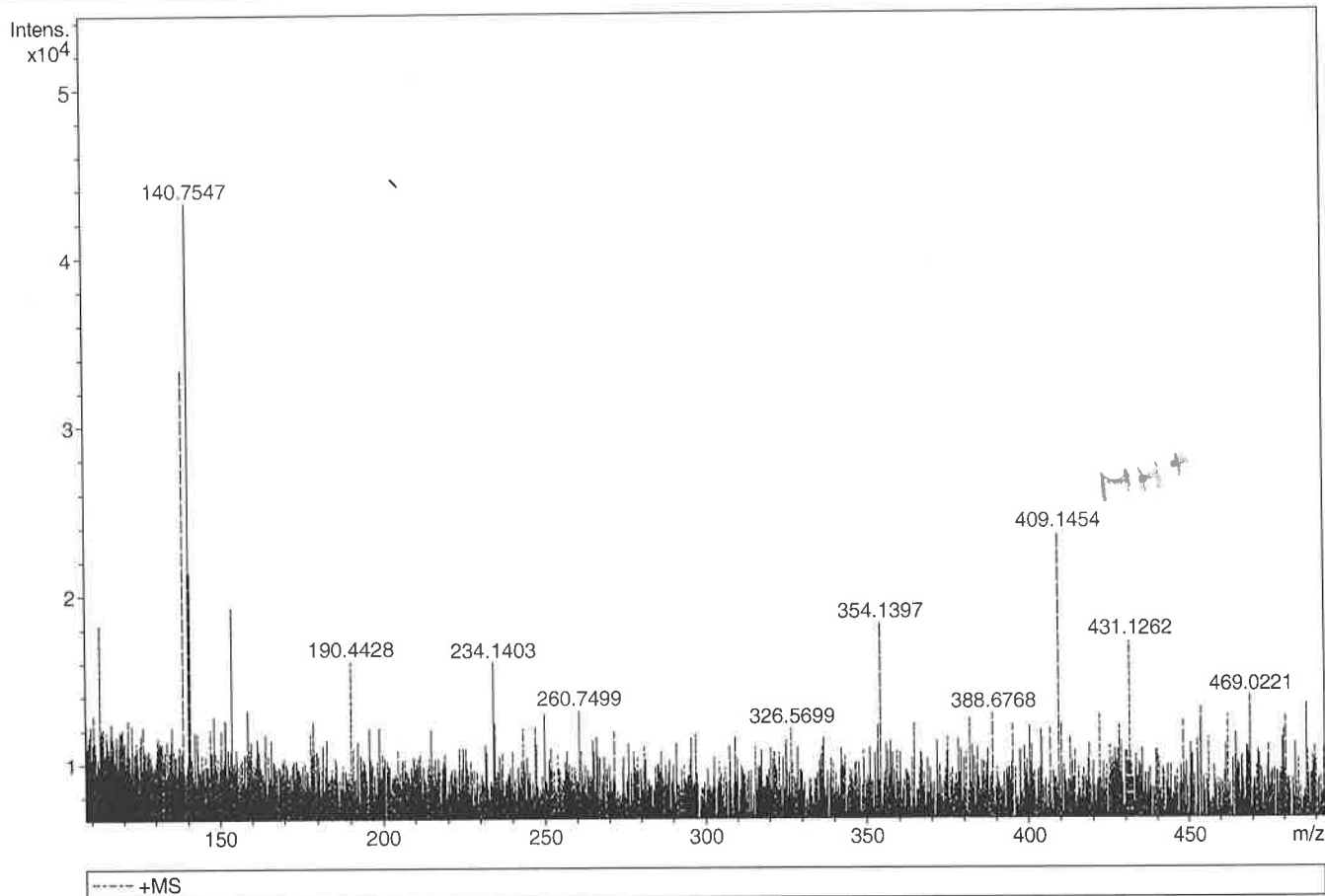
Generic Display Report

Analysis Info

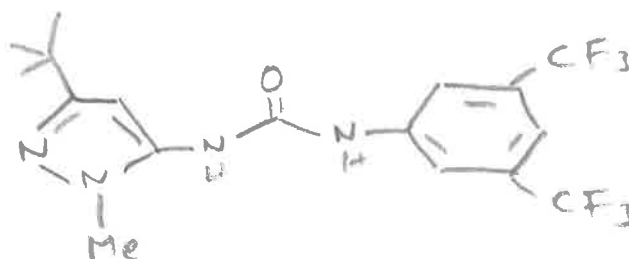
Analysis Name D:\Data\Alinanopos\JESS4934_000002.d
 Method pos20090608esi
 Sample Name POS ESI BO3JD190A
 Comment

Acquisition Date 23/03/2015 13:32:13

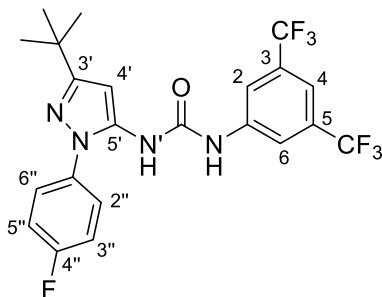
Operator Administrator
 Instrument apex-III



Sum Formula	Sigma	m/z	Err [ppm]	Mean Err [ppm]	Err [mDa]	rdB	N Rule	e ⁻
C 17 H 19 F 6 N 4 O 1	0.117	409.1458	0.83	0.83	0.34	7.50	ok	even



***N*-(3,5-Bis(trifluoromethyl)phenyl)-*N'*-(3-*tert*-butyl-1-(4-fluorophenyl)-1*H*-pyrazol-5-yl)urea (227F)**



¹H NMR spectrum (500 MHz, DMSO-*d*₆) for *N*-(3,5-bis(trifluoromethyl)phenyl)-*N'*-(3-*tert*-butyl-1-(4-fluorophenyl)-1*H*-pyrazol-5-yl)urea

B04JD001A DMSO.esp

M07(dd,7,11)

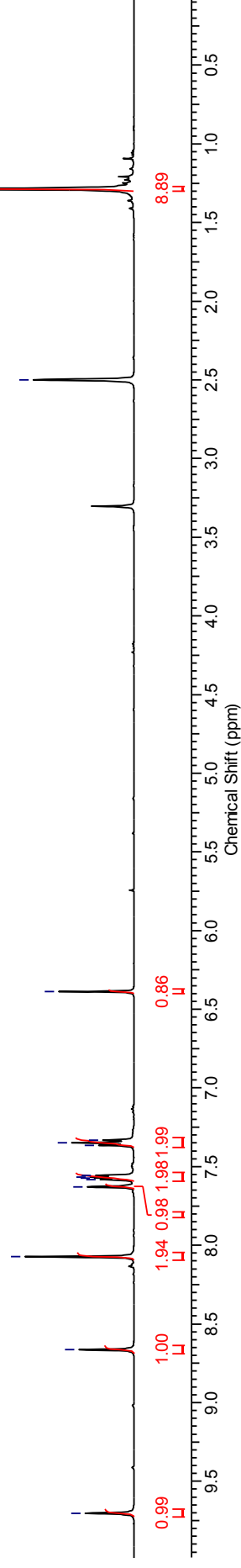
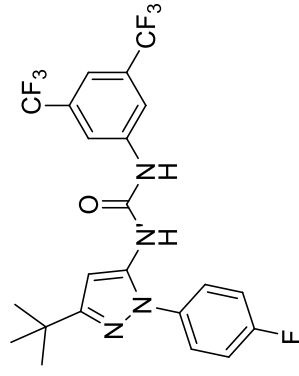
M04(s,26,22) M06(t,8,10)

M02(s,20) 9.70
M03(s,14) 8.66
M08(s,24) 7.63
7.58
7.57
7.56
7.37
7.35
7.33

M05(s,4) 6.39

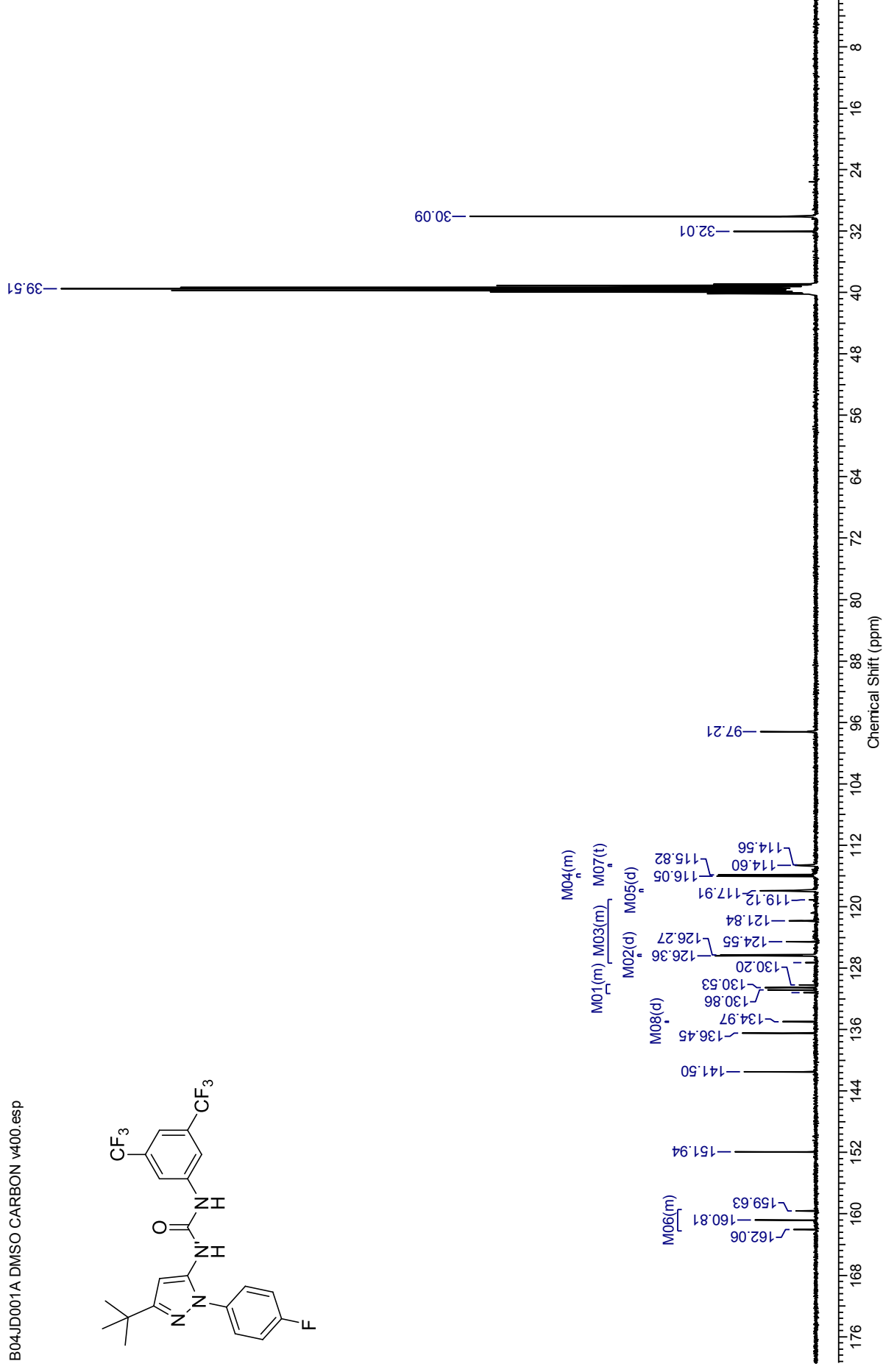
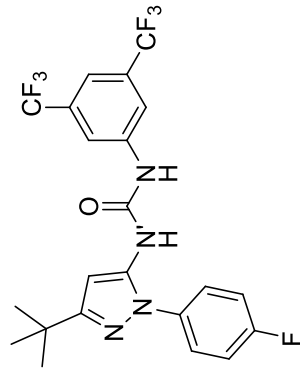
M01(s,18,13,19) 1.29

2.50



¹³C NMR spectrum (100 MHz, DMSO-*d*₆) for *N*-(3,5-Bis(trifluoromethyl)phenyl)-*N'*-(3-*tert*-butyl-1-(4-fluorophenyl)-1*H*-pyrazol-5-yl)urea

B04JD001A DMSO CARBON v400.esp



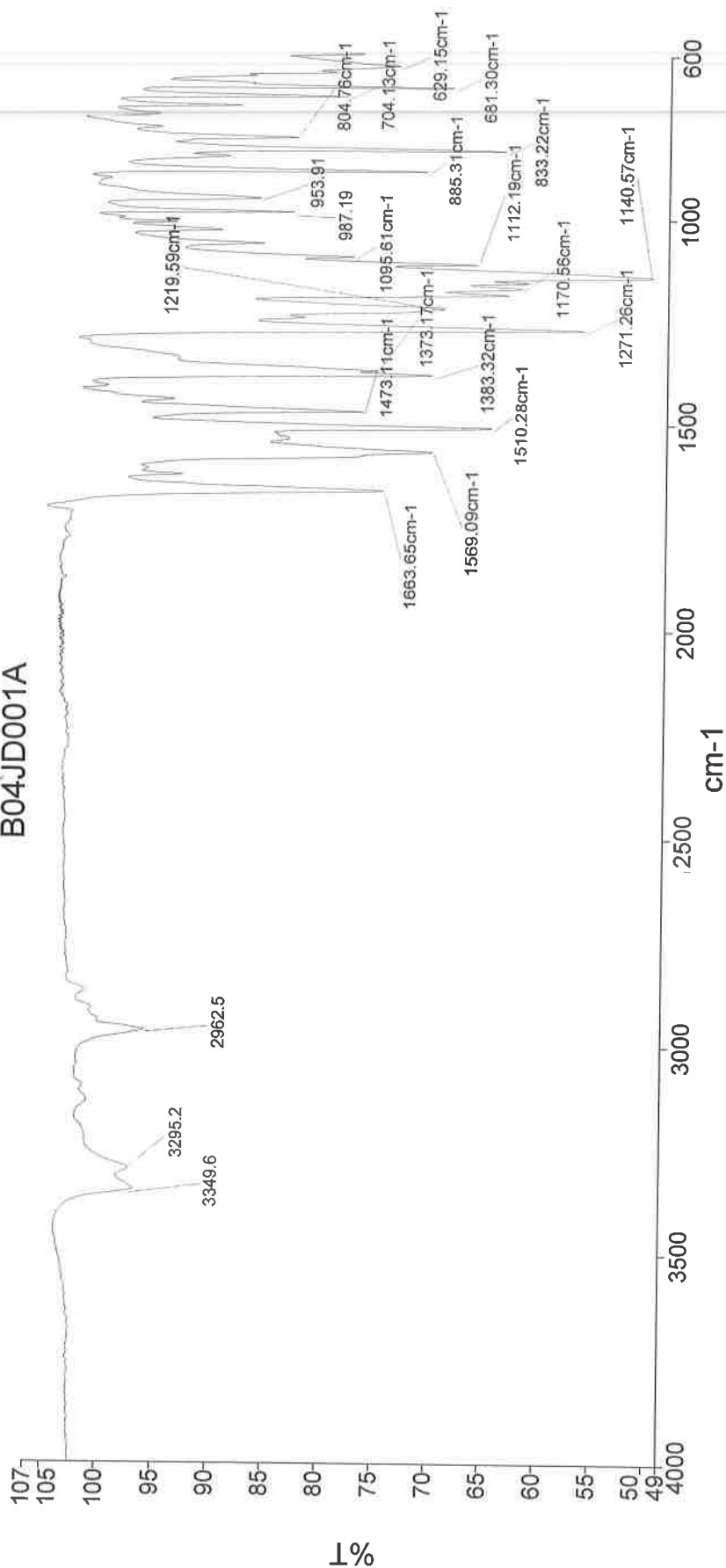


PerkinElmer Spectrum Version 10.03.08
28 May 2015 15:16

Analyst
Date

Administrator
28 May 2015 15:16

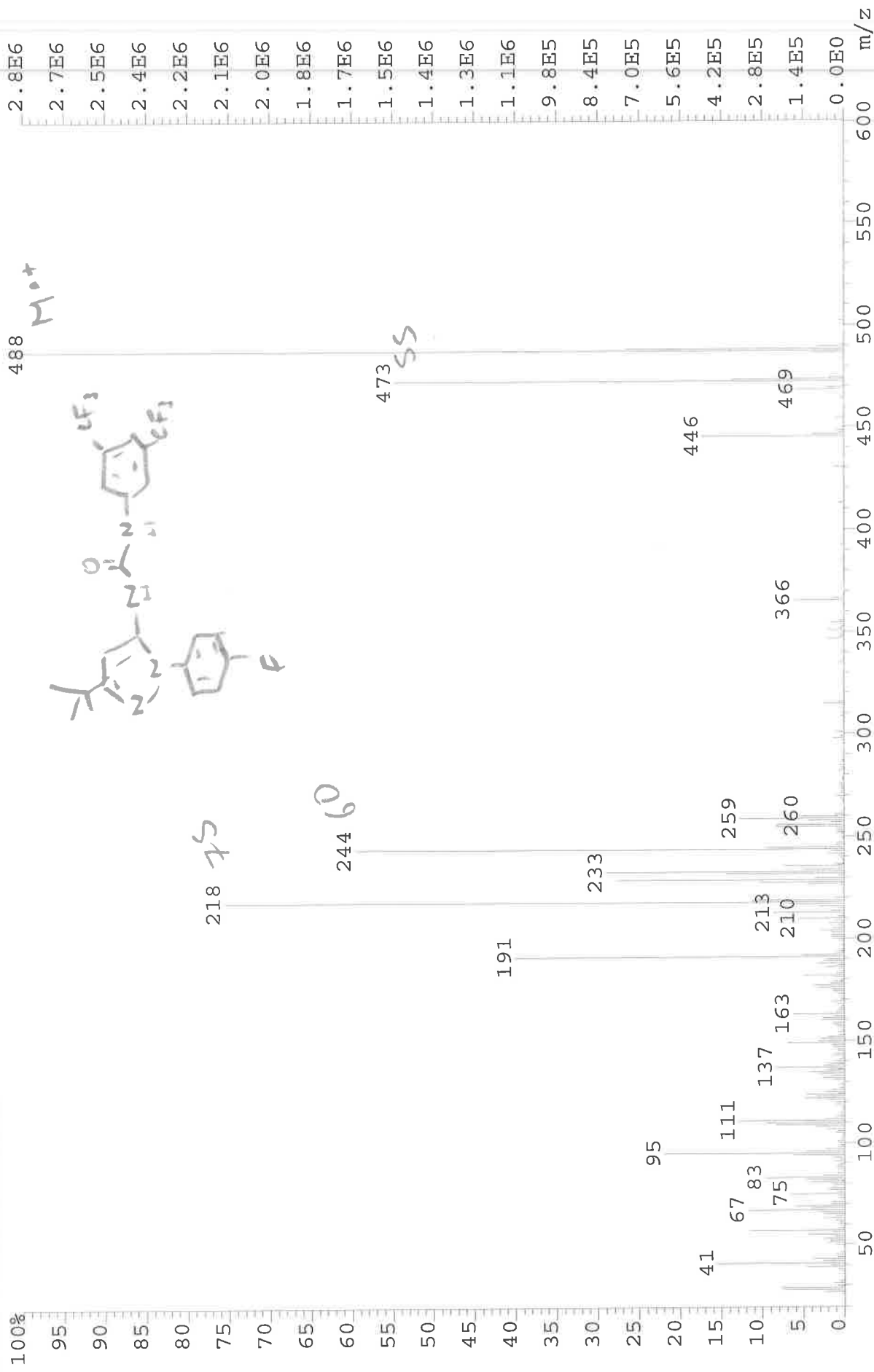
B04JD001A



3350 -N-H
2962 C-H
1664 C=O
1569 N-H
1510 N-H
1383 -C-H
1271 -C-N
1140 -C-F
833 -C-F

Administrator 31 Sample 031 By Administrator Date Thursday, May 28 2015

File: JESS4994 Ident: 38 Acq: 21-APR-2015 12:32:24 +2:23 Cal: CAL1
AutoSpecE EI+ Magnet BpI: 2795958 TIC: 30663172 Flags: HALL
File Text: B04JD001A



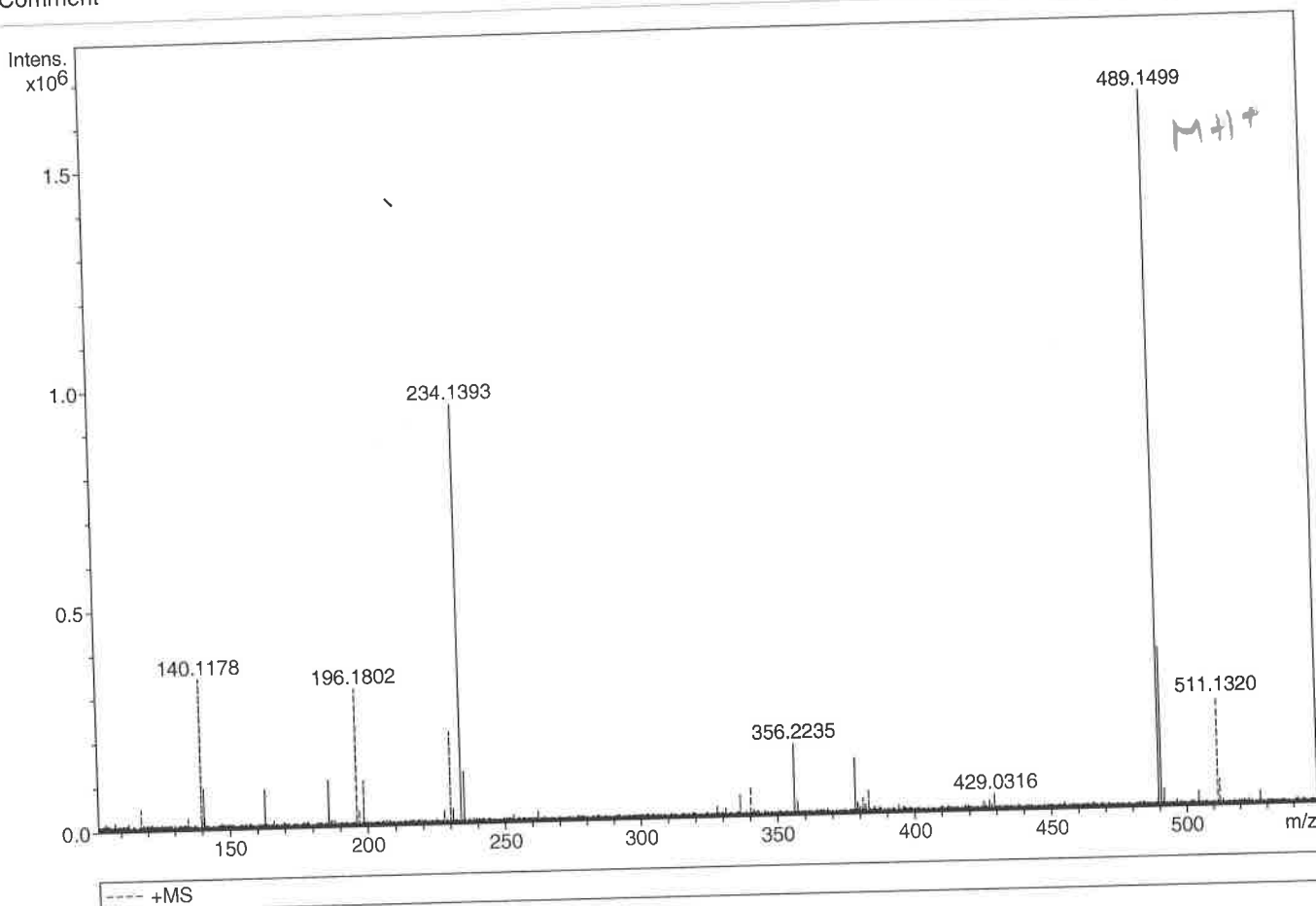
Generic Display Report

Analysis Info

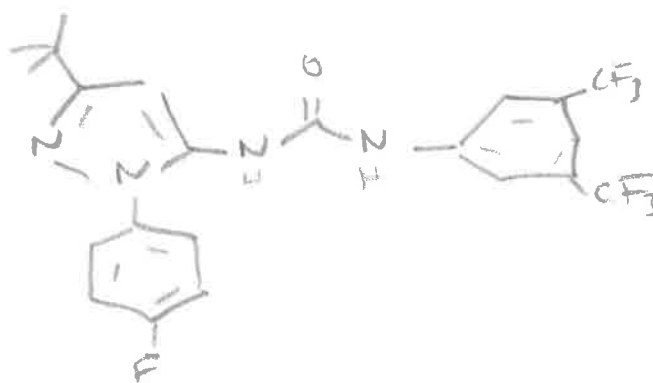
Analysis Name D:\Data\Alinanopos\JESS4994_000001.d
 Method pos20090608esi
 Sample Name POS ESI BO4JD001A
 Comment

Acquisition Date 21/04/2015 10:07:12

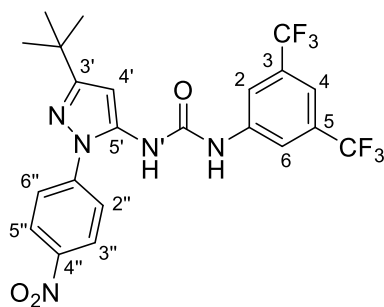
Operator Administrator
 Instrument apex-III



Sum Formula	Sigma	m/z	Err [ppm]	Mean Err [ppm]	Err [mDa]	rdb	N Rule	e ⁻
C ₂₂ H ₂₀ F ₇ N ₄ O ₁	0.036	489.1520	4.32	4.14	2.02	11.50	ok	even

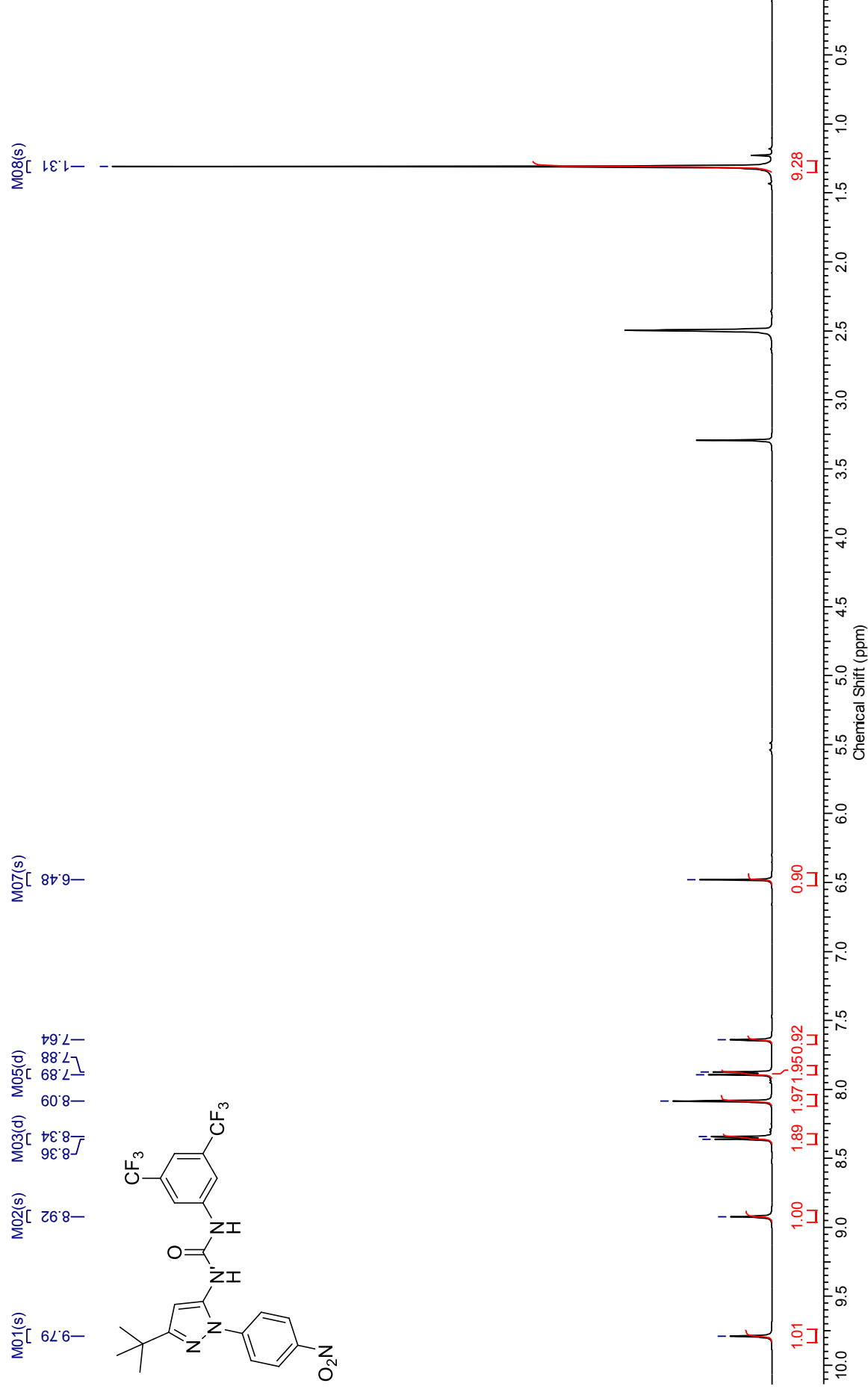


***N*-(3,5-Bis(trifluoromethyl)phenyl)-*N'*-(3-(*tert*-butyl)-1-(4-nitrophenyl)-1*H*-pyrazol-5-yl)urea (228F)**



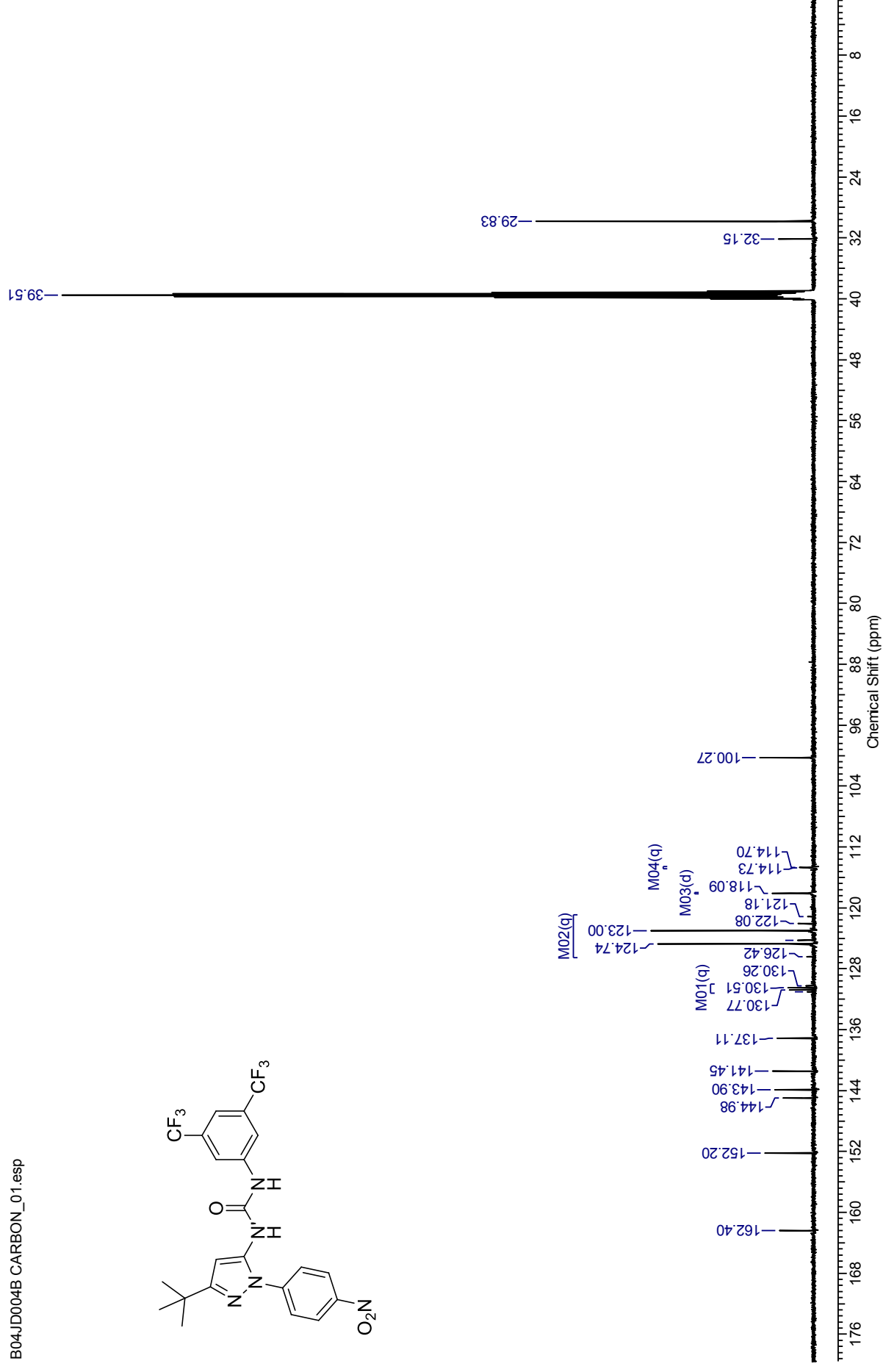
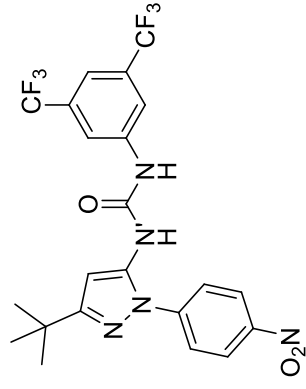
¹H NMR spectrum (500 MHz, DMSO-*d*₆) for *N*-(3,5-Bis(trifluoromethyl)phenyl)-*N'*-(3-(*tert*-butyl)-1-(4-nitrophenyl)-1*H*-pyrazol-5-yl)urea

B04JD004B proton for carbonDMSO-*d*₆ est



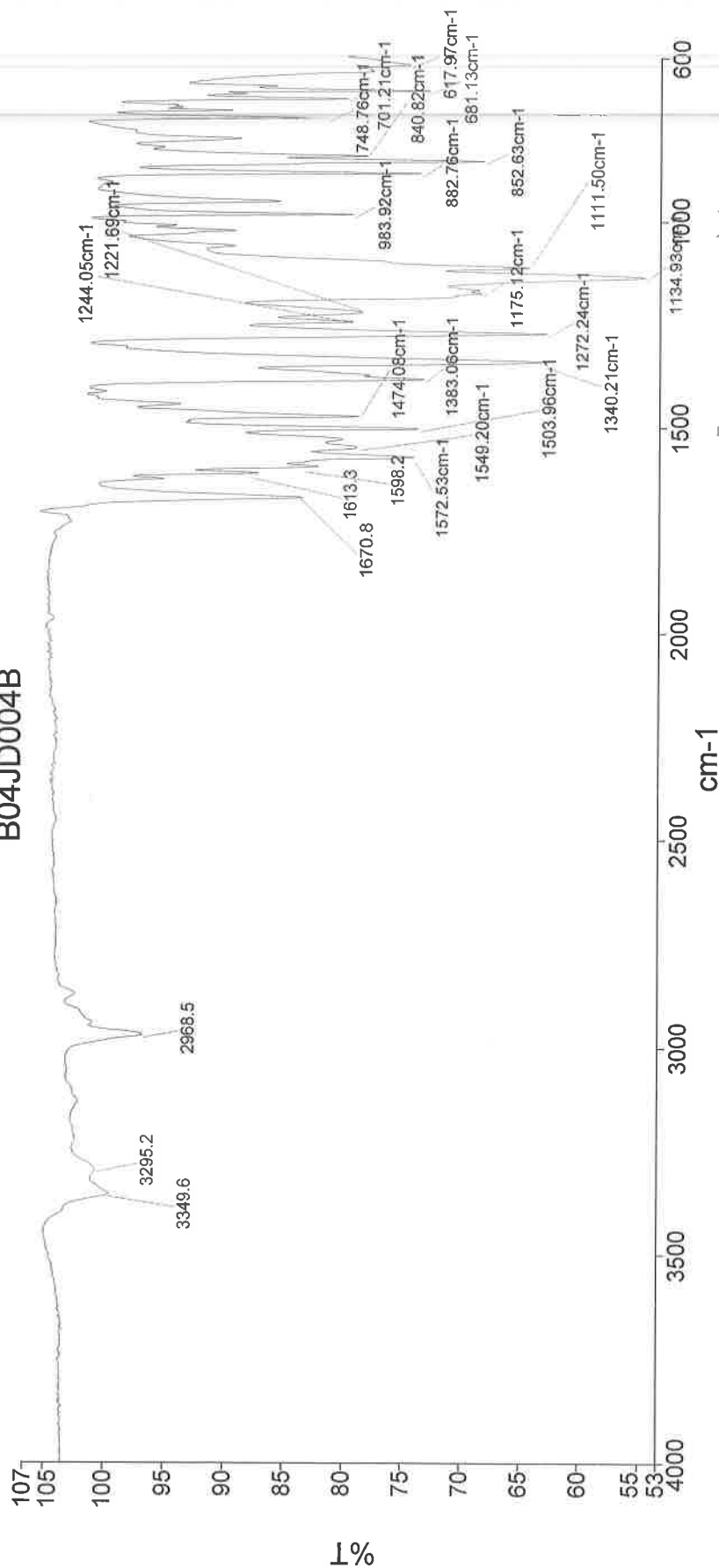
¹³C NMR spectrum (126 MHz, DMSO-*d*₆) for *N*-(3,5-Bis(trifluoromethyl)phenyl)-*N'*-(3-(*tert*-butyl)-1-(4-nitrophenyl)-1*H*-pyrazol-5-yl)urea

B04JD004B CARBON_01.esp



Analyst Date
Administrator
28 May 2015 15:29

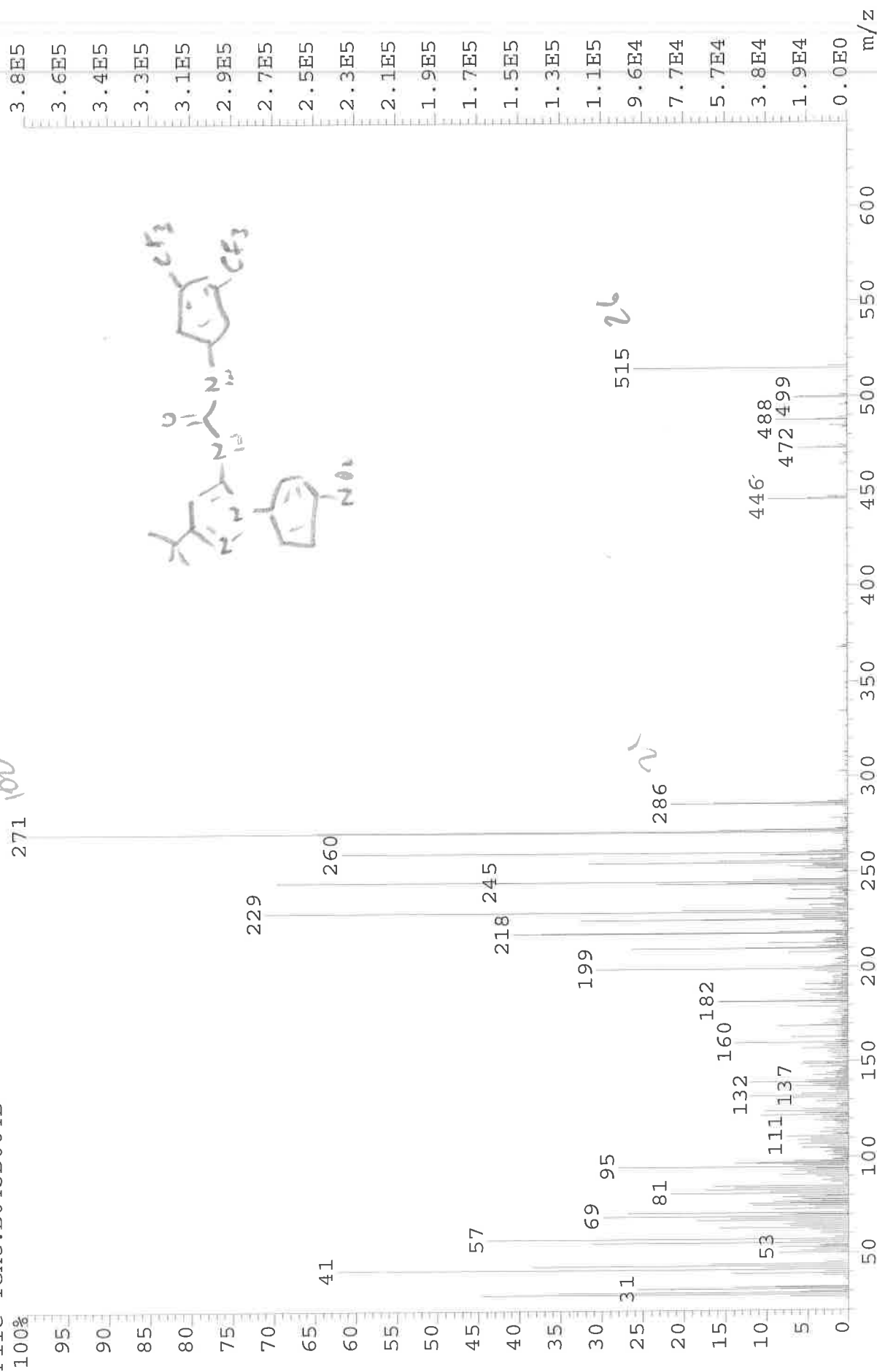
B04JD004B



3350 - N-H str
2968 - C-H str
1671 - C=O str
1572 - N-H bend
1504 - N-O
1340 - N-O
1272 - C-N
1175 - C-O
1135 - C-F
852 - C-H

Administrator 35 Sample 035 By Administrator Date Thursday, May 28 2015

File: JESS4996 Ident: 17 Acq: 21-APR-2015 12:39:19 +1:06 Cal: CAL1
AutoSpecE EI+ Magnet BpI: 382778 TIC: 11408222 Flags: HALI
File Text: B04JD004B



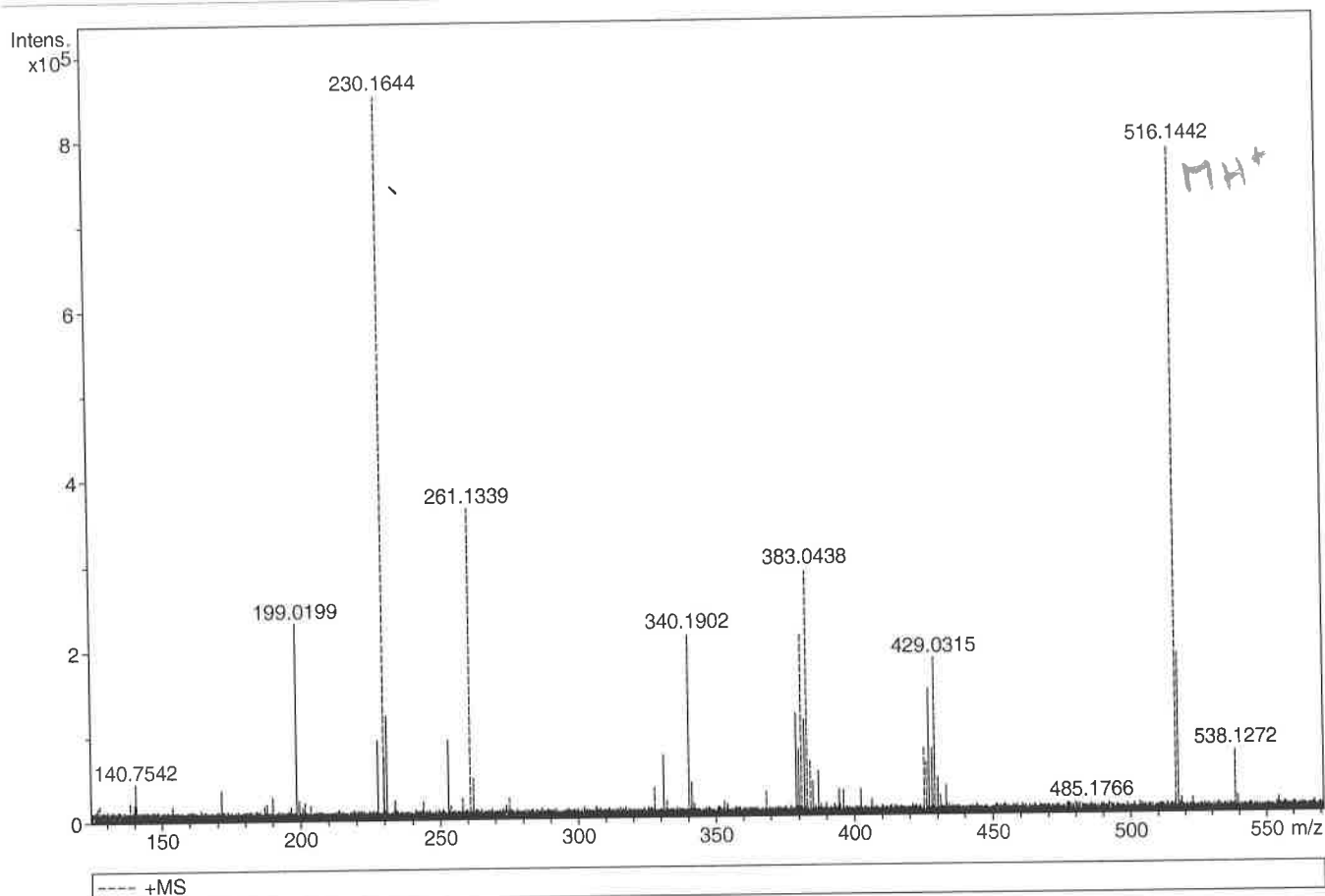
Generic Display Report

Analysis Info

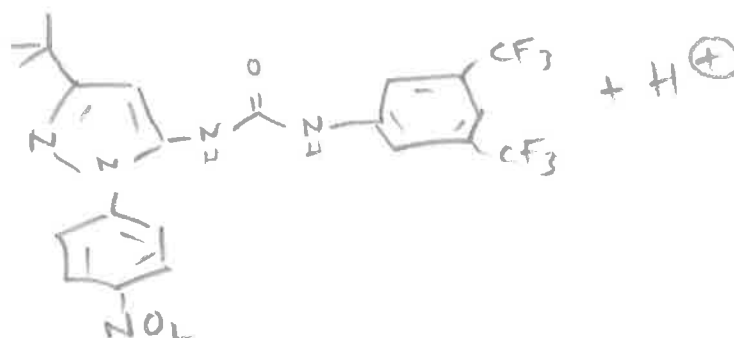
Analysis Name D:\Data\Alinariupos\JESS4996_000002.d
 Method pos20090608esi
 Sample Name POS ESI BO4JD004B
 Comment

Acquisition Date 21/04/2015 10:01:52

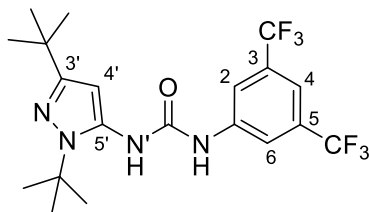
Operator Administrator
 Instrument apex-III



Sum Formula	Sigma	m/z	Err [ppm]	Mean Err [ppm]	Err [mDa]	rdb	N Rule	e ⁻
C 22 H 20 F 6 N 5 O 3	0.016	516.1465	4.45	3.94	2.04	12.50	ok	even



***N*-(3,5-Bis(trifluoromethyl)phenyl)-*N'*-((1,3-di-*tert*-butyl)-1*H*-pyrazol-5-yl)urea (229F)**



¹H NMR spectrum (500 MHz, DMSO-*d*₆) for *N*-(3,5-Bis(trifluoromethyl)phenyl)-*N'*-((1,3-di-*tert*-butyl)-1*H*-pyrazol-5-yl)urea

B04JD010 Proton DMSO.esp M03(s)

M01(m)
9.64

M02(s)
8.16
8.20

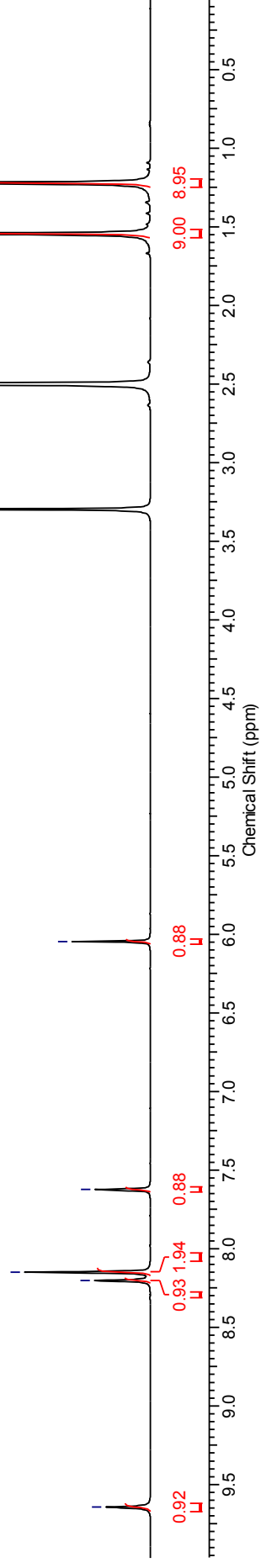
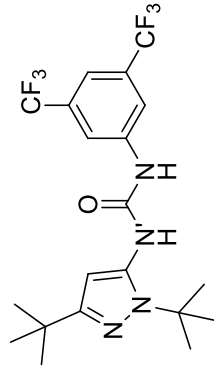
M04(s)
7.62

M05(s)
6.05

M06(s)

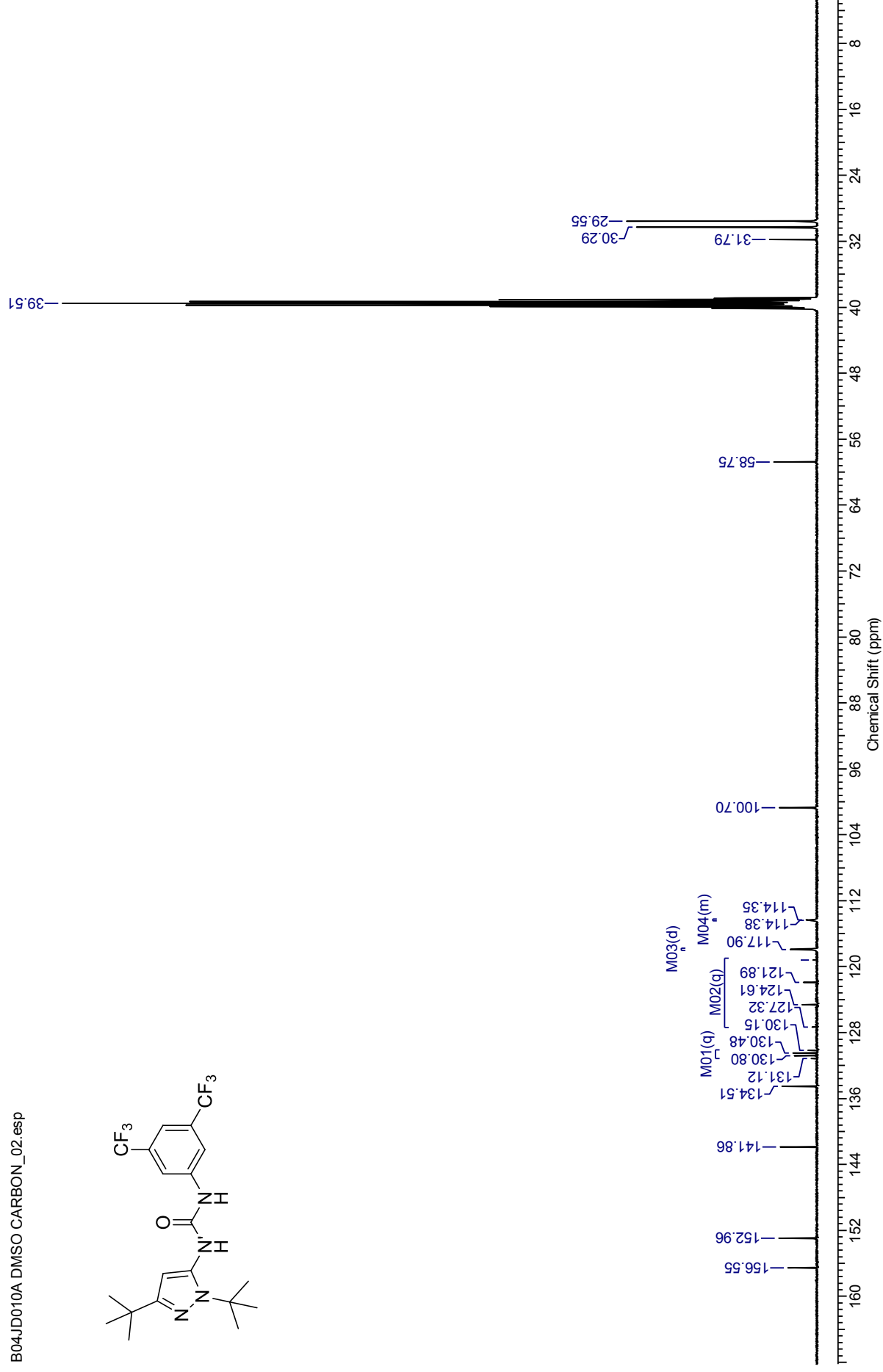
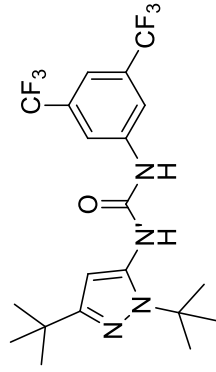
M07(s)
1.22
1.54

2.50



¹³C NMR spectrum (100 MHz, DMSO-*d*₆) for *N*-(3,5-Bis(trifluoromethyl)phenyl)-*N'*-((1,3-di-*tert*-butyl)-1*H*-pyrazol-5-yl)urea

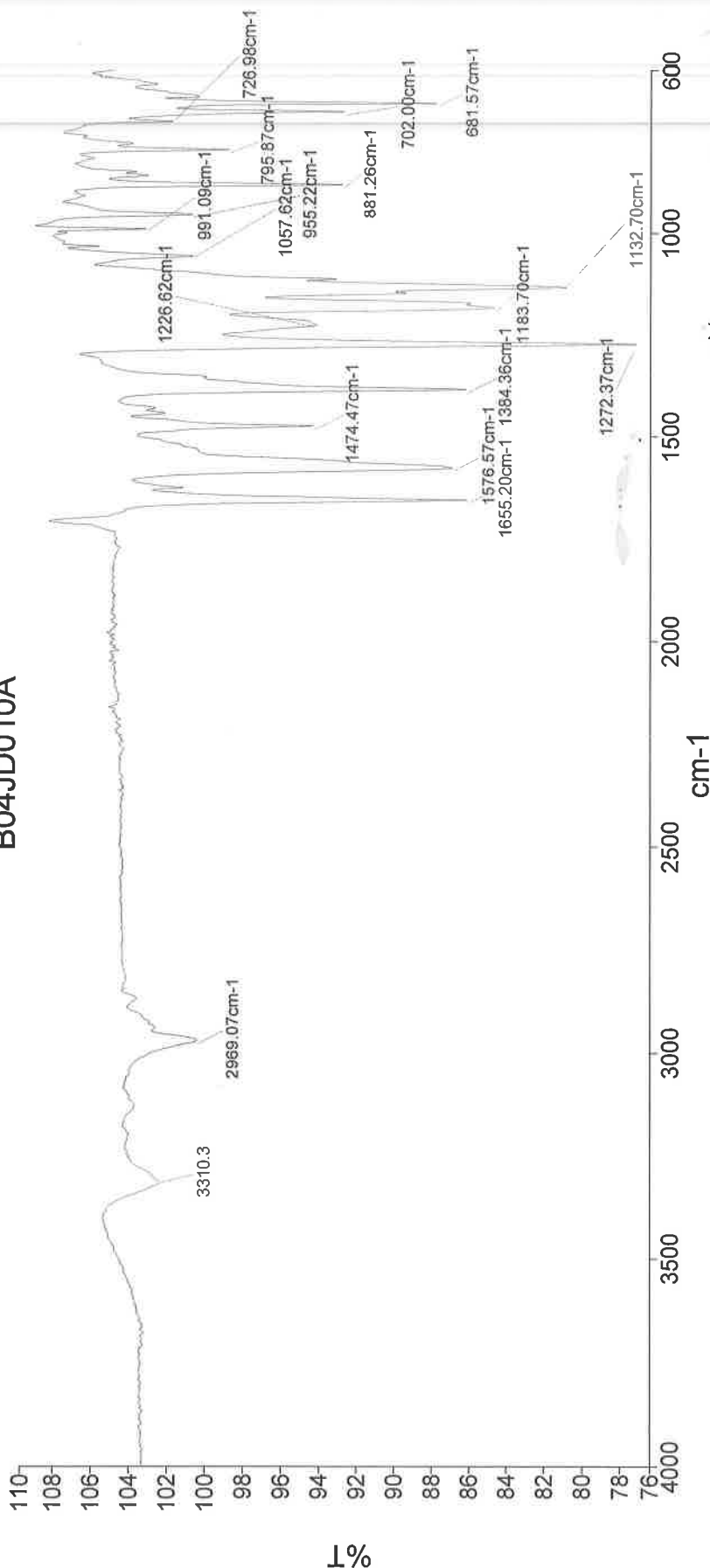
B04JD010A DMSO CARBON_02.esp



Analyst
Date

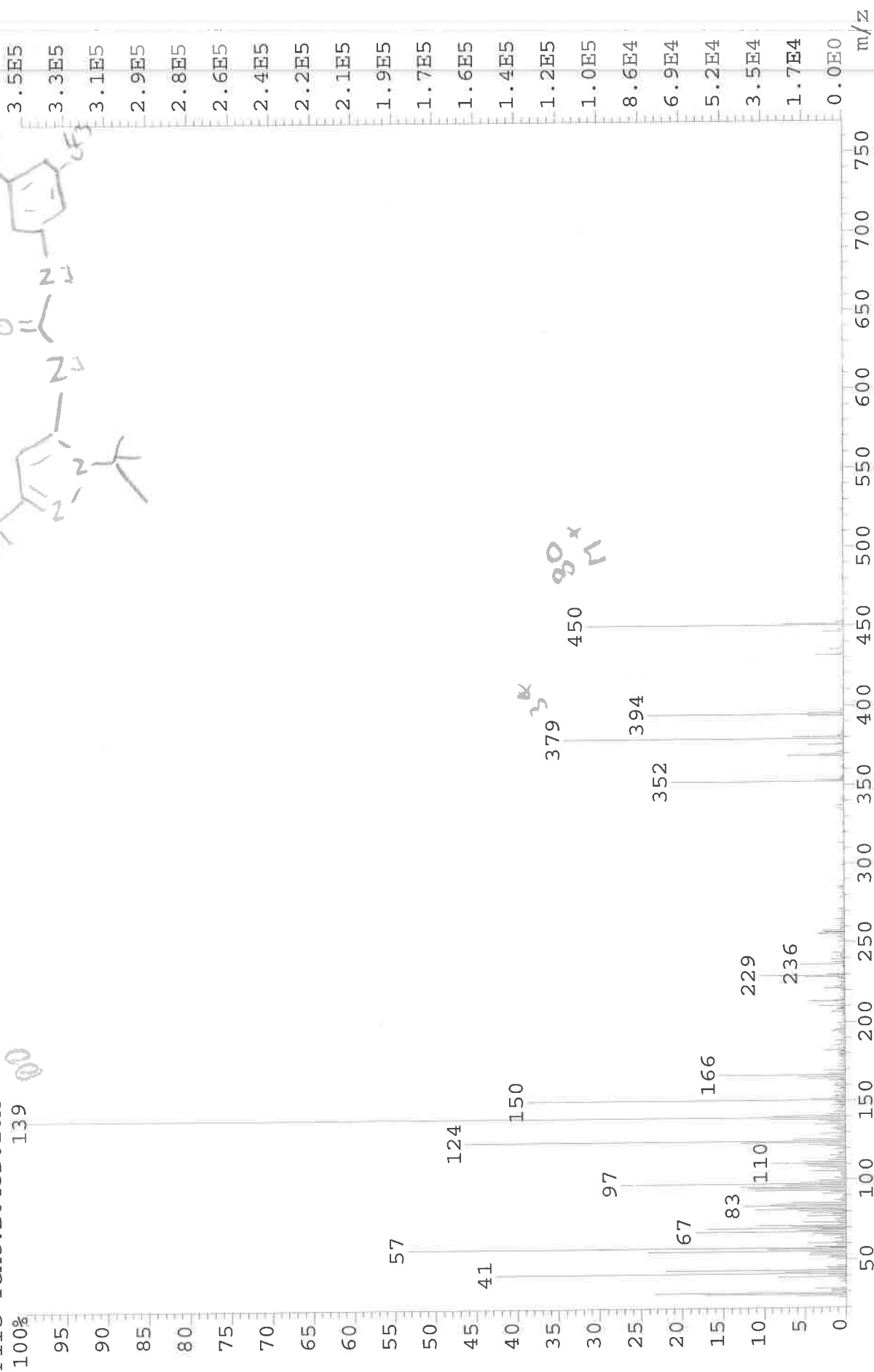
Administrator
28 May 2015 15:22

B04JD010A



3310 N-H str.
2969 C-H str. alk.
1655 C=O str.
1576 N-H bend
1474 C-H str.,
1384 C-H
1272 C-N str.
1184 C-O
1133 C-F str.

File: JESS5158 Ident: 18 Acq: 28-MAY-2015 15:52:21 +1:10 Cal: CALL
AutoSpecE EI+ Magnet BpI: 346037 TIC: 4028522 Flags: HALL
File Text: B04JD010A



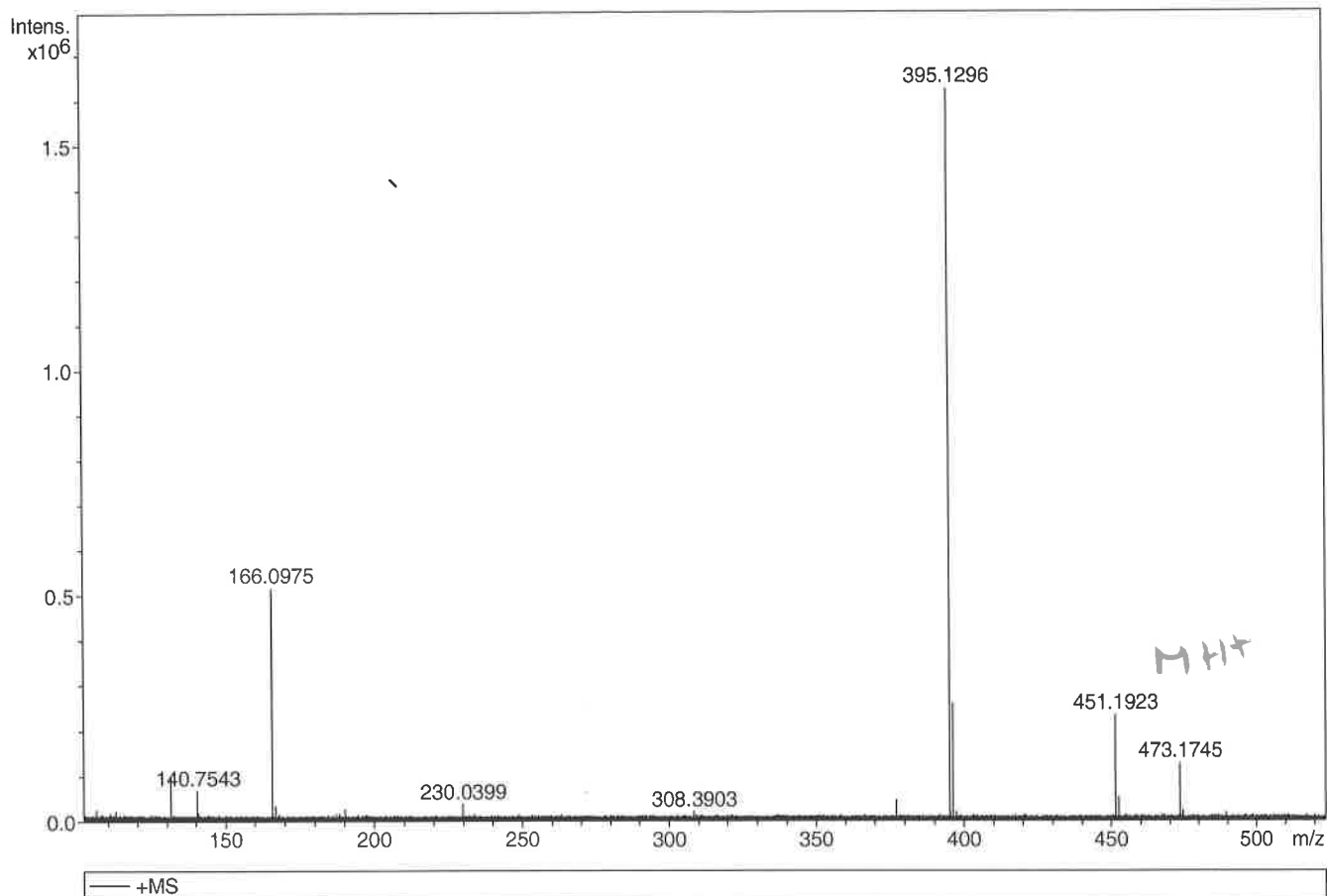
Generic Display Report

Analysis Info

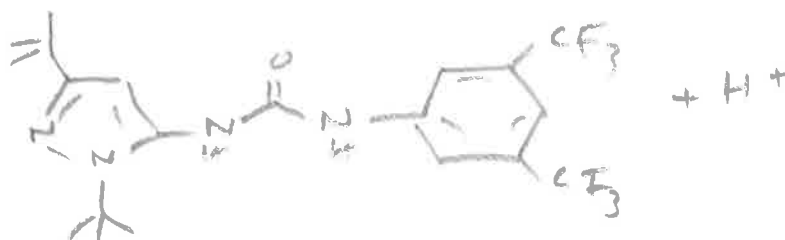
Analysis Name D:\Data\Alinanopos\JESS5158_000001.d
 Method pos20090608esi
 Sample Name POS ESI BO4JD010A
 Comment

Acquisition Date 28/05/2015 16:04:41

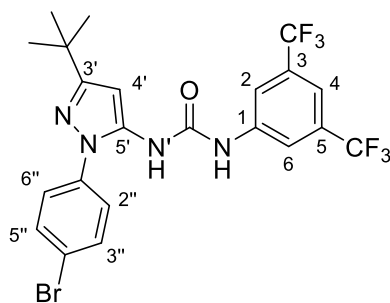
Operator Administrator
 Instrument apex-III



Sum Formula	Sigma	m/z	Err [ppm]	Mean Err [ppm]	Err [mDa]	rdb	N Rule	e ⁻
C 20 H 25 F 6 N 4 O 1	0.022	451.1927	0.89	-1.68	-0.76	7.50	ok	even

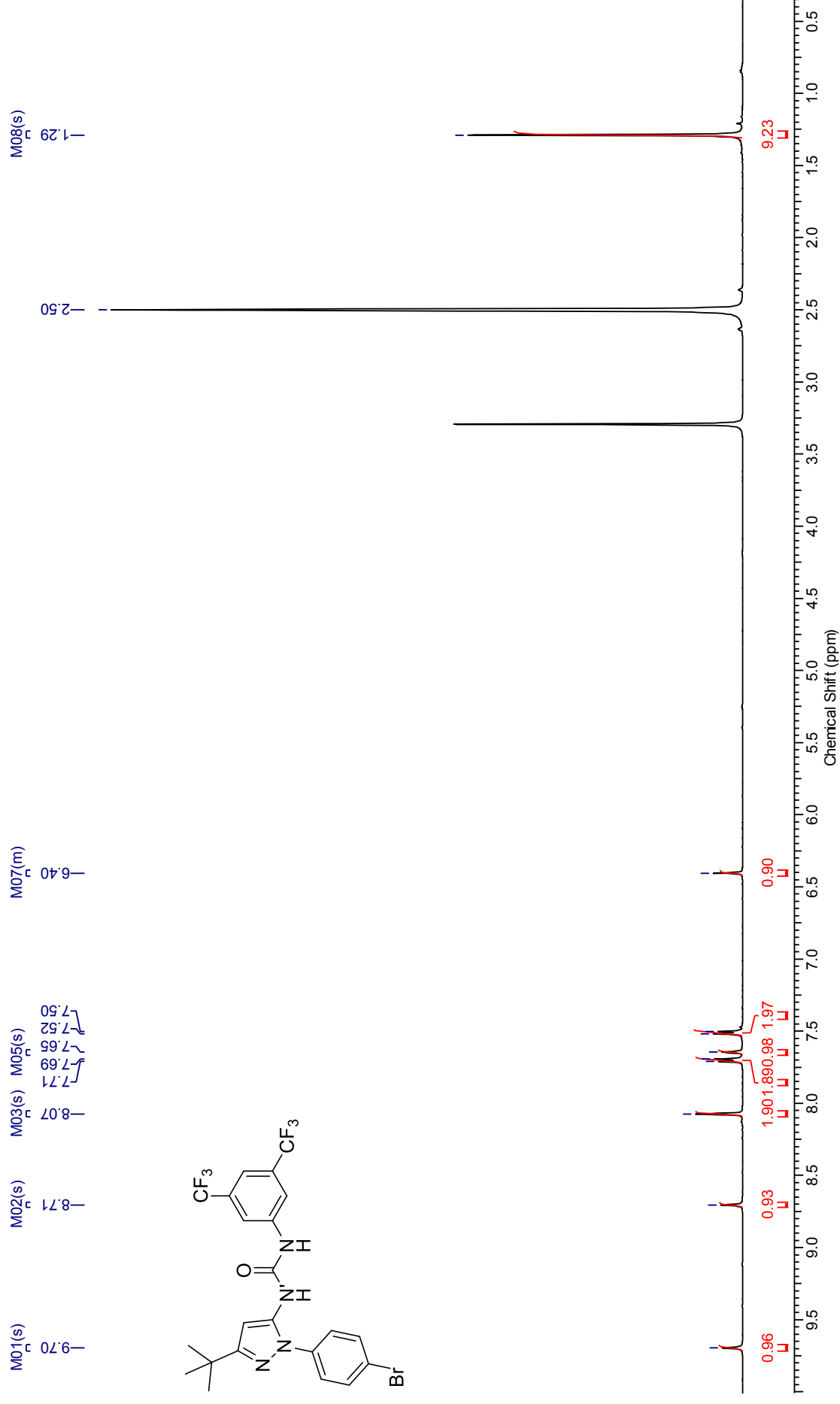
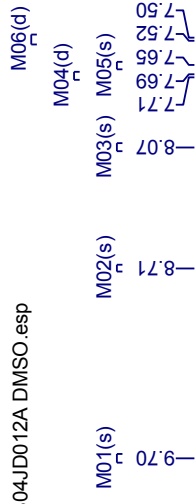


***N*-(3,5-Bis(trifluoromethyl)phenyl)-*N'*-(3-(*tert*-butyl)-1-(4-bromophenyl)-1*H*-pyrazol-5-yl)urea (230F)**



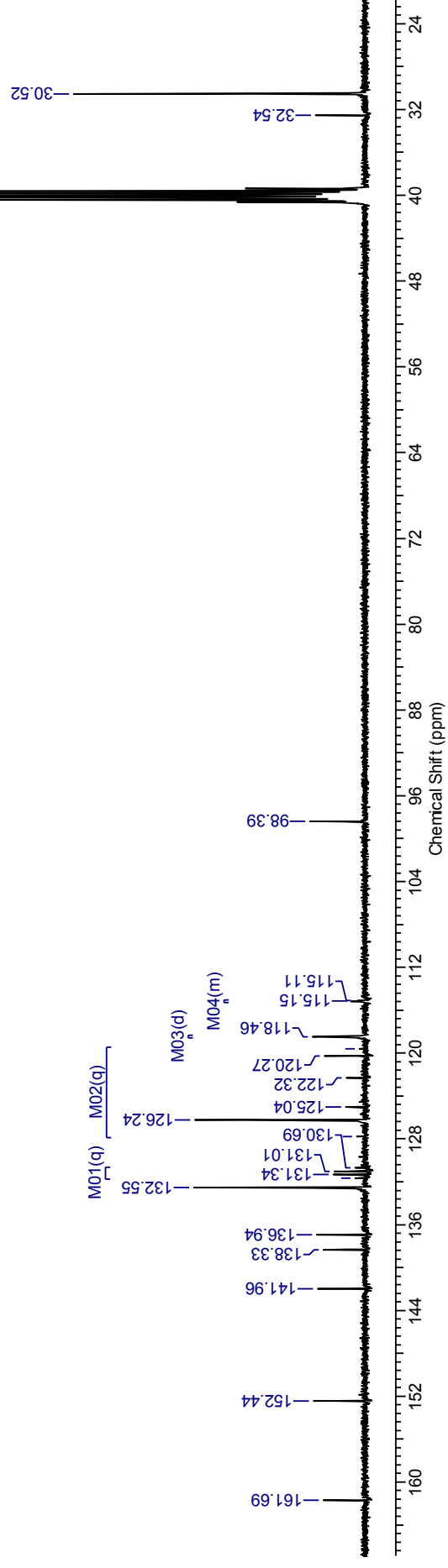
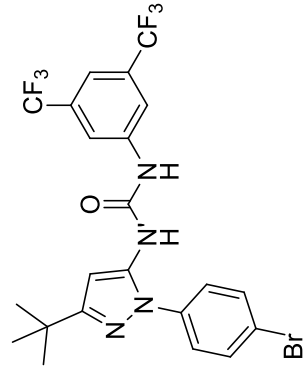
¹H NMR spectrum (500 MHz, DMSO-*d*₆) for *N*-(3,5-Bis(trifluoromethyl)phenyl)-*N'*-(3-(*tert*-butyl)-1-(4-bromophenyl)-1*H*-pyrazol-5-yl)urea

B04JD012A DMSO.esp



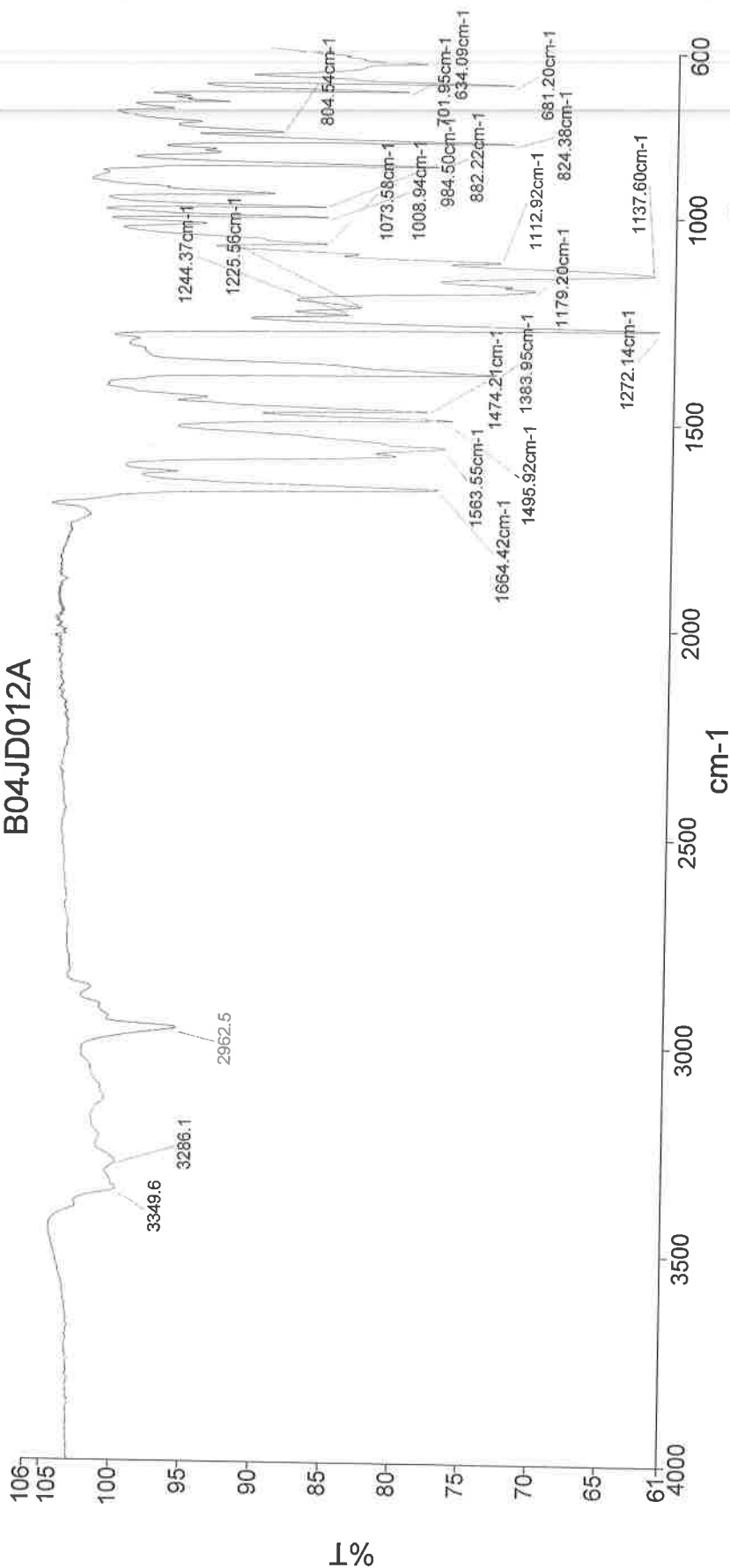
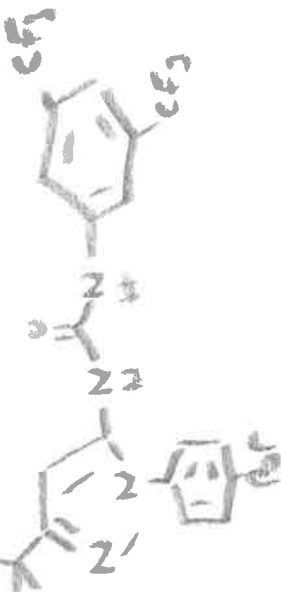
¹³C NMR spectrum (100 MHz, DMSO-*d*₆) for *N*-(3,5-Bis(trifluoromethyl)phenyl)-*N'*-(3-(*tert*-butyl)-1-(4-bromophenyl)-1*H*-pyrazol-5-yl)urea

B04JD012A DMSO CARBON_01.esp



Analyst
Date
Administrator
28 May 2015 15:08

B04JD012A



Administrator 29 Sample 029 By Administrator Date Thursday, May 28 2015

File: JESS5157 Ident: 25 Acq: 28-MAY-2015 15:58:34 +1:35 Cal: CAL1
AutoSpec EI+ Magnet BpI: 3632139 TIC: 62626640 Flags: HALL
File Text: B04JD012A



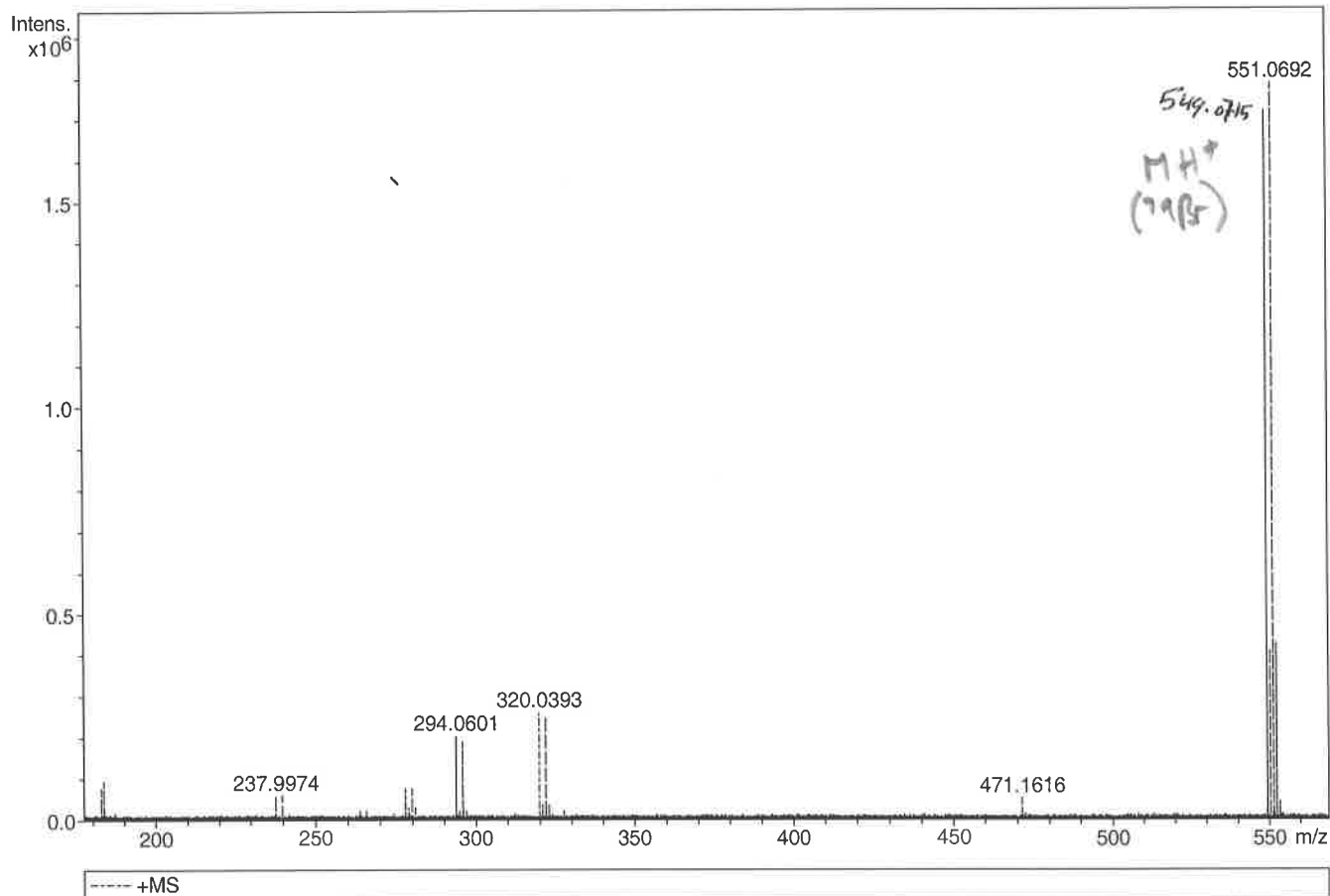
Generic Display Report

Analysis Info

Analysis Name D:\Data\Allnanopos\JESS5157_000001.d
 Method pos20090608esi
 Sample Name POS ESI BO4JD012A
 Comment

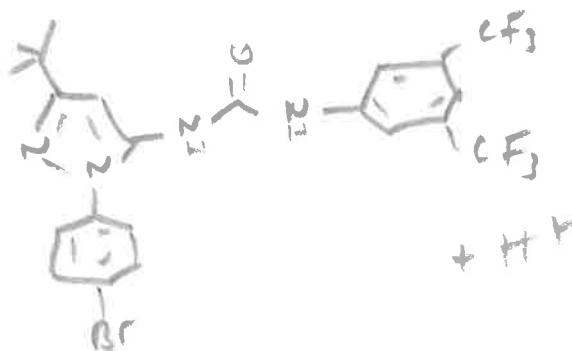
Acquisition Date 28/05/2015 16:14:16

Operator Administrator
 Instrument apex-III

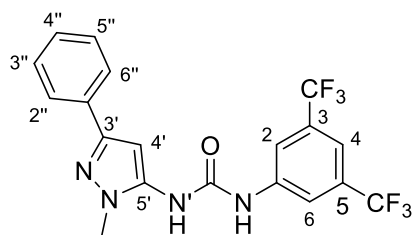


Sum Formula	Sigma	m/z	Err [ppm]	Mean Err [ppm]	Err [mDa]	rdb	N Rule	e ⁻
C 22 H 20 Br 1 F 6 N 4 O 1	0.016	549.0719	-1.36	-0.14	-0.08	11.50	ok	even

↑
79Br



***N*-(3,5-Bis(trifluoromethyl)phenyl)-*N'*-(1-methyl-3-phenyl-1*H*-pyrazol-5-yl)urea (231F)**



^1H NMR spectrum (500 MHz, $\text{DMSO}-d_6$) for *N*-(3,5-Bis(trifluoromethyl)phenyl)-*N'*-(1-methyl-3-phenyl-1*H*-pyrazol-5-yl)urea

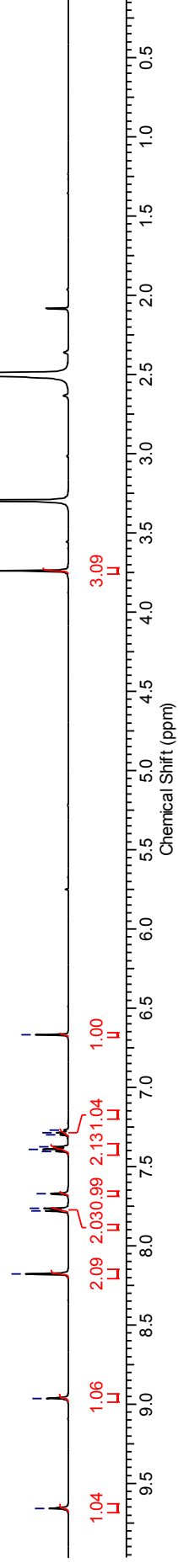
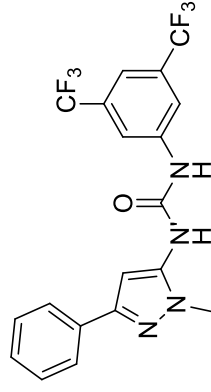
B04JD086A DMSO .esp

M06(t)

M04(d) M07(t)

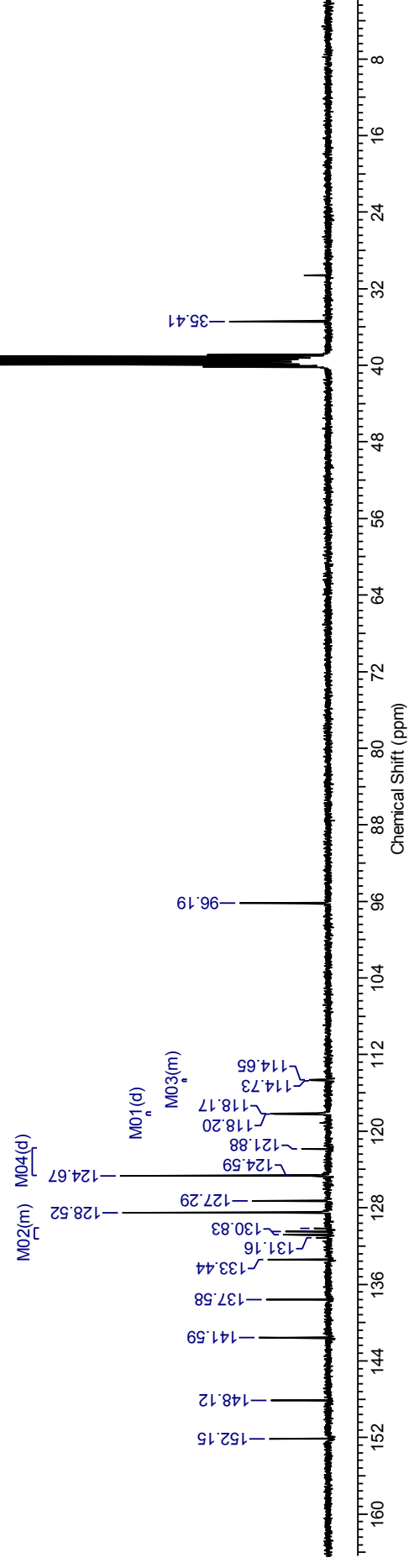
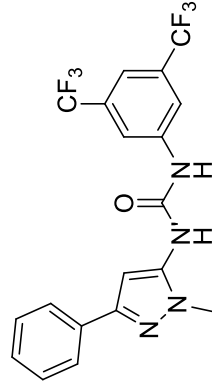
M01(s) M02(s) M03(s) M05(s) M10(m) M08(s)

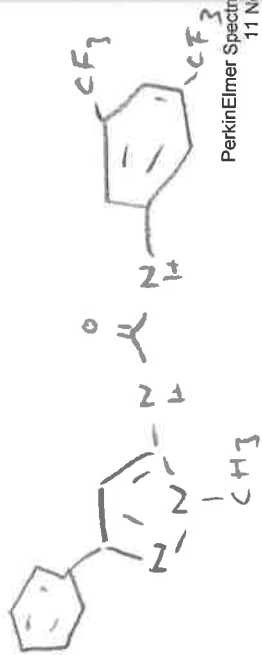
M09(s)



¹³C NMR spectrum (100 MHz, DMSO-*d*₆) for *N*-(3,5-Bis(trifluoromethyl)phenyl)-*N'*-(1-methyl-3-phenyl-1*H*-pyrazol-5-yl)urea

B04JD086A DMSO CARBON_01.esp

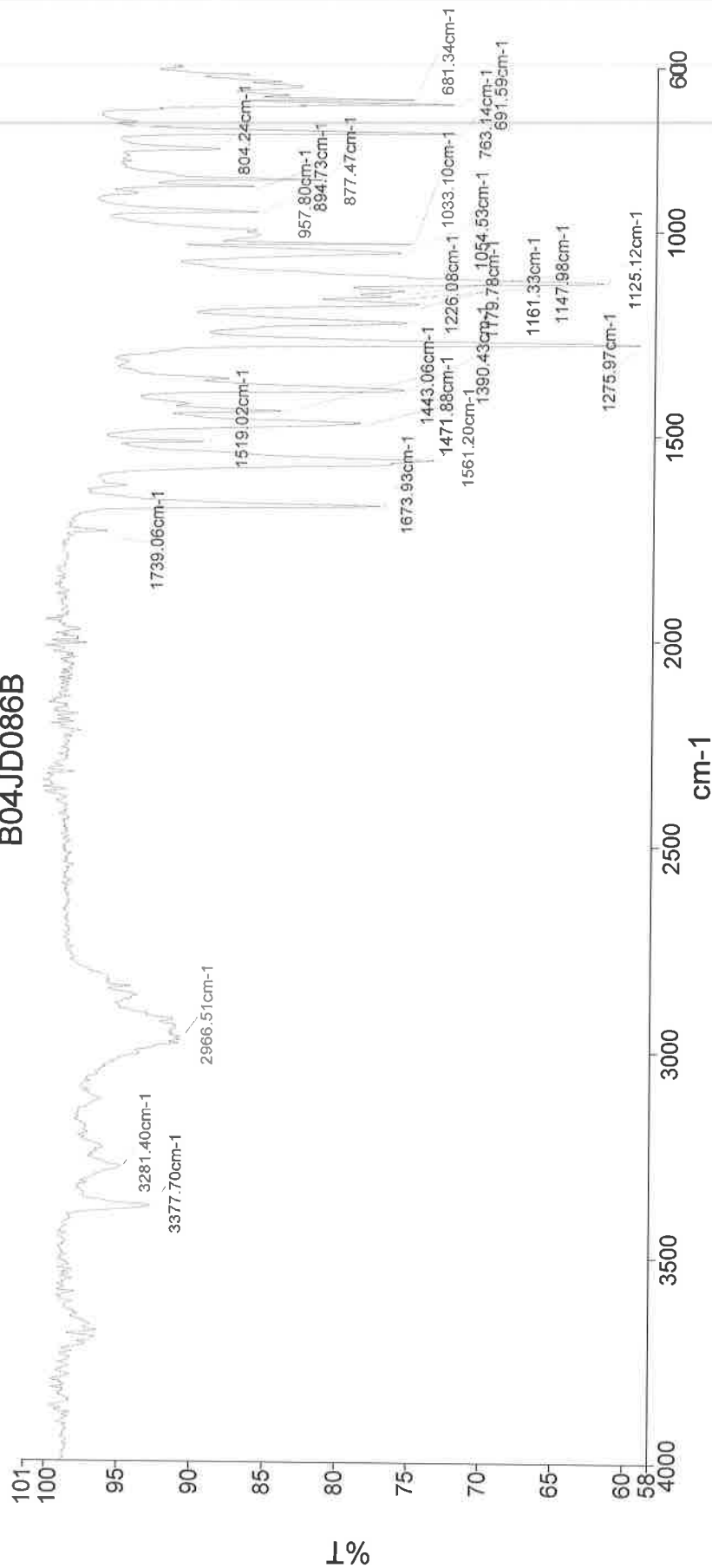




PerkinElmer Spectrum Version 10.03.06
11 November 2015 14:09

Analyst
Date
11 November 2015 14:09

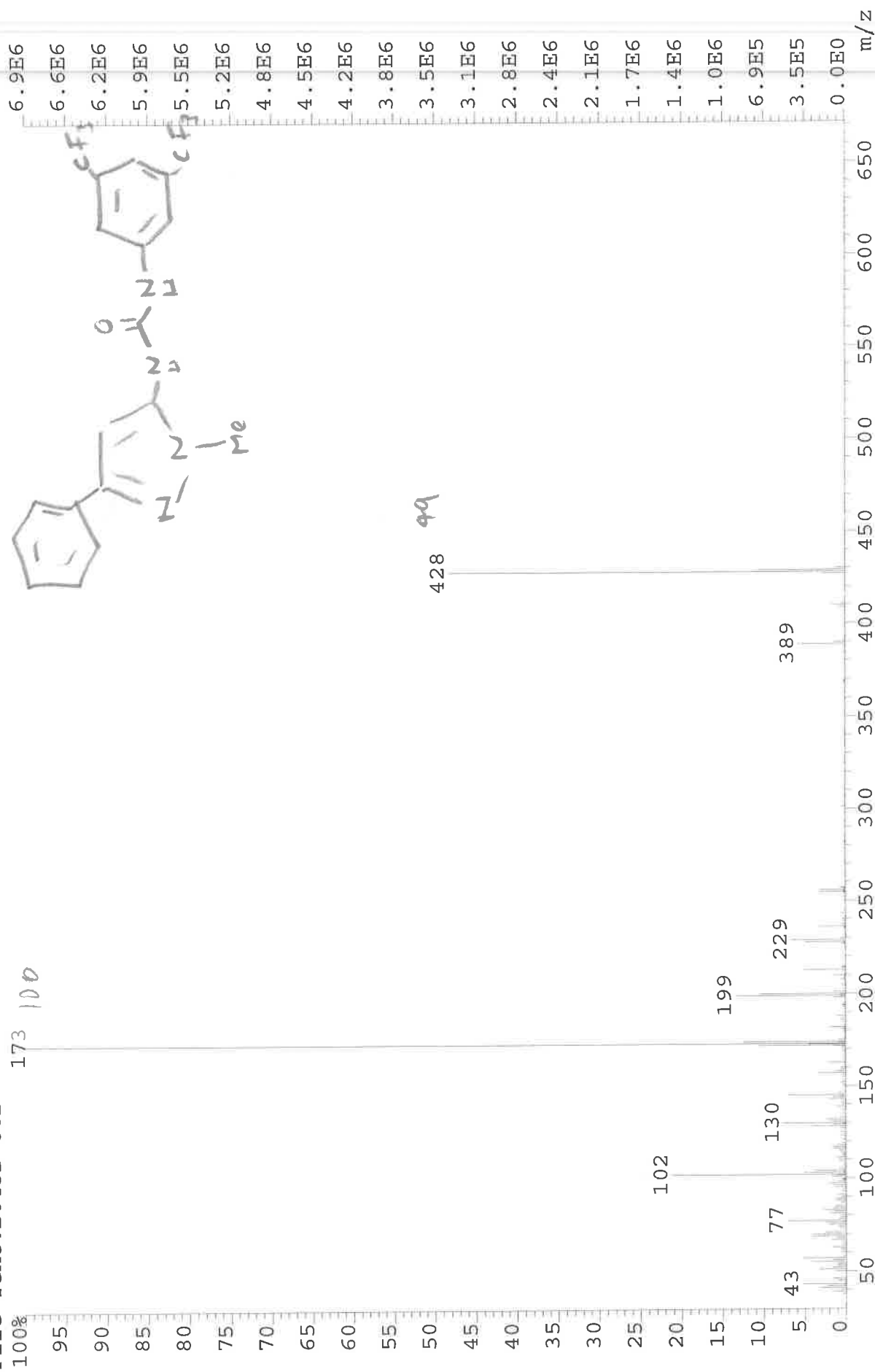
B04JD086B



3378 - N-H str.
2966 - C-H str.
1674 - C=O str.
1561 - C-H str.
1472 - C-C in ring
1443 - C-C str.
1276 - C-N str.
1125 - C-F str.
1054 - C-N str.

249-081 Sample 081 By Administrator Date Wednesday, November 11 2015

File: JESS6229 Ident: 3 Acq: 23-OCT-2015 15:33:14 +0:15 Cal: CAL1
AutoSpecE EI+ Magnet BpI: 6927776 TIC: 35249896 Flags: HALL
File Text: B04JD-86B



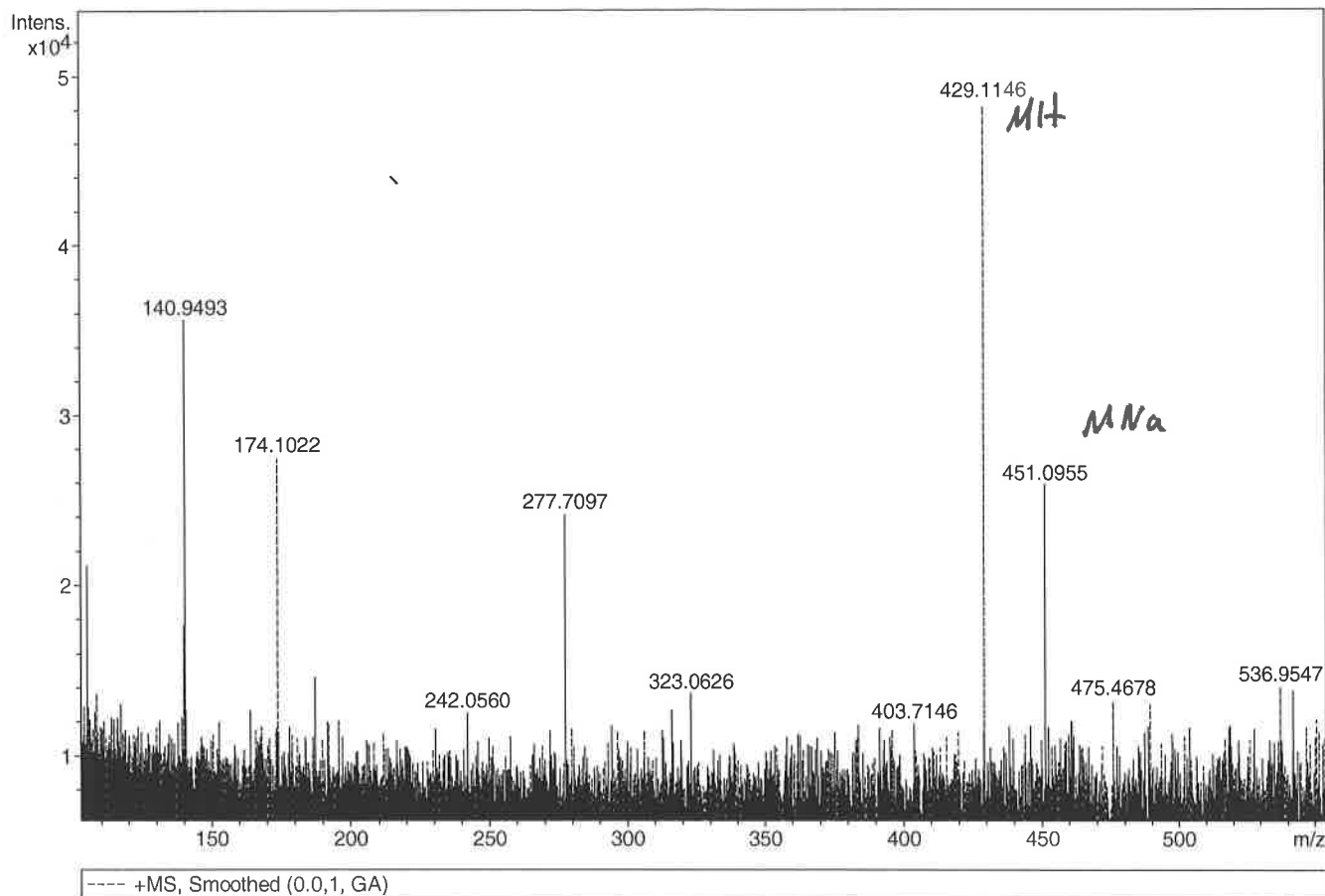
Generic Display Report

Analysis Info

Analysis Name D:\Data\Alinanopos\JESS6229_000001.d
 Method pos20090608esi
 Sample Name POS ESI BO4JD086B
 Comment

Acquisition Date 23/10/2015 15:40:36

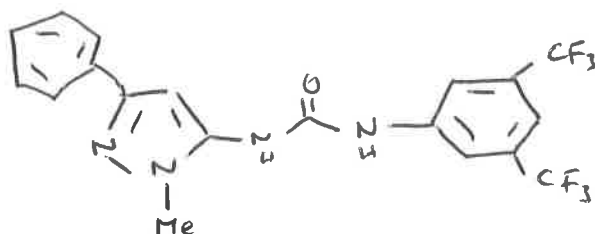
Operator Administrator
 Instrument apex-III



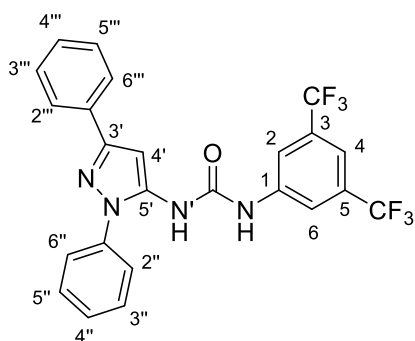
Sum Formula	Sigma	m/z	Err [ppm]	Mean Err [ppm]	Err [mDa]	rdB	N Rule	e ⁻
C ₁₇ H ₁₆ F ₆ N ₄ Na ₁ O ₁	0.113	429.1121	5.95	-20.40	-8.79	8.50	ok	even

C₁₉H₁₅F₆N₄O

429.1144 Da



***N*-(3,5-Bis(trifluoromethyl)phenyl)-*N'*-(1,3-diphenyl-1*H*-pyrazol-5-yl)urea (232F)**



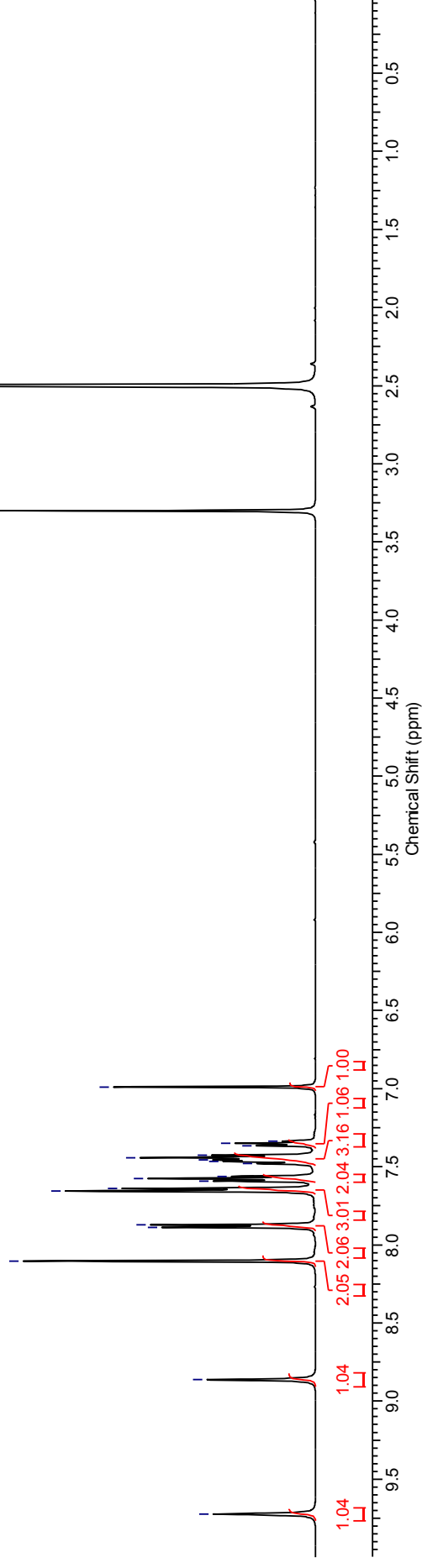
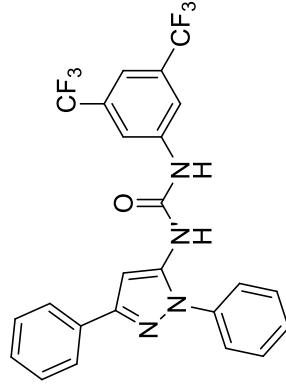
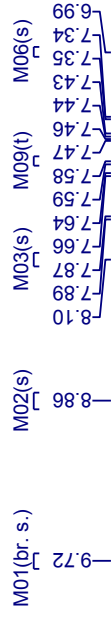
¹H NMR spectrum (500 MHz, DMSO-*d*₆) for *N*-(3,5-Bis(trifluoromethyl)phenyl)-*N'*-(1,3-diphenyl-1*H*-pyrazol-5-yl)urea

B04JD089B DMSO.esp

M08(m)

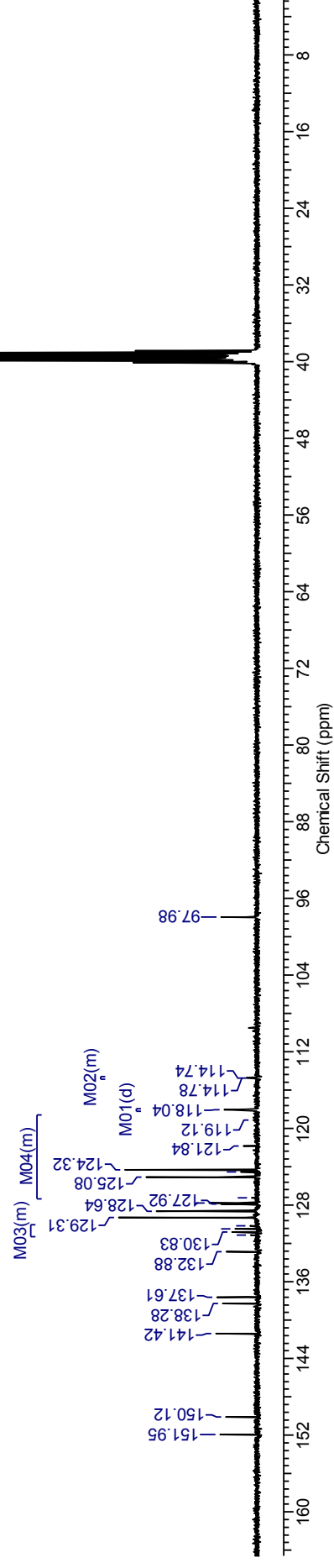
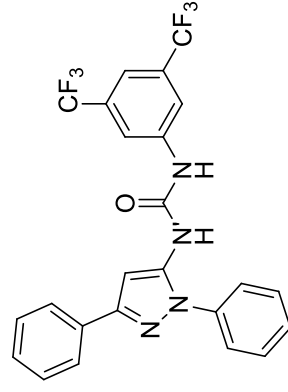
M04(d) M07(m)

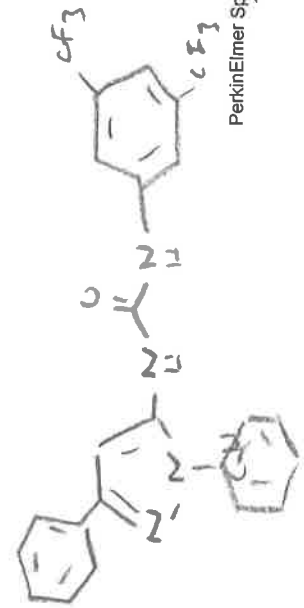
M05(d)



¹³C NMR spectrum (100 MHz, DMSO-*d*₆) for *N*-(3,5-Bis(trifluoromethyl)phenyl)-*N'*-(1,3-diphenyl-1*H*-pyrazol-5-yl)urea

B04JD089B DMSO CARBON_01.esp

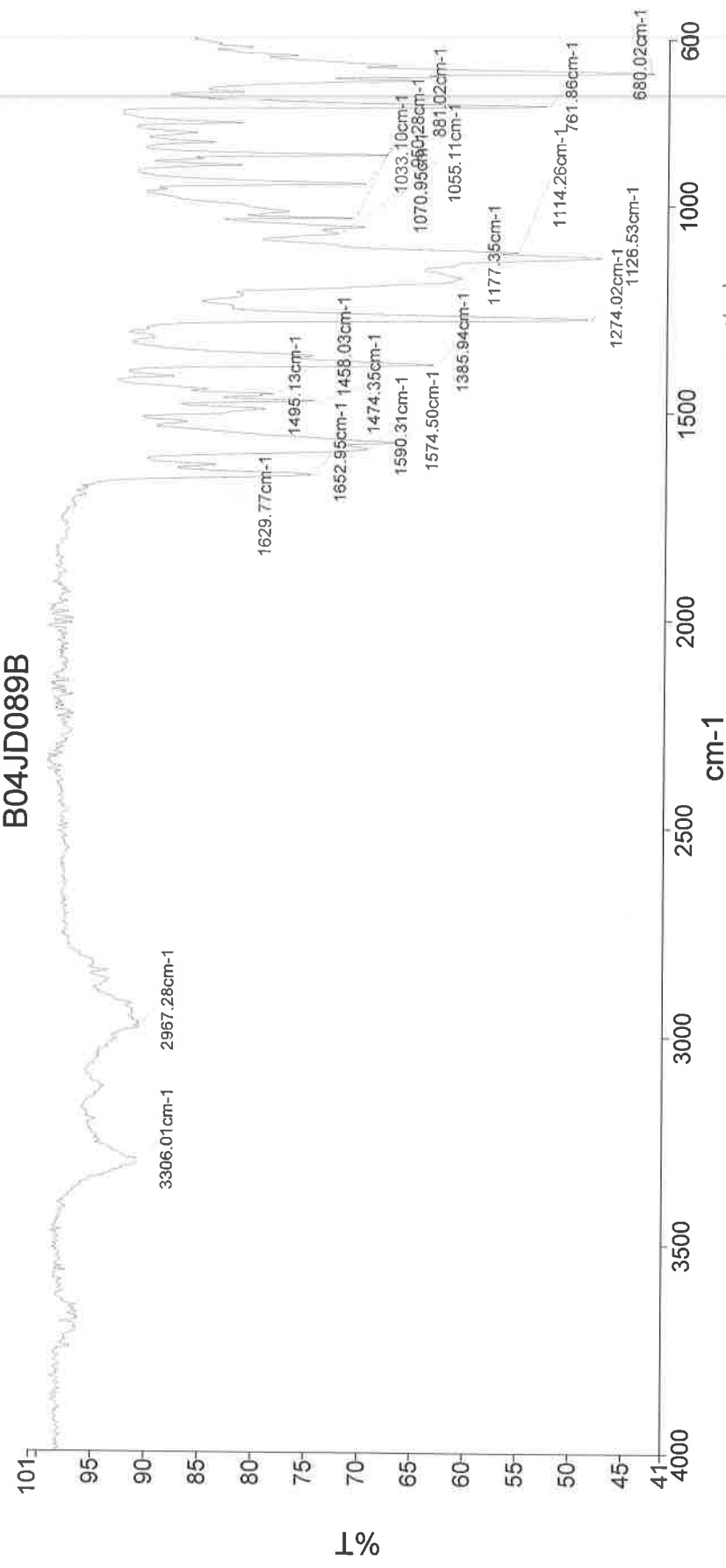




PerkinElmer Spectrum Version 10.03.06
11 November 2015 14:06

Analyst
Date
11 November 2015 14:06

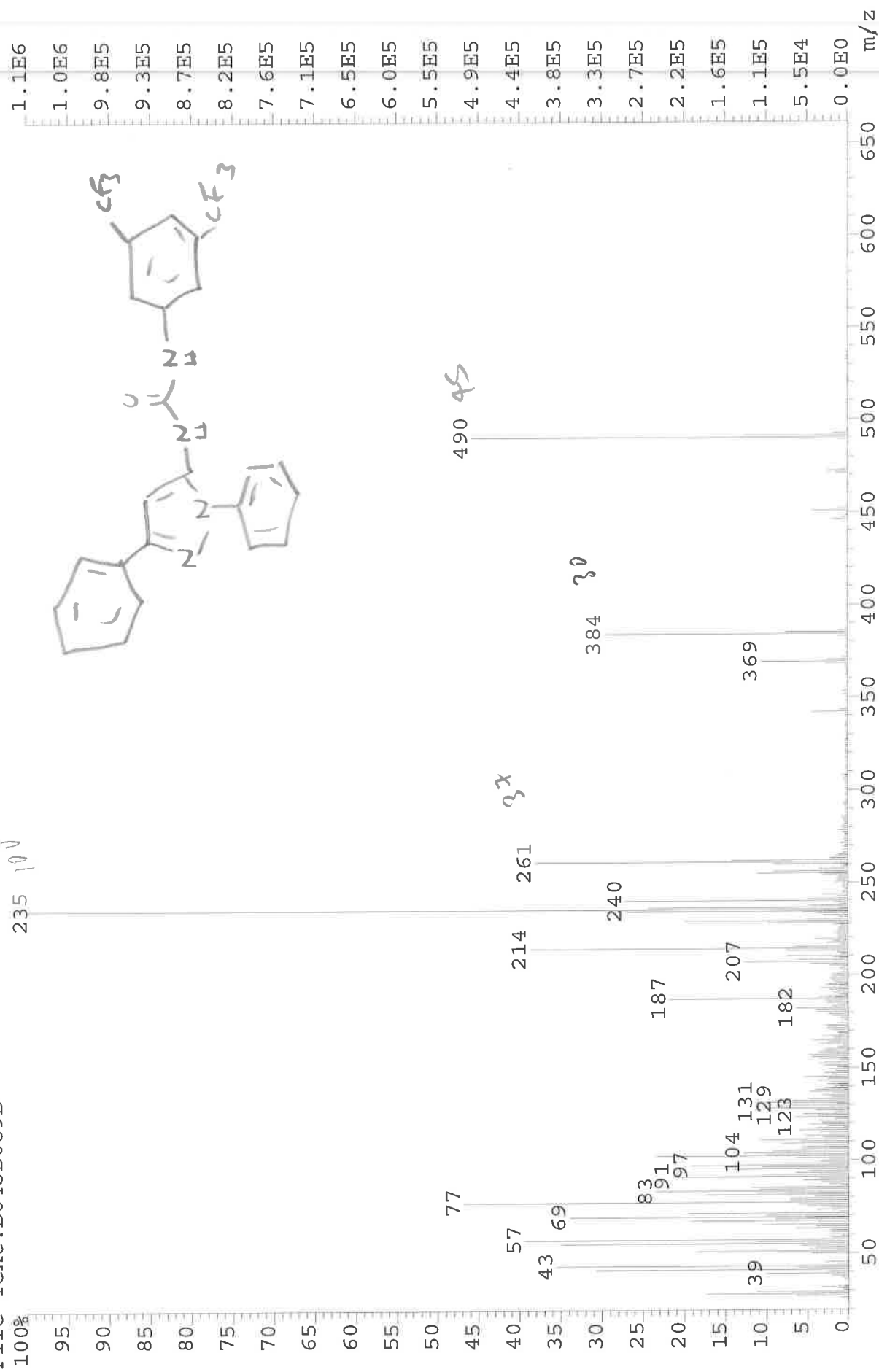
B04JD089B



3306 - N-H str.
2967 - C-H str.
1653 - C=O str.
1590 - N-H str.
1574 - N-H str.
1474 - C=C str.
1386 - C-N str.
1274 - C-N str.
1126 - C-F str.
1055 - C-N str.

249-080 Sample 080 By Administrator Date Wednesday, November 11 2015

File: JESS6252 Ident: 28 Acq: 29-OCT-2015 15:33:16 +1:46 Cal: CAL1
AutoSpecE EI+ Magnet BpI: 1091943 TIC: 19434442 Flags: HALL
File Text: B04JD089B



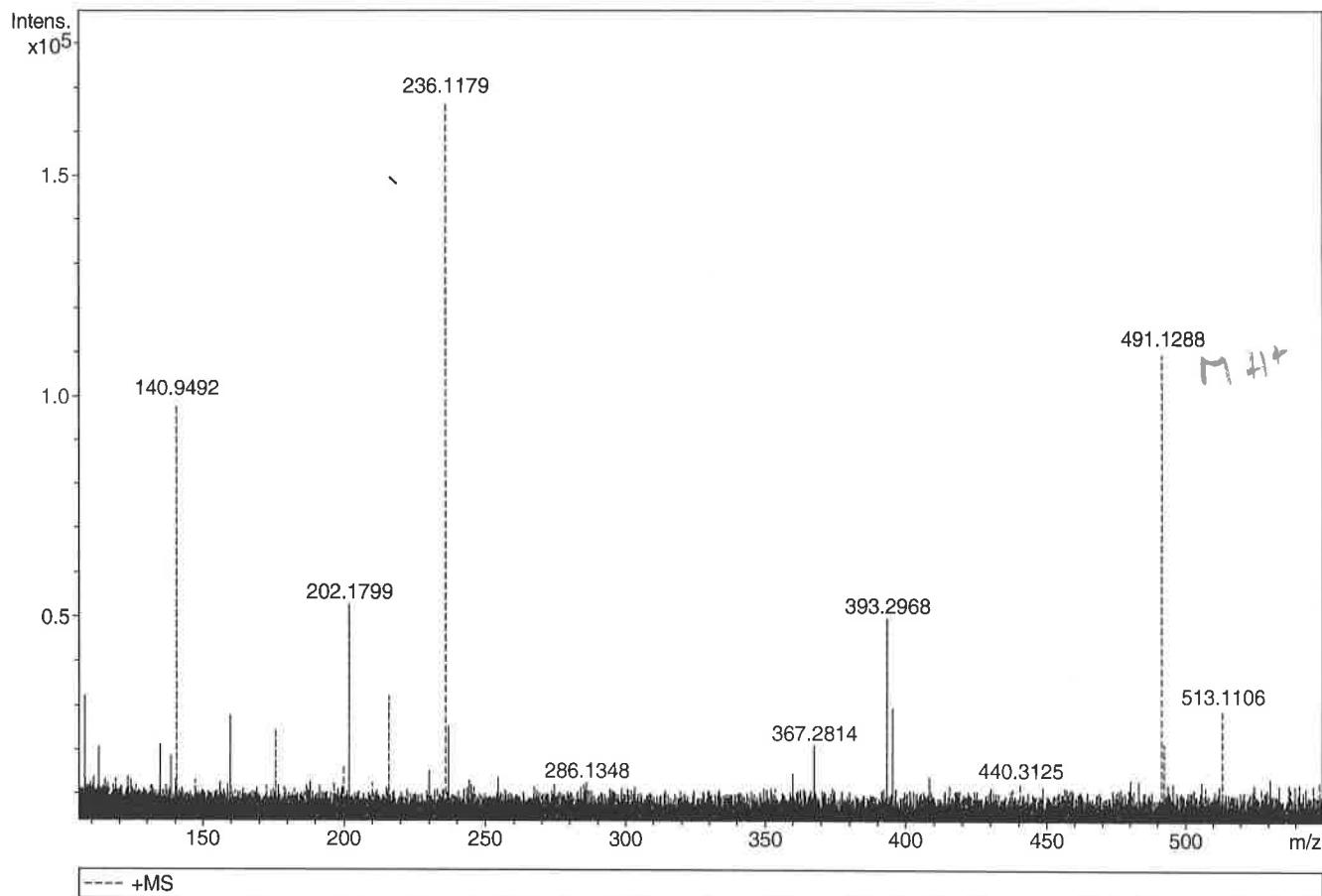
Generic Display Report

Analysis Info

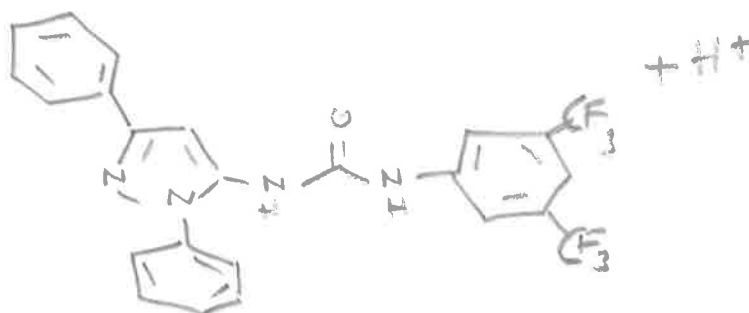
Analysis Name D:\Data\Alinanopos\JESS6252_000001.d
 Method pos20090608esi
 Sample Name POS ESI BO4JDO89B
 Comment

Acquisition Date 29/10/2015 13:39:34

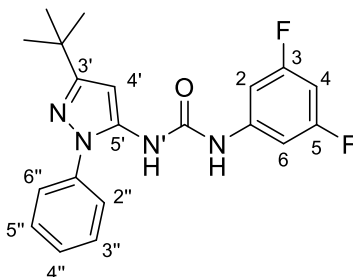
Operator Administrator
 Instrument apex-III



Sum Formula	Sigma	m/z	Err [ppm]	Mean Err [ppm]	Err [mDa]	rdB	N Rule	e ⁻
C ₂₄ H ₁₇ F ₆ N ₄ O ₁	0.053	491.1301	2.68	1.64	0.81	15.50	ok	even

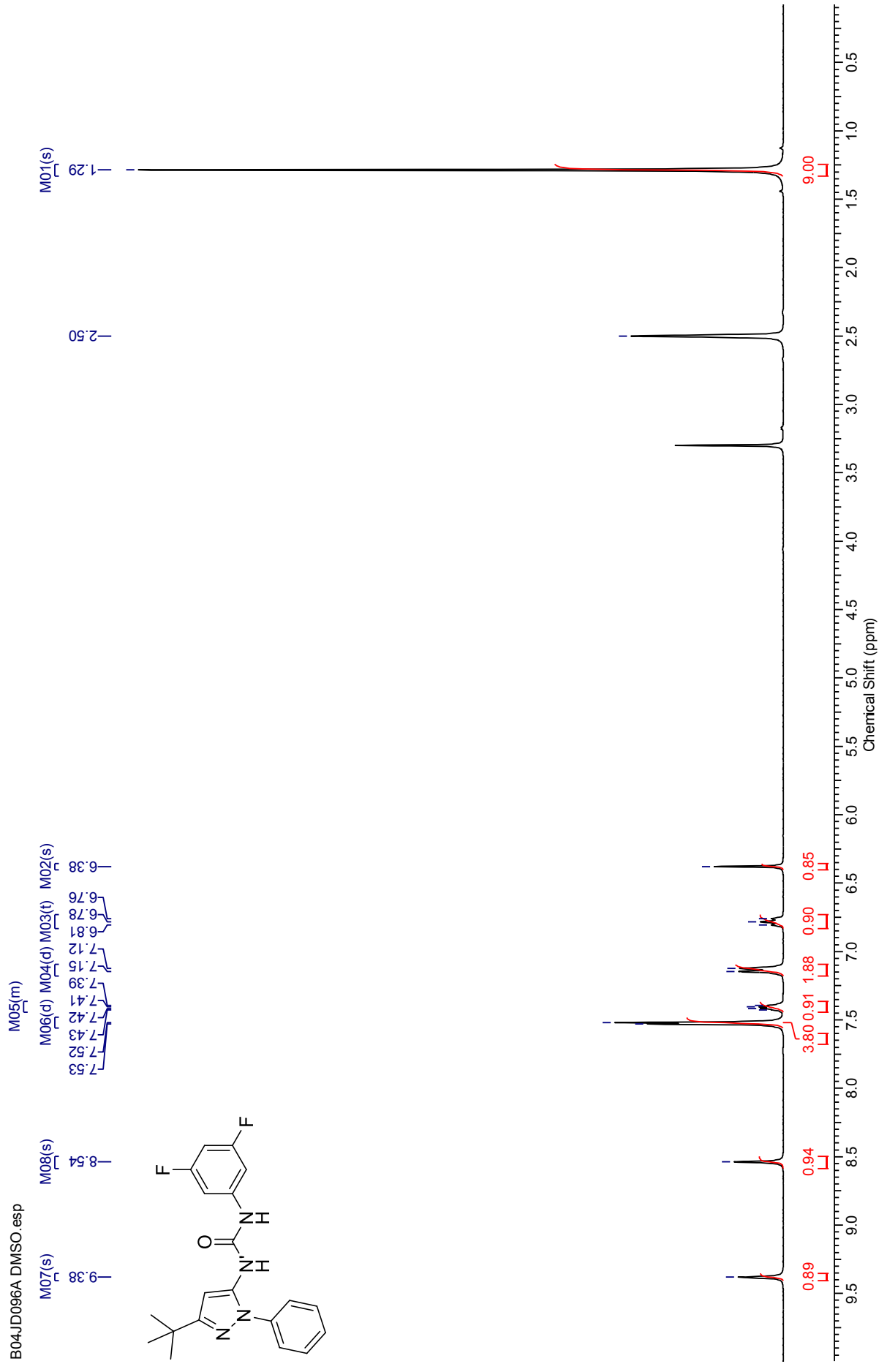


***N*-(3,5-Difluorophenyl)-*N'*-(3-(*tert*-butyl)-1-(phenyl)-1*H*-pyrazol-5-yl)urea (215O)**



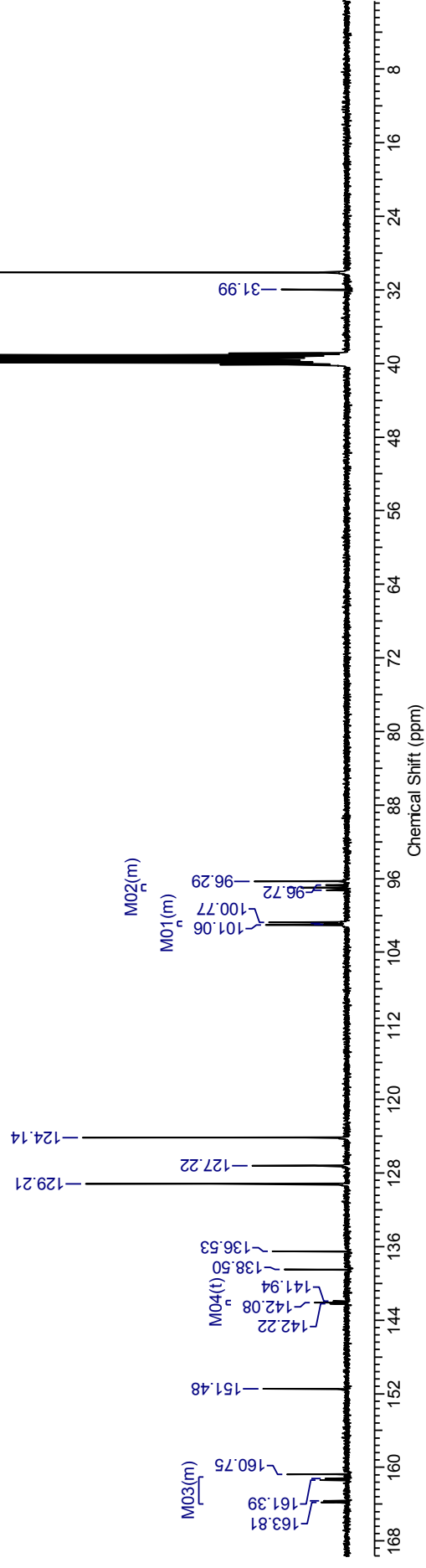
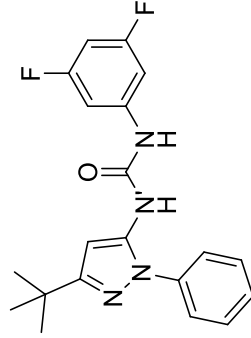
¹H NMR spectrum (500 MHz, DMSO-*d*₆) for *N*-(3,5-Difluorophenyl)-*N'*-(3-(*tert*-butyl)-1-(phenyl)-1*H*-pyrazol-5-yl)urea

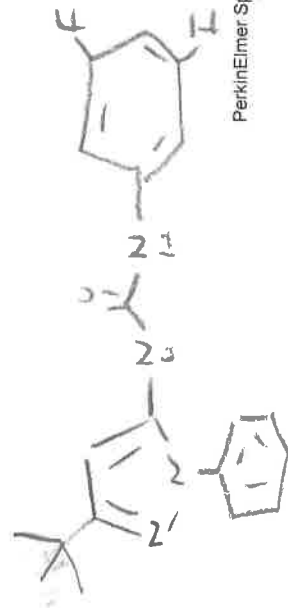
B04JD096A DMSO.esp



¹³C NMR spectrum (100 MHz, DMSO-*d*₆) for *N*-(3,5-Difluorophenyl)-*N'*-(3-(*tert*-butyl)-1-(phenyl)-1*H*-pyrazol-5-yl)urea

B04JD096CARBON_01.esp

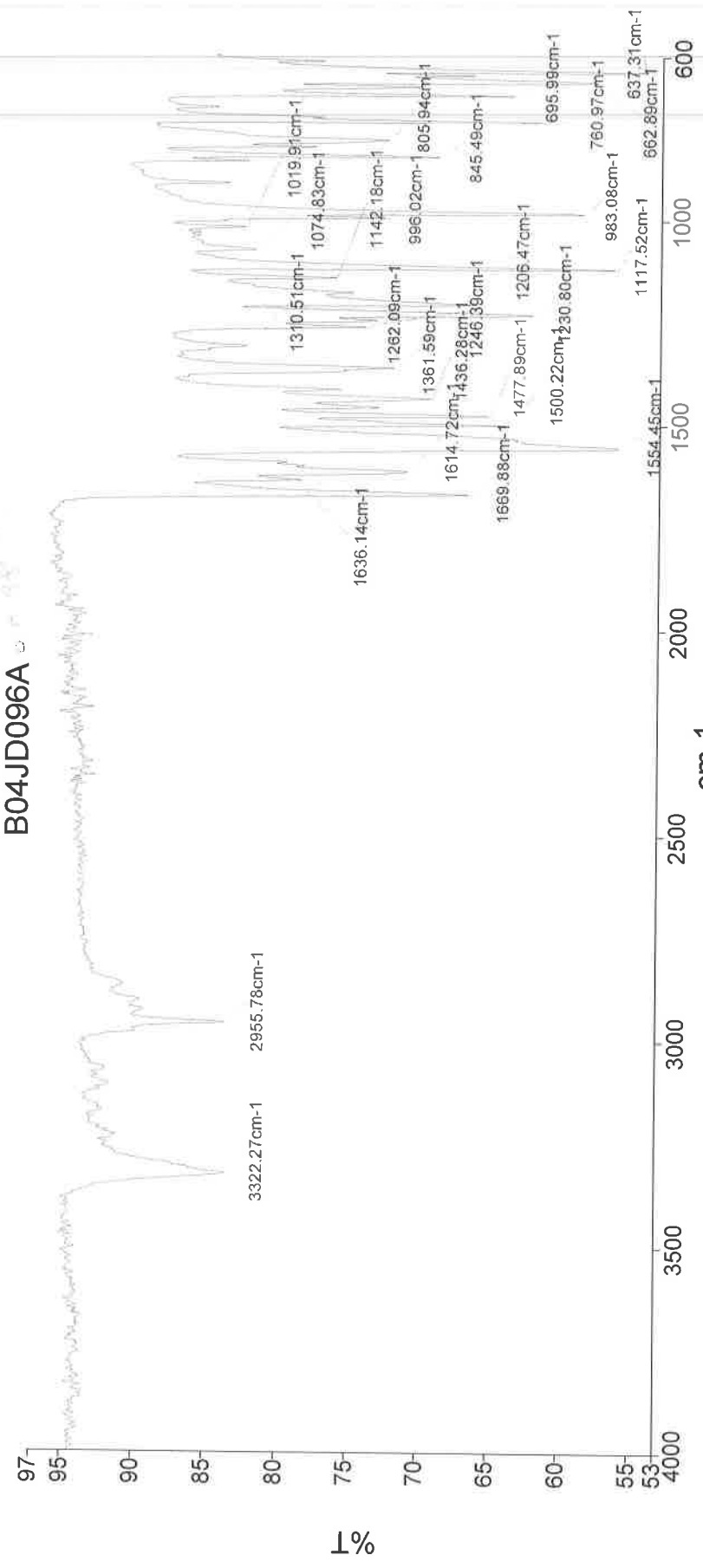




PerkinElmer Spectrum Version 10.03.06
11 November 2015 14:13

Analyst
Date
Administrator
11 November 2015 14:13

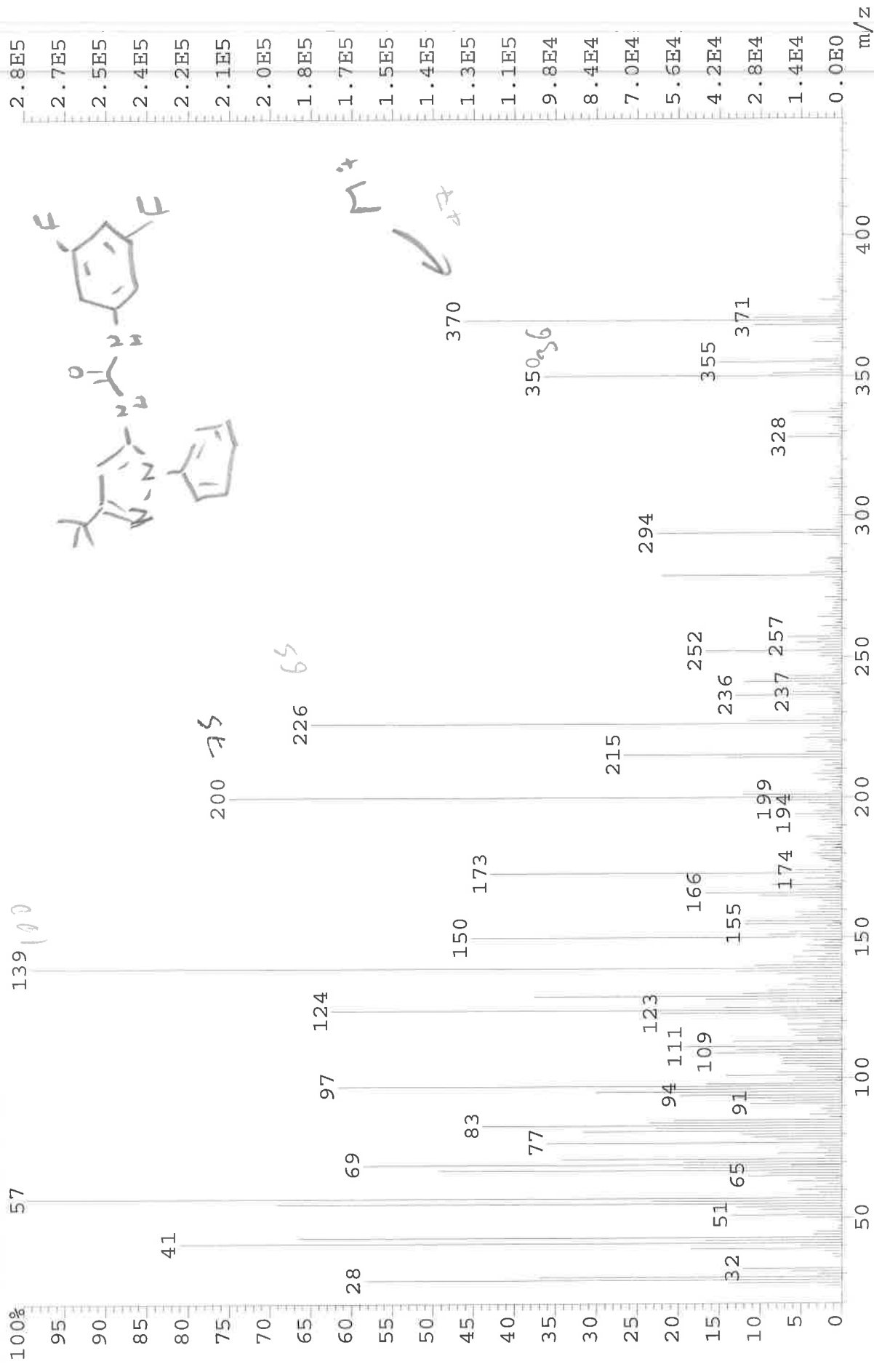
B04JD096A



3322 - N-H str.
2956 - C-H str.
1670 - C=O str.
1554 - N-H str.
1500 - C-C str.
1478 - C-C str.
1362 - CH₃
1231 - C-N str.
1117 - C-F str.

249-082 Sample 082 By Administrator Date Wednesday, November 11 2015

File: JESS6256 Ident: 22 Acq: 30-OCT-2015 17:19:40 +1:24 Cal: CAL1
AutoSpecE EI+ Magnet BpI: 279900 TIC: 7862755 Flags: HALL
File Text: B04JD096A



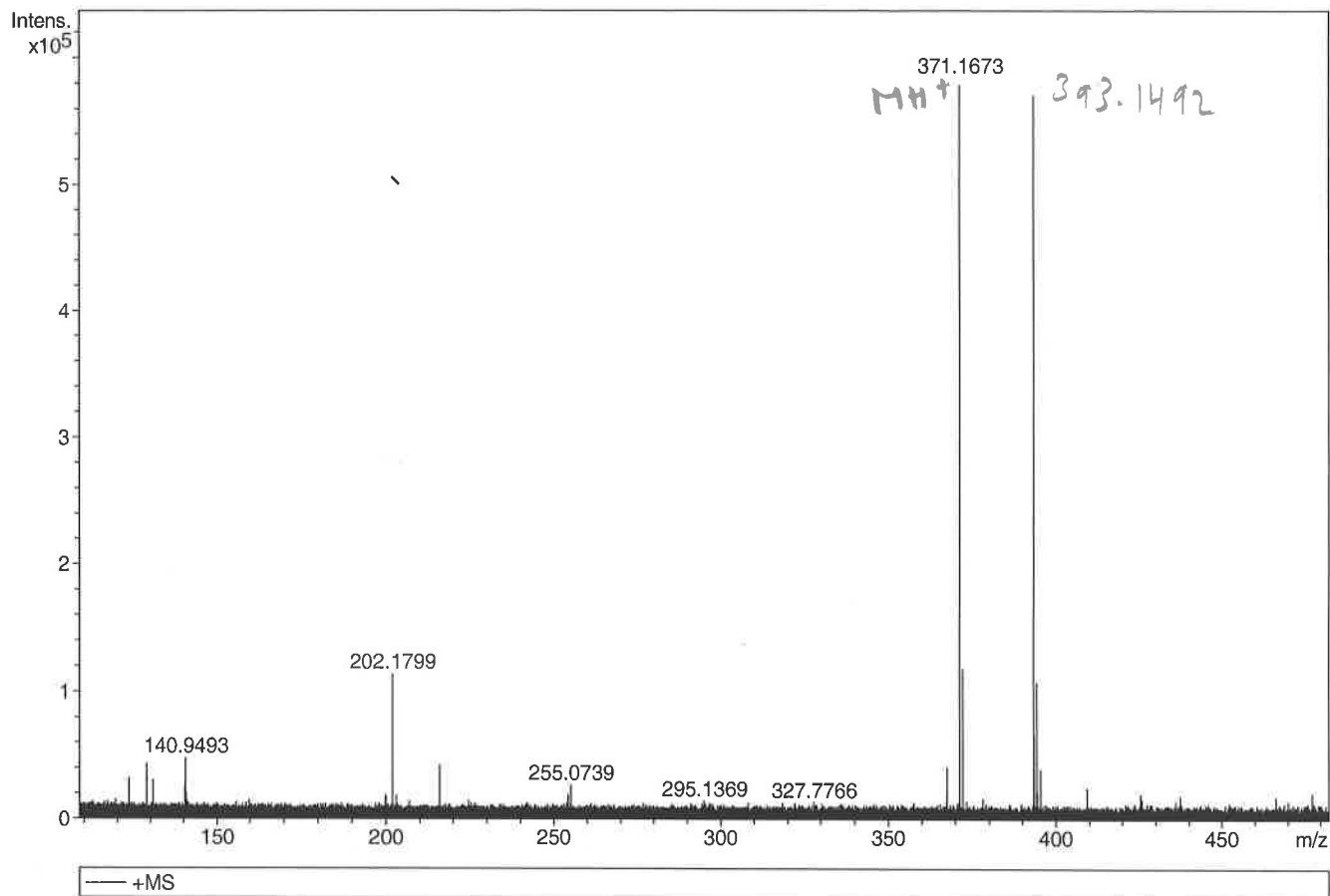
Generic Display Report

Analysis Info

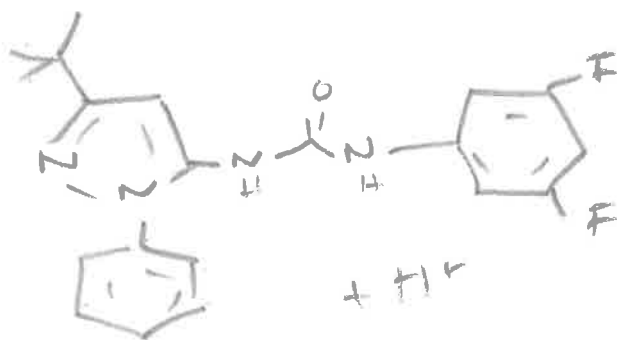
Analysis Name D:\Data\Alinanopos\JESS6256_000001.d
 Method pos20090608esi
 Sample Name POS ESI B04JD096A
 Comment

Acquisition Date 30/10/2015 12:51:05

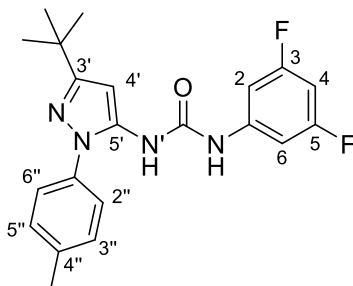
Operator Administrator
 Instrument apex-III



Sum Formula	Sigma	m/z	Err [ppm]	Mean Err [ppm]	Err [mDa]	rdb	N Rule	e ⁻
C ₂₀ H ₂₁ F ₂ N ₄ O	0.021	371.1678	1.36	0.39	0.15	11.50	ok	even

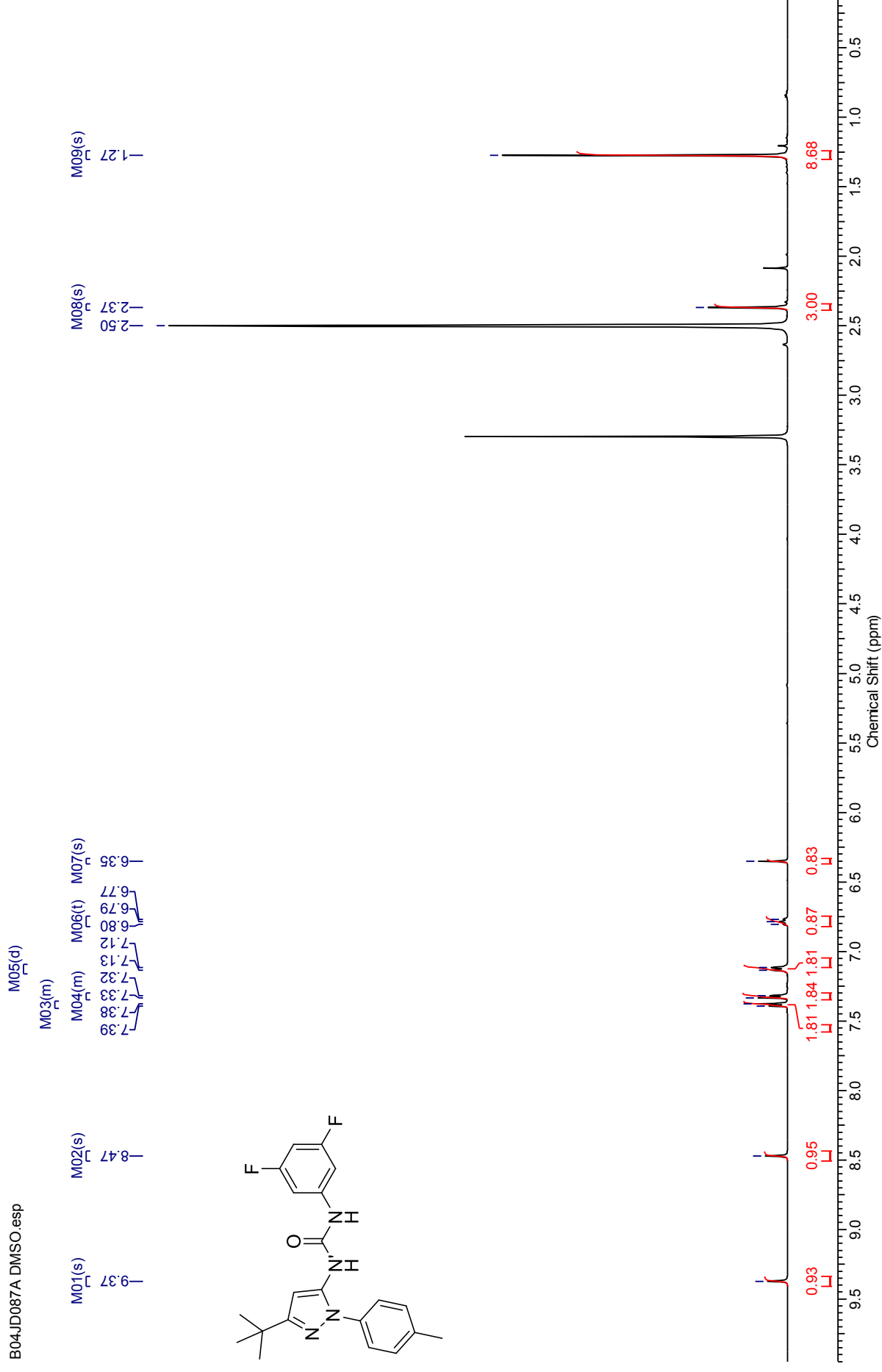


***N*-(3,5-Difluorophenyl)-*N'*-(3-(*tert*-butyl)-1-(*p*-tolyl)-1*H*-pyrazol-5-yl)urea (217O)**



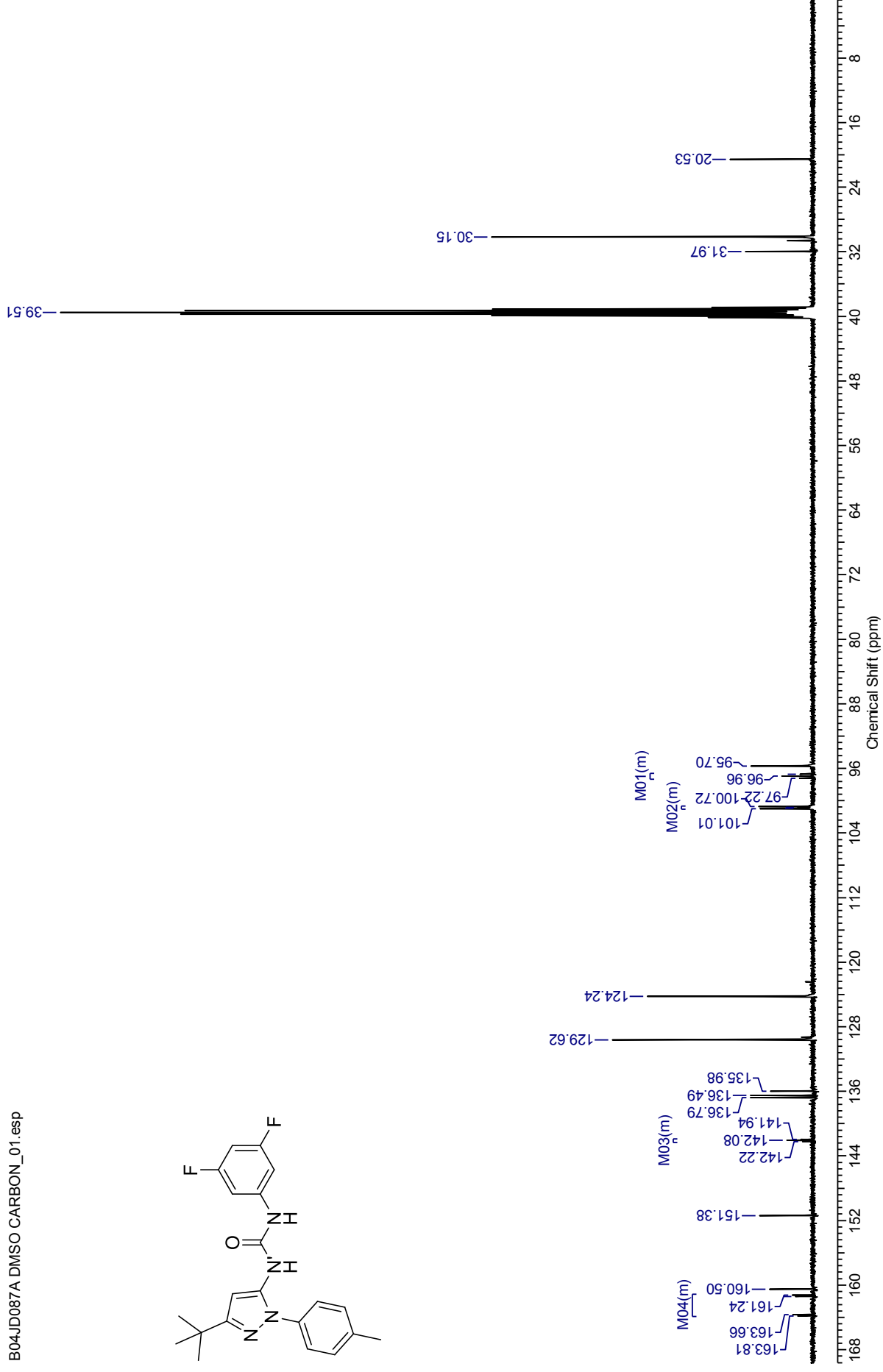
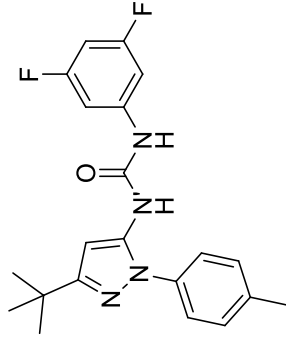
¹H NMR spectrum (500 MHz, DMSO-*d*₆) for *N*-(3,5-Difluorophenyl)-*N'*-(3-(*tert*-butyl)-1-(*p*-tolyl)-1*H*-pyrazol-5-yl)urea

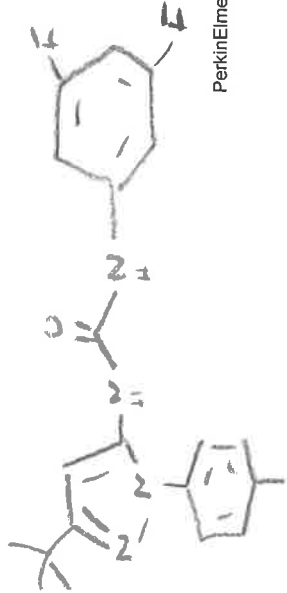
B04JD087A DMSO.esp



¹³C NMR spectrum (100 MHz, DMSO-*d*₆) for *N*-(3,5-Difluorophenyl)-*N'*-(3-(*tert*-butyl)-1-(*p*-tolyl)-1*H*-pyrazol-5-yl)urea

B04JD087A DMSO CARBON_01.esp

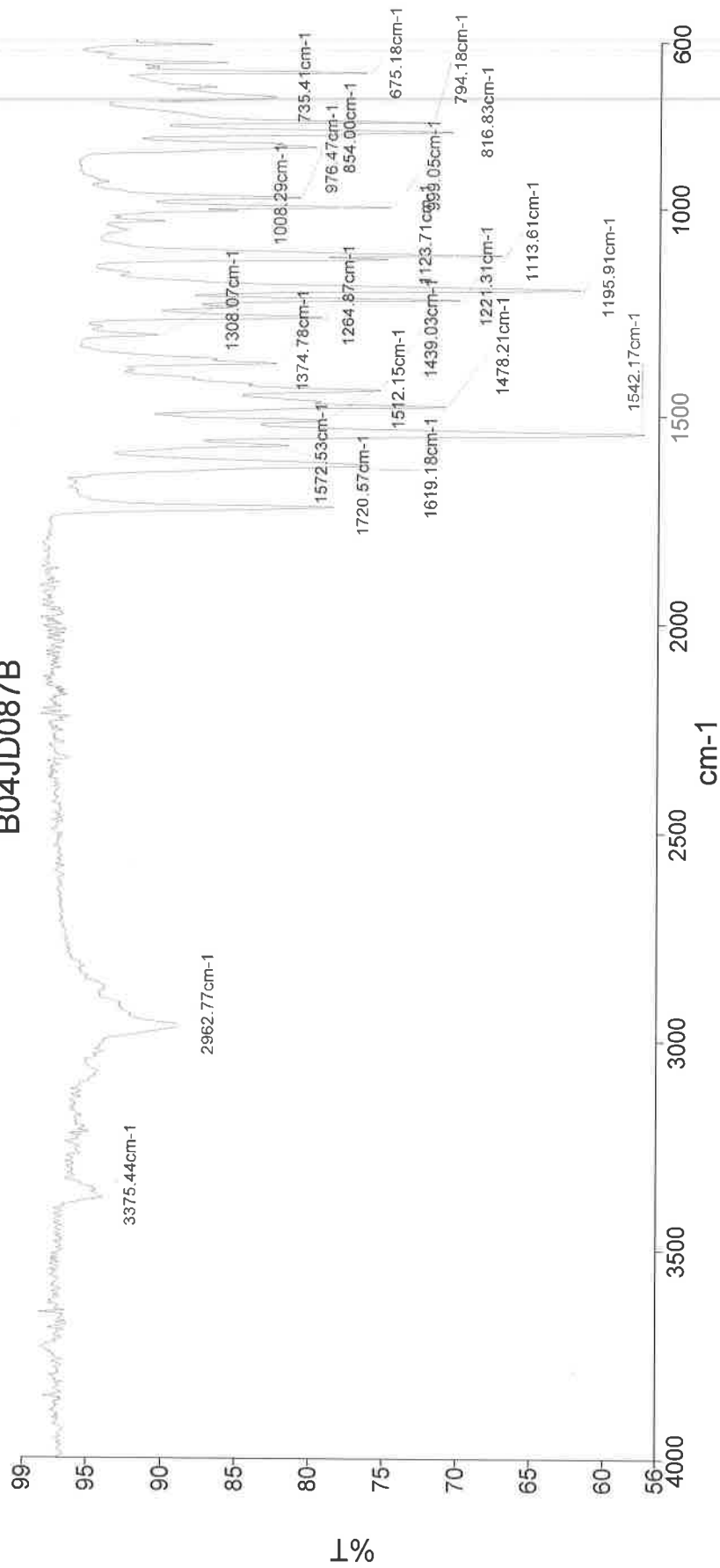




PerkinElmer Spectrum Version 10.03.06
11 November 2015 14:16

Analyst
Date
Administrator
11 November 2015 14:16

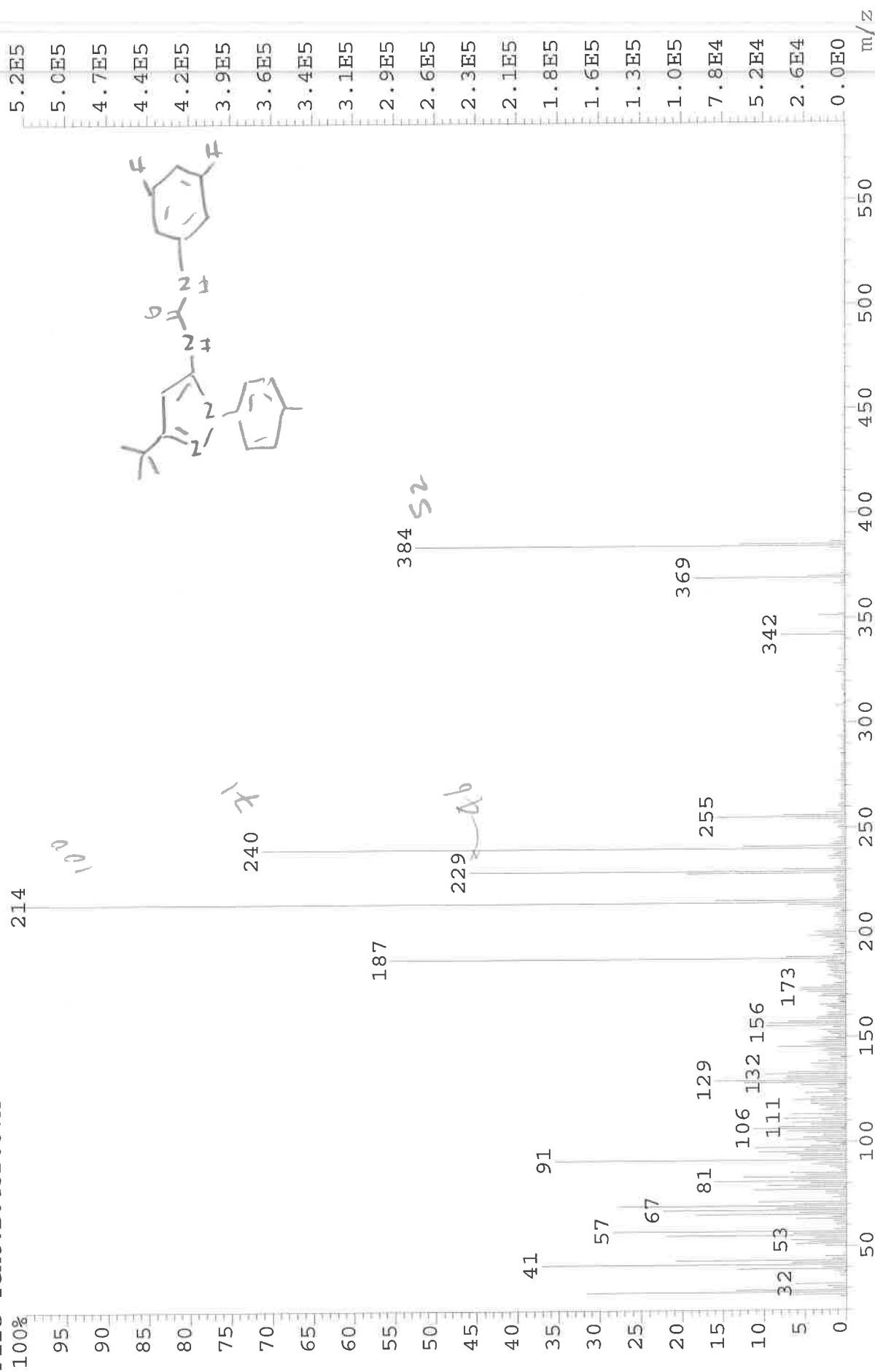
B04JD087B



3375 - N-H str.
2963 - C-H str.
1720 - C=O
1619 - N-H str.
1542 - N-H str.
1478 - C-C str.
1196 - C-N str.
1114 - C-F str.

249-083 Sample 083 By Administrator Date Wednesday, November 11 2015

File: JESS6250 Ident: 29 Acq: 29-OCT-2015 15:30:25 +1:50 Cal: CAL1
AutoSpecE EI+ Magnet BpI: 521148 TIC: 7795358 Flags: HALL
File Text: B04JD087A



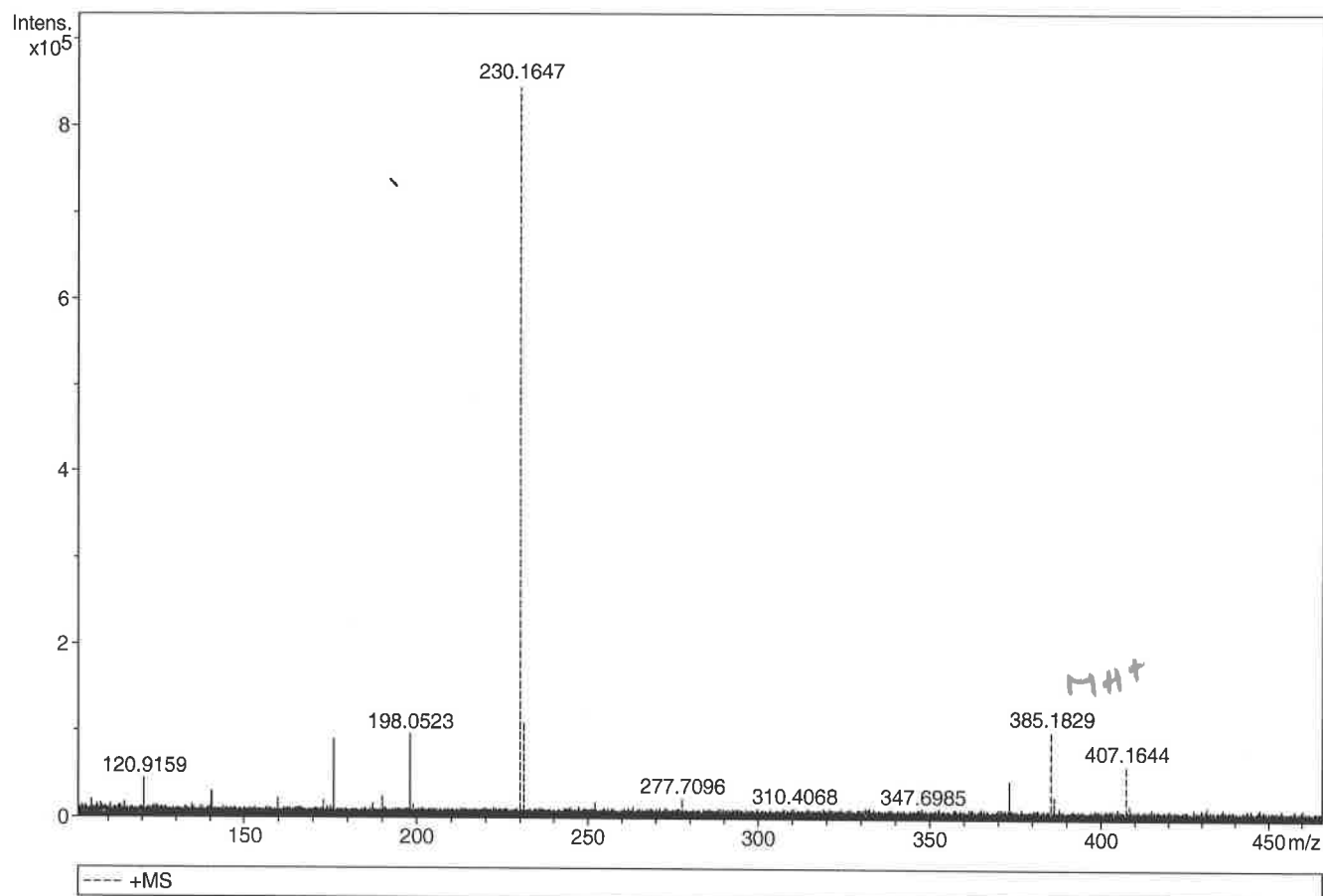
Generic Display Report

Analysis Info

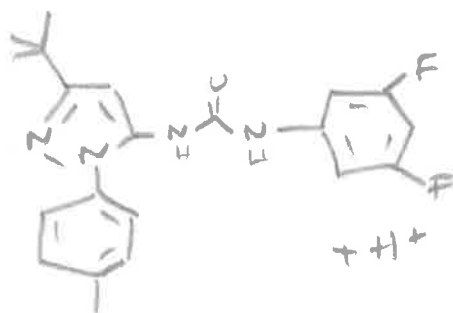
Analysis Name D:\Data\Alinanopos\JESS6250_000002.d
Method pos20090608esi
Sample Name POS ESI BO4JDO87A
Comment

Acquisition Date 29/10/2015 13:36:11

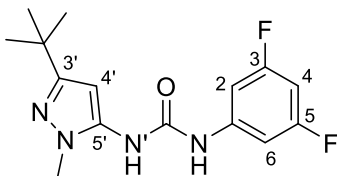
Operator Administrator
Instrument apex-III



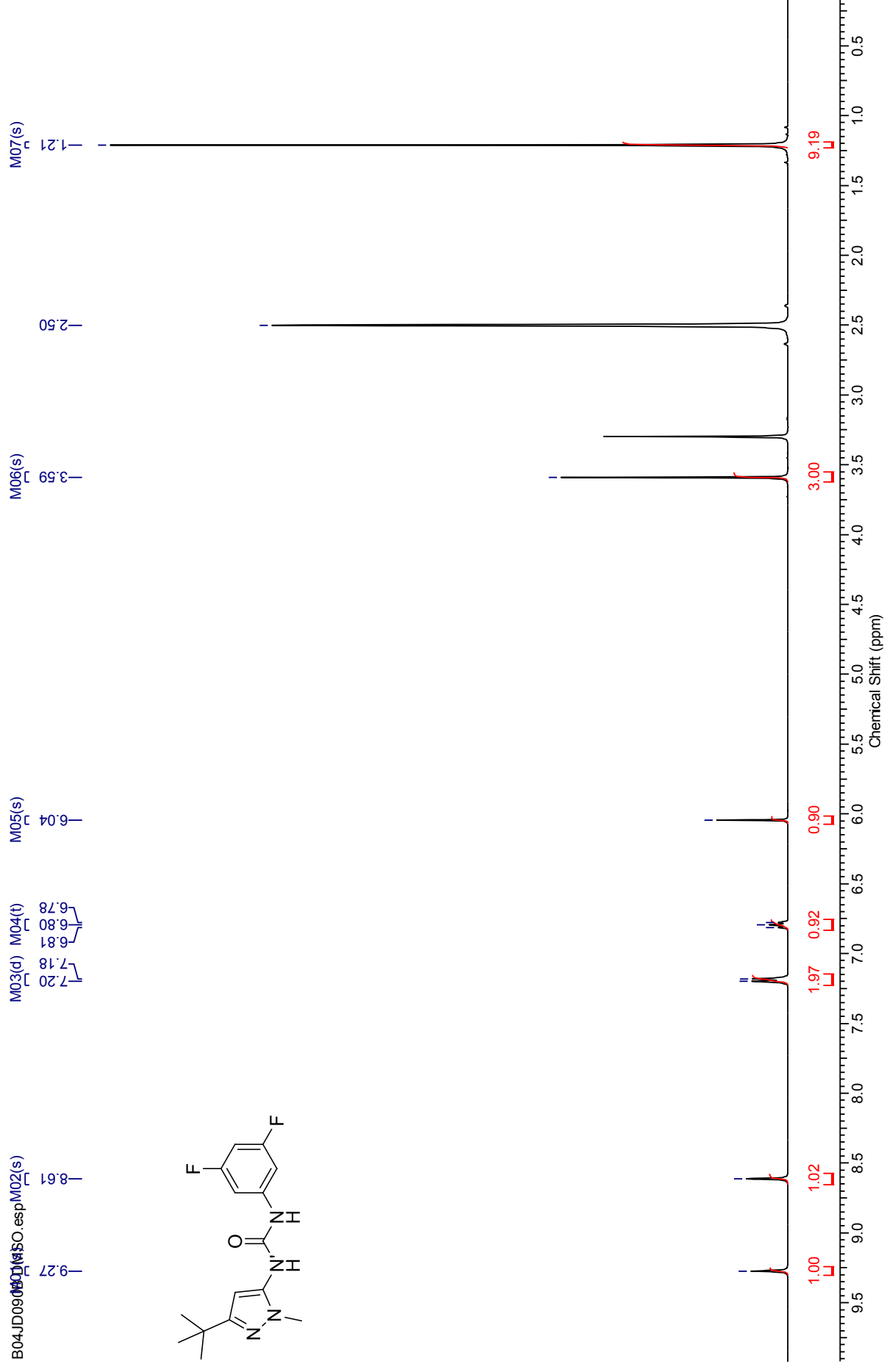
Sum Formula	Sigma	m/z	Err [ppm]	Mean Err [ppm]	Err [mDa]	rdb	N Rule	e ⁻
C 21 H 23 F 2 N 4 O 1	0.019	385.1834	1.39	0.97	0.37	11.50	ok	even



***N*-(3,5-Difluorophenyl)-*N'*-(3-*tert*-butyl-1-methyl-1*H*-pyrazol-5-yl)urea (226O)**

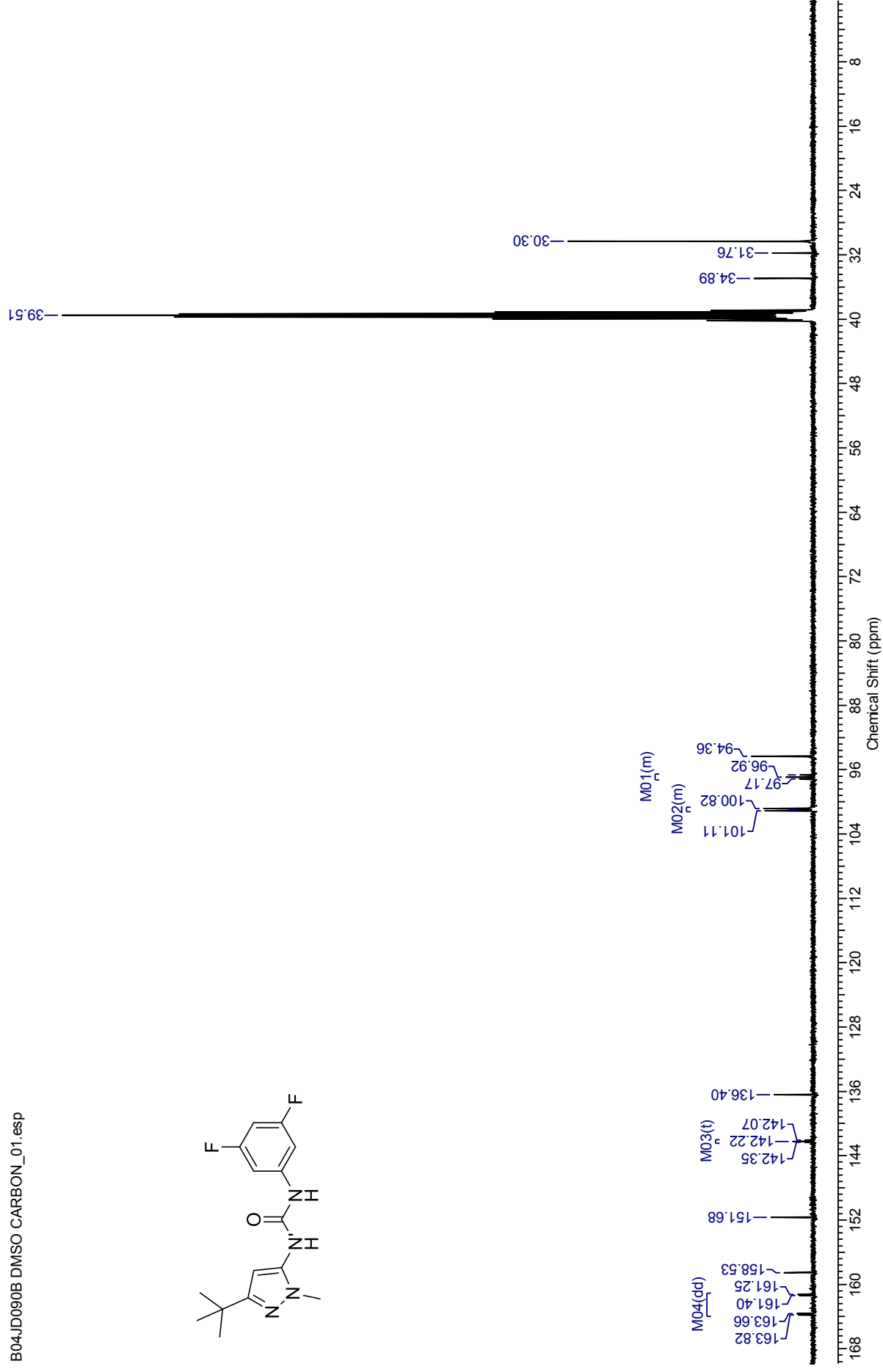
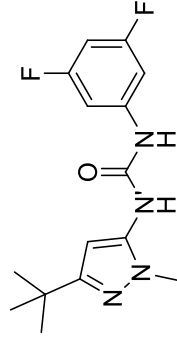


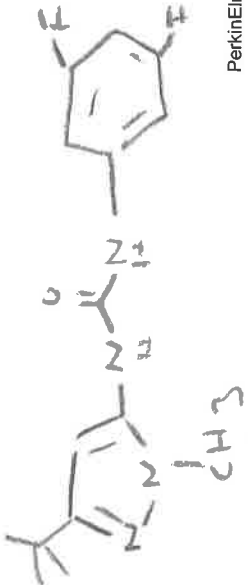
¹H NMR spectrum (500 MHz, DMSO-*d*₆) for *N*-(3,5-Difluorophenyl)-*N'*-(3-*tert*-butyl-1-methyl-1*H*-pyrazol-5-yl)urea



¹³C NMR spectrum (100 MHz, DMSO-*d*₆) for *N*-(3,5-Difluorophenyl)-*N'*-(3-*tert*-butyl-1-methyl-1*H*-pyrazol-5-yl)urea

B04JD090B DMSO CARBON_01.esp

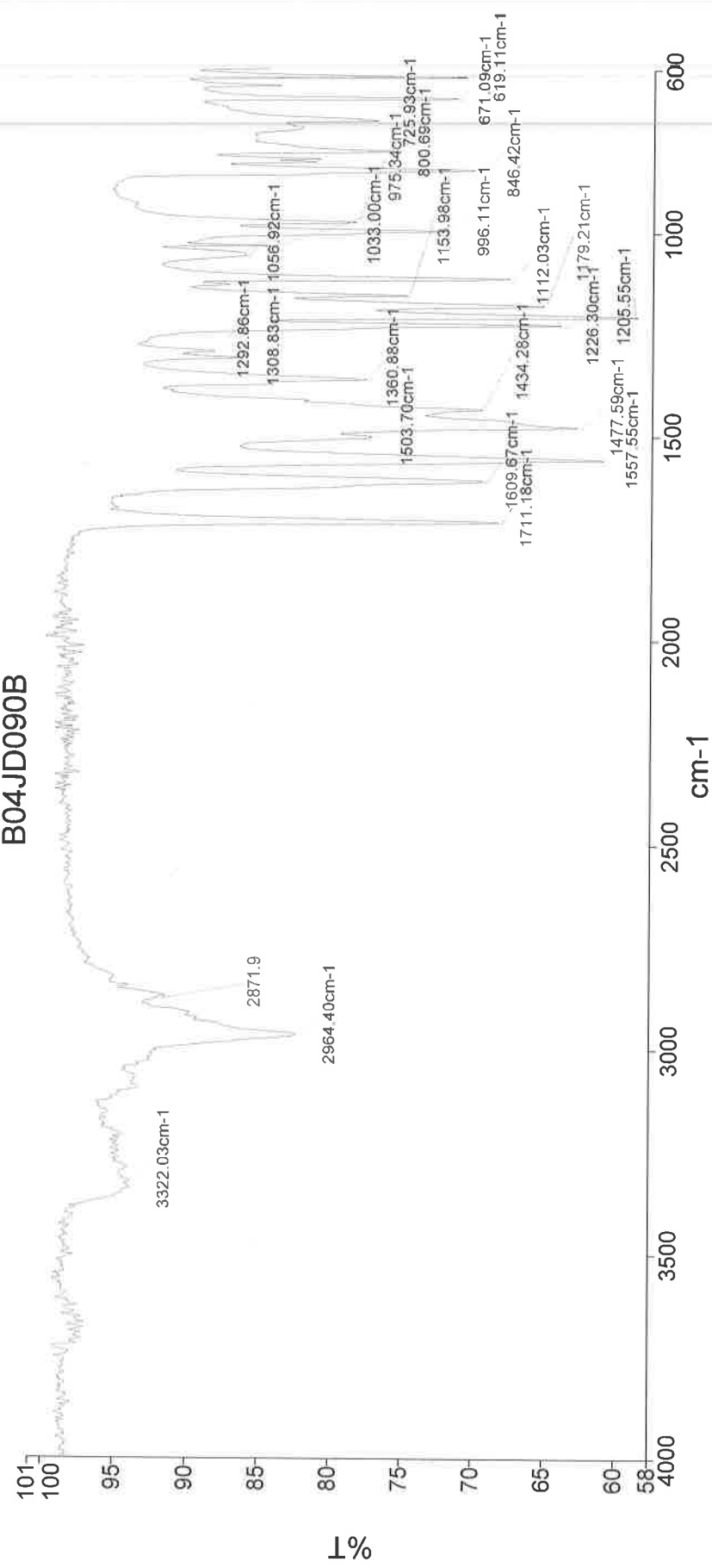




PerkinElmer Spectrum Version 10.03.06
11 November 2015 14:22

Analyst
Date
Administrator
11 November 2015 14:22

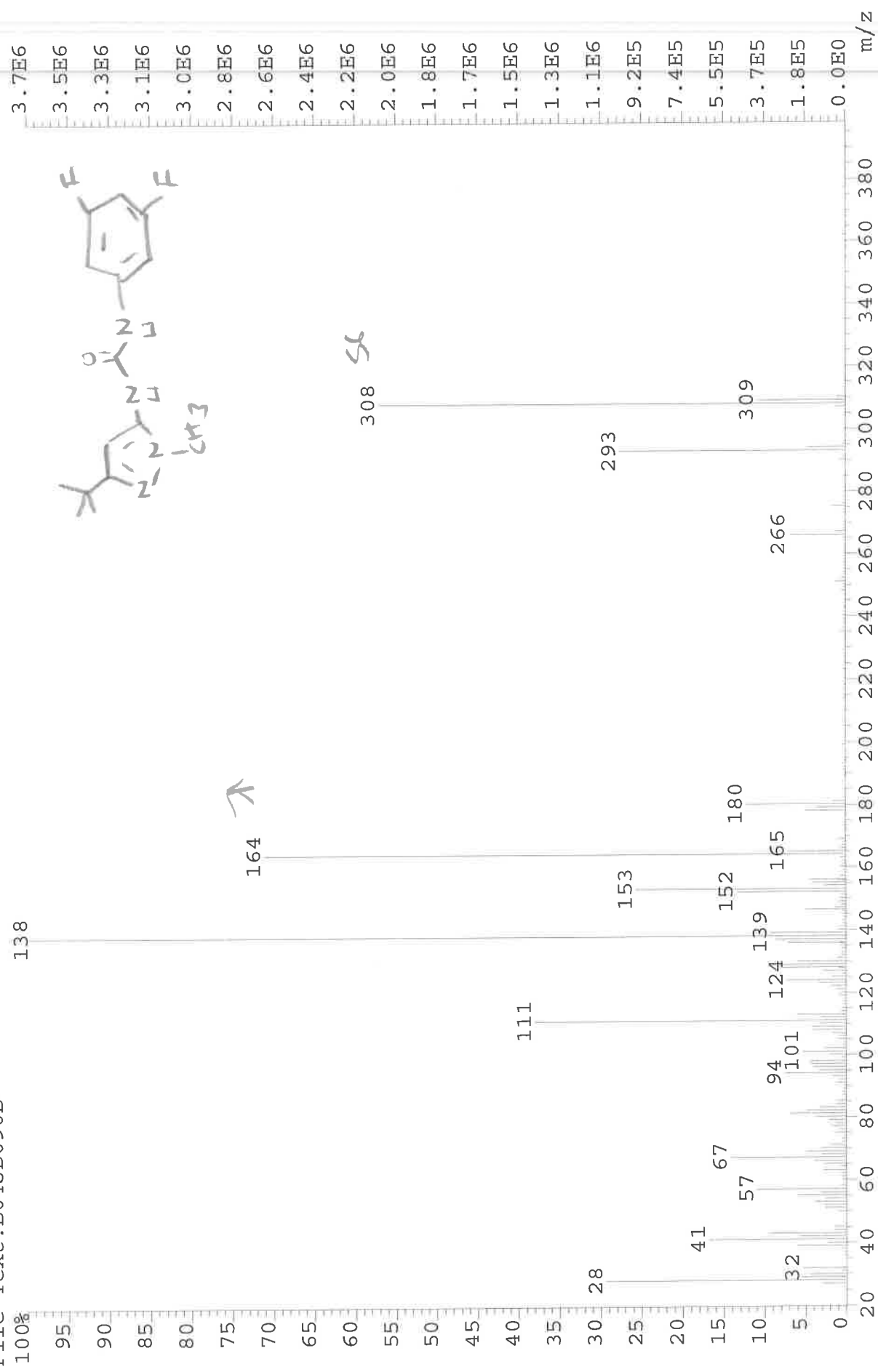
B04JD090B



3322 - N-H str
2964 - C-H str
1711 - C=O
1610 - N-H
1558 - N-H bend
1478 - C-H
1206 - C-N
1112 - C-F

249-085 Sample 085 By Administrator Date Wednesday, November 11 2015

File: JESS6251 Ident: 20 Acq: 29-OCT-2015 15:24:46 +1:17 Cal: CAL1
AutoSpecE EI+ Magnet BpI: 3696286 TIC: 29380120 Flags: HALL
File Text: B04JD090B



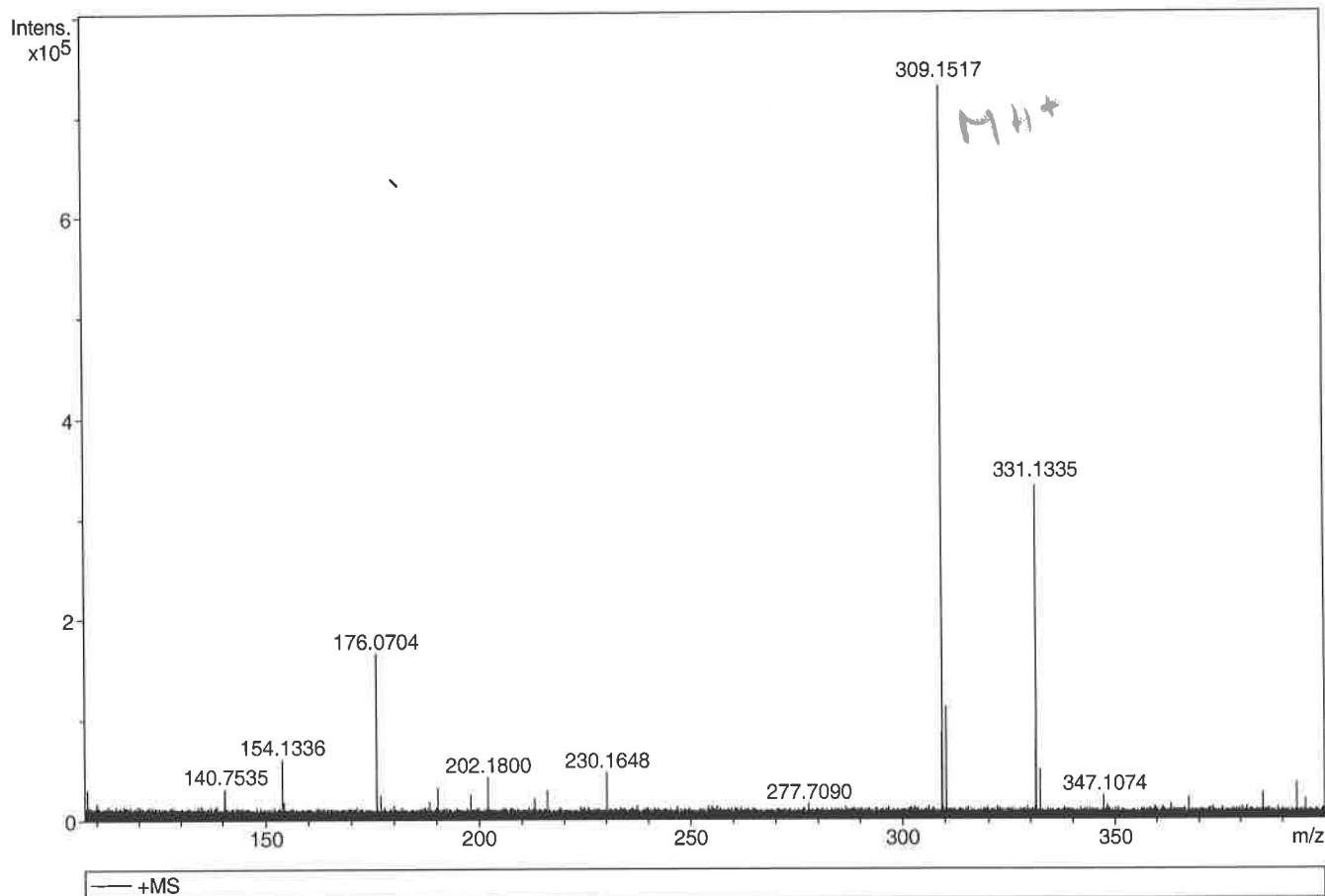
Generic Display Report

Analysis Info

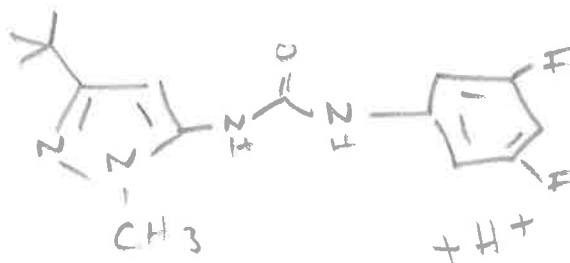
Analysis Name D:\Data\Alinanopos\JESS6251..000001.d
Method pos20090608esi
Sample Name POS ESI BO4JDO90B
Comment

Acquisition Date 29/10/2015 13:37:51

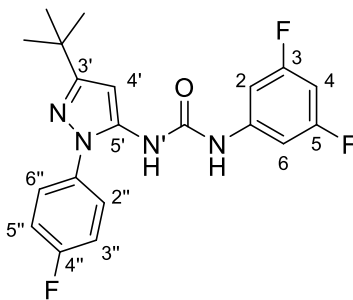
Operator Administrator
Instrument apex-III



Sum Formula	Sigma	m/z	Err [ppm]	Mean Err [ppm]	Err [mDa]	rdb	N Rule	e ⁻
C 15 H 19 F 2 N 4 O 1	0.027	309.1521	1.41	-0.65	-0.20	7.50	ok	even

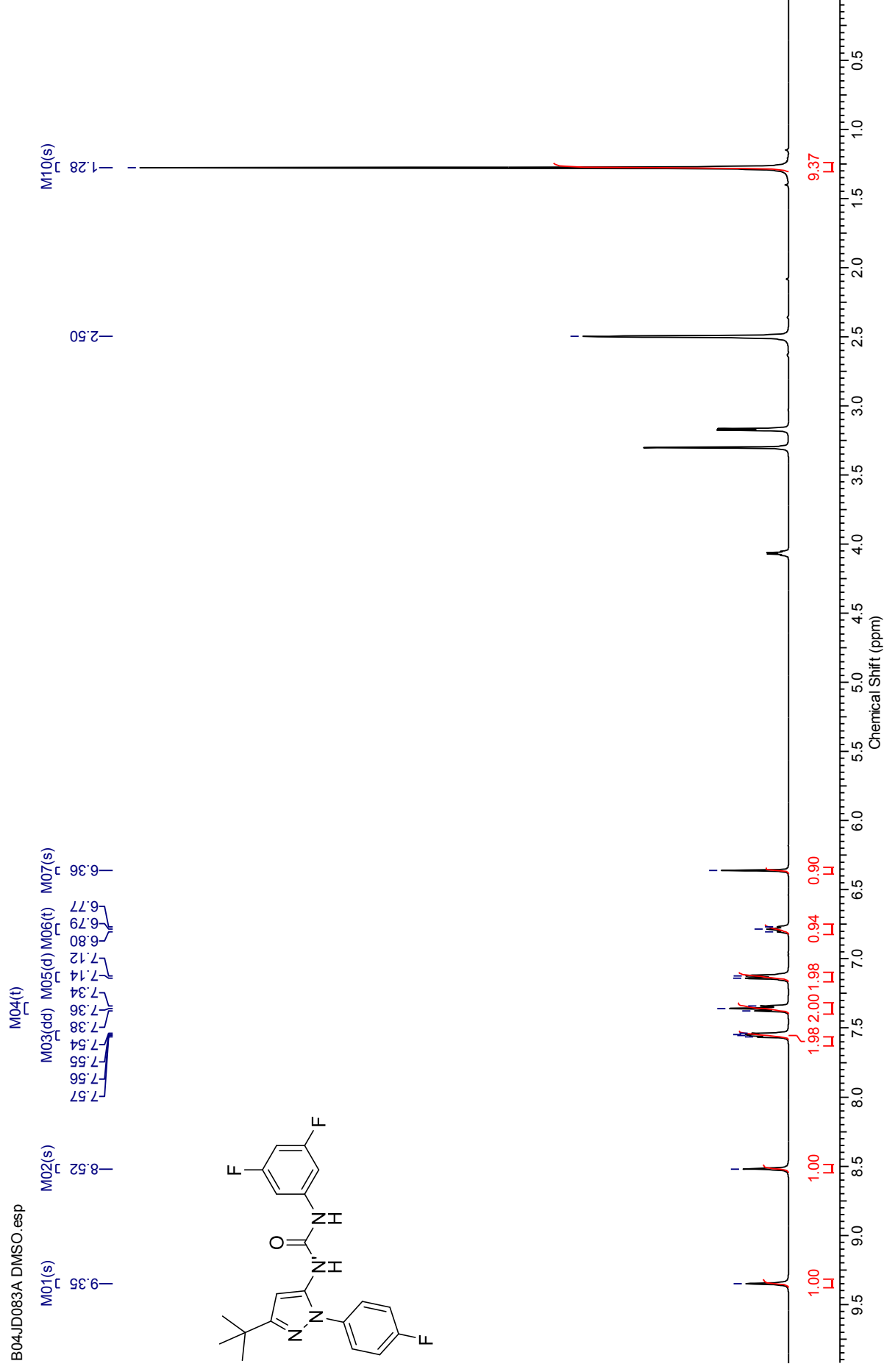


***N*-(3,5-Difluorophenyl)-*N'*-(3-(*tert*-butyl)-1-(4-fluorophenyl)-1*H*-pyrazol-5-yl)urea (227O)**



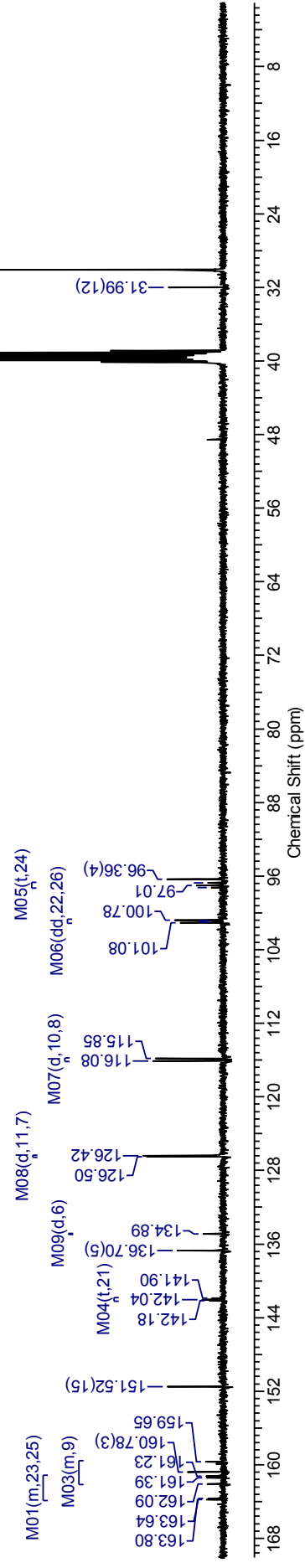
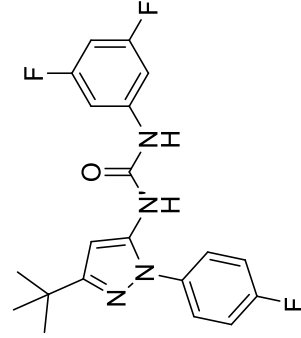
¹H NMR spectrum (500 MHz, DMSO-*d*₆) for *N*-(3,5-Difluorophenyl)-*N'*-(3-(*tert*-butyl)-1-(4-fluorophenyl)-1*H*-pyrazol-5-yl)urea

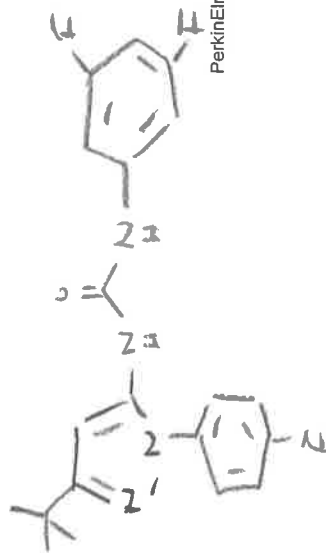
B04JD083A DMSO.esp



¹³C NMR spectrum (100 MHz, DMSO-*d*₆) for *N*-(3,5-Difluorophenyl)-*N'*-(3-(*tert*-butyl)-1-(4-fluorophenyl)-1*H*-pyrazol-5-yl)urea

B04JD083A CARBON_01 - mislabelled on 400.esp

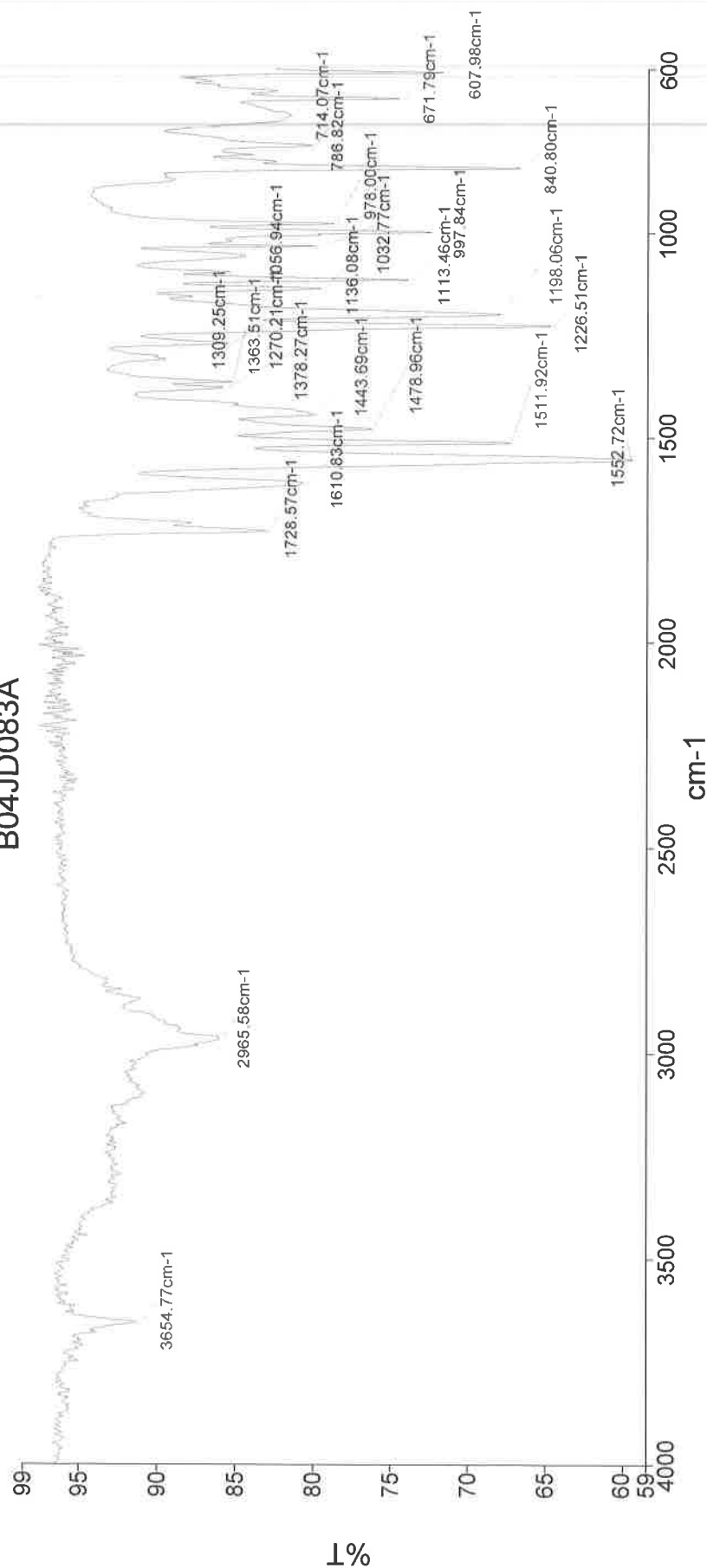




PerkinElmer Spectrum Version 10.03.06
11 November 2015 14:25

Analyst
Date
Administrator
11 November 2015 14:25

B04JD083A



2966 - C-H str.
1728 - C=O str.
1612 - N-H bend
1553 - N-H bend

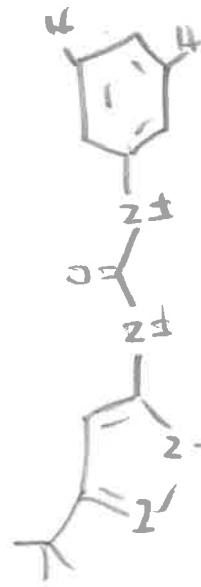
1226 - C-N str.
1113 - C-F

249-086 Sample 086 By Administrator Date Wednesday, November 11 2015

File Text:BO4JD083A

Chemical structure of compound 10j: CC(C)(C)C1=CC=C(C=C1)C(=C2C=CC(=C2)C(=O)N2C=CC(F)=CC(F)=C2)N3C=CC(F)=CC(F)=C3

m/z	Relative Intensity (%)
41	~25
57	~20
69	~25
81	~15
95	~30
110	~10
129	~15
149	~15
155	~10
177	~5
191	~55
218	100
234	~30
244	~60
261	~15
347	~10
374	~25
389	~10



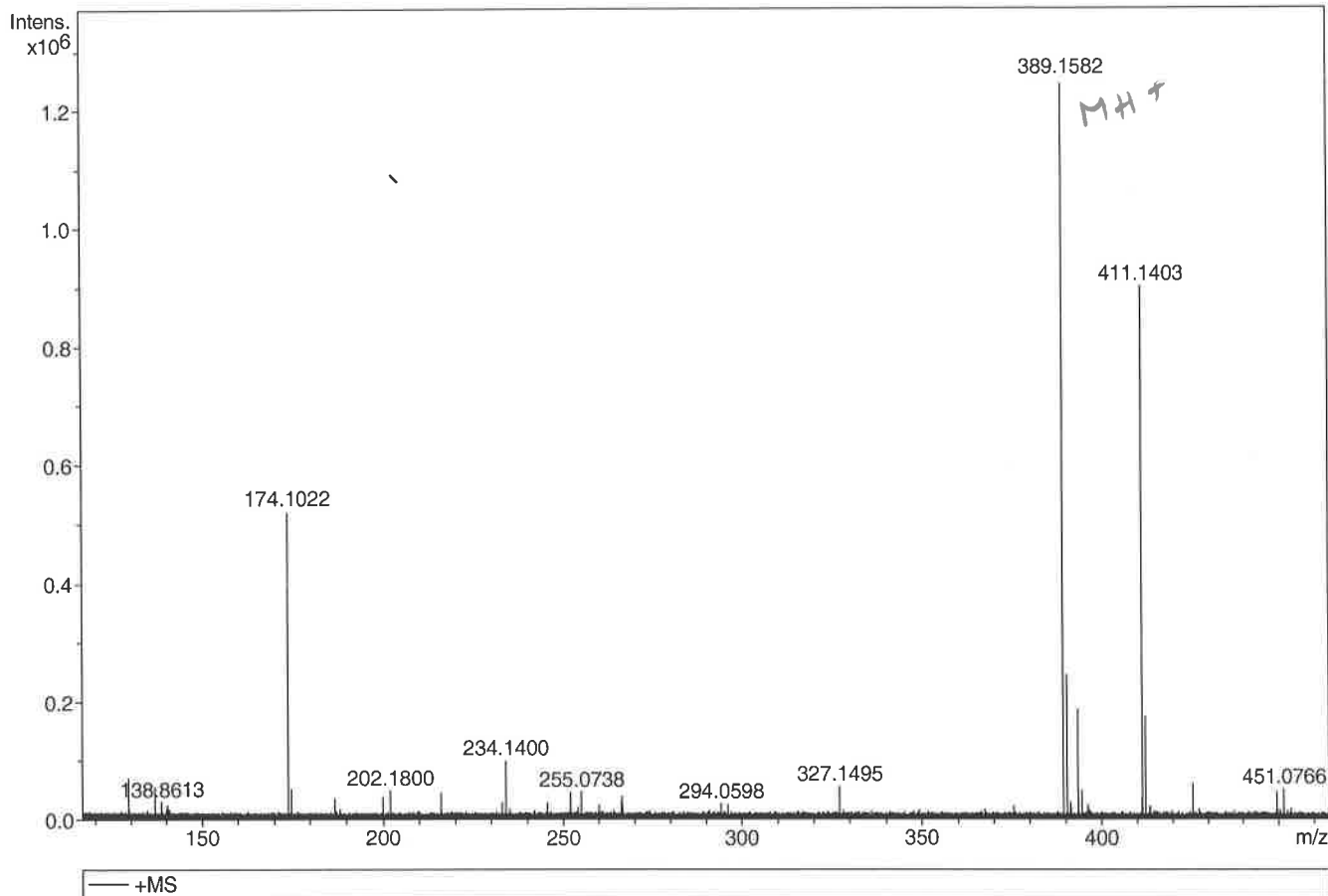
Generic Display Report

Analysis Info

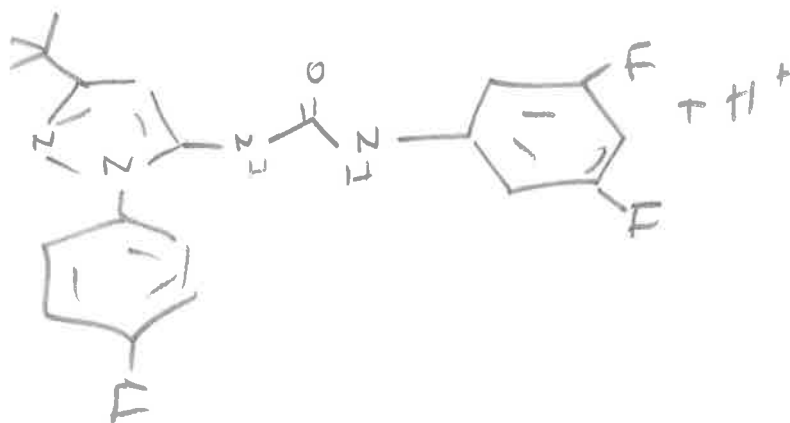
Analysis Name D:\Data\Allnanopos\JESS6210_000001.d
 Method pos20090608esi
 Sample Name POS ESI B04JD083A
 Comment

Acquisition Date 21/10/2015 10:32:58

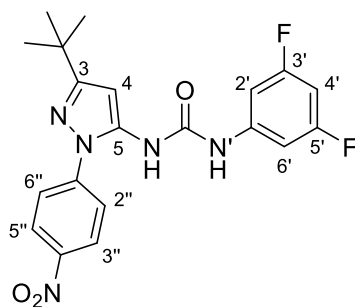
Operator Administrator
 Instrument apex-III



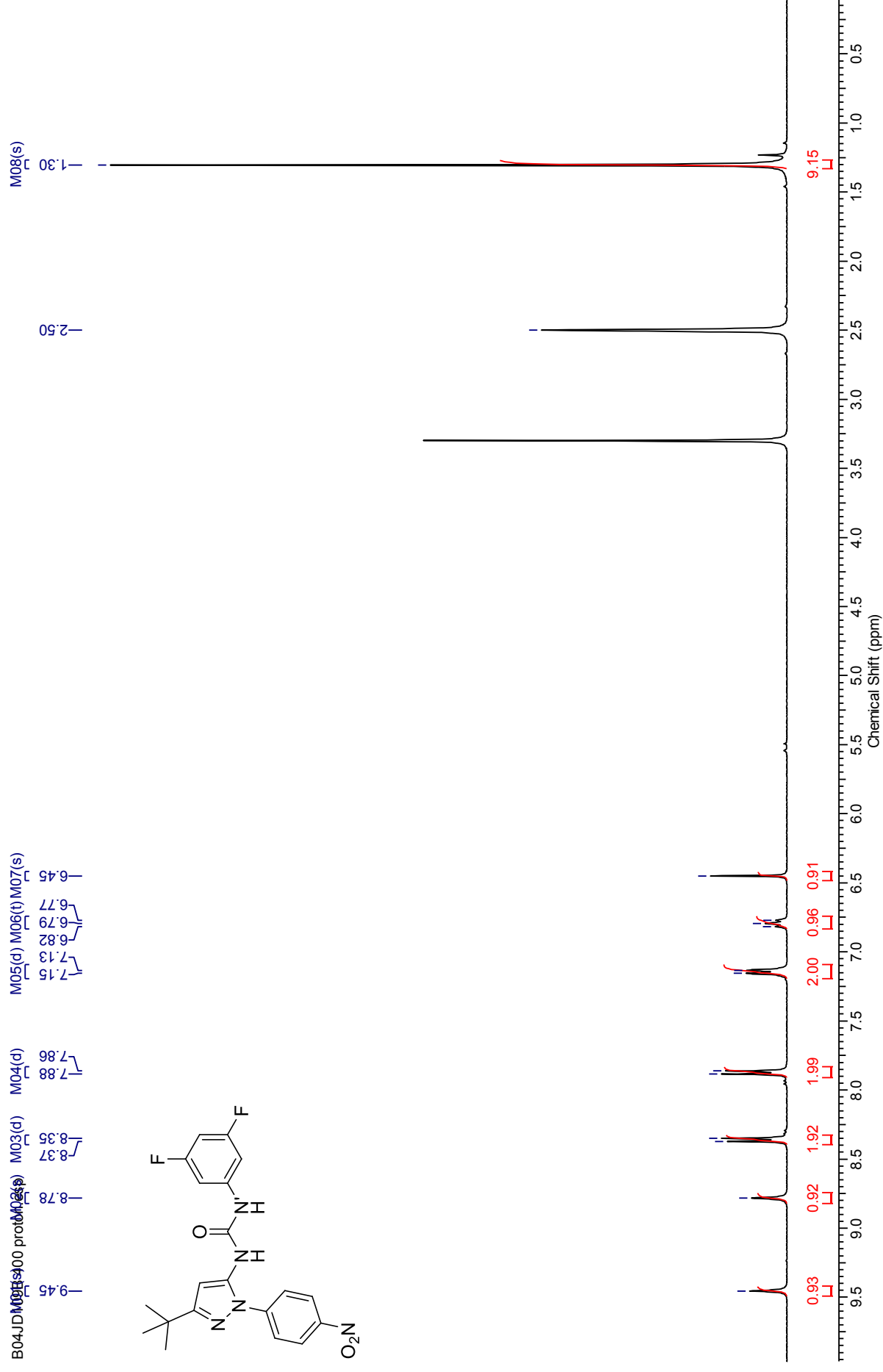
Sum Formula	Sigma	m/z	Err [ppm]	Mean Err [ppm]	Err [mDa]	rdb	N Rule	e ⁻
C 20 H 20 F 3 N 4 O 1	0.037	389.1584	0.56	-1.60	-0.62	11.50	ok	even



***N*-3-(*tert*-Butyl)-1-(4-nitrophenyl)-1*H*-pyrazol-5-yl)-*N'*-(3,5-difluorophenyl)urea (2280)**

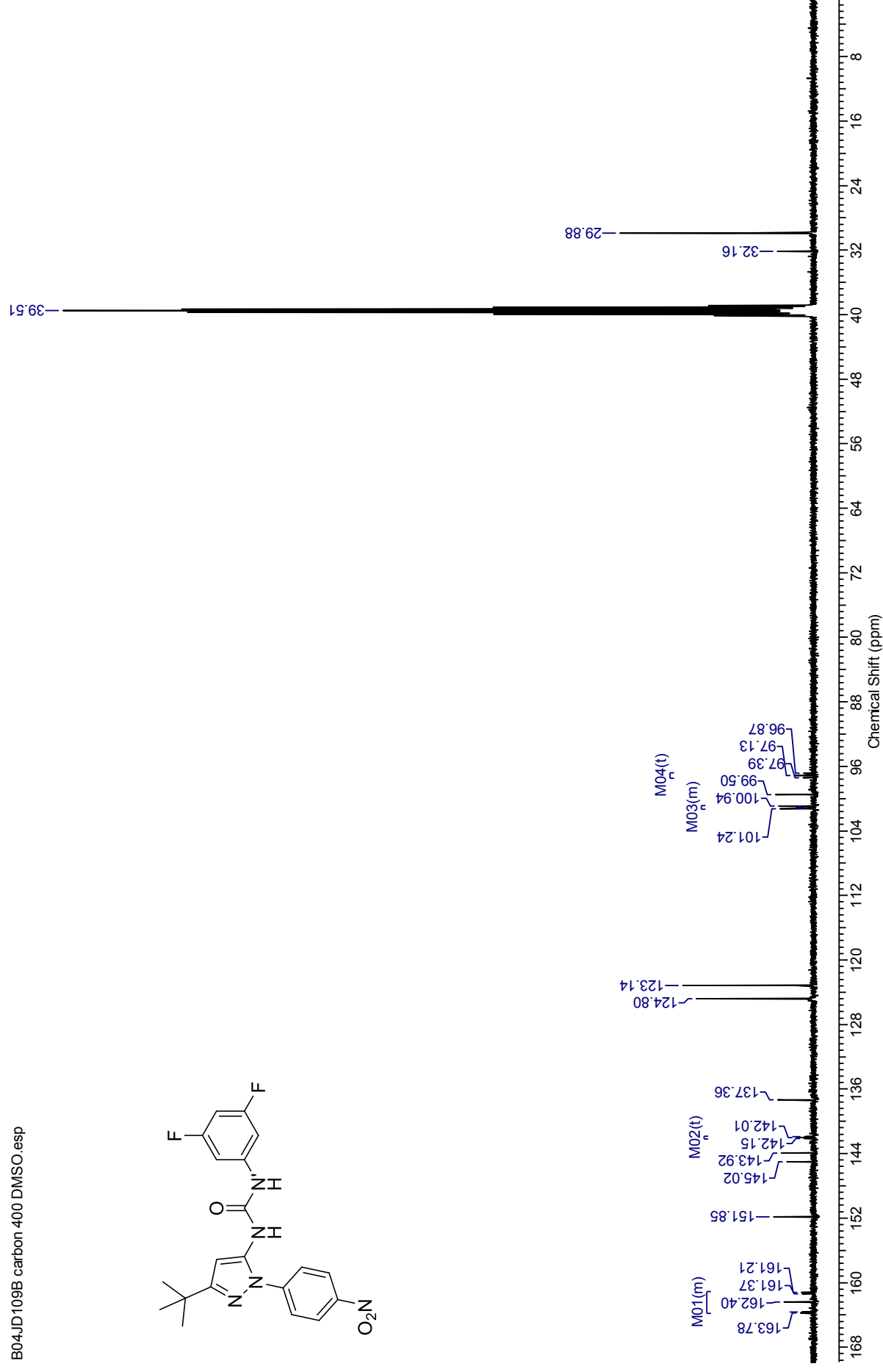
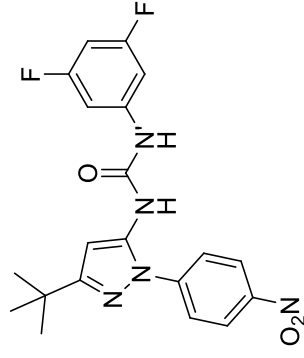


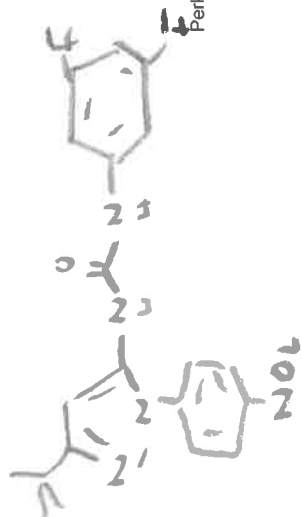
¹H NMR spectrum (399 MHz, DMSO-*d*₆) for *N*-3-(*tert*-Butyl)-1-(4-nitrophenyl)-1*H*-pyrazol-5-yl)-*N'*-(3,5-difluorophenyl)urea



¹³C NMR spectrum (100 MHz, DMSO-*d*₆) for *N*-3-(*tert*-Butyl)-1-(4-nitrophenyl)-1*H*-pyrazol-5-yl)-*N'*-(3,5-difluorophenyl)urea

B04JD109B carbon 400 DMSO.esp

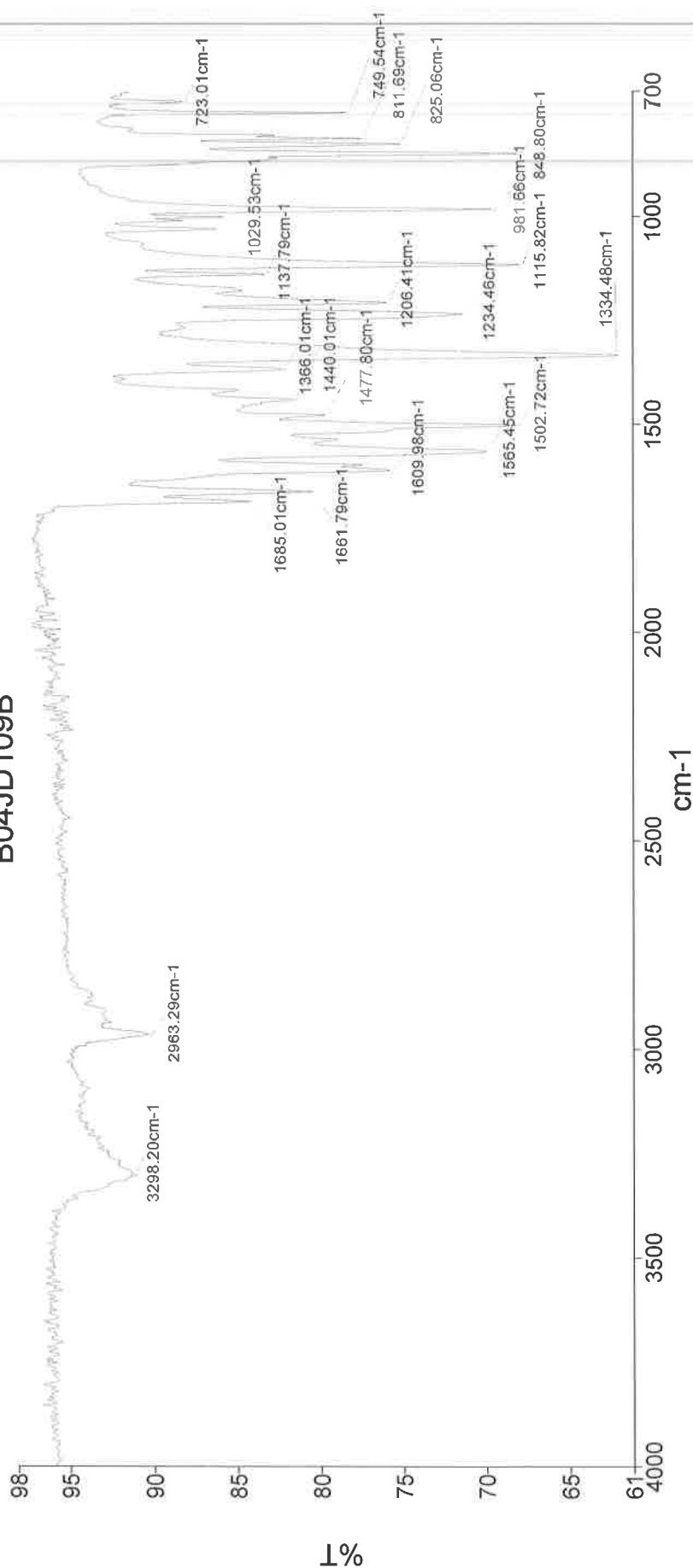




PerkinElmer Spectrum Version 10.03.06
18 November 2015 15:50

Analyst
Date
18 November 2015 15:50

B04JD109B



3298 - N-H str
2963 - C-H str
1662 C=O str.
1609 N-H str
1565 - N-H bend
1503 - N-O str.
1334 - N-O str.

File: JESS6345 Ident: 17 Acq: 25-NOV-2015 10:37:17 +1:06 Cal: CAL1
 AutoSpecE EI+ Magnet BpI: 743464 TIC: 17161112 Flags: HALL
 File Text: BO4JD109B



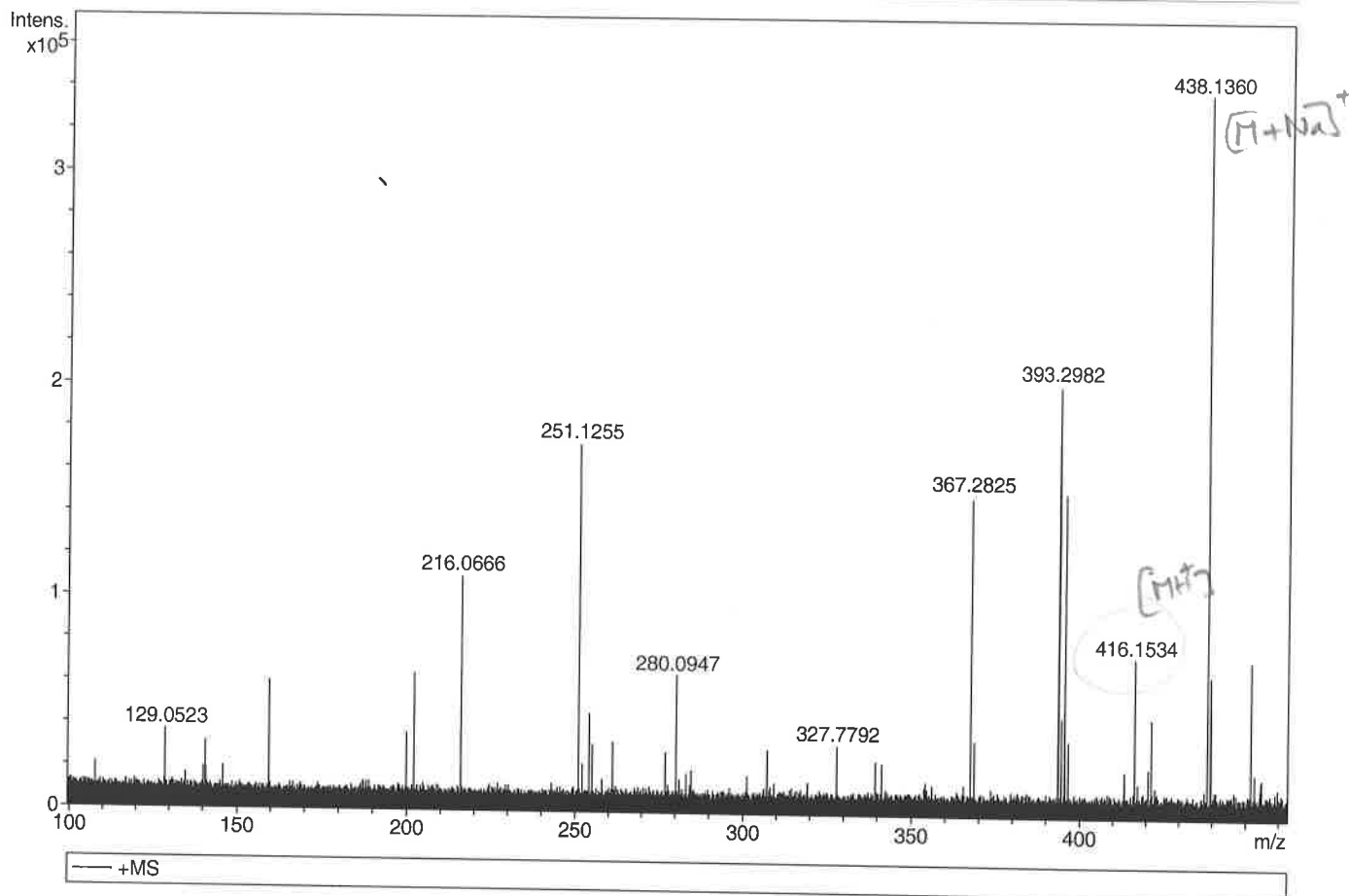
Generic Display Report

Analysis Info

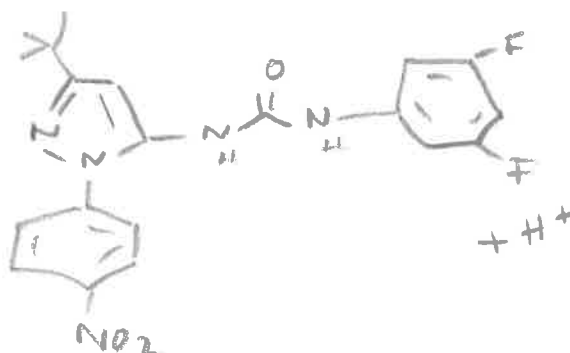
Analysis Name D:\Data\Alinanopos\JESS6345_000001.d
 Method pos20090608esi
 Sample Name POS ESI BO4JD109B
 Comment

Acquisition Date 25/11/2015 09:52:40

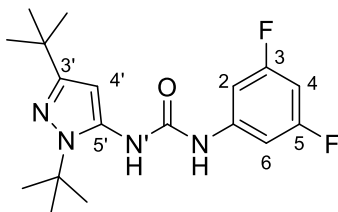
Operator Administrator
 Instrument apex-III



Sum Formula	Sigma	m/z	Err [ppm]	Mean Err [ppm]	Err [mDa]	rdb	N Rule	e ⁻
C 20 H 20 F 2 N 5 O 3	0.023	416.1529	-1.16	-1.60	-0.67	12.50	ok	even

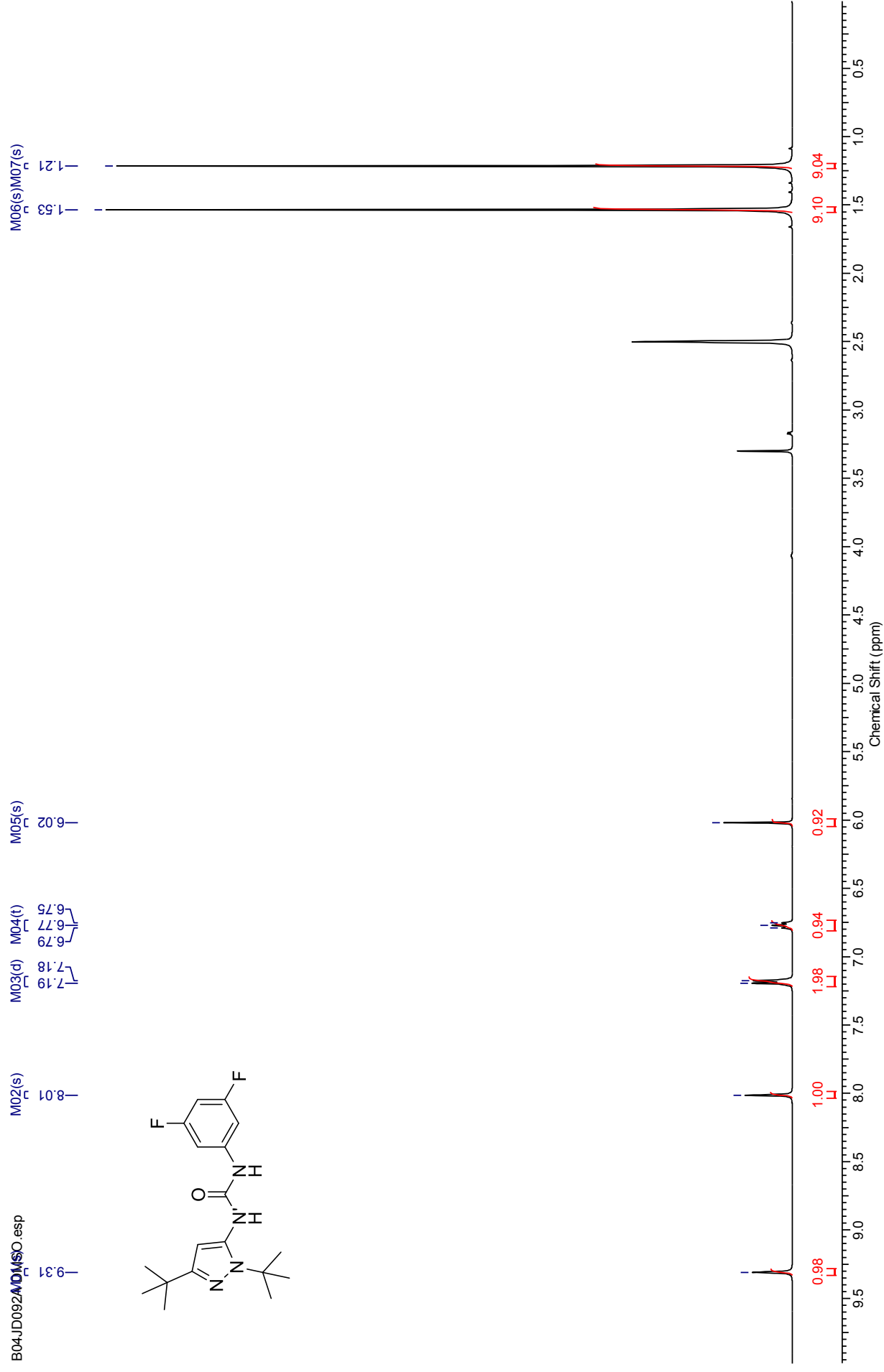


***N*-(3,5-Difluorophenyl)-*N'*-(1,3-(*tert*-butyl)-1*H*-pyrazol-5-yl)urea**
(2290)



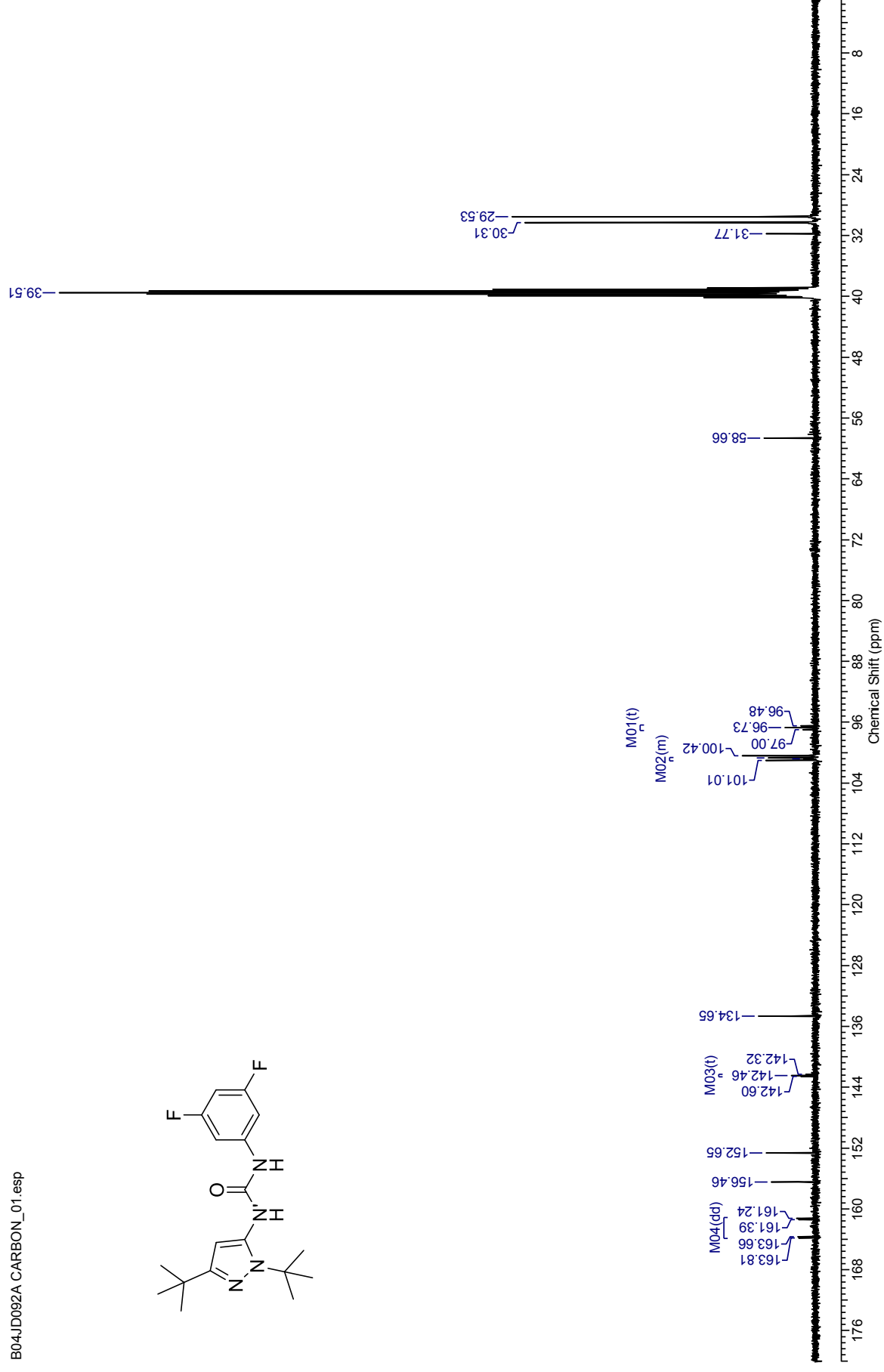
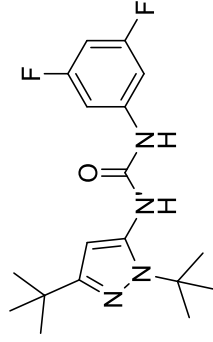
¹H NMR spectrum (500 MHz, DMSO-*d*₆) for *N*-(3,5-Difluorophenyl)-*N'*-(1,3-(*tert*-butyl)-1*H*-pyrazol-5-yl)urea

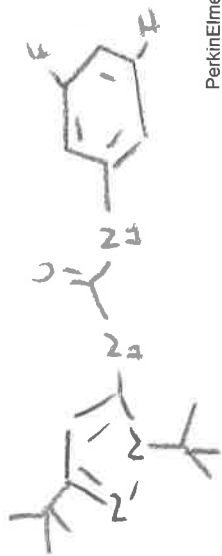
B04JD092401.DMSO esp



¹³C NMR spectrum (100 MHz, DMSO-*d*₆) for *N*-(3,5-Difluorophenyl)-*N'*-(1,3-(*tert*-butyl)-1*H*-pyrazol-5-yl)urea

B04JD092A CARBON_01.esp

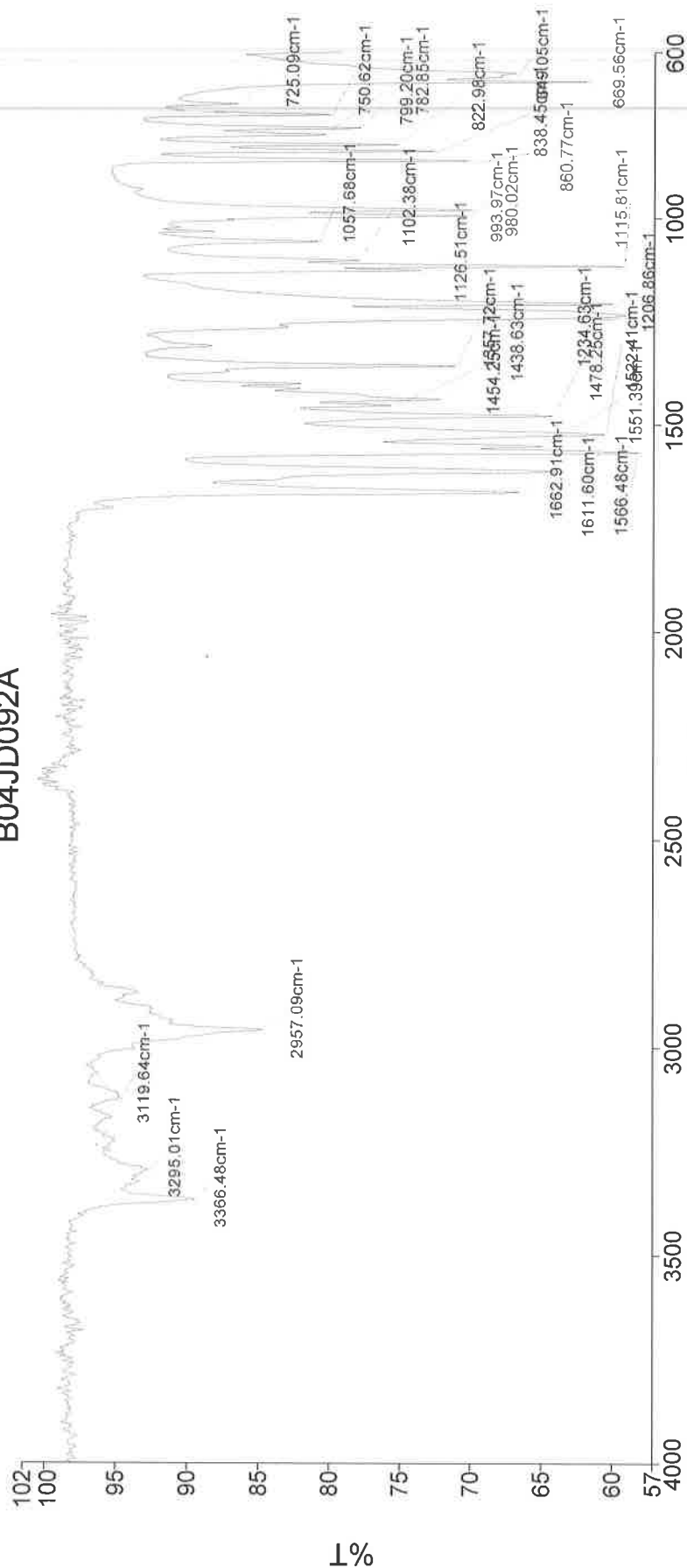




PerkinElmer Spectrum Version 10.03.06
11 November 2015 14:20

Analyst
Date
Administrator
11 November 2015 14:20

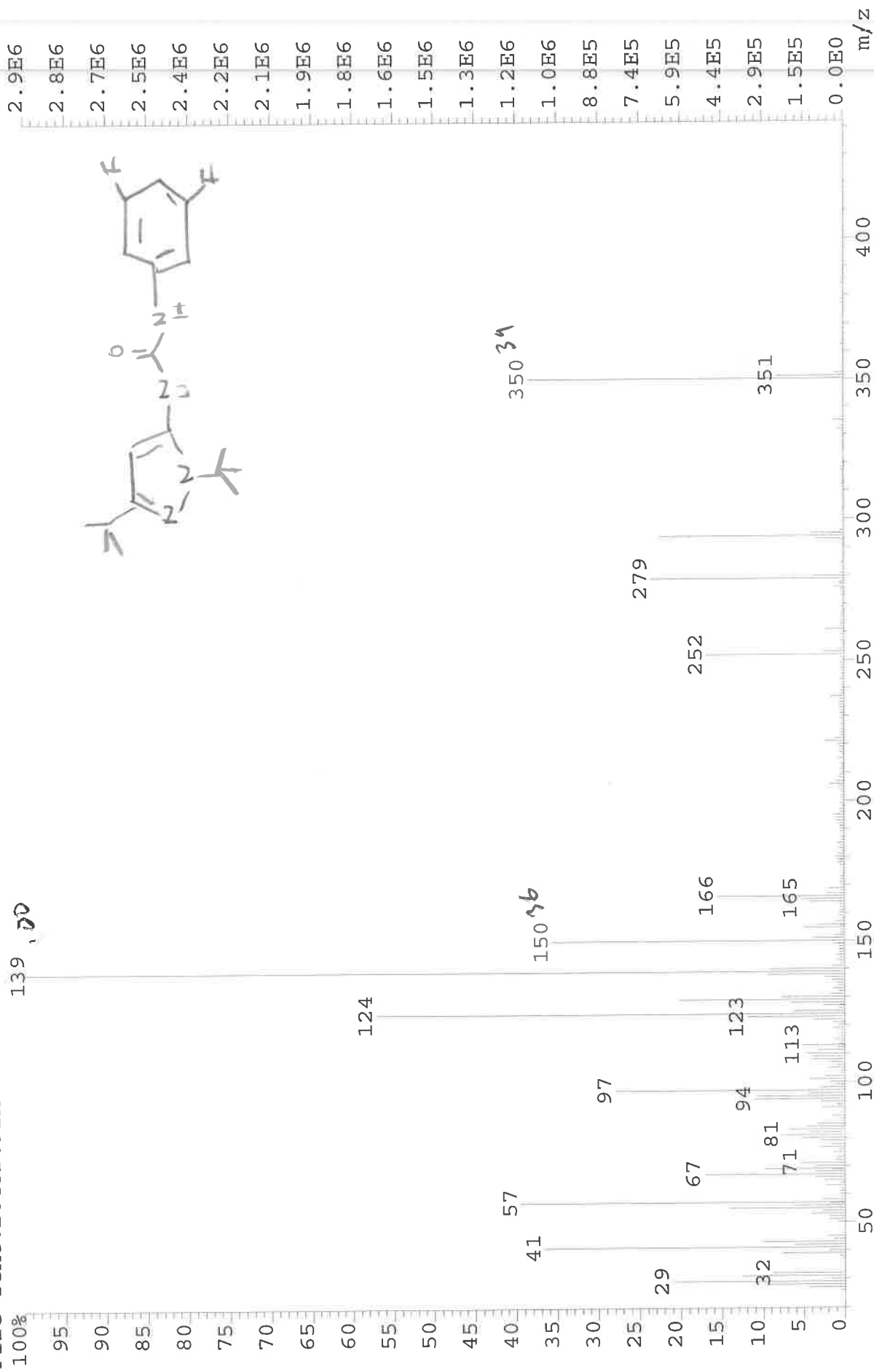
B04JD092A



3366 - N-H str.
2957 - C-H str.
1663 - C=O str.
1612 - N-H bend
1566 - N-H bend
1478 - C-H bend
1358 - C-N
1207 - C-N
1116 - C-F

249-084 Sample 084 By Administrator Date Wednesday, November 11 2015

File: JESS6255 Ident: 5 Acq: 30-OCT-2015 17:17:34 +0:22 Cal: CALL
 AutoSpecE EI+ Magnet BpI: 2948094 TIC: 28653820 Flags: HALL
 File Text: B04JD092A



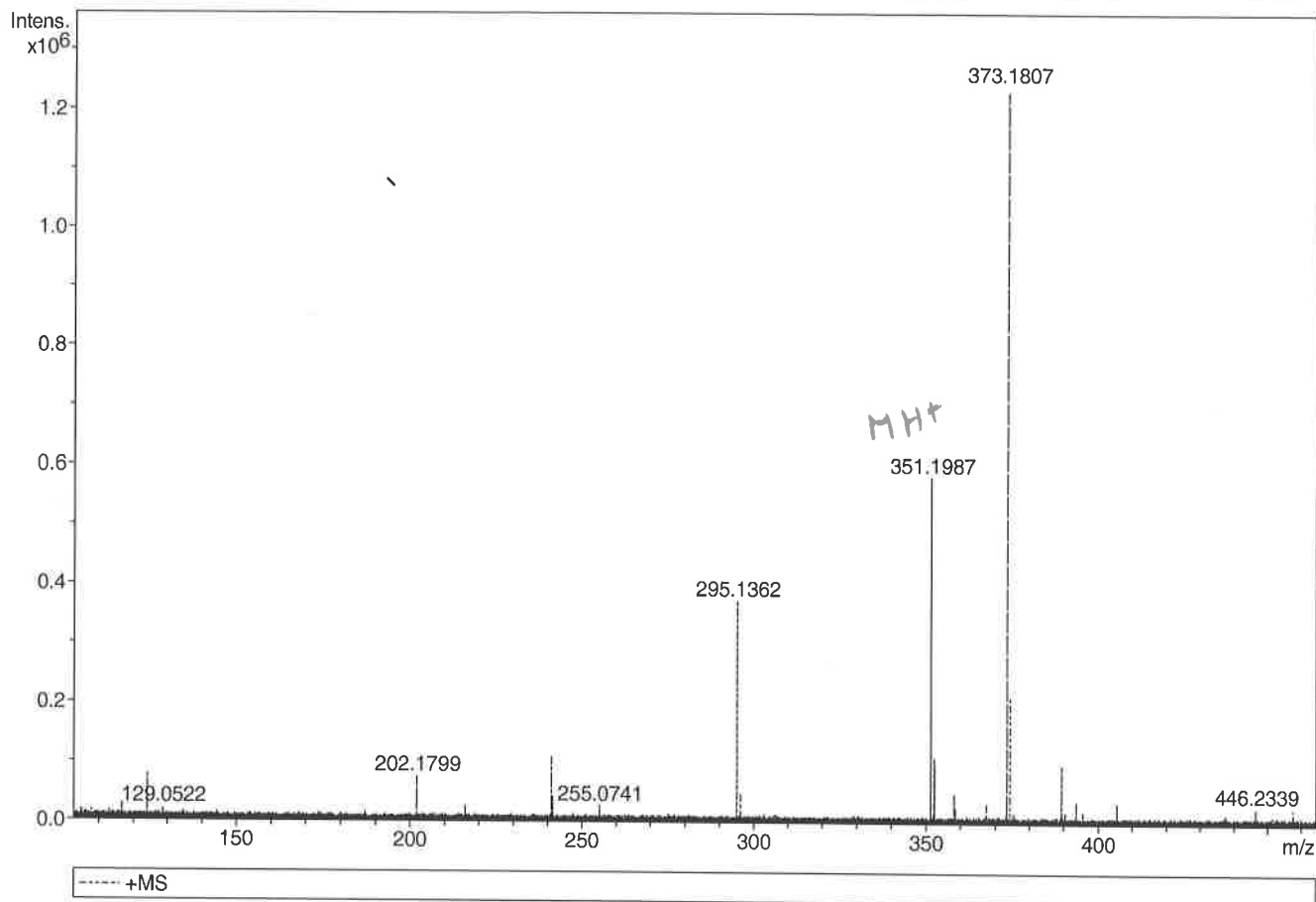
Generic Display Report

Analysis Info

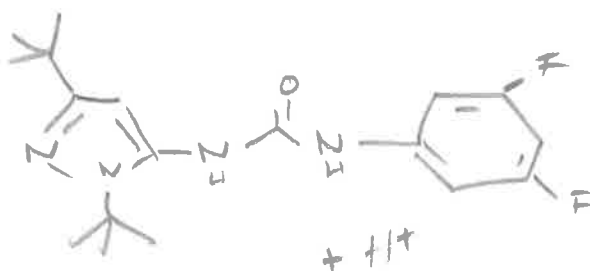
Analysis Name	D:\Data\Alinanopos\JESS6255_000001.d
Method	pos20090608esi
Sample Name	POS ESI B04JD092A
Comment	

Acquisition Date 30/10/2015 12:45:53

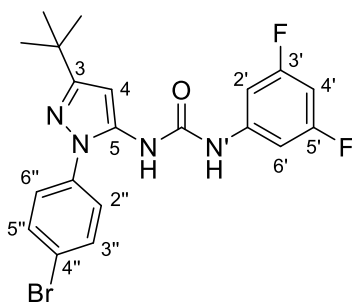
Operator	Administrator
Instrument	apex-III



Sum Formula	Sigma	m/z	Err [ppm]	Mean Err [ppm]	Err [mDa]	rdb	N Rule	e ⁻
C 18 H 25 F 2 N 4 O 1	0.026	351.1991	1.15	-2.14	-0.75	7.50	ok	even

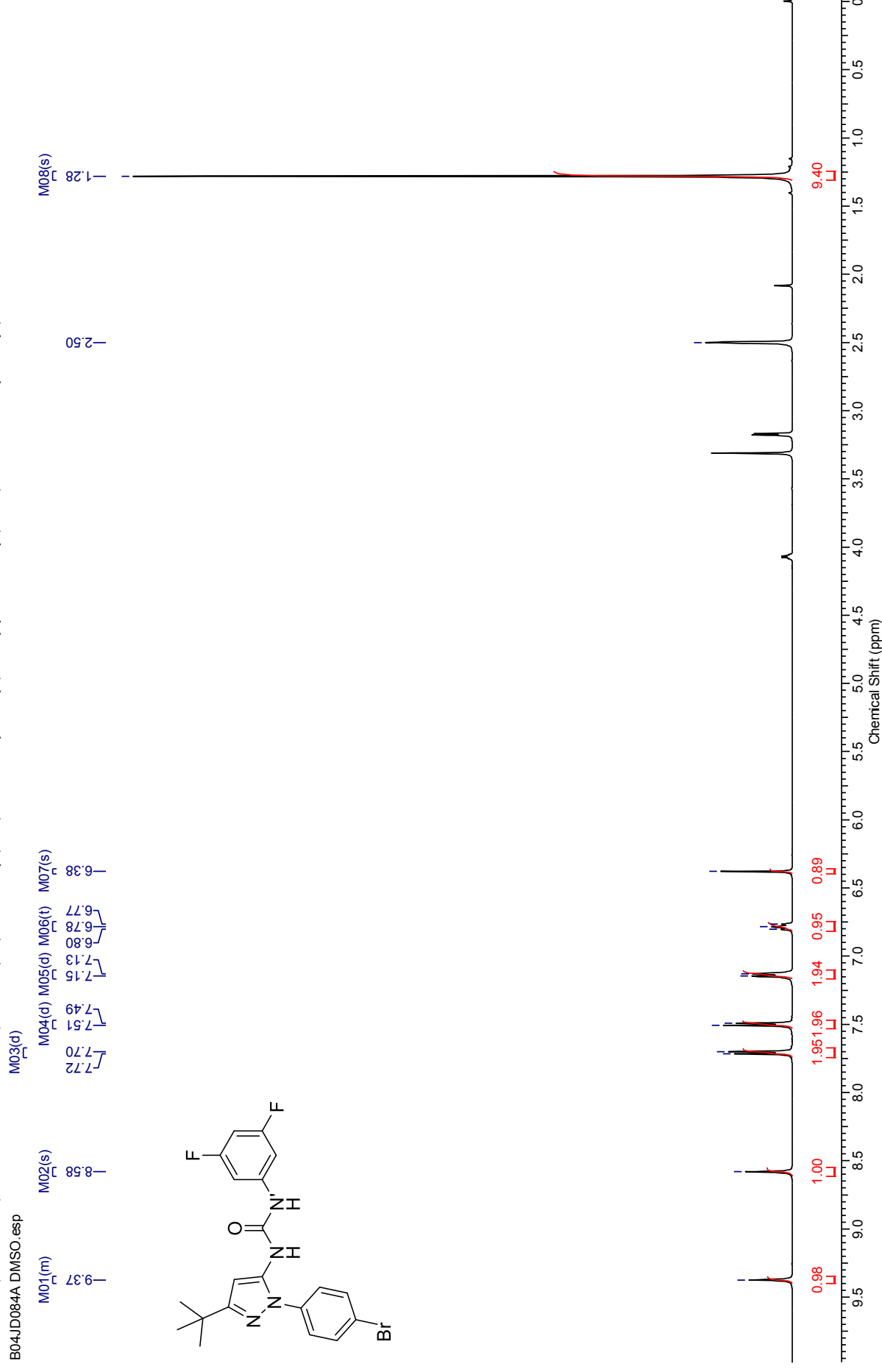


***N*-(3-(*tert*-Butyl)-1-(4-bromophenyl)-1*H*-pyrazol-5-yl)-*N'*-(3,5-difluorophenyl)urea (2300)**



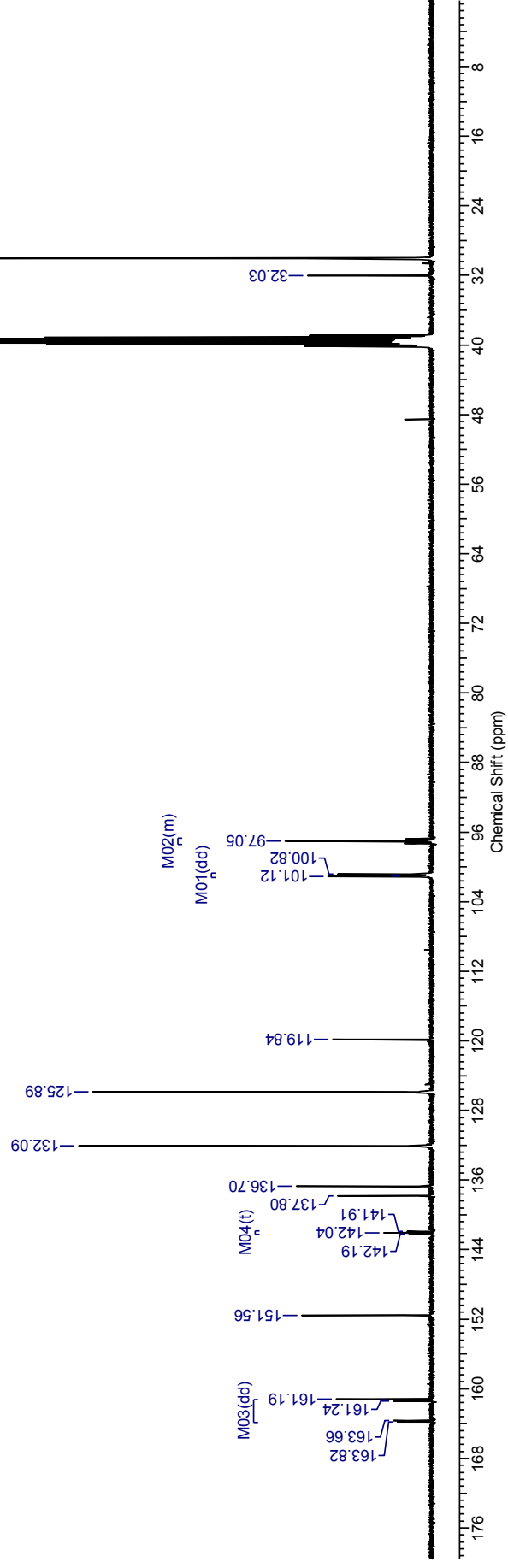
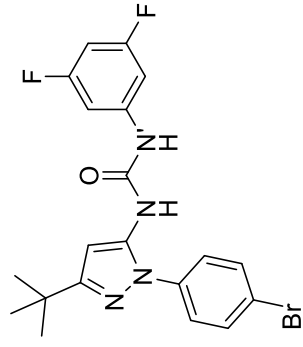
¹H NMR spectrum (500 MHz, DMSO-*d*₆) for *N*-(3-(*tert*-Butyl)-1-(4-bromophenyl)-1*H*-pyrazol-5-yl)-*N'*-(3,5-difluorophenyl)urea

B04JD084A DMSO esp



¹³C NMR spectrum (100 MHz, DMSO-*d*₆) for *N*-(3-(*tert*-Butyl)-1-(4-bromophenyl)-1*H*-pyrazol-5-yl)-*N'*-(3,5-difluorophenyl)urea

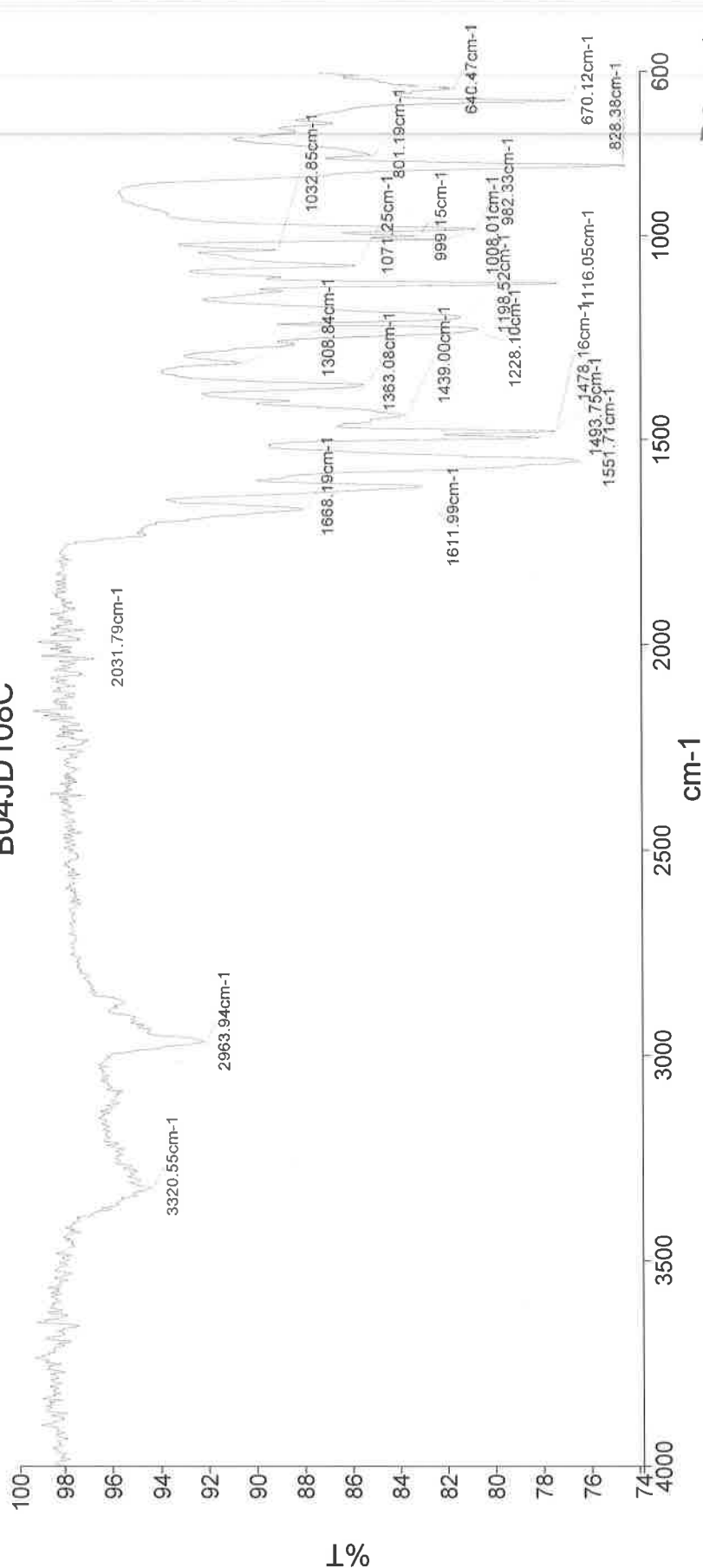
B04JD084A DMSO 400CARBON_01.esp



Analyst
Date

Administrator
18 November 2015 15:55

B04JD108C



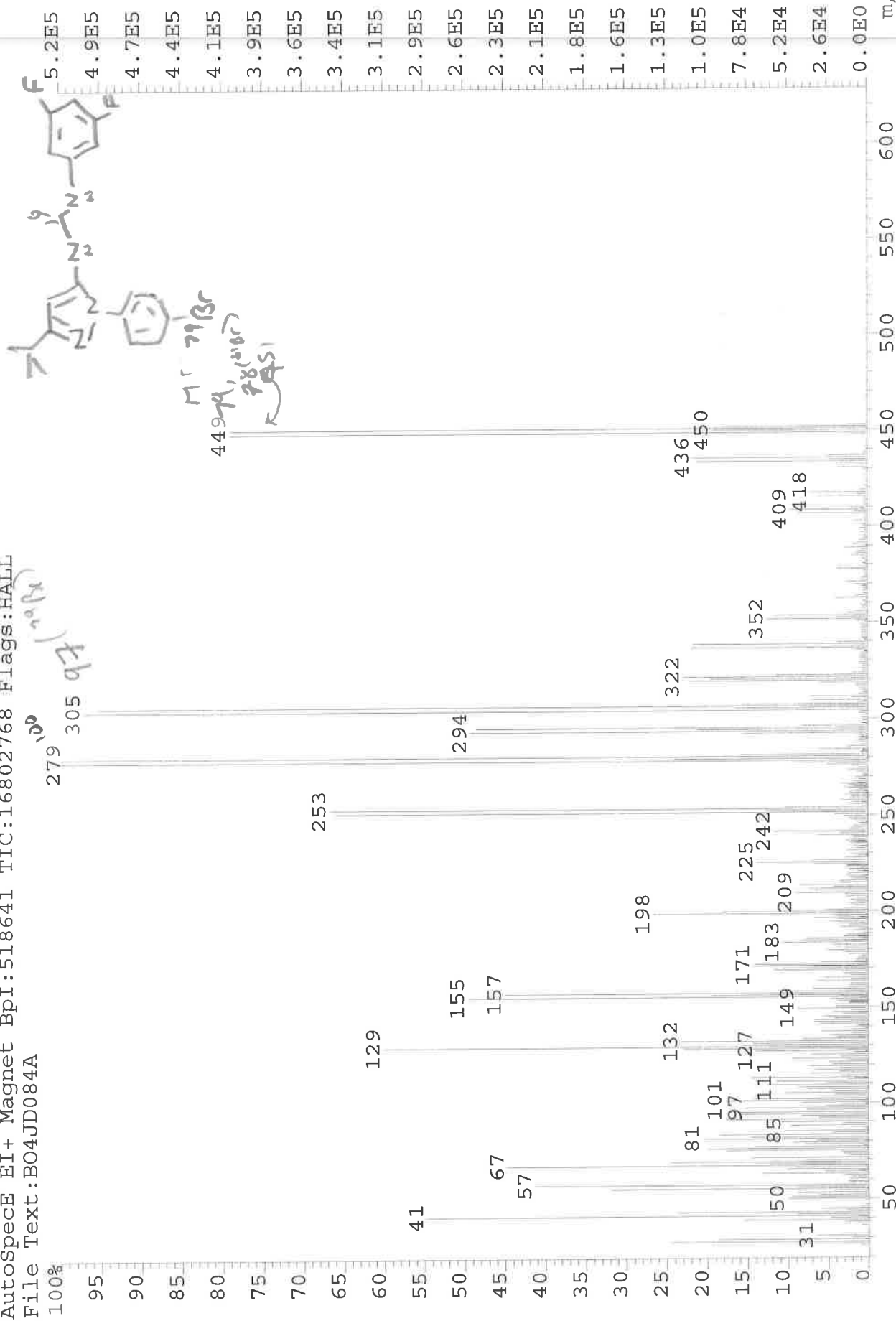
670-C-Br

3320 - N-H
2964 - C-H
1668 - C=O
1612 - N-H bend
1552 - N-H
1478 - C-C in ring str
1228 - C-N
1116 - C-C

File Text:BO4JD084A

Mass spectrum plot showing relative intensity (0-100%) versus m/z (50-600). The base peak is at m/z 279. Other significant peaks are labeled at m/z 305, 253, 294, 449, and 450. A chemical structure of a brominated amine is shown in the top right corner.

m/z	Relative Intensity (%)
279	100
305	95
253	70
294	55
449	45
450	40
322	25
352	15
409	10
418	8
198	25
129	60
155	50
157	48
132	25
81	20
101	18
171	15
225	12
242	10
149	10
183	8
209	8
50	5
31	2



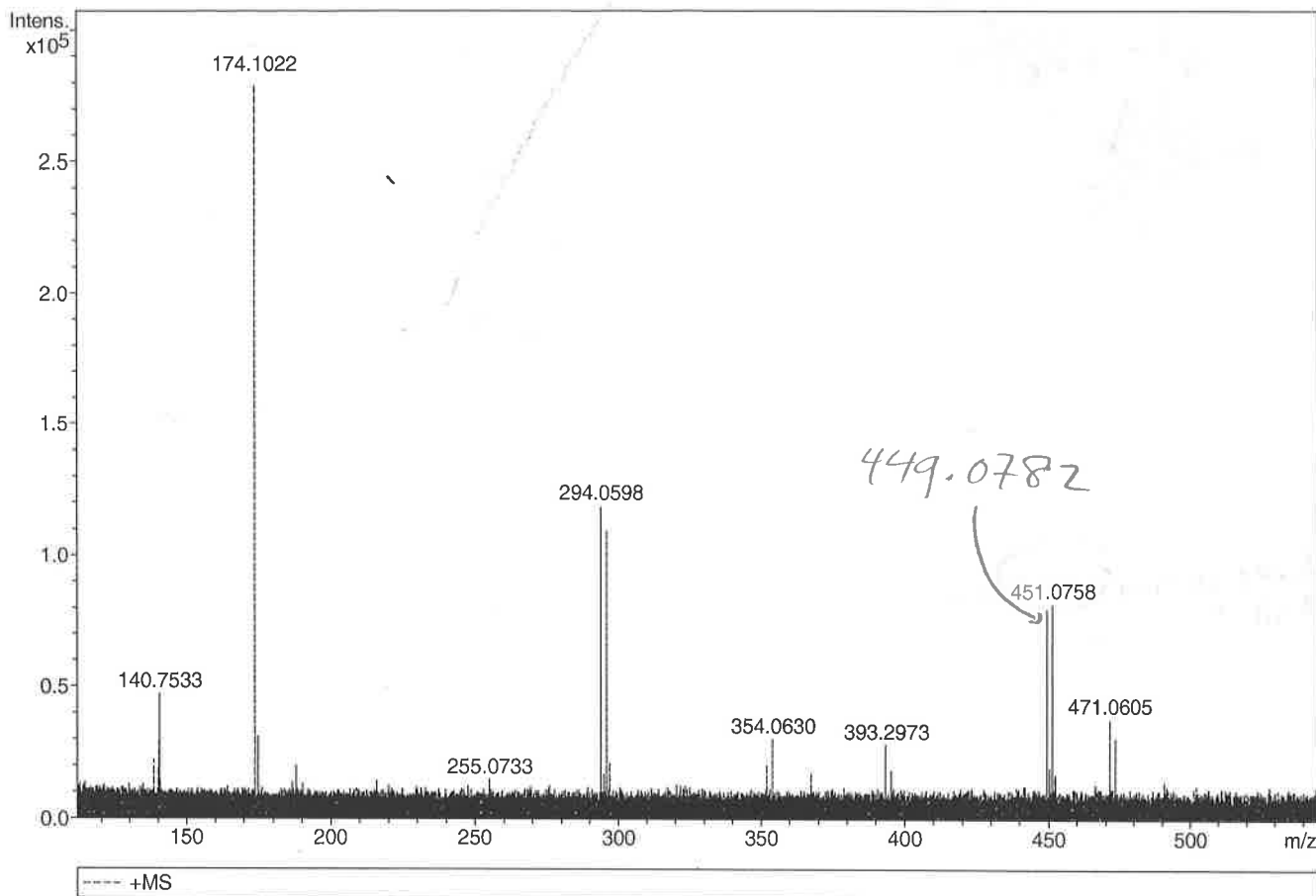
Generic Display Report

Analysis Info

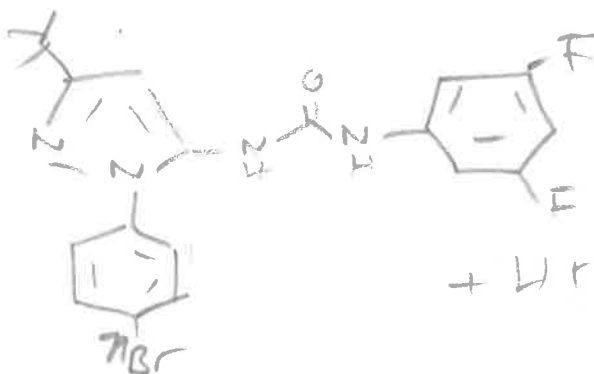
Analysis Name D:\Data\Alinanopos\JESS6211_000001.d
 Method pos20090608esi
 Sample Name POS ESI B04JD084A
 Comment

Acquisition Date 21/10/2015 10:39:08

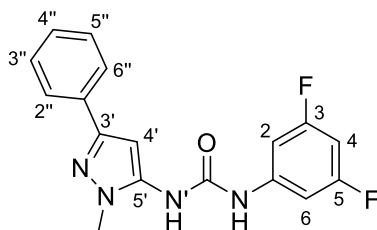
Operator Administrator
 Instrument apex-III



Sum Formula	Sigma	m/z	Err [ppm]	Mean Err [ppm]	Err [mDa]	rdB	N Rule	e ⁻
C 20 H 20 Br 1 F 2 N 4 O 1	0.021	449.0783	0.14	0.54	0.24	11.50	ok	even

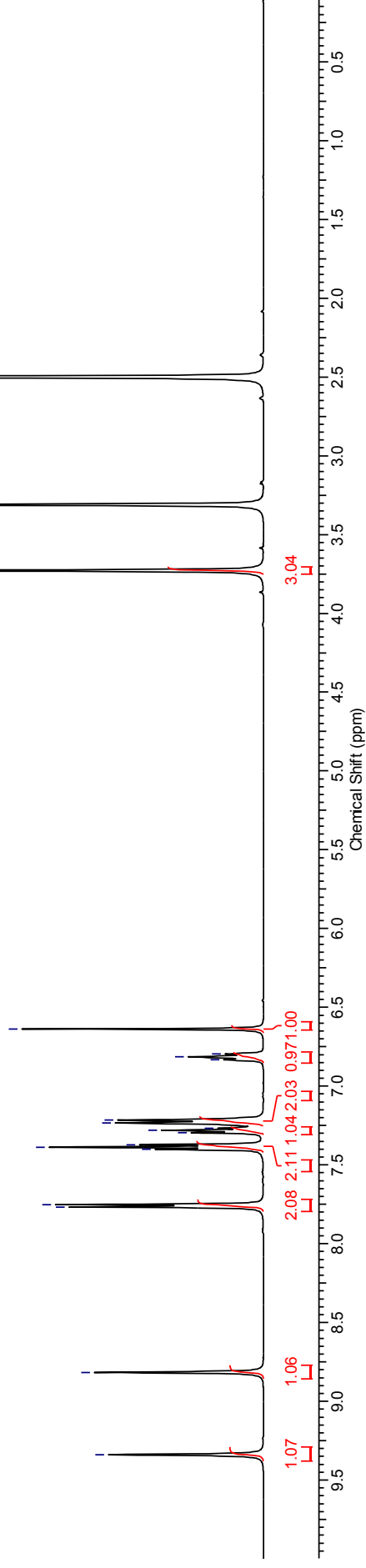
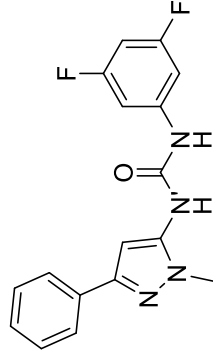
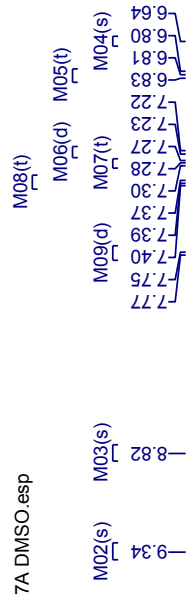


***N*-(3,5-Difluorophenyl)-*N'*-(1-methyl-3-phenyl-1*H*-pyrazol-5-yl)urea
(2310)**



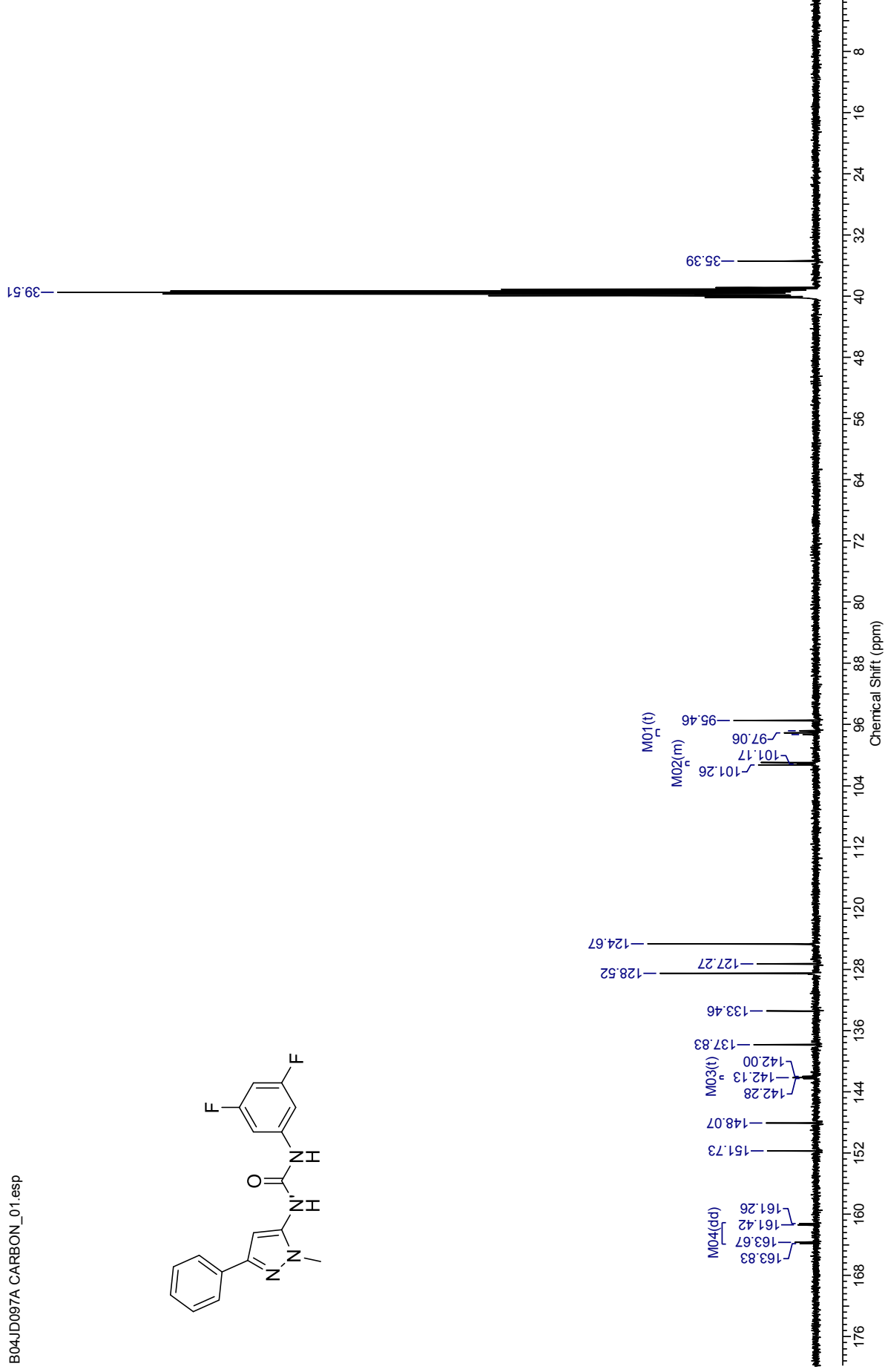
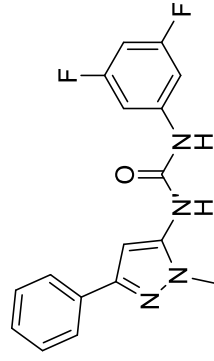
¹H NMR spectrum (500 MHz, DMSO-*d*₆) for *N*-(3,5-Difluorophenyl)-*N'*-(1-methyl-3-phenyl-1*H*-pyrazol-5-yl)urea

B04JD097A DMSO.esp



¹³C NMR spectrum (100 MHz, DMSO-*d*₆) for *N*-(3,5-Difluorophenyl)-*N'*-(1-methyl-3-phenyl-1*H*-pyrazol-5-yl)urea

B04JD097A CARBON_01.esp

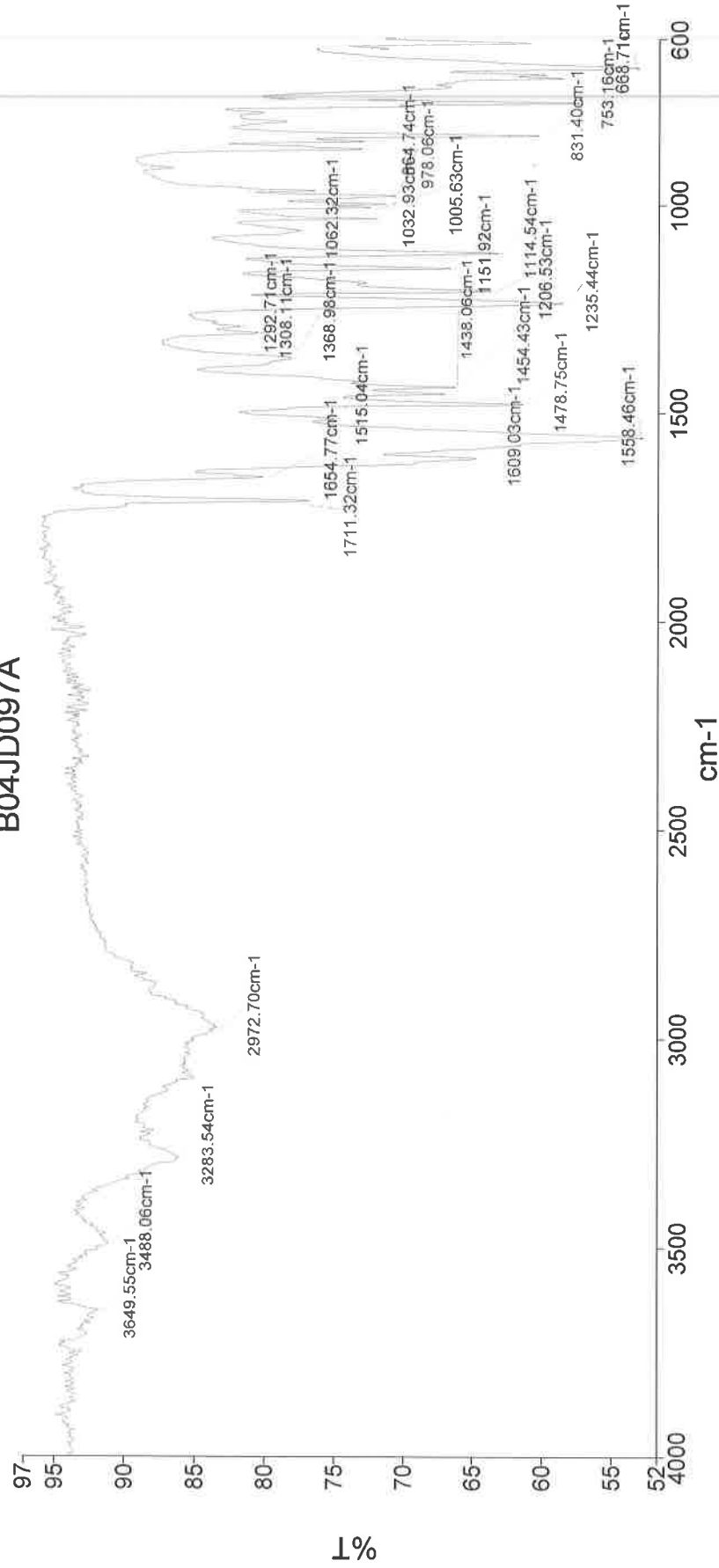


Analyst
Date

Administrator
11 November 2015 14:28

B04JD097A

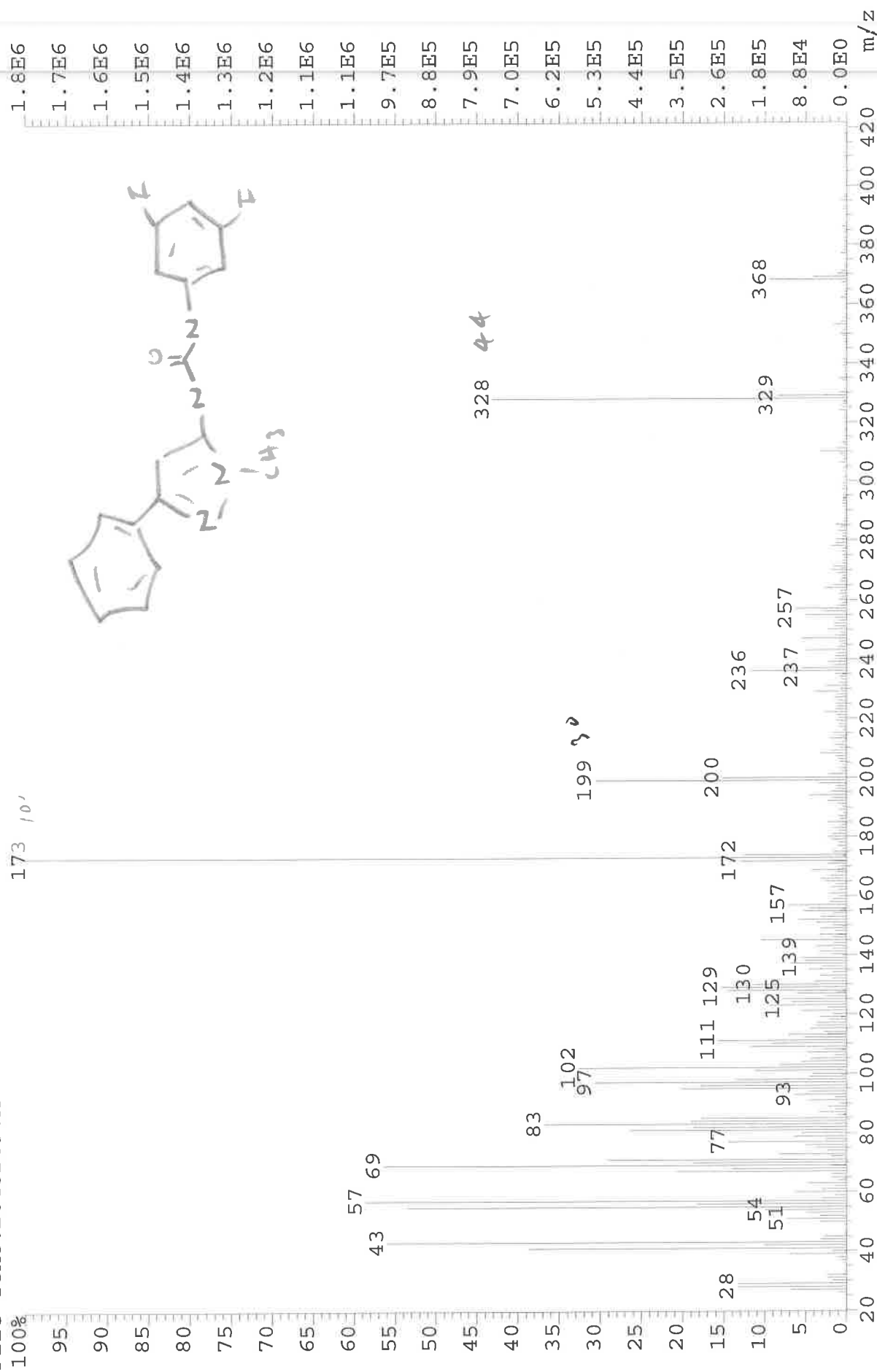
PerkinElmer Spectrum Version 10.03.06
11 November 2015 14:28



3284 - N-H str
2973 - C-H str
1711 - C=O
1609 - N-H bend
1558 - N-H bend
1479 - C-H bend
1235 - C-N
1114 - C-F

249-087 Sample 087 By Administrator Date Wednesday, November 11 2015

File: JESS6257 Ident: 30 Acq: 30-OCT-2015 17:22:17 +1:54 Cal: CAL1
 AutoSpecE EI+ Magnet BpI: 1758316 TIC: 28543596 Flags: HALL
 File Text: B04JD097A



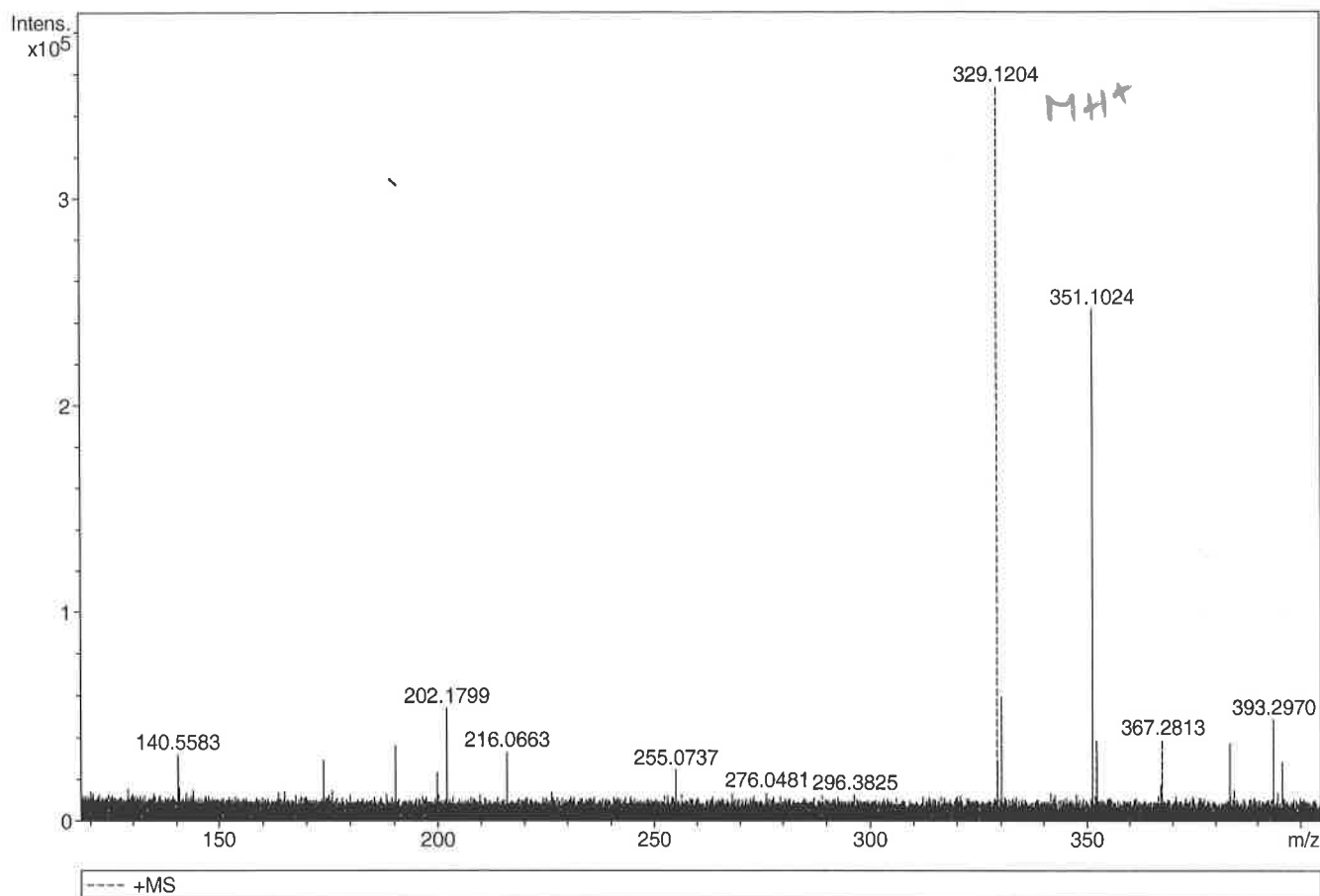
Generic Display Report

Analysis Info

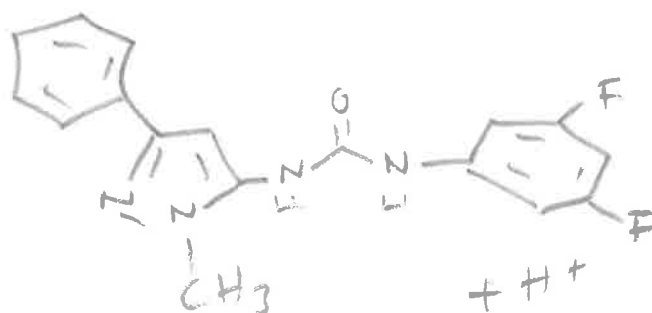
Analysis Name D:\Data\Alinanopos\JESS6257_000001.d
 Method pos20090608esi
 Sample Name POS ESI B04JD097A
 Comment

Acquisition Date 30/10/2015 12:55:56

Operator Administrator
 Instrument apex-III



Sum Formula	Sigma	m/z	Err [ppm]	Mean Err [ppm]	Err [mDa]	rdb	N Rule	e ⁻
C 17 H 15 F 2 N 4 O 1	0.007	329.1208	1.24	0.14	0.05	11.50	ok	even



BIRB_xtal3

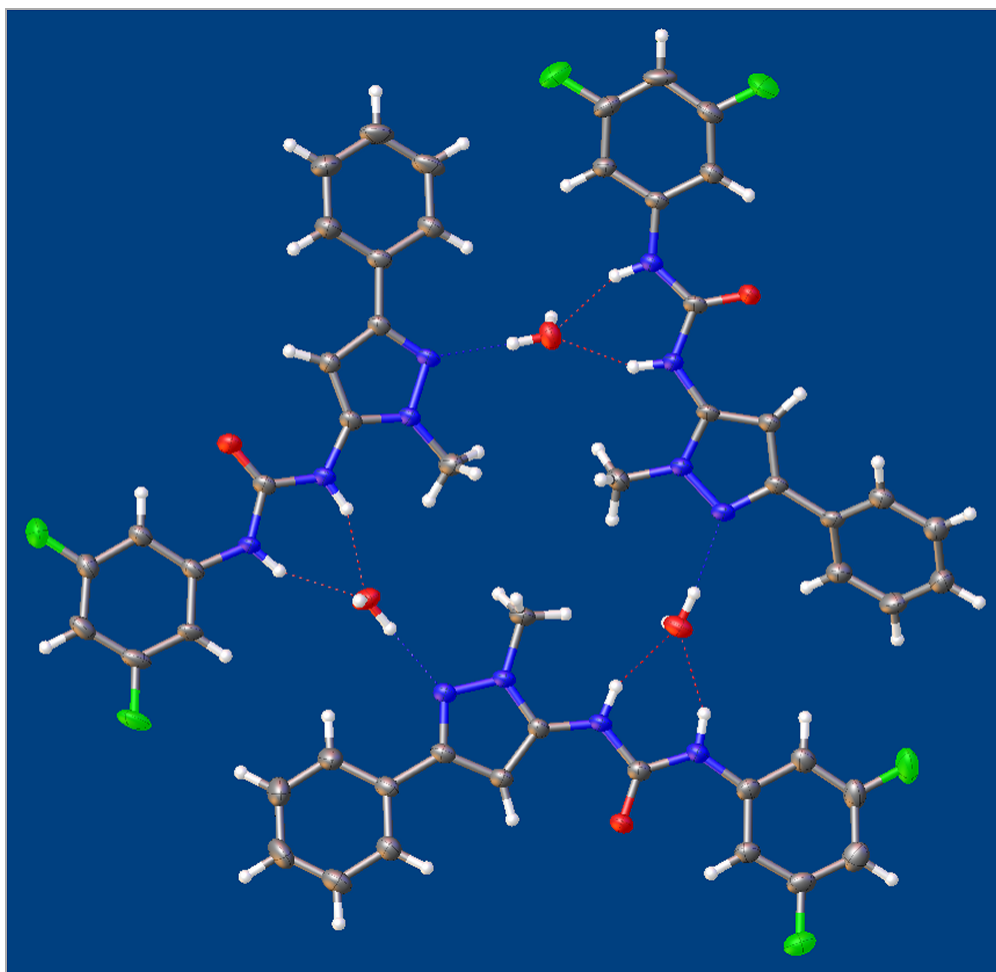


Table 1 Crystal data and structure refinement for BIRB_xtal3.

Identification code	BIRB_xtal3
Empirical formula	C ₁₇ H ₁₆ F ₂ N ₄ O ₂
Formula weight	346.34
Temperature/K	173.0
Crystal system	triclinic
Space group	P-1
a/Å	7.3053(6)
b/Å	19.0191(15)
c/Å	19.5624(16)
α/°	61.876(8)
β/°	85.618(7)
γ/°	86.500(7)
Volume/Å ³	2389.1(4)
Z	6
ρ _{calc} /g/cm ³	1.444
μ/mm ⁻¹	0.963
F(000)	1080.0
Crystal size/mm ³	0.6 × 0.1 × 0.1
Radiation	CuKα (λ = 1.54184)
2θ range for data collection/°	8.92 to 142.83
Index ranges	-8 ≤ h ≤ 8, -23 ≤ k ≤ 23, -23 ≤ l ≤ 19

Reflections collected	17105
Independent reflections	9017 [$R_{\text{int}} = 0.0700$, $R_{\text{sigma}} = 0.1049$]
Data/restraints/parameters	9017/0/688
Goodness-of-fit on F^2	1.101
Final R indexes [$I \geq 2\sigma(I)$]	$R_1 = 0.0997$, $wR_2 = 0.2767$
Final R indexes [all data]	$R_1 = 0.1383$, $wR_2 = 0.3044$
Largest diff. peak/hole / $e \text{ \AA}^{-3}$	0.40/-0.36

Table 2 Fractional Atomic Coordinates ($\times 10^4$) and Equivalent Isotropic Displacement Parameters ($\text{\AA}^2 \times 10^3$) for BIRB_xtal3. U_{eq} is defined as 1/3 of the trace of the orthogonalised U_{IJ} tensor.

Atom	<i>x</i>	<i>y</i>	<i>z</i>	$U(\text{eq})$
F1	8281 (6)	7075 (3)	1496 (2)	64.5 (12)
F2	10705 (6)	4462 (2)	2725 (2)	53.4 (10)
O1	8073 (6)	4293 (2)	5112 (2)	41.7 (10)
N1	7570 (7)	5615 (3)	4231 (3)	36.5 (11)
N2	6760 (7)	5169 (3)	5511 (3)	35.9 (11)
N3	5832 (7)	4880 (3)	6805 (2)	32.6 (10)
N4	5813 (6)	4281 (3)	7551 (2)	32.8 (10)
C1	8237 (8)	5628 (3)	3535 (3)	34.0 (12)
C2	7948 (8)	6342 (3)	2851 (3)	38.8 (13)
C3	8576 (9)	6385 (4)	2151 (3)	43.5 (14)
C4	9499 (9)	5762 (4)	2077 (4)	44.8 (14)
C5	9777 (8)	5087 (4)	2758 (4)	39.1 (13)
C6	9180 (8)	4988 (3)	3487 (3)	34.4 (11)
C7	7517 (8)	4973 (3)	4956 (3)	33.3 (11)
C8	6592 (7)	4635 (3)	6300 (3)	29.5 (11)
C9	7095 (8)	3837 (3)	6720 (3)	33.8 (12)
C10	6589 (7)	3647 (3)	7500 (3)	31.3 (11)
C11	6846 (8)	2872 (3)	8189 (3)	33.4 (11)
C12	7955 (9)	2285 (4)	8121 (3)	41.8 (14)
C13	8181 (10)	1542 (4)	8753 (4)	49.3 (16)
C14	7336 (12)	1374 (4)	9470 (4)	58.0 (19)
C15	6242 (12)	1965 (4)	9544 (4)	59 (2)
C16	6009 (10)	2704 (4)	8918 (3)	46.7 (15)
C17	5145 (9)	5673 (3)	6644 (3)	42.1 (14)
F3	5513 (6)	1664 (2)	11568 (2)	53.6 (10)
F4	2541 (7)	2822 (2)	13018 (2)	64.3 (13)
O2	1868 (6)	5201 (2)	10624 (2)	41.9 (10)
N5	3167 (7)	4304 (3)	10237 (2)	33.1 (10)
N6	2331 (6)	5558 (3)	9334 (2)	32.5 (10)
N7	1603 (6)	6805 (3)	8278 (2)	32.2 (10)
N8	881 (6)	7553 (3)	8108 (2)	32.4 (10)
C18	3408 (7)	3626 (3)	10952 (3)	31.3 (11)
C19	4332 (8)	2972 (3)	10924 (3)	34.7 (12)
C20	4607 (8)	2293 (3)	11602 (4)	38.4 (13)
C21	4031 (9)	2208 (3)	12327 (3)	41.9 (14)
C22	3141 (9)	2866 (3)	12326 (3)	40.2 (13)
C23	2806 (8)	3577 (3)	11667 (3)	35.2 (12)
C24	2401 (7)	5032 (3)	10112 (3)	31.0 (11)
C25	1646 (7)	6337 (3)	9052 (3)	30.1 (11)
C26	928 (8)	6773 (3)	9407 (3)	31.9 (11)
C27	458 (7)	7527 (3)	8792 (3)	29.6 (11)
C28	-431 (7)	8208 (3)	8862 (3)	31.4 (11)
C29	-800 (10)	8160 (4)	9584 (4)	48.1 (16)
C30	-1746 (12)	8769 (4)	9668 (4)	59 (2)
C31	-2313 (10)	9451 (4)	9019 (4)	51.9 (17)
C32	-1925 (9)	9507 (4)	8299 (4)	47.8 (15)
C33	-1002 (9)	8903 (3)	8208 (3)	40.7 (13)

C34	2147 (9)	6612 (3)	7661 (3)	40.6 (13)
F5	-886 (7)	11585 (3)	6958 (2)	64.5 (12)
F6	1380 (8)	13205 (2)	4413 (3)	70.9 (14)
O3	2746 (6)	10821 (2)	4208 (2)	40 (1)
N9	1574 (7)	10359 (3)	5460 (2)	32.4 (10)
N10	2859 (7)	9489 (3)	5062 (2)	32.7 (10)
N11	3846 (7)	8439 (3)	4785 (2)	33.3 (10)
N12	4611 (7)	8297 (3)	4195 (3)	35 (1)
C35	1117 (7)	11069 (3)	5506 (3)	30.1 (11)
C36	321 (8)	10994 (3)	6200 (3)	34.9 (12)
C37	-99 (9)	11678 (4)	6270 (3)	42.5 (14)
C38	222 (9)	12430 (4)	5681 (4)	46.6 (15)
C39	1016 (9)	12469 (3)	5014 (4)	42.7 (14)
C40	1476 (8)	11824 (3)	4883 (3)	37.0 (13)
C41	2422 (7)	10275 (3)	4864 (3)	29.2 (11)
C42	3636 (7)	9237 (3)	4546 (3)	29.9 (11)
C43	4256 (8)	9631 (3)	3777 (3)	32.1 (11)
C44	4851 (7)	9023 (3)	3584 (3)	30.6 (11)
C45	5663 (8)	9114 (3)	2840 (3)	31.6 (11)
C46	6580 (8)	9810 (3)	2343 (3)	36.1 (12)
C47	7332 (9)	9929 (4)	1618 (3)	41.8 (14)
C48	7180 (9)	9351 (4)	1396 (3)	44.3 (14)
C49	6269 (10)	8653 (4)	1882 (4)	45.5 (15)
C50	5506 (9)	8538 (3)	2596 (3)	40.2 (13)
C51	3507 (10)	7792 (3)	5554 (3)	46.7 (16)
O4	5128 (7)	6695 (2)	4552 (3)	44.6 (10)
O5	4792 (6)	4691 (3)	8725 (2)	44.4 (10)
O6	765 (6)	8694 (3)	6532 (2)	44.5 (10)

Table 3 Anisotropic Displacement Parameters ($\text{\AA}^2 \times 10^3$) for BIRB_xtal3. The Anisotropic displacement factor exponent takes the form:

$$-2\pi^2[h^2a^{*2}U_{11}+2hka^*b^*U_{12}+...].$$

Atom	U ₁₁	U ₂₂	U ₃₃	U ₂₃	U ₁₃	U ₁₂
F1	68 (3)	64 (3)	31.1 (17)	0.0 (17)	1.3 (17)	22 (2)
F2	61 (2)	51 (2)	54 (2)	-32.6 (18)	5.3 (17)	11.3 (18)
O1	59 (3)	24.5 (19)	32.3 (19)	-8.3 (15)	4.5 (17)	15.2 (17)
N1	49 (3)	23 (2)	31 (2)	-8.8 (18)	1.6 (19)	11.1 (19)
N2	48 (3)	22 (2)	31 (2)	-9.7 (17)	-0.4 (19)	15.1 (19)
N3	40 (3)	23 (2)	30 (2)	-11.3 (17)	-1.1 (18)	12.0 (18)
N4	38 (3)	27 (2)	30 (2)	-10.8 (17)	-1.5 (18)	10.2 (18)
C1	31 (3)	34 (3)	33 (3)	-15 (2)	4 (2)	6 (2)
C2	36 (3)	35 (3)	37 (3)	-11 (2)	-1 (2)	10 (2)
C3	40 (3)	47 (3)	28 (3)	-6 (2)	-2 (2)	8 (3)
C4	40 (3)	55 (4)	38 (3)	-22 (3)	-2 (2)	4 (3)
C5	33 (3)	40 (3)	48 (3)	-25 (3)	4 (2)	7 (2)
C6	33 (3)	31 (3)	38 (3)	-16 (2)	1 (2)	6 (2)
C7	36 (3)	28 (3)	33 (3)	-12 (2)	1 (2)	8 (2)
C8	30 (3)	25 (2)	28 (2)	-9 (2)	-0.3 (19)	9 (2)
C9	41 (3)	26 (3)	30 (2)	-11 (2)	-3 (2)	13 (2)
C10	33 (3)	24 (2)	35 (3)	-13 (2)	-4 (2)	8 (2)
C11	42 (3)	26 (3)	31 (2)	-13 (2)	-8 (2)	9 (2)
C12	48 (4)	33 (3)	36 (3)	-11 (2)	-1 (2)	10 (2)
C13	58 (4)	31 (3)	50 (3)	-13 (3)	-9 (3)	16 (3)
C14	86 (6)	33 (3)	38 (3)	-3 (3)	-9 (3)	11 (3)
C15	92 (6)	42 (4)	31 (3)	-11 (3)	6 (3)	6 (4)
C16	71 (5)	31 (3)	35 (3)	-15 (2)	3 (3)	9 (3)
C17	54 (4)	28 (3)	40 (3)	-14 (2)	0 (2)	18 (2)
F3	59 (2)	25.5 (17)	68 (2)	-16.6 (16)	-5.2 (18)	20.2 (16)
F4	100 (3)	42 (2)	30.4 (17)	-4.1 (15)	8.6 (19)	16 (2)
O2	54 (3)	31 (2)	32.7 (19)	-11.3 (16)	0.9 (17)	19.7 (18)
N5	43 (3)	22 (2)	29 (2)	-9.4 (17)	-1.5 (18)	15.8 (18)
N6	38 (2)	26 (2)	29 (2)	-10.5 (17)	-3.3 (17)	14.8 (18)
N7	40 (3)	24 (2)	27 (2)	-8.5 (17)	-3.6 (17)	14.5 (18)
N8	36 (2)	23 (2)	32 (2)	-9.3 (17)	-4.3 (18)	14.3 (18)
C18	32 (3)	21 (2)	32 (2)	-6 (2)	-3 (2)	7.3 (19)
C19	32 (3)	25 (3)	42 (3)	-14 (2)	2 (2)	12 (2)
C20	36 (3)	23 (3)	53 (3)	-16 (2)	-3 (2)	10 (2)
C21	46 (3)	22 (3)	44 (3)	-5 (2)	-3 (3)	7 (2)
C22	51 (4)	28 (3)	31 (3)	-6 (2)	1 (2)	4 (2)
C23	38 (3)	25 (3)	34 (3)	-8 (2)	-1 (2)	10 (2)
C24	31 (3)	26 (2)	31 (2)	-10 (2)	-5 (2)	12 (2)
C25	29 (3)	25 (2)	30 (2)	-9 (2)	-1.5 (19)	10.9 (19)
C26	36 (3)	27 (3)	28 (2)	-9 (2)	-3 (2)	10 (2)
C27	28 (3)	25 (2)	31 (2)	-11 (2)	-2.2 (19)	8.9 (19)
C28	28 (3)	26 (3)	37 (3)	-13 (2)	-1 (2)	9 (2)
C29	62 (4)	33 (3)	42 (3)	-14 (2)	2 (3)	16 (3)
C30	79 (5)	44 (4)	54 (4)	-27 (3)	10 (3)	17 (3)
C31	45 (4)	40 (3)	70 (4)	-28 (3)	4 (3)	16 (3)
C32	42 (3)	31 (3)	65 (4)	-19 (3)	-6 (3)	17 (3)
C33	49 (4)	28 (3)	38 (3)	-11 (2)	-4 (2)	14 (2)

C34	52 (4)	36 (3)	32 (3)	-16 (2)	-5 (2)	15 (3)
F5	86 (3)	60 (2)	54 (2)	-37 (2)	20 (2)	6 (2)
F6	111 (4)	23.2 (18)	62 (2)	-10.9 (17)	20 (2)	4 (2)
O3	57 (3)	24.8 (18)	27.7 (18)	-6.0 (15)	4.3 (16)	14.2 (17)
N9	40 (3)	22 (2)	29 (2)	-8.9 (17)	-0.2 (17)	10.8 (18)
N10	42 (3)	25 (2)	24.6 (19)	-8.2 (16)	0.0 (17)	14.7 (18)
N11	42 (3)	25 (2)	29 (2)	-10.7 (17)	-0.2 (18)	12.5 (18)
N12	44 (3)	25 (2)	33 (2)	-12.6 (18)	-0.8 (19)	14.7 (19)
C35	33 (3)	23 (2)	31 (2)	-12 (2)	-3 (2)	11 (2)
C36	42 (3)	29 (3)	31 (2)	-13 (2)	0 (2)	11 (2)
C37	47 (4)	45 (3)	40 (3)	-26 (3)	5 (2)	10 (3)
C38	50 (4)	35 (3)	64 (4)	-33 (3)	0 (3)	13 (3)
C39	52 (4)	22 (3)	45 (3)	-10 (2)	4 (3)	6 (2)
C40	44 (3)	25 (3)	33 (3)	-9 (2)	0 (2)	12 (2)
C41	27 (2)	24 (2)	34 (2)	-12 (2)	-2.8 (19)	11.3 (19)
C42	32 (3)	21 (2)	32 (2)	-10.8 (19)	-1 (2)	11.9 (19)
C43	40 (3)	24 (2)	27 (2)	-9.8 (19)	-2 (2)	12 (2)
C44	32 (3)	24 (2)	31 (2)	-11 (2)	-3 (2)	13 (2)
C45	35 (3)	26 (2)	32 (2)	-14 (2)	-4 (2)	16 (2)
C46	38 (3)	29 (3)	37 (3)	-13 (2)	-4 (2)	11 (2)
C47	44 (3)	37 (3)	38 (3)	-14 (2)	4 (2)	7 (2)
C48	55 (4)	38 (3)	33 (3)	-14 (2)	4 (2)	11 (3)
C49	63 (4)	38 (3)	40 (3)	-23 (3)	-1 (3)	11 (3)
C50	49 (3)	30 (3)	39 (3)	-16 (2)	2 (2)	7 (2)
C51	67 (4)	28 (3)	33 (3)	-7 (2)	3 (3)	14 (3)
O4	57 (3)	26 (2)	46 (2)	-13.9 (17)	-6 (2)	12.3 (18)
O5	57 (3)	43 (2)	39 (2)	-26.2 (18)	1.6 (18)	11 (2)
O6	52 (3)	36 (2)	30.4 (19)	-4.6 (16)	1.3 (17)	8.0 (19)

Table 4 Bond Lengths for BIRB_xtal3.

Atom	Atom	Length/Å	Atom	Atom	Length/Å
F1	C3	1.354 (7)	C19	C20	1.364 (8)
F2	C5	1.357 (7)	C20	C21	1.385 (9)
O1	C7	1.231 (7)	C21	C22	1.374 (8)
N1	C1	1.401 (7)	C22	C23	1.382 (7)
N1	C7	1.366 (7)	C25	C26	1.372 (7)
N2	C7	1.374 (7)	C26	C27	1.414 (7)
N2	C8	1.391 (7)	C27	C28	1.471 (7)
N3	N4	1.365 (6)	C28	C29	1.378 (8)
N3	C8	1.349 (7)	C28	C33	1.407 (7)
N3	C17	1.452 (6)	C29	C30	1.382 (9)
N4	C10	1.344 (7)	C30	C31	1.389 (10)
C1	C2	1.404 (8)	C31	C32	1.371 (10)
C1	C6	1.400 (7)	C32	C33	1.374 (8)
C2	C3	1.376 (8)	F5	C37	1.357 (7)
C3	C4	1.389 (9)	F6	C39	1.362 (7)
C4	C5	1.366 (9)	O3	C41	1.229 (6)
C5	C6	1.386 (8)	N9	C35	1.414 (7)
C8	C9	1.385 (7)	N9	C41	1.349 (7)
C9	C10	1.415 (7)	N10	C41	1.379 (7)
C10	C11	1.469 (7)	N10	C42	1.382 (7)
C11	C12	1.390 (8)	N11	N12	1.377 (6)
C11	C16	1.404 (8)	N11	C42	1.363 (7)
C12	C13	1.382 (8)	N11	C51	1.441 (7)
C13	C14	1.385 (10)	N12	C44	1.345 (7)
C14	C15	1.397 (10)	C35	C36	1.381 (7)
C15	C16	1.372 (9)	C35	C40	1.402 (7)
F3	C20	1.359 (6)	C36	C37	1.386 (8)
F4	C22	1.356 (7)	C37	C38	1.369 (9)
O2	C24	1.218 (7)	C38	C39	1.357 (9)
N5	C18	1.400 (6)	C39	C40	1.386 (8)
N5	C24	1.379 (6)	C42	C43	1.379 (7)
N6	C24	1.374 (7)	C43	C44	1.411 (7)
N6	C25	1.390 (6)	C44	C45	1.464 (7)
N7	N8	1.378 (6)	C45	C46	1.394 (8)
N7	C25	1.348 (7)	C45	C50	1.399 (8)
N7	C34	1.442 (7)	C46	C47	1.399 (8)
N8	C27	1.330 (7)	C47	C48	1.372 (9)
C18	C19	1.401 (7)	C48	C49	1.389 (9)
C18	C23	1.395 (8)	C49	C50	1.384 (8)

Table 5 Bond Angles for BIRB_xtal3.

Atom	Atom	Atom	Angle/°	Atom	Atom	Atom	Angle/°
C7	N1	C1	127.2 (5)	O2	C24	N5	124.7 (5)
C7	N2	C8	124.2 (4)	O2	C24	N6	123.5 (5)
N4	N3	C17	119.8 (4)	N6	C24	N5	111.8 (4)
C8	N3	N4	111.8 (4)	N7	C25	N6	119.2 (5)
C8	N3	C17	128.3 (4)	N7	C25	C26	107.9 (4)
C10	N4	N3	104.8 (4)	C26	C25	N6	132.9 (5)
N1	C1	C2	116.5 (5)	C25	C26	C27	104.9 (4)
C6	C1	N1	124.3 (5)	N8	C27	C26	111.0 (5)
C6	C1	C2	119.2 (5)	N8	C27	C28	122.1 (4)
C3	C2	C1	118.8 (5)	C26	C27	C28	126.8 (5)
F1	C3	C2	118.2 (6)	C29	C28	C27	120.0 (5)
F1	C3	C4	117.9 (5)	C29	C28	C33	118.2 (5)
C2	C3	C4	123.9 (5)	C33	C28	C27	121.7 (5)
C5	C4	C3	115.1 (6)	C28	C29	C30	121.2 (6)
F2	C5	C4	117.9 (5)	C29	C30	C31	120.2 (7)
F2	C5	C6	117.2 (5)	C32	C31	C30	118.9 (6)
C4	C5	C6	124.9 (6)	C31	C32	C33	121.5 (6)
C5	C6	C1	118.1 (5)	C32	C33	C28	120.0 (6)
O1	C7	N1	125.3 (5)	C41	N9	C35	128.5 (4)
O1	C7	N2	122.5 (5)	C41	N10	C42	123.9 (4)
N1	C7	N2	112.2 (5)	N12	N11	C51	120.9 (4)
N3	C8	N2	120.1 (4)	C42	N11	N12	111.0 (4)
N3	C8	C9	107.8 (4)	C42	N11	C51	127.9 (5)
C9	C8	N2	132.1 (5)	C44	N12	N11	105.1 (4)
C8	C9	C10	104.2 (4)	C36	C35	N9	117.3 (5)
N4	C10	C9	111.4 (4)	C36	C35	C40	120.6 (5)
N4	C10	C11	121.9 (5)	C40	C35	N9	122.1 (5)
C9	C10	C11	126.7 (5)	C35	C36	C37	118.8 (5)
C12	C11	C10	119.2 (5)	F5	C37	C36	117.4 (5)
C12	C11	C16	118.8 (5)	F5	C37	C38	119.5 (5)
C16	C11	C10	122.0 (5)	C38	C37	C36	123.1 (5)
C13	C12	C11	120.6 (6)	C39	C38	C37	115.6 (5)
C12	C13	C14	120.5 (6)	F6	C39	C40	116.4 (5)
C13	C14	C15	119.0 (6)	C38	C39	F6	117.8 (5)
C16	C15	C14	120.7 (6)	C38	C39	C40	125.7 (5)
C15	C16	C11	120.3 (6)	C39	C40	C35	116.1 (5)
C24	N5	C18	127.2 (5)	O3	C41	N9	125.3 (5)
C24	N6	C25	123.3 (4)	O3	C41	N10	122.3 (5)
N8	N7	C34	120.1 (4)	N9	C41	N10	112.4 (4)
C25	N7	N8	111.0 (4)	N11	C42	N10	118.9 (5)
C25	N7	C34	128.9 (4)	N11	C42	C43	107.5 (4)
C27	N8	N7	105.2 (4)	C43	C42	N10	133.5 (5)
N5	C18	C19	116.0 (5)	C42	C43	C44	105.2 (4)
C23	C18	N5	124.2 (5)	N12	C44	C43	111.1 (5)
C23	C18	C19	119.8 (5)	N12	C44	C45	121.0 (5)
C20	C19	C18	118.9 (5)	C43	C44	C45	127.9 (5)
F3	C20	C19	118.4 (5)	C46	C45	C44	119.0 (5)
F3	C20	C21	117.8 (5)	C46	C45	C50	118.4 (5)
C19	C20	C21	123.8 (5)	C50	C45	C44	122.5 (5)
C22	C21	C20	115.2 (5)	C45	C46	C47	120.8 (6)

F4	C22	C21	118.1 (5)	C48	C47	C46	119.6 (6)
F4	C22	C23	117.2 (5)	C47	C48	C49	120.5 (5)
C21	C22	C23	124.8 (6)	C50	C49	C48	120.0 (6)
C22	C23	C18	117.5 (5)	C49	C50	C45	120.7 (6)

Table 6 Torsion Angles for BIRB_xtal3.

A	B	C	D	Angle/°	A	B	C	D	Angle/°
F1	C3	C4	C5	179.1 (6)	C24	N5	C18	C19	-176.1 (6)
F2	C5	C6	C1	179.3 (5)	C24	N5	C18	C23	3.4 (10)
N1	C1	C2	C3	-179.9 (6)	C24	N6	C25	N7	-178.9 (5)
N1	C1	C6	C5	-179.5 (6)	C24	N6	C25	C26	0.4 (10)
N2	C8	C9	C10	178.7 (6)	C25	N6	C24	O2	0.1 (9)
N3	N4	C10	C9	-0.4 (7)	C25	N6	C24	N5	-179.1 (5)
N3	N4	C10	C11	179.4 (5)	C25	N7	N8	C27	-0.9 (6)
N3	C8	C9	C10	-0.7 (7)	C25	C26	C27	N8	-0.7 (7)
N4	N3	C8	N2	-179.0 (5)	C25	C26	C27	C28	177.6 (5)
N4	N3	C8	C9	0.5 (7)	C26	C27	C28	C29	3.5 (10)
N4	C10	C11	C12	-168.0 (6)	C26	C27	C28	C33	-173.4 (6)
N4	C10	C11	C16	11.9 (9)	C27	C28	C29	C30	-175.5 (7)
C1	N1	C7	O1	0.6 (10)	C27	C28	C33	C32	176.1 (6)
C1	N1	C7	N2	-179.5 (6)	C28	C29	C30	C31	-1.4 (13)
C1	C2	C3	F1	179.7 (6)	C29	C28	C33	C32	-0.9 (10)
C1	C2	C3	C4	-0.4 (11)	C29	C30	C31	C32	0.3 (13)
C2	C1	C6	C5	-0.6 (9)	C30	C31	C32	C33	0.4 (12)
C2	C3	C4	C5	-0.8 (10)	C31	C32	C33	C28	-0.1 (11)
C3	C4	C5	F2	-178.7 (6)	C33	C28	C29	C30	1.6 (11)
C3	C4	C5	C6	1.4 (10)	C34	N7	N8	C27	177.5 (5)
C4	C5	C6	C1	-0.7 (10)	C34	N7	C25	N6	1.7 (9)
C6	C1	C2	C3	1.1 (9)	C34	N7	C25	C26	-177.7 (6)
C7	N1	C1	C2	172.8 (6)	F5	C37	C38	C39	179.9 (6)
C7	N1	C1	C6	-8.3 (10)	F6	C39	C40	C35	179.3 (6)
C7	N2	C8	N3	179.9 (6)	N9	C35	C36	C37	178.3 (5)
C7	N2	C8	C9	0.6 (11)	N9	C35	C40	C39	-177.8 (6)
C8	N2	C7	O1	2.0 (10)	N10	C42	C43	C44	-178.5 (6)
C8	N2	C7	N1	-177.9 (5)	N11	N12	C44	C43	0.3 (6)
C8	N3	N4	C10	0.0 (6)	N11	N12	C44	C45	179.4 (5)
C8	C9	C10	N4	0.7 (7)	N11	C42	C43	C44	-0.5 (6)
C8	C9	C10	C11	-179.1 (6)	N12	N11	C42	N10	179.0 (5)
C9	C10	C11	C12	11.7 (10)	N12	N11	C42	C43	0.7 (7)
C9	C10	C11	C16	-168.4 (6)	N12	C44	C45	C46	-153.5 (5)
C10	C11	C12	C13	-178.1 (6)	N12	C44	C45	C50	28.5 (9)
C10	C11	C16	C15	178.2 (7)	C35	N9	C41	O3	-9.8 (10)
C11	C12	C13	C14	-1.3 (11)	C35	N9	C41	N10	172.0 (5)
C12	C11	C16	C15	-1.9 (11)	C35	C36	C37	F5	179.7 (6)
C12	C13	C14	C15	0.4 (13)	C35	C36	C37	C38	0.6 (10)
C13	C14	C15	C16	-0.3 (13)	C36	C35	C40	C39	1.0 (9)
C14	C15	C16	C11	1.0 (13)	C36	C37	C38	C39	-1.0 (11)
C16	C11	C12	C13	2.1 (10)	C37	C38	C39	F6	-179.4 (6)
C17	N3	N4	C10	-177.8 (5)	C37	C38	C39	C40	1.5 (11)
C17	N3	C8	N2	-1.4 (10)	C38	C39	C40	C35	-1.5 (11)
C17	N3	C8	C9	178.0 (6)	C40	C35	C36	C37	-0.6 (9)
F3	C20	C21	C22	179.3 (6)	C41	N9	C35	C36	-177.0 (6)
F4	C22	C23	C18	-179.6 (6)	C41	N9	C35	C40	1.8 (9)
N5	C18	C19	C20	-179.8 (6)	C41	N10	C42	N11	-173.7 (5)
N5	C18	C23	C22	179.9 (6)	C41	N10	C42	C43	4.1 (10)
N6	C25	C26	C27	-179.2 (6)	C42	N10	C41	O3	-2.2 (9)
N7	N8	C27	C26	1.0 (6)	C42	N10	C41	N9	176.1 (5)

N7 N8 C27 C28	-177.4 (5)	C42 N11 N12 C44	-0.6 (6)
N7 C25 C26 C27	0.2 (7)	C42 C43 C44 N12	0.1 (7)
N8 N7 C25 N6	179.9 (5)	C42 C43 C44 C45	-179.0 (6)
N8 N7 C25 C26	0.4 (7)	C43 C44 C45 C46	25.4 (9)
N8 C27 C28 C29	-178.3 (6)	C43 C44 C45 C50	-152.5 (6)
N8 C27 C28 C33	4.7 (9)	C44 C45 C46 C47	-178.3 (5)
C18 N5 C24 O2	2.7 (10)	C44 C45 C50 C49	178.9 (6)
C18 N5 C24 N6	-178.2 (5)	C45 C46 C47 C48	-0.6 (9)
C18 C19 C20 F3	-179.7 (5)	C46 C45 C50 C49	1.0 (9)
C18 C19 C20 C21	-0.4 (10)	C46 C47 C48 C49	0.7 (10)
C19 C18 C23 C22	-0.7 (9)	C47 C48 C49 C50	0.1 (10)
C19 C20 C21 C22	0.0 (10)	C48 C49 C50 C45	-0.9 (10)
C20 C21 C22 F4	179.9 (6)	C50 C45 C46 C47	-0.2 (8)
C20 C21 C22 C23	0.0 (10)	C51 N11 N12 C44	-175.8 (6)
C21 C22 C23 C18	0.3 (10)	C51 N11 C42 N10	-6.2 (9)
C23 C18 C19 C20	0.7 (9)	C51 N11 C42 C43	175.5 (6)

Table 7 Hydrogen Atom Coordinates ($\text{\AA} \times 10^4$) and Isotropic Displacement Parameters ($\text{\AA}^2 \times 10^3$) for BIRB_xtal3.

Atom	x	y	z	U(eq)
H1	7136	6072	4199	44
H2	6355	5663	5358	43
H2A	7331	6786	2872	47
H4	9907	5803	1587	54
H6	9405	4501	3941	41
H9	7652	3495	6529	41
H12	8563	2396	7635	50
H13	8922	1143	8696	59
H14	7499	864	9905	70
H15	5653	1855	10032	70
H16	5278	3104	8979	56
H17A	3903	5638	6884	63
H17B	5114	6013	6082	63
H17C	5955	5902	6860	63
H5	3546	4259	9821	40
H6A	2742	5392	8998	39
H19	4761	3001	10441	42
H21	4237	1729	12792	50
H23	2188	4015	11701	42
H26	780	6605	9949	38
H29	-396	7701	10031	58
H30	-2010	8720	10172	71
H31	-2958	9873	9074	62
H32	-2303	9974	7853	57
H33	-750	8955	7703	49
H34A	1285	6869	7247	61
H34B	2139	6032	7863	61
H34C	3386	6802	7455	61
H9A	1266	9913	5875	39
H10	2630	9127	5546	39
H36	67	10482	6621	42
H38	-91	12894	5735	56
H40	2005	11890	4398	44
H43	4278	10191	3448	39
H46	6696	10208	2498	43
H47	7945	10408	1281	50
H48	7701	9428	907	53
H49	6171	8255	1725	55
H50	4868	8064	2923	48
H51A	3492	7290	5530	70
H51B	2317	7884	5771	70
H51C	4480	7762	5886	70
H4A	4001	6556	4578	67
H4B	5140	7198	4431	67
H5A	5063	4552	8364	67
H5B	5797	4720	8921	67
H6B	-393	8799	6438	67
H6C	871	8341	7015	67

Experimental

Single crystals of $C_{17}H_{16}F_2N_4O_2$ [BIRB_xtal3] were [1]. A suitable crystal was selected and [1] on a **Xcalibur, Eos, Gemini ultra** diffractometer. The crystal was kept at 173.0 K during data collection. Using Olex2 [1], the structure was solved with the ShelXT [2] structure solution program using Direct Methods and refined with the ShelXL [3] refinement package using Least Squares minimisation.

1. Dolomanov, O.V., Bourhis, L.J., Gildea, R.J., Howard, J.A.K. & Puschmann, H. (2009), J. Appl. Cryst. 42, 339-341.
2. Sheldrick, G.M. (2008). Acta Cryst. A64, 112-122.
3. Sheldrick, G.M. (2008). Acta Cryst. A64, 112-122.

Crystal structure determination of [BIRB_xtal3]

Crystal Data for $C_{17}H_{16}F_2N_4O_2$ ($M = 346.34$ g/mol): triclinic, space group P-1 (no. 2), $a = 7.3053(6)$ Å, $b = 19.0191(15)$ Å, $c = 19.5624(16)$ Å, $\alpha = 61.876(8)^\circ$, $\beta = 85.618(7)^\circ$, $\gamma = 86.500(7)^\circ$, $V = 2389.1(4)$ Å³, $Z = 6$, $T = 173.0$ K, $\mu(\text{CuK}\alpha) = 0.963$ mm⁻¹, $D_{\text{calc}} = 1.444$ g/cm³, 17105 reflections measured ($8.92^\circ \leq 2\theta \leq 142.83^\circ$), 9017 unique ($R_{\text{int}} = 0.0700$, $R_{\text{sigma}} = 0.1049$) which were used in all calculations. The final R_1 was 0.0997 ($I > 2\sigma(I)$) and wR_2 was 0.3044 (all data).

Refinement model description

Number of restraints - 0, number of constraints - unknown.

Details:

1. Fixed Uiso

At 1.2 times of:

All C(H) groups, All N(H) groups

At 1.5 times of:

All C(H,H,H) groups, All O(H,H) groups

2.a Free rotating group:

O4(H4A,H4B), O5(H5A,H5B), O6(H6B,H6C)

2.b Aromatic/amide H refined with riding coordinates:

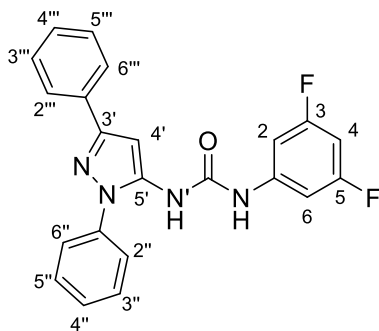
N1(H1), N2(H2), C2(H2A), C4(H4), C6(H6), C9(H9), C12(H12), C13(H13), C14(H14), C15(H15), C16(H16), N5(H5), N6(H6A), C19(H19), C21(H21), C23(H23), C26(H26), C29(H29), C30(H30), C31(H31), C32(H32), C33(H33), N9(H9A), N10(H10), C36(H36), C38(H38), C40(H40), C43(H43), C46(H46), C47(H47), C48(H48), C49(H49), C50(H50)

2.c Idealised Me refined as rotating group:

C17(H17A,H17B,H17C), C34(H34A,H34B,H34C), C51(H51A,H51B,H51C)

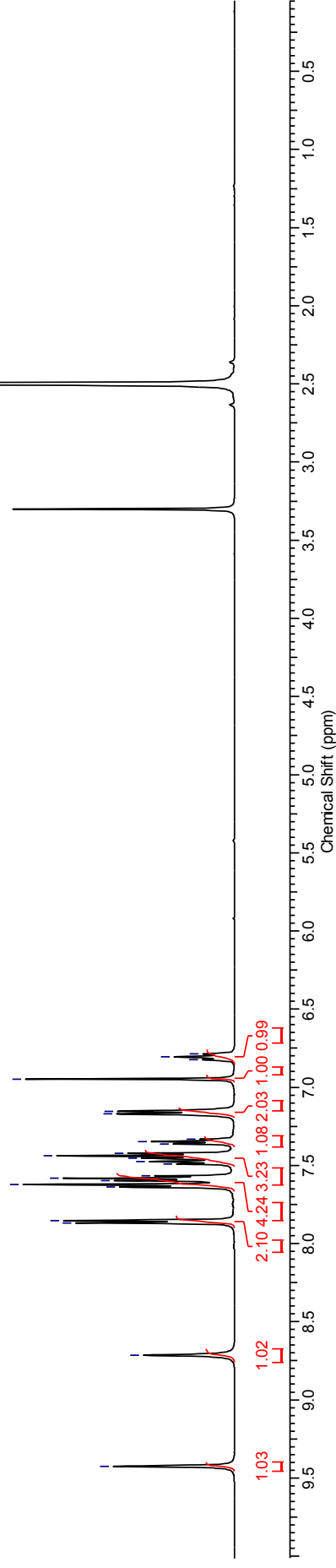
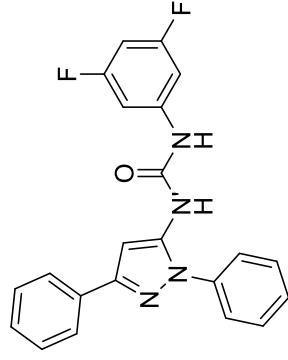
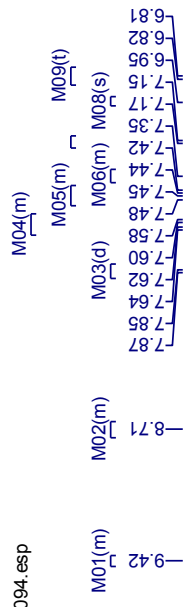
This report has been created with Olex2, compiled on 2014.09.19 svn.r3010 for OlexSys. Please [let us know](#) if there are any errors or if you would like to have additional features.

***N*-(3,5-Difluorophenyl)-*N'*-(1,3-diphenyl-1*H*-pyrazol-5-yl)urea**
(2320)



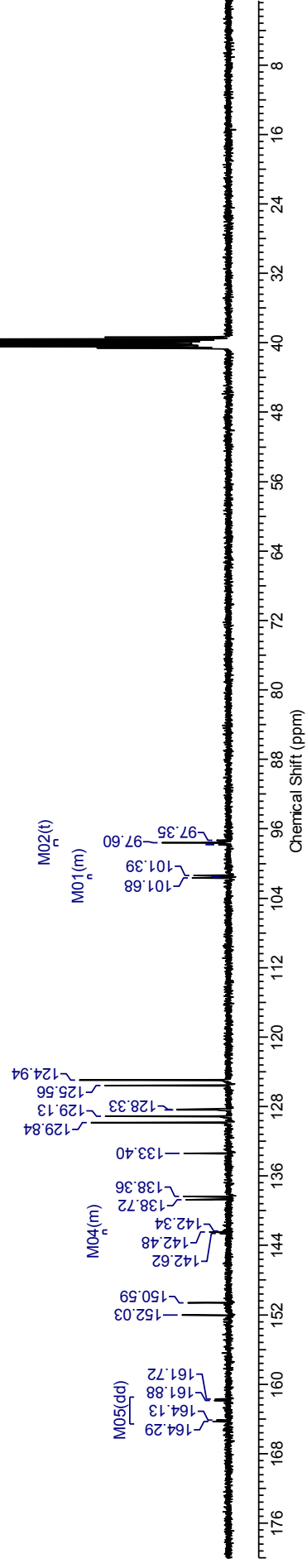
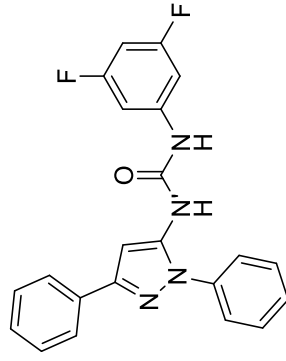
¹H NMR spectrum (500 MHz, DMSO-*d*₆) for *N*-(3,5-Difluorophenyl)-*N'*-(1,3-diphenyl-1*H*-pyrazol-5-yl)urea

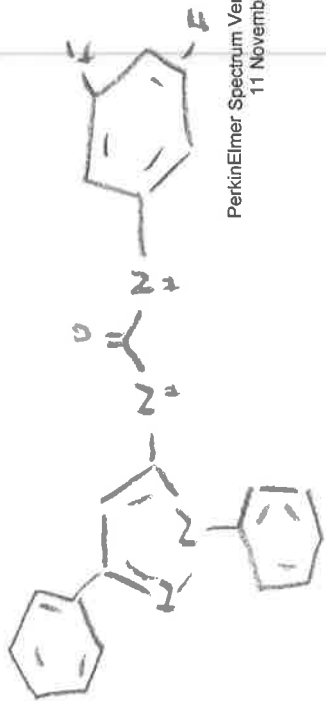
B04JD094.esp



¹³C NMR spectrum (100 MHz, DMSO-*d*₆) for *N*-(3,5-Difluorophenyl)-*N'*-(1,3-diphenyl-1*H*-pyrazol-5-yl)urea

B04JD094 CARBON_01.esp

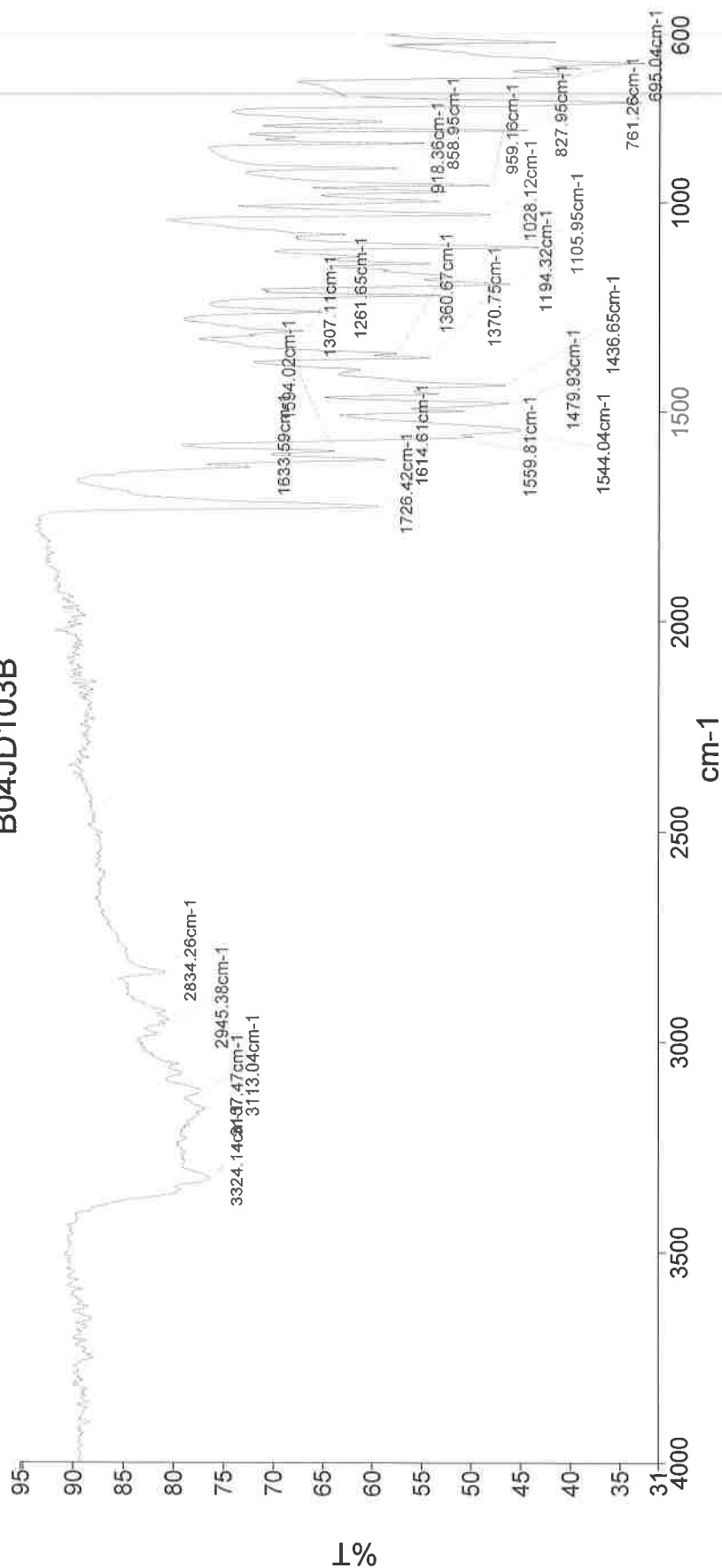




PerkinElmer Spectrum Version 10.03.06
11 November 2015 14:35

Analyst
Date
Administrator
11 November 2015 14:35

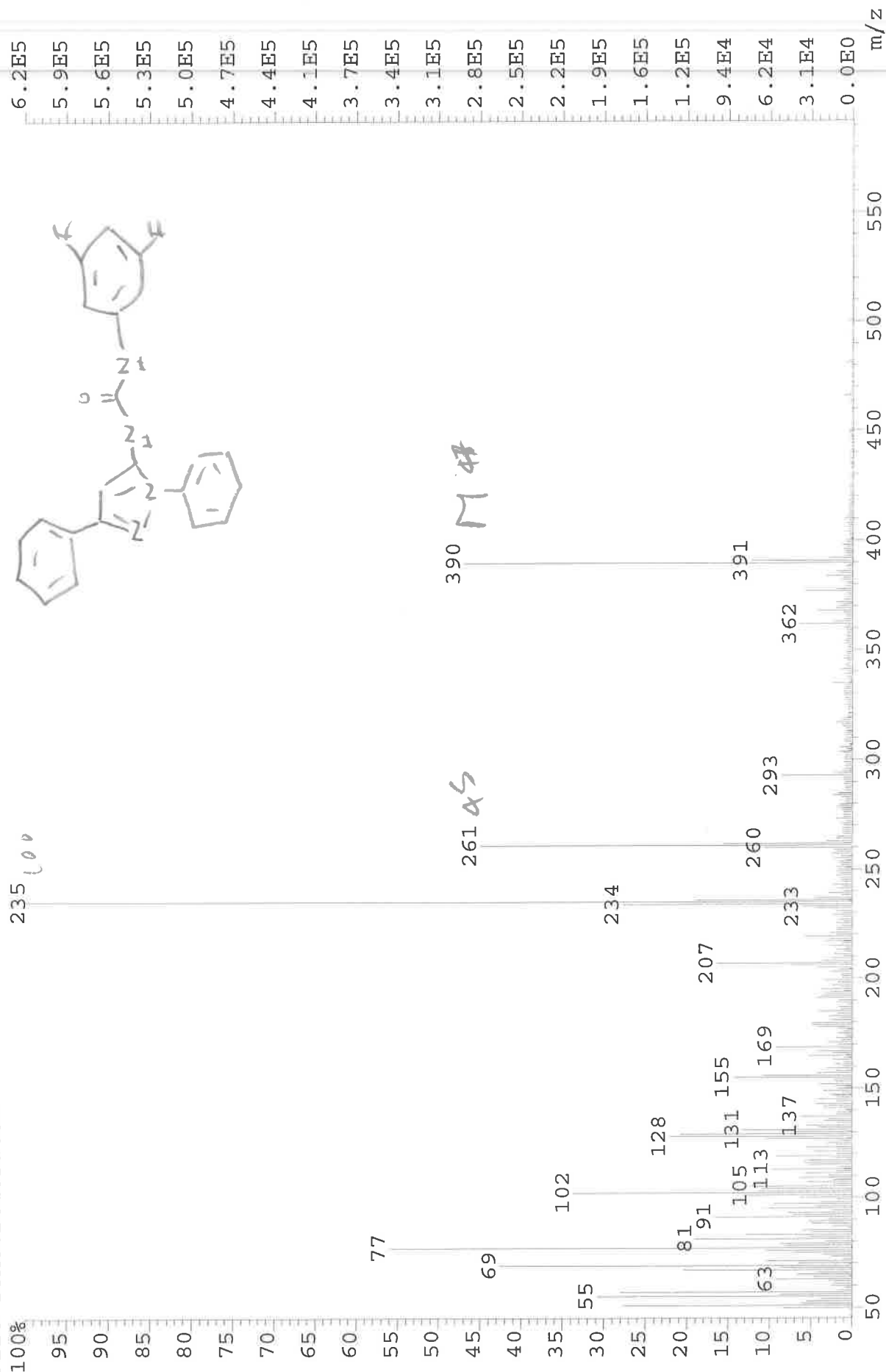
B04JD103B



3324 - N-H str
2945 - C-H str
1726 - C=O
1615 - N-H bend
1544 - N-H bend
1480 - C-C str
1194 - C-N str
1106 - C-F str

249-090 Sample 090 By Administrator Date Wednesday, November 11 2015

File: JESS6344 Ident: 18 Acq: 25-NOV-2015 10:31:26 +1:10 Cal: CAL1
 AutoSpecE EI+ Magnet BpI: 623896 TIC: 10897816 Flags: HALL
 File Text: BO4JD103B



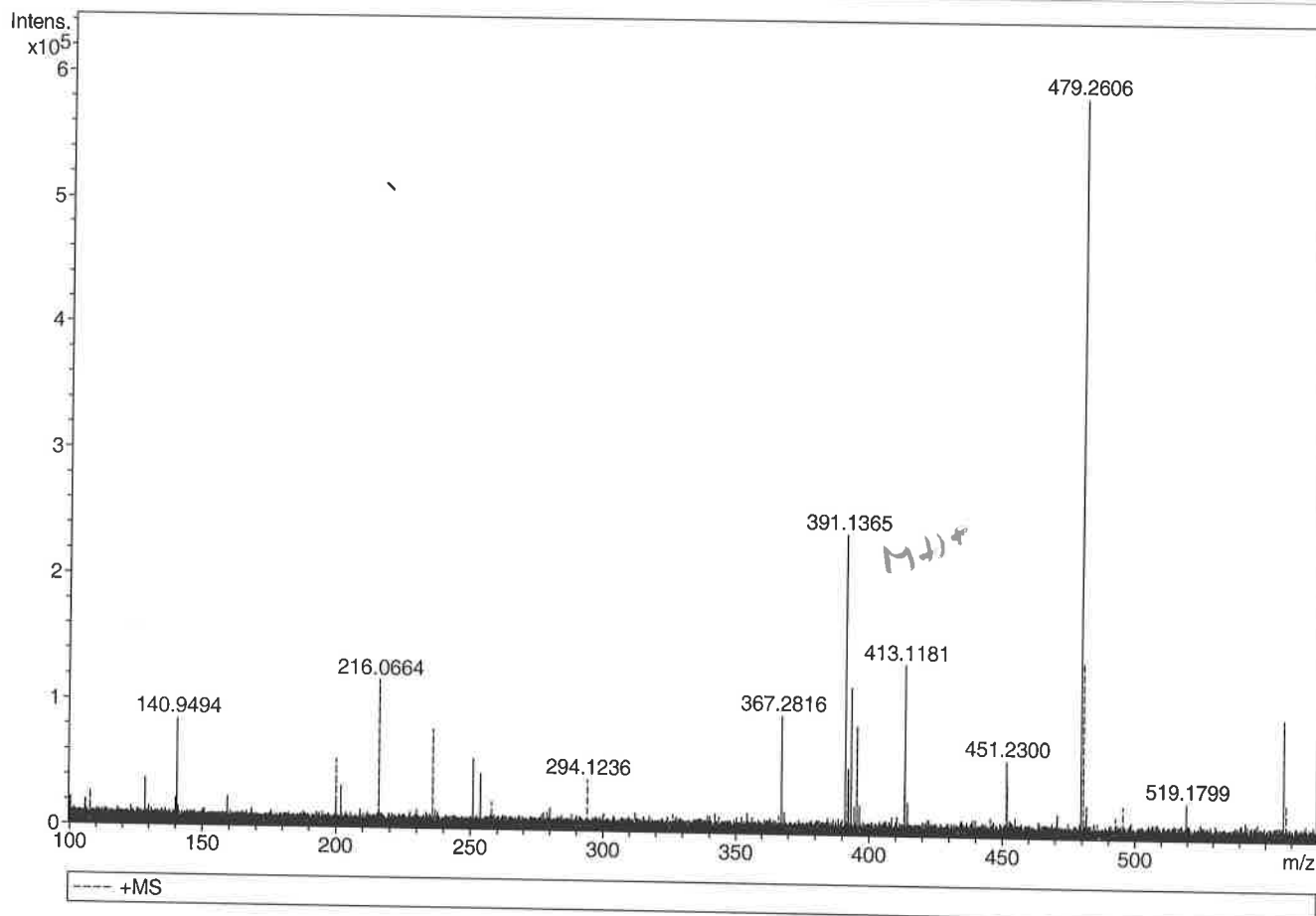
Generic Display Report

Analysis Info

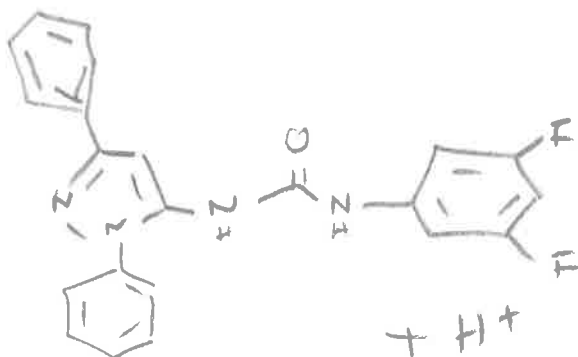
Analysis Name D:\Data\Alinanopos\JESS6344_000001.d
 Method pos20090608esi
 Sample Name POS ESI BO4JD103B
 Comment

Acquisition Date 25/11/2015 09:43:03

Operator Administrator
 Instrument apex-III

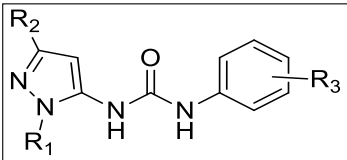
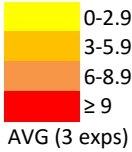


Sum Formula	Sigma	m/z	Err [ppm]	Mean Err [ppm]	Err [mDa]	rdb	N Rule	e ⁻
C 22 H 17 F 2 N 4 O 1	0.264	391.1365	0.08	-113.38	-44.43	15.50	ok	even



		SRPK1A	SRPK2A	MAPK14A	CLK1A	DYRK1AA	PIM1A
COMPOUND		AVG	AVG	AVG	AVG	AVG	AVG
1 s t B i r b L i b r a r y	B03JD133A	2.92	0.57	15.8	1.6	2.67	1.94
	B03JD137B	1.34	0.17	13.08	0.4	0.16	0.24
	B03JD138 A	8.55	1.58	10.64	3.17	4.19	3.08
	B03JD139C	8.02	1.04	7.59	2.21	1.79	2.28
	B03JD140B	7.13	0.82	12.25	1.82	0.96	1.46
	B03JD141B	9.19	1.45	2.03	3.07	3.87	2.8
	B03JD143B	5.75	0	4.56	4.4	0	1.82
	B03JD144B	4.39	0.44	7.88	1.5	1.31	1.64
	B03JD145C	2.82	0.54	12.09	1.4	1.19	1.2
	B03JD146B	11.69	2.36	12.43	3.98	3.15	3.03
	B03JD147A	3.91	0.41	12.3	1.25	0.87	0.92
	B03JD152	0	0	0	0.13	0.06	0.45
2 n d B i r b L i b r a r y	B04JD088B	9.95	1.34	1.17	2.79	2.97	2.41
	B03JD190A	11.8	1.52	1.24	2.08	2.13	2.03
	B04JD001A	11.81	1.35	0.82	2.65	2.12	2.76
	B04JD004B	-0.61	1.32	1.54	2.14	2.36	1.98
	B04JD010A	1.15	0.75	0.49	1.25	2.63	2.21
	B04JD012A	12.25	1.34	0.7	19.53	3.24	11.48
	B04JD086B	2.57	1.58	1.86	2.7	4.34	4.5
	B04JD89B	1.72	1.09	0.81	2.2	2.52	2.76
	B04JD096A	13.72	1.46	5.18	3.17	2.25	2.01
	B04JD087B	14.82	2.33	6.48	4.51	1.96	2.6
	B04JD090B	6.37	0.42	2.84	0.55	0.61	-0.15
	B04JD083A	12.62	1.51	5.33	2.83	1.98	1.93
	B04JD109B	14.15	2.14	7.51	3.87	1.69	1.56
	B04JD092A	0.14	0.13	0.1	-0.01	0.45	-0.04
	B04JD108C	12.72	1.94	5.1	3.18	2.71	2.35
	B04JD097A	1.34	0.37	0.22	1.41	1.74	1.2
	B04JD103B	2.27	1.23	2.59	2.07	3.48	2.87

R1	R2	R3
phenyl	tert-butyl	
phenyl	tert-butyl	1-Naphthyl
phenyl	tert-butyl	o-tolyl
phenyl	tert-butyl	2-naphthyl
phenyl	tert-butyl	4-ethoxyphenyl
phenyl	tert-butyl	4-fluorophenyl
phenyl	tert-butyl	bis-(3,5-CF3)Phenyl
phenyl	tert-butyl	3-benzyloxyphenyl
phenyl	tert-butyl	3,5-dimethylphenyl
phenyl	tert-butyl	5-fluoro-2-methylphen
phenyl	tert-butyl	3,4-difluorophenyl
phenyl	tert-butyl	phenyl
phenyl	tert-butyl	p-tosylate
phenyl	tert-butyl	3-methoxyphenyl
phenyl	tert-butyl	p-tolyl
R1	R2	R3
p-tolyl	tert-butyl	bis-(3,5-CF3)Phenyl
methyl	tert-butyl	bis-(3,5-CF3)Phenyl
4-fluorophenyl	tert-butyl	bis-(3,5-CF3)Phenyl
4-nitrophenyl	tert-butyl	bis-(3,5-CF3)Phenyl
tert-butyl	tert-butyl	bis-(3,5-CF3)Phenyl
4-bromophenyl	tert-butyl	bis-(3,5-CF3)Phenyl
methyl	phenyl	bis-(3,5-CF3)Phenyl
phenyl	phenyl	bis-(3,5-CF3)Phenyl
phenyl	tert-butyl	3,5-difluorophenyl
p-tolyl	tert-butyl	3,5-difluorophenyl
methyl	tert-butyl	3,5-difluorophenyl
4-fluorophenyl	tert-butyl	3,5-difluorophenyl
4-nitrophenyl	tert-butyl	3,5-difluorophenyl
tert-butyl	tert-butyl	3,5-difluorophenyl
4-bromophenyl	tert-butyl	3,5-difluorophenyl
methyl	phenyl	3,5-difluorophenyl
phenyl	phenyl	3,5-difluorophenyl



yl

- two nitro models very different results!!

LOSS OF ACTIVITY WITH BULK @ 1-N

LOSS OF ACTIVITY WITH 3-PHENYL

LOSS OF ACTIVITY WITH 3-PHENYL

- two nitro models very different results!!

LOSS OF ACTIVITY WITH BULK @ 1-N

LOSS OF ACTIVITY WITH 3-PHENYL

LOSS OF ACTIVITY WITH 3-PHENYL